16-17 November, Novi Sad, Serbia

16th International Scientific Conference

integration Novelty Design interdisciplinarity Sustainability

Proceedings

16th International Conference - integration, Novelty, Design, interdisciplinarity, Sustainability - Conference Proceedings

Editors: M. Trivunić, I. Džolev, M. Šešlija

DEPARTMENT OF CIVIL ENGINEERING AND GEODESY

iNDiS2023

16 iNDiS 2023

INTERNATIONAL SCIENTIFIC CONFERENCE

“Integration, Novelty, Design, Interdisciplinarity, Sustainability”

PROCEEDINGS

Novi Sad, Serbia, 16-17 November 2023

Editors:	Milan Trivunić Igor Džolev Miloš Šešlija
Technical organization of the meeting:	Department of Civil Engineering and Geodesy, Faculty of Technical Sciences, Novi Sad
Technical editor of the proceedings:	Miloš Šešlija
Graphic design:	Sara Koprivica
Publisher:	Department of Civil Engineering and Geodesy, Faculty of Technical Sciences, Novi Sad

CIP - Каталогизација у публикацији
Библиотеке Матице српске, Нови Сад

69.05(082)
624(082)
72:502.1(082)

INTERNATIONAL Scientific Conference „Integration, Novelty, Design, Interdisciplinarity, Sustainability" (16 ; 2023 ; Novi Sad)
Proceedings [Elektronski izvor] / 16th International Scientific Conference „Integration, Novelty, Design, Interdisciplinarity, Sustainability" iNDiS 2023, Novi Sad, Serbia, 16-17 November 2023. ; [editors Milan Trivunić, Igor Džolev, Miloš Šešlija]. - Novi Sad : Faculty of Technical Sciences, 2023

Način pristupa (URL): https://indis.gradjevinans.net/. - Nasl. sa naslovnog ekrana. - Opis zasnovan na stanju na dan 28.12.2023. - Bibliografija uz svaki rad.
ISBN 978-86-6022-615-2

а) Индустријска градња -- Зборници б) Грађевинске конструкције -- Зборници в) Архитектура -- Еколошка градња – Зборници

COBISS.SR-ID 134266377

PROGRAM COMMITTEE
Milan Trivunić, Chairman
Srđan Kolaković
Igor Peško
Andrija Rašeta
Miloš Šešlija
Vladimir Mučenski
Ivan Lukić
Marko Marković
Dragana Konstantinović
Igor Džolev
Slobodan Kolaković
Senka Bajić

ORGANIZING COMMITTEE
Igor Džolev, Chairman
Anka Starčev-Ćurčin
Vesna Bulatović
Vladimir Vukobratović
Milan Marinković
Jovana Topalić
Suzana Draganić
Goran Jeftenić
Đorđe Jovanović
Mehmed Batilović
Višnja Žugić
Tiana Milović
Slaviša Dumnić

SCIENTIFIC COMMITTEE
Zoran Matijević, Canada
Igor Džolev, Serbia
Miljana Zeković, Serbia
Anka Starčev-Ćurčin, Serbia
Darko Nakov, N. Macedonia
Damir Varevac, Croatia
Dušan Kovačević, Serbia
Paulo B. Lourenço, Portugal
Damir Markulak, Croatia
Sergio Ruggieri, Italy
Vladimir Vukobratović, Serbia
Slaviša Trajković, Serbia
Tahir Hanif, UK
Mitar Đogo, Serbia
Ksenija Janković, Serbia
Duško Lučić, Montenegro
Milan Trivunić, Serbia
Asterios Liolios, Greece
Vesna Bulatović, Serbia
Robert Pečenko, Slovenia
Zoran Brujić, Serbia
Mirjana Laban, Serbia
Michael C. Forde, UK
Dragan D. Milašinović, Serbia
Marko Mihić, Serbia
Gyorgy L. Balazs, Hungary
Miha Tomaževič, Slovenia
Biljana Šćepanović, Montenegro
Marija Nefovska-Danilović, Serbia
Meri Cvetkovska, N.Macedonia
Ana Trombeva-Gavriloska, N. Macedonia
Tomaž Hozjan, Slovenia
Milos Knezevic, Montenegro
Jelena Dobrić, Serbia
Koichi Kusunoki, Japan
Srđan Kolaković, Serbia
Nenad Fric, Serbia
Zoran Sušić, Serbia
Danijel Kukaras, Serbia
Mladena Luković, Netherlands
Aleksandar Pavić, UK
Ana Baričević, Croatia
Sofija Kekez, Poland
Ivan Ignjatović, Serbia
Luisa Giuliani, Denmark
Chiara Bedon, Italy
Zlatko Marković, Serbia
Marijana Serdar, Croatia
Emina Hadžić, BiH
Bojana Grujić, BiH

iNDiS 2023

Department of Civil Engineering and Geodesy, Faculty of Technical Sciences, University of Novi Sad, is organizing the sixteenth international scientific conference "iNDiS 2023" - integration, novelty, design, interdisciplinarity, sustainability. From this year, the modified format of the event starts, therefore the conference will be held biennial in the future.

Topic of the first conference, held in 1976, was "Industrial construction of apartments" because of its modernity in that period. Later, conferences were held with a considerably broader theme of "Construction Industrialization", and soon papers from all areas of construction appeared at the conference, from urban planning and design of buildings of various purposes, to maintenance and major interventions on the built construction stock. This led to the expansion of the area of expertise, covered by this conference, in which, in addition to civil engineers, urban planners, architects, engineers of other professions, who work in construction, sociologists, economists and others participate.

This conference, like several previous ones, covers the problems of planning, designing, construction and renovation of construction, geodesy, geoinformatics and risk management of catastrophic events, which have come across to an adequate response from researchers and engineers of various profiles, both from our country and abroad.

Members of the International Scientific Committee actively participated in the preparation of the conference, both as reviewers and authors. It is expected that the presentations of papers and discussions at the conference will enable the definition of the main directions of construction development, in accordance with modern trends, since many ideas and results, experimental and theoretical researches in the fields of construction have been promoted.

For this conference, the Proceedings consists of two books, namely Book 1. Papers in English and Book 2. Papers in Serbian, which enables better and more fruitful communication and exchange of experiences with colleagues from abroad.

Additionally, the possibility of establishing new and strengthening existing professional and collegial ties is also of the great importance. This year, authors from 13 countries are participating in the Conference, and the Proceedings Book 1 contains 94 papers in English, while the Book 2 contains 23 papers in Serbian, in total 117 papers.

The editors express their sincere gratitude to all the authors for the effort invested in writing the papers as well as for their contribution to this event.

Editors of the Proceedings

CONFERENCE SPONSORS

PLATINUM SPONSORS

- PROJECT BIRO UTIBER DOO NOVI SAD
- GAT DOO NOVI SAD

GOLDEN SPONSORS

- AXIS GRAĐEVINSKI BIRO DOO SREMSKA KAMENICA
- BECHTEL ENKA UK LIMITED OGRANAK BEOGRAD
- STRUCTURA CONCEPT

SILVER SPONSORS

- INŽENJERSKA KOMORA SRBIJE
- ČELIK DOO BAČKI JARAK
- “JADRAN“ D.O.O.
- ENERGOTEHNIKA JUŽNA BAČKA DOO NOVI SAD
- DELTA REAL ESTATE D.O.O. BEOGRAD
- AG INSTITUT DOO NOVI SAD

BRONZE SPONSORS

- INSTITUT IMS AD BEOGRAD
- PRO-ING DOO NOVI SAD
- GRAĐEVINSKI INSTITUT CPL DOO VETERNIK
- TEAMCAD DOO BEOGRAD
- DEL ING DOO BEOGRAD
- DT MAPPING KRALJEVO
- ASIP PREVENT DOO NOVI SAD
- MHM-PROJEKT DOO NOVI SAD
- CAD SOLUTIONS DOO
- MAPEI SRB D.O.O. BEOGRAD
- GP BEST IZGRADNJA DOO NOVI SAD
- IGOR AJDUKOVIĆ PR IZGRADNJA STAMBENIH I NESTAMBENIH ZGRADA AJDUKOVIĆ GRADNJA SREMSKA KAMENICA
- DOO PUT-INVEST NOVI SAD
- ELITA-COP DOO BEOGRAD-ZEMUN

FRIEND OF THE CONFERENCE

- GP GRADITELJ NS DOO
- KARIN KOMERC MD DOO VETERNIK
- GMP GRAMONT-NS DOO NOVI SAD
- MODERA DOO NOVI SAD
- ADOMNE DOO PROJEKTOVANJE I INJŽENJERING NOVI SAD
- A.D. "ROMANIJAPUTEVI" SOKOLAC
- HIDROZAVOD DTD AD NOVI SAD

- MBBM ING DOO ZA PROJEKTOVANJE, INŽENJERING, NADZOR I USLUGE
- VOJVODINAPUT-BAČKAPUT DOO NOVI SAD
- SAINT-GOBAIN GRAĐEVINSKI PROIZVODI DOO BEOGRAD
- AD VOJVODINAPROJEKT NOVI SAD
- BALDINISTUDIO INTERNATIONAL DOO NOVI SAD

CONTENTS

ARCHITECTURE AND URBAN PLANNING

GEODESY AND GEOINFORMATICS

DISASTER RISK MANAGEMENT AND FIRE SAFETY

SPONSORS

PLENARY LECTURES

SPENS: ENCLOSED CITY CENTRE – APPROACH AND DESIGN METHODOLOGY FOR RECONSTRUCTION OF "SPORTS AND BUSINESS CENTRE VOJVODINA"

*Dragana Konstantinović [1]**

Summary:

For the past three years, the planning process for the reconstruction of the "Sports and Business Center Vojvodina" has been underway, initiated with the creation of the *Spens Facility Development Strategy*[2]. The strategy outlines the future mission of the Spens Centre, emphasises its (new) social tasks, and establishes the basic principle for further development and reconstruction of the building as a sports-recreational and active social centre. The strategy's overall goal *outlines directions for sustainable reconstruction and development of Spens*. In connection with this, specific issues related to the facility's physical structure, spatial programming, and technical-technological systems have been concretised.

This important foundational document has guided the process of creating the Preliminary Design, which was carried out by the team from the Faculty of Technical Sciences in Novi Sad, in collaboration with partners Axis Construction Bureau from Novi Sad, as well as the companies Bexel and BSS from Belgrade. The multidisciplinary team's work on this project has raised numerous questions about the approach to reconstructing buildings from the second half of the 20th century, specific goals that should be set in the design process, and strategies for achieving these goals. As the Spens building is valued as a unique urban sports and social centre with authentic architectural and urbanistic values from the era it was built, the conceptual framework for its renovation has been determined. The Preliminary Design provides answers to identified programmatic, technical-technological, spatial, and design issues defined by the Project Assignment, in which all requirements and expectations of the client, as well as conditions for meeting the demands of future user groups, are clearly outlined. The specification of these requirements has defined the specific goals of the project: achieving adequate functioning of all envisaged sports processes in the facility in all required regimes (competitive, training, representative), as well as all other necessary activities in the facility that complement the functions of sports; improving the physical structure of the facility, which will significantly enhance the closer and broad urban context, as well as all aspects of facility use; contributing to the new visual and ambient value of the city through a sustainable approach to the reconstruction of the iconic building that symbolizes the urban values of Novi Sad; ensuring accessibility for all user groups - meeting the principles of "universal design"; achieving adequate thermal, acoustic, and visual comfort for users; establishing an energy-efficient facility in operation; implementing a system for using renewable energy sources; environmentally friendly selection of materials and technologies and minimizing environmental impact in all phases; rational structural and spatial solutions that will

[1] Assoc. prof., Faculty of Technical Sciences, University of Novi Sad, Serbia, konstan_d@uns.ac.rs
* On behalf of the team of engineers working on the Preliminary design project for the reconstruction, extension and building of the Sports and Business Centre Vojvodina–Spens

[2] Srđan Kolaković, Dragana Konstantinović, Miljana Zeković, Višnja Žugić, Maja Momirov, Slobodan Jović, Bojan Stojković, Igor Peško, Vladimir Mučenski, Strategija razvoja objekta Spensa: Spens – natkriveni gradski centar, Fakultet tehničkih nauka, Novi Sad, 2021.

affect building efficiency, relying on the principles and experience of the existing structure of Spens.

The conceptual framework developed in the Preliminary design project for the reconstruction, extension and building of the Sports and Business Centre Vojvodina–Spens represents an integral design solution for defined parameters. Also, it establishes the spatial, functional, ambient, and technological frameworks for future work on the project. All activities preceding the project—historical research, programmatic reassessment, development of the Development Strategy, and assessment of the facility's condition in spatial, functional, and technical-technological terms—were essential steps in creating a specific methodology for work on the project. This was necessary to clearly understand, conceptualise, design, and, in the future, achieve the conditions for the new life of the multifunctional, covered urban centre Spens.

Key words: architectural design; engineering; reconstruction; 20th-century heritage; Novi Sad, Spens

MANAGEMENT OF MAJOR INTERNATIONAL PROJECTS

Zoran Matijevic[1]

Summary

Although all projects involve the same set of project management knowledge areas, depending on their size and the locality of their execution, some specific management approaches and actions are required to maximize positive and minimize negative outcomes. This paper explains methods and systems to optimally manage major projects performed in the international environment by EPC (Engineering, Procurement, and Construction) and EPCM (Engineering, Procurement, and Construction Management) contractors.

Besides knowledge, the project manager's ability to adequately structure, staff, direct and motivate the project team, which shall, in return, gather, produce and process an immense volume of information and consistently make optimal decisions, is of critical importance. This paper provides optimal leadership approaches and team management tools for the successful execution of major international projects.

Keywords: Major International Projects, Project Phases, Project Delivery, Performance.

1 Project Director, Independent Consultant, Montreal, Canada, zoran.matijevic@yahoo.com

1. INTRODUCTION

1.1 PROJECT SIZE

Project size is usually defined based on its capital expenditure (CapEx) and complexity. Although there is a significant correlation between the two, it is not absolute, so both factors need to be taken into account while classifying projects based on their size, with CapEx leading the classification and complexity modulating it.

Project complexity depends on technical and societal challenges that need to be resolved. Technical challenges encompass engineering and organizational requirements, while societal challenges encompass stakeholder, regulatory, and geopolitical factors.

Therefore, at expected complexity for their size, small projects have CapEx up to \$10 million, medium-size projects between \$10 and \$100 million, major projects (also known as large or capital projects) between \$100 million and \$1 billion, mega projects between \$1 billion and \$10 billion and giga projects above \$10 billion. Increased complexity could drive the project to a higher category and vice versa. This paper is focused on major projects.

1.2 PROJECT LOCALITY

Based on the locality, projects can be classified as domestic and international. Domestic projects are executed in a single country, typically under the same legislation, with a common language, similar cultural and behavioral norms, a narrow specter of stakeholders, a similar climate, and relatively short supply chains. On the other hand, international projects are more complex - they are executed in more than one country, with often quite different geographical, climate, and societal environments, long supply chains, multiple local communities, a wide specter of stakeholders with often conflicting interests, and are influenced by geopolitical risks and opportunities. This paper analyzes international projects.

1.3 EXECUTION MODEL

Industrial projects are typically executed in the following provider options: directly by the client, EPC (Engineering, Procurement, and Construction), EPCM (Engineering, Procurement, and Construction Management), and Hybrid (combining elements of the previous three models) [1]. This paper analyzes EPC and EPCM models. Although it is not mentioned in their formal names, both models can, and mostly do include commissioning and startup of the project products. This paper considers the delivery of industrial projects in all their phases, from initiation to closure. As they are the most complex construction-driven projects, the findings can be applied to other project types through the elimination of non-applicable analysis segments.

In the EPC project delivery model, the contractor has most of the control over the project execution, especially under the lump-sum contract. The contractor is responsible for and has authority over all phases of the project execution, limited purely by compliance with the relevant legislation and the contractual stipulations. The contractor produces and hands over the project deliverables to the client, while the client's ability to direct the execution approach and its sequence is minimal. The client issues a head contract to the contractor, who in turn performs the work itself or subcontracts portions of the work as required, and bears full responsibility for its profit and loss.

In the EPCM model, the client retains significant control over the project execution. Typically, the contractor executes the engineering under the close oversight, and sometimes direction of the client, assists with the procurement process, and provides construction *management* services. The client issues direct contracts to all contractors -

the EPCM, suppliers, fabricators, logistics, construction, and commissioning. The contractor in this model typically operates on a cost-reimbursable basis.

1.4 PAPER OBJECTIVES

The primary objective of this paper is to provide real-life experiences and practical recommendations to project managers, with the goal of increasing their ability to successfully deliver major international projects, through: Examining the unique characteristics of the subject projects; Explaining the major challenges associated with such projects; and Providing management methods and systems, as well as leadership approaches and team management tools required for their successful execution.

1.5 PAPER METHODOLOGY

To achieve the research objectives, this paper will employ a review of the existing literature in the subject science area, as well as the author’s personal work experience on multiple large international projects and his work and interviews with leading industry experts.

1.6 PAPER STRUCTURE

This paper is structured to provide a systemic analysis of the major international projects' execution. It analyzes all significant project aspects and phases, in chronological order, from its initiation to closure, and provides major findings, recommendations, guidelines, and conclusions that have been produced during this research.

2. PROJECT INITIATION

As the project size grows, its initiation becomes more important. Successful project initiation encompasses the following:

- A *project charter* development. This document appoints the project manager, defines his or her responsibility and authority, defines the project team and its internal and external relationships, defines project strategy, scope, budget, milestones, and drivers;
- Identification of all known *stakeholders* and their relationship with the project;
- *Kickoff meeting*, which ensures the strategic alignment between the contractor and the client, especially when it comes to a definition of the project drivers, objectives, and success, the scope of facilities and services, key strategies, milestones, communication protocols, focus areas, and immediate project execution steps. High-quality kickoff meetings involve a robust and detailed discussion, last for several hours, and result in a common project delivery understanding and expectations;
- Based on the previous steps, a *project execution plan* is to be prepared to elaborate on and document all critical items. It includes sub-plans covering management of all project phases and aspects - engineering, procurement, logistics, construction, commissioning, contracting, project controls, and HSE (health, safety, and environment).

The key strategy for project initiation is to *frontload* the project, i.e. to make the project team demonstrate at the very beginning its ability to: understand the reasons for the project’s undertaking, define clear project results, and define the most important actions required to deliver results within the applicable regulative and contractual stipulations. However, it is of the utmost importance for all stakeholders to understand and allow *flexibility* in the project delivery, through *progressive elaboration*. As the information becomes available during the project execution, the project manager and project team need to be allowed and able to constantly adapt their actions and project activities (tactics and sometimes strategies) to achieve or improve the project results. “Projects cannot directly adopt only one uniform and explicit goal or method communicated by a top management representative of a single parent organization. In fact, the project must carefully position itself to its environment, and the goals and management methods of the project must be carefully matched with the situation at hand and the context.” [2].

Successfully completed project initiation is essential for feasible project execution, as the approximate (rule of thumb) ratio of costs incurred on *prevention versus rectification* of issues shows that for $1 spent during the project initiation and setup, $10 would be required during design, $100 during fabrication and preassembly, and $1,000 during construction and commissioning.

3. PROJECT PLANNING AND CONTROL

“In preparing for battle I have always found that plans are useless, but planning is indispensable”, Dwight D. Eisenhower. Therefore, the realistic goal of planning is to formalize the most feasible and probable execution scenario which will serve as a *framework* for day-to-day project activities in a continually changing environment and evolving constraints. Good planning, therefore, results in having a majority of activities planned and executed in the “business-as-usual” mode, providing a spare capacity to deal with unplanned ones in the emergency mode.

3.1 PROJECT SCHEDULE

The key strategies to developing a good project schedule are: progressive elaboration, early inclusion of key stakeholders in the schedule development, impartiality with float utilization, and frequent updates.

3.1.1 Progressive Elaboration

The certainty of decision-making changes significantly during the project execution [3], which makes progressive elaboration the optimal scheduling method - starting from a high level and working on detailing as the project progresses. Insistence on a high level of detail too early in the project (to prove a detailed understanding of the project execution) is misguided and should be resisted as much as possible, especially if the pressure is internal. The notion that all project activities and their sequence remain the same, with only dates changing would be false, especially on complex, large, long-duration projects. On successful projects, work methods change, and resequencing occurs several times before the optimal schedule configuration is reached, and it is usually relatively close to the time of the activity execution. To be expedient in resequencing, the *blocks of activities* suitable for fast manipulation are needed. One should handle dozens, rather than hundreds or thousands of activities. Too many details early in the project execution would significantly slow down the progressive elaboration, and make changes very difficult or even impossible in any practical sense.

A purely theoretical approach to preparing “a good schedule and just executing it” would be possible in the static system existing in a vacuum. On real projects though, subcontractors go bankrupt, key equipment becomes unavailable, or superior solutions become available. The project has to be adjusted continually to reduce risks and amplify opportunities. The scheduling is unavoidably affected by it.

On the other hand, one must be cautioned to avoid descending into improvisation, which would have devastating effects on major projects. A good progressive elaboration starts from the major milestones in the level one schedule, defining start, duration, finish, and connections between major project phases for each major project deliverable, for example: engineering, procurement, fabrication, logistics, construction, and commissioning. Then, based on the project strategy, defining major activities within each phase in the level two schedule, for example: basic engineering, detail engineering, procurement of long-lead items, number of ships to be utilized for sea transport, civil construction works, structural-mechanical construction, electrical, instrumentation and controls construction, pre-commissioning, and commissioning. Level three schedule defines more granular activities like the production of certain groups of drawings, fabrication of individual elements, installation of each mechanical component at the site, etc. The level four schedule provides details for hands-on work execution, like each work activity for installation of every mechanical item, for example: setting, initial alignment, connection, and final alignment, where durations are measured in no more than a few days. Finally, the level five schedule covers the most sensitive work-face activities and sequences the work steps, where durations are measured in hours, like: lock-out, set-up workspace, de-coupling, etc.

3.1.2 Key Schedule Development Stakeholders

The key stakeholders for schedule development are the project manager, the project phase and/or area managers, the planner, the project sponsor, and the client's representatives. All of them shall be involved in the schedule development as soon as practically possible. Depending on the size of the project, besides project functional managers (engineering, procurement, fabrication, preassembly, logistics, construction, commissioning, HSE), area managers may be appointed, acting as autonomous sub-project managers. Both categories of managers shall perform detailed planning for their areas of responsibility and work on the integration of their sub-project schedule segments into the overall project schedule. The project sponsor provides comments related to the incorporation of the subject project schedule into the overall company's business strategy. The client's representatives provide comments on the subject project's schedule alignment with the other client's activities. The project planner should operate the planning software, advise on the best scheduling approaches, as all other stakeholders, and create what-if scenarios sufficient to judge their feasibility. In the EPC execution model, it is the project manager who ultimately makes key decisions and takes full responsibility for them. In the EPCM model, the client owns the overall project schedule and ultimately makes key decisions.

3.1.3 Impartial Float Utilization

The impulse to plan schedule activities as late as possible, to allow as much time as available for their delivery should be resisted, as the project teams typically show a tendency to work towards the late schedule, albeit knowing it is creating risk. This approach would also allow clients to deliver their inputs as late as possible, and add schedule risk with no direct consequences to them. Therefore, the best approach is to plan activities commencement as early as possible and utilize schedule float to optimize project results in real-time, during the project execution.

3.1.4 Schedule Update Frequency

The schedule needs to be updated weekly, as the common practice of bi-weekly, or even monthly updates prevents timely understanding of the current project status and prevents undertaking the required preventive and corrective actions.

3.2 PROJECT ACTION TRACKERS

A project cannot be successfully managed by schedule alone, as all project actions are *not* listed in the schedule, and for successful project execution, the missing actions have to be identified, planned, and tracked. The common practice of project team members managing their actions individually is inadequate, primarily due to the subjective understanding that each person has related to project priorities and how to achieve them. Utilizing an individual approach, the project team typically fails to identify all required actions, performs unnecessary actions, has more than one team member performing the same action independently (thus wasting resources and creating conflicts), and finally, optimizes each individual action instead of the overall project. The solution for this common disconnect is a detailed *action tracker*, created by the project team in the weekly project/subproject/phase meetings. Trackers are getting increasingly important with the project size increase. On very small projects with compact teams of just a few individuals that know each other well, a single tracker has limited benefits. Small and medium-sized projects significantly benefit from a single project tracker. On the other end of the spectrum, major, mega, and giga projects require several trackers to get any chance of success - a master project tracker, accompanied by sub-trackers for each phase and/or area of the project.

Trackers should predominantly contain actions requiring *intensive collaboration* between the project team members, and must *not* have activities listed in chronological order or classified in any sense, as any attempt to achieve that would render them unusable. The trackers utilize rolling planning with a fuzzy time horizon. Actions are to be added as far in the future as the team can reasonably perceive them, in every weekly project meeting. The whole project management team shall participate in defining tracker input and in its maintenance, and each action owner shall make sure his or her dates are realistic, and inputs available, so he or she can realistically succeed. This is a positive form of self-micromanagement, thus creating a feeling of empowerment instead of resentment. An optimally structured tracker is a table, which contains the following columns:

- *Action number*. Once assigned, it shall not be reassigned. An action keeps its number indefinitely, even if it is canceled;
- *Action description*. Any team member can propose it. However, *the team* amends it to suit the overall project needs, and the project manager has to modify it as required and accept it as the one who is ultimately accountable for the overall project performance. This is where the project optimization versus individual action optimization, as well as the team synergy, starts occurring. The action description has to be *clear and simple*, for example, “Issue a purchase order for grounding testing in Sector A”, or “Obtain site access for foundations surveyor in Sector B”. It is *not a problem description*, it is *an action* that will *resolve the problem*. Too often the inadequate action trackers stop at describing the problems, with no directive on how to proceed, when, and by whom. Repetitive actions, like issuing daily reports, or conducting a pre-start meeting at the site do not belong in the tracker. However, an action like “Start issuing daily reports” at the beginning of the project, does. The same is applicable for project schedule activities, with the exemption of important milestones, which should be emphasized in the tracker, and highly visible to the team;
- *Action owner* - the person responsible and qualified to perform the action, even if he or she does not directly create results. The responsibility for an action cannot be delegated, only the physical work can;
- *Planned completion date*. The action owner proposes it based on the available information, from his or her own perspective. The whole team then has to analyze the impact of the proposal on their own activities, and work on the optimization, until the best solution for the overall project is found;
- Once the execution of the actions starts, other priorities may arise, resource availability could change, etc., affecting their completion. As the planned completion date cannot be changed, *the forecast completion date* is required. Similarly to the planned completion date, once the forecasted date is proposed, the buy-in of the rest of the team has to be obtained. It might result in further re-

prioritization or adding resources, changing technologies, paying premiums to achieve critical milestones, or acceptance of the delay if the action is not critical. Reforecasting is to be done every week as the team discusses each and every open item. In the end, it results in a single trajectory for the complete project team - synergy. Forecasting shall not be guessing, it has to be logical and based on facts and qualified assumptions. Delaying an action shall not be tolerated without a solid reason for it;

- Once an action is complete, *the actual completion date* is registered. An activity shall not be closed if it is not 100% physically completed;
- Finally, *a status column* defines the following action states: in progress, completed, cancelled, or on hold.

The notion that such trackers are unnecessary bureaucracy shall be resisted at any cost. Master tracker session typically takes an hour and a half per week, and sub-trackers an hour per week. In return, this effort prevents significant losses (time, cost, reputation). Accountability of the team members is the key element for the described approach's success, and it is achieved through weekly reports to the whole team by each action owner on successes, failures, and required support to achieve the planned results. Once every team member realizes that everyone is treated solely based on the merit of their work, that the required support is being delivered by the rest of the team in good faith, and that all adjustments are made solely for the benefit of the project, the synergy is fully established, and consequently, the project performance improves significantly.

3.3 WAR ROOM MEETINGS

War Room meetings were introduced by Winston Churchill during World War II, as a corrective action to his orders not being executed, either properly, or not at all. In project management, such meetings are to be utilized to resolve a significant crisis.
A whiteboard with individual tasks on “sticky notes” is the main tool for the war room meetings. It details every working step required to resolve the crisis, the step owner, the logical relationship between the steps, and the completion dates. This meeting is corrective in its nature (opposite from the weekly project meetings which are preventive), it involves all personnel directly performing the distressed project activities (opposite from the weekly project meetings which involve management personnel), and it is preferably performed having personnel standing, on a daily basis, with a very limited duration, usually 15 to 30 minutes.
The most significant schedule impacts practically always come from the fragmentation of the work process, lack of communication or miscommunication, performing unnecessary tasks, misinterpreting priorities, personal animosities, correcting instead of preventing mistakes, and technical incompetence of personnel. Such meetings surface all these issues, so they can be dealt with, starting from the ones with the biggest positive impact.

3.4 PHYSICAL PROGRESS MEASURING

As per Galileo Galilei’s “Measure what can be measured, and make measurable what cannot be”, it is of the utmost importance on the project to know exactly what the planned and actual physical project progress is, continually throughout project execution. Just tracking the costs and schedule is insufficient for successful project control.
Physical project progress measuring is based on *productive work*, expressed in *100% productive direct man-hours*, as only productive work can transform project inputs into outputs - build the project product. Indirect and overhead work, like management, engineering support, as well as machine work are ignored.
The first step in this analysis is to estimate the productive man-hours required to perform every activity in the schedule. Then, all the estimated man-hours need to be

summarized, which will represent 100% of the physical progress. Participation of every activity's man-hours in the total man-hours defines proportional participation of that activity in the physical project progress, expressed as a percentage. That is called *the rule of credit* and will provide an accurate measurement of physical progress.
It is important to note that man-hours spent and shown on timesheets (colloquially known as "burned" hours) are almost never equal to the productive (earned) man-hours. Earned hours are calculated by multiplying actually observed physical progress on any deliverable with man-hours estimated for its execution. Although there is an element of subjectivity in observing the physical deliverable progress, it can be practically eliminated by observing level three or four activities, where items can be clearly quantified. For example, if four out of eight motors are installed, the earned physical progress is at 50%. Transferred into 50% of estimated hours, it will provide its participation in the overall earned physical project progress. This exercise is to be done every week for every project activity and every project deliverable. The physical progress is observed and agreed to by both, the contractor's and client's representatives.

3.5 LESSONS LEARNED

Lessons learned exercise is typically performed at the end of the project, by documenting the most prominent issues and opportunities registered on the current project, for utilization in future projects. This approach, however, deprives the current project of systemically utilizing the knowledge gathered during its execution. The best approach, therefore, would be to commence the lessons learned process at the start of the project execution, document in detail every lesson, and utilize and refine the actions throughout the project execution. Although project phases do not last throughout the entire project, a significant number of activities within them repeat in other phases, which is an opportunity to prevent the reoccurrence of already detected issues. For example, the office and site engineering have similar activities, as well as preassembly and construction phases, etc. Administrative and HSE activities are practically the same throughout the project.
The key points on lessons learned are: They are critical for performance improvement on the current and future projects; All project team members have to be included and contribute, to cover all project aspects; Start on the first day of the project execution, and maintain until the end of the project, as it should not be a forensic tool, but an active project management tool; It has to list both issues and opportunities; Project manager owns and manages the document; All lessons have to be quantified (cost and/or duration); Description of the problem is not sufficient, and actions to reduce risk or emphasize opportunity have to be defined; All actions shall have owners, planned, forecast and completion dates, as well as status.

4. REPORTING

While it is relatively easy for a contractor's leadership or a client to personally and frequently observe a small, locally executed project, it is impossible to do the same on a major, globally executed one. Therefore, project reporting is getting more essential for the facilitation of project delivery with the increase in project size and geographic dispersion.

4.1 CLIENT REPORTING

On major international projects, reporting is done in layers: daily, weekly, and monthly. Daily reports are prepared for construction activities only, while weekly and monthly address the entire project. Besides providing information, reports should be also used as a team performance management tool, based on the feedback from many quarters that examine these reports. One of the first signs of poor project management is inadequately prepared or late reports.

4.1.1 Daily Reports

Daily reports are the first layer of reporting, providing factual information for a specific day, with no detail quantitative or qualitative analysis, except for cumulative man-hours calculation. Daily reports provide the following information: Project name; Contractor's name; Client's name; Site name; Date; Activities performed on the subject date, divided as per site zone or main deliverables; Schedule concerns; Commercial concerns; Manpower type, and quantity, for every performing entity, for the subject day, and cumulative; Equipment type, and quantity, for every performing entity, for the subject day; Weather conditions - temperature, humidity, rainfall, wind speed; Pictures of every work-front with adequate titles.

Besides communicating the status of the project, daily reports are important record of facts that is fundamental for any dispute resolution. Daily reports shall be issued by noon the next day, as issuing delays would defeat most of their purpose.

4.1.2 Weekly Reports

Weekly reports are the second layer of reporting, focused on short-term plans and results, providing extensive quantitative analysis: Variation requests status; Requests for Information status; QA/QC documentation status (Inspection and Test Plans, Non-conformance reports, and Manufacturer Data Records); Procurement status; Correspondence status; Updated schedule; Three weeks look-ahead; Progress Dashboard; Progress curves (entire project and separable portions); Manning Forecast (native file).

4.1.3 Monthly Reports

Monthly reports are a final reporting layer that provides medium-term focus and extensive qualitative and quantitative analysis: Executive summary, explaining progress status for the overall project and separable portions, major achievements in the previous reporting period, plans for the next period, and major issues and concerns; Health, Safety, and Environment status; Human Resources status; Engineering status; Procurement status; Fabrication status; Preassembly status; Logistics status; Construction status; Commissioning status; Progress status.

4.2 INTERNAL REPORTING

As the client reporting sufficiently covers internal daily and weekly information needs, the key difference between external and internal reporting is on the monthly level. While being mindful of contractual and commercial considerations, internal reporting shall provide sufficient detail and expose the root cause of the current situation, as well as the most probable forecasts of short and mid-term developments, and the final project results. This enables the company's executives to steer the project execution timely, in a controlled manner, avoiding abrupt reactions later and sudden changes of direction. Therefore, the internal reporting is based on the client's monthly reporting, with the addition of the SWOT (Strengths, Weaknesses, Opportunities, and Threats) and commercial analysis.

SWOT analysis shall provide the following information: Item - describing strengths, weaknesses, opportunities, and threats for the reporting period and the ones expected in the future; Actions - describing what actions have been taken to prevent or correct negative items, or to instigate or amplify positive items. "...our approach must be based on actual experience from concrete projects. The purpose is to ensure a realistic understanding of the issues at hand as well as proposals that are practically desirable and possible to implement." [4]

The commercial analysis shall provide the following information: Planned, actual, and estimate at completion total project value, planned gross and net profit and profit margins; Planned, actual, and estimate at completion commercial progress (cash-in, cash-out, and cash-flow); Planned, actual and estimate at completion internal hours; Planned, actual and estimate at completion costs for all phases of the project and risk reserves; Risk cost breakdown; Bank guarantees; Payments information; Variation request registers for all contracts.

5. COMMERCIAL AND CONTRACT MANAGEMENT

5.1 BUDGETING

There is a significant difference in philosophy between budget preparation for a proposal and budget management during work execution, especially in the level of detail. During the proposal phase, at least two methods of budget calculation should be utilized, to ensure accuracy: a detailed, bottom-up, activity-based analysis; and benchmarking. However, to manage the budget during the project execution effectively, in the lump-sum environment it needs to be restructured to summarize detailed budget positions into segments for which the contractor has exact and verifiable information. It results in precise expenditure reports, clear and accurate estimates to complete the job, less workload, and allows a sufficient frequency of budget updates (monthly). Such an approach also results in the project team using the budget as one of the tools to manage the project. In the EPCM, cost-reimbursable environment, the budget positions can remain the same, due to the high financial transparency of such a model, resulting from a very limited number of subcontracts.

5.2 RISK ANALYSIS

An effective project risk management characteristics: Corporate data on risk probability and consequences should be treated as guidelines instead of prescriptions, the project team shall be able to interpret these guidelines to get reliable cost implications for every risk, and these numbers have to go back into the project budgeting scenarios without further adjustments; All managers in the project team shall be involved in the risk register update; Risk register update shall be performed monthly, just before the budget update; Core project team members have to constantly think about risk mitigation and opportunity utilization, which in turn requires them to actively manage the existing ones and constantly add new items as the project progresses.

5.3 CONTRACT VARIATIONS

As the contracts are seldom entirely clear and explicit, even in their most important aspects, the contractor's ability to interpret the contract adequately and assert its rights, very often decides on the success or failure of the project. "Sometimes disputes are precipitated not by events but by realization by one of the parties that the deal they agreed to will not turn out as planned" [5]. Such situations get more frequent and prominent with the project size increase.

5.3.1 Outgoing Contract Variation Requests

Outgoing contract variations are submitted by the contractor to the client. Adequate requests must consider the financial and schedule aspect of the contract change. Major projects typically require hundreds of variations to build the product as envisioned.

The common pitfall is to consider any of these variations too small to be formally submitted, as their cumulative effect could significantly affect the project execution, if not financially, then certainly schedule-wise. The other common mistake is to treat each change in a vacuum, not considering their direct effect on other project activities. The solution is to have all relevant stakeholders engaged in the variation process (project personnel with first-hand knowledge of the item), from identification to pricing, execution, documenting, and closing. It is achieved through a robust change management system and associated trackers, detailing: Change description; Requested and awarded sum and time extension; Owner; Submission and resolution dates; Status.
Such a rigorous variation process will not only capture and compensate for all changes but discourage the client from adding any unnecessary items to the project scope. This benefit is often neglected, or even treated in a negative light as a loss of the business opportunity. This is certainly not the case on large projects, as the disruption that a multitude of changes causes to the overall project execution significantly outweighs any reasonable profit margin that can be assigned to each of them.
Finally, the contract variation financial aspect is often misinterpreted by treating it as regular project work. The more appropriate test for pursuing the request would be treating the *failure to pursue* the variation as *a direct and full profit loss*. At an approximate average of 5% net profit on successful major construction-driven projects, any amount of not pursued requests would require performance of 20 times larger project work to compensate. For example, $1 million of not pursued variations requires a stand-alone project of $20 million to be executed successfully to break even.

5.3.2 Incoming Contract Variation Requests

Incoming variation requests are submitted by suppliers and subcontractors to the contractor. The common pitfall in this scenario is the contractor's inability to draw a clear line between their responsibility to design a conforming product and the subcontractors' or suppliers' responsibility to deliver in accordance with the contract. For example, the identification of a suboptimal design resulting in more difficult fabrication than otherwise necessary is certainly a valuable lesson learned, but it cannot be accepted as a reason for the increased fabrication cost or time extension. The other common issue is the contractor's inclination to retain *corporate* relationships with the suppliers at the expense of a *project*, resulting in the contractor performing the supplier scope, or granting unwarranted cost increases and time extensions. These issues are resolved by having a strong project manager's position (operating in a strong matrix or projectized organizational structure), being responsible for all aspects of the project execution, able to overwrite any functional manager's decisions if necessary [6].

5.4 BACK-CHARGES

Most of the contracting companies do not pursue back-charges adequately, since it requires a counterintuitive thought process - the contractors are used to claiming money for the performed work from the client and expect the same from their subcontractors and suppliers. Back-charges reverse the direction of claims. The other common mistake is considering this process not worth pursuing, due to the size of the claims.
Back charging should be treated primarily as a matter of principle and good order. If one entity has performed the other entity's scope, it shall be reimbursed. Also, if an entity has not performed a portion of its work under contract, the other contracting party needs to get reimbursed. In both cases, an entity has already paid for the goods or services that have not been delivered. The contractor shall protect the planned margin, and help everyone else on the project do the same. By not protecting itself, the contractor is not only setting a poor precedent for the current project but for all its

projects in the future in the given market. Additionally, failure to pursue the back-charge is a net profit loss, the same in nature as a failure to pursue the variation.

6. ENGINEERING

6.1 CREATIVITY & REALITY

Engineering is one of the most creative parts of the project delivery, rivaled only by planning in terms of initial freedom. From the very beginning, when every conceivable option is worth examining, the goal of the engineering phase shall be to, through every engineering decision, reduce the number of options to one, which is called "the design freeze". From that point in time, the question is no longer *what* will be built, but *how*, *when*, and *by whom*.

Decision paralysis is a common issue in the engineering phase, and its consequences are growing exponentially with the size of the project. Too often the engineering remains fluid well into the fabrication, and even into the construction phase, affecting the project's key performance indicators. It is the project engineering manager's role to direct the engineering work with a clear focus on delivering results timely, and in the sequence which allows optimal execution of other project activities. On large projects, this cannot be achieved with functional management directing the work.
The optimal design process includes the involvement of experienced fabrication, preassembly, construction, commissioning, and operations SMEs (subject matter experts) from the inception stage. To understand that design significantly affects all other project phases, and learn to design more buildable and useful products, the design engineers should not only respond to rectification requests but personally face fabricators' and construction subcontractors' personnel when problems arise.

6.2 MODULARIZATION

Modularization is indispensable on remote projects, but it is also feasible on other projects if their site labor and equipment rates are high. The main postulate of modularization is to maximize utilization of the transportation envelope and weight limits, as well as to avoid significantly uneven distribution of the load. Transport frames and special tools for module transportation and installation shall be designed and produced together with the modules and tested prior to the commencement of the transportation, as they affect the product design and prevent the commencement of the transportation and installation if unavailable or inadequate.

6.3 3D MODELING

3D modeling is critical to completely eliminate expensive and time-consuming field-run activities, and its importance increases with the size of the project. Despite the actual abilities of the available software, the tendency to 3D model only "significant" elements, and leave the rest of the engineering work (tertiary structural steel, small pipes, ducts, cable trays, and ladders) to be performed in the field is still prevailing. Such practice should be avoided, as it only transfers increased engineering costs to the construction phase while reducing design accuracy and site safety, causing reworks at the site, and increasing fabrication and transportation costs. It is also important to note that chosen 3D modeling tool shall be able to integrate all disciplines to avoid disconnects between them.

7. PROCUREMENT

7.1 PROCUREMENT TRACKER

The procurement process takes inputs from the design phase and provides its outputs to all other project phases. The procurement tracker shall capture all items which are not part of the fabrication and construction packages, from cradle to grave, and includes: Item name or description; Supplier; Planned, forecast, and actual procurement input dates; Delivery type and its exact location; Planned, forecast, and actual delivery dates; Status. The number of items procured outside of the main procurement process shall be minimized, and applicable only to unforeseen, emergency corrections.

7.2 LONG LEAD ITEMS

Long lead items are defined by the effect that their production and delivery time has on the project schedule. Although long lead items delivery typically takes between 12 and 24 months, sometimes even much shorter lead times can affect the schedule due to engineering constraints, i.e. late input to the procurement process. Procurement of long lead items is a strategic, critical path activity, that significantly affects engineering, preassembly, and construction sequencing and timing. Ideally, while defining the project milestones, engineering can be scheduled to accommodate all long lead times, with sufficient contingencies for unimpeded execution of the preassembly and construction processes. If this is not the case, an independent design and procurement contract can be issued for long lead items in advance of the full EPC/EPCM project award.

7.3 OVERSIGHT

The equipment production process on major projects does not require continual contractor presence at suppliers' premises. However, the contractor's oversight through periodic meetings focused on the progress achieved in the given time period and addressing the supplier's requests for information, is a must, to ensure the planned production schedule and quality. The usual frequency of these meetings is every two weeks unless production issues require more intensive coordination. The oversight culminates with a factory acceptance test, which confirms the equipment's conformance with all relevant specifications and legislation.

8. FABRICATION

8.1 LOCATION

While choosing the optimal fabricator, attention should be paid to their location - they should be located near main traffic routes along which the terrain, traffic signs, buildings, and vegetation allow transportation of oversized loads and wide turns. A rail connection would be a major plus.

8.2 FABRICATION TRACKER

Fabrication phase takes inputs from the engineering phase and provides its outputs to the preassembly and construction phases. The fabrication tracker shall list every structural element, and its current production status - 3D model and shop drawings availability, material procurement, cut, tacked, welded, trial assembled, painted, ready for delivery, QA/QC completed, and delivered.

8.3 DESIGN OPTIMIZATION

In an attempt to protect their intellectual property, many contractors provide 2D drawings instead of 3D models to fabricators. This practice should be abandoned, as the fabricators have to re-create the 3D model from received 2D drawings, to be able to produce adequate shop drawings for fabrication. In essence, the contractors are spending resources on redundant drafting in-house, and at the same time, delaying the project and paying more to fabricators to re-create the model, while the re-created, and more accurate 3D model remains in the possession of the fabricator in the end.
Before issuing the model, while negotiating fabrication contracts in an open competition environment, the contractor shall review the 3D model with all proponents, and adjust the design to facilitate less expensive and faster fabrication, while keeping the design intent intact.

8.4 FABRICATION MANAGEMENT

Besides fabricators' own management, major projects require extensive engagement and personal presence of the contractor's fabrication manager, supervision, and QA/QC personnel, acting as immediate advisors, observers of the actual progress and resources engaged in the fabrication process, and contract variation preventers.

8.5 TRIAL ASSEMBLY

Trial assembly ensures that an adequate fit between the structural elements is checked, and necessary corrections are made, as even if each element is fabricated within its own tolerance, the cumulative imperfections might result in structural clashes and the inability to assemble complex structures. Although it adds time and cost to the fabrication process, this step is overall very cost-effective as it prevents rectification in the preassembly and construction phases.

8.6 PREPARATION FOR TRANSPORTATION

The final stage of the fabrication process is preparation for transportation - an activity often overlooked, with significant consequences. The load needs to be stable and secure to prevent transportation incidents, softeners need to be installed to prevent paint and even structural damage, and all permits need to be obtained and notifications sent so the load can be accepted at the final destination.

9. PREASSEMBLY

The main aim of the preassembly phase is to build modules as large and heavy as possible off-site to minimize the on-site work. These modules include structural, architectural, mechanical, electrical, and instrumentation elements. The only reason to not install any item would be due to logistics restrictions, to avoid exceeding the size, weight, or acceptable eccentricity of the module. As it is much easier to control the environment at the preassembly facility than at the construction site, preassembly results in higher labor productivity and satisfaction, at lower hourly rates, and more effective and efficient QA/QC and HSE processes.

9.1 LOCATION

The optimal location for the preassembly facility would be as close as possible to the main fabricators, suppliers, and the major source of the workforce, which makes the industrial zone of the nearest city or town the best choice, even if it is hundreds or thousands of miles away from the construction site. The more remoteness plays into the project parameters, the higher importance of the preassembly is, as the cost to mobilize the site, transport materials, and hourly rates increase. City-based preassembly facility ensures solid competition between fabricators and preassembly subcontractors, and any material shortages can be easily replenished from multiple sources. The micro-location should satisfy all conditions required for fabrication facilities, and additionally, it would be a major advantage if it is close to the harbor with berths capable of handling the biggest modules that associated ships can.

If the fabricators are located overseas, the preassembly can be organized there or in the country where construction takes place. If logistics can withstand it, the best option would be to organize the preassembly overseas, as the choice of fabricators already indicates lower labor and equipment rates. If this is indeed the case, the more work performed overseas, the more cost-effectiveness is achieved.

If the fabrication facilities are sufficiently large and equipped, the preassembly can be performed at the fabrication facility. Caution should be advised to not disperse the preassembly process to several fabricators, which could result in excessive management costs or inconsistencies, as well as to not overcommit to any one fabricator, which could be leveraged against the contractor if they underperform in the fabrication phase. The best approach is to leave all options open well into the fabrication process and choose the best fabricator for preassembly when their performance is adequately proven, providing they retain the same management team.

9.2 FACILITY PERFORMANCE

Preassembly facility characteristics and performance vary widely. Some cities develop state-of-the-art facilities which can be rented at affordable rates, which is usually the case when a strong industry exists in the vicinity for a long time, warranting the investment. Such facilities have enormous sheds protecting the work process from elements, bridge or gantry cranes, lighting, offices, power, water and air supply, internet, and security. On the other side of the spectrum, the contractor may have to create a minimally equipped yard, able to provide the necessary return on investment. Such a yard would encompass a well-compacted surface layer with a good drainage system, a fence around it, security, water, electrical power, trailers for offices, and mobile or tower cranes of sufficient capacity. In both cases, the preassembly has to be more feasible than the construction to be undertaken.

9.3 PREASSEMBLY MANAGEMENT

As the preassembly is in its essence construction work performed away from the construction site, to save time and money and increase overall project productivity, safety, and quality performance, the future project construction manager should manage the preassembly process. In this phase, the position is called a project preassembly manager. Preassembly is usually still progressing when the construction phase is due to start, but at that point in time the preassembly process is very well established, and the peak of the activities has passed, so the project fabrication manager’s scope can be extended to the preassembly, as the fabrication phase is winding down at that moment.

In this phase management authority gets consolidated, from parallel lines prevalent in the previous phases, into a powerful construction-driven hierarchy line. All preassembly supervisors, quality, and safety personnel, report to the preassembly manager, and he or she to the project manager.

9.4 PREASSEMBLY PROCESS

A few weeks before taking possession of the facility, the preassembly team shall perform a facility walk-down, to list all shortcomings and have them fixed before mobilization, as the facility is rarely fully functional at that stage. The next steps are to assign responsibilities to each team member, have a final review and adjustments of all work packages, and design the positions of all modules and for all stages of the preassembly process. Then a sufficient number of supports is to be delivered and placed in designated positions. Once the module is set in its location, it shall not be relocated until it's ready to be shipped out. Any in-process horizontal or vertical relocation would indicate a lack of preparation and disrupt the preassembly process, causing unnecessary costs and delays. All preassembly material is to be placed in such a way as to allow optimal installation access. Integration of different disciplines comes to the fore at this point. Items that have not been trial-fitted in the fabrication stage could and usually do not fit and need to be adjusted. Once all items are installed, all tripping hazards, pinch-points, and unfirm items can be identified and rectified. Once the structural steel is mostly installed, the installation of cable trays and ladders, cables, and pipes can commence. All grounding, dividing, tying, and spacing requirements need to be clearly understood and followed from the commencement of the preassembly. All installed piping on individual modules is to be tested. Once the testing is done, all signage and tags should be placed. Of particular importance is for every module or steel member to be equipped with well-protected connection accessories - encompassing all nuts, bolts, washers, cotter pins, etc. which are needed to connect it at the construction site. Finally, the transportation frames are fixed to modules, and they are ready for the transportation phase.

9.5 PREASSEMBLY PROCESS RESULT

A result of the successful preassembly process are maximally dressed modules mounted on the transport steel, all clashes are removed, specifications are conformed with, and all available testing is performed. Once delivered to the site, each module shall fit into the structure as designed and no rework shall be done intra-module. Inter-module clashes are unfortunately still possible.

10. LOGISTICS

10.1 LOGISTICS TRACKER

Major projects are large and complex enough that logistics cannot be tracked as a part of the procurement tracker. On smaller projects, such a practice would be acceptable. The logistics tracker shall provide the exact status of every single logistics element, classified as per their type - structural steel, procured items, produced items, etc., for easier navigation. For each element, planned, forecast and actual dates need to be set for their dispatch and receival, as well as the ship and truck numbers, release documentation status, and site permit status.

In case of delays, the following actions could be performed: The planned transportation start date could be accelerated by expediting predecessor activities; A superior transportation solution could be developed; A planned transportation end date could be delayed and successor activities expedited; or, The project could take calculated and controlled schedule impact. This tracker is to be updated on a weekly basis, and in the most critical period for the most critical items, daily.

10.2 LOGISTICS SUBCONTRACTORS MANAGEMENT

The main reason for having logistics personnel in the major project team is to avoid issues in this critical project phase through the alignment of the logistic subcontractor's culture and interests with the contractor's. While reviewing the number of vessels, and type of trailers, or sharing resources with other projects, the contractor shall make sure that optimization is done for the project, and not solely for the subcontractor's benefit.

10.3 LAND TRANSPORT

While overly large or heavy modules are obvious mistakes, the more implicit issues come from significant module eccentricity, causing instability of the trucks and overloading of trailer axles. To avoid that, the following actions can be taken: change the module size, change the dressing extent, and utilize eccentric transportation frames. The crucial element for such analysis is determining the exact position of the module's center of gravity. Its preliminary position is found utilizing software, and the final one is located during the trial lift. The measured (actual) center of gravity shall be permanently marked on the module and corresponding rigging requirements are to be conveyed to all other stages of the project execution.
The first leg of the land transport is usually short, from the preassembly facility to the vessel at the dispatch port. Large modules are usually transported by SPMTs (self-propelled modular transportation), which can withstand practically any kind of load and difficult terrain, while smaller ones are transported by truck-towed trailers. The second leg of land transportation, from the receiving port to the construction site, is usually much longer, often several hundred kilometers or more. If road infrastructure allows, truck-towed trailers should be utilized for all modules at this stage, due to their relatively low cost and high speed compared to the SPMTs. This approach, however, requires extensive design and planning due to the much lower bearing capacity and stability of the trailers compared to the SPMTs. Prior to the commencement of the second leg of transportation, conformity of the load configuration with the transportation drawings is to be checked, including lashing points and means, for each module. After that, the trailer configurations, condition, axle loads, and overall weight are to be checked. Finally, the removal of road signs and other obstacles along the route is to be verified.

10.4 SEA TRANSPORT

Due to the high fixed costs of sea transport - the ship mobilization, loading, unloading, and demobilization, sea transportation requires longer distances to be feasible on the same landmass, at least several hundred kilometers. Consequently, the sea transport duration is relatively long, and it takes from approximately one week for the shortest voyages up to eight weeks for the longest.
While planning the sea transport, the ship's waiting time is especially difficult to define. Although ships are typically berthing on a first come first served basis, priority vessels like cruise lines, ore transportation, etc., do not follow the queue, which makes duration estimating extremely difficult and inaccurate. So, for long-term planning, the most probable duration should be scheduled based on the experience. Then, as the date to book the actual ship approaches, typically a few weeks before the loading start date, a choice needs to be made based on the availability of suitable vessels in a few thousand kilometers radius from the dispatch port.
Work on the ship is much more dangerous than in the fabrication, preassembly, or construction environment. There are numerous unmarked and unprotected openings on the ship decks, very long vertical ladders without protective cages, deck configuration changes continually, working under artificial lighting on the lower decks is the norm, etc. Extreme caution is to be exercised continuously, to avoid severe injuries or fatalities on the ship.
The most significant challenge during the ship loading process is the communication with and within the ship crew, as every company and every vessel has different quality and enforcement of procedures and varying crew cohesion. This could lead to disconnects between berth and deck crews, and consequently to major incidents. Communication issues can be prevented by having the kick-off meeting with the ship management as soon as the ship arrives, to go through and fortify the rules of

engagement - who is making critical decisions, who is giving the orders, ship entry, and work on the ship protocol. It needs to be ensured that all the agreements are passed onto the crew in the daily prestart meetings. Finally, the work needs to be observed, and followed by interventions at the first sign that any of the stipulations are not being followed.

In case of unplanned clashes between the ship structure and modules, due to inadequate ship deck drawings or stow planning, robust management of change needs to be performed. The lift has to be aborted, the module temporarily stooled off, and the stowage plan adjusted. It disrupts the loading process at the preassembly facility and delays the ship's departure date.

Once the module is loaded on the deck, it needs to be secured for transport, as it shall not move during the voyage. It is achieved by using steel stoppers, lashing lugs, and lashing. These elements shall be designed along with the modules and the transport steel. Unfortunately, it is often not the case, and extensive welding is being done on already fabricated and painted modules, sometimes even during the load securing or voyage. This practice shall be discouraged, as the forces during the sea transport are high, and the consequences of modules getting loose could be catastrophic.

Once all modules are secured, all hatches closed, and all quality checks have been completed, the captain (and only the captain) makes the final call on the ship's readiness to leave the harbor.

11. CONSTRUCTION

The construction phase is the heart of the EPC or EPCM project, with the highest overall safety, reputational and financial risks of all project phases, for both client and the contractor. Therefore, it drives the overall project execution. The project and construction manager’s ability to visualize the completed product, as well as all stages of its delivery, and have every decision and action driven by that vision is indispensable. The building blocks of the construction phase are construction packages, detailing the exact work methods for every construction activity.

Construction site remoteness increases the hourly rates, as well as the cost of mobilization and demobilization of the personnel and equipment. These costs can be reduced by minimizing the number of people on site by reducing required construction man-hours, through maximal engineering and fabrication completeness and modularization. Fly-in and fly-out shifts can be organized to allow personnel an optimal amount of off-site time for maximum on-site performance. The construction sequence can be optimized through a focused heavy-lift campaign, limiting the engagement of the heaviest cranes.

11.1 PRE-START MEETINGS

Pre-start meetings are focused on the workforce at the construction site. The most effective pre-start meeting encompasses: The work completed the previous day, its comparison with the plan and relation with activities planned for the current day; A clear description of all work activities planned for the current day, for each construction zone, including associated HSE risks and mitigations; Simultaneous operations and interactions between the subcontractors; Weather forecast for the next week, wildfire and flooding reports and associated mitigating actions.

11.2 MOBILIZATION AND DEMOBILIZATION

Successful green-field mobilization of a remote construction site shall be executed in a short period of time. Hostile environments require adequate security elements. Pre-mobilization effort establishes a minimal infrastructure for the mobilization team,

accompanied by evacuation plans, to address serious uncontrollable events. An optimal composition of the pre-mobilization team is essential, as any skill missing at that point cannot be replenished without excessive costs and delays. The team needs adequate communication means, including satellite phones and the internet. The team shall have all equipment and material to build a base camp effectively - all-terrain vehicles, cranes, water, fuel and sewage trucks, trailers, etc. Once pre-mobilization is completed, a construction camp and offices are to be established. They shall provide all necessary services for the construction team - kitchen, mess, ambulance, security, living quarters, offices, leisure facilities, security, maintenance shops, etc. Once construction site mobilization is completed, the construction mobilization can commence - deployment of the construction crew, as well as delivery and assembly of heavy equipment.
Except for the surveying and geo-exploratory work, other construction activities shall not commence prior to the completion of the mobilization. Experience shows that starting significant construction activities before all infrastructure and systems are in place results in unsafe and unproductive work accompanied by substandard work results.
Demobilization shall be executed with the same sense of urgency as mobilization, and it shall start as soon as the first person or piece of equipment can be released from the project phase. Any missed opportunity to demobilize results in the escalation of costs, lowering the project’s performance.

11.3 AUXILIARY CREWS

To reduce overall construction costs on major projects, the contractor should engage auxiliary crews. These are small, autonomous complements, performing the majority of site rectifications and small additional works, like rectification of members or module clashes, small installations, limited welding, and painting.
Engagement of such crews causes additional overhead and indirect costs, as well as mobilization of additional equipment. However, by adding a crew that perceives extra work as their sole source of income, instead of a hindrance to their construction process, which is a usual perception of the large construction subcontractors, the contractor at the same time achieves a very efficient extra-work execution, and avoids disruption claims from its subcontractors for an excessive amount of extra works. It is important to bear in mind that although construction contracts usually have a provision stipulating that the subcontractor shall comply with all principal’s directives and execute all extra works, once the value of extra works exceeds approximately 10% to 15% of the original contract value, a disruption claim could be filed since scope grew significantly beyond the originally contracted one.
SMP (Structural, Mechanical, Piping) auxiliary crew shall have their own scaffolding capabilities, welding, structural and mechanical installations, painting, and aerial work platforms. EIC (Electrical, Instrumentation, Controls) auxiliary crew will perform only the EIC work and will depend on the SMP crew for access support. Crane support should be obtained from the main subcontractors.

11.4 SUBCONTRACTOR MANAGEMENT

11.4.1 Number of Subcontractors

The optimal number of subcontractors depends on the number of facilities to be constructed at the site, their geographic dispersion, and the disciplines involved. The EPC and EPCM contractors need to balance, on the one hand, the risk of creating excessive dependence on a single subcontractor or even creating future direct competition to themselves by awarding excessively large portions of work to a single

subcontractor, and on the other hand, fracturing the project scope and the construction process excessively with too many subcontractors and interfaces between them.
The optimal approach usually has one group of subcontractors for every significant facility, usually divided as per the discipline - civil, SMP, and EIC. The heaviest cranes, surveying, scaffolding, snow clearing, dust suppression, and similar services can be shared between facilities, often directly subcontracted to the contractor.

11.4.2 Management of Subcontractors

The contractor's personnel shall be careful to avoid directing the work of the EPC lump-sum subcontractors, except in emergency situations. However, if the subcontractor is underperforming, it needs to be addressed promptly and decisively. If the subcontractor fails to rectify the underperforming part of the work, with indications of further under-delivery, they should be descoped progressively, until the remaining work can be performed satisfactorily. Additionally, the contractor's construction management team should review all subcontractors' work packages and provide *comments* (not directives) on how to improve the work and do it more efficiently. If the first iteration of suggestions has a positive outcome, it builds rapport and acceptance of the contractor's advice. The next steps could involve full work-face planning, detailing every work step, logical connections between steps, and resourcing.
Effective contractor-subcontractor relationship is based on protecting each other's profit margins. During contract negotiation subcontractor offers and the contractor accepts costs containing expenses, risks, and profit. Both parties shall genuinely work on preventing either party's risks from materializing and thus protecting their profit. Although formally, each party should execute the contract regardless of their losses, in project reality, it practically always results in major friction, escalating losses on both sides and it finally obstructs the construction process, resulting in disputes and even legal proceedings. If the subcontractor's attitude is not constructive, and there is no will to rectify the inadequate performance, their construction management team or even the entire company is to be removed from the construction site. Although such action has negative short-term effects, in the long run, and especially strategically, on the market level, it has positive consequences. It sets a precedent and effectively discourages inadequate subcontractors from either planning to participate in the contractor's projects, or acting similarly.

11.5 MATERIAL RECEIVING AND MANAGEMENT

Logistics register is the basis for material receiving and management planning. Each load shall be inspected right after the transportation slings and chains are removed to determine the damage before unloading. Anything that would affect the functionality of the item shall be checked - disconnects, deformations, scratches, and water damage. All overages, shortages, and damages shall be documented and resolved. All crated, boxed and containerized items are to be opened and inspected.
All received material is to be stored and treated as per the manufacturer's instructions. For example, machined surfaces shall be protected from rusting and mechanical damages, large shafts need to be rotated periodically, electronic equipment cannot be stored in cold environments or exposed to rain, etc.
Site grid and a corresponding register for received material shall be prepared, facilitating fast material retrieval. Finally, the status of each received element shall be documented (stored, shipped for repair, or installed, with the accompanying dates).

11.6 CONSTRUCTION-COMMISSIONING INTERFACE

One of the most important construction site interfaces is the one between construction and commissioning activities. There are two management approaches to this interface -

the first has a construction manager and commissioning manager with equal authority, each practically independently optimizing their own scope, and the second has a construction manager responsible for all site activities, including commissioning, while the commissioning *lead* (not manager) autonomously manages the commissioning scope. The first approach results in friction between the processes, due to the duality in authority over site activities which cannot be resolved by the project manager effectively. The second approach is much more optimal, providing that the construction manager genuinely accepts full responsibility for all site activities, including commissioning, becoming a de facto construction *site* manager, instead of a construction *process* manager. The project manager's task is to ensure this is established and enforced.

11.7 CONSTRUCTION PHASE STAGES

11.7.1 Delineation Between Construction Stages

To optimize the overall project results, the point in the construction work execution should be defined up to which construction activities should be done in bulk, to gain as much as possible of the *overall* construction progress, and from which activities should be grouped in functional systems, to gain *targeted* construction progress. When approximately 80% of construction activities are completed, the focus is to be moved from bulk construction to the completion of functional systems in a sequence that is fully aligned with the planned commissioning activities.

11.7.2 Bulk Construction Stage

During the bulk construction stage practically all the civil, structural, and architectural works are to be performed, mechanical equipment installed, and practically all the piping, HVAC, and EIC works are to be completed. All equipment is to be aligned and cleaned, piping and cranes installed and tested, calibrations performed, and associated quality reports produced. The final step is the punch-list walk-down, which will verify the level of the bulk construction stage completeness, and provide the input to the system completion construction stage.

11.7.2.1 Site Modularization and Dressing

As the modularization in the preassembly phase is limited by the logistics constraints, the opportunity to additionally increase the size of the module before lifting it into its final position should be utilized at the construction laydown while respecting the crane capacity and installation location conditions.
If the elements are transported to the construction site in bulk instead of modules, modularization can be done in the laydown area, reducing installation of the individual elements at height (so-called "stick-build"). Besides being safer, such an approach is more productive, as the scaffold, aerial work platforms, and fall protection requirements are much lower at the ground level. Most of the quality control activities can be done at the ground level as well. Relatively small cranes are sufficient for modularization since the required reach is much smaller for the same loads. Once the module is fully dressed, a large crane is used to lift the entire module into its final position.

11.7.2.2 Non-Energized Testing

In the bulk construction stage, non-energized testing is to be performed to demonstrate that the product is ready for energized testing.
Non-Energized Piping Testing
Piping static testing should be done as much as possible off-site, in modules, or in individual spools. To reduce risks on-site, pneumatic testing is to be substituted with

hydro tests. Air entrapment, which would prevent the flow of the fluid through piping, shall be avoided by checking the adequate placement of high points vents in the piping systems design.
It is essential to perform fit-for-purpose testing instead of imposing unnecessarily strict testing requirements. For example, pressure testing should not be done for the piping that will be exposed to atmospheric pressure in operation, as service testing for such piping is sufficient. Such issues can be avoided by preparing the testing procedures and insisting on resolving them well in advance of the testing date.
Non-Energized EIC Testing
Non-energized EIC testing verifies the wiring integrity - the continuity of the wires (that the energy flows with sufficiently low resistance through the designed path), as well as their isolation and insulation (that current cannot flow between certain points and that there is no leakage of electrical energy through insulation). Due to the low safety risk of these activities, a good schedule-saving strategy would be to perform them, as well as all resulting rectifications, out of regular working hours.

11.7.3 System Completion Construction Stage

The systems completion stage is the interface between the bulk construction and no-load commissioning stages, so at its start, it is aligned with the bulk construction work status, and at its finish, with the no-load commissioning sequence. Based on the bulk construction punch list, the work in this stage should be focused on eliminating the highest priority items (safety and operability related) and minimizing the rest of them. As soon as all highest priority items are cleared, the construction verification certificate is issued, and the no-load commissioning phase can commence. All “work to go” from the bulk construction stage shall be completed during this stage of work as well. All red-line drawings have to be produced and available for use during commissioning.

11.7.3.1 Early Correction

Early correction of punch-list items is based on the daily site inspections, performed by commissioning leads simultaneously with the construction completion, focused on the construction non-conformances, for example: scaffold not removed before the walk down, piping and hoses not reinstated after the testing, gates not installed on the permanent ladders, malfunctioning hatches, loose bolts, inadequate grating and kick plate gaps, handrail, and lighting poles too flexible for the purpose due to inadequate supporting, etc. Successful early correction results in just a few category one and two snags, which can be expediently resolved prior to the commencement of commissioning.

11.7.3.2 Late Correction

The punch list is created during the punch list walk down, which is an official inspection between the contractor and the client to detect snags preventing the formal verification of the construction process completion and/or the start of the no-load commissioning phase. The highest category of snags is related to safety and operability risks that *have* to be addressed before commissioning is allowed to proceed. The second-highest category still needs to be addressed for construction to be verified as completed, but the no-load commissioning can proceed even if they are not addressed. The lowest category comprises so-called “wish list items” that are not safety or operability-related, not part of the contract, and may be addressed as a contract variation. The usual approach, to skip early correction, rectify the highest category items only, leave multiple non-critical snags unaddressed, and proceed with the no-load commissioning as soon as possible, should be discouraged, as once a facility is energized, the time to perform the same task is doubled or tripled.

Punch list items are to be addressed by taking a photo of each item, preparing a tracker with planned, forecast, and actual completion dates, and performing the rectifications by the construction team. The commissioning team verifies the intervention, by taking a picture of the rectified item, and sends the notification with photographic evidence to the client, which clears the item from the punch list after verifying its rectification.

12. NO-LOAD COMMISSIONING PHASE

No-load commissioning is performed without the substance which is planned to be processed in the facility, for example, run of mine ore or crude oil. It starts as soon as the construction completion certificate is obtained for each system or subsystem, once it is verified that the highest priority safety and operability-related shortcomings are rectified and it is safe to start bringing the product into working condition. The output of this phase is the certificate of mechanical completion, which means that the project product is ready for operational testing during the load commissioning phase.
The first step in this phase is to prove that all the facility's aspects conform to all applicable laws, specifications, and design. Remaining debris is to be cleaned, especially from piping and vessels, and a series of energized tests is to be performed, to prove that all systems are ready for operational testing. Finally, the commissioning walk-down takes place, where once again, all punch list items are listed, categorized, and cleared. The punch list items identified at this point could have been missed in the previous phase or could have been detected during the no-load commissioning. The latter is much more probable. For example, internal clashes between apron feeder pans or conveyor mistracking can be observed only when equipment is started.

12.1 CARE, CUSTODY, AND CONTROL IN NO-LOAD COMMISSIONING PHASE

The CCC (care, custody, and control) over the facility in the no-load commissioning phase is still held by the contractor. Compared with previous phases, the CCC in this phase is much more onerous. As the system gets temporarily or permanently energized, safety risks are increasing exponentially. The contractor has to ensure that no uncontrolled release of energy occurs, be it electrical, hydraulic, pneumatic, or mechanical. This phase brings a large change for the construction crew, as previously easily accessible facilities now require several hours to obtain access to, and PPE (personal protective equipment) requirements are much more extensive, for example, flame and ARC-flash resistant coveralls accompanied by natural fibers clothing become a must for entering the energized e-houses, etc. To ensure safety, firstly the energy shall be kept away from personnel authorized to work on the equipment and secondly unauthorized personnel shall be kept away from the work zone. This is achieved by locking out the equipment - physically disconnecting the equipment from the energy source, and placing a lock on the isolation point for every single individual working on the equipment, which will stay there until the work is done or stopped in a controlled manner, and every single individual removes their lock personally. Unauthorized personnel is kept from the working zone by taping and tagging the area out. At this phase the color of warning tapes and tags change, to clearly delineate construction from no-load commissioning activities.

12.2 CLEANING, FIRST FILL, AND FLUSHING

Cleaning can be expedited by performing it during the construction process. Extensive cleaning performed during commissioning directly delays the project completion. Adequate packaging and storage of the equipment and material are crucial for the efficient execution of the flushing activities. If the pollutants access the equipment and material, the duration of the flushing process, which is usually on the project's critical path, extends from just a few days to several weeks. First fill, as well as flushing, shall be done with adequate type and quantity of oil.

12.3 ENERGIZED TESTING

The tests in the no-load commissioning phase shall prove that the product is ready for operational testing, so all tests in this phase will be energized, both static and dynamic. However, there shall be no load introduced into any of the plant's facilities and equipment.
Locally controlled tests, where no programming is involved, are bump tests and run-ins of every motor in the plant, including alignments. The goal of the plant programming is to achieve its optimal functioning - maximize output and reliability while ensuring the health and safety of personnel and protecting the environment. Modern industrial plants are run through DCS (distributed control system), which is consisted of a network of PLCs (programmable logic controllers). Remotely controlled tests on this system are focused on programming adequacy, by simulating different scenarios, observing the system's responses, and correcting the inadequate ones.
The contractor needs the support of specialized subcontractors for most of the technical work in this phase, especially when it comes to testing the programmed equipment. To effectively manage the interface between the no-load commissioning subcontractors and construction work that is still ongoing in this phase, daily coordination meetings with a detailed seven days lookahead schedule are required. All subcontractors need to participate in them, and they should be held in the late afternoon, to have most of the information that can be acquired during the day available for planning purposes.

13. LOAD COMMISSIONING, STARTUP, AND PERFORMANCE TESTING PHASES

Although the load commissioning, startup, and performance testing are distinct phases, due to the CCC transfer to the client at the end of the no-load commissioning phase, to maximize their feasibility the contractor should treat these phases as a unified effort. In these phases, the client directs and manages the work, and the contractor provides support. Accordingly, the lump-sum project execution model transforms into the cost-reimbursable one.
The load commissioning phase starts at the end of the no-load commissioning phase, as soon as the second category punch-list items are rectified and a mechanical completion certificate is obtained. Based on that, the client issues a notice of readiness for commissioning. The output of the load commissioning stage is a "ready for startup" certificate. The output of the startup stage is the "first product" milestone, followed by the performance testing phase. Once it is proven that the plant can produce quantities and qualities of the product as per the contract, the client issues the final acceptance certificate, which marks the completion of the entire project scope.

13.1 SAFETY IN LOAD COMMISSIONING, STARTUP, AND PERFORMANCE TESTING PHASES

In these phases, the client controls the work and issues work permits. All equipment shall be treated as energized (as if it will start automatically at any moment), so safety awareness and performance shall be at their peak. It is achieved by having the core team transition from construction, through no-load commissioning, to these final phases, as this team gradually creates and adapts to the operational facility. A safety workshop shall be held before each new phase starts, to ensure the safe transition.

13.2 BUSINESS DEVELOPMENT IN LOAD COMMISSIONING, STARTUP, AND PERFORMANCE TESTING PHASES

Although the client controls the work in these phases and the work is performed on a cost-reimbursable basis, the most successful contractors utilize such configuration as a business development opportunity, through not only cooperating and genuinely caring for the outcome but actively proposing solutions to minimize the time and effort required to perform their tasks. The client's operations personnel manages these phases, with a focus on safety, production, productivity, and ease of maintenance. It is important to know that the same client's operations personnel is responsible for the operational maintenance works, schedules, and choice of contractors, as well as that they are first consulted when the development of new plants is contemplated. Demonstrating the contractor's competence to this group is essential for the new business opportunities with the client.

13.3 WORK SCOPE

In these stages, the equipment like conveyors and apron feeders are aligned *under* the load, as static and dynamic alignment of such equipment without the load is not sufficient. Only when the load is introduced, the alignment process can be truly finalized. All other equipment is to be run-in on system by system basis, with all production materials introduced, including water, reagents, solvents, steam, etc. While running these subsystems, the plant performance data is to be collected, and all devices are to be tuned and calibrated.

13.4 PERFORMANCE TESTING

Production quantity and quality, as well as the reliability and availability of the plant, are to be tested in the performance testing phase. Specified production rate and characteristics of the product are to be achieved for a sustained period of time, starting from hours, and ending with weeks of production within prescribed tolerances. A significant challenge in the performance testing phase is its potentially excessive duration when the plant is effectively used for production, but the warranty period does not start, which also affects the core team's availability for the next engagement.

14. PROJECT CLOSING

The volume of information (produced mainly by the project management personnel) and productive work (produced mainly by the labor) required for optimal project delivery varies significantly throughout the project life. The maximal number of parallel activities on the project, demanding the most personnel to manage and execute it, as well as the maximal information bandwidth is reached approximately with the first shipment in the preassembly phase. Up to that point, the project management personnel constantly ramps up. As soon as man-hours become available to earn, the resource shall be added. At a resource maximum plateau, work is being performed simultaneously on engineering, procurement, fabrication, preassembly, logistics, and construction phases, including all other supporting activities, like commercial, contractual, quality, health, safety, environment, and administration. The common resourcing pitfall is to perceive this maximum as a project's permanent configuration. It can be avoided through adequate resource reduction as soon as earnable hours diminish. If the person has more than one skill and can be successfully engaged in other project phases, it should be utilized as a major advantage, due to their understanding of the project culture and the possession of the historical data. For example, a highly competent project engineering manager can remain on the project for its entire duration. From the initiation phase through design to logistics management (or support), to preassembly and construction engineering support, to off-site commissioning management. The construction manager can also start very early on planning and engineering advising, and go through preassembly and construction, and on-site commissioning phases. The fabrication manager can work on the preassembly and construction phases as well. The maximal requirement of labor hours is usually reached in the later stages of bulk construction when practically all disciplines work simultaneously at the construction site. The principles of ramping up and down the labor are the same as for the management personnel.

If the project is scheduled adequately - the engineering, fabrication, preassembly, construction, and commissioning phases can be covered with only four technical managers (project, engineering, fabrication, and construction manager). This provides direct and instantaneous access to the gathered project knowledge throughout its execution, increasing its productivity and cost-effectiveness. At the culmination of the project execution, these managers would be fully focused on the two most expensive and the highest-risk project phases - construction and commissioning. Although information bandwidth reduces with the progression of the bulk construction and closure of the previous project phases, retaining all four top managers on the project until its completion is strongly advised to create some redundancy required to manage unplanned events. The lower layers of the project management team though have to be reduced, to keep the man-hours available for the most qualified personnel. Once construction and commissioning are completed and facilities are handed over to the client, the commercial discussions with the client and construction subcontractors still have to be finalized, which usually takes a few additional weeks. Once all open commercial items are closed, and the remaining project personnel is disbanded, the closing phase of the project is completed.

15. CONCLUSIONS

Management of major international projects requires a holistic approach to all aspects and phases of the project, integrating all project functions and team members' efforts into a coherent set of actions aimed at the achievement of all project goals, while maximizing its key performance indicators. At the heart of such an approach stands a knowledgeable and experienced project manager, able to build a synergistic, competent project team, as well as develop and implement the optimal framework for the execution of every project activity.

The project should be frontloaded in its initiation phase, to ensure an understanding of the reasons for the project's undertaking, define clear project results, and actions required to deliver them, while maintaining sufficient flexibility in the project delivery.

Project scheduling should be based on progressive elaboration, early inclusion of key stakeholders in the schedule development, impartiality with float utilization, and weekly updates. Project trackers are a positive form of self-micromanagement resulting in team synergy, created and maintained in the weekly project meetings, they utilize rolling planning with a fuzzy time horizon and contain actions requiring intensive collaboration between the project team members. "War room" meetings are corrective in their nature, performed on a daily basis, involving all personnel directly executing the distressed project activities. Besides tracking costs and the schedule, successful project control is also based on measuring and tracking physical project progress. The lessons-learned process should be treated as an active project management tool (instead of a forensic one), should commence at the start of the project, and result in the development, utilization, and further refinement of the preventative actions throughout the current and future execution of projects in the company.

Client reporting on major international projects is done in layers: daily, weekly, and monthly. Daily reports are prepared for construction activities only, while weekly and monthly address the entire project. Internal monthly reporting shall provide sufficient detail on and expose the root cause of the current situation, as well as provide the most probable estimate of potential developments. Besides providing information, reports should be also used as a team performance management tool. One of the first signs of poor project management is inadequately prepared or late reports.

Budgeting and risk analysis activities are interrelated and heavily depend on a contracting model. Updates of these systems should be done on a monthly basis, involving all managers on the project. The contractor's ability to interpret the contract adequately and assert its rights very often decides on the success or failure of the project. The failure to pursue or defend variations and back charges directly and fully affects the project profit.

Optimal engineering execution is based on initial openness to various strategies, but expedient achievement of the "design freeze" milestone, early engagement of the subject matter experts, and hands-on involvement of the engineering personnel in the design issues rectification. Designing large modules, while still respecting transportation envelope and weight limits, significantly benefit remote and all other projects with high labor and equipment rates. Every element of the project product should be 3D modeled and fabricated as a part of the engineering and fabrication phases, completely eliminating "field runs".

Successful procurement of long lead items is based on a timely supply of engineering information, which can be achieved either as a part of an overall project contract or through an independent accelerated design and supply contract for long lead items. The equipment production process requires the contractor's oversight through periodic meetings focused on progress, quality, and clarifications.

Fabrication shops should be located near the main traffic routes along which the terrain, traffic signs, buildings, and vegetation allow transportation of oversized loads and wide turns. Before issuing the model, while negotiating fabrication contracts in an open competition environment, the contractor shall review the 3D model with all proponents, and adjust the design to facilitate less expensive and faster fabrication, while keeping the design intent intact. Major projects require the contractor's continuous, hands-on, in-house, fabrication management presence. Trial assembly is a cost-effective method to prevent rectification in the preassembly and construction phases caused by the cumulative effect of individual elements' fabrication imperfections on complex structures.

The preassembly facility should be located as close as possible to the main fabricators, suppliers, road, and rail infrastructure, harbor, and source of the workforce. For overseas fabrication, providing that the logistics can support it, the best option would be to organize the preassembly overseas as well. If the fabrication facilities are sufficiently large and equipped, the preassembly can be performed at the fabrication facility. Management authority in this phase is to be consolidated into a powerful construction-driven hierarchy line.

Due to their significant cost, SPMTs can be feasibly utilized for land transport on short distances and for short engagements. Due to their large capacity, stability, and versatility, these are particularly useful for large modules and difficult terrain. Truck-towed trailers are utilized for large distances, due to their relatively low cost and high speed compared to the SPMTs. The trailers, however, require extensive design and planning, due to their much lower bearing capacity and stability compared to the SPMTs. In preparation for and during sea transport, extreme caution is to be exercised continuously, to avoid severe injuries or fatalities. Effective communication with and within the ship crew shall be ensured through the kick-off meeting and daily prestart meetings. Steel stoppers, lashing lugs, and lashing required to secure the load to the ship deck shall be designed together with the modules and the transport steel.

Mobilization of the construction site shall be performed in a short period of time, by the team possessing all skills and equipment required for independent execution of the task. No significant construction activities shall start prior to the completion of the mobilization. Demobilization shall start as soon as the first personnel position or piece of equipment can be permanently released from the construction site. The optimal subcontracting approach has one group of subcontractors for every significant facility, usually divided as per the discipline - civil, SMP, and EIC. If the subcontractor is underperforming, with insufficient signs of improvement, they should be descoped progressively, until the remaining work can be performed satisfactorily. If there is no will to rectify the inadequate performance, the subcontractor's construction management team or even the entire company is to be removed from the construction site. For the majority of site rectifications and small additional works, autonomous auxiliary crews are a better option than major subcontractors. The construction-commissioning interface is optimally managed by having the construction manager responsible for all site activities, including commissioning, while the commissioning lead autonomously manages the commissioning scope. When approximately 80% of construction activities are completed, the focus is to be moved from bulk construction (construction-driven approach) to systems completion (commissioning-driven approach), which shall fully align the construction completion sequence with the planned commissioning activities. Non-energized testing should be maximized during the preassembly phase. Successful early correction of construction punch-list items during the systems completion construction stage results in just a few category one and two snags, which can be expediently resolved prior to the commencement of commissioning.

As the contractor still holds the CCC over the facility in the no-load commissioning phase, they have to ensure site personnel safety by keeping the energy away from personnel authorized to work on the equipment (locking out the equipment) and keeping unauthorized personnel away from the work zone (taping and tagging out the working areas). Adequate packaging and storage of the equipment and material are crucial for the reduction of cleaning and efficient execution of the flushing activities. Static and dynamic testing, on locally and remotely controlled systems in the no-load commissioning phase, are performed in energized state. To effectively manage the interface between the no-load commissioning subcontractors and construction work that is still ongoing in this phase, daily coordination meetings between all parties present at the site are required.

Due to the CCC transfer to the client at the end of the no-load commissioning phase, the load commissioning, startup, and performance testing should be treated as a unified effort, to maximize their feasibility. The core team should be transitioned from construction, through no-load commissioning, to these final phases. Demonstrating the contractor's competence to the client's operations personnel, which manages these phases, is essential for the new business opportunities with the client, both on the new projects as well as on the operations support.

Management and labor should be ramped up and down based on the availability of earnable man-hours. It is a major advantage, due to their understanding of the project culture and the possession of the historical data, to utilize the same project personnel in multiple project phases, provided they poses adequate knowledge and skills. The project closing phase lasts throughout most of the project execution, from permanently closing the first project position to disbanding all project personnel.

ACKNOWLEDGMENTS

I would like to extend my sincere appreciation to my dear friend and mentor, Professor Milan Trivunic, whose friendship, insightful discussions, and support have been invaluable in shaping my personal and professional journey. If there was only one takeaway from Milan, and there were many, it would be his selfless sharing of knowledge and opportunities with new generations of scientists and practitioners, which I hope they appreciated and internalized as much as I think I did.

REFERENCES

[1] Hickson R., Owen T. (2015) *Project Management for Mining - Handbook for Delivering Project Success*. Society for Mining, Metallurgy & Exploration. The USA.

[2] Artto K., Kujala J., Dietrich P., Martinsuo M. (2008). *What is Project Strategy?* International Journal of Project Management. Volume 26, Issue 1, pp. 4-12.

[3] Trivunic M., Matijevic Z. (2006). *Technology and Organization in Construction - Handbook* (in Serbian). Faculty of Technical Sciences, Novi Sad. Serbia.

[4] Flyvbjerg B., Bruzelius N., Rothengatter W. (2003). *Megaprojects and Risk - An Anatomy of Ambition*. Cambridge University Press, Cambridge, United Kingdom.

[5] Samuels B., Sanders D. (2016). *Practical Law of Architecture, Engineering and Geoscience*. Pearson Canada. Canada.

[6] Matijevic Z. (2006). *Process-Oriented Transformation of the Industrial Systems in Construction*. Doctoral Thesis (in Serbian), University of Novi Sad, Serbia.

IS FLOOR VIBRATION SERVICEABILITY PROBLEM SOLVED FOR GOOD BY EMERGENCE OF COMMERCIAL ACTIVE MASS DAMPERS?

Aleksandar Pavić[1]

Summary:

Historically, structural engineers designing buildings tended to deal with many structural design uncertainties by the generous use of cheap construction materials, as no better approach existed. This paper identifies numerous uncertainties related to floor vibration serviceability that became a de facto governing design criterion for modern floors worldwide governing their size and shape.

With the need to stop wasting materials and the stated uncertainties that can render floor vibration design predictions unreliable and useless, the new active mass damping technology, that has just been launched in the UK, is potentially a game-changer. The mass-produced CALMFLOOR® mechatronics product means designers can avoid both the use of additional materials and the need for significant structural modifications, such as precious span reduction, simply to control tiny, but very perceptible by humans, floor resonant vibrations.

Key words: floor vibration serviceability, partitions, active mass damper, floor occupants

[1] Professor of Vibration Engineering, University of Exeter, United Kingdom

1. INTRODUCTION

The present climate emergency requires serious and fast re-thinking of how the construction sector operates worldwide. Construction and operation of buildings, and the construction industry in general currently generate 39% of 42Gt CO_2e of all annual emissions in the world. Of these, 28% is pertinent to buildings (construction and operation) and 11% to the rest of the construction industry. A good estimate [1] is that 10% of all worldwide annual emissions i.e., a staggering 4.2Gt CO_2e is due to – structural engineering decision making. This should be viewed in the context of the enormous size of the construction sector worldwide which creates and maintains the whole of the human-built environment and provides millions of jobs generating 13% of the world's Gross Domestic Product (GDP) [1]. However, in the process of doing this, the construction very clearly also - destroys the environment.
The UN Environment and International Energy Agency [2] estimates that the total building floor area on Earth will double by 2060 by 230bn m^2 of new floors. This is equivalent to adding one Paris to the planet every week for the next 38 years! This last fact emphasises the importance of building floors on the consumption of the CO_2e worldwide. On average, to construct one m^2 of a typical modern building floor in a multi-storey building requires 250kg CO_2e. Therefore, to create 230bn m^2 of floors in the next 38 years a total of 57.5Gt CO_2e is needed. This is more than what the entire world consumes in a single year. On average, this is about 1.5Gt CO_2e per year which is just over a third of the above mentioned 4.2 CO_2e for which structural engineers around the world are responsible. This is about 3% of the total CO_2e emissions annually generated by the entire world – just to build the floors in buildings needed for the growing human population demanding more quality space. Commercial aviation is responsible for about 2-3% of global carbon emissions, which is about the same amount as for the construction of building floors.
Therefore, as floors are omnipresent and by far the most frequent type of civil engineering structure, which is everywhere, the key question is: how are modern floors in buildings designed? Considering the huge floor area which needs to be built globally, any even small waste in the embodied carbon per m^2 of the floor should be identified as it could yield to enormous waste on a global scale. Such identified waste should be tackled and eliminated through immediate change of the design or construction practice.
There are many types and classifications of building floors. Classifications exist based on construction materials (concrete, composite, timber, etc.), construction method (in-situ cast, pre-cast, modular), ownership (private, commercial, mixed), type of utilisation (office, assembly structures, condominiums, retail, laboratories, schools, hospitals, gyms, etc.), and so on.
Out of all these, the commercial and assembly floors (offices, retail, airports, etc.) are particularly important as they normally require above average embodied carbon (CO_2e) while making a considerable proportion of all floors. For example, just in the UK every year over 1 million of m^2 of new office floors is built. The function and commercial viability of such floors dictate that they tend to be open plan, long-span and increasingly lightweight. Consequently, such floors have low stiffness, low natural frequencies, low damping and low mass. This, in turn, means that they are increasingly prone to high vibrations caused by footfall dynamic forces due to omnipresent walking of the human occupants of such floors.
Vibration performance of building floors in response to human-induced footfall dynamic loading, i.e. walking, is worldwide by far the most widely considered vibration serviceability requirement. It has rightly become a governing design criterion with growing number of reported problems with excessive vibrations of floors already meeting safety requirements of strength and fire resistance as well as thermal and sound insulation comfort requirements. Not surprisingly, over the last 10 years, I published

with my researchers and collaborators dozens of technical and scientific papers dealing with vibration serviceability of civil engineering structures, mostly about human-induced dynamic loading, such as walking on floors. The opening sentence of such papers typically reads:

> *"With the advent of stronger and lighter construction materials and advancements in construction technology, vibration serviceability has become a governing design criterion for lightweight and slender civil engineering structures occupied and dynamically excited by humans."*

This means that vibration, and not strength, considerations determine the size and shape of office floor structures. This is in turn dictates the carbon footprint of the floor structure which typically accounts for 60% of the total weight of a multi-storey building.

So, how are then the low-frequency floors designed today to avoid them vibrating excessively?

2. THE PROBLEM WITH DAMPING AND MASS

Design guidelines used worldwide [3, 4] invariably assume that human walking can cause a 'low (natural) frequency floor' to vibrate excessively in resonance. In resonance, the calculated floor acceleration response is inversely proportional to both modal damping ratio and modal mass [3]. Modal mass can at least be estimated (modelled) directly via physical mass, but damping can never be predicted, only estimated from real world measurements.

It is no surprise then that when checking floor vibration performance, there is a scramble for evidence supporting use of a high damping ratio to reduce the calculated response. Simply increasing damping from, say, 1.5% to 2.5%, reduces calculated vibration response by a whopping 40%! A previously failing floor now passes with flying colours.

Interestingly, similar questions are not usually asked about modal mass. Because values are generated by a formula or computer modelling, they are perceived to be more 'reliable' and less questionable and amendable. Modal mass comes from a calculation whereas the modal damping ratio gets assumed based on design guidelines and experience. So, there is a perception that the modal damping value is more 'flexible' to interpret and assume than its modal mass counterpart when it comes to calculating the resonant response.

However, those who – like me – spent their professional lives not only modelling but also – whenever possible – testing full-scale floors (and comparing the two sets of data) know that modal damping ratio and modal mass are together also the two most unreliable floor vibration modelling parameters. Moreover, they are quite difficult to measure and correlate with their counterparts used in the calculations. Hence, every time I use the assumed value of modal damping ratio and the calculated value of modal mass to get the floor's resonant response, I am worried about how different they could be in reality after the floor is constructed. Yet, as nothing better is available, we all keep using them in a calculation procedure that is overly sensitive to their values.

3. HOW MUCH DOES GOOD FLOOR VIBRATION COST?

As previously mentioned, and quite surprisingly, in the case of omnipresent open plan and long-span floors, it is not the *strength* (i.e., the threat of structural failure) but *vibration* (i.e., the threat of excessive dynamic motion) which dictates the size and shape of such structures nowadays. When I talk about this to lay people, they are often perplexed that anything other than serious structural failure and threat to life can dictate the use of literally millions of tonnes of construction materials and associated embodied

carbon to control structurally non-lethal vibrations. Very often, in situations like this, I get asked a simple question: *how much more material and embodied carbon is then needed just to have satisfactory floor vibrations*?
Here is an example illustrating the answer to this important question.

3.1. DOUBLING FLOOR WEIGHT TO CONTROL ONLY TINY FLOOR VIBRATIONS

Fig. 1 shows the contour plot of the so-called *response factors* (Willford and Young, 2006) due to walking over a 42m long and 27m wide (1,134m^2) floor plate consisting of nine floor panels, each spanning 14m and being 9m wide. So, it is a typical long-span composite steel-concrete floor which can be found in many modern commercial buildings in the UK and internationally. The floor, featuring the usual 14m long secondary beams to minimise the number of beam-to-beam connections, was optimised to have minimum weight and structural depth while satisfying all design criteria (strength, deflection, fire resistance, thermal comfort, and sound insulation) apart from the vertical floor vibrations. However, the maximum vertical vibrations allowed were set to response factor R<4, as appropriate for an office in accordance with the relevant, respected and widely used international standard ISO 10137 [5]. In the UK R<4 would be a criterion required for a 'quiet office'. The floor's 130mm deep lightweight concrete deck, beams, and columns had an admirably low mass of 231kg/m^2 and equally very reasonable embodied energy of only 201kgCO_2e. However, as Fig. 1 shows, about 25% of the floor area (warm coloured) had R>4 with the maximum R>14. The structurally very efficient floor clearly failed the vibration serviceability check.

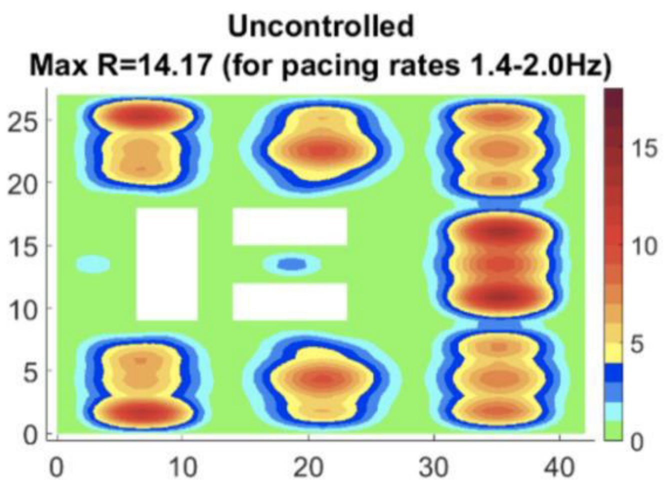

Fig. 1: Uncontrolled floor designed for minimum weight satisfying all design criteria apart from vibration serviceability.

The usual structural modifications followed, to improve the floor's vibration performance by increasing the sizes of the structural elements of the floor, while keeping the spans intact. After many iterations, again a floor structure with minimum weight and depth emerged, but this time satisfying the R<4 criterion over 99% of its area. However, the mass of that structurally modified floor almost doubled to 452kg/m^2 with the total floor depth being 260mm greater and embodied carbon 30% greater just for the floor structure before considering increased costs of bigger vertical support elements, foundations, construction, and decommissioning due to so much more mass needed. In addition, a typical multi-storey commercial building featuring floors like this would lose one entire usable floor level every dozen or so floors. The colossal consequential costs of structural modifications to meet the R<4 floor vibration serviceability requirements, which equate to a peak dynamic displacement around only *20*µm (micron i.e. 0.02mm!) for a 6Hz floor, are hardly acceptable. So, is there a better way?

3.2. 4<R<8 CAN AND DID CREATE EXCESSIVELY LIVELY FLOORS

A common approach is to relax the floor vibration serviceability requirement to R<6 or R<8. However, over the years I dealt with many problematic floors with 4<R<8 and unhappy tenants. Others have reported issues with such floors as well. I find little peer-reviewed scientific evidence that would justify $R>4$ for offices so using $R<8$ for offices seems to be driven by the obviously extremely high environmental and financial cost of achieving $R<4$. However, somehow $4<R<8$ has become a de-facto norm with an expectation that the floor will behave well but with the risk of complaints under certain conditions that need further scientific research to clarify. I described evidence [6] that the Institution of Structural Engineers (IStructE) gathered in a 2015 survey pointing that the ‘design guideline compliant’ building floors satisfying $4<R<8$ may have disappointing vibration behaviour.

Having all this in mind, what is then the way forward when: a) meeting $R<4$ criterion is prohibitively expensive, and b) not meeting $R<4$ can easily create an unduly lively floor attracting complaints and which is difficult to let and eventually fix?

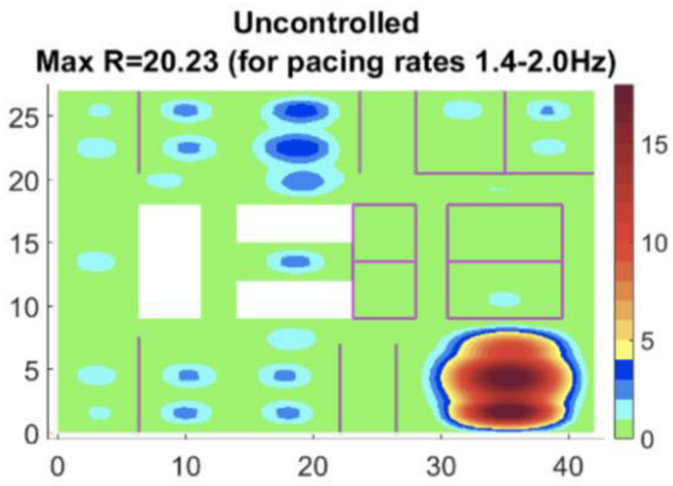

Fig. 2: The original lightweight composite floor not satisfying vibration serviceability, but with floor partitions modelled.

Fig. 2 shows the same floor as in Fig. 1, but now featuring full-height non-structural partitions (outlined in pink). These partitions are typically present in every office, but their stiffness is normally neglected. This even though there is a growing body of peer-reviewed evidence that effects of non-structural partitions can render calculations assuming bare unpartitioned floor potentially useless. This is very much the experience of anybody who witnessed a normally lively bare composite floor transforming into a well-behaving floor in the partitioned areas.

In our example, the vertical stiffness of the outlined partitions was modelled using simple vertical springs based on recommendations in peer-reviewed publications [1, 7]. The partitions very much suppressed vibrations in the partitioned areas, as expected. But, they also *amplified vibrations in the not-partitioned open-plan part of the floor*, boosting unexpectedly the maximum R-factor to over 20! Although the experience is also that not-partitioned areas of the floor are known to be lively, such a significant amplification of vibration is a surprising result.

When comparing contour plots in Figures 1 and 2, the response factors in the unpartitioned area of the floor (bottom right corner) are almost 50% greater than when calculated neglecting the presence of the partitions. This means that the common belief that neglecting partitions is a ‘safe’ assumption may well not be correct. This may concern many colleagues as it definitely concerns me.

3.3. OTHER PROBLEMS

There are other sources of uncertainty in response predictions: I tested an open plan floor in service with as many as 120 people working where, as usual, the calculation formulae assume that only a single person is walking and causing resonance. It is quite common is that occupants in such offices frequently walk simultaneously and very close to each other, very possibly causing greater responses than an individual walker. However, this is anecdotal evidence and there is no peer-reviewed evidence of that. Footbridge design guidelines have been dealing with multi-person loading for over a decade and also consider the likelihood of the pacing frequencies matching the natural frequency. Yet, floor design guides stick with quite a few irrational assumptions from

30-40 years ago including a single person walking. The logic has been that the wrong assumption of perfectly achieving resonance (conservative) will be cancelled by the wrong assumption of a single pedestrian (unconservative) so it is OK! Pass-fail criteria suitable for ultimate limit state calculations still prevail in floor vibration serviceability assessment where a more nuanced and informed probability-based approach of what is likely to happen in day-to-day operation is preferable.

Finally, the climate emergency means that it cannot be business as usual anymore, whereby the structural engineering profession throws vast amounts of construction materials and embodied energy at managing design risk and uncertainties relating to floor vibration serviceability. Increasing the mass and/or stiffness of the floor just to control tiny footfall-induced vibration of low-frequency floors is no longer a viable design option.

4. THE BIG QUESTION

So, knowing all this, the big question is: why do we keep designing up-front omnipresent low-frequency floor structures using uncertain structural parameters and unreliable loading models given the increasing evidence that our approach does not always work and is definitely not fit for purpose in a climate emergency? In partitioned areas of the floor the responses are easily considerably lower than calculated and in the unpartitioned areas they can easily be much higher! Adding mass and stiffness to control low-frequency floor resonance is plain wrong when damping is by far the most effective approach. Every textbook on structural dynamics is telling us that increasing damping and not mass and/or stiffness should be used to reduce resonant vibrations.

So, how about we stop doing all of that and instead start designing floor structures for everything *except* vibration serviceability?

In this rather radical change of the approach to designing building floors, we optimise the floor structure for the minimum embodied energy while meeting strength, deflection, concrete cracking, fire, sound and thermal comfort criteria (and whatever else is needed to be satisfied, just not the footfall-induced vibration criterion). We do not consider footfall vibrations at all when deciding spans and sizing structural elements. After all, what is the point designing the low-frequency floor structure for vibration serviceability when we know that:

- Significantly more (up to 100%) materials will be needed to achieve a code-compliant vibration serviceability design. This will severely impact material utilisation and destroy the green credentials of the building design knowing that about 60% of the total multi-storey building mass above the ground and corresponding embodied energy is in floors, as previously mentioned.
- Even when we do design a floor structure for acceptable vibration serviceability, the uncertain damping, inappropriate footfall loading model and effect of partitions will render the design calculations meaningless when compared with what is really happening on the real floor after it is constructed.

Granted, neglecting floor vibration serviceability in structural design will result in a very slender floor which will certainly be bouncy on its own under footfall dynamic loading, as shown in Fig. 1. We will have a safe and sustainable, but not fit for purpose floor. What then?

Well, then the floor will be constructed and partitions and other non-structural elements (installations, facade, furniture, etc.) will come in. These will certainly improve the floor vibration performance in many partitioned areas, so much so that they will often become quite satisfactory, but difficult to predict upfront. This is known to anybody who witnessed fitting out of an empty and rather lively floor and its transformation into a solid floor in the partitioned areas. The large non-partitioned areas of the floor are likely to remain lively requiring vibration control. However, this is likely to be just a fraction of the total floor area which would otherwise have required structural modification throughout, and the many millions of tonnes of steel and concrete wasted annually worldwide.

5. A SOLUTION FOR THE 21ST CENTURY: SOPHISTICATED VIBRATION ANALYSIS COUPLED WITH THE NEW CALMFLOOR® PRODUCT

Fig. 3: The 67kg CALMFLOOR AMD attached to a steel I-beam supporting a composite steel-concrete deck. Courtesy of FSD Active Ltd.

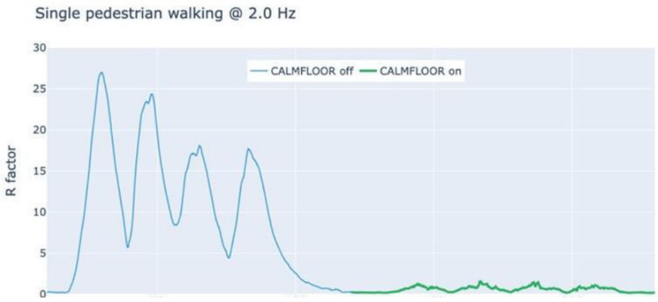

Fig. 4: CALMFLOOR performance on a real-life open plan office floor achieving vibration reduction of over 90%.

Throwing enormous amounts of steel and concrete at the problem goes against all the principles of *lean design*. Typically, floor design is woefully wasteful for today's climate emergency state in which we all are. There is an urgent need to reduce embodied energy in construction.

There is also a clear need for a new and better way to reduce resonant vibrations in floors. As previously mentioned, the best way to reduce resonant vibrations is by increasing damping, and this can be achieved by using either passive or active technology.

After multi-£m investment in years of research and development, UK-based start-up FSD Active Ltd has just brought first-to-market CALMFLOOR® mechatronics device, a novel Active Mass Damper (AMD), to solve the problem of the lively low-frequency floor for good (Fig. 3).

5.1. ACTIVE VS. PASSIVE COMMERCIALLY AVAILABLE TECHNOLOGY FOR REDUCING FLOOR VIBRATIONS

In principle, an AMD device of any kind is a potential game changer which enables design of very slender floor structures with optimal use of construction material spans unduly shortened just to meet the stringent floor vibration serviceability criteria. It ensures an outstanding vibration performance (Fig. 4) of long-span, open-plan, low-frequency commercial floors that is practically impossible to achieve using *constrained layer damping materials* and *tuned mass dampers* (TMDs) as the two key passive methods that are currently commercially available.

How is this possible?

Specifically in the case of the CALMFLOOR® device, by generating an active force proportional to the measured velocity of the floor structure to which CALMFLOOR® is attached, a huge increase in damping can be achieved typically resulting in more than 10% damping ratio in all modes of floor vibration it is controlling. This is far beyond anything existing or seen on the market to date. When factored in at the design stage of a new building, this autonomous mechatronics device could replace tens to hundreds of tonnes of traditional construction materials, such as steel and concrete. This is due to increasing damping by 5 or more times which is equivalent to increasing the floor mass by the same amount, which is practically impossible. The CALMFLOOR® technology makes it for the first time very possible now.

5.2. CALMFLOOR® TEHNOLOGY EXPLOITS SPECIFICS OF FLOOR VIBRATION PROBLEM

CALMFLOOR® AMD makes use of the simple yet underappreciated fact that the annoying but tiny oscillatory floor displacements are generated by small individual walking forces, of the order 100N. The mechatronics device continuously senses the floor vibrations and applies similar force levels to cancel them. This is a large-scale equivalent of noise-cancelling headphones.

Moreover, the CALMFLOOR® technology in principle resolves the following key issues hampering the wider application of the floor vibration control passive technologies:

1. CALMFLOOR® can control multiple modes of floor vibration simultaneously. This is crucial in floors where modes of vibration are often closely spaced due to structural near symmetry and repetitive geometry. TMDs can control one a single mode and multiple TMDs may be needed on a floor structure to control multiple modes. This in turn may cause interaction between TMDs with adverse effect on their overall performance.
2. CALMFLOOR® are identical mass-manufactured devices whereas TMDs are custom built for each floor and each mode.
3. CALMFLOOR® cannot be detuned in the same manner as TMDs are detuned if the floor usage changes.
4. CALMFLOOR® can engage easily at ultra-low levels of real floor vibration of only a few microns. At such low levels the passive technologies may struggle to engage in real floors.
5. CALMFLOOR® are an order of magnitude lighter than TMDs.
6. CALMFLOOR® are easy to install after the floor tenant moves in whereas passive solutions are not.
7. CALMFLOOR® can be moved flexibly around after the installation if needed to accommodate flexibly a new floor tenant and partitioning layout whereas passive technologies cannot.

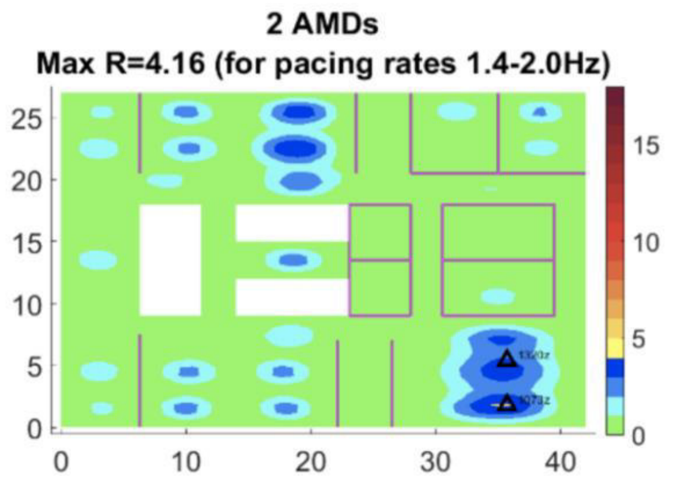

Fig. 5: The original long-span composite floor featuring full-height partitions and two CALMFLOOR® units reducing the maximum R-factor from highly problematic 20.2 to satisfactory 4.2 in the problematic unpartitioned area of the floor.

The contour plot in Fig. 5 shows R-factors for the structurally *unmodified*, original lightweight floor, featuring partitions and effects of only two CALMFLOOR® active mass dampers in the problematic unpartitioned area previously mentioned and shown in Fig. 2. The floor plate has satisfactory R<4 performance over its entire area with no need for either costly structural modifications or risky relaxation of vibration criteria.

The small carbon footprint (see Fig. 6) of the two CALMFLOOR® AMDs (relative to the mentioned structural modification) and their competitive costs are both many times lower than those of the structural modification to achieve the coveted R<4.

The usual argument against an approach that involves explicit modelling of the partitions is that it is normally not clear where the partitions are going to be until the tenant moves in. The counterargument is that eventually the floor partitions will be erected and then it will be clear where the unpartitioned areas are. The 67kg CALMFLOOR® units can then be installed in these locations very easily and with the full cooperation of the tenant after they move in. This huge level of flexibility is the *key transformative feature* of CALMFLOOR®: it is new and off-the-shelf technology (all

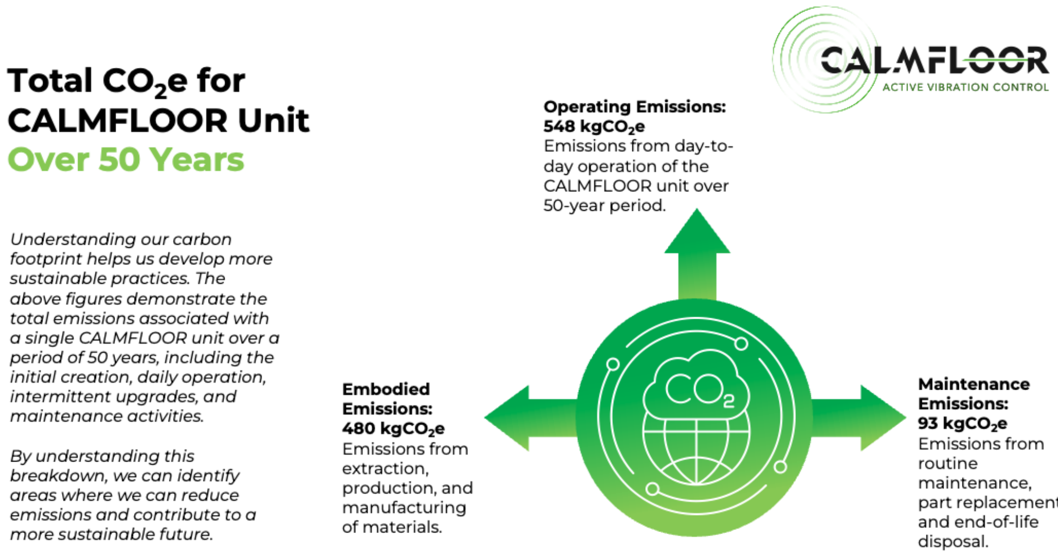

Fig. 6: Total embodied and operating carbon for a single CALMFLOOR® unit over 50 years.

CALMFLOOR® units are identical and suitable for mass production) that is simple to install. This is in stark contrast with other post-occupancy solutions to control floor vibrations such as:

- structural modification, and
- TMDs.

TMDs, being at least an order of magnitude heavier, more complex to install, cost overall no more (usually less) and still perform worse than CALMFLOOR®.

So, combining the sophisticated modelling of partitions with CALMFLOOR® units in the remaining unpartitioned floor areas is an innovative design approach that permits retention of long and very lightweight spans while achieving excellent vibration performance impossible by other means.

6. CONCLUSIONS

Historically, structural engineers designing buildings tended to deal with many structural design uncertainties by overuse of previously low cost construction materials, there being no better approach. The climate emergency means that such a practice must stop immediately, requiring a radically different innovative design approach to meeting increasingly stringent floor vibration requirements.

This paper identifies numerous uncertainties related to floor vibration serviceability: location of partitions, walking corridors, number and activity of office occupants, future tenant's vibration serviceability needs, etc. The perception of the floor partitions generally improving floor vibration response is shown to be wrong – partitions, surprisingly, can actually increase response in some unpartitioned floor areas. Therefore, a common practice of not modelling partitions is generally not conservative as far as floor resonant vibrations are concerned.

With the need to stop wasting materials, and with so much uncertainty about the floor vibration performance that can easily render floor vibration design predictions unreliable or useless, the new CALMFLOOR® active mass damping technology that has just been launched in the UK is potentially a *game-changer*. CALMFLOOR® can avoid the need for additional materials or significant structural modifications (including shortening of the precious spans) solely to control tiny floor resonant displacements that can still be annoying to human occupants of the floor. CALMFLOOR® offers unprecedented levels of flexibility when managing floor vibrations as it is an off-the shelf mass produced technology that can be deployed at short notice and only at floor vibration 'hotspots' after handover when the tenant and their needs are known.

REFERENCES

[1] Orr, J. J., Cooke, M., Ibell, T. J., Smith, C., Watson N., Algaard, W., Arnold, W., Butterfield, T. J., Darby, A. P, Gardner, H., Hawkins, W., Mandoki R., Marsh, E., Nuh, M., Oval, R., Peters, A. and Roynon, J. (2021). "Design for Zero". London, United Kingdom: The Institution of Structural Engineers.

[2] UN Environment and International Energy Agency (2021). "Towards a zero-emission, efficient, and resilient buildings and construction sector". UN Global Status Report for Buildings and Construction.

[3] Willford, M. R. and Young, P. (2006). "A Design Guide for Footfall Induced Vibration of Structures", CCIP-016, The Concrete Centre.

[4] Murray, T. M., Allen, D. E., Ungar, E. E. and Davis, D. B. (2016). "Vibrations of steel Framed Structural systems Due to Human Activity". Second Edition. American Institute for Steel Construction.

[5] International Standardisation Organisation. (2007). "Bases for design of structures – Serviceability of buildings and walkways against vibrations". ISO 10137, Second Edition.

[6] Pavic, A. (2019). "Results of IStructE 2015 Survey of Practitioners on Vibration Serviceability". SECED Conference. 9-10 September. Greenwich, London.

[7] Devin, A., Fanning, P. and Pavic, A. (2015). Modelling the Effect of Non-Structural Elements on Floor Modal Properties. Engineering Structures. Vol. 91, 58-69 (doi:10.1016/j.engstruct.2015.02.021).

TOWARDS A NEW VISION OF CIVIL ENGINEERING: DIGITAL INNOVATION APPLICATIONS FOR THE STRUCTURAL HEALTH MANAGEMENT OF EXISTING BRIDGE PORTFOLIOS

Sergio Ruggieri[1], Andrea Nettis[2], Mirko Calò[3], Alessandro Nettis[4], Angelo Cardellicchio[5], Giuseppina Uva[6]

Summary:

Bridges are one of the most critical components of road networks and their safety and preservation represent pivotal topics for management companies and scientific community. Bridges are usually subjected during their life to different phenomena provoking a continuous increment of vulnerability, such as aging, environmental aggressive conditions, natural hazards, which can result in the worst-case scenario in the occurrence of structural collapses. Taking as reference the Italian case, after the collapse of the Polcevera Viaduct, the Italian Ministry of Transportation proposed a multi-level safety evaluation procedure to apply on the entire national existing bridge stock, with the aim to provide a methodology for assessing critical cases to act on with risk mitigation interventions. For this scope, several phases should be processed, starting from the collection of the original documentation, passing for the performance of periodic onsite surveys to evaluate defects and degradation signs, up to the definition of a risk class that account for different hazard sources. To carry out the above phases, several problems arise, such as the unavailability of documentation for the older structures, the time- and cost-consuming phase of onsite inspections, the lack of objectivity in the visual definition of defects, the high demand for qualified personnel. To limit the above issues, traditional techniques could be supported by the possibilities provided from the world of digital innovation, whose goal is to develop new and reliable tools to support road management companies in safeguarding the heritage infrastructural asset. This paper addresses these topics, firstly proposing a panoramic about the multi-level approaches proposed by the Italian government and after by reporting the recent developments and new methodologies for assessing the health state of existing bridge portfolios. The use of cost-effective techniques, such as artificial intelligence, satellite data, and automated analytical models are explored, in order to assess bridge health state towards service conditions and to provide new means to exploit for purpose of risk assessment and priorization.

Keywords: Digital Innovation, Structural Health Management, Existing Bridge Management, Deep Learning, MTInSAR Data, Fragility assessment

[1] Asst. Prof., DICATECH Department, Polytechnic University of Bari, Via Orabona 4, Bari, Italy, sergio.ruggieri@poliba.it
[2] Post-Doc. Res., DICATECH Department, Polytechnic University of Bari, Via Orabona 4, Bari, Italy, andrea.nettis@poliba.it
[3] PhD Stud., DICATECH Department, Polytechnic University of Bari, Via Orabona 4, Bari, Italy, mirko.calo@poliba.it
[4] PhD Stud., DICATECH Department, Polytechnic University of Bari, Via Orabona 4, Bari, Italy, alessandro.nettis@poliba.it
[5] Post-Doc. Res., STIIMA, National Research Council of Italy, Bari, Italy, angelo.cardellicchio@stiima.cnr.it
[6] Full Prof., DICATECH Department, Polytechnic University of Bari, Via Orabona 4, Bari, Italy, giuseppina.uva@poliba.it

1. INTRODUCTION

The numerous incidents involving the collapse of existing bridges in Italy have significantly raised the public opinion regarding the safety of the infrastructure networks and then, the necessity to develop strategies to carry out reliable risk mitigation plans. The real watershed was the collapse of the Polcevera Viaduct, which prompted public institutions and the scientific community to release specific guidelines on the structural safety of existing bridges in 2021 [1]. These latter, which are nowadays mandatory for management companies, were developed on the base of a systematic multilevel approach, to be applied on the entire national bridge inventory and to accurately establish monitoring and maintenance strategies on the worst cases. In detail, the multilevel approach consists of six distinct levels of increasing complexity, to be sequentially implemented. The first three levels consist in a preliminary and simplified assessment of the infrastructural stock, aimed at identifying critical cases. Their application allows to determine the appropriate actions to perform on the prioritized infrastructures. The second set of three levels guides the decision-making process concerning whether a specific bridge should undergo demolished and reconstructed, retrofitted, or some restrictions should be imposed on the service conditions (e.g., limitation of traffic). However, a crucial role is played by the first three levels, because from the obtained output final decisions can be taken regarding the future of the focused bridges.

Talking about the first three levels, level 0 consists in a comprehensive collection of original documentation about bridges and viaducts within the network under study. Different data should be collected, such as structural characteristics, geometrical and mechanical parameters, constructive details. In addition, contextual information can be retrieved by using existing studies related to environmental risks around the structures. Level 1 consists in the visual inspection of the bridges within the road network, where instructed surveyors periodically observe the environment around each bridge and all structural elements (e.g., desk and beams, pillars, supports, abutments), in order to identify potential vulnerability sources and boundary conditions related to various risks, including structural, seismic, hydraulic, geotechnical, and geological hazards. If a significant risk affecting the safety of the bridge is identified, a specific report should be performed, and the procedures in levels 4, 5, and 6 should be employed. Otherwise, level 2 can be carried out. With this regard, a "risk class" is determined as result of all analysed risks, which are quantified through a specific sub-risk class (e.g., structural, seismic, hydraulic, and geological). As output of the level 2, the Italian guidelines propose five overall risk levels: low, medium-low, medium, medium-high, and high, defined according to a scheme to logically ascertain the global risk class. Based on the obtained risk classification, the management companies could determine the necessary actions to be taken. For instance, for bridges classified as high-risk, level 4 is mandatory, where assessment shall be performed according to different limit-states, such as transitability and operativity and, to enhance safety, structural monitoring is strongly recommended.

From the above framework, several problems arise for levels 0 and 1. For the level 0, the real enemy is represented by the unavailability of documentation, which could be absent when the structure is extremely old. Instead, for level 1, in-situ inspections constitute a fundamental and yet challenging phase, from which the success of the priorization task depends. Although visual observations offer a direct and quick way to identify issues or vulnerabilities, they come with certain drawbacks. In fact, subjectivity may arise in defining defects, their extent and severity, even if surveyors are well-instructed. Moreover, lapses in attention can introduce bias in defect assessment due to human factors, as well as, the inaccessibility of some bridge components, such as supports, could limit an accurate classification. Furthermore, it is worth specifying that

to conduct a careful survey of all structural elements belonging to about 4/5 bays requires one working day, which means that the time at disposal is extremely limited, especially if considering a high number of bridges vs. a low number of instructed surveyors.
In light of these situations, a consistent support is required to fulfil the demanding tasks attributed to the management companies, and the friend who can come to the rescue is the digital innovation. This latter has not the role of substituting the traditional techniques for purposes of inspections and monitoring, but it could support the usual practices by reducing time and efforts required in the field of bridge portfolios risk priorization. The paper deals with the use of new digital innovation techniques for purpose of bridges health management. On the base of the recent research carried out by the authors of this paper, the exploration of cost-effective techniques is presented, starting from the use of the artificial intelligence (AI) and deep learning (DL) approaches to involve an automated recognition of typical defects in existing reinforced concrete (RC) bridges, passing from the use of satellite data (i.e., Multi Temporal Interferometry Synthetic Aperture Radar, MTInSAR) for purpose of monitoring unexpected deformation in RC simple supported bridges over time, and finishing on the use of the fragility curves tool to rapidly and automatically assess the behaviour of prestressed RC bridges under service conditions (also in presence of degradation phenomena, as the corrosion). These methodologies (object of ongoing research) are employed to assess the health state of bridges, offering innovative ways to leverage risk assessment and prioritization purposes.

2. USE OF DEEP LEARNING TECHNIQUES TO PERFORM DEFECT DETECTION IN EXISTING RC BRIDGES

Over the last years, machine learning (ML) techniques have been widely employed in the field of structural engineering, with the aim to solve complex problems or to define input-output relationships [2-3]. Another way to use the powerful of ML principles is to retrieve data from images through DL techniques, as made in [4]. Analogously, when talking about existing RC bridges, DL techniques are widely spread in the literature, especially for crack detection (e.g., [5-7]). Instead, in the field of defect recognition, convolutional neural networks (CNNs) are usually employed, as made by Cha et al. [8] that automatically detected five types of damages by means of the videos collected during inspections, or as proposed by Zhu et al. [9], which combined transfer learning and CNNs for automatically detecting bridge defects. Cardellicchio et al. [10] employed and compared eight types of CNNs on seven kinds of typical defects in RC bridges, proposing new metrics for explaining the obtained prediction. However, interesting outcomes can be achieved by using object detection approaches, where to difference of CNNs, specific defects are recognized within an image by avoiding the high computational cost to scan the entire image. A popular approach is represented by the "you look only once" (YOLO) [11], which is a single stage detector that achieves a good accuracy with sustainable computational efforts. Few works are available on the defect detection through YOLO on existing bridges, such as made by Maeda et al. [12], which used single-stage detectors on a dataset of 9.053 road damage images. With the aim to use YOLO for purpose of defect detection in images, this work reports a summary of the previous research proposed in [13-14], where authors using the dataset in [10], and employed several versions of YOLOv5 to propose a tool for supporting the objectivity in onsite inspection.
The reference dataset contains 6580 images about several inspected bridges and for which different structural elements are available. On the dataset, authors performed a labelling to identify the visible defects, which were classified according to seven classes, i.e., cracks, corroded and oxidized steel reinforcements, deteriorated concrete,

honeycombs, moisture spots, pavement degradation, and shrinkage cracks. It is worth noting that a more refined classification of the defects is proposed by the Italian guidelines [1], but a first attempt was made with the most typical defects observed in the inspected bridges. From the available dataset, about 10831 labels were extracted as reported in Tab. 1.

Tab. 1 Number of available labels for each defect of the available dataset

Defect	No. of labels
Cracks	1138
Corroded and oxidized steel reinforcements	2928
Deteriorated concrete	2448
Honeycombs	1165
Moisture spots	2962
Pavement degradation	119
Shrinkage cracks	71

For purpose of training the object detector, several architectures of YOLOv5 were trained. For each model, the backbone (CNN-based architecture used by the model to extract relevant features from images), the neck (reduce the loss during the feature extraction process and introduce additional contextual information), and the head (convolutional layers representing the bounding boxes and the category information in the input image) were set and, to train the models on a relatively small dataset, transfer learning was used. Using a machine equipped with an Intel Core-i9 13900K as CPU, a 64 GBs DDR4 as RAM, and an NVIDIA GeForce 3090 with 24 GBs VRAM as GPU, all images were rescaled to 960 pixels and training/test and validation quantities were fixed to 75% and 25% of the dataset, respectively. Obtained results were assessed in terms of three metrics, that is, precision (P), recall (R), and mean average precision (mAP) and following defined:

$$P = \frac{TP}{TP + FP} \tag{1}$$

$$R = \frac{TP}{TP + FN} \tag{2}$$

$$mAP = \frac{1}{N}\sum_{i=1}^{N} AP_i \tag{3}$$

where TP, FP, and FN are the true positive, the false positive, and the false negative, respectively, while AP_i indicates the average precision for the i^{th} class. Among the trained models (for the sake of synthesis, all models are not reported but a complete overview can be found in [14]), YOLOv5x presented the best performance (P=86.90%, R=58.17%, mAP=54.52%), and results are shown in Fig. 1. In some case, the trained model is not able to correctly detect the defect (Fig. 1, top), while in other cases the prediction is good (Fig. 1, bottom).

Fig. 1 Comparison between labelled (left) and predicted (right) defects in some images of the available dataset

Overall, there is a number of missed detections, especially for defects as pavement degradation and shrinkage crack where the available number of labels is low. Instead, for defects with more labels (e.g., moisture spot, cracks), the model is able to detect defects with a relatively high confidence score.

Further investigations will be oriented in two main directions: (a) to enlarge the available database; (b) to train the most recent models of object detection.

3. USE OF MTINSAR DATA TO MONITOR DEFORMATIONS OVER TIME

In the last years, a new cost-effective technique to monitor the behaviour of existing bridges caught on, which consist in the use of the information contained in satellite data. In particular, the use of synthetic aperture radar (SAR) data is strongly recommended in Italy (for example the ReLuis consortium released specific guidelines for their treatment [15]) for purpose of structural evaluation. In general, the method allows to dispose of a low-cost technique for continuously monitoring large areas, and it is usually employed to monitor landslide and subsidence phenomena. Nevertheless, recent works employed this methodology to monitor the displacements and the velocities over the time of some bridges.

Briefly, as working principles, satellite data can be used by elaborating stacks of SAR images, which are characterized by features as amplitude and phase. The first characteristic is used to display the image, which is related to specific points, named persistent scatters (PSs) that usually belong to parts of structures and contain the information related to the displacement (and then the velocity). To obtain these points, multi temporal Interferometry Synthetic Aperture Radar (MTInSAR) techniques can be employed, which allow to compare the values of pixels phase between consecutive images, and to evaluate the difference of phase ($\Delta\varphi$). This parameter is used to evaluate the displacement along the Line-of-Sight (LoS) direction, named d_{LoS}, according to the following formulation:

$$d_{LoS} = \frac{\Delta\varphi * \lambda}{4\pi} \tag{4}$$

where λ represents the wavelength of SAR sensor. Obviously, a lower value of λ implies a higher resolution and this is the existing difference among the different typologies of satellites, e.g., Sentinel (SEN), COSMO-SkyMed (CSK). The main characteristics of PSs are the latitude, the longitude, the height, the d_{LoS}, the velocity over the LoS (v_{LoS}), and the coherence. This latter is used to quantify the consistency of the LoS

displacement time series according to a linear regression model (higher values of the coherence are desirable). As all the time series, some filtering actions are required on the phase value, as for example by eliminating the influence of topography, atmosphere, residual orbit error and noise sources. In the end, data can be used to check if unexpected displacements (with related quantification of the velocity) characterized parts of the focused structure.
Several examples exist in the scientific literature on the use of MTInSAR for purpose of bridge monitoring. In their work, Peduto et al. [16] introduced a procedure focused on investigating damages caused by bridge settlement in Amsterdam, by deriving empirical fragility curves to assess the vulnerability of bridges. Nettis et al. [17] proposed an automatic geo-processing chain for interpreting deformation scenarios, specifically aimed at monitoring bridges. The methodology employed MTInSAR with the aim to establish priority classes for bridge portfolios. In a similar vein, Farneti et al. [18] presented a methodology for evaluating multi-span bridges by leveraging satellite data. The assessment accounts for both systematic and random errors, which are influenced by the precision of the initial line-of-sight (LOS) measurements and the assumed direction of deformations. The application of this method was demonstrated on the Albiano-Magra Bridge, which unfortunately collapsed. With the aim to use MTInSAR for purpose of bridges monitoring, this work reports a summary of the previous research proposed in [19], where authors elaborated satellite data to derive displacements in existing bridges and proposed some thresholds for purpose of comparison. It is worth noting that the proposed methodology builds upon existing approaches, aiming to offer a semi-automatic solution for monitoring the displacements of existing bridges. This is achieved by harnessing satellite data in conjunction with other relevant sources of information, including environmental data and structural details.
In the proposed framework, developed for single or multi-span simply supported concrete girder bridges, the first step consists in the collection of the position of the bridge (i.e., coordinates) and the related structural features, among which bearings arrangement, properties of the deck and its beams, properties of the piles. Using MTInSAR technique, ascendent (ASC) and descendant (DSC) acquisition geometries should be available, according to the availability of CSK data (see [19] for more information about differences between SEN and CSK). Given satellite data, LoS displacement time series can be estimated, by means of the algorithm SPINUA [20]. From the available PSs, only the ones belonging to the bridge should be selected. Once selected the PSs, are elaborated and used for assessing unexpected behaviours. An application of the proposed method is provided, where for an existing bridge in the Fiumicino area (Rome, Italy), ASC and DSC PSs have been collected and elaborated (see Fig. 2).

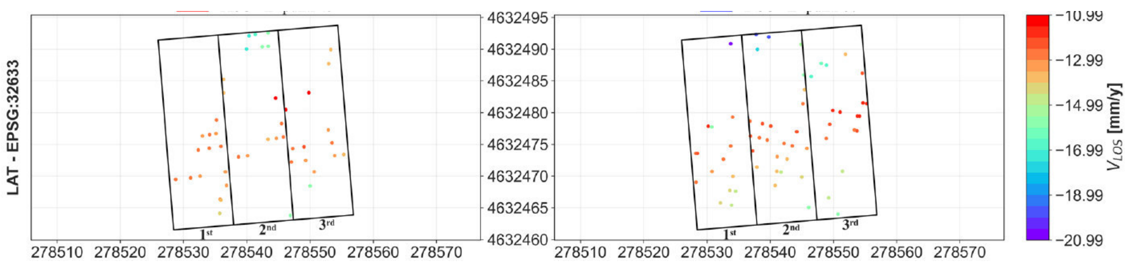

Fig. 2 Bridge footprint and selected PSs from the ASC (left) and DSC (right) datasets

From the elaboration, displacement components can be derived, as shown in Fig. 3. The analysis of the longitudinal seasonal component revealed displacements of the sub-regions near the supports, showing reverse phases in the 1st and 3rd zones. These relative displacement values oscillate within ±1.5 mm and are attributed to a static scheme featuring longitudinally mobile bearings on both abutments. Notably, the maximum vertical seasonal displacement of the 2nd sub-region doubled over a three-year period, from 2017 to 2020. This increment may be linked to a potential malfunctioning of the bearings. For longitudinal trends, from mid-2018, sub-regions started moving together towards the West direction, with a longitudinal velocity of -0.21 mm per year for the 3rd sub-region. Longitudinal displacements oscillated between -1.7 mm and 1.5 mm, while vertical displacements ranged from -2.2 mm to 4.5 mm. Considering a 5-year observation period and nearly 8 cm of vertical displacement in the localization area, the proposed elaboration revealed two different behaviours regarding longitudinal displacements: (i) prior to mid-2018, the 1st and 3rd sub-regions moved away from each other, and (ii) after mid-2018, both parts moved toward the West direction.

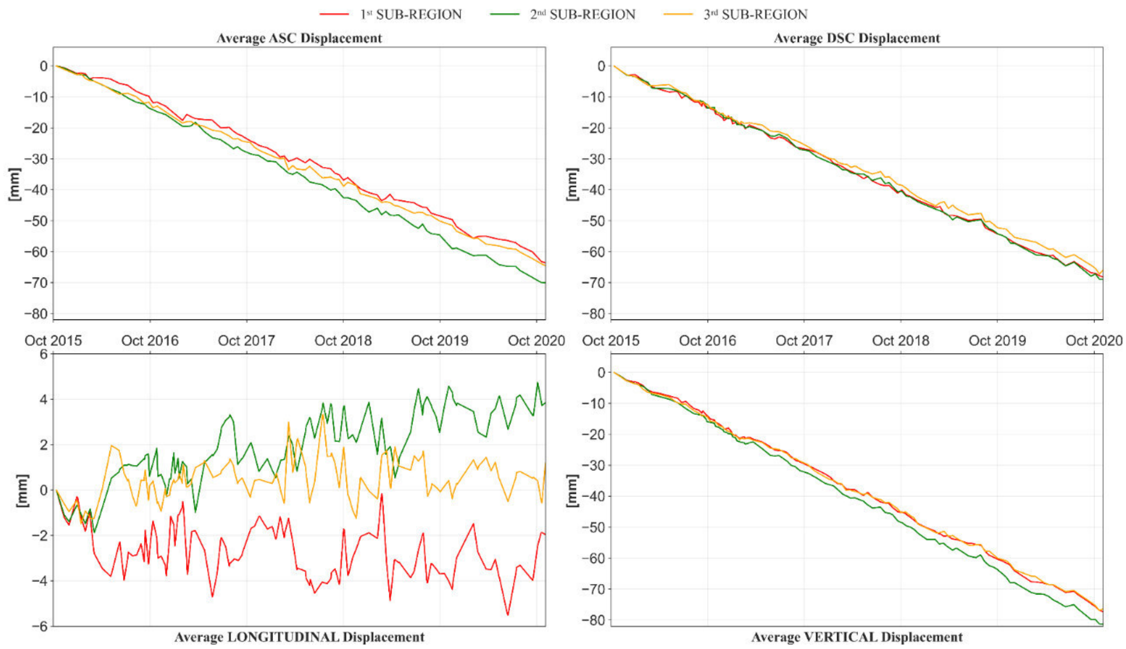

Fig. 3 Fiumicino (Rome) sub-regions seasonal displacement time-series

In conclusion, the proposed approach shows a certain powerful in a view of bridge behaviour prediction, despite traditional monitoring could reveal major details. Nevertheless, the reduced cost of the available data represents the reason for pushing the research in this direction. Further developments will be aimed to employ spatial resampling techniques, to improve the quantity of data, and some extensions could be elaborated to investigate other typologies of bridges.

4. FRAGILITY ASSESSMENT OF SERVICE CONDITIONS THROUGH AUTOMATED ANALYTICAL MODELS

As last topic of this paper, structural performance of existing bridges could be investigated trough some tools able to predict future losses due to service and natural hazard causes. Focusing on existing bridges, their behaviour could be severely undermined in the case of high degradation, as effect of aging and environmental conditions. This aspect could be visually assessed during onsite inspection, but to support management companies in the task of risk priorization, some predictive tools could be developed. Before to make predictions for natural hazards, a less intuitive study should be conducted on the behaviour of bridges under service conditions, i.e., traffic loads. Few studies are available about the topic, as provided by Fiorillo et al. [22], which employed real field truck data to conduct a fragility analysis of existing bridges, specifically focusing on the impact of overweight traffic loads. They investigate the vulnerability of these bridges under such conditions. Similarly, Miluccio et al. [23] performed a characterization of statistical distributions related to significant geometric and structural variables for a broad category of existing prestressed concrete girder superstructures. Subsequently, they carry out a fragility analysis, considering the effects of traffic loads. Both studies contribute valuable insights into assessing the resilience and structural integrity of existing bridges when subjected to various loading conditions, shedding light on potential risks, and providing essential information for effective bridge management and maintenance.

With the aim to predict the behaviour these structures under traffic loads, the authors of this paper developed a tool for evaluating the failure probability of prestressed concrete girder bridges, accounting for the presence of tendon corrosion [24-25]. The tool is fully probabilistic-based and propagation of epistemic uncertainties affecting geometric and structural parameters was considered by using sampling techniques. The typological study started by defining geometrical and mechanical parameters of prestressed concrete girder bridges. In detail, considering that a not specific case was investigated, existing probability distributions were considered from the available literature (e.g., [26-27]) to simulate different configuration of existing bridges. Given the distribution of the useful parameters, Latin Hypercube Sampling (LHS) technique was used to generate a random population of bridge models. Hence, a simplified modelling strategy was employed to model the simply supported superstructures, that is, the method by Courbon-Albenga [28], used for calculating maximum flexure and shear demands for the girders of a given bridge superstructure. Gravity loads were attributed by considering the self-weight of the generated structures, while traffic loads were imposed according to Eurocode 1-Part 2 [29]. At this point, demand parameters can be extracted, among which the maximum bending moment recorded at mid-span and the maximum shear stress recorded at the support. Demand quantities are then compared with the capacity, where for bending (M_R) and shear (V_R) stresses, the following models were considered:

$$M_R = \left(A_{sp} f_{p.01} + A_s f_y\right) z \tag{5}$$

$$V_R = 0.7 b_w d \sqrt{{f_{ct}}^2 + \sigma_{cp} f_{ct}} \tag{6}$$

where A_{sp} is the area of tendons, $f_{p,01}$ is conventional yield strength of prestressing steel, A_s is the area of steel reinforcement, f_y is the tensile strength of steel reinforcement, z is the internal lever arm, b_w is the girder web width; d is the distance of the reinforcing steel from the top compression side (equal to girder height minus concrete cover); f_{ct} is the concrete tensile strength; σ_{cp} is the average compressive concrete stress due to residual prestressing action σ_{sp}. The influence of the corrosion was accounted for through a percentage reduction of A_{sp}, given a corrosion degree, according to the proposal by Yu et al. [30]. Given the demand and the capacity of all random realizations, fragility curves can be computed according to the maximum likelihood method proposed by Baker [31].

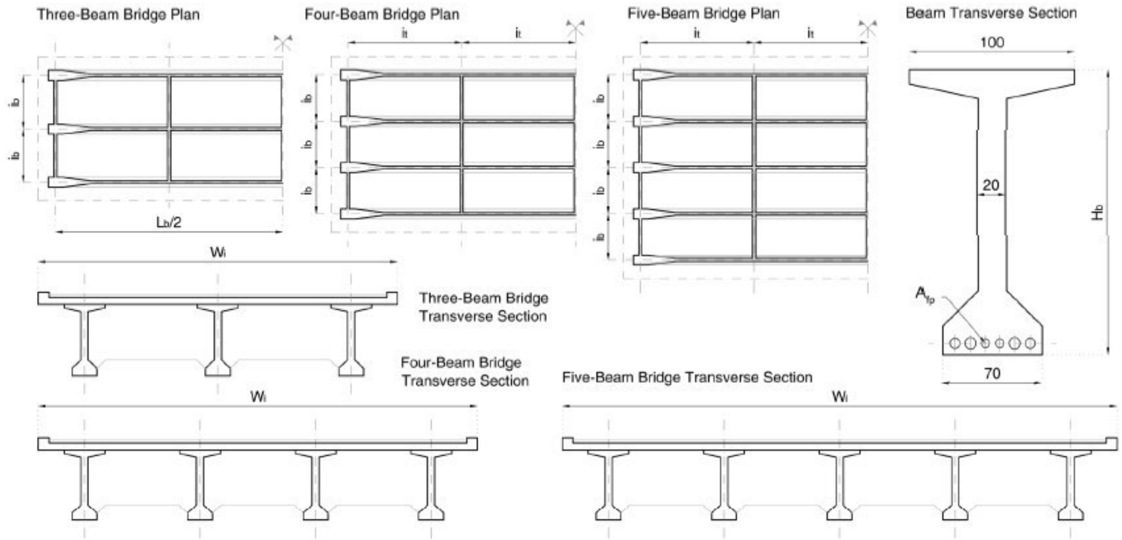

Fig. 4 Generated case studies [24]

The evaluation is repeated several times in order to account for the corrosion effect. The efficiency of the proposed procedure was tested on some case studies, as representative of the post-World-War bridges (see Fig. 4). Nine bridge typologies were defined using a simulated design approach (employing design rules of the old Italian bridge code), accounting for the combination of three different number of beams (3, 4, 5) and three different values of the span length (15 m, 35 m, 55 m). Values and distributions of the mechanical and geometrical parameters used are reported in Tab. 2, while three values of the corrosion degree (ξ) were considered (0%, 20%, 40%). Applying the proposed framework, fragility curves were derived, and they are reported in Fig. 5, accounting for flexural (F) and shear (S) collapse mechanisms.

Tab. 2 Statistical distribution of geometrical and mechanical parameters. S indicates the slab thickness, h_{bit} indicates the road pavement thickness

Parameter (unit measure)	Distribution type	Mean	COV (%)
f_{cm} (MPa)	Lognormal	38.5	11.4
f_{ym} (MPa)	Lognormal	451	7.2
$f_{p,01}$ (MPa)	Lognormal	1665	7.5
s (m)	Uniform	0.25	12.0
h_{bit} (m)	Uniform	0.14	24.7
σ_{sp} (MPa)	Uniform	600	11.5

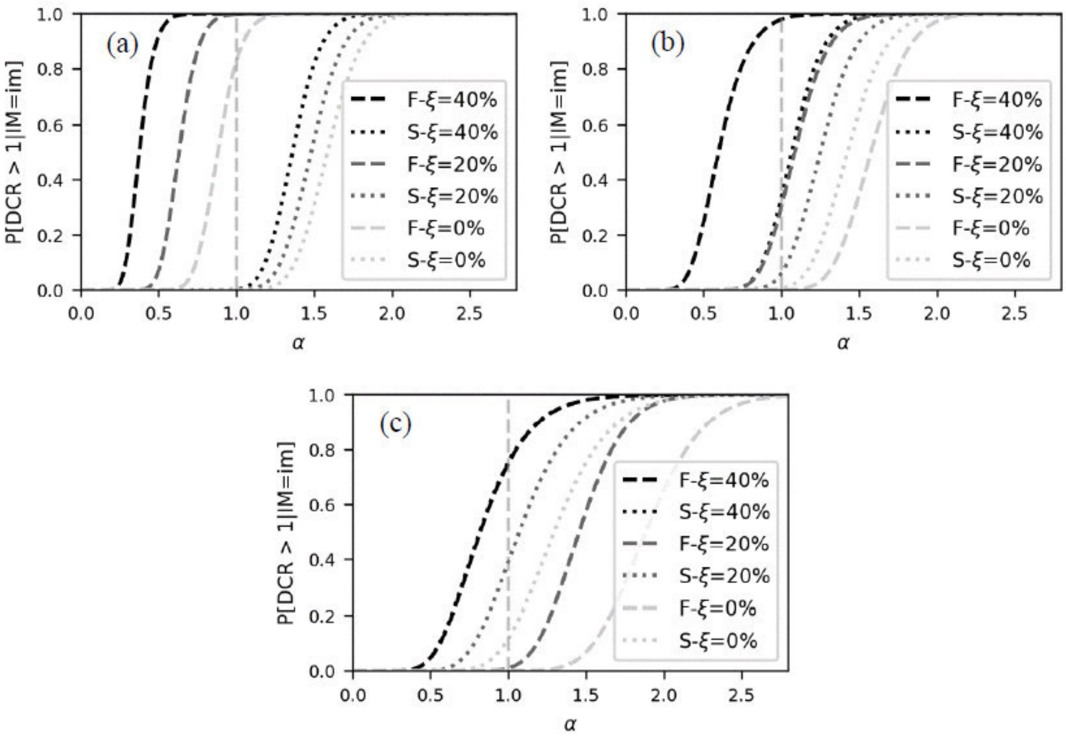

Fig. 5 Fragility curves obtained by combining all independent variables. DCR indicates the demand-capacity ratio, while the IM, indicated as α, is the traffic load amplification factor [24]

The fragility analysis conducted for different flexural and shear failure modes indicates that there is no clear dominant failure type for medium- and long-span bridge typologies. However, for short-span decks, flexural failure emerges as the dominant failure type. As the span length increases, the shear failure type becomes increasingly dominant, primarily due to the modelling approach used for the tendon area. Moreover, in the case of medium- and long-span typologies, it is observed that with an increase of corrosion, flexural failure tends to overshadow shear failure. This is attributed to the calculation algorithm, which considered a decrease in reinforcement for flexural strength, while shear strength is less influenced, mainly contributing to the compression state of the beam cross-section. Generally, the study indicates that variations in terms of geometric and mechanical characteristics have limited influence on the structural response, as fragility curves demonstrate low dispersion in most cases. Conversely, the state of prestressing tendon corrosion plays a crucial role in determining the structural behaviour. Additionally, the study reveals that short-span bridge typologies exhibit greater vulnerability compared to others. However, this conclusion should be further validated through future investigations to ensure its reliability. In the end, when prioritizing bridge inspections and allocating available resources, it is vital to focus on the condition of prestressing tendons, which significantly impacts the response. Further developments will increase the simulated scenarios and will account for other characteristics and aging effects.

5. CONCLUSIONS

The paper presents a summary of the ongoing research works that the authors of this paper are carrying out towards the topic of structural health management of the existing bridge portfolios. First, the paper reports a panoramic of the new approach proposed by the Italian government, focusing on the first three levels of the provided multi-level approach. In particular, critical issues are related to the activities within the levels 0 and 1, which are characterized by the collection of the original documentation and by the onsite inspections. Especially these latter represent an expensive part of the overall

work, which management companies should account for. To support this step, scientific research could provide new means to be made available and that can ease the working activities by exploiting the exponential growth of digital innovation. The paper demonstrates how the use of new and cost-effective techniques could improve the management of existing bridge portfolios, by providing tools developed for purpose of risk priorization. In the paper, three different approaches are provided: (a) the use of artificial intelligence to perform defect detection in existing RC bridges; (b) the use of satellite data to perform a continuous monitoring of bridges and part of them; (c) the use of automated analytical models, to predict probability of failure of bridges under service conditions and accounting for corrosion.
Further activities will be aimed at improving the proposed techniques, orienting them to develop new tools at high technology readiness level.

ACKNOWLEDGEMENT

The first author acknowledges funding by Italian Ministry of University and Research, within the project 'PON-Ricerca e Innovazione-2014–2020, CUP Code (D.M. 10/08/2021, n. 1062): D95F21002140006.

REFERENCES

[1] Ministero delle Infrastrutture e della Mobilità Sostenibili (2022). Decreto ministeriale numero del 01/07/2022: "Linee guida per la classificazione e gestione del rischio, la valutazione della sicurezza ed il monitoraggio dei ponti esistenti". GU Serie Generale n.196 del 23-08-2022 (in Italian)

[2] Xie Y., Ebad Sichani M., Padgett J.E., DesRoches R. (2020). The promise of implementing machine learning in earthquake engineering: a state-of-the-art review, *Earthquake Spectra* 36 (4) 1769–1801. https://doi.org/10.1177/8755293020919419.

[3] Sun H., Burton H.V., Huang H. (2020). Machine learning applications for building structural design and performance assessment: state-of-the-art-review. *Journal of Building Engineering*, 101816. https://doi.org/10.1016/j.jobe.2020.101816.

[4] Ruggieri S., Cardellicchio A., Leggieri V., Uva G. (2021). Machine-learning based vulnerability analysis of existing buildings. *Automation in Construction*, Volume 132, 103936. https://doi.org/10.1016/j.autcon.2021.103936

[5] Cha Y.J., Choi W., Büyüköztürk O. (2017). Deep Learning-Based Crack Damage Detection Using Convolutional Neural Networks. *Computer- Aided Civil and Infrastructure Engineering*, 32:361–78. https://doi.org/10.1111/mice.12263.

[6] Xu Y., Bao Y., Chen J., Zuo W., Li H. (2019). Surface fatigue crack identification in steel box girder of bridges by a deep fusion convolutional neural network based on consumer-grade camera images. *Structural Health Monitoring*. https://doi.org/10.1177/1475921718764873.

[7] Prasanna P., Dana K.J., Gucunski N., Basily B.B., La H.M., Lim R.S. (2016). Automated Crack Detection on Concrete Bridges. IEEE IEEE transactions on automation science and engineering. https://doi.org/10.1109/TASE.2014.2354314.

[8] Cha Y.J., Choi W., Suh G., Mahmoudkhani S., Büyüköztürk O. (2018). Autonomous Structural Visual Inspection Using Region-Based Deep Learning for Detecting Multiple Damage Types. *Computer-Aided Civil and Infrastructure Engineering*, 33:731–47. https://doi.org/10.1111/mice.12334.

[9] Zhu J., Zhang C., Qi H., Lu Z., (2020). Vision-based defects detection for bridges using transfer learning and convolutional neural networks. *Structure and Infrastructure Engineering*, 16(7), 1037-1049. https://doi.org/10.1080/15732479.2019.1680709.

[10] Cardellicchio A., Ruggieri S., Nettis A., Renò V., Uva G. (2023). Physical interpretation of machine learning-based recognition of defects for the risk management of existing bridge

heritage, *Engineering Failure Analysis* 149, 107237. https://doi.org/10.1016/j.engfailanal.2023.107237.

[11] Redmon J., Divvala S., Girshick R., Farhadi A., You Only Look Once: Unified, Real-Time Object Detection, in *2016 IEEE Conference on Computer Vision and Pattern Recognition (CVPR)*, 779–788, IEEE, Las Vegas, NV, USA, June 2016.

[12] Maeda H., Sekimoto Y., Seto T., Kashiyama T., Omata H. (2018). Road damage detection and classification using deep neural networks with smartphone images. *Computer-Aided Civil and Infrastructure Engineering*, 33(12), 1127-1141. https://doi.org/10.1111/mice.12387.

[13] Ruggieri S., Cardellicchio A., Nettis A., Renò V., Uva G. (2023) Using machine learning approaches to perform defect detection of existing bridges, Procedia Structural Integrity 44, 2028–2035. https://doi.org/10.1016/j.prostr.2023.01.259.

[14] Cardellicchio A., Ruggieri S., Nettis A., Mosca N., Uva G., Renò V. (2023) On the use of YOLOv5 for detecting common defects on existing RC bridges. In *SPIE Optical Metrology*, 26 - 29 June 2023, Munich, Germany

[15] IREA-CNR, DPC, ReLUIS (2021) Linee guida per l'utilizzo dei dati interferometrici satellitari ai fini dell'interpretazione del comportamento strutturale delle costruzioni (Version 1 – In Italian).

[16] Peduto D., Elia F., Montuori R. (2017) Probabilistic analysis of settlement-induced damage to bridges in the city of Amsterdam (The Netherlands). *Transportation Geotechnics*, 14, pp. 169-182. https://doi.org/10.1016/j.trgeo.2018.01.002.

[17] Nettis A., Massimi V., Nutricato R., Nitti D.O., Samarelli S., Uva G. (2023). Satellite-based interferometry for monitoring structural deformations of bridge portfolios. *Automation in Construction*, 147, pp. 104707. https://doi.org/10.1016/j.autcon.2022.104707.

[18] Farneti E., Cavalagli N., Costantini M., Trillo F., Minati F., Venanzi I., Ubertini F. (2022) A method for structural monitoring of multispan bridges using satellite InSAR data with uncertainty quantification and its pre-collapse application to the Albiano-Magra Bridge in Italy. *Structural Health Monitoring*, 22, pp. 353-371. https://doi.org/10.1177/147592172210836.

[19] Calò M., Ruggieri S., Nettis A., Uva G. Multi source Interferometry Synthetic Aperture Radar for monitoring existing bridges: a case study. In *Eurostruct- – 2nd conference of the European association on quality control of bridges and structures*, 25 – 29 September 2023, Vienna, Austria.

[20] Bovenga F., Nutricato R., Refice A., Guerriero L., Chiaradia M.T. (2005). SPINUA: A flexible processing chain for ERS / ENVISAT long term interferometry. European Space Agency (Special Publication), pp. 473–478.

[21] Ministero delle Infrastrutture e dei Trasporti (2018). Aggiornamento delle «Norme tecniche per le costruzioni» (In Italian).

[22] Fiorillo G., Ghosn M. (2018). Fragility analysis of bridges due to overweight traffic load', *Structure and Infrastructure Engineering*. vol. 14, no. 5, pp. 619–633. https://doi.org/10.1080/15732479.2017.1380675.

[23] Miluccio G., Losanno D., Parisi F., Cosenza E. (2021). Traffic-load fragility models for prestressed concrete girder decks of existing Italian highway bridges, *Engineering Structures*. vol. 249. https://doi.org/10.1016/j.engstruct.2021.113367.

[24] Nettis A., Nettis A., Ruggieri S., Uva G. Typological fragility assessment of prestressed concrete girder bridges subjected to traffic loads affected by corrosion. In *COMPDYN 2023 9th ECCOMAS Thematic Conference on Computational Methods in Structural Dynamics and Earthquake Engineering*, 12-14 June, Athens, Greece, 2023.

[25] Nettis A., Nettis A., Ruggieri S., Uva G. Fragility analysis of prestressed concrete girder bridges to traffic loads considering tendon corrosion. In *Eurostruct- – 2nd conference of the European association on quality control of bridges and structures*, 25 – 29 September 2023, Vienna, Austria.

[26] Zelaschi C., Monteiro R., Pinho R. (2016). Parametric Characterization of RC Bridges for Seismic Assessment Purposes, *Structures*, vol. 7, pp. 14–24. https://doi.org/10.1016/j.istruc.2016.04.003.

[27] Jacinto L., Pipa M., Neves L.A.C., Santos L.O. (2012) Probabilistic models for mechanical properties of prestressing strands. *Construction and Building Materials*, vol. 36, pp. 84–89. https://doi.org/10.1016/j.conbuildmat.2012.04.121.

[28] Albenga G. (1930) Lezioni di ponti. Torino: U.T.E.T. (In Italian).

[29] CEN (2003) Eurocode 1: Actions on structures - Part 2: Traffic loads on bridges', vol. EN 1991-2. Brussels, Belgium.

[30] Yu Q.Q., Gu X.L., Zeng Y. H., Zhang W.P. (2022). Flexural behavior of Corrosion-Damaged prestressed concrete beams. *Engineering Structures*. vol. 272. https://doi.org/10.1016/j.engstruct.2022.114985.

[31] Baker J.W. (2015). Efficient analytical fragility function fitting using dynamic structural analysis, *Earthquake Spectra*. vol. 31, no. 1, pp. 579–599. https://doi.org/10.1193/021113EQS025M.

DIGITAL CONCRETE: FROM TECHNOLOGIES TO MATERIALS

Luka Zevnik[1]

Summary:

The construction industry is experiencing a profound shift towards digitalization, driven by automation and reduction of environmental impact. "Digital concrete" emerges as a key concept, involving innovative concrete formulations infused with mineral and chemical additives to achieve unique properties. At the forefront of this transformation is 3D concrete printing (3DCP), a versatile technology implemented using various systems, including 3-axis gantry and robotic arms, offering design flexibility. Effective material flow control, especially in dry-mix concrete systems, is essential. Two common 3DCP systems, 1K and 2K, depend on different composition and binder-accelerator reactions to achieve successful printing. Monitoring early-stage rheology and strength gain is crucial for 3DCP, and ultrasonic methods offer reliable assessment shortly after extrusion. Overall, digitalization and 3DCP hold immense potential to enhance construction efficiency, reduce environmental footprints, and drive innovation in the concrete industry.

Key words: 3dcp, digital concrete, concrete formulation, ultrasonic measurement

[1] Dr., Zevnik Lab, Kranj, Slovenija, luka@zevniklab.com

CIVIL ENGINEERING

EXPERIMENTAL RESPONSES OF COMPRESSED I-SECTION SHORT COLUMNS WITH WEB OPENINGS

Maja Ranisavljević[1], Jelena Dobrić[2]

Summary:

This paper reports the experimental study on compressed I-section short columns with web openings aimed at providing insight on the specific mechanical behaviour underlying the local buckling of the web panel around the opening. The I-section elements with web openings possess a minute flexural stiffness caused by lack of web contribution to the cross-section deformation capacity. In the case of compresses columns, this structural feature implies the high combined stresses around openings caused by compression force, global bending moment and shear force developed during buckling, and local bending moments due to Vierendeel action. The four stub column tests on IPE300-sections with widely spaced (isolated) and closely spaced circular and square web openings (S275 steel grade) was performed to determine their susceptibility to local buckling. The generated experimental data allowed the quantitative assessment of design procedure stated in draft version of new European code prEN 1993-1-13, revealing its good accuracy.

Key words: web openings, compression, local buckling, Vierendeel action

[1] Associate, Faculty of Civil Engineering, University of Belgrade, Serbia, maja@imk.grf.bg.ac.rs
[2] Assoc. prof., Faculty of Civil Engineering, University of Belgrade, Serbia, jelena@imk.grf.bg.ac.rs

1. INTRODUCTION

Hot-rolled or welded steel beams with web openings combine function with flexibility. As alternative to trusses, these beams are lightweight and long-span structural elements that enable the passing of mechanical, electrical and plumbing pipes and ducts through the web openings reducing the floors depth and leading to an optimal use of space and steel material. They can be used in composite and non-composite structures, as simply supported members, cantilever elements or as part of moment or portal frames. The shape of the web openings depends on the purpose of the opening (the size of the installation route). Openings of regular shapes, such as circular, rectangular, hexagonal and sinusoidal are usually chosen.
Steel structural elements with web openings usually fabricated by flame cutting of hot-rolled profiles, following a specified path made in the web at the initial stage of the production process. After cutting, the two resulting Tee sections are reassembly (shear aligned) and then welded together (see Fig.1). The final element typically has a 40 to 50% higher cross-sectional height with a significant increase in flexural stiffness compared to the parent hot-rolled profile, all without increasing weight.

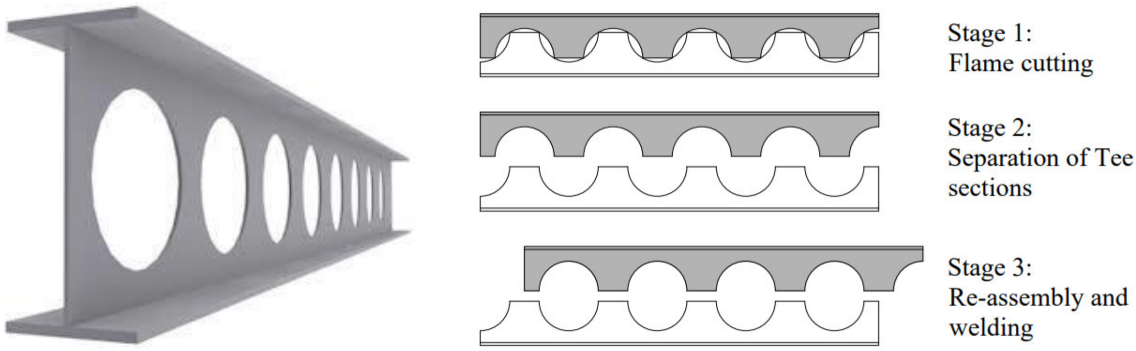

(a)final product [1] *(b) fabrication process*

Fig. 1 Fabrication process of steel beams with web openings

The web opening decreases both global and cross-section flexural stiffness of the beam resulting in larger deformations than the equivalent beam with solid webs. The failure modes are usually governed by the local yielding and plastic deformations of critical cross-section including opening. These structural features are caused by Vierendeel mechanism due to the local bending of web posts induced by the shear transfer around the openings. In the case of rectangular and hexagonal openings, the critical cross-section is located at the opening corners, considering that the Tee sections are uniform in upper- and lower-member's height along the opening length. However, for openings with perimeter variation along their length, the position of the critical cross-section is not straightforward and needs to be defined using a specific mathematical and numerical approach.
Nowadays, numerous experimentally-, numerically- and analytically-based scientific research have been performed to evaluate the structural responses and ultimate capacity of the beams with web openings [2-7].
The draft version of the new European code prEN1993-1-13 [8] gives supplementary design provisions and rules that extend the application of EN1993-1-1 [9] and EN1993-1-5 [10] to the design of rolled and welded steel I- or H-sections with various shapes of web openings. This pr-code accounts for the effect of the openings on the global behaviour of the beam, including lateral torsional buckling and covers the corresponding resistance verifications at the openings.
This paper presents an experimental investigation of short length IPE-section columns with circular and square web openings (also known as perforated webs), designed to

experience at cross-section local and/or distortional buckling modes. The axial load-strain curve relationships were obtained by measuring the longitudinal and transverse strains at characteristic locations along the openings, and at the column ends. The failure modes can be linked to the Vierendeel mechanism due to the plastic local bending of flanges and/or web around the openings.

2. EXPERIMENTS

2.1. TEST DESIGN AND PREPARATION

The test matrix includes commercially available IPE300-sections made from conventional carbon steel with a nominal yield stress of 275 MPa. The tests were carried out on 4 specimens, each 600 mm length. The webs of specimens were perforated by circular and square openings, according to the following description:

- Specimen 1 – one circular opening with radius equal to 200 mm positioned in the specimen centre designed as "ICO1x200", to account for influence of widely spaced openings;
- Specimen 2 – one square opening with dimension equal to 200 mm positioned in the centre designed as "ISO1x200", to account for influence of widely spaced openings;
- Specimen 3 – two equidistant circular openings with radius equal to 120 mm named as "ICO2x120", to account for influence of closely spaced openings;
- Specimen 4 – two equidistant square openings with dimension equal to 120 mm named as "ISO2x120", to account for influence of closely spaced openings.

Webs of all specimens are unstiffened around the openings. The nominal length of 600 mm is chosen so that global buckling failure mode does not occur. The dimensions of the openings and the distance between them fulfill the geometric range of validity in accordance with prEN 1993-1-13 (see Table 1).

Tab. 1 Limiting dimensions for unstiffened openings; symbol designations are given in [8]

Shape of opening	Maximum opening height, h_o	Maximum opening length, a_o	Minimum edge to edge spacing, s_o	Minimum depth of Tee in compression, d_t
Circular	0,8h	-	0,1h_o	max ($t_f + r$ + 10 mm; t_f + 30 mm)
Rectangular	0,75h	2,5h_o	max (0,5a_o; h_o)	max (a_o/12; 0,1h)

The dimensions of the square openings were chosen as the maximum possible for the corresponding specimen length and the used number of openings. The dimensions and position of the circular openings were chosen so that they stand for the equivalent of square openings, and for the sake of sensitivity and a comparative study of the influence of the opening shape on the cross-section stress and deformation capacity. Position of the openings, as well as their dimensions, are shown in Figure 2.

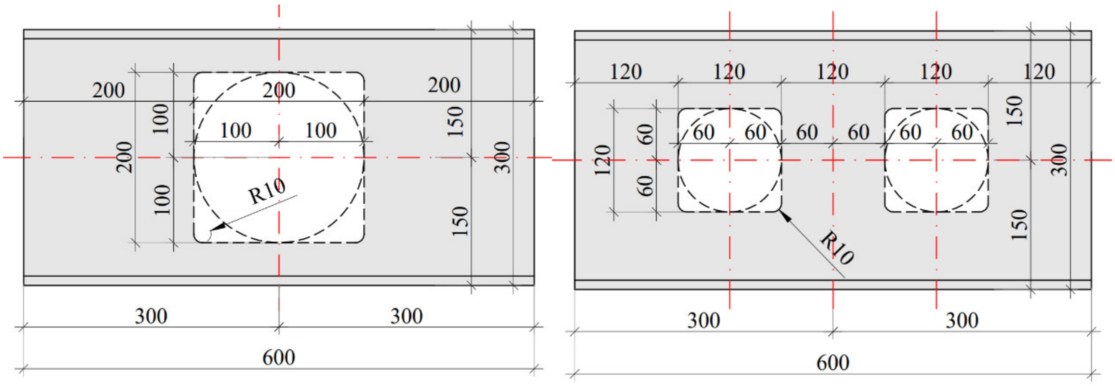

Fig. 2 Dimensions and positions of the openings at the specimens' webs

2.2. TEST SET-UP

The compressive load was applied using a strain-controlled Amsler hydraulic testing machine, with a capacity of 2500 kN. The parallel end plates were fixed against rotations and twist about any axis in order to achieve fixed boundary conditions.
End shortening of the stub columns was monitored by linear variable displacement transducers (LVDT) positioned at four points and placed on the upper plate of the testing machine. The stress-strain distribution fields in the specimen web, around openings, were measured using electrical strain gauges (SG). The test setup of stub column specimens with the position of the measuring equipment is shown in Fig. 3 and Fig. 4. A load cell was used to record the applied load. All experimental results: load, displacements and strains were recorded in one-second intervals on the data acquisition device.

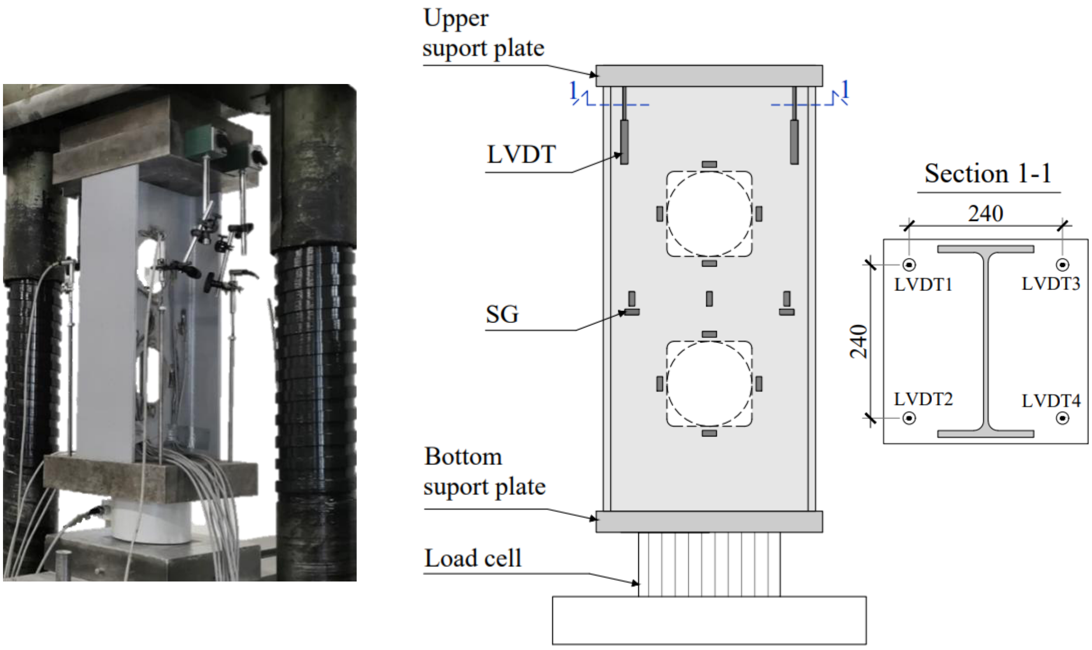

Fig. 3 Test set-up on the example of specimens with two openings

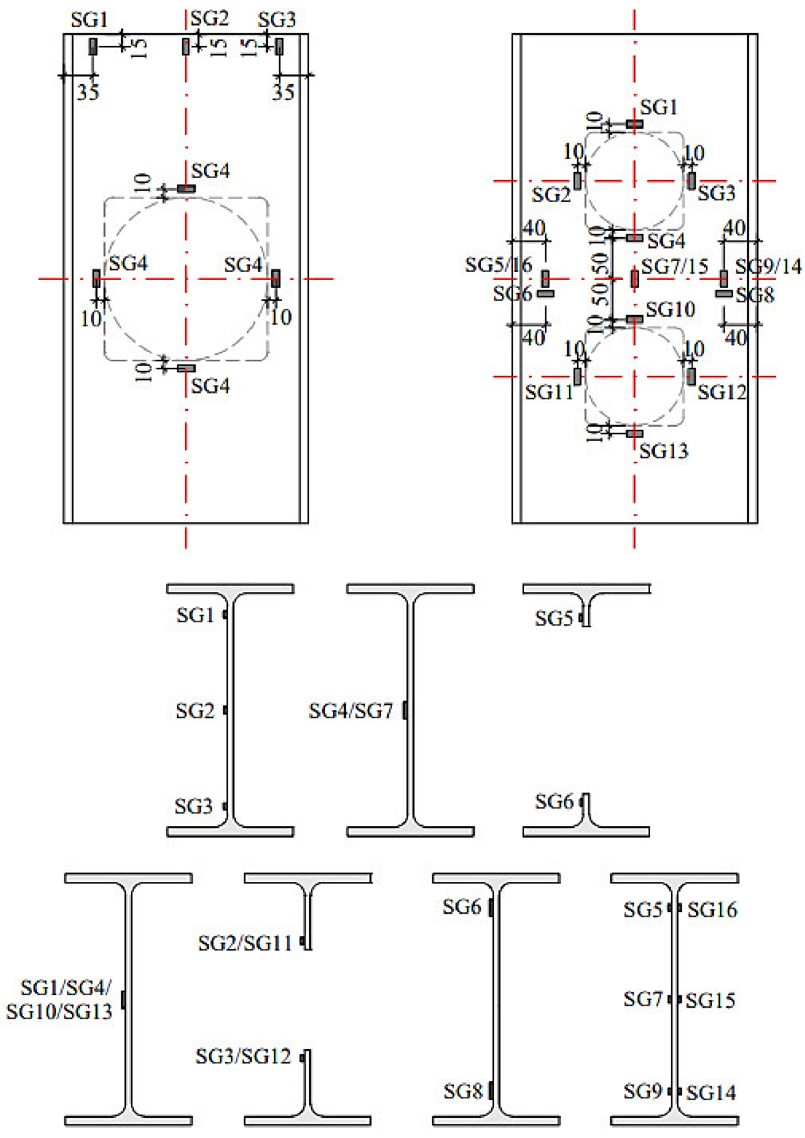

Fig. 4 Position of strain gauges

2.3. TEST RESULTS

The failure behaviours of the test specimens are shown in Fig. 5. All columns experienced local buckling occurred at the interface between the elastic and plastic stress regions. Local buckling of specimens with one opening was localised in the middle part of their height and characterised by the symmetric, one wave-shape deformations of the cross-section flanges in the opening area. The section web almost completely remained straight and angles between web and flanges did not change (see Fig.5a and Fig.5b). Local buckling of specimens with two closely spaced openings was also localised in the middle part of their height, however it was featured by the more wave-shape deformations of the cross-section flanges along the column length. The longitudinal deformation distributions at the ends of the same flange are of opposite signs, the convex deformation at one flange end corresponds to the concave deformation at the other flange end. The inflection planes are observed in the mid-length of both openings (see Fig.5c and Fig.5d).

(a)ICO1x200

(b)ISO1x200

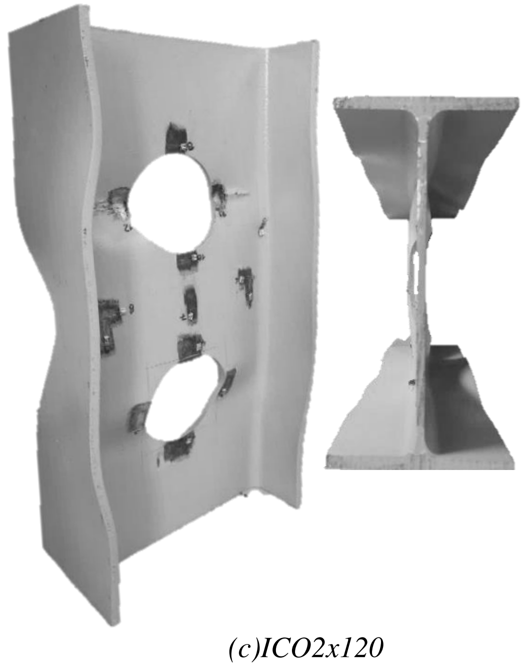

(c)ICO2x120

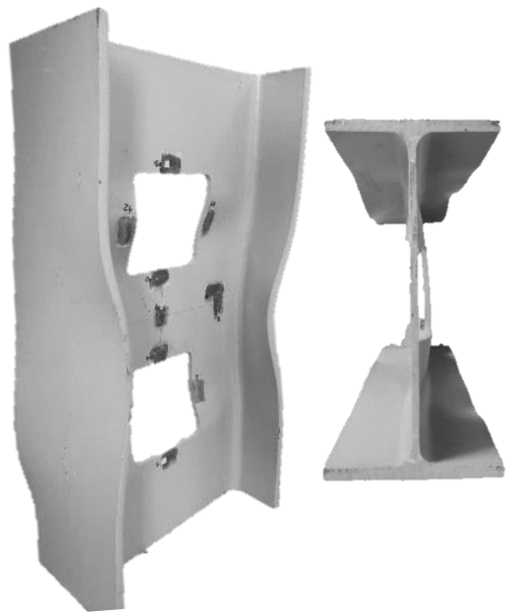

(d)ISO2x120

Fig. 5 Post-buckling deformed shape of specimens with web openings

The key experimental results for specimens ICO1x200 and ICO2x120 are summarized in Table 2, in which $N_{c,u}$ is the ultimate failure load, σ_b is the ultimate buckling stress reached at the web post, σ_{bo} is the ultimate buckling stress reached at the opening, both calculated by dividing the corresponding ultimate load $N_{c,u}$ and measured bruto or neto (account for opening) cross-section area, respectively. It can be seen from Table 2 that the failure mode of the specimens is governed by elastic-plastic local buckling; the predicted (design) stress values around openings σ_{bo} are higher, whereas the predicted stress values at the web post σ_b are lower than the measured yield strength f_y = 328 MPa, respectively. It was also found that the ultimate resistances of specimens with circular openings are higher than those measured for the corresponding specimens with square openings. Thus, the ultimate resistances and deformation capacity of the tested specimens significantly depends on the shape, size and number of web openings (that is, distance between openings).

Tab. 2 Summary of stub column test results under pure compression

Specimen	$N_{c,u}$ [kN]	σ_b [MPa]	σ_{bo} [MPa]
ICO1x200	1327,7	256,6	346,6
ICO2x120	1474,2	284,9	337,5

The axial load-longitudinal strain curves for specimens ICO1x200 and ICO2x120 are shown below in Fig. 6 and 7. The results are presented for each strain gauge separately, without their averaging, in order to more easily notice the differences in the structural behaviour of the specimens at web post and at the opening. It can be seen from Fig. 6 and 7 that the measured axial strains around openings are higher than the strains at the web post, indicating the shear transfer around the openings.

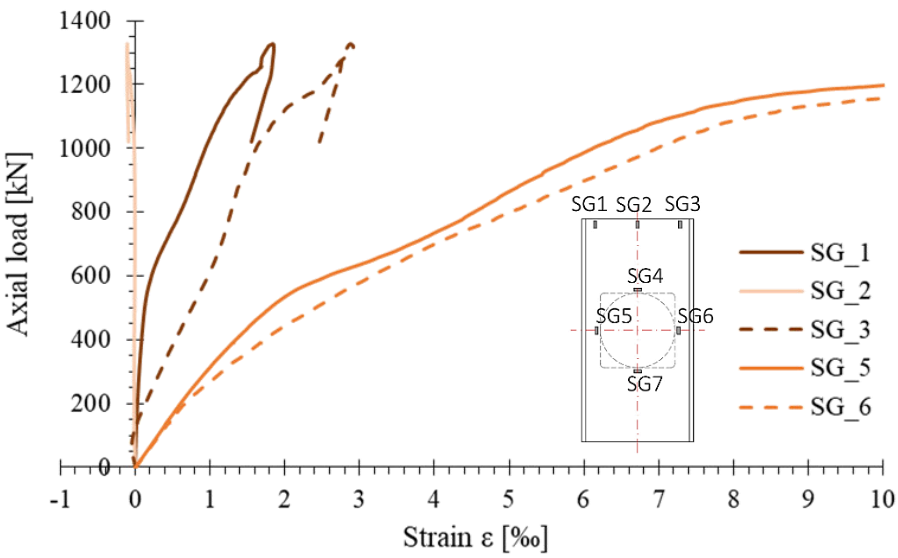

Fig. 6 Axial load-longitudinal strain curve for ICO1x200

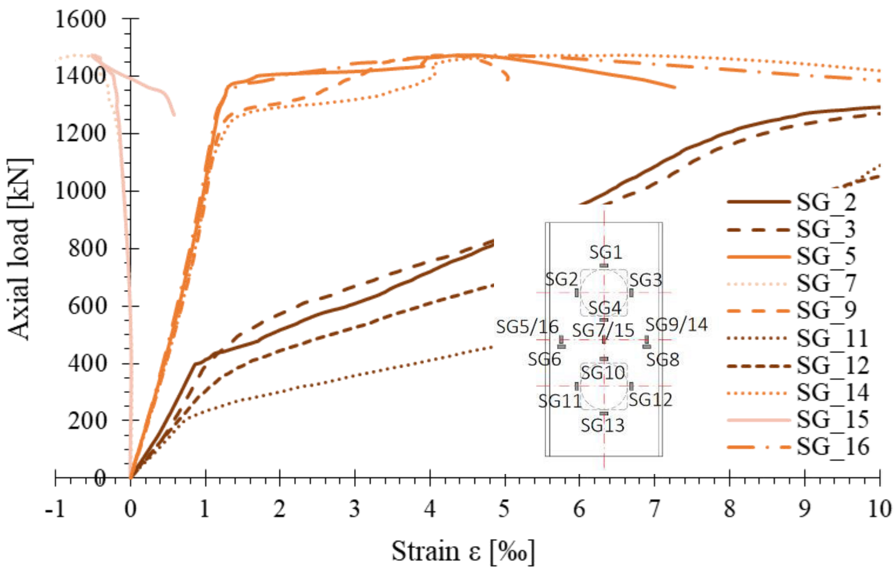

Fig. 7 Axial load-longitudinal strain curve for ICO2x120

3. EVALUATION OF prEN 1993-1-13 PREDICTIVE MODELS FOR CROSS-SECTION CLASIFIACTION

Based on the experimental results, an accuracy assessment of the cross-section deformation capacity, according to prEN 1993-1-13 was performed.

In accordance with prEN 1993-1-13, local buckling is accounted using the concept of cross-section classification and effective width based on an elastic-plastic material model, such as in the current code in use EN 1993-1-1. The cross-section class is determined by the classification of all cross-section elements, comparing their individual slenderness (width-to-thickness ratio) with the limit values prescribed in the code. In the case of perforated webs, cross-section should be classified at each web opening and web post. At the opening, both flanges and web are classified as outstand elements. The cross-section resistance is defined as buckling resistance of the compressed Tee sections, considering bending moments due to Vierendeel bending effects and axial force.

Fig. 8 shows a comparison of the slenderness of the outstand and internal parts of the cross-section with the limit values for classes 1 (green line), 2 (orange line) and 3 (red line) at pure compression (according to prEN 1993-1-13). The ultimate force obtained by tests is normalized by a value that represents the product of corresponding cross-section area and the measured yield strength. Diagrams are given separately for the cross-section at the opening and the cross-section outside the opening, for outstand (flanges) and internal (web) parts of the cross-section.

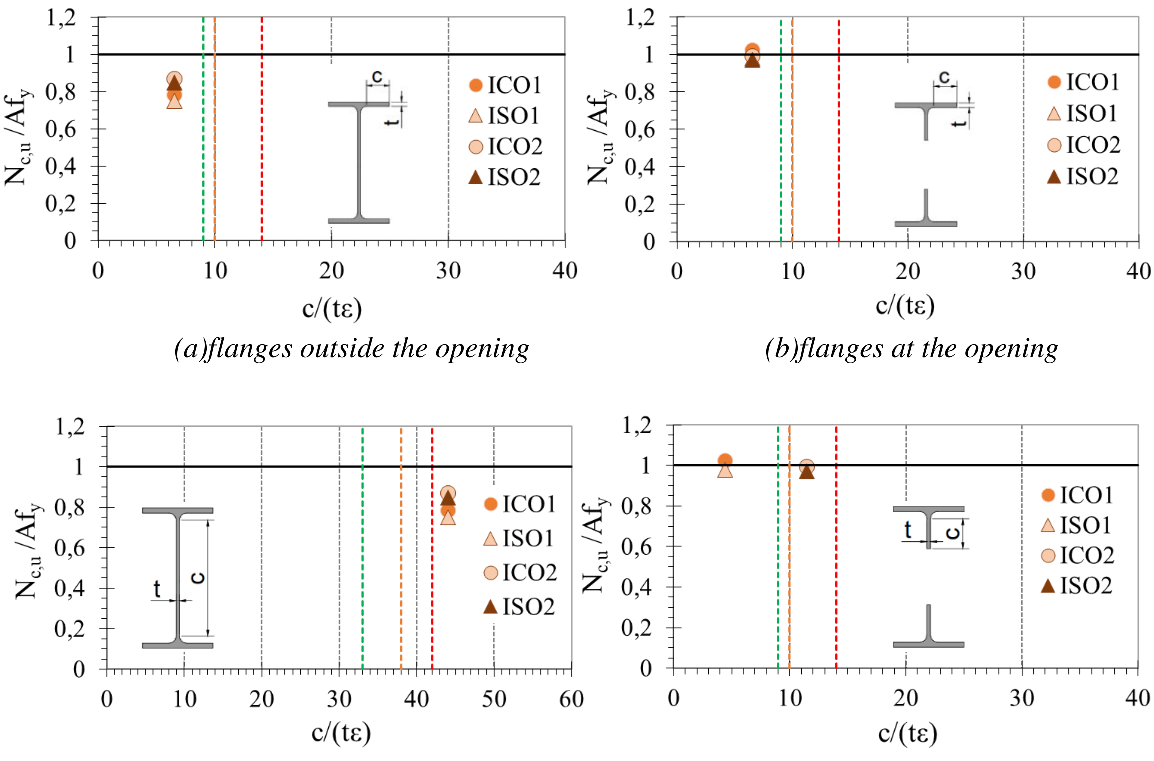

(a)flanges outside the opening *(b)flanges at the opening*

(c) web outside the opening *(d) web at the opening*

Fig. 8 Limit slenderness for pure pressure according to prEN 1993-1-13

It can be seen from Fig.8a and Fig.8b that the data points for flanges (outstand compressed element) are on left, safely side regarding to Class 1 slenderness limit. Similarly, Fig.8c shows that the Class 4 slenderness limit for web section (internal compressed element), outside the openings, corresponds to the experimental data points. However, considering the cross-section with web openings (Tee section web as outstand compressed element), the experimental data points for the specimens with one opening are on left, safely side regarding to Class 1 slenderness limit, while the experimental

data for the specimens with two openings lie between the Class 2 slenderness limit and the Class 3 slenderness limit for outstand compressed elements (see Fig.8d). Thus, related to analysed specimens, prEN 1993-1-13 provides a considerably precise prediction of the cross-section deformation capacity and classification under pure compression load.
Finite element models will be calibrated and validated against the presented tests and used to perform a parametric assessment of the ultimate capacity of short length columns with web openings, considering the column length, cross-section dimension, opening shape and distances between openings, see Fig. 9. The experimental and numerical data related to failure loads (ultimate resistances) will be compared with resistance predictions obtained using the codified design methods in prEN 1993-1-13.

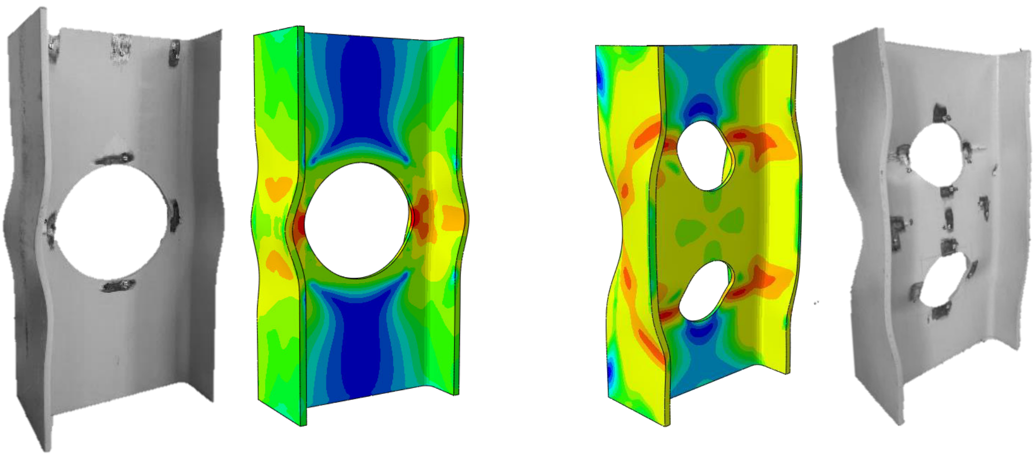

Fig. 9 Failure mode of FE models with circular web openings

4. CONCLUSIONS

An experimental investigation consisting of four IPE300-section columns with low slenderness was carried out under pure compression. The overall aim of the experiments was to investigate cross-section buckling modes and corresponding capacities and quantify the influence of shape and dimensions of the openings and their distances on the ultimate structural responses.
The failure mode of the tested specimens was local buckling triggered by the weakening of the section web by the openings and the consequent reduction of its flexural stiffness. The structural behaviour of specimens strongly depends on cross-section slenderness, opening shape and distance between openings.

ACKNOWLEDGEMENT

The authors are grateful to associate professor Milan Spremić, assistant professor Aljoša Filipović Faculty of Civil Engineering University of Belgrade, and the company EXING B&P Novi Sad for their support.

REFERENCES

[1] http://www.optimalbeams.com/index_undercons.html (september 2023)

[2] D. Kerdal, D.A. Nethercot, Failure modes for castellated beams, Journal of Constructional Steel Research 4 (1984) 295–315, https://doi.org/10.1016/0143-974X(84)90004-X.

[3] D.A.K.D. Nethercot, Lateral-torsional buckling of castellated beams, Journal of Structural Engineering (1982) 53–61.

[4] E. Ellobody, Interaction of buckling modes in castellated steel beams, Journal of Constructional Steel Research (2011) 814–825, https://doi.org/10.1016/j.jcsr.2010.12.012.

[5] E. Ellobody, Nonlinear analysis of cellular steel beams under combined buckling modes, Thin-Walled Structures 52 (2012) 66–79, https://doi.org/10.1016/j.tws.2011.12.009.

[6] F.P.V. Ferreira, A. Rossi, C.H. Martins, Lateral-torsional buckling of cellular beams according to the possible updating of EC3, Journal of Constructional Steel Research 153 (2019) 222–242, https://doi.org/10.1016/j.jcsr.2018.10.011.

[7] A.S. Carvalho, C. H. Martins, A. Rossi, V. M. Oliveira, S. G. Morkhade, Moment gradient factor for steel I-beams with sinusoidal web openings, Journal of Constructional Steel Research 202 (2023) 107775.

[8] Eurocode 3 – Design of steel structures – part 1-13, Rules for beams with large web openings prEN 1993-1-13, Brussels, Belgium, CEN, 2020.

[9] Eurocode 3 – Design of steel structures – part 1-1, General rules and rules for buildings EN 1993-1-1, Brussels, Belgium, CEN, 2006.

[10] Eurocode 3 – Design of steel structures – part 1-5, Plated structural elements EN 1993-1-5, Brussels, Belgium, CEN, 2006.

ASSESSMENT OF CONCRETE STRUCTURES USING GROUND PENETRATING RADAR (GPR): MAIN FINDINGS OF THE ASAP PROJECT

Ksenija Tešić[1], Ana Baričević[2], Marijana Serdar[3]

Summary:

To address safety concerns related to the ageing of reinforced concrete (RC), a proactive and timely inspection should be performed. However, such inspections are often overlooked due to their duration, high costs, and extensive scope. Ground penetrating radar (GPR) emerges as a non-destructive technique that can be used for diverse applications, including determination of the location of reinforcement, thickness of concrete cover, geometry of structural elements, and corrosion status. These investigations are carried out within the four-year project "Autonomous System for Assessment and Prediction of Infrastructure Integrity" - ASAP - coordinated by the Faculty of Civil Engineering, University of Zagreb. This paper aims to introduce the main results of the project ASAP on the condition assessment of concrete structures using GPR. By leveraging GPR technology, the project aims to revolutionize the inspection process, making it more efficient, cost-effective, and comprehensive.

Key words: condition assessment, reinforced concrete, GPR, corrosion.

[1] Assistant, University of Zagreb Faculty of Civil Engineering, Zagreb, Croatia, ksenija.tesic@grad.unizg.hr
[2] Assoc. prof., University of Zagreb Faculty of Civil Engineering, Zagreb, Croatia, ana.baricevic@grad.unizg.hr
[3] Assoc. prof., University of Zagreb Faculty of Civil Engineering, Zagreb, Croatia, marijana.serdar@grad.unizg.hr

1. INTRODUCTION

Autonomous System for Assessment and Prediction of Infrastructure Integrity, abbreviated ASAP, is a project directed by the Faculty of Civil Engineering in cooperation with the Faculty of Electrical Engineering and Computing and the Faculty of Mechanical Engineering and Naval Architecture at the University of Zagreb [1]. The four-year project is co-financed by the European Union from the European Regional Development Fund. The main goal of the project is to develop an autonomous system, a wall-climbing robot [2] and an unmanned aerial vehicle [3] equipped with sensors for the inspection of reinforced concrete (RC) structures.
Part of the project team at ASAP focused on developing reliable methods for inspecting structures using the ground penetrating radar (GPR) integrated into the robot. In particular, the aim was to investigate the accuracy of the GPR in detecting reinforcement and determining concrete cover thickness, as well as the ability of the GPR to detect corrosion of reinforcement. This paper presents the main results of the studies conducted both in the laboratory and in the field. The paper is divided into two sections, the first relating to the advantages and the second to the limitations and disadvantages of GPR in the inspection of RC structures.

2. ASSESSMENT OF RC STRUCTURES USING GPR

Ground penetrating radar is a non-destructive testing method based on the emission of electromagnetic (EM) waves in the radio wave range of spectrum [4]. The GPR device is dragged over the surface of the concrete being tested, Figure 1, and it triggers the emission of EM waves into the material. The waves are reflected back to the device by the objects or layers in the material. From the properties of the reflected waves, the sign, amplitude and travel time, information about the object, such as position, size, depth, or state of corrosion, can be obtained.
The following sections present the advantages and disadvantages of GPR in the inspection of structures, i.e., the areas where the signal can be unambiguously interpreted and those where this is not possible.

Fig. 1 The inspection of reinforced concrete wall with GPR.

2.1. ADVANTAGES OF METHOD

One of the main activities of the GPR is the detection of reinforcement in reinforced concrete structures. This is partly due to the fact that metallic objects (due to their dielectric properties) are best detected with the GPR. The penetration of electromagnetic radiation depends primarily on its position in EM spectrum, i.e., its frequency, and secondarily on the material properties. Figure 2 shows the detection of stirrups in a reinforced concrete column and the first reinforcement layer in a reinforced concrete slab. The hyperbolic reflection corresponds to the reinforcement in the radargram.

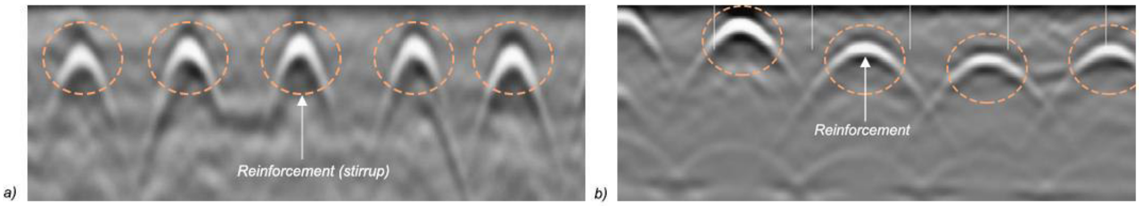

Fig. 2 The radargram of a row of a) stirrups and b) longitudinal reinforcement.

Figure 2 shows two cases where the reinforcement in a concrete element was easily detected. The radargrams were recorded perpendicular to the reinforcement under investigation. One of the most important findings is therefore that the first layer of reinforcement can be detected without doubt in the first 20 cm of the concrete if there is no other object between the surface and the reinforcement that could prevent the signal from penetrating.

The accuracy of the GPR in determining the concrete cover thickness depends on the input parameters used to calibrate the depth scale. Namely, the depth of objects is calculated based on the wave travel time measured with the GPR and the velocity of wave. The velocity of wave in turn, depends on the condition of the concrete. It can be estimated based on typical values of the dielectric constant from the literature [5], by calibration with an object of known depth [6], or by analysing the properties of hyperbolic reflections [7]. The first method is the least reliable. The latter method, on the other hand, is very demanding and requires knowledge of electromagnetism. Estimating the depth based on calibration with the known depth of the object is suitable if the condition of the concrete is quite similar along the area under investigation. If the condition varies in the investigated area, the velocity also varies, and several calibration procedures are required.

Tab. 1 The results on determining the concrete cover thickness using GPR.

No.	Real depth, x_R [mm]	GPR-measured depth, x_{GPR} [mm]	Δx [%]
1	65	64	2
2	69	70	-1
3	67	68	-1
4	66	65	2
5	65	65	0
6	69	67	3
7	66	66	0
8	66	67	-2
9	64	65	-2
10	69	71	-3

Table 1 shows the results of the determination of the concrete cover thickness with GPR. The investigations were carried out on a slab produced in the laboratory, with the reinforcement left 5 cm outside the concrete surface so that the concrete cover could be measured with a calliper. The velocity and hence the dielectric constant were calculated based on the signal travel time and the one known depth. It is assumed that the measured velocity is the same in the whole investigated area, as the slab did not show

any changes in condition. The results showed that the largest deviation from the actual thickness of the concrete cover was 3%, i.e., 2 mm difference. The mean difference between actual and measured thickness was 0%.
In [8], it was shown that the GPR was more effective in determining the concrete cover thickness compared to the cover meter at a depth of more than 8 cm. It was also able to detect the second reinforcement layer with greater accuracy than the cover meter.
One of the advantages of the GPR is also that it provides a graphical output, called a B-scan, so that other information, such as the geometry of the thickness of the structural element, can be obtained at the same time as determining the position of the reinforcement and the concrete cover thickness. Figure 3 shows the radargram in which the thickness of the column could be determined in the same radargram in which the position of the reinforcement was determined.

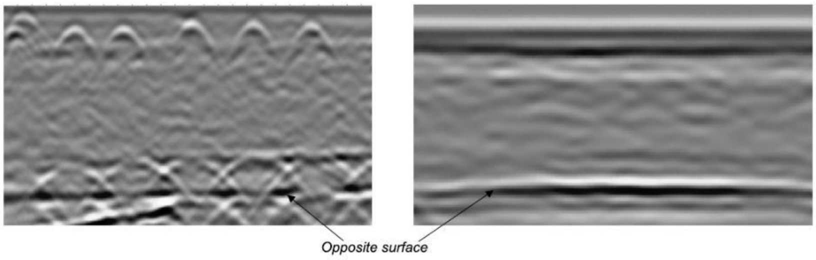

Fig. 3 Determination of thickness of concrete element from radargram.

In the [8], the detailed analysis of radargrams where the geometry of the mezzanine slab were reconstructed from the acquired radargrams.
One of the main advantages of GPR is the speed of inspection [9], especially the speed of data acquisition and analysis. The analysis varies depending on the structural element and type; however, the GPR has proven to be a great opportunity for automation [10,11].

2.2. LIMITATIONS AND DRAWBACKS

As already mentioned, the penetration depth of the wave depends on the centre frequency of the antenna and the properties of the material. For comparison, the penetration depth of the signal for the device with a centre frequency of 1 GHz is 1.5 m, while it is 0.5 m for 2 GHz [12]. In the investigations presented here, the GPR device with 2.7 GHz was used. Although the penetration depth is 0.6 m according to the manufacturer's specifications [13], the limitations in reinforcement detection are discussed in the following text.
The first limitation relates to the penetration depth in a disturbed concrete environment, especially concrete with high moisture and chlorides in the concrete pores. Figure 4 shows a) the concrete 4 months after casting, without chlorides, under laboratory conditions, and b) the same concrete but saturated and with a chloride concentration of 1.7% of the cement mass at the depth of the reinforcement. The concrete cover thickness was 5 cm.
The colours in the radargram indicate the signal strength. The higher the contrast between the hyperbolic reflection (white) and the surrounding space (grey), the stronger the signal reflected from the reinforcement. It can be seen that for the same concrete element, the signal is lost much more in chloride-contaminated concrete. Thus, one of the limitations of the GPR signal is penetration into concrete containing larger amounts of chlorides [14], moisture [15], and corrosion products [16]. Therefore, one of the findings is that the penetration depth of 0.6 m at 2.7 GHz is questionable for corrosive concrete environments.

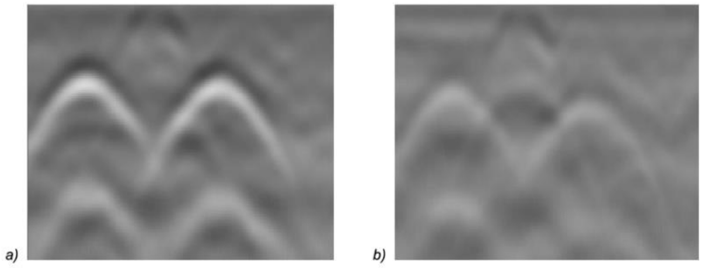

Fig. 4 Determination of thickness of concrete element from radargram.

The second limitation is the detection of reinforcement at depths close to the penetration depth (60 cm) when many reflections have occurred before the signal has penetrated to the reinforcement. Figure 5 shows the case of a ribbed floor structure where the reinforcement was detected near the bottom of the rib.

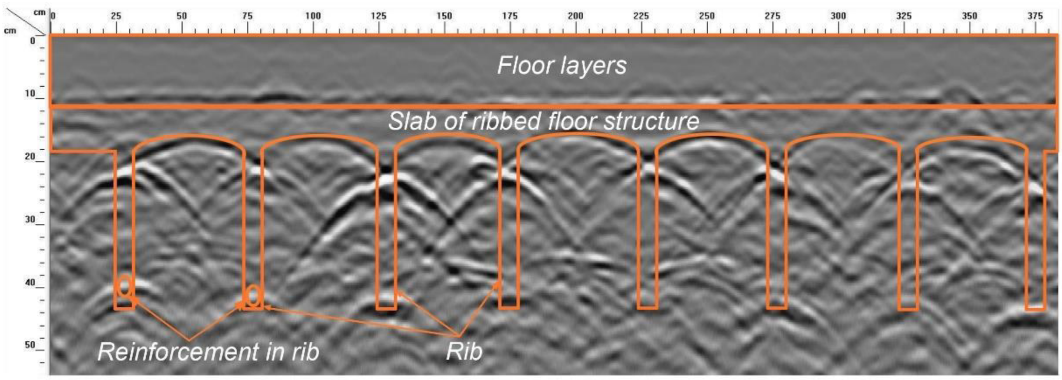

Fig. 5 Detection of reinforcement at depth near penetration depth [8].

Despite the additional signal processing applied to improve the interpretation of the radargram, the hyperbolic signs corresponding to rib reinforcement could easily be misinterpreted due to their low strength.

One of the limitations of inspecting structural elements with GPR could be the case when they have a wire lath in the final treatment. This is because if the wires of the lath are densely arranged, it behaves like a metal plate and prevents the signal from penetrating [8].

Inspection of GPR becomes a challenge when examining an element with small dimensions, such as the width of a beam, to determine the position of the longitudinal reinforcement. Although the dimensions of handheld GPR devices for inspecting concrete structures are relatively small (e.g., the GSSI Structure ScanMini XT is 23.6 x 18.4 x 15.7 cm [13]), element dimensions that are in the order of the dimensions of the GPR are cumbersome to inspect. This is because the GPR device emits EM waves when it spins the wheels of the device, so it requires an area larger than the device to detect the object in the material.

3. CONCLUSIONS

The conclusions of this work are summarised in Table 2.

Tab. 2 The advantages and limitations of GPR in the inspection of reinforced concrete structures.

Advantage
Detection of the first reinforcement in the first 20 cm of the concrete if there is no other object between the surface and the reinforcement that could prevent the penetration of the signal
Determination of the concrete cover thickness based on the calibration of the depth scale using the known object depth
Simultaneous determination of the element thickness and geometry from the radargram with the localisation of the reinforcement
Speed of data acquisition and data analysis
Possibility to automate the process of analysis and interpretation of results

Limitation
Penetration of the signal in concrete with a high concentration of chloride, moisture, and corrosion products
Analysis of the signal when the radargram contains a high number of reflections
The inspection of elements with small dimensions, e.g., the width of the beam

ACKNOWLEDGEMENT (STYLE: ZAHVALNOST)

This research was funded by the European Union through the European Regional Development Fund's Competitiveness and Cohesion Operational Program, grant number KK.01.1.1.04.0041, project "Autonomous System for Assessment and Prediction of infrastructure integrity (ASAP)".

REFERENCES

[1] Serdar M., Damjanović D., Švaco M., Jerbić B., Orsag M., Kovačić Z. (2021). Development of an autonomous system for assessment and prediction of structural integrity. *Gradjevinar*, Volume 73, pp. 1173–1184. https://doi.org/10.14256/JCE.3390.2021.

[2] Božić M., Ćaran B., Švaco M., Jerbić B., Serdar M. (2022). Mobile Wall-Climbing Robot for NDT inspection of vertical concrete structures, *NDT-CE 2022 - The International Symposium on Nondestructive Testing in Civil Engineering*, Zurich, Switzerland, 16-18 August. https://doi.org/10.58286/27295.

[3] Goricanec J., Ereiz S., Orsag M., Duvnjak I. (2023). Identification of the dynamic parameters of bridge elements using unmanned aerial vehicle, *Journal of Sound Vibration*, Volume 566. https://doi.org/10.1016/j.jsv.2023.117901.

[4] Daniels D.J. (2024). *Ground Penetrating Radar*, second ed., The Institution of Electrical Engineers, London, 2004.

[5] Cassidy N.J. (2009). Electrical and Magnetic Properties of Rocks, Soils and Fluids, in: H.M. Jol (Ed.), Ground Penetrating Radar Theory and Application, Elsevier, Amsterdam, pp. 41–72. https://doi.org/10.1016/B978-0-444-53348-7.00002-8.

[6] Clem D.J., Schumacher T., Deshon J.P. (2015). A consistent approach for processing and interpretation of data from concrete bridge members collected with a hand-held GPR device, *Construction and Building Materials*. Volume 86. pp. 140–148. https://doi.org/10.1016/j.conbuildmat.2015.03.105.

[7] Ma X., Liu H., Wang M.L., Birken R. (2018). Automatic detection of steel rebar in bridge decks from ground penetrating radar data, *Journal of Applied Geophysics*. Volume 158. pp. 93–102. https://doi.org/10.1016/j.jappgeo.2018.07.010.

[8] Tešić K., Baričević A., Serdar M. (2021). Comparison of cover meter and ground penetrating radar performance in structural health assessment: case studies, *Građevinar*. Volume 73. pp. 1131-1144. https://doi.org/10.14256/JCE.3323.2021.

[9] Omar T., Nehdi M.L., Zayed T. (2017). Performance of NDT Techniques in Appraising Condition of Reinforced Concrete Bridge Decks, *Journal of Performance of Constructed Facilities*. Volume 31. https://doi.org/10.1061/(asce)cf.1943-5509.0001098.

[10] Dinh K., Gucunski N., Zayed T. (2019). Automated visualization of concrete bridge deck condition from GPR data, *NDT&E International*. Volume 102. pp. 120–128. https://doi.org/10.1016/j.ndteint.2018.11.015.

[11] Dinh K., Gucunski N., Duong T.H. (2018). An algorithm for automatic localization and detection of rebars from GPR data of concrete bridge decks, *Automation in Construction*. Volume 89. pp. 292–298. https://doi.org/10.1016/j.autcon.2018.02.017.

[12] Solla M., Lorenzo H., Pérez-Gracia V. (2016). Ground penetrating radar: Fundamentals, methodologies and applications in structures and infrastructure, in: B. Riveiro, M. Solla (Eds.), Non-Destructive Techniques for the Evaluation of Structures and Infrastructure, CRC Press, Boca Raton, FL, USA. pp. 89–111. https://doi.org/10.1201/b19024-7.

[13] Geophysical Survey Systems, Inc. (2016). StructureScan MiniXT Manual. Geophysical Survey Systems, Inc. Nashua, New Hampshire, USA.

[14] Senin S.F., Hamid R. (2016). Ground penetrating radar wave attenuation models for estimation of moisture and chloride content in concrete slab, *Construction and Building Materials*. Volume 106. pp. 659–669. https://doi.org/10.1016/j.conbuildmat.2015.12.156.

[15] Laurens S., Balayssac J.P., Rhazi J., Klysz G., Arliguie G. (2005). Non-destructive evaluation of concrete moisture by GPR: Experimental study and direct modeling, *Materials and Structures*. Volume 38. pp. 827–832. https://doi.org/10.1007/BF02481655.

[16] Tesic K., Baricevic A., Serdar M., Gucunski N. (2022). Characterization of ground penetrating radar signal during simulated corrosion of concrete reinforcement, *Automation in Construction*. Volume 143. https://doi.org/10.1016/j.autcon.2022.104548.

METASTRUCTURES WITH A SINGLE VIBRATION ABSORBER: HOW TO DESIGN IT AND WHERE TO LOCATE IT TO ACHIEVE BROADBAND VIBRATION ATTENUATION?

Srđan Nikačević[1], Ivana Kovačić[2]

Summary:

Vibration absorbers have been used in structural engineering for decades. This interest has been renewed by the new concept of metastructures, which are modelled as oscillatory chains with absorbers designed as distributed tuned auxiliary oscillators. Such linear oscillatory chains are considered in this work as well, but the main question regards the use of a vibration absorber as a single discrete oscillator instead of an array of them. In this respect, this study aims to determine the optimal design parameters and appropriate location of the additional oscillator that would yield broadband low-frequency vibration attenuation. The methodology is based on the so-called equal-peak method. The case studies considered include the chains with two masses and the absorber attached to the first or to the second mass. The results obtained are expected to pave the way for practical realisation of a lightweight metastructure with a single, appropriately designed and positioned vibration absorber that would attenuate its first and second modal resonance.

Key words: vibration absorber, equal-peak method, oscillatory chain

[1] Teaching Assistant, Faculty of Technical Sciences, University of Novi Sad, Serbia, se.nika@uns.ac.rs
[2] Full Professor, Faculty of Technical Sciences, University of Novi Sad, Serbia, ivanakov@uns.ac.rs

1. INTRODUCTION

A vibration absorber (VA), consisting of one mass, one spring and one damper, is a well-known device for achieving vibration attenuation. A classical problem assumes attaching the VA as an auxiliary oscillator to a main oscillatory system modelled by a single-degree-of-freedom (SDOF) undamped harmonically excited oscillator [1], with the aim of finding the optimal properties of VA's spring and damper so as to maximize the vibration attenuation of the main mass.

The most famous optimum design method for the VA, the so-called equal-peak method or fixed-points theory, is described in detail in [1]. The essence of the method lies in the existence of two invariant points of the amplitude-frequency response curves of the main mass, which are independent from VA's damping parameter. These two invariant points, usually referred to as points P and Q, can be graphically shown as the intersection of any two amplitude-frequency response curves. For the sake of convenience, Figure 1 shows them for two distinctive cases: one when VA's damping parameter ζ approaches zero (depicted by the green dash-dotted line), and the other one when ζ approaches infinity (depicted by the green dashed line). In Figure 1, given on the horizontal axis is the frequency ratio, which is assumed as the ratio of the excitation frequency and the natural frequency of the main oscillatory system, and given on the ordinate is the non-dimensional amplitude, which is assumed as the ratio of the amplitude of the steady-state solution of the main oscillatory system and its static deflection. The optimal value of VA's stiffness parameter is defined as the one yielding equal amplitudes for the points P and Q, while its optimal damping is to be calculated as to the maxima at the points P and Q. The utilization of the VA with such optimal parameters results in the maximal attenuation for the response of the main system. The corresponding amplitude-frequency response curve is also shown in Figure 1 as the green solid line, and the attenuated region is marked by the grey shaded area.

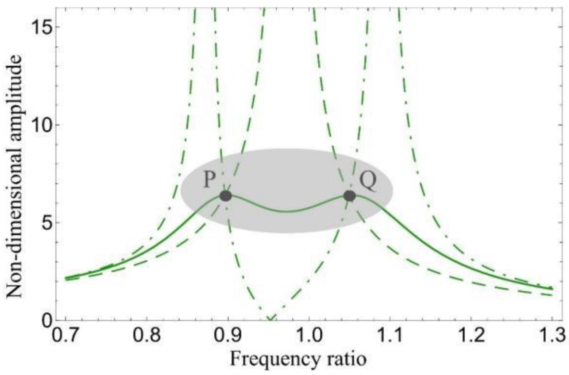

Fig. 1 Amplitude-frequency response curves of the SDOF main system with the VA attached [1], with optimal stiffness parameter when: $\zeta \to 0$ (green dashed-dotted line), $\zeta \to \infty$ (green dashed line), $\zeta \to$ optimum value (green solid line).

Multi-degree-of-freedom (MDOF) main systems with one VA attached have also been studied for decades. One of the seminal papers was written by Warburton [2,3], who described two-DOF system with an equivalent SDOF, and then used den Hartog's equal-peak method for its optimisation. Subsequently, Vakakis and Paipetis [4], applied a polynomial series method and derived the optimal absorber parameters for MDOF systems with the VA attached to the last discrete mass of the main system. An excessive overview of the development of VAs until the time of its publication was given by Sun, Jolly and Norris [5], while [6] provided a more recent overview of the state-of-the-art. One of the prominent contributions was made by Ozer and Royston [7], who extended the classical den Hartog's method for the use on MDOF undamped systems. Sims [8] considered the problem of chatter suppression in machining operations and introduced a

new analytical solution, using only the real part of the amplitude-frequency response function for deriving the optimal system parameters. Krenk and Hogsberg [9] provided an explicit design procedure for a linear VA attached to a flexible structure. By using the Laplace transform method, Shen *et al*. [10] obtained the analytical solution for optimal parameters of the VA with negative stiffness. Based on the concept of robust equal peaks, Dell'Elce, Gourc and Kerschen [11] introduced a new tuning approach for the linear VA to mitigate a specific resonance of a mechanical system with uncertainties. Using the method based on the equal peak method, Shen *et al.* [12] presented and investigated a new concept of the VA with a grounded stiffness and an amplifying mechanism.
In this study, oscillatory chains with the main system consisting of two masses and one VA are investigated in Section 2, where the VA is attached to the first or to the second main mass. Optimal parameters of the VA in both cases are presented in Section 3, with the aim of attenuating either the first or the second modal resonance. The methodology used is based on the previously described equal-peak method, and the optimal parameters and position of the VA are discussed in Section 4.

2. THEORY

The main system is modelled as an oscillatory chain with two-DOF, consisting of two discrete masses connected mutually via a linear spring, where the first mass is also attached to a moving base. In the first case, the VA is attached to the first mass of the main system, as shown in Figure 2a, and in the second case, it is attached to the second mass of the main system, as shown in Figure 2b.

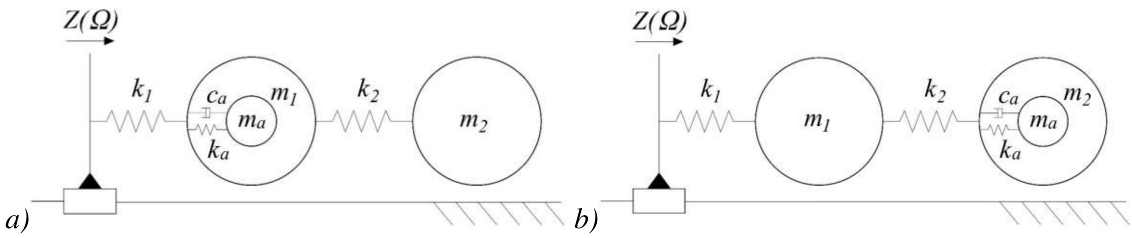

Fig. 2 Main system with the VA attached to: a) the first main mass; and b) the second main mass.

The mass, stiffness, and natural frequency of the main oscillators are denoted as m_n, k_n, and ω_n, respectively, where $n = 1, 2$. The corresponding parameters of the absorber have the subscript a, while its damping parameter is denoted by c_a. The base excitation is assumed to be harmonic with the angular frequency Ω and the amplitude Z_0, as follows:

$$Z = Z_0 e^{i\Omega t}. \tag{1}$$

It is assumed that the main masses are equal $m_1 = m_2 = m$, and so are the stiffness parameters $k_1 = k_2 = k$, leading to their natural frequencies being equal as well $\omega_1 = \omega_2 = \omega$. Natural frequencies of the main system and the VA are, thus, given by:

$$\omega = \sqrt{\frac{k}{m}}, \omega_a = \sqrt{\frac{k_a}{m_a}}. \tag{2a, b}$$

For the sake of convenience, the following non-dimensional parameters are introduced, representing the frequency ratio, damping ratio, mass ratio and excitation frequency ratio, respectively:

$$f = \frac{\omega_a}{\omega}, \zeta = \frac{c_a}{2m_a\omega_a}, \mu = \frac{m_a}{m}, \psi = \frac{\Omega}{\omega}. \tag{3a-d}$$

Non-dimensional amplitude of the first and second main mass is defined as:

$$H_n = \frac{A_n}{Z_0}, \tag{4}$$

where n = 1, 2 stands for the case of the first or the second main mass, respectively, while A_n represents the amplitude of the steady-state solution of the first and second main mass.

Treating the mass of the VA as a known parameter, the design problem involves finding the optimal stiffness and damping of the VA, i.e., finding the optimal frequency ratio f and damping ratio ζ. In addition, the design problem also involves finding the appropriate location of the VA.

In the following subsection, the methodology used for finding these optimal parameters will be shown via the example of the first case, illustrated in the Figure 2a, when the VA is attached to the first main mass.

2.1. OPTIMAL PARAMETERS

When the VA is attached to the first main mass (Figure 2a), the non-dimensional amplitude of the second main mass can be derived as:

$$|H_2| = \sqrt{\frac{A^2 + B^2\zeta^2}{C^2 + D^2\zeta^2}}, \tag{5a}$$

where:

$$\begin{aligned} A &= \psi^2 - f^2, \\ B &= 2f\psi, \\ C &= \psi^6 - 3\psi^4 + \psi^2 - f^2\big(1 + \psi^4(1+\mu) - \psi^2(3+\mu)\big), \\ D &= 2f\psi\big(1 + \psi^4(1+\mu) - \psi^2(3+\mu)\big). \end{aligned} \tag{5b-e}$$

2.1.1. Optimal frequency ratio

Following the steps of the equal-peak method [1], the positions of the invariant points should be found first and expressed in terms of the excitation frequency ratio ψ., Eq. (3d).

As the invariant points are independent of VA's damping, their positions in terms of the excitation frequency ratio can be found through the amplitude-frequency response function for the case when it is independent of VA's damping. Based on Eq. (5a), this independence can be achieved when:

$$\frac{A}{C} = \frac{B}{D}. \tag{6}$$

Using Eqs. (5b-e) and (6), a polynomial in terms of the excitation frequency ratio ψ, with the highest power being fourteen, can be derived:

$$B_{14}\psi^{14} + B_{12}\psi^{12} + B_{10}\psi^{10} + B_8\psi^8 + B_6\psi^6 = 0, \tag{7a}$$

where:

$$\begin{aligned} B_{14} &= 2 + \mu, \\ B_{12} &= -2\big(4 + \mu + f^2(1+\mu)\big), \\ B_{10} &= 8 + \mu + 4f^2(2+\mu), \\ B_{12} &= -2\big(1 + f^2(4+\mu)\big), \\ B_6 &= 2f^2. \end{aligned} \tag{7b-f}$$

Solving the polynomial, four invariant points are detected as four non-trivial real and positive solutions, which represent the positions of four invariant points. Their expressions are too cumbersome to be presented here, but they can be obtained by solving the polynomial (7a) in terms of ψ. It should be noted that in this case, only three of these solutions are the functions of the mass ratio and the frequency ratio as $\psi = \psi(\mu, f)$, while one of the solutions is constant and equal to unity. One constant invariant point does not appear only in the second case, when one uses the amplitude-frequency response of the first main mass. In this case, all invariant points are the functions of the mass ratio and the frequency ratio.

Four invariant points are shown in Figure 3a as the intersections of two amplitude-frequency response curves. The cases when the damping ratio ζ approaches zero and infinity are presented. Note that the logarithmic graphs are used for the sake of easier observation of the invariant points.

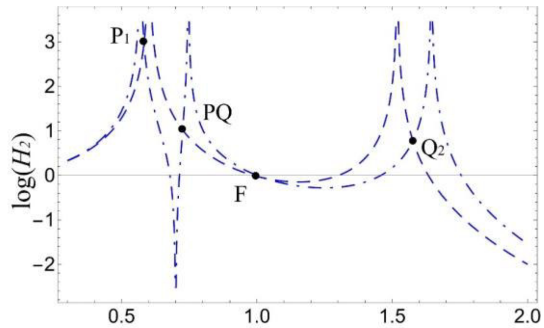

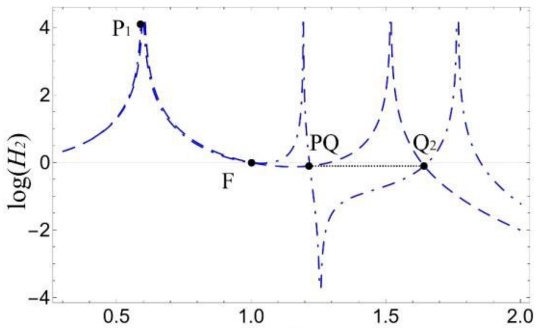

Fig. 3 Amplitude-frequency response curves of H_2 for $\mu = 0.2$, when $\zeta \rightarrow 0$ (blue dashed-dotted line) and $\zeta \rightarrow \infty$ (blue dashed line): a) $f = 0.7$; and b) $f = f_{opt} = 1.257$.

To find the optimal frequency ratio $f(\mu)$, the additional condition is needed. Following the classical den Hartog's case illustrated in Figure 1, one needs to set the amplitudes of the amplitude-frequency response at the invariant points to be equal. But the question is which two points to choose out of the four existing invariant points. This corresponding analysis is given subsequently. In terms of ψ, the location of the point F is always constant and equal to unity. The locations of points P_1, PQ and Q_2 depend on the mass ratio and the frequency ratio, but they do not behave in the same way with respect to the variation of the frequency ratio. When the frequency ratio is changed, the location of the point P_1 is always around the first modal resonance peak, and similarly, while Q_2 appears always around the second modal resonance peak. In addition, the location of the point PQ changes more apparently with respect to the frequency ratio. This can be seen when comparing the two graphs shown in Figure 3.

So, if the aim is to attenuate the second resonant mode, the amplitudes of the points PQ and Q_2 should be equated, and the additional condition can be written as:

$$\lim_{\zeta\to\infty}\left|H_2(\psi_{PQ})\right| = \lim_{\zeta\to\infty}\left|H_2(\psi_{Q2})\right|. \tag{8}$$

Solving this equation for the parameter f, the optimal frequency ratio is obtained, and consequently, the optimal VA stiffness as well. The locations of the invariant points in case of the mass ratio $\mu = 0.2$ and the optimal stiffness for attenuating second modal resonance $f_{opt} = 1.257$ are given in Figure 3b.

2.1.2. Optimal damping ratio

Optimal attenuation is obtained for the case when the local maxima around the aimed modal resonance peak are set to be at the invariant points. The corresponding amplitude-frequency response curve is shown in Figure 4 as the blue solid line, where the attenuated modal resonance is marked by the grey shaded area. For the optimal value of the damping ratio, the first derivative of the amplitude-frequency equation (5a) with respect to ψ should be equal to zero at the invariant points PQ and Q_2. The general expression for this condition can be written down as:

$$H'_2(\mu, \psi, f, \zeta) = \frac{\partial |H_2|}{\partial \psi} = 0. \tag{9}$$

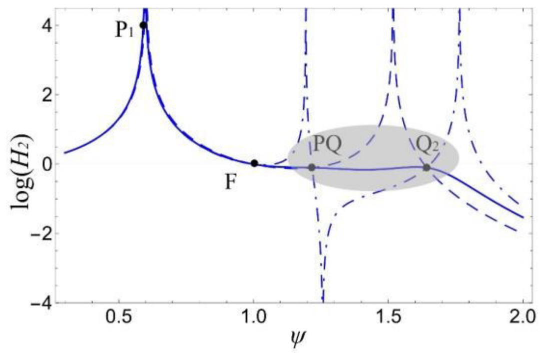

Fig. 4 Amplitude-frequency response curves of H_2 for μ = 0.2 and f_{opt} = 1.257 when: $\zeta \to 0$ (blue dashed-dotted line), $\zeta = \zeta_{opt}$ = 0.2593 (blue solid line), $\zeta \to \infty$ (blue dashed line).

It should be noted that there is no value of the damping ratio for which both local maxima would be at the invariant points PQ and Q_2 at the same time. Following the equal-peak method [1], one should find two values of the damping ratio: one for the local maximum to appear at the point PQ and the other one for the local maximum be at the point Q_2. Evaluating Eq. (9), an expression is obtained in terms of the mass ratio μ, excitation frequency ratio ψ, frequency ratio f and damping ratio ζ. Using the value of the optimal frequency ratio and the locations of the invariant points ψ_{PQ} and ψ_{Q2}, two expressions are obtained and can be represented as:

$$H'_2(\mu, \psi_{PQ}, f_{opt}, \zeta) = 0, H'_2(\mu, \psi_{Q2}, f_{opt}, \zeta) = 0. \tag{10a, b}$$

Solving Eqs. (10a, b) for the parameter ζ, two values of the damping parameter are obtained ζ_1 and ζ_2. Following the equal-peak method [1], the optimal damping ratio is obtained as an average value of these two solutions:

$$\zeta_{opt} = \frac{\zeta_1 + \zeta_2}{2}. \tag{11}$$

3. RESULTS

In this section, the optimal parameters of the VA for attenuation of the first or the second resonant mode of the main masses are presented. This is done for the case when the VA is attached to the first or the second main mass. These optimal parameters are obtained for different values of the mass ratio using the methodology shown in the previous section.

3.1. VA ATTACHED TO THE FIRST MAIN MASS

Tables 1 and 2 show the optimal parameters of the VA when it is attached to the first main mass, obtained through the responses of the first and second main mass, respectively. Three larger columns show the optimal parameters for different values of the mass ratio, and the first and second row for attenuation of the first or the second modal resonance, respectively. It can be concluded that by decreasing the mass ratio the value of VA's, the optimal damping ratio also decreases, while the value of VA's optimal frequency ratio increases, which is in accordance with the results given in [2, 4, 8]. Also, it can be noticed that when the VA is attached to the first main mass, the value of optimal damping is significantly larger when it is tuned for the attenuation of the second modal resonance.

Tab. 1 Optimal parameters of the VA attached to the first main mass, with respect to H_1.

Aimed modal res.	$\mu = 0.2$		$\mu = 0.1$		$\mu = 0.05$	
	f_{opt}	ζ_{opt}	f_{opt}	ζ_{opt}	f_{opt}	ζ_{opt}
1.	0.5815	0.1447	0.5994	0.1022	0.6086	0.0721
2.	1.4588	0.1940	1.5275	0.1497	1.5696	0.1111

Tab. 2 Optimal parameters of the VA attached to the first main mass, with respect to H_2.

Aimed modal res.	$\mu = 0.2$		$\mu = 0.1$		$\mu = 0.05$	
	f_{opt}	ζ_{opt}	f_{opt}	ζ_{opt}	f_{opt}	ζ_{opt}
1.	0.5910	0.1446	0.6044	0.1021	0.6112	0.0721
2.	1.2570	0.2593	1.4311	0.1641	1.5219	0.1156

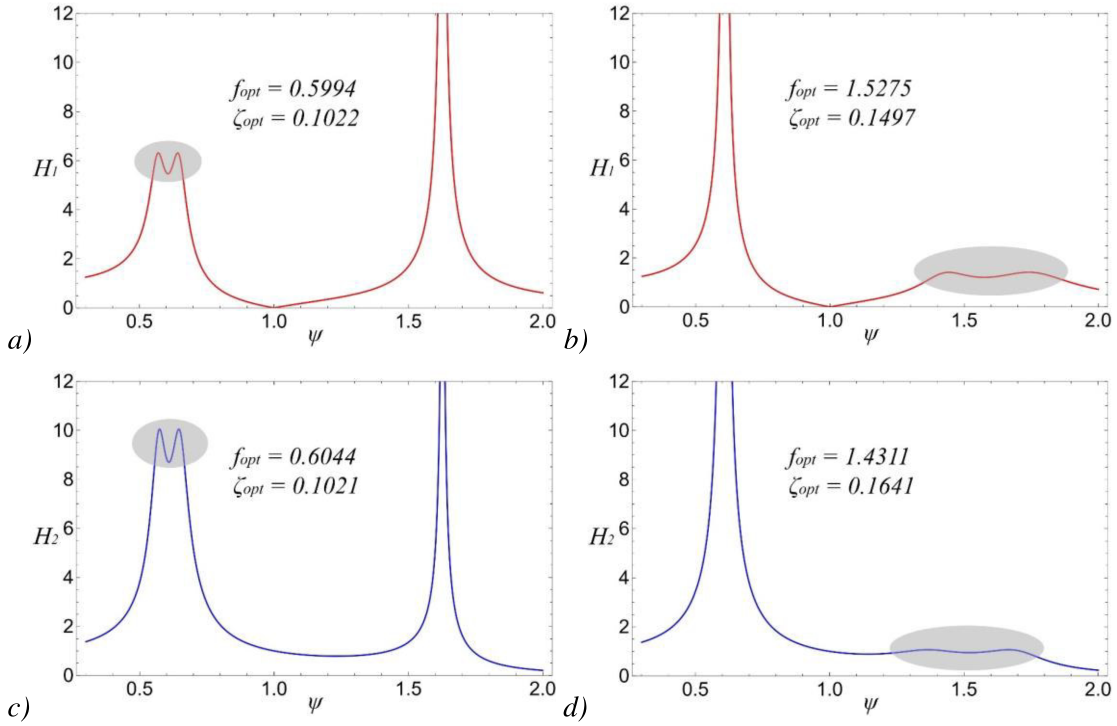

Fig. 5 Amplitude-frequency response curves for the case when the VA is attached to the first main mass for $\mu = 0.1$: a) H_1 for the VA tuned to the first modal resonance; b) H_1 for the VA tuned to the second modal resonance; c) H_2 for the VA tuned to the first modal resonance; and d) H_2 for the VA tuned to the second modal resonance.

Figure 5 presents the amplitude-frequency responses of the main masses with the tuned VA attached to the first main mass, when the mass ratio is $\mu = 0.1$. Graphs in Figure 5a and 5b show the amplitude-frequency responses of the first main mass (depicted by the red solid line) when the VA is tuned for attenuation of the first or the second modal resonance, respectively. Similarly, graphs in Figure 5c and 5d show the amplitude-frequency responses of the second main mass (depicted by the blue solid line). In these graphs the aimed (attenuated) modal resonance is marked with the grey area, and the optimal parameters of the VA, used in each case, are given in the graphs. In these graphs, one can see the effect of the VA tuned for attenuation of different modal resonances, for the responses of both first and second main mass, so as the possible attenuation in each case.

3.2. VA ATTACHED TO THE SECOND MAIN MASS

Shown in Tables 3 and 4 are the optimal parameters of the VA when it is attached to the second main mass, obtained through the responses of the first and second main mass, respectively. The arrangement of these tables is analogous to the one of Tables 1 and 2.

Tab. 3 Optimal parameters of the VA attached to the second main mass with respect to H_1.

Aimed modal res.	$\mu = 0.2$		$\mu = 0.1$		$\mu = 0.05$	
	f_{opt}	ζ_{opt}	f_{opt}	ζ_{opt}	f_{opt}	ζ_{opt}
1.	0.5397	0.2196	0.5764	0.1599	0.5965	0.1147
2.	1.3923	0.1256	1.4953	0.0948	1.5539	0.0694

Tab. 4 Optimal parameters of the VA attached to the second main mass with respect to H_2.

Aimed modal res.	$\mu = 0.2$		$\mu = 0.1$		$\mu = 0.05$	
	f_{opt}	ζ_{opt}	f_{opt}	ζ_{opt}	f_{opt}	ζ_{opt}
1.	0.5461	0.2205	0.5801	0.1602	0.5985	0.1149
2.	1.4495	0.0898	1.5243	0.0811	1.5684	0.0658

Similar behaviour of VA’s optimal parameters can be noticed in this case, too. The main difference is that in this case, the value of VA’s optimal damping is considerably larger when it is tuned for the attenuation of the first modal resonance.

Graphs shown in Figure 6 are analogous to those in Figure 5 but are given for the case when the tuned VA is attached to the second main mass. As in the previous figure, shown in Figure 6a and 6b are the amplitude-frequency responses of the first main mass (depicted by the red solid line), and in Figure 6c and 6d of the second main mass (depicted by the blue solid line). The optimal parameters of the VA used in each case are given in the graphs, and the grey shaded area marks the aimed modal resonance.

Comparing the amplitude-frequency responses of the same main masses given in Figure 5 and Figure 6, one can notice a few interesting phenomena. The attenuation of the first modal resonance is better when the VA is attached to the second main mass, and of the second modal resonance when the VA is attached to the first main mass. However, in both cases, the value of VA’s damping ratio is large, and it exceeds 0.1. On the other hand, attaching the VA in an opposite way leads to a significantly smaller value of the damping ratio, but also worsens the attenuation of the aimed modal resonance. This phenomenon will be further discussed in the following Section.

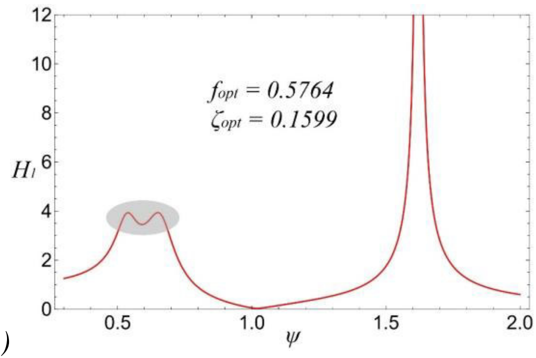

a)

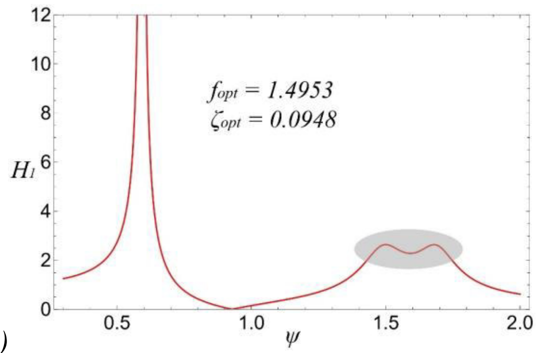

b)

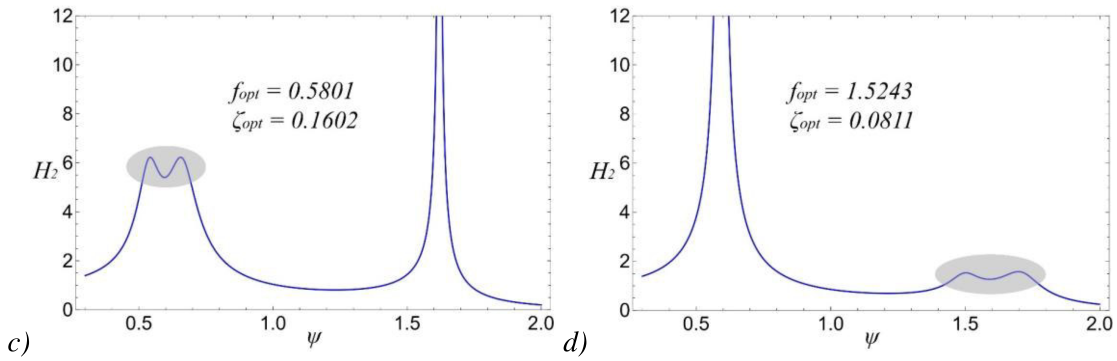

Fig. 6 Amplitude-frequency response curves for the case when the VA is attached to the second main mass for $\mu = 0.1$: a) H_1 when the VA is tuned to the first modal resonance; b) H_1 when the VA is tuned to the second modal resonance; c) H_2 when the VA is tuned to the first modal resonance; and d) H_2 when the VA is tuned to the second modal resonance.

4. DISCUSSION

It was shown in [7] that the VA should be attached to the most active main mass in order to achieve the maximal attenuation of a certain modal resonance of a MDOF system in that particular mode. Thus, to clarify the reason of better attenuation of the first or second modal resonance shown in the previous Section, one needs to find the most active main mass in both resonant modes. Since the main system considered herein is modelled as a linear oscillatory chain with two-DOF (Figure 2), so one can expect two oscillatory modes. Figure 7 shows the corresponding mode-shape illustration, for its first and second mode, where the main mass notation is given on the abscissa and the normalised amplitude is given on the ordinate. As shown in Figure 7 for a two-DOF main system in the first mode, the most active mass is the second main mass, while in the second mode, the most active mass is the first main mass.

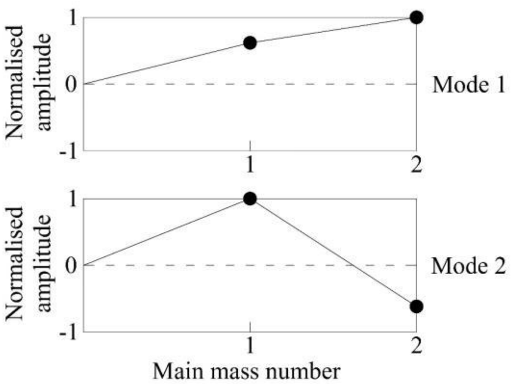

Fig. 7 Mode-shape illustration of the main system modes.

This analysis clarifies the reason why the better attenuation of the first or the second modal resonance is obtained if the VA is attached to the second or the first main mass, respectively. But in both cases, if the VA is positioned in this way, the problem remains with a very large value of VA's optimal damping ratio. Moreover, it is seen from Tables 1 to 4 that even for the mass ratio being 0.05 and the VA attached to the most active mass of a particular mode, the value of the optimal damping ratio still exceeds the value of 0.1.

On the other hand, if the VA is attached to the less active mass in a particular mode, the value of the optimal damping decreases. In order to lower the optimal damping ratio, due to practical limitations, the VA can be attached to the less active mass, and lower attenuation can be compensated by increasing VA's mass, if possible.

For example, if the aim is to achieve a maximal attenuation of the second modal resonance of the second main mass, the VA should be attached to the first main mass. In this case, with the mass ratio being 0.05, the optimal damping ratio is obtained as ζ_{opt} = 0.1156 and the non-dimensional amplitude of the second modal resonance is H_{2max} = 1.38. If the VA is attached to the second main mass, with a higher mass ratio being 0.2, the optimal damping ratio is obtained as ζ_{opt} = 0.0898 and the non-dimensional amplitude for second modal resonance is H_{2max} = 1.14. Both cases are depicted in Figure 8 by the blue dotted line and the blue solid line, respectively, where the attenuated modal resonance is marked with the grey shaded area.

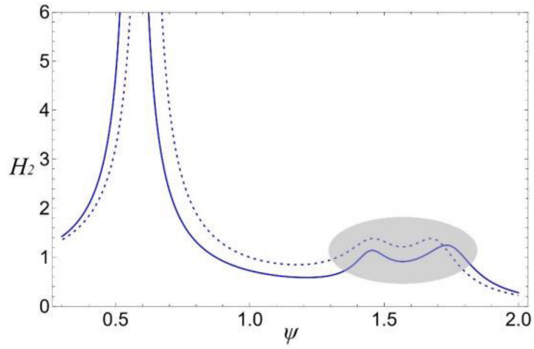

Fig. 8 Amplitude-frequency response curves of H_2 when the VA is attached to the first main mass with μ = 0.05, f_{opt} = 1.5219 and ζ_{opt} = 0.1156 (blue dotted line) and when it is attached to the second main mass with μ = 0.2, f_{opt} = 1.4495 and ζ_{opt} = 0.0898 (blue solid line).

5. CONCULSION

The aim of this case study has been to analyse the behaviour of a two-DOF oscillatory chain with the addition of one tuned VA. Depending on a different position and mass of the VA, its optimal design parameters have been obtained with respect to the first and second main mass.

The amplitude-frequency responses and the mode shapes considered have shown that attaching the VA to the most active main mass in a particular mode yields the maximal attenuation of the corresponding modal resonance. If the VA is positioned in this way, the optimal damping ratio has been obtained to be of a large value, which might be practically unattainable. To decrease this value, one can lower the mass of the VA, but this undesirably reduces the attenuation of the aimed modal resonance response.

If the VA is attached to the less active main mass in a particular mode, a smaller value of the optimal damping ratio is needed, but the attenuation gets worse. The difference in the attenuation can be compensated by using a larger mass of the VA, if possible, realising better attenuation, and still having a lower optimal value of the damping ratio. Thus, the positioning of the VA is a trade-off between the level of attenuation achieved and VA's design parameters.

Future research will be directed towards the investigations of multi-DOF oscillatory chains, so as to establish the foundation for practical realisation of a lightweight metastructure whose response will be attenuated not only at a certain resonance but in a wider frequency band that includes several of them.

ACKNOWLEDGEMENT

This research has been funded by the Ministry of Science, Innovation and Technological Development of the Republic of Serbia within the project 'Noise and Vibration Isolation through Nonlinear Metastructures' (acronym NOLIMAST).

REFERENCES

[1] Den Hartog J.P. (1956). *Mechanical Vibrations*. 4th ed., McGraw-Hill, New York.

[2] Warburton G.B. (1981). Optimum absorber parameters for minimizing vibration response. *Earthquake Engineering and Structural Dynamics*, Volume 9 (3), pp. 251-262. https://doi.org/10.1002/eqe.4290090306.

[3] Warburton G.B. (1982). Optimum absorber parameters for various combinations of response and excitation parameters. *Earthquake Engineering and Structural Dynamics*, Volume 10 (3), pp. 381-401. https://doi.org/10.1002/eqe.4290100304.

[4] Vakakis A.F., Paipetis S.A. (1986). The effect of a viscously damped dynamic absorber on a linear multi-degree-of-freedom system. *Journal of Sound and Vibration*, Volume 105 (1), pp. 49–60. https://doi.org/10.1016/0022-460X(86)90219-1.

[5] Sun J.Q., Jolly M.R., Norris M.A. (1995). Passive, adaptive and active tuned vibration absorbers – A survey. *Journal of Vibration and Acoustics, Transactions of ASME*, Volume 117 (B), pp. 234-242. https://doi.org/10.1115/1.2838668.

[6] Yang F., Sedaghati R., Esmailzadeh E. (2021). Vibration suppression of structures using tuned mass damper technology: A state-of-the-art review. *Journal of Vibration and Control*, Volume 28 (7-8), pp. 812-836. https://doi.org/10.1177/1077546320984305.

[7] Ozer M.B., Royston T.J. (2005). Extending Den Hartog's vibration absorber technique to multi-degree-of-freedom systems. *Journal of Vibration and Acoustics, Transactions of ASME*, Volume 127 (4), pp. 341-350. https://doi.org/10.1115/1.1924642.

[8] Sims N.D. (2007). Vibration absorbers for chatter suppression: A new analytical tuning methodology. *Journal of Sound and Vibration*, Volume 301 (3-5), pp. 592-607. https://doi.org/10.1016/j.jsv.2006.10.020.

[9] Krenk S., Hogsberg J. (2014). Tuned mass absorber on a flexible structure. *Journal of Sound and Vibration*, Volume 333 (6), pp. 1577-1595. https://doi.org/10.1016/j.jsv.2013.11.029.

[10] Shen Y., Peng H., Li X., Yang S. (2017). Analytically optimal parameters of dynamic vibration absorber with negative stiffness. *Mechanical Systems and Signal Processing*, Volume 85, pp. 193-203. https://doi.org/10.1016/j.ymssp.2016.08.018.

[11] Dell'Elce L., Gourc E., Kerschen G. (2018). A robust equal-peak method for uncertain mechanical systems. *Journal of Sound and Vibration*, Volume 414, pp. 97-109. https://doi.org/10.1016/j.jsv.2017.10.038.

[12] Shen Y., Xing Z., Yang S. Sun J. (2019). Parameters optimization for a novel dynamic vibration absorber. *Mechanical Systems and Signal Processing*, Volume 133, art. num. 106282. https://doi.org/10.1016/j.ymssp.2019.106282.

MAXIMIZING PROFIT THROUGH SUSTAINABLE OPTIMIZATION OF SIMPLY SUPPORTED BEAMS

Tomaž Žula[1], Stojan Kravanja[2], Primož Jelušič[3]

Summary:

This paper describes the optimization process for producing simply supported beams in civil engineering while maximizing sustainability profit and economic profit. Three material alternatives were proposed and optimized: structural steel, reinforced concrete, and glulam. The optimization models were developed using two objectives - economic profit and sustainability profit, which included environmental costs like global warming. The beams were evaluated based on design, resistance, and deflection constraints specified in Eurocode 2, 3, and 5. The mixed-integer nonlinear programming (MINLP) approach using GAMS/Dicopt was utilized to solve the non-linear discrete-continuous optimization problem. The study concluded that laminated timber beams offer the highest economic and sustainability profits. A numerical example is presented at the end of the article to illustrate the optimization process.

Key words: Sustainability profit, GHG emissions, Simply supported beams, Mixed-integer non-linear programming, MINLP

[1] Assist. Prof. dr. Tomaž Žula, DSc, BSc, University of Maribor, Faculty of Civil Engineering, Transportation Engineering and Architecture, Smetanova 17, 2000 Maribor, Slovenia, e-mail: tomaz.zula@um.si
[2] Prof. dr. Stojan Kravanja, DSc, MSc, BSc, University of Maribor, Faculty of Civil Engineering, Transportation Engineering and Architecture, Smetanova 17, 2000 Maribor, Slovenia, e-mail: stojan.kravanja@um.si
[3] Assoc. Prof. dr. Primož Jelušič, DSc, BSc, University of Maribor, Faculty of Civil Engineering, Transportation Engineering and Architecture, Smetanova 17, 2000 Maribor, Slovenia, e-mail: primoz.jelusic@um.si

1. INTRODUCTION

This paper focuses on the optimization of sustainability profits generated by the production of simply supported beams in the construction industry. The sustainability profit considered in this study is a combination of economic profit and the environmental cost of global warming. The study examines a range of simply supported beams made from three different material alternatives, including glulam, structural steel, and reinforced concrete. The objective of this work is to determine the optimal design of simply supported beams that maximize both economic and sustainability profits, using a mixed-integer nonlinear programming approach.
In the field of optimization and sustainability, researchers have proposed various optimization techniques and objectives. For example, Zaforteza et al. [1] utilized the Simulated Annealing algorithm to optimize the embedded CO_2 emissions and economic cost of reinforced concrete structures. Camp and Huq [2] proposed a hybrid Big Bang-Big Crunch algorithm for optimal design of reinforced concrete frames, aimed at minimizing total cost or CO_2 emissions. Alonso and Berdasco [3] presented the carbon footprint of sawn timber products, while Li et al. [4] introduced a topology optimizer for welded box-beam structures that emit fewer greenhouse gases using the Improved Ground Structure Method.

2. MINLP MODEL FORMULATION

It is generally accepted that a non-linear and non-convex optimization problem can be expressed as a Mixed-Integer Nonlinear Programming (MINLP) problem, which combines both continuous and discrete variables:

$$\min \ z = f(\mathbf{x},\mathbf{y})$$

$$\text{subjected to:} \quad g_k(\mathbf{x},\mathbf{y}) \leq 0 \quad k \in K$$

$$\mathbf{x} \in X = \{\mathbf{x} \in R^n: \ \mathbf{x}^{\mathrm{LO}} \leq \mathbf{x} \leq \mathbf{x}^{\mathrm{UP}}\}$$

$$\mathbf{y} \in Y = \{0,1\}^m$$

In the context of an MINLP problem, the decision variables are typically split into two types: continuous variables **x** and discrete variables **y**, where **y** can take on binary values (0 or 1). The objective function $f(\mathbf{x},\mathbf{y})$ represents both economic and sustainability profits, which take into account the environmental costs of global warming. Additionally, the constraints on the design, resistance, and deflection of the system are represented by $g_k(\mathbf{x},\mathbf{y})$.

3. NUMERICAL EXAMPLE OF SIMPLY SUPPORTED BEAMS

In this example, the optimization process is shown for 150 simply supported beams, each with a length of 8.5 meters and subject to the effects of dead-weight, permanent load of 13.0 kN/m (g) and an imposed variable load of 10.0 kN/m (q) as shown in Fig. 1. The beams have a selling price of € 2500.00 per piece.
The goal is to determine the optimal design for each beam using three different materials: laminated timber, structural steel, and reinforced concrete. Two objectives were considered for optimization: maximizing economic profit and sustainability profit. Six optimization models were developed using Dicopt by Grossmann [6], as the problem is a simple discrete and non-linear one. GAMS (General Algebraic Modelling System), see Brooke et al. [7], was used for mathematical modeling, with Eurocode

specifications for timber [8], steel [9], and reinforced concrete [10] being used to establish design, loading, and resistance constraints. The final design of the beams was checked for bending moment, and shear resistance, lateral torsional buckling resistance and deflection.

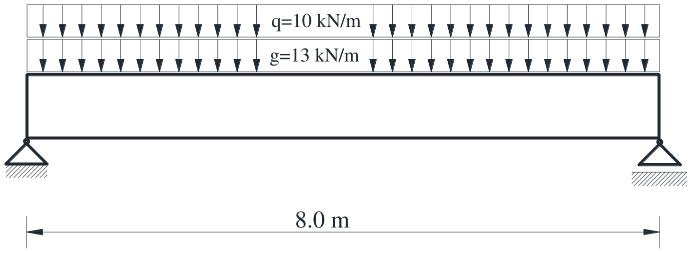

Fig. 1 Simply supported beam

The superstructure of the beam is simply supported and composed of three different materials. The laminated timber beam superstructure exhibits 101 variations in rounded dimension for section width and 131 variations in rounded dimension for section height. As for the steel beam superstructure, it is comprised of 3 different grades of steel and offers 8 distinct dimensional alternatives for both flanges and webs, along with 1051 rounded dimensional alternatives for flange width and 1301 rounded dimensional alternatives for web height. The reinforced concrete beam superstructure contains 7 different concrete grades, 13 standard reinforcement, and 131 rounded dimension alternatives for cross-section height, along with 101 rounded dimension alternatives for cross-section width, rounded up to the nearest whole centimeter.
Taking into account the aforementioned material and dimensional alternatives, a total of 13,231 design alternatives can be generated for the laminated timber beam, while the steel beam offers a staggering 262,531,392 unique design alternatives. The reinforced concrete beam, on the other hand, yields a total of 1,204,021 distinct design alternatives. These design alternatives are determined by binary variables.
Two different objective functions have been proposed for two different defined criteria. The first optimization criterion is to maximise the economic profit (P_E [€]) of 150 equal beams. The economic profit is determined as the sum of the selling price, self-manufacturing material and labour costs, and overhead costs. The objective function was defined separately for three different materials, see Eq. (1). N is the number of simply supported beams (N = 150), C_S [€] is the selling price of a single simply supported beam, $C_{\mathrm{M}i}$ [€/kg] represents the material unit prices of ($i \in I$: laminated timber, impregnation and protection paint for the timber beam; structural steel, electrodes, gas consumption and anticorrosion-resistant paint for the steel beam; and concrete, reinforcing steel bars and formwork slab-panels for the concrete beam). ρ_i [kg/m^3] is the corresponding unit of mass and V_i [m^3] is the volume. $C_{\mathrm{L}j}$ represents the hourly labour cost [€/h], t_j [h] are the times required for ($j \in J$: impregnating and painting the timber beam; cutting, welding and painting the steel beam, placing; cutting and placing the reinforcement and curing, vibrating, panelling the concrete beam), and f_O is an indirect overhead cost factor (f_O = 2). More details on the cost factors used in the economic objective function can be found in Jelušič [11], Kravanja [12] and Žula [13].

$$\max P_\mathrm{E} = N \cdot \left(C_\mathrm{S} - C_{\mathrm{M}i} \cdot \rho_i \cdot V_i - C_{\mathrm{L}j} \cdot t_j \cdot f_\mathrm{O} \right) \tag{1}$$

The next parameter involves the optimization of the sustainability profit (P_{SUS} [€]). This value was obtained by evaluating the economic profit and the environmental cost of producing 150 beams, taking into account the impact of global warming. This calculation was based on the Eco-costs/Value Ratio (EVR) model [14]. To accomplish this, a separate objective function was created for each of the three materials, as shown in Eq. (2). C_GW (€/kg CO_2 eq.) is a price of global warming, 0.116 €/kg CO_2 eq. EVR [14], ρ_k [kg/m^3] and V_k [m^3] are the corresponding mass and volume units, respectively, and $f_{\mathrm{CFEF}k}$ is the carbon footprint emission factor ($k \in K$; for the timber beam, steel beam, and for the reinforced concrete beam, respectively). The carbon footprint emission factor used in the study is 0.69 kg CO_2 eq./kg for timber, 1.72 kg CO_2 eq./kg for steel, 0.11–0.16 kg CO_2 eq./kg for concrete and 2.43 kg CO_2 eq./kg for the reinforcing steel bars.

$$\max P_{\mathrm{SUS}}=P_{\mathrm{E}}+N\cdot\left(-C_{\mathrm{GW}}\cdot f_{\mathrm{CFEF}k}\cdot\rho_k\cdot V_k\right) \qquad (2)$$

The results of the optimization process for two distinct objective functions and three different materials are illustrated in Table 1. It can be seen that the glulam beams outperformed the other materials in terms of both economic profit and sustainability profit. Conversely, the steel beams demonstrated the least favorable results across all three criteria. The optimal cross- sections of the simply supported beam have been provided in Figure 2.

Tab. 1 Results of the simply supported beam optimizations

Criterion		Timber GL24h	Steel S 235	Reinforced Concrete C 50/60
1.	**Economic profit (€)**	**178 136**	**104 655**	**171 993**
	b (mm)	290	338	350
	h (mm)	670	478	570
2.	**Sustainability profit (€)**	**169 041**	**83 277**	**149 139**
	b (mm)	290	338	350
	h (mm)	670	478	570

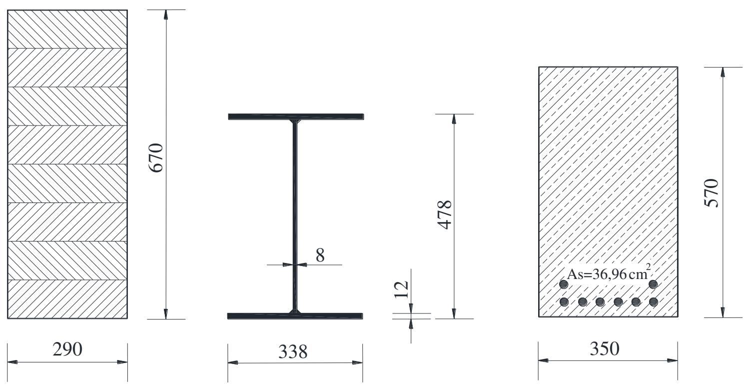

Fig. 2 Optimal cross-sections of the simply supported beam

4. CONCLUSION

In the field of civil engineering, this paper focuses on improving sustainability in the production of simply supported beams. To achieve optimal results, the study employs two different objective functions - economic profit and sustainability profit - while utilizing a mixed-integer non-linear programming (MINLP) approach to optimize the beam alternatives. The numerical example highlighted in the paper demonstrates that the laminated timber beams deliver the highest economic profit and sustainability profit. As a next step, the research aims to incorporate material recycling into the objective function to further improve sustainability.

ACKNOWLEDGEMENT

The authors gratefully acknowledge support from funds of the Slovenian Research Agency (research programs P2-0129 and P2-0268) and the GEOLAB project (grant number 101006512).

REFERENCES

[1] Zaforteza I.P., Yepes V., Hospitaler A., Vidosa F.G. (2009). CO_2-optimization of reinforced concrete frames by simulated annealing. *Engineering Structures*, 31, 1501-1508. DOI:10.1016/j.engstruct.2009.02.034

[2] Camp C.V., Huq, F. (2013). CO_2 and cost optimization of reinforced concrete frames using a big bang-big crunch algorithm. *Engineering Structures*, 48, 363-372. DOI:10.1016/j.engstruct.2012.09.004

[3] Alonso C.M., Berdasco, L. (2015). Carbon footprint of sawn timber products of Castanea sativa Mill. in the north of Spain. *Journal of Cleaner Production*, *102*, 127-135. DOI:10.1016/j.jclepro.2015.05.004

[4] Li B., Hong J., Liu Z. (2017). A novel topology optimization method of welded box-beam structures motivated by low-carbon manufacturing concerns. *Journal of Cleaner Production*, 142, 2792-2803. DOI:10.1016/j.jclepro.2016.10.189

[5] Kravanja Z. (2010). Challenges in sustainable integrated process synthesis and the capabilities of an MINLP process synthesizer MipSyn. *Comput. chem. eng*., 34, 1831-1848. DOI:10.1016/j.compchemeng.2010.04.017

[6] Grossmann I.E., Viswanathan J. (2002). DICOPT - Discrete and Continuous Optimizer. *Engineering Design Research Center (EDRC) at Carnegie Mellon University*, Pittsburgh, PA.

[7] Brooke A., Kendrick, D., Meeraus, A. (1998). *GAMS - A User's Guide*", Scientific Press, Redwood City, CA.

[8] Eurocode 5 (2004). *Design of timber structures.* European Committee for Standardization, Brussels.

[9] Eurocode 3 (2005). *Design of steel structures.* European Committee for Standardization, Brussels.

[10] Eurocode 2 (2004). *Design of concrete structures.* European Committee for Standardization, Brussels.

[11] Jelušič P., Kravanja S. (2017). Optimal design of timber-concrete composite floors based on the multi-parametric MINLP optimization. *Composite structures*, 179, 285-293. DOI:10.1016/j.compstruct.2017.07.062

[12] Kravanja S., Žula T., Klanšek U. (2017). Multi-parametric MINLP optimization study of a composite I beam floor system. *Engineering structures*, 130, 316-335. DOI:10.1016/j.engstruct.2016.09.012

[13] Žula T., Kravanja S., Klanšek U. (2016). MINLP optimization of a composite I beam floor system. *Steel and composite structures*, *22*(*5*), 1163-1192. DOI:10.12989/scs.2016.22.5.1163

[14] *The Model of the Eco-costs / Value Ratio (EVR)* (2021), Delft University of Technology, www.ecocostsvalue.com/

VIBRATION SERVICEABILITY ASSESSMENT OF A STRESS-RIBBON FOOTBRIDGE

Marija Nefovska-Danilović[1], Vitomir Racić[2]

Summary:

With advancements in structural modelling and construction techniques, contemporary footbridges have become increasingly susceptible to vibrations induced by human activities, such as walking, jogging and jumping. This study aims to evaluate pedestrian-induced vibrations of a stress-ribbon footbridge. A three-dimensional finite element model of the footbridge was developed, considering nonlinear behavior of the structure and staged construction. Vibration serviceability assessment was carried out using HIVOSS design guidelines. Numerical modal analysis showed that the lateral modes of vibration cannot be excited in resonance by pedestrians walking. However, the footbridge is prone to vertical pedestrian-induced vibrations. The first torsional mode shape is the most critical. It can be excited in resonance by the first harmonic of the vertical pedestrian loading, yielding vibration response beyond the suggested acceleration limit in some extreme scenarios of pedestrian loading.

Key words: pedestrian-induced loading, nonlinear behavior, modal analysis, numerical model, dynamic response

[1] Assoc. prof, Faculty of Civil Engineering, University of Belgrade, Belgrade, Serbia, marija@grf.bg.ac.rs
[2] Assoc. prof, Faculty of Civil Engineering, University of Belgrade, Belgrade, Serbia, vracic@grf.bg.ac.rs

1. INTRODUCTION

With advancements in structural modelling, building materials and construction techniques, footbridges are often designed as flexible structures [1]. Consequently, contemporary footbridges have become increasingly susceptible to vibrations induced by human activities, such as walking, jogging and jumping [2]. Human-induced vibrations are a serviceability issue, i.e. they do not cause structural damage but can cause discomfort and annoyance to pedestrians. Therefore, vibration serviceability assessment has become the governing criterion for the design of long-span footbridges.

Extensive studies have been carried out to address key challenges related to the vibration serviceability assessment of footbridges [1]. Damping generally features as one of the most uncertain structural parameters at the design stage. However, knowledge about dynamic loading induced by pedestrians is far more sparse and limited. So, it is commonly associated with the greatest level of uncertainty.

Stress-ribbon bridges are gaining popularity in the design and construction of medium and long-span footbridges due to their lightness, aesthetic appeal, high level of prefabrication, easy construction and low maintenance requirements [3]. Main load-bearing elements of the stress-ribbon footbridge are bearing tendons, catenary–type cables usually anchored at the concrete abutments. The bridge deck is usually made of precast concrete segments installed over the bearing tendons and linked together through a cast in-situ concrete layer. After the deck construction, the additional prestressing tendons are posttensioned, forming a composite section of the stress-ribbon footbridge with an increased stiffness. Such a design concept results in a very slender structure having large displacements, which requires application of the geometrically nonlinear analysis. In addition, stress-ribbon footbridges are particularly prone to human-induced vibrations, which has been confirmed through several experimental studies [4-5].

Caetano and Cunha [6] carried out both experimental and numerical investigation of a stress-ribbon footbridge to assess the modal properties and vibration levels due to pedestrian traffic. The measured vibration levels due to a single pedestrian were relatively high but within the acceptable limits. However, large vibration levels were recorded due to a high-density flow of pedestrians whose walking frequency closely matches the natural frequencies of the two experimentally identified vertical vibration modes around 2Hz. The measured damping factors were between 1.7% and 2.6%, indicating slightly higher damping factors than those specified in the guidelines (usually 1%).

This paper presents a numerical study of the modal properties and pedestrian-induced vibrations of a stress-ribbon footbridge. A three-dimensional finite element model of the footbridge was developed, considering geometrically nonlinear behavior of the structure and staged construction. Vibration serviceability assessment was carried out using HIVOSS design guidelines [7].

2. DESCRIPTION AND BEHAVIOUR OF THE BRIDGE

The footbridge was designed as a 30 cm thick stress-ribbon concrete slab with the span of 102 m, width of 3.8m and 2.3 m sag at the end of the construction, Fig. 1. A typical cross section of the footbridge is depicted in Fig. 2. The bearing cables are embedded in the concrete slab, providing a catenary shape to the bridge. The bridge goes through the following construction stages:

- Installation of the bearing cables between the abutments – the bridge behaves as a bare cable,
- Installation of a 3m-long precast concrete segments along the bearing cables – the bridge still behaves as a bare cable with additional dead load,

- Concrete is cast over the segments to achieve monolith and composite section with the bearing cables – the bridge still behaves as an additionally loaded bare cable, as long the concrete is wet,
- Posttensioning using the set of posttensioning tendons – the concrete section had hardened, and the bridge from this stage starts to behave as a stress ribbon (i.e. cables and prestressed concrete form a composite section),
- Application of superimposed dead load (fences, waterproofing etc.) – the bridge behaves as a stress-ribbon with the additional load – this is the end of the construction,
- Service life of the bridge (pedestrian loading, temperature, shrinkage, creep, relaxation) – the bridge behaves as a stress-ribbon.

Due to large displacements, geometrically nonlinear analysis was applied in each construction stage.

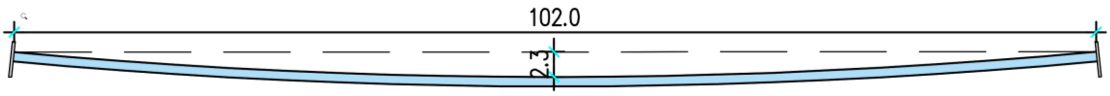

Fig. 1 Longitudinal section of the bridge

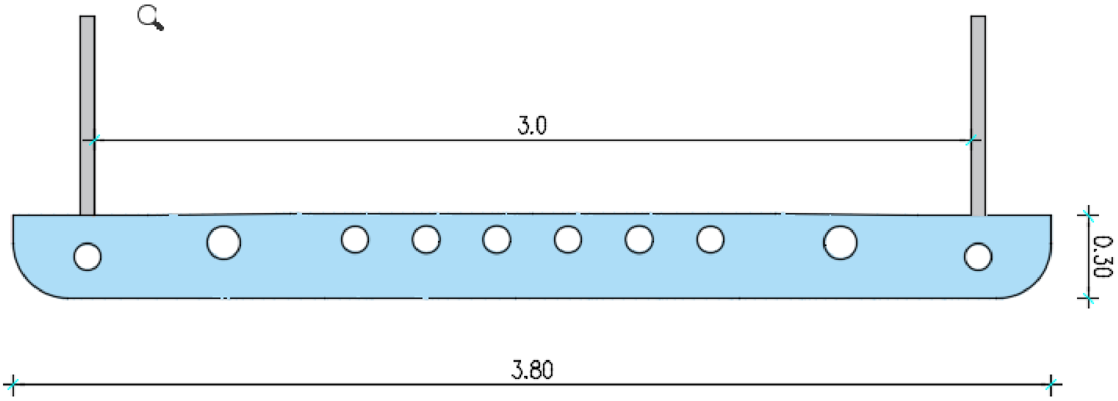

Fig. 2 Typical cross-section of the bridge

3. NUMERICAL MODEL AND ANALYSIS

To account for prescribed loads, geometry of the structure and forces in the cables that change at each construction stage of the stress-ribbon footbridge, a numerical model (Fig. 3.) was developed using the finite element-based software SAP2000 and applying geometrically nonlinear analysis. The finite element model consists of 1836 SHELL elements. The bearing cables were modelled using curved frame elements (CURVED FRAME), while the prestressing tendons were modelled using TENDON type finite elements, with their actual positions in the horizontal plane of the bridge cross-section. In this way, the real stiffness of the bridge in the horizontal plane was taken into account.

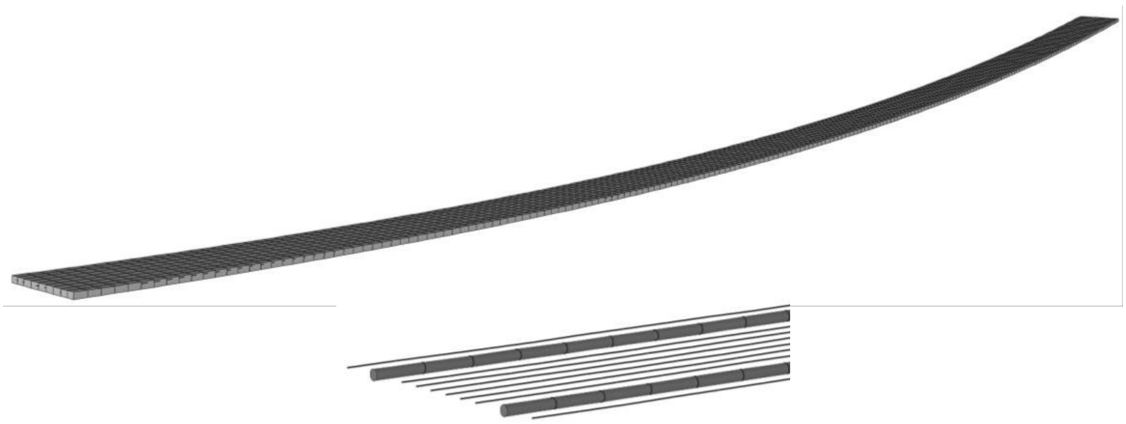

Fig. 3 Finite element model of the bridge: shell elements and position of bearing and prestressing cables

First, static analysis was carried out under the action of permanent loads (the self-weight of the bridge plus additional permanent loads) and prestressing, using geometrically nonlinear staged construction analysis. The change in axial stiffness of the cross-section due to concrete curing was taken into account, as well.
After the static analysis, a modal analysis was run to obtain the natural frequencies and mode shapes of the bridge. This was followed by a dynamic response analysis designed to calculate the maximum vertical acceleration induced by pedestrians crossing the bridge. The pedestrian harmonic loading was determined according to the HIVOSS guidelines [7], as well as the subsequent vibration serviceability evaluation. Considering the dimensions of the bridge deck along which pedestrians (P) can move freely, the bridge location, as well as its purpose, the expected level of pedestrian traffic on the bridge in most cases will not exceed density d = 0.2 P/m^2. This corresponds to a group of 60 pedestrians present on the bridge. Consequently, vibration serviceability assessment was carried out for two pedestrian-induced loading scenarios, i.e., traffic classes:

- TC1 – group of 15 pedestrians crossing the bridge,
- TC2 – traffic density d = 0.2 P/m^2.

The critical range of natural frequencies of the bridge according to HIVOSS is between 1.25 Hz and 2.3 Hz for the vertical and longitudinal direction. This frequency range corresponds to the typical range of walking frequencies (also called footfall rates) for the healthy human population. Moreover, vertical and longitudinal vibration modes with natural frequencies in the range between 2.5 Hz and 4.6 Hz can also be excited to the resonant vibrations by the second harmonic of the pedestrian force model. However, amplitudes of the second force harmonic are significantly lower than the amplitudes of the first harmonic across the whole range of footfall rates. This means that the resonant footbridge vibrations due to the second harmonic of pedestrian excitation are unlikely to reach critical values that might cause human discomforts [8].
HIVOSS suggests the minimum and the average damping factors 0.7% and 1%, respectively. In this study, the maximum acceleration response of the bridge was calculated assuming damping factors in the range between 1% and 2%.

4. RESULTS AND DISCUSSION

4.1. MODAL PROPERTIES

The first twelve natural frequencies (i.e. all bellow 5Hz) and directions of the corresponding modes (V – vertical, L – lateral, T – torsional) are presented in Tab.1, while the mode shapes are illustrated in Figs. 4-6. Note that the first vertical mode shape is asymmetric, which is influenced by the high axial stiffness of the cables in comparison to the bending stiffness of the footbridge deck. As the natural frequency of the lateral-torsional mode is out of the critical range between 0.5 Hz and 1.2 Hz for the lateral vibrations according to HIVOSS, the footbridge is unlikely to be excited by the pedestrians in the lateral direction. Therefore, only the vertical dynamic response of the bridge will be analyzed in the remaining part of the paper.

Tab. 1 First twelve natural frequencies of the bridge

Mode no.	f [Hz]	Mode direction
1	0.821	V1
2	0.960	V2
3	1.402	V3
4	1.430	LT1
5	1.771	V4
6	2.075	T1
7	2.355	V5
8	2.943	V6
9	3.409	LT2
10	3.646	V7
11	4.201	T2
12	4.394	V8

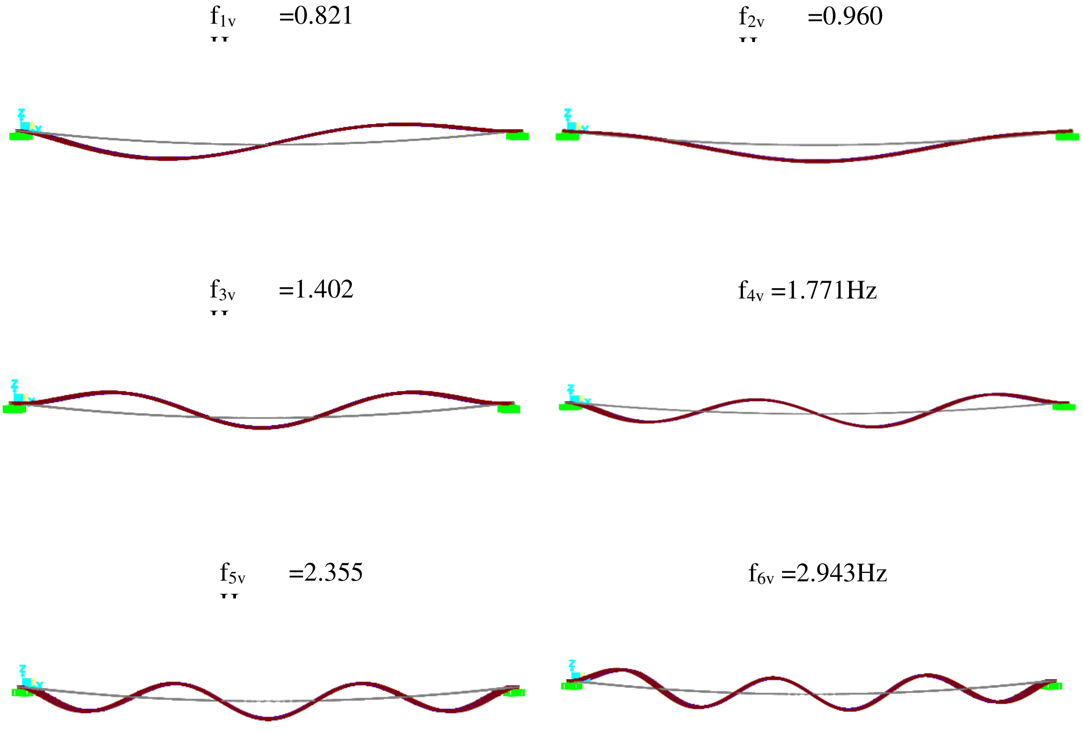

Fig. 4. First six vertical mode shapes of the bridge

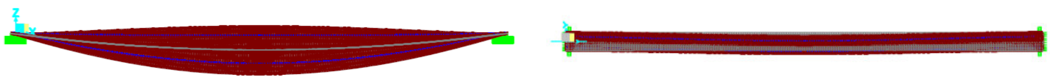

Fig. 5. First torsional mode shape of the bridge: top view (left), side view (right)

Fig. 6. First lateral-torsional mode shape of the bridge: top view (left), side view (right)

4.2. VIBRATION RESPONSE ANALYSIS

Results of the modal analysis elaborated in the previous section have shown that the vertical mode shapes V3 and V4, as well as the first torsional mode T1, are the most critical. This is because they can be excited in resonance by the first harmonic of the pedestrian-induced dynamic load. Therefore, a vibration response analysis was carried out to determine the maximum vertical acceleration response of the bridge considering only these three vibration modes. The results of numerical simulations considering relevant traffic classes and damping factors were summarized in Tabs. 2-4.

Tab. 2 Maximum vertical acceleration of the bridge considering mode V3

Traffic class	TC1 (15 P)			TC2 (0.2 P/m^2)		
Damping factor (%)	1.0	1.5	2.0	1.0	1.5	2.0
Acceleration (m/s^2)	0.10	0.08	0.07	0.19	0.16	0.14

Tab. 3 Maximum vertical acceleration of the bridge considering mode V4

Traffic class	TC1 (15 P)			TC2 (0.2 P/m^2)		
Damping factor (%)	1.0	1.5	2.0	1.0	1.5	2.0
Acceleration (m/s^2)	0.26	0.21	0.18	0.52	0.43	0.47

Tab. 4 Maximum vertical acceleration of the bridge considering mode T1

Traffic class	TC1 (15 P)			TC2 (0.2 P/m^2)		
Damping factor (%)	1.0	1.5	2.0	1.0	1.5	2.0
Acceleration (m/s^2)	0.43	0.35	0.30	0.87	0.71	0.61

The maximum acceleration responses of the bridge occurred when the walking frequency of the pedestrians matched the natural frequency of the first torsional mode shape. The damping factor, as the most uncertain parameter in the dynamic response analysis, can significantly affect the vibration levels of the bridge. According to HIVOSS, maximum pedestrian comfort due to the vertical bridge vibrations is assured by limiting the maximum acceleration to 0.5 m/s^2 (comfort class CL1). In this study, for vibration mode T1 the maximum acceleration is exceeded for all considered damping factors. On the other hand, for vibration mode V4 excessive accelerations are obtained only for 1% damping.

5. CONCLUSIONS

The finite element modelling of a stress-ribbon footbridge presented in the paper has shown that the structure exhibits complex dynamic behavior that requires a stage construction modelling approach and geometrically nonlinear analysis. This is in line with findings reported in experimental studies of already constructed stress-ribbon footbridges worldwide [4, 6].
Vibration serviceability assessment of the investigated footbridge was carried out using HIVOSS guidelines, considering two pedestrian-induced loading scenarios (i.e. two traffic classes).
The footbridge is not sensitive to lateral-induced vibrations as the natural frequency of the first lateral-torsional mode is out of the critical range for the lateral vibrations. However, there are two vertical modes and one torsional mode that can be excited in resonance by the first harmonic of the pedestrian-induced dynamic load. The torsional mode T1 was found to be the most critical, as maximum vertical acceleration response reached 0.87 m/s^2 for damping of 1%, which was beyond the acceleration limit of 0.5 m/s^2 corresponding to maximum pedestrian comfort according to HIVOSS.

ACKNOWLEDGEMENT

This research is supported by the Ministry of Science, technological development and innovations of the Republic of Serbia on Grant No. 200092.

REFERENCES

[1] Zivanovic S., Pavic A., Reynolds P. (2005). Vibration serviceability of footbridges under human-induced excitation: a literature review, *Journal of Sound and Vibration*, Volume 279, No. 1-2, pp. 1–74. https://doi.org/10.1016/j.jsv.2004.01.019.

[2] Heinemeyer C., Butz C., Keil A., Schlaich M., Goldack A., Trometer S., Lukic M., Chabrolin, Lemaire B. A., Martin P.-O., Cunha A., Caetano E. (2009). Design of Lightweight Footbridges for Human Induced Vibrations, *JRC Scientific and technical reports*.

[3] Georgiadis K., Ruiz-Teran A.M., Stafford P.J. (2022). Investigation of the static and the dynamic behaviour of stress-ribbon footbridges under pedestrian actions. *Footbridge 2022: Creating Experience*, Madrid, Spain, 07-09 September.

[4] Soria J.M., Diaz I.M., Garcia-Palacios J.H., Iban N. (2016). Vibration monitoring of a steel-plated stress-ribbon footbridge: uncertainties in the modal estimation, *Journal of Bridge Engineering*, Volume 21(8), paper ID C5015002.

[5] Zhang Y., He W., Yhang J., Dong H. (2021). Experimental and numerical investigation on dynamic properties and human-induced vibrations of an asymmetric steel-plated stress-ribbon footbridge, Advances in Civil Engineering, Volume 2021, article ID 2028378, https://doi.org/10.1155/2021/2028378.

[6] Caetano E., Cunha A. (2004). Experimental and numerical assessment of the dynamic behaviour of a stress-ribbon footbridge, *Structural Concrete*, Volume 5, Issue 1, pp. 29-38, DOI: 10.1680/stco.2004.5.1.29

[7] Hivoss (Human induced vibrations on steel structures): Design of Footbridges. Guideline. 08. September 2008.

[8] Racic, V., Pavic, A., Brownjohn, J.M.W. (2009). Experimental identification and analytical modelling of human walking forces: literature review. *Journal of Sound and Vibration*, Volume 326, pp. 1-49.

APPLICATION OF TERRESTRIAL LASER SCANNING TECHNOLOGY IN THE PROCEDURE OF CREATING AS-BUILT PROJECTS OF OBJECTS

Marijana Vujinović[1], Đuro Krnić[2], Mehmed Batilović[3], Vladimir Bulatović[4], Zoran Sušić[5]

Summary:

Terrestrial laser scanning (TLS) technology is attracting increasing interest in construction, architecture and engineering, with outstanding advantages such as highly automated, non-contact operations and the ability to collect a large amount of data in a short period of time. Today, many facilities lack the necessary technical documentation or have incomplete one, which is essential for the legalization of buildings, as well as for the maintenance and managing facility spaces, equipment, and energy systems. The paper presents the possibilities of using TLS technology to capture and update existing information about objects and create as-built documentation, using an industrial facility as an example.

Key words: terrestrial laser scanning, as-built documentation, civil engineering

[1] Teaching assistant, MSc, Faculty of Technical Sciences, University of Novi Sad, Novi Sad, Serbia, e-mail: marijana.petkovic@uns.ac.rs
[2] Teaching associate, BSc, Faculty of Technical Sciences, University of Novi Sad, Novi Sad, Serbia, e-mail: djuro.geo@uns.ac.rs
[3] Assistant professor, PhD, Faculty of Technical Sciences, University of Novi Sad, Novi Sad, Serbia, e-mail: mehmed@uns.ac.rs
[4] Full professor, PhD, Faculty of Technical Sciences, University of Novi Sad, Novi Sad, Serbia, e-mail: vbulat2003@uns.ac.rs
[5] Associate professor, PhD, Faculty of Technical Sciences, University of Novi Sad, Novi Sad, Serbia, e-mail:zsusic@uns.ac.rs

1. INTRODUCTION

The smooth management of building operations and maintenance relies on accurate and comprehensive as-built models and drawings. These essential documents not only facilitate efficient use of facility spaces, equipment, and energy systems, but also play a critical role in assessing building performance, guiding repairs and renovations, and supporting decommissioning processes [1] [2]. Despite their crucial significance, inefficiencies in generating, communicating, and updating as-built documents result in significant costs for building owners. An astonishing $1.5 billion is estimated to be lost annually due to unavailable or inaccurate as-built documents, causing delays and hindering Facilities Management (FM) personnel [3]. This problem is worsened by an additional annual expenditure of $4.8 billion on FM labour solely for validating existing as-built documentation [3].

Traditionally, verifying and creating as-built documentation has been labour-intensive and error-prone, involving manual measurements and surveys. Facility managers frequently use tape measures or laser devices to manually check dimensions, requiring a careful comparison with existing records. When predefined threshold levels are exceeded (typically around 2%), corrective actions become necessary. This has prompted the exploration of innovative remote sensing technologies like 3D laser scanning and terrestrial laser scanning, which capture accurate 3D spatial data non-invasively from a distance [4] [5].

In this context, TLS emerges as a promising and cost-effective solution, though its reliability hinges on favourable environmental conditions. For evaluating interior as-built documentation, particularly within occupied existing buildings, applying TLS technology demands rigorous real-world testing. While previous research has assessed TLS techniques in various scenarios, including historical facades [6] and construction sites [7], the intricate challenges posed by existing and occupied buildings have received limited attention.

Given this context, TLS technology has become a powerful tool in the fields of construction, architecture, and engineering. By utilizing laser-based instruments to capture precise spatial data, TLS offers unparalleled accuracy and efficiency in documenting existing structures and environments [8]. The significance of accurate as-built documentation cannot be overstated, serving as the foundation for legal compliance, effective facility management, and informed decision-making throughout a building's lifecycle. This paper aims to delve into the application of TLS technology specifically in the context of creating comprehensive as-built documentation for construction projects. By examining the capabilities, benefits, and real-world case studies, this study contributes to a deeper understanding of how TLS is revolutionizing the way we capture and utilize spatial information in civil engineering and related disciplines.

It is possible to create a comprehensive digital representation of a facility's design based on CAD models (as-designed condition). However, these models often lack detailed information regarding the actual construction of the facility (as-built condition) or its current state (as-is condition). Construction may deviate from the initial design, modifications can be made during renovations, or an accurate design model of an existing facility may not be available. These observations emphasize the need for methods to accurately document a facility's as-built or as-is conditions. Hereafter, we will use the term "as-built" for as-is.

The primary purpose of this paper is to comprehensively explore the application of TLS technology in the context of creating accurate and detailed as-built documentation for purpose of technical documentation and legalization. Through a blend of theoretical insights and practical examples, we hope to demonstrate the significant impact of TLS on the way we acquire and utilize spatial information in the construction industry.

2. TERRESTRIAL LASER SCANNING TECHNOLOGY

2.1. HOW TLS TECHNOLOGY WORKS

Terrestrial Laser Scanning (TLS) technology is a remarkable advancement in spatial data capture, essential in the fields of construction and engineering. At its core, TLS relies on highly precise laser-based instruments to acquire detailed 3D representations of physical environments. In recent years, the latest terrestrial laser scanners have shown significant improvements in performance and overall system functionality [9]. For instance, laser scanning technology has become an integral part of total stations [10]. As a result, TLS has evolved considerably, finding a wide range of practical applications.

The process starts with the TLS device emitting laser beams towards the area being examined, which could be inside a building or an outdoor construction site. When these laser beams hit surfaces within that area, they bounce back to the TLS device, creating a return signal. The length s' and two perpendicular angles, w_1 and w_2, are measured for each point where the laser beam reflects (as shown in Fig. 1). Using this data, along with the intensity of the reflected signal, the position of each point in the 3D local coordinate system can be determined. The intensity of the reflected signal is crucial for visualization, particularly in situations involving complex and dense point clouds [9].

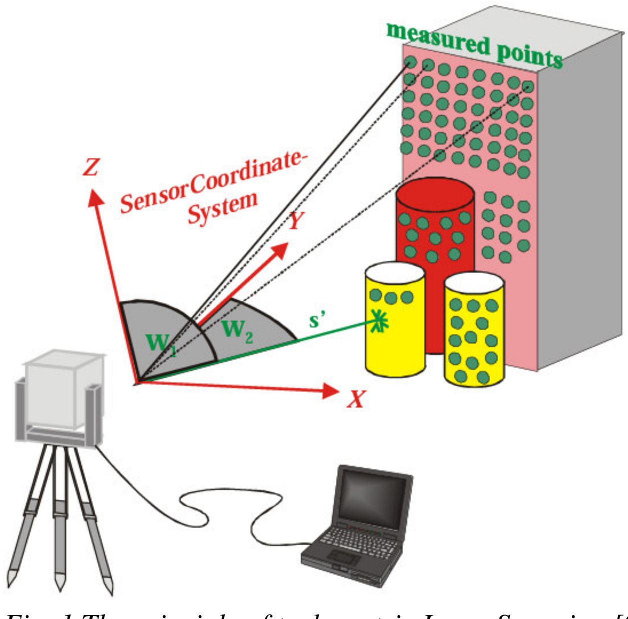

Fig. 1 The principle of tachymetric Laser Scanning [9]

TLS devices carefully measure the time it takes for the laser beams to travel to the target and back, which is known as time-of-flight measurement. This data allows for precise distance calculations, even down to millimetre-level accuracy [11].

To ensure complete coverage, multiple scans are conducted from various positions and angles. These scans are then integrated to form a comprehensive point cloud. A point cloud is a dense collection of individual data points, each representing a specific location in three-dimensional space.

Advanced software processes this point cloud data, transforming it into highly detailed 3D models, visualizations, and precise measurements. These digital representations become invaluable assets for engineers, architects, and construction professionals.

2.2. GENERAL OVERVIEW OF TLS SURVEYING PROCEDURE

Survey planning in TLS remains an area without established standard rules. However, it involves several key steps (shown in Fig. 2):

- Defining the survey area and conducting initial investigations;
- Determining the required point cloud resolution and accuracy, based on the intended final deliverables;
- Selecting an appropriate scanner;
- Identifying optimal scanning station locations to ensure sufficient coverage and accuracy and
- Choosing the types and placement of targets for registration and georeferencing.

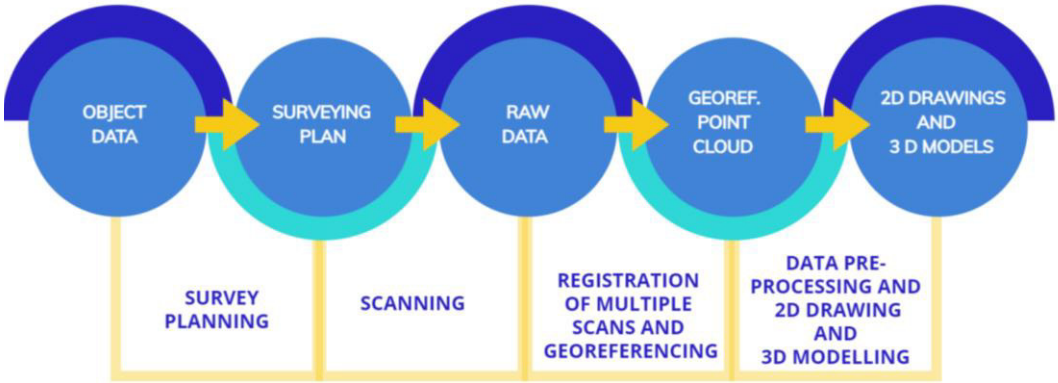

Fig. 2 TLS surveying procedure

Before commencing the scanning process, the operator positions the instrument at the designated location, specifies the 3D area to be scanned, and configures settings in the scanning software, such as sampling resolution, accuracy mode, number of scans, and pulse measurements. Throughout the scanning process, progress can be monitored on a device screen. After the scanning process is finished, the data is stored in a specified project file.

Since objects scanned with a laser scanner are often large and complex, multiple scans are typically conducted from different instrument cites. These individual point clouds are initially referenced to the scanner's internal coordinate system. To create a comprehensive representation of the scanned object, the point clouds must be registered, aligning them to a common coordinate system (e.g., the coordinate system of a chosen scan) [12]. This process is followed by combining the registered scans into a single dataset. Georeferencing involves transforming the data into the desired coordinate system, such as a national coordinate system.

Once the point clouds are registered and georeferenced, they can be used for modeling purposes and generation of 2D blueprints and drawings. The "raw" point clouds are not directly suitable for specific applications due to the presence of noise that needs to be filtered out, and the redundancy in scan overlaps must be reduced.

2.3. ADVANTAGES OF TERRESTRIAL LASER SCANNING (TLS) TECHNOLOGY

TLS technology has ushered in a transformative era in construction and engineering practices, offering a host of advantages that have reshaped the industry. TLS has the potential to be effectively used for inspection processes because of its capacity to rapidly capture objects with high precision, down to sub-millimeter accuracy [13]. This level of precision not only ensures that every detail is faithfully recorded but also substantially reduces errors and discrepancies that are more common in manual surveys.
Furthermore, TLS redefines efficiency in data acquisition. It significantly shortens project timelines by swiftly capturing copious data, even in intricate and cluttered environments. The technology's non-invasive approach enhances safety by minimizing the need for personnel to enter potentially hazardous sites or difficult-to-reach areas.
Despite an initial investment in TLS equipment and software, the efficiency and precision it offers often result in long-term cost savings, particularly in large-scale projects. This makes it a cost-effective choice, aligning with the industry's drive for increased efficiency.
The authors [14] have shown that laser scanning simplifies quality control for rebar and anchor bolt installation, reducing the need for time-consuming and labour-intensive traditional surveying methods.
The utilization of building information model (BIM) promotes information sharing and enhances communication among various managers and workers through the projects. Currently, BIM primarily relies on 2D CAD drawings, which do not faithfully represent the actual as-built state of structures or facilities (Fig. 3). This difference between the as-designed information and as-built conditions can impact the effectiveness of BIM. In recent times, the Scan-to-BIM approach has emerged as a viable solution for enhancing management during both the construction and maintenance phases by capturing dynamically updatable as-built data [15].

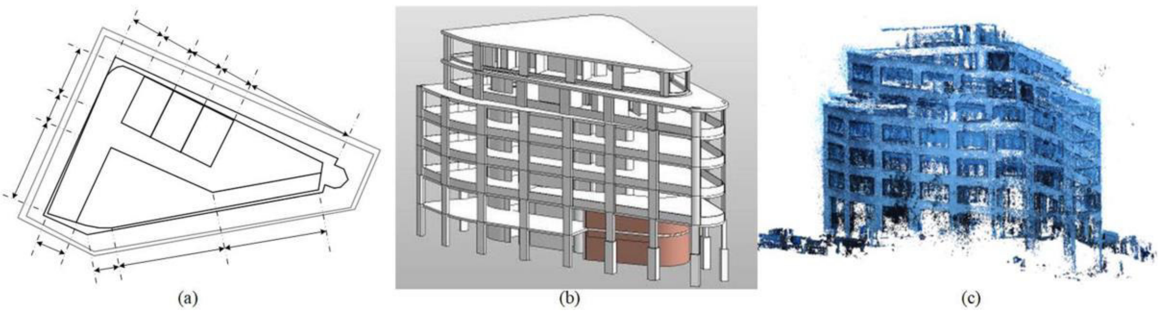

Fig. 3 Examples of a building. (a) 2D blueprint; (b) 3D BIM; (c) point cloud [15]

2.4. TLS VS. TRADITIONAL SURVEYING METHODS

When TLS technology is compared to traditional surveying methods, its significant impact on the industry becomes evident. TLS operates much faster, leading to a substantial reduction in project timelines compared to traditional surveys [8]. Additionally, extensive datasets are generated with a single scan, providing a more comprehensive view of the surveyed area than traditional methods.
Furthermore, safety is improved by TLS as it reduces the need for personnel to enter potentially dangerous or hard-to-reach locations, thus minimizing on-site risks. The non-invasive nature of the technology also decreases the risk of potential damage to structures, a concern in traditional approaches that may require physical interaction with the surveyed objects.

In terms of cost-efficiency, while there is an initial investment in TLS equipment and software, it frequently leads to cost savings over time due to increased efficiency and reduced labor requirements [13] [16].

3. NEED FOR AS-BUILT DOCUMENTATION

The need for as-built documentation arises due to the significance of precise technical documentation for buildings and facilities, the challenges posed by insufficient or missing documentation, and the legal and operational consequences of its absence.

Accurate technical documentation for buildings and facilities serves as the cornerstone of efficient facility management and maintenance. These records encompass comprehensive details about a structure's design, construction, and systems. They include essential information such as architectural plans, engineering drawings, equipment specifications, and utility layouts. The importance of these records spans the entire lifespan of a building.

Inadequate, outdated, or incomplete technical documentation introduces a lot of complications. Facility managers and maintenance personnel face difficulties in comprehending the building's systems, equipment, and spatial layout. This lack of clarity can lead to inefficient operations, increased maintenance costs, and safety concerns [17]. Inadequate documentation may also result in delays and errors during renovations, repairs, or system upgrades.

The absence of precise as-built documentation carries legal and operational ramifications. Many jurisdictions require building owners to maintain up-to-date technical records to comply with building codes and regulations. Non-compliance with these requirements can lead to legal consequences and regulatory issues. Furthermore, the absence of documentation can hinder real estate transactions, as potential buyers or lessees often require comprehensive records to assess the property's condition and adherence to regulations.

In summary, accurate technical documentation is not merely a bureaucratic formality; it is a fundamental tool for efficient facility management, safety, legal compliance, and informed decision-making throughout a building's lifecycle [17]. The lack of such documentation poses significant challenges and risks that impact both operational efficiency and legal standing in the realm of buildings and facilities.

4. CASE STUDY: AS-BUILT DOCUMENTATION FOR FACTORY

Once the point clouds are registered, they serve as the foundation for generating precise as-built models. These models include detailed information about the building's architecture, structural elements, utilities, and spatial layout. They offer a comprehensive view of the existing conditions, allowing for precise analysis, planning, and decision-making.

The utilization of TLS technology not only speeds up the data capture process but also enhances the accuracy of the resulting as-built documentation. The industrial facility which is the focus of our survey, is located in Crvenka, Vojvodina. This building includes the ground floor, an intermediate floor, the first and second floors. The Trimble TX8 terrestrial laser scanner (Fig. 4) was used for scanning each floor separately, as well as the exterior of the building.

As can be seen in Fig. 4, special markers were utilized for the registration and georeferencing of individual scans. These markers were instrumental in forming a unified point cloud within the coordinate system. During the survey, the TLS instrument is positioned at multiple locations to ensure comprehensive coverage.

Fig. 4 Trimble TX8 on cite and markers

Following data acquisition, the next crucial phase is data processing. The scans were uploaded into the Trimble Business Centre software and processed and registered into a unified coordinate system. This registration aligns the multiple scans to create a cohesive and accurate representation of the entire surveyed area. Georeferencing the TLS instrument requires a minimum of three known points to transform all TLS measurements into a common reference coordinate system. Fig. 5 visually represents the entire object as a point cloud, including and a part of the industrial facility.

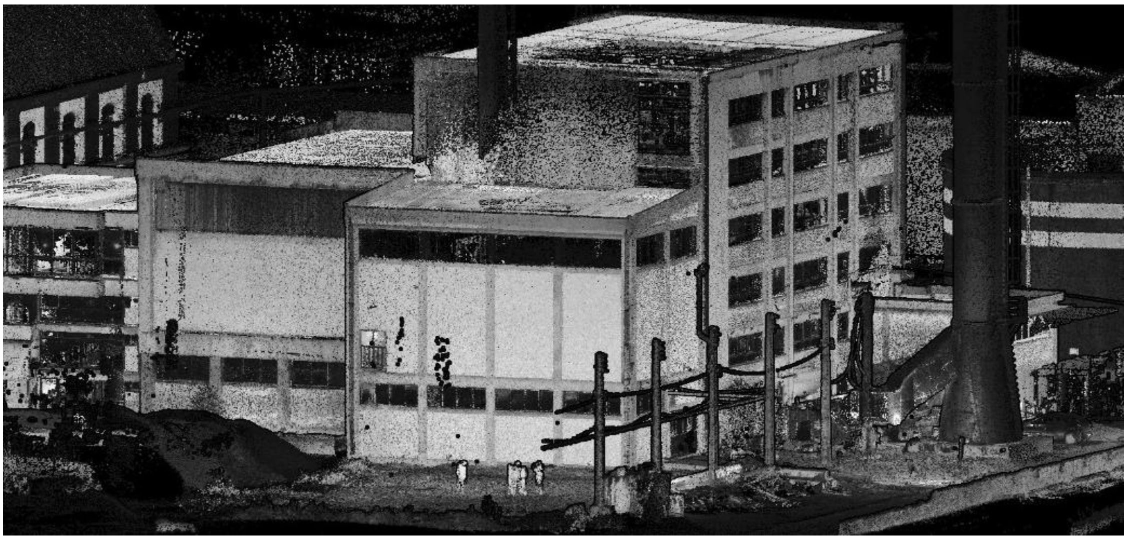

Fig. 5 Point cloud of scanned whole object

The fundamental components for 3D representation of spatial object forms are the three-dimensional coordinates of points. In addition to information about spatial coordinates, there is also data regarding light intensity. Given the fact that billions of collected points are involved, an essential aspect of processing high-resolution spatial data relates to the classification of point clouds to accurately determine their affiliation with specific floors and sections of the object.

Using the acquired point cloud data, the process of digitizing the building and all the surveyed floors was performed using MicroStation and AutoCAD, results are shown in Fig. 6. Industrial facilities pose unique challenges due to the presence of numerous specialized equipment, complex networks of pipes and cables, necessitating special attention during digitization.

Fig. 6 Floor plan of the building point cloud (left) and AutoCad drawing (right)

TLS provides a high level of accuracy in capturing facades and enables a detailed reconstruction of architectural features, including windows, doors, ornamentation, and other elements. Facade representations based on point clouds are often integrated into broader frameworks for digitizing construction projects, including BIM systems. Additionally, for the purpose of creating as-built documentation, it was necessary to create a vertical section of the object, as depicted in the Fig. 7.

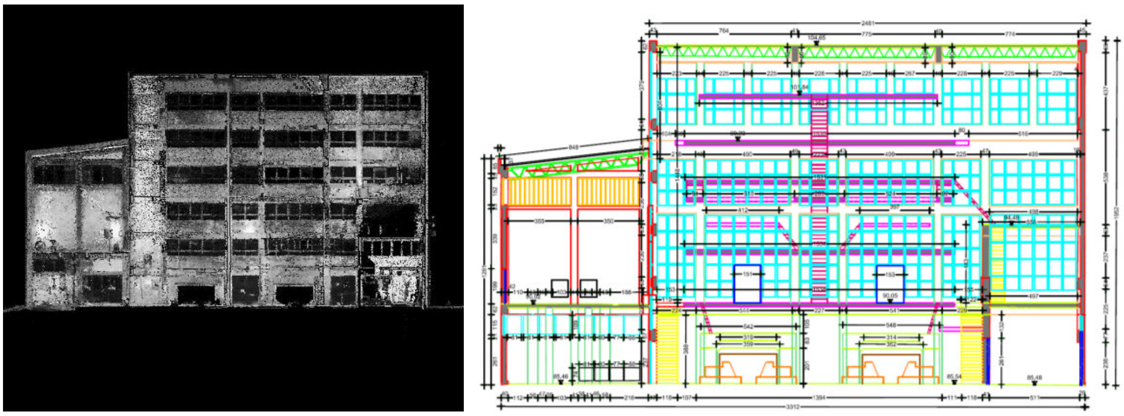

Fig. 7 Vertical section of the building point cloud (left) and AutoCad drawing (right)

5. BENEFITS, IMPACT, FUTURE TRENDS, AND CONSIDERATIONS

TLS technology offers a range of advantages. Its primary strength is its precision, providing exceptionally accurate spatial data that minimizes errors commonly associated with manual measurements. This precision also extends to efficiency, as TLS significantly reduces the time required for data capture compared to traditional methods, all while minimizing disruption to ongoing operations. TLS goes beyond simple data collection, it generates detailed as-built models that offer a comprehensive view, proving invaluable for various applications.

From a financial perspective, TLS can lead to substantial cost savings by reducing the need for repetitive surveys and manual verification. Ensuring legal compliance, especially for building legalization, is vital, and TLS technology excels in ensuring adherence to regulatory standards.

Furthermore, TLS greatly benefits facility management by providing facility managers with precise spatial data that streamlines maintenance, repairs, and renovations, reducing the need for frequent, costly, and disruptive manual surveys. The integration with BIM systems holds immense potential, allowing for real-time updates to BIM models and the creation of dynamic, comprehensive digital twins of facilities. This convergence is likely to become common practice in the construction and engineering industries.

The adoption of TLS is gradually becoming the industry standard [18]. Its potential for enhanced automation in surveys could further reduce the reliance on extensive manual post-processing, thereby increasing overall efficiency. Standardization and interoperability of TLS data across various software and systems are likely to improve data exchange and collaboration. Future TLS technology may also incorporate environmentally friendly features and data analysis methods to assess building sustainability, aligning with growing environmental considerations. Incorporating TLS into construction and engineering practices signifies not just a technological shift but a significant change in approach [7].

6. CONCLUSION

TLS technology is increasingly popular for capturing 3D objects in various applications and enables us to visualize our surroundings in 3D and 2D, which is valuable for tasks such as building restoration, renovation, design, monitoring, creation of as-built models, technical documentation and urban planning. This paper focuses on the practicality and importance of generating 2D blueprints and 3D models using TLS, demonstrating a method for obtaining information by scanning objects of interest and processing the acquired data, where almost no previous documentation existed.

It's important to note that point clouds generated in this manner (filtered and classified) provide a significant digital archive from which any spatial data of interest can be extracted later. The tools used for spatial data collection, along with cutting-edge software for processing and interpreting massive data, ensure the necessary quality and accuracy of the final data presented in the preceding tables.

In summary, this exploration of TLS technology highlights its significant impact on accurate and comprehensive "as-built" documentation. TLS technology represents a significant milestone in the construction and engineering fields. It transforms the approach to "as-built" documentation by providing efficient and precise spatial data capture. This not only enhances measurement accuracy but also provides a comprehensive perspective of construction and facility environments, reducing errors and improving documentation quality

Looking ahead, we see TLS evolving from a cutting-edge tool to a fundamental practice in construction and engineering. We trust that this paper has showcased the vast possibilities of TLS and encouraged industry experts to embrace and apply this technology in their work. By doing so, we can guide the industry toward a future characterized by heightened precision and efficiency.

ACKNOWLEDGEMENT

The research has been conducted within the project "Scientific theoretical and experimental research and improvement of educational process in the field of civil engineering", developed at the Department of Civil Engineering and Geodesy, Faculty of Technical Sciences, University of Novi Sad, Serbia.

REFERENCES

[1] Klein, L., Li, N., & Becerik-Gerber, B. (2012). Imaged-based verification of as-built documentation of operational buildings. *Automation in construction*, Volume 21, pp. 161-171. https://doi.org/10.1016/j.autcon.2011.05.023.

[2] Akcamete, A., Akinci, B., & Garrett, Jr, J. H. (2009). Motivation for computational support for updating building information models (BIMs). *In Computing in Civil Engineering*, pp. 523-532. https://doi.org/10.1061/41052(346)52.

[3] GCR, N. (2004). Cost analysis of inadequate interoperability in the US capital facilities industry. *National Institute of Standards and Technology (NIST)*, pp. 223-253.

[4] Brilakis, I., Lourakis, M., Sacks, R., Savarese, S., Christodoulou, S., Teizer, J., & Makhmalbaf, A. (2010). Toward automated generation of parametric BIMs based on hybrid video and laser scanning data. *Advanced Engineering Informatics*, Volume 24(4), pp. 456-465. https://doi.org/10.1016/j.aei.2010.06.006.

[5] Tang, P., Huber, D., Akinci, B., Lipman, R., & Lytle, A. (2010). Automatic reconstruction of as-built building information models from laser-scanned point clouds: A review of related techniques. *Automation in construction*, Volume 19(7), pp. 829-843. https://doi.org/10.1016/j.autcon.2010.06.007.

[6] Heras, V., Sinchi, E., Briones, J., & Lupercio, L. (2019). Urban heritage monitoring, using image processing techniques and data collection with terrestrial laser scanner (TLS), case study cuenca-Ecuador. *The International Archives of the Photogrammetry, Remote Sensing and Spatial Information Sciences*, Volume 42, pp. 609-613. https://doi.org/10.5194/isprs-archives-XLII-2-W11-609-2019.

[7] Wu, C., Yuan, Y., Tang, Y., & Tian, B. (2021). Application of terrestrial laser scanning (TLS) in the architecture, engineering and construction (AEC) industry. Sensors, Volume 22(1), pp.265. https://doi.org/10.3390/s22010265.

[8] Nguyen, T. A., Nguyen, P. T., & Do, S. T. (2020). Application of BIM and 3D laser scanning for quantity management in construction projects. *Advances in Civil Engineering*, *2020*, pp. 1-10. https://doi.org/10.1155/2020/8839923.

[9] Staiger, R. 10 years of terrestrial laser scanning-technology, systems and applications (2011). *Interexpo Geo-Siberia* (2011), pp. 43–55.

[10] Lachat, E., Landes, T., & Grussenmeyer, P. (2017). Investigation of a combined surveying and scanning device: The Trimble SX10 scanning total station. *Sensors*, Volume 17(4), pp. 730. https://doi.org/10.3390/s17040730.

[11] Teng, J., Shi, Y., Wang, H., & Wu, J. (2022). Review on the Research and Applications of TLS in Ground Surface and Constructions Deformation Monitoring. *Sensors*,Volume 22(23), pp. 9179. https://doi.org/10.3390/s22239179.

[12] Kuzmić, T., Marković, M., Batilović, M., & Bulatović, V. (2021). Application of Terrestrial Laser Scanning Technology for the Purpose of Creating 3D Models of Objects. *FIG-e Working Week (2021)*, Virtually in Netherlands, 21-25 June.

[13] Rashidi, M., Mohammadi, M., Sadeghlou Kivi, S., Abdolvand, M. M., Truong-Hong, L., & Samali, B. (2020). A decade of modern bridge monitoring using terrestrial laser scanning: Review and future directions. *Remote Sensing*, Volume 12(22), pp. 3796. https://doi.org/10.3390/rs12223796

[14] Hajian, H., & Brandow, G. (2012). As-built documentation of structural components for reinforced concrete construction quality control with 3D laser scanning. In *Computing in Civil Engineering (2012)*, pp. 253-260. https://doi.org/10.1061/9780784412343.0032

[15] Xu, Y., & Stilla, U. (2021). Toward building and civil infrastructure reconstruction from point clouds: A review on data and key techniques. *IEEE Journal of Selected Topics in Applied Earth Observations and Remote Sensing*, Volume 14, pp. 2857-2885. https://doi.org/10.1109/JSTARS.2021.3060568.

[16] Soni, A., Robson, S., & Gleeson, B. (2015). Structural monitoring for the rail industry using conventional survey, laser scanning and photogrammetry. *Applied Geomatics*, Volume *7*, pp. 123-138. https://doi.org/10.1007/s12518-015-0156-1.

[17] Woo, J., Wilsmann, J., & Kang, D. (2010). Use of as-built building information modeling. *Construction Research Congress 2010: Innovation for Reshaping Construction Practice*, Maz, pp. 538-548. https://doi.org/10.1061/41109(373)54.

[18] Badenko, V., Fedotov, A., Zotov, D., Lytkin, S., Volgin, D., Garg, R. D., & Liu, M. (2019). Scan-to-BIM methodology adapted for different application. *The International Archives of the Photogrammetry, Remote Sensing and Spatial Information Sciences*, Volume 42, pp. 1-7. https://doi.org/10.5194/isprs-archives-XLII-5-W2-1-2019.

IMPACT OF THE IMPERMEABLE LINING OF TAILINGS RESERVOIR TO THE HYDRODYNAMIC INSTABILITY OF TAILINGS DAM

Mircevska Violeta[1], Nanevska Ana[2]

Summary:

This paper discusses the second part of an analytical study on seepage related processes in a tailings dam-impoundment system. The analysis includes parameters such as potential field, pore pressure distribution, seepage velocities, critical and manifested hydraulic gradients, and the potential for piping and heave effects due to erosion. To demonstrate their importance in hydrodynamic dam stability, an existing tailings dam-impoundment system was assessed for three seepage boundary conditions of different impermeable lining conditions, for which the critical zones with potential for internal erosion were analyzed. The main conclusion of the study is that the installation of impermeable lining can significantly affect seepage velocities and pore pressure distribution, potentially triggering hydrodynamic instability in the dam. Therefore, when local environmental protection demands seepage barriers, a comprehensive engineering assessment of the expected negative hydrodynamic effects is essential.

Key words: finite element modeling, tailings dams, seepage analysis, seepage conditions, hydrodynamic stability

[1]Prof, Institute of earthquake engineering and engineering seismology, University St. Cyril and Methodius, Skopje, R. N. Macedonia, mircevska@iziis.ukim.edu.mk
[2]Assist. MSc., Institute of earthquake engineering and engineering seismology, University St. Cyril and Methodius, Skopje, R. N. Macedonia, nanevska@iziis.ukim.edu.mk

1. INTRODUCTION

Hydrodynamic effects are crucial for the design, construction, and operation of tailings dams. A profound knowledge is required to assess the overall stability of tailings dams, including the slope stability and the internal erosion processes that can lead to piping and heave failure. At sufficiently high hydraulic gradients, tailing dams may be subjected to permanent hydrodynamic deformations as a result of the mobilization of soil particles, such as erosion, suffusion, and heave effect. Numerous studies identified internal erosion due to poor compaction, differential settlement, frost action, desiccation, etc., as one of the main forms of hydrodynamic deformation behind failures of earth structures [1]. A special case of erosion is backward erosion, where the material first starts to erode at the free unfiltered exit of the seepage path followed by retrograde erosion, which may continue all the way to the dam`s upstream slope [2]. Piping refers to internal erosion along a seepage pathway with a formation of a low-pressure conduit allowing concentrated flow. Piping with sufficient velocity to erode the embankment face may generate local or general failure of the embankment [3].

Suffusion, on the other hand, is a type of erosion process occurring in internally unstable materials and manifested with selective dislodging of the fine particles from the coarser soil skeleton whose volume remains unchanged [3]. Taking place mainly in soils with bimodal structure, the suffusion gradually decreases the density and the coefficient of uniformity, increasing the porosity and the hydraulic conductivity and creating conditions favorable for internal erosion. The soil stability can also be compromised with the progressive decrease of the stress tensor as the pore pressure increases. The strength loss occurs because of the contractive nature of the loaded loose soil. Since the contraction is not allowed due to the incompressibility of the pore water, outward stresses are generated as counteraction which decreases soil stresses. The undrained soft and loose soils are as well prone to the effect of flow liquefaction resulting from the strain softening behavior concomitant with continuous reduction of the shear resistance and additional plastic shear strains [4]. During the stationary seepage in soft, loose, and mainly contractive soils, the outward pore pressures could eventually reduce the total mean and/or the total vertical stress generating a concentrated heave, also known as a blowout or static liquefaction. The static liquefaction is provoked, in general, by triggering mechanisms such as overloading (rapid raising rate, construction activities at crest), changes in pore pressure (rapid construction rate, intense rainstorms, high pond levels), overtopping, as well as by the reduction of lateral confinement (due to erosion) of the downstream slope [5].

The research conducted in this study is based on the analysis discussed in the first part of a comprehensive study of tailings dams, presented in the paper entitled "Finite element modeling and seepage analyses to assess the hydrodynamic effects of tailings dams under different seepage conditions" [6]. This paper focuses on analyzing seepage under various scenarios of seepage forces and confining static stresses using a coupled fluid-solid finite element model. The rate of seepage is estimated using a conventional flow net analysis, assuming steady seepage conditions. The study determines excess pore pressure, seepage velocities, and both manifested and critical hydraulic gradients.

2. CRITICAL HYDRAULIC GRADIENT

The hydrodynamic deformation processes and the embankment stability are directly related to the seepage rate. The potential of piping failure is determined by comparing the actual hydraulic gradient to the evaluated critical hydraulic, emphasizing the need for accurate knowledge of the expected critical hydraulic gradient. Traditionally, its assessment is based on empirical evidence in field conditions, laboratory measurements and theoretical and analytical studies.

A significant amount of research has been done studying quantitatively the hydraulic gradients critical to trigger internal erosion and their limit values for which the shear strength of confined soil is reduced by drag forces of the seeping water. Indraratna et al. [7] proposed a practical definition of the critical gradient as the ratio between the buoyant unit weight of soil and the unit weight of water. However, such definition may be quite inaccurate since the critical gradient in piping depends on inherent soil properties, such as grain size, gradation, and porosity, inter particle friction as well as the boundary friction, compaction, interlocking effect of the angular soil particles, etc. [2]. The gravity also has a significant influence on the material transport, and it is important to consider the flow direction, i.e., horizontal, upward, or downward flow. Richards et al. [8] developed a true triaxial piping test apparatus to measure the critical hydraulic gradient and the initiating critical velocity at which piping in cohesionless soil begins. The authors investigated the relationship between the seepage direction and gravity and demonstrated that the critical velocity provides more valuable information on piping initiation than is the critical gradient. On the other hand, Wan et al. [9] introduced the hole erosion and the slot erosion tests to study the erosion characteristics, such as the erosion rate index and the critical erosion shear stress at which erosion begins. Investigating the piping erosion in sand, confirmed was the increase of the critical hydraulic gradient with increased particle size and hydraulic conductivity of the material, and defined was the correlation between the critical gradient and the coefficient of uniformity C_u, [10].

The recent experimental study by Quanyi et al. [11] considered the internal erosion in homogeneous materials as function of the degree of compaction and particle roughness, where the soil compaction and clay content contributed to the increase of the critical hydraulic gradient from 10 to up to 70%. Jahanzaib et al. [12] conducted experimental investigations to quantify the critical hydraulic gradients in internally unstable non-uniform sand and gravel mixtures and stable uniform fine sands. It was concluded that for upward flow in unstable soil the critical hydraulic gradients are lower than unity. It was also found that the relative density in stable soils has a strong effect on the critical hydraulic gradients. Wan et al. [13] modified the expression for the critical hydraulic gradient, as given by Terzaghi et al. [14] introducing a hydraulic gradient at which particle erosion and boiling begin. In this paper, the critical hydraulic gradient is assessed considering the relatively simple expression of Perzlmaier [15] where two different critical gradients were considered for flow to an unfiltered exit and for flow within the soil matrix. The critical gradient for unfiltered exit, i_{crit}, is given with the following equation:

$$i_{crit} = \frac{(1-n)(\gamma_s - \gamma_w)}{\gamma_w} \tag{1}$$

where n is porosity, γ_s is the specific weight of soil and $\gamma_w$is the specific weight of water. For a seepage throughout the soil matrix the critical gradient value is reduced in the range of 70 to 80% of the critical gradient for unfiltered exit. The criterion for suffusion according to Perzlmaier [15] is correlated positively to the coefficient of uniformity,C_u , indicating higher risk for suffusion with the increase of C_u as follows,

$$i_{crit} = \begin{Bmatrix} 0{,}3\ to\ 0{,}4 & for & C_u < 10 \\ 0{,}2 & for & 10 \le C_u \le 20 \\ 0{,}1 & for & C_u > 20 \end{Bmatrix} \tag{2}$$

3. HYDRAULIC GRADIENTS

Figure 1 presents the distribution of the critical hydraulic gradient, which applies for the three considered models [6]. It was calculated for the sand embankment, starter dike and stone fill support applying the empirical equation 1, according to data given in Table 1 [6]. The estimated critical hydraulic gradient is below one within the sand embankment, except in the lower part where it varies between 1.0 and 1.4. The critical hydraulic gradient in the domain of the starter dike is, i_c=1.2. The maximum value of the critical hydraulic gradient, i_c=1.4 appears in the lower half of the supporting rockfill. The distribution of the manifested hydraulic gradients generated by the seepage forces in all three models is shown in Fig. 2a, Fig. 2b, Fig. 3a and Fig. 4a.

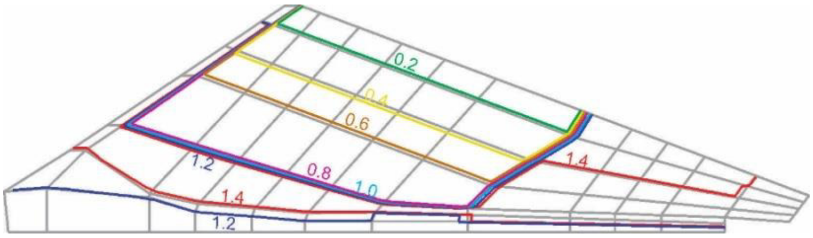

Fig. 1 Distribution of the critical hydraulic gradient.

Model A: The extreme hydraulic gradient of 5 occurs at the top of the starter dike, (Fig. 2a, Fig. 2b). Other zones with larger hydraulic gradients can also be observed, such as at the interface starter dike-send embankment-vertical drain with a value of 3. A few such zones are also located at the downstream slope of the sand embankment, varying between 1 and 3. Larger hydraulic gradient occurs as well at the toe of the drainage carpet and the outlet channel at the bottom age of the supporting rockfill. It is now possible to evaluate the zones which are critical for erosion of soil particles. They are completed when the ratio between the manifested (actual) hydraulic gradient and the allowable critical hydraulic gradient is higher than one (Fig. 2c and Fig. 2d). Several such zones can be observed: (i) at the top of the starter dike (ratio=4), (ii) on the downstream face of the sand embankment (ratio=10~15), and (iii) the zone at the interface of the sand embankment with the drain carpet at the downstream edge of the model (ratio=3). In addition to the high ratio, the erosion potential builds up when seepage occurs through cracks or compaction deficiencies in the upper relatively poorly compacted layers of the sand embankment.

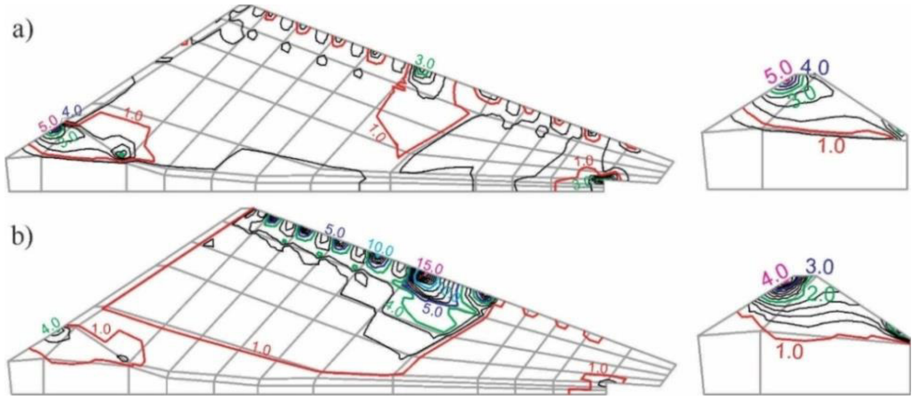

Fig. 2 Model A: a) manifested hydraulic gradients in the sand embankment, the starter dike and in the stone fill support, (equidistance 0.5), b) manifested hydraulic gradients in the starter dike, (equidistance 0.5), c) critical zones for soil erosion in the sand embankment and in the starter dike, (equidistance 1), and d) critical zones for soil erosion in the dike, (equidistance 0.2).

This means that hydraulic instability of the respective critical zones can endanger the stability of the entire dam. However, in well compacted soil environments, the critical gradient threshold can be increased as much as 70% with respect to values given in equation 1. Also, the presence of friction forces between the soil parts further opposes the movement of the particles. Consequently, the potential for erosion can be reduced respectively.

Model B: As opposed to model A, where the maximum manifested hydraulic gradient occurs at the upper part of the starter dike, here the maximum manifested hydraulic gradient occurs at the bottom of the starter dike at the upstream slope with a magnitude of 6.5 (Fig. 3a). Actually, in the whole domain of the starter dike, the manifested hydraulic gradient is larger than the allowable value of 1.2. The only exception is at the crown of the starter dike where the manifested hydraulic gradient equals the allowable. At the same time, the most critical zone for erosion appears at the bottom of the starter dike with 5.4 times higher ratio than the allowable, Fig. 3b. Although the critical gradient value increases for 70% in the well compacted soil just like the starter dike, and assuming that in this zone the potential of erosion is additionally reduced due to the presence of friction forces between the soil particles that further oppose their movement, the potential of erosion still exists.

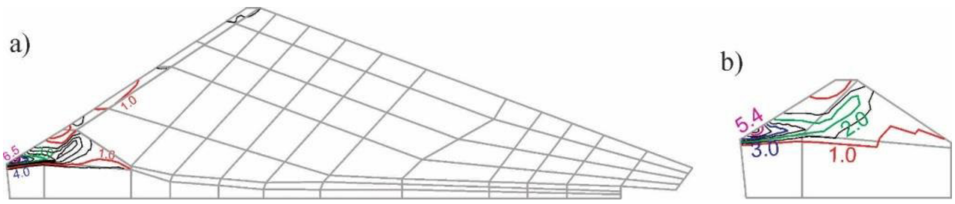

Fig. 3 Model B: a) manifested hydraulic gradient in the starter dike and sand embankment, (equidistance 0.5) b) critical zones for soil erosion in the starter dike, (equidistance 0.5).

Contrary to the seepage model A, where most critical zone appears in the upper part of the dike, in case of the model B it appears at the lower part of the starter dike close to the natural gravely sediments, which makes the hydraulic instability less likely to occur.

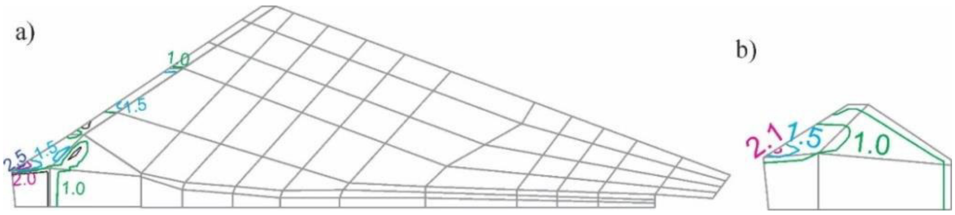

Fig. 4 Model C: a) manifested hydraulic gradient in the starter dike and sand embankment and b) critical zones for soil erosion in the starter dike, (equidistance 0.5).

Model C: Similarly to model B, the maximum manifested hydraulic gradient of 2.5 occurs at the bottom of the starter dike at the upstream slope (Fig. 4a). The remaining parts of the starter dike have hydraulic gradient close to the allowable. The critical zone for the erosion potential with a ratio of 2.1 times higher than the allowable is visible in Fig. 4b. However, respecting the substantial compaction in this zone as well as the positive impact of fiction between the soil particles, this potential becomes insignificant.

4. HEAVE POTENTIAL (STATIC LIQUEFACTION)

Static liquefaction or heave occurrence can trigger dam failures, manifested via internal erosion and/or slope instability. The heave effect is mainly generated by confined seepage flow concentrated in a high permeability layer overlaid by low permeability layer, under conditions of first filling of the reservoir, as well as in cases of pore pressures increase due to erosion or suffusion, or blockage of drains and pressure relief walls. In the considered tailings dam, the latter two phenomena can initiate heaving as a balance problem between upward pore water pressure due to buoyancy force and downward static loads resulting in a zero-effective stress. At the soil particle level, the pressure force acts outward, uniformly in all directions, whereas the spherical stress acts in the same manner, but in the opposite (inward) direction. The heave potential F can then be expressed by the following equation,

$$F = \frac{\sigma_0}{U} \tag{3}$$

where, σ_0 is the total spherical (mean) stress and U is the pore water pressure at the same stress point for flow in both horizontal and upward direction.

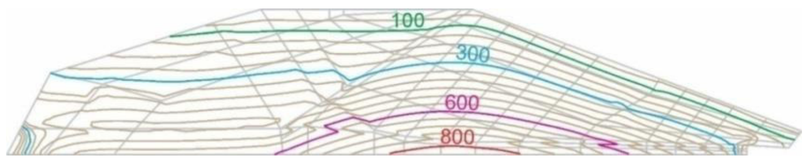

Fig. 5 Total spherical static stresses σ_0 (kPa). Equidistance is 50 (kPa).

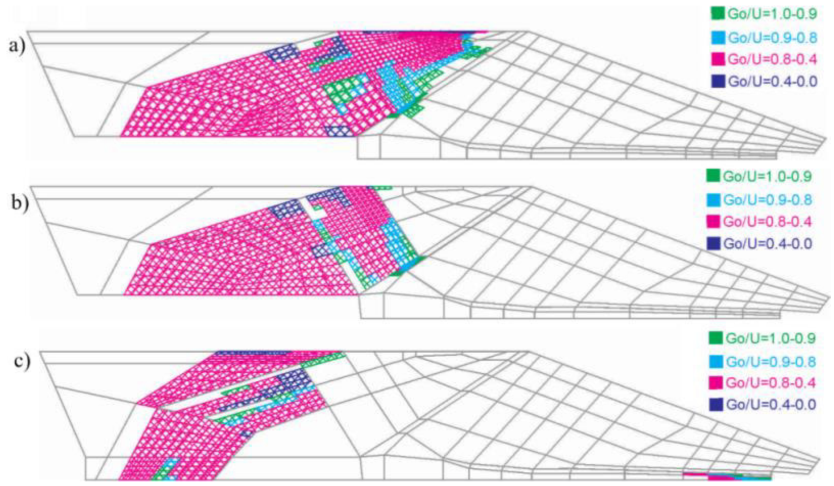

Fig. 6 Heave potential (static liquefaction): for: a) model A, b) model B, and c) model C.

Accordingly, the static liquefaction in the form of heave effect is possible in zones where the ratio between the spherical total stress and the pore pressure becomes equal or lower than 1. In the present analysis a factor of safety against heave of 1,5 is assumed to be compatible with the degree of uncertainty of the prediction pressure. The single lift static analysis conducted herein is based on the ideal elasto-plastic Mohr-Coulomb material model considering zones of increasing soil stiffness with depth. Since the softer soils of the dam start to exhibit nonlinear behaviour with the beginning of the loading, the stress state is defined considering the secant modulus corresponding to 50% of the soil strength E50, for each distinct soil stiffness zone. Figure 5 depicts the distribution of the total spherical static stresses for the example tailings dam-impoundment system.

Figure 6 shows the heave potential for the three seepage models. For model A, the small σ_0/U ratio in the range of 0.4~0.8, indicates that static liquefaction may occur in large part of the tailing's impoundment (Fig. 6a). Near the upstream slope of the starter dike, just below the crest, and in a narrow zone of send embankment in vicinity to the downstream slope of the starter dike, the ratio varies in the range of 0.9~1.0, whereas above the starter dike the ratio decreases slightly in the range of 0.8~0.9. The seepage model B displays a similar heave potential as that of model A (Fig. 6b). However, whereas the starter dike and the sand embankment above the dike crest exhibit similar heave potentials, the upper part of the impoundment near the upstream slope of the sand embankment appears not affected at all. In the case of model C, the heave potential is simulated only partially in the impoundment zones, distanced from the upstream slopes of the starter dike and sand embankment, and doesn't appear to impact the stability of the tailings dam-impoundment system (Fig. 6c).

5. CONCLUSIONS

The critical hydraulic gradient reflects the soil inherent properties and the compaction effect, while the manifested (actual) hydraulic gradient reflects the soil permeability and the seepage conditions. Critical zones with potential for internal erosion were identified when the ratio between the manifested hydraulic gradient and the critical hydraulic gradient was larger than one. For model A, critical zones were the top of the starter dike (ratio=4), the downstream slope of sand embankment (ratio=10~15), and the interface of the sand embankment with the drain carpet at the downstream edge of the model (ratio~3). The model B displayed critical zones for erosion at the bottom of the starter dike (ratio=5.4), which being on top of the natural gravely sediments is less prone to hydraulic instability. The model C showed the lowest potential for erosion, insignificant for tailings dam stability. The model A had also the highest susceptibility to static liquefaction, whereas the hydrodynamic stability of the model C was not affected since the detected liquefiable zones in the impoundment were located far from the upstream face of the starter dike and sand embankment.

The main conclusion of the seepage analyses is that the installation of impermeable lining can have significant impact on the seepage velocities and pore pressure distribution and can initiate hydrodynamic instability of tailings dam. Therefore, when local environmental settings require protection with seepage barriers, a comprehensive engineering assessment of the expected negative hydrodynamic effects has to be made.

6. REFERENCES

[1] Foster M., Fell R., Spannagle M. (2000). The statistics of embankment dam failures and accidents. *Canadian Geotechnical Journal*, Volume 37 (5), https://doi.org/10.1139/t00-030.

[2] Richards K. S., Reddy K. R. (2007). Critical appraisal of piping phenomena in earth dams. *Bulletin of Engineering Geology and the Environment*, Volume 66 (4), pp. 381-402, https://doi.org/10.1007/s10064-007-0095-0.

[3] Chang D. S., Zhang L. M. (2013). Extended internal stability criteria for soils under seepage. *Soils and Foundations*, Volume 53 (4), pp. 569-583, https://doi.org/10.1016/j.sandf.2013.06.008.

[4] De Jager R. (2006). The behaviour of solids during static liquefaction in geotechnical engineering. *Master thesis Delft University of Technology*, Netherlands.

[5] Fourie A. B., Tshabalala L. (2011). Initiation of static liquefaction and the role of K0 consolidation. *Canadian Geotechnical Journal*, Volume 42 (3), pp. 892-906.

[6] Nanevska A., Mircevska V. (2023). Finite element modeling and seepage analyses to assess the hydrodynamic effects of tailings dams under different seepage conditions. *In conference iNDiS 2023*,16-17 November 2023, Novi Sad, Serbia (presented in this conference).

[7] Indraratna B., Radampola S. (2002). Analysis of Critical Hydraulic Gradient for Particle Movement in Filtration. *Journal of Geotechnical and Geoenvironmental Engineering*. Volume 128 (4), pp. 347-350.

[8] Richards K. S., Reddy K. R. (2010). True Triaxial Piping Test Apparatus for Evaluation of Piping Potential in Earth Structures. *Geotechnical Testing Journal*, Volume 33 (1), pp. 83–95, https://doi.org/10.1520/GTJ102246.

[9] Wan C. F., Fell R. (2004). Investigation of Rate of Erosion of Soils in Embankment Dams. *Journal of Geotechnical and Geoenvironmental Engineering*, Volume 130 (4), pp, 373–380, https://doi.org/10.1061/(ASCE)1090-0241(2004)130:4(373).

[10] Schmertmann J. H. (2015). The Non-Filter Factor of Safety Against Piping Through Sand. *Proceedings of Geo-Congress' 98*, ASCE Geotechnical Special Publication 111, Reston, VA, pp. 65-132, https://doi.org/10.1061/9780784405376.006.

[11] Quanyi X., Jian L., Bo H., Hongtao L., Yuying L., Xuanzheng L. (2018). Critical Hydraulic Gradient of Internal Erosion at the Soil–Structure Interface. *Processes*, Volume 6 (7), pp. 92, https://doi.org/10.3390/pr6070092.

[12] Jahanzaib, I. Indraratna, B. (2019). Study of Critical Hydraulic Gradients for Seepage-Induced Failures in Granular Soils. *Journal of Geotechnical and Geoenvironmental Engineering*, Volume 145 (7), https://doi.org/10.1061/(ASCE)GT.1943-5606.0002062.

[13] Wan C. F., Fell R. (2008). Assessing the potential of internal instability and suffusion in embankment dams and their foundations. *Journal of Geotechnical and Geoenvironmental Engineering*, Volume 134 (3), pp. 401-407.

[14] Terzaghi K., Peck R. B. (1948). Theoretical Soil Mechanics in Engineering Practice, *A Wiley Inter Science Publication*, John Wiley & Sons Inc., New York.

[15] Perzlmaier S. (2007). Distributed filter speed measurement in dams (in German). *Ph.D. Thesis*, Technical University of Munich, Germany.

FINITE ELEMENT MODELING AND SEEPAGE ANALYSES TO ASSESS THE HYDRODYNAMIC EFFECTS OF TAILINGS DAMS UNDER DIFFERENT SEEPAGE CONDITIONS

Nanevska Ana[1], Mircevska Violeta[2]

Summary:

Comprehending hydrodynamic effects is crucial for tailings dam design, construction, and operation, as they impact the overall stability of the dam, including the downstream slopes and the risk of internal erosion leading to piping and heave failure. This study discusses the first part of a comprehensive study of tailings dams, focused on analysis of seepage under various seepage forces and static stresses using a coupled fluid-solid finite element model. The seepage rates are estimated through conventional flow net analysis, assuming steady seepage conditions. The study evaluates excess pore pressure, seepage velocities, and hydraulic gradients. In order to assess hydrodynamic stability, three different 3D models of isotropic stationary seepage were examined, each with a different impermeable lining option to mitigate environmental concerns. The evaluation of the stress tensor relies on finite element analysis, utilizing the Mohr-Coulomb material model as a "first-order" approximation of the soil's elasto-plastic behaviour.

Key words: finite element modeling, tailings dams, seepage analysis, seepage conditions, hydrodynamic stability

[1] Asist. MSc, Institute of Earthquake Engineering and Engineering Seismology, University St. Cyril and Methodius, Skopje, R. N. Macedonia, nanevska@iziis.ukim.edu.mk
[2] Prof., Institute of Earthquake Engineering and Engineering Seismology, University St. Cyril and Methodius, Skopje, R. N. Macedonia, mircevska@iziis.ukim.edu.mk

1. INTRODUCTION

Tailings dams are a by-product of the mining industry activities in the process of extracting minerals from the ore, are constructed incrementally, gradually integrating mine waste as the fill material. In this way, they can be considered as a type of embankment dam made predominantly from tailings material. Due to their resemblance, the procedures for design, construction and maintenance of tailings dams are largely based on established practices for embankment dams. However, it's important to note that numerous instances of heavy damage and collapse have occurred in tailings dams, a total of 351 failures have been recorded in the last 100 years [1] [2]. Their failure rate was estimated to be at about 1.0% over a century, a rate ten times higher than that of conventional embankment dams, which is also well above what is expected for geotechnical structures [3]. Moreover, a simple statistical analysis of the past decade showed that the occurrence rate of destructive failures has remained consistent with that of the preceding ten years [4]. These findings suggest that safe construction of tailings dams with graded tailings material is a complex issue, and the design procedures should not be solely based on methods suitable for all embankment dams [5].

Tailing dams possess several characteristics that render them susceptible to damage and danger to the environment [6]. First and foremost, they are constructed using local sandy soils and deposed tailings, resulting in gradual increase of the dam heigh along with the height and volume of the impoundment domain. Secondly, due to the substantial quantity of loose and saturated tailings material, these dams present significant hazard to the downstream environment, necessitating ongoing monitoring and maintenance throughout both the active mining phase and the post-exploration period. Thirdly, the absence of specific regulations for tailings dam often leads to ad-hoc engineering solutions to address all of the aforementioned shortcomings. Collapses of tailings dams can be attributed to several associated failure mechanisms [6]. According to ICOLD bulletins [7], these primary mechanisms encompass static and dynamic liquefaction, internal and external erosion, suffusion, inadequate foundation, overflow of water and tailings over the dam's crest, seismic instability and more.

A study conducted by Foster et al. [8] found that erosion, piping and heave effects contributed to around 30% of tailings dams failures globally. The most comprehensive data on 351 failures can be accessed through the Center for Science in Public Participation – CSP2 [2]. Piciullo et al. [1] utilized this dataset in their statistical analysis aimed at understanding the trend of tailings dam collapses from 1915 to 2019, revealing an average of 2.5 failures annually (Figure 1). Figure 2 illustrates the primary causes of tailings dams failures. According to this data, the most common reasons for these failures are overtopping at the dam crest and static and dynamic liquefaction, aligning with the findings of ICOLD [7]. The statistics also indicate that vertically constructed dams are particularly susceptible to damage (32%), mainly due to static liquefaction (slope instability) and dynamic liquefaction, resulting from hydraulic events. Other significant factors contributing to the past failures include internal erosion due to uncontrolled seepage or piping (21.6%), overtopping (20.6%), foundation issues (17.3%), seismic activity (17.0%), and other factors, such as mine subsidence and structural problems [3].

Comprehending the hydrodynamic effects is of utmost importance when it comes to analysing tailings dams. Since they undergo changes in safety and stability through their construction and operational phases due to the gradual consolidation settlement accompanied with pore pressure dissipation [9], they must meet rigorous criteria for long-term stability, ideally with minimal or no need for ongoing maintenance. This includes evaluating their impact on the overall stability, including factors such as the downstream slope and internal erosion processes that can lead to piping and heave, i.e. the mitigation of finer particles initiated by seepage pressure. The seepage pressure and rate is influenced by various factors, including the elevation of the phreatic surface, hydraulic gradient, grain size distribution, the progression of consolidation, internal structure, and more [10]. In order to address environmental concerns and prevent uncontrolled leaching and release of toxic substances into the surface and groundwater, liners in the form of seepage barriers are commonly employed. However, the influence of these liners on the seepage flow has to be analytically examined. The best approach for analysing the stability of the dam involves using coupled fluid-solid mathematical models that consider steady seepage with conventional flow net analysis [11] [12] and finite element approach to assessment of the stress field based on reliable constitutive material models [13].

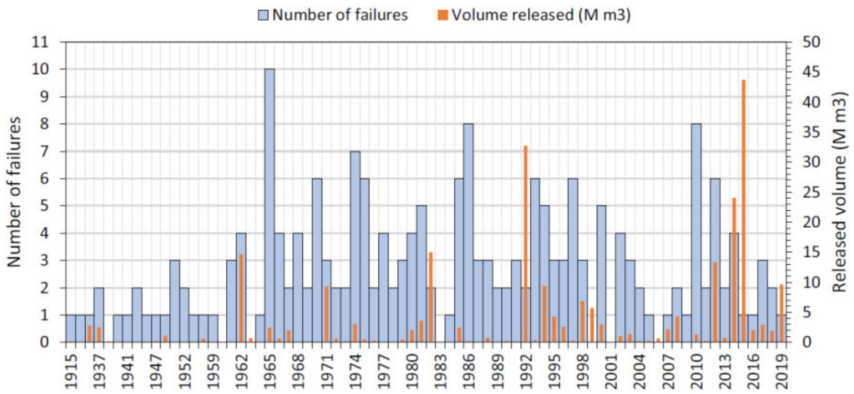

Fig. 1 Number of tailings dams' failures (blue colour) and material volume released (red colour) from 1915 [1]

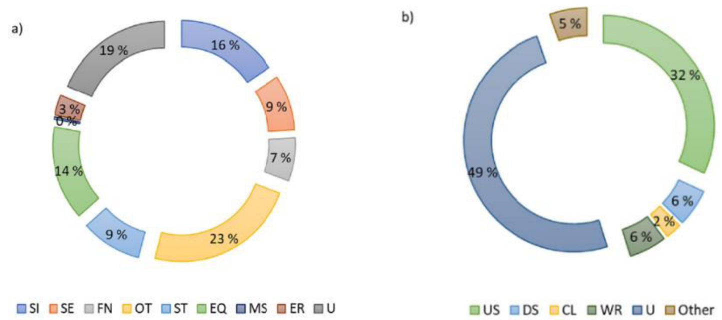

Fig. 2 Statistical analysis of 257 dam collapses: a) mechanism: static failure (SI), seepage and internal erosion (SE), foundation problems (FN), overtopping (OT), structural problems (ST), seismic instability (EQ), subsidence (MS), external erosion (ER), unknown (U); and b) type of construction: upstream (US), downstream (DS), central (CL), unknown (U) [1].

This study examines the first part of a research done in a previous study of tailings dam conducted by Mircevska et al. [14]. It specifically focuses on seepage analysis under various scenarios of seepage forces and stresses, for which three distinct impermeable lining options were considered in order to mitigate environmental impacts. The hydrodynamic stability analyses for all scenarios were conducted with a coupled fluid-solid finite element model for an existing 72 m high tailings dam in its final operational phase as an example. This phase, prior to the completion of the construction is the most critical construction phase, whereat the extreme head in the tailings pond establishes stationary filtration process and pore pressure in most of the dam domain. The analyses were conducted with ADAD-IZIIS FE-BE software written specifically for evaluation of static and dynamic behaviours of dams [15]. In the software, the seepage rate is estimated through a conventional flow-net analysis, with the assumption of steady seepage conditions. The soil behaviour and stress tensor distribution was modelled with the Mohr-Coulomb elasto-plastic constitutive relationship based on associated plasticity as a 'first-order' approximation.

2. FE ANALYSIS OF STATIONARY SEEPAGE THROUGH A COHERENT MEDIA

The equation of continuity that governs the stationary seepage process can be written with the *Laplace's differential equation*, as:

$$\frac{\partial}{\partial x}\left(k_{xx}\frac{\partial W}{\partial x}\right)+\frac{\partial}{\partial y}\left(k_{yy}\frac{\partial W}{\partial y}\right)+\frac{\partial}{\partial z}\left(k_{zz}\frac{\partial W}{\partial z}\right)=0 \tag{1}$$

where, $W(x,y,z)$ is the potential function that should satisfy the boundary conditions and k_{xx}, k_{yy}, k_{zz} are Darcy's permeability coefficients in the global x, y, z directions.
Two boundary conditions can be imposed along the contours of the seepage medium:

- **Essential boundary condition** that prescribes the potential acting along the surface contour S_1:

$$W=\overline{W} \tag{2}$$

- **Natural boundary condition** that determines the velocity V_n in direction of the normal *n* of the surface contour S_2:

$$V_n=-\left(k_{xx}\frac{\partial W}{\partial x}\cos(nx)+k_{yy}\frac{\partial W}{\partial y}\cos(ny)+k_{zz}\frac{\partial W}{\partial z}\cos(nz)\right)=\overline{V_n} \tag{3}$$

where, cosine functions define the direction of the normal with respect to the global coordinate system. The projections of seepage velocity in case of incompressible fluid in a 3D orthotropic medium (V_x, V_y, V_z) are also described by *Darcy's law*:

$$V_x=-k_{xx}\frac{\partial W}{\partial x};\ V_y=-k_{yy}\frac{\partial W}{\partial x};\ V_z=-k_{zz}\frac{\partial W}{\partial z} \tag{4}$$

In order to apply this concept within the finite element method, the integral expression of the analysed problem has to be transformed. The system of equation 1, 2 and 3 is herein solved with the method of virtual work:

$$\iiint_{\Omega}\left(k_{xx}\frac{\partial W}{\partial x}\frac{\partial \delta W}{\partial x}+k_{yy}\frac{\partial W}{\partial y}\frac{\partial \delta W}{\partial y}+k_{zz}\frac{\partial W}{\partial z}\frac{\partial \delta W}{\partial z}\right)dxdydz = \iint_{S2}\overline{V_n}\delta W ds=0 \tag{5}$$

Having in mind that explicit integration of equation 5 is difficult and often impossible, especially when the seepage domain Ω is of complex geometry, numerical integration has to be applied. This is transforming the integrals in an equivalent ensemble of discrete finite domains, Ω_i. Thus, the seepage domain is discretized with a number of 3D seepage finite elements, while the surface domain is divided into 2D sub-surfaces as follows:

$$\sum_{i=1}^{NEL}\int_{\Omega_i}\left(k_{xx}\frac{\partial W}{\partial x}\frac{\partial \delta W}{\partial x}+k_{yy}\frac{\partial W}{\partial y}\frac{\partial \delta W}{\partial y}+k_{zz}\frac{\partial W}{\partial z}\frac{\partial \delta W}{\partial z}\right)d\Omega-\sum_{i=1}^{NEL}\int_{S_2}\overline{V_n}\delta W ds = 0 \tag{6}$$

where, NEL is the number of finite elements constituting the seepage domain Ω.

3. FE MODELING OF AN EXAMPLE OF TAILING DAM

The study examines an existing tailings dam, constructed using a modified downstream method with a supporting stone fill on the downstream side. The characteristic cross section of the dam, with description of all its elements is presented in Figure 3. The total dam height of 72 m also includes the underlying riverbed sediments approximately 8-10 m thick. The base width of the tailings dam-impoundment system spans 406 m, with a crest width of 5 m, and upstream and downstream slopes of the sand embankment with ratios of 1:1.5 and 1:2.7, respectively. The tailings pond is enclosed by natural canyon walls, the downstream slope of the upper tailings dam and the upstream slope of sand embankment and the initial dike.

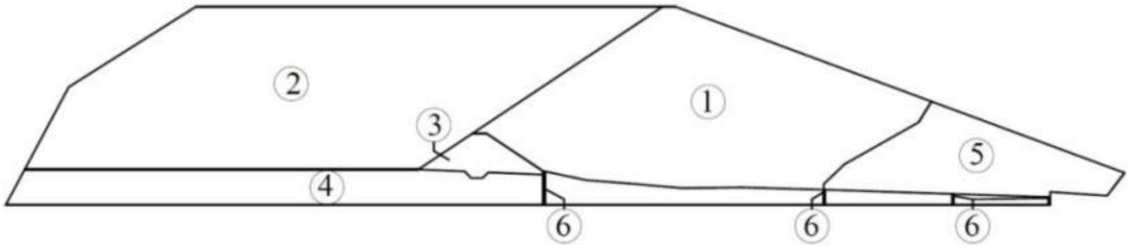

Fig. 3 Cross-section of the dam: 1) downstream sand embankment, 2) tailings pond, 3) starter dike of graphite shale, 4) gravel (8-10m), 5) downstream rockfill support, 6) drainage pipes.

The plans of analysed tailings and the 3D mathematical model of dam is not included in the paper. Herein, only the FE model of the main central section of the dam considered for the analyses is presented in Figure 4. The FE numerical model is composed of 220 structures. Each substructure is discretized by 100 finite elements, so the model comprises of 22,000 finite elements in total, assuming five subdivisions in the x- and z-direction, and four subdivisions in the y-direction. The model has 9911 external, i.e., "Guyan" nodes, representing 29733 degrees of freedom. Due to the small deformability of the gneiss rock in comparison to the deformability of the tailings, the dam-rock interaction has little or no significance to the response, thus the model was considered to be fixed at the base. The generated hydrodynamic forces at the fluid-tailings interface were simulated with the added mass method [16] [17].

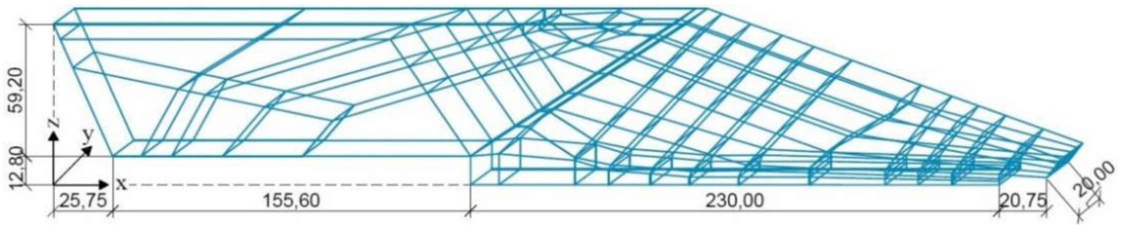

Fig. 4 FE model of the central section of the tailings dam.

The seepage bounding conditions direct the stationary seepage process, i.e., the seepage forces, velocities, pore pressure distribution and the manifested potential, which directly impact eventual internal instabilities triggered by suffusion and heave, as well as static and dynamic liquefaction within the complex tailings dam-impoundment system. In order to quantify and compare the impact of different lining options, three isotropic stationary seepage models were examined.

In Model A, the lining is applied to the reservoir walls, bottom, and the upstream slope of the starter dam. The lining effectively prevents the expected process of gradual water seepage through these components, ensuring that the tailings material remains completely submerged up to the crest of the dike. This disruption in the filtration process, redirects a significant amount of undrained water above the dike's crest towards areas in the sand embankment, in this way facilitating the necessary redirection in hydraulic potential. Model B, on the other hand, incorporates lining only on the reservoir walls and bottom, allowing for efficient water dissipation from the impoundment without significant disruption to the technological process. The pressure dissipation is directed through the starter dike, towards the drains located below the dike and the filtration carpets at the interface between the downstream sand embankment and the gravel deposits. As a comparison to these two models, Model C represents an option with no lining applied.

The seepage boundary conditions that govern the seepage process in a manner described above are assigned to the referent coordinate system, as presented in Figure 5. In the figure, the dashed blue line corresponds to the phreatic line, the light blue dot-dashed line denotes the constant potential boundary condition, the bold red line represents the restricted seepage condition, and for the rest of the area, an undisturbed seepage boundary condition is assigned to the model. The constant potential boundary condition of W=72 m is assigned to the free impoundment surface (BC and AB) in all three models. The phreatic surface, with a potential W=h, in model A is placed on the downstream face of the dam, which is in fact exposed to atmospheric pressure. For the other two models, due to directed seepage through the dike and sediments drainage system, the phreatic surface extends along the upstream slope of the sand embankment, the starter dam's downstream slope and the bottom of the embankment. Restricted seepage condition (with zero seepage velocities) is assigned to the bottom lining in models A and B, whereas in model C, undisturbed water seepage is allowed through the bottom of the impoundment.

Apart from the boundary conditions, the seepage process is significantly influenced by the hydraulic conductivities of the materials encompassed within the tailings dam-impoundment system. The distribution of the hydraulic conductivities with their values are given in Figure 6 and Table 1.

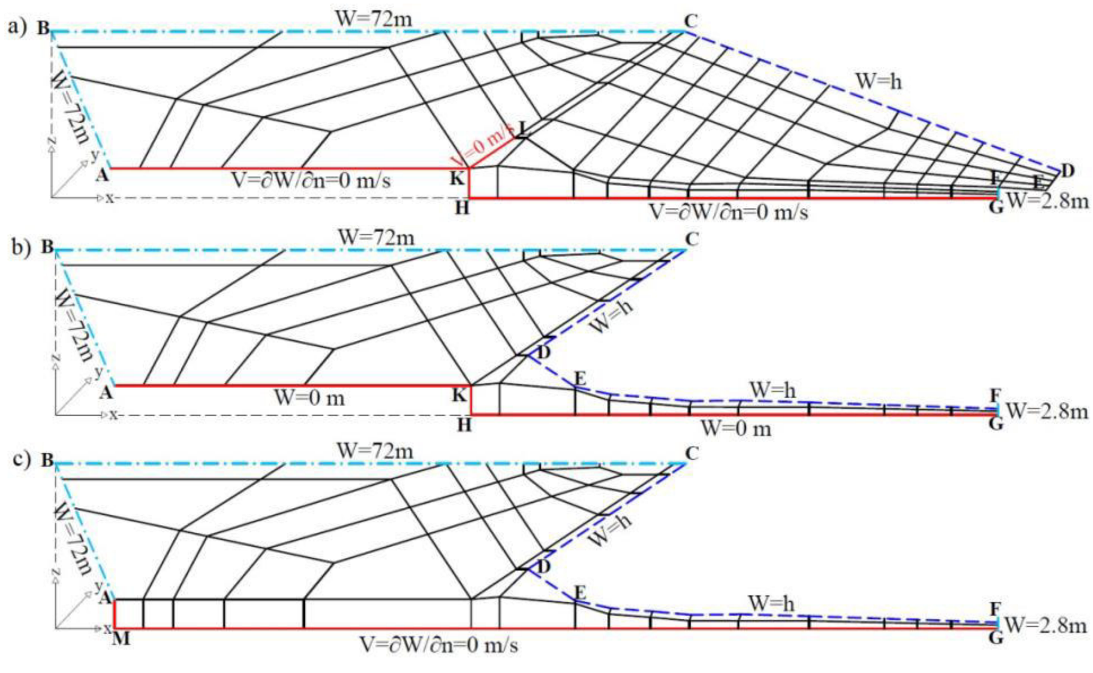

Fig. 5 Seepage boundary conditions for: a) model A, b) model B and c) model C

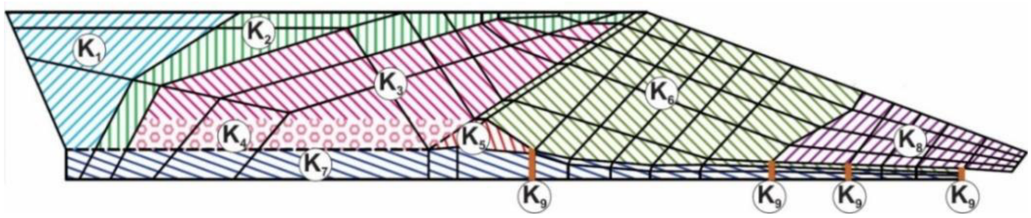

Fig. 6 Hydraulic conductivity of the distinct zones of the tailings dam-impoundment system.

Tab. 1 Hydraulic conductivity of the distinct zones (as shown in Figure 5)

Zone	Description	Isotropic hydraulic conductivity k_x=k_y=k_z (m/s)	Porosity N	γ_s [kN/m^3]	Youngs modulus Es [kPa]
1	tailings pond	K1=0.001	n/a	n/a	n/a
2	tailings pond	K2=0.00005	n/a	n/a	29,000
3	tailings pond	K3=0.0000015	n/a	n/a	36,000
4	tailings pond	K4= 0.000001	n/a	n/a	45,000
5	starter dike	K5=0.0000001	0.289	27.0	90,000
6	sand embankment	K6=0.000002	0.3-0.483	32.0	43,000-75,000
7	natural sediments	K7=0.0001	0.283	26.5	100,000
8	stone fill	K8=0.00001	0.315-0.375	32.0	25,000-57,000
9	drainage	K9=0.001	n/a	n/a	n/a

4. RESULTS OF STATIONARY SEEPAGE ANALYSES

The results of the stationary seepage analysis for the analysed dam are presented as potential field distribution (Figure 7), pore pressures distribution (Figure 8) and seepage velocities (Figures 9, 10 and 11) across the dam-impoundment seepage domains for all models.
The illustrated potential field distribution agrees well with the predefined seepage boundary conditions. The with maximum equipotential line equal to the height of the dam (72 m) is set at the free water surface, due to the fully saturated tailings. The minimum potential of 2.8 m is simulated at the edge of the downstream slope of the model, mimicking the outlet channel of the seepage flow.
In model A, as opposed to other models, the potential distribution extends across the entire tailings domain, including the much susceptible to damage sand embankment. The highest gradient of the potential field for this model is observed in the sand embankment and the starter dike (Figure 7a), while in the impoundment the potential drop is considerably lower, decreasing from 72 m at the water level to about 60 m at the crest of the starter dike. Models B and C exhibit similar pressure potentials (Figure 7b and 7c) with a higher potential gradient in the impoundment, dropping from 72 m to 30 m, with remaining potential dissipation within the dike and the drainage carpet. The higher gradient in this zone is due to the shorter seepage path of both models in comparison to model A. In model A, the equipotential lines at the interface between the tailings and the starter dike are noticeably discontinued, due to the influence of the impermeable lining. In contrast, in the other two models the equipotential lines at this interface remain continuous. The only noticeable distinction between models B and C is the result of the allowed seepage through the natural sediments at base of the tailings pond in model C (Figure 7c).

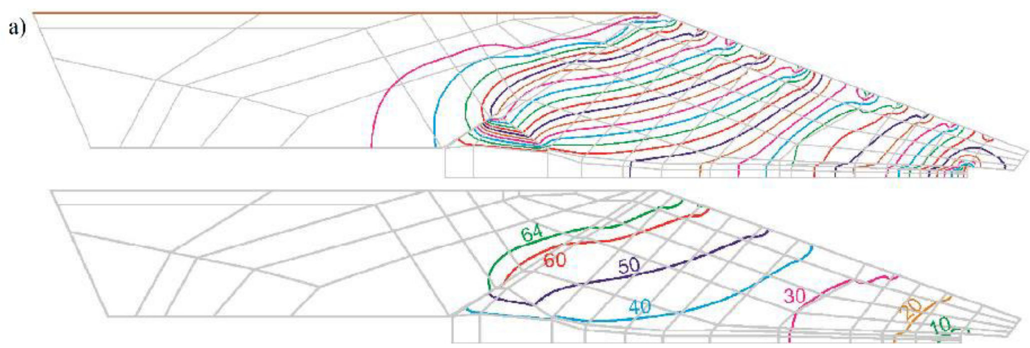

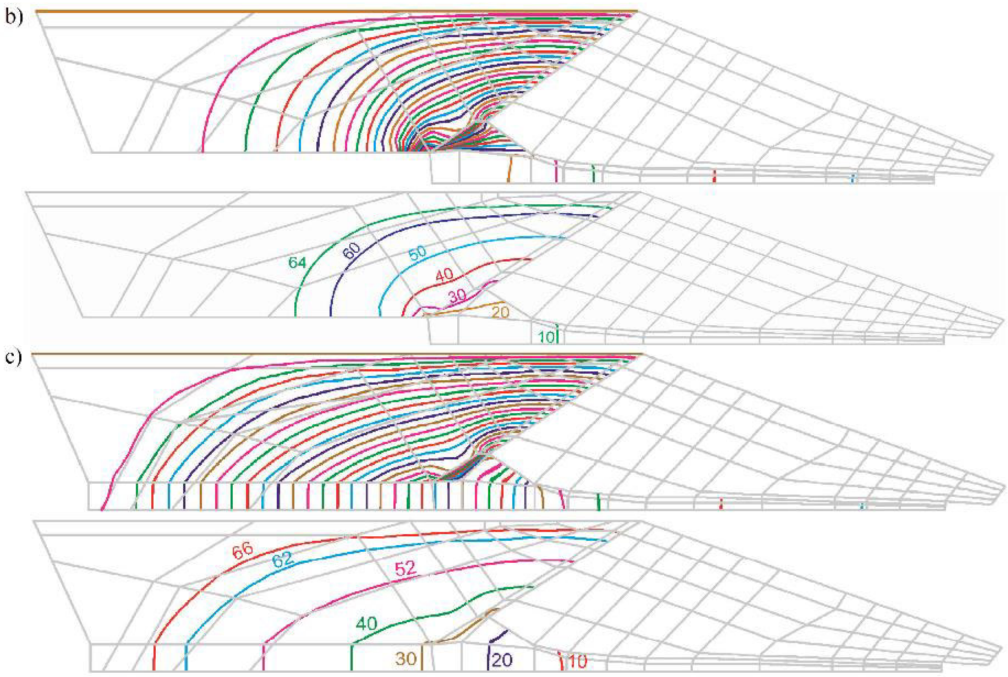

Fig. 7 Distribution of the potential fields throughout the seepage domain (equidistance 2 m) and selected equipotential lines for: a) model A, b) model B, and c) model C.

The pore pressure distribution within the seepage domain is highly influenced by the potential field, as illustrated in Figure 8 for the three models in form of isobars corresponding to distinct pore pressures. For all models, along the phreatic surface, zero pore pressure corresponding to atmospheric pressure is observed, which increases with depth. For models A and B, the maximum value of pore pressure is about 590 kPa at the bottom of the tailings pond, while for model C is 720 kPa. For model A, the continuity of the isobaric lines at the interface with the starter dike is interrupted again, which is in accordance with the boundary conditions.

Due to the established seepage and high potential gradient in the sand embankment in model A, high pore pressures are manifested in this zone as well (Figure 8a). Due to this larger seepage domain, the pore pressure increase in this model is practically constant. On the other hand, in models B and C, the pressure gradually increases from about 100 kPa at the starter dike, to the maximum value of 590 kPa at the downstream slope of the upper tailings dam (Figure 8b and 8c). Herein, no pore pressures are manifested in the highly susceptible to damage zone of sand embankment. In model C, the pore pressure in the impoundment increases further in the underlaying natural sediments, attaining a value of 720 kPa, (Figure 8c).

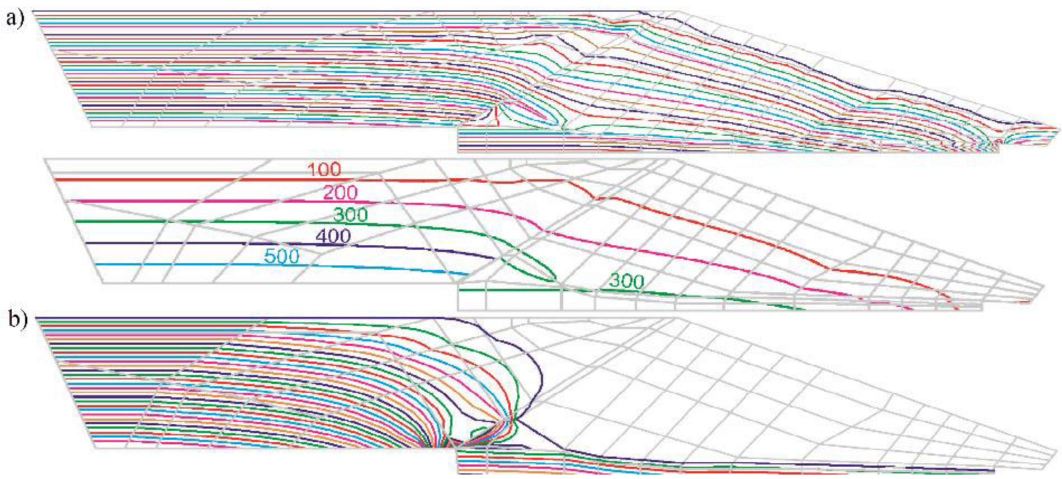

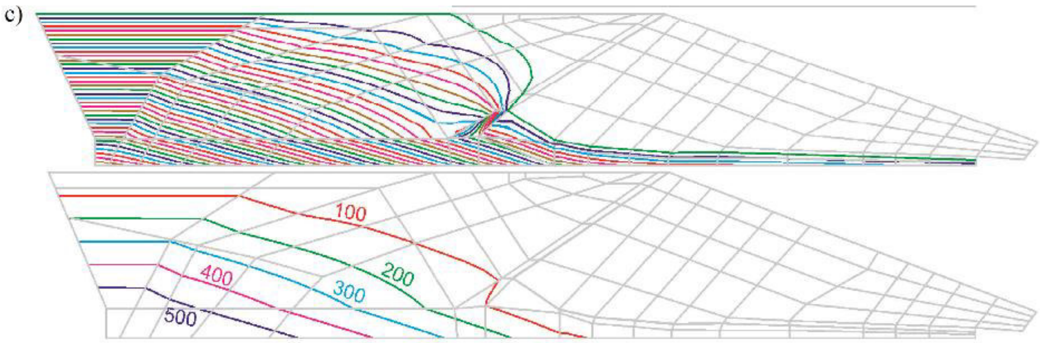

Fig. 8 Distribution of pore pressure through the seepage domain in [kPa] (equidistance of 20 kPa) and selected pore pressure isobars for: a) model A, b) model B, and c) model C.

The seepage velocities for all models in Figures 9, 10, and 11, respectively are given in form of vectors with length indicating the magnitude and arrow pointing out the direction of the seepage. The boundary condition of impermeable lining at the impoundment bottom and upstream face of the starter dike in Model A results in predominantly horizontal flow with low seepage velocities just above the bottom lining. Near the starter dike's slope, however, the velocities increase and gradually circumvent the dike (Figure 9b), after which the water overtops the dike and flows toward the sand embankment (Figure 9c). The increase of the seepage velocity just above the starter dike is a consequence of the significant potential variation in this zone. Most significantly, high velocity seepage in a vulnerable zone of the dam such as the sand embankment is manifested with maximum value of 5.4 x 10^{-6} m/s at the starter dike – embankment – vertical drain interface.

In model B, due to the abrupt potential drop along the shorter length of the path, the seepage velocities are notably higher compared model A, primarily in the tailings pond (Figure 10a). However, this zone doesn't carry significant implications for the overall stability of the dam. In the upper part of the starter dike, which is a zone crucial for stability, the respective seepage velocities are slightly lower compared with model A (Figure 10b). Most importantly, in this model no seepage is allowed in the sand embankment. Model C is characterized by predominantly horizontal seepage along the base and the starter dike, with the maximum seepage velocity reaching 270 x 10^{-6} m/s (Figure 11a). Within the tailings pond, the seepage velocities are higher than that observed in model B.

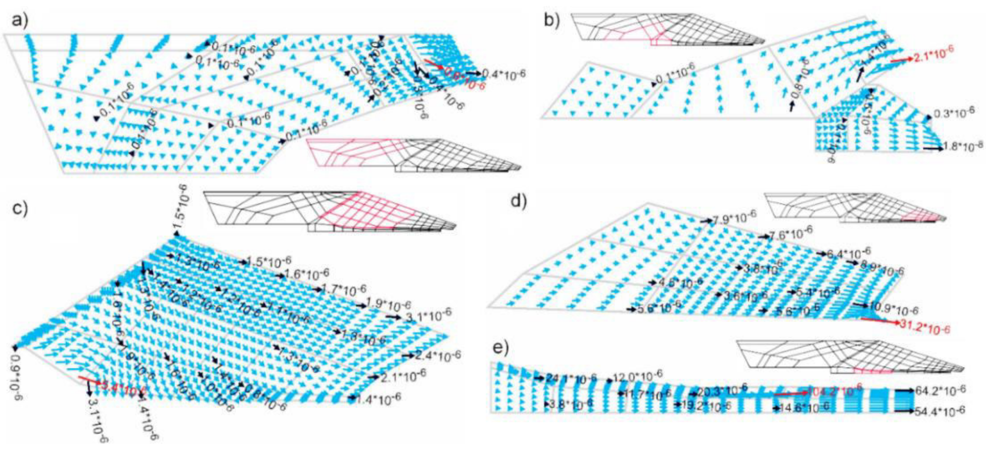

Fig. 9 Model A: Velocity of seepage (m/s) in characteristic parts of the seepage domain. The maximum velocity value is indicated in red.

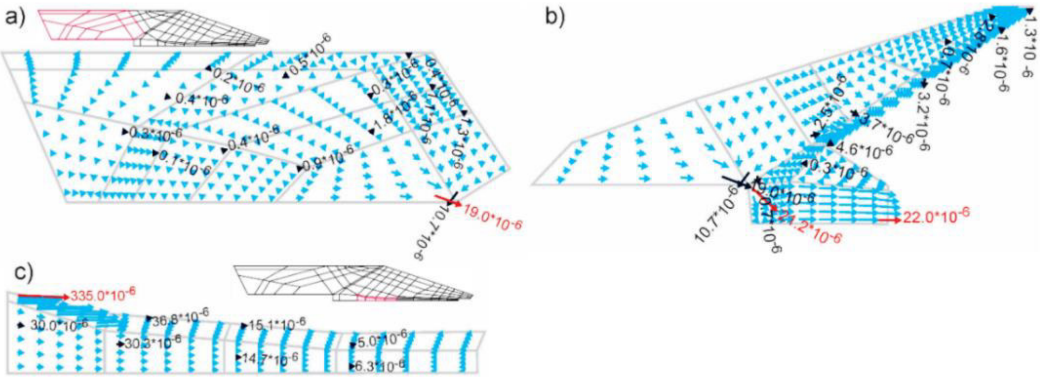

Fig. 10 Model B: Velocity of seepage (m/s) in characteristic parts of the seepage domain. The maximum velocity value is indicated in red.

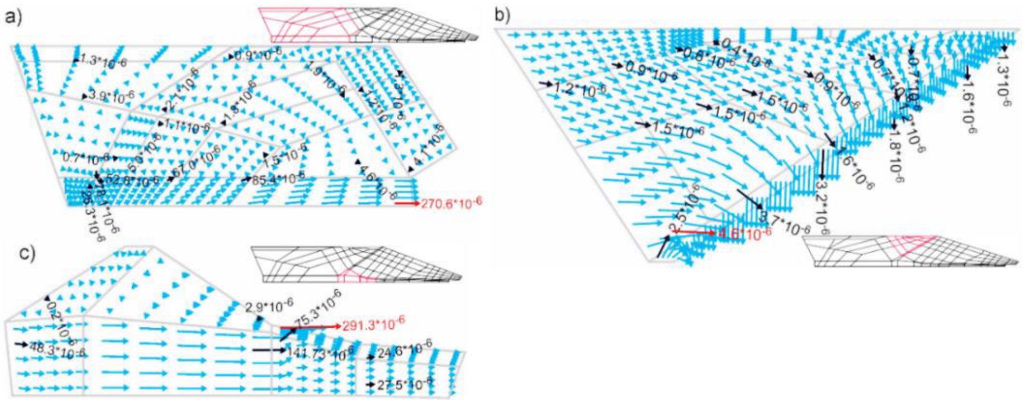

Fig. 11 Model C: Velocity of seepage (m/s) in characteristic parts of the seepage domain. The maximum velocity value is indicated in red.

5. CONCLUSIONS

In order to avert potential failures and resulting environmental consequences, it is imperative that tailings dams adhere to strict long-term stability requirements. An essential aspect in achieving this objective is gaining a comprehensive understanding of hydrodynamic effects that encompasses evaluation of their influence on the overall stability of the dam. To underscore the importance of the hydrodynamic dam stability, an analysis of existing tailing dam for three distinct seepage boundary conditions was conducted. The results of the study, including the calculated potential field, pore pressures and seepage velocities will serve as a foundation for determining critical and manifested hydraulic gradients, as well as the potential for issues such as erosion-induced piping and heave effect. The comprehensive finding regarding these effects and their implications for the dam's stability are presented in the second part of this study [14] [18], which is also included in the conference proceedings.

One of the primary conclusions drawn from the seepage analysis under different conditions is that the significant impact that the introduction of impermeable lining can have on seepage velocities and pore pressure distribution. This alteration in seepage behaviour can potentially trigger hydrodynamic instability in the tailings dam. Therefore, when local environmental protection considerations necessitate the use of seepage barriers, it becomes imperative to conduct a thorough and comprehensive engineering assessment of the expected and potential negative hydrodynamic effects that may arise.

REFERENCES

[1] Piciullo L., Briseid E., Zhongqiang L., Farrokh N., Lacasse S. (2022). A new look at the statistics of tailings dam failures, *Engineering Geology*, Volume 303, 106657, ISSN 0013-7952, https://doi.org/10.1016/j.enggeo.2022.106657.

[2] CSP2 – Tailings Dam Failures, 1915–2016. http://www.csp2.org/tsf-failures-from-1915.

[3] Zongjie L., Junrui C., Zengguang X., Yuan Q., Jing C. (2019). A Comprehensive Review on Reasons for Tailings Dam Failures Based on Case History, *Advances in Civil Engineering*, Article ID 4159306, https://doi.org/10.1155/2019/4159306.

[4] Small A., Herza J., Ashley M., Thorp J. (2019). A consequence-based tailings dam safety framework. *Proceedings of the ICOLD 2019 Symposium - Sustainable and Safe Dams Around the World*, Ottawa, Canada, 9-14 June, ISBN 9780367334222.

[5] GRIDA, 2016. Mine Tailings Storage: Safety is no Accident. A UNEP Rapid Response Assessment. *United Nations Environment Programme and GRID-Arendal*, Nairobi and Arendal, www.grida.no. ISBN: 978-82-7701-170-7.

[6] Rico M., Benito G., Díez-Herrero A. (2008). Floods from tailings dam failures, *Journal of Hazardous Materials*, Volume 154 (1–3), pp. 79-87. https://doi.org/10.1016 /j.jhazmat.2007.09.110.

[7] ICOLD (2001). Tailing Dams: Risk of Dangerous Occurrences - Lessons learnt from practical experiences, *Bulletin 121*, 2001.

[8] Foster M., Fell R., Spannagle M. (2000). The statistics of embankment dam failures and accidents. *Canadian Geotechnical Journal*, Volume 37 (5), https://doi.org/10.1139/t00-030.

[9] Psarropoulos P. N., Tsompanakis Y. (2008). Stability of tailings dams under static and seismic loading. *Canadian Geotechnical Journal*, Volume 45 (5), pp. 663-675. https://doi.org/10.1139/T08-014.

[10] Wang T., Zhou Y., Lv Q., Zhu Y., Jiang C. (2011). A safety assessment of the new Xiangyunphospho gypsum tailings pond. *Minerals Engineering*, Volume 24 (10), pp. 1084–1090.

[11] Hu S., Chen Y., Liu Y., Zhou S., Hu R. (2015). Effect of seepage control on stability of a tailings dam during its staged construction with a stepwise-coupled hydro-mechanical model. *International Journal of Mining Reclamation and Environment*, Volume 29 (2), pp. 125–140, https://doi.org/10.1080/17480930.2013.870693.

[12] Liu C., Shen Z., Gan L., Xu L., Zhang K., Jin T. (2018). The Seepage and Stability Performance Assessment of a New Drainage System to Increase the Height of a Tailings Dam. *Applied Sciences*, Volume 8 (10), pp. 1840, https://doi.org/10.3390/app8101840.

[13] Daouadji A., Hicher P. Y. (2009). An enhanced constitutive model for crushable granular materials. *International Journal for Numerical and Analytical Methods in Geomechanics*, Volume 34 (6), pp. 555–580, https://doi.org/10.1002/nag.815.

[14] Mircevska V., Nanevska A., Nastev M., Zafirov T. (2022) Containment Lining Solutions and Hydrodynamic Stability of Tailings Dam, *International Journal for Engineering Modelling*, Volume 36 (1), pp. 49-65, https://doi.org/10.31534/engmod.2023.1.ri.04a.

[15] ADAD-IZIIS software (2018). Analysis and design of arch dams – User's manual, *Institute of Earthquake Engineering and Engineering Seismology – IZIIS*, University of Ss. Cyril and Methodious, Skopje, R. N. Macedonia.

[16] Mircevska V., Bulajic I., Manova K. (2013). Comparison of added mass method with sophisticated analytical BEM-FEM approach using ADAD-IZIIS software. *Proceedings of the 15th World Conference of Earthquake Engineering*, Lisbon, Portugal.

[17] Westergaard H. M. (1933). Water pressure on dams during earthquakes. *Transactions of the American Society of Civil Engineers*, Volume 98 (2), pp. 418–472, https://doi.org/ 10.1061/ TACEAT.0004496.

[18] Mircevska V., Nanevska A. (2023). Impact of the impermeable linin of tailings reservoir to the hydrodynamic instability of tailings dam. *In conference iNDiS 2023*,16-17 November 2023, Novi Sad, Serbia (presented in this conference).

INVESTIGATION OF OBJECTS VERTICALITY USING TERRESTRIAL LASER SCANNER

Đuro Krnić[1], Marijana Vujinović[2], Mehmed Batilović[3], Marko Marković[4], Tatjana Budimirov[5]

Abstract:

Determining deviations from the verticality of tall structures is a very important criterion in assessing their condition and functionality. In this study, for the purpose of examining the verticality of a tall chimney within an industrial facility, terrestrial laser scanning technology was applied, where a point cloud was obtained as a result. The analysis of the chimney verticality was performed by generating horizontal sections of the chimney at specific heights from the point cloud. Since the chimney being tested for verticality is conical in shape, a circle with the corresponding radius was extracted from each horizontal section. Deviations from verticality were determined by comparing the centres of the circles. This research provides insight to the practical application of terrestrial laser scanning for assessing the verticality of tall objects and the advantages and challenges associated with this approach.

Keywords: verticality testing, terrestrial laser scanner, point cloud

[1] Teaching associate, BSc, Faculty of Technical Sciences, University of Novi Sad, Novi Sad, Serbia, e-mail: djuro.geo@uns.ac.rs
[2] Teaching assistant, MSc, Faculty of Technical Sciences, University of Novi Sad, Novi Sad, Serbia, e-mail: marijana.petkovic@uns.ac.rs
[3] Assistant professor, PhD, Faculty of Technical Sciences, University of Novi Sad, Novi Sad, Serbia, e-mail: mehmed@uns.ac.rs
[4] Associate Professor, PhD, Faculty of Technical Sciences, University of Novi Sad, Novi Sad, Serbia, e-mail: marko_m@uns.ac.rs
[5] Teaching assistant, MSc, Faculty of Technical Sciences, University of Novi Sad, Novi Sad, Serbia, e-mail: tatjana.kuzmic@uns.ac.rs

1. INTRODUCTION

During the 19th century, the Industrial Revolution initiated the construction of tall industrial chimneys throughout Europe as a consequence of the expansion of numerous factories and the need for proper smoke and gas exhaust. These facilities varied in height, adapting to different factors such as the type of industry, topography, meteorological conditions, and geographical location. Their main function was to evacuate smoke and gases produced by burning coal that was used in almost all industrial facilities [1]. Many factors such as topography, wind, type of industrial factory, nearness to cities, etc. [2] [3] influenced the height of the constructed chimney. Chimneys with varying heights, ranging from several tens to over one hundred meters, are used to prevent the harmful effects of waste gases and smoke on the environment and human health. Most industrial chimneys of that period are constructed from brick masonry [4] and are conical in shape [4], [5], [6]. Initially, these chimneys were constructed on the outskirts of cities, but due to urbanization, they are now commonly found in densely populated areas of cities. The presence of these chimneys in active areas of cities increases the risk of damage and casualties in case of structural collapses. The importance of analyzing the stability of old industrial chimneys is evident due to their potential hazards. The analysis of chimney stability is crucial to prevent catastrophic collapses that could cause material damage and human casualties. Therefore, it is necessary to conduct regular maintenance and monitoring of these chimneys to ensure their stability and prevent any potential hazards.

Numerous chimneys have received the status of protected structures due to their significant social and historical significance. Nevertheless, as they became obsolete within industrial contexts, a substantial number of these chimneys were disregarded for extended periods, resulting in swift deterioration. Consequently, evaluating their conservation status holds paramount importance when considering future restorative actions and preservation strategies. From a static point of view, one of the most important parameters to inspect during a stability assessment of a tall chimney is the inclination of the main body [2].

In past decades, traditional approaches to determining the verticality of chimneys relied on the use of optical theodolites, latter total stations, whose main drawback is the inaccessibility of points on the chimney and the need for measuring a larger number of points on the chimney's surface. [7] .

With today's advancements in engineering techniques, modern geodetic measurement technology, including terrestrial laser scanners, enables precise and contactless scanning of tall chimneys. This advanced approach allows quick and accurate monitoring of incline but also offers the possibility of continuous monitoring of changes over time. Terrestrial laser scanners (TLS), using the principle of active illumination and collecting reflected light, scan the chimney's surface, creating a dense cloud of points with high accuracy. This technique enables safe data collection from a distance, eliminating the need for physical contact with the structure while ensuring high precision and detail. Laser scanning is a popular solution to evaluate structural stability for many constructions [2], [8], [9], [10], [11].

From laser scanner measurements, Barazzeti, Previtali, and Roncoroni (2019) [2] extracted sections with approximately equal heights and utilized them to calculate the position of the object's axis at different levels. Two approaches were employed by the authors to determine the object's inclination: the first method was manual, involving the use of CAD software, while the second was automated, employing the least squares method to determine the center of each section. Quality results were obtained from both approaches; however, it should be noted that the traditional CAD software approach could not be utilized to assess the quality of the results obtained. Marjetič (2018) [12] [12] also has emploied laser scanning techniques for the analysis of industrial chimney verticality. The author emphasizes the advantage of speed in measurements conducted by laser scanners in this method. It is crucial to perform chimney verticality measurements within a minimal time frame to reduce the influence of weather-related changes on the results. In the research conducted by Zrinjski and colleagues (2020) [13], a three-dimensional linear regression method was applied to investigate the verticality of an industrial chimney. Measurements were taken from an existing geodetic foundation, and samples were collected along circular sections that were approximately at the same height on the structure. Subsequently, the centers of these circular sections were determined through circular regression modeling, while the chimney's axis was established using the linear regression method. One notable advantage of this approach is that quality assessments for all calculated parameters are accessible [14]. In their study, Kregar (2015) [15] used data obtained from laser scanner measurements to fit a cylinder to the measurements using the least squares method. Through this fitting process, they determined the inclination of a tall industrial chimney. In conclusion, the authors emphasize that this method allows for precise determination of the chimney's inclination, with minimal deviations compared to the results obtained using a total station.

This paper elaborates on a method based on laser scanning of points on the chimney's surface. A geodetic reference network established around the chimney serves as the basis for determining the coordinates of these points. The centers of chimney cross-sections are determined by extracting circles from profiles, while the vertical axis of the chimney is determined by connecting the centers of these circles on the profiles. Verticality analysis is compared to maximum allowable deviations defined according to the international standard EN 1993 EUROCODE 3 [16]. This paper is based on geodetic research and verticality analysis of a chimney in an industrial facility in Crvenka. Only key results and segments are presented and elaborated in the paper.

2. METHODOLOGY

2.1. DATA ACQUISITION AND PRE-PROCESSING

The ideal geometry of the chimney refers to the coincidence of the positions of the circles' centers at the bottom and top of the chimney in a two-dimensional (2D) plane. The points presented in this paper are represented in a Cartesian coordinate system, which is a mathematical system used to describe the position of points in space. A TLS is used to obtain these coordinates with the polar surveying method. The horizontal direction, zenith angle, and slope distance are measured at each point (Fig. 1). To obtain the Cartesian coordinates of the measured points the position and orientation of the instrument must be known [12].

In order to create a unique and precise 3D representation of the scanned area, point cloud registration is performed. Registration represents the alignment of a set of point clouds into a common coordinate system (coordinate system of the scanner), thus forming a single set of data.. To georeference the TLS instrument, at least three known points are required to calculate the transformation parameters between the scanner's coordinate system and the referential coordinate system. Once the georeferencing is performed, all TLS measurements can be transformed into a common reference coordinate system. The calculation of coordinates from raw terrestrial measurements is a common geodetic procedure and is not discussed in this paper.

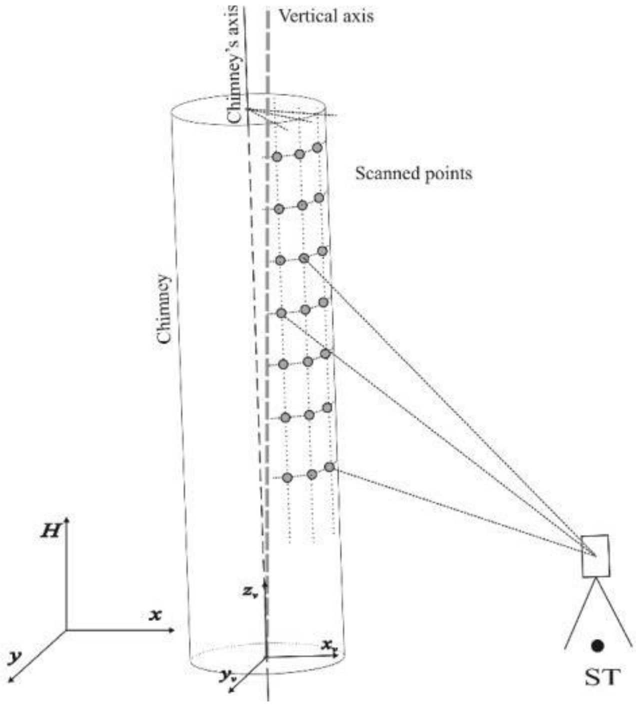

Fig. 1 Method of scanning points on chimney's surface [12]

To obtain the coordinates of all measured points from different stations, the position and orientation of the scanner must be known, and the distances need to be appropriately adjusted for meteorological and geometric corrections. Precise georeferencing of the considered TLS device and consequently the measured point clouds must be achieved using additional measurements with special markers. These markers must have known positions to ensure the accuracy and precision of the transformation parameters between the scanner's internal coordinate system and the external coordinate system, established by a geodetic network of known points [12].

2.2. CASE STUDY: INDUSTRIAL CHIMNEY

The chimney is located in Crvenka, in the municipality of Kula. The height of the chimney itself extends to just over 30 meters. As mentioned earlier in previous chapters, the TLS method was used, resulting in a dense point cloud that will be used for further analysis (Fig. 2).
For chimney scanning, the TLS used was the Trimble TX8. This scanner enables the discretization and measurement of a finite number of points, resulting in a dense point cloud. The coordinates of these points are determined in the reference coordinate system with the help of special markers whose coordinates are obtained by georeferencing. The quality of the obtained results in this research primarily depends on the selection of the appropriate instrument, equipment, scanning method, and the topography of the terrain where the measurements are conducted.

Fig. 2 View of the chimney in reality (left) and frontal view of the chimney in the point cloud (right)

2.3. THE METHOD

The method for representing the spatial axis of the chimney and analyzing its verticality, presented in this research, is based on precise drawing of horizontal profiles on the chimney. To assess the chimney's verticality, a specific number of profiles on the chimney will be analyzed according to its height and construction. All processing and analysis of the obtained point cloud data are performed using the *Terrasolid* software.The reference point used for assessing verticality represents the center of the circle representing the chimney's base. Based on the centers of the circles from each profile, the chimney axis, representing its inclination in space, will be drawn. In line with the initial assumption, the ultimate goal of data processing is to assess the chimney's verticality by comparing the positions of the circle centers.

3. RESULTS AND DISCUSSION

3.1. EXTRACTION OF PROFILES FROM THE POINT CLOUD

For the analysis of the verticality of the industrial facility, the chimney was divided into certain horizontal profiles. The reference profile corresponding to the bottom of the chimney is represented as Profile 0. The profiles are selected at certain distances, taking into account the breaking points on the object and the uniform distance between the profiles. During the selection of the profile count for the chimney, the objective was to encompass all the rings on the chimney's surface, ensuring a precise depiction of the industrial chimney's structure. Special attention was given to ensure that the chosen number of profiles does not compromise the accuracy of the chimney's verticality analysis (Figure 3). This approach enables a systematic assessment of chimney verticality using horizontal profiles as criteria for verticality testing.

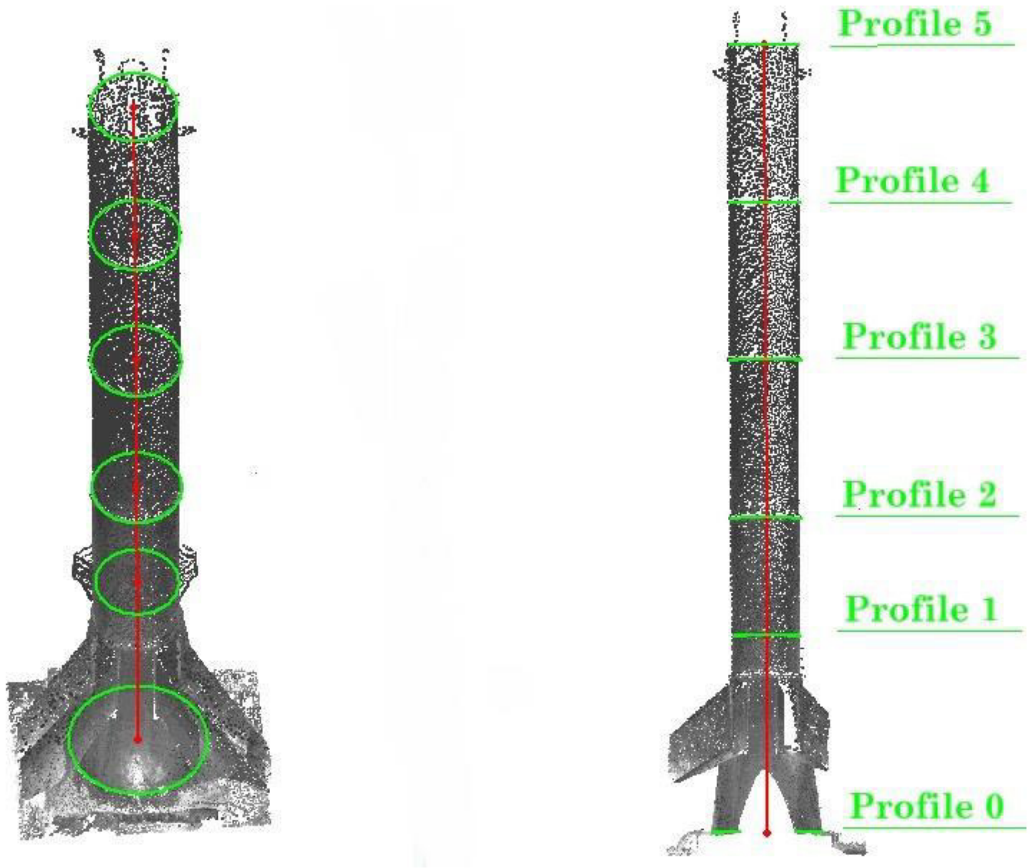

Fig. 3 Display of horizontal profiles and spatial axis of the chimney in the point cloud

Starting from each horizontal section, a series of circles was manually created in the point cloud. Three points were used to draw the circle shapes, while carefully checking the distance between the point cloud and the drawn profiles. Subsequently, the center of each circle could be easily calculated. The deviation was computed as the difference between the center at ground level and the centers of all other profiles. The profile positions, are shown in Figure 3.

3.2. RESULTS ANALYSIS

The coordinates of the chimney circle centers are crucial for this research. These coordinates serve as the fundamental data for the examination and analysis of the chimney's verticality. The coordinates of the circle centers related to horizontal profiles 0, 1, 2, 3, 4, and 5 are presented in Table 1**.**

Tab. 1 Coordinates of the circle centers

Profile	Y [m]	X [m]	Z [m]
0	7378557.524	5058784.252	0,000
1	7378557.491	5058784.250	7.920
2	7378557.478	5058784.243	12.400
3	7378557.451	5058784.241	18.420
4	7378557.412	5058784.232	24.420
5	7378557.379	5058784.285	30.440

These data provide the basis for further analysis of the chimney's verticality and the identification of potential irregularities in its construction. The coordinates of the circle center on different profiles enable the tracking of positional changes of the chimney along its vertical axis.

3.3. DEVIATIONS BETWEEN PROFILES

Each circle center is compared to the reference circle. As previously mentioned, the reference circle corresponds to the bottom of the chimney (Profile 0). The deviation values from the bottom of the chimney contribute to monitoring the position of the chimney axis and the analysis of verticality. Table 2 shows the deviation values for each chimney profile concerning Profile 0. Deviations are presented in terms of horizontal displacement, as well as the overall deviation expressed in millimeters.

Tab. 2 The values of vertical deviations from the bottom of the chimney

Deviations	ΔY [mm]	ΔX [mm]	Δ [mm]
0-1	32.7	1.8	32.7
0-2	46.2	8.6	47.0
0-3	73.3	11	74.1
0-4	112.0	19.8	113.7
0-5	144.6	-33.5	148.4

Based on the table, the deviations increase linearly with height. Profile 0-5 has the highest deviation and, consequently, the largest overall displacement. This indicates significant changes in the chimney's horizontal position concerning the bottom (Fig. 4).

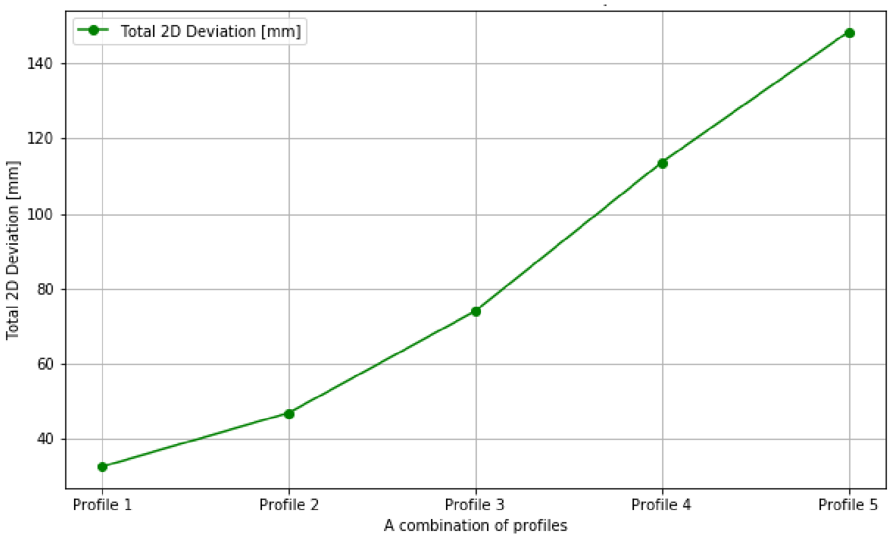

Fig. 4 Total deviation from the reference profile

The analysis of these deviations provides a deeper understanding of the dynamics of changes in the 2D plane along the vertical axis of the chimney. Identifying points with the largest deviations is crucial for further analysis and planning the necessary corrective measures to ensure the stability and safety of this industrial structure. In Table 3, values of deviations related to the coordinates of the circle centers between all remaining profiles are presented.

Tab. 3 The values of vertical deviations from each profile on the chimney

Deviations	ΔY [mm]	ΔX [mm]	Δ [mm]
1-2	-13.5	-6.8	15.1
1-3	-40.6	-9.2	41.6
1-4	-79.3	-18.0	81.3
1-5	-111.9	35.3	117.3
2-3	-27.1	-2.4	27.2
2-4	-65.8	-11.2	66.7
2-5	-98.4	42.1	107.0
3-4	-38.7	-8.8	39.7
3-5	-71.3	44.5	84.0
4-5	-32.6	53.3	62.5

When analyzing the differences in deviations between different profiles, significant changes in the positions of the circle centers are observed. It is noted that the largest deviation is detected in the combination of profiles 1 and 5. In this case, as expected, the largest horizontal deviation is observed between profiles 1 and 5, indicating the greatest differences in the positions of the circle centers between these two profiles (Fig. 5).

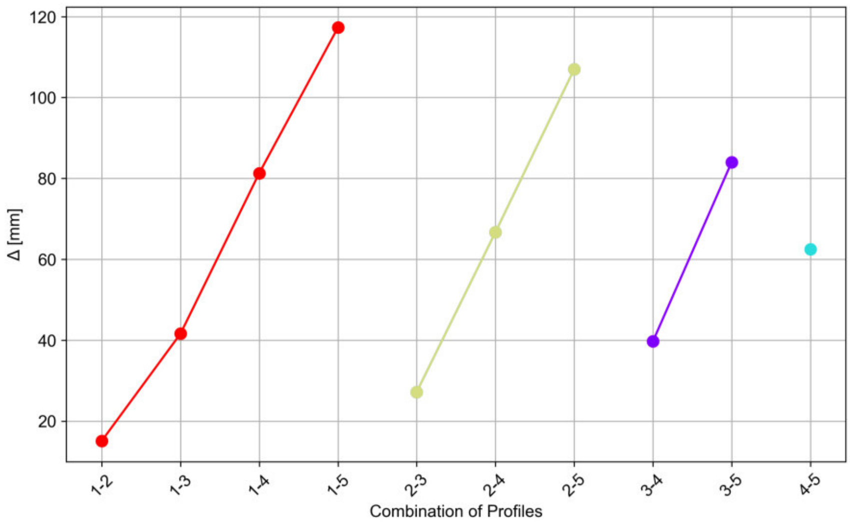

Fig. 5 Deviation based on profile combinations

The analysis of verticality in this case can identify points where changes in the position of circle centers are most pronounced, providing crucial information for planning necessary interventions to ensure the chimney's stability, safety and functionality.

3.4. CONFORMITY WITH INTERNATIONAL STANDARDS

In comparison to the allowable values established by international standards, the computed chimney inclinations provide valuable insights into its structural condition. The EUROCODE 3 standard Design of steel structures – Part 3-2: Towers, masts and chimneys–Chimneys prescribes the maximum permitted horizontal offset Δ of the steel circumference of standalone chimneys according to their height above the foundation [16]:

$$\Delta = \frac{H_d[m]}{1000}\sqrt{1+\frac{50}{H_d[m]}}, \tag{1}$$

where H_d represents the height of the chimney.
For a chimney with a height of 30.5 meters, the allowable horizontal deviation at the top is 5.01 cm. In the case of the industrial chimney under investigation, the deviation exceeds the allowable limits.

4. CONSIDERATIONS AND CONCLUSIONS

Based on the analysis of the results, it can be concluded that the industrial chimney is not entirely vertical. Deviations in the horizontal position, with a particular emphasis on the higher profiles of the chimney, strongly indicate irregularities in its construction. These results reveal that there are deviations from verticality throughout the structure of the chimney, which can affect its stability and safety.
Identifying the causes of these variations and taking corrective measures is the crucial next step. Precise verticality of the chimney is essential for maintaining structural integrity and safety, especially in industrial facilities. Therefore, the focus should be on conducting additional research and analysis to gain a more in-depth understanding of the dynamics and causes of these deviations.
In future research, additional measurement and analysis techniques can be applied to gain a deeper understanding of the dynamics and causes of deviations from verticality. Additionally, monitoring these variations over time can provide valuable insights into the stability of the chimney and any changes in its structure.
It is crucial to note that the precise assessment of chimney verticality has direct applications in engineering and the maintenance of industrial facilities. Any irregularities in verticality can affect the functionality of the chimney and the safety of the surrounding environment. Therefore, it is essential to carefully monitor and analyze these parameters.
In conclusion, the analysis of chimney verticality measurement results using terrestrial laser scanning provides valuable insights into the stability and structure of these building objects. Further research and monitoring are necessary to ensure the sustainability and safety of industrial chimneys.

ACKNOWLEDGEMENT

The research has been conducted within the project "Scientific theoretical and experimental research and improvement of educational process in the field of civil engineering", developed at the Department of Civil Engineering and Geodesy, Faculty of Technical Sciences, University of Novi Sad, Serbia.

5. REFERENCES

[1] Zrinjski, M., Tupek, A., Barković, Đ., & Polović, A. (2021). Industrial masonry chimney geometry analysis: A total station based evaluation of the unmanned aerial system photogrammetry approach. *Sensors*, Volume 21(18), pp. 6265. https://doi.org/10.3390/s21186265.

[2] Barazzetti, L., Previtali, M., & Roncoroni, F. (2019). The use of terrestrial laser scanning techniques to evaluate industrial masonry chimney verticality. *The International Archives of the Photogrammetry, Remote Sensing and Spatial Information Sciences*, Volume 42, pp. 173-178. https://doi.org/10.5194/isprs-archives-XLII-2-W11-173-2019.

[3] Ivorra, S. (2014, October). Old industrial masonry chimneys: Repairing and maintenance. In *Proceedings of the 9th International Conference on Structural Analysis of Historical Constructions, Mexico City, Mexico* pp. 14-17.

[4] Guedes, J. M., Lopes, V., Quelhas, B., Costa, A., Ilharco, T., & Coelho, F. (2019). Brick masonry industrial chimneys: assessment, evaluation and intervention. *Philosophical Transactions of the Royal Society A*, Volume *377*(2155). https://doi.org/10.1098/rsta.2019.0012.

[5] Pallarés, F. J., Ivorra, S., Pallarés, L., & Adam, J. M. (2011). State of the art of industrial masonry chimneys: A review from construction to strengthening. *Construction and building materials*, Volume 25 (12), pp. 4351-4361. https://doi.org/10.1016/j.conbuildmat.2011.02.004.

[6] Dawood, A. O., Sangoor, A. J., & Al-Rkaby, A. H. (2020). Behavior of tall masonry chimneys under wind loadings using CFD technique. *Case Studies in Construction Materials*, Volume *13*. https://doi.org/10.1016/j.cscm.2020.e00451.

[7] Marjetic, A., Ambrozic, T., & Kogoj, D. (2011). DOLOCITEV NEVERTIKALNOSTI VISOKIH DIMNIKOV/DETERMINATION OF THE NONVERTICALITY OF HIGH CHIMNEYS. *Geodetski vestnik*, Volume *55*(4),pp. 701.

[8] Głowacki, T., Grzempowski, P., Sudoł, E., Wajs, J., & Zając, M. (2017). The assessment of the application of terrestrial laser scanning for measuring the geometrics of cooling towers. *Geomatics, Landmanagement and Landscape*, (4), pp. 49-57. doi: 10.15576/GLL/2016.4.49.

[9] Muszyński, Z. (2014). Application of robust estimation methods to calculation of geometric distortions of a cooling tower shell. In *14th International Multidisciplinary Scientific GeoConference SGEM 2014*, pp. 65-72.

[10] Pandžić, J., Pejić, M., Božić, B., & Erić, V. (2016). Tls in determining geometry of a tall structure. In *Engineering geodesy for construction works, industry and research, proceedings of the international symposium on engineering geodesy*, pp. 279-290.

[11] Pesci, A., Casula, G., & Boschi, E. (2011). Laser scanning the Garisenda and Asinelli towers in Bologna (Italy): Detailed deformation patterns of two ancient leaning buildings. *Journal of cultural heritage*, Volume *12*(2), pp. 117-127. https://doi.org/10.1016/j.culher.2011.01.002.

[12] Marjetič, A. (2018). TPS AND TLS LASER SCANNING FOR MEASURING THE INCLINATION OF TALL CHIMNEYS. *Geodetic Courier/Geodetski Glasnik*, Volume 52.

[13] Zrinjski, M., Tupek, A., Barković, Đ., Polović, A., Novosel, T., & Vidoš, M. (2020, October). Determination and analysis of chimney inclination. In *Proceedings of the 8th International Conference on Engineering Surveying & 4th Symposium on Engineering Geodesy* , pp. 155-166. Zagreb, Croatia: Croatian Geodetic Society.

[14] Hamzić, A., & Hamzić, D. K. (2021). ISPITIVANJE VERTIKALNOSTI OBJEKATA SA KRUŽNOM BAZOM: KOMPARACIJA METODA. *Geodetic Courier/Geodetski Glasnik*, Volume 55.

[15] Kregar, K., Ambrožič, T., Kogoj, D., & Marjetič, A. (2015). Determining the inclination of tall chimneys using the TPS and TLS approach. *Measurement*, Volume *75*, pp. 354-363. https://doi.org/10.1016/j.measurement.2015.08.006.

[16] EN 1993 EUROCODE 3, „Design of steel structures – Part 3-2: Towers,“.

ANALYSIS AND APPLICATION OF TERRESTRIAL LASER SCANNING ALGORITHMS FOR DAM MONITORING

Milka Šarkanović Bugarinović[1], Miro Govedarica[2], Aleksandar Ristić[3], Željko Bugarinović[4], Igor Ruskovski[5]

Summary:

In this paper, existing point cloud processing algorithms are analyzed in order to monitor dams using terrestrial laser scanning. The introductory part describes the methodology of terrestrial laser scanning and the advantages that this method provides in relation to other acquisition methods of spatial data. In the following, existing algorithms and their application for monitoring dams, as a specific type of object, are analyzed. In addition, there are also examples of the application of terrestrial laser scanning in dam monitoring, such as crack detection, deformation monitoring, erosion measurement and analysis of changes in the dam environment.

Key words: monitoring, dam, TLS, algorithms, point cloud

[1] Istraživač pripravnik, Fakultet tehničkih nauka, Univerzitet u Novom Sadu, Srbija, milkasb@uns.ac.rs
[2] Redovni profesor, Fakultet tehničkih nauka, Univerzitet u Novom Sadu, Srbija, miro@uns.ac.rs
[3] Redovni profesor, Fakultet tehničkih nauka, Univerzitet u Novom Sadu, Srbija, aristic@uns.ac.rs
[4] Asistent sa doktoratom, Fakultet tehničkih nauka, Univerzitet u Novom Sadu, Srbija, zeljkob@uns.ac.rs
[5] Asistent-master, Fakultet tehničkih nauka, Univerzitet u Novom Sadu, Srbija, rus_igor@uns.ac.rs

1. INTRODUCTION

By continuous collection of spatial data and analysis of deformations on buildings and terrain, serious consequences caused by their deformations can be avoided. Traditional methods for deformation monitoring mainly use levelers, total stations, GNSS [1] and close-range photogrammetry that provide observation and analysis of individual points [2, 3, 4, 5]. However, with this approach, there are too few points that are observed and they cannot provide a comprehensive analysis of objects like dams. In addition, due to inaccessibility on the ground, it is often difficult to set control points on complex objects such as dams, and the period for obtaining results is usually quite long, which greatly affects the effectiveness of monitoring object deformations [6, 7]. In this paper, the advantages of applying terrestrial laser scanning in dam monitoring will be presented, as well as the ways in which this technology can be applied to improve the safety of dams. Also, the basic characteristics of terrestrial laser scanning and the way it is used in this process will be described.
Terrestrial laser scanning (TLS) is one of the most advanced technologies used for environmental scanning and mapping. The principle of operation of terrestrial laser scanning includes the following steps:

1. **Emitting a laser beam.** Scanning begins with the emission of a directed laser beam towards the desired surface.
2. **Reflection from the surface.** When the laser beam hits the desired surface, part of the laser beam is reflected towards the scanner. In this process, the scanner sensor records the time required for the laser beam to return to the scanner. Given the known speed of propagation of the laser beam through the air, the distance between the scanner and each reflected point from the surface is calculated (Fig. 1).
3. **Scanner rotation.** To scan an entire surface/object, the scanner usually rotates to cover a wider scanning area.
4. **Formation of point clouds.** All measured points on the surface of the object of interest are combined to create a point cloud with 3D coordinates (Fig. 1). The point cloud is the result of TLS representing different objects at different scales and levels of complexity [8].

   Data processing. After scanning, the point cloud can be further processed to remove errors, noise, perform classification or generate surface, terrain or object models.

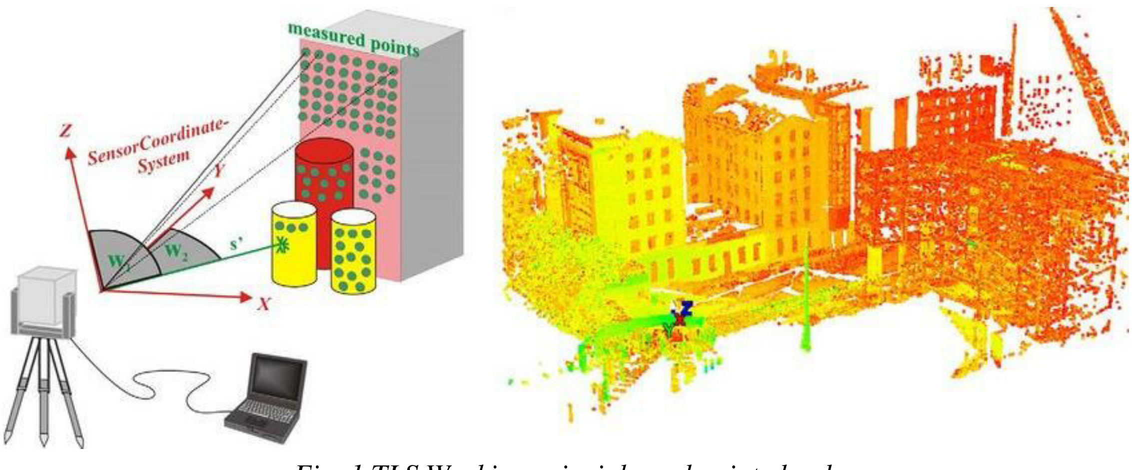

Fig. 1 TLS Working principle and point cloud

Terrestrial laser scanning finds application in various fields, including the creation of digital terrain models, cartography, the automotive industry, architecture, archeology, geology, the video game industry, where it is used to create accurate 3D models for various purposes (Figure 2).

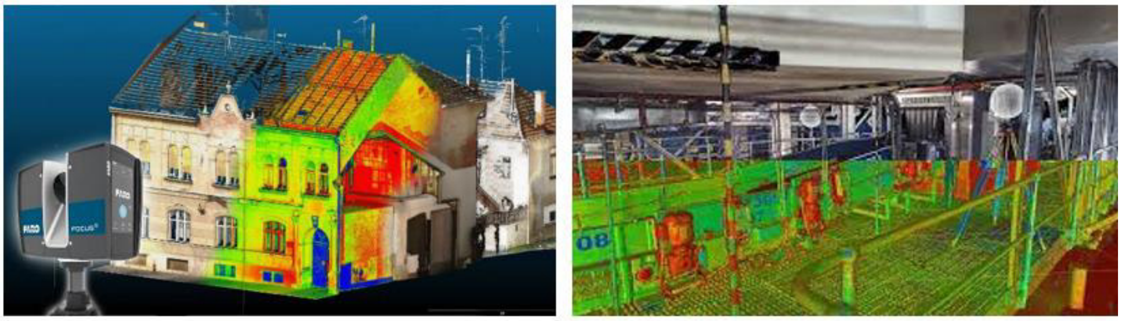

Fig. 2 Variety of TLS results application

Lately, with the aim of faster, automated and non-contact data collection, TLS technology has also been used for tracking terrain and objects [9]. This paper deals with the application of TLS in order to monitor dams. Safety of dams is crucial for their normal operation, therefore their continuous monitoring is important in order to prevent any dangerous effects of dams [10]. Traditional methods of dam monitoring, such as visual inspection, require a lot of time and human resources. In addition, the classic approach does not provide a detailed insight into the condition of the dam. Terrestrial laser scanning can significantly improve the dam monitoring process. This technology enables precise mapping and creation of detailed 3D models of dams, which gives a detailed insight into its condition and possible problems that may arise. In addition, terrestrial laser scanning can also detect minor changes in the surface of the dam, which can indicate potential problems. In this way, early detection of problems is ensured, which gives time to react before serious consequences occur.

The main advantage of TLS is reflected in the observation of deformations as a whole and not only in individual points. Namely, although TLS generally cannot measure the same point twice compared to other techniques, resulting in a loss of precision at a single point, strain tracking based on TLS can provide discrete 3D surface data, avoiding the locality and unilaterality of stress-strain analysis based on single point tracking data. At the same time, the application of TLS can improve the efficiency, accuracy, and variety of data types, which ensures that TLS-based surface slope deformation monitoring has a wide application area.

TLS also has great potential in inspection processes due to its ability to scan objects moving at high speeds with sub-millimeter accuracy.

2. RELATED WORK

In the past decade, a large number of studies have proven the feasibility of TLS in strain monitoring, and strain monitoring has been applied to surfaces, buildings, dams, tunnels, and the like [11]. In paper [12], an algorithm for dam monitoring based on spherical projection was proposed, which used a triangulation algorithm to construct a 3D surface model. The total deformation of the dam is obtained by comparing the cloud data of the different reference point with the created model of the reference surface. In paper [13], NURBS technology was used to model dam point cloud data and create a high spatial resolution model of an earthen dam with an accuracy of 2mm. This method enables precise modeling of smooth surfaces, which is especially important from the aspect of monitoring complex objects such as dams. In the paper [14], the authors propose a processing procedure for deformation extraction, the basic idea of which was to achieve high accuracy of point cloud registration in an iterative way using the ICP algorithm for different time periods in the reference region, which shows the undeformed geometry in each time period (stable locations) . The minimum detectable deformation was in the range below 10.0mm if numerical surface generation errors were removed. A registration algorithm based on the normal distribution was proposed in [15], which improved the original progressive triangulation filter algorithm. Due to the monitoring of the dam on a smaller surface, the accuracy in monitoring the deformations of the dam was at the millimeter level (the root mean square error in the movement of the settlement of the dam was about 1.98mm).

In addition to geodetic sensors, geotechnical sensors such as piezometers [16], inclinometers, extensometers, measuring tapes, measuring cells and others are increasingly used for monitoring buildings and terrain. These sensors are most often placed inside buildings/ground, in order to obtain comprehensive information about deformations. Their main advantage is reflected in the sub-millimeter accuracy and no visual inspection of the analyzed points is required. Also, some studies take into account only individual external influences, such as the influence of temperature in concrete dams [17, 18].

3. ALGORITHMS

Different algorithms are used for point cloud processing. In a general sense, all stages of point cloud processing can be grouped into several units, namely:

1. **Point cloud registration**. With TLS, multiple scans are usually combined to get a complete picture of the object. Point cloud registration is the process of aligning and merging different scans into a single coordinate system. There are various algorithms for point cloud registration, such as iterative nearest neighbor (ICP) [19], variants of the closest point method [20] and others. In order to achieve submillimeter accuracy, the authors in paper [21] propose a novel 3D deformation measurement method based on image guided point cloud registration, while in paper [22] the first fast algorithm for the registration of two sets of 3D points with a high degree of outlier correspondences is proposed.
2. **Noise removal**. Scans may be subject to noise and unnecessary data. To eliminate these types of interference, different point filtering algorithms can be used, such as the distance-based noise removal algorithm, algorithms for removing outliers or a combination with the principal component analysis (PCA) technique [23, 24]. In general, point cloud denoising techniques are diverse and can be grouped into three classes: filter-based, optimization-based, and deep learning-based algorithms [25] (Fig. 3).

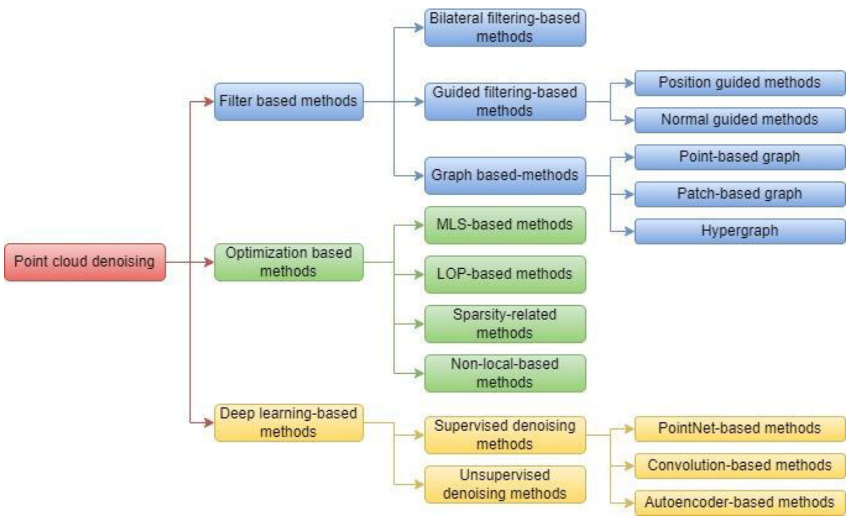

Fig. 3 Noise removal algorithms classification [25]

3. **Segmentation and classification.** To obtain more comprehensive information about the dam, segmentation of the point cloud should be performed. This procedure involves dividing points into different segments, such as dam walls,

dam crown, overflow channels, and others. For the automated grouping of adjacent points with similar characteristics, different segmentation algorithms can be used (Fig. 4), such as the Region Growing algorithm [26]. After segmentation, some of the algorithms for automatic classification of point clouds can be applied. Modern algorithms are based on machine learning methods (eg Support Vector Machines or Random Forest). The classification procedure involves classifying the points for each segment into a certain segment class (eg wall, crack, damage). Classification of point clouds is a very current area of research [27 - 30].

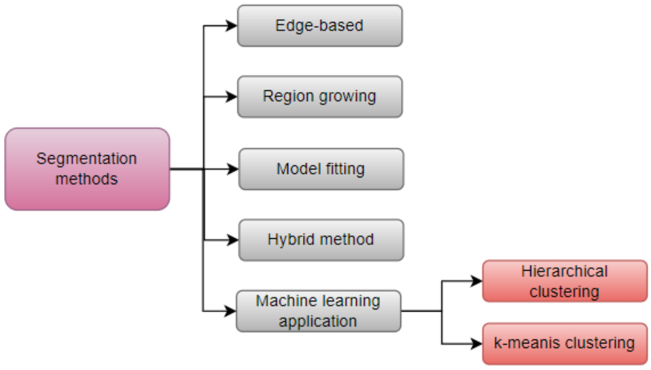

Fig. 4 Point cloud segmentation methods

4. **Change detection.** Comparing point clouds from different measurement periods can reveal displacements, cracks or other changes in the dam. Change detection algorithms typically include methods such as differential scanning, statistical analysis, or machine learning. Algorithms can be applied to the entire dam model to detect cracks and dam damage. This may include analysis of surface geometry, as well as the use of edge and texture detection algorithms. Also, point analysis algorithms, such as the RANSAC (Random Sample Consensus) algorithm, can be used to identify linear structures that indicate cracks or damage.
5. **Analysis of deformations.** Deformation analysis algorithms are used to quantify the nature of the deformations. These algorithms can calculate displacements, rotations, bulges, or other parameters that describe changes in the dam. For this type of analysis, different methods can be applied, such as least squares methods [31], interpolation or more advanced methods based on numerical analysis.
6. **Visualization of results.** Various visualization algorithms are used to display the results of measurements and analyses. This can include displaying a point cloud as a 3D model of the dam, a colored deformation map, or an animation showing changes over time, as well as generating reports and graphical displays. Algorithms for surface reconstruction, such as the triangulation algorithm or the Closest Point Method, can be applied to generate a three-dimensional dam model that can be used for further analysis and visualization.

The emphasis in this paper is on the algorithms that deal with the detection of changes and the analysis of deformations, therefore they are analyzed in more detail in the rest of the work.

3.1. CHANGE DETECTION

With the accelerated development of 3D laser scanning technology and progress in point cloud processing, these data are increasingly used in change detection algorithms [32-37]. The detection of changes is a key step in the analysis of TLS data when monitoring deformations on dams. The basic idea is to compare two or more clouds for the same object that were taken at different time periods, and to identify areas where changes have occurred. There are different approaches and algorithms for TLS change detection, such as:

1. **Differential scanning.** This method involves directly comparing point clouds from two different measurement periods to identify changes. Subtracting the coordinates of points from one cloud with the corresponding points from another cloud can reveal displacements, rotations or deformations of the object. Larger differences in coordinates indicate larger changes.
2. **Statistical analyses.** This method focuses on analyzing the statistical characteristics of point clouds to identify regions of change. For example, point density analysis or point height analysis can be used to detect regions of sudden changes or irregularities.
3. **Machine learning.** More advanced change detection techniques use machine learning algorithms. As input information, these algorithms can use different information such as distance, color, intensity of reflection and other.

Change detection is an iterative process that may involve multiple steps and parameter settings. A high level of accuracy and precision is required from the change detection algorithm, because the detection and monitoring of even small changes in the dam is of great importance for its safety. A combination of multiple change detection methods can provide the best results and reduce the possibility of errors or false positive/negative detections.

3.2. DEFORMATION ANALYSIS

There are different algorithms for the application of TLS in the monitoring of deformations on dams, which can be classified into one of the following groups:

1. **Algorithms for modeling shapes and deformations.** They are used to create a 3D model of the dam based on data obtained by laser scanning. After that, the model is used to analyze shape changes and deformations over a certain period of time. NURBS (non-uniform rational B-splines) is another algorithm that can be used to process point clouds on the basis of which NURBS curves and surfaces are created. NURBS curves can be used to model the cross section of dams, while NURBS surfaces can be used to model the surface of dams [14]. When used to process point clouds, the NURBS method uses mathematical curves that pass through specific points in the cloud. These curves are then combined to create a smooth surface that passes through all the point clouds and represents a smooth approximation of the point cloud.
2. **Algorithms for the detection of cracks and leaks.** These algorithms are used to detect and monitor changes in dam cracks, such as changes in crack shape and size. To detect concrete dam cracks, the authors in [38] use k-nearest neighbor (kNN) and principal components analysis (PCA) algorithms. Algorithms from the domain of artificial intelligence are being used more and more recently. Through a review paper [39], the authors show on the example of an earthen dam that machine learning algorithms, neural networks and hybrid models are more popular than other techniques.
3. **Algorithms for identifying risk zones.** Algorithms from this group analyze the data obtained by laser scanning to determine the areas that change most rapidly over time and that could represent a potential danger.

Deformation analysis focuses on measuring and evaluating changes in dam geometry and shape. This process involves various steps and techniques to calculate the various parameters that describe the deformations. Some of the common algorithms used in deformation analysis are:

1. **The method of least squares.** Algorithms applying least-squares methods try to find the best approximate transformations that minimize the squared errors. Based on this information, displacements, rotations and deformations on the dam can be calculated.
2. **Interpolation.** Interpolation is used to calculate continuous strain values from discrete measurement points. Interpolation algorithms use mathematical models or functions to fill the gaps between the measured points and obtain a smooth and continuous surface. This technique is useful for identifying areas with a high concentration of deformations or for visualizing deformations in the form of a continuous map.
3. **Numerical analysis.** These methods are based on dividing the dam structure into smaller elements and applying mathematical models to calculate the deformations in each element. This type of analysis allows for a more detailed understanding of the stress and strain distribution on the dam.

In order to ensure the most accurate analysis of the condition of the dam and determine potential risks, the existing TLS deformation algorithms are often combined with other techniques, such as geodetic and geotechnical measurements. The choice of the appropriate algorithm for deformation analysis depends on the specific characteristics of the dam, such as its size, the time required for the analysis, the desired level of accuracy, and others.

4. CONCLUSION

The application of TLS can improve the efficiency, accuracy and variety of data types, which ensures that TLS-based surface slope deformation monitoring has a wide application area. Using point clouds from several epochs of measurement, it is possible to model the dam, detect changes, and detect deformations. In this paper, a number of algorithms for the processing of point clouds are included in order to extract information that is important for dam monitoring. Based on the performed analyses, it is concluded that an increasing number of papers deal with the application of machine learning algorithms from each of the analyzed domains (detection of changes, deformations, and others). There is a large number of papers for concrete dams, although many algorithms can also be applied to earthen dams.

ACKNOWLEDGEMENT

This research (this paper) is supported by the Ministry of Science, Technological Development and Innovation through project number 451-03-47/2023-01/200156 "Innovative scientific and artistic research in the field of activities of FTN". The authors wish to express their deepest gratitude and warmest recognition to the Geoinformatics Laboratory of the Faculty of Technical Sciences in Novi Sad.

REFERENCES

[1] Vazquez-Ontiveros, J. R., Martinez-Felix, C. A., Vazquez-Becerra, G. E., Gaxiola-Camacho, J. R., Melgarejo-Morales, A., & Padilla-Velazco, J. (2022). Monitoring of local deformations and reservoir water level for a gravity type dam based on GPS observations. *Advances in Space Research*, 69(1), pp. 319-330.

[2] Holst, C., & Kuhlmann, H. (2016). Challenges and present fields of action at laser scanner based deformation analyses. *Journal of applied geodesy*, 10(1), pp. 17-25.

[3] Chen, Z. H., & Zhao, M. (2014). A method of metro tunnel deformation measurement based on the theory of close range photogrammetry. *Applied Mechanics and Materials*, *488*, pp. 755-758.

[4] Zhao, S., Kang, F., Li, J., & Ma, C. (2021). Structural health monitoring and inspection of dams based on UAV photogrammetry with image 3D reconstruction. *Automation in Construction*, *130*, 103832.

[5] Arbad, A. P., Arifin, Z. N., Martina, N., Nindya, E. P., & Nurfa, M. A. (2023). Monitoring Work Progress of Dam Construction based on Photogrammetric Point Clouds and BIM: Practical Approach to Teaching Industry. *The International Archives of the Photogrammetry, Remote Sensing and Spatial Information Sciences*, *48*, pp. 1-5.

[6] Berberan, A., Ferreira, I., Portela, E., Oliveira, S., Oliveira, A., & Baptista, B. (2011). Overview on terrestrial laser scanning as a tool for dam surveillance. In *6th International Dam Engineering Conference. LNEC, Lisboa*.

[7] Tsakiri, M., Lichti, D., & Pfeifer, N. (2006) Terrestrial Laser Scanning for Deformation Monitoring. *In Proceedings of the 3rd IAG/12th FIG Symposium*, Baden, Austria

[8] Di Stefano, F., Chiappini, S., Gorreja, A., Balestra, M., & Pierdicca, R. (2021). Mobile 3D scan LiDAR: A literature review. *Geomatics, Natural Hazards and Risk*, *12*(1), pp. 2387-2429.

[9] Wu, C., Yuan, Y., Tang, Y., & Tian, B. (2021). Application of terrestrial laser scanning (TLS) in the architecture, engineering and construction (AEC) industry. *Sensors*, *22*(1), 265.

[10] Hamzic, A., Avdagic, Z., & Besic, I. (2020). Multistage cascade predictor of structural elements movement in the deformation analysis of large objects based on time series influencing factors. *ISPRS International Journal of Geo-Information*, *9*(1), 47.

[11] Kaartinen, E., Dunphy, K., & Sadhu, A. (2022). LiDAR-based structural health monitoring: Applications in civil infrastructure systems. *Sensors*, *22*(12), 4610.

[12] Wang, J., & Zhang, C. C. (2014). Earth-Rock dam deformation monitoring based on three-dimensional laser scanning technology. *Advanced Materials Research*, *926*, pp. 1918-1921.

[13] Xu, H., Li, H., Yang, X., Qi, S., & Zhou, J. (2018). Integration of terrestrial laser scanning and nurbs modeling for the deformation monitoring of an earth-rock dam. *Sensors*, *19*(1), 22.

[14] Xiao, P., Zhao, R., Li, D., Zeng, Z., Qi, S., & Yang, X. (2022). As-built inventory and deformation analysis of a high rockfill dam under construction with terrestrial laser scanning. *Sensors*, *22*(2), 521.

[15] Chuanxun, Y., Ji, Y., Yong, L. I., Liusheng, H., & Shuisen, C. (2021). 3D laser scanning point cloud analysis method for dam deformation monitoring. *Bulletin of Surveying and Mapping*, (10), 54.

[16] Luo, J., Zhang, Q., Li, L., & Xiang, W. (2019). Monitoring and characterizing the deformation of an earth dam in Guangxi Province, China. *Engineering Geology*, *248*, pp. 50-60.

[17] Bowen, W., Zhaoxing, L., & Dongyang, Y. (2023). Optimized deformation monitoring models of concrete dam considering the uncertainty of upstream and downstream surface temperatures. *Engineering Structures*, *288*, 115950.

[18] Pan, J., Liu, W., Wang, J., Jin, F., & Chi, F. (2022). A novel reconstruction method of temperature field for thermomechanical stress analysis of arch dams. *Measurement*, *188*, 110585.

[19] Rusinkiewicz, S., & Levoy, M. (2001). Efficient variants of the ICP algorithm. In *Proceedings third international conference on 3-D digital imaging and modeling*, pp. 145-152. IEEE.

[20] Besl, P. J., & McKay, N. D. (1992). Method for registration of 3-D shapes. In *Sensor fusion IV: control paradigms and data structures*, Vol. 1611, pp. 586-606. Spie.

[21] Yuan, Y., Ge, Z., Lai, B., Guo, X., Zhang, Y., Liu, X., ... & Yu, Q. (2023). Three dimensional deformation measurement method based on image guided point cloud registration. *Optics and Lasers in Engineering*, *161*, 107399.

[22] Yang, H., Shi, J., & Carlone, L. (2020). Teaser: Fast and certifiable point cloud registration. *IEEE Transactions on Robotics*, *37*(2), pp. 314-333.

[23] Cheng, D., Zhao, D., Zhang, J., Wei, C., & Tian, D. (2021). PCA-based denoising algorithm for outdoor Lidar point cloud data. *Sensors*, *21*(11), 3703.

[24] Jia, C. C., Wang, C. J., Yang, T., Fan, B. H., & He, F. G. (2019). A 3D point cloud filtering algorithm based on surface variation factor classification. *Procedia Computer Science*, *154*, pp. 54-61.

[25] Zhou, L., Sun, G., Li, Y., Li, W., & Su, Z. (2022). Point cloud denoising review: from classical to deep learning-based approaches. *Graphical Models*, *121*, 101140.

[26] Grilli, E., Menna, F., & Remondino, F. (2017). A review of point clouds segmentation and classification algorithms. *The International Archives of the Photogrammetry, Remote Sensing and Spatial Information Sciences*, *42*, pp. 339-344.

[27] Rabbani, T., Van Den Heuvel, F., & Vosselmann, G. (2006). Segmentation of point clouds using smoothness constraint. *International archives of photogrammetry, remote sensing and spatial information sciences*, *36*(5), pp. 248-253.

[28] Weinmann, M., Jutzi, B., Hinz, S., & Mallet, C. (2015). Semantic point cloud interpretation based on optimal neighborhoods, relevant features and efficient classifiers. *ISPRS Journal of Photogrammetry and Remote Sensing*, *105*, pp. 286-304.

[29] Weinmann, M., Jutzi, B., & Mallet, C. (2013). Feature relevance assessment for the semantic interpretation of 3D point cloud data. *ISPRS Annals of the Photogrammetry, Remote Sensing and Spatial Information Sciences*, *2*, pp. 313-318.

[30] Niemeyer, J., Rottensteiner, F., & Soergel, U. (2014). Contextual classification of lidar data and building object detection in urban areas. *ISPRS journal of photogrammetry and remote sensing*, *87*, pp. 152-165.

[31] Gruen, A. (1985). Adaptive least squares correlation: a powerful image matching technique. *South African Journal of Photogrammetry, Remote Sensing and Cartography*, *14*(3), pp. 175-187.

[32] Stilla, U., & Xu, Y. (2023). Change detection of urban objects using 3D point clouds: A review. *ISPRS Journal of Photogrammetry and Remote Sensing*, *197*, pp. 228-255.

[33] Chen, B., Deng, L., Duan, Y., Huang, S., & Zhou, J. (2015). Building change detection based on 3D reconstruction. In *2015 IEEE international conference on image processing (ICIP)*, pp. 4126-4130. IEEE.

[34] Teo, T. A., & Shih, T. Y. (2013). Lidar-based change detection and change-type determination in urban areas. *International journal of remote sensing*, *34*(3), pp. 968-981.

[35] Zeibak, R., & Filin, S. (2008). Change detection via terrestrial laser scanning. *Technion-Israel Institute of Technology, Faculty of Civil and Environmental Engineering*, pp. 430-435.

[36] Qin, R., Tian, J., & Reinartz, P. (2016). 3D change detection–approaches and applications. *ISPRS Journal of Photogrammetry and Remote Sensing*, *122*, pp. 41-56.

[37] Liu, D., Li, D., Wang, M., & Wang, Z. (2021). 3D change detection using adaptive thresholds based on local point cloud density. *ISPRS International Journal of Geo-Information*, *10*(3), 127.

[38] Ge, Y., Liu, J., Zhang, X., Tang, H., & Xia, X. (2023). Automated Detection and Characterization of Cracks on Concrete Using Laser Scanning. *Journal of Infrastructure Systems*, *29*(2), 04023005.

[39] Beiranvand, B., & Rajaee, T. (2022). Application of artificial intelligence-based single and hybrid models in predicting seepage and pore water pressure of dams: A state-of-the-art review. *Advances in Engineering Software*, *173*, 103268.

PROPOSAL OF DECREE ON CONSTRUCTION SITES IN SLOVENIA

Mateja Držečnik[1], Uroš Klanšek[2]

Summary:

The paper introduces a novel proposal of decree on construction sites in Slovenia. Its core part addresses conditions for construction site arrangements, i.e. marking, environmental protection and emissions reduction measures, temporary facilities, reuse of uncontaminated soil and other naturally occurring material, waste management, construction site layout plan and construction logbook. The obligations of the participants in the construction process are also revealed. The present article is aimed to serve as an informative source to nearby countries with a similar construction regulations and contractors from abroad, as well as to share key facts about the subject under consideration among a wider international professional audience to incite discussion and suggestions for improvement.

Key words: construction operations, construction site arrangement, regulations, decree on construction sites.

[1] Asst. dr., University of Maribor, Faculty of Civil Engineering, Transportation Engineering and Architecture, Smetanova ulica 17, 2000 Maribor, Slovenia, e-mail: mateja.drzecnik@um.si
[2] Prof. dr., University of Maribor, Faculty of Civil Engineering, Transportation Engineering and Architecture, Smetanova ulica 17, 2000 Maribor, Slovenia, e-mail: uros.klansek@um.si

1. INTRODUCTION

Before starting construction, it is necessary to establish the conditions for organized work on the construction site. The scope of the preparatory activities necessary to establish the mentioned conditions is influenced by many factors, among which the type and size of the construction together with the materials that need to be included in the production processes and the available time in which the work needs to be carried out stand out [1]. Applicable legislation, technical restrictions, conditions of production processes, characteristics of devices and safety requirements are additional general influencing factors. Construction site arrangements are also influenced by specific factors, such as contractual agreements, economy of the production, characteristics of the company, peculiarities of the location, properties of the building, etc.
The aim of construction site arrangements is to organize and equip workplaces on the construction site so that the construction can be completed on time, in the agreed quality and economically while simultaneously fulfilling all the conditions dictated by the aforementioned influencing factors. Interventions in the built environment have to follow the public interest [2], as must the construction site arrangements. In this way, the paper introduces a novel proposal of decree on construction sites in Slovenia. Its core part addresses conditions for construction site arrangements [3], i.e. marking, environmental protection and emissions reduction measures, temporary facilities, reuse of uncontaminated soil and other naturally occurring material, waste management, construction site layout plan and construction logbook. Subsequently the obligations of the participants in the construction process are revealed. Finally, conclusions are given towards the end of the paper.

2. CONDITIONS FOR CONSTRUCTION SITE ARRANGEMENTS

2.1. MARKING

In general, the construction site should be marked with a construction board. According to the proposal, the said board must be made for every construction site where facilities will be built, for which a building permit has been obtained, except for those that are undemanding and in case of changes in the purpose of buildings or their parts. It should provide the data about the: (i) investor, (ii) name of construction, (iii) number and date of the building permit, the date of its validity/finality and the authority that issued such permit, (iv) date of registration of the start of construction, (v) designer of detailed design, (vi) name and surname of design manager with an identification number, (vii) supervisor, (viii) name and surname of head of supervision with an identification number, (ix) name and surname of the coordinator for safety and health at work during the construction phase, (x) contractor, and (xi) name and surname of the construction manager. Whenever the said data changes, the related update on the construction board must also be done.
The construction board can be made entirely in physical form or partially in physical form with data accessible via a QR code. In the latter case, the mentioned board needs to contain, in physical form, at least information about the investor and the name of the construction, as well as the QR code that is linked to eConstruction platform [4], which enables conducting business electronically. The physical construction board is required to be placed in a visible place at the entrance to the construction site. When building linear facilities, such as roads, transport infrastructure objects, pipelines, communication networks, energy lines, etc., the construction board should be placed at the beginning or end of the route or at a location next to the construction office.

2.2. ENVIRONMENTAL PROTECTION AND EMISSIONS REDUCTION MEASURES

It is necessary to assure the implementation of measures to prevent the leakage, spreading or leaching of loose and other building materials, liquids as well as waste from the construction site. When performing works either on point sources of air pollution (e.g., places of cleaning, grinding, milling or chiselling) or on those that are dispersed (e.g., traffic on construction routes; transhipment or storage of building materials; excavation, transhipment or transport of soil; handling of construction waste; etc.), several measures should be carried out at construction site to prevent and reduce particle emissions.

Dust deposits must be removed by vacuuming, damp or wet process, and it is forbidden to remove them by blowing, with compressed air or dry sweeping. They need to be bound on all surfaces, including unpaved construction roads, by maintaining the humidity of these surfaces, such as by automatically controlled or manual water spraying. During the execution of works with construction machinery or other devices for processing construction materials, like cutting plates or grinders, it must be assured that measures are taken to reduce dust, such as wetting, capturing or vacuuming dust or other suitable dust removal technique. Moving and transhipment of construction waste should be performed from a height that is not greater than the height of caissons or containers for collecting and transporting construction waste. If this is not technically possible, downpipes or covered gutters are required to be used, and parts of the downpipe must be connected with cuffs in an impermeable manner for dust emission.

Demolition or dismantling of buildings should be accomplished in large pieces wherever technically possible and using covers and barriers to prevent dust from spreading. In case of removing a large-area buildings or blasting a larger facilities where it is not possible to assure covers and barriers, adequate alternative particle containment such as heavy wetting or a water curtain must be provided. Conveyor belts for loose materials should be completely covered, closed or continuously wetted with a water mist, while the conveyor systems themselves must operate at low exit speeds. Stored loose materials need to be covered, moistened or shielded from wind to reduce dust.

Paved construction roads are required to be cleaned regularly with efficient dust-free sweepers or wet cleaning. Construction roads that will be used for more than twelve months must be covered with a bearing asphalt or other anti-dust base. At exits from construction roads or construction sites to public areas, it must be ensured that the wheels and chassis of vehicles are washed. In case of pollution or damage to the public area, immediate cleaning or repair must be provided. The speed of vehicles on the construction site should be limited to a maximum of 20 km/h. The parking and supply of working machines with fuels or lubricants must be arranged in such a way that the leakage, seepage and release of these substances into the environment is prevented. In case of leakage, seepage or release of these substances into the environment, they must be contained and their safe disposal must be ensured.

2.3. TEMPORARY FACILITIES

Temporary facilities are allowed to be erected on the construction site area exclusively for the construction period. During construction, the contractor is obliged to provide sanitary facilities with a closed municipal waste water collection system or a connection to public sewage, electricity, drinking water, and a closed space where workers can withdraw from precipitation. As soon as it is expected that workers will reside or sleep on the construction site during construction, it must be additionally ensured on it heated or air-conditioned places for sleeping and socializing, a kitchen and sanitary facilities with showers that provide hot water and are connected to a closed municipal waste water system or to public sewage system. Municipal waste water that accumulates in a closed system must be collected and transported to the treatment plant. All temporary facilities must be removed from the construction site before obtaining an operating permit for the built objects.

2.4. REUSE OF UNCONTAMINATED SOIL AND OTHER NATURALLY OCCURRING MATERIAL

The investor must ensure that the excavated soil is preferentially used for construction at the place where it was excavated. In this context, the construction site layout plan should provide details about estimated volume of the excavation caused by construction work on the construction site and planned handling of it. It is also necessary to indicate the volume of excavated soil intended for use on the construction site, which will not result from the implementation of construction works on it. The volume of uncontaminated soil, which in its original condition will be certainly employed for construction on the same construction site where it was excavated, should be specified too. However, in doing so, it is needed to give information about any associated analyses and present the supporting documents in the attachments.

2.5. CONSTRUCTION WASTE MANAGEMENT

Construction waste management must be performed in accordance with the EU construction and demolition waste management protocol [5] and the guidelines for the waste audits before demolition and renovation works of buildings [6], which are both published on the central website of the state administration. When handling materials containing asbestos, polychlorinated biphenyls or terphenyls, the provisions of the special regulations [7-8] governing this must also be taken into account. Therefore, the construction site layout plan needs to contain information on the type and mass of construction waste to be: (i) generated at the construction site as a result of the construction itself; (ii) hazardous and disposed before the removal or reconstruction of the facility; (iii) collected separately at the construction site; (iv) processed at the construction site including data on treatment procedure; (v) delivered to a construction waste collector; and (vi) handed over to a construction waste treatment contractor.

On large construction sites, it is not allowed to treat with crushing, breaking or grinding processes with devices, unless: (i) they are equipped to capture and clean the exhaust air; (ii) they are automatically controlled and continuously employed to create a water mist or water curtain on all conveyor belts including at entry and exit openings; or (iii) the water is used in cleaning operations. However, on the construction site, it is banned to treat construction waste from other construction sites by crushing, breaking or grinding procedures, including the processing of construction waste in mobile devices.

2.6. CONSTRUCTION SITE LAYOUT PLAN

Principally, the construction site layout plan must be drawn up for all construction sites that are required to be marked. In addition, the said plan should be also made when building facilities on large construction sites for which a building permit has not been obtained. It is an independent documentation prepared by an expert certified on basis of regulations governing architectural and engineering activities, which must be attached to the notification of the start of construction. For legal constructions on large construction sites that do not require a building permit, the construction site layout plan must be available on-site in paper or electronic form. This plan is allowed to be changed due to the construction progress itself, but the revised version must be reported.

The content of construction site layout plan should be structured in the following appendices, which need to provide extensive data required by regulation: 1A Introductory Sheet, 1B Construction Information, 1C Construction Site Information, 1D Environmental Protection, and 1E Excavated Earth Handling and Waste Management.

The scope of data depends on the size and complexity of the construction site and the estimated execution time. The presentation for different technological phases can be made separately, however this must be taken into account according to the nature, extent and hazards of works. If the construction will be performed on a part of the area of the airport, infrastructure facilities, devices and systems of navigation services of air traffic, road, railway or port, which will be simultaneously in function, it is necessary to ensure the safe and uninterrupted operation of these facilities with the construction site layout plan. Likewise, the possibility of intervention and fire safety in the construction area and neighbouring buildings must not be impaired by the construction.

2.7. CONSTRUCTION LOGBOOK

As specified by regulation, the construction logbook must be kept for all constructions for which a building permit has been issued, except for those that are undemanding and in instance of changes in the purpose of buildings. Exceptionally, it is also required to keep construction logbook for constructions on large sites for which a building permit has not been obtained. The construction logbook must be kept from the day the first contractor is introduced to work, or from the beginning of construction site arrangements, until the construction is completed.

The construction logbook must be maintained in eConstruction platform. It must be accessible for entries to all participants in the construction process, as well as to the conservator/archaeologist, opinion-providers and authorized inspectors until the completion of construction. Authority for entries in the construction logbook is assigned by the investor to the head of supervision and the design manager, and to the construction manager by the head of supervision after the contractor is introduced to work. The investor and the head of supervision do not have the right to revoke the granted access, except in case of termination of the contract. The construction logbook includes: 2A Introductory Sheet, 2B Construction Site Daily Sheets, and 2C Contractor's Daily Sheets.

Introductory Sheet contains basic information about participants in the construction process and is filled out by the supervisor. Construction Site Daily Sheets must provide daily data on the construction site and on the execution of works and measures on it. The data is entered in this sheets by the construction manager or the construction site manager, if there are several contractors active at the construction site. An authorized subordinate can also do this entries, however the data confirmation must be executed by the construction (site) manager. The designer, conservator/archaeologist, opinion-providers, and inspectors also enter their findings in this sheets.

Contractor's Daily Sheets are intended for daily entries of each individual contractor. Other participants in the construction process also enter their notes into them. Data relating to the works execution and to the construction itself, including descriptions of permissible minor deviations, are entered into the said sheets. Minutes, proofs, drawings, statements, letters and other documents can be entered in the construction logbook as attachments.

3. OBLIGATIONS OF PARTICIPANTS IN CONSTRUCTION PROCESS

Contractors, construction managers and the construction site manager are required to ensure that the measures specified in the construction site layout plan are carried out. The supervisor and the head of supervision must assure that the compliance of the implementation of measures with the construction site layout plan is checked on the construction site during the supervision. If a discrepancy between the implementation of the measures and the construction site layout plan is found, they must immediately inform the investor, and the findings and suggestions for achieving a suitable compliance must be entered in the construction logbook.

In the event that the contractors, their construction managers, or the construction site manager do not comply with the request entered by the head of supervision or otherwise do not implement measures in accordance with the construction site layout plan, the head of supervision must immediately inform the authorized inspector and the investor as well as enter the finding of non-compliance in the construction logbook. On the basis of such notice from the supervisor, the investor must, in accordance with the construction contract, promptly request in writing from the contractor to immediately implement measures in accordance with the construction site layout plan, and inform the supervisor correspondingly.

4. CONCLUSION

To a great extent, the considered proposal of decree on construction sites maintains the currently valid rules on construction sites [9]. A major change compared to the current regulation is that the construction site layout plan, the construction waste management plan and the study on the prevention and reduction of particle emissions from the construction site have been combined into a common document that can be prepared in digital form over the eConstruction platform. The combined document is expected to improve environmental protection as well as the transparency in the construction waste management, tracking and control of its flow.

A significant innovation is also the obligation to keep an electronic construction logbook on a special module in the eConstruction platform. The construction logbook is no longer linked to a contractor, but to the construction site, which prevents its duplication in cases when several contractors are located there at the same time, and therefore provides a more transparent insight into the daily happenings on the construction site. Through the eConstruction platform, it is possible to enter the construction logbook for all authorized persons, including inspection supervision. A step towards digitization of construction site arrangements is also that it is not necessary to write all the contents on the construction board, but they can be seen via the QR code.

ACKNOWLEDGEMENT

The authors acknowledge the financial support from the Slovenian Research Agency (Research Core Funding No. P2-0129).

REFERENCES

[1] Schach R., Otto J. (2017). Baustelleneinrichtung: Grundlagen – Planung – Praxishinweise – Vorschriften und Regeln. 3. Auflage, Springer Vieweg, Wiesbaden, Germany.

[2] Šuman N., Dolaček-Alduk Z., Klanšek U. (2018). Construction procedures for public goods on roads of local interest in Slovenia. Tehnički vjesnik, Volume 25, pp. 231-239. https://doi.org/10.17559/TV-20170721124145.

[3] Decree on Construction Sites, Government act record: 2022-2550-0019 (in Slovenian), https://e-uprava.gov.si/drzava-in-druzba/e-demokracija/predlogi-predpisov/predlog-predpisa.html?id=13853.

[4] Building Act. Official Gazette of the Republic of Slovenia, No. 199/21.

[5] EU Construction and Demolition Waste Management Protocol. European Commission: Directorate-General for Internal market, Industry, Entrepreneurship and SMEs, 2016.

[6] Guidelines for the Waste Audits Before Demolition and Renovation Works of Buildings. European Commission: Directorate-General for Internal market, Industry, Entrepreneurship and SMEs, 2018.

[7] Decree on Management of Waste Containing Asbestos. Official Gazette of the Republic of Slovenia, No. 34/08.

[8] Decree on the Disposal of Polichlorinated Biphenyls and Polichlorinated Terphenyls. Official Gazette of the Republic of Slovenia, No. 34/08 and 9/09.

[9] Rules on Construction Sites. Official Gazette of the Republic of Slovenia, No. 55/08 and 54/09.

MEASURING COST AND TIME OVERRUNS IN INFRASTRUCTURE PROJECTS IN CHINA

Jelena M. Andrić[1]

Summary:

Infrastructure projects are of essential importance for the modern societies due to their contribution to socio-economic development and prosperity of country. During their project lifecycle, infrastructure projects are exposed to multiple and serious risks which cause budget overruns and delays in project completion. The aim of this study is to analyze the cost and time performance of infrastructure projects in China and to examine the relation between cost and time overruns over the project size and implementation period, as well as correlation between cost and time overruns. A sample of 58 infrastructure projects including railways, roadways and energy sector in China is collected and analyzed using descriptive statistical analysis method. The results show that the mean value of cost overruns is 14.83% and the mean value of time overrun is 26.51% in infrastructure projects in China.

Key words: Cost overruns, Time overruns, Infrastructure projects, Descriptive statistical analysis, China

[1] Assistant Professor, Xi'an Jiaotong-Liverpool University, Suzhou, China, Jelena.Andric@xjtlu.edu.cn

1. INTRODUCTION

Infrastructure is of essential importance for the modern societies since it has role to enable the undisrupted flow of goods, energy, information, and people. Governments of many countries have invested a large capital in infrastructure in order to contribute to socio-economic development and prosperity of their country. The Chinese Government has established Belt and Road Initiative with the aim to build major infrastructure projects such as railways, seaports, highways, bridges, tunnels in order to sustain economic growth, and enable the connectivity and cooperation between China and other Asian, European and African countries [1, 2]. During the whole project lifecycle infrastructure projects are exposed to multiple risks due to their complexity, large-scale, dynamic, geotechnical conditions along the route and large number of stakeholders involved in project [2]. Generally, many risks which appear during the whole project lifecycle can result in the unwanted outcomes such as budget overruns and delays in project completion [3]. One of the examples from construction industry practise is the completion of Hong Kong-Zhuhai-Macau Bridge which connects Special Administrative Regions Hong Kong and Macau with Mainland China. This project was delayed for one-year due to unstable supply materials, a labor shortage, a height restriction and a legal challenge regarding the environmental impact [4]. Historically and geographically, infrastructure projects were prone to cost and time overruns [5]. Considering their frequent appearance in infrastructure projects, cost and time overruns have become an integral part of construction projects worldwide [6]. Overruns in infrastructure projects are global phenomenon [7]. Cost overrun is defined as the amount by which actual cost exceeds estimated cost, with cost measured in the local currency, constant prices and against a consistent baseline [8]. Cost overruns have occurred in different infrastructure projects type across different countries, such as railway projects in Australia [9], Dutch transport infrastructure projects [10], Italian transport projects [11], Belgian transport infrastructure projects [12], public projects in Qatar [13], megatransport projects in Hong Kong [14], Norwegian transport projects [15], road projects in the USA [16], and others. Similarly, delay in construction projects is defined as the extra time required or incurred either beyond the stipulated completion date or beyond the project stakeholders' date to complete the project [17]. Time overruns have appeared in many infrastructure projects worldwide such as, infrastructure projects in the UK and the USA [18], public projects in Qatar [13], and others. The current literature reveals there are more publications related to cost overruns in transport infrastructure projects compared to time overruns in similar projects. Additionaly, the majority of these publications related to cost performance and cost overruns in infrastructure projects are focused on the European countries, the USA, Australia, however there is a less research related to cost and time performance in infrastructure projects in Asian countries. Also, there are no relevant studies related to cost and time performance of infrastructure projects in China even though a large number of infrastructure development projects is currently ongoing in China. Therefore, the aims of this paper are following: (1) to analyse the cost and time performance of infrastructure projects in China; (2) to examine the influence of two independent variables, project size and the length of implementation period on cost and time overruns in infrastructure projects. A sample of 58 infrastructure projects completed in China is collected in order to determine the characteristics of cost and time perfromance by statistical methods and the correlation between project size and implementation period and cost and time overruns by regression analysis. The results has application in planning and managing the similar infrastructure projects in the future.

2. LITERATURE REVIEW

Regarding cost overruns, there are many literature related to measuring the performance and the size of cost overruns in infrastructure project. The initial studies on the cost performance and the size of cost overruns in transport infrastructure projects was introduced by Flyvbjerg et al. [19]. According to this study, the performance of 258 transport projects located in Europe and North America is measured and the average cost overrun of this sample was 28%. The average cost overrun in transport infrastructure projects in Netherlands was 16.5% which was estimated in research carried out by Cantarelli et al. [20]. Further, Huo et al. have conducted investigation on cost performance of mega transport projects in Hong Kong and it is determined that the average cost overrun is 39.18% [14]. The results of cost perofrmance analysis of transport infrastructure projects in Slovenia have revealed that the size of cost overruns were 19% [21]. For the studied transportation projects in Belgium, the final cost prices are on average 10.26% higher than in the initial phase [12]. In some studies, the focus was on one type of transport infrastructure projects. Particularly for railway projects in Australia, the research has shown that the magnitude of cost overrun is 23% [9].
In case of time overruns in infrastructure projects, some of the earliest research in this area is conducted by Assaf and Al-Hejji [22]. In this research, the average time overrun for projects in Saudi Arabia was between 10% and 30% of original duration of project. For projects in the UK and the USA, the average schedule delay was 23.19% [18]. The other literature is more focused on the causes of delays and cost overruns in infrastructure projects.

3. METHODOLOGY

A methodology for this study is developed in order to provide answers related to cost and time overruns in infrastructure projects in China. Data collection of completed infrastructure projects in China is carried out in order to analyze project performance and overruns. In total, data of 58 completed infrastructure projects in China are collected. Infrastructure projects include: railways (16), roadways (31), and energy sector (11). Data for each project includes: name of the project, year of decision to build, the infrastructure type, the estimated cost, the actual cost, the estimated duration and the actual duration of project. Further, this paper gives analyses of two variables on the size of cost and time overruns, as well as the analysis of correlation between cost and time overruns. The selected variables are: project size and implementation period. The relations between the variables and the size of cost and time overruns is determined by a different probability and statistical methods for data analysis.
Cost overruns is defined as the difference between the forecast and actual construction cost (Love et al., 2014). In mathematical terms, cost overruns are calculated as the ratio between the additional cost of project over the appraisal estimated cost. The following equation is applied:

$$Cost\ overrun = \frac{Actual\ cost - Appraisal\ cost}{Appraisal\ cost} * 100\% \tag{1}$$

where, *actual cost* – the total cost of project after completion; *appraisal cost* –the estimated cost of project after the formal decision to build is made.
If the actual cost is higher than appraisal cost, then cost overrun has appeared on the project and it is expressed as a percentage point above 0%. In case, if actual and appraisal cost are the same, then project is completed on budget and it hasn't experienced overrun or underrun. When the actual cost is less than estimated cost, then the project has expressed cost underrun and its value is shown as a percentage point below zero.

Similarly, the general definition of delay in construction projects is the time overrun beyond completion date specified in contract or beyond the date that the parties agreed upon for delivery of a project [22]. Hence, schedule delay represent the additional time needed to complete the project. Correspondingly, time overruns can be described and calculated. Precisely, according to definitions time overruns can be calculated and provided by the following equation:

$$Time\ overrun = \frac{Delay}{Appraisal\ duration} * 100\% \tag{2}$$

When the definition of delay is applied than time overrun is given as following:

$$Time\ overrun = \frac{Implementation\ period - Appraisal\ duration}{Appraisal\ duration} * 100\% \tag{3}$$

where, *implementation period* – represents the total time in months after which was completed the project; *appraisal duration* – is determined the duration of project in months after the formal decision to build is made; *delay* – the additional time in months needed to complete project.

Generally, if implementation period is longer than appraisal duration, then delay has occurred and the value of time overrun is expressed as a percentage point above 0%. The second scenario is that implementation period is equal to appraisal duration and there is no delays and no time overrun in project. The third scenario is that implementation period is shorter than appraisal duration and project experienced time underrun and the value as percentage point is below 0%.

For data analysis, some of the probability and statistical methods include: Binominal test, Mann-Whitney U-test, F-test, and linear regression analysis [23]. The binominal test is a parametric hypothesis test that applies when the population can be divided into two classes: each observation of this population will belong to one or the other of these two categories [24]. The application of the binominal test in this study is to determine whether projects with cost overrun and cost underrun, as well as time overrun and with time underrun are equally likely to occur. Mann-Whitney U-test is a nonparametric counterpart of the t-test and gives the most accurate estimates of significance, especially when sample sizes are small and when the data do not approximate a normal distribution [25]. Linear regression analysis is used to determine whether there is a relationship between the dependent y-variable and the x-explanatory factor. The task of this analysis is to evaluate if the explanatory factor is a statistically significant predictor of outcome [26]. Fisher's exact test is a statistical test which is applied to confirm if there are nonrandom associations between two variables, X and Y. For all statistical analysis in this research and Figures, *Matlab* is applied.

4. COST AND TIME OVERRUNS IN INFRASTRUCTURE PROJECTS

4.1. THE CHARACTERISTICS OF COST PERFORMANCE

Figure 1 shows histogram of cost overruns distribution in infrastructure projects. This histogram displays that the range of cost overrun is between -30% and 90%, and bins with time overrun between -15% and 0%, and between 0% and 15% have the highest number of projects compared to other bins, 16 and 17, respectively. However, these two bins of projects were no different from other bins when project type, project size and implementation period are considered. The statistical analysis of sample represents the characteristics of cost overruns as following:

- the range of cost overrun in infrastructure projects is between -29.88% and 88.00%;
- the mean value of cost overrun is 14.83% (SD =27.44);

- the number of projects experienced cost overrun is 62.07%; 5.17% projects have completed on budget and 32.76% projects were cost underrun;
- projects with cost overrun are common as projects with cost underrun (p=0.0195, Binominal test);
- the average cost overrun is 29.20% (SD=25.01) in projects with overruns; and
- the average cost underrun is -10.16% (SD=8.33) in projects with underruns (Mann-Whitney U-test, U=0.00, p < 0.0001)

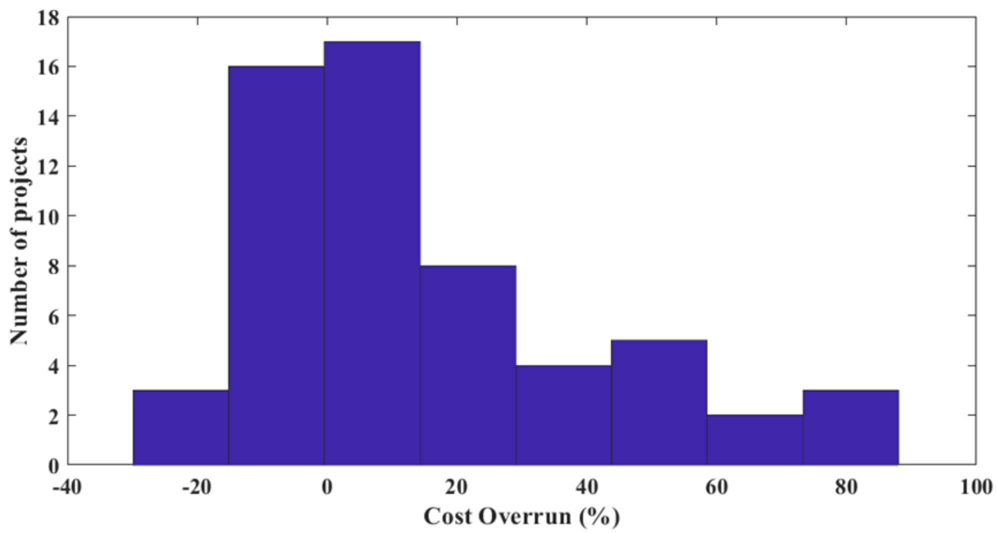

Fig. 1 Histogram of cost overruns in infrastructure projects

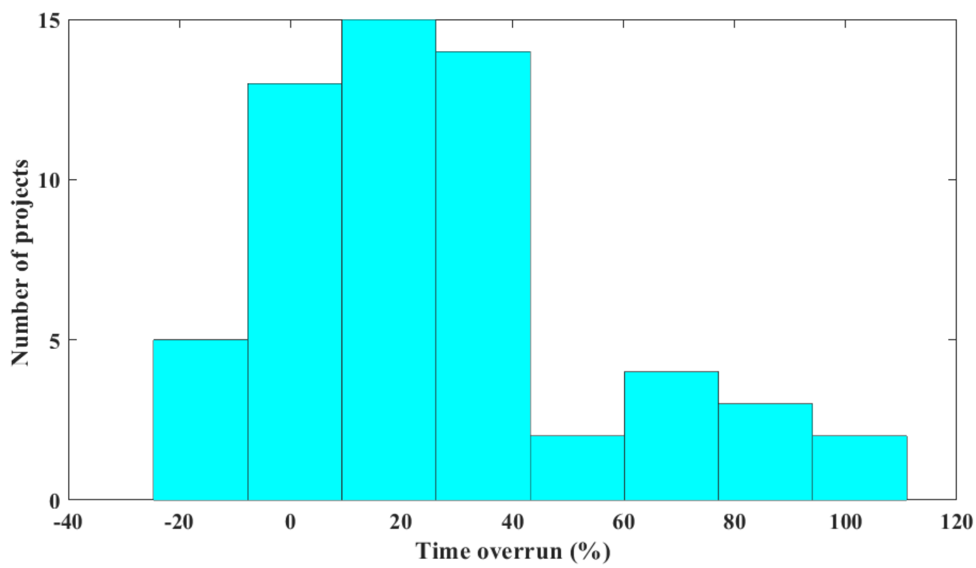

Fig. 2 Histogram of time overruns in infrastructure projects

4.2. THE CHARACTERISTICS OF TIME PERFORMANCE

A histogram of time overruns distribution in infrastructure projects is provided in Figure 2. Time overrun ranges between -25% and 115%. The statistical analysis of sample shows the characteristics of time overruns as following:

- the range of time overrun in infrastructure projects is between – 24.64% and 111%;
- the mean value of time overrun is 26.51% (SD = 30.57);
- the number of projects experienced overrun is 77.58%; 10.34% projects have completed on time and 12.07% projects were completed ahead of schedule;

- projects with time overrun are common as projects with time underrun (p=0.00001095, Binominal test);
- the average time overrun is 36.11% (SD = 27.76) in projects with time overruns and the average time underrun is -12.47% (SD = 7.88) in projects with time underrun (Mann/Whitney U-test, U=0.00, p < 0.0001)

4.3. COST AND TIME OVERRUN OVER PROJECT SIZE

The influence of project size on cost overrun and time overrun is examined by linear regression analysis. The analysis has shown that there is a correlation between the project size and cost overrun (*F-test*, F = 39.6, p < 0.001). Mathematically, the regression line for cost overrun over project size is given by the following equation:

$$C = 0.007283 * A + 4.7132 \quad (4)$$

in which, *C* – cost overrun, and *A* – actual cost after the project completion.
Figure 3 depicts a regression line for cost overrun over the project size. On the other hand, there is no correlation between time overrun and project size for infrastructure projects in China (*F-test*, F=0.00019, p = 0.989).

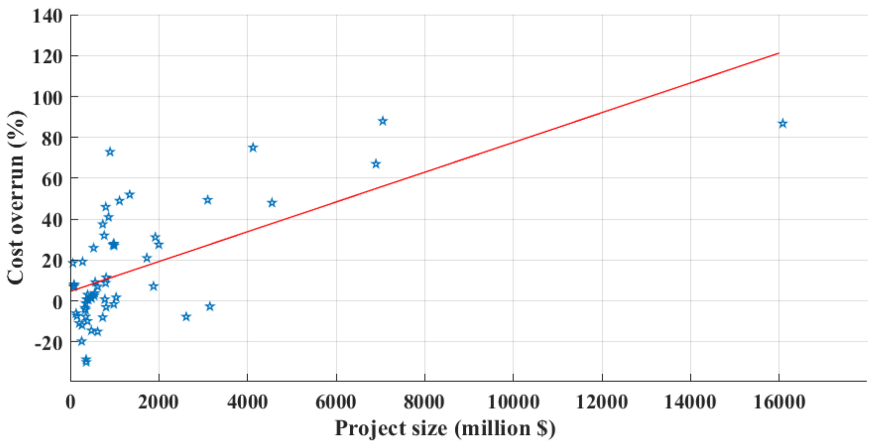

Fig. 3 Cost overrun over project size

4.4. COST AND TIME OVERRUN OVER IMPLEMENTATION PERIOD

To examine the relationship between the implementation period and cost overrun and implementation period and time overrun, the linear regression analysis is performed. In view of cost overrun, the result show that there is a correlation between cost overrun over implementation period (*F-test*, F = 39.6, p < 0.001). Mathematically, the linear regression model for cost overruns over implementation period is provided as:

$$C = 0.3174 * T - 8.5869 \quad (5)$$

in which, *C* – cost overrun, and *T* – implementation period of project.
Figure 4 displays a graph of cost overrun over the implementation period.
Regarding time overruns, there is a correlation between time overrun over implementation period (*F-test*, F = 31.38, p < 0.001). The statistical equation of time overrun over implementation period is given as following:

$$\Delta T = 0.896 * T - 39.6112 \quad (6)$$

in which, *ΔT* – time overrun, and *T* – implementation period of project.
Figure 5 illustrates a graph of time overrun over the implementation period.

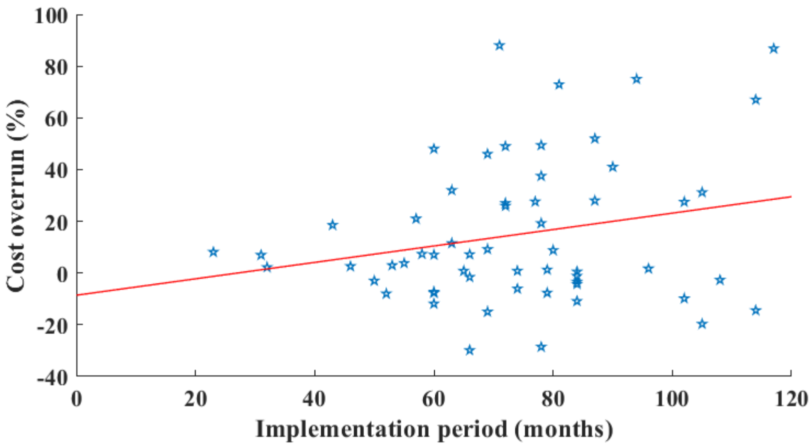

Fig. 4 Cost overrun over implementation period

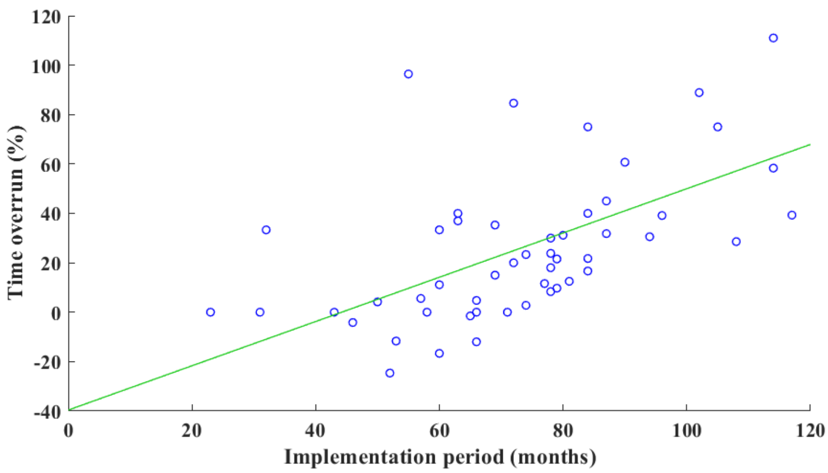

Fig. 5 Time overrun over implementation period

4.5. THE CORRELATION BETWEEN TIME AND COST OVERRUNS

In order to determine whether the size of cost overruns influence time overruns ininfrastructure projects, regression analysis is applied. The result show that there is no correlation between the cost overrun and time overrun in this projects in China (*F-test*, F=0.00074, p = 0.978). Hence, there is no influence of project delays on cost overruns.

5. CONCLUSIONS AND FURTHER RESEARCH

In this paper, the cost overrun and time overrun in infrastructure projects in China is investigated, the influence of project size and the length of implementation period on cost and time overruns are studied and estimated. The following conclusions can be drawn from this study:

- Cost overruns in infrastructure projects in China are as common as cost underruns and the mean value of cost overrun (29.20%) is higher than cost underrun (-10. 16%).
- Time overruns in infrastructure projects in China are as common as time underruns and the mean value of time overrun (36.11%) is higher than time underrun (-12. 47%).

- Regarding the project size, there is a statistical dependence between project size and cost overruns, however there is no correlation between time overrun and project size.
- Regarding the implementation period, there is a correlation between cost overruns and duration of project, as well as between time overrun and duration of project.
- There is no correlation between time overrun and cost overrun in projects.

Comparing the average cost overrun in China (14.83%) to worldwide, it is similar to the average cost overrun in Belgium (10.26%) and Netherlands (16.5%). However, it is significant lower compared to Hong Kong (39.18%) and projects in Europe and North America (28%).
The performance of infrastructure projects in China provides a significant information for the potential investors, contractors, designers and other project stakeholders in construction industry. Further studies should be conducted in order to provide more detailed information related to project types, year of decision to be build and causes of cost and time overruns.

ACKNOWLEDGEMENT

We acknowledge Xi'an Jiaotong-Liverpool University for attending the conference.

REFERENCES

[1] Andrić, J. M., Wang, J., & Zhong, R. (2019a). Identifying the critical risks in railway projects based on fuzzy and sensitivity analysis: A case study of belt and road projects. *Sustainability*, *11*(5), 1302. https://doi.org/10.3390/su11051302

[2] Andrić, J. M., Wang, J., Zou, P. X., Zhang, J., & Zhong, R. (2019). Fuzzy logic–based method for risk assessment of belt and road infrastructure projects. *Journal of Construction Engineering and Management*, *145*(12), 04019082. https://doi.org/10.1061/(ASCE)CO.1943-7862.0001721

[3] Gondia, A., Siam, A., El-Dakhakhni, W., & Nassar, A. H. (2020). Machine learning algorithms for construction projects delay risk prediction. *Journal of Construction Engineering and* Management, 146(1), 04019085. https://doi.org/10.1061/(ASCE)CO.1943-7862.0001736

[4] Bridge Design and Engineering, https://www.bridgeweb.com/Hong-Kong-announces-delay-in-mega-bridge-completion/3892, access on August 7th, 2023

[5] Flyvbjerg, B., Skamris Holm, M. K., & Buhl, S. L. (2004). What causes cost overrun in transport infrastructure projects?. *Transport reviews*, *24*(1), 3-18. https://doi.org/10.1080/0144164032000080494a

[6] Rosenfeld, Y. (2014). Root-cause analysis of construction-cost overruns. *Journal of construction engineering and management*, *140*(1), 04013039. https://doi.org/10.1061/(ASCE)CO.1943-7862.0000789

[7] Cantarelli, C. C., Flyvbjerg, B., & Buhl, S. L. (2012). Geographical variation in project cost performance: the Netherlands versus worldwide. *Journal of Transport Geography*, *24*, 324-331. https://doi.org/10.1016/j.jtrangeo.2012.03.014

[8] Flyvbjerg, B., Ansar, A., Budzier, A., Buhl, S., Cantarelli, C., Garbuio, M., ... & Van Wee, B. (2018). Five things you should know about cost overrun. *Transportation Research Part A: Policy and Practice*, *118*, 174-190. https://doi.org/10.1016/j.tra.2018.07.013

[9] Love, P. E., Zhou, J., Edwards, D. J., Irani, Z., & Sing, C. P. (2017). Off the rails: The cost performance of infrastructure rail projects. *Transportation Research Part A: Policy and Practice*, *99*, 14-29. https://doi.org/10.1016/j.tra.2017.02.008

[10] Cantarelli, C. C., Van Wee, B., Molin, E. J., & Flyvbjerg, B. (2012). Different cost performance: different determinants?: The case of cost overruns in Dutch transport infrastructure projects. *Transport Policy*, *22*, 88-95. https://doi.org/10.1016/j.tranpol.2012.04.002

[11] Cavalieri, M., Cristaudo, R., & Guccio, C. (2019). On the magnitude of cost overruns throughout the project life-cycle: An assessment for the Italian transport infrastructure projects. *Transport Policy*, *79*, 21-36. https://doi.org/10.1016/j.tranpol.2019.04.001

[12] Molinari, L., Haezendonck, E., & Mabillard, V. (2023). Cost overruns of Belgian transport infrastructure projects: Analyzing variations over three land transport modes and two project phases. *Transport Policy*, *134*, 167-179. https://doi.org/10.1016/j.tranpol.2023.02.017

[13] Senouci, A., Ismail, A., & Eldin, N. (2016). Time delay and cost overrun in Qatari public construction projects. Procedia engineering, 164, 368-375. https://doi.org/10.1016/j.proeng.2016.11.632

[14] Huo, T., Ren, H., Cai, W., Shen, G. Q., Liu, B., Zhu, M., & Wu, H. (2018). Measurement and dependence analysis of cost overruns in megatransport infrastructure projects: Case study in Hong Kong. *Journal of construction engineering and management*, *144*(3), 05018001. https://doi.org/10.1061/(ASCE)CO.1943-7862.0001444

[15] Odeck, J. (2014). Do reforms reduce the magnitudes of cost overruns in road projects? Statistical evidence from Norway. *Transportation Research Part A: Policy and Practice*, *65*, 68-79. https://doi.org/10.1016/j.tra.2014.04.005

[16] Ellis Jr, R. D., Pyeon, J. H., Herbsman, Z. J., Minchin, E., & Molenaar, K. (2007). Evaluation of alternative contracting techniques on FDOT construction projects.

[17] Radman, K., Babaeian Jelodar, M., Ghazizadeh, E., & Wilkinson, S. (2021). Causes of delay in smart and complex construction projects. *Journal of Legal Affairs and Dispute Resolution in Engineering and Construction*, *13*(4), 05021006. https://doi.org/10.1061/(ASCE)LA.1943-4170.000050

[18] Park, J. E. (2021). Schedule delays of major projects: what should we do about it?. *Transport Reviews*, *41*(6), 814-832.https://doi.org/10.1080/01441647.2021.1915897

[19] Flyvbjerg, B., Skamris Holm, M. K., & Buhl, S. L. (2003). How common and how large are cost overruns in transport infrastructure projects?. *Transport reviews*, *23*(1), 71-88. https://doi.org/10.1080/01441640309904

[20] Cantarelli, C. C., Molin, E. J., van Wee, B., & Flyvbjerg, B. (2012). Characteristics of cost overruns for Dutch transport infrastructure projects and the importance of the decision to build and project phases. *Transport Policy*, *22*, 49-56. https://doi.org/10.1016/j.tranpol.2012.04.001

[21] Makovšek, D., Tominc, P., & Logožar, K. (2012). A cost performance analysis of transport infrastructure construction in Slovenia. *Transportation*, *39*, 197-214. https://doi.org/10.1007/s11116-011-9319-z

[22] Assaf, S. A., & Al-Hejji, S. (2006). Causes of delay in large construction projects. *International journal of project management*, *24*(4), 349-357. https://doi.org/10.1016/j.ijproman.2005.11.010

[23] Ang, A. H. S., & Tang, W. H. (2007). Probability concepts in engineering: emphasis on applications in civil and environmental engineering 2nd Edition, John Wiley & Sons.

[24] Dodge, Y. (2008). *The concise encyclopedia of statistics*. Springer Science & Business Media.

[25] Smalheiser, N. R. (2017). Chapter 12-nonparametric tests. *Data literacy*, 157-167.

[26] Kissell, R., & Poserina, J. (2017). *Optimal sports math, statistics, and fantasy*. Academic Press.

SITE FRONTIER - SOFTWARE FOR PROCESS OPTIMIZATION DURING STEEL STRUCTURE ERECTION WORKS

Vitomir Nikola[1], Biočanin Dušan[2], Dr Petronijević Predrag[3]

Summary:

Efficient data management during the construction of large-scale steel structures such as industrial facilities is crucial due to the extensive amount of data and the numerous element state changes during the erection process. Swift and accurate data management is necessary for making important decisions on time. The traditional assemblies tracking approach based on technical drawings carries a higher risk of errors due to human factors. The software system Site Frontier successfully addresses these challenges by employing an advanced mathematical model that considers the interdependencies of structure elements, as well as the conditions and constraints at the construction site. By utilizing the Site Frontier software, significant savings can be achieved in material costs, labor hours, and the resources of engineers and equipment.

Key words: BIM, Construction management, Process coordination, Steel structures, Industrial facilities, Site Frontier

[1] MSc, NV Technologies DOO, Belgrade, Serbia, nvitomir@yahoo.com
[2] MSc, Dušan Biočanin PR Concrit Hub, Kraljevo, Serbia, dusanbiocanin@hotmail.com
[3] Assoc. prof., Faculty of Civil Engineering, University of Belgrade, Belgrade, Serbia, pecap@grf.rs

1. INTRODUCTION

During construction of industrial facilities diverse types of work are performed and intersected in a relatively small area. Steel structures erection represents one of the most important factors in organizing works on the construction site itself as it connects different disciplines. Steel structures are placed on concrete supports and then pipes, equipment and electrical installations are mounted on them. Therefore, steel structures erection is the process which is mainly applied in the critical path during construction of this kind of facilities, and as such, it requires flawless functionality.

2. PROBLEMS OF MONITORING STEEL STRUCTURES ERECTION IN THE CURRENT PRACTISE

Industrial facilities often consist of a great number of steel structures which can be the main objects of certain manufacturing processes or additional objects intended for enabling communication of pipelines and electric cables between the main objects. It is typical for steel structures that every element of the structure has its place, and number of different elements frequently exceeds several thousand on one object. On construction sites that exceed 5,000 tons, the number of elements goes over 100,000 elements (elements average weight may vary from structure to structure but at industrial facilities it is approximately 50kg/pcs[1]).

Due to a big number of elements and its uniqueness, the warehouse of a steel construction site occupies a large area and requires a good organization of handling input and output of material. The elements are delivered to the warehouse from factories that make them for the need of the construction site. Due to the financial reasons and serial production, structure elements do not often arrive to the construction site warehouse in the correct erection order.

The delivered elements to the construction site warehouse are subject to an analysis resulting in determining the possibility to erect every single element and this result represents an open workfront for erection. Determining workfront is the most comprehensive process as it is necessary to mark the elements delivered to the warehouse on the drawings or in 3D view of the structure, and then based on the view, determine which elements can be installed at the given moment. The challenging circumstances when marking the elements delivered to the warehouse is, that it is impossible to determine an optimal position of the elements delivered to the construction site in insufficient quantity. It is especially difficult when it comes to connecting elements or bolts because of their abundance. In addition, due to their small size in PDF or 3D view, it is difficult to graphically present the delivered connection details and bolts in such a way so that it can be concluded with certainty whether a given part of structure has become an open workfront for erection.

During erection, each element goes through numerous states. In order to ensure quality monitoring of the erection process and generating relevant reports, it is necessary to enable monitoring of elements passing through all the states on all the objects on the construction site:

- Pending - the element can be erected
- Ordered - the element has been ordered from the warehouse for the need of the construction site
- Delivered - the element has been delivered to the construction site
- Erected - the element has been erected in the projected position

[1] For example, average weight of one element on fifteen random structures at AMMONIA/UREA PLANT KINGISEPP 2 where software Site Frontier was used equals 55.79kg/pcs

- RFI - the element is being approved by the contractor
- Approved - the element has been approved and it is the final state of an element

Besides the basic ones, it is possible that some elements go through the following states as well:

- Assembled - the element belongs to a group of elements that are assembled on the ground and afterwards erected together in the projected position
- Blocked - the element has been damaged or its erection is impossible due to another reason
- Postponed - the element whose erection depends on blocked elements

Currently, during the work execution process, printed drawings or PDF files, as well as 3D models of worked out structures are used for monitoring. Regardless the monitoring method, the state changes of elements are entered manually and individually. State changes record in tabular form for periodic reports is also kept manually and individually for each element. As a result of the entire monitoring process there are numerous reports that have to be created and archived. A big number of engineers is required in order to realize all the processes.

Due to this work procedure, the intensity of work execution and interconnection of the elements, errors caused by human factor are common and keep accumulating. Further, the efficiency of the use of engineers, manpower, equipment and materials is disputable.

Modern development of information technologies opens up a possibility for improving the current method of planning and monitoring steel structure erection works on industrial facilities which has resulted in creating Site Frontier software system.

3. SITE FRONTIER SOFTWARE SYSTEM

3.1. INTRODUCTION AND IDEA

Site Frontier is a 3D software built for the visualization, optimization and monitoring of processes that occur during the erection of steel structures with the aim of optimal use of resources such as material, technology, labor and engineering personnel. It is intended for construction sites where it is necessary to process a large amount of data in a short time, mainly industrial complexes with a planned average steel structure erection of at least 300 tons per month. Site Frontier is a real-time application that is launched via a browser, and is applied exclusively to structures exported from software compatible with BIM logic, such as Tekla, Revit, etc. In a carefully designed system, on the same models, multiple users, of various levels of competence, simultaneously make changes in real time. It contains a large number of mathematical calculations with the aim of achieving maximum automation in data processing and avoiding errors caused by the human factor.

The initial idea of creating this software is the necessity to timely determine the optimal open workfront in steel structures erection based on the information about the delivered construction elements at the warehouse and dependencies between the model elements, defined in accordance with the steel structure erection technologies, taking into account the physical conditions for carrying out works on the construction site and the state of the delivered elements. In the further development of the software, automated processes have also been developed:

- localization of elements in the warehouse
- ordering elements from the warehouse
- delivering elements to the construction site
- erection of elements on the construction site
- as well as the inspection of the erected structure by the contractor

3.2. ORGANIZATIONAL STRUCTURE OF THE CONSTRUCTION SITE AND STEEL STRUCTURE ERECTION TECHNOLOGY

3.2.1. Model validation and hierarchy

The model obtained when exported from some BIM software is compared to the project specification of the given model. Provided that all the elements of the project can be found in the exported file, the given export is uploaded to the Site Frontier platform while taking over just the necessary data from the exported file.

The model hierarchy on Site Frontier platform is ensured by organizational structure as follows: construction site / zone / structure. Correct model positioning and its organization provides a possibility to load simultaneously more models of one zone or of the entire construction site, which is relevant for evaluating the erection process at a higher level.

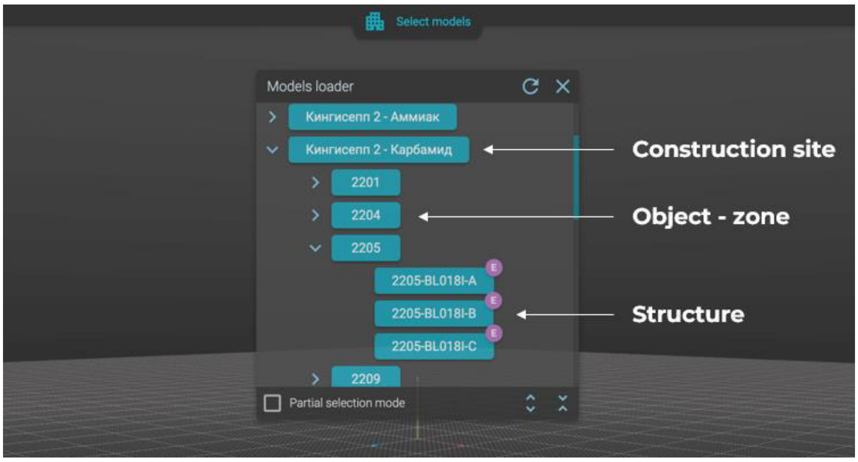

Fig. 1 Display of the model hierarchy on the platform Site Frontier

3.2.2. Steel structure erection technology

Steel structure erection technology represents the correct order of the elements during steel structure erection works, depending on the available equipment in accordance with the structural requirements defined by the project. The process of erection in Site Frontier software system includes the following operations:

- assigning types to elements in the model
- defining the order of erection between two elements
- defining sets of elements that must be erected simultaneously under the name “frame”
- forming a group of elements with same erection priority called “section”

In every model it is necessary to assign types to elements in order to obtain groups of elements with a specific function in constructive sense, and also to facilitate defining of mutual relations among the elements. Each element that has been assigned a type is included in the model specification and thus the user can define project quantities in the model which can also include entities that are not a part of the given structure in the project. Types of elements in Site Frontier system:

- main types (connecting elements, beams, columns, bracings and construction elements)
- secondary (gratings, steps, handrails, ladders and secondary elements)

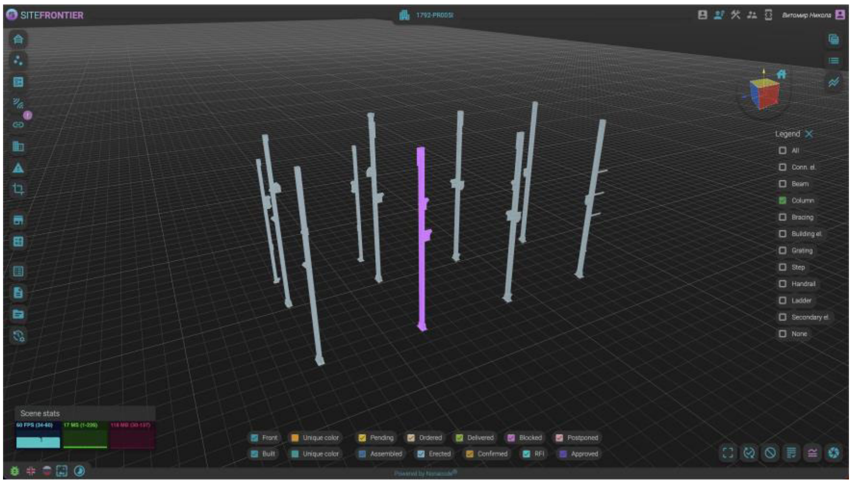

Fig. 2 Display of elements to which the type "Columns" has been assigned isolated using the tool "Legend"

The hierarchy between model elements is defined by creating a parent - child relation between two elements in models, by adding connecting elements and bolts in the relation, which are used to make the relation. Thus, a network of interdependent elements is formed with a lower or higher level of dependence compared to other elements of the structure, and in such a way so as to keep the order of erecting all the model elements.

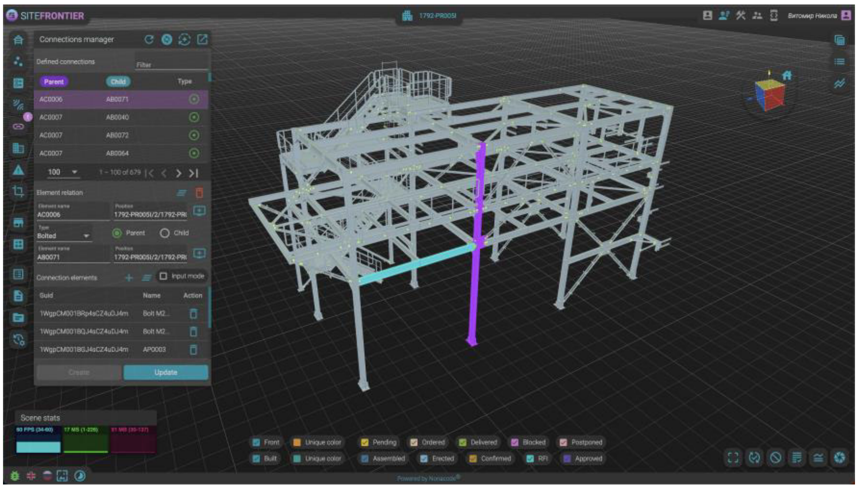

Fig. 3 Display of parent (column) - child (beam) relationship

Although one model can represent an entire structure, more often objects are divided into many smaller entities represented by separate models. The given models rely on one another through individual elements. Site Frontier software also possesses a functionality for defining interdependencies among the elements of different models.

Various kinds of works are often intertwined on this type of construction sites and therefore, it may happen that in spite of fulfilling all the conditions for the erection of the elements in a constructive sense, another type of works could, for a certain time, prevent the erection of the elements that would represent open workfront for erection. It is for these situations that a functionality which draws a 'blocking zone' in 3D scene was designed to prevent any element located in it from becoming an open workfront for erection.

3.2.3. Levels of Competence

Within the SF software, there is an organized division of duties and responsibilities of different software co-workers depending on the level of software usage:

- Administrator - the leader of a group of engineers who organizes the entire work on the construction site and assigns roles to other users of the software
- Engineer - a lower level of competence than the administrator, deals with all the activities described in this paper on a certain number of models that are under his jurisdiction
- Site Manager - indicates which elements are assembled or erected on the models assigned to him
- Observer - all other software users not having a right to make changes, but who have insight into the processes and access to all reports

3.2.4. Construction site warehouse

Given that the organization of elements in the warehouse is important for a more efficient delivery to the construction site, there is a functionality for keeping records of the delivered elements at the construction site warehouse and for updating the warehouse state with each new delivery at the construction site. The warehouse is divided at the construction site itself into sections whose dimensions and position can be shown in Site Frontier application as well.

3.3. OPEN WORKFRONT CALCULATION

3.3.1. The data structure and the calculation algorithm

The basis for workfront calculation is a mathematical model based on combinatorics and the theory of graphs. A Site Frontier application user indirectly creates an information model of structure while doing the initial processing of the model and determining relations among elements (nodes).

The basis of the mathematical model consists of:

- nodes - a mathematical representation of construction elements interconnected with surrounding construction elements
- references - relations between nodes that have the same root graph node (internal reference) and nodes that do not have the same root graph node (external reference). These relationships represent interdependencies between elements of the parent-child type and are determined by the way the elements are supported, i.e. the natural flow of the construction assembly process.

Given that the structure, almost for sure, has a multiple number of basic nodes, the model itself consists of a group of general graphs whose nodes can be mutually referenced in one-way.

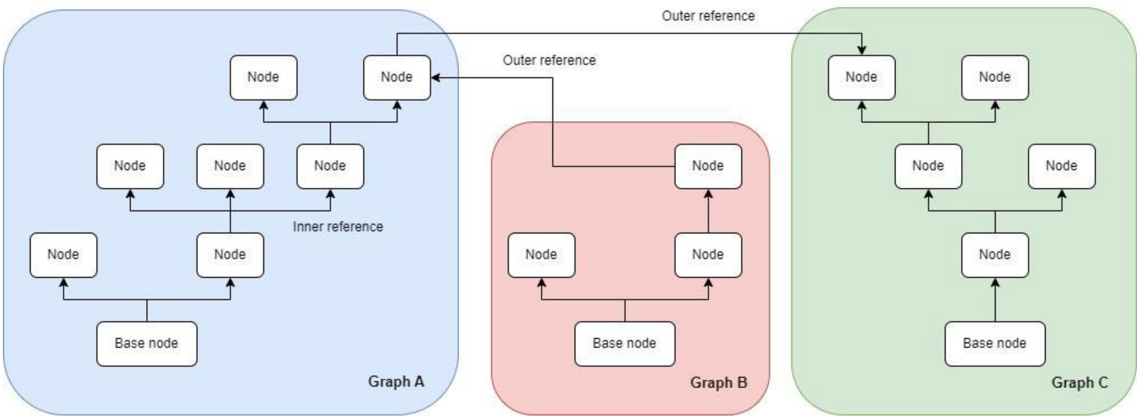

Fig. 4 Graphs with inner and outer references (parent -child relation)

3.3.2. The basis of calculation

Variations of the elements in the recursive algorithm are performed by calculation, taking into account:

- the status of elements
- relations between elements
- availability of elements (their quantity in the warehouse)
- limiting factors dictated by the construction site conditions

Having in mind the recursive nature of algorithm and its subprocesses based on combinatorics, it is clear why the number of resulting groups of elements belonging to workfront in practice goes from a few, in special cases, to several tens of million. Therefore, the critical parts of algorithm have been optimized primarily for optimum use of computer memory. Nevertheless, the basic use value of the calculation is in its duration, which in common computer systems is measured in tens of seconds.

The calculation also includes a number of constraints and among them, the connecting elements which are necessary to realize the relationships between the elements, have the biggest influence on the complexity of the algorithm. Examining the availability of connecting elements (bolts and connecting plates) and their classification in the front raises the erection process optimization to a new level. On the other hand, in addition to going into details, the algorithm also offers a possibility of segregating elements into sections, subsequently treating them as super-elements. Afterwards, the iterative calculation procedure can be continued.

The final result of the calculation is a previously defined number of groups of elements that can become the workfront and satisfy the basic limiting factor - the sum of element weights. The result form itself has several noticeable features:

• the possibility of having a set of discrete workfronts
• convergence in case of variations of the same elements that are not entirely available

3.3.3. A set of discrete workfronts as a result of calculation

One of the common types of calculation results is a smaller set (up to several tens) a group of workfronts in case of taking predefined sections into account. Unlike the ordinary calculation, which is characterized by the variation of individual elements (Figure 5), this type of calculation treats sections of elements as super-elements, which leads to a more discrete distribution of results.

Apparently the most simple, this kind of calculation also involves a great number of availability checks of the necessary connecting elements and the relations among them.

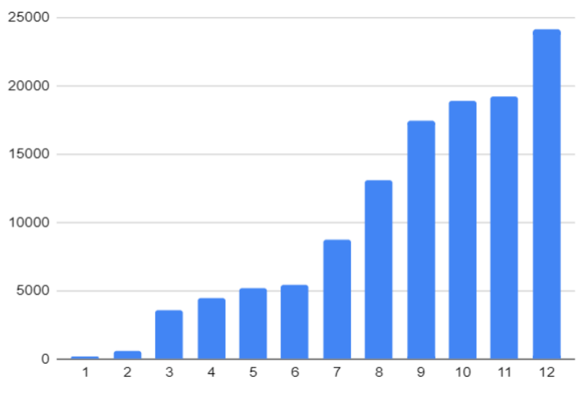

Fig. 5 Chart showing the common distribution of the total workfront weights when sections are taken into account

The horizontal axis shows the serial number of the iteration of the calculation, and the vertical shows the total weight of all elements of the front in the corresponding iteration (in kg)

3.3.4. Convergence in case of variations of the same elements that are not entirely available

In case there are more elements (N) which in the iterative calculation rely on previously calculated elements and facts that they are not entirely available (their warehouse state is M<N), we come to a position variation of the above-mentioned elements by whose processing the calculation is ended or continued in a new direction. By checking the number of variations and additionally calculated graph branches, it becomes obvious that such cases are almost impossible to comprehend without the application. It is exactly in such situations that the users of Site Frontier program open up previously unavailable possibilities for erection optimization.

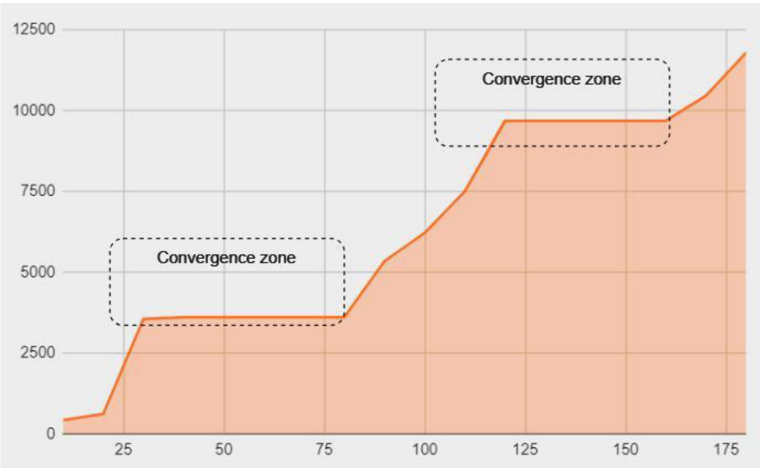

Fig. 6 Chart showing the common distribution of the workfronts total weights in the case of element variations

The horizontal axis shows the serial number of the iteration of the calculation, and the vertical shows the total weight of all elements of the front in the corresponding iteration (in kg)

3.4. MODEL PREPARATION FOR USE

A user has to perform the following activities prior to using the model in the erection process:

- assigning types to elements in the model and thus aligning the model specification with the project specification
- defining all parent-child interdependencies within the model, with a great number of cross checkings, so that all the connections that exist in reality are created
- grouping elements in frames
- creating sections and determining priorities
- determining interdependencies of elements from various models

Upon completing the listed activities, several validation processes, which can identify possible errors and correct them, are performed and the model is ready for use.

3.5. ELEMENT STATE CHANGES DURING THE PROCESS OF ERECTION

3.5.1. Element localization at the construction site warehouse

Upon delivering the material at the construction site warehouse, information about the delivered construction elements for certain structure, together with the information about the location of unloading, are imported on the Site Frontier platform. For each structure, there is a list of elements that were not delivered at the warehouse, the ones that were partially delivered and those available in the full project quantity.

3.5.2. Open workfront calculation

Open workfront is obtained as a result of the given mathematical calculation based on the implemented erection technology and information about the delivered elements at the construction site. Two types of calculations are implemented depending on the planned erection technology:

- Calculation that takes sections (priorities) into account
- Calculation that does not take sections (priorities) into account

Sections represent a group of elements that are not necessarily erected simultaneously, but that is advisable, in order to get the erection of a certain part of construction completed and ensure optimum performance of the equipment. The calculation that takes sections into account requires all the section elements to fulfill simultaneously the conditions for becoming open workfront for erection.

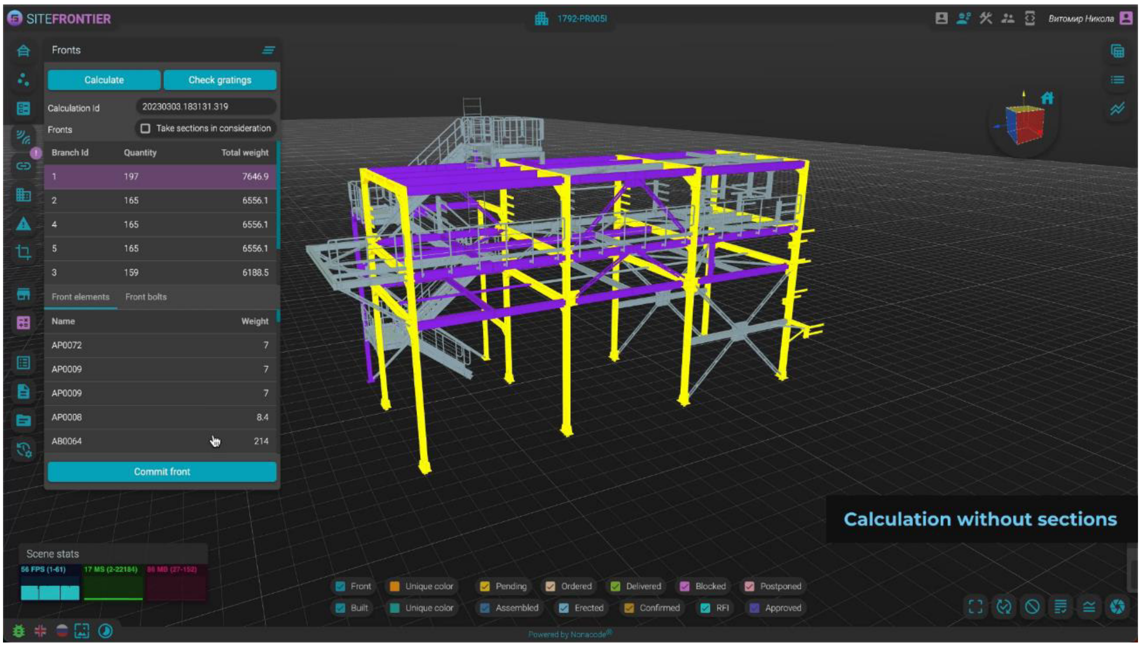

Fig. 7 Display of calculation that does not take sections (priorities) into account

The calculation result potentially offers variations of workfronts and the user chooses the appropriate one according to a visual analysis. All elements of a fixed workfront have state ‘pending’ when the corresponding status (color) is assigned to the elements in the scene. The user gets an insight in the list of workfront elements, the quantity of all the elements and weight of the newly received workfront.

3.5.3. Ordering elements from the warehouse and delivering to the construction site

On a separate panel, by selecting in scene or using a table, the user selects a certain quantity of elements and orders them from the warehouse for the erection works. Then, an automatically generated report is obtained with all the necessary data, and the element state is changed from ‘pending’ into ‘ordered.’ According to the previously entered information about the delivered elements to the construction site warehouse, the user gets an insight about the location of all the necessary elements at the warehouse and sends the information to the employees in the warehouse. The elements are delivered from the warehouse to the construction site and the information which warehouse section the elements were delivered from is sent. The given information is entered in Site Frontier platform and the elements get a ‘delivered’ status, while their quantities are decreased in the warehouse.

All the orders are archived in the application database and a visual checking about whether they have been realized can be performed any time.

3.5.4. Erection

The user, Site Manager, in his work mode enters the elements that were assembled and those that were erected and assigns them corresponding states ‘assembled’ and ‘erected.’ At the start of a new working day, and before sending a new report about erection process, a user, an Engineer, responsible for the given structure in the Site Manager’s work mode, checks the correctness of the Site Manager’s entries. As a result of this activity, the elements with an ‘erected’ status, get an ‘approved’ status and there opens a possibility of recognizing the elements erected in the last reporting period.

After that, the general report for all construction sites models is created, which is then forwarded to all the interested individuals through Site Frontier platform, and upon that, it is archived in the system database.

3.5.5. Handing over steel structure to the contractor

Upon the final positioning of the elements in the project position with bolts tightened to their final tightening torque there comes the stage of handing over the steel structure to the contractor. The elements that are taken into account for the final handing over are the elements with a ‘confirmed’ status. By selecting, in the scene, the part of the construction which is ready for handing over, the elements get a new ‘RFI’ status together with a corresponding report. After checking is done on the construction site by the quality control service of the contractor and subcontractor, a verified document is obtained containing the elements that have passed the approval stage. The given document is archived on the Site Frontier platform assigning the final ‘approved’ status for the elements that passed the approval, and for the elements that did not pass the approval, their status goes back to ‘confirmed.’ Thus, if disputes occur, it is always possible to prove easily the realized handing over of the steel structure to the contractor.

4. CONCLUSION

The existing commercial BIM software do not have a possibility of calculations that results in automatic changes in the state of a group of elements depending on the fulfilled conditions and based on the rules that apply in steel structure erection.

In practice, it has been proved that twice as few engineers were required on the construction sites where Site Frontier software was used and with much better control of the information flow. By inspecting the location of the elements in the warehouse and ordering only the elements needed for the erection at a given time period, elements and bolts loss on the construction site is avoided. Knowing the open workfront for erection on multiple locations, enables selecting the location with the biggest open workfront and keeping the equipment on a specific location for a longer period. If the equipment moving is minimized, its performance per tonnage increases and the equipment work hours decrease. As the entire process of determining the open workfront for erection and ordering the elements from the warehouse is transferred to engineers, the site managers can spend more time on the construction site itself, which directly improves the workers’ performance.

For Site Frontier use, it is necessary to provide:

- IFC2x3 files obtained by exporting from one of the software with BIM logic (Tekla, Revit, etc.)

- Specification of the model elements given in the form of an excel document
- Construction site plan with construction site zones and facilities for model positioning
- Shipments from steel manufacturing factories given in the form of an excel document

Site Frontier software offers the following benefits:

- Cost-cutting - savings in resources: materials, equipment, manpower and engineers
- Reliability - eliminating errors caused by the human factor
- Operability - optimum data processing speed
- Professionalism - a high level of digitalization directly leads to a higher transparency of the erection process and a better cooperation with the contractor

CONSTRUCTION OF NEW MARIBOR PUBLIC LIBRARY IN ROTOVŽ CENTRE AND CONSERVATION WORKS ON ITS OLDEST COMPLEX "LEDENICE"

Rok Cajzek[1], Uroš Klanšek[2], Mateja Držečnik[3]

Summary:

This article presents the construction of the new Maribor Public Library in the Rotovž Centre and conservation works on its oldest complex called "Ledenice". The project is implemented by companies GIC GRADNJE d.o.o. and Pomgrad d.d. in cooperation with the Municipality of Maribor and co-financed by the Ministry of Culture. Rotovž Centre is in the old city square of Maribor, which is fully protected as an urban monument. The project implementation includes measures to protect and preserve the cultural heritage and interventions in the buildings, which have the status of cultural monuments of the highest level. Students from the University of Maribor, Faculty of Civil Engineering, Transport Engineering and Architecture, are also being trained on construction site of this project through practical exercises on fields of construction management and technology.

Key words: construction, Rotovž Centre, Ledenice, cultural heritage.

[1] dr., GIC GRADNJE d.o.o., Sv. Florijan 120, 3250 Rogaška Slatina, Slovenia, e-mail: rok.cajzek@gic.si
[2] Prof. dr., University of Maribor, Faculty of Civil Engineering, Transportation Engineering and Architecture, Smetanova ulica 17, 2000 Maribor, Slovenia, e-mail: uros.klansek@um.si
[3] Asst. dr., University of Maribor, Faculty of Civil Engineering, Transportation Engineering and Architecture, Smetanova ulica 17, 2000 Maribor, Slovenia, e-mail: mateja.drzecnik@um.si

1. INTRODUCTION

The Maribor Public Library was founded in 1949 [1] and is one of the most extensive libraries in Slovenia. Throughout its history, it has undergone numerous renovations and expansions that have consolidated its status as an important cultural institution in the heart of Maribor. What makes the Maribor Public Library special is that it is housed in the historic Rotovž building. This architectural jewel has been carefully preserved as a municipal monument and is of great historical importance. The integration of the library into this architectural monument emphasizes its unique character and is a living testimony to the rich heritage of the city. The Rotovž Library plays a central role in promoting literature, education and culture in the region. It provides comprehensive access to a wide range of library resources and services and acts as a focal point for learning and cultural enrichment within the community.
In 2008, an architectural competition was launched to revitalize the Rotovž Centre, an important square in the old town of Maribor [2]. The goal was to give wider purpose to this historic place. At the same time, this renovation project was an opportunity to solve the spatial problems of the Maribor Public Library, which has long been an important cultural element of the square. Unfortunately, the project could not be realized at that time. In 2019, the Municipality of Maribor reconsidered this solution and planned to add various functions to the square and the building, which was originally intended exclusively for the library. With this goal in mind, the decision was made to transform the building into an Innovative Centre, focused on promoting literature, education, culture and digitization. As part of this process, a program review [3] was conducted in 2019 to explore the possibilities for incorporating additional elements, including extensive exhibition space to meet the needs of the Maribor Art Gallery and a city cinema. The program review confirmed the feasibility of including all three programs, with the necessary architectural adjustments and the relocation of the Maribor Public Library archive to another location.
In 2020, investment documentation [4] was prepared, followed by the development of project documentation focused [5] on the new program content. In 2021, the Municipality of Maribor received a legally binding building permit [6] for the project, which was simultaneously renamed Rotovž Centre - an Innovative Centre for the promotion of literature, education, culture and digitization. In addition, a financing agreement was concluded with the Ministry of Culture and successful public tenders were held for the construction and craft works for the Rotovž Centre. Construction works started in February 2022 with an expected construction period of two years. After the completion of the construction works, the delivery and installation of equipment will take place, followed by the issuance of the occupancy permit. The move of users into the building is planned for 2024 [7].

2. ARCHITECTURAL FEATURES OF THE BUILDING

2.1. PRESERVING CULTURAL HERITAGE IN THE BUILDING

The building at Rotovž Square 2, the former seat of the Maribor City Library, is registered in the Register of Cultural Heritage as "a "one-story building with a simple eight-bay facade" [8]. The original building at this location was built in the late 19th century in Neo-Gothic style [9]. A search in the archival records of the Maribor Regional Archives [10] revealed that two older buildings were actually erected on this site shortly before the renovation around 1930. The new building, built around 1930 (Fig. 1) [11], is clearly different from its predecessors and is considered a new construction, although it does not retain the architectural features of the time. It was severely damaged during World War II but was extensively restored and rebuilt after the war [12].

Fig. 1 Photo before 1930 at Rotovž Square 2 location [11]

This building combines elements of Neo-Gothic and Neo-Renaissance styles (Fig. 2) and was included in the register mainly because of its location in the city centre, between Rotovž Square and Lekarniška Street, and its proximity to important historical monuments [13]. From the floor plans, the facades and the as-is condition, it is clear that the only high-quality part of the interior is the vaulted cellar, into which the cellars of the two earlier buildings were integrated. These cellars, known as 'Ledenice - ice houses', were originally used to store ice, as the building was known as a pub and brewery [14]. It was proposed to demolish the upper part of the building called Maribor – House Rotovž Square 2 keeping the two vaulted cellars. This would allow a more rational use of the space for the library content and optimize the floor plan and floor heights, which would be feasible within the cultural protection conditions for the preservation of the urban monument Maribor - City Centre [15]. In its long history, the Maribor City Library has undergone many renovations and expansions to meet the needs of its readers and visitors.

Fig. 2 Photo of the building at Rotovž Square 2 from 1960 [13]

2.2. A NEW FUTURE IN AN OLD LOCATION: THE CITY PUBLIC LIBRARY PROJECT

Since the existing buildings of the Rotovž Centre do not meet the current seismic safety requirements [16], it was necessary to make interventions in the existing building complex. It was decided to remove two buildings that are not protected monuments. The existing building (Fig. 3), which housed the library, was located on the west side of Rotovž Centre, and was bordered on the north and south by two other buildings. The ground plan was simple and roughly rectangular. The building is about 36m long and 16m wide. The height of the building to the eaves was about 8m. The entire area of the building had a cellar. The bottom of the existing cellar is located at a depth of about – 5.00 m in relation to the existing external wall. The main supporting structure of the basement part of the building consists of 40cm and 35cm thick reinforced concrete walls and a reinforced concrete core in the north and in the south, respectively. These walls and cores are connected by an 80cm and 120cm thick reinforced concrete floor slab under the cores, respectively, and by a 35cm thick reinforced concrete floor slab with a 0.00 angle. Between the floors, a reinforced concrete slab was built at a depth of approximately –4.00 m. The eastern edge of the basement will be 'open' towards Rotovž Centre to connect it with the hall [17].

Fig. 3 Maribor Public Libary before its demolition in 2022 [author: R.Antolič]

The newly constructed building at Rotovž Square 2, which will be attached to the preserved cellars - Ledenice - will be used as the new central branch of the Maribor Library. Fig. 4 shows a visualization of a cross-section of the library.

Fig. 4 Visualization of library cross-section [2]

The visualization of the cross-section through the new Maribor Public Library in the Rotovž Centre clearly highlights the preservation of the basement parts of the building that preserve its historical value, while also showing the diversity of the library's overall programme, including the lending of library materials, study rooms, a variety of events, digital resources, and an important part of the preservation of cultural heritage. Through this picture, the past and present are brought together in a library experience that enriches the community.

3. CONSTRUCTION TECHNOLOGY

Top-down construction technology was used in this particular project (Fig. 5). The said approach is suitable for the construction of multi-story basements, underground parking garages, foundations for underground infrastructure (e.g., subways), and other projects that require the execution of underpasses or deep excavations. This approach allows for better control of construction, minimizes ground movement, and allows construction in confined spaces. However, this technology is complex and risky, requiring careful planning and the use of specialized equipment and skilled labour.
The top-down design process usually involves several consecutive steps [18]:

- Preparation and construction of the top level: first, the construction site is prepared on the surface on which the first level of the structure is built. This may be an above-ground building or a platform that serves as the starting point for construction.
- Once the upper level is built, excavation below ground begins. Various excavation methods are used, such as drilling, pile driving, etc. At the same time, measures are taken to prevent the collapse of walls and floors, such as anchors, support piers or linings.
- Construction at lower levels: construction work continues to the desired depth, with walls and floors being reinforced and retrofitted to ensure stability and safety. After construction at depth is completed, the process is repeated at deeper levels as needed. Each time, construction takes place on a new level and then descends deeper.

Fig. 5 Top-down construction technique on Ledenice

The preserved part of Ledenice, which includes the southern half, has undergone some changes. The eastern basement outer wall facing the square was replaced in one phase by a reinforced concrete frame, while the northern part was completely removed. Before concreting the southern basement, the vaults were restored. The layers down to the supporting structure were removed, and the vaults were cleaned and grouted as needed. Prior to placing the floor concrete, a connecting slab of reinforced concrete was constructed to ensure a 0.00 angle alignment. The south basement was concreted in sections (Fig. 6) using the top-down method, with each section secured with temporary bar anchors. In the undercut section, the backfill soil was stabilized with low-pressure grouting. The depth of the linear subgrade concrete under the walls is approximately 2.30m. The campadas were followed by an 80cm or 120cm thick floor slab, depending on the load requirements. After completion of the floor slab, excavation of the back walls and temporary openings for excavation support for the reinforced concrete basement back walls was started [17].

Fig. 6 Concrete campadas

4. CONSTRUCTION SITE AS AN INTERACTIVE CLASSROOM

At the University of Maribor's Faculty of Civil Engineering, Transport Engineering, and Architecture, education goes beyond traditional classrooms. As a forward-thinking institution, it has recognized the immense potential of using construction sites as interactive classrooms that offer students a unique opportunity to learn through hands-on experience.

In a groundbreaking initiative, faculty students actively participate in the construction management and technology aspects of an ongoing project. The university has partnered with a construction company GIC GRADNJE d.o.o. to provide prospective civil engineers and architects with a real construction site as a practice ground (Fig. 7).

Through hands-on exercises at the construction site, students gain valuable insight into the complexities of managing a construction project. They experience first-hand how project planning, scheduling, and resource allocation play a critical role in successful project execution. By working with real-world professionals, students learn to apply theoretical knowledge to real-world situations, improving their problem-solving and decision-making skills. The interactive classroom experience also extends to technology-oriented areas. Students have the opportunity to learn about the latest construction technologies and machinery.

Fig. 7 Students on the construction site

However, it is essential to ensure that the interactive classroom environment meets safety standards and that students are adequately supervised. Collaboration between educational institutions and construction companies can help establish guidelines and ensure seamless integration of the learning experience.

In summary, the construction site as an interactive classroom provides a rich learning experience that bridges the gap between theory and practice. With this innovative approach, educators can bring in well-rounded individuals who have both the knowledge and skills needed to succeed in the construction industry and beyond. In addition, students can develop a deeper understanding of the importance of their academic studies and how they contribute to real-world projects, making learning a truly rewarding endeavor.

The connection between industry and faculty is critical to providing a quality education and preparing students for the challenges they will face in their careers. Working with construction companies allows colleges to tailor their curricula to industry needs and ensure that students develop the skills employers demand.

5. CONCLUSION

The construction of the new Maribor Public Library in the centre of Rotovž and the preservation of the historical complex "Ledenice" is an ambitious project. GIC GRADNJE d.o.o. and Pomgrad d.d. in cooperation with the Municipality of Maribor are building an important investment in the preservation of cultural heritage and the development of a modern infrastructure. The fact that the project is co-financed by the Ministry of Culture underlines its national importance. The Rotovž Centre is located in the heart of the Old Town Square of Maribor, a fully protected urban monument, and embodies historical significance. The careful approach to the protection and preservation of cultural heritage is commendable, especially when it comes to buildings classified as cultural monuments of the highest level. In addition, the involvement of students underscores the educational dimension of the project and its potential long-term impact on the local community. In essence, the new Maribor Public Library and the extensive efforts to preserve it represent a harmonious blend of tradition and innovation that underscores the importance of cultural heritage, education, and sustainable development in the municipality of Maribor.

REFERENCES

[1] Fras Popović, S., Kramberger, D. (1999). Na temeljih preteklosti snujemo prihodnost: 1949-1999: Zbornik ob 50-letnici Mariborske knjižnice. Maribor.

[2] Žnidaršič R., et al. (2008). Ureditev Rotovškega trga z Rotovžem in Mariborsko knjižnico, Medprostor Arhitekturni Atelje d.o.o. (in Slovene).

[3] Izvedbeni načrt Trajnostne urbane strategije Mestne občne Maribor (TUS-MOM), (2017). Razvojni izziv: urejeno in prenovljeno mesto kot regionalni kulturni center. Ukrep 22: prenova javnih površin (in Slovene).

[4] Izdelava projektne dokumentacije za »Prenovo Mariborske knjižnice z Rotovškim trgom in Rotovžem (2019). Medprostor Arhitekturni Atelje d.o.o., Referenčna številka dokumenta: 41001-805/2019 (in Slovene).

[5] Projekt za izvedbo (2019). Št projekta 0179-2019, Medprostor Arhitekturni Atelje d.o.o. (in Slovene).

[6] Building permit (2020). No.: 351-1818/2020-29, UE Maribor.

[7] Izvedba gradbeno obrtniških in inštalacijskih del potrebnih za izgradnjo Centra Rotovž (2021). Pogodba št. 4102-650/2021-41, Mestna občina Maribor (in Slovene).

[8] SI_PAM/0011/108/00001_005_01 - Rotovški trg 2, Maribor: gradbeni spisi in gradbena dokumentacija., 1925-1934 (in Slovene).

[9] SI_PAM/0057/024/00371_00005 Gradbeni načrt za prezidavo prvega nadstropja na Rotovškem trgu, Maribor, investitor Franc Tscheligi, gradbeni mojster Nebesky, 1864 (in Slovene).

[10] SI_PAM/0057/024/00371 Tscheligi, Franz, Maribor: gradnje v Mariboru [danes Rotovški trg 2 in Koroška cesta 2] in Pekrah: gradbena zadeva Okrajnega urada Maribor, 1861-1864 (in Slovene).

[11] SI_PAM/0011/108/00001 MA/1367 - Rotovški trg 2, Maribor: gradbeni spisi in gradbena dokumentacija., 1925-1934 (in Slovene).

[12] SI_PAM/0057/024/00016 Denzel, Jakob, Maribor: gradnja ledenice v hiši št. 147 [danes Rotovški trg 2], 1856.02.01-1856.04.0 (in Slovene).

[13] SI_PAM/0057/024/00015 Denzel, Jakob, Maribor: prijava nezakonite gradnje na Apothekergassel 147 [danes Rotovški trg 2], 1856.02.27-1856.02.28 (in Slovene).

[14] SI_PAM/0057/024/00371_00001 Gradbeni načrt za gradnjo pomožne zgradbe ob pivnici na Rotovškem trgu, investitor Franc Tscheligi, gradbeni mojster Pregl, 1861 (in Slovene).

[15] Cultural heritage protection institute (2020). 35107-0691/2020-3 ES OE Maribor, Slomškov trg 6, 2000 Maribor.

[16] Elaborat o stanju nosilnih konstrukcij štirih zgradb na Rotovškem trgu v Mariboru (2010). DN 2003776 Pogodba št. 101 / 2010 ZRMK – Center za materiale in konstrukcije (in Slovene).

[17] Temlin J. (2022). Concrete structures implementation project, no. 146_1.5/2022, POMGRAD d.d., GIC GRADNJE d.o.o.

Chew M. Y. L. (2000). Construction Technology for Tall Buildings 2nd Edition. World Scientific Book. https://doi.org/10.1142/9789812791887_0005

INTRODUCING A NOVEL DECISION SUPPORT TOOL FOR BUILDING RENOVATION MANAGEMENT

Suzana Draganić[1], Mirjana Laban[2], Mirjana Malešev[3], Srđan Popov[4], Marko Z. Marković[5]

Summary:

The research paper introduces the *Digital Building Repository*, a novel decision support tool for building renovation management. The proposed building repository incorporates comprehensive information on the building's performance in terms of energy efficiency, durability and fire safety, as well as potential measures for improvement, enabling a holistic approach to renovation planning. It represents a valuable tool for efficient data management, optimizing the renovation process, ensuring transparency and facilitating informed decision-making during building renovations. The integration of the presented tool with relevant publicly available digital platforms would enable easy access, retrieval and exchange of information among various stakeholders involved in the building renovation process.

Key words: Building renovation, Digital building repository, Decision support tool, Energy efficiency, Durability, Fire safety

[1] Assist. prof., Faculty of Technical Sciences, University of Novi Sad, Serbia, suzanav@uns.ac.rs
[2] Full prof., Faculty of Technical Sciences, University of Novi Sad, Serbia, mlaban@uns.ac.rs
[3] Full prof., Faculty of Technical Sciences, University of Novi Sad, Serbia, miram@uns.ac.rs
[4] Full prof., Faculty of Technical Sciences, University of Novi Sad, Serbia, srdjanpopov@uns.ac.rs
[5] Assoc. prof., Faculty of Technical Sciences, University of Novi Sad, Serbia, marko_m@uns.ac.rs

1. INTRODUCTION

Supporting the European Union's (EU) transition to decarbonized, intelligent, and sustainable buildings requires a fundamental shift in both the technical and methodological aspects of current design and (re)construction processes [1]. The European Commission (EC) considers the digitalisation of buildings and construction technologies as essential drivers for improving energy efficiency and emphasizes the role of digitalisation and data in the acceleration of the planning, implementation, control and monitoring of the renovation plans' outcomes, as well as for a more efficient planning and management of energy [2].

The construction sector is underdeveloped in terms of overall digitalisation and data applications in comparison with other industry sectors. During building's life cycle a great amount of information is generated. Despite the existence of large amount of building-related data, the data is often scarce, of unreliable quality and limited accessibility and there is a lack of strategies to efficiently manage and correlate them [3,4].

To encourage deep energy renovations and overcome barriers in building renovations, the EC has mandated the use of Digital Building Logbooks (DBL) [5]. DBL is considered as a key solution to bridge the gap between the vast amount of data and information generated throughout the building's lifecycle and the lack of methodologies and tools to safely manage, organise, structure, and share this data [1]. There are several initiatives on DBLs at the national level in Europe. However, these initiatives differ greatly in terms of their focus, digitalization features, and the integration of building data [1]. Although some important progress has been made in that direction, a common European DBL model has not yet been implemented [6] as some crucial aspects are still under development, such as the identification of the main functionalities, the target groups and their needs, the interoperability with external data sources, and the indicators it should include to further support informed decision making [1,4].

The research paper introduces the *Digital Building Repository (DBR)*, a novel decision support tool for building renovation management, that can be considered as an original version of DBL, developed according to Serbian needs as a part of a doctoral dissertation [7]. The proposed building repository incorporates comprehensive information on the building's performance in terms of energy efficiency, durability and fire safety, as well as potential measures for improvement, enabling a holistic approach to renovation planning.

2. EUROPEAN DIGITAL BUILDING LOGBOOK MODELS

DBL was first introduced as an autonomous tool by the *Renovation Wave initiative* [8] in 2020 and first defined within the proposal for a recast of the *Directive on Energy Performance of Buildings* (EPBD) in 2021[9] and redefined in 2023 [10]. Before the publication of these two documents, several European countries had already taken steps to implement the DBL at the regional and national levels [6].

EPBD recast [10] defines DBL as a common repository for all relevant building data, including data related to energy performance such as energy performance certificates, building renovation passports and smart readiness indicators, as well as on the life-cycle Global Warming Potential and indoor environmental quality, which facilitates informed decision making and information sharing within the construction sector, among building owners and occupants, financial institutions and public authorities. DBLs can be also integrated with the digital twin (DT) and building information models (BIM) [11-13], however DT and BIM data is limited to new buildings, given the ease of using the methodology from the initial process of building design and construction [1].

The definition of DBL has been also proposed as part of the *Study on the Development of a European Union Framework for Digital Building Logbooks* [3], based on a thorough stakeholder consultation, interviews with experts and detailed analysis of 40 existing DBL initiatives across Europe and beyond. DBL is defined as a dynamic tool that allows a variety of data, information and documents to be recorded, accessed, enriched and organised under specific categories. It represents a record of major events and changes over a building's lifecycle, such as change of ownership, tenure or use, maintenance, refurbishment and other interventions. As such, it can include administrative documents, plans, description of the land, the building and its surrounding, technical systems, traceability and characteristics of construction materials, performance data such as operational energy use, indoor environmental quality, smart building potential and lifecycle emissions, as well as links to building ratings and certificates. As a result, it also enables circularity in the built environment.

The results of comprehensive review of existing European DBL models, conducted by [1,5,14], indicate that much of the recent DBL research is related to projects funded by the EU Horizon programme. Ten H2020 projects and four Horizon Europe project, which implements DBL concepts, were identified. The most recent project, *EUB SuperHub* (2021-2024)[1], has developed an online platform offering DBL as a methodology and technology for data integration, with the goal of revolutionising building certification and rating systems.

To deliver a comprehensive and continuously evolving evaluation of building lifecycle, a unified European framework for DBLs is currently under development [3, 15]. The framework aims to integrate building and human-centric performance factors, while making efficient use of real-time building information and data. Such a framework needs to provide secure and flexible data exchange among stakeholders, raising awareness, fostering collaboration and synergies, as well as to provide high levels of interoperability across various services [1].

3. PROPOSED DIGITAL BUILDING REPOSITORY

3.1. THE CONCEPT OF DIGITAL BUILDING REPOSITORY

The DBR represents one of the outcomes of the strategic model for the renovation of concrete facades of high-rise residential buildings. The strategic model is the result of theoretical and research work presented within a doctoral dissertation [7], with a specific focus on buildings constructed in Novi Sad between 1961 and 1990. According to the proposed model, the building renovation process consists of eight phases whose realization requires a multidisciplinary approach involving the combined application of methods, technologies, and digital tools commonly used in contemporary science and engineering practice.

To test and validate the proposed model, a case study was conducted on a selected building. All collected data and obtained results have been consolidated and systematized in a directory structure, and then integrated into the open-source geographic information system Quantum GIS, which resulted with multi-layered georeferenced interactive database (Fig. 1).

Developed database enables generation of DBR for analyzed building, containing comprehensive information on the building's performance in terms of energy efficiency, durability and fire safety, as well as potential measures for improvement, enabling a holistic approach to renovation planning.

[1] https://eubsuperhub.eu/

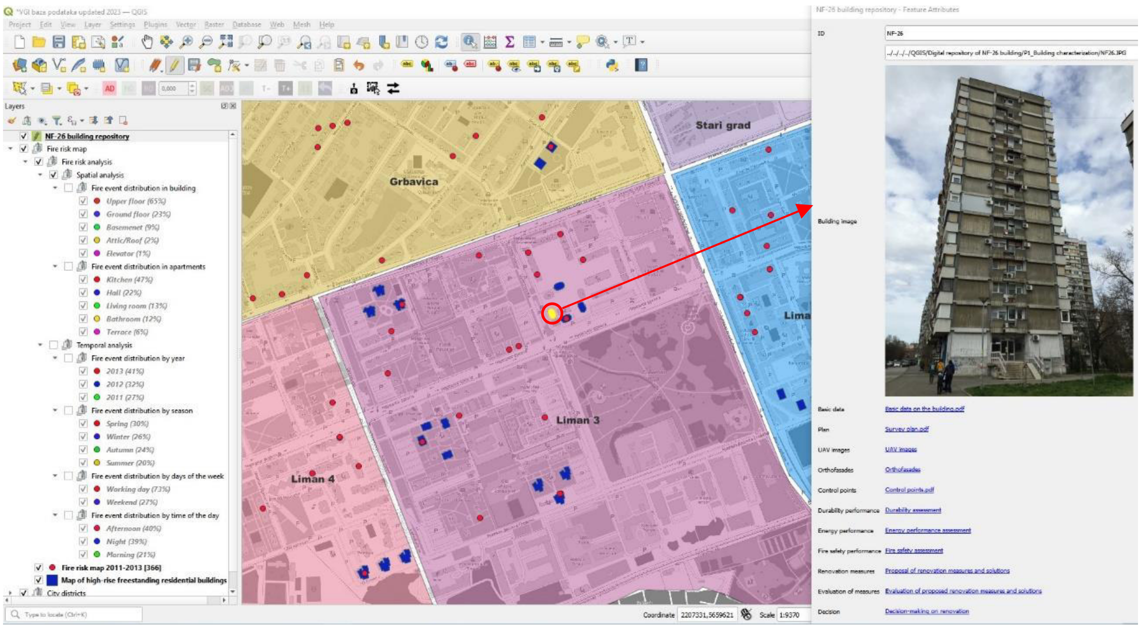

Fig. 1 Building repository within the developed multi-layered georeferenced interactive database

3.2. THE DIGITAL BUILDING REPOSITORY DATA STRUCTURE

The DBR data structure reflects the fundamental renovation model structured into eight phases and, thus, is organized into eight modules in parallel:

1. Basic data on the building
2. Building survey plan
3. Building photographs and coordinates of reference points
4. Orthomosaic and orthofacades
5. Building facades performance
6. Proposed renovation measures and solutions
7. Evaluation of proposed renovation measures and solutions
8. Renovation decision

The information provided by DBR is presented in the form of descriptive files, photographs, lists, maps, tables, diagrams and trees.
Modules are briefly presented in following chapters.

3.2.1. Module 1: Basic data on the building

The DBR module *Basic data on the building* (Fig. 2) contains the following data categories:

- General building information
- Data on building morphology
- Data on building structure
- Data on technical building system

Collection of basic data on the building is carried out within first phase of renovation model (P1: Building characterization) through the analysis of available documentation and a preliminary inspection of the building. The data was collected through a form created for this purpose. The aim of conducted activities is to analyze the building and its surroundings and make an initial assessment of the building's and environmental conditions.

3.2.2. Module 2: Building survey plan

The DBR module *Building survey plan* (Fig. 2) consists of unmanned aerial vehicle (UAV) mission plan and a geodetic measurement plan, that are prepared within the second phase of renovation model (P2: Preparation and organization of building survey).

UAV mission plan defines flight parameters, which include: flight mode, flight pattern, flying distance from the building, UAV take off positions, camera orientation, ground sampling distance (GSD), image overlap percentage and capture intervals. Geodetic measurement plan contains the positions of the surveying instrument, as well as the number and positions of reference points.
Building survey plan also includes data on the performance of available equipment for survey and information on survey limitations identified during the preliminary inspection of the building.

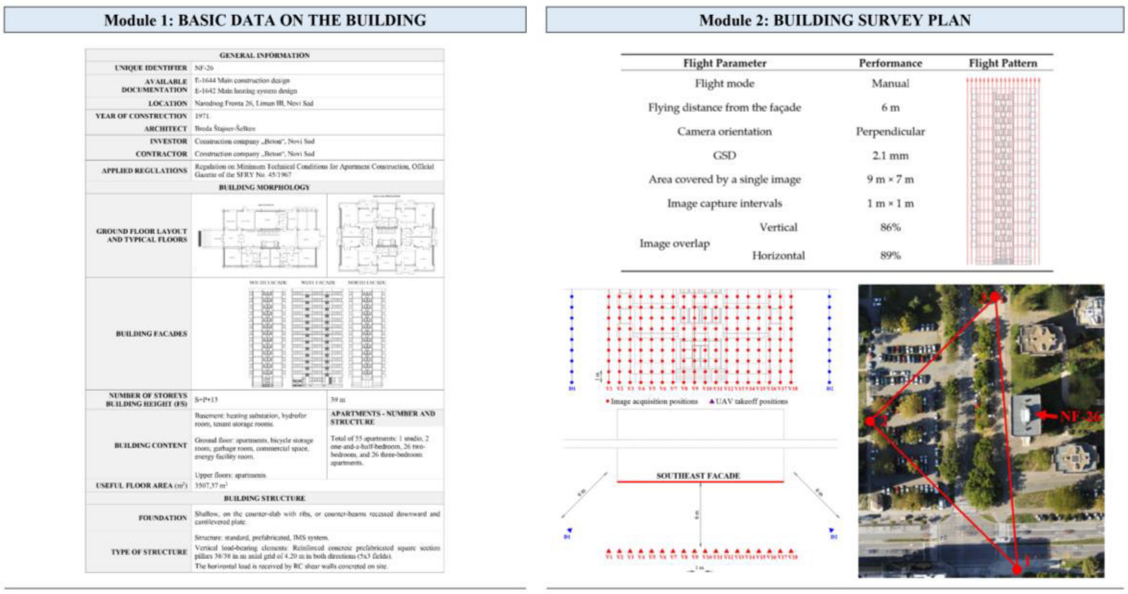

Fig. 2 Overview of the DBR Module 1 - Basic data on the building and Module 2 - Building survey plan

3.2.3. Module 3: Building photographs and coordinates of reference points

The overview of DBR module *Building photographs and coordinates of reference points* is presented in Fig. 3.
Building photographs and 3D coordinates of selected points (on the ground and on facades) are collected within third phase of renovation model (P3: Building survey), according to the guidelines and instructions provided by Building survey plan.
Data collection is carried out using three methods:

1. Aerial photogrammetry method
2. Precise electronic tachymetry method
3. GNSS Real Time Kinematic (RTK) method

3.2.4. Module 4: Orthomosaic and orthofacades

The DBR module *Orthomosaic and orthofacades* (Fig. 3) contains orthofacades, orthomosaic, and digital surface model of the residential block where the building is located, as well as quality reports generated from photogrammetric software within renovation model phase four (P4: Orthomosaic and ortofacades generation). The collected images and 3D coordinates of reference points serve as input data for the tool.

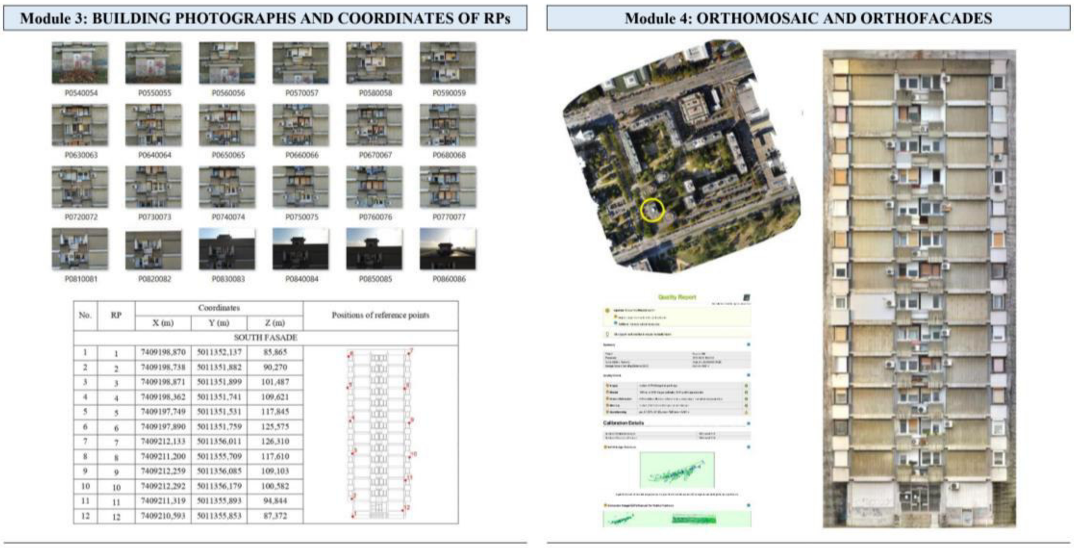

Fig. 3 Overview of the DBR Module 3 - Building photographs and coordinates of reference points and Module 4 - Orthomosaic and orthofacades

3.2.5. Module 5: Building facades performance

The DBR module *Building facades performance* is divided into three sub-modules:

- Sub-module 5.1 – Durability performance of building facades
- Sub-module 5.2 – Energy performance of building
- Sub-module 5.3 – Fire safety performance of building

The sub-module *Durability performance of building facades* (Fig. 4) provides information about:

- Identified damages and defects
- Potential causes of identified damages and defects
- Classification of damages and defects
- Quantification of the degradation

Durability of building facades is assessed within the first segment of the fifth renovation model phase (P5.1: Durability assessment of building facades). To assess the durability of the facades, the model proposes the application of a modern approach based on a visual inspection of the generated orthofacades, application of novel computer code for automatic crack detection and the utilization of a numerical degradation model.

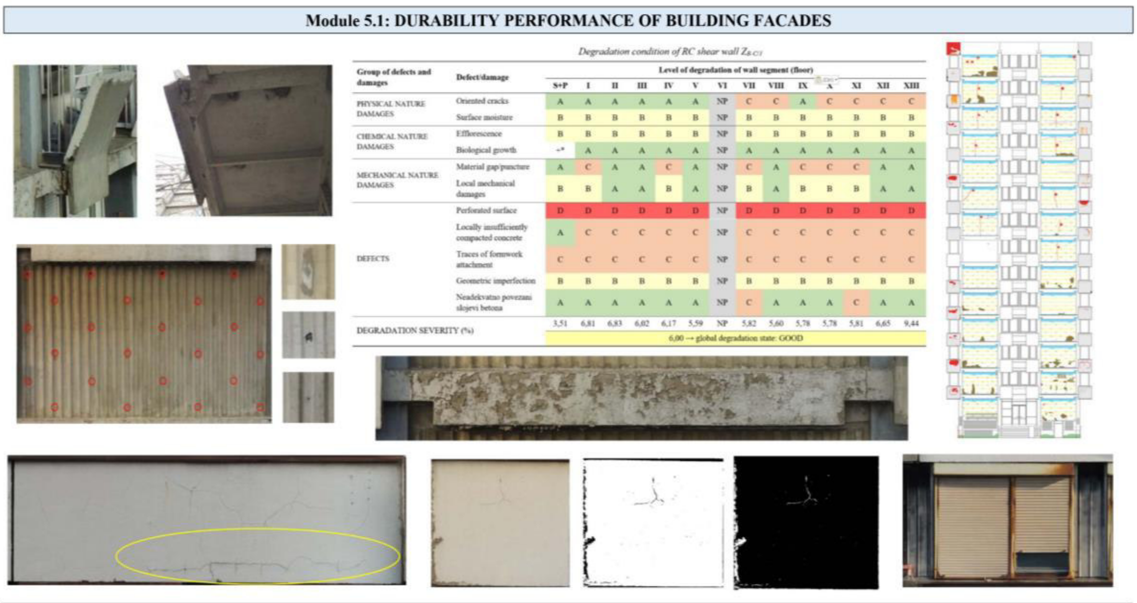

Fig. 4 Overview of the DBR Module 5.1 - Durability performance of building facades

Through *Energy Efficiency Elaborate* of the analyzed building, the sub-module *Energy performance of building* (Fig. 5) provides information about:

- Elements of building envelope
- Basic thermal-technical performance of building envelope
- Thermal bridges in the building envelope
- Required energy for heating of the building
- Building energy class

Elaborate is developed within the second part of the fifth renovation model phase (P5.2: Energy performance assessment), which involves evaluation of the thermal protection of the building and its components.

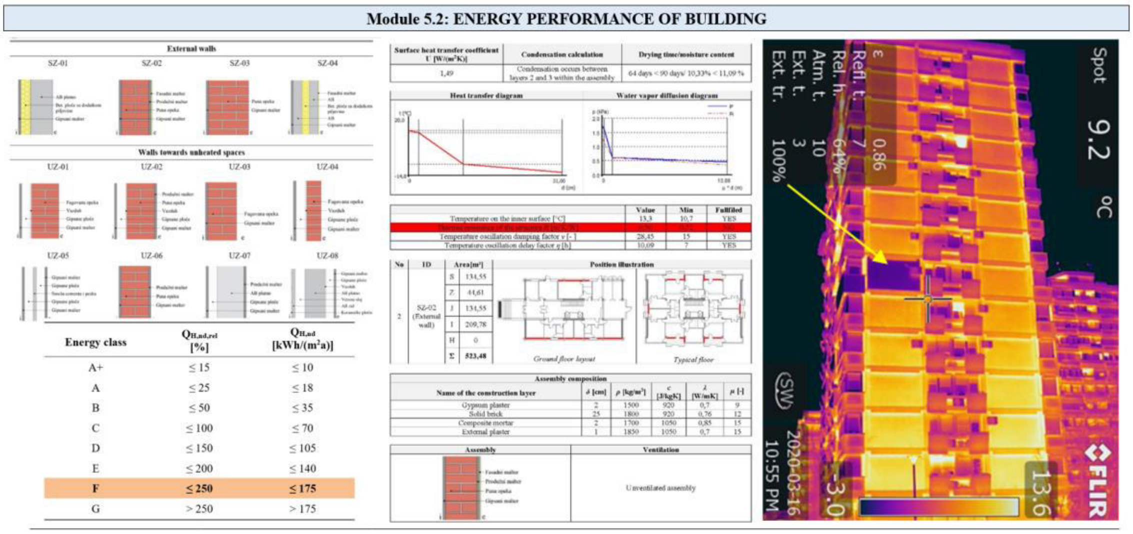

Fig. 5 Overview of the DBR Module 5.2 - Energy performance of building

The sub-module *Fire safety performance of building* (Fig. 6) is a result of a third segment of the fifth renovation model phase (P5.3: Fire safety assessment), conducted using a multi-step methodology developed as part of the doctoral dissertation.

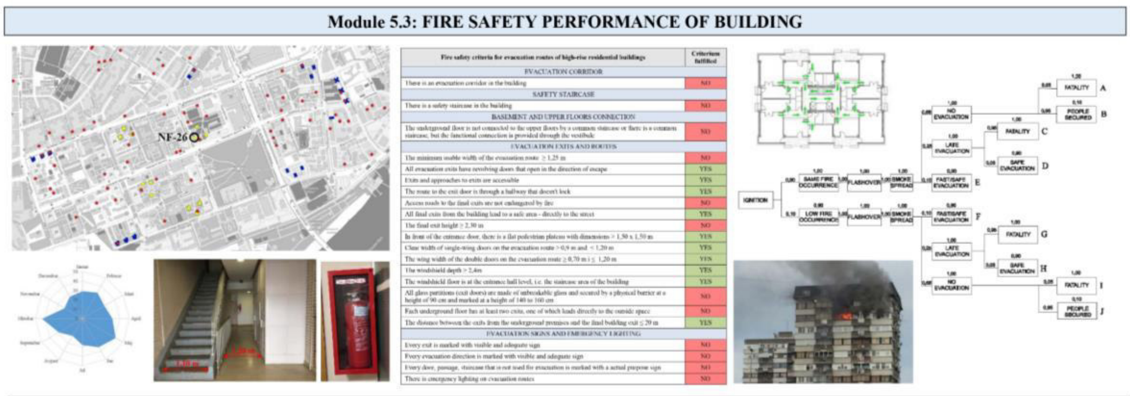

Fig. 6 Overview of the DBR Module 5.3 - Fire safety performance of building

The 5.3 sub-module provides information on the following aspects:

- Spatio-temporal analysis of fire distribution in residential buildings, through the newly created *Fire hazard map*.
- Fire risk in high-rise residential buildings, as indicated by the newly generated *Fire risk map*.
- The quality of building’s fire safety performance, determined by a qualitative method, using the newly created *Checklist*.
- The building's fire risk in terms of fire protection system requirements, evaluated using the semi-quantitative Euroalarm method.
- The building's fire risk, quantified by the event tree method.

3.2.6. Module 6: Proposed renovation measures and solutions

The overview of DBR module *Proposed renovation measures and solutions* is presented in Fig. 7. Measures and solutions have been proposed within two possible scenarios: (1) preserving the building's identity entirely and (2) partially preserving the building's identity.
Renovation measures and technical solutions for their implementation are proposed within the sixth renovation model phase (P6: Proposal of measures and solutions for facade renovation). Technical solutions may include selection of methods and principles for repairing identified damages, as well as selection of various thermal insulation materials and systems for retrofitting external building walls, and more.

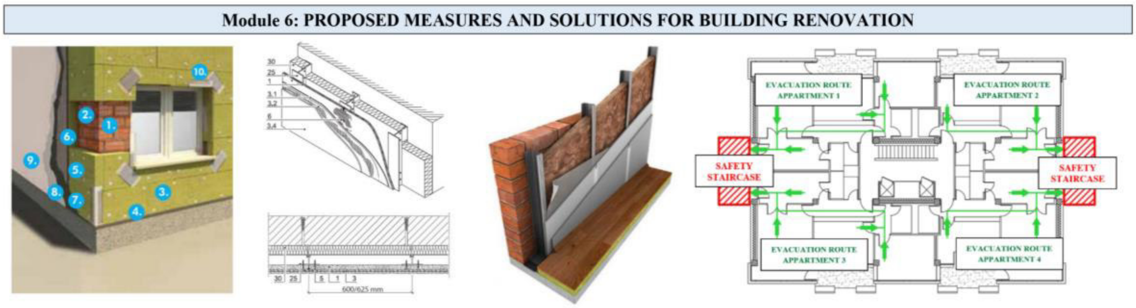

Fig. 7 Overview of the DBR Module 6 - Proposed renovation measures and solutions

3.2.7. Module 7: Evaluation of proposed renovation measures and solutions

The overview of DBR module *Evaluation of proposed renovation measures and solutions* is presented in Fig. 8.

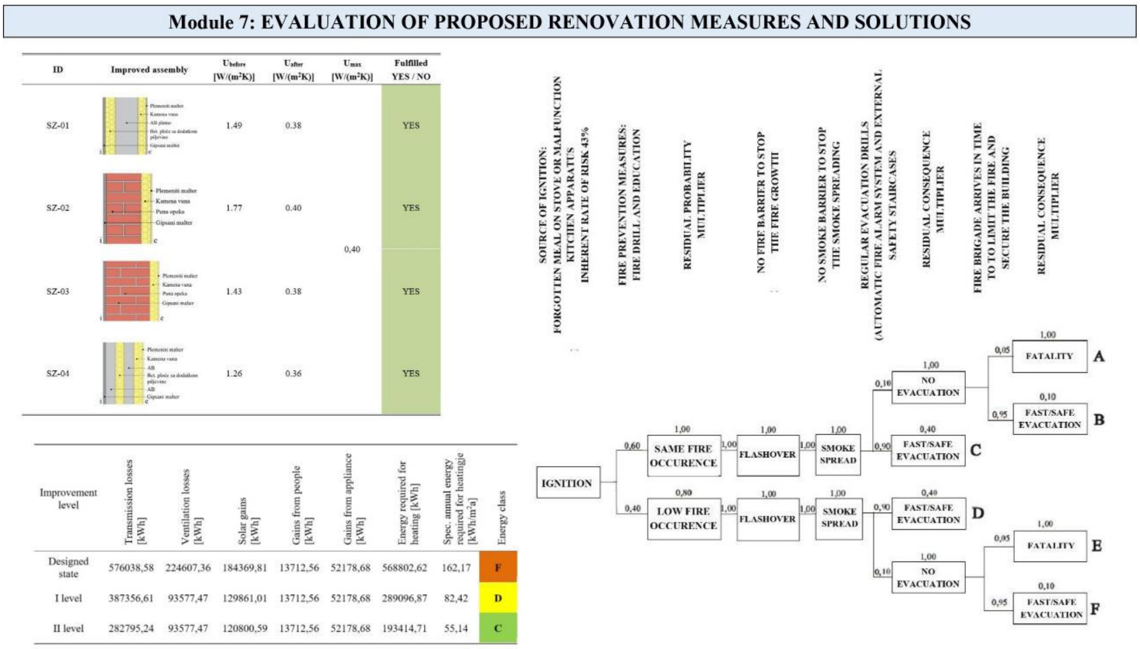

Module 7: EVALUATION OF PROPOSED RENOVATION MEASURES AND SOLUTIONS

ID	Improved assembly	U_{before} [W/(m²K)]	U_{after} [W/(m²K)]	U_{max} [W/(m²K)]	Fulfilled YES / NO
SZ-01	Plemeniti malter, Kamena vuna, AB platno, Bet. ploče sa dodatkom piljevine, Gipsani malter	1.49	0.38	0,40	YES
SZ-02	Plemeniti malter, Kamena vuna, Puna opeka, Gipsani malter	1.77	0.40		YES
SZ-03	Plemeniti malter, Kamena vuna, Puna opeka, Gipsani malter	1.43	0.38		YES
SZ-04	Plemeniti malter, Kamena vuna, AB, Bet. ploče sa dodatkom piljevine, AB, Gipsani malter	1.26	0.36		YES

Improvement level	Transmission losses [kWh]	Ventilation losses [kWh]	Solar gains [kWh]	Gains from people [kWh]	Gains from appliance [kWh]	Energy required for heating [kWh]	Spec. annual energy required for heatingje [kWh/m²a]	Energy class
Designed state	576038,58	224607,36	184369,81	13712,56	52178,68	568802,62	162,17	F
I level	387356,61	93577,47	129861,01	13712,56	52178,68	289096,87	82,42	D
II level	282795,24	93577,47	120800,59	13712,56	52178,68	193414,71	55,14	C

Fig. 8 Overview of the DBR Module 7 - Evaluation of renovation measures and solutions

The DBR module 7 is a result of seventh renovation model phase (P7: Evaluation of proposed renovation measures and solutions). In this phase an analysis and evaluation of proposed measures and alternative solutions are conducted based on defined parameters, with the aim of verifying the appropriate selection. The verification of the suitability of the proposed measures and solutions involves conducting a comparative analysis between the current state and the improved state. If the newly designed condition meets the established requirements, the next step is to make a decision on renovation. Otherwise, renovation measures are reviewed.

3.2.8. Module 8: Renovation decision

The DBR module *Renovation decision* is a result of final, eight, renovation model phase (P8: Decision-making on renovation). In the final phase, based on the previously conducted evaluation of the proposed renovation solutions, a decision is made regarding the implementation of measures, i.e., the realization of the renovation in the context of established goals. Measures can be implemented either entirely or in phases, according to the prioritization of the work.

4. CONCLUSION

In 10 years, the buildings of Europe will be the microcosms of a more resilient, greener and digitalised society, operating in a circular system by reducing energy needs, waste generation and emissions at every point and reusing what is needed [8].
The importance of DBLs, which contain all relevant building-related data throughout the entire life cycle of a building, is evident in the era of digitalisation, and interest in this topic is growing at the EU level.
The research paper introduced a novel decision support tool for building renovation management, with a particular focus on facades, that can be considered as an original version of DBL, developed according to Serbian needs. The proposed building repository represents a valuable tool that supports building renovation management in a holistic manner, with a simultaneous focus on three critical aspects of building performance: energy efficiency, durability and fire safety. Developed repository serves as a valuable tool for efficient data management, optimizing the renovation process, ensuring transparency and facilitating informed decision-making during building renovations.
The integration of the presented tool with relevant publicly available digital platforms, such as geoportal GeoSrbija[2], would enable easy access, retrieval and exchange of information among various stakeholders involved in the building renovation process.
The repository can also serve as a basis for development of a computer model (application/expert system) that enables the operator (engineer) to quickly and simultaneously assess the durability, energy performance, and fire safety of high-rise residential buildings, and also suggests measures and solutions to improve these performances.

ACKNOWLEDGEMENT

The research has been conducted within the project "Scientific theoretical and experimental research and improvement of educational process in the field of civil engineering", developed at the Department of Civil Engineering and Geodesy, Faculty of Technical Sciences, University of Novi Sad, Serbia.

REFERENCES

[1] Alonso R. Olivadese R., Ibba A., Reforgiato Recupero D. (2023). Towards the definition of a European Digital Building Logbook: A survey. *Heliyon*, Volume 9. https://doi.org/10.1016/j.heliyon.2023.e19285.

[2] GeoSrbija is centralized platform for accessing various geospatial data, maps, and services related to the territory of Republic of Serbia.

[2] European Parliament (2020). Maximising the energy efficiency potential of the EU building stock. European Parliament resolution of 17 September 2020 on maximising the energy efficiency potential of the EU building stock (2020/2070(INI)).

[3] European Commission (2021). Study on the Development of a European Union Framework for Digital Building Logbooks: Final Report. https://data.europa.eu/doi/10.2826/659006.

[4] Gómez-Gil M., Sesana M., Salvalai G., Espinosa-Fernández A., López-Mesa B. (2022). The Digital Building Logbook as a Gateway Linked to Existing National Data Sources: The Cases of Spain and Italy. *Journal of Building Engineering*, Volume 63. https://doi.org/10.1016/j.jobe.2022.105461.

[5] Malinovec Puček M., Khoja A., Bazzan E., Gyuris P. (2023). A Data Structure for Digital Building Logbooks: Achieving Energy Efficiency, Sustainability, and Smartness in Buildings across the EU. *Buildings*, Volume 13, 1082. https://doi.org/10.3390/buildings13041082.

[6] Gómez-Gil M., Espinosa-Fernández A., López-Mesa B. (2022). Contribution of New Digital Technologies to the Digital Building Logbook. *Buildings*, Volume 12, 2129. https://doi.org/10.3390/buildings12122129.

[7] Draganić S (2022). Strategic model for planning and designing the renewal of concrete facades of free-standing high-rise residential buildings from the aspect of energy efficiency, durability and fire safety (in Serbian), doctoral dissertation, University of Novi Sad, Faculty of Technical Sciences, https://nardus.mpn.gov.rs/handle/123456789/20850.

[8] European Commission (2020). A Renovation Wave for Europe - greening our buildings, creating jobs, improving lives. Communication from the Commission to the European Parliament, the Council, the European Economic and Social Committee and the Committee of the Regions. COM/2020/662. Brussels, Belgium.

[9] European Union (2021). Proposal for a Directive of the European Parliament and of the Council on the energy performance of buildings (recast). Brussels, Belgium.

[10] European Union (2023). Directive of the European Parliament and of the Council on energy efficiency and amending Regulation (EU) 2023/955 (recast). Brussels, Belgium.

[11] Mêda P., Calvetti D., Hjelseth E., Sousa H. (2021). Incremental Digital Twin Conceptualisations Targeting Data-Driven Circular Construction. *Buildings*, Volume 11, 554. https://doi.org/10.3390/buildings11110554.

[12] Daniotti B., Masera G., Bolognesi C., Spagnolo S., Pavan A., Iannaccone G., Signorini M., Ciuffreda S., Mirarchi C., Lucky M., Cucuzza M. (2022). The Development of a BIM-Based Interoperable Toolkit for Efficient Renovation in Buildings: From BIM to Digital Twin, *Buildings*, Volume 12, 231. https://doi.org/10.3390/buildings12020231.

[13] Rosa F. (2022). Digital Twin Solutions to Historical Building Stock Maintenance Cycles. *IOP Conference Series: Earth and Environmental Science*, Volume 1073. doi:10.1088/1755-1315/1073/1/012013.

[14] Gómez-Gil M., Espinosa-Fernández A., López-Mesa B. (2022). Review and Analysis of Models for a European Digital Building Logbook. *Energies*, Volume 15, 1994. https://doi.org/10.3390/en15061994.

[15] European Commission (2023). Technical study for the development and implementation of Digital Building Logbooks in the EU. Meeting report.

INTERNATIONAL SCIENTIFIC CONFERENCE
INTEGRATION, NOVELTY, DESIGN,
INTERDISCIPLINARITY, SUSTAINABILITY

iNDiS2023

A REVIEW OF METHODS FOR FLOOD RISK ASSESSMENT

Jelena M. Andrić[1], Aleksandar Pujović[2]

Summary:

Floods are the most frequent disasters around the world since flooding is a natural phenomenon that affects all river basins in some regular intervals. In this paper, a literature review on methods for flood risk assessment in different parts of the world is conducted. In total, 50 papers from 2002 to 2023 are collected related to flood risk assessment in different countries in order to analyse the applied methods for risk assessment. Since Asian continent is prone to floods hence there are a significant number of publications compared to other continents. The various methods for flood risk assessment are used: remote sensing and GIS, flood risk index, probabilistic and statistical approach, fuzzy approach, machine learning, AHP and GIS, and others. However, the results show that the majority publications have applied remote sensing and GIS for flood risk assessment. In addition, machine learning has the great potential for future research in this field.

Key words: Floods, Risk assessment, Remote sensing, GIS, Flood risk index, fuzzy approach, probabilistic and statistical approach, AHP, Machine learning

[1] Assistant Professor, Department of Civil Engineering, School of Design, Xi'an Jiaotong-Liverpool University, Suzhou, China, Jelena.Andric@xjtlu.edu.cn

[2] Teaching Assistant, Department of Civil Engineering and Architecture, Western Serbia Academy of applied studies, Užice, Serbia, aleksandarpujovic@gmail.com

1. INTRODUCTION

Floods are the most frequent natural disaster around the world since flooding is a natural phenomenon that affects all river basins in some regular intervals [1]. The consequences of floods can be critical and dangerous and it can influence different communities around the World. The definition of floods is as following: "*an overflow of water beyond the normal limits of watercourse*", which is given by the Australia Bureau of Meteorology [2]. The occurrences of flood hazards are rising due to the extreme rainfalls, which are the results of changing global climate and human activities on the environment. Climate change is the main factor that contributes to floods in urban areas [3]. With the increased number of flood disasters occurrence, the impact is becoming more severe. It is noted that floods caused a great impact on the society, serious economic losses, and social loss. The unwanted effects of flooding on society are a long-term and severe impact on human health or immediate drowning and death, physical trauma, infections and other diseases. Aftermaths of flooding can be serious including damage of the critical infrastructure systems such as power lines, electrical distribution systems, railways, roadways, water supply systems, wastewater services and others. According to the statistics data, the annual occurrence of floods is raising [4]. In the period between 1990 and 2019, floods were the most frequent disasters compared to other disasters such as: storms, earthquakes, landslides extreme temperature drought, wildfire and volcanic activity as shown in Table 1 [5].

Tab. 1 Statistics about the occurrence of disasters

Disaster	Number of occurrences	Percentage
Floods	4119	41.5%
Storms	2942	29.6%
Earthquakes	818	8.2%
Landslides	551	5.6%
Extreme temperature	524	5.3%
Drought	475	4.8%
Wildfire	341	3.4%
Volcanic activity	154	1.6%

Floods as natural disasters have occurred worldwide in different regions and parts of the Worlds during different time periods. In summer 2023, Beijing, China's capital, has recorded the heaviest rainfall in last 140 years. Beijing and Hebei province have been hit by severe flooding due to large amount of the rainfall and the level of waters rise to dangerous levels [6]. Flood destroyed roads and knocked out power and pipes caring drinking water (Figure 1). The mostly impacted area by floods is Asia. In total, 41% of global flooding incidents with the 1.5 billion people affected have occurred on Asian continent [7]. More precisely, the reason for this high number of flood disasters in South Asia is due to the extreme riverside flooding in countries such as India, Pakistan, Sri Lanka, Bangladesh and Nepal. Due to climate change in this area, there is a strong confirmation that the occurrence of extreme rainfalls is increasing [8]. These extreme events are becoming more unpredictable and chaotic, hence even forecasting models cannot predict. In June 2013, floods in India have caused a huge number of fatalities, in total 6054 fatalities [7].

Fig. 1 Recent floods in Beijing in 2023

Beside South Asia, China has experienced a significant number of catastrophic flood disasters, especially in coastal cities such as Shenzhen, Guangzhou, Wuhan, Yangcheng and others [9-11]. During the heavy floods in Guangzhou, subway stations, cars, taxis and buses were submerged [11]. In addition, there have been a major amount of floods in 2020 caused by heavy rainfall in the People's Republic of China [12]. A total number of 21 floods occurred in major rivers across China during 2020. Since 1998, the People's Republic of China has experienced its worst flood leading to economic loss of $38.194 billion.

Not only limited to Asia, floods are common in other parts of the World. Given that most of cities in Europe are located near major rivers since this land is highly attractive for different forms of use, the appearance of urban floods are common [13]. During the heavy rainfall in 2012, 25 properties in Bristol were flooded [14]. Floods are also the most damaging natural hazards in Costa Rica [15]. Historically, Australia has been impacted by floods in regions where extreme rainfalls have occurred. In 2021 and 2022, major flood events have occurred in New South Wales [16]. Between 1900 and 2005, a total of 241 floods have occurred in Canada and have resulted in more than 200 losses of human lives with damage of over CAD $2 billion [17]. This statistics has shown that floods are the most frequent natural disaster across Canada.

Flood risk assessment represents a complex process which can be divided into simple steps in order to obtain the result. Generally, disaster risk assessment consists of three steps: risk identification, risk analysis and risk assessment [18]. With the application of the mentioned process on the flood disasters, the following flood risk assessment process entail: 1.) flood risk identification; 2.) flood risk analysis; and 3.) flood risk assessment. Thus, risk is the probability that exposure to hazard will result in a negative consequences. Risk assessment can be a quantitative or qualitative measure of risk related to situation or threat [9]. In case that risk assessment is represented as a quantitative measure, it is calculated by two components the probability of hazard occurrence and the magnitude of potential loss.

2. METHODOLOGY

This paper performs a systematic literature review including articles related to floods and flooding, flood hazard, flood risks, flood risk assessment, flood mitigation and flood management. The review process can be divided into four steps: identification phase, screening phase, eligibility phase and analysis phase. The proposed methodology is presented in Figure 2. The identification phase is the initial phase and the aim is to identify the most relevant articles. The keywords typed in search field are: "*floods*", "*flood risk assessment*", "*flood hazards*", "*flood risks*", and "*flooding*". The research is conducted through Web of Science and Scopus, and the type of literature was limited to peer-review articles. The second stage is limiting search to the articles in which floods risk assessment is conducted by a particular methods. A certain number of articles were excluded since the focus was not related to the flood risk assessment, or without proposed methods for flood risk assessment. The third phase is related to identifying and classifying the methods which are used in the process for flood risk assessment. There are single methods and also a combination of two or more methods which are applied to assess the flood risks. Finally, the descriptive analysis of 50 articles is conducted. The descriptive analysis contains the number of articles published per year, the geographic distribution of publications, and the analysis of applied methods for flood risk assessment.

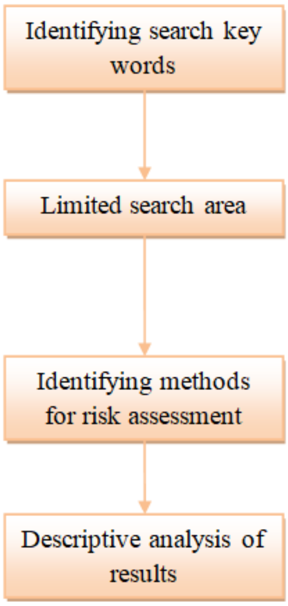

Fig. 2 The proposed approach for literature review

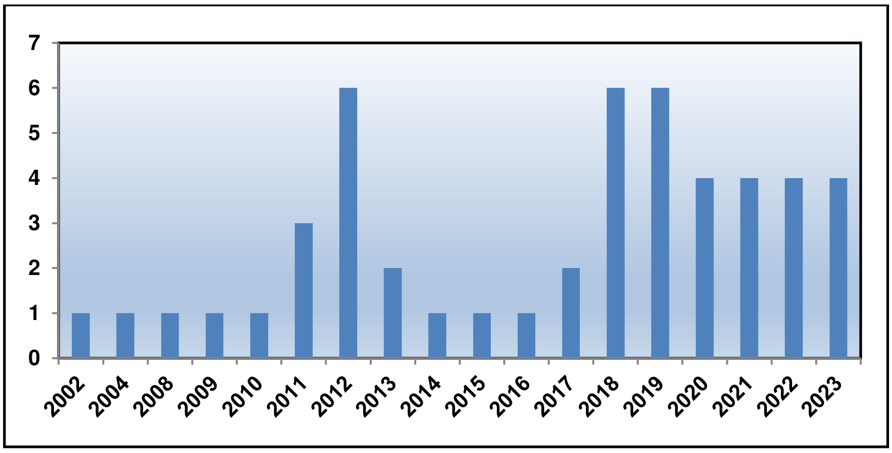

Fig. 3 Number of publications per year

3. RESULTS

Firstly, the year of publications has been analysed in Figure 3. The considered articles have been published between 2002 and 2023. The numbers of articles published during 21 year-period has increased from 1 paper in 2002 and 2004 to 4 papers in the recent years 2020 – 2023. Also, the two surges are experienced in 2012 and the period 2018 and 2019 with 6 papers per year.

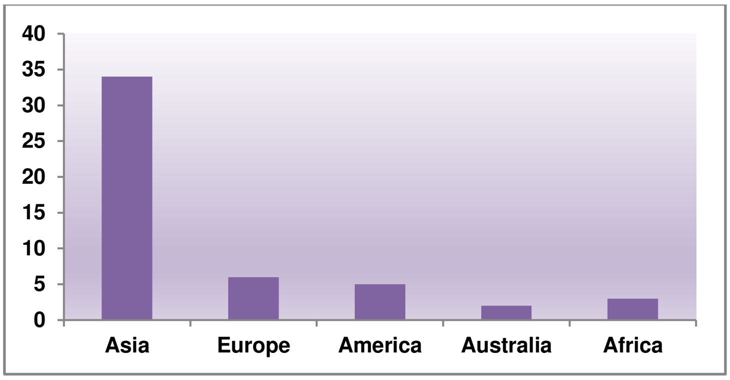

Fig. 4 Number of publications per year

In Figure 4, it is displayed the number of articles per continent. According to this Figure, Asian countries have published the majority of research related to risk assessment of flooding since Asia is seriously affected by floods in different regions and countries. In total, 34 of 50 papers are focused on flood risk assessment in Asia. On the other hand, Australia and Africa have the least research articles. Geographically, data have been considered for floods risk assessment from 28 different countries: China (12), India (4), Malaysia (4), Sri Lanka (2), Australia (2), Saudi Arabia (2), Canada (2), Netherlands (2), Nepal (1), Iran (1), South Korea (1), Japan (1), Indonesia (1), Vietnam (1), Cambodia (1), Pakistan (1), Bangladesh (1), USA (1), Costa Rica (1), Argentina (1), Portugal (1), Spain (1), Germany (1), Belgium (1), Togo (1), Niger (1), and Ethiopia (1). The most articles are published from China, which is expected since China is prone to flood disasters. It is followed by other three Asian countries, India, Malaysia, and Sri Lanka which are also seriously affected by flooding.

Tab. 2 Methods for flood risk assessment

Methods	Number of publications
Remote sensing and GIS	12
Flood risk index	7
Probabilistic and statistical approach	7
Fuzzy approach	6
Machine learning	6
GIS and AHP	5
GIS and MCDM	3
Other	4

Regarding methodology, the results are given in Table 2. There are several methods used for flood risk assessment such as remote sensing and GIS, flood risk index, probabilistic and statistical approach, fuzzy approach, Machine learning, GIS and AHP, GIS and MCDM and others. According to the analysis, the common methodology for flood risk assessment is remote sensing and GIS as a coupling method. Remote sensing is useful tool for obtaining information such as flooded areas, inundation duration, and mapping and monitoring of surface and sub-surface waterlogged areas. The observed data from satellites play a crucial role in disaster forecast system along with data made by terrestrial sensors which are assimilated into global and regional Numerical Weather Prediction models to provide improved forecast [19]. With the application of remote sensing, it can be promptly collected information about study area before and after the flood. Further, this information is used as input in GIS tools for spatial analysis. The integration of remote sensing and GIS is serves as a useful guide for the selection of training areas for classification and update a database for the assessment of spatially and temporally dynamic distribution of flood [11, 20-30].

Flood risk index is a method that is based on the three indexes, the flood hazard index, the exposure index, and the vulnerability index [15-16, 31-35]. The flood hazard index is calculated by the percentage of flood-prone hazard areas in municipal areas, the mean municipal slope degree, and the mean municipal value for rainfall intensity-duration-frequency curves. The flood exposure index is determined by the interaction of the population density, the mean infrastructure density and the percentage of non-forested area. The flood vulnerability index is established by the social development index, which includes economic, public health, educational, security and civic participation variables of the national municipalities. The general formula which can be applied to estimate the flood risk index is as follows [16]:

$$Flood\ risk\ =\ Hazard\ x\ Exposure\ x\ Vulnerability \qquad (1)$$

Probabilistic and statistical approach is widely used for modelling floods and flood risk assessment [36-42]. In this particular approach, the historical data related to flood inundation and exposure to disaster, the number of affected households, loss and damages is applied for the prediction of future perspectives of floods. The mathematical statistics is used for analysis and some of the methods such as Monte Carlo Simulation are practical for predictions. For example, one of the proposed models for flood assessment combines three simple modules, flood frequency analysis (peak discharge and frequency), inundation depth, and damage and loss assessment [36]. Also, rainfall data analysis can be used to provide vulnerability curves and quantitative and qualitative flood risk analysis are conducted based on this data.

Fuzzy approach is very convenient method for flood risk assessment due to their advantage in the complex uncertainty problem-solving [43-48]. The statistical data analyses method has a disadvantage since it is prone to incomplete data, data interruptions and other similar situations. In order to bridge the disadvantage of the lack of data or incomplete data, there are different fuzzy approach methods for flood risk assessment such as fuzzy multi-criteria approach, fuzzy comprehensive evaluation, fuzzy sets, fuzzy classifications and other. A unique model for flood disaster assessment that unifies fuzzy comprehensive evaluation assessment, fuzzy classification and fuzzy similarity methods is built [44]. Furthermore, a model that combines fuzzy comprehensive evaluation methods with GIS technique is developed based on three input factors: the hazard, the exposure and the vulnerability, and all factors are put into GIS to achieve overlay analysis and fuzzy matrix calculations [45].

Machine learning methodology for flood risk assessment is a recently method which appear with the development of computer technology [19, 49-53]. This method is based on the learning algorithms that learn the characteristics of flood hazard and vulnerability such as flood inundation, rainfall and other. Besides, the accuracy of results widely depends on the completeness and reliability of the input of the sample dataset. Machine learning methods include artificial neural network, logistic model trees, support vector machine, random forest, logistic regression, neural-fuzzy, adaptive neuro-fuzzy inference system and other. For instance, a machine learning based flood depth prediction model using the least square support vector machine is developed in order to estimate flood risks [49].

Other methods which are used for flood risk assessment are AHP [54, 55], Bayesian network (BN) [56], and combination of two methods GIS and AHP [9, 57-60], GIS and multi-criteria decision making (MCDM) [61-63], and GIS and BN [64]. With the application of AHP, different flood indicators are generated and it enables different indexes on multiple layers to consider and evaluate for the process of flood risk assessment [50]. In one of the proposed AHP models, the index layer for flood risk consists of two indexes, hazard and vulnerability [60]. The factors considered for layer hazard include extreme rainfall, elevation, terrain slope, drainage density, reservoir storage modulus, and flood detention basin modulus. For the layer vulnerability, three factors are taken into account: population, GDP and sown area of farm crops.

4. CONCLUSIONS

A total of 50 journal articles related to flood risk assessment published in the period between 2002 and 2023 are analysed. Asian continent is prone to severe flooding hence the majority of publications are related to flood risk assessment in Asian countries, China, Malaysia, India, Sri Lanka, Pakistan and other. This result is expected since the most of these articles are particularly focused on the flood risk assessment in China. Regarding the year of publications, there is a recent increase in the number of publications compared to the initial years in 2000s. Furthermore, this study has shown that the remote sensing coupling with GIS is widely used method for flood risk assessment following by flood risk index method, probabilistic and statistical approach, fuzzy approach and machine learning methods. Machine learning methods have a great potential to be widely used for flood risk assessment. The further research for flood risk assessment should be focused on the application of deep learning algorithms and training datasets for the prediction of flood disasters.

ACKNOWLEDGEMENT (STYLE: ZAHVALNOST)

We acknowledge Xi'an Jiaotong-Liverpool University for attending the conference.

REFERENCES

[1] Cloke, H., Di Baldassarre, G., Landeg, O., Pappenberger, F., & Ramos, M. H. (2017). Hydrological risk: floods, Science for disaster risk management 2017: knowing better and losing less, Publications Office of the European Union, pp.198 -238.

[2] AUSTRALIAN BUREAU of METEOROLOGY (BoM). (2022). *Understanding Floods*; Australian Government Bureau of Meteorology: Melbourne, Australia, Available online at: https://www.bom.gov.au/australia/flood/knowledge-entre/understanding.html

[3] Zhou, Q. (2014). A review of sustainable urban drainage systems considering the climate change and urbanization impacts. *Water*, *6*(4), pp. 976-992.

[4] Li, C., Sun, N., Lu, Y., Guo, B., Wang, Y., Sun, X., & Yao, Y. (2022). Review on Urban Flood Risk Assessment. *Sustainability*, *15*(1), 765. https://doi.org/10.3390/su15010765

[5] Vision of humanity, Available online at: https://www.visionofhumanity.org/global-number-of-natural-disasters-increases-ten-times/

[6] People's Daily online, 40 flights cancelled as heavy rains batter Beijing, Available online at: http://en.people.cn/n3/2023/0801/c90000-20052116.html

[7] Manandhar, B., Cui, S., Wang, L., & Shrestha, S. (2023). Urban Flood Hazard Assessment and Management Practices in South Asia: A Review. *Land*, *12*(3), 627. https://doi.org/10.3390/land12030627

[8] Mukherjee, S., Aadhar, S., Stone, D., & Mishra, V. (2018). Increase in extreme precipitation events under anthropogenic warming in India. *Weather and climate extremes*, *20*, 45-53. https://doi.org/10.1016/j.wace.2018.03.005

[9] Lyu, H. M., Sun, W. J., Shen, S. L., & Arulrajah, A. (2018). Flood risk assessment in metro systems of mega-cities using a GIS-based modeling approach. *Science of the Total Environment*, *626*, 1012-1025. https://doi.org/10.1016/j.scitotenv.2018.01.138

[10] Lyu, H. M., Shen, J. S., & Arulrajah, A. (2018). Assessment of geohazards and preventative countermeasures using AHP incorporated with GIS in Lanzhou, China. *Sustainability*, *10*(2), 304. https://doi.org/10.3390/su10020304

[11] Lyu, H. M., Wang, G. F., Shen, J. S., Lu, L. H., & Wang, G. Q. (2016). Analysis and GIS mapping of flooding hazards on 10 May 2016, Guangzhou, China. *Water*, *8*(10), 447. https://doi.org/10.3390/w8100447

[12] Xu, W., Xie, Y., Yu, Q., & Proverbs, D. (2023). An Evaluation of Factors Influencing the Resilience of Flood-Affected Communities in China. *Hydrology*, *10*(2), 35. https://doi.org/10.3390/hydrology10020035

[13] Löschner, L., Eder, M., Herrnegger, M., Hogl, K., Nordbeck, R., Scherhaufer, P., ... & Habersack, H. (2022). RegioFEM–Informing future‐oriented flood risk management at the regional scale (Part I). *Journal of Flood Risk Management*, *15*(1), e12754. https://doi.org/10.1111/jfr3.12754

[14] Sánchez-Muñoz, D., Domínguez-García, J. L., Martínez-Gomariz, E., Russo, B., Stevens, J., & Pardo, M. (2020). Electrical grid risk assessment against flooding in Barcelona and Bristol cities. *Sustainability*, *12*(4), 1527. https://doi.org/10.3390/su12041527

[15] Quesada-Román, A. (2022). Flood risk index development at the municipal level in Costa Rica: A methodological framework. *Environmental Science & Policy*, *133*, 98-106. https://doi.org/10.1016/j.envsci.2022.03.012

[16] Kelly, M., Schwarz, I., Ziegelaar, M., Watkins, A. B., & Kuleshov, Y. (2023). Flood Risk Assessment and Mapping: A Case Study from Australia's Hawkesbury-Nepean Catchment. *Hydrology*, *10*(2), 26. https://doi.org/10.3390/hydrology10020026

[17] Singh, J., Ghosh, S., Simonovic, S. P., & Karmakar, S. (2021). Identification of flood seasonality and drivers across Canada. *Hydrological Processes*, *35*(10), e14398. https://doi.org/10.1002/hyp.14398

[18] Andrić, J. M., & Lu, D. G. (2016). Risk assessment of bridges under multiple hazards in operation period. *Safety science*, *83*, 80-92. https://doi.org/10.1016/j.ssci.2015.11.001

[19] Lammers, R., Li, A., Nag, S., & Ravindra, V. (2021). Prediction models for urban flood evolution for satellite remote sensing. *Journal of Hydrology*, *603*, 127175. https://doi.org/10.1016/j.jhydrol.2021.127175

[20] Chowdary, V. M., Chandran, R. V., Neeti, N., Bothale, R. V., Srivastava, Y. K., Ingle, P., ... & Singh, R. (2008). Assessment of surface and sub-surface waterlogged areas in irrigation command areas of Bihar state using remote sensing and GIS. *agricultural water management*, *95*(7), 754-766. https://doi.org/10.1016/j.agwat.2008.02.009

[21] Pathak, S., Liu, M., Jato-Espino, D., & Zevenbergen, C. (2020). Social, economic and environmental assessment of urban sub-catchment flood risks using a multi-criteria approach: A case study in Mumbai City, India. *Journal of Hydrology*, *591*, 125216. https://doi.org/10.1016/j.jhydrol.2020.125216

[22] Suriya, S., & Mudgal, B. V. (2012). Impact of urbanization on flooding: The Thirusoolam sub watershed–A case study. *Journal of hydrology*, *412*, 210-219.
https://doi.org/10.1016/j.jhydrol.2011.05.008

[23] Rijal, S., Rimal, B., & Sloan, S. (2018). Flood hazard mapping of a rapidly urbanizing city in the foothills (Birendranagar, Surkhet) of Nepal. *Land*, *7*(2), 60. https://doi.org/10.3390/land7020060

[24] Wijeratne, V. P. I. S., & Li, G. (2022). Urban sprawl and its stress on the risk of extreme hydrological events (EHEs) in the Kelani River basin, Sri Lanka. *International Journal of Disaster Risk Reduction*, *68*, 102715. https://doi.org/10.1016/j.ijdrr.2021.102715

[25] Ntajal, J., Lamptey, B. L., Mahamadou, I. B., & Nyarko, B. K. (2017). Flood disaster risk mapping in the lower Mono river basin in Togo, West Africa. *International journal of disaster risk reduction*, *23*, 93-103. https://doi.org/10.1016/j.ijdrr.2017.03.015

[26] Jamali, B., Löwe, R., Bach, P. M., Urich, C., Arnbjerg-Nielsen, K., & Deletic, A. (2018). A rapid urban flood inundation and damage assessment model. *Journal of Hydrology*, *564*, 1085-1098. https://doi.org/10.1016/j.jhydrol.2018.07.064

[27] Dawod, G. M., Mirza, M. N., & Al-Ghamdi, K. A. (2011). GIS-based spatial mapping of flash flood hazard in Makkah City, Saudi Arabia. *Journal of Geographic Information System*, *3*(03), 225. doi:10.4236/jgis.2011.33019

[28] Thanh Son, N., Thi Thu Trang, N., Bui, X. T., & Thi Da, C. (2022). Remote sensing and GIS for urbanization and flood risk assessment in Phnom Penh, Cambodia. *Geocarto International*, *37*(22), 6625-6642. https://doi.org/10.1080/10106049.2021.1941307

[29] Haq, M., Akhtar, M., Muhammad, S., Paras, S., & Rahmatullah, J. (2012). Techniques of remote sensing and GIS for flood monitoring and damage assessment: a case study of Sindh province, Pakistan. *The Egyptian Journal of Remote Sensing and Space Science*, *15*(2), 135-141. https://doi.org/10.1016/j.ejrs.2012.07.002

[30] Islam, M. M., & Sado, K. (2002). Development priority map for flood countermeasures by remote sensing data with geographic information system. *Journal of hydrologic engineering*, *7*(5), 346-355. https://doi.org/10.1061/(ASCE)1084-0699(2002)7:5(346)

[31] Anuar, A., Abdullah, J., & Muhammad, N. S. (2023). Quantifying the flood risk index of the Malaysian "rice bowl". *Journal of Hydrology: Regional Studies*, *46*, 101324. https://doi.org/10.1016/j.ejrh.2023.101324

[32] Weerasinghe, K. M., Gehrels, H., Arambepola, N. M. S. I., Vajja, H. P., Herath, J. M. K., & Atapattu, K. B. (2018). Qualitative flood risk assessment for the Western Province of Sri Lanka. *Procedia engineering*, *212*, 503-510. https://doi.org/10.1016/j.proeng.2018.01.065

[33] Silva, S. F., Martinho, M., Capitão, R., Reis, T., Fortes, C. J., & Ferreira, J. C. (2017). An index-based method for coastal-flood risk assessment in low-lying areas (Costa de Caparica, Portugal). *Ocean & Coastal Management*, *144*, 90-104.
https://doi.org/10.1016/j.ocecoaman.2017.04.010

[34] Camarasa-Belmonte, A. M., & Soriano-García, J. (2012). Flood risk assessment and mapping in peri-urban Mediterranean environments using hydrogeomorphology. Application to ephemeral streams in the Valencia region (eastern Spain). *Landscape and Urban Planning*, *104*(2), 189-200. https://doi.org/10.1016/j.landurbplan.2011.10.009

[35] Li, K., Wu, S., Dai, E., & Xu, Z. (2012). Flood loss analysis and quantitative risk assessment in China. *Natural Hazards*, *63*, 737-760. https://doi.org/10.1007/s11069-012-0180-y

[36] Oubennaceur, K., Chokmani, K., Nastev, M., Lhissou, R., & El Alem, A. (2019). Flood risk mapping for direct damage to residential buildings in Quebec, Canada. *International journal of disaster risk reduction*, *33*, 44-54. https://doi.org/10.1016/j.ijdrr.2018.09.007

[37] de Moel, H., Bouwer, L. M., & Aerts, J. C. (2014). Uncertainty and sensitivity of flood risk calculations for a dike ring in the south of the Netherlands. *Science of the Total Environment*, *473*, 224-234. https://doi.org/10.1016/j.scitotenv.2013.12.015

[38] Mouri, G., Minoshima, D., Golosov, V., Chalov, S., Seto, S., Yoshimura, K., ... & Oki, T. (2013). Probability assessment of flood and sediment disasters in Japan using the Total Runoff-Integrating Pathways model. *International Journal of Disaster Risk Reduction*, *3*, 31-43. https://doi.org/10.1016/j.ijdrr.2012.11.003

[39] Kheradmand, S., Seidou, O., Konte, D., & Batoure, M. B. B. (2018). Evaluation of adaptation options to flood risk in a probabilistic framework. *Journal of Hydrology: Regional Studies*, *19*, 1-16. https://doi.org/10.1016/j.ejrh.2018.07.001

[40] Chubey, M. S., & Hathout, S. (2004). Integration of RADARSAT and GIS modelling for estimating future Red River flood risk. *GeoJournal*, *59*, 237-246. https://doi.org/10.1023/B:GEJO.0000026693.87089.83

[41] De Moel, H., Aerts, J. C., & Koomen, E. (2011). Development of flood exposure in the Netherlands during the 20th and 21st century. *Global Environmental Change*, *21*(2), 620-627. https://doi.org/10.1016/j.gloenvcha.2010.12.005

[42] Van Steenbergen, N., Ronsyn, J., & Willems, P. (2012). A non-parametric data-based approach for probabilistic flood forecasting in support of uncertainty communication. *Environmental Modelling & Software*, *33*, 92-105. https://doi.org/10.1016/j.envsoft.2012.01.013

[43] Jun, K. S., Chung, E. S., Kim, Y. G., & Kim, Y. (2013). A fuzzy multi-criteria approach to flood risk vulnerability in South Korea by considering climate change impacts. *Expert Systems with Applications*, *40*(4), 1003-1013. https://doi.org/10.1016/j.eswa.2012.08.013

[44] Jiang, W., Deng, L., Chen, L., Wu, J., & Li, J. (2009). Risk assessment and validation of flood disaster based on fuzzy mathematics. *Progress in Natural Science*, *19*(10), 1419-1425. https://doi.org/10.1016/j.pnsc.2008.12.010

[45] Cai, T., Li, X., Ding, X., Wang, J., & Zhan, J. (2019). Flood risk assessment based on hydrodynamic model and fuzzy comprehensive evaluation with GIS technique. *International Journal of Disaster Risk Reduction*, *35*, 101077. https://doi.org/10.1016/j.ijdrr.2019.101077

[46] Li, Q., Zhou, J., Liu, D., & Jiang, X. (2012). Research on flood risk analysis and evaluation method based on variable fuzzy sets and information diffusion. *Safety Science*, *50*(5), 1275-1283. https://doi.org/10.1016/j.ssci.2012.01.007

[47] Fariza, A., Basofi, A., Prasetyaningrum, I., & Pratiwi, V. I. (2020). Urban flood risk assessment in sidoarjo, indonesia, using fuzzy multi-criteria decision making. In *Journal of Physics: Conference Series* (Vol. 1444, No. 1, p. 012027). IOP Publishing. doi:10.1088/1742-6596/1444/1/012027

[48] Lv, H., Guan, X., & Meng, Y. (2020). Comprehensive evaluation of urban flood-bearing risks based on combined compound fuzzy matter-element and entropy weight model. *Natural Hazards*, *103*, 1823-1841. https://doi.org/10.1007/s11069-020-04056-y

[49] Ziya, O., & Safaie, A. (2023). Probabilistic modeling framework for flood risk assessment: A case study of Poldokhtar city. *Journal of Hydrology: Regional Studies*, *47*, 101393. https://doi.org/10.1016/j.ejrh.2023.101393

[50] Pham, B. T., Luu, C., Van Dao, D., Van Phong, T., Nguyen, H. D., Van Le, H., ... & Prakash, I. (2021). Flood risk assessment using deep learning integrated with multi-criteria decision analysis. *Knowledge-based systems*, *219*, 106899. https://doi.org/10.1016/j.knosys.2021.106899

[51] Mojaddadi, H., Pradhan, B., Nampak, H., Ahmad, N., & Ghazali, A. H. B. (2017). Ensemble machine-learning-based geospatial approach for flood risk assessment using multi-sensor remote-sensing data and GIS. *Geomatics, Natural Hazards and Risk*, *8*(2), 1080-1102. https://doi.org/10.1080/19475705.2017.1294113

[52] Kia, M. B., Pirasteh, S., Pradhan, B., Mahmud, A. R., Sulaiman, W. N. A., & Moradi, A. (2012). An artificial neural network model for flood simulation using GIS: Johor River Basin, Malaysia. *Environmental earth sciences*, *67*, 251-264. https://doi.org/10.1007/s12665-011-1504-z

[53] Khosravi, K., Shahabi, H., Pham, B. T., Adamowski, J., Shirzadi, A., Pradhan, B., ... & Prakash, I. (2019). A comparative assessment of flood susceptibility modeling using multi-criteria decision-making analysis and machine learning methods. *Journal of Hydrology*, *573*, 311-323. https://doi.org/10.1016/j.jhydrol.2019.03.073

[54] Dano, U. L. (2020). Flash flood impact assessment in Jeddah City: An analytic hierarchy process approach. *Hydrology*, *7*(1), 10. https://doi.org/10.3390/hydrology7010010

[55] Wu, J., Chen, X., & Lu, J. (2022). Assessment of long and short-term flood risk using the multi-criteria analysis model with the AHP-Entropy method in Poyang Lake basin. *International Journal of Disaster Risk Reduction*, *75*, 102968. https://doi.org/10.1016/j.ijdrr.2022.102968

[56] Li, G., Wu, X., Han, J. C., Li, B., Huang, Y., & Wang, Y. (2023). Flood risk assessment by using an interpretative structural modeling based Bayesian network approach (ISM-BN): An urban-level analysis of Shenzhen, China. *Journal of Environmental Management*, *329*, 117040. https://doi.org/10.1016/j.jenvman.2022.117040

[57] Roy, S., Bose, A., Singha, N., Basak, D., & Chowdhury, I. R. (2021). Urban waterlogging risk as an undervalued environmental challenge: An Integrated MCDA-GIS based modeling approach. *Environmental Challenges*, *4*, 100194. https://doi.org/10.1016/j.envc.2021.100194

[58] Seejata, K., Yodying, A., Wongthadam, T., Mahavik, N., & Tantanee, S. (2018). Assessment of flood hazard areas using analytical hierarchy process over the Lower Yom Basin, Sukhothai Province. *Procedia engineering*, *212*, 340-347. https://doi.org/10.1016/j.proeng.2018.01.044

[59] Chen, Y., & Alexander, D. (2022). Integrated flood risk assessment of river basins: Application in the Dadu river basin, China. *Journal of Hydrology*, *613*, 128456. https://doi.org/10.1016/j.jhydrol.2022.128456

[60] Wu, Y., Zhong, P. A., Zhang, Y., Xu, B., Ma, B., & Yan, K. (2015). Integrated flood risk assessment and zonation method: a case study in Huaihe River basin, China. *Natural Hazards*, *78*, 635-651. https://doi.org/10.1007/s11069-015-1737-3

[61] Fernández, D. S., & Lutz, M. A. (2010). Urban flood hazard zoning in Tucumán Province, Argentina, using GIS and multicriteria decision analysis. *Engineering Geology*, *111*(1-4), 90-98. https://doi.org/10.1016/j.enggeo.2009.12.006

[62] Ogato, G. S., Bantider, A., Abebe, K., & Geneletti, D. (2020). Geographic information system (GIS)-Based multicriteria analysis of flooding hazard and risk in Ambo Town and its watershed, West shoa zone, oromia regional State, Ethiopia. *Journal of Hydrology: Regional Studies*, *27*, 100659. https://doi.org/10.1016/j.ejrh.2019.100659

[63] Meyer, V., Scheuer, S., & Haase, D. (2009). A multicriteria approach for flood risk mapping exemplified at the Mulde river, Germany. *Natural hazards*, *48*, 17-39. https://doi.org/10.1007/s11069-008-9244-4

[64] Wu, Z., Shen, Y., Wang, H., & Wu, M. (2019). Assessing urban flood disaster risk using Bayesian network model and GIS applications. *Geomatics, Natural Hazards and Risk*, *10*(1), 2163-2184. https://doi.org/10.1080/19475705.2019.1685010

THE MANAGEMENT RISKS IN THE RISK ASSESSMENT MODEL MADE FOR WASTEWATER TREATMENT PLANT

Jovana Topalić[1], Vladimir Mučenski[2]

Summary:

This paper analyses the management risks in the risk assessment model made for wastewater treatment plants. This group of risks was identified during the doctoral research conducted with the Delphi method. In the risk assessment model, six groups of risks are identified and evaluated within a team of the Delphi method: legal, financial and economic, logistics, environmental protection, management, and design risks. The management risk group has seven identified risks. These risks are specified after the literature review and previous project experiences. From project management in construction, these risks can be further upgraded with tools such as SWOT and PESTEL methods.

Key words: risk, management, model, wastewater treatment plant

[1] Research Associate, Faculty of Technical Sciences, University of Novi Sad, Serbia, jovanatopalic90@uns.ac.rs
[2] Assoc. prof., Faculty of Technical Sciences, University of Novi Sad, Serbia, mucenskiv@uns.ac.rs

1. INTRODUCTION

The group of management risks in the preliminary risk assessment model is the part of the model made during doctoral research. It is a unique model made after detailed literature research, which included a review of journals, legal acts, and books, and collection of information about operational plants [1]. This is the specific part of the project management and there is no unified methodology like this made specifically for construction process of wastewater treatment plants.

The model was developed because there is no unified methodology for identifying and quantifying risks connected to the civil engineering processes for wastewater treatment facilities. This model was created after detailed research using the Delphi method, with six groups of identified risks. One of the risk groups, which is important for the planning and design phase of construction, is the managerial group of risks. The other groups include legal, financial and economic risks, logistics risks, ecological risks and design risks.

This topic is important because of the problem of wastewater treatment in the Republic of Serbia. Every country has laws regulating specific issues such as wastewater treatment and reuse. The European Union established many procedures and directives regarding wastewater treatment (European Union, 2000). According to [2] legal regulation plays a significant role in developing and applying wastewater treatment processes. The Republic of Serbia adopted all the necessary regulations on wastewater treatment, but the main problem is the adherence to the laws and bylaws in practice [3].

The German ATV standard [4] and the instructions from the book Wastewater Treatment Disposal and Reuse [5] are most frequently used in Europe. In practice, risk factors in the design instructions ([4],[5]; [6]) are based on the improvement of the design that meets the requirements of the effluent (such as ammonia content or total nitrogen content) but not the construction elements and processes of the project. This model is made up of a construction group of risks. Because it is very important to implement planning and design processes in the risk analysis.

For the past couple of years there has been an interest in risk management in the civil engineering industry. With risk identification, there is a formed base of risks, which is necessary for analysis and control. This can improve the knowledge about the issues in the civil engineering industry and the risks. If this analysis is well implemented, risk identification ensures successful management of the risk because an unknown risk becomes clear [7].

Construction risks i.e. the risks of construction projects are related to design, logistics, legal acts, environmental protection, management, finances, but also state policy [8]. For the past couple of years there has been an interest in risk management in the civil engineering industry. With risk identification, there is a
formed base of risks, which is necessary for analysis and control. This can improve the knowledge about the issues in the civil engineering industry and the risks. If this analysis is well implemented, risk identification ensures successful management of the risk because an unknown risk becomes clear [7].

The risk structure formed for the purpose of this research had 37 risks divided into six groups. Every group of risks was created on the basis of considering the issues on the project and the benefits of treating these risks at the beginning of the project. The first iteration was to send the risk structure to the group of experts who were qualified for the Delphi method. Each expert had to rate the risk with points from 1 to 5 (the Likert scale). Their decisions were based on the knowledge and experience in their professional work.

The risk model, which was developed as a part of the doctoral thesis is different from the standard guidelines because it includes 37 risks strictly connected to the civil engineering aspects of projects. This model is essential in the initial phases and design phases, when poor decisions can subsequently lead to poor efficiency and financial losses. For Serbia, it is crucial to know how to manage the risks, because there will be many future projects for wastewater treatment plants required for Serbia's EU accession.

2. MANAGEMENT RISKS

The greatest responsibility for identifying risks, analyzing them, and responding to them lies with the investor and their management team. Risk analysis provides the best results when performed at the very beginning of the project, although it is also important in other phases due to the disturbances that may occur [9]. It is important to emphasize risk identification in the first phase of the project (investor selection, financial issues, location requirements, contracts with public utility companies, environmental organisations, etc.) as well as in the design phase [2].
Civil engineering risks can be analysed differently based on their consequences, probability, types, and origin. According to [8], civil engineering risks relate to design, logistics, legal acts, management, environmental protection, finances, and politics.
The management risks will be defined after a detailed literature analysis, laws and bylaws, and projects. This group of risks comprises seven risks. Evidence for every risk can be found in the literature. These risks are the following [10]:

1. Lack of qualified staff working in public companies (based on interviews with experts and experience of authors)
2. Bad communication between the participants (designers) on the project
3. Insufficient professionalism of the investor in the design phase in terms of providing information for the designer
4. Slow investor decisions that slow down the designing process
5. Inadequate structure of the team for realization of the investment
6. Missing the project leader by the investor
7. Unrealistic project deadline planning by the investor.

These risks are explained and defined for the preliminary risk assessment model [10]:

1. Lack of qualified staff working in public companies (based on interviews with experts and experience of authors)

This risk is identified by experience.
Risk explanation: Many people employed in public utilities have yet to have the opportunity to meet with the construction projects of the water treatment plant. Therefore, it comes to problems when making important decisions related to Wastewater treatment plants.

2. Bad communication between the participants (designers) on the project

This risk is identified in [11].
Risk explanation: The work of designers on the project must be coordinated. If the participants (investor, designer, public institutions, and other interested parties) do not communicate constantly and do not keep records of current changes in the project, errors occur in design.

3. Insufficient professionalism of the investor in the design phase in terms of providing information for the designer

This risk is identified in [11]
Risk explanation: The environmental problem is caused by a lack of knowledge about wastewater treatment and the realization of investments by investors. If he is not sufficiently familiar with the issue, or he does not have enough knowledge, he cannot convey his requirements to the designer. Also, an investor does not know his obligations, from the aspect of realising the investment.

4. Slow investor decisions that slow down the designing process
This risk is identified in [12]
Risk explanation: A common problem when designing is investors' decision-making when the designer waits too long for decisions on the offered solutions.
5. Inadequate structure of the team for the realization of the investment
This risk is identified in [13]
Risk explanation: It is possible that problems may arise in the project if the most important parts are missing, projects are given to the most inexperienced member of the team, or they become essential due to unforeseen circumstances, decisions are made spontaneously "ad-hoc", without the involvement of all team members and interested parties sides for the observed problem. The investment implementation team includes the following structure: investors or representatives of investors, contractors, planners, consultants, designers, professional supervision and ecological engineers or other people in charge of decision-making.
6. Missing the project leader by the investor
This risk is identified in [13]
Risk explanation: In front of the investor, there may be a team in charge of the management project or just the project manager, who, in addition to technical problems, also handles all the other necessary activities for the investor.
7. Unrealistic project deadline planning by the investor
This risk is identified in [13]
Risk explanation: If a realistic plan is not made at the beginning of the project and the risks are not assessed with which all interested parties will be familiar, the works on the project may undoubtedly exceed the deadline, which leads to financial losses and even termination contracts, for example. When project deadlines are unrealistically planned, delays occur to the project and unplanned risks affect the very realization of the project.
The described risks are identified in this way for the first time and it is important to note that they are used for the Delphi method. These risks are connected to the risks in the creation and design phase of the project. All risks presented are rated by the experts, the participants in the Delphi method. After two rounds, the respondents reached a consensus, which was confirmed by the methods of descriptive statistics.
This research was conducted to fully meet the needs of the project managers when planning risk management. Therefore, it is important that everything is available with information on whether and how project managers create management plans risks. If they create them, this model will help them go through the definition more easily risk and create a plan for making the same.
The main significance of the created model is a better understanding of risk factors which can lead to the reduction in financial losses and better sustainability of the project. The limitations of the research are small number of experts with managerial experience in the Delphi team and the fact that experts participating in this research were from only two countries, Serbia and Bosnia and Herzegovina. The discussed preliminary risk assessment model can be implemented as a part of future research and can then be used in the PESTEL or the SWOT method. These methods are qualitative, but also essential for the beginning of project implementation.

3. CONCLUSION

This paper analysed the management risks of the preliminary risk assessment model for the construction process of wastewater treatment plants. The managerial aspects were defined as a special risk group for creating the model. This Risk Group was identified as a separate risk group with seven specified risks. The defined risks were specified after a literature review and the previous project experiences. From project management in construction, these risks can be further upgraded with tools such as PESTEL and SWOT methods.

ACKNOWLEDGEMENT

This research (paper) has been supported by the Ministry of Science, Technological Development and Innovation through project no. 451-03-47/2023-01/200156 "Innovative scientific and artistic research from the FTS (activity) domain".

REFERENCES

[1] Topalić Marković J., Mučenski V., Savić D., Velkovski T., Peško I., Tomaš L.: Risk Assessment Model for Planning and Design Processes of Wastewater treatment plants, Periodica Polytechnica Civil Engineering, 2020

[2] Riffat, R.: Fundamentals of Wastewater Treatment and Engineering, CRC Press, Boca Raton, FL, USA, 2012

[3] Topalić Marković J., Mučenski V.: Legal aspects of the risk assessment model created for wastewater treatment plants, 19th International Conference Man and working environment OESEM, Niš, 2022

[4] ATV: German ATV Rules and Standards: "ATV – A 106E Design and Construction Planning of Wastewater Treatment Facilities", GFA, Hennef, Germany, 1995 [online]

[5] Tchobanoglous, G., Burton, F. L., Stensel, H. D.: Wastewater Engineering, Treatment and Reuse, 4th ed., McGraw-Hill Education, New York, NY, USA, 2003

[6] Grady, Jr., C. P. L., Daigger, G. T., Love, N. G., Filipe, C. D. M.: Biological Wastewater Treatment, 3rd ed., IWA Publishing, London, UK, 2011

[7] Renault, B. Y., Agumba, J. N.: Risk management in the construction industry: a new literature review, MATEC Web of Conferences 66, Article number: 00008, 2016.

[8] Kishan, P., Bhatt, R., Bhavsar, J. J.: A Study of Risk Factors Affecting Building Construction Projects, International Journal of Engineering, Research & Technology, 3(12), pp. 831–835, 2014, [online]

[9] Boznak, R. G.: On the horizon - a 24-month car, the question is, who will achieve it?, Project Management Journal, 22(3), pp. 11–16, 1991. [online]

[10] Topalić Marković J.: Model preliminarne procjene rizika za proces građenja postrojenja za prečišćavanja otpadnih voda, doktorska disertacija, Univerzitet u Novom Sadu, Fakultet tehničkih nauka, 2022

[11] Aziz, R. F.: Ranking of delay factors in construction projects after Egyptian revolution, Alexandria Engineering Journal 52(3), pp. 387–406, 2013.

[12] Wideman, R. M. (ed.): Project and Program Risk Management: A guide to managing project risks and opportunities, Project Management Institute, Newtown Square, PA, USA, 1992.

[13] Walewski, J. A., Gibson, Jr., G. E., Vines, E. F.: Risk identification and assessment for international construction projects, [pdf] In: Global project management handbook, 2nd ed., McGraw-Hill, New York, NY, USA, 2006.

METHODS OF MEASURING WORKER PRODUCTIVITY FOR ENEGRY-EFFICIENT CONSTRUCTION IN THE NORMENG PROJECT

Zvonko Sigmund[1], Matej Mihić[2], Anita Cerić[3], Ivona Ivić[3], Sonja Kolarić[3], Meho Saša Kovačević[3], Lana Lovrenčić Butković[3], Mladen Vukomanović[3], Ivica Završki[3]

Summary:

Standardisation of works in the construction industry is an ongoing topic through many decades, due to technical innovations and overall increase in productivity. This paper will present the current research status of the EU funded project titled Development of automated resource standardization system for energy-efficient construction (NORMENG). A continuing issue in Croatia and in the neighbouring countries is that there are no universally accepted standards for worker productivity and materials consumption per unit of measure. The project aims to provide such standards for works related to energy efficiency and this paper specifically presents the use of advanced imaging hardware and software, such as LIDAR and photogrammetry to measure the quantity of work performed in a unit of time. The use of hardware and software were first tested in laboratory setting, followed by on a real construction site.

Key words: Productivity, NORMENG, Energy-efficient construction, Standards, LIDAR, Photogrammetry

[1] Associate professor, University of Zagreb Faculty of Civil Engineering, Zagreb, Croatia, zvonko.sigmund@grad.unizg.hr
[2] Assistant professor, University of Zagreb Faculty of Civil Engineering, Zagreb, Croatia, matej.mihic@grad.unizg.hr
[3] University of Zagreb Faculty of Civil Engineering, Zagreb, Croatia

1. INTRODUCTION

Construction industry in most countries employs 6 to 10% of the workforce [1] and in the Europe contributes around the same percentages of GDP [2], meaning that it has a large impact on any national economy and therefore that proper planning and monitoring is of great importance. To plan, and during construction to monitor, both the costs and the duration of construction works, labour productivity standards are essential. These standards show what type of construction workers are needed and how much time it would take for them to complete a unit of work, which can be expressed in meters, square or cubic meters, kilograms, pieces and so on. The standard itself is then expressed in hours per unit of work, such as h/m^2, h/m^3, h/kg,... In addition to time, the standards can also state how much materials are needed per unit of work, for example, how much cement in kilograms is needed for one cubic meter of concrete, but this is not the focal point of this research.

Many construction standards do exist, however, due to the more or less evident differences in construction practices in different countries, standards from one country may not be accurate in another. Another issue is that to be of use to the entire industry of one country, they need to represent the average productivity of workers employed in various different construction companies and working in different conditions. Larger construction companies often have their own internal standards, but they are based on their own work processes, and they are quite reasonably unwilling to share their competitive advantage to the rest of the market.

This all brings us to the issue that is the cornerstone of the project of the project titled "Development of automated resource standardization system for energy-efficient construction (NORMENG)". In Croatia and in its neighbouring countries, the last universal construction standards were published more than 35 years ago [3]. The goal of the project was therefore to see how a model for such standards can be developed, which would correspond to the institutional, legal, and economic frameworks of the environment of the Republic of Croatia and additionally the principles of green building at the same time.

The project itself was to be implemented through two phases, first one was industrial research and lasted 24 months and the second one was experimental development and it lasted 12 months.

The industrial research phase itself was divided into three activities. During the first activity knowledge will be gathered in the from available literature, existing construction standards and through interviews with industry experts both from Croatia and from other members of the EU. Focus groups will also be formed, consisting of public entities in Croatia, professional associations and representatives of the construction industry. As a result the concept of the construction standards model was to be developed, including the components essential for construction works which effect the building's energy efficiency.

The second phase of the industrial research focuses on the analysis of existing technologies and trends in the field of standardization of energy-efficient construction. Analytical studies of new technologies for the implementation of works related to environmentally sustainable construction will be conducted, which would result in the formulation of a conceptual form of a model for the standardization of energy-efficient construction. During this stage, innovation is expected in the area of using new technologies, namely 3D scan data, for measuring quantities of work performed in chosen unit of time.

In the third activity, the proposed use of innovative technologies will be tested in a controlled environment. Validation was planned on a test site where a structure was constructed specifically for the purpose of measuring construction workers' performance.

Finally, in the last year of the project, two activities will be conducted. One is the testing and fine tuning the construction standards model based on the measurements on a real construction site, and the other, last activity, will be the digitalization of the database on standards and the development of a software solution.
This paper specifically, will present the initial findings of measuring worker productivity using 3D scan data as a part of the second phase and third activity of the industrial research of the project.

2. METHODOLOGY

The basis of this research is the literature review undertaken in the field of construction productivity and more specifically in the use of 3D scan data for progress monitoring and consequently productivity estimation. Sources for the literature review were journal and conference papers collected by searching through academic databases, libraries, indexing sites and search engines, such as Scopus, Web of Science and Google Scholar. Due to a larger number of search results, the paper titles were first screened to establish relevance to the topic. Then the abstracts and keywords were read to further conclude the relevance to the topic. Finally, all paper that were deemed relevant were read in full and used as a theoretical background for this research.
Following the theoretical part of the research, a practical part was planned in two parts. The first one was to test the 3D scan data tools in a controlled environment (laboratory setting) and the second one to test them in a real construction site environment. For the purpose of the laboratory setting, a provisional building was constructed specifically for the purpose of its construction to be measured. Specific details will be shown in section 4. of this paper.

3. USE OF 3D SCAN DATA FOR PROGRESS MONITORING AND MEASURING WORKER PRODUCTIVITY

Three-dimensional (3D) scan data are the point cloud models of buildings, objects or terrain collected through one of, or a combination of, vision-based sensing technologies [4]. Vision-based sensing technologies are a subtype of remote sensing technology that collect information from visual data gathered from photographs, video or laser scanners with varying degrees of complexity in the sensor system [5]. Photogrammetry and laser scanning are the most common [6,7] and both can be either aerial or terrestrial.
Laser scanning or LIDAR (laser detection and ranging) is a technology that uses data collected from terrestrial laser scanners (TLS) or from drone-mounted LIDAR scanners to generate 3D point clouds. It works by measuring the time it takes for an emitted pulse of laser light to be reflected back and then calculating the distance to the target [6]. After the scanner receives the reflected signal (relative locations of the surrounding surfaces from the base station are calculated based on the time taken for the signal to return [8]), a data point is created and given x, y and z coordinates [9]. The coordinated points from each of the scans are then used to construct a 3D point cloud [9]. Generally, LIDAR is the most accurate of the vision-based sensing technologies able to produce extremely high-resolution models [10].
Photogrammetry is the other most common vision-based sensing technology for generating 3D point cloud models from 2D images [11]. Through the use of complex algorithms, it is able to reconstruct the position, orientation, shape and size of objects from pictures, which may be obtained via conventional photography or digital photography [12,13]. Photogrammetry includes more than just taking photographs, but is also "the processing of images; the development of 2D and 3D model reconstruction; the classification of objects for mapping or thematic applications; and the visualization

of maps" [14]. Videogrammetry is virtually the same as photogrammetry, since videos are sets of photographs taken in a short interval.
No matter if the source is from a TLS or photographs the end result is a set of data points in a 3D coordinate system [15], usually defined by the x, y and z coordinates of points that are present on the external surfaces of an object. It is a 3D model of a real object, but however the raw point cloud model shows only the surface of the scanned objects, with elements themselves being hollow in the point cloud model before postprocessing in other software.
For both photogrammetry and LIDAR, data collection can be both aerial and terrestrial, with aerial meaning that the sensor is located most likely on an UAS (unmanned aerial System) and terrestrial meaning that the sensor is on the ground level. Both also have the option of using commercial-grade and professional-grade hardware. There are certain quality requirements regarding the resolution of the but most modern smartphones are equipped with camera sensors of sufficient quality for photogrammetry making it more affordable. LIDAR has also started to be found on some smartphones and tablets, but is not accurate enough to generate point clouds that could be used for quality and quantity control and professional terrestrial scanners are therefore used.
It was mentioned before that LIDAR produces more accurate scans and that photogrammetry is more affordable. But each has other advantages and disadvantages. Previous research into this [4] has identified significant issues with using both technologies for progress monitoring. This is why both were chosen to be tested for this project.
Even when disregarding potential issues, there are still a large number of construction works whose quantity cannot be measured through point clouds created by LIDAR or photogrammetry. Formwork and reinforcement in the concrete can have issues due to occlusion when taking photographs and making scans. Other works which result in small changes often within the error range cannot be accurately measured. Electrical wiring or even more evident, almost all finishing works, result in voluminously small changes that cannot be picked up by photogrammetry and sometimes even LIDAR. This drastically reduces the possible works whose progress can be monitored to those which result in large changes in the environment such as earth works, concrete works, masonry work, assembly of prefabricated elements and so on.
Finally, when it comes to measuring productivity, only one method can be used, dividing progress with the time input into the activity. The differences in volume of elements between two subsequent scans are calculated and divided by the time between scans, or work time measured by other means.

4. MEASUREMENTS ON A TEST SITE AND AT A REAL CONSTRUCTION SITE

As it was mentioned before, the technologies were first tested out in a controlled environment, in "laboratory" conditions. The progress tracking was tested out on six different work types: masonry works, plastering works, façade works, drywall works, carpentry works, roof decking works. For testing purposes, a simple object was designed and constructed which contained previously mentioned works while at the same time representing almost realistic on-site situations. Figure 1 shows the blueprints of the object and Figure 2 shows the object when it was nearly completed. All figures in the paper were made by the authors.

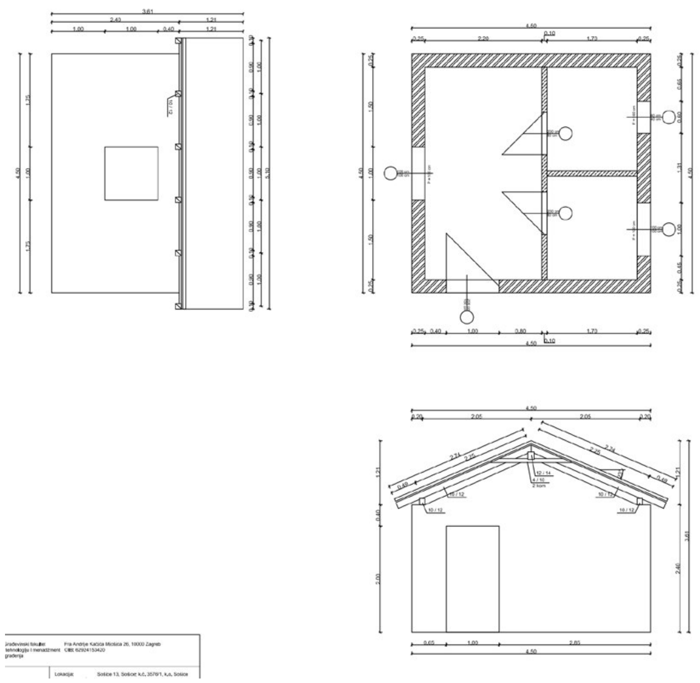

Fig. 1 Blueprints of the object planned for construction

Fig. 2 Construction phase at the test site

The main aims of the test site were to define the best possible post-processing procedure that enables qualitative assessment of the work that was done with taking post-processing (3D modelling) into account.

For the data capturing part of the problem three types of possible advanced progress tracking techniques were chosen. Those were:

- terrestrial LIDAR 3D scanning – excels at 3D data capturing with high accuracy, but requires a rather slow data collection process,
- photogrammetry using UAS – superior at aerial open-space data capturing but with very limited capabilities when it comes to operations in enclosed spaces,
- continuous video recording of the processes – a precise data recording process requiring very time-consuming post-processing or advanced programming capabilities of the user.

As for the data postprocessing phase, the following four software solutions were used:

- Agisoft Metashape – a very powerful software for point cloud creation using either photos or videos with limited point cloud analysis capabilities,

- Faro Scene – necessary software for LIDAR data management- excels at point cloud stitching and registration especially for FARO LIDAR scanner data,
- Faro BuildIt – general point cloud analysis software which brings certain point cloud analysis capabilities mostly tendering the needs of land surveyors employed with different construction sites,
- PointCab – a powerful CAD software providing the user with different point cloud analysis capabilities mostly aimed at specialists capturing the as-built state of buildings and similar surroundings.

4.1. DEFINING THE PROCEDURE FOR PROGRESS TRACKING

4.1.1. Terrestrial LIDAR 3D scanning

As the progress tracking should namely take place during the construction period it is to be expected that there are going to be materials, equipment, and workers around the site, thus this issue had to be taken into consideration. Still, as laser scanning is the most precise procedure, we first tested out the possibility of tracking the process with a LIDAR scanner.

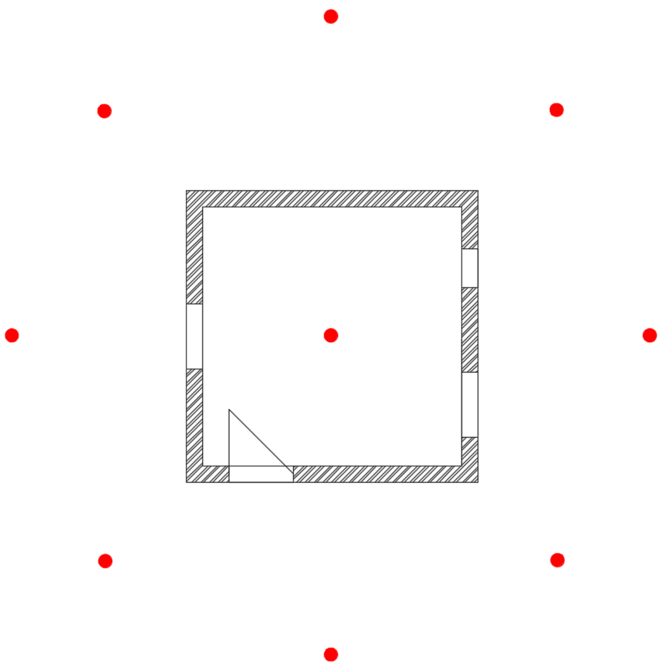

Fig. 3 Stand points for LIDAR scanning process.

For the scan the cover all the areas, one should plan the scanning procedure considering that all scanned areas should have at least 60% of overlap between scans to have a good enough scan which can be replicated on a computer. Additionally, one should bear in mind that even though a laser scanner is very precise it can scan only areas visible to it from its standing point.

To take advantage of its great capabilities, recording points should be considered before starting to record the construction site (or any other object). The stand-point plan should be conducted, an example of which is presented in the figure 3.

To record the construction site, the person recoding the site should go over all standing points. Each of the recordings can take from 1,5 min to 5 min depending on the decision to record the site in colour or not.

Considering a construction site is a living surrounding with workers moving and equipment placed in certain places to have a precise recording of the building one should plan to have at least one or 2 stations per enclosed room more than initially planned. Thus, a recording of our experimental site took from 13 min to 45 minutes,

during which if one is to evade the obstruction of the recording by workers the construction site had to be worker free (or they need to be standing still).
This was a major drawback for this recording process, as it is next to impossible to have the building site clear so one could interrupt the recording process.

4.1.2. Photogrammetry using UAS

For the UAS recording, at our disposal we had 3 types of UAS:

- DJI Matrice 300 RTK with Zenmuse P1 camera – UAS with a high-definition camera (maximum take-off weight 9 kg)
- DJI Inspire 2 with Zenmuse X7 camera – UAS with a high-definition camera (maximum take-off weight 4.25 kg)
- DJI Air 2s camera drones - UAS (maximum take-off weight 0.59 kg)

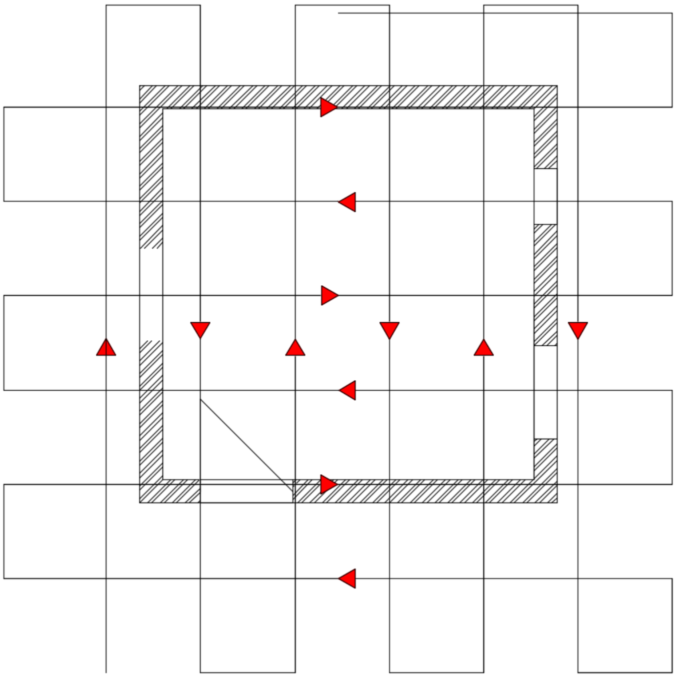

Fig. 4 Flight pattern for site recording using a video.

Each of these drones excels as a UAS within its designated usage area. The Matrice 300 is optimal for capturing footage from significant heights in vast open spaces where movement isn't a major hindrance to the final recording quality. Being an enterprise-grade UAS, the Matrice 300 is equipped with robust mission planning software. On the other hand, the Inspire 2 is a formidable flying machine designed for stable, high-speed flights, complemented by a camera tailored for high-definition, high-speed recording. The DJI Air 2s, being lightweight, boasts a high-resolution camera that ensures stable flights, both indoors and outdoors. However, it's worth noting that neither the Inspire 2 nor the Air 2s come with pre-installed mission planning software.
For a purely photogrammetric recording process, where each image must overlap by 70+% with the adjacent one in every direction, capturing our test site would consistently take between 7 to 10 minutes, regardless of the drone used. Yet, still images present a significant drawback: during post-processing, it is essential to ensure the site is free of workers. This ensures that all construction zones are visible when the camera records from a high vantage point.
Given this, we opted to capture footage of the site by recording a video during the flight. This approach allowed us to easily exclude movable objects, like workers, by simply omitting frames where they appear. Such recordings wouldn't exceed 5 minutes.

However, this method would necessitate adjusting the flight path to suit the new recording style.

4.1.3. Continuous recording of the processes

For the continuous recording of the processes two DJI Osmo Action - handheld cameras were placed on the building site. The main drawbacks of these recording techniques are that the analysis of the work process is a tedious process with no capability of a 3D display of the progress.

4.1.4. 3D displays of recording processes.

Upon analysing the progress recorded during the working hours at the construction site, we compared still photo photogrammetry and video photogrammetry.
In the case of still photo photogrammetry, the construction site was devoid of any ongoing work, resulting in images without workers. Conversely, the video photogrammetry captured scenes with workers actively engaged on the site.
Our benchmark for an acceptable video photogrammetry result was a minimal geometric alteration while retaining a high-quality outline comparable to both LIDAR scans and still photo photogrammetry.
Case 1: No Workers on Site (figures 5 and 6)
This illustrates the 3D modelling outcomes when the site was cleared of workers.

Fig. 5 Photograph of the first case

Fig. 6 3D modelling result of the still photo photogrammetry process

Fig. 7 Frame from a video used for the photogrammetry with a worker on the premises

Fig. 8 3D modelling result of the photogrammetry process using a video

Case 2: Workers Present but Excluded in 3D Modeling (figures 7 and 8)
This scenario features workers on the site, but they're excluded from the 3D model without necessitating any post-processing, such as point deletion. The displayed results informed the recording protocol for this construction site.
Both methods proved satisfactory for volume assessment, as seen in the subsequent images. However, video photogrammetry has a slight edge, especially when monitoring construction progress in environments where workers' presence might influence the results.
Still, the authors would suggest 3D modelling from still images for construction sites where workers do not present a major obstruction to the volume estimations. For instance, next are shown results of progress tracking on a building site stretching over an area of 8000 m^2, where workers present a minor obstruction.

Fig. 9 3D modelling of a building site – state 1

Fig. 10 3D modelling of a building site – state 2

As one can see, a volumetric contribution of a number of workers is in this case irrelevant, here a major contribution would be the possibility to filter out the machines automatically. Authors are still in the process of the research on how to have a clear representation of the object that is recorded without the objects that are obstructing the view.

5. CONCLUSION

This paper presents the first practical application of visual sensing technologies for monitoring construction progress on the NORMENG project. First, the laboratory test site was used to test out the possibilities of LIDAR, photogrammetry/videogrammetry and of continuous video recording in a completely controllable environment. The main advantage was that researchers were in control of the building process and therefore able to take measurements in any point in time, with workers and without workers on the site.

Preliminary results showed that when workers are on the site, they and more specifically their movement, present a real challenge to the monitoring process. This is most evident for LIDAR scanning, followed by photogrammetry. Videogrammetry on the other hand, provided better results, due to the fact that the frames where workers are moving can be

easily removed from the point cloud generation process. Drawback of videogrammetry is that only short videos can be taken, due to the limited flight time of UAS.
On the larger construction site, different conclusions can be drawn. Due to the size of the site and the earthworks carried out, the movement of workers is negligible when compared to the total volume of works. In that case, machinery such as excavators and dump trucks present larger problems. However, since there is considerable overlap of images due to the flight path, ground points could still be identified and occlusion issues avoided, making photogrammetry more than suitable for large construction sites.
Further research will continue with experimenting using all three techniques on a real construction site, to determine from practical experience, the benefits and drawbacks of each. Finally, the goal of this strand of the project's research will be to determine which technique is best for what purpose, what size of construction site and what work types, not just from the data collection standpoint but also from postprocessing standpoint.

ACKNOWLEDGEMENT

This research and the APC were funded by the European Union through the Competitiveness and Cohesion Operational Program, European Regional Development Fund, as a part of the project KK.01.1.1.07.0057 Development of automated resource standardization system for energy-efficient construction (NORMENG). The content of the publication is the sole responsibility of the University of Zagreb Faculty of Civil Engineering.

REFERENCES

[1] Raheem, A.A.; Hinze, J.W. (2014). Disparity between construction safety standards: A global analysis. *Safety Science*, Volume 70, pp. 276-287, https://doi.org/10.1016/j.ssci.2014.06.012.

[2] United Nations Economic Commission for Europe. (2022). Share of construction in GDP. Available online: https://w3.unece.org/PXWeb/en/CountryRanking?IndicatorCode=8 (accessed on 30.08.)

[3] Višnjić, M. (1986). *Normativi i standardi rada u građevinarstvu,*; Građevinska knjiga: Beograd

[4] Mihić, M.; Sigmund, Z.; Završki, I.; Butković, L.L. (2023). An Analysis of Potential Uses, Limitations and Barriers to Implementation of 3D Scan Data for Construction Management-Related Use: Are the Industry and the Technical Solutions Mature Enough for Adoption? *Buildings,*Volume *13*, pp. 1184, https://doi.org/10.3390/buildings13051184

[5] Arabshahi, M.; Wang, D.; Sun, J.; Rahnamayiezekavat, P.; Tang, W.; Wang, Y.; Wang, X. (2015). Review on Sensing Technology Adoption in the Construction Industry. *Sensors*, Volume 21, pp. 8307. https://doi.org/10.3390/s21248307

[6] Omar, T.; Nehdi, M.L. (2016). Data acquisition technologies for construction progress tracking. *Automation in Construction*, Volume 70, 143-155, https://doi.org/10.1016/j.autcon.2016.06.016.

[7] Liu, Y.; Kang, J. (2014). Application of Photogrammetry: 3D Modeling of a Historic Building. *Proceedings of the Construction Research Congress 2014*, pp. 219-228.

[8] Maalek, R.; Ruwanpura, J.; Ranaweera, K. (2014). Evaluation of the State-of-the-Art Automated Construction Progress Monitoring and Control Systems. *Construction Research Congress 2014*, pp. 1023-1032.

[9] Motawa, I.A.; Kardakou, A. (2018). Unmanned aerial vehicles (UAVs) for inspection in construction and building industry. Proceedings of the 16th International Operation & Maintenance Conference, Cairo, Egypt, p. 10.

[10] Golparvar-Fard, M.; Bohn, J.; Teizer, J.; Savarese, S.; Peña-Mora, F. (2011). Evaluation of image-based modeling and laser scanning accuracy for emerging automated performance monitoring techniques. *Automation in Construction*, Volume 20, pp. 1143-1155, https://doi.org/10.1016/j.autcon.2011.04.016.

[11] Dering, G.M.; Micklethwaite, S.; Thiele, S.T.; Vollgger, S.A.; Cruden, A.R. (2019). Review of drones, photogrammetry and emerging sensor technology for the study of dykes: Best practises and future potential. *Journal of Volcanology and Geothermal Research*, Volume 373, pp. 148-166, https://doi.org/10.1016/j.jvolgeores.2019.01.018.

[12] Kraus, K. (2007). *Photogrammetry: Geometry from Images and Laser Scans*. De Gruyter, Berlin, Germany

[13] Hackl, J.; Adey, B.T.; Woźniak, M.; Schümperlin, O. (2018). Use of Unmanned Aerial Vehicle Photogrammetry to Obtain Topographical Information to Improve Bridge Risk Assessment. *Journal of Infrastructure Systems*, Volume 24, https://doi.org/10.1061/(ASCE)IS.1943-555X.0000393.

[14] Baltsavias, E.P. (1999). A comparison between photogrammetry and laser scanning. *ISPRS Journal of Photogrammetry and Remote Sensing*, Volume 54, pp. 83-94, https://doi.org/10.1016/S0924-2716(99)00014-3.

[15] Wang, Q.; Kim, M.-K. (2019). Applications of 3D point cloud data in the construction industry: A fifteen-year review from 2004 to 2018. *Advanced Engineering Informatics,* Volume 39, pp. 306-319, https://doi.org/10.1016/j.aei.2019.02.007.

INTERNATIONAL SCIENTIFIC CONFERENCE
INTEGRATION, NOVELTY, DESIGN,
INTERDISCIPLINARITY, SUSTAINABILITY

iNDiS2023

A PRACTICAL METHOD FOR STRUT-AND-TIE MODELLING OF THE BRIDGE PILE CAP

Goran Milutinović[1], Nenad Pecić[2], Rade Hajdin[3], Snežana Mašović[4], Duško Bobera[5],

Summary:

Pile cap is a typical example of a discontinuity region, where the classical beam theory does not apply. Therefore, strut-and-tie (STM) model is considered appropriate for the analysis of pile caps. Although, the strut-and-tie method is a powerful tool, one of its shortcomings is the need for guidelines for the standardized models. Otherwise, it is left to the designer to come up subjectively with the STM model, which is a sensitive task. In literature, usually simple loading (axial compression or compression with bending only in one direction) on a four-pile cap is discussed. In practice, for real bridge structure, usual loading is alternate biaxial bending, along with compression, on much larger number of piles, making the typical four-pile caps models useless. A practical methodology for creating pile cap model with large number of piles and with complex loading is presented step-by-step. It is further illustrated for the cases with six piles and eight piles from the actual bridge structures, where the method was applied in practice.

Key words: pile cap, strut-and-tie

[1] Bridge Designer at DB Inženjering, Belgrade, Serbia, and PhD Student at University of Belgrade, Faculty of Civil Engineering, Serbia, gormilutin@gmail.com
[2] Professor at University of Belgrade, Faculty of Civil Engineering, Serbia, peca@imk.grf.bg.ac.rs
[3] Full Professor at University of Belgrade, Faculty of Civil Engineering, Serbia, and President of Infrastructure Management Consultants (IMC) GmbH, Switzerland, rade.hajdin@grf.bg.ac.rs
[4] Professor at University of Belgrade, Faculty of Civil Engineering, Serbia, smasovic@grf.bg.ac.rs
[5] President of DB Inženjering, Belgrade, Serbia, dusko_bobera@yahoo.com

1. INTRODUCTION

Pile cap is a typical example of a discontinuity region, where the classical beam theory does not apply. Therefore, strut-and-tie (STM) model is considered appropriate for the analysis of pile caps. Although, the strut-and-tie method is a powerful tool, one of its shortcomings is the need for guidelines for standardized models, since it is left to the designer to come up subjectively with the STM model, which is a sensitive task. In literature, usually simple loading (axial compression or compression with bending only in one direction) on a four-pile cap is discussed. In practice, for real bridge structure, usual loading is alternate biaxial bending, along with compression, on much larger number of piles, making the typical four-pile caps models useless. A practical methodology for creating pile cap with large number of piles and with complex, but realistic loading is presented step-by-step. The method is further illustrated for the cases with six piles and eight piles from the actual bridge structures, where the method was applied in practice. The intent is to make the unique model for one pile cap where numerous load combinations can be easily applied with complex alternating loading.
Strut-and-tie method, in general, is a practical application of the static theorem of plasticity [1]. The consequence is that the solution of the STM model is safe as long as the forces are in equilibrium. The structure will eventually come to the assumed strut-and-tie model force equilibrium, but if it is not the appropriate model, a severe unacceptable cracking and redistribution of forces will occur first. Therefore, a standardized procedure for constructing the STM model for each application (pile cap in this case) is needed, for its accurate and fast application in practice. The strut-and-tie method, when applicable, in general provides usually less required reinforcement than the classical beam theory, and moreover the reinforcement will be on the more appropriate (accurate) locations[2]. The intent of the paper is to be of the immediate benefit to the practicing engineers. The presented method can be used for the design of new bridge structures, as well as for evaluation of the existing bridges. Its application, however, is possible only for pile caps with two or more rows of piles; the single-row pile caps strut-and-tie models are inherently unstable for bending moment around pile-cap longitudinal direction.

2. LITERATURE REVIEW

A brief literature review is presented. In the fib Bulletin 100 [3], a STM model for four-pile cap loaded with only axial compression is discussed. Williams et al [4] studied the STM analysis of the four-pile cap with two load cases, each being compression with bending in one direction. Model from [4] is shown in Fig. 1, where red solid lines represent ties and green dashed lines represent struts; compression and one-directional bending is resolved in four forces applied on the top of the truss elements. Different model is needed for each load case, as the model become unstable once the loading is changed. This model becomes unstable also, for example, when bending in the other direction is added to the shown load combination, to obtain biaxial bending, what is the load case almost always encountered in practice.
Similarly, Schlaich et al [5] proposed a simple STM model for pile cap on four piles, supporting the wall (Fig. 2). Numerous other research has been published, regarding the pile cap STM modelling, but almost always a four-pile pile cap, with simple loading, is considered [6]–[15].

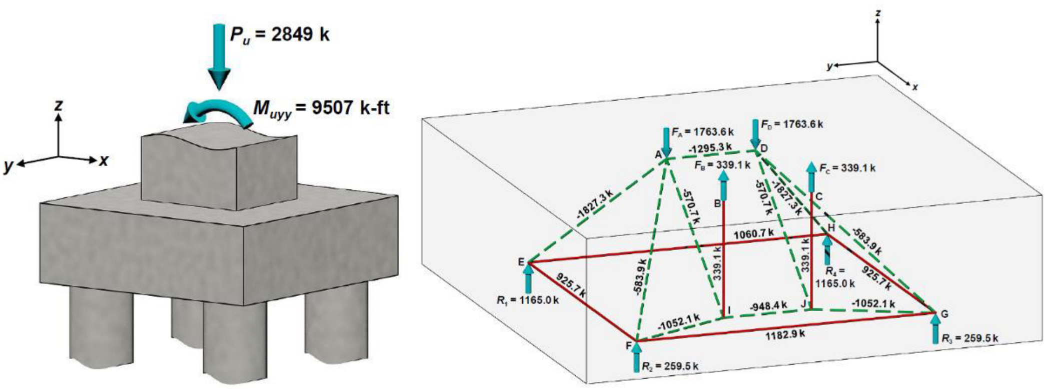

Fig. 1 - A strut-and-tie model for pile cap with four bored piles and one-directional bending load case [4]

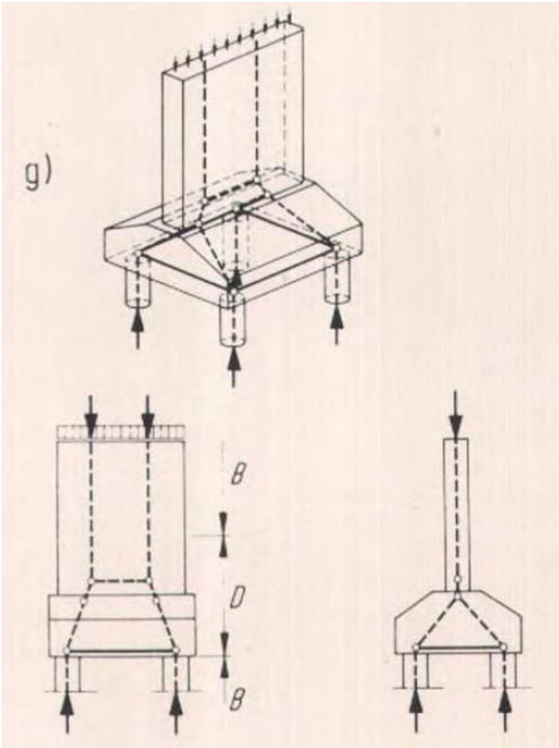

Fig. 2 - Strut-and-tie model for four-pile cap supporting the wall [5]

3. METHOD OVERVIEW

In this chapter, the step-by-step methodology for creating the STM truss models, using a typical finite-element software, for a pile cap with large number of piles and with complex realistic loading will be presented. The final goal is fast creation of safe and accurate STM model of the pile cap with any number of piles and any pile arrangement. The intent is to make the unique model, where numerous load combinations can be applied with alternating biaxial bending and compression force. The design checks for ties and struts according to the applicable code is considered determined and known to the reader/user of the method; they are not the focus of the paper.

However, as the strut-and-tie models are a simplified analogy with the stress field method, 3D node regions should be studied, since several 3D space members intersect in one point, which is not usually the case in strut-and-tie applications. This topic, however, is not the focus of this paper, and it will not be considered herein, although it should be a topic of future research.

The step-by-step procedure is presented below, followed by two examples of pile caps with six and with eight piles on two actual bridge structures, where the method had been applied in the practice.

3.1. STEP 1 – CREATE THE PILES

At the location of piles, create the beam elements with the actual geometric dimensions and concrete material properties of the piles. These are the only beam elements in the model. Appropriate spring stiffnesses representing the soil horizontal stiffness needs to be applied along the piles. Determination of the spring stiffnesses is considered to be outside of the scope of the paper.

3.2. STEP 2 – CREATE MAIN TIES (REINFORCEMENT)

Connect the top of each pile with truss element in an orthogonal grid. These truss elements represent the steel reinforcement connecting the piles at the lower face of the pile cap. The main rule is that the ties need to be in the orthogonal directions to match direction of the usual reinforcement layout. The forces in these ties determine the reinforcement quantity in the strips above the piles (connecting the piles) at the lower face of the pile cap. This is the main output of the analysis.

3.3. STEP 3 – CREATE TOP STIFF PLATE ELEMENT, WHERE THE CONCENTRATED LOAD IS APPLIED

Create the plate element at the connection between pile cap and column. Top surface elevation of the top plate element should correspond to the top surface elevation of the pile cap. The layout dimensions of the plate element should be equal to the layout dimensions of the column. Plate thickness should be one fifth of the pile cap thickness at the column face, and modulus of elasticity of the plate should be ten times the modulus of elasticity of the pile cap concrete. This stiffness is suggested based on the parametric study discussed later, in order to properly distribute the applied loads. This top stiff plate element is the element where the concentrated forces (compression and bending moment in two directions, obtained by the analysis of the global model of the bridge structure) is applied in the centroid of the plate.

3.4. STEP 4 – CREATE MAIN CONCRETE STRUTS

Divide the top stiff plate in (n-1)*(m-1) equal-area segments, where m and n are the number of piles in two orthogonal directions. Consequently, pile grid will be projected to stiff top plate. Connect the top of the piles and corresponding corners of top stiff plate segments with relatively massive concrete strut, using the compression-only truss element. The angle of approximately 45 to 60 degrees from main concrete strut to the horizontal at the pile cap lower face will usually be constructed for pile caps justifying the D-region assumption. Top plate element is connecting the main struts, making them and entire model stable. Modulus of elasticity should be the same as the pile cap material and dimensions should be the same as pile dimensions or slightly smaller. These main concrete struts follow the main compression flow of forces.

3.5. STEP 5 – CREATE PERIMETER CONCRETE DIAGONAL STRUT

Make one bracing per perimeter (inclined) face of the pile cap model (similar as bracing in building design), by connecting the top of one main concrete strut to the bottom of adjacent main concrete strut with compression-only truss element. If, in one direction of the pile cap, there are more than two piles, create two diagonal struts per face, each in adjacent bay, to form a K-bracing. If, in one direction of the pile cap, there are only two piles, create two diagonal struts (not connected to each other, but crossing each other) to form a X-bracing in that one bay. Create bracing in the mid zone of the perimeter face, as pile-cap corners are expected to be more loaded, with the assumption of the pile cap rotating as a rigid body. The material properties should be the same as the pile cap concrete, and cross sectional area should be two or three times smaller than the main concrete struts. These compression-only truss element represent the key elements for the stability of the model for different load combinations with alternate biaxial bending – they are forming, together with the main strut, the “outer core” of the space truss model.

3.6. STEP 6 – CREATE THE VERTICAL TIES REPRESENTING THE PILE CAP ANCHORS TO THE COLUMN

Create the vertical ties as vertical truss element at the four corners of the top plate element representing the anchors from the pile cap to the columns. These ties are connected at the top with stiff plate, and supported at the bottom by three struts located in 3D orientation. These ties usually attract large tensile forces, but they do not require special proportioning for the reinforcement, since they represent the column reinforcement, with significant amount of the cross-sectional area already determined during the column design. These ties will show forces obtained by the column reaction moment arm and are necessary to introduce the column moment in the pile-cap space-truss model.

3.7. STEP 7 – CREATE AUXILIARY DIAGONAL CONCRETE STRUTS

Create auxiliary diagonal concrete struts (as compression-only truss elements) between lower joint of the vertical column ties and the upper joint of the adjacent vertical column tie, forming four “X” bracing in four directions (two intersecting struts forming the bracing are not connected to each other). Together with the vertical ties, these auxiliary diagonals form the “inner core” of the pile-cap space-truss model. The column bending moment reaction is resolved by the compression in the main struts and the tension in the vertical ties (column anchors) on the opposite side – this tension is finally introduced in the space truss system with the “inner core” created in this step. The material properties should be the same as the pile cap concrete, and cross sectional area should be two or three times smaller than the main concrete struts.

3.8. STEP 8 – CREATE BOTTOM LEVEL DIAGONAL CONCRETE STRUTS

Connect the bottom of column anchor vertical ties (from Step 6) with top of the corner piles, with compression-only truss element in a horizontal brace in the level of reinforcement. The material properties should be the same as the pile cap concrete, and cross sectional area should be two or three times smaller than the main concrete struts. These compression-only truss element represent one of the key elements for the stability of the model for different load combinations with alternate biaxial bending.

4. DISCUSSION

Usually, the main challenge is to make the truss model stable for different complex alternate loading cases, i.e. for introduction of the bending moment in the space truss model of the pile cap. In the presented method, bending moment is introduced in the pile-cap space-truss system by the means of vertical column anchors (ties from the Step 6) and auxiliary compression struts (from Steps 7 and 8). The model obtained by the proposed approach is statically indeterminate, bringing the uncertainty in the analysis, corresponding to the appropriate selection of the truss element stiffness and consequent force distribution. However, the use of the compression-only elements for the struts reduces the statical indeterminacy of the system, as often there are zero-force truss elements or truss elements with small value of compression, for certain load combination. Further, the statical indeterminacy of the system (and related consequences of the element stiffness choice), can be justified by the static theorem of plasticity (the base for the STM), stating that the configuration is safe as long as the forces are in equilibrium. Further, for the STM it stands that the structure will eventually come to the assumed strut-and-tie model force equilibrium, but if it is not the appropriate model, a severe unacceptable cracking and redistribution of forces will occur first. However, the model set in this approach and corresponding flow of forces seems intuitive and appropriate, enabling multiple biaxial load combination. An advantage of the proposed approach is that ties are located only in the direction where the main reinforcement already exists in the conventional pile cap reinforcement layout. These are the locations of the horizontal orthogonal reinforcement and vertical column anchors. The use of compression-only truss elements requires the use of nonlinear finite-element analysis, since the stiffness matrix depends on the displacements (i.e. it is not constant). The iterative process for nonlinear analysis is incorporated in most modern finite-element softwares.

The main output of the analysis is the reinforcement quantity obtained from the tensile forces in the main ties. Compression in the strut usually does not represent a large unacceptable loading (although need to be checked of course), since the pile cap is a massive concrete block, allowing for enough concrete to be activated in the strut. One of the advantages of the proposed method is that the only one model is made, on which different numerous load combinations can be easily applied, allowing for its fast application in practice.

Parametric study of the top plate stiffness, analysing the distribution of the tensile forces in the main ties, was performed. The top stiff plate thickness (t_{plate}) is modelled as one-fifth of the pile cap thickness (t_{pile_cap}) to have geometrically meaningful dimensions, and modulus of elasticity of the plate element (E_{plate}) was varied from the same as the pile cap concrete ($E_{concrete}$), to two, four, eight, ten, and 15 times the pile cap concrete modulus of elasticity, in order to obtain the realistic stiffness. The layout dimensions of the plate element are modeled equal to the layout dimensions of the column. The forces in ties for each case are shown in Fig. 3. It is concluded that relatively soft plate (for example, $t_{plate} = 1/5 * t_{pile\_cap}$ and $E_{plate} = E_{concrete}$) does not distribute well the forces between different ties in the horizontal tie network – the most loading goes to the middle ties. However, with increasing the top plate stiffness, the force distribution between different ties is improved, and start to converge at one point, showing well-distributed tie forces. It has been suggested to use one fifth of the pile cap for the top plate thickness and to increase the modulus of elasticity of pile cap concrete by ten times, to obtain the appropriate stiffness of the top plate.

Further, it has been discussed in the literature that zones above the piles (where the ties end) are in highly compressed region (due to pile compression force), so the tie reinforcement can be anchored only by the straight bars extended to the pile cap face [16]. However, from the constructability point of view, it should not be a problem to provide a 90-degree hook. Only one layer of the main bottom-level tie reinforcement is usually necessary. The reinforcement in the main ties is the only reinforcement obtained from the structural calculation – however, reinforcement between strips/main ties, skin reinforcement on side faces, and reinforcement in the top surface of the pile cap should be also provided. It should be in the amount of at least 0.1% of the cross sectional area of the pile cap (a requirement of the Eurocode). For a 2m-deep and 8m-wide pile cap, this corresponds to minimum Ø20/15 for top mat reinforcement and side reinforcement. Often large portion of diagonal struts will not be activated for certain load combination – only those diagonal required for the stability of the model for the specific load case will be activated and will receive the compression force. Its application, however, is possible only for pile caps with two or more rows of piles; the single-row pile caps strut-and-tie models are inherently unstable for bending moment around pile-cap longitudinal direction.

The method can be applied not only to the pile caps with bored piles (drilled shafts), but also to other pile types, such as driven steel HP piles, often used in the U.S.A. [17]. The proposed method is also very useful when additional piles, due to unnapropriate construction of a pile (the case often happened in practice), are added to the pile cap, making pile cap shape irregular.

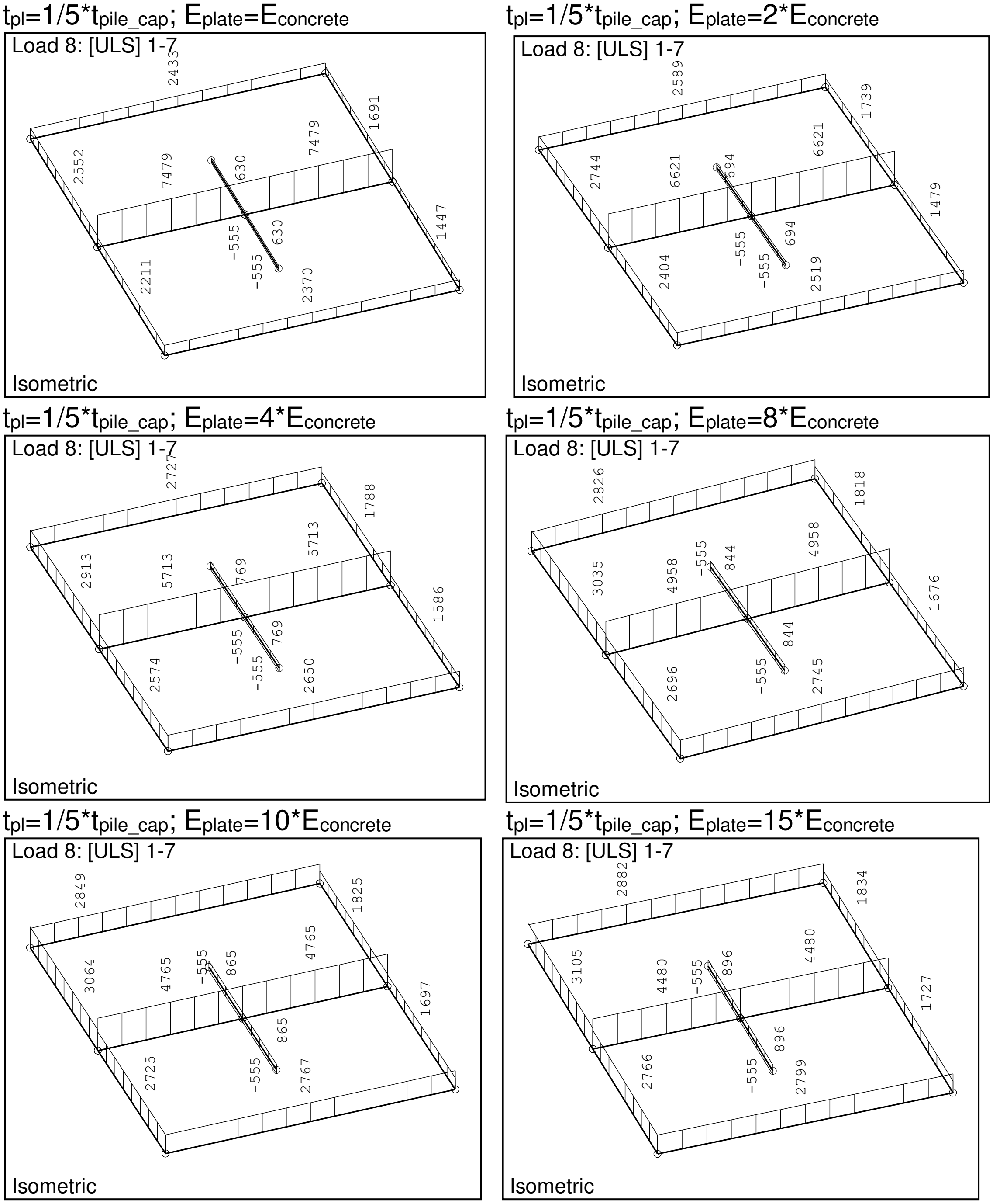

Fig. 3 - Tie forces distribution for different concrete modulus of elasticity and fixed top plate thicknesses

5. CASE STUDY 1 – PILE CAP WITH SIX PILES

The method proposed in this paper has been applied in the practice to the actual bridge structure shown in Fig. 4, for a 2m-thick pile cap with six bored concrete piles with 1.2m diameter. One model is built (Fig. 5), on which concentrated column-base reactions from the global model were applied, for all applicable Eurocode load combinations, including seismic ones.

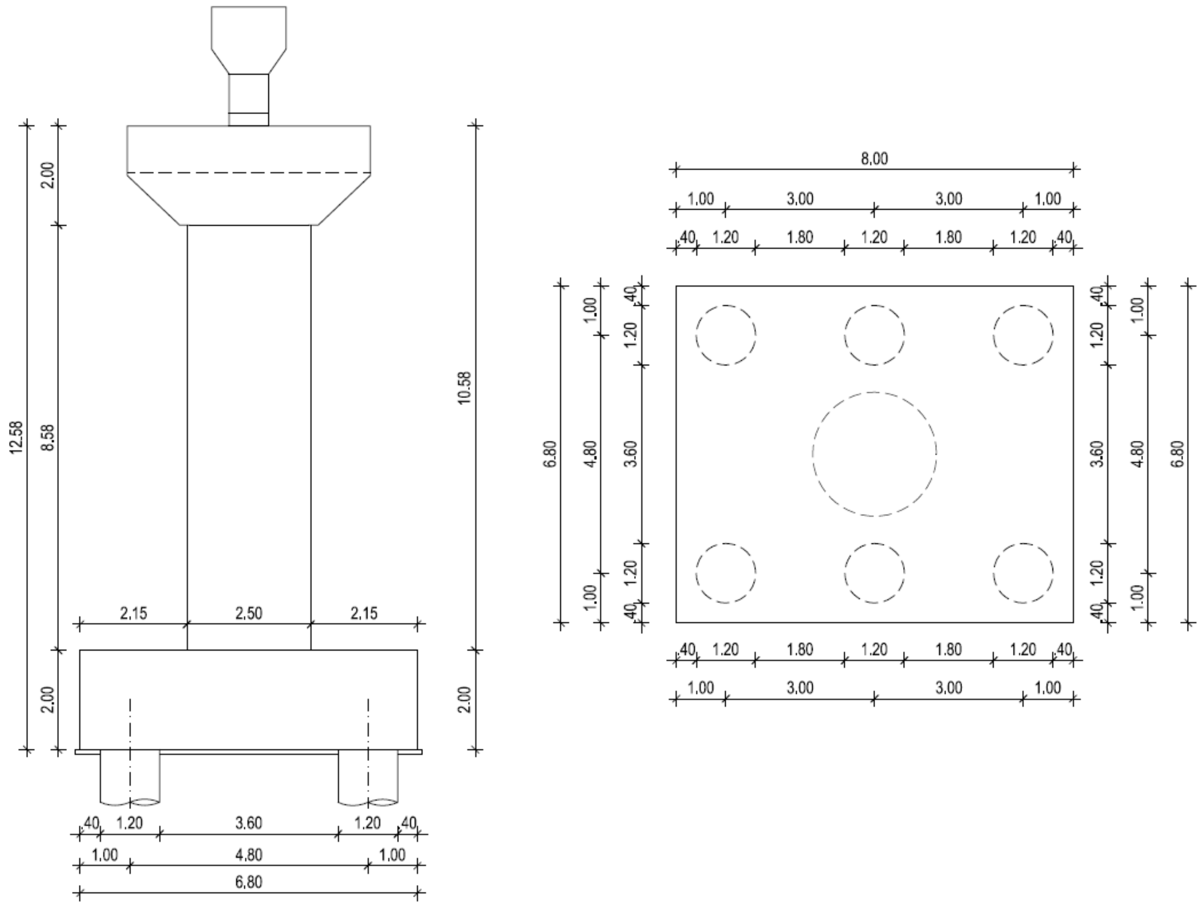

Fig. 4 – Pile cap at bridge at Morava Corridor in Serbia (at km 15+759, near Kruševac)

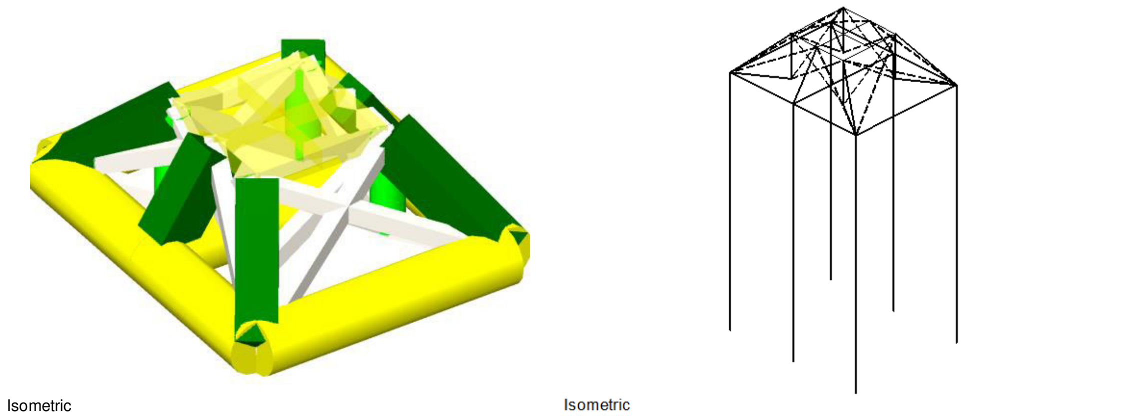

Fig. 5 - 3D rendering of the STM pile cap model with six piles (left full rendering shown without piles present in the model)

In Fig. 6, the decomposition of the model is shown: (1) main ties, in the upper left corner, created in the step 2 of the method; (2) main concrete struts, in the upper right corner, created in the step 4 of the method; (3) concrete perimeter diagonals, in the lower left corner, created in step 5 of the method, forming the “outer core”; and (4) the “inner core”, in the lower right corner, created in the steps 6, 7 and 8 of the method.

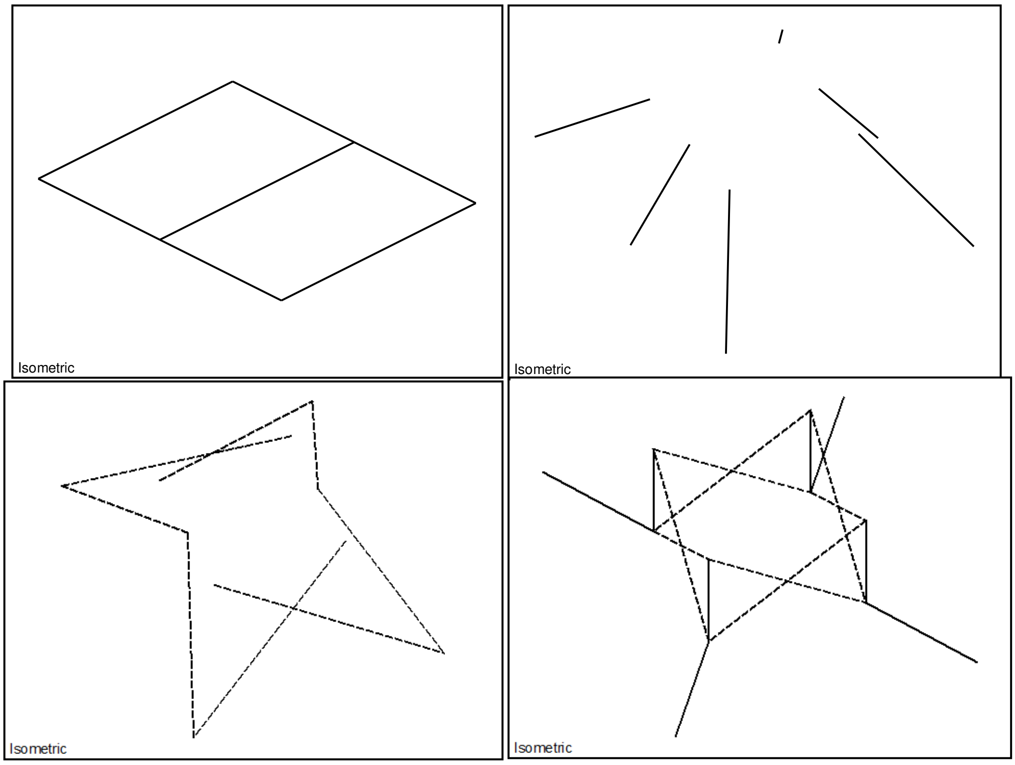

Fig. 6 - Upper left: ties (reinforcement) at strip above the piles; upper right: main concrete struts; lower left: concrete diagonals; lower right: the "inner core"

6. CASE STUDY 2 – PILE CAP WITH EIGHT PILES

The method proposed in this paper has been also applied in the practice to the actual bridge structure shown in Fig. 8, for a 2.2m-thick pile cap with eight bored concrete piles with 1.2m diameter. Again, one model is built (Fig. 7), on which concentrated column-base reactions from the global model were applied, for all applicable Eurocode load combinations, including seismic ones.

In Fig. 9, the decomposition of the model is shown: (1) main ties, in the upper left corner, created in the step 2 of the method; (2) main concrete struts, in the upper right corner, created in the step 4 of the method; (3) concrete perimeter diagonals, in the lower left corner, created in step 5 of the method, forming the "outer core"; and (4) the "inner core", in the lower right corner, created in the steps 6, 7 and 8 of the method.

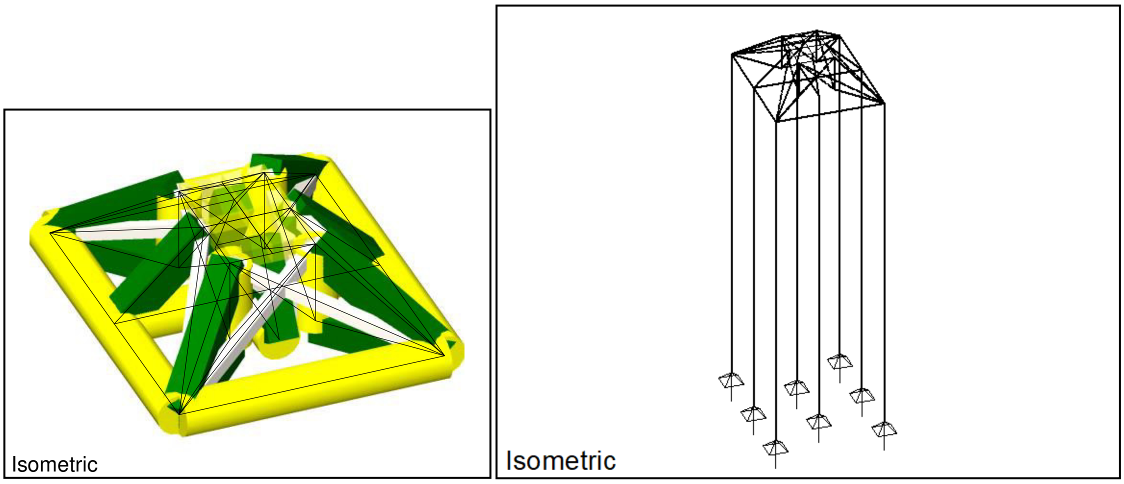

Fig. 7 - 3D rendering of the STM pile cap model with eight piles (left full rendering shown without piles present in the model)

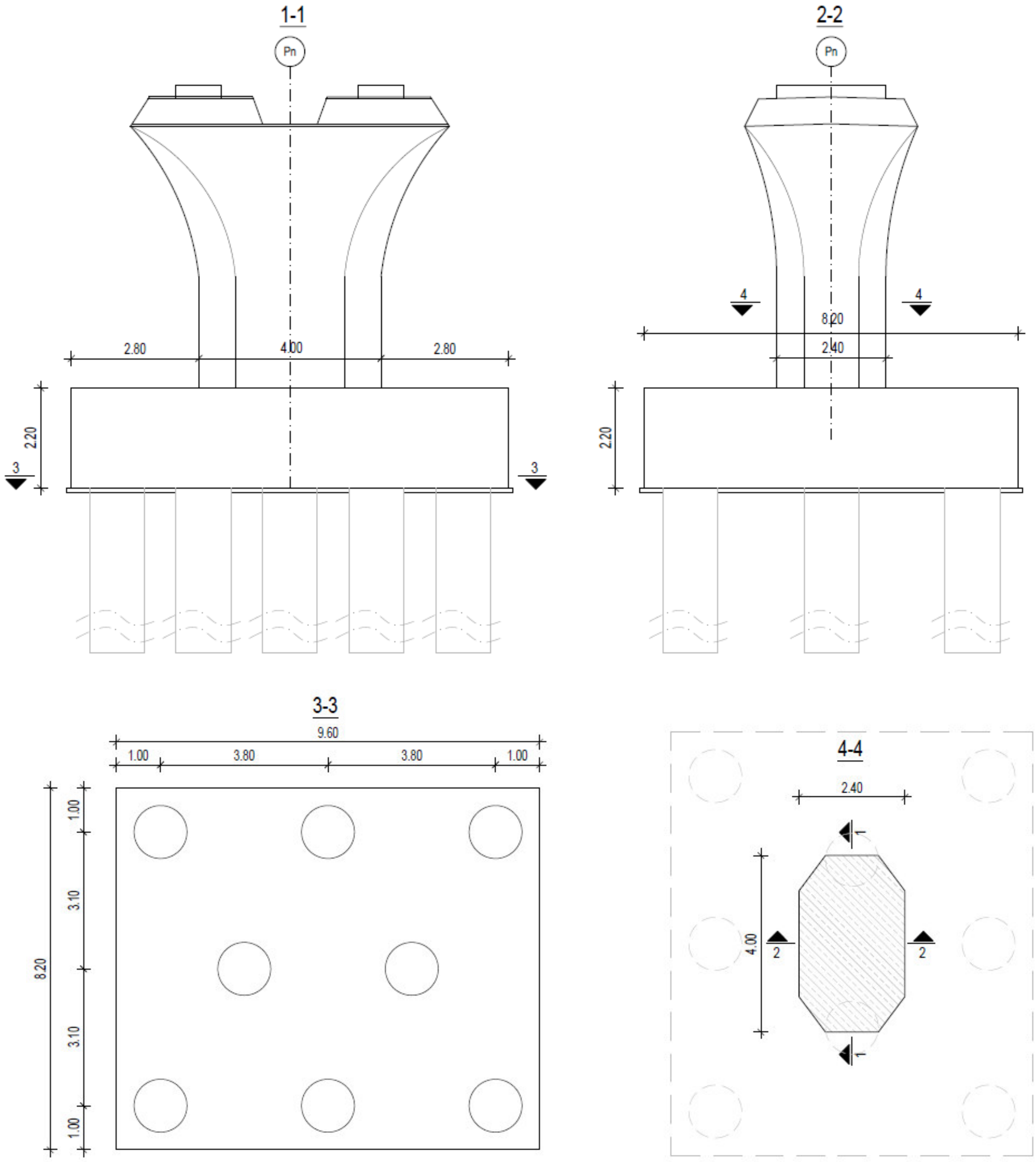

Fig. 8 – Pile cap at bridge at Novi Sad - Subotica - State border high-speed railway in Serbia (viaduct at km 117+155, near Vrbas)

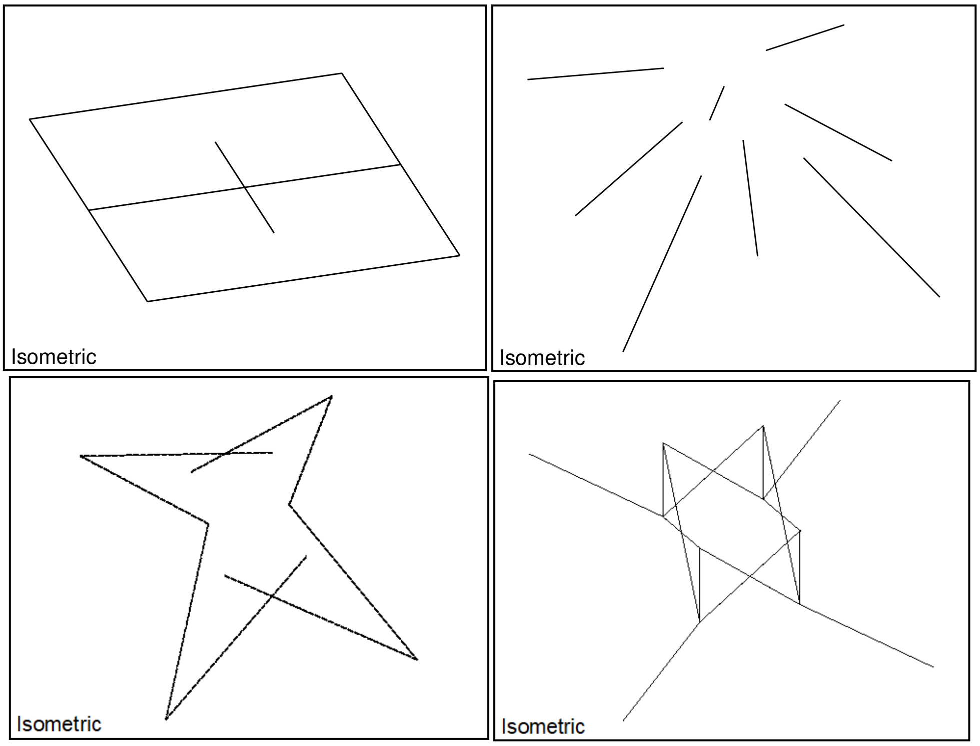

Fig. 9 - Upper left: ties (reinforcement) at strip above the piles; upper right: main concrete struts; lower left: concrete diagonals; lower right: the "inner core"

7. CONCLUSION

A standardized procedure for constructing the STM model for each application (pile cap in this case) is needed, for its safe and fast application in practice. A practical methodology for creating pile cap, usually encountered in practice, with large number of piles and with complex, but realistic loading is presented. The method is illustrated for the cases with six piles and eight piles from the actual bridge structures, where the method was applied in practice. The main advantage of the model is that the unique model for the specific pile cap is made in a fast and accurate manner, where numerous load combinations can be easily applied with realistic alternating loading (compression and biaxial bending). The method can be used for the design of new bridge structures, as well as for evaluation of the existing bridges. The paper is intended to be a practical guideline to the practicing engineers.

REFERENCES

[1] Rade Hajdin, *Primena teorije plasticnosti u proracunu armiranih i prethodno napregnutih betonskih konstrukcija (in Serbian)*. Naucna Knjiga, 1991.

[2] G. Milutinovic and D. Bobera, "COMPARATIVE ANALYSES OF BRIDGE PIER CAP USING STRUT-AND-TIE AND BEAM MODEL," presented at the MASE 2023, Skopje, Macedonia.

[3] "fib Bulletin 100: Design and assessment with strut-and-tie models and stress fields: from simple calculations to detailed numerical analysis," 2021.

[4] C. Williams, D. Deschenes, and O. Bayrak, "Strut-and-Tie Model Design Examples for Bridges: Final Report," FHWA / Texas DOT, 2012.

[5] J. Schlaich, K. Schafer, and M. Jennewein, "Toward a Consistent Design of Structural Concrete," *PCI Journal*, vol. 32, no. 3, pp. 74–150, May 1987, doi: 10.15554/pcij.05011987.74.150.

[6] Y. M. Yun, H.-S. Chae, and J. A. Ramirez, "A Three-Dimensional Strut-and-Tie Model for a Four-Pile Reinforced Concrete Cap," *Journal of Advanced Concrete Technology*, vol. 17, no. 7, pp. 365–380, Jul. 2019, doi: 10.3151/jact.17.365.

[7] R. Souza, D. Kuchma, J. Park, and T. Bittencourt, “Adaptable Strut-and-Tie Model for Design and Verification of Four-Pile Caps,” *ACI Structural Journal*, vol. 106, no. 2, 2009, doi: 10.14359/56352.

[8] W. Cavers and G. A. Fenton, “An evaluation of pile cap design methods in accordance with the Canadian design standard,” *Canadian Journal of Civil Engineering*, vol. 31, no. 1, pp. 109–119, Jan. 2004, doi: 10.1139/l03-075.

[9] J. M. de Araújo, “Design of Rigid Pile Caps through an Iterative Strut-and-Tie Model,” *Journal of Advanced Concrete Technology*, vol. 14, no. 8, pp. 397–407, Aug. 2016, doi: 10.3151/jact.14.397.

[10] S. Ahmad, A. Shah, and S. Zaman, “Evaluation of the shear strength of four pile cap using strut and tie model (STM),” *Journal of the Chinese Institute of Engineers*, vol. 32, no. 2, pp. 243–249, Mar. 2009, doi: 10.1080/02533839.2009.9671501.

[11] J. Park, D. Kuchma, and R. Souza, “Strength predictions of pile caps by a strut-and-tie model approach,” *Canadian Journal of Civil Engineering*, vol. 35, no. 12, pp. 1399–1413, Dec. 2008, doi: 10.1139/L08-062.

[12] R. Folić, B. Folić, and I. M. Miličić, “STRUT – AND – TIE MODEL FOR ANALYSIS OF PILES CAP,” *Contemporary achievements in civil engineering 20. April 2018. Subotica, SERBIA*, vol. 34, pp. 33–40, 2018, doi: 10.14415/konferencijaGFS2018.002.

[13] L.-J. Leu, C.-W. Huang, C.-S. Chen, and Y.-P. Liao, “Strut-and-Tie Design Methodology for Three-Dimensional Reinforced Concrete Structures,” *ASCE Journal of Structural Engineering*, vol. 132, no. 6, pp. 929–938, Jun. 2006, doi: 10.1061/(ASCE)0733-9445(2006)132:6(929).

[14] P. Adebar, D. Kuchma, and M. Collins, “Strut-and-tie models for the design of pile caps: An experimental study,” *ACI Structural Journal*, Feb. 1990.

[15] S. Dey and M. M. Karthik, “Modelling four-pile cap behaviour using three-dimensional compatibility strut-and-tie method,” *Engineering Structures*, vol. 198, p. 109499, Nov. 2019, doi: 10.1016/j.engstruct.2019.109499.

[16] M. Przulj, *Mostovi (in Serbian)*. Izgradnja, 2014.

[17] G. Milutinovic, R. Hajdin, and D. Bobera, “Differences in bridge engineering between the U.S.A. and Serbia,” in *DGKS*, Arandjelovac, Serbia: DGKS, 2022.

DAMAGE OF MASONRY INFILLED RC STRUCTURES IN FEBRUARY 2023 EARTHQUAKES SEQUENCE IN TURKEY. DECOUPLED INFILL AS A SOLUTION FOR BETTER BEHAVIOUR

Marko Marinković[1], Christoph Butenweg[2]

Summary:

The predominant form of damage observed during the February 2023 earthquakes in Turkey was the extensive failure of infill walls. This paper offers an insight into the repercussions of these earthquakes on infills, as well as their consequences for both the building inventory and the inhabitants. The unsatisfactory performance and significant destruction resulting from the interaction between flexible frames and rigid infill walls underscored the conceptual inadequacy of traditional infill systems (with mortar connections between frames and infills) in seismically active regions. Consequently, this paper proposes the isolation of infill walls as a viable solution to mitigate such devastating effects. This isolation system aims to offer designers, construction companies, and workers a functional and easily applicable solution. Full-scale experimental tests on isolated infilled RC frame specimens are presented, affirming the efficacy of the isolation system for infills with windows, doors, and full walls.

Key words: In-plane, out-of-plane, seismic loading, decoupling, RC frames

[1] Ass. Prof., Chair of Engineering Mechanics and Theory of Structures, Faculty of Civil Engineering, University of Belgrade, Belgrade, Serbia, mmarinkovic@grf.bg.ac.rs
[2] Full Prof., Center for Wind and Earthquake Engineering, RWTH Aachen University, Aachen, Germany, butenweg@lbb.rwth-aachen.de

1. INTRODUCTION

On the morning of Monday, February 6, 2023, at 4:17 AM, a powerful earthquake measuring 7.7 on the Richter scale struck the central region of Turkey and the northwest part of Syria. The epicenter of this seismic event was located in close proximity to the town of Pazarcik, with its hypocenter situated at a depth of 8.6 kilometers beneath the Earth's surface. Later that same day, around 1:24 PM, another significant earthquake with a magnitude of 7.5 occurred, originating from a depth of 7.0 kilometers. The epicenter of this second quake was situated near the town of Elbistan, approximately 95 kilometers north-northwest of the epicenter of the initial earthquake. These devastating tremors were followed by an extensive series of aftershocks, numbering over 18,000 as of June 2023. Among these aftershocks, three were of magnitude greater than 6.0, and more than twenty others registered magnitudes exceeding 5.0. These subsequent seismic events exacerbated the destruction, leading to further damage and, in some instances, the collapse of structures already weakened by the earlier shocks.

In the immediate aftermath of the earthquakes, the Turkish Disaster and Emergency Management Authority (AFAD) launched an assessment campaign to evaluate the extent of building damage. This initiative involved the participation of over 7,000 engineers and architects from across the country [1]. A staggering total of 230,000 buildings sustained significant damage or collapsed entirely, necessitating the construction of new edifices. An additional 40,000 structures experienced moderate damage, while around 430,000 buildings exhibited minor damage [2]. Numerous settlements, including the historically significant city of Antioch (Antakya), suffered near-total devastation. As anticipated, the residential sector bore the brunt of the losses, accounting for approximately 53% of the overall damage. Non-residential buildings accounted for 28% of the losses, while the remaining 19% was attributed to damage incurred by essential infrastructure [1].

This article provides a concise overview of the outcomes derived from the collaborative reconnaissance investigation conducted by members of the Serbian Association for Earthquake Engineering (SUZI-SAEE) and ETH Zurich. In response to the destructive earthquakes that struck Turkey, the SUZI team undertook a comprehensive field study encompassing 16 urban centers, numerous villages surrounding major cities, industrial complexes, hospitals, educational establishments, bridges, and water towers. The primary objective of this reconnaissance mission was to meticulously record the repercussions of the seismic activity on various construction assets and critical infrastructure. Additionally, the study aimed to outline the strategies and initiatives formulated for the rehabilitation and revitalization of the southern regions of Turkey that were profoundly impacted by the earthquakes.

The paper presents key observations concerning the seismic performance of reinforced concrete (RC) buildings during the February 2023 earthquakes. The primary focus lies on masonry infill walls, which emerged as the predominant type of damage during this seismic event, a recurring pattern evident in numerous prior earthquakes [3-5]. Given the persistent and widespread failure of infill walls during medium to strong earthquakes, the authors dedicated several years of research towards devising a solution capable of enhancing the behavior of these vulnerable components. Through an extensive process of iterative refinement involving comprehensive experimental campaigns and sophisticated numerical simulations, the authors developed an innovative system for isolating/decoupling infill walls from the surrounding structural framework. The resulting system represents a practical and effective approach that addresses the challenges posed by infill walls. The details of this decoupling system are presented within the paper, providing valuable insights for the earthquake engineering community. This system introduces a potential breakthrough for improving infill wall performance, offering promising avenues for significant advancements in the field.

2. DAMAGE OF RC STRUCTURES WITH INFILL WALLS DURING THE FEBRUARY 2023 EARTHQAUKES IN TURKEY

This study delves into the examination of masonry infill damage, which emerged as the predominant and main type of destruction. A more intricate exposition of the earthquake's impacts was unveiled during a seminar held on May 29, 2023 [6]. During this seminar, the team presented the findings from the site visits within the earthquake's epicentral zone. Of notable significance, the most profound structural deterioration manifested in reinforced concrete (RC) frame structures with masonry infill. Widespread damage to masonry infills was spanning in all regions affected by the earthquake. Interestingly, examples of infill damage were also observed within buildings incorporating a dual system, characterized by RC frames coupled with walls. From the team's observations it can be concluded that the main reason for such a huge damage was interaction of RC frame structures with masonry infill. The connection between infill and frame emerged as a crucial point, having an obvious influence on the out-of-plane (OOP) infill collapse. Illustrated in Fig. 1 shows substantial infill damage, notably manifesting as out-of-plane collapse, documented across a substantial number of residential structures.

Fig. 1 Damage and OOP collapse of infills in RC buildings

Fig. 2 Soft story collapse of buildings

A predominant portion of the damaged residential buildings were RC frame structures, with a substantial number of these constructions having been erected within the last two decades. The prevalent patterns of damage can be categorized as follows: buckling and/or rupture of longitudinal reinforcement; shear failure of RC columns, beams, and walls; soft-story; and structural overturning. Specifically, the occurrence of soft-story was observed, frequently arising in scenarios involving an open ground floor coupled with masonry infill present in the upper stories (Fig. 2). In several instances, the ground floor served as a garage area, while in certain cases (Fig. 2b), the topmost floor was added subsequently, as per info provided by local residents.

Examples of the “short column” effect (Fig. 3), resulting from the interaction of columns with partially infilled masonry panel, have also been observed. In this case, the interaction between the masonry infill and the RC column, along with constrained deformations of the column throughout its height, led to an increase in shear force in the "free" portion of the column. Shear cracks developed, despite the presence of 15 cm spaced and 135-degree hooked ties.

Fig. 3 “Short column” effect due to partial height infill/frame interaction

Fig. 4 Damage and collapse of infills in a hospital in Iskenderun, due to use of foam for infill/frame connection

Cases of deficient performance in non-structural components, notably infill walls and brick façade walls within RC frame structures, have been observed. These elements exhibited poor behaviour during the earthquake event. The seismic forces subjected infill walls to both in-plane and out-of-plane loading, culminating in a notable decrease in the load-bearing capability of the infill under out-of-plane forces. One of the causes of the damage was use of polyurethane foam for connection top of the infill to the frame (Fig. 4). It is imperative to highlight that this method of connecting infill to the surrounding RC structure has gained considerable popularity and adoption across numerous construction sites. However, it is obvious that polyurethane foam fails to provide a robust and enduring connection between the wall and the structure. Consequently, any perpendicular acceleration experienced by the wall can lead to the collapse of the infill in out-of-plane.

The visit to Antioch (Antakya) left the strongest impression mark on the team members, as they were confronted with a scene of absolute devastation and catastrophe. In March 2023, an intense effort was underway to clear and demolish nearly all structures that had borne the effect of the earthquake's impact. The ruins of many collapsed residential buildings were predominantly of RC structures. However, a notable number of older family houses constructed from stone masonry also suffered substantial damage or complete collapse. RC buildings featuring frames and/or a dual system were also vulnerable, with their masonry infill sustaining notable damage. In numerous instances, these infills damaged and collapsed in OOP on the lower levels (Fig. 5). The mechanism behind this phenomenon is rooted in the combined influence of in-plane (IP) and out-of-plane (OOP) loading on the infill walls. As the RC structure deflects, the IP load is transferred to the infills as a result of interstory drift-induced displacement. Simultaneously, the acceleration experienced by each floor generates inertia forces perpendicular to the wall surfaces (OOP load). The greatest interstory drift occurs in the lower stories, thus precipitating IP damage to infill walls or causing the detachment of infills from the adjoining RC elements. These infill walls are particularly vulnerable to OOP forces. Moreover, infills that have become detached and lack connection (contact) with the RC frame are even more vulnerable to OOP loads. The magnitude of these forces need not be substantial to prompt the collapse of infills in out-of-plane.

Fig. 5 Damage and collapse of infill walls on the lower stories

In March 2023, the SUZI team talked with locals about rebuilding villages and towns hit by the earthquake. Funding and lack of knowledge on reconstruction methods were key issues, particularly in rural areas. Urban zones used tunnel formwork for fast RC building construction, though this might not fully protect masonry infill from damage. Fear persists months after the quake, with many still in tents despite their buildings being structurally safe (but with widespread infill damage). People are hesitant to return to buildings with infill damage due to traumatic memories of the earthquake. This has led to decisions to demolish structures with perceived severe infill damage.

This chapter briefly compresses the multitude of factors that have pushed the efforts of numerous researchers and practicing engineers to confront the challenge of mitigating masonry infill damage during seismic events. Although the study of this subject spans several decades, the pressing urgency to address it has escalated, underscoring the imperative need to find effective solutions that can stop similar catastrophes in times to come.

3. ISOLATION OF INFILLS AS A SOLUTION

Considerable efforts have been dedicated to investigating the behavior of infilled RC frames, both through experiments and numerical analysis, with the objective of finding the solution. Within a range of proposed enhancements, the most promising strategy involves the isolation of infill walls. This approach facilitates the separation of non-structural elements from the frames, enabling deformation while postponing the engagement of infill elements. Although the creation of gaps between infills and frames achieves a fundamental in-plane separation, supplementary connections are essential to out-of-plane capacity. This method provides design benefits by introducing minimal deviations from current practices and has gained notable traction in recent times. While the efficacy of these decoupling techniques in augmenting seismic performance is undeniable, their practical implementation remains constrained by economic factors, including the expenses associated with materials and the installation of integrated components. Nevertheless, the viability of this approach endures, necessitating continued actions for the advancement of solutions. Consequently, revised guidelines pertaining to masonry infill walls should prioritize improved seismic performance and incorporate provisions for decoupling infill panels from the adjacent RC frames as a feasible solution.

These conditions have encouraged investigations and the creation of solutions to decrease unfavorable interactions between masonry infill walls and concrete structures. Alongside experimental tests and enhancements in the design of traditional infills, novel approaches have been under exploration. This article introduces a system consistent with this goal, seeking to establish a pragmatic construction technique that tackles these challenges. The objective is to provide engineers with a straightforward method that doesn't necessitate intricate numerical models.

3.1. DESCRIPTION OF INFILL ISOLATION SYSTEM

Currently, no economically viable masonry infill systems fulfill a diverse group of requirements. This study was undertaken to develop a seismic safety solution for infills. The intended system had to guarantee seismic resistance across varying loads, enable practical on-site installation, accommodate different types of bricks, and prove cost-effective. In response to these criteria, a decoupling methodology was chosen, building upon prior research by Marinković and Butenweg [7]. This approach involves the incorporation of recycled rubber material between the RC frame and the infill, aimed at preventing brittle behavior. By doing so, the initiation of infill engagement is delayed until higher levels of drift are reached, thus preventing stress within both the RC frame and the infill. The rubber strips take on the drift of the RC frame without inflicting damage on the infill, thereby mitigating potential harm during seismic events. By adjusting the stiffness and thickness of the rubber material, the system can be designed to accommodate different seismic loads. Moreover, the viscoelastic characteristics of the rubber joints contribute to an increased damping capacity for the building.

This innovative solution uses recycled rubber material, providing an economically efficient approach that can be flexibly adapted to various brick types and seamlessly integrated into on-site construction practices. The decoupling system contains of three recycled rubber strips: central strip that is fixed with mortar to the RC frame, and outer strips mortared to the masonry bricks (Fig. 6). Thicker strips with lower stiffness positioned between the infill and columns are intended absorbing in-plane frame deformations, thereby delaying the initiation of infill activation. Conversely, thinner strips with higher stiffness positioned at the top and bottom serve to maintain out-of-plane stability, constraining displacements until infill arching is activated. This design approach enables substantial in-plane drifts and simultaneous management of significant out-of-plane forces.

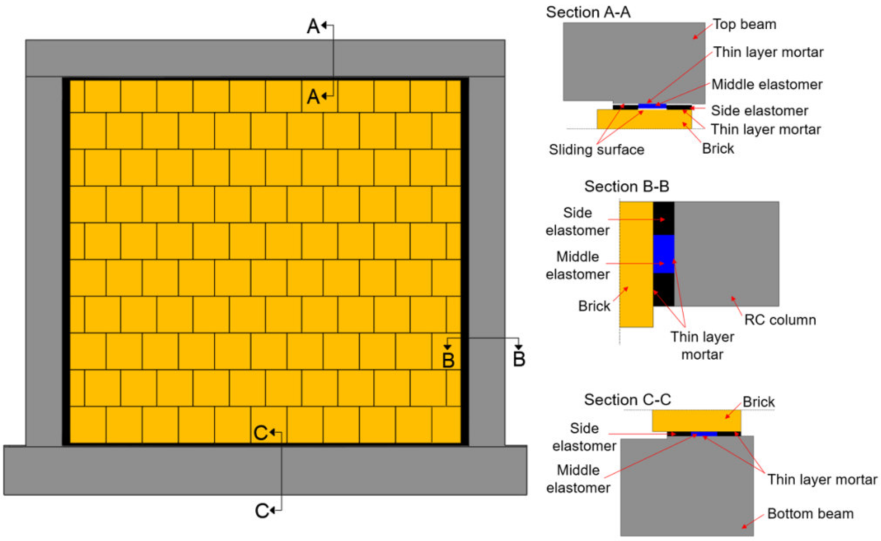

Fig. 6 Details of the infill isolation/decoupling system

The system's capacity for adaptability is truly noteworthy. Through the choice of rubber thickness and stiffness between columns and infills, based on the desired interstorey drift, effective safeguarding against in-plane damage for masonry infills can be easily accomplished. Importantly, this concept smoothly translates to infills featuring openings, avoiding any additional interventions. This breakthrough has the potential to fundamentally transform the seismic performance of masonry infills, increasing their capacity and stability, all the while simplifying the construction process.

3.2. TESTING CAMPAIGN

An experimental campaign involving a total of 18 specimens was executed. The tests were carried out on full scale RC frames with decoupled infills, systematically inspecting their behavior under distinct in-plane and out-of-plane loads, both individually and in combination. The investigation encompassed both complete infill walls and those featuring windows and doors. A comparative analysis was undertaken, using the outcomes of nine tests conducted on RC frames employing the decoupling system (D1-D9) with an equivalent number of tests performed on traditionally infilled frames (T1-T9). These tests and their details are extensively elaborated in Milijaš et al. [8]. The principal difference lies in the utilization of the decoupling system in D1-D9, while preserving same infill configurations and load application protocols. This allows a direct and comparison between the performance of traditional and decoupled infill walls. This paper primarily focuses on presenting the results derived from simultaneous in-plane and out-of-plane tests (T3, D3, T6, D6, T9, D9).
The experimental setup in Fig. 7 enables application of different loading conditions to the test specimen, such as pure in-plane, out-of-plane, as well as combined loading scenarios. Vertical forces were applied through the utilization of hydraulic presses, positioned on the columns of the reinforced concrete (RC) frame. The transmission of tension forces for vertical loads was facilitated by means of crossbeams and steel rods. For the purpose of cyclic in-plane loading, servo hydraulic actuators (with a cumulative capacity of 500 kN) were fixed to a reaction wall and the upper beam of the RC frame. The application of displacements was enabled by horizontal steel tie rods. Out-of-plane loading was executed employing four airbags, positioned between the infill wall and a rear reaction wall constructed from timber, thereby inducing outward pressure on the

wall. The reaction wall for out-of-plane loading was linked to the RC frame beams via four threaded rods, each of which was equipped with load cells capable of measuring forces up to 500 kN. Anchors situated at the end of the strong-floor (Fig. 7) served to stabilize the RC frames, having been preloaded with 400 kN. The prevention of slippage between the RC frame and the strong-floor was ensured through the utilization of steel supports and wedges situated on both sides.

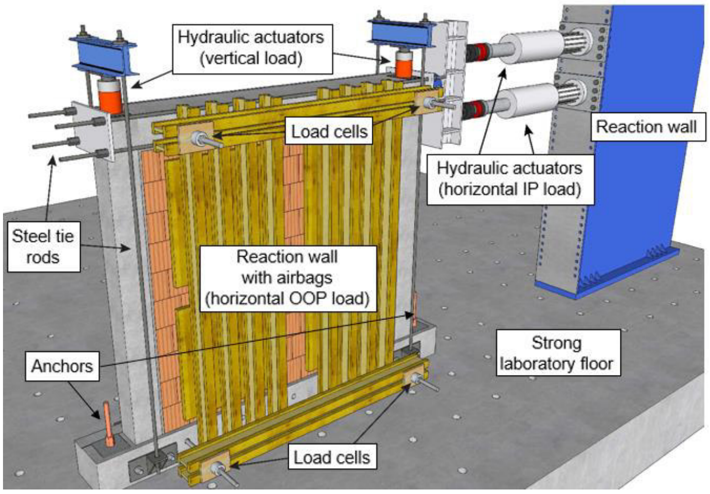

Fig. 7 Test setup [8]

To ensure a direct and meaningful comparison of experimental results, both the RC frames with traditional infills and those with decoupled infills were configured with identical frame and infill geometries. The construction of the RC frame entailed the utilization of concrete with a strength classification of C30/37, coupled with ductile B500B reinforcing steel. Columns were designed in the form of 25/25 cm squares, while the beams featured rectangular cross-sections measuring 25/45 cm. Details about the distribution of reinforcement and material characteristics for bricks, mortar, and masonry can be seen in Milijaš et al. [8].

The masonry infills were constructed employing Thermoplan SX10 clay bricks, that have slender vertical voids. These bricks are contemporary, highly thermally-insulating units, characterized by significant thickness (30cm). The use of these bricks was followed with the use of Maxit 900D thin layer mortar, only applied to the bed joints. The assembly of head joints was achieved using dry tongue and groove connections.

Fig. 8-10 show comparison of hysteretic curves of RC frames with traditional and decoupled infills, for each infill configuration. The hysteretic curves of RC frames with traditional infills are characterized by a high initial stiffnesses and pinching effect. Maximum force in full traditional infill of test T3 is 195 kN at 0.64 % of in-plane drift and the test is stopped due to the substantial damage at 1.4 % of in-plane drift (Fig. 8). On contrary, at 1.4% of in-plane drift, force in the decoupled infill is only 35.8 kN in test D3 (Fig. 8). In test T6, maximum contribution force of 125.8 kN is reached at 0.8 %, whereas in test D6 contribution force is only 16.7 kN (Fig. 9). The decoupled infills with door openings in test D9 remain completely isolated from the RC frame with negligible contribution forces, which are measured only after 2.0 % of in-plane drift (Fig. 10). On the other side, traditional infill with door opening experiences complete collapse at at 1.0 % of in-plane drift due to the adverse effect of combined in-plane and out-of-plane loads (Fig. 10).

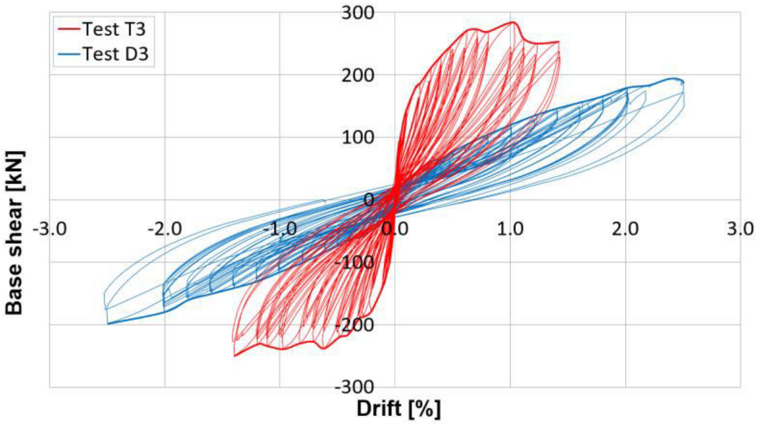

Fig. 8 Experimental results on traditional (T) and isolated/decoupled (D) for full infills

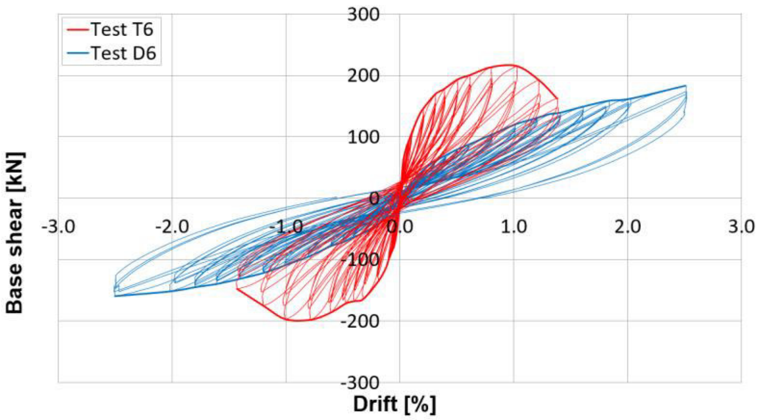

Fig. 9 Experimental results on traditional (T) and isolated/decoupled (D) infills with windows

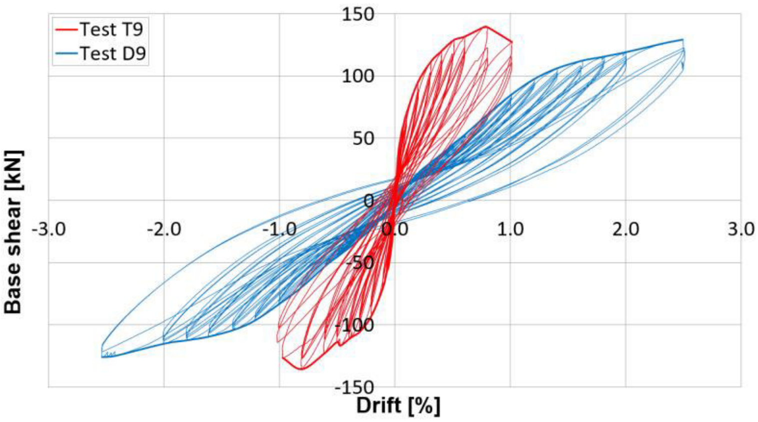

Fig. 10 Experimental results on traditional (T) and isolated/decoupled (D) infills with doors

Fig. 11 shows comparison of the envelope curves of the experimental tests carried out on traditional and decoupled infills, and bare frame (Test A). It can be seen that traditional specimens activate high IP forces quite quick and thus get damaged at very low drifts. On contrary, decoupled infills have almost the same force activation until 1% of drift, but also afterwards at higher drifts difference between bare frame and decoupled infills base shear force is not big. This is a strong argument for the use of isolated infills since they allow design of RC structures with infills without modelling infill walls, which is not the case with traditional infills. In that sense only assignment of the design engineer is to choose appropriate thickness of the rubber of the INODIS RP system.

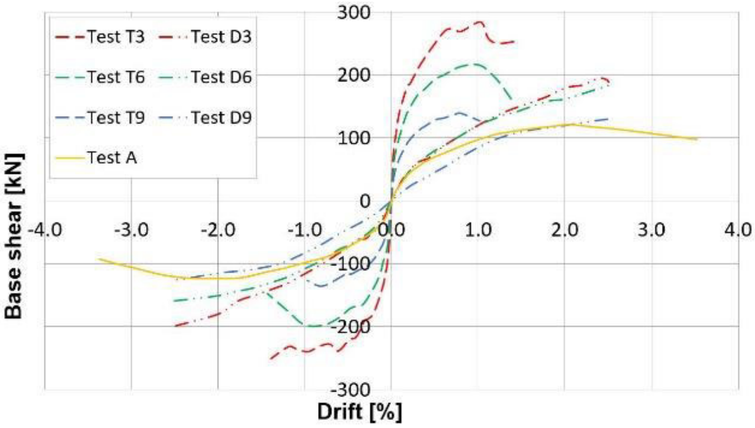

Fig. 11 Envelope curves for tests on traditional (T) and isolated/decoupled (D) infills

4. SUMMARY

The paper investigates the catastrophic aftermath of the earthquakes that struck Turkey in February 2023. The primary focus of the paper is directed towards the masonry infill walls, which emerged as the predominant source of damage during these seismic events. The paper highlights the unfavorable performance of infill walls, drawing upon data obtained from extensive field observations conducted during a reconnaissance mission. The research presents an inadequate behavior exhibited by infills. This is backed with the data collected from the field. The paper systematically shows representative cases of the characteristic modes of failure. These illustrative examples serve to summarize the extent of damage on infills. By taking into account the on-site investigations, the paper points out the profound impact of earthquakes on RC structures with infill walls. The cumulative effect of the evidences from the filed pushes the search for a solution directed at addressing the vulnerabilities characteristic for infill walls. This pressure is emphasized by the economic losses incurred, the considerable hindrance posed to the recovery process, and the critical jeopardy posed to human lives due to the vulnerability of these walls to damage and subsequent collapse during seismic events.

This paper introduces an isolation system as a promising solution for the challenges posed by infill walls, explaining its qualities through a methodically conducted experimental campaign. The findings derived from these tests emphasize a essential distinction: the initial in-plane stiffness exhibited by decoupled masonry infills, regardless of whether they possess centrally positioned openings or not, remains nearly indistinguishable from the initial in-plane stiffness of the bare frame. This stands in contrast to traditional infills, where all configurations induce a significant increase in the in-plane initial stiffness. Consequently, the decoupling system shows a distinct advantage by having both the lateral stiffness of the bare frame and thus keeping the dynamic characteristics in the same range of the RC structure itself. This fact sets it apart from traditional infills, wherein modifications to dynamic characteristics become evident upon implementation.

The comparative analysis of experimental findings between traditional and decoupled infills serves to underline the pronounced benefits offered by the decoupling system, thereby constituting the central outcome of the experimental investigations. Traditional infills exhibit cracking at remarkably low levels of in-plane drift. Maximum in-plane loads for RC frames with traditional infills are reached within a drift range of 0.8% to 1.0%, corresponding to states of considerable damage in the masonry infills. In sharp contrast, the tests conducted on RC frames endowed with decoupled infills attain peak in-plane loads at significantly higher drift values, spanning from 2.8% to 3.25%. This important difference is attributed to the delayed activation of the infills in the decoupled system. Furthermore, the observed damage in decoupled infills, at the state of significant damage limit conditions, becomes perceptible only around the 3.0% of in-plane drift for both solid infills and infills with windows. Remarkably, the configuration with a central, full-height door opening remains entirely unharmed. It is important to point out that isolated infills incorporated with the INODIS RP system demonstrate a remarkable capacity to withstand substantial out-of-plane loads even under very high levels of in-plane drift. These findings serve as a foundational basis upon which a design concept, readily applicable within the daily routine of engineering practice, can be derived. These results offer a practical framework for enhancing the seismic resilience of RC structures having infill walls.

In combination with the ongoing construction of tunnel form buildings in Turkey, the construction of RC frame structures is anticipated to persist, primarily owing to a multitude of advantages encompassing rapid and efficient construction, adaptability to meet architectural specifications etc. In light of this, addressing the challenge of masonry infill failure during seismic events becomes imperative. Many of the issues identified in both recent and prior earthquakes can be mitigated by the application of the INODIS RP infill isolation system. The fundamental objective of this study is to offer valuable insights to designers, contractors, and investors involved in the construction of buildings incorporating masonry infills. This paper effectively bridges the gap in construction practices by introducing an isolation/decoupling system developed for infills, signifying a decisive step towards improving the performance of masonry infills.

ACKNOWLEDGEMENT

The authors are grateful to the Serbian Association for Earthquake Engineering (SUZI-SAEE) and ETH Zurich for the initiative and financial support which enabled the visit to earthquake-affected areas of Turkey and gain valuable experience regarding the building damage and other consequences. The team members are grateful for the cooperation during and after the visit to the ACI-133 and following colleagues: Prof. Polat Gulkan, Prof. Ayhan Irfanoglu, Prof. Alper Ilki, Prof. Murat Altuğ Erberik, Dr. Kurtuluş Atasever, Gözde Özgün, Dr. Recep Cakir, Prof. Orhan Tatar, Filiz Tuba Kadirioğlu, Prof. Svetlana Brzev, Nursen Büyükasik, Fuat Büyükaşık, Murat Akpinar, Dr. Şerife Özata, Dr. Zeynep Ünsal Aslan. The assistance of these colleagues, their knowledge and experience, were critical for the success of the reconnaissance visit.

Part of the work on connection tests was done during the STSM of COST Action CA18120 (CERTBOND – https://certbond.eu/), supported by COST (European Cooperation in Science and Technology).

REFERENCES

[1] World Bank (2023). Global Rapid Post-Disaster Damage Estimation (GRADE) Report, February 6, 2023 Kahramanmaraş Earthquakes, Türkiye Report. Global Facility for Disaster Reduction and Recovery (GFDRR). https://documents1.worldbank.org/curated/en/099022723021250141/pdf/P1788430aeb62f08009b2302bd4074030fb.pdf

[2] SBB (2023). 2023 Kahramanmaraş and Hatay earthquakes report. Presidency of Strategy and Budget, Government of Türkiye. https://www.sbb.gov.tr/wp-content/uploads/2023/03/2023-Kahramanmaras-and-Hatay-Earthquakes-Report.pdf

[3] Braga, F., Manfredi, V., Masi, A., Salvatori, A., & Vona, M. (2011). Performance of non-structural elements in RC buildings during the L'Aquila, 2009 earthquake. Bulletin of Earthquake Engineering, 9(1), 307-324.

[4] Brzev, S., Pandey, B., Maharjan, D. K., & Ventura, C. (2017). Seismic vulnerability assessment of low-rise reinforced concrete buildings affected by the 2015 Gorkha, Nepal, earthquake. Earthquake Spectra, 33(1_suppl), 275-298.

[5] Marinković, M., Baballëku, M., Isufi, B., Blagojević, N., Milićević, I., & Brzev, S. (2022). Performance of RC cast-in-place buildings during the November 26, 2019 Albania earthquake. Bull. of Earth. Eng., 1-54.

[6] SUZI&ETH (2023). https://suzi-saee.rs/akcije/online-suzieth-seminar-u-vezi-zemljotresa-u-turskoj

[7] Marinković, M., & Butenweg, C. (2019). Innovative decoupling system for the seismic protection of masonry infill walls in reinforced concrete frames. Engineering Structures, 197, 109435.

[8] Milijaš, A., Marinković, M., Butenweg, C., Klinkel, S. (2023). Experimental results of reinforced concrete frames with masonry infills with and without openings under combined quasi-static in-plane and out-of-plane seismic loading, Bulletin of Earthquake Engineering (2023). https://doi.org/10.1007/s10518-023-01664-4

COMPOZITE LIGHTWEIGHT PANEL WITH INTEGRATED LOAD-BEARING STRUCTURE

Domagoj Tkalčić[1], Bojan Milovanović[2], Mergim Gaši[3], Marija Jelčić Rukavina[4], Ivana Banjad Pečur[5]

Summary:

The primary objective of this study was to develop a novel method for constructing LSF (Lightweight Steel Frame) structures, leveraging the advantages of prefabricated construction to address labour shortages. The research employed a combination of experimental methods and modelling. Properties of each individual component were determined, forming the basis for the model. Following that, real panels were constructed based on the model, followed by testing for thermal and acoustic properties. The key findings of the research indicate that while challenges related to thermal conductivity in LSF construction persist, potential solutions are presented in this article. The proposed construction method is feasible, although certain limitations warrant attention.

Key words: LSF, hygroscopic properties, acoustic properties, thermal properties, prefabricated construction

[1]Mag. ing. aedif., Faculty of Civil Engineering, University of Zagreb, Croatia, domagoj.tkalcic@grad.unizg.hr
[2] Assoc. prof., Faculty of Civil Engineering, University of Zagreb, Croatia, bojan.milovanovic@grad.unizg.hr
[3] Dr. sc., Faculty of Civil Engineering, University of Zagreb, Croatia, mergim.gasi@grad.unizg.hr
[4] Assoc. prof., Faculty of Civil Engineering, University of Zagreb, Croatia, marija.jelcic.rukavina@grad.unizg.hr
[5] Prof., Faculty of Civil Engineering, University of Zagreb, Croatia, ivana.banjad.pecur@grad.unizg.hr

1. INTRODUCTION

Lightweight steel frame buildings (LSF) have a relatively long history and a well established reputation in the construction industry. Frames are assembled on site, primarily using bolt connections. Once the framework is in place, thermal insulation is installed between the frames, and the structure is enclosed with sheathing panels on both sides of the steel framework [1,2].

In the construction of traditional LSF buildings, challenges arise in terms of quality control, the availability of skilled labour and assembly time. To address these challenges, the composite lightweight panel with integrated load-bearing structure (hereinafter referred as KLIK panel) has been devised. This type of panel comprises a steel structure enclosed by cladding panels, with the interior filled with PUR foam for thermal and acoustic insulation purposes. The entire panel is manufactured in a factory under controlled conditions. Upon completing the steel structure, it is enclosed by cladding panels, which also serve as molds during the injection of the PUR foam. After production, the panel is transported to the construction site, where it is assembled into a unified structure using bolted connections. In its current phase of development, the panel is designed for constructing single-story nZEB buildings.

Based on the idea and preliminary calculation, the draft of KLIK panel was made (Fig. 1, a)). Through comprehensive lab testing of individual components (Tab. 1), and determining their properties at room and high temperatures, as well as diffusive properties, the collective properties of the KLIK panel were determined, allowing for the execution of the panel (Fig. 1, b)). Tests for whole panels acoustic properties, and thermal transmittance coefficient (*U* - value) were conducted.

Tab. 1. Test samples and equipment

Sample		
PUR foam	Firepanel	Gypsum-fiber board
		

Test			
Change of mass as a function of temperature	Specific heat capacity change as a function of temperature	Change of thermal conductivity as a function of temperature	Hygroscopic properties
			

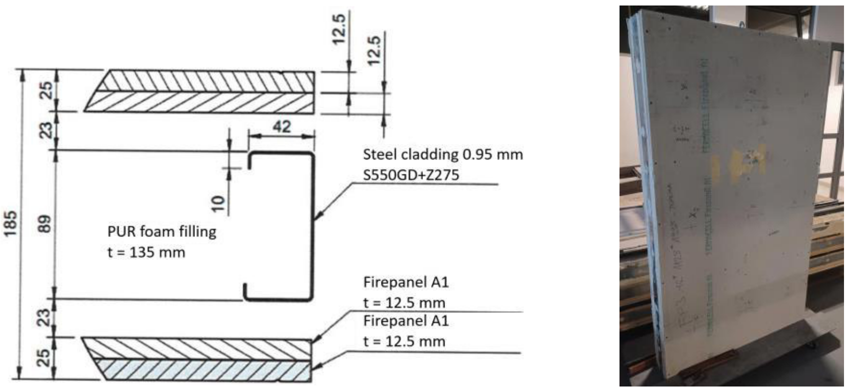

a) b)

Fig. 1. a) KLIK panel draft, b) KLIK panel

In this scientific article, we delve deeper into the advantages and innovations brought forth by LSF panels with integrated load-bearing construction. Through careful examination and empirical evidence, we aim to demonstrate how this transformative construction method stands as a testament to the industry's commitment to progress, offering a brighter and more sustainable future for the built environment.

2. HYGROSCOPIC PROPERTIES

To assess moisture levels within a structure and gain insight into moisture transport processes such as drying or wetting through the observed building material, it is essential to establish sorption curves. These curves illustrate the moisture content that the examined material can retain at specific relative humidity levels in its surrounding environment. The moisture retention capacity of the material is primarily influenced by its inherent structure, including porosity and permeability, as well as the prevailing hygrothermal conditions [3]. In order to simulate the hygroscopic properties of the entire panel, the hygroscopic properties of each component were determined individually. Sample properties are shown in Tab. 2. Changes in the sample's mass over time were monitored. It has been decided to conduct the static gravimetric method using a desiccator and saturated solutions in accordance with the EN ISO 12571:2021 [4] standard.

Tab. 2. Sample properties for hygroscopic testing

Sample label	Material	Nominal density [kg/m^3]	Length [mm]	Width [mm]	Thickness [mm]	Sample number
PUR 40	PUR foam	40	150	150	20	10
PUR 45		45				
PUR 50		50				
PUR 60		60				
GVP 12,5	Gypsum-fiber board	1030	100	90	12,5	6
GVP 15					15	
FP 12,5	Fire panel	1230	70	90	12,5	6
FP 15					15	

The examination of sorption using the static gravimetric method was conducted in two phases. The first phase involved determining the absorption behavior (exposing samples to increasing humidity levels), while the second phase involved determining the desorption behavior (exposing samples to decreasing humidity levels). The selected environmental humidities for these phases were 9, 33, 75, 85, and 93%. Figure 2 display the results of sorption and desorption measurements as the average equilibrium moisture content u [kg/kg] at specific relative humidity levels for 40 kg/m³ density PUR foam. The presented results for the PUR foam represent the mean values obtained from measuring 10 samples.

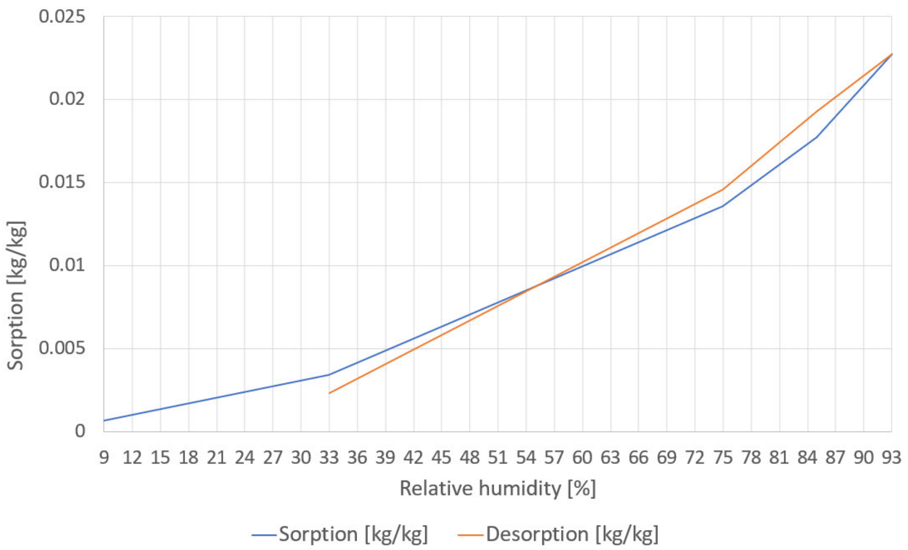

Figure 2. Sorption curves

The hygroscopic properties of each component individually serve as an input parameter in creating a model for the entire panel. This allows for the consideration of multiple factors, including wind-driven rain, all three forms of heat transfer, solar influence, the presence of embedded moisture, and more. Instead of employing the Glasser method, advanced models have been developed [5] to predict moisture transfer through the panel, aiming to capture the intricate interaction among various factors and panel components.

3. ACOUSTIC PROPERTIES

Sound absorption is the process of attenuating sound as it passes through a medium or crosses over a surface. The absorption of materials varies for different frequencies, increasing with frequency for single-layer materials [6].
Sound insulation of partition structures essentially refers to the difference between the transmission and reception levels of sound power between two rooms in a building. Sound power levels can be converted into sound pressure levels depending on the type of room (dominantly free or diffuse field), so sound pressure levels are typically measured and used to calculate partition sound insulation parameters. To standardize measurement results, sound level differences must be adjusted to the acoustics of the receiving room. Therefore, all parameters for expressing sound insulation are normalized with respect to the sound-absorbing properties of the receiving room. During testing, individuals should not be present in the transmitting room to avoid hearing damage [7], [8].
In building acoustics, it is prescribed that sound insulation should be presented in one-third octave bands, within the frequency range from 100 Hz to 3150 Hz. In this case, this range is extended to higher frequencies up to 5000 Hz and lower frequencies down to 50 Hz. Approximate values of sound insulation can also be presented in octaves. Airborne and structure borne sound insulation of partitions can be calculated based on given input parameters (mass per square meter, construction thickness, material type,

additional lining), and the result is specified in the form of a curve called the normalized curve [7].

In this part of the study, three versions of the Klik panel were tested. The manufacturer installed the test samples (Tab. 3) in a test opening which is made in a solid brick wall that devides for the purpose of testing sound insulation. All three panels were installed in the same manner (Figure 3, a)). The panel was placed in the opening, suspended on two guides, allowing it to be supported from below and secured on both sides with screws and a steel flat profile at one point per height.

Tab. 3. Sample properties for acoustic testing

Sample label	Sample thickness [m]	Sample width [m]	Sample height [m]	Dual-sided external cladding	Sample weight [kg]	Filling
S1	0,185	1,13	2,0	2x FP	330	PUR 45 kg/m³
S2	0,185	1,13	2,0	3x FP	465	
S3	0,21	1,13	2,0	2x GVL 1x FP	465	

After installing the sample, a sound signal is emitted into the transmitting room using speakers. On the other side of the wall, there is a receiving room equipped with microphones to record information about the sound signal that has passed through the sample. Using the acquired data, a single-number weighted sound reduction index R_w is calculated according to EN ISO 717-1:2020 [9] and EN ISO 10140-2 [8]. While all three curves share a similar shape (Figure 3, b), c), d)), a more substantial overlap is observed between the curves of samples S2 and S3. The greater contribution to improved sound reduction between sample S1 and samples S2 and S3 is attributed to the change in mass. Samples S2 and S3 have equal mass, resulting in an identical sound reduction index and a more similar curve shape.

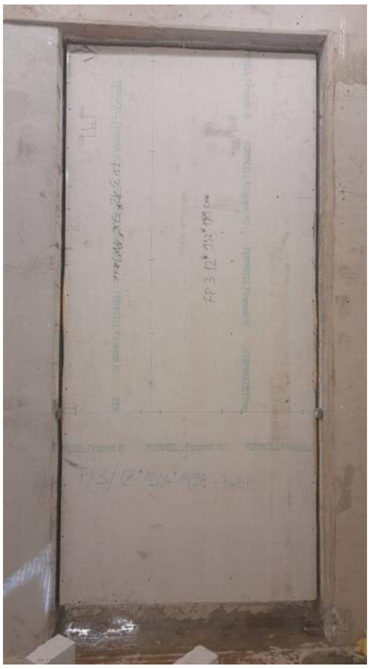

a) Installed sample ready for testing

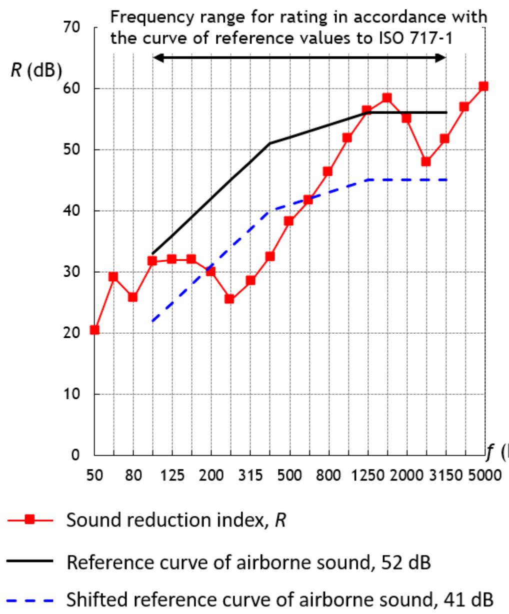

$R_W(C; C_{tr})$ = 41 (-2;-5) dB

b) S1

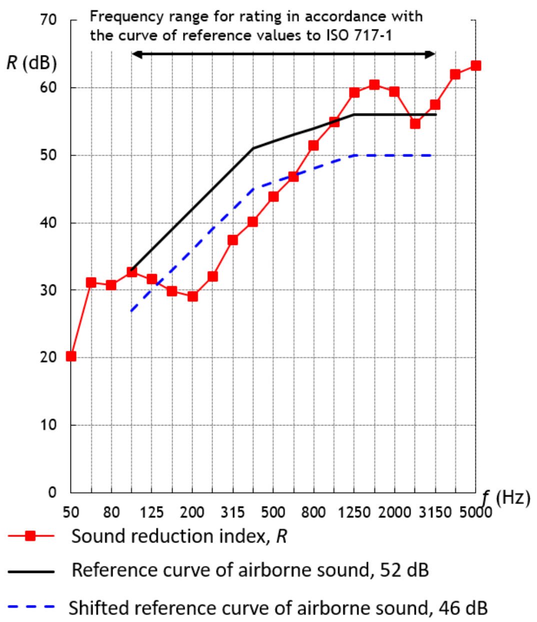

$R_W(C; C_{tr})$ = 46 (-2;-6) dB

c) S2

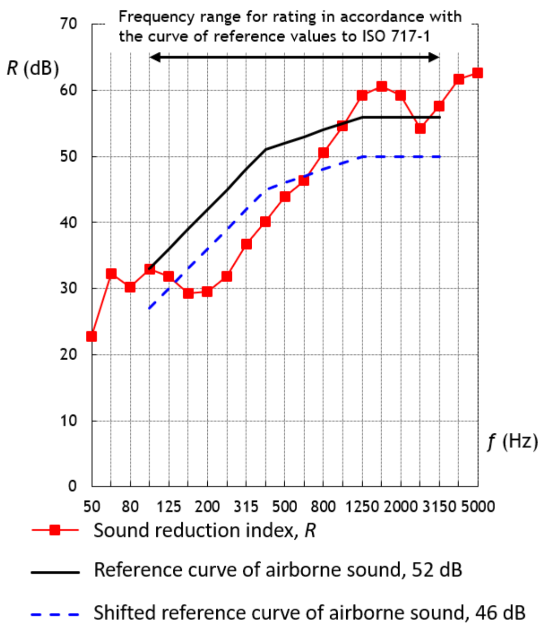

$R_W(C; C_{tr})$ = 46 (-2;-6) dB

d) S3

Figure 3. a) Installed sample, b) Result for sample S1, c) Results sample S2, d) Results for sample S3

4. THERMAL PROPERTIES

To determine the thermal transmittance coefficient (*U* - value) of the KLIK panel, the hot-box testing method was selected. The testing was conducted following the EN ISO 8990 standard [10]. The *U* - value testing chamber consists of hot and cold chambers with the test sample placed in between. To ensure an adiabatic surface, the sample is mounted within a frame made of EPS of the same thickness as the test sample. The panels are freely supported within the chamber frame and sealed around the edges with acrylic putty. All four samples were installed in the same manner.

After installing the sample into the frame, it is placed inside the testing chamber, where thermocouples are attached to it. There are nine thermocouples on both the hot and cold sides of the sample. The hot side of the chamber is heated to 20°C, while the air temperature in the cold chamber is maintained at 0°C. Defined temperatures are sustained for 36 hours to achieve a steady thermal flux through the element, during which air temperature in the chamber, surface temperature of the sample, relative humidity, and air flow velocity in the chamber are recorded.

Heat is transferred to and from the sample through radiation exchange with other surfaces in the hot chamber and through conduction on the surface of the sample. The heat transfer intensity for the first mechanism depends on the average radiation temperature established on the test panel, while for the second mechanism, it depends on the ambient air temperature. The thermal flux through the sample is influenced by both radiation and air temperature on each side of the sample [10].

Tab. 4 displays the characteristics of the samples subjected to testing, along with the results. The testing was conducted on a total of four samples, which differ from each other in terms of diagonal reinforcements, and number of cladding panels.

Tab. 4. Sample properites for testing U - values

Sample label	Sample thickness [m]	Measured U_{eff} [W/m^{2}K]	Diagonal reinforcement	Dual-sided external cladding	Filling
H1	0,185	0,395	With	2x FP	PUR 45 kg/m^3
H2	0,185	0,387	Without	2x FP	
H3	0,21	0,364	With	2x GVL 1x FP	
H4	0,21	0,364	Without	2x GVL 1x FP	

The difference between samples H1 and H2 lies in the diagonal reinforcements. Despite having the same thickness, they exhibit different U - values, attributed to the metal diagonal reinforcements that increase thermal conductivity. Interestingly, the distinction between samples H3 and H4 is also in diagonal reinforcements, however, in this case, there is no disparity in U - values.

The difference in panel thickness between samples H1 and H2, and samples H3 and H4, results from an additional cladding panel, which causes samples H3 and H4 to have lower U - values.

Paper [11] proposes solutions to reduce the U - values of KLIK panels and lower the impact of thermal bridges associated with steel frame and connections to other building components.

5. CONCLUSION

The increasing application of LSF construction, combined with prefabrication, addresses challenges related to the shortage of skilled labour, quality control of executed LFS structures, and the speed of installation. By subjecting each component to detailed testing, the individual performance is optimized, contributing in the creation of complete KLIK panels. These panels were subjected to acoustic and thermal property testing to validate computational models and the interaction of individual components. The various design variations provide flexibility in terms of acoustic and thermal performance. Additional thermal insulation can be applied to these panels to further reduce the panel's U - value, and minimize airtightness of the external envelope.

FUNDING

This research was funded by the European Union through the European Regional Development Fund’s Competitiveness and Cohesion Operational Program, grant number KK.01.1.1.07.0060, project “Composite lightweight panel with integrated load-bearing structure (KLIK-PANEL)”.

ACKNOWLEDGEMENT

The authors extend their gratitude to the companies Tehnoplast profili d.o.o. and Palijan d.o.o. for their assistance with inputs in the construction technology.

REFERENCES

[1] B. Milovanović, M. Bagarić, M. Gaši, N. Vezilić Strmo, “Case Study in Modular Lightweight Steel Frame Construction: Thermal Bridges and Energy Performance Assessment,” *Applied Sciences (Switzerland)*, 12, br. 20, 2022.

[2] M. J. Rukavina, D. Skejić, A. Kralj, T. Ščapec, B. Milovanović, “Development of Lightweight Steel Framed Construction Systems for Nearly-Zero Energy Buildings,” *Buildings*, 12, br. 7, 2022.

[3] M. Bagarić, “Higrotermalno ponašanje ventiliranih teških ovojnica zgrada,” University of Zagreb, Faculty of Civil Engineering, 2020.

[4] The European Committee for Standardization, “EN ISO 12571 2021; Hygrothermal performance of building materials and products - Determination of hygroscopic sorption properties.” The European Committee for Standardization, Brusels, Belgium, 2021.

[5] Fraunhofer Institute for Building Physics, “WUFI-WIKI, Moisture Storage Function.” [Online]. Available: https://www.wufi-wiki.com/mediawiki/index.php/Details:MoistureStorageFunction.

[6] B. Milovanović, “Građevinska fizika - Zaštita od buke - 11. predavanje.” University of Zagreb, Faculty of Civil Engineering, Department of Materials, Zagreb, 2017.

[7] A. A. Petošić, M. Suhanek, “Osnove akustike , buka okoliša i zvučna izolacija te mjere za zaštitu od buke u otvorenom i zatvorenom prostoru,” 2018.

[8] Hrvatski zavod za norme, “HRN EN ISO 10140-2; Acoustics - Laboratory measurement of sound insulation of building elements - Part 2: Measurement of airbourne sound insulation.” Hrvatski zavod za norme.

[9] Hrvatski zavod za norme, “HRN EN ISO 717-1; Acoustics - Rating of sound insulation in buildings and of building elements - Part 1: Airbourne sound insulation.” Hrvatski zavod za norme, 2021.

[10] The European Committee for Standardization, “EN ISO 8990_1998; Thermal insulation - Determination of steady-state thermal transmission properties - Calibrated and guarded hot box.” 1998.

[11] D. Tkalčić, B. Milovanović, M. Gaši, M. J. Rukavina, I. B. Pečur, “Optimization of Thermal Bridges Effect of Composite Lightweight Panels with Integrated Steel Load-Bearing Structure,” pp. 1–24, 2023.

EXPERIMENTAL CAMPAIGN FOR DETERMINATION OF MECHANICAL CHARACTERISTICS OF DOWEL LAMINATED TIMBER

Tomaž Pazlar[1], Martin Hladnik[2], Boris Azinović[3]

Summary:

Dowel Laminated Timber (DLT) might present a sustainable alternative to glued Cross Laminated Timber (CLT). DLT has – in terms of mechanical characteristics – certain limitations if being compared to CLT. However, with the thoughtful design of DLT (number of layers, orientation of layers, position and number of dowels, wood species, boards with tongue / groove, etc.) the mechanical behaviour of elements can be significantly improved. Paper presents an experimental campaign for determination of mechanical characteristics of DLT. Presented research focused on in-plane shear tests (including cyclic testing) and on buckling tests of DLT wall elements with main goal to develop slim but robust products.

Key words: Dowel Laminated Timber (DLT), Cross Laminated Timber (CLT), in-plane shear tests, buckling tests.

[1] Tomaž Pazlar, Ph. D. (Civ. Eng.), ZAG, Ljubljana, Slovenia, tomaz.pazlar@zag.si
[2] Martin Hladnik, BSc. (Mech. Eng.), iQwood d.o.o., Mengeš, Slovenia, martin.hladnik@iqwood.si
[3] Boris Azinović, Ph. D. (Civ. Eng.), ZAG, Ljubljana, Slovenia, boris.azinovic@zag.si

1. INTRODUCTION

Dowel Laminated Timber (DLT) structural elements are solid wood elements made from multiple layers of softwood timber species such as spruce, fir and pine. DLT elements may be compared to cross laminated timber, with the difference that the layers are connected mechanically. No glue is used. For the analysed DLT, mainly spruce from the Slovenian Alpine region (Picea abies) is used, which allows DLT elements to be constructed in a visible quality [1]. From the inside the DLT elements can therefore be visible or not, however, on the outside, the DLT should be protected by a water-repellent facade to prevent atmospheric moisture entering the structure and other water damage. Preventing of wetting the structure will ensure that the building may last much longer than its normal life expectancy, which should be at least 50 years.
The DLT wall consists of timber laminations (timber boards) with various thicknesses, which are arranged in layers longitudinally and transversely (90°) or longitudinally and diagonally (+/- 45°). Between the layers, the laminations are connected by wooden dowels made of beech wood. The dowels assure connection between boards and make DLT a suitable structural system for the wall elements of primarily single-family houses and also as multi-apartment buildings, as well as public buildings such as schools, kindergartens, nursing homes and other. The individual layers of timber laminations range in thickness from 22.5 mm to 30 mm, depending on the type and availability of raw timber. The number of layers varies from 3 up to 10. DLT elements can be produced in widths of up to 3.5 m and lengths of up to 16.0 m.
As part of the development and optimisation of production, the shear tests were first carried out on small samples of three and five-layered DLT, which, compared to the previous production, were expected to have better in-plane shear characteristics due to a better dowel arrangement [1]. In addition, the orientation of the central layer (either horizontal or diagonal laminations) also has a major influence on the shear capacity of DLT elements.
A first experimental campaign of full size DLT elements was conducted in 2011 and then in 2021 at the Slovenian National Building and Civil Engineering Institute (ZAG), covering in-plane shear and buckling tests [2] for five different test series varied in number of layers, orientation of the mid layer(s) and dowel arrangement. The experiments have proved the effectiveness of the newly proposed dowel arrangement [3] – [5]. To further optimize the production, experimental investigations of DLT without the use of tongue / grove system was recently performed [6], [7]. In the paper, the experimental campaign from 2023 is presented [6], [7], while the obtained shear stiffness and buckling forces are compared to the values obtained in testing in 2021 [4], [5].

2. DESCRIPTION OF DLT SPECIMENS

DLT panels were made of planned spruce boards connected with profiled beech dowels inserted in predrilled holes. The panels differed regarding the number of layers; boards were planned without tongue / grove. Orientation of layers can also differ: layers are in general perpendicular or with some variants diagonal inner (mid) layers. Timber boards with width 16 cm and strength class C24 (min. 70 %) and C16 / C18 (max. 30 %) are used. Certain percentage of butt jointed boards in mid layer(s) is allowed in DLT for both, horizontal and diagonal layer. The outer layers are always arranged in longitudinal direction of the elements - for wall elements this is the vertical direction.
The dowels can be 80 - 110 mm long connecting 3 or 4 layers (depending on the DLT product). The diameter of dowels varies from 10 mm (bottom) to 17 mm (top). Profiled beech dowel is presented in Figure 1.

Fig. 1 Hardwood dowels connecting DLT elements

Information about the types of test specimens is given in Table 1. Some test series were tested only at in-plane shear (type 12E and 12C), while the others were additionally tested also in compression (type 9D and 9B), additional tests are foreseen. Before mechanical testing the geometry (length, width and thickness), weight and moisture content measurements were performed on all specimens [6] [7]. Type 9B and 12C have diagonal mid layers, which are rotated under 45° in relation to the outer layer orientation. The dowelling schema is presented in detail for each series in [6].

Tab. 1 Detailed description of specimens

Type	Nr. of layers	Thickness* [mm]	Orientation of layers	Nominal dimensions (b x h) [cm]	Test	Nr. of tests
Type 9D	3	3 x 30= 90	VHV	150 x 270	buckling	3
Type 9B	3	3 x 30 = 90	VDV	150 x 270	buckling	3
Type 9D	3	3 x 30 = 90	VHV	240 x 270	shear	3
Type 9B	3	3 x 30 = 90	VDV	240 x 270	shear	3
Type 12E	4	4 x 30 = 120	VHVH	240 x 270	shear	3
Type 12C	4	4 x 30 = 120	VDDV	240 x 270	shear	3

* Boards without tongue / grove.

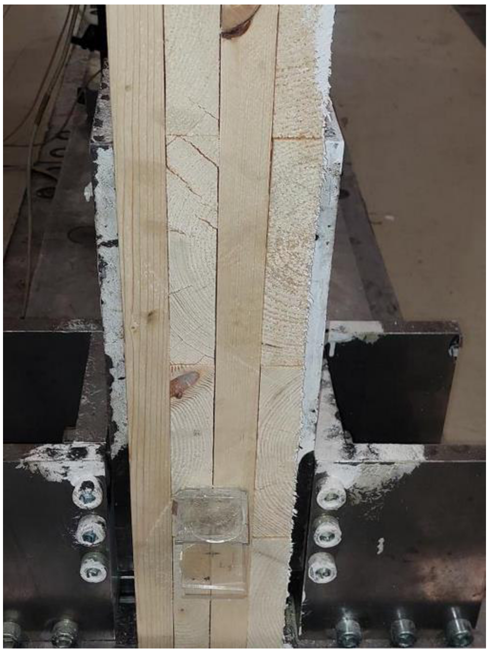

Fig. 2 Two types of DLT – with and without tongue / grove [6]

3. TEST SETUP AND TEST PROCEDURE

3.1. IN-PLANE COMPRESSION TESTS

The in-plane compression / buckling resistance of the panels were determined by a compression test in a hydraulic press by gradual increase of vertical force. The test method defines the vertical load resistance of DLT panels which fail in buckling as shown in Figure 3. The test method was designed as such that no additional resistance is induced; the panel is only laterally supported. Since the support of the specimens was not hinged but clamped, an evaluation of the failure loads needs to consider the support conditions.

The test setup and displacement measurements are shown in Figure 3. The vertical load F_v is introduced from the bottom, while the steel support at the top is fixed. The steel support at the bottom is additionally restrained, so that the out of plane movement is prevented. Specimens were loaded using the hydraulic press Amsler 500 MPa with a force controlled procedure for applying the vertical load. The vertical load F_v was increased until $F_{v,max}$ was reached. The rate of loading was adjusted to approximately 2 kN/s, so that most of the specimens reached $F_{v,max}$ in the target time recommendation (300 ± 120 s). The $F_{v,max}$ was determined when the vertical load of the DLT panel begins to significantly reduce. At least three specimens were tested for each test series. Average and characteristic values were determined according to EN 14358:2016 [8].

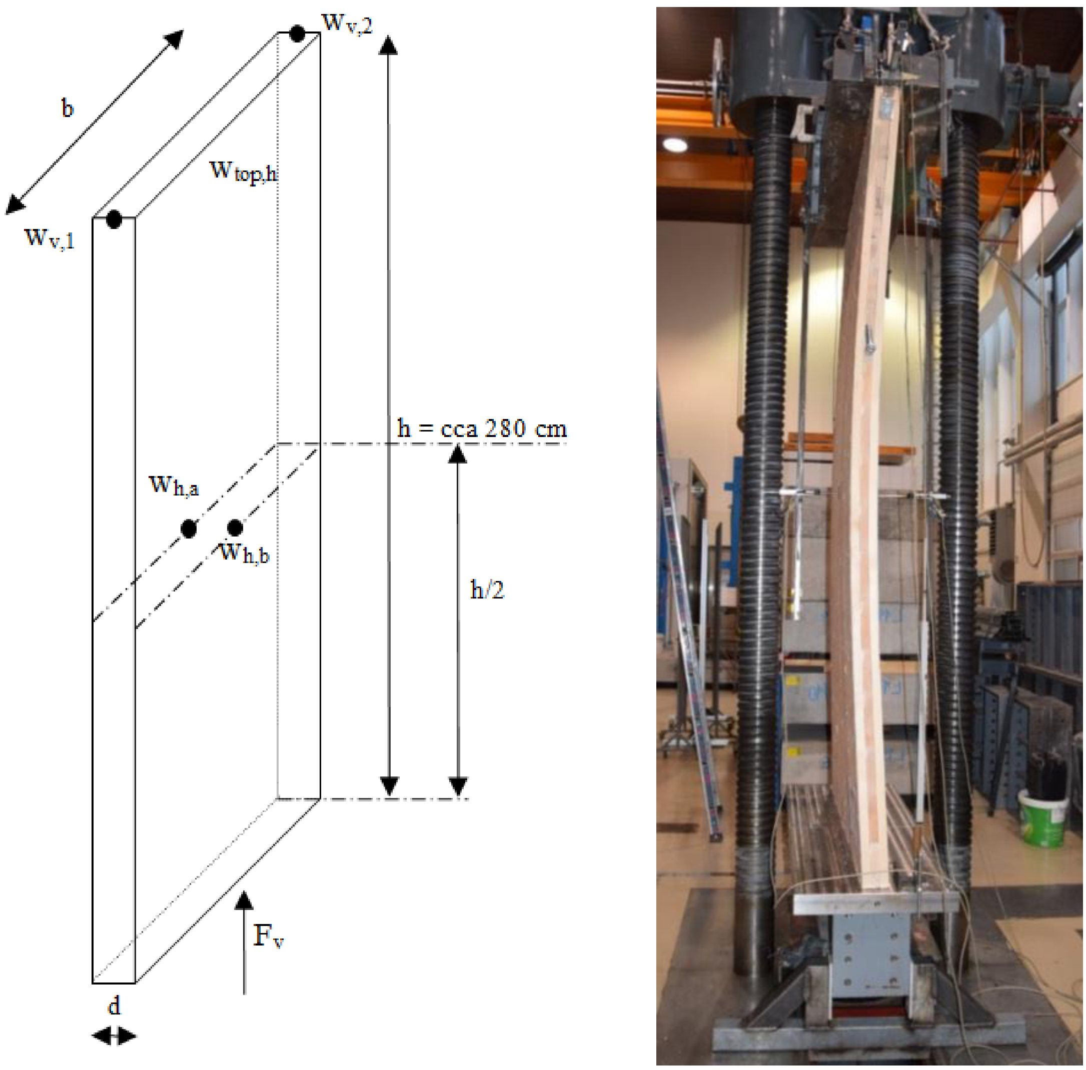

$w_{v,i}$ … vertical displacement of wall ($w_v = (w_{v,1} + w_{v,2}) / 2$)
$w_{h,i}$ … horizontal displacement of wall (perpendicular to wall) ($w_h = (w_{h,a} + w_{h,b}) / 2$)
$w_{top,h}$ … differential horizontal displacement of wall (parallel to wall at the top)

Fig. 3 In-plane compression test arrangement and typical buckling failure mode when subjected to axial compression load

3.2. IN-PLANE SHEAR TESTS

The purpose of testing was to evaluate in-plane shear characteristics, for this reason two types of tests were performed:

- Racking strength and stiffness tests - “monotonic tests” (without and with vertical load 25 kN/m) according to EN 594:2011 [9],
- Cyclic in plane shear tests (“cyclic tests”) according to ISO 16670:2003 [10].

Specimens were fixed on a rigid supports as presented in Figure 4. Horizontal and vertical loads were applied using hydraulic actuators ($F_{hor,max}$ = 250 kN). Due to the high-level shear resistance of specimens with diagonal layer a slightly different system for applying loads and supporting specimens was applied. Testing details are given [6].

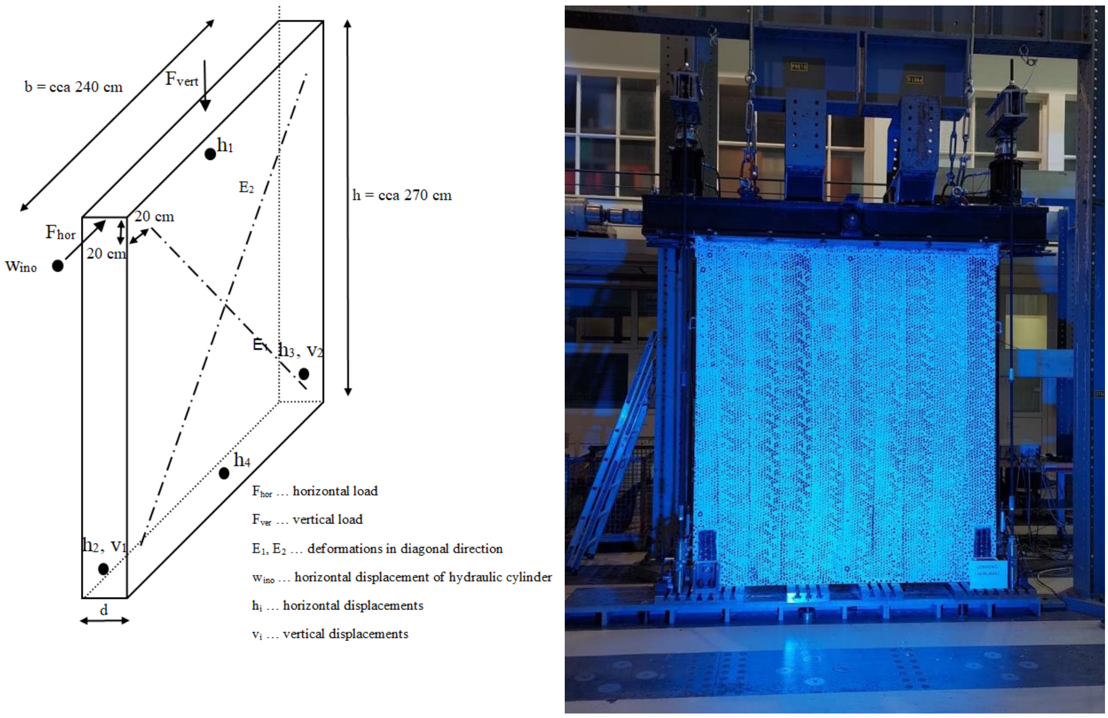

Fig. 4 In-plane shear test arrangement and test setup showing horizontal and vertical load insertion as well as measurements of displacements with optical system

4. TEST RESULTS

4.1. IN-PLANE COMPRESSION TESTS

Main points of interest were the vertical loads (F_v) and the horizontal displacements in the middle of the wall panels (w_h calculated from $w_{h,a}$ and $w_{h,b}$). For the sake of test control, also the vertical displacements ($w_{v,1}$ and $w_{v,2}$) were measured at the edge of the panel and horizontal displacements at the top of the panel ($w_{top,h}$). The buckling load ($F_{v,max}$) is calculated both as mean and characteristic value. Characteristic 5-percentile values of the buckling load-bearing capacity were determined according to EN 14358:2016 [8]. The results are listed in Table 2 and presented in Figure 5.

Tab. 2 Summary of in-plane compression test results

Type	Specimen nr.	$F_{v,max}$ [kN]	$w_{h,max}$ [mm]	$w_{v,max}$ [mm]	$L_{1c,max}$ [mm]
Type 9D	1 - 3	775.0	6.6	34.8	6.6
	1 - 1	625.1	3.8	38.7	3.8
	1 - 2	574.3	2.9	30.5	2.9
Type 9B	4 - 1	666.3	86.4	37.9	2.4
	4 - 2	609.6	51.7	44.1	9.2
	4 - 3	631.8	76.3	40.7	18.9

The failure mechanism of all specimens was similar. All specimens buckled as a whole, where no visual separation of layers/boards could be noticed. No visual damage could also be noticed on outside boards and dowels. The buckling loads (maximum vertical load - $F_{v,max}$) were recorded when a significant drop on the force-displacement curve was evident (Figure 5). Characteristic buckling loads ($F_{v,k}$) were determined separately for each test series. The characteristic load $F_{v,k}$ for type 9D equals 401.3 kN and for type 9B 551.9 kN, while the average $F_{v,av}$ is 658.1 kN for type 9D and 635.9 kN for type 9B respectively. The difference in the average buckling load capacity between the different test series is expected, although the differences between series 9D and 9B were not that significant. The difference in characteristic load is due to the small number of samples. Maximum vertical displacements were in range from cca. 2.4 mm to 18.9 mm. Maximum horizontal displacements were in the range from cca. 30.5 mm to 44.1 mm. As expected, in the buckling phenomenon the standard deviation is high, since this is a stability limit state and therefore occurs suddenly (Figure 5).

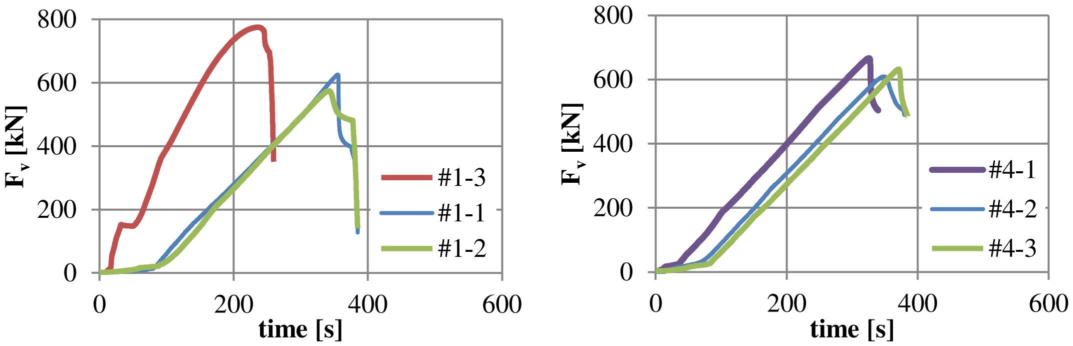

Fig. 5 In-plane compression test diagrams

4.2. IN-PLANE SHEAR TESTS

The purpose of in-plane shear testing was to evaluate the in-plane shear characteristics of DLT panels. The results are summarized in Table 3 for the main points of interest (values that were denominated in Figure 4), typical force-displacement diagrams are presented in Figures 6 and 7.

Tab. 3 Summary of in-plane shear test results

Type	Specimen nr.	Test type	Vertical load	$F_{L1,max}$ [kN]	$L_{1,max}$ [mm]	$F_{L1,max,c}$ [kN]	$L_{1c,max}$ [mm]
Type 9D	1-1 (D)	Monotonic	NO	73.2	164.2		
	1-2 (D)	Monotonic	25 kN/m	71.4	161.7		
	1-3 (D)	Cyclic	25 kN/m	80.7	100.0	77.2	100.0
Type 9B	2-1 (D)	Monotonic	25 kN/m	159.8	86.4		
	2-3 (D)	Cyclic	25 kN/m	152.8	51.7	253.3	58.1
	2-4 (D)	Monotonic	NO	149.5	76.3		
Type 12E	3-1 (H)	Monotonic	NO	80.6	165.1		
	3-2 (H)	Monotonic	25 kN/m	126.8	140.3		
	3-3 (H)	Cyclic	25 kN/m	145.4	100	152.3	100.0
Type 12C	4-1 (D)	Cyclic	25 kN/m	236.4	46.9	246.8	50.8
	4-2 (D)	Monotonic	25 kN/m	227.7	52.1		
	4-3 (D)	Monotonic	NO	204.5	47.2		

The following **c**onclusions based on performed tests can be made:

- Samples with no diagonal layers (Type 9D and Type 12E, Figure 8): The failure mechanism of all specimens is similar; when horizontal load was applied the boards in panel rotated / slipped: Dowels deformed and impressed into boards. The target displacement 100 mm with monotonic tests was possible to reach. With cyclic testing expected symmetry of force-displacement curve was confirmed with experiments (Figure 6).

- For the samples with diagonal layers (Type 9B and Type 12C, Figure 8) different failure mechanism applies. Diagonal layers assure the high level of rigidity of panels before deformation of dowels and their impressing into boards occurs. Consequently, an improved restraining system was set up due to the local damage on samples (separation of layers, compression crushing of timber at supports and at points of applying the horizontal loads). The gradient of force-displacement curves (Figure 7) indicates that stiffness of discussed panels with diagonal layers is much higher than the stiffness of panels with non-diagonal layers. Therefore, the target displacement as defined in EN 594 could not be reached. Buckling of outer layers occurred and was visible with bare eye for 12 cm thick specimens.
- Due to the relatively small number of specimens and due to relatively low level of vertical load no conclusions about the effects of vertical load can be made.
- With some specimens, locally, beech dowels reached brittle shear failure as well as brittle failure of timber boards occurred.

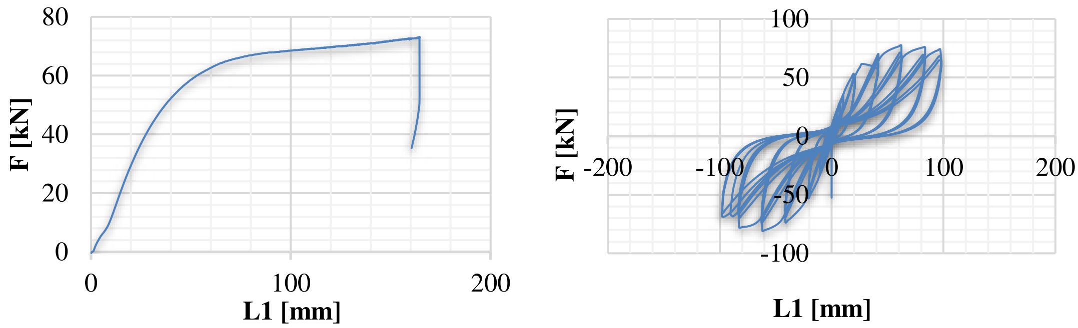

Fig. 6 Typical force-displacement diagrams, samples Type 9D, monotonic (left) and cyclic (right) loading

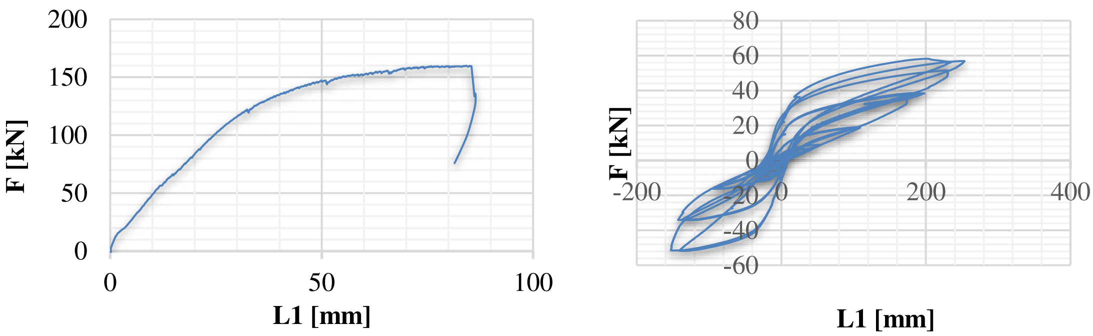

Fig. 7 Typical force-displacement diagrams, samples Type 9B, monotonic (left) and cyclic (right) loading

Fig. 8 Typical specimen with no diagonal layers (type 12E) at high lateral deformation (left), typical specimen with diagonal layers at max. displacement (right).

5. DISCOUSSION AND CONCLUSIONS

The main purpose of the presented tests was to evaluate the response of DLT panels for their in-plane shear as well as buckling/compression response. The performed experimental campaign consisted of DLT, which was assembled by timber boards without tongue / groove.

When comparing the DLT with non-profiled boards and the equivalent DLT using the tongue / groove boards, the load-bearing capacity reduces especially for in-plane shear.

With the most comparable samples tested in 2021 (thickness of boards, number and orientation of layers, doweling schema but with the presence of tongue / grove), the following results were obtained:

- Type 9D, monotonic, no vertical load, $F_{L1,max}$ = 131.42 kN,
- Type 9D, monotonic, vertical load 25 kN/m, $F_{L1,max}$ = 111.58 kN,
- Type 9D, cyclic, vertical load 25 kN/m, $F_{L1,max}$ = 107.98 kN, $F_{L1,max,C}$ = 107.98 kN
- Type 9B, monotonic, no vertical load, $F_{L1,max}$ = 249.98 kN,
- Type 9B, monotonic, vertical load 25 kN/m, $F_{L1,max}$ = 244.89 kN.

Tested samples therefore demonstrate relatively high reduction of the in-plane shear load-bearing capacity, up to amount of 35 - 45 % with the monotonic load protocol and 25 - 35 % with the cyclic load protocol. No significant difference has been identified regarding orientation of mid layer (horizontal, diagonal). Since the doweling schema has also been slightly modified the difference in mechanical behaviour cannot be assigned purely to the tongue / grove presence/absence.

On the other hand, the mean buckling load-bearing capacity of comparable 3 layer DLT with a diagonal mid layer with ($F_{v,av}$ = 678,6 kN) and without ($F_{v,av}$ = 658,1 kN) tongue / grove is less than 7 %. The difference in mean buckling load-bearing capacity with 3 layers DLT with a horizontal mid layer seems to be higher, similar as with in-plane shear tests. Additional in-plane compression tests are foreseen to study / analyse the influence of parameters on buckling phenomena of DLT.

ACKNOWLEDGEMENT

The research was supported by the Slovenian Research and Innovation Agency (Research Core Funding No. P4-0430 and No. P2-0273). The company iQwood d.o.o. is also gratefully acknowledged for providing the specimens for testing.

REFERENCES

[1] Dujič B., Jančar J., Kocina B., Bogataj M. (2021). iQwood – Lesena masivna križno mozničena večslojna stena brez lepil. *42. Zborovanje gradbenih konstruktorjev Slovenije*, Rogaška Slatina, Slovenia, 7-8 October, pp. 123–132.

[2] EOTA. (2015). EAD 130002-00-0304 Solid wood slab element – element of dowel jointed timber boards to be used as a structural element in buildings.

[3] ETA-14/0334 (2020). iQwood Timber Elements.

[4] Pazlar, T. (2021). Report No. 921/20-640-2 about the shear tests of cross layered dowel jointed timber wall panels – iQwood. Slovenian National Building and Civil Engineering Institute (ZAG), Ljubljana, Slovenia.

[5] Pazlar, T. (2021). Report No. 921/20-640-1 on the compression/buckling resistance of cross layered dowel jointed timber wall panels. Slovenian National Building and Civil Engineering Institute (ZAG), Ljubljana, Slovenia.

[6] Pazlar, T. (2023). Report No. 318/23-640-1-EN about the shear tests of cross layered dowel jointed timber wall panels - iQwood. Slovenian National Building and Civil Engineering Institute (ZAG), Ljubljana, Slovenia.

[7] Azinović, B. (2023). Report No. 297/23-640-1-EN on the compression/buckling resistance of cross layered dowel jointed timber wall panels - iQwood. Slovenian National Building and Civil Engineering Institute (ZAG), Ljubljana, Slovenia.

[8] EN 14358:2016 - Timber structures - Calculation and verification of characteristic values.

[9] EN 594:2011 - Timber Structures - Test methods - Racking strength and stiffness of timber frame wall panels.

[10] ISO 16670:2003 - Timber structures - Joints made with mechanical fasteners - Quasi-static reversed-cyclic test method.

DEVELOPMENT OF MAGNESIUM PHOSPHATE CEMENT USING LIGHT BURNED MAGNESIUM OXIDE

Branka Mrduljaš[1], Marin Šepuka[2], Ana Baričević[3]

Summary:

Magnesium phosphate cements (MPCs) are formed at room temperature by reaction between magnesium oxide (MgO) and an acidic phosphate source. The reaction proceeds rapidly, and retarders such as boric acid are used to control the setting time. Normally, dead-burned magnesium oxide, obtained by calcination at 1500 – 2000 °C, is used to produce MPCs. However, a more environmentally friendly solution can be achieved by using light burned magnesium oxide. This type of MgO is calcined in a temperature range of 750 - 1000 °C, which results in sufficient reactivity.

In this study the influence of light burned MgO, metakaolin, fly ash and boric acid content on workability, temperature, and compressive strength of MPC paste is investigated.

Key words: Light burned MgO, Fly ash, Metakaolin

[1]Department od Materials, Faculty of Civil Engineering/University of Zagreb, Zagreb, Croatia, branka.mrduljas@grad.unizg.hr
[2] Department od Materials, Faculty of Civil Engineering/University of Zagreb, Zagreb, Croatia, msepuka@student.grad.hr
[3] Department od Materials, Faculty of Civil Engineering/University of Zagreb, Zagreb, Croatia, ana.baricevic@grad.unizg.hr

1. INTRODUCTION

Innovative approaches have been developed to meet the global demand and reduce CO_2 emissions. Among these approaches, MgO-based cements have been attracted attention due to their over 150 years long industrial use of and their remarkable ability to absorb CO_2 [1]. MgO, or magnesium oxide, has unique property of absorbing carbon dioxide (CO_2) from the atmosphere, forming carbonates and hydroxycarbonates [2]. This makes MgO cement effectively “carbon neutral”.

There are two main methods for producing MgO: wet calcination, in which MgO is extracted from $Mg(OH)_2$ precipitates from water or brine, and by dry calcination, which uses magnesia-based minerals, such as magnesite [3]. Importantly, calcining magnesite can result in net CO_2 emissions that are a remarkable 73% lower compared to ordinary Portland cement (OPC) [4].

Magnesium oxide (MgO) manufactures usually divide it into three categories, regardless of its source: (i) light burned MgO (LBM), which is produced at temperatures between 700 and 1000°C; (ii) hard burned MgO (HBM), which is produced at temperatures between 1000 and 1500°C; and (iii) dead burned MgO (DBM), which is produced at temperatures between 1500 and 2000°C [1]. The reactivity of MgO decreases by increase of calcination temperature, which is accompanied by a decrease in porosity and surface area, as noted by [5]. In particular, the hydration rate of MgO is primarily affected by its specific surface area [3]. In the cement industry, MgO calcined at lower temperatures is commonly referred to as “reactive magnesia” [5]. Namely, the reactivity of magnesia is directly proportional to its particle size and surface area. Finer particle size with greater surface area exhibits higher reactivity, leading to faster formation of hydration products [6]. Conversely, higher calcination temperature result in a larger particle size. It is also worth noting that uncalcined MgO particles have irregular particle surfaces, while calcination process produces MgO particles with more regular spherical surfaces, as shown in Fig. 1[7].

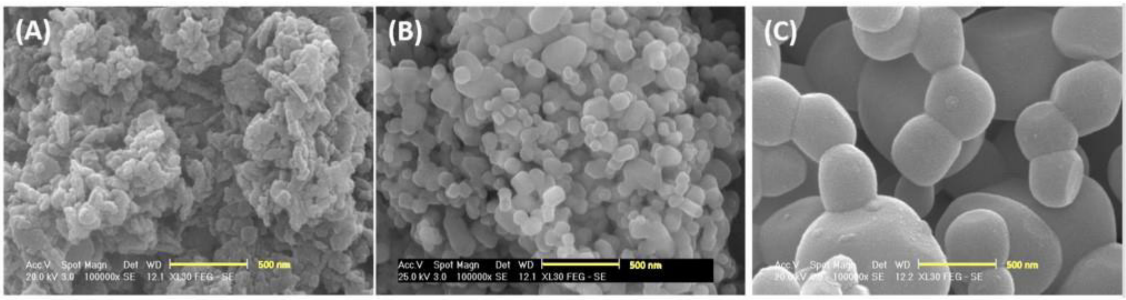

Fig. 1 Morphology of MgO obtained by SEM; a) without calcination, b) calcinated at 900 °C for 2 h and c) calcined at 1100 °C for 2 h [7]

Magnesium phosphate cements (MPCs) are clinker-free cements sometimes referred to as chemically bonded ceramics. These cements are formed at room temperature by a rapid aqueous reaction between calcined magnesia with soluble acid phosphate. This reaction results in the formation of insoluble magnesium phosphate salts with cement-like properties [8].

Phosphate sources commonly used in this process include ammonium dihydrogen phosphate ($NH_4H_2PO_4$) or potassium dihydrogen phosphate (KH_2PO_4). The acid–based reaction is inherently rapid and requires the addition of retarders such as boric acid (H_3BO_3), borax $Na_2B_4O_7$ x 10 H_20, or sodium triphosphate ($Na_5P_3O_{10}$) are required. The addition of a setting retarder reduces the acid-base reaction and effectively delays the setting time. This delay ensures that the cement paste, or mortar remains workable.

Existing literature [9] indicates that several factors play a critical role in determining the properties of MPC hardened cement paste. These key factors include the reactivity of

MgO, the molar ratio of MgO to phosphate (referred to as the M/P ratio), the presence of a retarder, and the amount of water involved in the process. The water content is crucial as it has a significant effect on the crystallisation of the hydration products, and consequently, on the formation of K-struvite.

A Mg/PO_4 molar ratio of 1 is sufficient for the formation of K-struvite, the primary hydration product, and should result in satisfactory material performance [10]. Higher molar ratios of $Mg/PO_4 \geq 4$ are generally used in the production of magnesium phosphate cements (MPC) for rehabilitation purposes. On the other hand, $Mg/PO_4 \leq 4$ molar ratios are more commonly used for waste immobilization due to their lower pH. In the study conducted by Xu et al [10], it was found that in MPC systems using DBM magnesia, especially at high Mg/PO_4 molar ratios, excess of unreacted magnesia leads to problems related to brucite production and subsequent volume expansion. If the MgO content is too high, it will result in an inadequate phosphate to water ratio. This deficiency leads to insufficient formation of hydration products, which ultimately results in a lack of strength or even a complete absence of strength. On the other hand, if the MgO content is too low, this will affect the performance of MPC due to the coarse particle size of the hydration products and excessive shrinkage and deformation due to high hydration exotherm [9]. The recommended range for the addition of retardants is typically between 5 and 15% of the amount of MgO [9].

Compared to OPC, MPC with DBM exhibit superior mechanical properties. Remarkably, it achieves an early strength of 25 MPa within only one hour after moulding [11]. The studies conducted by Volpe et al [12] focused on MPCs with LBM. These materials generally exhibit brittle behaviour. After 7 days of curing, the flexural strength tends to decrease, while compressive strength increases, primarily due to the development of K -struvite. It is worth noting that limited data is available on MPC based on LBM in the literature. However, values for compressive strength after 7 days typically range from 3.5 MPa up to 6 MPa [12], [13].

MPC containing DBM offers a number of advantages in construction. These include fast setting time, high early strength, low shrinkage, excellent resistance to high temperature, as well as an excellent adhesion to OPC substrates [10], [11]. However, it is important to recognize certain challenges associated with the use of MPC in construction. These challenges include too short setting time, relatively high cost, almost double that of OPC, and water resistance is concerns [14].

An effective approach to reduce the high cost of MPC is to substitute MgO with mineral additives such as fly ash and metakaolin. According to Zheng et al. [9], the role of fly ash in MPC cements is controversial. Some consider it an inert filler, while others believe that it actively participates in hydration, affecting early strengths but possibly reducing strength in the later stages. Similarly, metakaolin is also suitable as a substitute for MgO and is known to participates in the acid-base reaction [9]. Metakaolin is also credited with improving the compressive strength, moisture content and freeze-thaw resistance of MPC, by up to 30 %.

This paper aims to investigate the contribution of low temperature calcined magnesium oxide (LBM) further contributing to a reduced ecological footprint. MgO was partially replaced with supplementary cementitious materials, fly ash and metakaolin to reduce the cost of MPC. The effect of parameters like w/b, molar ratio M/P, and borax acid content on setting time and strength development of MPC pastes with light burned MgO were analysed.

2. MATERIALS AND METHODS

A cement paste based on light burned magnesium oxide (MgO) and potassium dihydrogen phosphate (KH_2PO_4) was prepared, to which tap water, boric acid as a retarder, and mineral additives (metakaolin and fly ash) as MgO substitutes were added.

Magnesium oxide from Carlo Erba Ltd, calcined at a temperature of 850 °C, was used (Tab. 1).

Tab. 1 Chemical composition of magnesium oxide

Component	MgO	SO_4	Fe_2O_3	CaO	PbO
Mass fraction [%]	98.00	≤ 1.0	≤ 0.05	≤ 1.50	≤ 0.3

The molar mass of the magnesium oxide used is 40.29, the pH is 10.3, and the density is 3.58 g/cm^3. Potassium dihydrogen phosphate (KH_2PO_4), manufactured by Fischer Scientific Ltd, was used as the phosphate source (Tab. 2). The purity of the phosphate used is more than 99.5%, and the proportions of the other components are shown in Table 2. The molar mass of the phosphate used is 136.09, and its density is 2.34 g/cm^3. Its pH value is between 4.4 and 4.7.

Tab. 2 Chemical composition of potassium dihydrogen phosphate (KDP)

Component	KH_2PO_4	Sulphates	Insoluble substances	Chlorides
Mass fraction [%]	99,5	0,003	0,01	0,0005

Boric acid, produced by Gram - Mol Ltd, was used as a retarding agent. The purity of boric acid (H_3BO_3) is 99.5%, while its density is equal to 1.44 g/cm^3.

MgO was partially replaced by metakaolin (MA) and fly ash (FA). Metakaolin Metaver® M from Newchem Ltd with a density of 2.74 g/cm^3 and FA from Holcim Ltd with a density of 2.46 g/cm^3 were used, which belongs to class F according to the ASTM C 618:2019 [15] (Tab. 3).

Tab. 3 Chemical composition of FA and MA

Component	SiO_2	Al_2O_3	Fe_2O_3	TiO_2	CaO	MgO	K_2O	Na_2O	SO_3
FA	57,2	25,1	5,8	0,9	4,8	1,7	1,5	1,1	0,8
MA	50-56	40-43	≤1,0	0,0	0,0	0,0	≤ 2,0	0,0	0,0

The experimental part is divided into two phases. In the first phase, influence of the molar (M/P) and water to binder (w/b) ratio were investigated on 8 mixtures, while in the second phase, 6 mixes were prepared, varying the proportions of setting retarders (boric acid) and mineral additives (fly ash and metakaolin). The aim was to determine the optimum composition in terms of compressive strength and setting time.

Tab. 4 Mix Designs in the First Experimental Phase

Mix ID	MgO [%]	M/P	w/b	Boric acid [%]
Mix1	100	2	0.50	5
Mix2	100	4	0.50	5
Mix3	100	2	0.50	10
Mix4	100	4	0.50	10
Mix5	100	2	0.60	5
Mix6	100	4	0.60	5
Mix7	100	2	0.60	10
Mix8	100	4	0.60	10

Tab. 5 Mix Designs in the Second Experimental Phase

Mix ID	MgO [%]	FA [%]	MA[%]	M/P	w/b	Boric acid [%]
Mix1	100	-	-	2	0.50	5
Mix3	100	-	-	2	0.50	10
Mix1FA	100	40	-	2	0.50	5
Mix1MA	100	40	-	2	0.50	10
Mix3FA	100	-	40	2	0.50	5
Mix3MA	100	-	40	2	0.50	10

The mixing process started with the addition of MgO, either with or without a mineral additive (metakaolin or fly ash), followed by the addition of water. After 30 seconds, KDP and boric acid were added to the mixture. Mixing proceeded for another 45 seconds to ensure thorough integration of all ingredients. Once mixing was completed, the resulting paste was poured into prismatic molds (4 x 4 x 16 cm).
The specimens were stored at a relative humidity of 60% and an air temperature of 21±2° C. The compressive strength of the specimens was tested according to the standard HRN EN 1015-11-2019 [16] at the age of 1 and 7 days, with a force increase of 250 N/s. In the second phase, in addition to the compressive strength, the initial and final setting times were recorded according to HRN EN 196-3:2016 [17].

3. RESULTS AND DISCUSSION

3.1. FIRST EXPERIMENTAL PHASE

In the first experimental phase, a study to determine the effect of three key factors: the w/b ratio, the M/P ratio and boric acid content was conducted, figure 2.
The effect of varying boric acid content on the compressive strength of magnesium phosphate cement (MPC) mixture shows interesting trends. When M/P is set at 2, an increase in boric acid content results in an increase in compressive strength. However, when the M/P ratio is set at 4, an increase in boric acid content leads to a decrease in compressive strength. Although certain authors believe that an excess of MgO creates a skeleton and thus contributes to the mechanical properties, Ribeiro et al. [18] believe that a lower molar ratio and the presence of a retardant contribute to a lower porosity of the system, where the retardant contributes to a slight increase in crystallinity of the hydrated phases.

In addition, increasing the w/b ratio to 0.60 leads to a significant decrease in compressive strength, ranging from 55 to 69% compared to mixtures with a w/b ratio of 0.5. This decrease is a common behaviour observed in various cementitious materials. According to Ribeiro et al [18], MPC produced with a higher water content tends to form struvite crystals whose size and mean diameter decreases. Interestingly, this phenomenon occurs independently of the calcination temperature of the MgO.

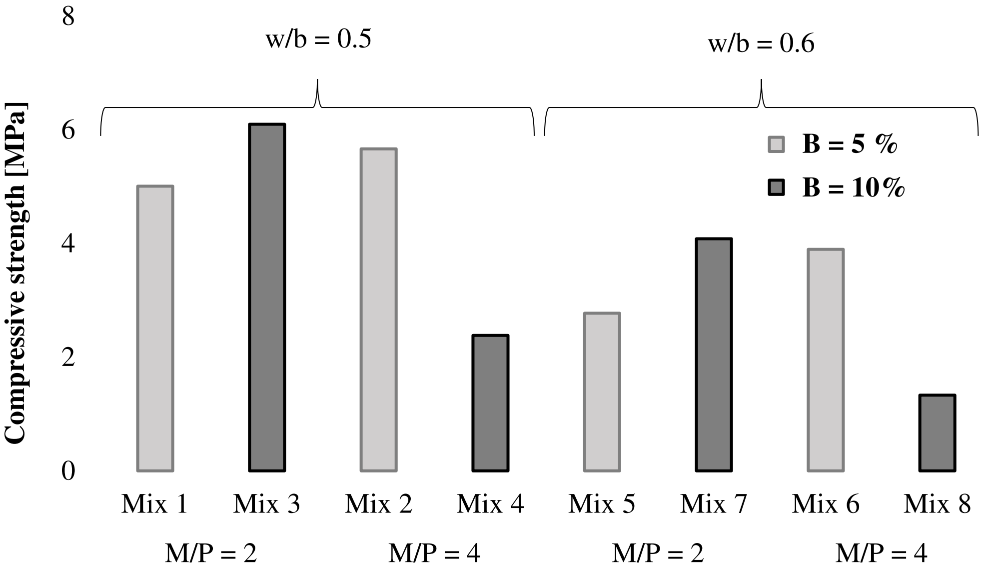

Fig. 2 Graphic representation of the 7th day compressive strength trend depending on: a) the boric acid content, b) the molar ratio and c) the water to binder ratio.

3.2. SECOND EXPERIMENTAL PHASE

In the second phase of the study, the effect of mineral admixtures, namely fly ash and metakaolin, was investigated. It is important to note that in this phase a constant water to binder ratio (w/b) of 0.50 and a fixed molar ratio (M/P) at 2 were maintained, as optimally indicated by the results of the first phase. Therefore, the experimental work proceeded using mixtures labelled Mix 1 and Mix 3 as referent.

The Fig. 3 and table 6 shows the values for the initial and final setting time of MPC pastes from the second phase. The addition of 10% boric acid leads to an increase in setting time, which is consistent with the findings of the previous literature on MPC with DBM. Similar, the addition of mineral additives also have a positive effect on the setting time, with the strongest effect observed for fly ash. This is consistent with the studies of Liu et al [19], where FA was found to have a greater effect on rheological properties and setting time compared to metakaolin.

Although rheological properties, such as consistency, were not specifically measured in this study, the use of fly ash appeared to be a more favourable choice than metakaolin, resulting in better workability of the MPC paste.

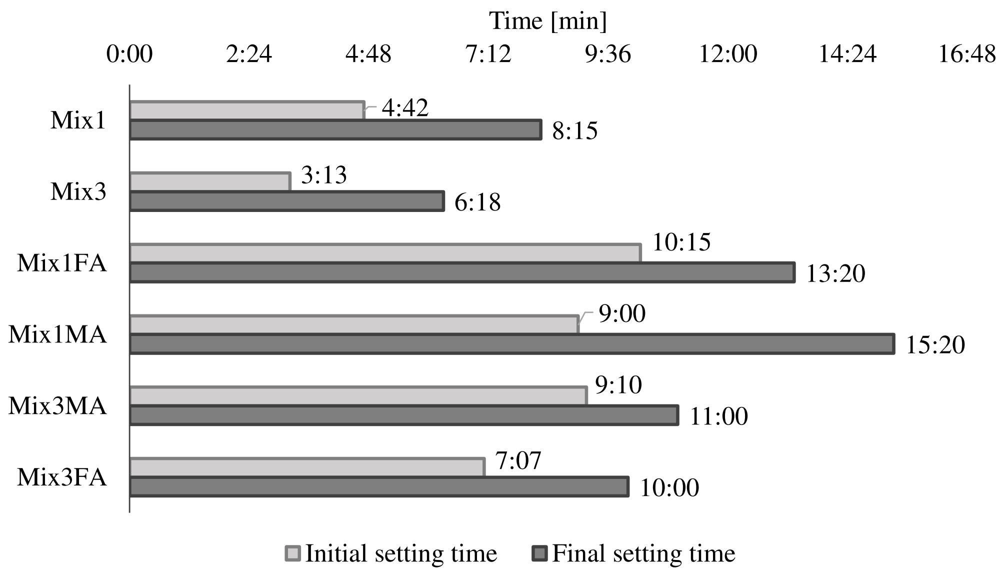

Fig. 3 The initial and final setting time for the mixtures from second phase

Tab. 6 The influence of MgO replacement by mineral additives on the setting time

Type of MPC	**Average delay analysis**	
	initial setting time	final setting time
with FA	118 %	62 %
with MA	95 %	33 %

The difference in results between Fig. 2 and Fig. 4 becomes clear when identical mixtures are compared in the first and second phases are compared. Especially, the mixtures in the second phase show higher results. This difference can be attributed to the different methods of specimen preparation. In the first phase, the specimens were mixed manually, while an automatic mixer was used in the second phase. These led to promising results, as the compressive strength values exceed than reported in the literature [12]. In this study, a maximum value of 15.10 MPa was obtained, which is 34 % higher than the maximum value of 9.98 MPa reported in the literature for LBM.

When comparing the results of the reference mixes Mix1 and Mix3, a clear pattern emerges: a 5% increase in boric acid content leads to a 21 % increase in compressive strength. However, the trend reverses when MgO is partially replaced by mineral additives. This behaviour has already been described in the literature [9], and it can be expected that the compressive strength of MPC specimens shows a tendency to increase first and then to decrease as the content of fly ash and metakaolin gradually increases. In cases where 40% of the MgO is replaced by fly ash (FA), the compressive strength decreases by an average of 6% after 7 days in mixtures with addition 5 % of boric acid. When 10% boric acid and FA are added, the compressive strength decreases by an average of 49 %. With an equivalent substitution by metakaolin (MA), the compressive strength decreases by 21 % after 7th day with boric acid content of 5 %, and with addition of 10 % boric acid the decrease is 41 %.

Therefore, the increase in compressive strength during the first 7 days is more modest when MgO is partially replaced by mineral additives. This finding can be clearly seen in Tab. 7 and is consistent with the results in the existing literature [19]. However, considering the potential cost savings resulting from these substitutions, the reduction in compressive strength considered acceptable depending on the intended end use of MPC.

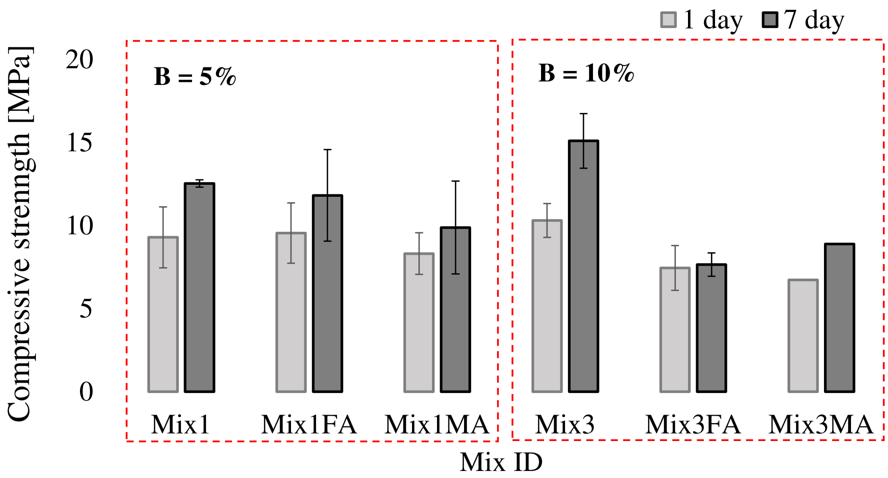

Fig. 4 Graphic representation of the 1st and 7th day compressive strength trend depending on: a) the boric acid content, and b) the mineral additives content.

Tab. 7 Average Compressive Strength Increase in MPC from day 1 to day 7

Type of MPC	**Increase of compressive strength**	
	B = 5 %	B = 10 %
No substitution	35 %	46 %
with FA	24 %	3 %
with MA	19 %	32 %

4. CONCLUSIONS

In the present work, the properties of MPC pastes based on light burned magnesia with variations of w/b ratio, molar ratio of M/P and addition of mineral additives were studied. Based on the results, the following conclusions can be drawn:

- MPC with LBM shows a strongly exothermic process with a very short setting time.
- Mixtures with a higher content of boric acid show an increase in compressive strength, only for M/P = 2, attributed to the reduced specimen porosity.
- Mineral additives, particularly fly ash, significantly influence setting time, leading to favourable effects.
- While the addition of mineral additives may lead to a decrease in compressive strength, it does contribute to cost reduction in MPC production.
- The compressive strength results achieved in this study surpass those documented in the exiting literature.

These results contribute to the understanding of MPC with LBM and the effects of mineral admixtures on setting time and compressive strength. Future research should focus into the evolution of hydration products and their influence on strength development.

ACKNOWLEDGEMENT

The research presented here was carried out as part of the projects "Cement Composites Reinforced with Waste Fibers" - Rewire (UIP-2020-02-5242) and "Career Development of Young Researchers - Training of New Doctors of Science" (DOK-2021-02-4884) at the Faculty of Civil Engineering, University of Zagreb, both funded by the Croatian Science Foundation.

REFERENCES

[1] S. A. Walling and J. L. Provis, "Magnesia-Based Cements: A Journey of 150 Years, and Cements for the Future?," *Chem. Rev.*, vol. 116, no. 7, pp. 4170–4204, 2016, doi: 10.1021/acs.chemrev.5b00463.

[2] N. José, H. Ahmed, E. Luis, and J. de Brito, "Magnesia (MgO) Production and Characterization, and Its Influence on the Performance of Cementitious Materials: A Review," *Materials (Basel).*, no. 13, 2020, doi: 10.3390/ma13214752.

[3] L. Huang, Z. Yang, and S. Wang, "Influence of calcination temperature on the structure and hydration of MgO," *Constr. Build. Mater.*, vol. 262, p. 120776, 2020, doi: 10.1016/j.conbuildmat.2020.120776.

[4] M. G. Gardeh, A. A. Kistanov, H. Nguyen, H. Manzano, W. Cao, and P. Kinnunen, "Exploring Mechanisms of Hydration and Carbonation of MgO and Mg(OH)2in Reactive Magnesium Oxide-Based Cements," *J. Phys. Chem. C*, vol. 126, no. 14, pp. 6196–6206, 2022, doi: 10.1021/acs.jpcc.1c10590.

[5] A. S. Wagh, *Chemically Bonded Phosphate Ceramics Chemically Bonded Phosphate Ceramics British Library Cataloguing-in-Publication Data*. 2016.

[6] Y. Dai and C. Wu, "Study on properties of magnesium phosphosilicate cement using different reactive magnesia," *J. Ceram. Soc. Japan*, vol. 129, no. 8, pp. 540–550, 2021, doi: 10.2109/jcersj2.21022.

[7] D. V. Ribeiro, G. R. Paula, and M. R. Morelli, "Effect of boric acid content on the properties of magnesium phosphate cement," *Constr. Build. Mater.*, vol. 214, pp. 557–564, 2019, doi: 10.1016/j.conbuildmat.2019.04.113.

[8] D. A. Hall, R. Stevens, and B. El Jazairi, "Effect of water content on the structure and mechanical properties of magnesia-phosphate cement mortar," *J. Am. Ceram. Soc.*, vol. 81, no. 6, pp. 1550–1556, 1998, doi: 10.1111/j.1151-2916.1998.tb02515.x.

[9] Y. Zheng, Y. Zhou, X. Huang, and H. Luo, "Effect of raw materials and proportion on mechanical properties of magnesium phosphate cement," *J. Road Eng.*, vol. 2, no. 3, pp. 243–251, 2022, doi: 10.1016/j.jreng.2022.06.001.

[10] B. Xu, F. Winnefeld, J. Kaufmann, and B. Lothenbach, "Influence of magnesium-to-phosphate ratio and water-to-cement ratio on hydration and properties of magnesium potassium phosphate cements," *Cem. Concr. Res.*, vol. 123, no. May, p. 105781, 2019, doi: 10.1016/j.cemconres.2019.105781.

[11] B. Fang *et al.*, "Research progress on the properties and applications of magnesium phosphate cement," *Ceram. Int.*, vol. 49, no. 3, pp. 4001–4016, 2023, doi: 10.1016/j.ceramint.2022.11.078.

[12] S. Volpe, A. Petrella, V. Sangiorgio, M. Notarnicola, and F. Fiorito, "Preparation and characterization of novel environmentally sustainable mortars based on magnesium potassium phosphate cement for additive manufacturing," *AIMS Mater. Sci.*, vol. 8, no. 4, pp. 640–658, 2021, doi: 10.3934/matersci.2021039.

[13] Y. T. Lim, S. Y. So, and H. S. Jang, "Effect of calcination temperature on the light burned MgO matrix and its physical properties," *J. Asian Archit. Build. Eng.*, vol. 21, no. 2, pp. 500–510, 2021, doi: 10.1080/13467581.2020.1869021.

[14] Y. Li and B. Chen, "Factors that affect the properties of magnesium phosphate cement," *Constr. Build. Mater.*, vol. 47, pp. 977–983, 2013, doi: 10.1016/j.conbuildmat.2013.05.103.

[15] ASTM, "ASTM C618:2023-Standard Specification for Coal Ash and Raw or Calcined

Natural Pozzolan for Use in Concrete." ASTM International (ASTM), p. 5, 2023.

[16] HZN Standard Publication, "Methods of test for mortar for masonry -- Part 11: Determination of flexural and compressive strength of hardened mortar (EN 1015-11:2019)." Croatian Standard Institute, Zagreb, Croatia, p. 16, 2019.

[17] HZN Standard Publication, "Methods of testing cement -- Part 3: Determination of setting times and soundness (EN 196-3:2016)." Croatian Standard Institute, Zagreb, Croatia, p. 14, 2016.

[18] D. V. Ribeiro, G. R. de Paula, and M. R. Morelli, "Effect of water content and MgO / ADP ratio on the properties of magnesium phosphate cement," *Mater. Res.*, vol. 23, no. 3, 2020, doi: 10.1590/1980-5373-MR-2020-0018.

[19] H. Liu, Q. Feng, Y. Yang, J. Zhang, J. Zhang, and G. Duan, "Experimental Research on Magnesium Phosphate Cements Modified by Fly Ash and Metakaolin," *Coatings*, vol. 12, no. 7, 2022, doi: 10.3390/coatings12071030.

PHYSICOMECHANICAL AND DEFORMATION PROPERTIES OF REPAIR CEMENT MORTARS MODIFIED WITH SLAG

Tiana Milović[1], Vesna Bulatović[2], Milan Marinković[3], Anka Starčev-Ćurčin[4]

Summary:

Due to the deterioration of aging concrete infrastructure worldwide, there is an increasing demand for the repair of reinforced concrete structures. The aim of this work was to evaluate the physicomechanical and deformation properties of repair cement-based mortars that contain 0%, 10%, 20% and 30% ground-granulated blast furnace slag as SCM, prepared with a water-to-binder ratio of 0.5. Applied slag was a by-product from the company Hesteel Serbia, located in Smederevo, Serbia. Following the standard EN 1504-3, the compressive strength of mortars and their modulus of elasticity in compression were determined at the age of 28 days, and additionally at the age of 60 days. Furthermore, flexural strengths of 28 and 60 days old mortars were determined, while the unrestrained shrinkage of mortars was followed up to the age of 63 days. All tested mortars fulfilled the requirement for class R4 of structural repair mortars in terms of compressive strength and elastic modulus.

Key words: ground-granulated blast furnace slag, EN 1504-3, compressive strength, flexural strength, elastic modulus, unrestrained shrinkage

[1] Res. Assoc., Faculty of Technical Sciences, University of Novi Sad, Serbia, tiana.milovic@uns.ac.rs
[2] Assoc. prof., Faculty of Technical Sciences, University of Novi Sad, Serbia, vesnam@uns.ac.rs
[3] Asst. prof., Faculty of Technical Sciences, University of Novi Sad, Serbia, milan.marinkovic@uns.ac.rs
[4] Assoc. prof., Faculty of Technical Sciences, University of Novi Sad, Serbia, astarcev@uns.ac.rs

1. INTRODUCTION

Due to a vast number of structures and infrastructure worldwide that approaching the end of their expected service life, there is an increasing demand for the maintenance and repair of reinforced concrete structures. In order to restore the performance of the deteriorated structures, conventional cement mortars are widely used, although they exhibit inadequate performance such as high shrinkage, and other durability issues [1]. The partial replacement of ordinary Portland cement (OPC) with supplementary cementitious materials (SCMs) in repair cement mortars, besides the environmental benefits, could have mechanical, physical and durability advantages.

Ground-granulated blast furnace slag (SL) is a by-product of iron and steel production, and therefore it is considered a green construction material. Due to its chemical and physical properties, SL is commonly used for cement production or as a partial replacement of OPC in mortar or concrete production, i.e. as type II addition in accordance with standard EN 206 [2].

Islam et al. [3] investigated the effects of SL on strength development of mortar that contained up to 60% SL as OPC substitution. Compressive as well as tensile strength of the mortar specimens were determined after 3, 7, 14, 28, 60, 90 and 180 days of curing. Test results showed that strength increased with the increase of SL up to an optimum value, beyond which, strength values started to decrease with further addition. The optimum amount of OPC replacement with SL in mortar was around 40%, and that provided 22% higher compressive and 23% higher tensile strength compared to OPC mortar, after 180 days of curing. Hammat et al. [4] examined the compressive strength and total shrinkage of self-compacting mortars containing SL. A total of seven mortar mixes were prepared, with water-to-binder ratio of 0.38, while cement was partially replaced with 0%, 15% and 30% SL (three different finenesses of SL: 3500 cm^2/g, 4200 cm^2/g and 5000 cm^2/g). Incorporating SL, compressive strength of mortars was reduced at early age, while the long-term compressive strength of mortars containing SL was higher than that of control mortar. At later ages, mortars with higher SL fineness had higher compressive strengths for substitution of 15%. However, for 30% replacement, the compressive strengths of mortars were similar regardless of the SL fineness. The results showed a reduction in the total shrinkage of mortars as the content and fineness of SL increased. Wang [5] investigated effect of OPC substitution with 5-100% SL on modulus of elasticity of paste prepared with water-to-binder ratio of 0.47. Obtained results showed that with an increase in the proportion of SL, there was a decrease in the modulus of elasticity of the tested pastes (at a temperature of 25°C).

The objective of the research presented in this paper was to evaluate the physicomechanical and deformation properties of repair cement-based mortars that contain 0%, 10%, 20% and 30% SL as SCM, prepared with a water-to-binder ratio of 0.5. Applied SL was a by-product from the company Hesteel Serbia, located in Smederevo, Serbia. Following the standard EN 1504-3 [6], the compressive strength of mortars and their modulus of elasticity in compression were determined at the age of 28 days in accordance with standards EN 12190 [7] and EN 13412 [8], respectively, and additionally at the age of 60 days. Furthermore, flexural strengths of 28 and 60 days old mortars were determined, while the unrestrained shrinkage of mortars was followed up to the age of 63 days.

2. MATERIALS AND METHODS

2.1. COMPONENT MATERIALS AND MORTAR MIXTURES

In order to examine the effect of SL as SCM on compressive strength, modulus of elasticity in compression of the repair blended cement mortars as well as flexural strength and unrestrained shrinkage, the following component materials were used for the repair mortars preparation:

- Ordinary Portland cement CEM I 42.5R (Lafarge-BFC Serbia),
- SL, sieved (through a sieve opening 125 µm) and additionally ground, from the company Hesteel Serbia, located in Smederevo, Serbia,
- CEN standard sand, in accordance with EN 196-1 [9],
- Deionized water.

True densities of OPC (3.126 g/cm^3) and SL (2.766 g/cm^3) were determined in accordance with EN 1097-7 [10], while the specific surfaces of OPC (4188.6 cm^2/g) and SL (5855.3 cm^2/g) were determined in accordance with the procedure specified in standard EN 196-6 [11]. The SL activity index was determined in accordance with the standard EN 15167-1 [12], and after 7 and 28 days SL activity indexes were 74% and 87%, respectively.

Four different cement/cement-based potential repair mortars were made with 0%, 10%, 20% and 30% of SL as SCM, by mass, to determine their compressive strength, flexural strength, modulus of elasticity in compression and unrestrained shrinkage. Mortar mixtures were prepared with a water-to-binder ratio of 0.5 according to EN 12190 [7]. Composition of mortar mixtures is shown in Table 1.

Tab. 1 Composition of cement-based repair mortar mixtures that contain SL as SCM

Component material	PC	SL10	SL20	SL30
CEM I 42.5 R (g)	450	405	360	315
SL (g)	-	45	90	135
Standard sand (g)	1350	1350	1350	1350
Deionized water (g)	225	225	225	225

2.2. METHODS

2.2.1. Flexural strength

The flexural strength of the mortars was determined according to the standard EN 196-1 [9] using prism-shaped specimens with dimension of 40 mm × 40 mm × 160 mm, at the age of 28 and 60 days, after recommended curing resume (covered in film for 24 h, demoulded after 24 h and cured under water at (21 ± 2)°C until testing). The mean strength values were obtained by testing the three prisms per mortar mixture. The load at failure was determined using the Michaelis scales.

2.2.2. Compressive strength

The compressive strength of the mortars was determined according to the standard EN 12190 [7] on the halves of the prisms remained from flexural strength testing, at the age of 28 and 60 days. The mean strength values were obtained by testing the six prism halves per mortar mixture. The load at failure was determined using a hydraulic press with a capacity of 150 kN.

2.2.3. Modulus of elasticity in comprassion

Modulus of mortars elasticity in compression was determined according to Method 2 given in the standard EN 13412 [8] using prism-shaped specimens with dimension of 40 mm × 40 mm × 160 mm, at the age of 28 and 60 days, as it is shown in Fig. 1. After recommended curing resume and conditioning (covered in film for 24 h, demoulded after 24 h and cured under water at (21 ± 2)°C until testing; immediately prior to testing, the test specimens were conditioned for at least 24 h under the standard laboratory climate, of (21 ± 2)ºC and (60 ± 10)% RH). The elastic modulus was established by measuring the change in the strain in the specimen when loaded to produce a stress of between 1.0 N/mm^2 and one-third of the compressive strength of the specimen. Compression testing machine with a capacity of 150 kN was used for pre-loading as well as for the test loading.

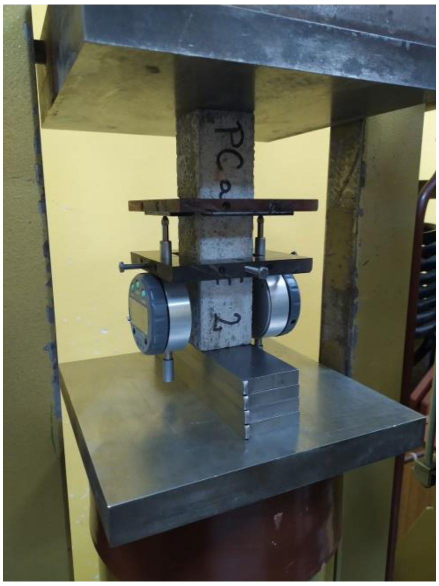

Fig. 1 Testing the modulus of mortar elasticity in compression

2.2.4. Unrestrained shrinkage

Unrestrained shrinkage of the mortars was determined in accordance with the method described in EN 12617-4: Chapter 6 [13]. The standard mortar prisms were used for this purpose. After demoulding, the specimens were stored in a climate chamber at a temperature of (21 ± 2) °C and (60 ± 10) % RH. Unrestrained shrinkage of specimens was measured after 1, 3, 7, 14, 21 and 28, 35, 42, 49, 56 and 63 days from demoulding.

3. RESULTS AND DISCUSSION

3.1. COMPRESSIVE STRENGTH

The compressive strength results of mortars containing SL as SCM, at the ages of 28 and 60 days, and prepared with a water-to-binder ratio of 0.5, are shown in Fig. 2. Based on the obtained results at the age of 28 days, the mortars made with SL as SCM fulfilled the requirement for class R4 of structural repair mortars according to the standard EN 1504-3 [6] in terms of compressive strength [7] i.e. their mean compressive strength values were higher than 45 MPa.

The ranges of compressive strength after 28 and 60 days of curing were from 50.16-52.92 MPa and from 54.06-58.44 MPa, respectively. It can be seen that the mortar containing 20% SL as SCM had the highest compressive strength at both tested ages. At the age of 28 days, the compressive strengths of SL10, SL20 and SL30 were higher by 1.1%, 5.5% and 0.1% than that of the reference mortar, respectively. After 60 days of curing, SL10 and SL20 had higher compressive strength for 3.3% and 6.4%, respectively, while SL30 had lower by 1.6%. With an increase in the age of the mortars from 28 to 60 days, there were the increase in PC, SL10, SL20 and SL30 compressive strength by 9.6%, 11.9%, 10.4% and 7.7%, respectively.

Considering that the differences in compressive strength of cement-slag mortars were less than 10% compared to reference cement mortar, it can be concluded that the level of substitution of OPC with SL up to 30% did not have a significant impact on the 28-

day and 60-day compressive strengths of blended cement mortars made with the water-to-binder ratio of 0.5, while compressive strengths were influenced by the duration of the curing time.

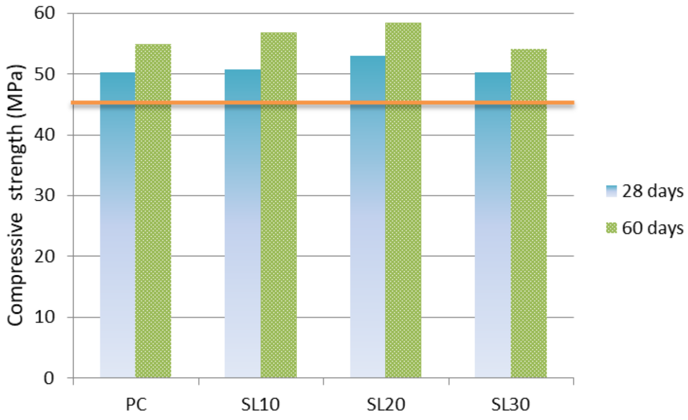

Fig. 2 Compressive strength of blended cement mortars

3.2. FLEXURAL STRENGTH

The 28-day and 60-day flexural strength results of mortars containing SL as SCM, prepared with a water-to-binder ratio of 0.5, are shown in Fig. 3.

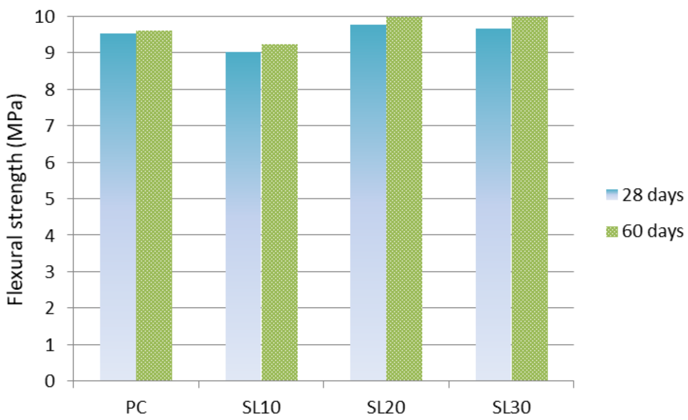

Fig. 3 Flexural strength of blended cement mortars

The ranges of flexural strength after 28 and 60 days of curing were: 9.01-9.77 MPa and 9.26-9.99 MPa, respectively. As in the case of compressive strength, mortar containing 20% SL as SCM had the highest flexural strength values for both curing times. Mortar with 10% SL had lower flexural strengths by 5.5% and 3.8% in comparison to the reference mortar at age of 28 and 60 days, while mortar SL20 had higher strength by 2.4% and 3.7%, as well as mortar SL30, for 1.2% and 3.7%, respectively. With an increase in the age of the mortars from 28 to 60 days, there were the increase in PC, SL10, SL20 and SL30 compressive strength by 0.9%, 2.8%, 2.2% and 3.5%, respectively. Since the differences were less than 10% compared to reference cement mortar, it can be concluded that the level of substitution of OPC with SL up to 30% as well as the increase in curing period from 28 to 60 days did not have a significant effect on the 28-day and 60-day flexural strengths of blended cement mortars made with the water-to-binder ratio of 0.5.

3.3. MODULUS OF ELASTICITY IN COMPRESSION

The elastic modulus results of mortars containing SL as SCM, at the ages of 28 and 60 days, and prepared with a water-to-binder ratio of 0.5, are shown in Fig. 4. Based on the obtained results at the age of 28 days, the mortars made with SL as SCM fulfilled the requirement for class R4 of structural repair mortars according to the standard EN 1504-3 [6] in terms of modulus of elasticity in compression [8] i.e. their mean values were higher than 20 GPa.

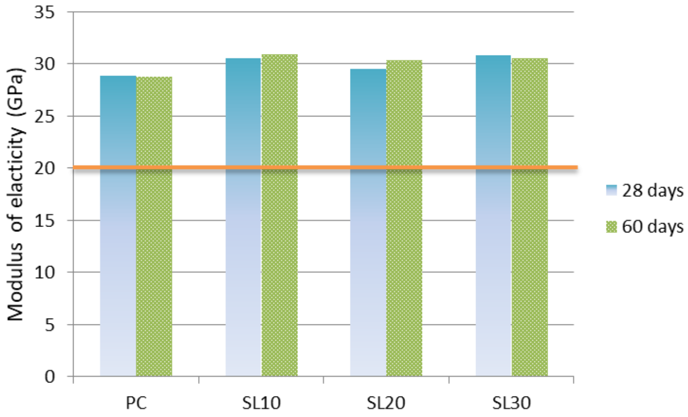

Fig. 4 Modulus of elasticity in compression of blended cement mortars

The ranges of the modulus of elasticity in compression of blended cement mortars after 28 and 60 days of curing were: 28.9-30.8 GPa and 28.8-31.0 GPa, respectively. After 28 days, the modulus of elasticity of SL10, SL20 and SL30 were 5.6%, 2.1% and 6.6% higher in comparison with reference one, while at the age of 60 days were higher for 7.6%, 5.6% and 6.2%, respectively. With the extension of the curing time from 28 to 60 days, there was a slight increase in the modulus of elasticity of the mortars SL10 and SL20, for 1.5% and 3.1%, respectively.
Based on the presented results, it can be concluded that the increase in the curing period from 28 to 60 days practically did not affect the 28-day and 60-day elastic modulus of cement and blended cement mortars containing SL as SCM, made with the water-to-binder ratio of 0.5, while the level of substitution of OPC with SL up to 30% had a certain impact although the difference was less than 10%.

3.4. UNRESTRAINED SHRINKAGE

The effect of SL on unrestrained shrinkage dilatations of blended cement mortars was followed up to the age of 63 days. The obtained results are presented in Fig. 5. As it can be seen, the application of SL as a SCM in blended cement mortars led to a decrease in unrestrained shrinkage. Until the age of 21 days, the highest value of unrestrained shrinkage had mortar SL10, followed by the reference mortar, while mortars SL20 and SL30 had lower unrestrained shrinkage in comparison to the SL10 reference one, respectively. At the age of 28 and 63 days, the unrestrained shrinkage of SL10 was slightly lower (by 8% and 12%) than that of the reference mortar, while in the case of SL20 and SL30, shrinkage was lower by 16% and 34% at the age of 28 days, and by 22% and 36%, respectively.

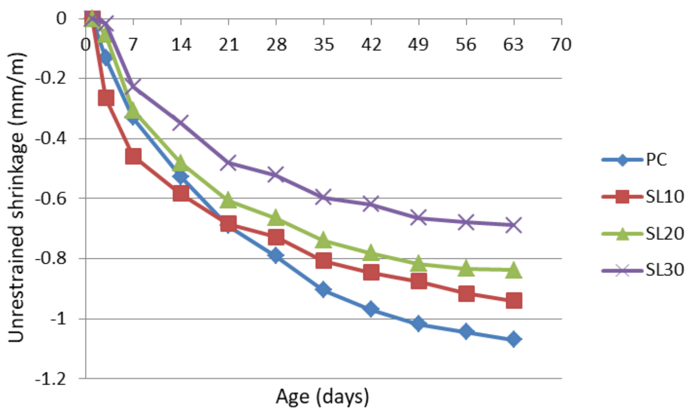

Fig. 5 Unrestrained shrinkage of blended cement mortars

Based on the presented results, it can be concluded that the substitution of OPC with 20-30% SL had a significant effect on decreasing the unrestrained shrinkage, while for the mortar that containing 10% SL shrinkage was a lower after 21 days from mortar casting, in comparison to the reference value.

4. CONCLUSION

Based on the obtained experimental results, in terms of the compressive strength, flexural strength, modulus of elasticity in compression and unrestrained shrinkage of the repair cement mortars that contain 0%, 10%, 20% and 30% SL as SCM, prepared with water-to-binder ratio of 0.5, the following can be concluded:

- Mortars containing up to 30% SL as SCM fulfilled the requirement for class R4 of structural repair mortars according to the standard EN 1504-3 in terms of compressive strength and elastic modulus;
- The level of OPC substitution with SL up to 30% did not have a significant effect on the 28-day and 60-day compressive and flexural strengths of blended cement mortars made with the water-to-binder ratio of 0.5;
- Compressive strengths were influenced by the duration of the curing time (from 28 to 60 days);
- The level of substitution of OPC with SL up to 30% did not have a significant impact on blended cement mortars modulus of elasticity in compression, as well as the duration of the curing time (from 28 to 60 days);
- The substitution of OPC with 20-30% SL had a significant effect on decreasing the unrestrained shrinkage of the blended cement mortars, while for the mortar that containing 10% SL shrinkage was a lower after 21 days from mortar casting, in comparison to the reference value.

Therefore, SL in an amount up to 30% (recommended level of OPC substitution with SL is 30%) can be used as SCM in repair cement mortars, in terms of the compressive strength, flexural strength, elastic modulus and unrestrained shrinkage.

ACKNOWLEDGEMENT

This research has been supported by the Ministry of Science, Technological Development and Innovation through project no. 451-03-47/2023-01/200156 “Innovative scientific and artistic research from the FTS domain”.

REFERENCES

[1] Ahmed S.F.U. (2011). Mechanical and Durability Properties of Mortars Modified with Combined Polymer and Supplementary Cementitious Materials. *Journal of Materials in*

Civil Engineering, Volume 23, No. 9, pp. 1311-1319. https://doi.org/10.1061/(ASCE)MT.1943-5533.0000300

[2] *SRPS EN 206-1:2011* - Concrete - Part 1: Specification performance, production and conformity.

[3] Islam M., Alam T., Islam S. (2017). Strength behavior of mortar made by using supplementary cementitious material as partial replacement of cement. *Journal of Civil Engineering*, Volume 45, No. 1, pp. 1-10.

[4] Hammat S., Menadi B., Kenai S., Khatib J., Kadri El-H. (2021). Properties of Self-Compacting Mortar Containing Slag with Different Finenesses. *Civil Engineering Journal*, Volume 7, No. 5, pp. 840-856. http://dx.doi.org/10.28991/cej-2021-03091694

[5] Wang H.Y. (2008). The effects of elevated temperature on cement paste containing GGBFS. *Cement & Concrete Composites*, Volume 30, pp. 992–999. https://doi.org/10.1016/j.cemconcomp.2007.12.003

[6] *BS EN 1504-3:2005* - Products and systems for the protection and repair of concrete structures - Definitions, requirements, quality control and evaluation of conformity - Part 3: Structural and non-structural repair.

[7] *BS EN 12190:1999* - Products and systems for the protection and repair of concrete structures - Test methods - Determination of compressive strength of repair mortar.

[8] *BS EN 13412:2006* - Products and systems for the protection and repair of concrete structures - Test methods - Determination of modulus of elasticity in compression.

[9] *SRPS EN 196-1:2008* - Methods of testing cement - Part 1: Determination of strength.

[10] *BS EN 1097-7:2008* - Tests for mechanical and physical properties of aggregates, Part 7: Determination of the particle density of filler – Pycnometer method.

[11] *BS EN 196-6:2010* - Methods of testing cement, Part 6: Determination of fineness.

[12] *BS EN 15167-1:2006* - Ground granulated blast furnace slag for use in concrete, mortar and grout - Part 1: Definitions, specifications and conformity criteria.

[13] *BS EN 12617-4:2002* - Products and systems for the protection and repair of concrete structures, Test methods – Part 4: Determination of shrinkage and expansion.

COMPARATIVE ANALYSIS OF CONCRETE TEST RESULTS WITH DIFFERENT AMOUNTS OF ELECTROFILTER ASH ADMIXTURES

Dušan Kocić[1], Jelena Bijeljić[2], Nenad Ristić[3]

Summary:

It is possible to improve the characteristics of cement concrete by adding or partially replacing the basic binder with appropriate admixtures or supplements. This paper presents the results of testing the characteristics of concrete mixes where cement was used as the basic binder. Four concrete series were tested. The first series of concrete was made only with cement as a binder and was called the standard. In other concrete mixes, cement was partially replaced with an industrial by-product - fly ash (FA) in the percentage-mass amount of 10% to 30%, at a replacement step of 10%. Testing of concrete in its fresh state was carried out after preparation, while testing of mechanical characteristics of concrete was carried out after reaching the age of 7, 28 and 56 days. According to the obtained test results, it can be concluded that the use of FA in concrete affects the change in the mechanical characteristics of concrete.

Keywords: Concrete, Fly ash, Compressive strength, Splitting tensile strength

[1] Asistent, Akademija tehničko-vaspitačkih strukovnih studija, Niš, Republika Srbija, dusan.kocic@akademijanis.edu.rs
[2] Viši predavač, Akademija tehničko-vaspitačkih strukovnih studija, Niš, Republika Srbija, jelena.bijeljic@akademijanis.edu.rs
[3] Vanredni profesor, Građevinsko-arhitektonski fakultet, Niš, Republika Srbija, nenad.ristic@gaf.ni.ac.rs

1. INTRODUCTION

World trends in the field of ecology, which are also transferred to construction, promote a more rational use of building materials and the reduction of their harmful impact on the environment. In recent years in Serbia, special attention has been drawn to construction waste and industrial by-products [1]. By-products that can be used as binding materials are numerous and are produced in many branches of heavy and light industry. The most commonly used by-product in construction is fly ash (FA), and there are several crucial reasons for this. First, it is available in large quantities, and then, its favorable physical properties. FA is defined as a fine powder obtained by electrostatic or mechanical deposition of powder particles from the flue gases of furnaces fired with pulverized coal [2].
The energy system of Serbia is mainly based on thermal power plants. There are eight active thermal power plants whose main activity is energy production, and lignite ore is used as the main fuel. In just two thermal power plants "Kolubara" and "Kostolac" close to 32 million tons of lignite originating from mining basins are burned annually. On that occasion, close to 6 million tons of waste is created in the form of fly ash, which is most often deposited. If we take into account that fly ash can be used as a basic binder for making geopolymers, it is clear that Serbia has the potential to develop in this area. Greater use of fly ash would reduce environmental pollution, and the space planned for disposal would be used more rationally [3].

2. DETAILS OF THE EXPERIMENT

In this study cement and fly ash were used as binder materials. CEM II 42.5 R produced by the company "Titan" from Kosjerić was used as the basic binder for concrete production. The volumetric mass of the cement used is up to 360 kg/m^3. FA originates from thermal electric power plant Kostolac "B''. Previously, FA was passed through the sieve with 0.09 mm openings. The chemical compositions of cement and FA were given it Table 1.

Tab. 1 Chemical composition of fly ash and cement

SiO_2	Fe_2O_3	Al_2O_3	CaO	MgO	SO_3	P_2O_5	TiO_2	Na_2O	K_2O
Fly ash									
51,68	11,58	20,16	7,43	2,41	1,02	0,12	1,04	0,88	1,04
Cement									
19,3	2,87	4,28	62,8	2,2	3,05	0,06	0,01	0,21	0,91

Aggregate used, for the production of all concrete samples, three-fraction river aggregate originating from South Morava was used. The total volumetric mass of the aggregate is 1820 kg/m^3.
For the purposes of testing, four series of different concrete mixtures were made in which partial replacement of cement was carried out in the amount of 10% - 30% with a replacement step of 10% in relation to the mass of the binder. The first concrete mixture was called the reference mixture and was marked with the symbol "E". The mixture made with 90% by weight of cement as a binder and 10% fly ash was named "10 P". The mixture made with 80% by mass percentage of cement as a binder and 20% fly ash was called "20 P". A similar labeling analogy was adopted for the mixture made with 30% by weight of fly ash as a binder, so the mixture was labeled "30 P". The mix design of the mentioned mixtures for 1 m^3 of concrete

mixture is given in Table 2. Master Glenium Sky 695 BASF plasticizer was used during the preparation of the concrete mix.

Tab. 2 Mix design of tested concrete mixtures for 1m³ of concrete

Name of the mixture	Mixture						
	Cement kg/m³	Fly ash kg/m³	Aggregate 0/4 kg/m³	4/8 kg/m³	8/16 kg/m³	Additive kg/m³	Water kg/m³
E	360	-	840	290	690	14,25	180
10 P	330	30	830	290	680	14,12	180
20 P	300	60	805	280	665	23,28	195
30 P	270	90	785	275	650	22,98	205

3. EXPERIMENTAL RESEARCH

Mixing of cement mixtures was carried out in a laboratory counter-current mixer manufactured by "Metalika Sopot". The mixer used is with a vertical shaft and a mixing drum capacity of 50 liters. During the preparation of cement concrete mixtures with the addition of FA, the preparation process began with wetting the mixer drum, after which the aggregate was measured and poured into the mixer drum. Then, in order to wet the aggregate more evenly, half of the projected amount of water for making concrete was added. The mixing of the aggregate and water lasted for 30 seconds, after which the other components were added. The total time of mixing the concrete in the mixture drum was 5 minutes [4].

The determination of the volumetric mass of concrete in the fresh (embedded state) was carried out according to the standard - SRPS EN 12350-6:2019 [5]. After preparation, fresh concrete was poured into a metal vessel with a volume of 8 liters, after which the concrete was measured on a laboratory scale manufactured by "Fuzhou Kerndy Electronics". Consistency was determined by the slump flow test method. The test was performed according to the standard - SRPS EN 12350-8:2019 [6]. Figure 1 shows concrete of the fourth series, with a share of 30% of fly ash, after testing by the settlement method. Testing of the air content in fresh concrete was performed according to the SRPS EN 12350-7:2019 standard [7]. The content of entrained air was determined using a device called a porosimeter by the manufacturer "Testing" whose container volume is 8 liters. Figure 1 (left) shows concrete after preparation and pouring into plastic molds, while Figure 1 (right) shows concrete of the same batch after testing the percentage of entrained air in the fresh concrete mix.

A compressive strength test was performed on the hardened concrete cube-shaped samples, while the tensile strength test was performed on the cylinder-shaped concrete samples. For each batch of concrete mix, three cube-shaped test specimens and three cylinder-shaped test specimens were made. The dimensions of the cube-shaped test specimens are 100x100x100 mm, and the dimensions of the cylinder-shaped test specimens are 100 mm in height and 99 mm in diameter. The appearance of the concrete samples after preparation is given in Figure 1.

Fig. 1 (left) Appearance of concrete samples after pouring into plastic molds, (right) examination of the percentage of entrained air in the fresh concrete mass

4. RESULTS AND DISCUSSION

After the concrete was made, the volume of the mass in the fresh state, the consistency parameters using the settling method and the percentage of entrapped air in the fresh concrete mixture were tested. The test results are given in Table 3.

Tab. 3 Results of concrete testing in fresh state

Name of the mixture	Tested parameters			
	Volumetric mass in the fresh state kg/m^3	Temperature ^{o}C	Consistency by settling method mm	Percentage of entrained air %
E	2362	22,8	170	3,1
10 P	2362	22,8	165	3,1
20 P	2310	22,9	160	3,4
30 P	2279	22,8	110	3,5

The concrete settlement of test bodies of the "E" series was 170 mm. Also, the percentage of entrained air was determined and it is 3.1% for this mixture. The settlement of the "10 P" series concrete was 165 mm (Figure 2 left), while the measured percentage of entrained air was 3.1 %. The total amount of entrained air is 3.1% (Figure 2 right). On the third batch of concrete, labeled "20 P", which was made so that its binder composition made up 20% of FA, the measured concrete temperature was 22.9^{o} C. The settlement of this batch of concrete was 160 mm, while the percentage of entrained air was 3.4%. Finally, the characteristics of fresh concrete of the "30 P" series were measured. The temperature of fresh concrete was 22.8^{o} C. The measured settlement of this batch of concrete was 110 mm, while the percentage of entrained air was 3.5%.

Fig. 2 (left) Consistency test using the settling method, (right) test of the percentage of entrained air in fresh concrete mass

After reaching the required age of the concrete, the mechanical characteristics of the concrete were examined. The results of the compressive strength test of concrete are given in Figure 3, while the results of the tensile test using the splitting method are given in Figure 4. According to the results of the compressive strength test given in Figure 3, it can be clearly seen that there is a trend of decreasing compressive strength between the tested samples a mixture of "10 P" and "20 P".

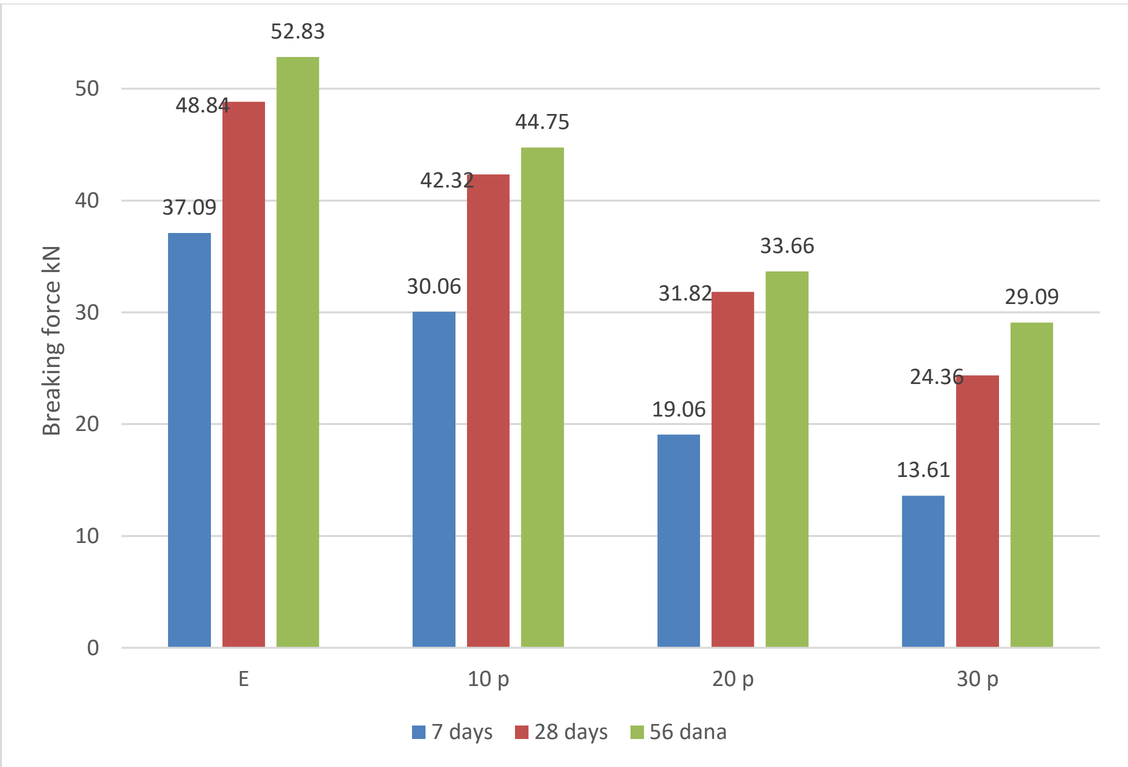

Fig. 3 The results of concrete compressive strength tests

The biggest difference in compressive strength occurs in samples tested after 7 days. In fact, the test concrete body with 20% FA has a lower compressive strength by 36.59% than the concrete samples made with 10% FA. This difference in the same series of samples tested after 28 and 56 days amounts to approximately 25%. The smallest difference in compressive strength was measured in samples aged 56 days, labeled "20 P" and "30 P". The measured difference in compressive strength of the mentioned series was 13.58%. The trend of decreasing breaking force as a function of the change in the proportion of FA was observed in all tested series. The value of the breaking force, for the tested samples after 56 days, decreased by 44.94%. The samples tested after 7 days recorded a decrease in the value of the breaking force by 63.31%, which is expected.

The difference in compressive strength of the series of specimens tested after 28 and 56 days is negligible compared to the difference that can be observed by comparing the results after 7 and 28 days.
Figure 4 shows the results of the tensile strength test. The test was carried out on cylinder-shaped samples. According to the presented results, it can be concluded that the biggest difference in tensile strength at splitting was measured on the samples of the "20 P" and "30 P" series. The mentioned difference amounted to 31.17%. The smallest difference in tensile strength at splitting was measured on samples "10 P" and "20 P", which is 7.42%. The total drop in breaking strength between samples of standard "E" and series of concrete marked "30 P" amounted to 45.01%.

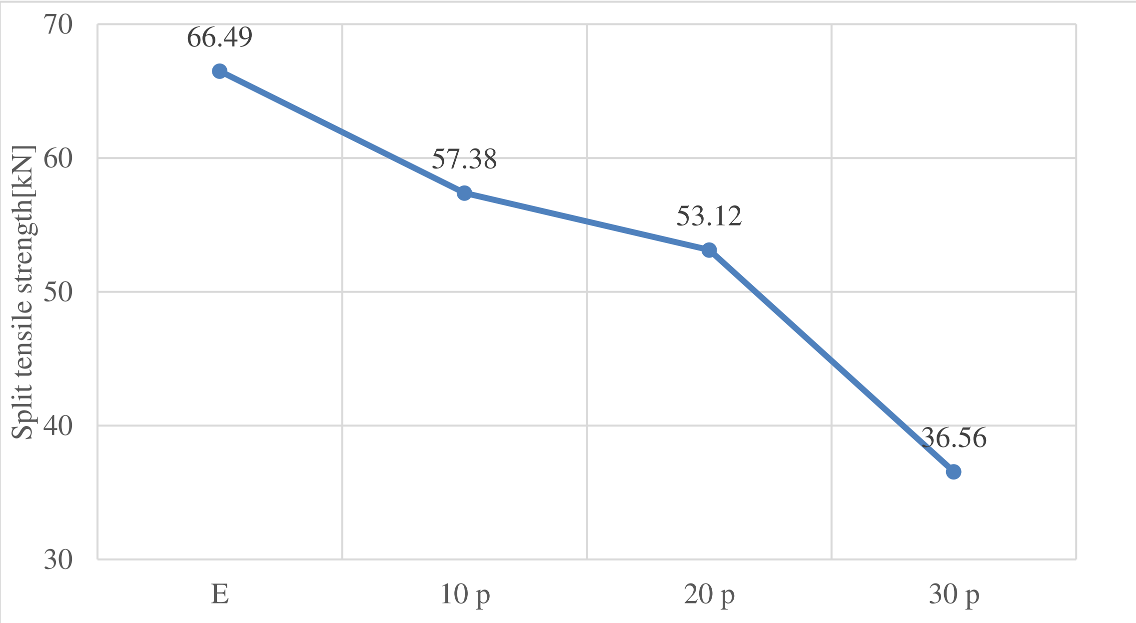

Fig. 4 Results of concrete tensile strength test using splitting method

5. CONCLUSION

In the present paper, a study of the effect of different fly ash percentage per mass ration on fresh and hardened state of concrete was carried out. Concrete mixtures were designed by using Portland cement and fly ash in the amount of up to 30 % of the cement mass, in replacement step od 10 %, in order to improve concrete properties.
The results can be summarized as follows:

- a decrease in the volumetric mass value was observed with an increase in the proportion of fly ash;
- the value of the settlement of the narrow standard and the "P30" sample is 35.29%. The percentage of the concrete's slump value increases rapidly as a function of the increase in the amount of fly ash;
- the difference in compressive strength shows a constant decreasing trend. The difference of the values itself decreases as a function of time.
- tensile strength by splitting shows the biggest difference, in relation to the standard, on the sample "P30". The "P20" sample can be considered as the optimal amount of fly ash, in terms of reducing tensile strength by splitting.

LITERATURE

[1] M. M. Životić, D. D. Stojiljković, A. M. Jovović, V. V. Čudić (2012): „Mogućnost korišćenja pepela i šljake sa deponije termoelektrane „Nikola Tesla“ kao otpada sa upotrebnom vrednošću“, Hemijska industrija, Vol. 66(3), pp. 403-412

[2] SRPS EN 450-1:2014: Leteći pepeo za beton — Deo 1: Definicija, specifikacije i kriterijumi usaglašenosti

[3] J. Bijeljić (2020): „Mogućnost primene industrijskih nusproizvoda u geopolimernim malterima i betonima na bazi elektrofilterskog pepela“, doktorska disertacija, Univerzitet u Nišu, Građevinsko – arhitektonski fakultet Niš

[4] I. Despotović (2015): „Svojstva samougrađujućeg betona spravljenog sa recikliranim agregatom i različitim mineralnim dodacima“, Građevinski materijali i konstrukcije, Vol. 58(4), pp. 3-20

[5] SRPS EN 12350-6:2019: Ispitivanje svežeg betona – Deo 6: Zapreminska masa

[6] SRPS EN 12350-8:2019: Ispitivanje svežeg betona – Deo 8: Samougrađujući beton – Ispitivanje rasprostiranja sleganjem

[7] D. Adak, M. Sarkar, S. Mandal (2014): „Effect of nano-silica on strength and durability of fly ash based geopolymer mortar“, Construction and building materials, Vol. 70, pp. 453–459

CONCRETE SURFACE CHARACTERISATION WITH HANDHELD XRF: EFFECT OF WATER-TO-CEMENT RATIO, CURING TIME AND RELATIVE HUMIDITY

Laura Sofía Gómez Jaramillo[1], Marcel Hermans[2],Marija Nedeljković[3]

Summary:

Recycled concrete aggregates (RCA) have been recognised as a sustainable solution to address the environmental impacts of the concrete industry. However, engineers and contractors still have reservations about RCA due to their heterogeneous origin and lower quality compared to natural aggregates. Understanding the chemical composition of the original concrete is crucial before demolishing structures to trace the source of the raw materials, yet this has never been done before. This study aims to asses the impact of water-to-cement (w/c) ratios ranging from 0.35 to 0.76, curing time of 1 day, 14 days and 28 days, and surface relative humidity (RH) ranging from 0 to 95% on the surface chemical composition analysis of concrete with handheld X-ray fluorescence (hXRF). The hypothesis was that the chemical analysis using hXRF reveal consistent levels of key oxides on the concrete surface, regardless of w/c, curing time, or RH. Lastly, this study provides knowledge of factors influencing the detection of oxides in cementitious materials.

Keywords: concrete; chemical composition; handheld X-ray fluorescence; non-destructive testing

[1] Faculty of Mechanical, Maritime and Materials Engeering, Delft University of Technology, The Netherlads

[2] Faculty of Mechanical, Maritime and Materials Engeering, Delft University of Technology, The Netherlads

[3] [a] Faculty of Civil Engineering & Geosciences, Delft University of Technology, The Netherlands

[b] Rijkswaterstaat, Dutch Ministry of Infrastructure and Environment, The Netherlands

1. INTRODUCTION

The construction sector has a crucial impact on materials consumption and carbon emissions. Concrete, being one of the most employed building materials, not only adds to carbon emissions and energy consumption but also heavily relies on natural resources like sand, stone, or gravel in excessive quantities [1]. Research for obtaining the high-quality of recycling concrete materials has been ongoing over the past decade. Currently, the most applied practice for concrete recycling involves crushing and producing recycled concrete aggregates (RCAs) [2]. The RCAs are often used for applications such as road base constructions, indicating that only a small percentage of demolished concrete is recycled for applications with the same or higher quality as the original material [3]. Some countries like The Netherlands and Belgium are already facing a problem of saturation of low-quality RCAs in the aggregates market [4]. Additionally, construction engineers, concrete producers, and real state owners still have doubts about using RCA because RCA are often inconsistent in composition and have lower quality compared to natural aggregates (NA). Structural engineers, in particular, encounter uncertainties when tasked with designing structural members using concrete with RCAs [3] [5]. This emphasises the significance of investigating novel technologies to improve the quality of RCAs while reducing their expenses in comparison to natural aggregates.

RCAs are distinguished by their higher water absorption and lower specific gravity compared to natural aggregates. Additionally, RCAs exhibit a weak interfacial zone between the mortar and the aggregate. This leads, for high replacement percentages, to increased permeability, higher shrinkage, and reduced compressive strength of the resulting concrete, ultimately affecting its overall quality [6] [7].

Some studies [6], [8] have indicated that the quality of RCAs is primarily influenced by the quality of the original demolished concrete. Furthermore, understanding the origin and properties (chemical, physical and mechanical) of the parent concrete can help improving predictions regarding the impact of the RCAs on the properties of the new concrete with RCAs [9]. A potential strategy to enable effective quality control of RCAs involves implementing selective demolition. This approach entails the gradual disassembly of concrete structures, enabling sorting processes [4] [5] [10]. Lately, a systematic method has been introduced for assessing concrete through non-destructive testing techniques before its demolition, particularly in cases where information about the original concrete is absent. This classification of concrete relies on factors such as concrete strength and chemical composition [5].

Testing the chemical composition of the original concrete before demolition provides two types of information. Firstly, it provides insight into the primary components of the concrete, such as cement and aggregates. Secondly, it identifies potential minor elements and contaminants. Knowing the type of cement used in original concrete is particularly valuable for determining the future applications of recycled materials. For instance, knowing the cement type allows decisions about whether the fine recycled concrete aggregates can be used as a raw material for clinker manufacturing, as a pozzolanic material, or as a filler. Remarkably, research has not yet delved into the chemical composition of the original concrete before demolition of concrete structures, specifically in the context of selective demolition [12].

Methods for characterising the concrete chemical composition necessitate the extraction of concrete samples from the concrete structure, followed by laboratory analysis. The extraction process can be demanding and time-consuming [10].

Non-destructive methods were not explored for testing the chemical composition of concrete in situ. One such method is the handheld X-ray fluorescence analyzer (hXRF). This method provides an advanced non-destructive analysis for characterizing the chemical composition of cementitious materials. It has been applied in various fields, including mineral exploration [11], geology [12], cultural heritage [13] [14] [15], archaeology [16], art [17], and environmental science [18], as well as the analysis of cementitious materials and concrete [9] [19] [10] [20] [21]. The primary advantages of hXRF include its ability to rapidly gather substantial amounts of data and its flexibility in sample preparation, which can vary from none (for in-situ, non-destructive analysis) to extensive (involving sample collection, homogenization, and pellet production), depending on the user's preferences [22]. Some researchers aimed to investigate the chemical composition of various cement types and concretes [9], as well as the influence of different factors (measurement time, moisture, surface carbonation, and matrix effect) on concrete composition using hXRF [10]. However, the effects of ageing, different water-to-cement ratios, and a wide range of relative humidities on the detection of concrete's characteristic oxides have not been investigated.

Taking all of this into consideration, this study investigates the effect of water-to-cement ratio, ageing and relative humidity on the testing of concrete surfaces with hXRF. Understanding the effect of these parameters is crucial for in situ assessment of concrete chemical composition with hXRF and for development of a testing guideline.

2. EXPERIMENTAL PROGRAM

The experimental program consisted of three Test Series: (1) testing chemical composition of concrete mixtures with different water-to-cement (w/c) ratios ranging from 0.35 to 0.76; (2) testing chemical composition of concrete after curing of 1 day, 14 days, and 28 days; and (3) testing concrete chemical composition under varying surface relative humidities of 0%, 40%, 60%, 75%, and 95%.

2.1. MATERIALS

The following materials were used for the production of the concrete specimens: CEM I 42.5 N (Portland cement), CEM III/B 42.5 (GGBFS cement), sand 0-4 mm, gravel 4-16 mm, and water.

To achieve relative humidity (RH) conditions of 60% and 75%, the following salts were used: sodium bromide (NaBr) and sodium chloride (NaCl).

2.2. CONCRETE PRODUCTION

2.2.1. Mix design

The consitency class was selected with a slump of 100 mm to 150 mm according to NEN-EN 206+NEN 8005:2017. Therefore, the water content was equal to 190 kg/m^3. The volume of air was considered to occupy 2% of the total concrete volume.

Tab. 1 shows seven different concrete mix designs (M1-M7) used in this study. For Test Series 1, the mixtures had different water-to-cement (w/c) ratios of 0.35, 0.38, 0.42, 0.48, 0.54, 0.63, and 0.76. In Test Series 2 and Test Series 3 concrete cubes were cast with a w/c ratio of 0.54 (M3).

Tab. 1 Proportions of concrete mixtures (kg/m^3)

	Concrete mixtures						
	M1	M2	M3	M4	M5	M6	M7
w/c	0.76	0.63	0.54	0.48	0.42	0.38	0.35
Water	190	190	190	190	190	190	190
CEM III/B 42.5N (CEM I 42.5N)	250	300	350	400	450	500	550
Sand 0-4 mm	841.02	820.80	800.59	780.38	760.17	739.96	719.74
Gravel 4-16 mm	1027.91	1003.20	978.50	953.80	929.09	904.39	879.69

2.2.2. Sample preparation

The raw materials were placed in a 40 L mixer in the specified order: coarse aggregates, fine aggregates, cement, and water. The sand and gravel were mixed for 1 minute. Then, the cement was added, and the mixture was further mixed for 1 minute. Finally, the water was added, and all components were mixed for an additional 3 to 5 minutes, depending on the desired consistency of the mixture.

The concrete cubes were cast into moulds 150 × 150 ×150 mm³. For each mixture three cubes were cast, Cube 1 (C1), Cube 2 (C2), and Cube 3 (C3). The moulds were oiled before casting in order to prevent the paste from adhering. Next, the moulds were placed on a compaction table, and the concrete was poured into two layers. After filling the moulds halfway, they were compacted for 10 seconds to eliminate trapped air. Following this step, the smooth surface of the fresh concrete was leveled using a straight edge.

The samples were demoulded 24 hours after casting. In order to proceed with the first set of experiments (Test Series 1), seven concrete cubes (one cube from each mix) were used. The rest of the samples were wrapped in a plastic film, and placed inside large plastic bags. Then, cubes were stored in a room maintained at a temperature of 20 °C and a relative humidity of 50% (see Fig. 1), until they were needed for the tests. The decision to wrap the concrete specimens in plastic film and store them in large plastic bags was made to prevent surface efflorescence.

(a) (b) (c)

Fig. 1 Demoulding and wrapping of concrete cubes (a) After casting, (b) Wrapping of the specimens with the plastic film, (c) Placing samples in plastic bags

In order to conduct measurements for Test Series 1 using handheld X-ray fluorescence (hXRF), Wavelength-Dispersive X-ray Fluorescence (WDXRF) and Environmental Scanning Electron Microscope and Energy-Dispersive X-ray Spectroscopy (ESEM-EDS), it was necessary to reduce the size of the concrete cubes. As a result, lines were drawn on two surfaces of each concrete cube using a carbon pencil to indicate where to make cuts in order to obtain smaller concrete specimens. For the Test Series 1 and Test

Series 2 specimens of 30 mm × 30 mm × 20 mm were used. For the Test Series 3 specimens of 50 mm × 50 mm × 20 mm were used.
The specimens were cut using two different saws. The first saw, with a blade thickness of 3 mm, was used to cut the two surfaces (SI and SII) from each cube. The second saw, with a blade thickness of 1 mm, was used to cut the smaller cubes. Both cutting sessions were conducted under wet conditions for safety reasons. Dry cutting results in the release of a significant amount of dust into the air.
After cutting, the samples were first submerged in ethanol for approximately 10 seconds and then dried with compressed air (about 20 seconds per sample). However, it was observed that some parts of the samples remained wet. Consequently, it was decided to place the specimens in an oven at 105 °C for 15 minutes to ensure that the sample surfaces were thoroughly dried.
Finally, the samples were labeled as shown in Tab. 2, Tab. 3, Tab. 4, depending on their test series. In Test Series 1, the concrete cubes were produced using CEM III/B 42.5N, and three size-reduced concrete samples (1, 2, and 3) were taken from C1 for each mixture, specifically for the hXRF measurements. For the measurements using WDXRF and ESEM-EDS only sample 1 from each mixture was tested.
In Test Series 2, the sample M3-SI-1 from Test 1 was used for the hXRF measurements.
In Test Series 3, the concrete cubes were cast using both CEM I 42.5N and CEM III/B 42.5N. Three size-reduced concrete samples (1, 2, and 3) were taken from either C1 or C2 and used for hXRF measurements.

Tab. 2 Labelling concrete specimens for Test Series 1

CEM III/B 42.5 N	M1-SI-1 M1-SI-2 M1-SI-3	M2-SI-1 M2-SI-2 M2-SI-3	M3-SI-1 M3-SI-2 M3-SI-3	M4-SI-1 M4-SI-2 M4-SI-3	M5-SI-1 M5-SI-2 M5-SI-3	M6-SI-1 M6-SI-2 M6-SI-3	M7-SI-1 M7-SI-2 M7-SI-3

Tab. 3 Labelling concrete specimens for Test Series 2

CEM III/B 42.5 N	M3-SI-1

Tab. 4 Labelling concrete specimens for Test Series 3

	0%	40±5%	60±5%	75±5%	95±5%
CEM I 42.5 N	M3-C2-SII-1 M3-C2-SII-2 M3-C2-SII-3	M3-C2-SII-1 M3-C2-SII-2 M3-C2-SII-3	M3-C1-SI-1 M3-C1-SI-2 M3-C1-SI-3	M3-C2-SII-1 M3-C2-SII-2 M3-C2-SII-3	M3-C2-SII-1 M3-C2-SII-2 M3-C2-SII-3
CEM III/B 42.5 N	M3-C2-SII-1 M3-C2-SII-2 M3-C2-SII-3	M3-C2-SII-1 M3-C2-SII-2 M3-C2-SII-3	M3-C1-SII-1 M3-C1-SII-2 M3-C1-SII-3	M3-C1-SII-1 M3-C1-SII-2 M3-C1-SII-3	M3-C1-SII-1 M3-C1-SII-2 M3-C1-SII-3

2.3. METHOD AND INSTRUMENTATION

Once the samples were cut and dried, those intended for Test Series 1 (M1-SI-1, M2-SI-1, M3-SI-1, M4-SI-1, M5-SI-1, M6-SI-1, and M7-SI-1) were selected for the analysis of their surface chemical composition using hXRF. Subsequently, measurements using WDXRF were conducted seven days later. Testing with ESEM-EDS was carried out a day after tests with WDXRF. During periods when the samples were not in use, they were stored in zipper bags and placed in a vacuum chamber. This approach aimed to preserve the material's original properties by minimising exposure to external factors that could potentially lead to degradation or changes.
This research employed a Bruker S1 TITAN 800 handheld XRF analyser (Fig. 2a) with specific features, including a rhodium tube for X-ray emission and a high-resolution

Silicon Drift (SDD) detector with a 145 eV resolution. To prevent direct contact with materials, there is a plastic film covering both the detector and the X-ray tube. Despite the option to use filters for better element detection, this study opted not to. Previous findings reported more precise measurements without filters [14], especially when analyzing historical mortars resembling concrete. The accelerating voltage was set at 15 keV. For measurement time, it was decide to set it at 30 seconds, following recommendations from previous studies that found this duration to be suitable for concrete analysis [19] [10]. Additionally, 10 consecutive measurements were taken without moving or lifting the sample between measurements.

Samples were also analyzed using a Panalytical Axios Max Wavelength Dispersive X-ray Fluorescence (WDXRF) spectrometer with an X-ray tube power of 4 kW (Fig. 2b). This instrument features an X-ray tube that serves as the source to irradiate the sample. The resulting fluorescence emitted by the sample is detected using a wavelength dispersive system. Analyzing crystals are components used to separate X-rays based on their wavelengths or energies, enabling the identification of each element's characteristic radiation. This analysis can be conducted either sequentially, measuring X-ray intensities at various wavelengths one by one, or simultaneously, where X-ray intensities at different wavelengths are measured all at once [23].

The ESEM-EDS analysis was performed with a Thermo Fisher™ Ultradry EDS detector (Fig. 2c). It operates with an energy beam ranging from 6 to 50 kV and has a beam size of 125 μm, which can be reduced to analyse a smaller area. Unlike hXRF, the ESEM-EDS can work in a vacuum and uses a windowless Silicon Drift Detector (SDD) that provides high-resolution detection for lighter elements like Beryllium (Be), with a resolution of 129 eV. The analysis was performed at an accelerating voltage of 15 keV. To analyze the chemical composition of concrete, elements associated with expected concrete oxides (MgO, Al_2O_3, SiO_2, P_2O_5, SO_3, K_2O, CaO, TiO_2, MnO and Fe_2O_3) were selected in the ESEM-EDS software.

(a) (b) (c)

Fig. 2 Instrumentation for composition analysis of concrete (a) hXRF, (b) WDXRF, (c) ESEM-EDS

The area analysed in each sample by hXRF, WDXRF, and ESEM-EDS is shown in Fig. 3. On one hand, the size of the area analysed with hXRF was a disc with a diameter of 5 mm, corresponding to the size of the X-ray beam emitted by the device. On the other hand, the area examined with WDXRF corresponded to a diameter of 27 mm. Finally, the area under analysis with ESEM-EDS was a rectangle measuring 3.3 mm × 2.2 mm, observed at a magnification of 125×.

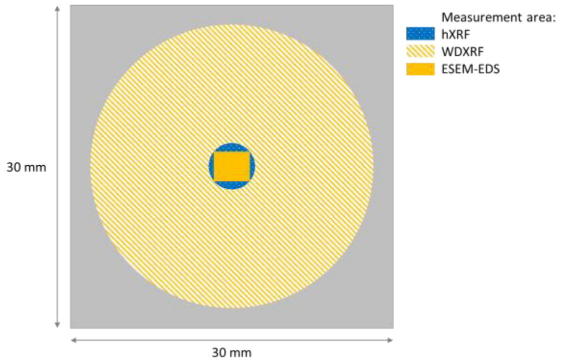

Fig. 3 Measurement areas with hXRF,WDXRF, and ESEM-EDS

For Test Series 2, the sample M3-SI-1 was used. The measurements conducted with hXRF during Test Series 1 provided results for day 1, and then measurements were performed at 14 days and 28 days. The sample was stored in the vacuum chamber during periods when testing was not being conducted.

For Test Series 3, various setups were defined to create the necessary environmental conditions for conducting this experiment. Tab. 5 shows the techniques or equipment used, along with the temperatures and relative humidities considered in this Test Series.

Tab. 5 Specifications for Test Series 3

RH	0%	40%	60%	75%	95%
Temp.	40 °C	20 °C	20 °C	20 °C	20 °C
Equipment/materials used	Oven	Climate chamber	Salt-saturated solution sodium bromide (NaBr)	Salt-saturated solution sodium chloride (NaCl)	Curing room

As found in the literature [24], to achieve a relative humidity of 60% and 75%, the salts sodium bromide (NaBr) and sodium chloride (NaCl) can be respectively used. Therefore, salt-saturated solutions were prepared with these salts and placed in plastic containers. To ensure and monitor the desired RH levels, an EL-USB-2 Humidity-Temperature Datalogger was placed in the containers during 24 hours. It was considered that the concrete samples were in equilibrium with their environment or had reached the respective relative humidity when their weight remained almost the same for two consecutive days. The samples were estimated to have reached the desired relative humidity after approximately 10-13 days. After this period, the hXRF measurements were performed.

3. RESULTS AND DISCUSSIONS

Cement primarily consists of clinker minerals, with the most common ones being tricalcium silicate (C3S), dicalcium silicate (C2S), tricalcium aluminate (C3A), and tetracalcium aluminoferrite (C4AF). When cement is mixed with water, it undergoes a chemical reaction known as hydration. During this process, hydration products are formed, including calcium silicate hydrate (C-S-H) gel, calcium hydroxide (CH), and ettringite [25]. These products play a crucial role in determining the strength and durability of concrete. Therefore, different water-to-cement ratios in a concrete mix design affect properties like workability and strength of concrete. It is hypothesized that there is no change in the chemical composition of concrete when different water-to-cement ratios are used. The chemical reactions during hydration involve cement compounds and water, without altering the original chemical composition of the cement [25]. Fig. 4 illustrates this hypothesis, showing that the concentration of characteristic element oxides in concrete, as measured with hXRF, remains nearly constant regardless of the water-to-cement ratio.

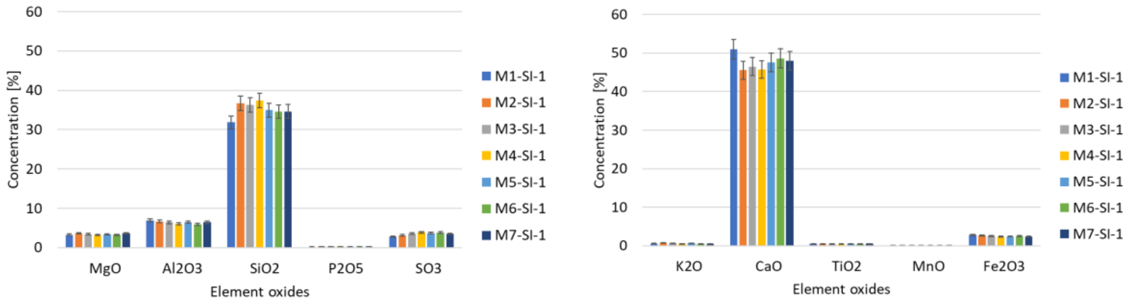

(a) (b)

Fig. 4 Effect of different water-to-cement ratios

Tab. 6 gives an overview of hXRF, WDXRF and ESEM-EDS results for surface chemical composition of the concrete samples M1-SI-1, M2-SI-1, M3-SI-1, M4-SI-1, M5-SI-1, M6-SI-1, and M7-SI-1. It can be seen that there are variations in the results for some oxide concentrations among the different methods. For instance, when examining SiO2, the element concentrations obtained with hXRF differs by nearly 8% compared to the other two methods. Similarly, for CaO, the difference is approximately 10%. However, there is an agreement between hXRF and WDXRF results for MnO and Fe2O3. These variations in chemical composition values can be attributed to several factors, including sample preparation, sample heterogeneity, and the presence of calcite crystals on the surface. Calcite crystals may have formed due to surface carbonation of the samples during the transportation of samples from one location to another for testing and during the testing process with WDXRF and ESEM-EDS methods.

Tab. 6 Chemical composition of concrete surfaces

Sample	w/c	Method	MgO	Al_2O_3	SiO_2	P_2O_5	SO_3	K_2O	CaO	TiO_2	MnO	Fe_2O_3
M1-SI-1	0.76	hXRF	3.28	6.92	31.85	0.18	2.80	0.58	50.96	0.49	0.15	2.83
		WDXRF	2.81	7.20	24.50	0.20	2.05	0.75	57.89	0.52	0.16	2.83
		EDS	2.42	6.35	23.77	0.08	1.66	1.09	60.72	0.60	0.00	2.69
M2-SI-1	0.63	hXRF	3.64	6.68	36.71	0.23	3.15	0.75	45.50	0.49	0.15	2.72
		WDXRF	3.58	6.65	29.73	0.25	2.11	0.79	52.76	0.49	0.16	2.56
		EDS	3.63	6.32	29.41	0.15	2.64	0.92	53.88	0.68	0.00	2.36
M3-SI-1	0.54	hXRF	3.42	6.43	36.25	0.21	3.56	0.61	46.46	0.46	0.14	2.49
		WDXRF	3.31	6.41	28.69	0.24	2.33	0.64	54.29	0.53	0.15	2.50
		EDS	3.11	5.99	27.28	0.14	2.82	1.10	56.66	0.61	0.00	2.31
M4-SI-1	0.48	hXRF	3.25	6.06	37.43	0.21	3.86	0.57	45.72	0.45	0.14	2.37
		WDXRF	3.27	6.32	26.76	0.22	2.80	0.55	55.91	0.69	0.15	2.59
		EDS	2.63	5.24	25.58	0.16	3.87	0.86	59.91	0.07	0.22	1.46
M5-SI-1	0.42	hXRF	3.35	6.46	34.98	0.23	3.71	0.69	47.56	0.46	0.15	2.44
		WDXRF	3.31	6.24	25.78	0.21	2.37	0.65	57.40	0.50	0.17	2.48
		EDS	2.85	5.24	24.88	0.23	2.93	1.08	60.20	0.81	0.00	1.78
M6-SI-1	0.38	hXRF	3.24	5.89	34.61	0.23	3.81	0.56	48.61	0.46	0.15	2.48
		WDXRF	3.31	6.21	24.57	0.23	2.85	0.53	58.10	0.58	0.16	2.70
		EDS	3.53	5.56	23.47	0.13	4.50	0.86	59.45	0.57	0.00	1.93
M7-SI-1	0.35	hXRF	3.66	6.43	34.64	0.25	3.50	0.55	48.00	0.47	0.15	2.37
		WDXRF	3.45	6.38	25.51	0.24	2.42	0.48	57.62	0.47	0.17	2.45
		EDS	3.12	6.66	25.05	0.07	3.40	0.98	57.30	0.81	0.18	2.43

Fig. 5 shows the element oxide concentrations measured on the concrete surfaces after 1 day, 14 days and 28 days of curing. The characteristic oxides remain similar regardless of the sample's curing time. This suggests that the hXRF measurements are independent of the curing time of the concrete specimens.

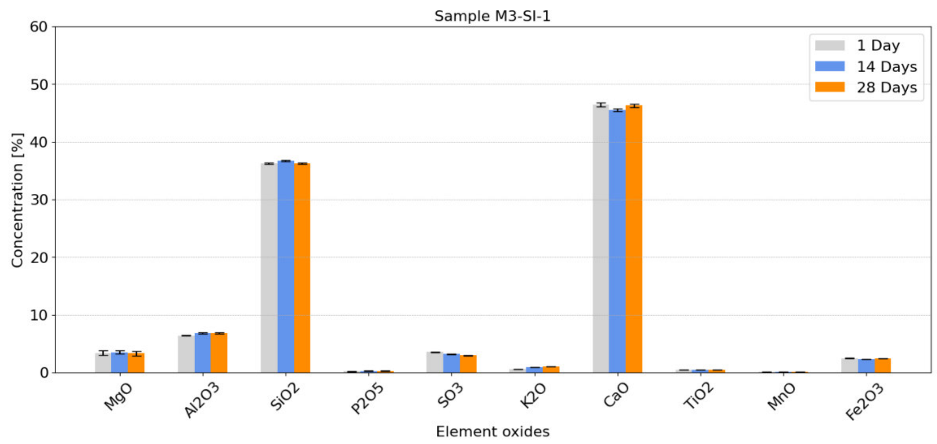

Fig. 5 Effect of curing time on the chemical composition analysis of concrete surfaces

The results of the chemical composition for the concrete specimens, which were exposed to drying conditions and relative humidities of 40%, 60%, 75%, and 95%, are presented in Fig. 6. It is important to highlight that the grey label specified as 'before' refers to the initial moment when the hXRF measurements were conducted on each specimen. The labels 'dried condition' and 'after 40%, 60%, 75%, and 95%' refer to the hXRF measurements taken after the samples were exposed to those respective conditions, which occurred approximately 10-13 days later.

It can be observed that at relative humidities of 40%, 60%, and 75%, the concentrations of characteristic elemental oxides remain similar. However, at 95% RH, there is a significant increase in calcium oxide concentration. This increase can be attributed to the presence of both CO2 and H2O in the environment where the samples were located. In such conditions, several chemical reactions occur, including the diffusion of CO2 at the gas/liquid interface, its dissolution in water as carbonic acid (H2CO3), subsequent dissociation into HCO_3^- and CO_3^{2-} ions, the dissolution of solid Ca(OH)2 (calcium hydroxide) with the release of calcium Ca^{2+} and hydroxyl OH^- ions, and the precipitation of Ca^{2+} with CO_3^{2-} to form CaCO3 (calcium carbonate) [26] [27].

According to López-Arce et al. [26] relative humidity higher than 75% lead to the formation of amorphous calcium carbonate, monohydrocalcite, calcite, aragonite, and vaterite with larger particle sizes and higher crystallinity than at the lower RH. These findings can explain the observed increase in calcium oxide at the sample surfaces exposed to 95% RH.

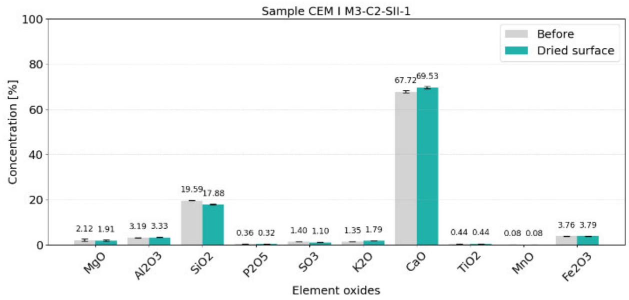

(a)

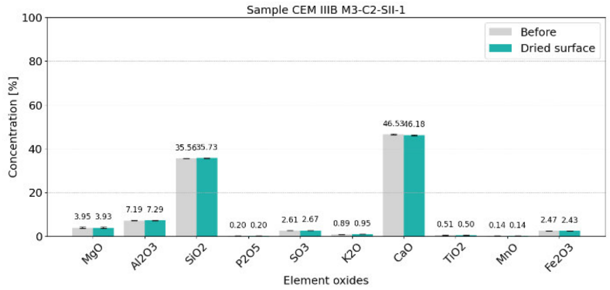

(b)

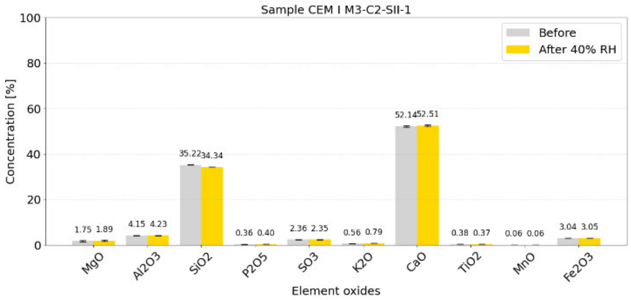

(c)

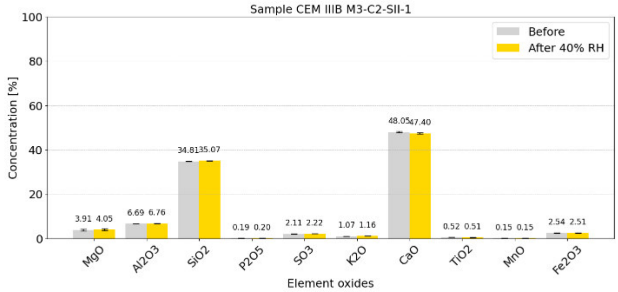

(d)

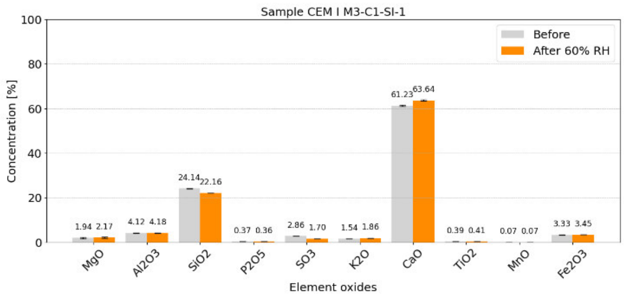

(e)

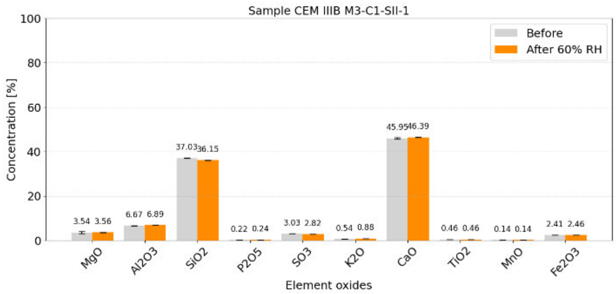

(f)

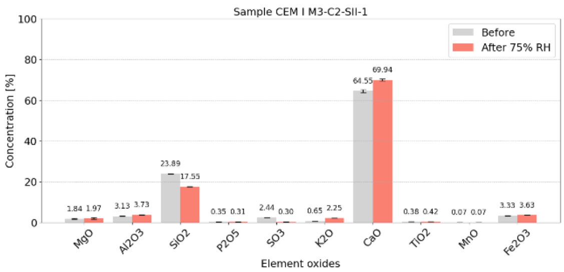

(g)

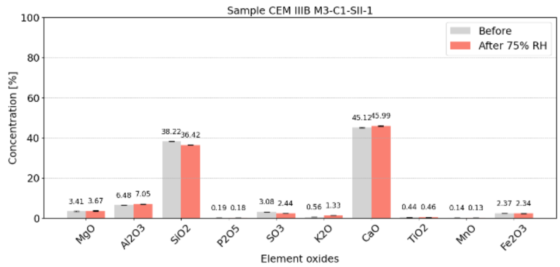

(h)

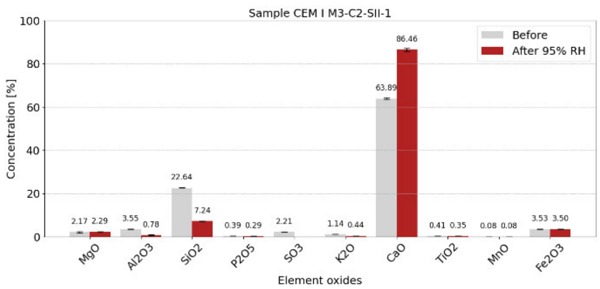

(i)

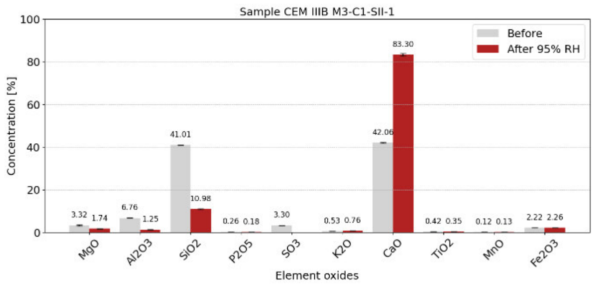

(j)

Fig. 6 Effect of relative humidity on the chemical composition analysis of concrete surfaces

4. CONCLUSIONS

In this study three Test Series were performed to understand the effect of concrete mix designs with different water-to-cement ratio, the concrete samples' age, and the samples being exposed to different relative humidities on the analysis of their surface chemical composition with hXRF. The following conclusions can be drawn:

1. The hXRF measurements are independent of the water-to-cement ratio and age of the concrete specimens.
2. Higher relative humidity conditions than 75% affect the measurements with hXRF, potentially posing challenges in terms of data reproducibility and cement type recognition.
3. Detecting the cement type with hXRF in-situ can be challenging, considering that concrete structures are typically exposed to various environmental conditions during their service life. However, a more in-depth analysis can focus on concrete's characteristic oxides that are less influenced or unaffected by environmental conditions. The oxides, such as MnO and Fe_2O_3 can serve as characteristic oxides for cement type identification.

ACKNOWLEDGEMENT

The first author acknowledges the funding provided by the Ministry of Infrastructure and Water Management of the Netherlands (Rijkswaterstaat). Special thanks to Maiko van Leeuwen, Arjan Thijssen, Ton Blom for assistance with laboratory testing and concrete casting.

REFERENCES

[1] W. M. Shaban, J. Yang, H. S. H. Mo, L. Li and J. Xie, "Quality Improvement Techniques for Recycled Concrete Aggregate: A review," 10 April 2019. [Online]. Available: https://doi.org/10.3151/jact.17.151

[2] C. Zhang, M. Hu, X. Yang, B. Miranda-Xicotencatl, B. Sprecher, F. D. Maio, X. Zhong and A. Tukker, "Upgrading construction and demolition waste management from downcycling to recycling in the Netherlands," 22 Arpil 2020. [Online]. Available: https://doi.org/10.1016/j.jclepro.2020.121718.

[3] B. M. Xicotencatl, "Scenarios for concrete-rubble recycling in the Netherlands," 2017. [Online]. Available: https://repository.tudelft.nl/islandora/.

[4] A. D. Maria, J. Eyckmans and K. V. Acker, "Downcycling versus recycling of construction and demolition waste: Combining LCA and LCC to support sustainable policy making," 3 February 2018. [Online]. Available: https://doi.org/10.1016/j.wasman.2018.01.028.

[5] M. Nedeljković, N. Tošić, E. Schlangen and S. Fennis, "Pre-demolition concrete waste stream identification classification framework," 30 March 2023. [Online]. Available: https://doi.org/10.5937/GRMK2301001N.

[6] C. S. Rangel, R. D. T. Filho, M. Amario, M. Pepe, G. d. C. Polisseni and G. P. d. Andrade, "Generalized quality control parameter for heterogenous recycled concrete aggregates: A pilot scale case study," 12 October 2018. [Online]. Available: https://doi.org/10.1016/j.jclepro.2018.10.110.

[7] V. W. Tam, M. S. and A. C. J. Evangelista, "Quality improvement of recycled concrete aggregate by removal of residual mortar: A comprehensive review of approaches adopted," 3 April 2021. [Online]. Available: https://doi.org/10.1016/j.conbuildmat.2021.123066.

[8] I. Khaliq and M. Khan, "Effect of parent concrete on the performance of recycled aggregate concrete," 2021. [Online]. Available: www.academicjournal.in.

[9] M. Nedeljkovic, N. Tosic, P. Holthuizen, F. F. d. M. Filho, O. Copuroglu, E. Schlangen and S. Fennis, "Non-destructive screening methodology based on handheld XRF for the classification of concrete: cement type-driven separation," 15 March 2023. [Online]. Available: https://doi.org/10.1617/s11527-023-02147-3.

[10] J. Aoustin, "Identification of the cement type at the concrete surface with ordinary Portland cement and supplementary cementitious materials with a handheld X-ray Fluorescence analyser," 2023.

[11] G. E. Hall, G. F. Bonham-Carter and A. Buchar, "Evaluation of portable X-ray fluorescence (pXRF) in exploration and mining: Phase 1, control reference materials," May 2014. [Online]. Available: https://doi.org/10.1144/geochem2013-241.

[12] A. Steiner, R. Conrey and J. Wolff, "PXRF calibrations for volcanic rocks and the application of in-field analysis to the geosciences," 20 February 2017. [Online]. Available: https://doi.org/10.1016/j.chemgeo.2017.01.023.

[13] A. Gianoncelli, J. Castaing, E. D. L. Ortega, J. Salomon, P. Walter, J.-L. Hodeau and P. Bordet, "A portable instrument for in situ determination of the chemical and phase compositions of cultural heritage objects," March 2008. [Online]. Available: https://doi.org/10.1002/xrs.1025.

[14] F. M. Filho, H. Morillas, H. Derluyn, M. Maguregui and D. Grégoire, "In-situ versus laboratory characterization of historical site in marine environment using X-ray fluorescence and Raman spectroscopy," 22 February 2019. [Online]. Available: https://doi.org/10.1016/j.microc.2019.02.014.

[15] C. García-Florentino, M. Maguregui, H. Morillas, I. Marcaida and J. M. Madariaga, "A fast in situ non-invasive approach to classify mortars from a construction of high historical value," 24 March 2017. [Online]. Available: https://doi.org/10.1016/j.microc.2017.03.020.

[16] "Non-destructive screening methodology based on ED-XRF for the classification of medieval and post-medieval archaeological ceramics," 28 March 2019. [Online]. Available: https://doi.org/10.1016/j.ceramint.2019.02.138.

[17] P. Moioli and S. C., "Analysis of Art Objects Using a Portable X-ray Fluorescence Spectrometer," September 1999. [Online]. Available: https://www.scopus.com/record/display.uri?eid=2-s2.0-0034412101&origin=inward.

[18] R. N. Brent, H. Wines, J. Luther, N. Irving, J. Collins and B. L. Drake, "Validation of handheld X-ray fluorescence for in situ measurement of mercury in soils," 6 January 2017. [Online]. Available: https://doi.org/10.1016/j.jece.2016.12.056.

[19] E. Yurdakul, P. Taylor and H. Ceylan, "The Application of X-Ray Fluorescence to Assess Proportions of Fresh Concrete," July 2012. [Online]. Available: https://www.researchgate.net/publication/278329076_The_Application_of_X-Ray_Fluorescence_to_Assess_Proportions_of_Fresh_Concrete.

[20] S. Chinchón-Payá, J. E. T. Martín, A. S. Toledo and d. J. S. Montero, "Quantification of Chlorides and Sulphates on Concrete Surfaces Using Portable X-ray Fluorescence. Optimization of the Measurement Method Using Monte Carlo Simulation," 20 December 2021. [Online]. Available: https://doi.org/10.3390/.

[21] S. Chinchón-Payá, J. E. T. Martín, N. R. Ramos and J. S. Montero, "Use of a Handheld X-ray Fluorescence Analyser to Quantify Chloride Ions In Situ: A Case Study of Structural Repair," 26 January 2021. [Online]. Available: https://doi.org/10.3390/ma14030571.

[22] J. Pringle, A. Jeffery, A. Ruffell, I. Stimpson, D. Pirrie, E. Bergslien, C. Madden, K. Wisniewski, J. Cassella, N. Lamont, S. Gormley and J. Partridge, "The use of portable XRF as a forensic geoscience non-destructive trace evidence tool for environmental and criminal investigations," 4 January 2022. [Online]. Available: https://doi.org/10.1016/j.forsciint.2022.111175 .

[23] "Wavelength Dispersive X-Ray Fluorescence (WDXRF)," Malvern Panalytical , [Online]. Available: https://www.malvernpanalytical.com/en/products/technology/xray-analysis/x-ray-fluorescence/wavelength-dispersive-x-ray-flourescence. [Accessed September 2023].

[24] L. Greenspan, "Humidity Fixed Points of Binary saturated Aqueous Solutions," 22 October 1976. [Online]. Available: https://nvlpubs.nist.gov/nistpubs/jres/81a/jresv81an1p89_a1b.pdf.

[25] N. B. Winter, Understanding Cement. An introduction to cement production, cement hydration and deleterious processes in concrete, 2012.

[26] M. Nedeljković, "Carbonation mechanism of alkali-activated fly ash and slag materials," 2019. [Online]. Available: https://doi.org/10.4233/uuid:97b9eabe-159e-43e1-8b35-edc61b1aa682.

[27] P. López-Arce, L. Gómez-Villalba, S. Martínez-Ramírez, M. Á. d. Buergo and R. Fort, "Influence of relative humidity on the carbonation of calcium hydroxide nanoparticles and the formation of calcium carbonate polymorphs," 29 September 2010. [Online]. Available: https://doi.org/10.1016/j.powtec.2010.09.026.

DURABILITY PROPERTIES OF GEOPOLYMER CONCRETE MADE OF GROUND GRANULATED BLAST FURNACE SLAG

Dr Jelena Bijeljić[1], Dr Nenad Ristić[2], Dušan Kocić[3], Dr Dušan Grdić[4], Dr Zoran Grdić[5], Dr Gordana Topličić-Ćurčić[6]

Summary:

This paper presents the results of testing the durability properties of geopolymer mortar and concrete mixtures. Fly ash was used as the basic binder, while its replacement was performed with ground granulated blast furnace slag. Compressive and flexural strength, but also sulfate resistance, were tested on hardened geopolymer mortar and concrete. Based on the most optimal results of mortar testing, the composition of concrete was determined, and durability properties, as well as sulfate resistance, were tested. According to the results of durability properties of geopolymer mortar and concrete mixtures made of 20 % ground granulated blast furnace slag as a binder showed better results than reference mixtures made only with fly ash.

Key words: Geopolymers, mortar, concrete, slag, fly ash

[1] Higher lecturer, Academy of Technical Vocational Studies Niš, Niš, Serbia, neimar.jelena@gmail.com
[2] Assoc. prof., Faculty of Civil Engineering and Architecture, University of Niš, Serbia, nenad.ristic@gaf.ni.ac.rs
[3] Assistant, Academy of Technical Vocational Studies Niš, Niš, Serbia, dusan.kocic@akademijanis.edu.rs
[4] Assistant. prof., Faculty of Civil Engineering and Architecture, University of Niš, Serbia, dusan.grdic@gaf.ni.ac.rs
[5] Full prof., Faculty of Civil Engineering and Architecture, University of Niš, Serbia, zoran.grdic@gaf.ni.ac.rs
[6] Full prof., Faculty of Civil Engineering and Architecture, University of Niš, Serbia, gordana.toplicic.curcic@gaf.ni.ac.rs

1. INTRODUCTION

Nowadays there is a growing number of reasons for the increasing interest in the field of geopolymers, and especially in their environmental advantages. As stated by numerous researchers in this field [1], in excess of 2/3 of anthropogenic emission of CO_2 is generated due to the use of energy and production. The largest global environment polluter is industrial production with around 36 % of the total emission of CO_2 in the manufacturing process of five groups of products: steel, cement, plastics, paper and aluminium. It is closely followed by the Construction industry with around 33 % CO_2. It is well known that in the making of cement, some industrial by-products can be used, such as fly ash, blast furnace slug etc. However, it is the current practice in our country not to combine the by-products very often, but rather the high value waste is mostly placed in landfills. A higher use of industrial by-products would create a certain economic gain, both through the reduction of disposal costs and through the selling of the waste as a raw material [2]. According to Stengel et al. [3], the environmental benefits due to the use of geopolymer concrete could be exhibited in the reduction of CO_2 emission, which would, according to some predictions range between 25 % and 45 %. In comparison with Portland cement, the production of alkali activated cement requires 60 % less energy [4], while the emission of CO_2 is around 6 times lower [2]. One can be acquainted with the environmental and economic benefits of geopolymer from the research conducted by Hardjito and Rangan [5]. The proved that one ton of fly ash can be used for the production of 2.5 m^3 of high-quality concrete whose cost is lower than the Portland cement concrete [6]. The environmental benefits are reflected in the implementation of waste materials into the geopolymer composition. Namely, alumina-silicate raw materials needed for making of geopolymer can be found in their natural state, such as the Earth's crust materials, but they are more often industrial by-products. The alkali activators such as strong bases in combination with silicate compounds are most often used for making geopolymers [7]. Accordingly, theoretically speaking, any solid material which, in its chemical composition, contains oxides of silicon, calcium and aluminium can be alkali activated, and the final product of activation is a material of polymer structure and high mechanical properties. [8][9]. Some of the most frequently used materials are waste materials originating from the industrial production such as: fly ash, blast furnace granulate slag, red mud, metakaolin, rice husk ash etc. [10]. Numerous authors tested the effects of granulated blast furnace slag on the geopolymer properties. Kim and Kim [11] examined the effect of replacement of fly ash with the slag in the mass percentage of 0 %, 50 % and 100 % the geopolymer mortar properties. According to the test results of mortars of 1, 7 and 28 days of age, the compressive strength increases with the increase of the percentage of slag in mortar. Aydin [12] also examined geopolymers made with granulated slag in the mass percentage of 60 %, 80 % and 100 %. Test results are in agreement with the results of other authors who conducted similar research [11]. The effect of the granulated blast furnace slag to compressive strength, in a somewhat different mass percentage ratio was examined also by Puertas et al. [13]. At the polymer age of 28 days, the flexural strength ranged between 6.8 and 7.8 MPa. At the same age of the specimens, the compressive strength ranged between 30 MPa and 89.5 MPa. Based on the obtained results of these authors, the lowest flexural strength and compressive strength measured on the samples of the mortar made with 50 % of fly ash and 50 % of granulated blast furnace slag. Researching on geopolymer concrete made by adding ground granulated blast furnace slag was not on the quantity level as geopolymer mortar. Provis et al [14] examined the compressive strength of concrete cured in ambient conditions. They used the following binders: fly ash, granulated blast furnace slag and metakaolin for the making. For making concrete base on fly ash, the w/b ratio was 0,223 (concrete labeled FA2) and 0,253 (concrete labeled FA8). Concrete with a lower w/b ratio was designed as a high-performance concrete. At the age of concrete of 28 days, in both series, it was observed that there was obvious dispersion of the results. Yet, at the ages of 28 to 56 days, an increase of mean values of compressive strength was measured. Nath and Sarker [15] tested the geopolymer concrete made at the conditions of laboratory curing temperature, and the obtained values of compressive strength ranged between 0 and 63 MPa. Somewhat better test results of the compressive strength were obtained by Nath and Kumar [16]. After making, the samples were cured at a curing temperature of 110 ºC for 8 h. Measured values of compressive strength ranged between 5 and 93,4 MPa. In addition to the mechanical tests, the durability tests are also very important. Owing to the long duration of the tests and the complexity of conducting them, the number of available scientific papers is low. Geopolymers were tested by Ristić et al. [17]. In their experiment, they tested the strength of geopolymer concrete made with the addition of hazardous waste vitreous enamel material. The mentioned authors concluded that the examined concrete exhibited resistance to the external sulfate action. The effects of sulfate action on geopolymer concrete on the basis of fly ash cured at 60 ºC for 24 hours were tested by Wallah and Rangan [18]. Concrete samples were immersed in the 5 % solution of Na_2SO_4 for one year. Like in the testing of the previous group of authors, these geopolymer concrete specimens showed good resistance to external sulfate solution. There were no visible changes on the samples regarding surface erosion, cracks, or fissures. Bakharev et al [19] tested the geopolymer samples made with the addition of slag which were exposed to the action of a 5 % solution of Na_2SO_4 for a year. On testing specimens was no visible extension and propagation, and the measured strength increase was up to 17 %.

2. EXPERIMENTAL RESEARCH

In this study, FA and GGBFS were used as binder materials. Fly ash originates from thermal electric power plant Kostolac "B", while GGBFS is a by-product of iron ore processing in the Smederevo still mill. The chemical compositions of FA and GGBFS were given it Table 1. Previously, granulated slag was pulverized in steel-ball mill and passed through the sieve with 0.09 mm openings. Also, fly ash was sifted through the same sieve. Sodium hydroxide and sodium silicate were used as alkali activators for making geopolymer mixtures. Sodium hydroxide of molarity 10M was mixed with sodium silicate of the starting module Ms 2,2 (Ms = SiO_2/NaO). That way, an activator with the content of 10% Na_2O of the solid binder mass was obtained, whereas Ms in sodium silicate was reduced. A solution prepared this way was used for making all geopolymer mixtures. Standard tap water was used in mortar production in all mixtures. The aggregate used in this research was river sand from South Morava (Serbia) with a maximum grain size of 2 mm and rock aggregate from „Rakov dol"of grain size 4/8 and 8/16 mm.

2.1. MIX DESIGN

Six geopolymer mortar mixtures were made and marked as "0 MS", "20 MS", "40 MS", "60 MS", "80 MS", and "100 MS". In mentioned mixtures, ground granulated blast furnace slag was used to replace fly ash at 0%, 20%, 40%, 60%, 80%, and 100% by weight, respectively. According to the mechanical and durability properties of geopolymer concrete, geopolymer concrete mixtures were made. Two geopolymer concrete mixtures were made and marked as "0 CS" and "20 CS". In mentioned mixtures, ground granulated blast furnace slag was used to replace fly ash at 0%, and 20% by weight, respectively. The mix proportions of geopolymer mortar and concrete mixtures are given in Table 1. The moulds with samples of geopolymer were after demoulding, and until the testing, wrapped in a plastic foil to prevent moisture loss. Two cement mortar and two cement concrete mixtures were made by using cement CEM II A-L 42,5R and CEM III/B 32,5 N-LH/SR. Those mixtures were made as etalon. Depending on the cement type, mixtures were named “E II”, “E III”, “E II”, and “E III”.

Tab. 1 Mix design of geopolymer mortar and concrete mixtures

Mix design	FA	GGBFS	CEM II	CEM III	NaOH	Na_2SiO_3	Sand	Aggr.	Additive %	Extra water
MORTAR [g]										
0 MS	450	-	-	-	56,16	303,23	1350	-	2	20
20 MS	360	90	-	-	56,16	303,23	1350	-	1,5	20
40 MS	270	180	-	-	56,16	303,23	1350	-	1,4	20
60 MS	180	270	-	-	56,16	303,23	1350	-	1,2	20
80 MS	90	360	-	-	56,16	303,23	1350	-	1	20
100 MS	0	450	-	-	56,16	303,23	1350	-	0,8	20
E II	-	-	450	-	-	-	1350	-	0,2	225
E III	-	-	-	450	-	-	1350	-	0,5	225
CONCRETE [kg/m^3]										
0 CS	400	-	-	-	50	270	618	928	-	-
20 CS	320	80	-	-	50	270	618	928	-	-
E II	-	-	450	-	-	-	890	890	1,2	195
E III	-	-	-	450			890	890	1,1	195

2.2. METHODS

When testing the mortar in the hardened state, the mechanical characteristics were first examined at the age of 2, 7, 28, 56 and 90 days according to standard EN 196-1. The flexural strength test was performed on three prism-shaped specimens measuring 4×4×16 cm. After measuring the flexural strength, the compressive strength test was performed Durability testing of geopolymer mortar was performed on prism-shaped samples measuring 4×4×16 cm. After reaching the age of 28 days, the sulfate resistance test according to the technical report recommendation CEN/TR 15697 for 180 days.

After measuring the mortar properties, the tests were conducted on concrete. Flexural strengths of geopolymer concrete were measured according to standard EN 12390-5 by applying two-point forces at the thirds of the span. The test was performed on three prism-shaped specimens, having dimensions 10×10×40 cm at the age of 90 days. The compressive strength test was conducted according to standard EN 12390-3 on cube-shaped specimens having sides of 10 cm at the ages of 2, 7, 28, and 90 days. The sulfate resistance of geopolymer concrete was tested by using the performance of technical report CEN/TR 15697. After achieving the age of 28 days the samples of concrete were completely immersed in Na_2SO_4 solution of 5% for 90 and 180 days. Three samples of each mixture were exposed to the sulfate solution, while the other three samples of concrete of the same composition served as reference samples. Reference samples were cured in ambient conditions until the time of testing. According to the used testing report, the tested samples are considered resistant to external sulfate action if the ratio of compressive strength of tested and reference samples of the same composition is higher than 80%. This criterion was used for concrete as well as mortar.

3. RESULTS AND DISCUSSION

The compressive and flexural strength of mortar bars are the most important mechanical properties of mortar mixtures, and they might be useful in determining concrete properties. The compressive and flexural strength of 2, 7, 28, 56, and 90 days old specimens of geopolymer mortar are summarized in Figures 1a) and 1b). Three samples from each mixture were taken to specify physical and flexural strength characteristics, while for the compressive strength test, six samples were used.

a)

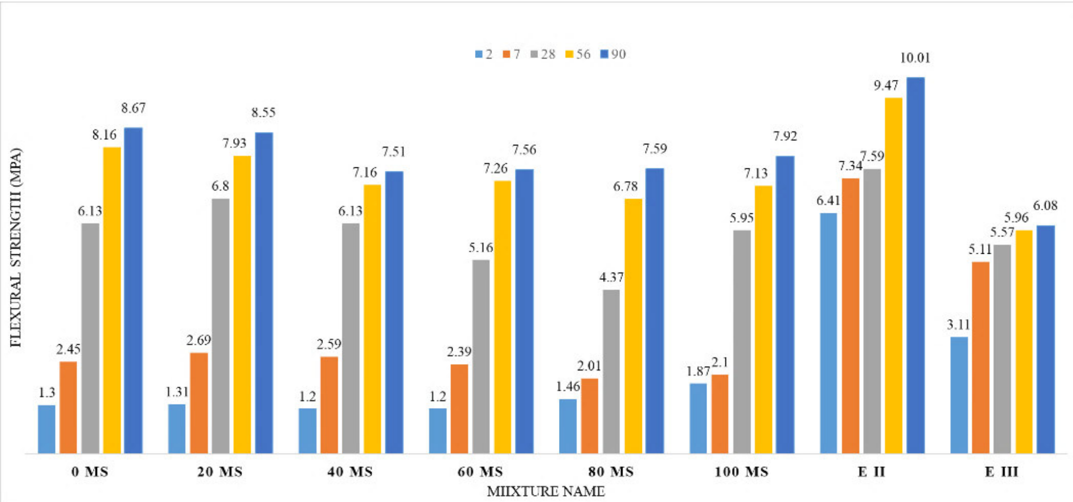

b)

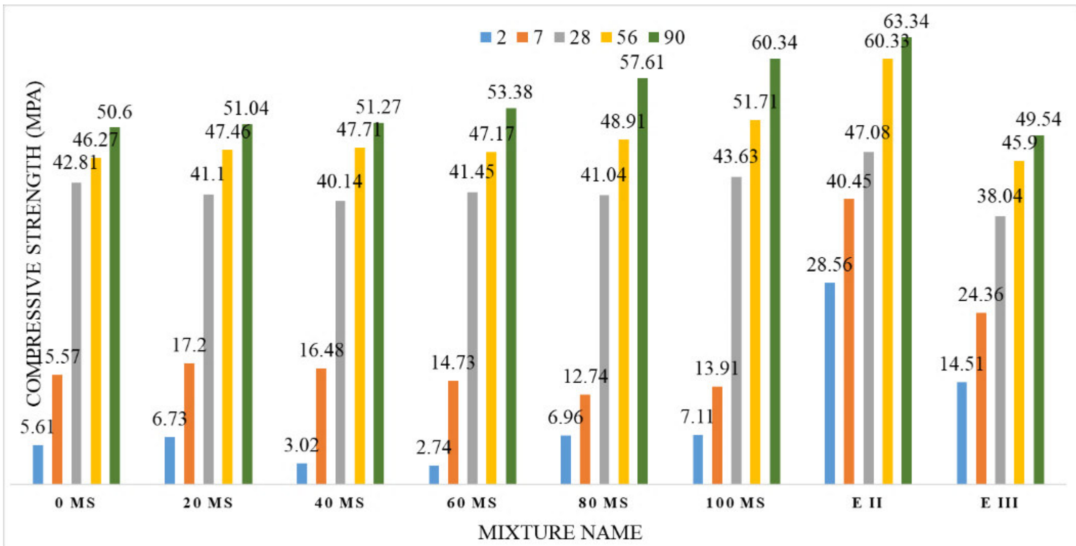

Fig. 1 Testing results of mortar a) flexural strength; b) compressive strength

According to the test results of the mortar at the age of 2 and 7 days, it can be concluded that the addition of ground granulated blast furnace slag has a positive effect on flexural strength, except in mixtures “60 MS”, “80 MS” and “100 MS”. At the age of mortar of 28 days, it is observed that the mixture marked as „100 MS“ has the highest flexural value (6.80 MPa) which is higher than the flexural strength measured on the reference mixture marked as “0 MS”. The trend of the increase of strength by age was observable in almost all mixtures, but at the ages of 56 to 90 days it is negligibly small in comparison to the increase of strength in early ages.

According to the test results of the compressive strength of the mortar at early ages, it can also be concluded that the addition of a ground granulated blast furnace has not a positive impact on compressive strength. At the age of 28 days, the compressive strength of the mixture marked as „20 MS"was slightly higher than "0 MS" and amounted to 6.80 MPa. As well as flexural strength, the trend of the increase of strength by age was observable in almost all mixtures, but at the ages of 56 to 90 days it is negligibly small in comparison to the increase of strength in early ages.

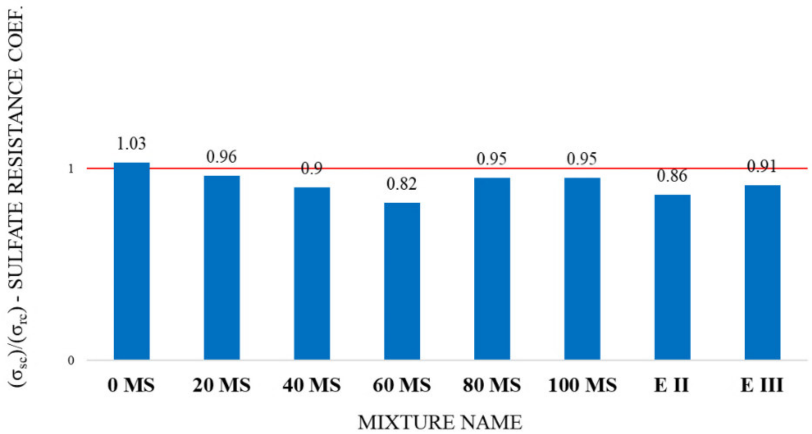

Fig. 2 Testing results of mortar sulfate strength resistance

Figure 2 presents test results of the compressive strength resistance of geopolymer mortar after one year of immersion in 5% Na_2SO_4. The test results of geopolymer concrete indicate good sulfate resistance under the implemented test requirements. The sulfate resistance coefficient is higher than 0.80 for all mixtures. The highest resistance coefficient was measured on the mixture marked as "0 MS", but also "20 MS". Physical changes on the tested samples were not observable. The good resistance of geopolymer concrete to the sulfate effects is accounted for by the fact that the process of polymerization continues unimpaired even after exposing the samples to the aggressive action of sulfate solution.

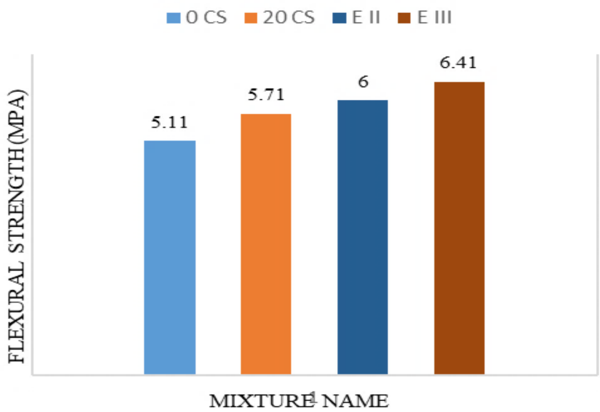

Fig. 3 Testing results of concrete flexural strength at the age of 90 days

The test results of flexural and compressive strengths of geopolymer concrete are presented in Figure 3 and 4. Observing the flexural strength diagram at the sample age of 90 days, it can be observed that the mixure named „0 CS" (5.11 MPa) has the lowest value. The achieved geopolymer concrete flexural strengths at the age of 90 days are higher for 15-20 % lower than the strengths measured on cement concrete samples.

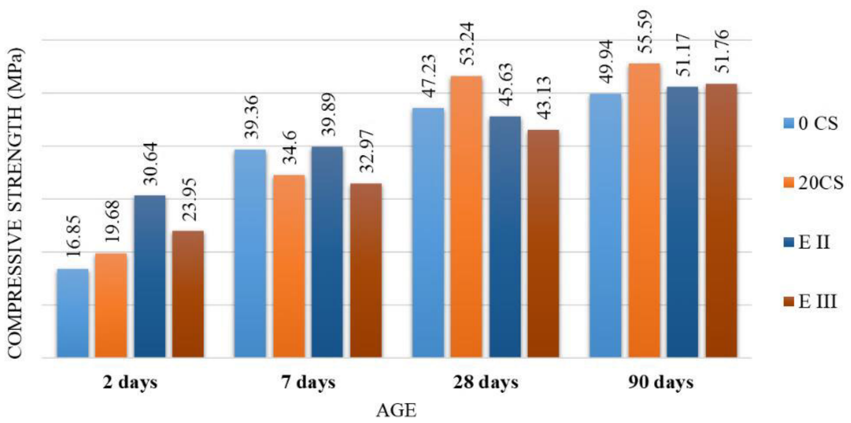

Fig. 4 Testing results of concrete compressive strength at the age of 2, 7, 28 and 90 days

According to the concrete compressive strength test results of the samples at 28 days of age, all mixtures exhibited approximately the same values. Yet, the „20 CS“ mix exhibited a higher value (53.24 MPa) and it is about 6,01 MPa higher than the „0 CS“ mixture. Such a trend is observable at the age of 90 days when the strength of the „20 CS“ mix was 55.59 MPa. It can be concluded that ground granulated blast furnace slag has a positive effect on the initial increase of compressive strength of the geopolymer concrete samples cured in ambient conditions.

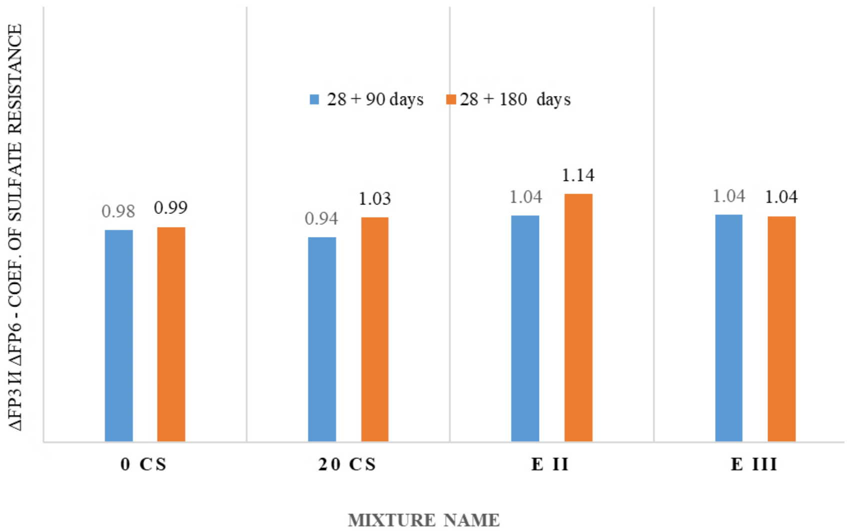

Fig. 5 Testing results of concrete sulfate resistance

The measured values of compressive strength of concrete specimens immersed in the sulfate solution for 90 and 180 days were presented in Figure 5. According to the result is a visible permanent increase of compressive strength with respect to the reference specimens of the same composition which were not exposed to the sulfate solution action. As opposed to the specimens of reference mixtures where a decrease of strength was not measured. The specimens of all series of geopolymer concrete mixtures continued to increase strength, and the coefficient of compressive strength resistance was in the range 0,94 to 1.14 (in the mixtures „0 CS“ and „20 CS“, respectively). Physical changes on the tested specimens were not visible.

4. CONCLUSION

Based on the test results presented in this paper, the following conclusions can be drawn:

- The increase of strengths after 28 days is high in the series of geopolymer mortar made with fly ash as binder and mortar in which the binder was granulated blast furnace slag. At the age of samples of 90 days, all mixtures made with the granulated blast furnace slag achieved higher strengths than the mortar made with only fly ash as a binder. Eventually, it can be concluded that granulated blast furnace slag causes the ultimate compressive strengths to increase.
- As the compressive strengths, the early flexural strengths of geopolymer mortar are low. The highest increase of strength was realized at the concrete ages of 7 to 28 days, while at the ages of 28 to 90 days, the increase is negligible.
- Due to the immersion of samples of geopolymer mortar in the 5 % solution of Na_2SO_4 for 180 days, geopolymer mortar continued to harden. The created polymer bonds retained stability, and the polymerization process continued until the end of the experiment.
- Geopolymer concretes cured in ambient conditions are characteristic for somewhat lower compressive strengths which increase in time, and at the age of around 90 days reach the maximum values. Granulated blast furnace slag at the mentioned age had a positive effect on the compressive strength of concrete.
- Based on the test results of the flexural strength, it can be concluded that the replacement of a part of fly ash with granulated blast furnace slag at the mass percentage of 20 % caused the increase of strength in comparison with the concrete made with only fly ash, as a binder
- According to the test results of sulfate resistance of concrete, after 3 months, it can be considered that the partial replacement of fly ash with granulated blast furnace slag has no notable effect on the resistance coefficient. However, a slight increase of the resistance coefficient at the test conducted after 180 days was observed. Geopolymer binder and alkali solution continue to maintain their interior bonds stable, with no reaction to external impacts.

REFERENCES

[1] Allwood J.M., Cullen J.M., Milford R.L. (2010). Options for achieving a 50% cut in industrial carbon emissions 2050. *Environmental science technology*, Vol. 44, pp. 1888-1894

[2] McLellan B. C., Williams R. P., Lay J., van Riessen A., Corder G. D. (2011). Costs and carbon emissions for geopolymer pastes in comparison to ordinary portland cement. *Journal of cleaner production*, Vol. 19, pp. 1080-1090

[3] Stengel T., Reger J., Heinz D. (2009). Life cycle assessment of geopolymer concrete - what is the environmental benefit. *Proceeding of the 24th Biennial Conference of the Concrete Institute of Australia*

[4] Li Z., Ding Z., Zhang Y. (2004). Development of sustainable cementitious materials. *International workshop on sustainable development and concrete technology*, Beijing, China, pp. 55–76

[5] Hardjito H., Rangan R. V. (2005). Development and properties of low-calcium fly ash based geopolymer concrete. Research report GC1, Curtin University of Technology Faculty of Engineering, Perth, Australia

[6] Ken P. W., Ramli M., Ban C. C. (2015). An overview on the influence of various factors on the properties of geopolymer concrete derived from industrial by-products. *Construction and building material*s, Vol. 77, pp. 370-395

[7] Gorhan G., Kurklu G. (2014). The influence of the NaOH solution on the properties of the fly ash-based geopolymer mortar cured at different temperatures. *Composites: Part B.* Vol. 58, pp. 371-377

[8] Palomo A., Grutzek M. W., Blanc M. T. (1999). Alkali-activated fly ashes. A cement for the future. *Cement and concrete research*. Vol. 29 (8), pp. 1323–1329

[9] Torgal F. P., Gomes J. C., Jalali S. (2008). Alkali-activated binders: A review. Part 2. About materials and binders manufacture. *Construction and building materials.* Vol. 22, pp. 1315-1322

[10] Islam A., Alengaram U. J., Jumaat M. Z., Bashar I. I. (2014). The development of compressive strength of ground granulated blast furnace slag-palm oil fuel ash-fly ash based geopolymer mortar. *Materials and design*. Vol. 56, pp. 833-841

[11] Hyunjung K., Yooteak K. (2012). Characteristics of the geopolymer using fly ash and blast furnace slag with alkaline activators. *4th international conference on chemical, biological and environmental engineering*. IPCBEE, Singapore, Vol. 43 (32), pp. 154–159

[12] Serdar A. (2013). A ternary optimization of mineral additives of alkali activated cement mortar. *Construction and building materials.* Vol. 43, pp. 131–138

[13] Puertas F., Amat T., Fernandez-Jimenez A., Vazquez T. (2003). Mechanical and durable behaviour of alkaline cement mortars reinforced with polypropylene fibres. *Cement and concrete research*. Vol. 33, pp. 2031-2036

[14] Provis J. L., Arbi K., Bernal S. A., Bondar D., Buchwald A., Castel A., Chithiraputhiran S., Cyr M., Dehghan A., Daube K. D., Dubey A., Ducman V., Gluth G. J. G., Nanukuttan S., Peterson K., Puertas F., van Riessen A.,. Carrasco M. T, Ye G., Zuo Y. (2019). RILEM TC 247-DTA round robin test: mix design and reproducibility of compressive strength of alkaliactivated concretes. *Materials and structures*, Vol. 52:99

[15] Nath P., Sarker P. K. (2014). Effect of GGBFS on setting, workability and early strength properties of fly ash geopolymer concrete cured in ambient condition. *Construction and building materials*. Vol. 66, pp. 163-171

[16] Nath S. K., Kumar S. (2013). Influence of iron making slags on strength and microstructure of fly ash geopolymer. *Construction and building materials*. Vol. 38 pp. 924–930

[17] Ristic N. Bijeljic J., Grdic D., Toplicic-Curcic G., Grdic Z. (2023). Sulfate resistance of geopolymer concrete produced with hazardous waste vitreous enamel generated in the production process of heating devices. *International conference synergy of architecture and civil engineering*. University of Nis

[18] Rangan B. V. (2008). Fly ash – based geopolymer concrete. *Research report GC4.* Curtin University of Technology, Engineering Faculty Perth, Australia

[19] Bakharev T., Sanjayan J. G., Cheng Y. -B. (2002). Sulfate attack on alkali-activated slag concrete. *Cement and concrete research*. Vol. 32, pp. 211-216

USING MATHEMATICAL MODELS TO PREDICT SORPTION BEHAVIOUR OF PUR

Bojan Milovanović[1], Domagoj Tkalčić[2], Mergim Gaši[3], Marija Jelčić Rukavina[4]

Summary:

One of the most significant hygrothermal characteristics of porous building materials is the sorption isotherm, which is often assessed using a static gravimetric test. In order to increase test efficiency because the static gravimetric test typically takes weeks or months to perform, it is beneficial to use mathematical models to predict sorption behaviour of porous building materials. In this paper, 9 existing mathematical models used to describe the sorption behaviour of materials were tested and fitted to laboratory measurement results of polyurethane (PUR) foam samples. Only PELEG model was proved to be correct, IBPmod and IBP proved to be acceptable for RH up to 85% while other models are not advisable to describe sorption behaviour of PUR.

Key words: sorption isotherm, PUR, mathematical models, KLIK

[1] Associate professor, University of Zagreb, Faculty of Civil Engineering, Zagreb, Croatia, bojan.milovanovic@grad.unizg.hr
[2] Assistant, University of Zagreb, Faculty of Civil Engineering, Zagreb, Croatia, domagoj.tkalcic@grad.unizg.hr
[3] Dr.sc., University of Zagreb, Faculty of Civil Engineering, Zagreb, Croatia, mergim.gasi@grad.unizg.hr
[4] Associate professor, University of Zagreb, Faculty of Civil Engineering, Zagreb, Croatia, marija.jelcic.rukavina@grad.unizg.hr

1. INTRODUCTION

Because of their ease of handling and combination of unique properties, polyurethane foams (PURs) are one of the most adaptable engineering polymeric foams [1]. They are used in a wide range of high-performance applications, from acoustic insulation materials used in transportation to thermal and electrical insulation materials used in refrigeration technology, construction and building industries, furniture, and appliances. PURs are in greater demand than ever, and since thermal conductivity is one of the most significant characteristics of polyurethane foams [2], this makes it frequently used in the field of energy saving.

On the other hand, the idea of a nearly zero energy building (nZEB) has emerged in recent years due to the demand for energy-efficient structures as well as an increasing awareness of sustainability [3]. The construction industry is looking for novel solutions that enable quicker and easier construction without compromising the quality of works in order to fulfil the high standards for performance quality, indoor air quality, and minimal energy usage. In this context, the building of nZEBs is increasingly using LSF (Light Steel Frame) panels [4]–[6].

University of Zagreb, Faculty of Civil Engineering, Tehnoplast profili d.o.o. and Palijan d.o.o. have developed composite lightweight panel with an integrated load-bearing structure (hence referred to as the KLIK panel) [4], [7]. The sheathing panels are joined to an LSF load-bearing structure. The spaces between the sheathing panels and the steel structure are filled with polyurethane (PUR) foam.

When developing new building products or systems, understanding moisture storage and transport phenomena is essential to preventing moisture-related issues in building components and enclosures. Foam materials are hygroscopic, which means they can absorb and release moisture depending on the environment.

To analyse the moisture condition within the structure and comprehend the moisture transport (drying or wetting processes) through the observed construction material, it is necessary to establish sorption isotherms. Sorption isotherms depict the moisture content that the examined material can retain at specific relative humidity levels in its surrounding environment. The moisture content a material can store primarily depends on the material's structure (its porosity and permeability) and the hygrothermal conditions of the environment [8]. Sorption isotherms are adjusted based on experimentally obtained moisture content values at various relative humidity levels using different mathematical models. The following will succinctly outline the physical background of moisture transfer and the associated phenomena crucial for understanding the sorption behaviour of porous construction materials.

2. SORPTION

Porous construction materials have a complex pore structure. Pore surfaces in contact with water vapor tend to adsorb and localize water molecules onto themselves. This phenomenon is called adsorption. The process of drawing moisture from the environment into the material's structure is known as absorption. The maximum amount of moisture that the observed material can absorb depends on temperature, relative humidity (RH), and the surface area of the material's pores, and is referred to as the equilibrium moisture content (EMC) under those conditions. Furthermore, each material has its characteristic affinity for water, often referred to as hygroscopicity. The EMC of the material is typically represented as a function of the relative humidity of the external air in the form of a moisture sorption curve. A more accurate term would be moisture sorption isotherm or simply sorption isotherm, as EMC also depends on temperature [9] and is usually determined at a constant temperature. Every sorption isotherm can be defined as an absorption or desorption isotherm. An absorption isotherm describes the equilibrium moisture content that a material absorbs when exposed to increasing humidity levels (the "wetting" process). On the other hand, a desorption isotherm depicts the EMC of the material when exposed to decreasing humidity levels (the "drying" process). Typically, the material retains more moisture during desorption than it can absorb at any given relative humidity (RH). This phenomenon is called hysteresis, [9].

The static gravimetric method is typically used to calculate sorption isotherms. The fundamental idea behind this technique is to subject test samples to rising/falling RH sequences. The EMCs at various RHs can be determined by comparing the starting dry mass with the equilibrium wet mass at each RH level. Numerous standards, including HRN EN ISO 12571 [10] and ASTM C1498 [11], give thorough explanations of the test technique.

Due to the technical limitations of the laboratory (lack of a chamber for simulating different conditions of humidity and temperature), it was decided to perform the static gravimetric method using a desiccator and saturated solutions in accordance with the HRN EN ISO 12571 standard [10]. The temperature of the test room was maintained at 23 ± 0.5 °C. In the first phase of the test, the samples were dried to a constant mass at a temperature of 60-80 °C over a period of 4 days. The sorption properties were tested for samples (150 ×150×20 mm) made of polyurethane foam (PUR) with a density of 40 kg/m^3. The samples were then successively exposed to different humidity conditions, in increasing order of the relative humidity of the environment (Fig. 1). The mentioned phase represents the wetting of the material and serves to determine the absorption behaviour of the material. The sample is exposed to a certain relative humidity until a state of equilibrium with the environment is established, which implies that the mass of the sample does not change. The sample is considered to have a constant mass if the change in mass between three consecutive weighing, with the time interval between weighing being at least 24 h, is less than 0.1% of the total mass of the sample.

a) b) c)

Fig. 1 a) PUR foam samples, b) PUR foam samples in the desiccator, c) sample weighing

Tab. 1 shows the salts used to achieve the target humidity, and all in accordance with the recommendations from HRN EN ISO 12571 [10].

Tab. 1 Selected humidity and necessary salts according to HRN EN ISO 12571

Salts	Potassium hydroxide KOH	Magnesium chloride hexahydrate $MgCl_2 \cdot 6H_2O$	Sodium chloride NaCl	Potassium chloride KCl	Potassium nitrate NO3
Relative humidity [%]	9	33	75	85	93

2.1. SORPTION TEST RESULTS

Fig. 2 shows the results of sorption measurements as the average equilibrium moisture content in [kg/m^3] at the tested relative humidites of the environment for PUR foam with a density of 40 kg/m^3. The presented PUR foam results are mean values obtained based on the measurement of 10 samples.

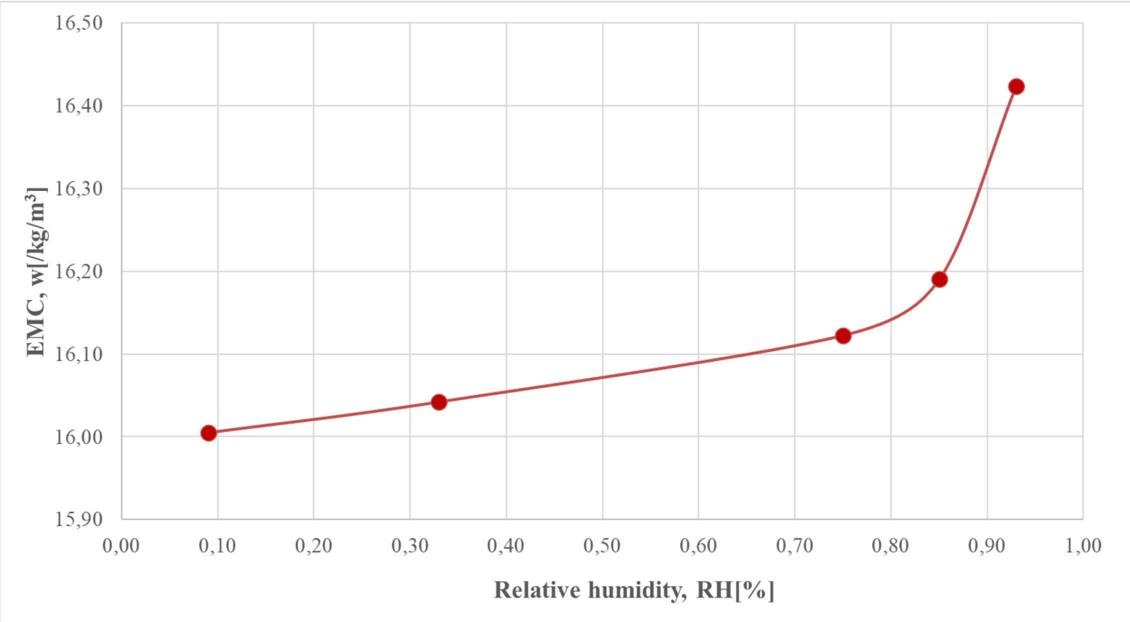

Fig. 2 Results of sorption moisture content for RH of a PUR foam sample (density 40 kg/m3)

3. MATHEMATICAL MODELS OF SORPTION

Adjustment of the sorption curve to discrete experimental results was carried out up to a relative humidity of 93%. The results of fitting of sorption isotherms for PUR 40 kg/m^3 samples are presented below. Using non-linear regression, coefficients of different sorption models calculated according to mathematical models were determined (Tab 2.), while tab. 3 shows the coefficients for the mentioned models.

Tab. 2 Mathematical models for constructing sorption isotherms

Model	Mathematical expression	Adjustment coefficients
IBPmod	$w(RH) = \frac{a}{1 + b \cdot (-\ln(RH))^c}$	*a, b, c*
IBP	$w(RH) = \frac{a}{1 + \left(\frac{p_c}{b}\right)^c}$	*a, b, c*
WUFI-BET	$w(RH) = a \cdot RH \cdot \frac{b-1}{b-RH}$	*a, b*
Feng-Janssen [12]	$w(RH) = ln\left[\frac{(100 \cdot RH + 1)^a}{(1-RH)^b}\right] + c \cdot \exp(100 \cdot RH)$	*a, b, c*
Peleg [13]	$w(RH) = a \cdot RH^b + c \cdot RH^d$	*a, b, c, d*
Oswin [14]	$w(RH) = a \cdot \left(\frac{RH}{1-RH}\right)^b$	*a, b*
Caurie [15]	$w(RH) = e^{a+b \cdot RH}$	*a, b*
GAB [16]	$w(RH) = \frac{c \cdot a \cdot b \cdot RH}{(1 - a \cdot RH)[1 + (c-1) \cdot a \cdot RH]}$	*a, b, c*
Hansen [17]	$w(RH) = a \cdot \left(1 - \frac{\ln(RH)}{b}\right)^{-\frac{1}{c}}$	*a, b, c*

The assessment of the suitability of a particular model for sorption behaviour, i.e. the quality of curve fitting, was carried out using statistical tools, primarily the coefficient of determination R^2:

$$R^2 = 1 - \frac{\sum_{i=1}^{n}(w_i - w_{fitting})^2}{\sum_{i=1}^{n}(w_i - w_{average})^2} \tag{1}$$

Where:

w_i – experimentally determined equilibrium moisture content [kg/m^3]

$w_{fitting}$ – moisture equilibrium position predicted by the model [kg/m^3]

$w_{average}$ – mean value of experimentally determined equilibrium moisture content [kg/m^3]

Since the coefficient of determination is insufficient for independent assessment of the suitability of different models, the sum of squares of residual deviations RSS was used as an additional assessment tool.

$$RSS = \sum_{i=1}^{n}(w_i - w_{fitting})^2 \tag{2}$$

Where, the smaller the RSS coefficient, the better the matching of the mathematical model curves with the discrete results of the sorption test.

Tab. 3 Coefficients of the used sorption models for PUR foam with R^2 and RSS

Model	Adjustment coefficients	Values	R^2	RSS
IBPmod	a	335,917	0,8421	0,0173
	b	19,922		
	c	0,00696		
IBP	a	34,75445	0,8404	0,01752
	b	607,263		
	c	0,01235		
WUFI-BET	a	16,157	0,046	0,1052
	b	0,0000		
Feng-Janssen	a	0,00000	0,9032	0,0106
	b	14,42675		
	c	0,00000		
Peleg	a	16,101	0,996	0,00038
	b	0,0026		
	c	0,8256		
	d	12,865		
Oswin	a	16,1211	0,7652	0,02577
	b	0,00455		
Caurie	a	2,7668	0,6915	0,03386
	b	0,02629		
GAB	a	15,9047	0,5688	0,04732
	b	0,04807		
	c	5000,00		
Hansen	a	16,2698	0,564	0,0478
	b	5,4428		
	c	19,461		

It should be emphasized that the sum of the squares of the residual sums RSS was calculated using the equilibrium moisture content expressed by the volume of the samples w [kg/m^3]. A large deviation of the coefficient of determination R^2 for the analysed models is visible (Tab. 3), so it is necessary to reject the WUFI-BET model. Fig. 3 shows a graphical comparison of mathematical models. The models IBPmod, IBP, Feng-Janssen and Peleg show a good correlation with the coefficient of determination R^2 >0.8. Although the Feng-Janssen model shows a satisfactory R^2, when drawing the curve, a large deviation from the laboratory test is observed (Fig. 4 - left), and thus the Feng-Janssen model must be rejected. Similar is observable for GAB model, for which results do not follow the laboratory measurements (Fig. 4 - right). If an additional high limit of $R^2 = 0.99$ is set for the quality of the model fitting, then it can be concluded that only Peleg's model satisfies the set condition. For this reason, only Peleg's model is considered suitable for describing the sorption behavior and constructing the sorption isotherms of PUR 40 (Fig. 5).

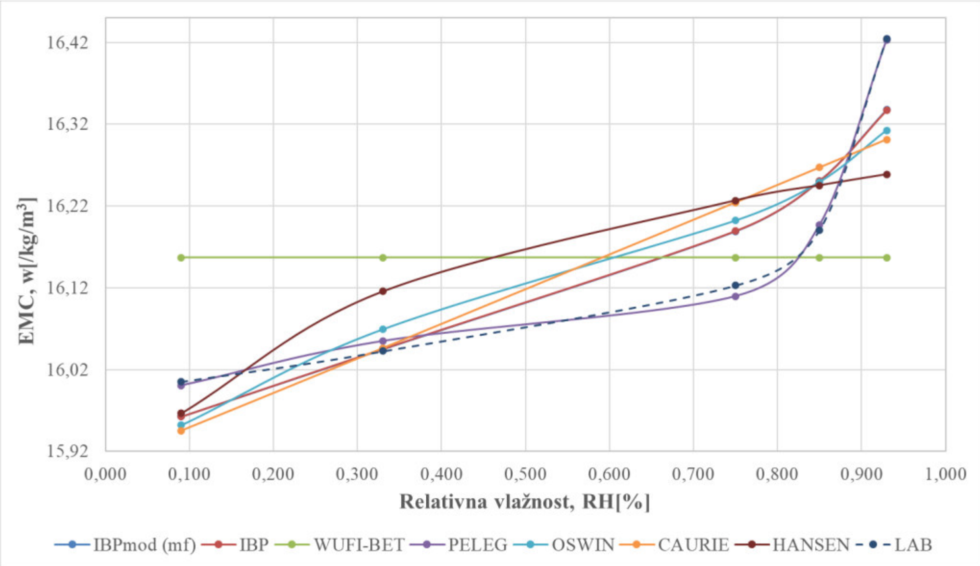

Fig. 3 Comparison of absorption isotherms for laboratory measurements and models

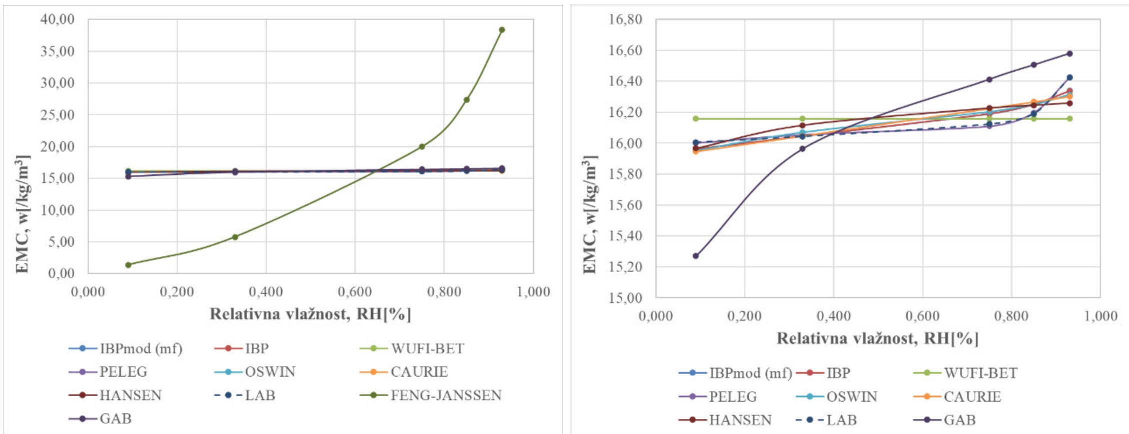

Fig. 4 Comparison of absorption isotherms for laboratory measurements and models including Feng-Janssen model (left) and GAB model (right)

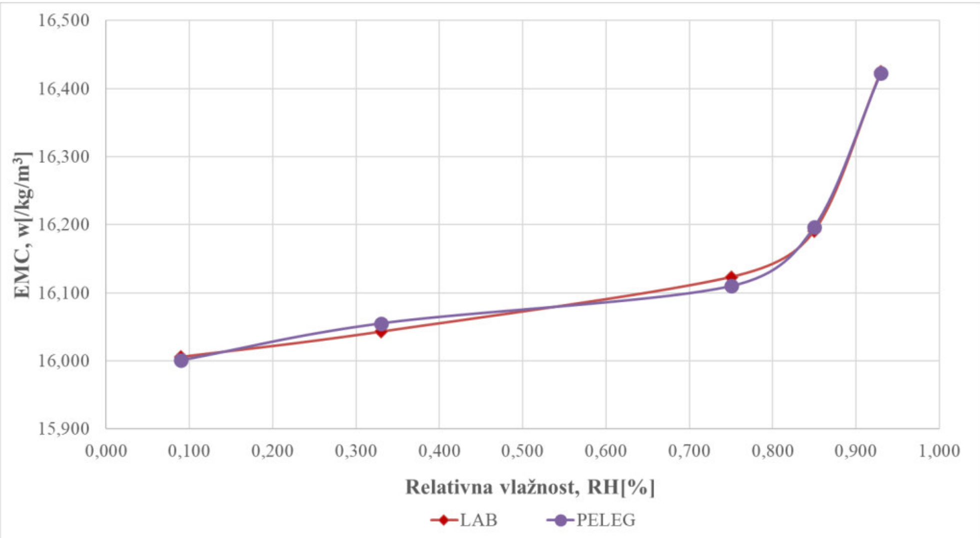

Fig. 5 Comparison of absorption isotherms for laboratory measurements and PELEG model

It is also evident from Fig. 3 that for low RHs models underestimate the moisture content in the samples, while for medium and high RH (up to 85 %) models overestimate the moisture content in PUR samples. It is also of critical importance to notice that all models but PELEG underestimate moisture content in the capillary (free) moisture region (>95 % RH) and supersaturated region (Fig. 3). which can significantly influence the c

4. CONCLUSIONS

Three areas make up the storage of moisture in building materials. The so-called hygroscopic equilibrium moisture contents are indicated by the first region. The capillary water zone, which has water contents up to capillary saturation, is next in line for capillary-active materials. The sorption isotherm defines the storage role for the hygroscopic moisture zone.

Up to 95% RH, the sorption isotherm can be determined gravimetrically, which is a very easy but time-consuming process. Because most building materials' sorption isotherms are particularly steep at higher relative humidities, precisely specified sorption measurements, as well as the correlation of water content with relative humidity are no longer possible above this value. Experimentally, the maximum moisture content in the material is present when the process takes place in a vacuum, eg pressure plate measurements have to be applied to determine the sorption curves in the high humidity range. This means the measurement process can be quite costly, complicated and time consuming. Thus accurate model for prediction of moisture content above 95 % RH is essential. The resulting liquid moisture retention curve is a prerequisite for simulations involving liquid moisture transport. Furthermore, accurate knowledge about sorption isotherms is essential for so-called HAM modelling (Heat, Air and Moisture - HAM) of mass transport through building envelopes. This non-stationary calculation approach can capture the influence of shorter time events such as hourly changes in boundary conditions in the observed time period. HAM modelling offers the possibility of better predicting the hygrothermal behaviour of building elements than the traditional Glaser method.

ACKNOWLEDGEMENT

This research was funded by the European Union through the European Regional Development Fund's Competitiveness and Cohesion Operational Program, grant number KK.01.1.1.07.0060, project "Composite lightweight panel with integrated load-bearing structure (KLIK-PANEL)".

REFERENCES

[1] C. T. Pham *et al.*, "Comprehensive Investigation of the Behavior of Polyurethane Foams Based on Conventional Polyol and Oligo-Ester-Ether-Diol from Waste Poly(ethylene terephthalate): Fireproof Performances, Thermal Stabilities, and Physicomechanical Properties," *ACS Omega*, vol. 5, no. 51, pp. 33053–33063, Dec. 2020, doi: 10.1021/acsomega.0c04555.

[2] H. Zhang, W.-Z. Fang, Y.-M. Li, and W.-Q. Tao, "Experimental study of the thermal conductivity of polyurethane foams," *Appl Therm Eng*, vol. 115, pp. 528–538, Mar. 2017, doi: 10.1016/j.applthermaleng.2016.12.057.

[3] E. Parliament and the Council of the European Union, "Directive (EU) 2018/844 of the European Parliament and of the Council amending Directive 2010/31/EU on the energy performance of buildings and Directive 2012/27/EU on energy efficiency." European Parliament, pp. 75–91, 2018. [Online]. Available: http://data.europa.eu/eli/dir/2018/844/oj

[4] M. J. Rukavina, D. Skejić, A. Kralj, T. Ščapec, and B. Milovanović, "Development of Lightweight Steel Framed Construction Systems for Nearly-Zero Energy Buildings," *Buildings*, vol. 12, no. 7, p. 929, Sep. 2022, doi: 10.3390/buildings12070929.

[5] E. Rodrigues, N. Soares, M. S. Fernandes, A. R. Gaspar, Á. Gomes, and J. J. Costa, "An integrated energy performance-driven generative design methodology to foster modular

lightweight steel framed dwellings in hot climates," *Energy for Sustainable Development*, vol. 44, pp. 21–36, Sep. 2018, doi: 10.1016/j.esd.2018.02.006.

[6] B. Milovanović, M. Bagarić, M. Gaši, and N. V. Strmo, "Case Study in Modular Lightweight Steel Frame Construction: Thermal Bridges and Energy Performance Assessment," *Applied Sciences (Switzerland)*, vol. 12, no. 20, 2022, doi: 10.3390/app122010551.

[7] D. Tkalčić, B. Milovanović, M. Gaši, M. Jelčić Rukavina, and I. Banjad Pečur, "Optimization of Thermal Bridges Effect of Composite Lightweight Panels with Integrated Steel Load-Bearing Structure," *Energies (Basel)*, vol. 16, no. 18, p. 6474, Sep. 2023, doi: 10.3390/en16186474.

[8] D. Zirkelbach, S.-R. Mehra, K.-P. Sedlbauer, H.-M. Künzel, and B. Stöckl, "A hygrothermal green roof model to simulate moisture and energy performance of building components," *Energy Build*, vol. 145, pp. 79–91, 2017, doi: https://doi.org/10.1016/j.enbuild.2017.04.001.

[9] M. Bagarić, "Higrotermalno ponašanje ventiliranih teških ovojnica zgrada," PhD, Sveučilište u Zagrebu, Građevinski fakultet, Zagreb, 2020.

[10] Croatian Standards Institute, "HRN EN ISO 12571:2021(en) Hygrothermal performance of building materials and products — Determination of hygroscopic sorption properties." International Organization for Standardization, 2021.

[11] ASTM, "ASTM C1498-04a(2016) Standard Test Method for Hygroscopic Sorption Isotherms of Building Materials." ASTM, 2016.

[12] C. Feng, Q. Meng, H. Janssen, and Y. Feng, "Effect of temperature on the sorption isotherm and vapor permeability," in *2nd central European symposium on building physics*, 2013.

[13] M. PELEG, "ASSESSMENT of A SEMI-EMPIRICAL FOUR PARAMETER GENERAL MODEL FOR SIGMOID MOISTURE SORPTION ISOTHERMS," *J Food Process Eng*, vol. 16, no. 1, pp. 21–37, Feb. 1993, doi: 10.1111/j.1745-4530.1993.tb00160.x.

[14] C. R. Oswin, "The kinetics of package life. III. The isotherm," *Journal of the Society of Chemical Industry*, vol. 65, no. 12, pp. 419–421, Dec. 1946, doi: 10.1002/jctb.5000651216.

[15] M. CAURIE, "A new model equation for predicting safe storage moisture levels for optimum stability of dehydrated foods," *Int J Food Sci Technol*, vol. 5, no. 3, pp. 301–307, Jun. 2007, doi: 10.1111/j.1365-2621.1970.tb01571.x.

[16] C. Berg and S. Bruin, "Water activity and its estimation in food systems: theoretical aspects," 1981.

[17] P. Hansen, "Freiesleben:'Coupled moisture/heat transport in cross-sections of structures,'" *Beton og Konstruktionsinstitutet (BKI), Denmark*, 1985.

AEROGEL BASED MATERIALS POTENTIAL IN CIRCULAR ECONOMY, ENERGY EFFICIENCY AND CULTURAL HERITAGE BUILDINGS' RENOVATION

Liljana D. Sofronievska[1], Meri Cvetkovska[2], Ana T. Gavriloska[3], Teodora Mihajlovska[4]

Summary:

Improving the energy efficiency (EE) and sustainability of the buildings is crucial for meeting EU climate targets. Circular economy (CE), especially in the building sector, strive to reduce the pollution, extend the building's lifespan, reduce the material waste and use long-lasting products. Proper renovation by using sustainable materials with low embodied energy will lead to the fulfilment of both goals, EE and CE. Aerogel-based building products are currently considered to be promising insulation materials due to their great thermal performances with limited thickness and their low embodied energy This paper aims to explore the potential that aerogel materials have not only in terms of EE and CE principles but as well as the cultural heritage impact after the renovation process. Comparing to all of the researched types of aerogel based materials, the silica aerogel thermal plaster proved to be the most appropriate solution in terms of E efficiency, sustainability, circularity and historical buildings' compatibility.

Key words: circular economy, energy efficiency, aerogel based materials

[1] Teaching Asitent, Faculty of Architecture, Ss. Cyril and Methodius University, Skopje, N.Macedonia, dimevska.liljana@arh.ukim.edu.mk
[2] Prof.PhD, Faculty of Civil Engineering, Ss. Cyril and Methodius University, Skopje, N.Macedonia,
[3] Prof.PhD, Faculty of Architecture, Ss. Cyril and Methodius University, Skopje, N.Macedonia,
[4] Teaching Assistant, Faculty of Architecture, Ss. Cyril and Methodius University, Skopje, N.Macedonia,

1. INTRODUCTION

The scientific interest in nano and biomaterials in energy efficient buildings has significantly increased in the last decade, especially after the introduction of "Nearly zero - energy buildings" - NZEB) according to Directive on the energy performance of buildings, 2010/31/EU - EPBD [1]. That means that the new building's energy consumption should be close to zero by 2030, which leads to great tightening of energy efficiency (EE) criteria and increase of thermal insulation materials thickness, which has important economic and technical consequences, especially high insulation costs [2]. Not only the material's thickness emphasizes the need for research and development of new materials, but more significant factors such as: finding solutions for reducing the embodied energy used for production and transportation, reducing toxicity and environmental pollution, as well as reducing material waste, favorite the use of long-lasting building materials and extending the building's lifespan. All these measures mark a new moment in the construction industry known as circular economy (CE). On the other hand, new buildings have a limited impact on overall energy reduction because they represent small part of the existing building stock [3]. It is estimated that only 1% of the buildings in Europe, per year are new buildings. Therefore, existing buildings represent the greatest opportunity for CE implementation. Moreover, new buildings use 4-8 times more resources than renovated ones [4], which is a sustainable argument in favour of buildings' renovation. An additional problem that arises during renovations is the preservation of the building's architectural appearance, that shouldn't be compromised. The selection of right materials and methods for application in renovation process are crucial for both, the EE and CE improvement, as well as for authenticity preservation.

This paper aims to explore the state of the art nanomaterials in the building sector, not only in terms of EE (energy consumption ad cost improvements), but also in terms of CE (reduction of embodied energy, environmental toxicity, recyclability, adaptive reuse, as well as the relationship of the new materials to the cultural heritage buildings). The research brings the nanomaterials based on silica aerogel as well as the nano ceramic coatings are the most promising building materials, according to all of the above-mentioned criteria. This paper highlights the potential that aerogel have in EE and CE of the building sector, and therefore, the further analysis refer only to aerogel-based materials. Comparing to all of the researched types of aerogel based materials, the silica aerogel thermal plaster proved to be the most appropriate solution in terms of energy efficiency, sustainability, circularity and historical buildings' compatibility.

2. NANOMATERIAL SELECTION CRITERIA

In terms of improving the energy efficiency, the following commercially available nanomaterials have been developed so far:

- Expanded polystyrene with graphite powder based products (graphite nanotubes or carbon particles are added to the granular structure of polystyrene [94];
- Aerogel-based products - have a wide range of products for insulating transparent or non-transparent surfaces [5];
- VIPs - vacuum thermal insulation panels, based on nano particles, with high thermal insulation power and very low thickness [6];
- Nano-ceramic thermal insulation coatings (extra thin film coatings) for insulating transparent or non-transparent surfaces [7];
- PCMs - phase change materials based on paraffin nanoparticles and salt hydrate, whose paraffin globules with a diameter between 2 and 20 nm are encapsulated in a plastic shell. They can be integrated into building materials, whereby, with a concentration of about 3 million such capsules in one square centimeter, they

change their aggregate state from solid to liquid when the temperature changes, and thus maintain the required temperature in buildings [8].

The five types of building facade nanomaterials are analysed in this paper according to their properties in relation to the following established criteria, shown of Fig.1:

- Criteria 1 - thermal conductivity;
- Criteria 2 - environmental impact (toxicity, pollution and embodied energy);
- Criteria 3 - material thickness;
- Criteria 4 - cultural heritage impact.

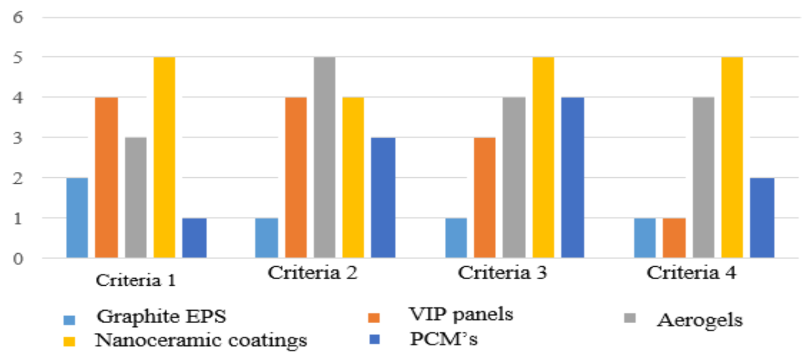

Fig. 1 Nanomaterials evaluation according to their properties and established criteria

From the conducted research, it can be concluded that aerogel based products and nano-ceramic coatings showed the best results in terms of the established criteria. These materials have the lowest rate of toxicity to the environment, low embodied energy and pollution in their production process, high thermal insulation properties (thermal conductivity), availability in extremely small thicknesses and above all, small impact on the original architectural appearance after façade renovations.

3. SILICA AEROGEL BASED MATERIALS

Aerogel-based building products are currently considered to be promising insulation materials mostly due to their high thermal properties with small thickness. Furthermore, they have quite low embodied energy, lower than traditional insulation products and other nanomaterials [9]. Different types of aerogel-based building nanomaterials are investigated in this paper, in order to give an overview of the state of the art use of aerogel nanomaterials in construction industry and their potential and significance for the EE improvement, CE implementation and cultural heritage proper renovation. Silica aerogels have amazing thermal properties, ie. they have a density of 1.9kg/m³, a volume porosity of 99.8% or a specific surface of 400 – 1000 m²/g. Pure silica has an extremely low thermal conductivity λ = 0.014 W/mK, while for different silica aerogel products \ it varies (0.01-0.02 W/mK)[10]. They are great sound absorbers, especially due to their high porosity with a pore size of 1-100 nm. Due to the silanol in their composition, they are waterproof. Thermal insulation materials based on silica aerogel are present in many forms and under different commercial brands. The most common forms are: aerogel panels, blankets, plasters, light concrete, granules, transparent films etc. (Fig.2).

a) b) c) d) e)

Fig.2 Silica aerogel products a)blankets; b)panels; c)light concrete; d)granules; c)plaster

4. AEROGEL BASED PRODUCTS ANALYSYS AND RESULTS

From the analysed types of aerogel-based products, it can be concluded that each of them has a similar composition, excellent thermal performances and above all, all of the aerogel based materials are sustainable, eco-friendly and since the silica based aerogel is mineral, it can be reused as an insulation material after a recycling process, which meets the CE criteria. Silica aerogel material has many applications and it can be modified to meet a number of specific purposes required by CE, since they have low embodied energy, lower than traditional insulation products [11][12]. Aerogel can be mixed to develop a green building material with unique characteristics and have a great potential for an application in green and sustainable buildings [12][13]. However, one of the criteria, such using the aerogel as a façade material in cultural heritage buildings is not possible for all types of aerogel based products, which also has an impact to the CE principles since building renovation and adaptive reuse is one of the main CE goals.

Tab. 1 Aerogel based products comparisons according to their cultural heritage impact

Type of aerogel product	Authenticy	Integrity	Reversibility	Compatibility
Aerogel blanket	Can be used where proportions cannot be changed (windows, doors) or where not enough space is available. Flexible for uneven surfaces	Removal and replacement of original material and necessary anchoring points should be minimised	Reversibility of the application is required. Possible addition to existing façade. Visual difference to original material is positive	Physical compatibility with historical materials and techniques is required. Vapour openness can be influenced by exterior render. Scientific proof of compatibility should be given
Panel/ board	The authentic appearance should be preserved and cannot be covered by boards. Boards can only be used in the interior if there are no protected parts.	Removal and replacement of original material and anchoring points should be minimised. Boards can be used without anchors, but glued by glue.	Reversibility of the application is required. Possible addition to existing façade. Visual difference to original material is positive	Physical compatibility with historical materials and techniques (vapour open, durable) is required. Vapour openness can be influenced by exterior render. Scientific proof of compatibility should be given
Plaster/ render	The original visual appearance of the building is possible to be reproducted by plasters. On uneven surfaces, mouldable render can be used for artistic and architectural details	Removal and replacement of original material should be minimised. The aerogel render can be an addition to the existing render	The aerogel plaster is considered reversible and can be removed down to original layers with a trowel and residues by hard brush. Its softness is considered a positive property	Physical compatibility with historical materials and techniques (vapour open, durable) required. Proof should be given scientifically.
Granular form	Authenticity not affected by filling of a cavity with granules if it is not exposed	Addition of granules do not affect the integrity of building	Reversible to previous status	Material can cause decrease of adhesion of other materials. If dust escapes, it can lead to skin and eye irritation. Increased hydrophobicity
Translucent panel	Daylighting of interior with diffusive effect can be achieved. Translucent elements are recognisable from original glazing. Better noise protection is achieved	Replacement of old translucent panels possible without change of integrity, depending on original frame. Additional structural frame might be required	Reversible to previous status	Compatibility is comparable with original forms of glazing. Panels might fit into original frames. Panels made out of glass and polycarbonate used for outer part of layered panel are considered as compatible

For this purpose, analysis of different types of aerogel based products are carried out terms to their methods of application in cultural heritage buildings and the results are explained in Table 1. The technical characteristics of the different aerogel products and their use and impact in the processes of cultural-historical heritage restoration and renovation are explained, according to four significant criteria for cultural heritage: authenticity, integrity, reversibility and compatibility. From the conducted analysis, it can be concluded that the most appropriate aerogel based material for renovation and preservation of historical buildings are the aerogel thermal insulation plasters (Table 1). Despite the fact that aerogel particles have the smallest impact of the authenticity and integrity, it is very difficult to be used in existing buildings. They are used to fill new hollow walls, to mix with the concrete or other materials in the process of creating the product, which usually correspond to smaller parts of the building such as architectural details, etc. but not to the façade walls which are responsible for the EE improvement.

The aerogel based thermal plasters or renders have the biggest potential in the application in existing buildings, especially cultural heritage buildings because of their soft texture and flexibility in applying on different surfaces [12][13]. According to the criteria for protection of historical buildings, aerogel plasters have a mild impact on their authenticity, but it is important that they are compatible with the chemical composition of the original materials, and can be easily removed without damaging them with no need for additional fastening that would damage the original material [14]. The application of the new material will not only improve the energy efficiency and sustainability of the building but also it will protect it from climate conditions and expand its lifespan. Due to the composition and method of application, aerogel plasters are available in different textures and colors and they can perfectly mimic the existing materials making it difficult for distinguishing, while the original material remains preserved (see Fig. 3 and 4).

Fig.3 Old renaissance building façade [15] original material before aerogel plaster application (left); after aerogel plaster application (right)

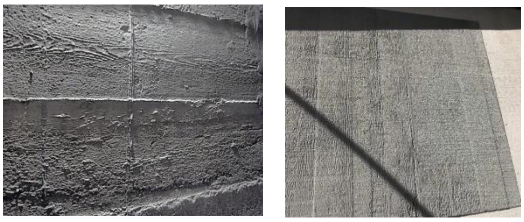

Fig.4 Old natural concrete façade, original material, before aerogel plaster (left), after aerogel plaster application (right)

5. DISCUSSION AND CONLUSION

Improving the energy efficiency and sustainability of the building stock is critical for meeting EU climate targets. Circular economy (CE), especially in the building sector, strive to reduce the pollution, extend the building's lifespan, reduce the material waste and favour the use of long-lasting building materials and products. Adopting the CE principles in building sector can reduce the quantity of materials used for the renovation of existing buildings, improve their energy performance and sustainability and minimize harmful emissions embodied in building materials. This paper aims to show the potential that different aerogel based materials have, because of their excellent thermal properties, low embodied energy and different products and methods of application in the building sector. The analyses of different types of aerogel materials bring the conclusion that the aerogel plaster is the most convenient product according to all of the established criteria. By applying the aerogel thermal plaster, the EE of the of the building will be improved, along with the thermal comfort, sustainability and lifespan. Also, by applying the thermal insulation from the outside, thermal bridges will be eliminated and the façade will be protected from external influences, preventing premature aging and carbonization of the original materials. By keeping the authenticity, integrity, reversibility and compatibility of the historical building in the process of renovation, together with improvement of the thermal comfort which leads to cutting the buildings emissions for heating and cooling, aerogel thermal plaster application has a great potential in EE, CE and cultural heritage renovation criteria and practices.

ACKNOWLEDGEMENT

The research has been conducted within the COST Action CircularB. The authors of this paper would like to thank the European Union for funding and COST (European Cooperation in Science and Technology) for supporting the COST Action CircularB CA21103, www.circularb.eu

REFERENCES

[1] Pacheco F. T., Buratti C., Kalaiselvam S., Granqvist C., Ivanov V.(2016) *Nano and Biotech Based Materials for Energy Building Efficiency*, DOI 10.1007/978-3-319-27505-5, Springer International Publishing Switzerland

[2] Attia S., Kurnitski J., Kosiński P., Borodiņecs A., Belafi D. Z., István K., Krstić H., Moldovan M., Visa I., Mihailov N., Evstatiev B., Banionis K., Čekon M, Vilčeková S., Struhala K., Brzoň R., Laurent O. (2022). Overview and future challenges of nearly zero-energy building (nZEB) design in Eastern Europe, Energy and Buildings, Volume 267, https://doi.org/10.1016/j.enbuild.2022.112165.

[3] Xing Y., Hewitt N., Griffiths P. (2011) Zero carbon buildings refurbishment—a hierarchical pathway. Renew Sustain Energy Rev 15:3229–3236

[4] Power A (2008) Does demolition or refurbishment of old and inefficient homes help to increase our environmental, social and economic viability? Energy Policy 36:4487–4501

[5] Bozsaky D. (2016). Special Thermal Insulation Methods of Building Constructions with Nanomaterials, Széchenyi István University, Department of Architecture and Building, Construction, Hungary, Vol. 9, No. 1, pp. 29-41, DOI:10.14513/actatechjaur.v9.n1.391

[6] Lakatos A., Deak I. Berardi U.(2018). Thermal characterization of different graphite polystyrene. Int. Rev. Appl. Sci. Eng. 9 (2018) 2, 163–168DOI: 10.1556/1848.2018.9.2.12

[7] Bozsaky D. (2017). Thermodynamic tests with nano-ceramic thermal insulation coatings, Pollack Periodica 12. pp. 135-145. doi: https://doi.org/10.1556/606.2017.12.1.11

[8] Baetens R., Bjorn Petter J., Gustavsen A.(2010). Phase change materials for building applications: A state-of-the-art review. Energy and Buildings 42(9):1361-1368, DOI: 10.1016/j.enbuild.2010.03.026

[9] Curto D. D., Cinieri V. (2020). Aerogel-based plasters and energy efficiency of historic buildings. Literature review and guidelines for manufacturing specimens destined for thermal tests. Sustainability. 12, 9457; http://dx.doi.org/10.3390/su12229457

[10] Berardi U. (2017). Aerogel-enhanced systems for building energy retrofits: Insights from a case study, Energy and Buildings 159 (2018) 370–381. Elsevier

[11] Handojo D. U., Xiaodong L., Eng T. J.N. (2022). Sustainable production in circular economy: aerogel upscaling production. Environmental Science and Pollution Research 29:20078–20084, Springer

[12] Ganobjak M.(2019) Aerogel materials for heritage buildings: Materials, properties and case studies", Journal of Cultural Heritage, Elsevier

[13] Castro-Díaz M., Osmani M., Cavalaro S., Parker B. Lovato T., Needham P., Thompson J., Philippe K., Ruiz F. (2022). Impact of Circular Silica Aerogel on Plasterboard Recycling. Loughborough, University.https://hdl.handle.net/2134/21435765.v1

[14] Carty L.(2017)Analysis of the effects of aerogel insulation on the thermal performance of existing building envelopes, Edinburgh Napier University, 09013398

[15] Ganobjak M., Brunner S., Wernery J.(2019). Aerogel materials for heritage buildings: Materials, properties and case studies, Journal of Cultural Heritage, Volume 42, Pages 81-98, https://doi.org/10.1016/j.culher.2019.09.007.

THE INFLUENCE OF GYPSUM-FIBER BOARDS ON HEAT TRANSFER THROUGH LSF COMPOSITE PANELS WITH COMBUSTIBLE INSULATION

Marija Jelčić Rukavina[1], Davor Skejić[2], Ivana Banjad Pečur[3], Martina Mataković[4]

Summary:

The main objective of this paper is to analyse, by means of experimental tests, the effects of different configurations of gypsum fiberboards on the fire behavior of light steel frame (LSF) composite panels. For this purpose, a standardized fire resistance test was performed on two specimens consisting of a steel frame, polyurethane (PUR) foam as a thermal insulation layer and three layers of gypsum fiberboards on both sides of the specimen. The configurations differed by the type of gypsum fiberboard, and during testing, the temperature rise through the cross-section of the boards was monitored. In addition, a thermogravimetric analysis of the gypsum fiberboards was performed. The results show that regardless of the type of board used in the LSF panel, the same class of fire resistance is achieved in terms of insulation properties, but a faster temperature rise was observed in the panel in which gypsum fiberboards with a lower fire performance were used.

Key words: lightweight composite panels, gypsum fibre boards, polyurethane insulation, heat transfer

[1] Assoc. Prof., University of Zagreb, faculty of Civil Engineering, Zagreb, Croatia, marija.jelcic.rukavina@grad.unizg.hr
[2] Prof., University of Zagreb, Faculty of Civil Engineering, Zagreb, Croatia, davor.skejic@grad.unizg.hr
[3] Prof., University of Zagreb, Faculty of Civil Engineering, Zagreb, Croatia, ivana.banjad.pecur@grad.unizg.hr
[4] MSc student, University of Zagreb, Faculty of Civil Engineering, Zagreb, Croatia, martina.matakovic@student.grad.hr

1. INTRODUCTION

Light gauge steel framing (LSF) systems are among the most popular wall systems in today's construction industry. The higher strength-to-mass ratio associated with cold-formed steel construction results in lighter structures, leading to significant savings in construction time, transportation costs, and labour requirements [1], [2]. Because the high thermal conductivity of the steel, it is important to consider the poor energy efficiency of cold-formed steel structures and ensure adequate thermal insulation with different types of thermal insulation materials, which may or may not be combustible [2]. Furthermore, LSF structures are sensitive to heat exposure, fire-resistant wall panels are used as passive fire protection. The most commonly used fire-resistant panels are gypsum boards due to its non-combustible core and good thermal properties. To determine the fire resistance of a structure, fire tests are usually carried out by subjecting test specimens to one-sided fire exposure based on the temperature-time curve specified in the standard ISO 834 [3]. The fire resistance of LSF walls depends on both their thermal and structural performance in fire. The thermal performance (temperature evolution) depends on the type, thermal properties, and thicknesses of the sheathing panels and insulation, as well as on the quality of the sheathing joints, while the structural performance depends on the thermal performance, the shapes and sizes of the steel sections, and the degradation of the mechanical properties of the steel used [4]. A brief literature search revealed that knowledge on the fire performance of LSF structures is extensive, but there are few studies on the fire performance of LSF structures with combustible insulation materials, which in most cases have lower thermal conductivity than non-combustible thermal insulation materials. Therefore, in the research project *'Composite lightweight panel with integrated load-bearing structure - KLIK PANEL*" [5], an LSF panel with improved thermal performance was developed by replacing the typical mineral wool insulation with polyurethane (PUR) foam. Due to the combustibility of PUR, the project, beside other goals, aims to analyse the type and number of gypsum boards that will provide the required fire resistance of minimum 90 minutes. In this paper, a part of the project results is presented, with the focus of the thermal performance of two LSF panels obtained by fire tests. The tested panels differ in the type of gypsum fiberboards used. First, a thermogravimetric analysis (TG) of the GFBs used was performed and discussed to show the differences between them.

2. EXPERIMENAL TESTING

2.1. THERMOGRAVIMETRIC ANALYSIS OF GYPSUM FIBREBOARDS

Two types of 12.5 mm GFBs were used from the same manufacturer (Fermacell GmbH): 1. GFB with density 1250 ± 50 kg/m^3 and reaction to fire A1, (A1 GFB onwards) and 2. GFB with density 1150 ± 50 kg/m^3 and reaction to fire A2, s1-d0 (A2 GFB onwards), Figure 1.

a) b)

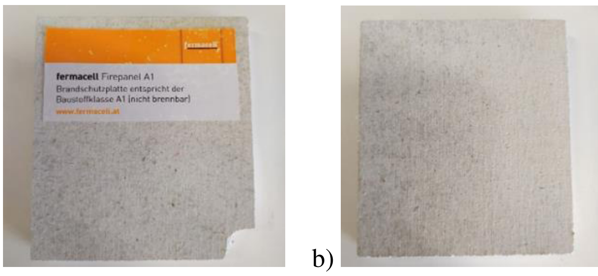

Fig. 1 Fibre-gypsum boards (GFB): a) A1 GFB; b) A2 GFB

A thermogravimetric (TG) analysis by TA instruments was conducted on the both GFB specimens to compare mass loss of two used boards when exposed to rising temperature. The temperature program for measurements started at room temperature and was then increased to 900°C at a rate of 10 °C/min. A small specimen's size (1-3 mg) was used in an air atmosphere.

2.2. FIRE TESTING OF PANELS

The fire resistance tests were performed on two specimens with dimensions of 1500 mm (width) and 2995 mm (height), with the configuration presented in Table 1.

Tab. 1 Configuration of the tested panels

Specimen	Cross-section	Configuration of the LSF panels
PANEL 1	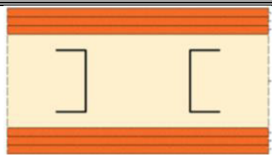	2xGFBe-PUR-2xGFBe
PANEL 2	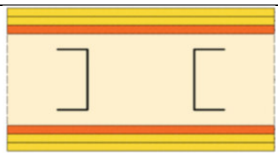	GFBe-2xGFB-PUR-2xGFB-GFBe

The steel frame consisted of studs, tracks, noggings and diagonal segments. A steel frame formed of C-shaped CFS members with dimensions 42x89x10x0.95 mm and steel grade S 550 GD were used, as shown in Figure 2.

Fig. 2 Steel frame of the tested LSF walls

Fig. 3 Testing specimen in the furnace before testing

With the aim to achieve FRR of 90 min, both specimens were sheathed with three layers of GFB s – specimen 1 with three layers of A1 GFB and specimen 2 with one A1 GFB, as the base layer, and two layers of A2 GFBs. Z-shaped spacers were placed on the noggings and studs to separate the wallboards from steel members and minimise the effect of thermal bridges. The specimens constructed in this way were then filled with PUR foam. The density of the PUR foam was 45 kg/m³ ± 5% and the added flame retardants in the mixture accounted for about 10-30% of the mass of the polyol. The total thickness of the specimens was 210 mm. The fire tests were performed in accordance to EN 1365-1 [6]. Therefore, the fire maintained the ISO 834 fire curve according to EN 1363-1 [7] with 6 radiant burners. Type K (NiCr-Ni) thermocouples were placed to monitor the temperatures on the unexposed side of the panel, but also to monitor development through the cross section of LSF walls. The Ø0.5 mm thermocouple wires were welded to 0.2 mm thick copper disks, which were attached to the wallboards with screws and welded to the steel frame. Figure 4 shows the placement of the thermocouples through the thickness of the specimens. The thermocouples were placed vertically at two heights, 1600-1650 mm and 2500-2550 mm from the bottom track.

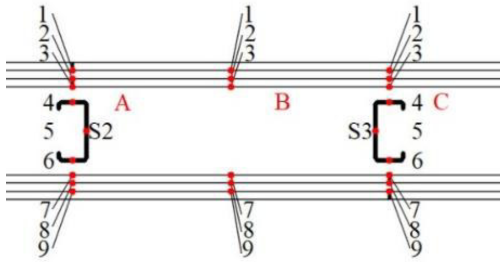

Fig. 4 Position of the thermocouples through thickness of the specimens

Each specimen was placed in the test rig and loaded with a total vertical load of 37.5 kN using hydraulic jacks. In addition, displacement transducers were placed on the specimens between the load beam and the fixed frame. They recorded the distances between the load beam and the fixed frame, which changed due to the deformations of the specimen. However, since this paper deals only with the thermal performance of the tested panels, the structural performance results will be presented elsewhere.

3. RESULTS AND DISCUSSION

3.1. THERMOGRAVIMETRIC ANALYSIS

Figure 5 shows the variations in mass loss for both GFBs. Significant mass losses occurred in the temperature range of 80°C–153°C, and 285°C- 393°C, reaching mass losses of 16% and 23% for A1 GFB and 14% and 23% for A2 GFB. Further mass losses occurred earlier for A2 GFB, peaking at 650°C and 732°C for A1 GFB. After 393°C, a 2% higher mass loss was observed for A2 GFB.

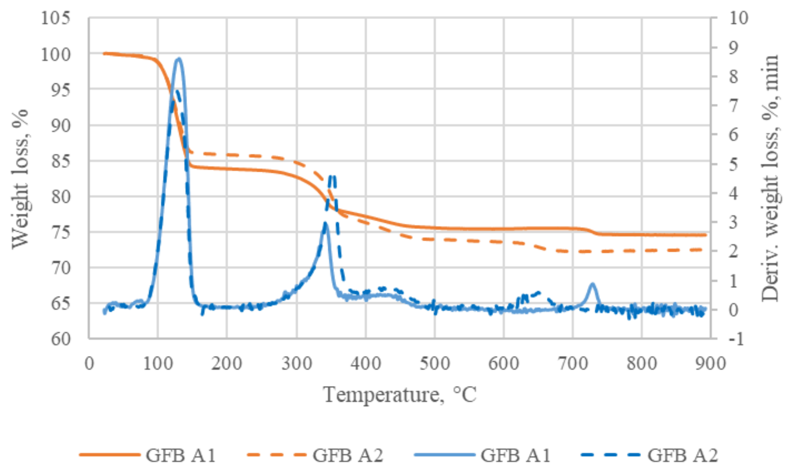

Fig. 5 Results of TG and DTG analysis of GFB used in the study

3.2. TEMPERATURE DEVELOPMENT THROUGH THE PANELS DURING FIRE RESISTANCE TESTS

The temperature exposure of panel 1 lasted 107 minutes, and 97 min for panel 2, but temperatures for both panels were recorded up to 120 minutes. Figure 6 shows the ambient sides of the specimens after testing. This side of the specimens remained intact throughout the test, and no discoloration, smoke, flames, or cracks were observed, as confirmed by the detailed post-test observations.

a) b)

Fig. 6 Appearance of the unexposed side of tested specimenat the end of testing: a) Panel 1 and b) Panel 2

The temperature-time curves recorded between the wallboards positioned at the exposed side of the specimens (T1-T3) for both specimens are shown in Figure 5a), on the steel profiles (T4-T6) in Figure 5b), and on the unexposed side (T7-T9) in Figure 5c).

a) b) c)

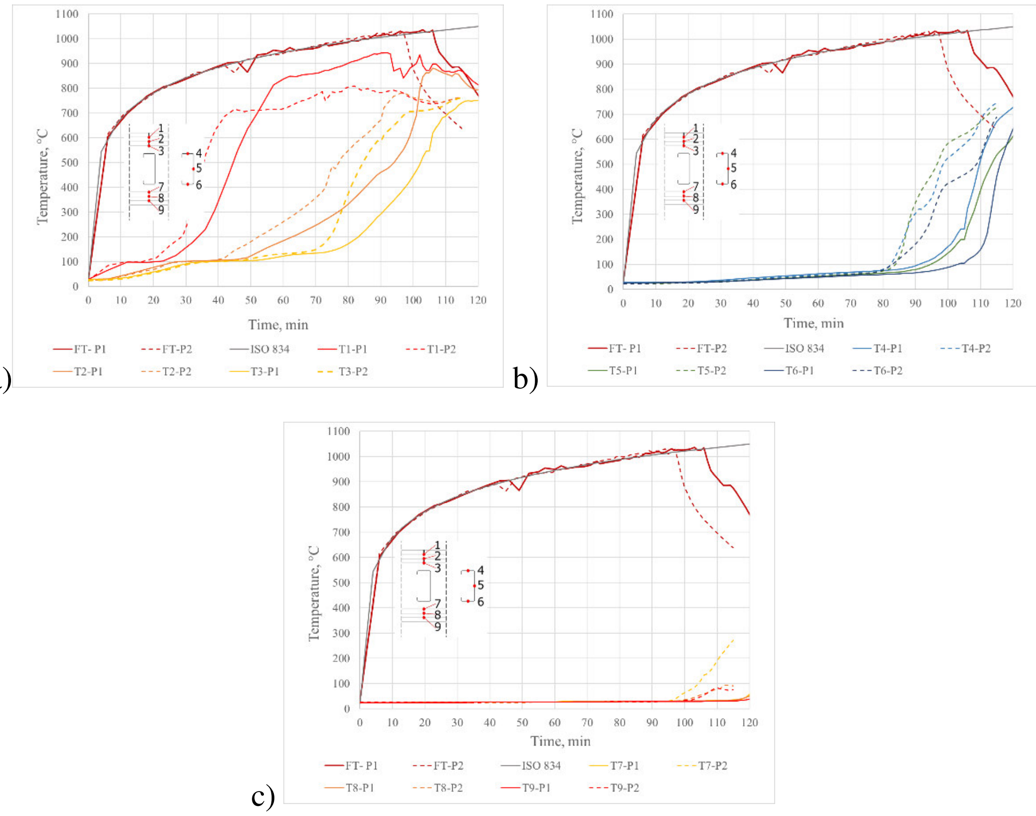

Fig. 7 Temperatures vs.time recorded a) between GFBs at the exposed side, b) at steel profiles and c) between GFBs at the un-exposed side of the panel

From the Figure 5a), a plateau around the temperature of 100°C is observed at each thermocouple position for both tested specimens. This is primarily due to the dehydration processes that occur in fire protective wallboards. Used wallboards contain about 20% bound water and 3-4% free water, evaporation of which prevents a temperature rise, but also at other locations of specimens, including the steel profiles. Nevertheless, an earlier temperature rise was observed on specimen 2 at all thermocouple positions. After 90 minutes of thermal exposure, temperatures at the hot flange, web and cold flange of steel profiles recorded at specimen 1 were 95°C, 80°C and 67°C, respectively, while those recorded on specimen 2 at the same locations were 305°C, 348°C and 182°C, respectively. These temperatures are below critical temperatures for steel, but after 90 minutes of fire exposure, rapid temperature rise was observed at steel profiles on both specimens. At the positions of unexposed wallboards (T7-T9), the temperatures of around 30°C were recorded after 90 minutes of fire exposure for both specimens, implying that insulation criterion was not reached.

4. CONCLUSIONS

This paper presents the results of fire tests related to the thermal behaviour of two LSF wall specimens insulated with PUR thermal insulation and lined with three layers of GFBs with different fire properties. Although the specimens were made with combustible thermal insulation, the results showed that this LSF composition can be used for 90 minutes. The structural criterion was not analysed in this work, but the temperatures obtained on the steel sections were lower than the critical temperatures of steel. The evaporation of bound and free water in the microstructure of GFBs prolongs the temperature evolution in the whole assembly. Nevertheless, the specimen consisting of two GFBs with fire reaction A2 experienced an earlier rapid temperature rise compared to the specimen consisting of three GFBs with fire reaction A1. Thermogravimetric analysis showed a higher mass loss of the A2 GFB after 355°C. As soon as the gypsum fiberboards lost their protective properties on the exposed side of the specimen, the temperatures in the remaining part of the specimen increased rapidly.

ACKNOWLEDGEMENT:

This research was funded by the European Union through the European Regional Development Fund's Competitiveness and Cohesion Operational Program, grant number KK.01.1.1.07.0060, project "Composite lightweight panel with integrated load-bearing structure (KLIK-PANEL)"

REFERENCES

[1] Perera D. et al. (2020) Fire performance of cold, warm and hybrid LSF wall panels using numerical studies, Thin-Walled Struct., vol. 157, doi: 10.1016/j.tws.2020.107109.

[2] Soares N., Santos P., Gervásio H., Costa J. J. and Simões da Silva L. (2017) Energy efficiency and thermal performance of lightweight steel-framed (LSF) construction: A review, Renew. Sustain. Energy Rev., vol. 78, pp. 194–209, doi: 10.1016/j.rser.2017.04.066.

[3] Ščapec T., Skejić D., Rukavina M. J (2023) Experimental Study on Fire Performance of Polymer Foam Cavity Insulated Light Steel Framed Walls, ce/papers, vol. 6, no. 3–4, pp. 2114–2119, doi: 10.1002/cepa.2443.

[4] Kesawan S., Mahendran M. (2018) A Review of Parameters Influencing the Fire Performance of Light Gauge Steel Frame Walls, vol. 54, no. 1. Springer US.

[5] Jelčić Rukavina M., Skejić D., Kralj A., Ščapec T., Milovanović B. (2022) Development of Lightweight Steel Framed Construction Systems for Nearly-Zero Energy Buildings, Buildings, vol. 12, no. 7, p. 929, doi: 10.3390/buildings12070929.

[6] CEN The European Committee for Standardization (2012), EN 1365-1 Fire resistance tests for loadbearing elements -- Part 1: Walls. Brussels, Belgium.

[7] CEN The European Committee for Standardization (2020), EN 1363-1 Fire resistance tests - Part 1: General requirements. Brussels, Belgium.

THE EFFECT OF THERMAL BRIDGES ON TOTAL HEAT LOSSES OF LSF WALLS

Mergim Gaši[1], Bojan Milovanović[2], Domagoj Tkalčić[3], Marija Jelčić Rukavina[4]

Summary:

New trends in the construction industry are leading to lightweight structures that combine both structural elements such as steel with thermal insulation materials such as polyurethane foam or mineral wool. Although these elements have lower heat losses compared to conventional concrete or brick walls, the impact of thermal bridges on the total heat losses of these walls can be significant. In this paper, numerically calculated and experimentally measured results are compared to show the difference in total heat losses through these walls, and it is emphasised that numerical analysis is necessary since experimental results can be misleading if measurement is not performed appropriately.

Key words: lightweight steel frame structures, LSF, Numerical analysis, Heatflowmeter, HFM

[1] PhD, University of Zagreb, Faculty of Civil Engineering, Zagreb, Croatia, mergim.gasi@grad.unizg.hr
[2] Associate professor, University of Zagreb, Faculty of Civil Engineering, Zagreb, Croatia, bojan.milovanovic@grad.unizg.hr
[3] Assistant, University of Zagreb, Faculty of Civil Engineering, Zagreb, Croatia, domagoj.tkalcic@grad.unizg.hr
[4] Associate professor, University of Zagreb, Faculty of Civil Engineering, Zagreb, Croatia, marija.jelcic.rukavina@grad.unizg.hr

1. INTRODUCTION

Sustainability and CO2 emission reduction are top priorities [1], as the building sector is responsible for 40 % of energy consumption and 36 % of CO2 emissions [1]. Many of the aging buildings in the European Union (EU) are not energy efficient [2]. In response, the EU has mandated that all public buildings must meet near-zero energy buildings (nZEB) standards starting in 2019, and all new buildings must follow these standards starting in 2021 [3].

The Fit for 55 package aligns EU policy with climate targets and aims to reduce CO2 emissions from buildings by 2030 [4]. The European Parliament protected these targets in the European Climate Change Act, making them legally binding [5]. By 2028, all new buildings must be zero-emission buildings (ZEBs) [6], with public buildings achieving this by 2026 [6], exceeding the nZEB standards.

Lightweight steel frame (LSF) structures offer numerous advantages over conventional materials [7–10], but are at risk of thermal bridging due to the conductivity of steel [11–15]. To address this, increased thermal insulation is required to solve this problem.

Quality control methods such as infrared thermography (IRT) and heat flow meter (HFM) help evaluate thermal performance after construction. The U-value, a critical parameter in the evaluation of energy consumption, is determined according to the standard ISO 6946 [16]. There are several methods for calculating the U-value, including experimental, numerical, and analytical methods. Numerical methods provide high accuracy but are less common due to their complexity and computational cost, especially for LSF elements with steel columns [17,18].

The objectives of this study include comparing U-value calculation methods – experimental and numerical – for LSF elements and investigating the effects of lightweight steel structures on surface heat flux, especially for the HFM method, considering the effects of sensor placement on U-value measurements [15,19].

2. WALL SPECIMENS

Five different specimens were evaluated (Tab. 1), consisting of different wall segments and an EPS reference specimen (Fig. 1). The wall specimens consisted of a steel framework filled with polyurethane foam and coated with double and triple fire protection cladding panels. An EPS reference specimen with a known thermal conductivity was also evaluated to validate the test results. The material properties are shown in Tab. 2.

The load-bearing structure of the wall specimens consists of steel C-sections, and some specimens also have diagonal stiffeners (Fig. 1a and 1b). Two different wall thicknesses were investigated, as these specimens were optimized for improved sound insulation with additional fire protection panels on both sides. The wall thicknesses of the specimens were 185 mm and 210 mm, while the reference specimen had a thickness of 185 mm. All specimens had the same external dimensions of 1130 x 2000 mm (width × height) with an area of 2.26 m^2.

Tab. 1 Specimens

Specimen name	d [mm]	Number of fireboards	Diagonal stiffeners
S1-185-DS	185	2	YES
S1-185-WDS	185	2	NO
S2-210-DS	210	3	YES
S2-210-WDS	210	3	NO
EPS-185-RS	185	--	--

Tab. 2 Material properties

Specimen name	d [cm]	λ [W/(m K)]
PUR	13.5	0.036
Gypsum boards	12.5	0.38
Steel	8.9	50
EPS	18.5	0.033

a) b)

Fig. 1 Wall specimens and heat-flow-meter positioning: a) without diagonal stiffeners; b) with diagonal stiffeners

3. HEAT-FLOW-METER METHOD

The Heat Flow Meter (HFM) is a method for determining the U-value on site. It involves simultaneous measurements of heat flux with a flowmeter and indoor and outdoor temperatures with a pair of thermocouples (Fig. 2), as described in the standard ISO 9869. Typically, heat flux data is averaged over an extended period of time to compensate for daily variations in air temperature and heat flux over the area under study. However, in cases where heat flux and temperature have semi-stationary characteristics during the measurement, as is the case in this study, the measurement time can be shortened.

The equipment used in this study is the TRSYS01 heat flux measurement system from Hukseflux (Fig. 3), which meets all the requirements listed in the standard ISO 9869.

The indoor and outdoor temperatures were simulated by a hotbox chamber on which the wall specimens were installed. In the chamber, a steady-state heat transfer through the wall was achieved with 20 °C on the warm side and 0 °C on the cold side of the installed specimen.

Heat transfer coefficient (U-value) is calculated from HFM measurement using the average method given in ISO 9869 as:

$$U = \frac{\sum_{i=1}^{n} q_i}{\sum_{i=1}^{n}\left(T_{int}^{i} - T_{ext}^{i}\right)} \tag{1}$$

Where q_i is heat flux density in W/m^2 and T_{int} and T_{ext} are internal and external temperature in °C.

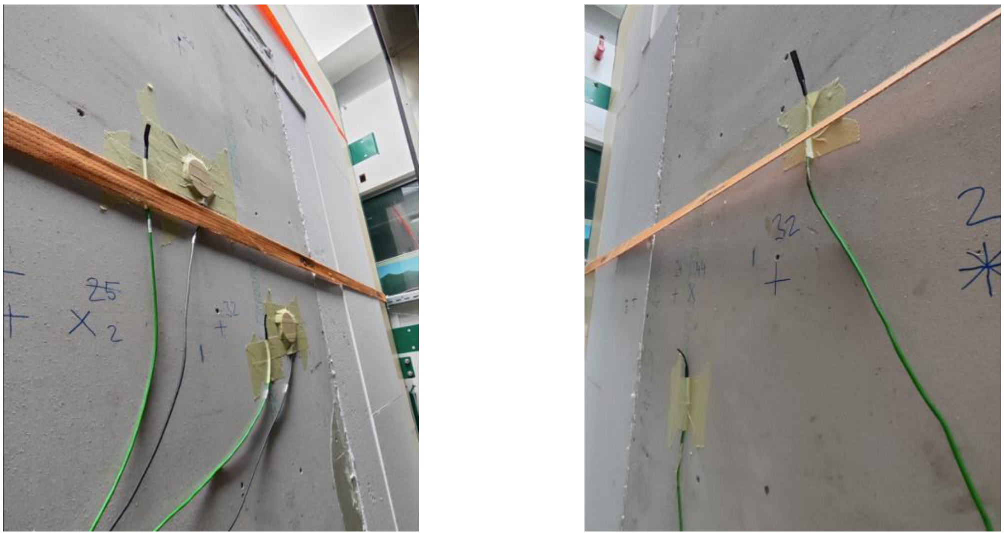

a) b)

Fig. 2 Installation of heat-flow-meter apparatus: a) indoor environment; b) outdoor environment

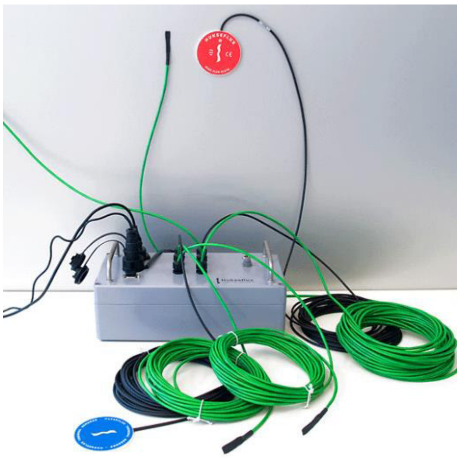

Fig. 3 Heat-flow-meter apparatus

4. NUMERICAL ANALYSIS

Three-dimensional thermal calculations were carried out using a software tool called AnTherm, designed specifically for estimating heat loss in building materials and structures. These calculations were based on geometric models representing the steel framework filled with polyurethane foam, including all the different layers like fireboard and polyurethane foam shown in Fig. 4a and 4b.
However, it is important to note that these geometric models did not consider certain details, such as the space between the steel framework and the fireboard layer or the openings in the steel framework that are designed to distribute the polyurethane foam evenly throughout the sample. These aspects were not considered during the calculations.

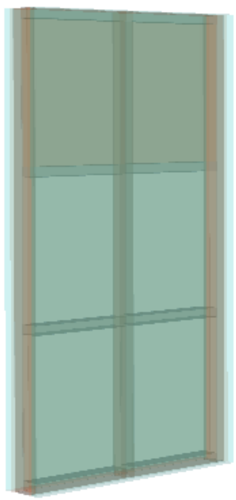

a)

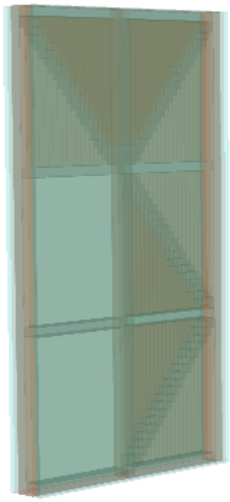

b)

Fig. 4 Geometrical models: a) without diagonal stiffeners; b) with diagonal stiffeners

Heat transfer coefficients on the internal and external surface were calculated using the procedure described in ISO 8890 standard (Tab. 3).

Tab. 3 Surface heat transfer resistances

Specimen name	R_{si} [(m^2 K)/W]	R_{se} [(m^2 K)/W]
S1-185-DS	0.07	0.04
S1-185-WDS	0.05	0.06
S2-210-DS	0.11	0.05
S2-210-WDS	0.11	0.05
EPS-185-RS	0.08	0.04

Result of the 3D numerical analysis is L3D or thermal conductivity coefficient in W/K from which the U-value is calculated as:

$$U = \frac{L_{3D}}{A} \tag{1}$$

Where A is the area of the specimen in m^2.
Total heat flux for reference EPS specimen is calculated as 1D due to the fact the specimen is homogenous.

5. RESULTS

5.1. HFM

Fig. 5a-e show the results of the HFM measurements while Tab. 4 shows the measured heat fluxes and U-values calculated using the average method (Eq. 1).

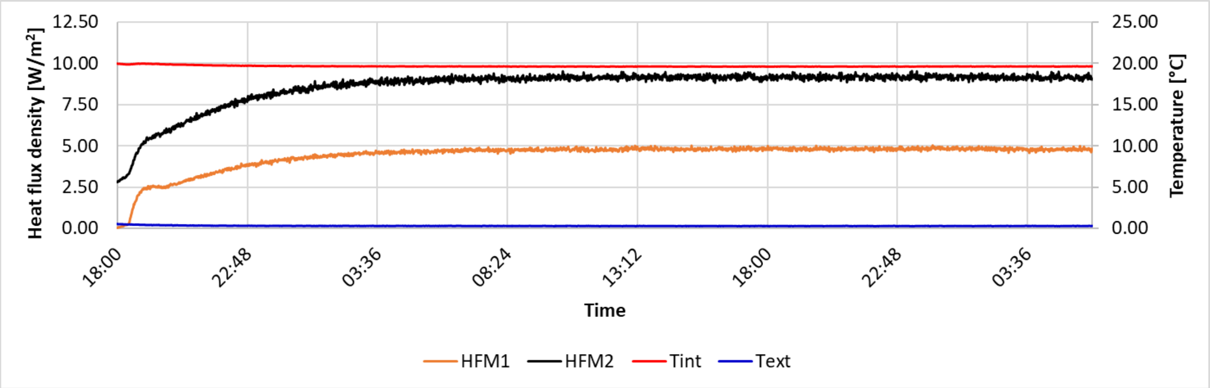

a) S1-185-DS

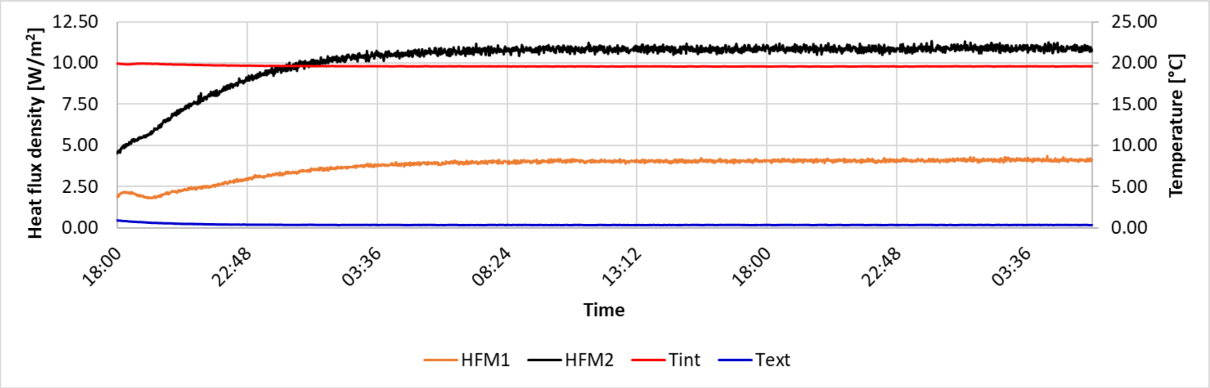

b) S1-185-WDS

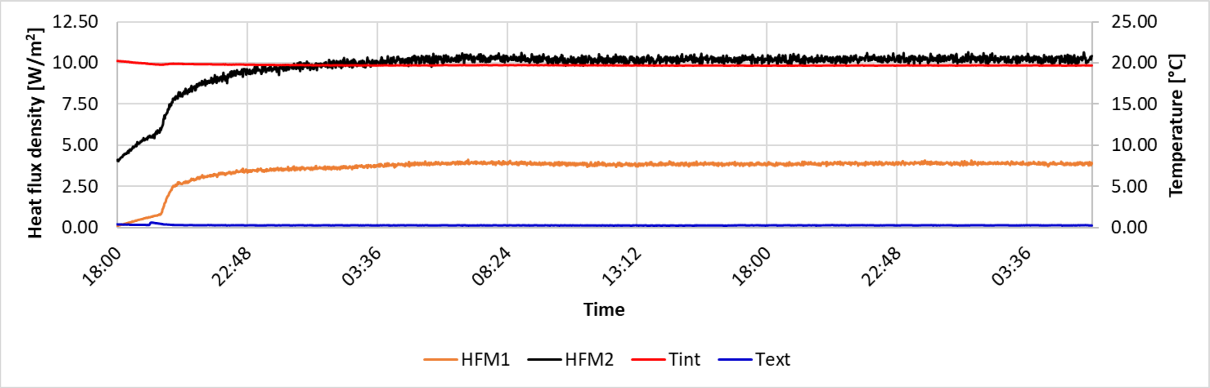

c) S2-210-DS

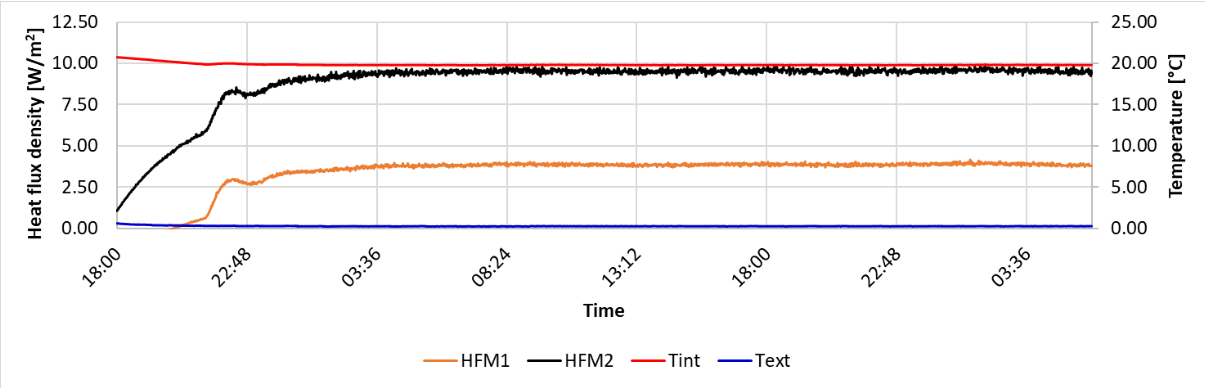

d) S2-210-WDS

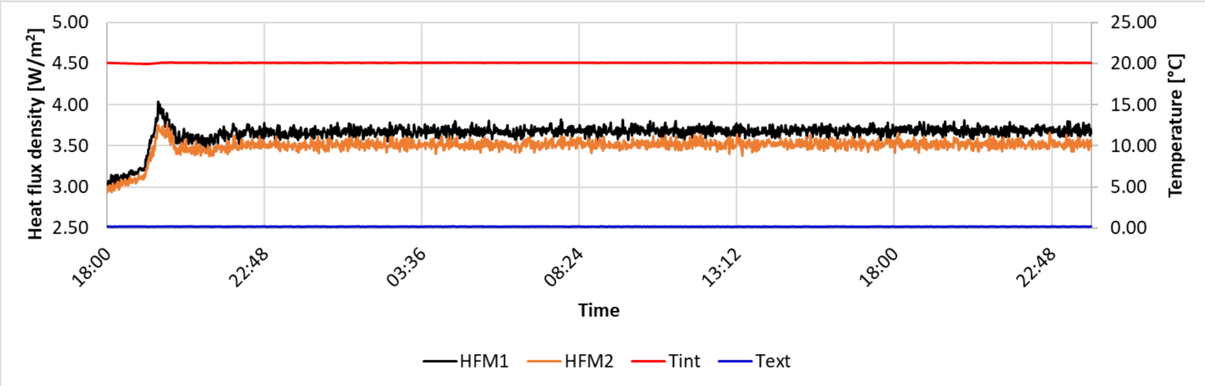

e) EPS-185-RS

Fig. 5 HFM measurement results

Tab. 4 U-values (HFM)

Specimen name	q_{HFM1} [W/m²]	q_{HFM2} [W/m²]	U-value [W/(m² K)]		
			Min	Max	Av
S1-185-DS	3.883	10.221	0.200	0.526	0.363
S1-185-WDS	3.887	9.542	0.199	0.489	0.344
S2-210-DS	4.815	9.144	0.249	0.474	0.361
S2-210-WDS	4.052	10.839	0.208	0.556	0.382
EPS-185-RS	3.677	3.518	0.177	0.185	0.181

5.2. NUMERICAL ANALYSIS

Fig. 6a-d shows the results of the 3D numerical analysis while Tab. 5 shows the heat fluxes calculated on the same locations as where the HFM measurements were carried out (Fig. 1). Tab. 5 shows the U-values calculated for each specimen according to Eq. 2.

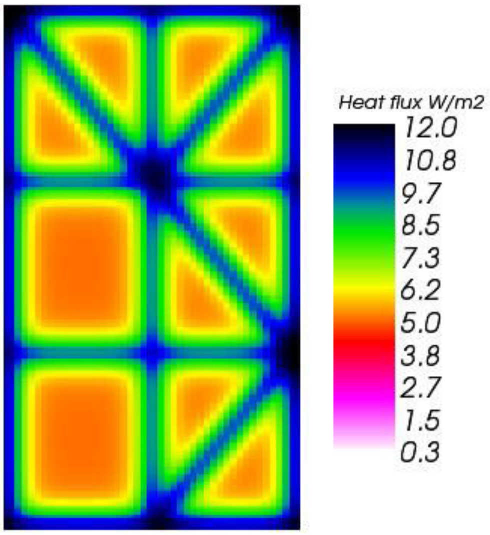

a) S1-185-DS

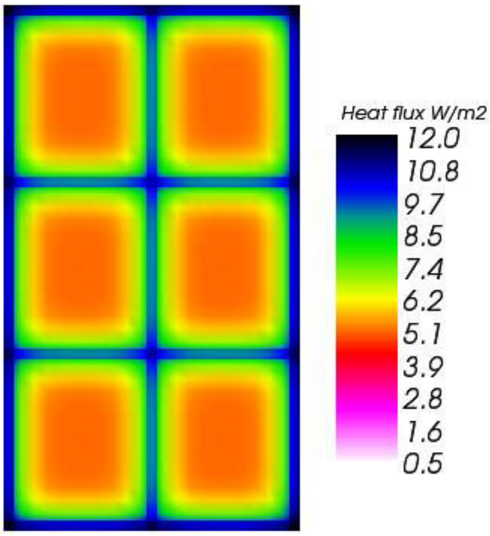

b) S1-185-WDS

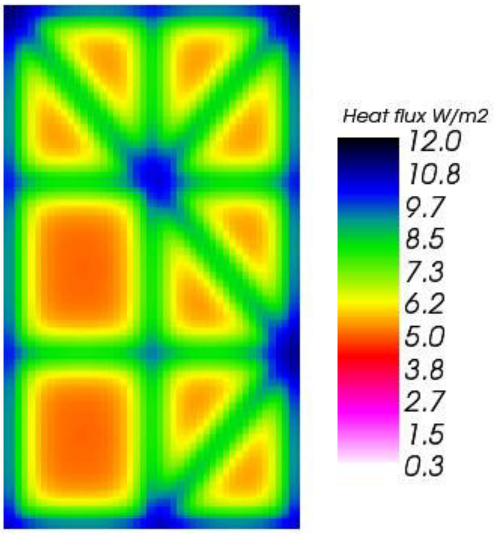

c) S2-210-DS

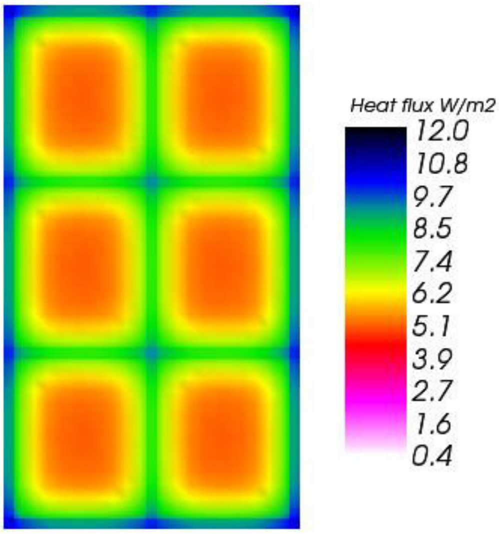

d) S2-210-WDS

Fig. 6 Numerical analysis results

Tab. 5 U-values (Numerical analysis)

Specimen name	q_{HFM1} [W/m^2]	q_{HFM2} [W/m^2]	L_{3D} [W/K]	U-value [W/(m^2 K)]
S1-185-DS	5.230	11.540	0.846830	0.375
S1-185-WDS	4.970	10.710	0.768692	0.340
S2-210-DS	4.880	10.990	0.809656	0.358
S2-210-WDS	4.930	9.160	0.737786	0.326
EPS-185-RS	3.500		--	0.175

5.3. COMPARISON OF THE RESULTS

Fig. 7a and 7b show the comparison of heat flux densities measured with HFM heat-flow-meters and those calculated numerically. The difference between these heat flux densities ranges from 1.35 to 34.69% for the 1D heat flux measured/calculated in the area where no steel stiffeners are present, and from 0.51 to 20.20% for the heat flux measured/calculated at the point where the heat flux is maximum, i.e., at the point where four or six stiffeners meet (depending on whether diagonal stiffeners are present or not).

Fig. 7c shows the comparison between the U-values calculated with the HFM and the numerically calculated values. With the HFM, the U-values are calculated as the average U-value between the minimum and maximum heat flux densities, while the numerically calculated U-values take into account the total heat flux that flows through the wall surface (L3D). Fig. 7d shows that the U-values calculated by these two methods correlate very well, with the maximum difference of 14.66 (17.18) % for specimen S2-210-WDS. This difference can be attributed to the incorrect positioning of the HFM sensor.

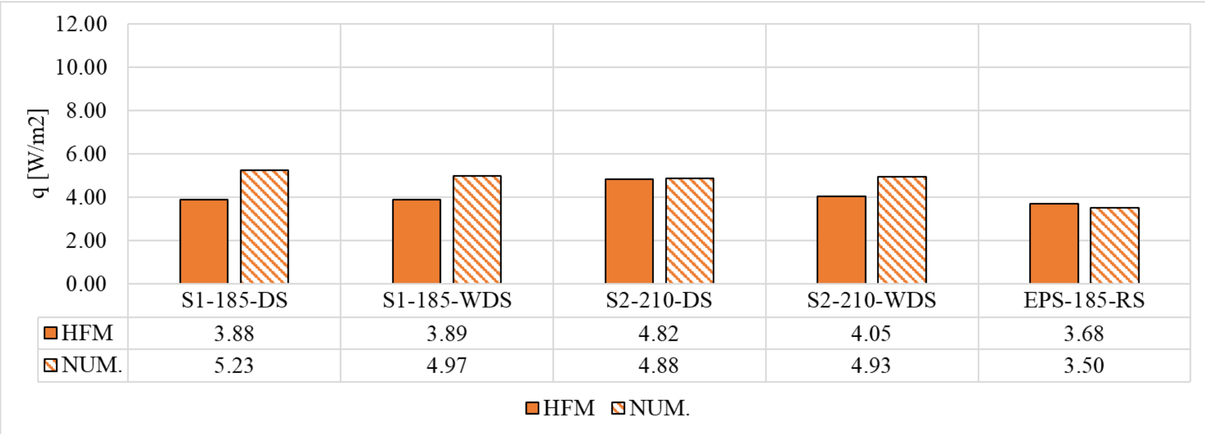

a) Minimal heat flux densities (HFM1)

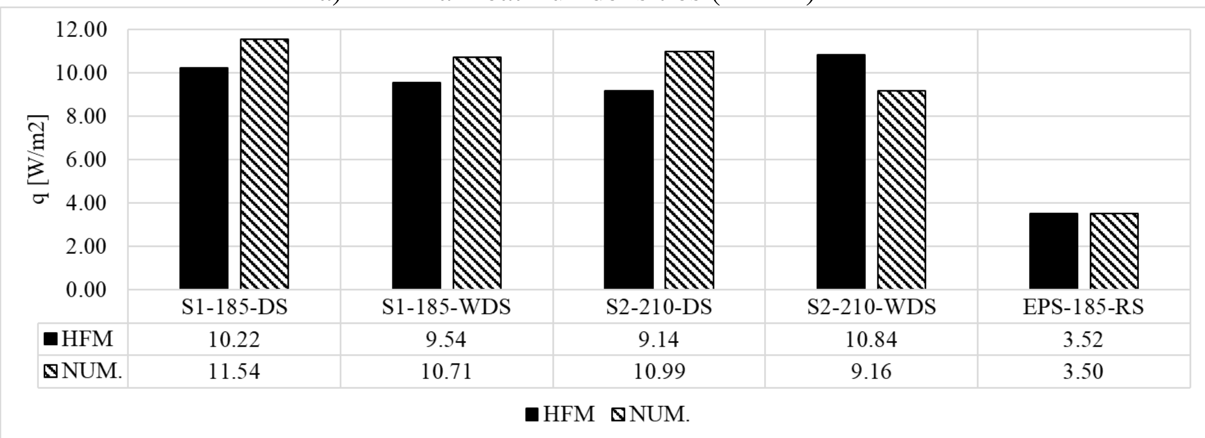

b) Maximal heat flux densities (HFM2)

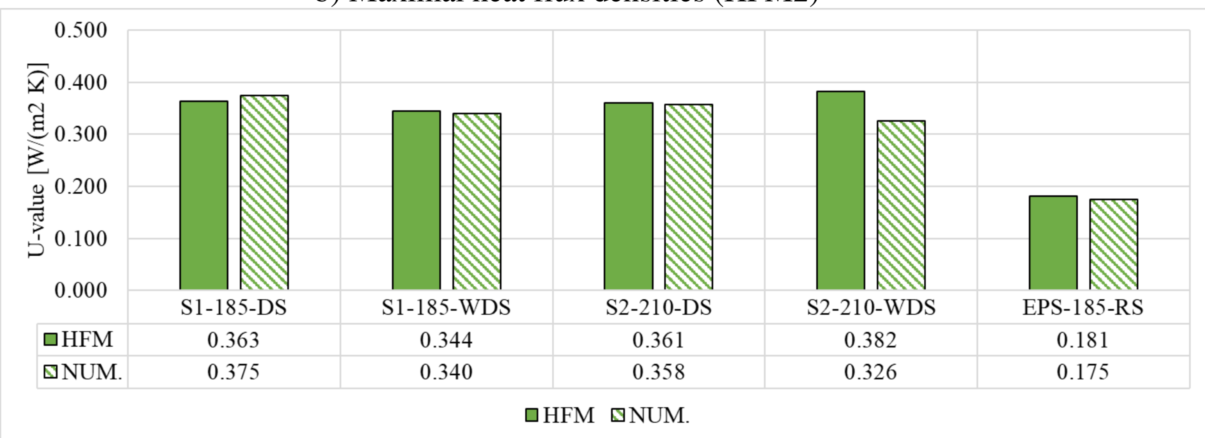

c) U-values

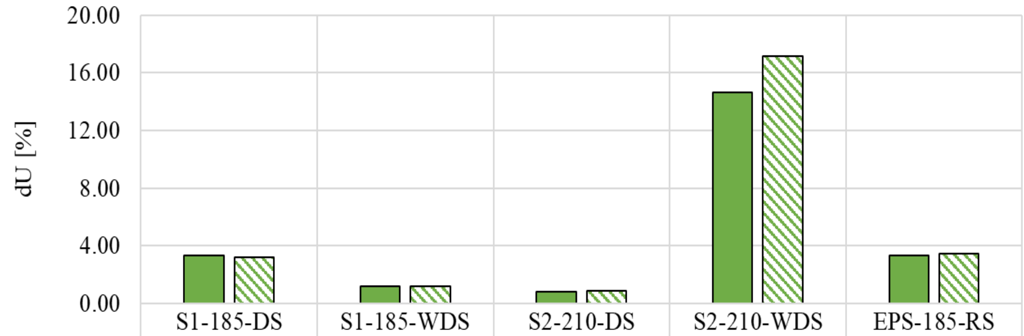

	S1-185-DS	S1-185-WDS	S2-210-DS	S2-210-WDS	EPS-185-RS
|UHFM - UNUM|/UHFM	3.31	1.16	0.83	14.66	3.31
|UHFM - UNUM|/UNUM	3.20	1.18	0.84	17.18	3.43

|UHFM - UNUM|/UHFM |UHFM - UNUM|/UNUM

d) U-value differences

Fig. 7 Comparison of results (HFM Vs. Numerical analysis)

6. CONCLUSION

In this work, four different LSF wall specimens and one EPS reference wall specimen were experimentally evaluated and numerically calculated to compare the heat flux densities and heat transfer coefficients (U-values) calculated by these two methods. The experimental results were carried out using the HFM method, in which heat flux densities are measured directly, from which the U-value is calculated according to the average method described in the standard ISO 9869. The numerical analysis was performed using a special computer software for the calculation of heat transfer in building physics – AnTherm. A three-dimensional numerical analysis was performed, and the result of the numerical analysis was the coefficient L_{3D}, from which the total U-values of the wall specimens were calculated.

After the measurement and analysis were done, the heat flux densities were compared, and the results show a difference between the heat flux densities from 1.35 to 34.69% for the 1D heat flux measured/calculated in the area where there are no steel stiffeners, and from 0.51 to 20.20% for the heat flux measured/calculated at the point where the heat flux is maximum, i.e., at the point where four or six stiffeners meet (depending on whether diagonal stiffeners are present or not).

The main objective of this work was to show the potential of the HFM method for in-situ measurement of the U-value in LSF walls, using the numerically calculated U-value as a reference. The comparison of the U-values shows a good agreement between these two methods with a maximum difference of 14.66 (17.18) % for specimen S2-210-WDS. This difference can be attributed to the incorrect positioning of the HFM sensor.

This effect can also be seen in the results of the heat flux densities. If the sensor is placed at the part of the LSF wall where there are no steel elements, the heat flux is one-dimensional, but if the sensor is placed at the junction of the steel elements, the heat flux is three-dimensional, and the difference between these two heat flux densities can be more than 200% compared to the one-dimensional heat flux. When using the HFM method in situ, the position of the steel elements should be known in advance, or a non-destructive technique such as infrared thermography or a device such as concrete rebar locator scanner should be used to identify the position of the steel studs.

ACKNOWLEDGEMENT

This research was funded by the European Union through the European Regional Development Fund's Competitiveness and Cohesion Operational Program, grant number KK.01.1.1.07.0060, project "Composite lightweight panel with integrated load-bearing structure (KLIK-PANEL)".

REFERENCES

[1] European Commission: In focus: Energy efficiency in buildings. Available at: https://commission.europa.eu/news/focus-energy-efficiency-buildings-2020-02-17_en (accessed on 23 June 2023)

[2] M. Economidou a, V. Todeschi a b, P. Bertoldi a, D. D'Agostino a, P. Zangheri a, L.C. a: Review of 50 years of EU energy efficiency policies for buildings, (2020). Doi: https://doi.org/10.1016/j.enbuild.2020.110322

[3] European Commission: Energy performance of buildings directive. Available at: https://energy.ec.europa.eu/topics/energy-efficiency/energy-efficient-buildings/energy-performance-buildings-directive_en (accessed on 23 June 2023)

[4] European Parliament: BRIEFING Towards climate neutrality: Fit for 55 package, (2021)

[5] European Commission: European Climate Law. Off J Eur Union:17, (2021)

[6] Fokaides, P.A.; Kylili, A.; Kyriakides, I.: Boundary conditions accuracy effect on the numerical simulations of the thermal performance of building elements. Energies 11(6), (2018). Doi: 10.3390/en11061520

[7] Soares, N.; Santos, P.; Gervásio, H.; Costa, J.J.; Simões, L.: Energy e ffi ciency and thermal performance of lightweight steel-framed (LSF) construction : A review 78(April):194–209, (2017). Doi: 10.1016/j.rser.2017.04.066

[8] Perera, D.; Upasiri, I.R.; Poologanathan, K.; Gatheeshgar, P.; Sherlock, P.; Hewavitharana, T.; Suntharalingam, T.: Energy performance of fire rated LSF walls under UK climate conditions. J Build Eng 44(September):103293, (2021). Doi: 10.1016/j.jobe.2021.103293

[9] Rukavina, M.J.; Skejić, D.; Kralj, A.; Ščapec, T.; Milovanović, B.: Development of Lightweight Steel Framed Construction Systems for Nearly-Zero Energy Buildings. Buildings 12(7), (2022). Doi: 10.3390/buildings12070929

[10] Atsonios, I.A.; Mandilaras, I.D.; Kontogeorgos, D.A.; Founti, M.A.: Two new methods for the in-situ measurement of the overall thermal transmittance of cold frame lightweight steel-framed walls. Energy Build 170:183–94, (2018). Doi: 10.1016/j.enbuild.2018.03.069

[11] Santos, P.; Lopes, P.; Abrantes, D.: Thermal Performance of Lightweight Steel Framed Facade Walls Using Thermal Break Strips and ETICS : A Parametric Study. Energies 16(4), (2023). Doi: https://doi.org/10.3390/en16041699

[12] Santos, P.; Abrantes, D.; Lopes, P.: Experimental and Numerical Performance Evaluation of Bio-Based and Recycled Thermal Break Strips in LSF Partition Walls. Buildings 12(8), (2022). Doi: https://doi.org/10.3390/buildings12081237

[13] Moga, L.; Petran, I.; Santos, P.: Thermo-Energy Performance of Lightweight Steel Framed Constructions : A Case Study. Buildings 1(3), (2022). Doi: https://doi.org/10.3390/buildings12030321

[14] Santos, P.: The Importance of Stud Flanges Size and Shape on the Thermal Performance of Lightweight Steel Framed Walls. Sustainability 13(7):1–22, (2021). Doi: https://doi.org/10.3390/su13073970

[15] Santos, P.; Lemes, G.; Mateus, D.: External Facade LSF Walls : A Parametric Study. Energies (1):1–20, (2019). Doi: https://doi.org/10.3390/en12142671

[16] EN ISO 6946: Building components and building elements — Thermal resistance and thermal transmittance — Calculation methods, (2017)

[17] Pomada, M.; Adamus, J.; Boruszewski, A.: Numerical and Experimental Analysis of Heat Flow at Window-to-Wall Interface. Energies 15(10), (2022). Doi: 10.3390/en15103837

[18] Santos, P.; Mateus, D.; Ferrandez, D.; Verdu, A.: Numerical Simulation and Experimental Validation of Thermal Break Strips' Improvement in Facade LSF Walls. Energies 15(21), (2022). Doi: 10.3390/en15218169

[19] Roque, E.; Santos, P.: The effectiveness of thermal insulation in lightweight steel-framedwalls with respect to its position. Buildings 7(1), (2017). Doi: 10.3390/buildings7010013

BUCKLING OF CONCRETE PANELS UNDER BIAXIAL COMPRESSION ACCORDING TO RHEOLOGICAL-DYNAMICAL THEORY

Aleksandar Pančić[1], Dragan D. Milašinović[2]

Summary:

This paper is concerned with experimental verification of inelastic buckling and failure analysis of concrete panels according to rheological dynamical theory (RDT). Iterative modulus calculation of buckling stress is presented and verified for concrete panels under biaxial and axial compression. For biaxial compression, three different concrete mixtures with two stress ratios are considered. Some experimental results from literature are also used to verify RDT calculation for concrete panels under axial compression as well as analytical expressions for concrete wall panel in two-way action. Besides normal concrete strength, this calculation can be used for fibre-reinforced ultra-high performance concrete UHPC. The calculation according to RDT had shown that the values of material parameters of such modulus of elasticity and Poisson's ratio have a significant influence on the structural material constant as well as buckling stress results. The calculation of buckling stress which is necessary for RDT calculation was carried out using the corresponding model in Abaqus software.

Key words: Rheological-Dynamical theory, Concrete Panels, Buckling Analysis, Biaxial Compression of Concrete, Stability of Concrete Panels

[1] PhD, Faculty of Civil Engineering Subotica, University of Novi Sad, Serbia, pancic2707@hotmail.com
[2] Prof. dr, Faculty of Civil Engineering Subotica, University of Novi Sad, Serbia, ddmil@gf.uns.ac.rs

1. INTRODUCTION

Compression members such as walls and columns have a very important role for the stability of buildings, industrial objects etc. There are many scientists and engineers, who have studied the structural stability problems. Leonhard Euler developed mathematical solution for columns under compression. With Euler's equations the critical buckling load of elastic material columns under various end conditions can be calculated. Timoshenko, S.P. and Gere J.M (1961) [1] have studied the theory of elastic stability of thin panels. They derive the mathematical solutions for plates under axial and biaxial compression.
Biaxial concrete strength has been topic of interest of many researchers. The results by Kupfer et al. (1969) [2] have shown that the compressive strength under biaxial compression is only 16 % larger than under uniaxial compression. Hussein A. and Marzouk H. (2000) [3] have studied the normal and high strength concrete panels specimens with dimensions 150 x 150 x 40 mm under biaxial loading. Their results show that the ultimate strength of concrete under biaxial compression was higher than under uniaxial compression. The maximum biaxial strength occurred at a biaxial stress ratio of 0,5 for all specimens tested. Load bearing behavior and stability of concrete wall panels have been investigated by several researchers, where some of the basic mathematical variations of different parameters were researched. This includes the variation of panel dimension (slenderness, thickness), steel reinforcement, eccentricities, concrete strength, and support condition. Many studies have investigated the behavior of concrete wall panel in one or two-way action. Two-way action considers the buckling of concrete walls, with side supports and axial compression. An overview of researches can be found in the paper by Doh J. H. et al. (2001) [4]. Fehling E. et al. (2008) [5] carried out experimental studies on reinforced concrete panels with and without fibres to biaxial compression-tension loading. The panels were 1000 mm long in the tensile direction, 500 mm high in the compression direction and 100 mm thick. The results have shown the reduction of the compression strength of the cracked reinforced concrete with and without steel fibres. A material model for cracked reinforced concrete with and without fibres is derived. Methods for design concrete walls are also a part of many codes and standards. Most of the mathematical equations are based on experimental investigations or some empirical solutions. Eurocode 2 [6] refers to reinforced concrete walls with a length to thickness ratio of 4 or more and in which the reinforcement is taken into account in the strength analysis. For walls subjected predominantly to out-of-plane bending, the rules for slabs apply. Second order effects may be ignored, if they are less than 10 % of the corresponding first order effects. Bourada M. et al. (2019) [7] proposed a new simpler formula of the Euler buckling stress of isotropic rectangular panels under axial compression loading in one and two orthogonal directions. This formula takes into account the transverse shear effect in an uniform manner across the thickness of the panel. The numerical verification was made on steel panels using the finite element method.
This paper shows the calculation and experimental verification of biaxial buckling load using the RDT. RDT is a mathematical-physical analogy proposed by Milašinović D. D. and it describes inelastic and time-dependent problems. This theory describes the critical mechanical behavior of viscoelastoplastic (VEP) materials under the cyclic stress variation. The scheme of the RDA modulus iterative method is already presented by Milašinović D. D. et al. (2018) [8]. This method was numerically verified for stability problems of steel panels. The experimental verification of this method on concrete panels is presented in this paper. Chapter 2 contains a short overview of the theory and RDA modulus iterative method. In chapter 3 is presented the experiment and in chapter 4 the verification on examples from literature.

2. BUCKLING ACCORDING RHEOLOGICAL-DYNAMICAL THEORY

2.1. RDA-A SHORT OVERVIEW

Since 2000 Milašinović D. D. developed a mathematical-physical analogy called rheological-dynamical analogy (RDA) which describes inelastic problems related to the load-bearing capacity of structural members (such as buckling and VEP deformation, fatigue of metals etc.). Mathematical analogy is given between rheological and dynamical model. The rheological body is shown in Figure 1 using the following symbols: N for the Newtonian dashpot, StV for Saint-Venant's body, H for the Hookean spring, "|" for a parallel connection and "—" for a connection in a series.

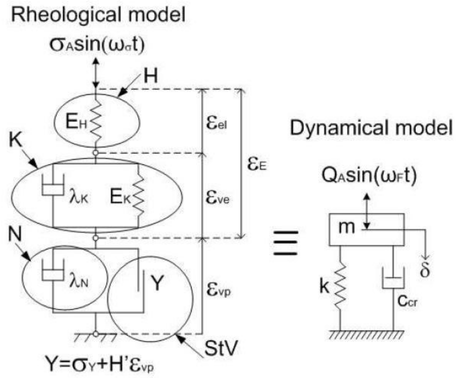

Fig. 1 Analogy between rheological and dynamical model - Milašinović D. D. (2015) [9]

Since the Hookean spring, Kelvin's body (K = H|N) and viscoplastic body (StV |N) are connected in a series, the stress loads in all the bodies are equal. The total axial strain is the sum of three components: elastic (instantaneous), viscoelastic and viscoplastic. Milašinović D. D. (1996) [10] gives differential equation for this model,

$$\begin{aligned}\ddot{\varepsilon}(t) + \dot{\varepsilon}(t)\cdot\left(\frac{E_K}{\lambda_K}+\frac{H'}{\lambda_N}\right) + \varepsilon(t)\cdot E_K\cdot\frac{H'}{(\lambda_K\cdot\lambda_N)} = \\ \ddot{\sigma}(t)\cdot\frac{1}{E_H} + \dot{\sigma}(t)\cdot\left[\frac{E_K}{(\lambda_K\cdot E_H)}+\frac{H'}{(\lambda_N\cdot E_H)}+\frac{1}{\lambda_K}+\frac{1}{\lambda_N}\right] + \\ +\sigma(t)\cdot\left[\frac{(E_K+H')}{(\lambda_K\cdot\lambda_N)}+E_K\cdot\frac{H'}{(\lambda_K\cdot\lambda_N\cdot E_H)}\right] - \sigma\gamma\cdot\frac{E_K}{(\lambda_K\cdot\lambda_N)}\end{aligned} \tag{1}$$

where E_H is Young's modulus and σ_Y is the uniaxial yield stress. The four material constants in fixed steps of time are: coefficient of viscoelastic viscosity λ_K and viscoplastic viscosity λ_N, and moduli E_K (viscoelastic) and H´ (viscoplastic). Milašinović D. D. (2000) [11] derived the solution of the differential equation and presented the inelastic response of viscoelastic and viscoplastic material under cyclic stresses with constant amplitude. The solution of the differential equation is also presented in [12] and [13]. Additionally to these solutions the RDA modulus for homogeneous isotropic inelastic material was derived in RDT, which is shown in the Equation (2),

$$E_R = E_H\cdot\frac{1+\delta^2+\varphi}{(1+\varphi)^2+\delta^2} \tag{2}$$

where E_H is Young's modulus, δ is the ratio of the load or the stress frequency to the frequency of natural vibrations and φ is the creep coefficient. The RDA modulus is used in different inelastic problems for mechanic as well as for stability issues.

Milašinović D. D. (2015) [9] derived relation between Poisson's ratio and creep coefficient which is based on the Bernoulli energy theorem. This relation is given by Equation (3),

$$\varphi = \frac{2 \cdot \mu}{1 - 2 \cdot \mu} \tag{3}$$

where μ is Poisson's ratio.

2.2. RDA MODULUS ITERATIVE METHOD

Milašinović D. D. et al. (2018) [8] derived RDA equations for isotropic 3D continua. The RDA modulus for homogeneous isotropic inelastic material is presented in other form, which is given in the Equation (4),

$$E_R = \frac{3 \cdot E_H}{(5 - 4 \cdot \mu) + 2 \cdot (1 + \mu) \cdot \varphi} \tag{4}$$

The second relation, given by Eq. (5) assumes the linear relationship between the stress σ and the creep coefficient. Milašinović D. D. (2015) [9] has introduced this assumption and named it the law of flow,

$$\sigma(t) = \frac{\sigma_E}{\varphi^*} \cdot \varphi(t); \quad \sigma_E = \frac{1}{K_E} \cdot \varphi^* \tag{5}$$

where K_E is the structural material constant and φ^* the creep coefficient at the limit of elasticity. This coefficient K_E can be defined on concrete cylinders and is presented by Milašinović D. D. (2015) [9] with the Equations (6) and (7),

$$\lambda_E = \pi^2 \cdot \frac{i^3}{I} \cdot \frac{1}{\gamma\varphi} \tag{6}$$

$$K_E = \lambda_E \cdot \frac{i^3}{I} \cdot \frac{1}{E_H \gamma} \tag{7}$$

where γ is the specific weight of the material, i is the minimum radius of gyration, λ_E is the slenderness ratio at the limit of elasticity and I is the minimum moment of inertia of the cross section. Taking into account Eqs. (4) and (5) a mathematical function between RDA modulus and critical stress is made. The RDA modulus in first iteration can be calculated using the Equation,

$$E_R^{(1)} = \frac{3 \cdot E_H}{(5 - 4 \cdot \mu) + 2 \cdot (1 + \mu) \cdot \sigma_{cr} \cdot K_E} \tag{8}$$

The buckling stress σ_{cr} causes the decrease of stiffness and is the input parameter for the next iteration. The corresponding modulus after (n) iterations is given by the following Equation,

$$E_R^{(n)} = \frac{3 \cdot E_H}{(5 - 4 \cdot \mu) + 2 \cdot (1 + \mu) \cdot {\sigma_{cr}}^{(n-1)} \cdot K_E} \tag{9}$$

Equation (9) is used to calculate the buckling stress of concrete panels under biaxial compression. The buckling stress is calculated using the finite element method in the Abaqus software. The RDA modulus changes in each iteration from the buckling stress and for each iteration a buckling calculation in Abaqus is required. This iterative procedure can be simplified by using a linear numerical function between modulus and buckling stress. This numerical function was found using several buckling stress calculations for different E-modulus and is used in Equation (9). This procedure is described in Chapter 3.

3. EXPERIMENTAL VERIFICATION

3.1. MATERIALS AND TEST SPECIMEN

The concrete panel specimens used in this study were 500 x 500 x 50 mm in dimension. The panels are reinforced with a Q84 reinforcing mesh on both sides that has a bar thickness of 4 mm. Concrete cover is 10 mm. The edges of the panel are additionally reinforced with stirrups of 4 mm, that are welded on reinforcement mesh. All reinforcement is constructive and in theoretical consideration is not taken into account. Reinforcement should exclude early failure of the corners. Self-compacting concrete with 8 mm aggregate size was used. Normal weight concrete mixtures with three different concrete strengths are tested. The reinforcement as well as formwork of panels are presented in Figure 2. The care and storage of all concrete samples until the test was carried out within the company Binis Beton in Banja Luka (Bosnia and Herzegovina), where the concrete strength on cubes 150 mm are tested. Concrete cylinders d / h = 150 mm / 300 mm are tested at the University of Novi Sad - Serbia (Laboratory of Civil Engineering Subotica). The elastic modulus, Poisson's ratio and density are tested on cylinders. The results are shown in Table 1.

Fig. 2 Reinforcement and formwork of concrete panels

3.2. EXPERIMENTAL SET-UP

The experiments were performed in the company Selena d.o.o. in Banja Luka (Bosnia and Herzegovina) with a hydraulic machine (No. 000100). The machine was upgraded for the biaxial compression tests. Horizontal compression was realized by two parallel-bonded hydraulic cylinders (Product Lukas with 100 tons per cylinder) which are placed in the same steel frame with concrete panels. The steel frame is coated with fat on the inside to reduce the friction allocation between the panel and the steel frame. Eccentricity of load was zero. The experimental set-up is shown in Figure 3.

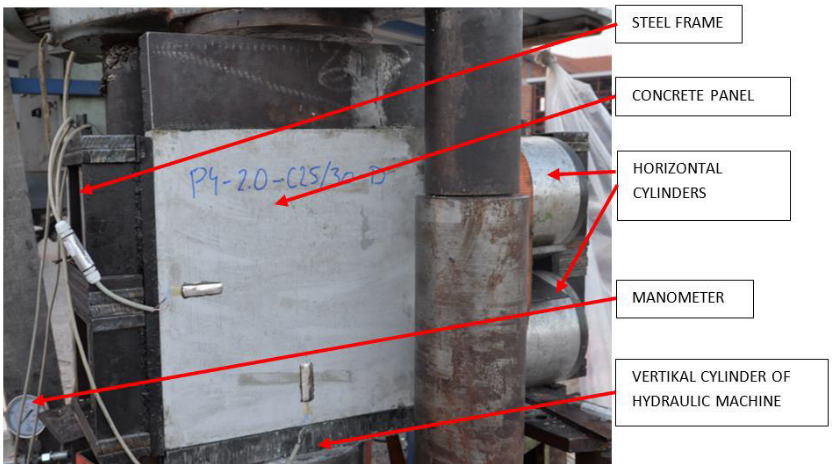

Fig. 3 Experimental set-up

Two different biaxial stress ratios for compression were considered. For tests with stress ratio 1,0 it was necessary to use a pressure booster because the horizontal and vertical cylinders deliver different forces. A pressure booster is a cylinder with different surfaces of the front and dorsal sides whose surfaces throughout the mechanism are obtained by applying Pascal's law. These surfaces are approximately aligned with the surfaces of the horizontal cylinders and the vertical cylinder of the press. The vertical cylinder has the following dimensions $D_1 = 320$ mm ($A_1 = 804$ cm^2), while two horizontal cylinders with a diameter of $D_2 = 171{,}5$ mm together give the area $A_2 = 462$ cm^2 and the ratio of their surfaces is 0,57. To obtain a ratio of 1,0, a pressure booster is used, which has a cylinder diameter of 62 mm and a piston rod of 45 mm. The ratio of the dorsal and front surfaces is 2,11; thus, the pressure in the horizontal cylinders will be many times greater than the pressure in the vertical cylinder. Without considering the influence of friction forces in cylinders the ratio of the horizontal and vertical forces would be 0,57 x 2,11 = 1,2. This ratio was corrected by measuring the friction of the cylinder. The influence of the friction in the cylinder was determined using one horizontal cylinder which was placed in the ram press. The separate measurement was carried out by first suppressing the upper cylinder with the lower cylinder and at the same time reading pressures. The measurement was also made in the opposite direction by pumping with a manual pump and moving the cylinders down. Loss due to friction in the cylinder was determined to be about 10 %. Taking into account the loss due to friction in the pressure booster the stress ratio was corrected to 1,08. For the stress ratio 0,57 the pressure booster was not necessary. Figure 4 shows the entire tying scheme.

In this experiment the stress ratios of horizontal and vertical force 1,08 and 0,57 were applied. Pressure readings on the manometer are converted into pressure on the concrete surface 50 x 5 cm and a coefficient of 0,9 is used due to the influence of friction in the cylinders. The approximate load rate range was about 0,2 - 0,6 MPa/s. This was made using a force increment regulator. The measuring of the concrete strain in two directions was carried out on a few samples using a strain gauge (HBM-1-LY41-50/120) and the corresponding Catman software, which is owned by the Institute for Testing Materials and Structures in Banja Luka (Bosnia and Herzegovina). The strain measurements in the edge area (distance from edge 7,5 cm) was used only to control the real stress ratios during the experiment. All pressure measurements were recorded with a camera until concrete panel failure.

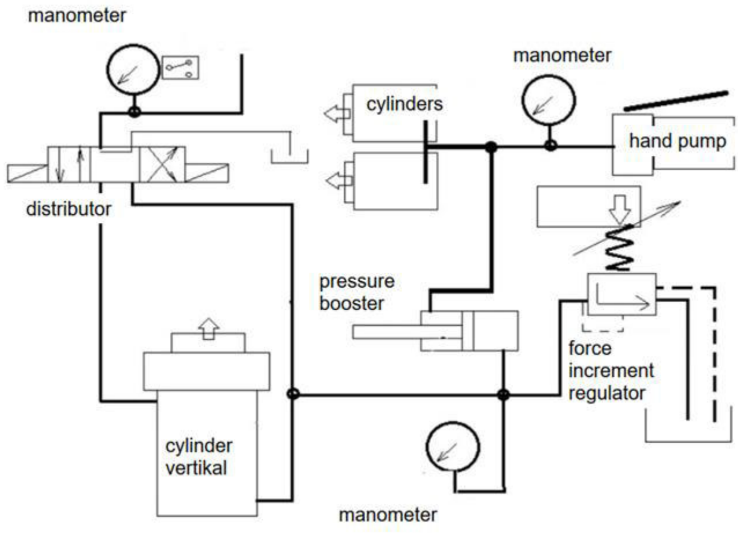

Fig. 4 Experimental tying scheme

3.3. TEST RESULTS

The test results on cubes and cylinders are shown in Table 1 and the measurement on concrete panels under biaxial compression with stress ratios 1,08 and 0,57 is shown in Table 2. Failure of concrete panels is shown in Figure 5.

Fig. 5 Failure of concrete panel (stress ratio 1,08 left) / (stress ratio 0,57 right)

Tab. 1 Material parameters for three different concrete mixtures

No.	Mixture	Age (days)	Density γ (kg/m3)	Modulus of Elasticity E (MPa)	Poisson's ratio μ	Compressive strength $f_{c,cylinder}$ (MPa)	Compressive strength $f_{c,cube}$ (MPa)
1	A	119	2416,33	36602,62	0,110	41,64	47,29
2		179	2405,01	36200,00	0,120	38,25	44,01
3		179	2397,46	38320,39	0,110	39,61	46,11
average values			2406,26	37041,00	0,113	39,83	45,80
4	B	179	2463,48	38800,00	0,100	45,04	57,51
5		179	2444,62	37722,22	0,125	59,30	58,89
6		116	2471,03	39180,61	0,120	48,66	58,88
average values			2459,71	38567,61	0,115	51,00	58,42
7	C	157	2442,73	38175,52	0,104	58,17	72,27
8		111	2476,69	38985,85	0,090	58,17	72,91
9		179	2450,28	39357,14	0,103	48,67	73,43
average values			2456,57	38839,50	0,099	55,00	72,87

Tab. 2 Vertical buckling stress on concrete panels under biaxial compression - test results

Concrete panel	Vertikal buckling stress σ_v (MPa)	
P1-1,08-A	20,3	Stress ratio $\sigma_h/\sigma_v = 1{,}08$
P7-1,08-B	20,3	
P8-1,08-B	18,8	
average value	19,6	
P9-1,08-C	24,6	
P10-1,08-C	26,0	
average value	25,3	
P1-0,57-A	27,5	Stress ratio $\sigma_h/\sigma_v = 0{,}57$
P2-0,57-A	26,1	
P3-0,57-A	31,8	
P4-0,57-A	28,9	
average value	28,6	
P5-0,57-B	34,7	
P6-0,57-B	28,9	
P7-0,57-B	30,4	
P8-0,57-B	31,3	
average value	31,3	
P9-0,57-C	35,3	
P10-0,57-C	43,4	
P11-0,57-C	37,6	
P12-0,57-C	32,4	
average value	37,2	

3.4. VERIFICATION OF TEST RESULTS ACCORDING TO RDT

The calculation method according to the RDA modulus iterative method is shown in this chapter for concrete panels (stress ratio 0,57 and mixture A); other results can be found in Table 4. The first iteration for the calculation of the buckling stress is made using the finite element method in Abaqus (with finite element type S3), where the linear elastic model with modulus elasticity and Poisson's ratio from Table 1 are considered. To avoid a repeated calculation in Abaqus, a linear function between modulus of elasticity and buckling stress is used and thus the iterative method is accelerated. The Abaqus model and the linear function for the stress ratio of 0,57 are shown in Figure 6. The coefficient K_E was calculated using Eq. (6) and (7). The values for mixtures A, B, and C were 0,07; 0,06 and 0,08 respectively. The iterative method was performed using Eq. (9) and is shown in Table 3.

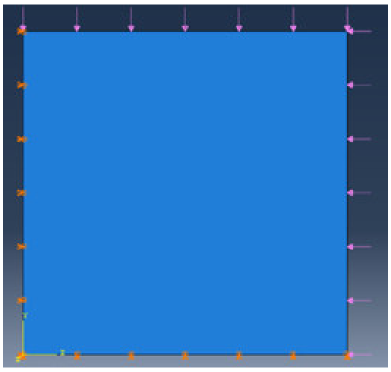

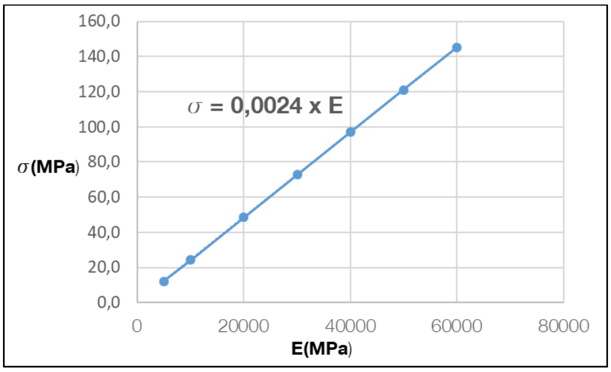

Fig. 6 Abaqus model (left) / Linear function between modulus of elasticity and buckling stress (right)

Tab. 3 RDA modulus iterative calculation for mixture A and stress ratio 0,57

Modulus of Elasticity E (MPa)	Poisson's ratio μ	K_E	RDA modulus E_R (MPa)	Vertikal buckling stress σ_v (Mpa)
37041	0,113	0,07	37041,00	88,90
37041	0,113	0,07	5976,82	14,34
37041	0,113	0,07	16307,68	39,14
37041	0,113	0,07	10355,17	24,85
37041	0,113	0,07	13113,05	31,47
37041	0,113	0,07	11672,71	28,01
37041	0,113	0,07	12383,07	29,72
37041	0,113	0,07	12022,24	28,85
37041	0,113	0,07	12202,86	29,29
37041	0,113	0,07	12111,77	29,07
37041	0,113	0,07	12157,53	29,18
37041	0,113	0,07	12134,50	29,12
37041	0,113	0,07	12146,08	29,15
37041	0,113	0,07	12140,25	29,14
37041	0,113	0,07	12143,19	29,14

The buckling stress on concrete panels according to RDT is 29,14 MPa, which was very well matching with the experimental value of 28,60 MPa. A comparison between the RDT calculation and the experiment values are shown in Table 4. The buckling mode 1 of concrete panels in Abaqus in first iteration is presented in Figure 7.

Tab. 4 Comparison between RDT calculation results and experiment values

Stress ratio / Mixture	Vertikal buckling stress σ_v (Mpa) - Test	Vertikal buckling stress σ_v (Mpa) - RDA	η (-)
1,08 / A	20,3	23,9	0,85
1,08 / B	19,6	24,7	0,79
1,08 / C	25,3	24,2	1,05
0,57 / A	28,6	29,1	0,98
0,57 / B	31,3	29,9	1,05
0,57 / C	37,2	29,3	1,27

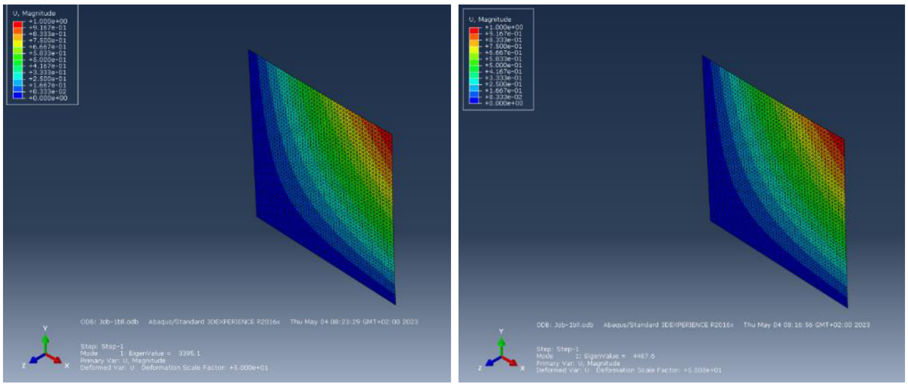

Fig. 7 Buckling mode 1 of concrete panels in Abaqus in first iteration (stress ratio 1,08 left) / (stress ratio 0,57 right)

4. VERIFICATION AGAINST RESULTS FROM LITERATURE

4.1. EXAMPLE 1

In addition to the experiment from chapter 3 in this example the verification of the RDA iterative method for stability of concrete panels under axial compression is shown. The experimental results from Lechner T. and Fischer O. (2015) [14] are used. They researched the load bearing behavior and stability of slender wall panels made of normal strength plain concrete and fibre-reinforced ultra-high performance concrete UHPC under axial compression. They considered different eccentricity values as well as the panel thickness. For this example only concrete panels with dimensions b x h x t = 1200 mm x 400 mm x 60 mm with an eccentricity of 10 mm are considered. Material parameters were measured on cubes 100 mm and cylinders 150 mm x 300 mm. Since for the calculation of the structural material constant K_E the measured values of modulus of elasticity and Poisson's ratio are necessary, this was partially taken into account. For normal concrete mixture (with the name C50/60) and for mixture of UHPC (with the name B5Q) modulus of elasticity 37000 MPa and 51000 MPa are used respectively. Poisson's ratio 0,15 and density 2400 kg/m3 was used for both mixtures. The structural material constant K_E for C50/60 and B5Q were calculated 0,05 and 0,04 respectively. The experimental set up and Abaqus model used for this example are shown in the Figure 8. Analogous to calculation in chapter 3.4, the same calculation method was used. For every mixture are used two concrete panels. The test results of buckling forces for two concrete panels with mixtures C50/60 and B5Q are (510,0 kN, 483,0 kN) and (836,0 kN, 941,0 kN) respectively. The RDT calculation results for C50/60 and B5Q are 694,4 kN and 933,6 kN respectively.

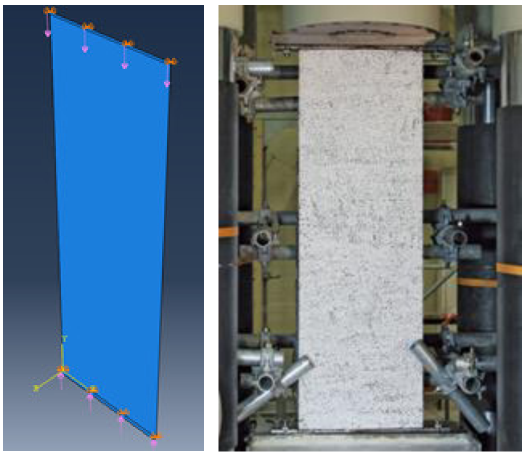

Fig. 8 Abaqus model (left) and experimental set up from Lechner T., Fischer O. [14] (right)

4.2. EXAMPLE 2

For further verification of the RDA iterative method in this example analytical expressions from literature on two-way action concrete panel were used. Swartz S. E. and Rosebraugh V. H. (1974) [15] tested 24 rectangular, reinforced concrete panels. The analytical expression as well as the results can be found in the paper by Doh J. H. et al. (2001) [4]. This expression is given in the Eq.(10),

$$f_{cr} = 0{,}425 \cdot f_c' \cdot B \cdot [-B + (4 + B^2)^{0{,}5}]; \qquad B = \frac{\pi^2 \cdot (\frac{1}{L} + L)^2 \cdot (h/b)^2}{6 \cdot \varepsilon_0 \cdot (1 - \rho)} \tag{10}$$

where L = a / b, if a / b < 1 and L = 1, if a / b ≥ 1. a, b, h are panel length, width and thickness, respectively. Average ultimate strain of concrete after 28 days was assumed for this example ε_0=0,0035 and the total reinforcement ratio ρ for this example was zero.

For the calculation of this example a concrete panel with length a = 4 m, width b = 2 m and thickness h = 0,05 m was used because Swartz S. E. and Rosebraugh V. H. (1974) [15] tested the concrete panels with aspect ratio a / b = 2,0, slenderness b / t = 75 to 128,51 and concrete strength f_c' = 16,65 to 27 MPa. For the calculation concrete with strength of f_c' =25 MPa was used. The modulus of elasticity of 28960,4 MPa was calculated with Eurocode 2 [6]. Poisson's ratio 0,20 and density 2400 kg/m3 was used for the calculation on this example. The structural material constant K_E = 0,04 was calculated. The calculation results of buckling stress according Eq. (10) and RDT calculation are 17,1 MPa and 17,7 MPa respectively.

5. CONCLUSIONS

In this paper was presented and experimentally verified the RDA iterative modulus method for the calculation of biaxial buckling stress of concrete panels. The experimental results from chapter 3 showed a very well matching with RDT calculation for both compression stress ratios. The measured values of modulus of elasticity, Poisson's ratio, and density have a significant influence on the structural material constant K_E as well as buckling stress results according to RDT. The first iteration of buckling stress was calculated using a model in Abaqus where the end conditions as well as the finite element mesh have influence on results. For further iterations (without Abaqus), a linear function between buckling stress and modulus of elasticity was used in this paper and has enabled faster calculations. In chapter 4.1 the RDA iterative modulus method used for calculation of buckling stress of concrete panels under axial compression is discussed. It was shown that this method can be used on normal strength plain concrete and fibre-reinforced ultra-high performance concrete UHPC. In chapter 4.2 the RDT calculation was compared with the analytical expression from literature on two-way action concrete panel. This results also show a very good matching.

As presented in this paper the RDA iterative modulus method in combination with finite element method can be used for the calculations of axial and biaxial buckling stress for different concrete mixtures, where it is necessary to have the material parameters values. The time of calculation according to RDT is faster and simpler because of using linear-buckling analysis in combination with RDA modulus equation. Initial increment assumption as well as the iterative results for deformation are not necessary beacuse of using correlation between elastic modulus and buckling stress. RDT is especially worth using in the biaxial compression analysis.

ACKNOWLEDGEMENT

The present work has been supported by The Provincial Secretariat for Higher Education and Scientific Research, Autonomous Province of Vojvodina, Republic of Serbia (Project No. 142-451-2640/2021-01).

REFERENCES

[1] Timoshenko S. P., Gere M. (1961). Theory of Elastic Stability. New York: 2nd ed, McGraw-Hill.

[2] Kupfer H., Hilsdorf H., Rusch H. (1969). Behavior of Concrete under Biaxial Stresses. *ACI Journal Proceedings,* vol. 66, no. 8, pp. 656-666.

[3] Hussein A., Marzouk H. (2000). Behavior of High-Strength Concrete under Biaxial Stresses, *ACI Journal Proceedings,* vol. 97, no. 1, pp. 27-36.

[4] Doh J. H., Fragomeni S., Kim J. W, (2001). Brief Review of Studies on Concrete Wall Panels in One And Two Way Action, *International Journal of Ocean Engineering and Technology,* vol. 4, no. 1, pp. 38-43.

[5] Fehling E., Leutbecher T., Röder K. F. (2008). Biaxial Compression-Tension-Strength of Reinforced Concrete and Reinforced Steel Fibre Concrete in Structural Panels, *Structural Materials and Engineering Series*, No. 11, Kassel University Germany.

[6] Eurocode 2 (2010). Design of concrete structures – Part 1-1: General rules and rules for buildings, German version EN 1992-1-1: 2004 + AC.

[7] Bourada M., Bouadi A., Bousahla A. A., Senouci A., Bourada F., Tounsi A., Mahmoud S. R. (2019). Buckling behavior of rectangular plates under uniaxial and biaxial compression, *Structural Engineering and Mechanics,* vol. 70, no. 1, pp. 113-123.

[8] Milašinović D. D., Majstorović D., Vukomanović R. (2018). Quasi static and dynamic inelastic buckling and failure of folded-plate structures by a full-energy finite strip method, *Advances in Engineering Software,* vol. 117, pp. 136-152.

[9] Milašinović D. D. (2015). Rheological-dynamical continuum damage model for concrete under uniaxial compression and its experimental verification, *Theoretical and Applied Mechanics,* vol. 42, no. 2, pp. 73-110.

[10] Milašinović D. D. (1996). Reološko-dinamička analogija, *Mehanika materijali i konstrukcije*, Naučni skup srpske akademije nauka i umjetnosti, Knjiga LXXXIII, Odjeljenje tehničkih nauka, Knjiga 2, pp. 102-110.

[11] Milašinović D. D. (2000). Rheological-dynamical analogy: prediction of buckling curves of columns, *International Journal of Solids and Structures,* vol. 37, no. 29, pp. 3965-4004.

[12] Milašinović D. D. (2006), Rheological-Dynamical Theory of Visco-Elasto-Plasticity and Fatigue: Part 1, *Multidiscipline Modeling in Materials and Structures,* vol. 2, no. 1, pp. 1-30.

[13] Milašinović D. D. (2007). Rheological–dynamical analogy: Prediction of damping parameters of hysteresis damper, *International Journal of Solids and Structures,* vol. 44, pp. 7143-7166.

[14] Lechner T., Fischer O. (2015). Stabilitätsversagen von schlanken Wandscheiben aus Normal- und Ultrahochleistungsbeton, *Beton und Stahlbetonbau*, Ernst & Sohn, Verlag für Architektur und technische Wissenschaften GmbH & Co. KG, Berlin, Heft 5.

[15] Swartz E. S., Rosebraugh H. V. (1974). Buckling of reinforced concrete plates, *Journal of Structural Engineering, American Society of Civil Engineering,* vol. 100, pp. 195-208.

TYPES OF SAFETY SCAFFOLDING IN CONSTRUCTION

Dragan Hristovski[1]

Summary

The safety of workers at construction sites is one of the major concerns in the construction industry. It is well recognized that the construction industry is one of the most dangerous industries in which to work. The reasons for these dangers are the hazards faced by the workers in this industry. The equipment they use on the construction sites is the cause of many of these hazards. One of the equipment with which injuries and death commonly occur among workers is working with scaffolds. Scaffolds play their role by providing a passageway, supporting the structure, and as a working platform. Scaffolding is a temporary structure that supports the original structure, and workers use it as a platform to carry out construction work. The types of scaffolding differ depending on the type of construction work. Scaffolding is made of wood or steel. It should be stable and strong to support workers and other construction materials placed on it.

Key words: Scaffolding, scaffolding safety, scaffolding standards

[1] MSc. Industrial Engineering, Expert consultant, Occupational Safety Association 28 April, Skopje, N.Macedonia, vestak.hristovski@gmail.com

1. DEFINITIONS

"Adjustable suspension scaffolding" means a suspension scaffolding equipped with a crane that can be operated by scaffold employees. "Girder" means the horizontal transverse member of the scaffold (which may be supported on beams or guides) on which the platform of the scaffold rests and which joins the scaffold posts, posts and similar members. "Operator chair" means a single-point adjustable suspension scaffold consisting of a seat or harness designed to support one employee in a seated position. "Body belt (safety belt)" means a strap with means both for securing it about the waist and for attaching it to a lanyard, lifeline, or deceleration device [4].
"Body harness" means a design of straps that can be fastened around the employee in such a way as to distribute the force of fall arrest over at least the thighs, pelvis, waist, chest and shoulders, with means of attachment for other components of the personal fall arrest system. "Brace" means a rigid connection that holds one member of a scaffold in a fixed position relative to another member, or to a building or structure. "Mason's Square Scaffold" means a supporting scaffold consisting of framed squares supporting a platform. "Carpentry bracket scaffold" means a support scaffold consisting of a platform supported by brackets attached to the walls of a building or structure. "Catenary Scaffolding" means a suspension scaffold consisting of a platform supported by two substantially horizontal and parallel ropes attached to structural members of a building or other structure. Additional support can be provided by vertical risers. "Chimney Hoist" means a multi-point adjustable suspension scaffold used to provide access to work within a chimney. "Wedge" means a structural block used at the end of a platform to prevent the platform from sliding off its supports. Cleats are also used to provide a footing on inclined surfaces such as crawling boards.
"Competent person" means a person who is capable of identifying existing and foreseeable hazards in the environment or working conditions that are unsanitary, hazardous, or hazardous to employees and who has the authority to take prompt corrective action to eliminate them. "Continuously Moving Scaffold" (Adjustable Scaffold) means a suspended two-point or multi-point adjustable scaffold that is constructed using a series of interconnected joined scaffold elements or support structures erected to form a continuous scaffold. "Coupling" means a device for joining the pipe of the pipe and the scaffolding of the coupling. "Crawling board (chicken ladder)" means a supported scaffold consisting of boards spaced and fixed with pegs to provide a base, for use on inclined surfaces such as roofs. "Retarding device" means any mechanism, such as a rope grab, rip cord, specially woven rope, break or deform rope, or automatic self-retracting life belt, which dissipates a significant amount of energy during a fall arrest or limits the energy imparted to the employee during arrest during a fall. "Double Pole (Independent) Scaffold" means a supported scaffold consisting of a platform(s) supported on cross beams (girders) supported on beams and a double row of posts independent of support (other than ties, grabs, braces) from any structure.
"Equivalent" means an alternative design, material, or method of protection against hazards that the employer can demonstrate will provide an equal or greater degree of safety to employees than the method, material, or design specified in the standard. "Eye" means a loop with or without a thimble at the end of the wire rope. "Exposed Power Lines" means power lines that are accessible to employees and are not protected from contact. Such lines do not include extension cords or cords for power tools. "Manufactured floors and planks" means manufactured platforms made of wood (including laminated timber and solid-sawn timber planks), metal, or other materials. "Manufactured Frame Scaffolding (Welded Tubular Frame Scaffolding)" means scaffolding consisting of a platform(s) supported on manufactured end frames with integral posts, horizontal girders, and intermediate members.

"Failure" means failure of load, breakage, or separation of components. Load rejection is the point at which ultimate strength is exceeded. "Formwork Scaffold" means a supported scaffold consisting of a platform supported by brackets attached to the formwork. "Guard rail system" means a vertical barrier, consisting of, but not limited to, top rails, middle rails, and posts, erected to prevent employees from falling from a scaffold platform or walkway to lower levels. "Crane" means a manual or electric mechanical device for raising or lowering a suspended scaffold. "Horse Scaffold" means a support scaffold consisting of a platform supported by construction horses(horses). Horse scaffolds made of metal are sometimes called horse scaffolds.

2. CONSTRUCTION OF THE SCAFFOLDING PLATFORM

(1) Each platform on all working levels of the scaffolding must be completely covered or placed between the front posts and the supports of the guardrail as follows:
(1.1) Each platform unit (e.g., scaffold board, fabricated plank, fabricated deck, or fabricated platform) shall be installed so that the clearance between adjacent units and the space between the platform and posts is not more than 1 inch (2.5 cm).) wide, except when the employer can demonstrate that a wider space is required (for example, to fit around posts when side supports are used to extend the platform) [3].
(1.2) When the employer has made a demonstration, the platform shall be boarded or decked as completely as possible, and the remaining open space between the platform and the posts shall not exceed 24.1 cm.
The requirement to provide full formwork does not apply to platforms that are used exclusively as walkways or exclusively by employees performing the assembly or dismantling of scaffolding. In these situations, only the formwork determined by the employer to ensure safe working conditions is required.
(2) each platform and scaffolding path must be at least 46 cm wide.
(2.1) Each ladder scaffold, top plate support scaffold, roof support scaffold, and pump jack scaffold must be at least 30 cm wide. There is no minimum width for operator chairs.
(2.2) Where scaffolding must be used in areas
which the employer can demonstrate are so narrow that platforms and walkways cannot be at least 46 cm wide, such platforms and walkways shall be as wide as possible and employees on such platforms and walkways shall be protected from fall hazards by using guardrails and/or personal fall arrest systems.
(3) The front edge of all platforms shall not be more than 36 cm from the front edge, unless guardrail systems are installed along the front edge and/or personal fall arrest systems are used in accordance to protect employees from falling.
(3.1) The maximum distance from the edge of the scaffolding for the supports shall be 8 cm;
(3.2) The maximum distance from the face for plastering and coating operations must be 46 cm.
(4) Each end of a platform, unless braced or otherwise secured by hooks or equivalent means, shall extend beyond the center line of its support by at least 15 cm.

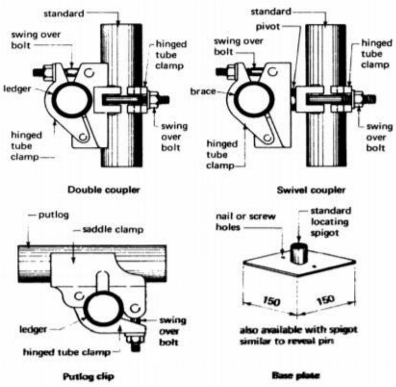

Fig. 1 Scaffolding attachment method [6]

(5) (5.1) Each end of a platform 10 feet or less in length shall not extend beyond its support more than 30 cm unless the platform is designed and installed so that the cantilevered portion of the platform can support personnel and/or materials without overturning or has guardrails that block employee access to the console end.
(5.2) Any platform more than 10 feet in length shall not extend beyond its support more than 46
cm, unless it is designed and installed so that the cantilevered portion of the platform can support employees without tipping over, or has guardrails to block employee access to the cantilevered portion of the platform. the end.
(6) On scaffolds where planks rest to form a long platform, each leaning end must rest on a separate supporting surface. This provision does not preclude the use of common support members, such as "T" sections, to support planks that abut or attach to platforms designed to rest on common supports.
(7) On scaffolds where the platforms overlap to form a long platform, the overlap shall occur only over supports and shall not be less than 30 cm unless the platforms are nailed together or otherwise restrained to prevent movement.
(8) At all points of scaffolding where the platform changes direction, such as turning a corner, any platform resting on a girder at an angle other than right shall be placed first, and platforms resting at right angles on the same girder shall be placed second, to the top of the first platform.
(9) Wooden platforms shall not be covered with an opaque finish, except that the edges of the platform may be covered or marked for identification. Platforms may be periodically coated with wood preservatives, fire retardant finishes, and
slip-resistant coatings, however, the coating may not obscure the top or bottom surfaces of the wood.
(10) Scaffold components manufactured by different manufacturers shall not be mixed unless the components fit together without force and the structural integrity of the scaffold is maintained by the user. Scaffolding components manufactured by different manufacturers shall not be modified to mix with each other unless a competent person determines that the resulting scaffolding is structurally sound.
(11) Scaffolding components made of different metals shall not be used together unless it has been determined by a competent authority that galvanic action will not reduce the strength of any component to a level [1].
The safety of workers at construction sites is one of the major concerns in the construction industry. It is well recognized that the construction industry is one of the most dangerous industries in which to work.

3. TYPES OF SCAFFOLDING USED IN CONSTRUCTION

3.1. SINGLE SCAFFOLDING

Individual scaffolds are commonly used for brickwork and are also called bricklayer scaffolds. Individual scaffolding consists of standards, slats, pavement, etc., which are parallel to the wall at a distance of about 1.2 m. The distance between the standards is about 2 to 2.5 m. Ledgers connect standards at a vertical distance of 1.2 to 1.5 m. Stakes are taken out of the hole left in the wall at one end of the ridge. Putlog is placed at a distance of 1.2 to 1.5 m.

Fig. 2 Individual scaffolding[5]

3.2. DOUBLE SCAFFOLDING

Double scaffolds are mainly used for stone masonry, so they are also called masonry scaffolds. In stone walls, it is difficult to make holes in the wall to support the logs. So, two rows of scaffolding were made to make it strong. The first row is 20-30 cm away from the wall, and the second is 1 m from the first row. Then stakes are placed that are supported on both frames. To make it stronger, rakes and cross supports are provided. This is also called independent scaffolding. They are frequently used in finishing scaffold which is erected for bldg face, painters, etc., but their modular frames can also be stacked several stories high for use on large-scale construction jobs [2].

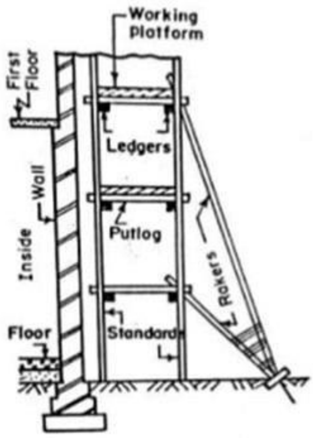

Fig. 3 Double scaffolding[5]

3.3. CANTILEVER SCAFFOLDING

This is a type of scaffolding where the standards are supported by a series of pins and these pins are pulled out through holes in the wall. This is called a single-frame scaffold. In the second type, the pins are inserted into the floors through holes and this is called independent or double frame type scaffolding. Care should be taken in the construction of cantilever scaffolding.

Fig. 4 Cantilever scaffolding[5]

3.4. HANGING SCAFFOLDING

With suspended scaffolding, the working platform is suspended from the roofs with the help of wire ropes or chains, etc., and can be raised or lowered to the desired level. This type of scaffolding is used for repairs, display, painting, etc.

Fig. 5 Hanging scaffolding[5]

3.5. MOBILE SCAFFOLDING

In mobile scaffolding, the working platform is supported on movable tripods or ladders. This is mainly used for indoor works, such as painting, repairs, etc., up to a height of 5m.

Fig. 6 Mobile scaffolding[5]

3.6. STEEL SCAFFOLDING

Steel scaffolding is made of steel pipes that are attached with steel connectors or couplings. It is very easy to construct or dismantle. It has greater strength, greater durability, and greater fire resistance. It is not economical, but it will provide greater safety for workers. So, it is widely used today.

Fig. 7 Steel scaffolding[5]

3.7. PATENTED SCAFFOLDING

Patented scaffoldings are made up of steel but these are equipped with special couplings and frames etc., these are readymade scaffoldings which are available in the market. In this type of scaffolding working platform is arranged on brackets which can be adjustable to our required level.

Fig. 8 Patented scaffolding[5]

4. SCAFFOLD STABILITY

4.1. THREE-TO-ONE RULE

The ratio of height to least lateral dimension must not exceed 3 to 1 unless the scaffold is

- Tied to a structure, as discussed in the section on Tie-in Requirements
- Equipped with outrigger stabilizers to maintain the ratio of 3 to 1 [7]
- Equipped with suitable guy wires.

Fig. 9 Patented scaffolding[7]

5. CONCLUSION

Scaffolds play their role by providing a passageway, supporting the structure, and as a working platform. Scaffolding is a temporary structure that supports the original structure, and workers use it as a platform to carry out construction work. The types of scaffolding differ depending on the type of construction work. Scaffolds enable workers to move around a building safely in any direction needed to complete their tasks. The use of scaffolding is crucial in providing a safe and protected workplace where workers are required to work at a variety of heights. Its equipment provides support on height while ensuring workers' safety. It enables crew to maintain balance, therefore reducing the risk of accidents for workers and pedestrians alike. These structures are widely used on sites to get access to areas that would otherwise be challenging to get to. Scaffolding provides a solution to complications and problems posed by high-rise construction.

6. REFERENCES

[1] Norzalili Abu Bakar, Mohd Rodzi Ismail and Tan Guat Lin (2008), Scaffolding safety assesment in construction sites in Penang, 2nd International Conference on Built Environment in Developing Countries (ICBEDC 2008).

[2] Jaydeep Desai, Prof. Jayeshkumar Pitroda, Prof. J. J. Bhavsar (2014), Scaffolding: Safety and Economical Aspect for Scaffoldings in Construction Industry, National Conference on: "Trends and Challenges of Civil Engineering in Today's Transforming World"

[3] www.osha.gov.

[4] Occupational Safety and Health Administration (2002), A Guide to Scaffold Use in the Construction Industry

[5] www.theconstructor.org

[6] www.sjce.ac.in

[7] www.ihsa.ca

ANALYSIS OF THE STABILITY, WITH A TECHNICAL SOLUTION FOR STRENGTHENING, OF A FIRST CATEGORY BUILDING IN BITOLA

Elena Delova[1], *Aleksandar Zlateski*[2], *Angela Poposka*[3], *Zhivko Bozhinovski*[4], *Veronika Shendova*[5]

Summary:

This paper will present a detailed analysis of the seismic stability of the existing masonry structure "KPU Prison" in Bitola, and also demonstrates the necessity for its strengthening. Through a detailed analysis it is established that according to the national regulations the existing structure does not satisfy the required strength and deformation capacities, when it is subjected to horizontal seismic loads. With the main aim of obtaining seismic stability and reliability of the structure, it is concluded that the building needs to be repaired and strengthened. Considering the possibilities for interventions, and the required strength and deformation capacities of the structure, a traditional solution has been chosen for repair and strengthening of the structure, which includes new reinforced concrete jackets on their own foundations. Analysis to obtain the strength and deformation capacities was carried out, which showed that the strengthened structure exhibits significantly increased strength, in accordance with the national regulations.

Key words: Repair, Strengthening, Masonry, Capacity Analysis

[1] MSc, Young Research Assistant, Ss Cyril and Methodius University in Skopje, Institute of Earthquake Engineering and Engineering Seismology (IZIIS), Skopje, North Macedonia, delova@iziis.ukim.edu.mk
[2] MSc, Research Assistant, IZIIS, Skopje, North Macedonia, azlate@iziis.ukim.edu.mk
[3] MSc, Research Assistant, IZIIS, Skopje, North Macedonia, angela@iziis.ukim.edu.mk
[4] PhD, Professor, IZIIS, Skopje, North Macedonia, zhivko_bozhinovski747@yahoo.com
[5] PhD, Professor, IZIIS, Skopje, North Macedonia, veronika@iziis.ukim.edu.mk

1. INTRODUCTION

Masonry structures, as a traditional type of construction, are especially present in the Balkan region. With cross-analysis of the statistical data from the last censuses from 1991 and 2002 and the available data from the State Statistical Office, it can be summarized that one third of the buildings in the Republic of North Macedonia belong to this type of constructions. Most of them were built in the second half of the XX century, before enactment of first seismic code in the country, and constructed on the basis of experiential knowledge. The most important and undeniable fact is that these buildings are still operating as buildings of vital importance for the society (schools, hospitals, cultural-historical monuments, etc.), *Shendova et al. (2019)*.

The building of “KPU Prison” in Bitola (Fig. 1), belongs to this type of buildings. This paper will present a detailed analysis of the stability of the existing structural system of the “KPU Prison” building, the need for repair and strengthening of the building, the selection of the most adequate solution for repair and strengthening, as well as analysis of the stability of the strengthened structural system of the building. For that purpose, the multidisciplinary approach developed in the Institute of Earthquake Engineering and Engineering Seismology in Skopje (UKIM-IZIIS) was applied. This approach is based on gathered experience in the field of earthquake protection. It includes detailed technical and experimental investigations of the facility, in order to determine the actual input parameters for the analysis, and then analysis for the load-bearing elements in order to determine the limit state of strength, deformability and ability of load-bearing elements and the system as a whole to dissipate seismic energy, *Bozinovski, Dojcinovski et al. (2019)*.

Fig. 1 Photo of the analysed wing (41.6m x 10.1m) of the building “KPU Prison – Bitola”

2. ANALYSIS OF THE EXISTING BUILDING

2.1. DESCRIPTION OF THE STRUCTURAL SYSTEM OF THE EXISTING BUILDING “KPU PRISON” IN BITOLA

The building by its function is a prison building, consisting of two wings, connected in the shape of the letter "L", with dimensions at the base of 7.0m x 12.3m and 41.6m x 10.1m on each wing respectively. Since the object of analysis is one wing of the prison (41.6m x 10.1m), the geometrical and material characteristics of the analysed wing of the building will be shown.

For the purposes of the analysis, visual inspection of the building was carried out, with visual inspection, control measurements of building dimensions and structural elements, indoor visual inspection for identification/verification of the structural system. Based on

this, technical drawings were prepared for: characteristic floor plans and cross sections (Fig. 2).
The dynamic characteristics of the building were determined by applying the ambient vibration technique and were used to calibrate the mathematical models in the analyses, specify the input parameters and conduct a realistic analysis of the structure.
It was established that from a structural point of view, the analysed wing of the prison is a masonry structure which consists of a basement and a ground floor with a total height of 7.08m. The load-bearing structural system consists of load-bearing stone walls on the ground floor and load-bearing walls of solid brick on the first floor, in both orthogonal directions. Each floor is covered with ribbed reinforced slab, while the foundation structure consists of foundation strips of stone.
The building was found in good condition without significant structural damage. The input values for quality of the masonry of the load-bearing walls of the building, expressed through the modulus of elasticity, compressive and tensile strength, were assumed based on the experiences of examined elements of similar quality and construction time, and were confirmed by experimental testing. Therefore, the following input parameters are adopted:

- modulus of elasticity E = 750MPa,
- shear modulus G = 75MPa,
- compressive strength f_c = 1MPa,
- tensile strength f_t = 0,1MPa.

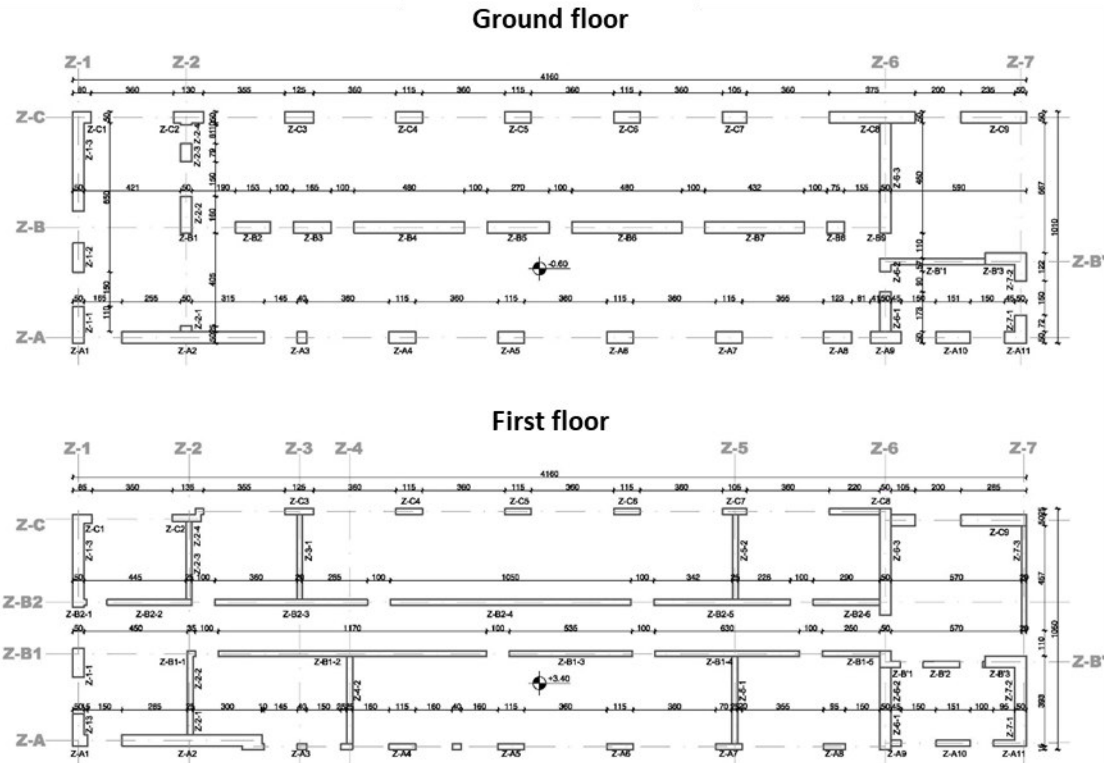

Fig. 2 Floor plan for ground floor and first storey of the "KPU Prison" building in Bitola (existing state)

2.2. ANALYSIS OF THE BEARING AND DEFORMATION STRUCTURAL CAPACITY

Based on the defined geometry of the structural systems of the building, the physical-mechanical characteristics of the embedded materials and the load of the elements, an

analysis was performed to determine the load-bearing capacity and deformability of the building, with the main purpose of defining its behaviour under seismic action.
To determine the real strength and deformation characteristics depending on the quantity and quality of the embedded materials, the computer program developed in UKIM-IZIIS was used. The program determines the displacement and the lateral force at yielding point (Δy and Qy), the ultimate displacement and lateral force (Qu and Δu), for each individual element of the storey, i.e. the initial stiffness and the stiffness at yielding point. In this way, the force-displacement relationship are obtained for each element of each storey separately, whereby, the load-bearing and deformation capacity of each storey is defined. The deformation capacity also defines the displacement ductility capacity for each floor as μ = Δu / Δy. The load-bearing and deformation capacity are determined for both orthogonal directions. The strength capacity is shown in the form of the ultimate storey shear force, which compared to the equivalent seismic force gives the safety factor.

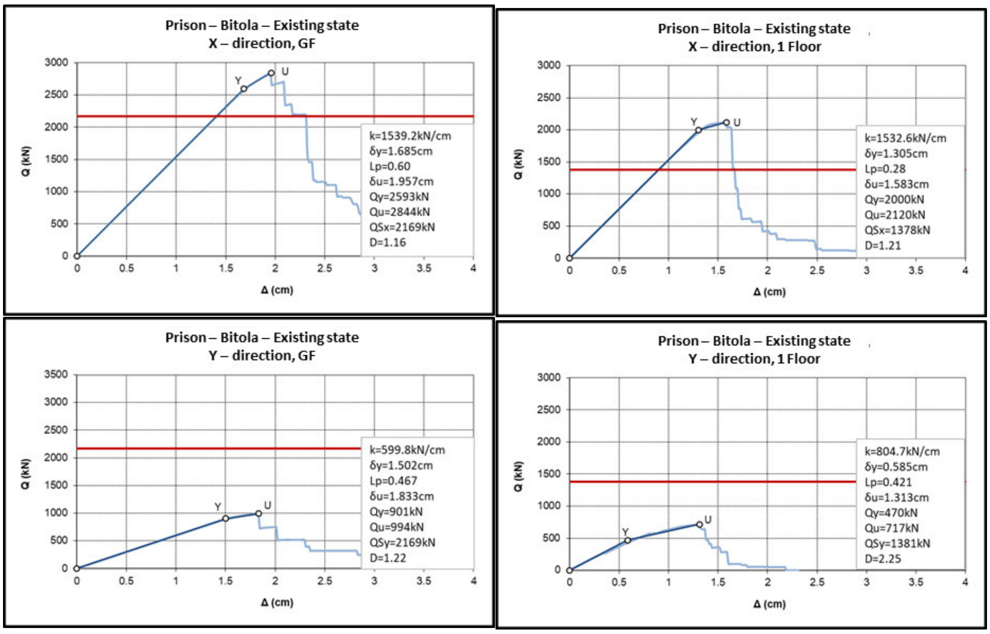

Fig. 3 Storey Q-Δ relationship (existing state) for both orthogonal directions

The results of the analysis, in the form of summary storey Q - Δ diagrams for the two orthogonal directions respectively, are shown in Fig.3. The bilinear diagrams with the characteristic yield points "Y" and the ultimate point "U" are shown in blue, while the required load capacity of each floor is marked in red. Table 1 summarizes the obtained and required load-bearing capacities of the structure for each storey.

Tab. 1 Structural bearing capacity for the existing structure

Existing state, x-direction						
level	M [kN]	Qy [kN]	Qu [kN]	Qs [kN]	Qy/Qs	Qu/Qs
1st floor	6884	2593	2844	2169	1,195	1,311
GF	5907	2000	2120	1378	1,451	1,538
Existing state, y-direction						
level	M [kN]	Qy [kN]	Qu [kN]	Qs [kN]	Qy/Qs	Qu/Qs
1st floor	6884	901	994	2169	0,415	0,458
GF	5907	470	717	1378	0,341	0,520

Based on the performed analysis of the existing structure and the obtained results, it was concluded that the strength capacity of the building for y-direction does not meet the requirements according to the regulations, PIOVS (1981). The ductility capacity for both directions is relatively small. Expressed through the percentage of the structures' mass, it amounts to 7-15%, while according to the code requirements for this type of structures it should be equal or larger than 20%. The structure does not have sufficient strength for y - directions, also the bearing capacity and deformability is relatively small for both directions, Bozinovski, et al. (2019a). According to the analysis results, it is necessary to provide adequate strength and sufficient deformability, providing structural elements with greater ductility and increasing the integrity of the structure in both directions.

3. REPAIR, STRENGTHENING AND ANALYSIS OF THE STRUCTURAL SYSTEM

3.1. DESCRIPTION OF THE TECHNICAL SOLUTION FOR STRENGTHENING OF THE EXISTING STRUCTURE

Based on the required strength and deformation characteristics of the elements and the whole structural system, several variant solutions for strengthening of the structure were considered. During the selection of the repair and strengthening solution a few aspects were considered including the possibilities for interventions in the building and the economic aspect. Also for each variant solution a preliminary analysis was obtained (for the structure stability for the two orthogonal directions). Comparison was made of the strength and deformability characteristics obtained with the required by the regulations.
From several variant solutions, a traditional solution for strengthening has been selected, the most appropriate from the economic aspect and from the aspect of assuring the strength and deformation requirements, according to the current technical regulations.
The solution for strengthening of the structural system includes the following, shown in Figures 4, 5, 6, 7, and 8, *Bozinovski, et al. (2019a)*:

- Strengthening of load-bearing masonry walls with reinforced concrete jacketing with 12cm thicnkess in longitudinal and transverse direction along with the new foundations;
- Connecting the RC jacketings with horizontal reinforced concrete belt courses, in transverse and longitudinal direction;
- Reinforced concrete walls on the ground floor and first floor with thickness of 20cm

The new reinforced concrete elements are intended to be of quality MB30 concrete and reinforcement of the type RA400/500-2. Reinforced concrete elements of the structure are proportioned according to the theory of limit loads, i.e., according to *PBAB (1987)*.

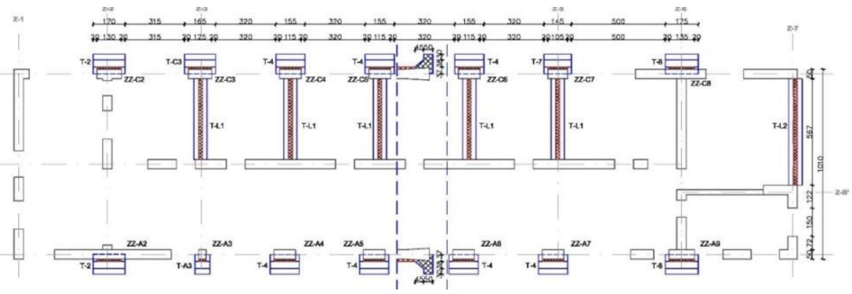

Fig. 4 Formwork plan of the foundations for the proposed strengthening solution

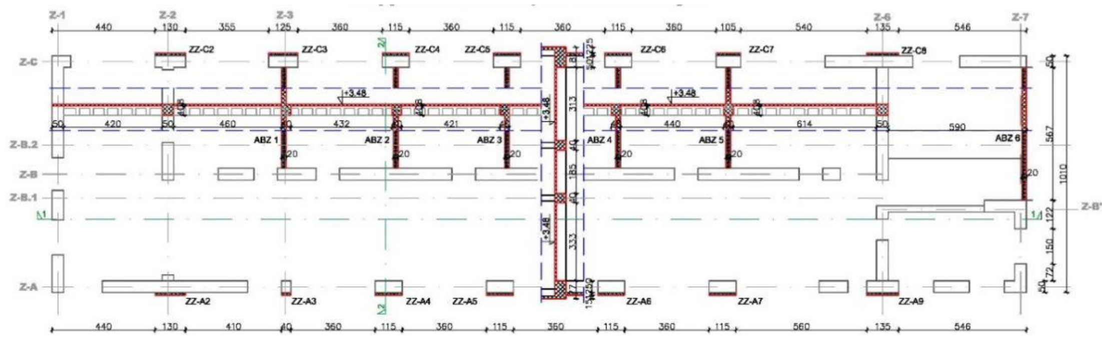

Fig. 5 Formwork plan of the ground floor for the proposed strengthening solution

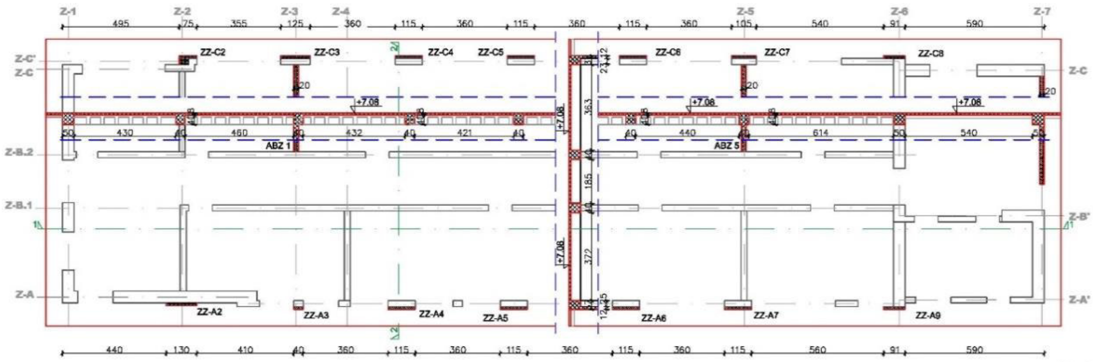

Fig. 6 Formwork plan of the first floor for the proposed strengthening solution

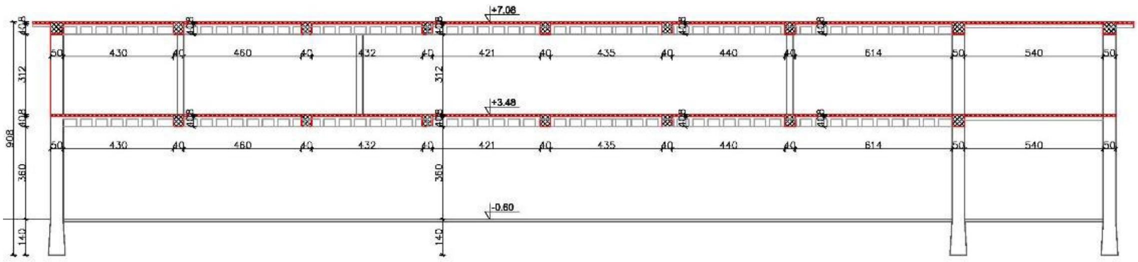

Fig. 7 Characteristic cross sections for the proposed strengthening solution: longitudinal cross section

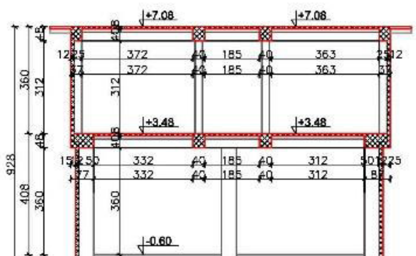

Fig. 8 Characteristic cross sections for the proposed strengthening solution: transverse cross section

3.2. ANALYSIS OF THE BEARING AND DEFORMATION CAPACITY FOR THE STRENGTHENED STRUCTURAL SYSTEM

For verification of the proposed technical solution for repair and strengthening of the building, the procedure shown in Chapter 2.2 was applied again, through which the load-bearing and deformation capacities are defined, but this time of the strengthened structure. The computer program recalculates the displacement and shear force at yielding point (Qy and Δy), as well as at the ultimate point (Qu and Δu) for each individual element of each storey, but for the integrated structural system of masonry and reinforced concrete elements, with the corresponding characteristics of the built-in material. The results are presented in the form of summary storey Q - Δ diagrams for the two orthogonal directions respectively. The bilinear diagrams with the characteristic yield points "Y" and the ultimate point "U" are shown in blue, while the required load capacity of each floor is marked in red (Fig. 9). Table 2 summarizes the obtained and required load-bearing capacities of the building by storey and directions, showing the new calculated safety factor.

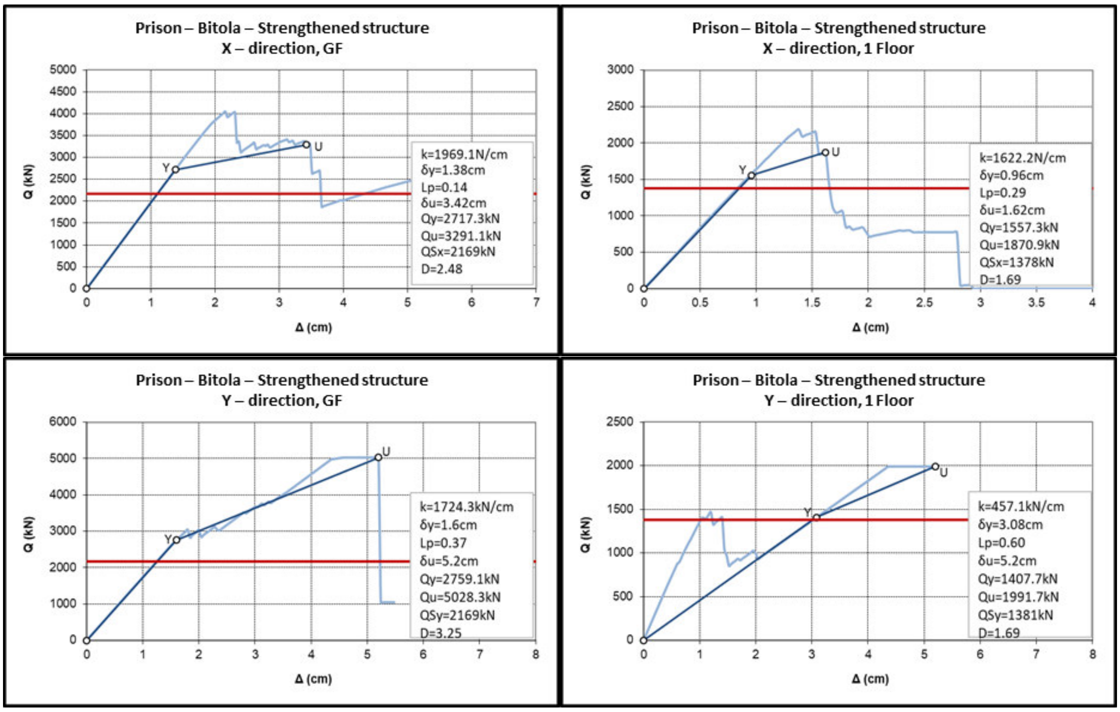

Fig. 9 Storey Q-Δ relationship (strengthened structure) for both orthogonal directions

Tab. 2 Structural bearing capacity for the strengthened structure

Strengthened structural system, x-direction						
level	M [kN]	Qy [kN]	Qu [kN]	Qs [kN]	Qy/Qs	Qu/Qs
1st floor	13556	2717,3	3291,1	2169	1,253	1,517
GF	8612	1557,3	1870,9	1378	1,130	1,358
Strengthened structural system, y-direction						
level	M [kN]	Qy [kN]	Qu [kN]	Qs [kN]	Qy/Qs	Qu/Qs
1st floor	13556	2759	5028,3	2169	1,272	2,318
GF	8612	1407,7	1991,7	1378	1,022	1,445

From the results of the analysis of the repaired and strengthened structure, it is noted that the capacity of the strength in both orthogonal directions amounts to 22.6-46.0% of the building's total mass for x – direction, and 20.5-46.7% for y – direction. The obtained strength capacity is significantly greater than the required limit capacity according to the regulations, *PIOVS (1981)*, or 16% of the total weight of the building. The bilinear diagrams show an increase in the deformation capacity of each of the storeys in both directions respectively, with an increase in the ductility capacities. This leads to the conclusion that the strengthening will increase the ability of the system for greater dissipation of energy, *Bozinovski, Zlateski et al. (2019)*. This is especially important for this type of buildings in case of seismic excitations. By increasing the deformation capacity, the input energy in the system would be consumed, which would greatly increase the seismic safety and security of the building, *Bozinovski et al (2021)*.

4. CONCLUSIONS

Based on the results from the performed analysis of the existing structure it can be easily concluded that the structure does not have sufficient strength capacity according to the valid regulations (PIOVS'81) and state of the art knowledge, also the deformation capacity is relatively small. According to the analysis results, the need for repair and strengthening is justified and necessary in order to improve the strength and deformation capacity and achieve the desired dynamic response during future earthquakes.

From several analysed variants, a traditional solution for strengthening has been selected, the most appropriate from the economic aspect, satisfying the strength and deformation requirements according to the current technical regulations in Republic of N. Macedonia.

The analysis of the repaired and strengthened structure of the "KPU Prison" building, clearly show that the strengthened system has significantly increased strength (load-bearing capacity) in both orthogonal directions and satisfies the required limit load capacity in accordance with current regulations. At the same time the results of the strengthened structure show an increase in the deformation capacity of each of the storeys in both directions respectively, i.e. an increase in the ductility. This leads to the conclusion that the proposed strengthening will increase the ability of the system to greater dissipation of energy, which is especially important for this type of buildings in case of seismic excitations.

The strengthening practically increases the stiffness, strength and deformability of the structural system, whereby, by optimizing these three characteristics, we obtain a structure that will satisfy the required strength and deformation characteristics, i.e. will ensure satisfactory seismic stability and reliability of the building.

REFERENCES

[1] Bozinovski, Z., Necevska-Cvetanovska, G., Delova, E., Zlateski, A. (2021). IZIIS Methodology for Design, Repair and Strengthening of Earthquake Resisting Masonry and Reinforced Concrete Structures, 1st Croatian Conference on Earthquake Engineering 22-24 March 2021, Zagreb, (Croatia).

[2] Bozinovski, Z., Zlateski, A., Gjorgjievska, E., Delova, E., Poposka, A. (2019). Analysis of Seismic Stability with Technical Solution for Seismic Strengthening of the Reconstructed Prison Building – "KPU Zatvor", in Bitola, Report IZIIS 2019-33, April 2019

[3] Bozinovski, Lj. Z., Dojcinovski, D., Delova, E., Poposka, M. (2019). Identification, Repairing, Strengthening and Revitalization of Existing Masonry and RC Buildings Structures in Seismic Prone Areas, Workshop on Earthquake Disaster Prevention and Mitigation in the "Road & Belt" countries, September 3-14 2019, Dalian (China).

[4] Bozinovski, Z., Shendova, V., Stojanoski B., Gjorgjievska, E., Necevska-Cvetanovska G., Apostolska, R., Jekikj G. (2011). "Strengthening of the Principal Structural System of the Parliament Building of Republic of Macedonia – Technical solution and construction", 14th International Symposium of MASE, 2011

[5] Krstevska, L., Manojlovski, F., Poposka, A., Shoklaroski, A., Naumovski, N. (2019). Definition of the Dynamic Characteristics of the Building of KPU Prison in Bitola, by the Ambient Vibration Method, Report IZIIS 2019-24, May 2019

[6] Shendova, V., Apostolska, R., Vitanova M., (2019). Structural Classification of Building and Bridge Assets in R. N. Macedonia, SERA Balkans Seismic Risk Workshop, EU Horizon 2020, ID 730900, June 2019, Belgrade, Serbia

[7] PIOVS (1981): Rulebook on Technical Regulations for Construction of Buildings in Seismic Regions, (OG SFRY No. 31/81, Amendments 49/82, 29/83, 21/88 and 52/90)

[8] PBAB (1987): Rulebook on Technical Regulations for Concrete and Reinforced Concrete, (OG SFRY No. 11/87)

THE USE OF WASTE CARBON FIBRES FOR THE PRODUCTION OF CONDUCTIVE CEMENTITIOUS MATERIALS

Katarina Didulica[1], Alen Ćenanović[2], Branka Mrduljaš[3], Ana Baričević[4]

Summary:

Conductive cementitious materials are produced by incorporating a form of carbonaceous material into a cement matrix, resulting in a multifunctional material. These materials are mostly used within de-icing and snow melting systems, electromagnetic shielding, support for a corrosion resistance (cathodic protection) or integrated in smart infrastructure serving as a sensor network. In this work, waste carbon fibres (wCF) from the production of high-performance technical textiles were used to demonstrate the possibility of obtaining a high performance conductive material. The fibres were added in two lengths (6 and 12 mm) and three dosages (0.5, 1.0, and 2.0 vol %) to monitor the effects of the fibres on fresh state properties, i.e., pore content, density, temperature, and consistency, and on mechanical and conductive properties. All results with wCF, were compared with a mix without fibres (REF) and a mix with factory-produced carbon fibres (fCF).

Key words: cement mortar, waste carbon fibre, conductive material

[1] Department of Materials/ Faculty of Civil Engineering/University of Zagreb, Zagreb, Croatia, katarina.didulica@grad.unizg.hr
[2] Department of Materials/ Faculty of Civil Engineering/University of Zagreb, Zagreb, Croatia acenanovic@student.grad.hr
[3] Department of Materials/ Faculty of Civil Engineering/University of Zagreb, Zagreb, Croatia branka.mrduljas@grad.unizg.hr
[4] Assist. Prof., Department of Materials/ Faculty of Civil Engineering/University of Zagreb, Zagreb, Croatia
ana.baricevic@grad.unizg.hr

1. INTRODUCTION

Concrete has been the most used building material for many years and is likely to remain the dominant material in the future. It is an essential part of the built environment around the world, from repair materials and non- structural elements all the way to large structures such as dams and bridges. Although widely used, there is a growing awareness of the environmental impact of cementitious materials. It is estimated that CO_2 emissions associated with the use, transportation, manufacture and demolition of cement and concrete accounted for nearly 10 % of global energy-related CO_2 emissions in 2019 [1], [2]. In addition, there are a growing number of buildings that are reaching their service life and need to be repaired or replaced. The increasing need for the development of environmentally and economically sustainable materials requires the immediate development of multifunctional materials that are able to meet multiple requirements in different environments. One such material is a conductive cementitious material, i.e. a composite material modified by the addition of conductive materials to reduce electrical resistance and achieve conductivity of the cementitious material by forming conductive networks within the cement matrix [3], [4]. This behaviour is achieved by using steel, carbon, graphene, or other materials in various forms such as fibres, shavings, powders, or nanomaterials. Carbonaceous materials have been shown to improve the electrical performance of cementitious materials more efficiently compared to steel fillers, as the corrosion properties of steel can lead to a degradation [3]. In addition, carbon fibres have been shown to perform better compared to powder materials [3]. It was concluded also that the size and distribution of the fibres in the composites are more important than the conductivity of the fibre material itself [4].

Further progress in obtaining low-cost multifunctional cementitious materials is evident in the use of recycled and waste materials [5], [6]. Considering that the percentage of material recycling is below 10 %, it is clear that additional efforts are needed to enable a more rational and sustainable use of resources. In this way, new opportunities for landfilled carbon fibres will be created to obtain high value-added products. Most of the recycled carbon fibres commercially available may contain remnants of matrix elements or can be obtained by pyrolysis, largely retaining the properties compared to virgin fibres (up to 90 %) [6]. There are also waste fibres that do not undergo any thermal treatment and do not exhibit differences in terms of mechanical properties compared to factory made fibres, but only surface damage from the weaving machine [5]. In this way, the economic and environmental requirements are met, but the effects on the properties of the material still need to be studied in more detail.

Carbon fibre mortars can be used for different purposes, mechano- electrical effect is used for structure monitoring [7], the electro- thermal effect is used to melt snow and ice on paving surfaces [8], [9], also for electromagnetic wave defence and cathodic protection of reinforced concrete [4].

The aim of this work was to evaluate the effects of waste carbon fibres on the mechanical and conductivity properties of cementitious materials. Accordingly, two lengths of carbon fibres (6 and 12 mm) were added to the high strength cementitious matrix in different amounts (0.5, 1.0, and 2.0 % by volume). The effects of the waste fibres (wCF) on the properties of the fresh and hardened material were determined together with the conductive properties in comparison with a reference mix without fibres (REF) and a mix with factory-made fibres (fCF) in both lengths (6 mm and 12 mm) and the amount of 1.0 % by volume.

2. MATERIALS AND METHODS

Cement CEM I 52.5 N, aggregate, water, and superplasticizer Master Glenium® ACE 430 were used for the mortars tested. The aggregate consisted of the following fractions: limestone filler 0.005/ 0.125 mm, quartz sand 0/ 1.0 mm and dolomite fractions 0.1/ 0.6 mm, 0.6/ 1.25 mm, and 1.25/ 2.0 mm. The water/ binder ratio was kept constant at 0.4, while the superplasticizer was predetermined to 0.45 % on the mass of cement but had to be increased depending on the amount of fibres. In this work, waste carbon fibres (wCF) and factory- made carbon fibres (fCF) with the properties given in Table 1, were used. Used waste fibres are free of impurities and do not require cleaning, but preparation in the form of combing and cutting with knives at 6 and 12 mm length was necessary. Combing was done in order to maintain fibre length uniformity during cutting.

A total of nine mixtures were prepared with the designation wCF and fCF for waste or factory- made glass fibres respectively, and a number indicating the volume fraction of the fibres used (0.5, 1.0 and 2.0 % V) followed by a number indicating the length (6 or 12). Another difference between the fibres was the sizing, where the sizing for waste fibres was determined as polyurethane and for factory made fibres of 6 mm polyurethane and for 12 mm glycerine. Waste fibres used in this paper were previously studied and their properties are available in previously published papers [5], [10].

Table 1 Characteristics of the carbon fibres

Property	Density [g/cm^3]	Diameter [µm]	Tensile Strength	Modulus of elasticity [GPa]	Elongation [%]
wCF	1.77	7.0	4.3	250	1.7
fCF	1.80	7.0	4.0	240	1.7

During the mixing process, the superplasticizer and the water were first mixed with the fibre addition. All powdered materials were previously mixed in the dry state to improve homogeneity and then added in a mixer. The total mixing time was predominantly set to 6 minutes, of which 1 minute at the first speed, then a 1 minute with dry mix on first speed and 1 min on second speed, followed by 1.5 minute break and 2 minutes mixing at the second speed. The same procedure was followed for the other mixes, with the difference of extending last step due to superplasticizer addition with the increase in fibre amount.

Immediately after mixing, the properties were tested in the fresh state, while samples for hardened state properties tests were stored under laboratory conditions for 24 hours and then in a water bath until testing. All the tests were conducted as stated in Table 2.

Table 2 Test in fresh and hardened state

Property	Standard	Dimensions (mm)	No. of samples per mix
Consistency	HRN EN 1015-3:2000	-	-
Density	HRN EN 12350-6:2019		
Fresh air content	HRN EN 1015-7:2000		
Flexural Strength	HRN EN 1015-11:2019	40 x 40 x160	3
Compressive strength			
Electrical Conductivity		150 x 100	3

3. EXPERIMENTAL RESULTS

3.1. FRESH STATE PROPERTIES

The properties in the fresh state are given in Table 3, together with the amount of superplasticizer used. The higher superplasticizer requirement, i.e. lower consistency values, with increase in fibre content was also found in previous work [6], [11]. Achieving the same consistency class for the mixtures was not possible due to the limitation of the maximum amount of superplasticizer, while for fCF1.0-6 mixture there was no need for SP amount increase. Although the fibre sizing in this mixture was polyurethane, same as the waste fibres, they are not following the same trend of fresh state properties.

From the results, it can be seen that the density values with fCF and wCF deviate only insignificantly from those of the reference mix (up to ± 1.3 %).

Fresh air content values obtained with fibres are higher than those obtained on REF mixture, up to 18 %. The same trend in results was also observed in the literature [12], [13], but on the contraire to [5]. Higher values may also be caused by prolonged mixing time, i.e., more entrapped air [14]. Significant difference is again seen on mixture fCF1.0-6, where fresh air content value is almost 70 % lower compared to reference mix and around 63 % lower compared to mixture with waste fibres of the same length.

Table 3 Fresh state properties.

Mix	REF	wCF 0.5-6	wCF 0.5-12	wCF 1.0-6	wCF 1.0-12	wCF 2.0-6	wCF 2.0-12	fCF 1.0-6	fCF 1.0-12
Consistency [mm]	224	160	150	145	130	115	110	285	120
Density [g/cm^3]	2.237	2.199	2.204	2.212	2.203	2.167	2.189	2.263	2.183
Fresh air content [%]	5.5	5.6	6.1	5.3	6.0	6.4	6.0	1.8	6.5
Temperature [°C]	26.0	26.5	26.2	27.5	27.6	27.7	27.6	23.9	22.9
Superplasticizer [% m_c]	0.45	0.55	0.55	0.90	0.65	0.95	0.95	0.45	0.65

3.2. HARDENED STATE PROPERTIES

The properties in the hardened state are presented below. The compressive strength was tested on the prisms after 28 days to test the influence of fibres on the properties of the high strength composites with expected strength between 50 and 100 MPa. The obtained values are shown in Fig. 1, representing the average strength value measured on 3 samples with standard deviation. The results obtained indicate that all of the mixtures meet the criteria for achieving a high-strength classification. However, the impact of fibre content on strength is not distinctly defined.

For mixtures with 6 mm fibre lengths, it was found that only the addition of 2 % of fibres by total volume was sufficient to improve compressive strength. Conversely, in mixtures containing 12 mm fibres, the strength values exhibited only marginal increase. Notably, in mixtures incorporating both factory fibre lengths, a reduction in the compressive strength value was observed.

Previous studies have demonstrated that a wide range of compressive strength values can be achieved, depending on various factors such as treatments for improved dispersion, the mixing process, and the properties of added fibres [8], [11]. The challenges encountered during mixing and difficulties in moulding, particularly with a higher fibre content, could potentially result in increased air entrapment within the mixture. This, in turn, may have led to less favourable outcomes in terms of compressive strength.

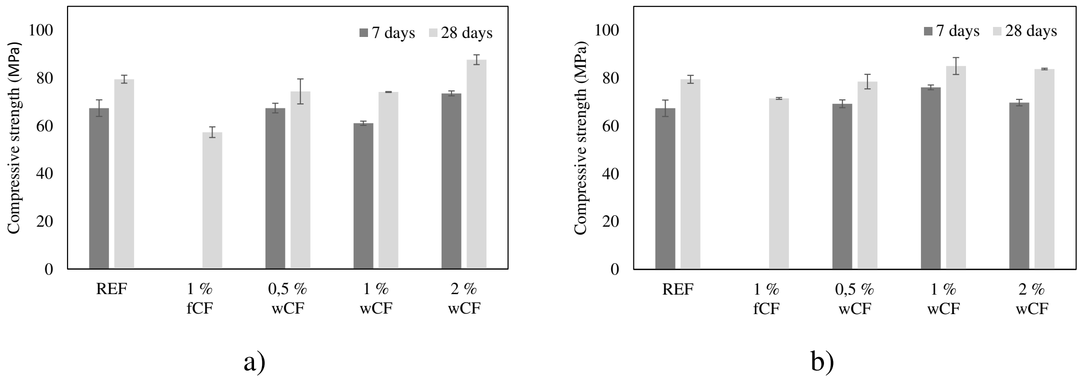

Fig. 1 Compressive strength values after 7 and 28 days: a) fibre length 6 mm, b) fibre length 12 mm.

In contrast to the compressive strength, the values for flexural strength exhibit a positive correlation with the presence of waste carbon fibres. This trend aligns with the findings reported in the previous literature [8], [11]. It's worth noting that the behaviour of factory-made fibres with polyurethane sizing differs from this trend. The variation in obtained values on mixture fCF 1.0-6, compared to the mixes with waste fibres (wCF 0.5-6, wCF 1.0-6, wCF 2.0-6) could be attributed to differences in sizing. Polyurethanes are naturally hydrophobic and insoluble in water, which can prevent the dispersion of fibres, i.e., keeping the fibres in bundles. However, some modifications are possible to also disperse them in water [15]. While as previously discussed in Mrduljaš et al. [10], ATR-FTIR spectra of waste carbon fibres did not reveal polyurethane absorptions but rather very weak absorptions of amino groups between 1600 and 1500 cm^{-1}, Fig. 2, suggesting that the sizing used might differ from polyurethane, i.e. it might be an organic amino- silane. Silane sizing is commonly used on glass fibres focusing on four silanes containing amino-, epoxide-, methacryloxy- or vinyl- function with significative improvement of adhesion [16].

A 12 mm fCF contained glycerol, a common humectant used to reduce moisture loss, as a sizing. Glycerol is very soluble in water which can contribute to the dispersion of the fibres and serve to improve compatibility and adhesion between the fibres and the cementitious matrix. In this study, a similar effect was observed in both fCF 1.0-12 and wCF specimens, both of which were 12 mm in length.

Additionally, it has been established in prior research [7], that fibres with a higher aspect ratio tend to form agglomerations, which not only diminish the mechanical properties but also increase the resistance of the composite.

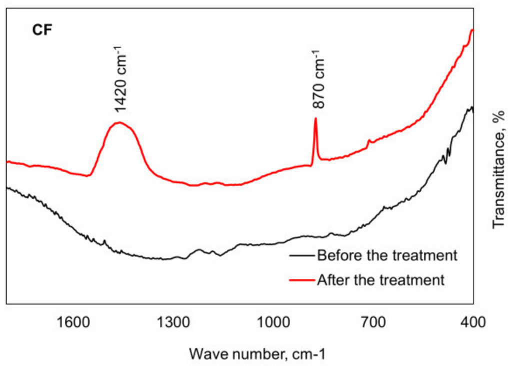

Fig. 2 ATR- FTIR Spectra of waste carbon fibres [10].

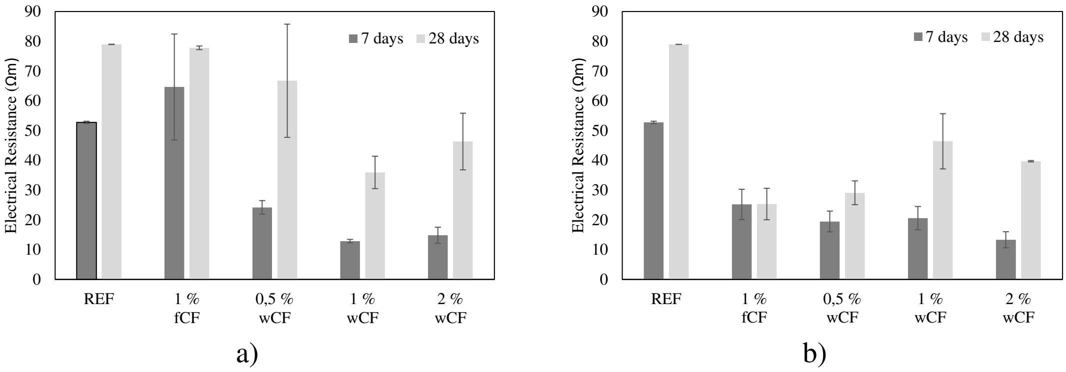

Fig. 3 Electrical resistivity values after 7 and 28 days for: a) 6 mm carbon fibres, b) 12 mm carbon fibres.

Fig. 3 presents the electrical resistivity results of cement mortars containing 6 mm and 12 mm carbon fibres. The results reveal a consistent trend: as the fibre content increases, the electrical resistance generally decreases, with one notable exception in the case of mixture fCF 1-6. These findings are in line with those reported in prior research [8], [11].

However, it is important to highlight that the results for mixture fCF 1.0-6 differ significantly from the other mixtures, considering that the values are close to the values of the reference mixture, one can say that the influence of the fibres was not present in this case. This difference becomes evident when examining the visual appearance of the cross-sections of mixtures containing waste fibres and factory fibres, where the similarity between waste fibres and factory fibres treated with glycerine sizing is apparent. In contrast, mixture fCF 1.0-6 stands out with noticeable distinctions in the dispersion and distribution of the fibres in the cross-section, as shown in Fig. 4.

These variation in electrical resistivity can be attributed to the concept of reduced connectivity, wherein the absence of a contact network of conductive material leads to increased resistance, thus reducing the conductivity of the mixture.

wCF 1.0-6	fCF 1.0-6	wCF 1.0-12	fCF 1.0-12

Fig. 4 Visual appearance of the mixtures with 1.0 % carbon fibres

4. CONCLUSION

This paper delves into the potential for developing multifunctional materials that not only have a reduced environmental impact but also take into account economic factors. Conductive, high- strength mortar has been produced using waste carbon fibres, which exhibit minimal differences in mechanical properties compared to factory-produced fibres.

While this study did not reveal a distinct impact of these fibres on the compressive strength, it’s important to note that these mixtures still fall under the category of high-strength cement composites. Furthermore, they exhibit a considerable positive influence on the flexural strength. Additionally, a favourable impact on the electrical conductivity

properties was observed. Importantly, this influence becomes more pronounced as the fibre content increases.
Results also highlight that both the fibres themselves and the sizing have a significant influence on dispersion and distribution within the composite. This, in turn, directly affects the materials overall behaviour and properties.
Future objectives in this area should be focused on the study of fibre sizing impact on distribution and dispersion, as well as the research on the resulting microstructural changes of cement composites reinforced with waste and factory made carbon microfibres.

ACKNOWLEDGEMENT

The research presented here is part of the scientific project entitled "Cementitious composites reinforced with waste fibres" – ReWire (UIP-2020-02-5242) and "Career Development of Young Researchers - Training of New Doctors of Science" (DOK-2021-02-4884). Both projects are founded by the Croatian Science Foundation and conducted at the University of Zagreb Faculty of Civil Engineering. The authors would like to express their sincere gratitude to Kelteks Ltd and Samoborka Ltd for their generous provision of resources and continuous support throughout the duration of the ReWire project.

REFERENCES

[1] F. Belaid, “How does concrete and cement industry transformation contribute to mitigating climate change challenges?,” *Resour. Conserv. Recycl. Adv.*, vol. 15, no. 200084, 2022.

[2] A. Belli, A. Mobili, T. Bellezze, and F. Tittarelli, “Commercial and recycled carbon/steel fibers for fiber-reinforced cement mortars with high electrical conductivity,” *Cem. Concr. Compos.*, vol. 109, May 2020, doi: 10.1016/j.cemconcomp.2020.103569.

[3] L. Wang and F. Aslani, “A review on material design, performance, and practical application of electrically conductive cementitious composites,” *Constr. Build. Mater.*, vol. 229, p. 116892, 2019, doi: 10.1016/j.conbuildmat.2019.116892.

[4] B. Han, L. Zhang, and J. Ou, “Smart and multifunctional concrete toward sustainable infrastructures,” *Smart Multifunct. Concr. Towar. Sustain. Infrastructures*, pp. 1–400, 2017, doi: 10.1007/978-981-10-4349-9.

[5] A. Baričević, K. Didulica, M. Frančić Smrkić, and M. Jelčić Rukavina, “Cementitious Composites Reinforced with Waste Fibres from the Production of High-Quality Construction Textiles,” *Materials (Basel).*, vol. 15, no. 4, 2022, doi: 10.3390/ma15041611.

[6] G. Faneca, I. Segura, J. M. Torrents, and A. Aguado, “Development of conductive cementitious materials using recycled carbon fibres,” *Cem. Concr. Compos.*, vol. 92, pp. 135–144, Sep. 2018, doi: 10.1016/j.cemconcomp.2018.06.009.

[7] J. Han, J. Pan, J. Cai, and X. Li, “A review on carbon-based self-sensing cementitious composites,” *Constr. Build. Mater.*, vol. 265, p. 120764, 2020, doi: 10.1016/j.conbuildmat.2020.120764.

[8] X. Jing and Y. Wu, “Electrochemical studies on the performance of conductive overlay material in cathodic protection of reinforced concrete,” *Constr. Build. Mater.*, vol. 25, no. 5, pp. 2655–2662, 2011, doi: 10.1016/j.conbuildmat.2010.12.015.

[9] O. Galao, L. Bañón, F. J. Baeza, J. Carmona, and P. Garcés, “Highly conductive carbon fiber reinforced concrete for icing prevention and curing,” *Materials (Basel).*, vol. 9, no. 4, 2016, doi: 10.3390/ma9040281.

[10] B. Mrduljaš, A. Baričević, I. Pucić, I. Carević, and K. Didulica, “Alkali resistance of selected waste fibres to model cement environment,” *Case Stud. Constr. Mater.*, vol. 19, no. August, 2023, doi: https://doi.org/10.1016/j.cscm.2023.e02411.

[11] B. Han, L. Zhang, C. Zhang, Y. Wang, X. Yu, and J. Ou, “Reinforcement effect and mechanism of carbon fibers to mechanical and electrically conductive properties of cement-based materials,” *Constr. Build. Mater.*, vol. 125, pp. 479–489, 2016, doi: 10.1016/j.conbuildmat.2016.08.063.

[12] D. C. González, M. Rahman, J. Mínguez, M. A. Vicente, and R. Hindi, "Influence of fibers and curing conditions on the pore morphology in plain and fiber-reinforced high-performance concrete through the use of computed tomography scan technology," *Appl. Sci.*, vol. 10, no. 12, 2020, doi: 10.3390/app10124286.

[13] J. Mínguez, M. A. Vicente, and D. C. González, "Pore morphology variation under ambient curing of plain and fiber-reinforced high performance mortar at an early age," *Constr. Build. Mater.*, vol. 198, pp. 718–731, 2019, doi: 10.1016/j.conbuildmat.2018.12.010.

[14] J. L. da Silva and A. C. Lordsleem, "Influence of mixer type and mixing time on the multipurpose mortars properties," *Case Stud. Constr. Mater.*, vol. 15, no. November 2020, p. e00562, 2021, doi: 10.1016/j.cscm.2021.e00562.

[15] H. Honarkar, "Waterborne polyurethanes: A review," *J. Dispers. Sci. Technol.*, vol. 39, no. 4, pp. 507–516, 2018, doi: 10.1080/01932691.2017.1327818.

[16] J. L. Thomason, "Glass fibre sizing: A review," *Compos. Part A Appl. Sci. Manuf.*, vol. 127, no. May, 2019, doi: 10.1016/j.compositesa.2019.105619.

OVERVIEW OF A TECHNICAL-TECHNOLOGICAL AND ORGANIZATIONAL STUDY FOR ROAD CONSTRUCTION OF MIDDLE SECTION BUDVA BYPASS

Željka Beljkaš[1], Biljana Ivanović[2], Njegoš Beljkaš[3] Mladen Gogić[4]

Summary:

The Budva bypass Budva is about 30 km long and consists of three sections: North, Middle, and South. The priority during the development of the technical documentation was to elaborate the documentation for the Middle section. The ToR required the preparation of a Technical-Technological and Organizational Study for the construction elements of all structures along the section and route. This paper provides an overview of the Study for the construction of the route. The Middle section is about 8 km long and connects to the main road M1 via an access road that is 2.2 km long. This section includes two interchanges, Bratešići and Budva, as well as four deviations. Along the route of the Middle section, there are five tunnels, 14 bridges, two underpasses, and one overpass. The Study determined the technical and technological solutions for construction, the network plan structure for implementing the proposed solutions, an approximate estimation of the duration and costs of construction, and an assessment of the cash flow during the construction of the route.

Keywords: Study, bypass, route, duration, costs

[1] Docent, Građevinski fakultet Univerzitet Crne Gore, Podgorica, Crna Gora, zeljkab@ucg.ac.me
[2] Docent, Građevinski fakultet Univerzitet Crne Gore, Podgorica, Crna Gora, biljanai@ucg.ac.me
[3] MSc, VE Inženjering 021, Novi Sad, Srbija, njegos77@gmail.com
[4] Viši stručni saradnik, Građevinski fakultet Univerzitet Crne Gore, Podgorica, Crna Gora, mladeng@ucg.ac.me

1. INTRODUCTION

During the development of the project documentation, current regulations, guidelines, methodologies, strategic plans, and reports were used. [1] [2] [3] [4] [5] [6] [7] [8] [9] [10] [11] [12] [13] [14] [15] [16] [17].
The route of the Budva Bypass starts in the zone of the interchange “Bratešići”. The 2.2 km long access road connects the main road M-1 with the Bypass. After the interchange, the route of the Middle Section goes through the hilly hinterland above Budva, and then, after 9 km, it intersects with the existing main road M10 Budva-Cetinje-Podgorica in the immediate vicinity of the settlement Markovići. The intersection of the main direction and the main road was solved by the interchange "Budva".
The route continues through the hilly hinterland above Bečići and ends in the zone of the village of Vrijesno. Due to the intersection of the existing road network, four deviations were designed.
On the Middle section of the bypass, the construction of 14 bridges is planned. On the access road Bratešići, 4 bridges are designed (Table 1), and on the main route, 10 double bridges are projected (Table 2).

Tab. 1 Bridges on the access road ***Bratešići***

No	Bridge	Chainage		Lenght
		Start	End	
1	Bratešići 1	680	752	72
2	Bratešići 2	1257	1329	72
3	Bratešići 3	1605	1789	184
4	Bratešići 4	1984	2110	126

Tab. 2 Bridges on the main route

No	Bridge	Chainage (left)		Lenght	Chainage (right)		Lenght
		Start	End		Start	End	
5	Rakita	680	752	72	459.62	615.62	156
6	Kralj 1	1257	1329	72	2012	2280	268
7	Kralj 2	1605	1789	184	2365	2521	156
8	Drenovštica	1984	2110	126	4660	5326	707
9	Duletići	6838.66	6857.16	18.5	6882.03	6990.53	18.5
10	Piratac	7780	7942	162	7780	7987	207
11	Vještica	8695.6	8947.6	252	8700	8997	297
12	Budva	9377.162	9629.162	252	9377.162	9629.162	252
13	Šamički potok	10060	10496	436	10056	10520	464
14	Bečica	11280	11712	432	11270	11702	432

The total length of the bridges of main route is 5692m.
On the route of the Middle section of the Bypass, five tunnels have been designed. An overview of the tunnels with their stationing is provided in Table 3.

Tab. 3 Tunnels on the main route

No	Tunnel	Chainage			Lenght
		Portal	Tunnels work	Portal	
1	Bogovina	2+500.00	2+560.00 – 3+425.00	3+441.62	942.62
		2+545.00	2+605.00 – 3+432.11	3+448.74	903.74
2	Duletići	5+430.00	5+445.00 – 6+815.00	6+819.00	1389.00
		5+445.00	5+460.00 – 6+858.00	6+862.00	1417.00
3	Markovići	7+125.00	7+240.00 – 7+651.79	7+720.00	595.00
		7+245.00	7+4325.00 – 7+685.00	7+705.00	460.00
4	Stanišići	10+550.00	10+670.00 – 11+020.00	11+220.00	670.00
		10+650.00	10+745.00 – 11+015.00	11+235.00	585.00
5	Babac	11+723.00	11+730.00 – 13+050.00	13+100.00	1377.00
		11+740.00	11+755.00 – 13+010.00	13+060.00	1320.00

The total length of the tunnel is 9658,36m.

2. ROUTE

2.1. TYPICAL CROSS SECTION

The elements of a typical cross-section are determined based on the specified design velocities.The widths of the individual elements of the typical cross-section of the main alignment (100km/h) are:

- traffic lanes 4x3.50m
- edge strips 4x0.35m
- dividing belt min 2.50m
- shoulder 2.00m
- berm 1.25m
- grid 0.9m
- inflow-outflow strip 3.50m.

Emphasizing the requirement of harmonization with TEM standards, the TOR defined the width of the dividing strip as at least 3.00m. In accordance with these standards, the width of the central dividing strip encompasses the edge strips. Therefore, in this particular scenario, the width as per TEM specifications is calculated as 2.5m plus twice the width of the edge strip, which is 0.35m on each side. This calculation results in a total width of 3.2m, surpassing the minimum required width for the central dividing strip, which is 3.00m. The dimensions of the elements of the typical cross-section of the connecting roads are:

- traffic lanes 2x 3.00m
- edge strips 2x0.30m

- shoulder 1.50m
- berm 0.75m
- grid 0.9m
- widening of the carriageway in the curve for passing two heavy goods vehicles with a trailer.

The elements of the typical cross-section of one-way, one-lane ramps have the following widths:

- traffic lane 1x3.50m
- edge strip 1x0.35m
- protective belt 1x1.65m

The minimum transverse slope of the road is 2.5%, and the maximum in the curve is 7.0%.

A typical cross-section of the main alignment is shown in the Figure 1.

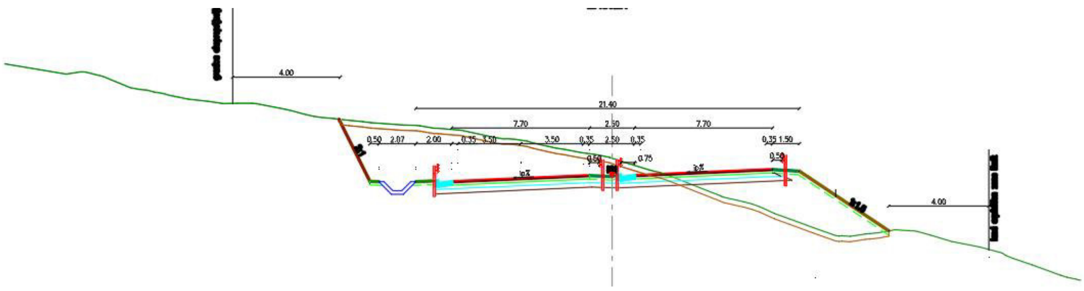

Fig. 1 Typical cross-section of the main alignment

The land acquisition limit of the bypass is defined at 4.00m from the last point of the cut, i.e. the foot of the embankment. For the connection road and the main road, the limit is defined at 2.00m, and for deviations at 1.00m.

2.2. BOUNDARY ELEMENTS OF THE PLAN AND PROFILE

The following elements of the plan and profile were adopted and given in Table 4. These elements are based on the given design speed, standards of the surrounding countries, and TEM:

Tab. 4 Adopted elements of the plan and profile

		label	regulation	design
Layout plan	***Minimum radius of horizontal curvature***	***min R***	***450m***	***450m***
	Minimum radius of the horizontal curvature in the counter-slope	***min R***	***3000m***	***-***
	Minimum transition curve parameter	***min A***	***180***	***200***
	Maximum direction length	***max L***	***2000m***	***1512m***
Longitudinal profile	***Maximum longitudinal slope***	***max in***	***5%***	***4%***
	Minimum longitudinal slope	***min in***	***0.5 %***	***0.68%***
	Minimum radius of convex roundness (in = 0%)	***min Rv konv***	***6000m***	***10 000m***
	Minimum radius of concave curvature	***min Rv konk***	***4000m***	***10 000m***

The geometric layout of the bypass route was established based on the predetermined boundary elements of the plan and profile. The challenging topography, coupled with the need for numerous structures such as tunnels and bridges, significantly influenced this layout. To accommodate these complexities, especially the requirement to maintain a 30m separation between tunnel axes, the alignment, and elevation of the right and left lanes of the bypass were individually defined on two distinct sections. Conversely, a common alignment and elevation were maintained on two other sections.
Furthermore, specific professional requirements, such as the maximum height distance between the right and left lanes within the tunnels (ranging from 2.5 to 3.0m to facilitate transverse evacuation connections) and the design plans for tunnels and bridges, made it infeasible to have a more separate alignment and elevation for the right and left lanes.

2.3. LAYOUT PLAN

The horizontal geometry elements of this route variant are designed for a design speed of Vr = 100 km/h. The minimum radius applied for curves on the open roadway is 450 meters, while in tunnels, the minimum radius is set to 1000 meters.
The Middle section of the route commences at Bratešići. The "Bratešići" interchange is configured as a rhombus shape with a central roundabout. To connect the bypass and the access road, one-way ramps are provided in all four quadrants of the roundabout. This design, despite limited space availability, ensures short distances on the subordinate road, clear navigation for drivers, and sufficient traffic capacity. It's especially advantageous in challenging terrain conditions.

The one-way ramps extend further into entrance and exit zones, with their lengths determined based on specified speeds and acceleration/deceleration requirements. The design of the entrances and exits on the main route is carried out using so-called "parallel" exit and entry lanes. The flow part of the roadway at the entry and exit zones is widened by an additional lane with a width of t_d=3.5m, which is the same width as the main route lane and extends over the deceleration (l_d), or acceleration (l_a). length of the road. Together with the access part, it forms the exit or entry, with lengths represented a $L_{izl-ul} = l_c + l_{d-a}$.

2.4. LONGITUDINAL PROFILE

The level of the main direction is designed with a maximum longitudinal slope of 4% at a length of 1369m. The minimum longitudinal slope is 0.68%. Special care has been taken to strategically position the inflection points in such a way that changes in the elevation profile predominantly occur within the middle section of the horizontal curves.
A significant focus has been placed on ensuring the proper alignment of the elevation profile, especially as it passes through the landslide-prone area in Markovići.

2.5. ACCESS ROAD

The access road at Bratešići serves as a connection between the main road Kotor-Budva and the Middle section route of the Bypass. The design of the horizontal and vertical geometry for this access road is tailored to a designated speed limit of 60 km/h. Additionally, there are plans to include a toll booth on the access road and allocate space for the Traffic Control and Management Center. The intersection of the access road and the Middle section of the Bypass is configured as a three-branch interchange.
This access road intersects with the existing local road network at four different points. Each of these intersections is meticulously designed to suit the specific terrain conditions and its role within the broader road network. In practical terms, these intersecting roads fall into the lowest rank, which is Class 5 for mountainous areas. Consequently, the design speed for these intersections is set at Vr=40(30) km/h, along with all other necessary minimum geometric characteristics to ensure safe and efficient traffic flow.

2.6. DEVIATIONS

In the Middle section of the project, two interchanges have been meticulously designed: "Bratešići" and "Budva."
The "Bratešići" interchange is specifically intended for the intersection of the access road "Bratešići," which branches off from the main road M1 Kotor-Budva, with the Middle section route. This interchange has been configured as a rhombus interchange featuring a central roundabout. To connect the Bypass and the access road seamlessly, one-way ramps have been strategically positioned in all four quadrants. The relatively small space requirement, short required distances in the subordinate road direction, good orientation on the subordinate road, as well as sufficient traffic capacity, classify this type of intersection as a favorable solution, especially in challenging terrain conditions.
The one-way ramps at the "Bratešići" interchange extend into entry and exit lanes, the lengths of which are carefully determined based on prescribed speeds and acceleration/deceleration requirements.
Additionally, there is an interchange "Budva" designed to facilitate the connection between the Budva-Cetinje highway and the Middle section route.

3. TECHNICAL - TECHNOLOGICAL SOLUTIONS FOR CONDUCTING WORKS ON OPEN ROUTES FOR PREPARATORY AND MAIN WORKS

This article outlines the technical and technological solutions recommended for the execution of work on the open route in the Middle section of the project. To efficiently handle earthwork operations, it is advisable to employ a significant degree of mechanization, with manual labor used where necessary to meet the project's specified dimensions.

For reinforced concrete work, the article suggests utilizing pre-fabricated reinforcement components manufactured off-site and then transported to the construction site as finished products. Concrete mixing should be done mechanically, and transportation should make use of both external and internal transport machinery. Installation should be carried out with the aid of high-quality particle board or steel formwork.

The specific machinery required is not detailed in this document, as it will depend on various factors such as chosen work methods, construction technology, the condition of available machinery, the contractor's financial resources, the machinery market, the workforce, and the ability to maintain machinery. The selection of machinery will be influenced by these considerations to ensure the successful execution of the project. capabilities.

3.1. CALCULATION OF HOURS SPENT ON WORK EXECUTION ON AN ANNUAL BASIS

Taking into account differences in weather conditions, specific work methodologies in different seasons, as well as all national holidays, the number of working days in a year for the construction of the route has been determined.

3.2. PRELIMINARY AND PREPARATORY WORKS

The following preliminary and preparatory works will be carried out on the open route:

- Marking the route and structures.
- Clearing shrubs and trees and site cleaning.
- Removing all shrubs and trees and fully clearing the site along the route to provide access to the construction sites and facilitate work execution.
- Demolishing existing residential buildings.
- Removing all residential buildings located within the road alignment.
- Demolishing existing asphalt surfaces.
- Removing all existing asphalt surfaces within the construction site boundaries.
- Demolishing existing earthen roads.
- Removing all existing earthen roads within the construction site boundaries.

3.3. PROCUREMENT OF MATERIALS, ENERGY, AND OTHER RESOURCES

Materials to be used in the execution of works on the open route will be primarily procured in Montenegro or from neighboring countries, as follows:

- Cement will be transported to the construction site by trucks from Serbia and Albania.
- Aggregates and sand will be transported to the construction site by trucks from Montenegro.
- Concrete additives will be transported to the construction site by trucks from Serbia.
- Steel materials will be transported to the construction site by trucks from the Federation of Bosnia and Herzegovina, Serbia, or Turkey.
- Waterproof foil and geotextile will be imported from foreign countries to the Port of Bar and then transported to the construction site by vehicles.

- Explosives and detonators will be transported to the construction site by trucks from Serbia.
- Fuel will be transported to the construction site by trucks from Montenegro or neighboring countries.
- Equipment arriving through the Port of Bar will be transported by vehicles to the construction site. The remaining equipment arriving from neighboring countries will be delivered to the construction site by trucks.
- Asphalt will be transported from an asphalt base in Montenegro to the construction site by trucks.

3.4. ACCESS ROADS

On the entire open route, it is necessary to construct access roads to facilitate the planned works. Some existing roads that are suitable will also be used for this purpose.

3.5. WATER AND ELECTRICITY SUPPLY

The water to be used during construction will be supplied using a mobile water tanker. In addition to water from mobile tankers, local water will also be utilized.
At the beginning of the work, the construction site will be powered by generators. After the completion of the electrical line, the construction site will be supplied with electricity through a substation.

3.6. CONSTRUCTION SITE ORGANIZATION PLAN

On the construction site, it is necessary to plan the setup of temporary facilities: offices, dining area, workers' locker room, toilets, water tanks, and machinery parking.
Transportation for the workers to and from the construction site needs to be arranged.

3.7. THE MAIN WORKS ON THE OPEN ROUTES

On the open route, it is envisaged that the main works will be divided into earthworks and road construction works.

3.7.1. Earthworks

In earthworks, the following positions are planned:

- Removal of the surface layer of degraded rock mass and humus with a thickness of 30cm.
- Wide excavations in rock mass of categories 3-6 (cuts, embankments).
- Material transport.
- Construction of stepped excavations for embankment construction.
- Construction of embankments using crushed rock material from excavations (cuts, embankments, tunnels).
- Machine processing of the bedding.
- Humus and grassing with a thickness of 20cm on embankment slopes, shoulders, berms, and median strips.

3.7.2. Road pavement

For the construction of the road pavement on the open route, the following positions are envisaged:

- Construction of a subgrade from unbound granular material from excavations.
- Construction of a lower base layer from crushed stone material from excavations.
- Construction of a bituminous base layer BNS 22sA.
- Construction of a leveling protective layer AB16 with PmB 45/80-65 on bridges.
- Construction of a wearing asphalt layer of SMA 0/11s (stone mastic asphalt).
- Construction of a wearing asphalt layer of AB11s with PMB 45/80-65.
- Construction of a wearing layer of AB11.

- Construction of a wearing layer of concrete slabs.
- Construction of paving with concrete pavers.
- Construction of concrete gutters, under-gutter drainage, concrete channels, curbs, pedestrian paths, and shoulders.

4. NETWORK DIAGRAM STRUCTURE

An initial list of project activities has been established based on the required work operations. This list was generated using MS Project 2013 software. Activities are linked together with dependencies that indicate the order in which tasks should be carried out, forming a structured network plan. This plan was developed using network planning techniques. In total, there are 41 activities within the network plan structure. The detailed list of these activities can be found in Table 5.

Tab. 5 The list of activities

ID	i	Task Name
1		**CONSTRUCTION OF THE ROUTE/IZGRADNJA TRASE**
2		**Construction of the main route/Izgradnja glavne trasa**
3		Trasa/Route
4		Potporni zidovi/Retaining walls
5		MSE i kosine/MSE, slopes
6		**Pristupni put Bratesici/Acces road Bratesici**
7		Trasa/Route
8		Potporni zid/Retaining wall
9		Kosine/Slope
10		**Denivelisana raskrsnica Bratesici/Interchange**
11		Trasa/Route
12		MSE/MSE
13		Kosine/Slope
14		**Devijacija 1/Deviation 1**
15		Trasa/Route
16		Potporni zid/Retaining wall
17		**Devijacija 2/Deviation 2**
18		Trasa/Route
19		Potporni zid/Retaining wall
20		Kosine/Slopes
21		**Denivelisana raskrsnica Budva/Interchange**
22		Trasa/Route
23		Potporni zid/Retaining wall
24		Kosine/Slopes
25		**Devijacija 3/Deviation 3**
26		Trasa/Route
27		**Devijacija 4/Deviation 4**
28		Trasa/Route
29		Potporni zid/Retaining wall'
30		Kosine/Slopes
31		SsiO/Traffic signaling and equipment
32		Zidovi za zastitu od buke/Noise protection walls
33		Zastita od pozara/Fire protection
34		Pejzazno uredjenje/Landscape
35		**Instalacije/Installations**
36		Hidrotehnicke instalacije/Hydrotechnics
37		Elektroinstalacije jake struje/High voltage
38		Elektroinstalacije slabe struje/Low voltage
39		Sistem nadzora i upravljanja saobracajem/TCMS
40		**CONSTRUCTION OF PAVEMENT/IZRADA KOLOVOZNE KONSTRUKCIJE**
41		Construction of pavement/Izrada kolovozne konstrukcije

The network plan is shown in the Figure 2.

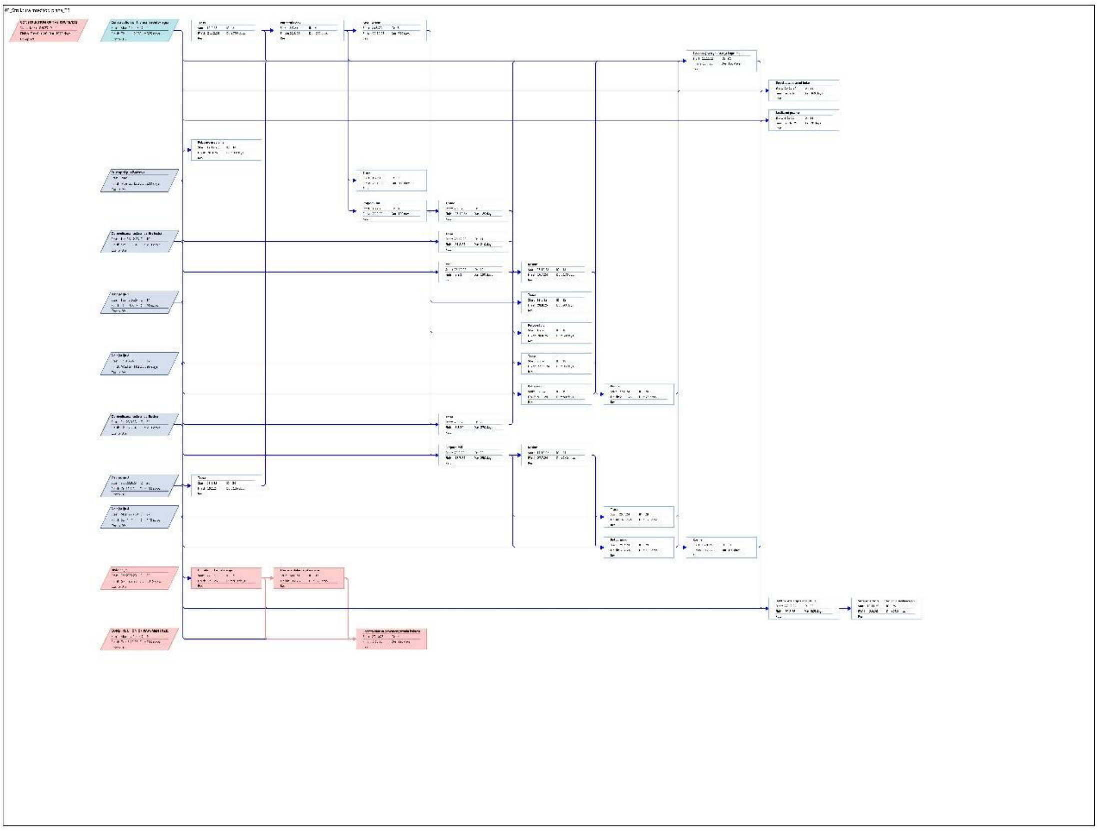

Fig. 2 Network plan

5. APPROXIMATE ESTIMATION OF THE DURATION OF THE WORKS

The project is scheduled to run six days a week, with a daily working duration of nine hours, inclusive of a one-hour break. State holidays are considered as non-working days. Activity durations have been estimated based on the work quantities outlined in the Preliminary Project (Figure 3). By creating a network diagram that links these activities, the project's completion deadline has been calculated. The entire construction process is expected to take 1075 working days. The schedule is illustrated in Figure 4 as a Gantt chart, outlining the timeline for the various activities and their dependencies.

ID	Task Name	Duration
1	**CONSTRUCTION OF THE ROUTE/IZGRADNJA TRASE**	**1075 days**
2	**Construction of the main route/Izgradnja glavne trasa**	**825 days**
3	Trasa/Route	790 days
4	Potporni zidovi/Retaining walls	710 days
5	MSE i kosine/MSE, slopes	790 days
6	**Pristupni put Bratesici/Acces road Bartesici**	**200 days**
7	Trasa/Route	200 days
8	Potporni zid/Retainig wall	120 days
9	Kosine/Slope	185 days
10	**Denivelisana raskrsnica Bratesici/Interchange**	**210 days**
11	Trasa/Route	210 days
12	MSE/MSE	190 days
13	Kosine/Slopes	170 days
14	**Devijacija 1/Deviation 1**	**90 days**
15	Trasa/Route	90 days
16	Potporni zid/Retaining wall	50 days
17	**Devijacija 2/Deviation 2**	**95 days**
18	Trasa/Route	95 days
19	Potporni zid/Retaining wall	80 days
20	Kosine/Slopes	75 days
21	**Denivelisana raskrsnica Budva/Interchange Budva**	**270 days**
22	Trasa/Route	270 days
23	Potporni zid/Retaining wall	250 days
24	Kosine/Slopes	240 days
25	**Devijacija 3/Deviation 3**	**100 days**
26	Trasa/Route	100 days
27	**Devijacija 4/Deviation 4**	**120 days**
28	Trasa/Route	120 days
29	Potporni zid/Retaining wall	110 days
30	Kosine/Slopes	100 days
31	SSiO/Traffic signaling and equipment	180 days
32	Zidovi za zastitu od buke/Noise protection walls	369 days
33	Zastita od pozara/Fire protection	20 days
34	Pejzazno uredjenje/Landscape	90 days
35	**Instalacije/Installations**	**1015 days**
36	Hidrotehnicke instalacije/Hydrotechnical	810 days
37	Elektroinstalacije jake struje/High voltage	820 days
38	Elektroinstalacije slabe struje/Low voltage	505 days
39	Sistem nadzora i upravljanja saobracajem/TCMS	250 days
40	**CONSTRUCTION OF PAVEMENT/IZRADA KOLOVOZNE KONSTRUKCIJE**	**290 days**
41	Construction of pavement/Izrada kolovozne konstrukcije	290 days

Fig 3 Estimated duration of activities

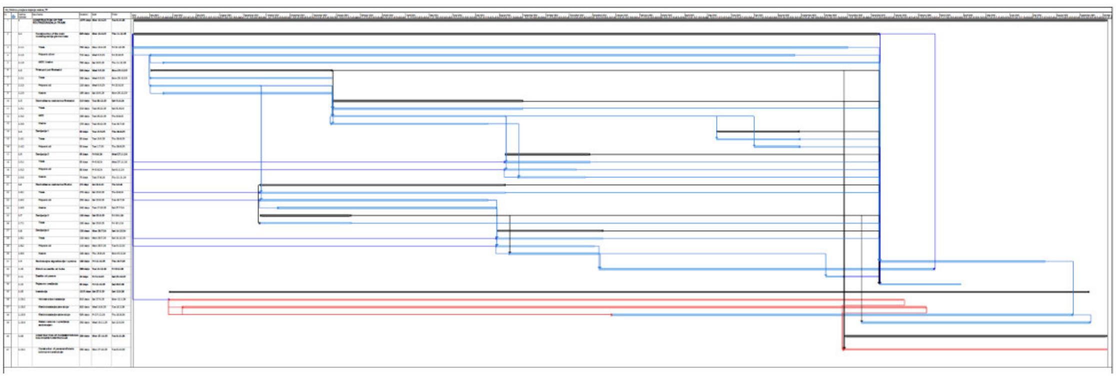

Fig. 4 Gantt chart

6. APPROXIMATE COST ESTIMATION

Approximate cost estimation was made based on the unit prices that were given in the Preliminary designs. The total construction costs, without unpredicted works and VAT, amount to 68.932.777,80 €. Costs by type of work are as follows:

- Construction of the main route with associated retaining walls, MSE, and slopes 34.045.161,14 €
- Construction of link road Bratesici with associated retaining walls and slopes 3.200.587,40 €
- Interchange Bratesici with associated retaining walls, MSE, and slopes 4.056.818,28 €
- Deviation 1 with associated retaining walls 70.486,70 €
- Deviation 2 with associated retaining walls 300.705,43 €
- Interchange Budva with associated retaining walls and slopes 2.529.656,18 €
- Deviation 3 3 059,40 €
- Deviation 4 with associated retaining walls 1.113.477,74 €
- Traffic signalization and equipment 3.155.501,44 €
- Noise protection walls 505.600,00 €
- Fire protection 4.740,00 €
- Landscape 456.847,56 €
- Installation (hydro technics, high and low voltage, Central and distance traffic control and management system) 11.427.059,38 €
- Construction of pavement 8.063.077,15 €

7. APPROXIMATE CASH FLOW ESTIMATION

According to the cash flow, the highest costs during construction occurred in March 2024 in the amount of 2.096.197,46 €. On the other hand, the lowest costs during construction occurred in October 2026 in the amount of 139.018,57 €.
The center of gravity of the investment is determined based on the diagram and the cumulative cost curve. The center of gravity is in November 2024.
In addition to the estimation of the cash flow, cost diagrams were prepared by type of work, as well as the percentage participation of each type of work in the total amount of costs. According to this, the highest cost is the cost of Construction of the main alignment of 34.045.161,17 €. Percentage participation in the total amount of costs is 49,39%. The lowest cost is the cost of Construction of Deviation 3 in the amount of 3.059,39 €. Percentage participation in the total amount of costs is 0,004%.

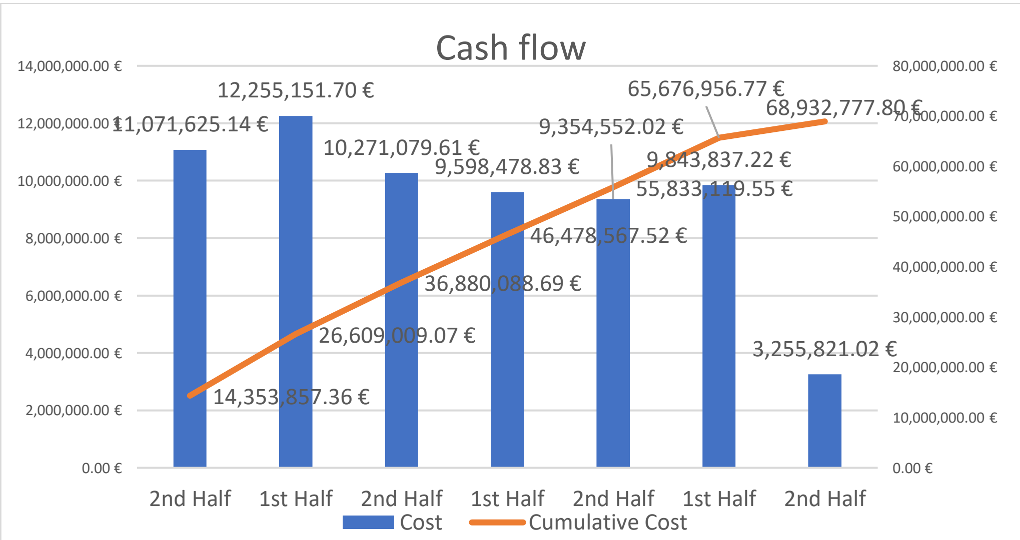

Fig. 5 Cash flow

8. CONCLUSION

The Middle section of the Budva Bypass spans approximately 8 kilometers and connects to the M1 main road through a 2.2-kilometer-long access road. This section comprises two interchanges, Bratešići and Budva, along with four deviations. Along the Middle section route, there are five tunnels totaling 9658.36 meters in length, as well as 14 bridges, two underpasses, and one overpass with a combined length of 5692 meters. The challenging terrain and numerous structures along the route significantly influenced the geometric design of the road.
After a thorough analysis, technical and technological solutions were proposed for the open route construction. An initial list of activities was formulated based on these solutions, using MS Project 2013 software. This list comprises a total of 41 activities, interconnected to reflect the sequence of operations during construction, forming a structured network plan created using network planning techniques.
By utilizing the constructed network diagram, the project's completion deadline was determined, requiring 1075 working days for construction. The total construction costs for the project amount to €68,932,777.80. The primary focus of the investment is expected to be in November 2024.

LITERATURE

[1] Vlada Crne Gore, Ministarstvo kapitalnih investicija (2021). Inovirani projektni zadatak za izradu Idejnog projekta obilaznice Budve.

[2] Zakon o putevima, Sl.list RCG 42/04.

[3] Zakon o uređenju prostora i izgradnji objekata, Sl.list CG br. 64/2017 i 44/2018.

[4] Smjernice za projektovanje, građenje, održavanje i nadzor na putevima (2005). Sarajevo/Banja Luka.

[5] Pravilnik o načinu izrade i sadržini tehničke dokumentacije za složene inženjerske objekte, Sl. list CG br. 71/18

[6] Zakon o procjeni uticaja na životnu sredinu, sl.list RCG br. 80/05 i Sl.list CG 27/13

[7] Zakon o geološkim istraživanjima, sl.list RCG 28/93

[8] Metodologija projektovanja puteva (1993). Građevinski fakultet Beograd.

[9] Projektovanje puteva (1983). Građevinski fakultet Beograd.

[10] Ministarstvo održivog razvoja i turizma Crne Gore (2019). Urbanističko-tehnički uslovi 1063-4222/14.

[11] Uprava za zaštitu kulturnih dobara, Područna jedinica Kotor (2019). Rješenje o konzervatorskim uslovima za izgradnju obilaznice oko Budve na trasi brze saobraćajnice, opštine Kotor i Budva.

[12] IGH (2009). Brza saobraćajnica duž Crnogorskog Primorja Prethodna studija opravdanosti, Zagreb.

[13] IGH (2009). Brza saobraćajnica duž Crnogorskog Primorja Generalni projekat, Zagreb.

[14] Systema and CeS.Cowi (2017). Priprema Studije izvodljivosti za prioritetnu obilaznicu na Crnogorskom Primorju (SEETO Route 1). WYG Int.

[15] Mott MacDonald CONNECTA Consortium (2018). Finalizacija Idejnog projekta prioritetne obilaznice Jadransko-Jonske dionice (Obilazak Budve poddionica 1.1) – EU standardi.

[16] Smart Environment Solutions (2018). Izvještaj o strateškoj procjeni uticaja na životnu sredinu Prostornog plana područja posebne namjene za Obalno područje Crne Gore.

[17] Mott MacDonald CONNECTA Consortium (2018). Geološki izvještaj urađen u okviru Finalizacija Idejnog projekta prioritetne obilaznice Jadransko-Jonske dionice (Obilazak Budve poddionica 1.1) – EU standardi.

RC JOINT STRENGTHENING WITH FRP

Daniel Tomic[1], Igor Gjorgjiev[2]

Summary:

Premature shear failure of beam-column joints is one of the main cause limiting the structural seismic capacity. Many post earthquake inspections confirmed that partially confined (exterior, corner) joints of RC existing buildings are the most vulnerable structural part due to the lack of adequate confinement, internal transverse stirrups and detailing. Local strengthening of beam-column joints with fiber-reinforced materials with polymeric matrix (FRP) increase the seismic capacity of structures and is widely used as a strengthening method. The strengthening method consists of several stages of construction: (1) steel sheets to prevent damage by infill, (2) joint panel shear strengthening, (3) column confinement and (4) U wraps on RC beam with carbon fibers. All stages are calculated in accordance with Italian CNR-DT 200 and improve the global capacity of under-designed RC structures in terms of global deformation and energy dissipating capacities.

Key words: seismic strengthening, seismic capacity, FRP

[1] M. Sc., Doctoral student, Institute of Earthquake Engineering and Engineering Seismology (IZIIS), University “Ss. Cyril and Methodius” in Skopje, Skopje, N. Macedonia, danielt@pluto.iziis.ukim.edu.mk
[2] Prof., Institute of Earthquake Engineering and Engineering Seismology (IZIIS), University “Ss. Cyril and Methodius” in Skopje, Skopje, N. Macedonia, igorg@iziis.ukim.edu.mk

1. INTRODUCTION

In FRP materials, fibers provide both loading, carrying capacity and stiffness to the composite while the matrix is necessary to ensure sharing of the load among fibers and to protect the fibers themselves from the environment [1]. Most FRP materials are made of fibers with high strength and stiffness, while their strain at failure is lower than that of the matrix as shown in figure 1. FRP material has lower stiffness than fibers and fails at the same strain, $\varepsilon_{f,max}$ of the fibers themselves. In fact, beyond such ultimate strain, load sharing from fibers to the matrix is prevented.

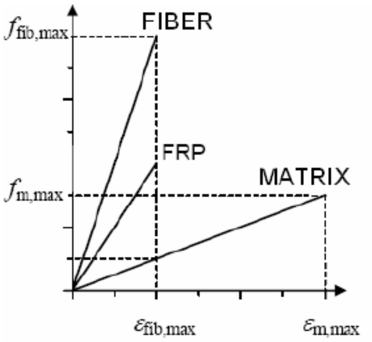

Fig. 1 Stress-strain relationship of fibers, matrix and FRP (CNR-DT 200)

When strengthening reinforced concrete members with FRP composites, the role of the bond between concrete and FRP is of great relevance due to the brittleness of the failure mechanism by debonding (loss of adhesion) [2]. According to the capacity design criterion, such a failure mechanism shall not precede flexural or shear failure of the strengthened member.

The FRP materials in a ''wet-layup system'' are widely used for strengthening since they can ensure the best compliance to the structural member shape. Wet lay-up systems - manufactured with fibers lying in one or more directions as FRP sheets or fabrics and impregnated with resin at the job site to the support. Carbon fibers (CFRP) are preferred in the case of external application while glass ones (GFRP) for internal application of strengthening.

The application of FRP composites in the field of strengthening started in the 1980s for providing additional confinement to RC columns or as flexural strengthening for RC bridges, a sudden increase in the use of FRPs was observed in Japan after the 1995 Hyogoken-Nanbu earthquake [3].

Local retrofitting of beam-column joint (corner) is presented in accordance with Italian CNR-DT 200 (Guide for the design and construction of externally bonded FRP systems for strengthening existing structures) on beam with base 45 cm and height 85 cm with bottom reinforcement 3 RØ16 and top reinforcement 5 RØ16. The column is with dimensions 45/55 cm with 4 RØ16 in corners and other 4 RØ12 with one at middle on the column side. Design concrete compressive strengths in calculations are 13.33 MPa for flexure calculations and 8.89 MPa for shear calculation. This values are obtained for existing structures with simulated design in accordance with relevant practice and materials with default values in accordance with the standards of the time of construction – limited knowledge with confidence factor 1.35. Mean value of concrete tensile strength is 1.39 MPa, elastic modulus of concrete 26 242.45 MPa. Joint panel is without transverse reinforcement or with transverse reinforcement where stirrups spacing are higher than 20 cm. Normalized axial load in column is 0.2. The local retrofitting of corner beam-column subassembly with FRP is presented in four stages of strengthening:

- design to resist infill action
- joint panel shear strengthening

- column end confinement
- calculations for U wraps on beam

Exterior joint FRP strengthening system increase joint panel shear capacity and energy dissipation [6]. The experimental results presented by Di Ludovico [7] highlighted the effectiveness of the FRP to improve global performance of under-designed RC structures in terms of global deformation and energy dissipating capacities. The FRP retrofit beam-column joints in structures is able to withstand a seismic level of PGA in two directions about 1.5 times higher, than that applied to the 'as built' structure without significant damages [7]. After a lot of tests on RC structures retrofitted with FRP, after removing of FRP is shown that the RC core was neither cracked or damaged [8].

2. DESIGN TO RESIST INFILL ACTION

Under seismic action the compression provided by infill at column end and joint panel may produce diagonal cracks on joint panel or horizontal, diagonal cracks on column end. In order to withstand the horizontal component of the infill strut force, SRP composites (steel sheets with polymer) in the form of uniaxial systems can be installed around the beam-column joint both in the case of corner or exterior joints. SRP is used for reason that steel is isotropic material. In our case 2 layers of one-directional SRP is adopted with b_f = 19 cm (as shown in figure 2 and 3) based on the seismic horizontal component of the force acting by infill. The seismic horizontal component of the force acting by infill H_0 is calculated according to expresions 1 and 2 [4].

$$H_0 = min\left[\frac{f_{vko}*l*t}{0.6*\emptyset}; 0.8*\frac{f_k}{\emptyset}*cos^2\theta*\sqrt[4]{\frac{E_c}{E_m}*I*h*t^3}\right] = min(500;\ 411.53) = 411.53\ \text{KN} \quad (1)$$

where,

f_{vko} – characteristic shear strength of masonry
f_k – characteristic compressive strength of masonry
θ – arctg $\frac{h}{l}$, the angle between diagonal of the panel compared to the horizontal axis
$\emptyset$ – reduction factor
E_c – elastic modulus of concrete
E_m – elastic modulus of masonry
I – moment of inertia

$$H = max\left[\frac{H_0}{2};\ H_0 - 0.4*N\right] = \max(205.76; 147.59) = 205.75\ KN \quad (2)$$

$$F_1 = \frac{H}{\cos 30} = 237.6\ KN$$

$$f_f = 1700\ MPa$$

$$E_s = 195\ 000\ MPa$$

$$\varepsilon_{su} = 0.87\ \%$$

$$A_{srp} = 3.77\ {mm^2}/{cm}$$

$$A_s = \frac{F_1}{f_f} = 139.76\ mm^2$$

$$W_s = \frac{A_s}{A_{srp}} = 37.77 = 38\ cm\ (adopted\ 2\ layers\ with\ b_f = 19\ cm)$$

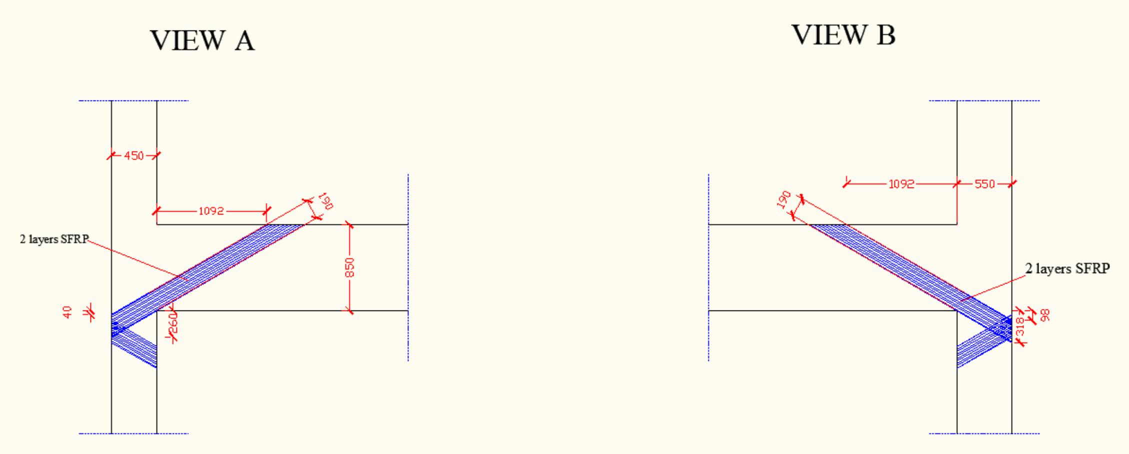

Fig. 2 Strengthening stage to resist infill action

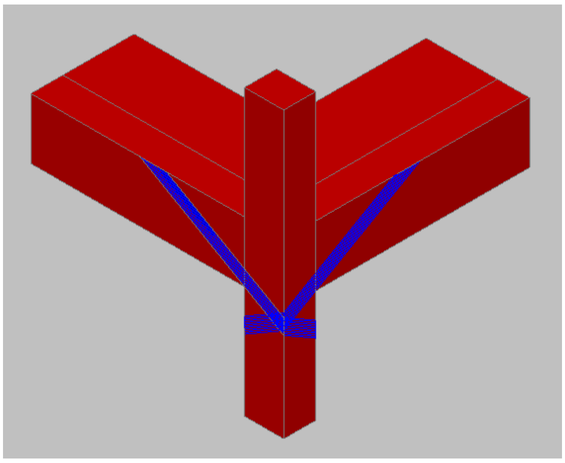

Fig.3 Strengthening stage to resist infill action – 3d view

3. JOINT PANEL SHEAR STRENGTHENING

A shear capacity increase of beam – column joint panel with the shear increase of beam column joint can be achieved through the application of composites with fibers placed along the principal tensile stresses (i.e. four-directional FRP sheets) for a corner joint and for an exterior one.

Shear strengthening is deemed necessary when the applied shear demand is greater than the corresponding member's shear capacity. The shear capacity of existing beam-column joints can be enhanced by epoxy-bonding FRP materials with fibers transverse to the axis of the shear cracks, in a way similar to adding shear strength through internal stirrup reinforcement, or perpendicular to potential shear cracks. In our case 2 layers of four-directional CFRP sheets is adopted on the joint panel extended 20 cm on beam and 10 cm on the column (as shown in figure 4 and 5). The calculation for the replacement of transverse reinforcement with FRP is with the expression 3 and 4 [4].

$$A_{sh} * f_{ywd} \geq \gamma_{RD} * A_{s2} * f_{yd} * (1 - 0.8 * \vartheta_d) = 202.57\ KN \quad [4] \tag{3}$$

$$A_{sh} * f_{ywd} = t_f * h_{beam} * f_{fd} + 2 * (t_f * h_{beam} * f_{fd} * \cos 45) = 200.12\ KN\ for\ one\ layer, 400.24\ KN\ for\ 2\ layers - 2\ layers\ are\ adopted \tag{4}$$

$A_{sh} * f_{ywd}$ - represent the amount of stirraps as in a building code (Eurocode) which is replaced with FRP layers

$\varepsilon_{fk} = 2.1\ \%$

$E_f = 230\ 000\ MPa$

$\varepsilon_{fd} = 0.004$
$f_{fd} = 920\ MPa$
$t_f = 2 * 0.106 = 0.212\ mm$

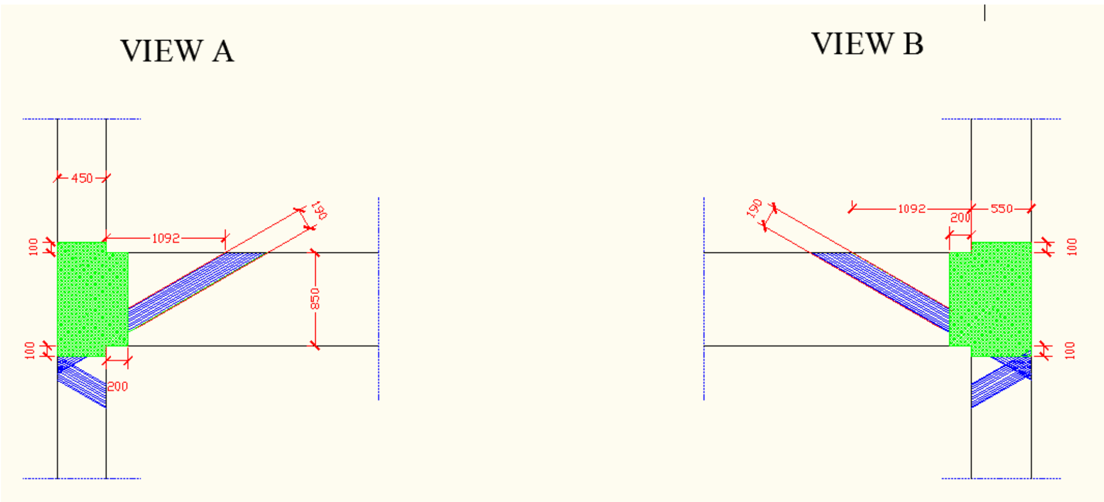

Fig. 4 Joint panel shear strengthening stage

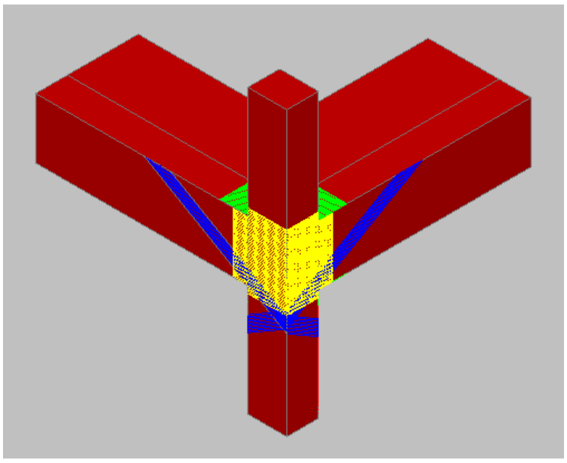

Fig. 5 Joint panel shear strengthening stage – 3d view

4. COLUMN END CONFINEMENT

Column end confinement significantly increase the deformation capacity in a plastic hinges zones with a corresponding enhancement of global structural ductility. The confinement is also effective to prevent longitudinal bars buckling and to sustain the shear action, at the top of the column, due to the infill strut force.
Wrapping of columns with fibers orthogonal to the member axis has been widely used in practice as a strengthening tool to achieve significant enhancements in both strength and ductility of axially loaded columns strength increase is due to the lateral pressure provided by confining devices restraining the lateral dilation of compressed concrete. Increased ductility of a section results from the ability to develop greater compressive strains in the concrete before failure leading to greater displacement capacities of the confined structural members.
Depending on accessibility, the strengthening can be provided by partial or full wrapping of FRP system around the member. Full wrapping is the most efficient strengthening scheme commonly used in the applications of columns where access to all sides of the member is usually available. In our case 120 cm continuous wraping with

CFRP is adopted with an overlap of 10 cm (as shown in figure 6 and 7). Unless a more detailed analysis is performed, the evaluation of the ultimate curvature of a FRP confined concrete member under combined bending and axial load may be accomplished by assuming a parabolic-rectangular approach for the concrete stress-strain relationship, characterized by a maximum strength equal to f_{cd} and ultimate strain ε_{ccu}, computed as follows [5]:

$$\varepsilon_{ccu} = 0.0035 + 0.015 * \sqrt{\frac{f_{1,eff}}{f_{cd}}} = 0.00879 = 0.879\ \% \tag{5}$$

$$f_{1,eff} = k_{eff} * f_1 = 1.661\ MPa\ (CNR - DT200(2004)) - effective\ confinement\ lateral\ pressure$$

$$f_{cd} = design\ strength\ of\ unconfined\ concrete$$

$$t_f = \frac{600}{1800} = 0.333\ mm - FRP\ thickness$$

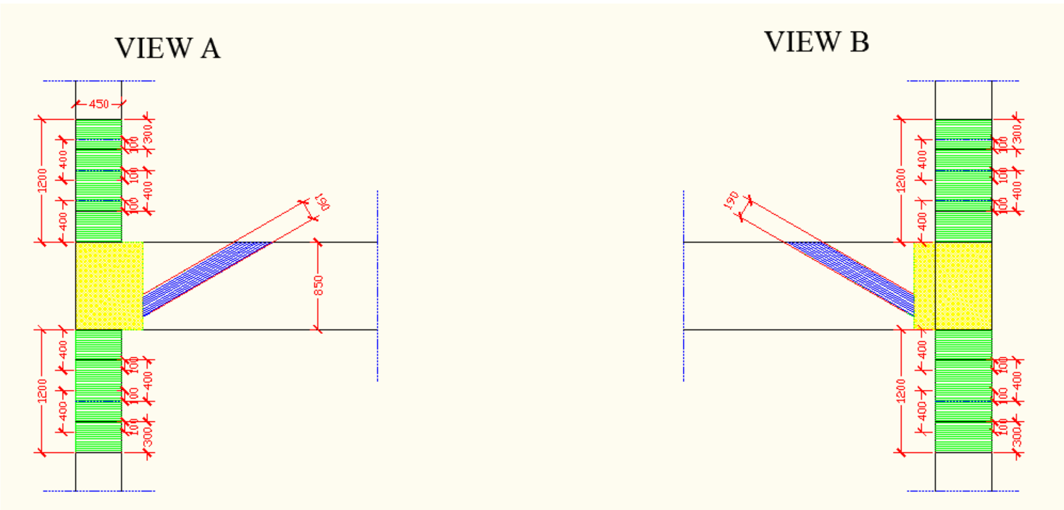

Fig. 6 Column end confinement

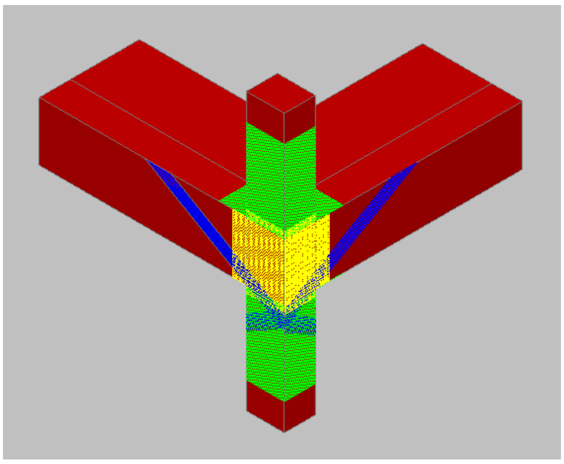

Fig. 7 Column end confinement – 3d view

5. CALCULATIONS FOR U-WRAP ON BEAM

A shear capacity increase of beams with the use of U-wrap FRP laminates increase the beam end shear capacity (in the zone of maximum shear demand in case of seismic action) and at the same time can be very useful in order to provide a mechanical anchorage to the four-directional CFRP sheet applied to the joint panel. U-wraps prevent the premature debonding of such panel and thus the effectiveness of the whole strengthening scheme. In our case 130 cm of CFRP is adopted (as shown in figure 8 and 9). The FRP contribution to the shear capacity shall be calculated according to the Moersch truss mechanism as follows [5]:

$$\vartheta_{RD,f} = \frac{1}{\gamma_{RD}} * 0.9 * d * f_{fed} * 2t_f * (\cot\beta + \cot\theta) * \frac{w_f}{p_f} = 69.2\,KN\,(CNR - DT200(2004)) \quad (6)$$

$\vartheta_{RD,f} -$ *FRP contribution to the shear capacity*
$f_{fed} -$ *effective FRP design strength* $(CNR - DT200(2004))$
$t_f = 0.166\ mm$

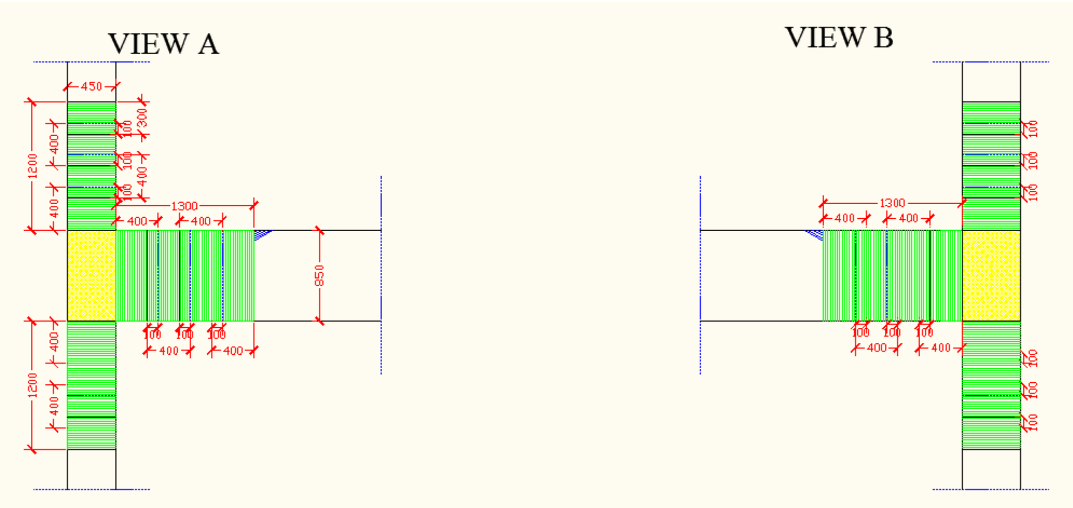

Fig. 8 Beam end strengthening stage with U-wrap

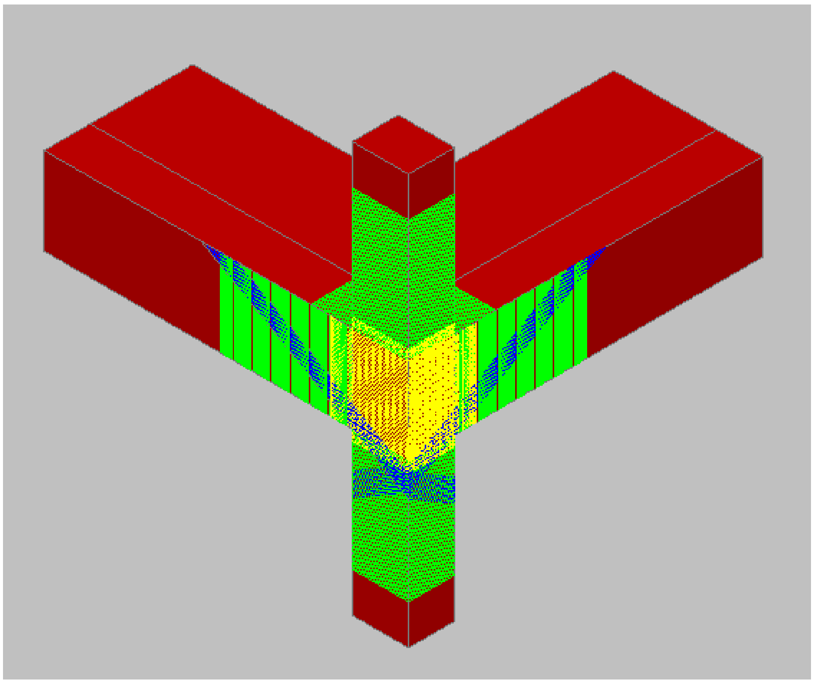

Fig. 9 Beam end strengthening stage with U-wrap – 3d view

6. CONCLUSIONS

FRP materials are widely adopted in strengthening the beam-column joints of existing structural systems. Their effectiveness is demonstrated by a large number of experimental tests on joint subassemblies and entire structural systems. Strengthening existing RC structures, especially when their seismic load capacity is not known, requires extensive analysis and calculations. By using the four stages of strengthening the beam-column joints, the seismic capacity of the structure is increased without the use of additional calculations and as a quick and effective method in increasing the seismic capacity.

An FRP wrapping increases the ultimate compressive strain of concrete, thus determining an increase of cross-section ultimate curvature and of corresponding member rotational capacity in plastic hinges zones. Thus, a global structural ductility enhancement and energy dissipation can be attained without changing the hierarchy of strength and moving of plastic hinges.

When the retrofitting is aimed to enhance the deformation capacity of the structure and all possible brittle failures have been prevented, it is necessary to assess to which extent the structure could exploit its ductility. This can be done, for example, through a nonlinear pushover analysis, now adopted and codified in the most modern seismic codes. Usually, it is requested to check if the structure can actually ensure a given ductility or if it is able to attain a given target displacement. Such analysis allows identifying the elements whose local collapse, due to ductility exhaustion, prevents the structure from exploiting its global ductility and from reaching the target displacement.

REFERENCES

[1] Balsamo, A., Di Ludovico M., Lignola, G. P., Prota, A., Manfredi, G. and Cosenza, E. (2012). Composites for structural strengthening. DOI: 10.1002/9781118097298.weoc038

[2] Di Ludovico, M., Ceroni, F., Lignola, G. P., Prota, A., Manfredi, G. and Cosenza, E. (2012). Externally bonded reinforced concrete structures. DOI: 10.1002/9781118097298.weoc078

[3] Katsumata, H., Kobatake, Y., Takeda T. (1987). A study on the strengthening with carbon fiber for earthquake-resistant capacity of existing reinforced concrete columns. Proceedings of the workshop on repair and retrofit of existing structures, U.S.–Japan panel on wind and seismic effects, U.S.–Japan Cooperative Program in Natural Resources, Tsukuba, Japan.

[4] Dolce, M., Manfredi, G., Di Ludovico, M., Lignola, G.P., Moroni, C. and Prota, A. (2015). Appendice B: Esempio di calcolo su rafforzamento locale di nodi con materiali composite.

[5] CNR (National Research Council). (2004). Guide for the design and construction of externally bonded FRP systems for strengthening existing structures. Rome, Italy: Advisory Committee on Technical Recommendation for Construction of National Research Council.

[6] Di Ludovico, M., Prota, A., Manfredi, G., et al. (2008). Seismic strengthening of an under-designed RC structure with FRP. Earthquake Eng Struct Dyn. 37:141–162 (ISSN: 0098-8847).

[7] Di Ludovico M, Balsamo A, ProtaA, et al. (2008). Comparative assessment of seismic rehabilitation techniques on a full-scale 3-story RC moment frame structure. Struct Eng Mech. 28(6):727–747.

[8] Di Ludovico, M., Manfredi, G., Mola, E., et al. (2008). Seismic behavior of a full-scale RC structure retrofitted using GFRP laminates. ASCE—J Struct Eng. 134(5):810–821.

SEISMIC UPGRADING OF TELECOMUNICATION CENTER IN SKOPJE

Aleksandar Zhurovski[1], Aleksandar Zlateski[2], Elena Delova[3] Goran Jekic[4] Roberta Apostolska[5] Veronika Shendova[6] Zivko Bozinovski[7]

Summary:

The complex of the Telecommunications Center in Skopje, North Macedonia was constructed during the seventies of the last century. To define the possibilities and conditions to meet the technical criteria for level TIER III defined by the standard TIA-942-A (Revision of TIA -942, August 2012), performed was the analysis of the stability and reliability of the existing structural system. The necessary interventions to strengthen the structure to meet the required technical standards were defined based on (i) input data from limited in situ technical investigations, (ii) assessment of the seismic potential of the site and (iii) analysis of the load-bearing structure for the newly predicted loads while simultaneously providing the required structural stability and reliability for gravity and earthquake actions according to the existing seismic code in North Macedonia. Findings from the performed analysis impose the need for both global and local structural strengthening.

Key words: telecommunication center, nondestructive testing, bearing and deformation capacity, time- history analysis, seismic strengthening

[1] Asisstant, IZIIS, Ss Cyril and Methodius University of Skopje, Macedonia, zurovski@iziis.ukim.edu.mk
[2] Asisstant, IZIIS, Ss Cyril and Methodius University of Skopje, Macedonia, azlate@iziis.ukim.edu.mk
[3] Asisstant, IZIIS, Ss Cyril and Methodius University of Skopje, Macedonia, delova@iziis.ukim.edu.mk
[4] Asst. Prof, IZIIS, Ss Cyril and Methodius University of Skopje, Macedonia, jekic@iziis.ukim.edu.mk
[5] Prof, IZIIS, Ss Cyril and Methodius University of Skopje, Macedonia, beti@iziis.ukim.edu.mk
[6] Prof, IZIIS, Ss Cyril and Methodius University of Skopje, Macedonia, veronika@iziis.ukim.edu.mk
[7] Prof, IZIIS, Ss Cyril and Methodius University of Skopje, Macedonia, zivko@iziis.ukim.edu.mk

1. INTRODUCTION

The complex of the Telecommunications Center in Skopje, North Macedonia was constructed during the seventies of the last century as a representative of the reinforced concrete buildings typical for the post-earthquake communist period, (Fig.1). This creation of the Macedonian architect Janko Konstantinov was exposed at the 2018 New York MoMA exhibition on the topic "Concrete Utopia - Architecture in Yugoslavia 1948-1980", as a representative from North Macedonia. Like other similar buildings from this period, the construction of the building is characterized by bold structural solutions, large spans and storey heights, followed by robust dimensions of the structural elements and the inevitable facade made of popularly called “nature-concrete”.

Fig. 1 The complex of Telecommunication Center in Skopje, North Macedonia.

To define the possibilities and conditions to meet the technical criteria for level TIER III defined by the standard TIA-942-A [1], which was set as a need for the possible future function of the facility, analysis of the stability and safety of the existing structural system of the Telecommunication Center facility in Skopje was carried out. Considering that it is a building of the high importance in terms of its function, built more than fifty years ago, it was necessary to evaluate its existing stability. Accordingly, the purpose of the analysis is to examine the need for additional strengthening of load-bearing structural elements in order to perform an initial cost estimation. For this purpose, in accordance with the multidisciplinary integrated approach developed in Institute of Earthquake Engineering and Engineering Seismology, IZIIS-Skopje [2], the following activities were carried out:

- Assessment of the seismic potential of the site
- On-site building inspection and investigation for providing relevant input structural data for further analysis, which encompasses (i) review of the available technical documentation, (ii) detailed inspection of the building and identification of its main structural system, (iii) definition of quality of built-in materials by non-destructive testing of structural elements and (iv) determination of dynamic characteristics of the structure by experimental in-situ testing using ambient vibration technique
- Analysis of stability of existing building for gravity and seismic loading, consisting of (i) 3D static and equivalent seismic FE structural analysis for the verified structural system and built-in materials, (ii) analysis of the bearing and deformation capacity of the existing structural system with identified quality and

quantity of built-in materials, and (iii) dynamic response including nonlinear time history analyses of building structure for earthquakes of different intensity and frequency content expected on the considered site.

The knowledge gained through the above investigations and analysis has been used to define preliminary technical solution for strengthening of individual structural elements with a cost-estimation for its realization, considering the current conditions of the market and the specifics arising from the method of execution, thus, to define the justification of entering such a process.

2. ASSESSMENT OF THE SEISMIC SITE POTENTIAL AND IDENTIFICATION OF THE LOAD-BEARING STRUCTURE

2.1. ASSESSMENT OF THE SEISMIC SITE POTENTIAL

Considering the given limited time framework, the necessary field investigation to define the seismic potential of the particular site have not been done, however, data and results of detailed research for several locations near the existing facility were considered. The seismic potential was assessed based on the results of the investigated location of the Mother Teresa monument, which is the closest to the location of the Telecommunication Center, (Fig 2).

Fig. 2 Telecommunication Center in relation to the location of the Mother Teresa monument.

The expected average maximum accelerations at the bedrock for near and far source earthquakes were estimated based on the seismic hazard analysis carried out for the location of the Mother Teresa monument. The upper limit of the average maximum accelerations of the bedrock for a return period of 475 years is 0.29g and at the foundation level is 0.36g due to the estimated dynamic amplification factor. The level of acceptable seismic risk for TK-Center was defined by the standard TIA-942-A [1]. For time-history analysis of the seismic response of the structure the following set of recorded earthquakes have been selected:

- ACC1: Ulcinj (Albatros) E-W, recorded during the Montenegro earthquake of 15.04.1979 with a magnitude of M=7.0.
- ACC2: El Centro N-S, USA, 1940, with magnitude M=6.7.
- ACC3: Robic N-S, recorded during the Furlania (Italy) earthquake of 15.09.1976 with magnitude M=6.1.
- ACC4: Petrovac (Oliva) N-S, recorded during the Montenegro earthquake of 15.04.1979 with a magnitude of M=7.0
- ACC5: Bar, N-S, recorded during the Montenegro earthquake of 15.04.1979 with a magnitude of M=7.0.

2.2. IDENTIFICATION OF THE LOAD-BEARING SYSTEM

Overview of available technical documentation: The complex of the Telecommunications Center - Macedonian Post Office in Skopje was built in three phases in the period between 1974 and 1982, (Telecommunications Center, Administration and Counter Hall, Fig. 3). The subject of analysis is the Telecommunication Center (Fig. 3 upper), which together with the tower, from which it is separated by an expansion joint, constitutes the first phase of the construction of this complex. From the available (uncompleted) technical documentation, the following was observed [3,4]:

- The structural system represents a moment resisting frame consisted of reinforced concrete columns and beams and reinforced concrete floor slabs
- The design calculations are carried out for a live load of 8 kN/m^2
- Seismic analysis is provided as for building with high importance (I category) in a zone with seismicity of IX+ degrees according to MCS, corresponding to the first seismic code in the country, (Temporary Technical Provisions for Building in Seismic Regions, Official Gazette SFRJ 39/64), valid for the time when the building was designed
- The proportioning of the load-bearing elements is carried out for concrete quality class of 30MPa (MB30) and plain reinforcement GA 240/360

Fig. 3 The Macedonian Telecommunication Complex, Telecommunication center (upper), Administration (lower left), Counter Hall (lower right).

On-site investigations of the structural elements: In order to obtain/confirm the structural system and the existing state of bearing elements, additional technical investigations and control measurements of the geometry of structural elements were performed in-situ. Considering the daily function of the building, non-destructive testing (categorized as an informative method), followed by a minimum number of semi-destructive investigations for identification of the built-in reinforcement in the selected structural elements were carried out. As a result, formwork plans of the individual storeys and characteristic cross-sections of the building have been prepared, (Fig. 4).

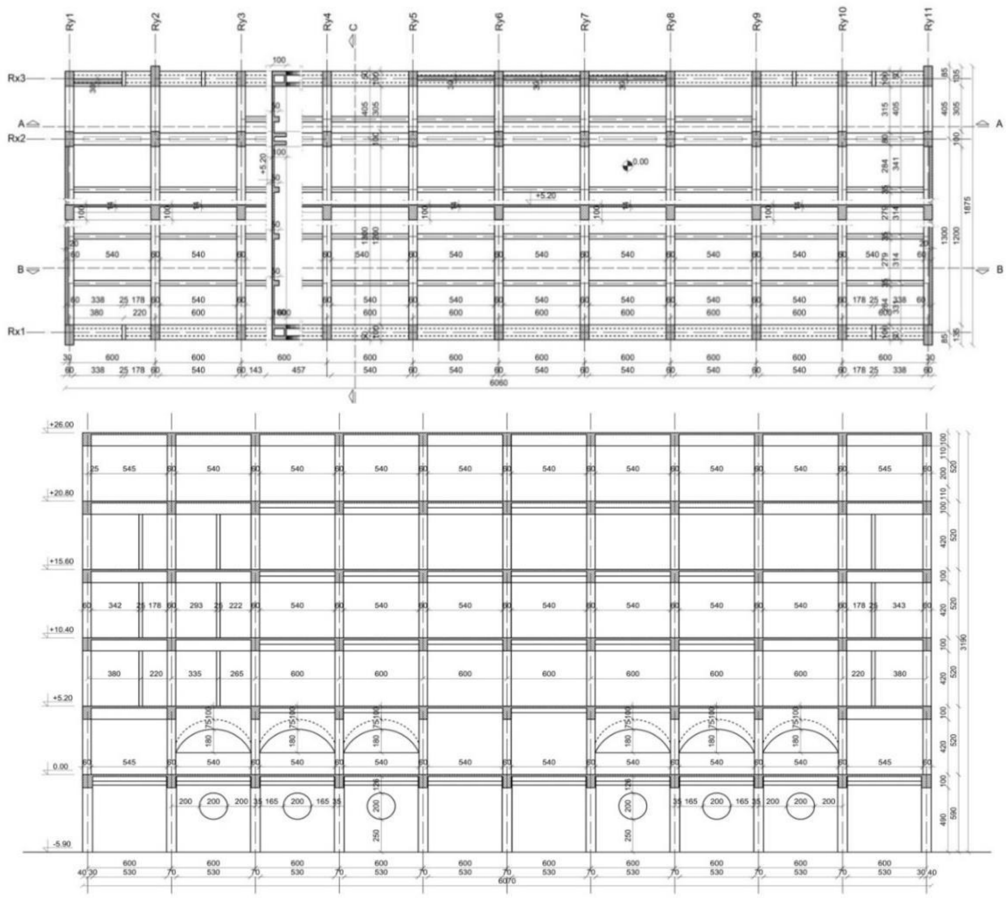

Fig. 4 Layout of the ground floor (upper) and longitudinal cross-section (lower) of the building.

Profometer Digi-Schmid Tromino

Fig. 5 Nondestructive testing equipment.

The NDT measurements have been done by the following modern equipment for determination of concrete grade and steel rebar disposition in the bearing elements, (Fig. 5):

- PROFOMETER 5+ (V2.3.0, 55.60312) (rebar detection system) for identifying the presence of built-in reinforcement, giving information about the cover layer and approximate diameter of the detected metal,
- DIGI-SCHMID 2000, (Modell ND) mechanical device designed to define the compressive strength of a material (primarily concrete),
- TROMINO® - portable ultra-mobile seismometers for definition of structural fundamental dynamic characteristic, (natural frequencies).

Majority of measurements were conducted and recorded in the basement and on the ground floor, while for the upper floors the critical positions were only confirmed. A total of 24 measurements were performed on selected available reinforced concrete elements, (Fig. 6).

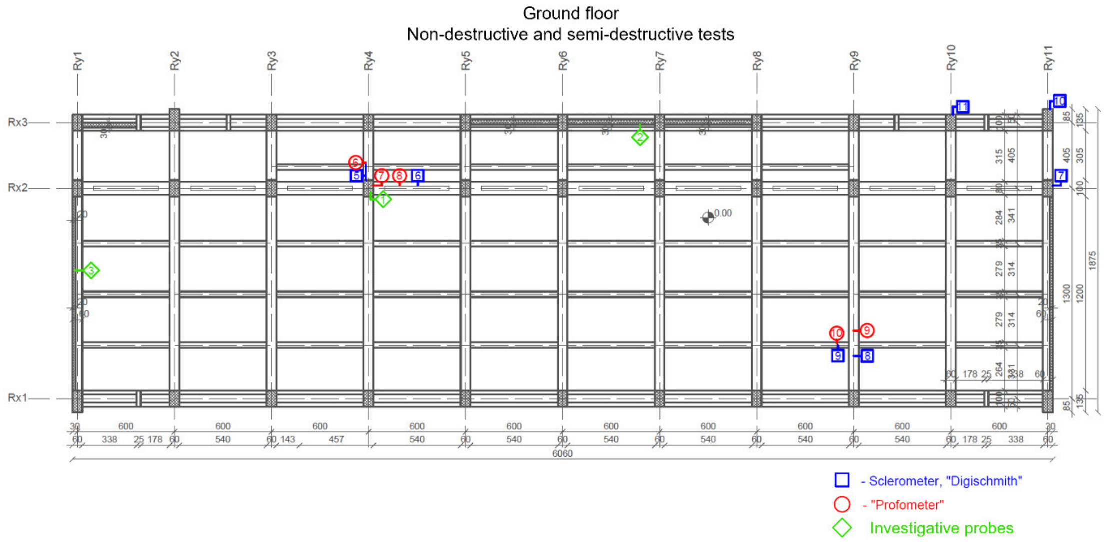

Fig. 6 NDT meaurement points on ground floor

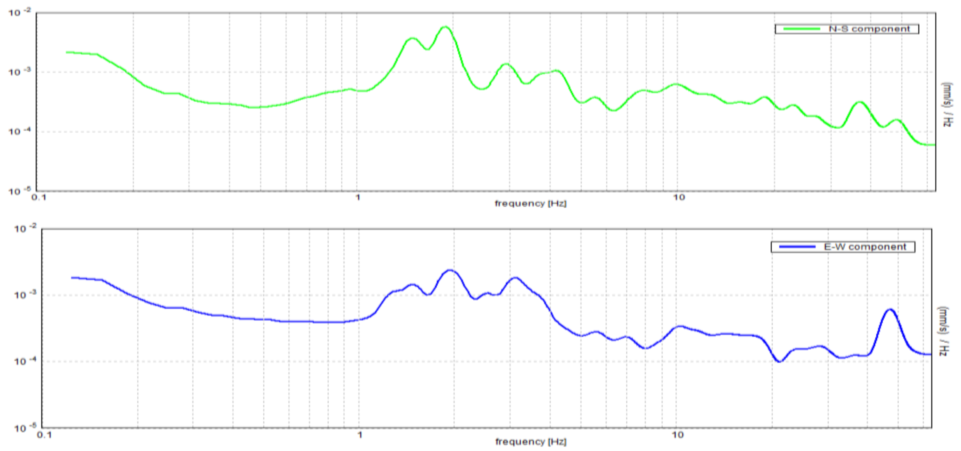

Fig. 7 Natural frequency in N-S and E-W direction.

The dynamic characteristics of the sturture were determined using the ambient vibration method, non-destructive "in situ" method based on measurement of structural vibrations caused by ambient forces. The experimentally obtianed dynamic characteristics is of particular importance when calibrating the mathematical models, for a more relevant analysis during the assessment of structural seismic stability, (Fig. 7). To confirm the exact rebar diameter minimum number of destructive investigation probes, were carriod out (Fig. 8).

Fig. 8 Column rebar diameter measurement (investuigation probe 1)

Summary on building structure investigation: The overall site investigations resulted in identification of the main load-bearing structure of the building in its current state, (Fig. 4). The principal structural system represents a reinforced concrete frame system. Selected important information are listed below:

- The compressive strength of the built-in concrete in the columns is higher than 40MPa (MB40), while in the shear walls, beams, and floor structure is 30MPa, (MB 30).
- Reinforcement configuration in beams, columns, and floor structures is defined.
- The distance of the shear reinforcement in the columns is 20/40 cm and in the beams is 15/30cm
- The natural periods of the structure in both directions are TN-S=0.55s, TE-W=0.52s.
- The columns are reinforced by longitudinal bars with 40 mm diameter and stirrups with 12mm diameter placed on 20-40 cm, (Fig. 8).
- Floor plate thickness is d=14cm.

During the visual inspection of the building, no structural damage was found, no settlements or structural distresses, nor damage or repairs due to previous earthquakes were observed. The general conclusion is that the structure has been designed and analysed according to regulations (gravity and seismic codes) at the time of construction on the building, built with exceptional quality and very well maintened.

However, considering that the building was built before the adoption of the current seismic code PIOVS'81 [5], which prescribes additional criteria that the facilitiy should satisfy, it is necessary to perform an analysis of the existing structure for the anticipated imposed gravity and seismic loads.

3. ANALYSIS OF EXISTING STRUCTURE ACCORDING TO TIA-942-A STANDARD

To assess the need for structural interventions in order to satisfy the required technical criteria for level TIER III of the TIA-942-A standard, the following structural analyses were performed for gravity and seismic actions: (1) elastic 3D analysis of a mathematical model by application of the finite element method, (2) Analysis of the bearing and deformation capacity, and (3) Nonlinear time-history analysis for the seismic parameters defined in Section 2.1 [3, 4].

3.1. LINEAR-ELASTIC 3D FINITE ELEMENT ANALYSIS FOR GRAVITY AND SEISMIC ACTIONS

For the mathematical model of the defined structural system, (Fig. 9), static and lateral force method of analysis for shear base coefficient equivalent to 15% of the total building weight (according to PIVOS'81) have been performed applying the RadImpex TOWER 7.0 Gravitational load analysis was carried out taken into consideration the crucial technical requirements for TIA-942-A - TIER III, as follows:

- additional live load of 12 kN/m^2 on the third and fourth floor structure
- additional live load of 2.4 kN/m^2, suspended on the bottom side of the third and fourth floor slab.

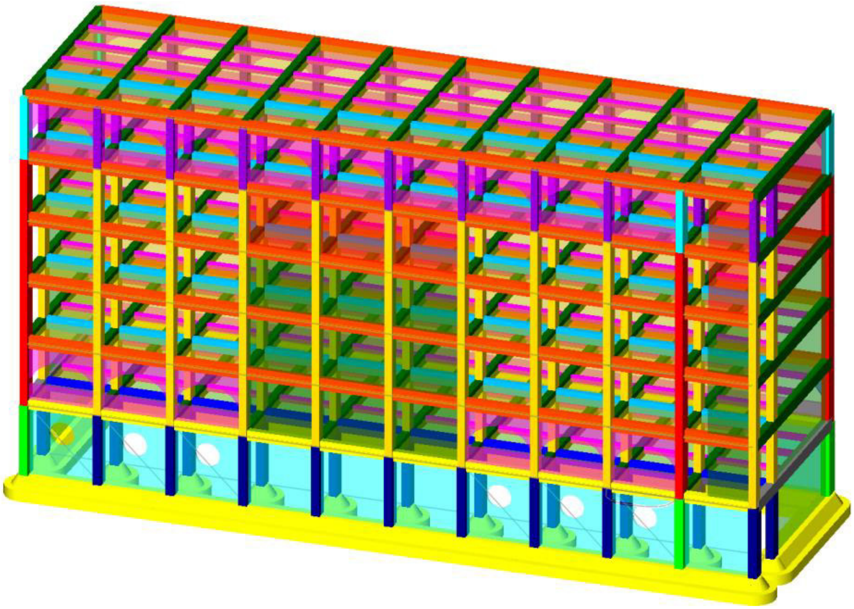

Fig. 9 3D Finite element mathematical model.

The building structure has six storeys (basement, ground floor and four stories), with a total weight of 147759 kN and a total seismic force of 21722 kN. The obtained natural periods were $T^{N\text{-}S}$=0.582s, $T^{E\text{-}W}$=0.525s, and they are very similar to the experimentally measured ones, (Fig.7). The total horizontal displacement of 1.76 cm and 2.01 cm are obtained for transversal and longitudinal direction respectfully, which are less than the maximum allowed (4.33cm), according to the PIOVS'81.

The obtained axial stresses in the columns meet the criteria against brittle failure from vertical loads prescribed in PIOVS'81, (σ_0^{max}=6.90 MPa < $\sigma_0^{allowed}$=7.175 MPa). However, certain requirements for reinforcement detailing of load-bearing elements to avoid brittle failure due to seismic actions are not fully met. This especially applies to the distance of shear reinforcement. The distance of the stirrups in the columns is 20cm near the joints and 40cm in the midsection, which is in accordance with the 1964 seismic code, but not completely in accordance with the PIOVS'81 that prescribes 15 cm in the midsection and 7.5 cm near to the joints.

As expected, in most cases the built-in reinforcement in the beams and slabs on the third and fourth storey is less than the required one, which is due to the additional live loading according to the TIA-942-A standard. At the floor levels where there are no such live loads, the built-in reinforcement corresponds to the required one obtained from the analysis.

Consequently, the elastic analysis of the structure carried out according to the current seismic code in the country, shown that the building exposed to the additional loads according to the TIA-942-A - TIER III requirements and seismic actions does not meet the overall safety criteria.

3.2. BEARING AND DEFORMATION CAPACITY

Bearing and deformation capacity at element level (Qi-δi relationship) is calculated by inhouse developed software [6]. The cumulative storey Q-δ relationship represents sum of the bearing and deformation capacity of each element, at that story level and considering direction. The storey ductility capacity is defined as ratio between maximum story displacement (δ_u) and displacement at the yield point (δ_y), i.e., $\mu = \delta_u / \delta_y$.

Bearing capacity of the ground floor, selected as most critical one, is presented on Fig.10 and it is larger than the required design criteria for shear base coefficient (see 3.1).

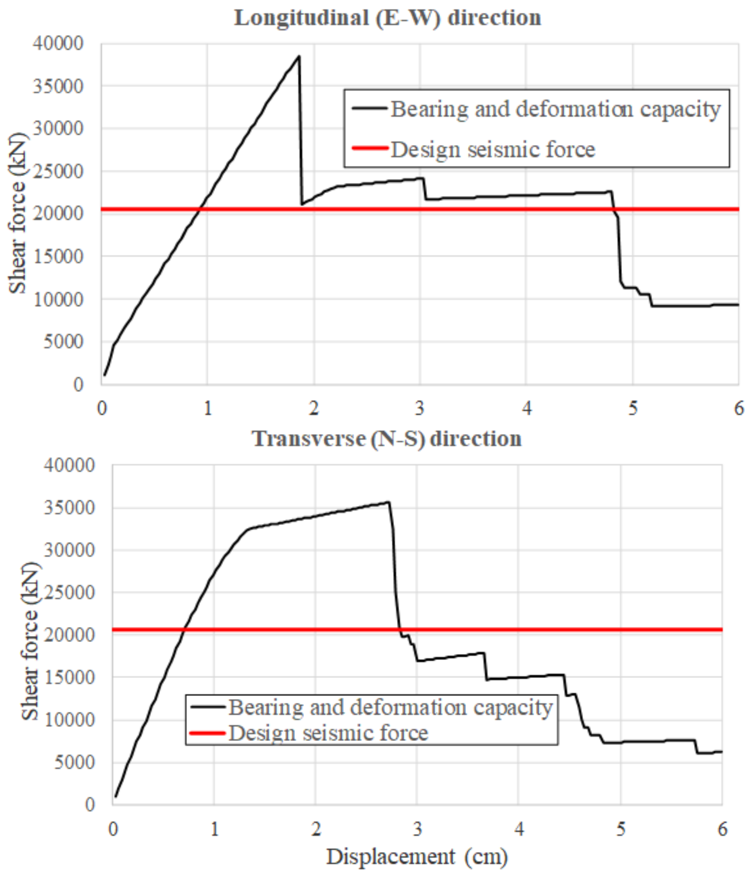

Fig. 10 Bearing and deformation capacity for ground floor.

3.3. NONLINEAR TIME-HISTORY ANALYSIS

Nonlinear time-history analysis has been performed by inhouse developed software [6], on the lump-mass structural model that assumes concentration of structural characteristics at story level and using the Q-δ bilinear relationship obtained from the analysis of bearing and deformation capacity, (Fig.10).

The results from the dynamic analysis are used for evaluation of the structural performance in nonlinear domain, i.e., verification of the capacity of the structure in respect to the demand for different earthquakes and different levels of input acceleration, as follows: (1) displacement capacity of the structure (δu) in respect to the displacement demand due to an earthquake (δ_{RQ}); (2) displacement ductility capacity of the structure (μ) in respect to the ductility demand ($\mu_{RQ} = \delta_{RQ}/\delta y$).

In accordance with the above:

- if $\delta_{RQ} \leq \delta y$, i.e., $\mu_{RQ} \leq 1$ – the system is in the elastic state,
- if $\delta y \leq \delta_{RQ} \leq \delta u$, i.e., $\mu \geq \mu_{RQ} > 1$ - the system is in the nonlinear range,
- if $\delta_{RQ} > \delta u$, i.e., $\mu_{RQ} > \mu$ - the system experiences deep nonlinearity and possible failure.

A nonlinear time-history analysis has been performed for the structure according to the described procedure and applying selected earthquakes (Section 2.1) with gradual increase of the intensity, (0.24g, 0.27g, 0.30g, 0.33g and 0.36g). Fig.11 illustrates storey displacements required by the earthquakes with selected intensity of 0.30g (design earthquake) and 0.36g (maximum expected earthquake), compared to the capacity displacement in points "Y" and "U". Ductility capacity of the ground floor level versus ductility demand for each of the earthquakes is presented on Fig. 12.

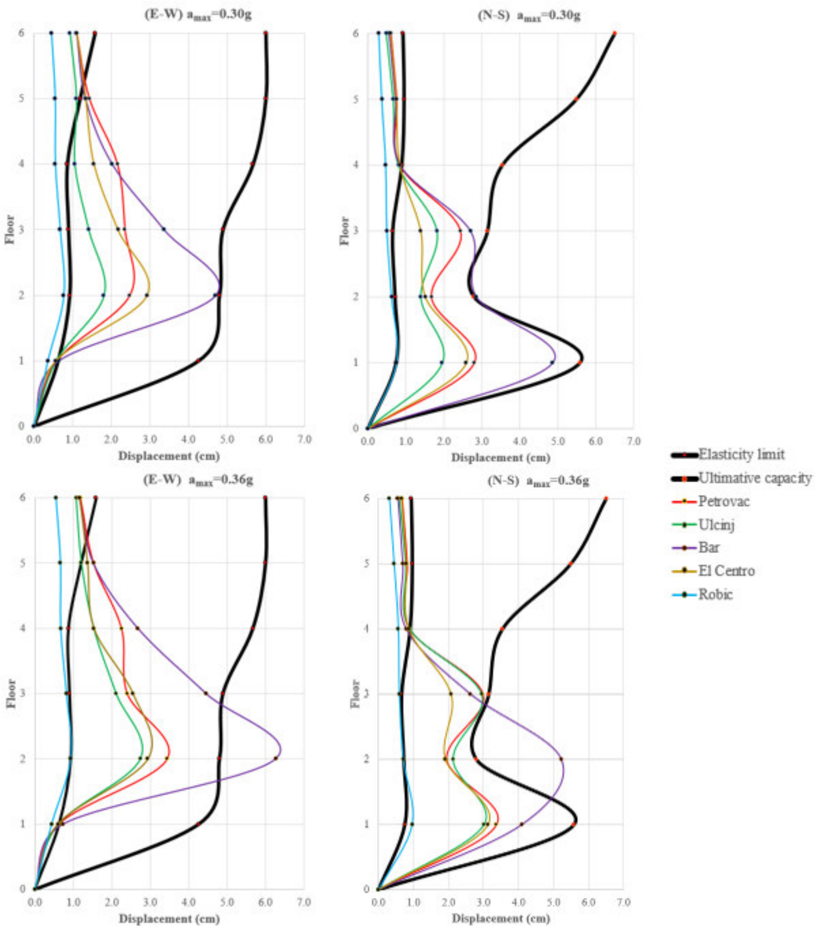

Fig. 11 Comparison of required displacements with deformation capacity for longitudinal (E-W) direction (left) and transverse (N-W) direction (right).

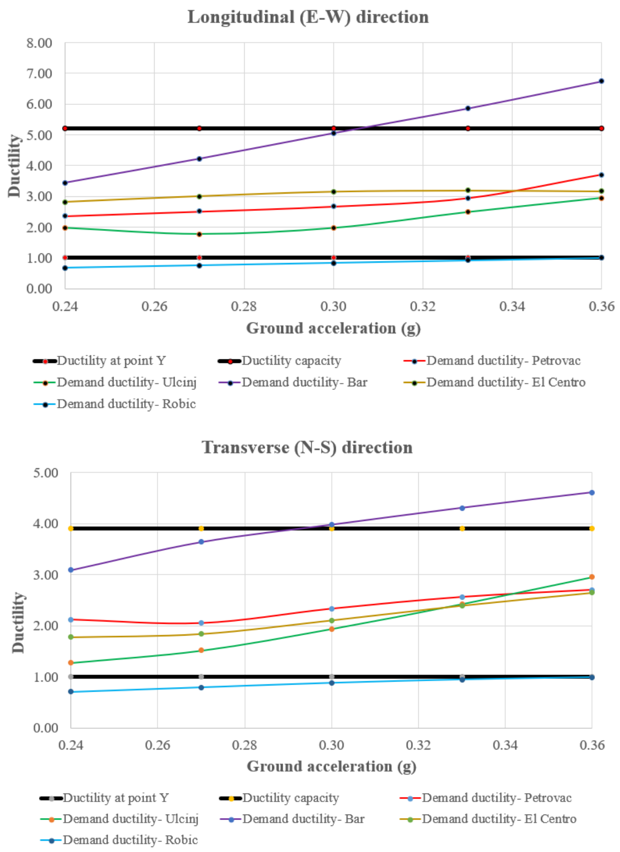

Fig. 12 Comparison of demand ductility to ductility capacity for ground floor for longitudinal (E-W) direction (top) and transverse (N-S) direction (bottom).

3.4. SUMMARY ON THE STRUCTURAL STABILITY AND SAFETY

As a result of the overall investigations and analyses shown in the previous Sections, it can be concluded that the structural system was originally designed for gravitational and seismic actions, (according to the seismic code at the time of design) and was built and maintained with high quality.

However, it does not satisfy completely the requirements according to the current seismic code in the country PIOVS'81 and the new requirements according to the standard TIA-942-A - TIER III. This is primarily due to the additional criteria related to the importance class of the building and rules for reinforcing detailing of the load-bearing elements to avoid brittle failure during seismic actions.

The vertical load-bearing elements (columns and shear walls) possess the necessary bearing capacity for seismic actions defined according to PIOVS'81, (Fig. 10), however the time-history analysis shows that the ground floor does not have sufficient deformation capacity and ductility for maximum expected earthquake actions (Figs. 10 and 11). Also, the horizontal RC elements on 3rd and 4th floor have not enough bearing capacity due to additional exploitation loads according to TIER III.

Finally, according to the structural analysis results, there is a need for global and local strengthening of the building's structure to satisfy completely the current seismic code PIOVS'81 and the specific TIER III criteria.

4. PRELIMINARY SOLUTION FOR SEISMIC RETROFITTING OF THE EXISTING STRUCTURE

The proposed solution for seismic retrofitting, based on building's specifics and the conditions for execution, consists of:

[1] Strengthening of the reinforced concrete slab on the third and fourth floor due to the additional imposed load, according to TIA-942-A - TIER III standard. It anticipates new secondary steel beams, (Fig.13, left). The beam is formed by inserting steel profiles below and above the slab, interconnected one to another and coupled with the existing slab.

[2] Strengthening of the longitudinal main reinforced concrete beams on the third and fourth floor due to the additional imposed load, according to the TIA-942-A - TIER III standard. It anticipates inserting steel profiles to reach the required bending moment capacity in the midspan, (Fig.13, right).

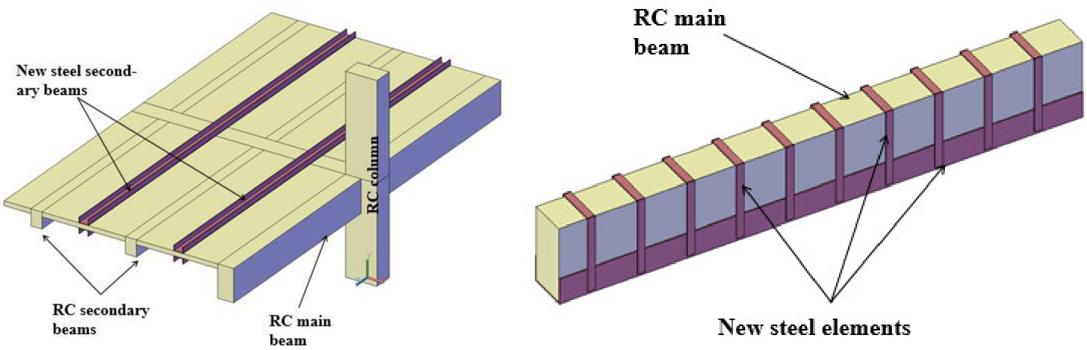

Fig. 13 Strengthening of the 3rd and 4th storey: slab (left) and main RC beam (right)

[3] Strengthening of reinforced concrete beam-column joints due to seismic action, which anticipates interconnected steel strips, mounted on the top and the bottom edge of the beam (Fig. 14).

[4] Strengthening of the reinforced concrete columns due to the additional imposed load and seismic action, which anticipates strapping with steel strips which are interconnected and connected to the strips on the strengthened beams, (Fig.14).

[5] Global strengthening of the structure for horizontal seismic action. Introducing additional reinforced concrete shear walls from the basement to the 2nd storey, on their own foundations, at locations where they will not interfere with the equipment and regular functioning of the facility, will reduce structural flexibility, and prevent non-structural damage due to the frequent earthquakes.

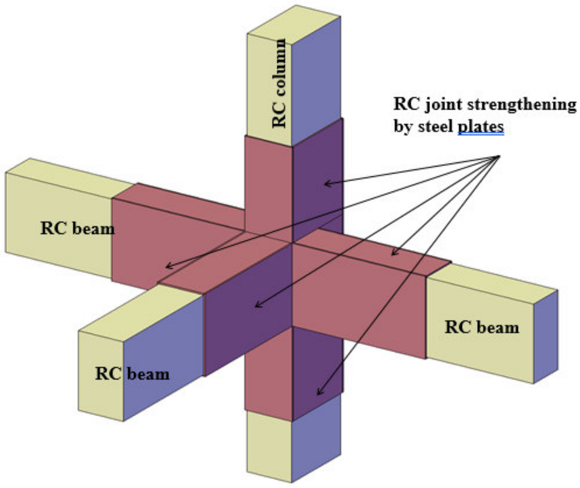

Fig. 14 Strengthening of RC columns, beams and joints.

5. CONCLUSIONS

Telecommunication Center facility in Skopje has existed for more than fifty years. Due to the requirement for eventual change of the building function, detail analysis of the stability and safety of the existing structural system has been carried out according to current seismic code and required technical standard TIA-942-A. The necessity for structural strengthening has been proved and the most appropriate technical solution for strengthening that satisfies the strength and deformability requirements has been proposed.

REFERENCES

[1] Telecommunications Industry Association, Standards and Technology Department, Telecommunications Infrastructure Standard for Data Centers, TIA-942-A, (Revision of TIA-942), August 2012.

[2] R. Apostolska, R., V. Shendova, G. Necevska-Cvetanovska, The need of integrated renovation of the existing buiding stock in North Macedonia, European Journal of Environmental and Civil Engineering, doi/full/10.1080/19648189.2020.1798816, 2020.

[3] Z. Bozinovski, V. Shendova, G Jekic, A. Zurovski, E. Delova, Analysis and cost estimation of the retrofitting of the existing structure TK-Center in Skopje, IZIIS Report 2018-24, 2018.

[4] Z. Bozinovski, V. Shendova, G. Jekik, A. Zlateski, A. Zurovski, E. Delova, Analysis of the existing structure of the building "Block" and "Tower" of the TK Center in Skopje, IZIIS Report 2019-64, 2019.

[5] Rulebook for the construction of buildings in seismic regions” - PIOVS’81, Official Gazette 31/81 of RM, 1981.

[6] G. Necevska Cvetanovska, R. Apostolska, Methodology for seismic assessment and retrofitting of RC building structures, Proc. of 15 World Conference on Earthquake Engineering, Lisboa, (Paper ID 2149),, 2012.

ESTIMATING CONCRETE QUANTITIES USING AI-BASED MODELS FOR RECYCLING AND REDUCING CO_2 EMISSIONS

Milena Senjak Pejić[1], Mirjana Terzić[1], Dragana Stanojević[1], Igor Peško[1], Maja Petrović[2], Mirna Kapetina[3], Vladimir Mučenski[1]

Summary:

The construction industry is responsible for a third of total greenhouse gas emissions. Carbon dioxide (CO_2) has the largest share in the global distribution of greenhouse gases, amounting to 76%. Annual concrete production is estimated at 12 billion tons, which results in large amounts of CO_2 emissions. The paper aims to estimate the amount of concrete from existing buildings that can be recycled and used as an aggregate while producing new carbon-negative concrete. In that way, it contributes to the reduction of carbon dioxide emissions, the planning of reducing the consumption of natural resources and the planning of waste management. Models based on machine learning (ML) and artificial neural networks (ANN) were formed and compared. The ANN model achieved an accuracy of 90%, while the Huber Regressor, as the optimal algorithm, achieved an estimation accuracy of 93%.

Key words: artificial intelligence, carbon emissions, recycled concrete, construction industry.

[1] University of Novi Sad, Faculty of Technical Sciences, Department of Civil Engineering and Geodesy, Novi Sad, Serbia
[2] University of Novi Sad, Faculty of Technical Sciences, Department of Environmental Engineering, Novi Sad, Serbia
[3] University of Novi Sad, Faculty of Technical Sciences, Department of Computing and Control Engineering, Novi Sad, Serbia

1. INTRODUCTION

In the context of the green agenda, addressing global warming has emerged as an urgent priority for the entire global population. Carbon dioxide (CO_2), nitrous oxide, fluorinated gases, and methane are emitted daily and contribute to the greenhouse effect. According to the 2014 report from The Intergovernmental Panel on Climate Change [1], global carbon dioxide emissions account for over 75% of the total.

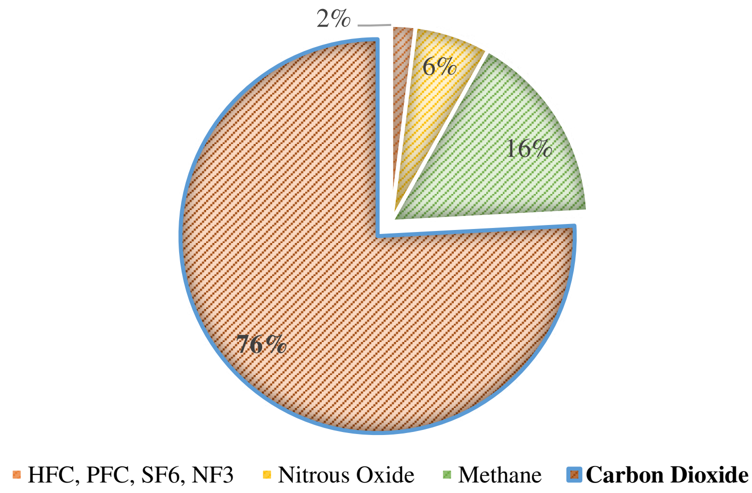

Fig. 1 Global distribution of greenhouse emissions [1]

Figure 1 shows the global distribution of greenhouse gases, indicating that emissions of all other greenhouse gases constitute one-quarter of the total, while carbon dioxide is responsible for the remainder. Given the significant role of CO_2 emissions in global warming, it is considered one of the foremost environmental protection priorities [2].
There are two types of carbon dioxide emissions: embodied carbon and operational carbon. Embodied carbon represents carbon emissions that are generated in the stages of extraction of raw materials, production and installation of materials, transportation, renovation activities, or removal of buildings [3], [4], [5], [6]. Operational carbon represents the emissions generated due to the exploitation of the facility during maintenance, lighting, air conditioning, and ventilation [4], [6]. In concrete construction, embodied carbon is a crucial consideration. Numerous studies indicate that the construction sector plays a significant role in managing and reducing carbon dioxide emissions during construction activities [7].
Concrete production is responsible for 7-8% of the total greenhouse gas emissions [8]. Presently, concrete production is estimated to be around 12 billion tons per year [9], whereas cement production between 2013 and 2022 exceeded 4 billion tons per year [10]. These statistics underscore the significant potential for emissions reduction in the concrete production sector.
Chen et al. [11] replaced aggregate in concrete with biochar, a carbon-based material obtained from waste, and were able to sequester 59 kg of CO_2 per ton of concrete. Their innovative approach resulted in a negative carbon footprint, as they sequestered a greater amount of CO_2 compared to the emissions generated during production. Unlike natural aggregate, recycled concrete has lower strength. However, it contains cement mortar rich in calcium hydroxide and calcium silica hydrate.
This composition presents a potential source of calcium that enables CO_2 sequestration, leading to the formation of the termodynamically stable carbonate minerals [12]. Current studies mostly focus on the "low carbon" concept to achieve "carbon neutrality". Researchers have discovered that it is possible to produce concrete that absorbs more carbon dioxide than it emits, resulting in the production of carbon-negative concrete. This accomplishment significantly advances progress towards

achieving the objective of "carbon neutrality" compared to the concept of low-carbon building. Numerous buildings lack electronic project records and are stored away in archives, making it impossible to access information regarding the quantities of materials used. The objective of this research is to assess the concrete volume within existing structures for the purpose of recycling and generating carbon-negative concrete.

2. RECYCLED CARBON-NEGATIVE CONCRETE

The total concrete mass consists of 11% cement, 67% aggregate, 16% water and 6% air [13]. Van der Zee and Zeman proposed a procedure for recovering cement from waste concrete by mineral carbonation. Concrete waste is crushed, and then, with the help of hydrochloric acid (HCl), calcium is separated with impurities. Through the application of the pH swing method, specific impurities are eliminated. Subsequently, a chemical reaction with a sodium carbonate solution (Na_2CO_3) results in the formation of calcium carbonate ($CaCO_3$) or precipitated calcium carbonate (PCC).The subsequent steps involve the processing of sodium chloride (NaCl), which is further separated into HCl and NaOH through electrodialysis. The HCl solution is then recycled in a new process designed for leaching calcium from waste concrete. Meanwhile, the NaOH is exposed to gaseous CO_2 to produce Na_2CO_3. During the formation of precipitated calcium carbonate (PCC) in the form of $CaCO_3$, CO_2 is permanently sequestered rather than remaining in the atmosphere [13].

The researchers experimentally confirmed that this method effectively sequesters more CO_2 within the concrete than is emitted during the entire process, thereby achieving the production of carbon-negative concrete. The treatment of concrete waste in this manner also enables the separation of sand, which can be subsequently utilized as an aggregate. Essentially, this approach allows for the complete elimination of physical waste.

2.1. AGGREGATE FOR CARBON-NEGATIVE CONCRETE

Due to its high porosity, concrete has the capacity to absorb CO_2 through a process known as carbon dioxide mineralization, wherein CO_2 is trapped within the rocks as a solid mineral. Carbon mineralization is considered a promising solution due to its inherent ability to sequester CO_2 without the need for additional energy input during the capture process. Crucially, research has demonstrated that the carbon dioxide mineralization of waste concrete aggregate can result in the creation of new concrete possessing enhanced physical and mechanical properties, including increased compressive strength. Approaches of this kind have numerous advantages:

- if the compressive strength of concrete increases, it is possible to reduce the proportion of cement, which certainly affects the reduction of cement manufacturing and CO_2 emissions,
- new concrete is used to store CO_2 permanently. On the other hand, that CO_2 would be emitted into the atmosphere [14],
- large quantities of concrete from the removed structures will not be disposed of in landfills but will end up in recycling plants,
- the amount of extraction of natural raw materials would be reduced, which is certainly already too little.

In order to evaluate the recycling capacities and facilitate the planning of new concrete production capable of sequestering more CO2 than it emits, an artificial intelligence-based model is being developed.

3. ARTIFICIAL INTELLIGENCE

John McCarthy defined the term "artificial intelligence" back in 1955, and it represents a type of technology that can imitate human intelligence. It involves building a machine

or program designed to process data for learning and making intelligent decisions enabling them to take predictive actions in pursuit of a specific objective. AI combines multiple technologies, such as machine learning, neural networks, deep learning, natural language processing, inference algorithms, and computer vision [15].
One of the three key drivers of AI is the availability of data. The performance of the model, specifically its accuracy, depends on the availability and amount of data. The greater the number of samples available for processing, the higher the expectation of improved generalization and inference-making capabilities.

3.1. DATABASE DESCRIPTION

The data set used to estimate the amount of material based on the building's structure consists of 100 samples, each with nine characteristics. This set includes numerical attributes (amount of material, area and height of the building, grids of columns, etc.) as well as categorical variables (complexity of building, type of floor structure and type of support floor structure). The structure of the database is shown in Table 1.
The data was extracted from projects for building permits on the territory of Novi Sad. Only buildings with a skeletal structural system, which is the most common system in Novi Sad, were considered.

Tab. 1 The structure of the database of input and output data of the AI model

Complexity of building	Total gross area [m^2]	Average gross floor area [m^2]	Building height [m]	Number of stiffening	Transverse and longitudinal disposition [m]	Type of floor structure	Type of supporting floor structure	Quantity of concrete [m^3]
Simple (1)	1000 – 9500	200 – 2000	13 -27	0 – 13	2 – 7	Full RC slab (1)	Direct support (1)	420 – 4500
Medium complex (2)						Semi-prefabricated ceiling type “Fert" (2)	Girder support (2)	
Complex (3)								

Construction complexity is divided into three categories. The first category is simple and implies a rectangular base shape without floor changes. The second category is a medium-sized complex with an "L"-shaped base and small changes per floor. The third category is a complex with an "H"-shaped base, i.e. a loose base with larger changes per floor. As the goal is to calculate material quantities based on readily available features of the object when the design is not available, the areas for analysis in the database are net areas. The height of the object is is determined by measuring the height from the elevation of the terrain to the ridge, which represents the highest point of the object.The number of reinforced concrete walls for stiffening buildings is important because it directly affects the amount of concrete and represents the number of walls within one floor. The transverse and longitudinal spans of the columns affect the dimensions and number of supporting elements and, thus, the amount of material. The two types of floor constructions in the observed buildings are semi-prefabricated FERT type construction and monolithic reinforced concrete construction. The foundation includes two types of support: direct support on columns and linear support. If the direct support is on the columns, the beams are omitted as a transitional linear element, which indicates a smaller amount of material.

Before modelling, a systematic approach to data processing was applied, including cleaning, scaling, and outlier handling. Due to the limited number of samples, feature selection and dimensionality reduction were considered the most important steps. Feature selection was performed using correlation matrices and analytical techniques to identify and retain the most influential features while eliminating redundancy.
The input data, which includes the characteristics of the object, were selected to effectively describe the volume of the object, recognizing that alterations to these characteristics have a direct influence on the quantity of material required. In addition to the domain of professional knowledge upon which the input data was selected, the sensitivity of the input and output variables was assessed. This involved calculating the correlation matrix.

3.2. CORRELATION

Correlation is a statistical method used to assess the direction and strength of influence between two variables. The influence of two variables is measured by the correlation coefficient, which ranges from 1 to -1, where these threshold values indicate a perfect correlation. The value of the correlation factor -1 indicates a strong negative correlation, which means that if one variable's value increases, the other's value decreases. The value of the correlation factor 1 indicates a strong positive correlation, which means that if one variable's value increases, the other's value also increases. If the correlation factor equals 0, it indicates no correlation between the two observed variables [16].

3.2.1. Correlation coefficients

Spearman's rank correlation coefficient is used when the data does not have a normal distribution, nor is there necessarily a linear relationship between the two variables. Also, the data distribution is monotonic [17].
By checking the data distribution, it was observed that not all features have a normal data distribution. The data distribution is monotonic, so it was decided to use Sperman's correlation coefficient. Spearman's coefficient is calculated according to the formula:

$$r_s = 1 - \frac{6\sum d_i^2}{N(N^2-1)} \quad (1)$$

where d is the difference in the rank values of the two observed variables, and N is the total number of samples.
Guidelines for interpreting the magnitude of the correlation of variables are provided by Xiao et al. [17] as follows:

Value of *r*	Strength of relationship
-1.0 to -0.5 or 0.5 to 1.0	Strong
-0.5 to -0.3 or 0.3 to 0.5	Moderate
-0.3 to -0.1 or 0.1 to 0.3	Weak
-0.1 to 0.1	None or very weak

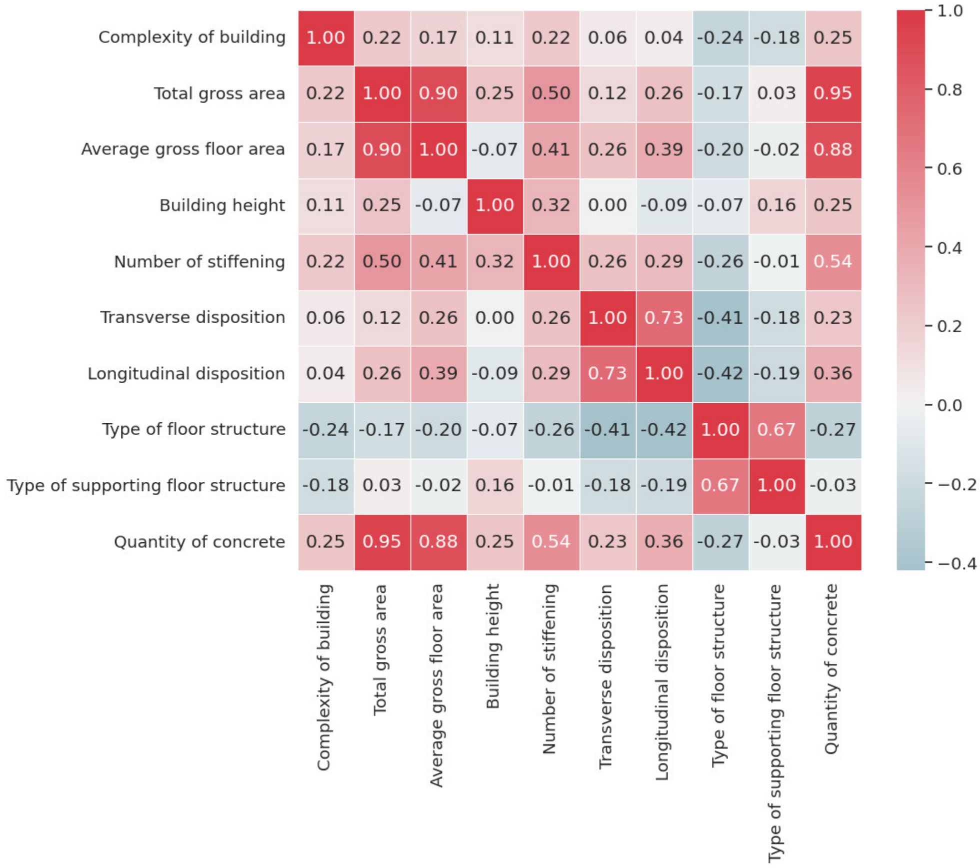

Fig. 2 Spearman correlation matrix for the existing database

Correlation matrices for the existing dataset were computed using Python packages, and the results were visualized in Figure 2. Upon analysing the obtained data, it was discerned that features total gross area, average gross floor area, and number of stiffening exhibited the highest absolute correlation values with the quantity of concrete. Consequently, these features were judiciously selected for further use as inputs for the machine learning mode.

4. ML-BASED PREDICTION MODEL

Machine learning-based prediction models are built in the Python programming language. Python is open source, allowing people to build small programs they can easily share. Thanks to the large developer base and the characteristics of the open-source model, Python has a rich library of modules for solving various tasks of numerous engineering problems [18].

Various model types and architectures, including Artificial Neural Networks (ANN) and various regression models, were meticulously trained and evaluated to obtain the best model. This comprehensive exploration aimed to uncover the most suitable model for accurately predicting material quantities.

The ANN models were constructed using popular deep learning frameworks such as TensorFlow and PyTorch, harnessing their powerful capabilities for complex pattern recognition and prediction tasks and other models the ML model was obtained using the PyCaret library, facilitating the streamlined experimentation and evaluation of various algorithms and configurations.

4.1. ANN MODEL

During model building, the database is divided into two sets. The dataset was then divided into training (80%), validation (10%), and test (10%) sets, using five-fold cross-validation to gauge model performance.

During the building of the ANN assessment model, to achieve the highest level of generalization, the foundational database was utilized in three distinct ways:

- A raw database with raw qualitative data (DB.1),
- Raw database where qualitative data has been converted into numerical data using the method of ordinal numbers (DB.2),
- The database which contains input data selected based on correlation analysis (DB. 3). This database contained input data: Total Gross Area, Average Gross Area, Number of Stiffeners, Longitudinal Disposition, and Type of Floor Construction.

Also, the following hyperparameters were varied:

- the number of hidden layers,
- the number of neurons in hidden layers,
- the activation function of hidden and output layers,
- the number of epochs and
- learning step and batch size.

Building an ANN model is an iterative procedure of hyperparameter tuning. Table 2. shows the models and their hyperparameters. The models were compared according to Mean Absolute Percentage Error (MAPE). MAPE represents the average absolute value of the percentage difference between the actual and estimated model values. It is calculated using the formula:

$$MAPE = \frac{1}{n}\sum\left(\left| \frac{(actual\ value - estimated\ value)}{actual\ value} \right| \right) * 100 \qquad (2)$$

n – the number of samples.

The model M9 that makes the smallest MAPE (9.23%) when estimating the amount of concrete over the test data has five hidden layers, with 100 neurons per layer. The activation function in the hidden and output layers is the Exponential Linear Unit. The number of learning epochs is 1000, and the learning rate is 0.0002. Bach size is 5.

Tab. 2 Comparison of ANN models built in Python based on the MAPE parameter

Model	Input data	Number of hidden layers	Number of neurons in hidden layers	Activation function for hidden neurons	Activation function for output neurons	Number of epochs/learning rate	Bach size	MAPE
M1	DB.2	3	128-64-16	ReLU	Linear	300/0.0001	10	10.46%
M2	DB.2	3	100-20-5	ReLU	Linear	300/0.0001	10	10.45%
M3	DB.2	2	64-16	ELU	Linear	100/0.0001	3	10.49%
M4	DB.1	5	120 per layer	ELU	Linear	1000/0.0002	3	9.91%
M5	DB.1	5	100 per layer	ELU	Linear	1000/0.0002	3	9.59%
M6	DB.1	5	100 per layer	ReLU	Linear	1000/0.0002	3	9.67%
M7	DB.3	3	128-64-16	ReLU	Linear	100/0.0002	3	10.40%
M8	DB.3	5	128 per layer	ReLU	Linear	1000/0.0002	3	9.78%
M9	DB.3	5	100 per layer	ELU	Linear	1000/0.0002	5	9.23%
M10	DB.3	5	120 per layer	ELU	Linear	1500/0.0002	5	10.01%

A smaller number of hidden layers, as well as a small number of epochs, negatively affects the accuracy of the estimation model, i.e. the model is not able to learn enough. Increasing these hyperparameters ensured that the network was able to learn. Bach size

represents the number of samples from the training set processed in each epoch before updating the network weights. It was shown that a smaller value of bach size enables the model to generalize better.
The M10 model shows that when increasing the number of neurons per hidden layer and the number of epochs, the network may be overtrained, and the estimation error may increase. Overfitting of the ANN means that in the training and validation phase, the network adapted too much of the data from this set and lost the ability to make general conclusions. This leads to an increase in estimation error over new unseen data.
Activation functions like sigmoid, hyperbolic tangent and softmax were unsuitable for this problem. The estimation model with these activation functions adopted produced an estimation error of over 99%.

4.2. PYCARET'S REGRESSION MODELS

The database is divided into two sets. The set size for training and validation is 90% of the total data, while 10% is set aside for testing. The cross-validation method is also applied to the training and validation set.
After that, the models based on machine learning are compared based on the following parameters: Mean Absolute Error (MAE), Mean Squared Error (MSE), Root Mean Squared Error (RMSE), Coefficient of Determination (R2), Root Mean Squared Logarithmic Error (RMSLE) and mean absolute percentage error (MAPE). These parameters help when interpreting the performance model. A parameter for selecting the model during training and validation is MAPE.
Table 3. shows 19 machine learning algorithms and their comparison based on the mentioned six parameters for the database described in Chapter 3.1. The Huber Regressor produces the smallest mean absolute percentage error (MAPE) during estimation, thus establishing itself as the optimal model for further construction and performance evaluation on test data.

Tab. 3 A comparison of machine learning algorithms in Python based on six parameters

Model	MAE	MSE	RMSE	R2	RMS LE	MAP E
K Neighbors Regressor	197.44	71814.21	246.70	0.79	0.16	0.14
Random Forest Regressor	197.35	74152.47	251.80	0.77	0.16	0.13
Extra Trees Regressor	210.95	80892.94	264.74	0.76	0.17	0.14
AdaBoost Regressor	208.87	76229.54	260.91	0.76	0.17	0.15
Extreme Gradient Boosting	205.90	79859.22	267.98	0.74	0.17	0.14
Gradient Boosting Regressor	203.20	79548.55	270.03	0.74	0.16	0.13
Huber Regressor	175.45	74568.79	237.79	0.71	0.14	0.11
Orthogonal Matching Pursuit	201.47	82632.83	267.46	0.71	0.16	0.13
Bayesian Ridge	206.52	86537.05	274.13	0.70	0.16	0.13
Elastic Net	207.20	89954.32	274.26	0.70	0.17	0.13
Ridge Regression	217.92	97915.91	291.33	0.66	0.20	0.15
Lasso Regression	219.05	98337.84	292.26	0.66	0.20	0.15
Lasso Least Angle Regression	219.05	98338.15	292.26	0.66	0.20	0.15
Linear Regression	220.92	99452.04	294.25	0.66	0.20	0.15
Decision Tree Regressor	237.71	98818.10	298.67	0.64	0.20	0.17
Least Angle Regression	230.91	108394.99	310.20	0.62	0.22	0.16
Passive Aggressive Regressor	267.58	127287.43	343.88	0.51	0.21	0.18
Light Gradient Boosting Machine	311.28	185930.87	400.88	0.48	0.24	0.21
Dummy Regressor	582.68	593402.71	719.08	-0.59	0.49	0.49

Huber regression is a machine learning model for regression problems with little sensitivity to extreme values. This algorithm combines the advantages of the least squares method (MSE loss) and the absolute deviation method (MAE loss). The goal of this algorithm is to minimize the Huber loss function:

$$l\alpha\,(x) = \begin{cases} 2\alpha^{-1}|x| - \alpha^{-2} & if \;\; |x| > \alpha^{-1} \\ x^2 & if \;\; |x| \leq \alpha^{-1} \end{cases} \tag{3}$$

which is squaring for small values of x and linear for large values [19]. If only a quadratic loss function were used, the extreme values would be large due to squaring, while in the case of a linear loss function, the extreme values would be ignored, affecting the accuracy. The parameter α controls the transition point between these two functions.

After building the model, the hyperparameters are adjusted to achieve better model performance. After adjusting the model's hyperparameters, the MAPE over the test data was 7.31%.

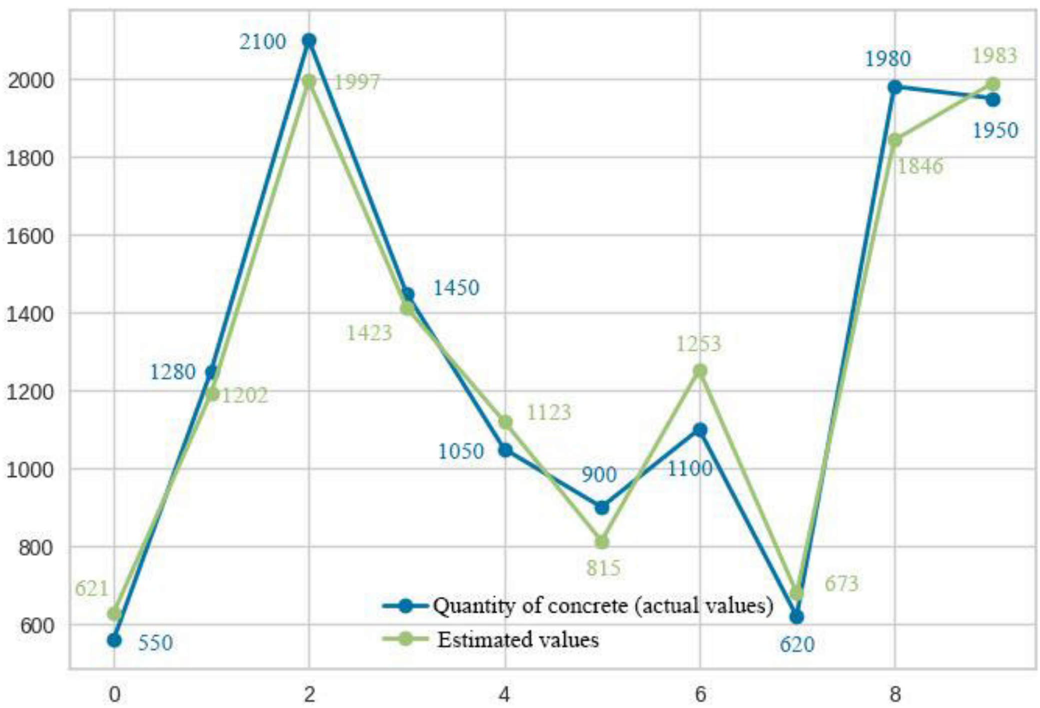

Fig. 3 The estimation error of the Huber regressor model for the amount of concrete – test data

Figure 3 shows a graph comparing the actual values of the amount of concrete with the estimated values of the adopted ML model. The values shown are above the test data.

5. CONCLUSION

Estimating the amount of concrete for recycling ensures material circularity, improves waste management practice, and resource planning. There is a need to demolish buildings that lack electronic project documentation, with many of these projects lost in archival storage. Consequently, determining the quantities of installed materials within these buildings is an insurmountable challenge. The production of carbon-negative concrete offers a means to mitigate CO_2 emissions by reducing the demand for cement production and permanently sequestering a greater quantity of CO_2 from the atmosphere than is emitted during its production. The significant advantages of utilizing recycled concrete as aggregates in the production of carbon-negative concrete are evident in the following:

- A decrease in the cement content, resulting in reduced overall cement production, which is responsible for approximately 7% of total CO_2 emissions;
- The permanent sequestration and storage of CO_2 within the new concrete;
- The utilization of waste concrete as a valuable resource, eliminating the need for landfill disposal;
- The reduction in the consumption and extraction of natural resources for concrete production.

AI-based models have demonstrated satisfactory accuracy in estimating concrete quantities. The ANN model achieved an estimation accuracy of 91%, while the Huber Regressor achieved an accuracy of almost 93%. The comparison of these models and the assessment of their performance were carried out using the mean absolute percentage error (MAPE), revealing that the Huber regressor machine learning algorithm outperformed other models for this specific problem. During the construction of the ANN model, a rigorous iterative process was undertaken, involving more than 35 iterations and the selection of 10 models to showcase the influence of changing hyperparameters on estimation accuracy. The highest-performing ANN model featured 5 hidden layers, each with 100 neurons, and employed Exponential Linear Unit (ELU) activation functions.

Furthermore, the reduction in database dimensionality, based on correlation factors, had a positive impact on the model's accuracy. Notably, the input data related to Total Gross Area, Average Gross Area, Number of Stiffeners, Longitudinal Disposition, and Type of Floor Construction were identified as the most influential factors contributing to estimation accuracy.

It's crucial to emphasize that the accuracy of the data within the database plays a pivotal role in shaping the model's performance. Structuring the database according to preliminary measurements from the BIM model, rather than relying on electronic project documentation, would enhance model reliability while minimizing the potential for human error.

Further research would focus on evaluating other building materials and examine emissions associated with their recycling.

ACKNOWLEDGEMENT

This research (paper) has been supported by the Ministry of Science, Technological Development and Innovation through project no. 451-03-47/2023-01/200156 “Innovative scientific and artistic research from the FTS (activity) domain”.

REFERENCES

[1] IPCC, 2014: Climate Change 2014: Mitigation of Climate Change. Contribution of Working Group III to the Fifth Assessment Report of the Intergovernmental Panel on Climate Change [Edenhofer, O., R. Pichs-Madruga, Y. Sokona, E. Farahani, S. Kadner, K. Seyboth, A. Adler, I. Baum, S. Brunner, P. Eickemeier, B. Kriemann, J. Savolainen, S. Schlömer, C. von Stechow, T. Zwickel and J.C. Minx (eds.)]. Cambridge University Press, Cambridge, United Kingdom and New York, NY, USA.

[2] Farahzadi, L., & Kioumarsi, M. (2023). Application of machine learning initiatives and intelligent perspectives for CO_2 emissions reduction in construction. Journal of Cleaner Production, 384, 135504. https://doi.org/10.1016/j.jclepro.2022.135504

[3] Chen, T. Y., Burnett, J., & Chau, C. K. (2001). Analysis of embodied energy use in the residential building of Hong Kong. Energy, 26(4), 323–340. https://doi.org/10.1016/s0360-5442(01)00006-8

[4] Ding, G. K. C. (2018). Embodied Carbon in Construction, Maintenance and Demolition in Buildings. Embodied Carbon in Buildings, 217–245. https://doi.org/10.1007/978-3-319-72796-7_10

[5] Teng, Y., Li, K., Pan, W., & Ng, T. (2018). Reducing building life cycle carbon emissions through prefabrication: Evidence from and gaps in empirical studies. Building and Environment, 132, 125–136. https://doi.org/10.1016/j.buildenv.2018.01.026

[6] Rodrigo, M.N.N., Perera, S., Senaratne, S., Jin, X. (2019). Embodied Carbon Mitigation Strategies in the Construction Industry. CIB World Building Congress 2019, Hong Kong SAR, China, 17 – 21 June 2019.

[7] Hu, X., Si, T., & Liu, C. (2017). Total factor carbon emission performance measurement and development. Journal of Cleaner Production, 142, 2804–2815. https://doi.org/10.1016/j.jclepro.2016.10.188

[8] IEA. Technology Roadmap - Low-Carbon Transition in the Cement Industry.(2018). Accessed date 28.07.2023. at https://www.iea.org/reports/technology-roadmap-low-carbon-transition-in-the-cement-industry

[9] Center for Low Carbon Built Environment. CARBON SEQUESTRATION. Accessed date 27.07.2023. at https://lowcarbonfuture.umich.edu/carbon-negative-concrete/

[10] Statista. Cement production global 2022. Accessed date 27.07.2023. at https://www.statista.com/statistics/1087115/global-cement-production-volume/

[11] Chen, L., Zhang, Y., Wang, L., Ruan, S., Chen, J., Li, H., Yang, J., Mechtcherine, V., & Tsang, D. C. W. (2022). Biochar-augmented carbon-negative concrete. Chemical Engineering Journal, 431, 133946. https://doi.org/10.1016/j.cej.2021.133946

[12] Lu, B., Shi, C., Zheng, J., & Ling, T.-C. (2018). Carbon dioxide sequestration on recycled aggregates. Carbon Dioxide Sequestration in Cementitious Construction Materials, 247–277. https://doi.org/10.1016/b978-0-08-102444-7.00011-3

[13] Van der Zee, S., & Zeman, F. (2016). Production of carbon negative precipitated calcium carbonate from waste concrete. The Canadian Journal of Chemical Engineering, 94(11), 2153–2159. Portico. https://doi.org/10.1002/cjce.22619

[14] Rosa, L., Becattini, V., Gabrielli, P., Andreotti, A., & Mazzotti, M. (2022). Carbon dioxide mineralization in recycled concrete aggregates can contribute immediately to carbon-neutrality. Resources, Conservation and Recycling, 184, 106436. https://doi.org/10.1016/j.resconrec.2022.106436

[15] L. Patel. (2020). LEAN AI. How Innovative Startups Use Artificial Intelligence to Grow. 1st ed., O'Reilly Media, United States, America.

[16] Swinscow TDV. (1997). Statistics at Square One. Nineth Edition, Copyright BMJ Publishing Group, University of Southampton.

[17] Xiao, C., Ye, J., Esteves, R. M., Rong, C. (2015). Using Spearman's correlation coefficients for exploratory data analysis on big dataset. Concurrency Computation: Practical Experience, 28(14), 3866-3878. doi: 10.1002/cpe.3745

[18] Nagar, S. (2017). Introduction to Python for Engineers and Scientists, Copyright by Sandeep Nagar, Apress, New York, USA.

[19] Fan, J., Li, Q., & Wang, Y. (2016). Estimation of High Dimensional Mean Regression in the Absence of Symmetry and Light Tail Assumptions. Journal of the Royal Statistical Society Series B: Statistical Methodology, 79(1), 247–265. https://doi.org/10.1111/rssb.12166

AN APPROACH FOR RAILWAY PROJECT MANAGEMENT

Zlatko Zafirovski[1], Ivona Nedevska[2], Vasko Gacevski[3], Riste Ristov[4], Slobodan Ognjenovic[5], Marijana Lazarevska[6], Saso Kostadinovski[7]

Summary:

This paper aims to solve this problem, which has recently become more common in railway projects. The key is in a planned approach and organization from the beginning of the project, which the candidate considers by elaborating a Methodology for the construction of the site in the form of a document. This methodology solves all the above and helps lead the project from its beginning to the end with a positive result. The scope of the methodology for the construction of a facility includes several scientific disciplines directly related to the realization of the facility, such as law, economics, ecology, quality management, construction, etc. Therefore, it should cover all matters in these areas and provide solutions and courses of action at the beginning and in the development phase of the site to adapt to possible needs and to be finalized. The conclusion is that the application of such a Methodology for the construction of the site is necessary, or it could be freely said that it is mandatory.

Key words: methodology, fidic, railway projects, quality management

[1] Associate Professor, Ss. Cyril and Methodius University in Skopje, Faculty of Civil Engineering, N. Macedonia, , zafirovski@gf.ukim.edu.mk
[2] Assistant, Ss. Cyril and Methodius University in Skopje, Faculty of Civil Engineering, N. Macedonia, nedevska@gf.ukim.edu.mk
[3] Assistant, Ss. Cyril and Methodius University in Skopje, Faculty of Civil Engineering, N. Macedonia, gacevski@gf.ukim.edu.mk
[4] Assistant, Ss. Cyril and Methodius University in Skopje, Faculty of Civil Engineering, N. Macedonia, ristov@gf.ukim.edu.mk
[5] Associate Professor, Ss. Cyril and Methodius University in Skopje, Faculty of Civil Engineering, N. Macedonia, ognjenovic@gf.ukim.edu.mk
[6] Associate Professor, Ss. Cyril and Methodius University in Skopje, Faculty of Civil Engineering, N. Macedonia, marijana@gf.ukim.edu.mk
[7] Civil engineer, POOR Macedonia, sk2408967@gmail.com

1. INTRODUCTION

For obtaining larger projects that are financed by various financial institutions and funds and which are almost regularly realized according to the rules of FIDIC Con-tracts, candidates are usually larger international companies or consortia formed specifically for the fulfilment of the project in question.
In addition to the basic rules of the FIDIC Agreements that provide correct relations, Investors, to protect their interests and the interests of the state, supplement the Agreements by using the section of Particular FIDIC conditions and setting specific requirements with which usually the entire (or almost all) the risk is transferred to the Contractor. Bidding companies cannot influence this, and their only option is to accept the proposed Contracts in the tender procedures as they are. The proposed Con-tracts in the tender documents are not usually "favoured" by the future Contractor.
The most important aspects of this topic are:

- the methodology is not just a document. It is a fundamental base that will al-low achieving a positive (or expected) financial result at the end of the project,
- the building is being built within the planned construction period,
- construction quality is achieved,
- the reputation of the Contractor is protected and increased,
- the Contractor company's rights are protected in future disputes between the two parties to the Agreement.

The methodology achieves proper organization and work guidelines and guarantees the facility's construction following the rules of the Agreement signed by both parties.

2. OBJECTIVES OF THE METHODOLOGY

The methodology will locate all potential problems and risks that can lead to the extension of construction deadlines and cause a negative financial result for the project.
The methodology itself will list all expected possible aspects and needs necessary to be considered, planned, prevented, and realized as part of such a methodology, with the aim of successful implementation of the project and a positive result. In addition, the method should provide preventive actions and measures to avoid (or minimize) all problems and risks.
The methodology is a sublimation of knowledge from many areas, planning, and management at the highest expert and scientific level. It unites construction, electrici-ty, contact network, signaling, telecommunications, railway construction, law, finance, quality systems, FIDIC, etc.). The methodology coordinates and implements: management of complex processes, knowledge from different fields of science (con-struction, law, finance, etc.), experts from various fields, design with actual performance, work with human resources, coordinating and harmonizing with public services, associations and citizens, ecology, and protection of the human environment, safety at work, correct organization of construction, etc.
Railway projects are specific, as they require specialized equipment, machinery, and personnel. There are almost no such capacities in the area of the Balkans. There are some remnants of the old socialist companies that are in the process of collapse, or individuals have appeared who do not have any resources but present themselves as executors for the upper management or a contact network.
A general finding in railway projects is that the Contractor firms were much more successful than the Contractor-Consortiums. Also, Contractors who did some plan-ning at the very beginning and followed through on the project realized better results than those who had no conception.
In our country, the following FIDIC projects have been worked on before:

Tab. 1 Project in Republic of North Macedonia

Project	**Contractor**	**Deadline (months)**	**Total working time (months)**	**Status**	**Results**
Tabanovce-Kumanovo Miravci-Smokvitsa	*JV "Alpine&WIEBE"*	12	24	Completed	Negative
Nogaevci-Negotino	*"SK 13 Holding JSC"*	12	36	Not finished	Negative
Bitola-Kremenica 1	*JV "Bitola - Kremenica"*	18	15	Not finished	Negative
Bitola-Kremenica 2	"STRABAG AG"	18	18	Completed	Positive
Kumanovo-Beljakovce	*"WIEBE GMBH"*	32	60	Discontinued project	Negative

There is a similar analysis for neighboring countries:

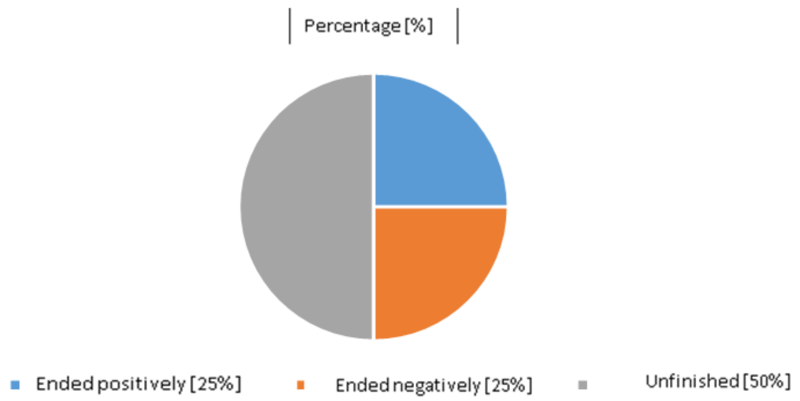

Fig. 1 Success rate of projects in neighboring countries

3. METHODOLOGY FOR THE CONSTRUCTION OF RAILWAY PROJECTS UNDER FIDIC AGREEMENT

Paper should The Project Manager is directly responsible for preparing and implementing the methodology. He is appointed by the company that performs the building. He makes the Preliminary Methodology for construction together with the Preliminary Project team formed by the primary heads of various departments, such as the Technical Head, Financial Head, Legal Head, Quality Head, FIDIC Head, and Program Engineer, as well as persons responsible for Occupational Safety, Human resources and for the protection of the human environment.

Its further elaboration and detailing until finalization, as well as all additional primary documents of the project, are produced under the control of the managers mentioned above.

For the entire time, the overall work for the full development and detailing of the plan is under the coordination and constant supervision of the Project Manager.

With the Construction Methodology, all crucial aspects of the project should be touched upon and solved: project team, documents required for contracts according to Fidic rules, quality management, the legal aspect, the economic-financial aspect, and the construction-operational part.

The project team is the one who manages the project for the entire period of project implementation. At the very beginning, the so-called Preliminary Project Team was formed by the fundamental managers of various sectors. These include the Project Team, managing it, and supplementing it as needed. Around the Project Team, the following stages should be completed: Preliminary Project Team, managers and their tasks, Formation of a complete Project Team, and Logistics of the Project Team.

Documents required for Contracts according to FIDIC rules are the following: Preliminary working program, Working Technology, Employer's mistake report, Quality system management plan (Quality plan), Protection and Safety plan, Environment protection plan, and Risk plan for project implementation.

The first task of the Quality Manager is to deliver the Quality Management Plan. Project management depends on the prompt and quality application of the quality management plan. To apply the quality plan, it is necessary to work according to the following activities: Quality Management Service, Application of ISO standards-QMS plan, Project documentation, Trials and tests, Safety and security at work, Environmental protection and Ecology. By fulfilling them, the project will be able to guarantee quality in all areas of the project.

When you have officially received a notification that the project has been received and you are invited to sign an Agreement and its implementation should begin, it is very important to analyze the construction contract. The legal part of the project covers the following aspects: Legal services for monitoring the project, the construction contract analysis, and the possibilities from FIDIC.

The analysis of the Construction Contract from the point of view of local legislation and the point of view of FIDIC, the rules of the Contract are very important for the final realization of the project because it often happens after the completion of the project that the Contractor starts a procedure before the court of the country in question or before the Assessment Board of disputes under FIDIC rules (Dispute Adjudication Board-DAB).

Upon receiving the project and starting its realization, it is necessary to immediately approach the review of the project from an economic-financial aspect. Therefore, it is required to make the essential analyzes and documents as follows: Economic service for monitoring the project, Analysis of the offer and price, Creating a plan for financing the project - Cash flow plan, Risk-chance table, Creating a functional calculation.

The economic and financial documents start working immediately after the formation of the Preliminary Team for the implementation of the project. After the analysis made by the technical manager and the legal service, the table for risks and chances is made (Risk-chance table).

Construction-operational part of the project

Since it is a construction project, as a rule, it is the essential part of the methodology for the realization of the project and the region by which the entire organization and technology of the project are made. Therefore, it should define everything that will guarantee a quick, efficient, high-quality, and timely realization of the project. Only some things that would violate the planned construction deadline must be allowed - all possible documents and plans for the completion and finalization of the project are based on it.

It is necessary to uncompromisingly: penetrate the technical regulations of the country in which the work is carried out, ensure all the required certifications of personnel and machines, plan the construction technology that is most suitable for the project, prepare a sufficient number of mechanization, plus spare engines, plan the maintenance system and repairs of the machines, provide adequate personnel (technical and working), carry out with their capacities the main parts of the projects that lead the project (for example, if it is a railway project, the upper system dictates the project), makes a careful selection of local Subcontractors with constant control over their work.

The parts that need to be planned and implemented are the following: Construction site organization, Work technology, Work program, Personnel, and Mechanization.

Correct solutions for the points mentioned above will guarantee the project's successful realization. In general, for each topic, we will list introductory provisions that should be paid attention to during the development of the construction-operational part of the project.

4. CONSTRUCTION-OPERATIVE SECTION BY EXAMPLE OF ONE PROJECT

4.1. CONSTRUCTION SITE ORGANIZATION

The right solutions will guarantee the successful realization of the project. In general, for each point, we will list introductory provisions that should be paid attention to during the development of the construction-operational part of the project.
The project's very opening starts with the construction site's organization and preparation for work. It is necessary to complete the following tasks in a concise period of time:

- Office space;
- Landfills and warehouses for old and new materials;
- Places for parking railway and construction machinery;
- Access roads to the facility;
- Field laboratory;
- Point for medical assistance;
- Transportation of machinery.

4.2. TECHNOLOGY FOR PROJECT WORK

Work technology defines:

- Scope of work,
- Basic technology for various types of project work,
- Phases for working on the project.

4.3. WORK PROGRAM

The working program is made in a suitable program, usually MS Project. This document is the subject of development based on long-established and approved work technology. In the beginning, it is a Preliminary work program. Still, after that, it should become an accurate and detailed work program that defines the time for the construction of the project, as well as the necessary resources.

4.4. PERSONNEL

The project staff is composed of the following:

- Project team,
- Personnel for work on the upper system,
- Personnel responsible for maneuvers and traffic within the project,
- Personnel for work on the lower system,
- Staff for working on a contact network,
- Signaling staff,
- Staff for building work,
- Personnel for construction work (bridges, culverts, overpasses, underpasses, etc.),
- Personnel for work on various types of cuts (water supply, sewerage, heating, etc.),
- Personnel for work on electrical and telecommunications cuts,
- Staff for working with metal structures (pedestrian overpasses).

The Work Program generally defines the number of staff. However, it varies and is in proportion to the starting job positions. Specific personnel should constantly be present at the building (superstructure, KM, and signaling) to fulfill the tasks and be able to intervene in all kinds of situations. The rest of the staff are tied to work-by-work phases.

4.5. CONSTRUCTION MACHINES

As well as the Personnel, the Work Program also defines the necessary machines for project construction. They are also divided into specific and classic mechanization. Specific machines are part of the teams to fulfill components such as the upper system, KM, and signaling.
This project requires the following:

- Mechanism for the upper system,
- Mechanism for KM,
- Signaling mechanism,

Classic construction machinery.

Fig. 2 Special excavators for the dismantling of rail fields

Fig. 3 Plasser und Theurer 08-32U

Fig. 4 GEISMAR PTH 350

5. CONCLUSION

The railway project management methodology provides results so that the project has:

- Positive financial results,
- Ensures timely completion of the project,
- Ensures high-quality construction,
- Preserves and improves the reputation of the Contractor company.

Also, the Methodology for managing a railway project can be considered a scientific paper that enables the successful realization of the project and a positive result. It acts preventively and minimizes all project risks.

Methodology for the management of a railway project is a sublimation of planning and management at an expert and scientific level, which unites knowledge from the fields of various sciences (railway construction, quality management, law, finance, ecology, human resources, safety at work, etc.). Preparatory work, proper planning, prevention, and, if possible, complete elimination of all objective and subjective risks are essential.

All this leads to the only recommendation that this paper sends, which is to develop a Methodology for managing a railway project at the very beginning of the project. It is the only guarantee for the successful realization of the project. In addition, it guarantees personal satisfaction and professional upgrading of all involved parties in a successfully realized project.

REFERENCES

[1] Clark, D., Toth, T., Dick, M., Maldonado, R.: V/TI Monitor Cluster Analysis and Implementation, AREMA 2015 annual conference & exposition, Minneapolis (USA), 2015.

[2] Esveld, C.: Modern Railway Track, Second Edition, MRTProductions, Zaltbommel, The Netherlands, 2001., ISBN 90- 800324-3-3.

[3] Fédération Internationale des Ingénieurs-Conseils (FIDIC) - Conditions of Contract for Plant and Design-Build (Yellow Book), First Edition 1999

[4] Fédération Internationale des Ingénieurs-Conseils (FIDIC) - Conditions of Contract for EPC/Turnkey Projects (Silver Book), First Edition 1999

[5] Fédération Internationale des Ingénieurs-Conseils (FIDIC) - Conditions of Contract for Construction (Red Book), First Edition, 1999

[6] Gianess, S., Pascoschi, G.: ARCHIMEDE - The first European diagnostic train for global monitoring of railway infrastructure, WCRR2003 World Congress on Railway Research, Edinburgh, 2003.

[7] Hunt, G.: Computer-aided Track Management, IQPC Asset Management for Railway Infrastructure 2002 Conference, Workshop B, London, 2 (2002).

[8] Uzarski, D., McNeil, S.: Technologies for planning railroad track maintenance and renewal, Journal of transportation engineering, 120 (1994), pp. 807., doi: http://dx.doi.org/10.1061/(ASCE)0733- 947X(1994)120:5(807)

[9] UIC Code-719R: Earthworks and track-bed layers for railway lines, International Union of Railway, Paris, France (www.uic. org), 1994.

[10] Xie J., Fu Q., Yan J. (2019). Compressive behaviour of stub concrete column strengthened with ultra-high performance concrete jacket. *Construction and Building Materials*, Volume 204, pp. 643–658. https://doi.org/10.1016/j.conbuildmat.2019.01.220.

[11] Crank J. (1975). *The Mathematics of Diffusion*. 2nd ed., Clarendon Press, Oxford, Great Britain.

[12] Kusunoki K., Yeow T., Kajiwara K. (2021). Tackling earthquake disaster by using E-defense shaking table facility. *15th International Scientific Conference iNDiS – Planning, Design, Construction and Building Renewal*, Faculty of Technical Sciences, Novi Sad, Serbia, 24-26 November, pp. 32–43.

[13] Hozjan T. (2009). Nelinearna analiza vpliva požara na sovprežne linijske konstrukcije. Doctoral thesis (in Slovenian), University of Ljubljana, Slovenia.

[14] Jelena Dimitrijević, Zoran Bonić, Dragan Milićević, Zlatko Zafirovski, CONTEMPORARY METHODS FOR SOIL AND WATER PROTECTION FROM THE IMPACT OF RAILWAY TRAFFIC, FACTA UNIVERSITATIS Series: Architecture and Civil Engineering, https://doi.org/10.2298/FUACE221224001D, march 2023

OPTIMAL NUMERICAL MODEL OF A NON-STATIONARY HEAT TRANSFER THROUGH A WALL

Snežana Ilić[1], Igor Džolev[2], Mirjana Laban[3]

Summary:

The problems of steady-state and transient heat conduction for a given geometry can be solved analytically and numerically. While the use of analytical solutions is limited, numerical methods can be used to solve heat transfer problems in complex geometries with more intricate boundary conditions, using computer simulations. Complex geometries are discretized to form an efficient numerical mesh for solving the given problem. This paper focuses on the calculation of one-dimensional, transient heat transfer for a wall with a thickness of 4 cm. The wall temperatures are calculated for each mesh node at a given moment in time. Unsteady, one-dimensional heat conduction through a flat wall is solved by the Finite Difference Method, and comparison is made with results obtained by ANSYS software. A parametric study was performed in order to analyse the influence of spatial and temporal step size on the accuracy of the solution. Finally, the optimal solution was determined to obtain temperature results with the lowest relative error within the wall nodes, while maintaining the efficiency of the computational model.

Key words: heat conduction, numerical model, FEM analysis, wall, ANSYS

[1]PhD student, Institute IMS, Belgrade, Serbia, snezana.ilic@institutims.rs
[2]Ass. prof., Faculty of Technical Sciences, University of Novi Sad, Serbia, idzolev@uns.ac.rs
[3]Full prof., Faculty of Technical Sciences, University of Novi Sad, Serbia, mlaban@uns.ac.rs

1. INTRODUCTION

The laws of heat transfer are crucial in designing and operating various forms of steam generators, furnaces, preheaters, heat exchangers, coolers, evaporators, and condensers in numerous industries [1]. For the heat transfer to occur, there must be a temperature difference. This difference can exist between parts of a single body or between two or more uninsulated bodies. Heat transfer consists of a series of distinct processes divided into three groups: heat conduction (conduction), heat transfer through a fluid (convection), and heat radiation (radiation). Figure 1 illustrates the processes of heat transfer. In addition to this classification, heat transfer can be categorized as steady-state and transient. In steady-state heat transfer, the temperatures of individual points within a body do not change with time (although they may vary spatially). In contrast, in transient heat transfer, these temperatures change with time [2]. If the temperature changes over time, energy is stored within the body or transferred to another body.
Heat conduction problems, both stationary and transient, for a given geometry, can be solved analytically and numerically. Analytical solutions apply to "simpler" geometric domains with straightforward boundary conditions. Numerical solutions for heat conduction problems are employed in cases of complex geometries with intricate boundary conditions, necessitating computer-based approaches when analytical solutions are not feasible. Complex geometries are approximated to create an efficient numerical grid for solving the given problem. A numerical mesh is formed within the observed geometric domain, where there are n unknown temperatures. To determine these n unknowns, systems of algebraic equations with n unknowns must be established. Solving these systems of algebraic equations yields the temperature distribution (temperature profile) within the observed geometric domain. The obtained temperature values are often referred to as temperature values at discrete points, while the mesh points are commonly called numerical nodes. In the scope of this work, numerical methods for solving heat conduction problems were primarily analysed [3], while analytical solutions for heat conduction problems can be found in the literature [4].
In general, numerical methods used for solving heat conduction problems include:

- Finite Element Method (FEM),
- Finite Difference Method (FDM),
- Finite Strip Method (FSM),
- Boundary Element Method,
- Energy Balance Method for Control Volume.

The study presented in this paper is focused on the calculation of one-dimensional, transient heat conduction for a 4 cm thick wall, using FDM. The wall mesh consists of nodes, and for each of these nodes, temperatures need to be computationally determined. To verify calculated temperature values, ANSYS software and FEM analysis was used. Regarding the spatial step, values of 0.02 m, 0.01 m, and 0.005 m were used, while for the time step, the chosen values were 12s, 6s, 3s, 1.5s, 1s, 0.5s, and 0.25s.By comparing the two calculation methods in a specific example, it was determined that the obtained solution accuracy is satisfactory.

2. NUMERICAL ANALYSIS

Numerical analysis for a 4 cm thick wall was conducted using the ANSYS software. To solve this problem numerically, the Finite Difference Method was used. First, it is necessary to set up a discrete grid and consider how temperature evolves, using the heat conduction differential equation. Setup:

- Wall thickness, L = 0.04 m,
- Thermal conductivity, k = 28 W/mK,
- Thermal diffusivity, a = 12.5 x 10^{-6} m^2/s,

- Initial wall temperature, $T_{initial}$ = 23 °C = 296 K,
- Heat source within the wall, e_{dot} = 5 x 10^6 W/m^3,
- Ambient temperature on one side of the wall, $T_{ambient}$ = 20 °C = 293 K,
- Convective component on the other side of the wall, $T_{infinity}$ = 30 °C = 303 K,
- Heat transfer coefficient, h = 45 W/m^{2}K.

The numerical grid has three nodes: the left node, the central node, and the right node. The central node will be in the middle of the wall thickness, and the left and right nodes will be at the boundaries of the wall. During the calculation, both the time and spatial steps were altered. With each change made in comparison to the initial example, different values for the Fourier number were obtained. The time duration of the numerical analysis was limited to one minute to facilitate a more straightforward comparison with the results obtained analytically, as the computational results were generated for one minute.

2.1. FINITE DIFFERENCE METHOD (FDM)

By applying the Finite Difference Method, temperature values within the nodes of the numerical grid for a wall with a thickness of 4 cm were obtained. The analysis was conducted by varying both the time and spatial steps. The temperature monitoring period was set to conclude after one minute for analytical calculation. The following Figures (1-3) visually represent the temperatures obtained at 12-second intervals, with varying time and spatial step parameters.

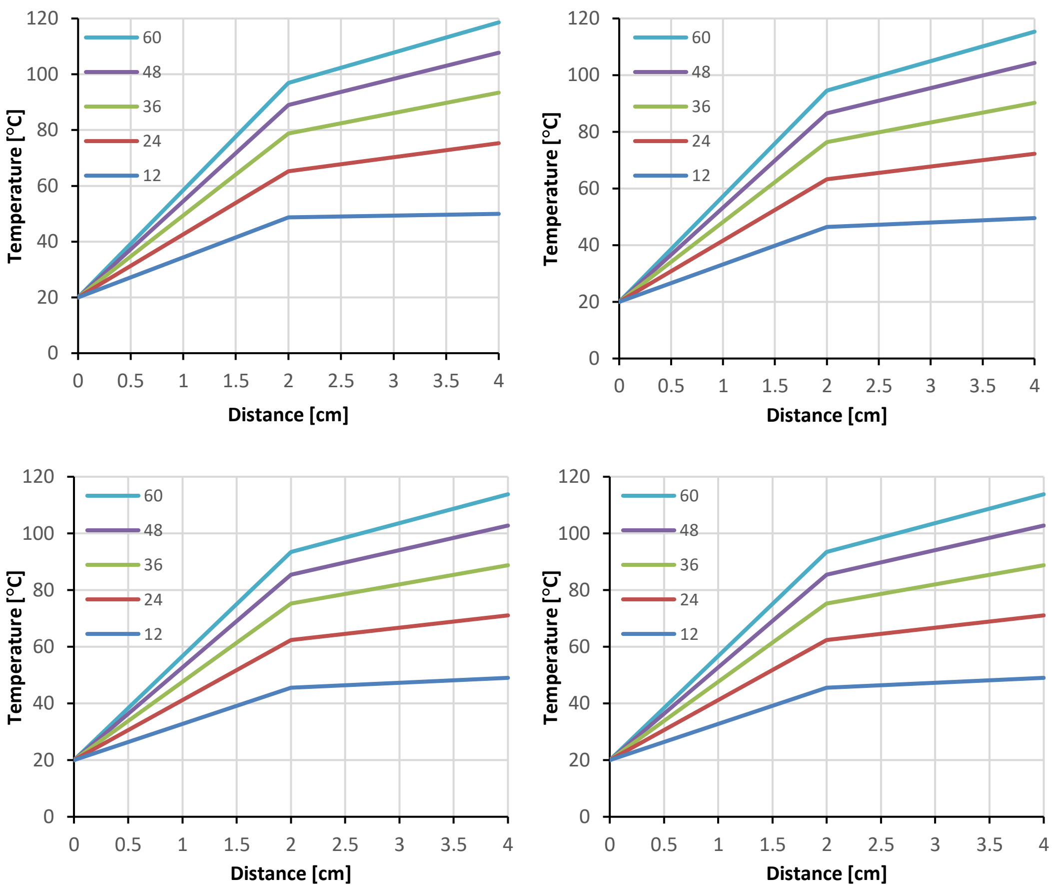

Fig. 1 Temperatures within the nodes of a 4 cm thick wall, using a spatial step of 0.02 m and a time step of 12s (top left), 6s (top right), 3s (bottom left), and 1.5s (bottom right)

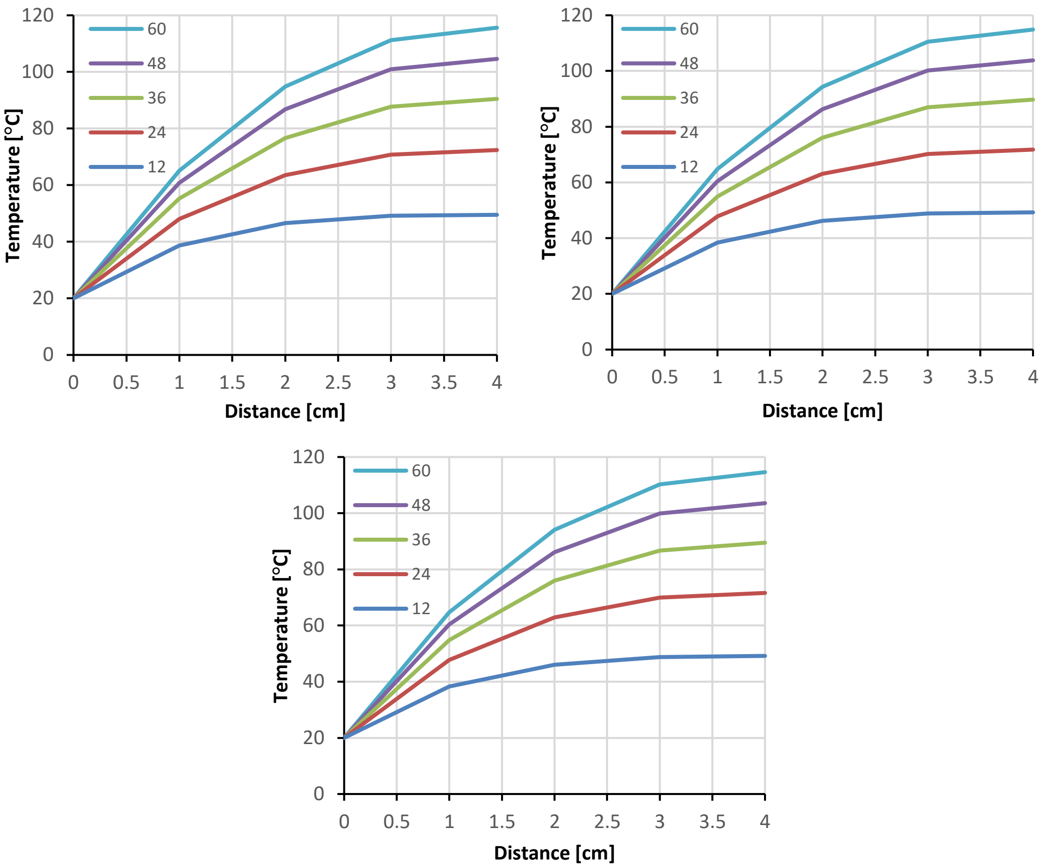

Fig. 2 Temperatures within the nodes of a 0.04 m thick wall, using a spatial step of 0.01 m and a time step of 3s (top left), 1.5s (top right), 1s (bottom)

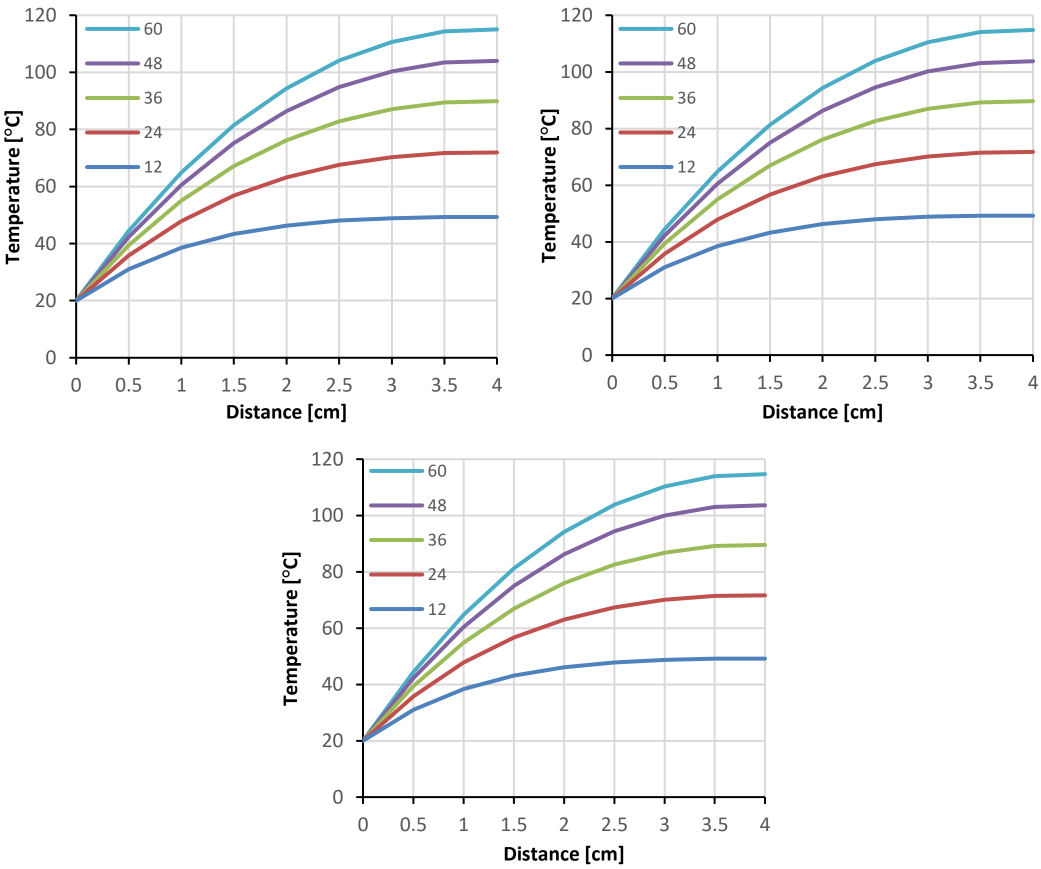

Fig. 3 Temperatures within the nodes of a 0.04 m thick wall, using a spatial step of 0.005 m and a time step of 1s (top left), 0.5s (top right), 0.25s (bottom)

Based on the previous diagrams, it can be concluded that using a denser numerical grid and setting lower values for the time step results in a smoother temperature curve.

2.2. FINITE ELEMENT METHOD (FEM)

In the next step, a parametric analysis was conducted using the Finite Element Method (FEM Analysis). The analysis was also performed for some time lasting one minute, and it focused on a 4 cm thick wall. Figure 4 illustrates curves based on the number of elements, with temperature values observed at the centre of the wall (central node) and the end of the wall (last node) over one minute.

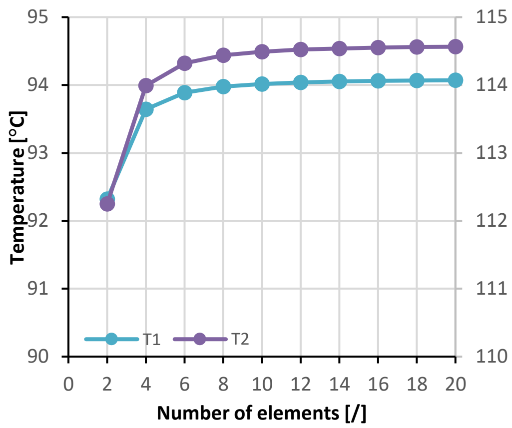

Fig. 4 Temperatures obtained at the central node and the node located at the end of the wall as a function of the number of elements

Figure 5 shows the relative error, expressed in percentages, for temperatures obtained at the central node and the node located at the end of the wall as a function of the number of elements (ranging from 2 to 20 elements).

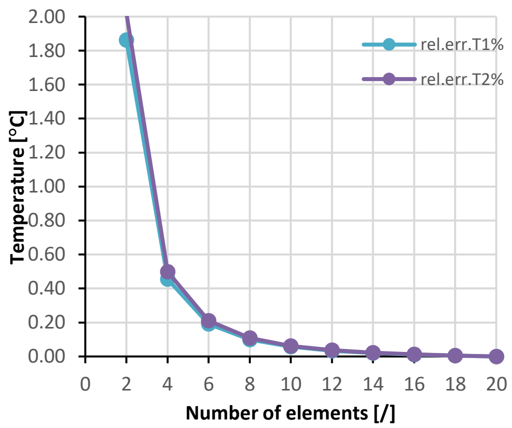

Fig. 5 Relative error for temperatures obtained at the central node and the node located at the end of the wall as a function of the number of elements

From Figure 5, it can be observed that the relative error is higher when the number of elements is lower (2 elements). Then, already at the number of elements 4, this error sharply decreases, and such a trend continues further until the number of elements 18, where the value of the relative error is 0%. Therefore, as the number of elements increases, more accurate temperature values at the mesh nodes are calculated.
In the following Figures (6-8), the relative error is shown, with variations in time and spatial step. The observation period is one minute, and relative errors are displayed every 12 seconds. The subject of analysis is a 4 cm thick wall. In Figure6 (left), relative

errors are shown during numerical analysis for the temperature within the central node of a 0.04 m thick wall, using a spatial step of 0.02 m, with variations in the time step (12s, 6s, 3s, and 1.5s). The number of elements is 2. From the figure, it is evident that the smallest error was achieved using a time step of 6 seconds. Figure 6 (right) presents the same scenario as shown in the previous diagram, but it observes temperatures at the end of the wall (last node). When observing temperatures at the end of the wall, it can be seen that the smallest relative error is achieved using time steps of 3 seconds and 6 seconds.

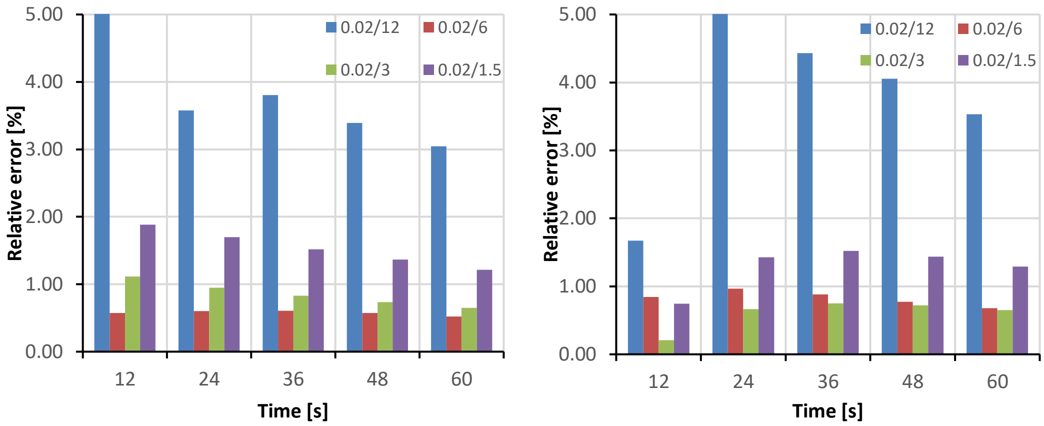

Fig. 6 Relative error for temperatures obtained at the centre of the wall (left) and at the end of the wall (right) using a spatial step of 0.02 m, with time steps of 12s, 6s, 3s, and 1.5s

In Figure 7 (left), relative errors during numerical analysis for the temperature within the central node of a 0.04 m thick wall are depicted. It uses a spatial step of 0.01 m, with variations in the time step (3s, 1.5s, and 1s). The number of elements is 4. Figure 7 (right) refers to temperatures obtained at the end of the wall. From Figure7, it is evident that the smallest error is achieved using a time step of 1 second. Although the smallest error is obtained with a time step of 1 second, it can be noticed that using time steps of 3s or 1.5s results in a relative error value below 1%, which can be considered satisfactory.

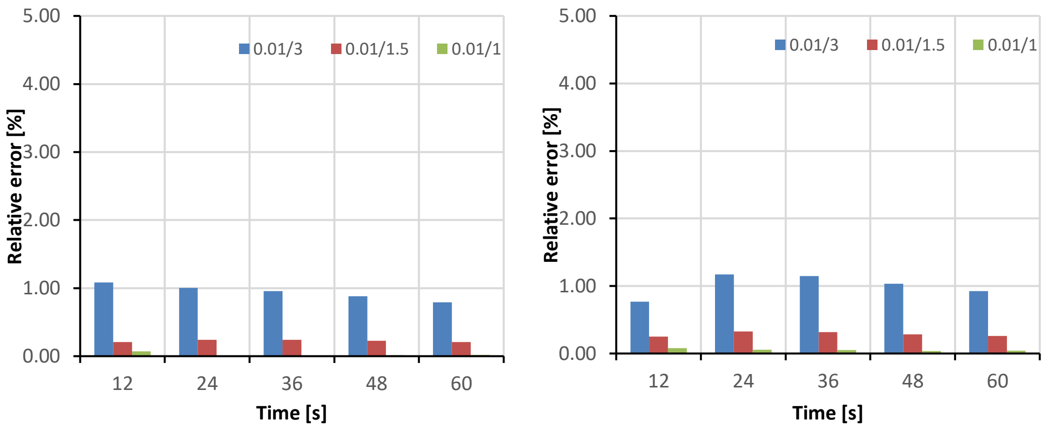

Fig. 7 Relative error for temperatures obtained at the centre of the wall (left) and at the end of the wall (right) using a spatial step of 0.01 m, with time steps of 3s, 1.5s, and 1s

In Figure 8 (left), relative errors during numerical analysis for the temperature within the central node of a 0.04 m thick wall are shown. It uses a spatial step of 0.005 m, with variations in the time step (1s, 0.5s, and 0.25s). The number of elements is 8. From Figure8, it is clear that the smallest error is achieved using a time step of 0.25 seconds.

Nevertheless, using time steps of 0.5s and 1s still provides fairly accurate values since their relative error values are below 1%.

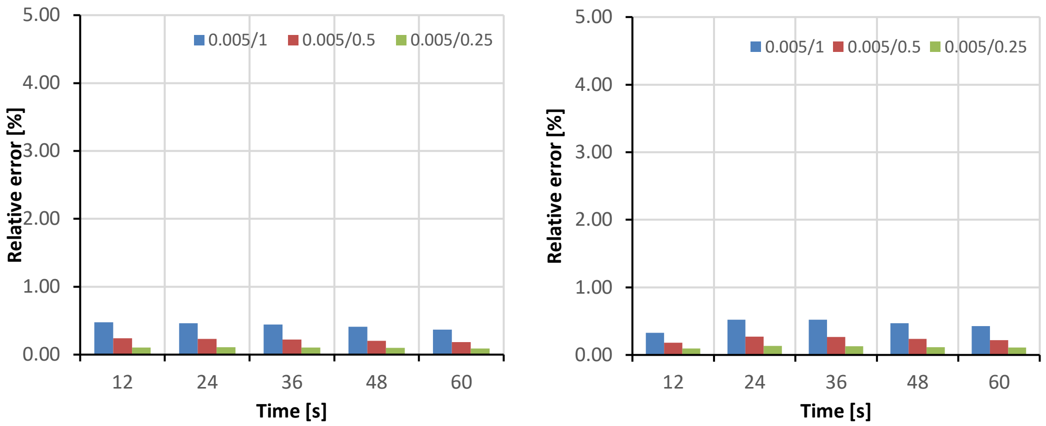

Fig. 8 Relative error for temperatures obtained at the centre of the wall (left) and at the end of the wall (right) using a spatial step of 0.005 m, with time steps of 1s, 0.5s, and 0.25s

2.3. RELATIVE ERRORS

The following diagrams show relative errors obtained using the Finite Difference Method (FDM) and the Finite Element Method (FEM). Temperatures within the nodes of the numerical grid for a 4 cm thick wall were analysed. The varied parameters were spatial and time steps. The analysis was conducted over a one-minute duration. Before the analysis, it was adopted that any relative error value below 1%, between two consecutive time step variations, represents satisfactory accuracy in obtaining temperatures within the numerical grid nodes.Figure9 (left) illustrates the relative error using a spatial step of 0.01 m and consecutive time steps (12s-6s, 6s-3s, 3s-1.5s). The number of elements for this example is 2, and temperatures were observed at the centre of the wall. From Figure 9, it can be concluded that using a time step variation of 3s-1.5s results in a relative error below 1%. In Figure9 (right), significant oscillations in the relative error values can be observed depending on the moment of temperature observation (12s, 24s, 36s, 48s, and 60s), indicating that a larger time step increases the likelihood of result inaccuracies.

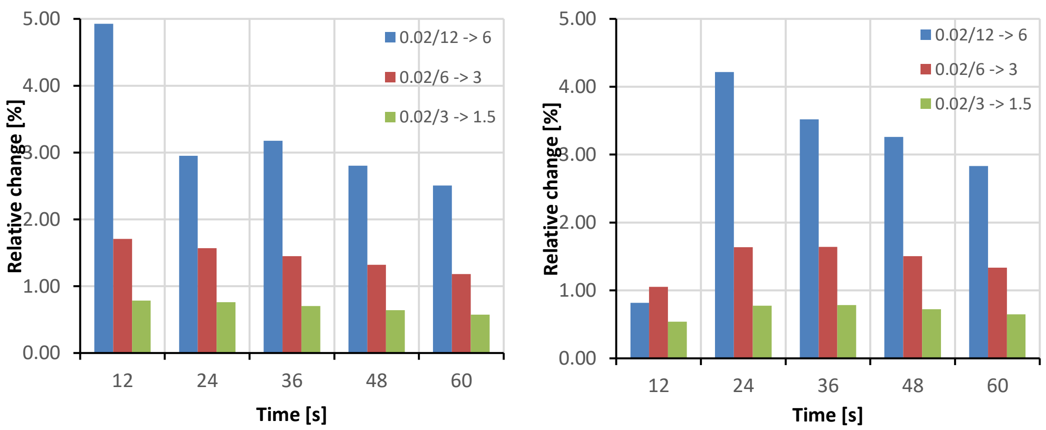

Fig. 9 Relative error using FDM and FEM analysis with a spatial step of 0.02 m, with time step variations (12s-6s, 6s-3s, 3s-1.5s) for temperatures observed at the centre of the wall(left) and at the end of the wall (right)

In Figure10 (left), a spatial step of 0.01 m and a time step variations (3s-1.5s and 1.5s-1s), were used. It is visible that a smaller time step results in a lower relative error value.

However, using time steps of (12s-6s and 6s-3s) still provides a relative error value below 1%, with 1% being considered as the acceptable threshold. In this example, 4 elements were used, and temperature values were observed at the centre of the wall (Figure 10, left) and the end of the wall (Figure10, right).

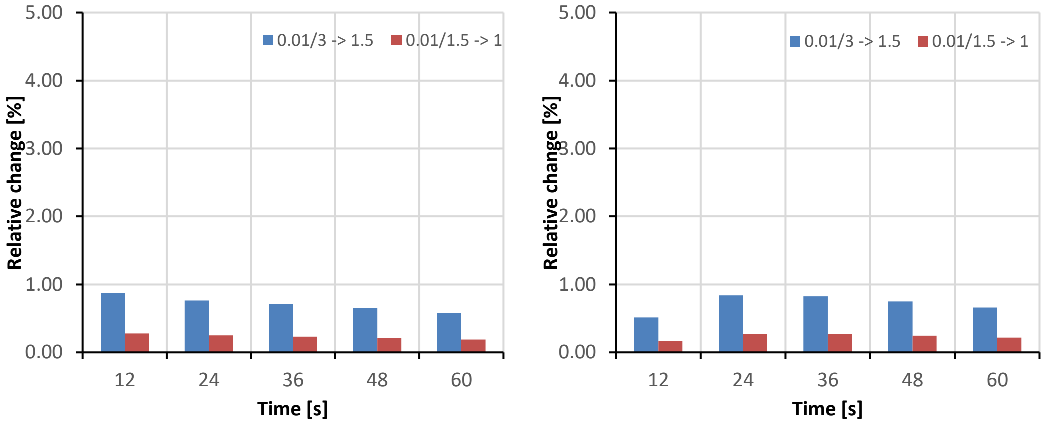

Fig. 10 Relative error using FDM and FEM analysis with a spatial step of 0.01 m, with time step variations (3s-1.5s and 1.5s-1s) for temperatures observed at the centre of the wall(left) and at the end of the wall (right)

Figure11 (left) presents an example where a spatial step of 0.005 m was used, while the time step variation was (1s-1.5s and 0.5s-0.25s). A smaller time step resulted in a lower relative error value in both cases. However, in both scenarios, the relative error values were well below 1%, which is considered satisfactory. In this example, 8 elements were used, and temperature values were observed at the centre of the wall (Figure11, left) and the end of the wall (Figure11, right).

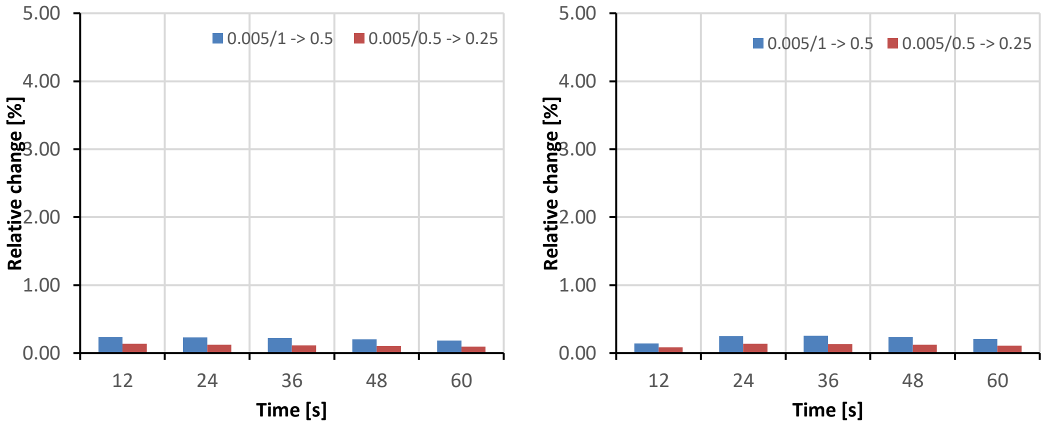

Fig. 11 Relative error using FDM and FEM analysis with a spatial step of 0.005 m, with time step variations (1s-0.5s and 0.5s-0.25s) for temperatures observed at the centre of the wall(left) and at the end of the wall (right)

Figure12 shows a comparative analysis of temperatures through a 4 cm thick wall using FDM and FEM analysis. The analysis was conducted at time intervals of 12s, 24s, 36s, 48s, and 60s.

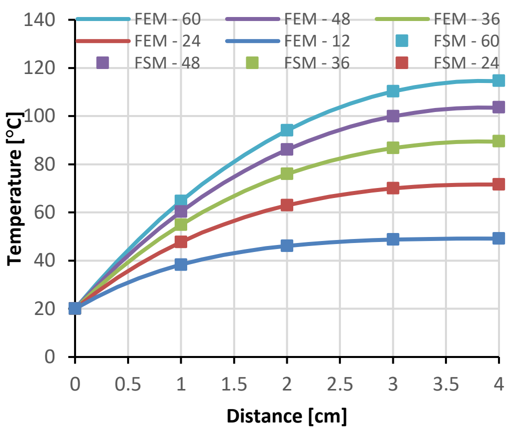

Fig. 12 Comparison of temperature results obtained for a 4 cm thick wall using FDM and FEM methods at 12s, 24s, 36s, 48s, and 60 seconds

3. CONCLUSION

The paper presents an example of one-dimensional, transient heat conduction through a 4 cm thick wall divided into three nodes. Temperature values for each of these points were calculated using the Finite Difference Method (FDM), with a time step of 0.2 minutes. The calculation was stopped after obtaining temperature values after one minute. Solution convergence was monitored through sensitivity analysis of the time and spatial step parameters until optimal values were determined in terms of solution accuracy and computation time. Additionally, as an external verification of the computational model, a model was created in the ANSYS software based on the Finite Element Method (FEM). By comparing the results of the two calculation methods in this specific example, it was determined that the achieved accuracy of the solution was satisfactory.

Regarding the spatial step, three values were used: 0.02 m, 0.01 m, and 0.005 m, and for the time step, the following values were considered: 12s, 6s, 3s, 1.5s, 1s, 0.5s, and 0.25s. After conducting all the analyses and variations, it was concluded that the best approach is to use a spatial step of 0.01 m and a time step of 1s to obtain values with the smallest relative error for temperatures within the nodes of the wall. The obtained values for the spatial and time steps are considered optimal, and further refinement of the numerical grid would increase the number of spatial points, potentially leading to rounding error accumulation, which can result in an increased error accumulation.

ACKNOWLEDGEMENT

This research has been supported by the Ministry of Education, Science and Technological Development through project no. 451-03-47/2023-02/200012.

REFERENCES

[1] Mak-Adams V. H. (1969). *Prostiranje toplote*, Građevinska knjiga, Belgrade, Serbia.

[2] Kozić Đ. G. (2019).*Termodinamika – inženjerski aspekti,*2nd ed.,Faculty of Mechanical Engineering, University of Belgrade, Serbia.

[3] Cengel Y. A., Ghajar A.J. (2015).*Heat and Mass Transfer Fundamentals & Applications.* 5th ed.,McGraw-Hill Education, University of Nevada, Oklahoma State.

[4] Baehr H. D., Stepfan K. (2011). *Heat and mass transfer,* 3th ed.,Mc-Graw Hill Education, New York.

ONE IMPLEMENTATION OF ARTIFICIAL INTELLIGENCE SOFTWARE FOR SEGMENTATION AND WALL COMPRESSION STRENGTH PREDICTION

Bojan Milošević[1,2], Nenad Kojić[2], Vladimir Mandić[1], Milena Čančarević[3] and Luka Lukić[3]

Summary:

The compressive strength of the wall is determined using an empirical expression defined by EuroCode 6 (EC 6). The calculation of such a value is based on a larger number of input parameters, so mathematically, each individual problem can be viewed as a vector with a larger number of elements. The work uses an artificial intelligence algorithm: Machine learning, which is very popular today and gives good results in data segmentation and prediction. Starting from the tree-based model, a solution was proposed that is its improved option: random forest. In accordance with the advantages of the random forest model, a solution was proposed that includes the way of creating the input data set, the algorithm for segmentation and prediction, with the aim of testing the possibility of segmentation and prediction of the training input data set with unknown wall pressure strength after training the algorithm with previously known data.

Key words: Artificial intelligence, machine learning, random forest, wall pressure strength, segmentation

[1] Assoc. prof., Faculty of Mechanical and Civil Engineering Kraljevo, University of Kragujevac, Kraljevo, Serbia, milosevic.b@mfkv.kg.ac.rs, mandic.v@mfkv.kg.ac.rs
[2] Professor of applied studies, Academy of Technical and Art Applied Studies Belgrade, Serbia, nenad.kojic@ict.edu.rs, bojan@vggs.rs
[3] Assistant, Academy of Technical and Art Applied Studies Belgrade, Department: School of Information and Communication Technologies, Belgrade, Serbia, milena.cancaravic@ict.edu.rs, luka.lukic@ict.edu.rs

1. INTRODUCTION

Masonry structures play an important role in the field of civil engineering. A large part of the buildings that are being built today, as well as the buildings that are part of the architectural heritage, were made as masonry systems. Masonry constructions are represented today in the field of construction of individual, residential, business, administrative, public and industrial buildings and as such are an indispensable factor in construction engineering [1].

The mechanical characteristics of the wall depend on the mechanical characteristics of the constitutive materials used for its construction, so masonry walls belong to inhomogeneous and anisotropic materials. Determining the mechanical characteristics of the wall is not an easy task because it is seen as a simultaneous effect of the constituent materials of the wall [1]. Defining the mechanical characteristics of the wall can be done experimentally and numerically using empirical expressions. When designing new buildings, the mechanical characteristics of the wall are generally defined using empirical expressions that define the dependence between the compressive strength of the masonry element and the applied binder [2].

Eurocode 6 is a standard for the design of masonry structures that was published in the form of a draft in 1988 and, after a long-term revision process, was first published in the form of a standard in 1995. Within this regulation, part 1-1 includes general rules for buildings and the procedure for determining the mechanical characteristics of masonry walls [1]. The materials used for the construction of masonry constructions must also meet the requirements defined in the relevant European standard.

As the calculation of wall compressive strength is relatively complex, and requires the analysis of a large number of empirical indicators and knowledge, this paper will offer a software solution that should enable faster and simpler work in everyday application. Considering the existence of a large number of parameters that influence the calculation, this can be seen as a classification problem along with a prediction problem. Classification can generally enable the analysis of input data to form a model that can be trained with previously known data with the aim of classifying the known input data [3]. In this way, after training the artificial intelligence algorithm, the unknown input data set can be automatically classified and assigned to one of the previously defined output sets and thus quickly obtain a conclusion of the compressive strength of the wall depending on the input data.

In the last two decades, artificial intelligence has a large number of concrete implementations that can significantly improve certain processes and work results [4]. One type of implementation of artificial intelligence algorithms is machine learning [5]. Machine learning is a set of different models that are applied for some specific applications [6]. One of the machine learning models is the tree-based model [7]. The very name of this model indicates the existence of a program-generated tree that is used for decision-making purposes. Using this model, sets of different input data can be analyzed with the aim of finding mutual dependencies and regularities between them, all with the aim of classification and value prediction [6]. Additional improvements of this model were realized through the Random forest model [7]. This model is created with a random selection of a smaller number of input parameters, so it is implemented faster in the code and has a lower degree of complexity during calculation. Various applications of the Random forest model show that this algorithm is very suitable for solving sophisticated problems of classifying or predicting information.

This paper is organized in four chapters: After the introduction, in the second chapter there are empirical expressions for the calculation of the compressive strength of the wall, in the third chapter the basic principles of SVM operation and the use of kernels are given. The fourth chapter defines the proposed model for the classification of data used to calculate the compressive strength of the wall, where the elements for masonry made of clay that are represented in the territory of the Republic of Serbia with the appropriate binders are considered. After that, the results of the proposed model for real data in the observed construction area are presented. At the end, the conclusion and further guidelines in the research of this matter are given, as well as the literature used.

2. CALCULATION OF SOLID STRENGTH UNDER WALL PRESSURE USING EC 6

Masonry walls belong to composite materials that consist of masonry elements and an applied binder that has the role of connecting the masonry elements to each other and thus forms a masonry structure. Research carried out so far, as well as regulations for the design of masonry structures, show that the compressive strength of the wall depends on various factors, such as the compressive strength of the masonry elements, the shape of the masonry element, the thickness of the binding material, and its strength. Defining a universal mathematical expression for determining the compressive strength of a wall that takes into account all the factors that affect the mechanical characteristics of the wall is almost impossible.

The empirical expression given in Eurocode 6 for calculating the compressive strength of the wall takes the ratio between the compressive strength of the masonry elements and the binder. On the basis of empirically defined coefficients, the shape of the applied masonry element (dimensions, belonging to a certain group), the type of applied binding agent and the surface between the masonry elements are taken into account. The compressive strength of a masonry wall in the general case can be defined by the following function [1]:

$$f_k = F(f, f_m, h_m, K) \tag{1}$$

wherein:

- K – empirical coefficient defined on the basis of the element for masonry, belonging to the group of the element, type of applied binding material
- f – compressive strength of masonry elements,
- fm – compressive strength of the applied binder,
- hm – thickness of the applied binder.

When designing masonry structures when the mechanical characteristics of the masonry elements are known, the characteristic value of the wall's compressive strength is determined in accordance with the empirical formula given in Eurocode 6 and has the following general expression:

$$f_k = K f_b^{\alpha} f_m^{\beta} \tag{2}$$

- f_b – normalized compressive strength of the masonry element,
- f_m – compressive strength of mortar,
- K – a constant (empirical) that depends on the characteristics of the elements used for construction and the type of applied veyive means (Table 1),
- α i β – constants.

The relationship between the characteristic value of the compressive strength of the masonry structure fk, the normalized mean value of the compressive strength of the masonry elements fb and the strength of the mortar can be determined depending on the type of mortar used:

- for masonry construction made with the use of general-purpose mortar and lightweight aggregate mortar,

$$f_k = K \cdot f_b^{0,7} \cdot f_m^{0,3} \tag{3}$$

- for masonry construction made with the use of thin-layer mortar, when the horizontal joints are 0.5 mm to 3.0 mm thick and with the use of group 1 and group 4 clay elements, calcium-silicate elements, concrete elements and autoclaved cellular elements of concrete,

$$f_k = K \cdot f_b^{0,5} \tag{4}$$

- for masonry construction made with the use of thin-layer mortar, when the horizontal joints have a thickness of 0.5 mm to 3.0 mm, and with the use of group 2 and group 3 clay elements,

$$f_k = K \cdot f_b^{0,7} \tag{5}$$

In the case of applying thin-layer mortar (for thin joints), the coefficient β is zero, which means that the compressive strength of the mortar is considered insignificant for the compressive strength of the wall with thin joints..

Tab. 1 Values for K for the use of general-purpose mortars, thin-layer or lightweight aggregate mortars [1]

Elementi za zidanje		Malter opšte namene	Tankoslojni malter (≥0,5 mm i ≤3mm)	Lakoagregatni malter, zapreminske mase	
				600-800	800-1300
Glina	Grupa 1	0,55	0,75	0,30	0,40
	Grupa 2	0,45	0,70	0,25	0,30
	Grupa 3	0,35	0,50	0,20	0,25
	Grupa 4	0,35	0,35	0,20	0,25

Attention should be paid to the determination of the normalized compressive strength of masonry elements, which was introduced into the calculation in an attempt to apply the empirical formula to
building elements of different geometric characteristics. In this way, the average compressive strength of the masonry element, using the shape coefficient, is translated into the normalized compressive strength of the 100x100mm masonry element. The form factor includes the height and smallest width of the masonry element. The empirical formula given in Eurocode 6 shows that the compressive strength of masonry elements has the greatest influence on the compressive strength of the wall, the relationship is based on experimental research to determine the compressive strength of masonry elements.

3. ARTIFICIAL INTELLIGENCE TOOLS

Artificial intelligence is a scientific discipline that aims to create intelligent machines and computer programs that represent the simulation of human intelligence [3]. In this way, the machine should be able to learn and make decisions just as a human brain would go through that process. There is a greater number of artificial intelligence in relation to the way the learning process and the goals for which they are applied [3]. One of the types of artificial intelligence is machine learning [4]. This discipline focuses on the advanced processing and analysis of data and algorithms with the aim of detecting dependencies and rules among the analyzed data, in accordance with the logic of human reasoning.

3.1. MACHINE LEARNING (TREE-BASED MODEL)

Machine learning uses several tools that are suitable for its work [4]. One of the models that is often used is the tree-based model [6]. This model uses a decision tree to show how different input data can be analyzed, described and as such used to predict some desired value [5]. Tree-based models have proven to be very successful for classification applications and solving regression problems [6].

Tree-based models belong to the concept of supervised classification [4]. Like a physical tree, it starts from the root where the branches branch and finally ends with leaves. The set of input data is divided in relation to some criteria into two groups. Such divisions are made until some stopping condition is met. A node is where branches branch off and represent a particular characteristic or state, while the branches themselves represent a range of possible values. Upon reaching the leaf, the possibility of further branching ends, and a concrete value defined by the problem itself is obtained there [7].
As an example of a tree-based model representation, consider a two-dimensional problem, with respect to the k and i axis, in which the various elements of the set N are located, Fig. 1.

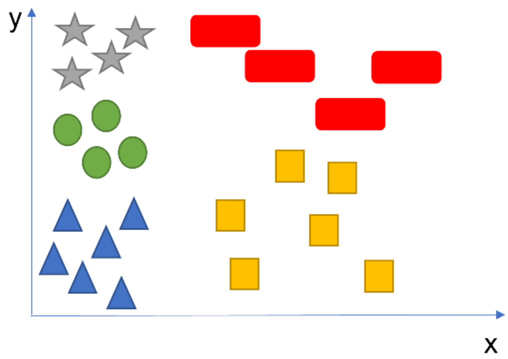

Fig. 1 An initial set N that has five types of similar elements of the set

The goal is to achieve segmentation of the elements of the set by recursive division, provided that the space is divided with lines parallel to one of the axes, Fig. 2.

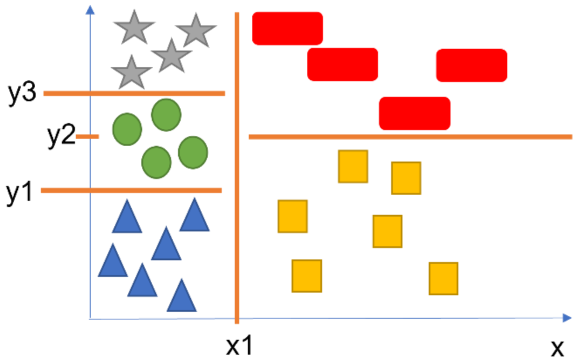

Fig. 2 Division of the initial set with lines parallel to the x and y axes with the aim of separating the elements of the set

Starting from the root of the set, in accordance with Fig. 2, the first criterion can be divided along the x axis into values that are smaller or larger than the value of x_1. After that, the values that are smaller than x_1 can be further divided in relation to the value on the y-axis, according to the criterion of whether they are smaller or larger than the value of y_1. In case they are less, we got elements of the set (triangle). In case they are greater than y_1, they can be further divided on the condition that they are less than or greater than y_3. Then the elements of two sets (stars and circles) are uniquely obtained. A branch started with respect to elements for which x is greater than the value of x_1 can be further split with respect to the value of y_2. Thus, for all elements for which y is less than the value of y_2, elements that are squares are obtained, while for those that are greater than y_2, rectangles are obtained.

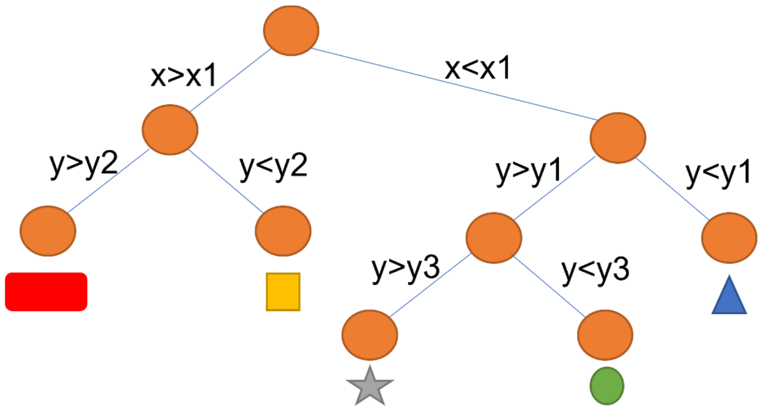

Fig. 3 One tree structure for the classification problem defined in Fig. 2

It is clear that the obtained tree can be made in several different ways depending on which division is made first and then which one is made next. Thus, trees can have different depths. The most common branch splitting criterion in the data classification process is the entropy derived from Shannon's source coding theorem [8].
In each node of the tree, the entropy is defined by a formula:

$$E = -\sum_{i=1}^{c} p_i \times \log(p_i) \tag{6}$$

Where: c is the number of unique classes, and p_i is the probability of each of those classes. When the entropy is maximum then the most information is obtained at each split in the node and it is the most optimal form. According to the condition for creating a tree, there is a frequent problem that is based on a big change in the structure and depth of the tree when the structure of the input data is slightly changed. This can complicate the tree creation process itself, but also lead to a low general prediction accuracy, which is also called generalization accuracy.

3.1.1. Random forest model

Analyzing the problem of increasing the accuracy, Xo introduced a new idea in 1995 to approach the two-stage approach of modifying the Tree-based model [5]. Both approaches are based on random selection of existing input elements. Thus, the creation of a random subset of input data is defined and an individual tree is created for each of them [7]. Braiman formally presents this idea in 2001 and introduces the term random forest tree, considering the obtaining of a large number of randomly obtained trees [3]. As each input data can be described by n characteristics, the division of random selection can be done both by random selection of input elements of the set and by random selection of m out of n characteristics of the input element. Thus, a two-stage approach to randomization of input data is achieved, which results in a new set of samples - bootstrap samples.
In this way, a large number of trees are obtained, which have a smaller number of input data, and which are therefore executed faster, but also obtain potentially different results. If all of the n characteristics of the input set were used in each tree, ie if their correlation is high, the overall result would also have a high error [3]. By using random forest tree, the number of input parameters is reduced, so the correlation of input sets in different stables is also reduced, which will lead to a smaller overall error, on the one hand. However, a smaller input set may be unrepresentative to obtain an accurate result and will result in an increase in error. It has been mathematically proven that the size of the error always has a convergence trend when the number of trees increases [3].
It is thus clear that the number of trees should be as large as possible, with a quality choice of the number of input parameters for each of the trees. The optimal number or

range for a given subset of input data can be determined by repeating the tests defined in [9].
Thus, with each individual tree, a separate decision on classification is made, and the final decision is based on the solution obtained by the majority in the individual trees.

3.1.2. Applications of Random forest model in construction

Examples of the use of random forest models of artificial intelligence are very common and give extremely good results in the field of data classification, regression and prediction. In the professional literature there is a large number of the most diverse applications in all aspects of the engineering profession. In the paper [10], the authors show the application of the random forest model for the semantic classification of buildings and precise categorization. The mentioned model also showed good results in predicting the strength of rubberized concrete [11]. In the paper [12], the authors presented the prediction results based on wind pressure on objects. Finding the optimal ratio of carbon emissions in the construction phase and design parameters based on 38 buildings in China is presented in paper [13]. In the paper [14], the authors applied random forest on the example of the material intensity coefficient (MIC), which is of vital importance for material inventory calculations. Random forest was also applied in the case of predicting building types using footprint and city zoning [15]. The problem of identifying moisture content in brick walls in historical buildings was also solved by applying the aforementioned model, presented in the paper [16]. There are still a large number of different applications in the field of construction, but it should be emphasized that random forest has the possibilities of a wide range of applications in all situations when it is necessary to classify or predict certain information.

4. PROPOSED ALGORITHM AND RESULTS

Based on the explained principles of the random forest tree algorithm, the first step is the formation of the input data set.
For these purposes, a data set was used for which the characteristic compressive strength of the wall was pre-calculated in accordance with EC 6. This was done on an initial set of 6965 samples. Each input data x is represented as a vector having i=5 array elements:

- Minimum width of the masonry element
- Minimum height of the masonry element
- Compressive strength of the masonry element
- Characteristic compressive strength of the binder after 28 days
- Group of elements for masonry

The values of each input element x_i represent the technical characteristics for the masonry element of different width, length and height: brick (12/26/6.5), giter block (19/25/19), Porotherm 20-50 Profi (20/50/ 24.9), Porotherm 25 Profi (25/37.5/24.9), Porotherm 25-38 IZO Profi (25/37.5/24.9), Porotherm 20 S P+E (20/37.5 /23.8), Porotherm 250 S P+E (25/37.5/23.8), and Porotherm 25 AKU (20/37.5/23.8).
For each of the 6965 samples, the compressive strength of the wall was calculated in accordance with EC 6. This data was used as a criterion for classification and prediction.
The Orange software package was used for the entire work. The block diagram of the proposed system is given in Figure 4. The input data set is first separated into two groups of data, one of which is used to create trees in accordance with the described random forest tree methodology. The second group (30%) is used to test the obtained solution. Thus, both outputs go to the prediction block, which checks the overall solution of the proposed system, Fig. 4.

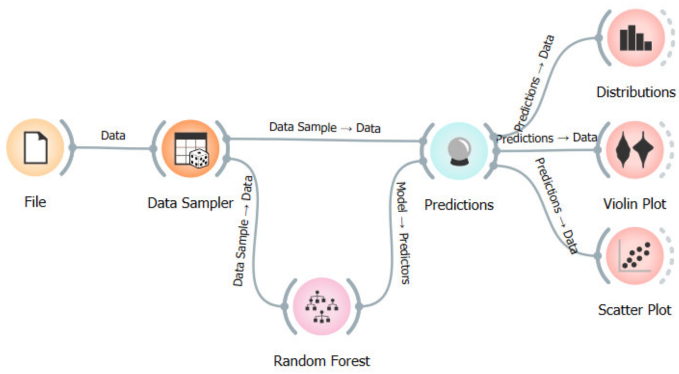

Fig. 4 Block diagram of the proposed algorithm

The quality of the obtained solution will be visually presented with three types of diagrams (data distribution, violin plot and scatter plot) and a tabular presentation.

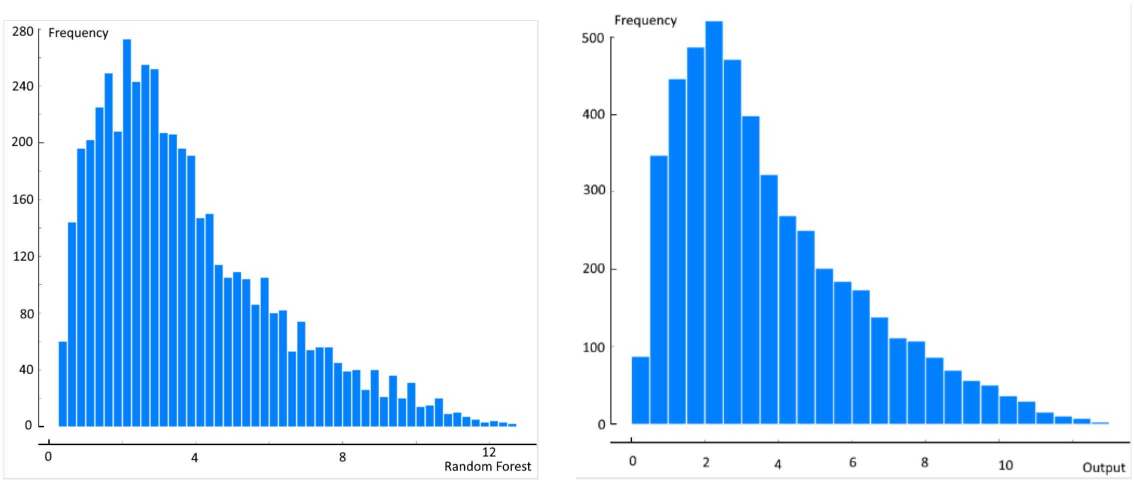

Fig. 5 Display of the distributions of the output data set after prediction for the Random forest tree algorithm in relation to the original set of calculated values of the characteristic compressive strength of the wall in accordance with EC 6

Fig. 5.a shows the obtained distribution of the output data set obtained by predicting the proposed solution, while Fig. 5.b shows the distribution of the calculated values of the observed wall strength. The shape of the curve indicates the extremely good result obtained by the proposed algorithm based on the testing of marked samples.
If the data is viewed at a mathematical level, the comparison of four characteristic parameters is often practiced: Mean Square Error (MSE), Root Mean Square Error (RMSE), Mean Absolute Error (MAE) and the degree of determination (coefficient of determination - R2). These results are shown in Table 2.

Tab. 2 Comparative analysis of four statistical indicators for the result obtained by the proposed algorithm

	MSE	RMSE	MAE	R2
Random forest	0,237	0,487	0,295	0,961

The obtained results show very satisfactory values and small error values obtained on the entire spectrum of observed input data, which indicates that the proposed algorithm can be one of the favorable solutions for the classification of such a defined input data set.
An additional indicator is the result of a comparative analysis of the predicted results in relation to all 5 observed characteristics of the input element. Fig. 6 shows the

dependence of the exact values of the observed wall strength calculated in accordance with EC 6 on the values obtained using the proposed algorithm.

Different colors indicate the elements of the vector x_i. It can be seen that the correlation obtained in this way is very high, that in addition to the very narrow data scattering curve around the diagonal, there is a high correlation by color grouping, which shows a relatively good way of classification according to each of the observed elements of the input vector.

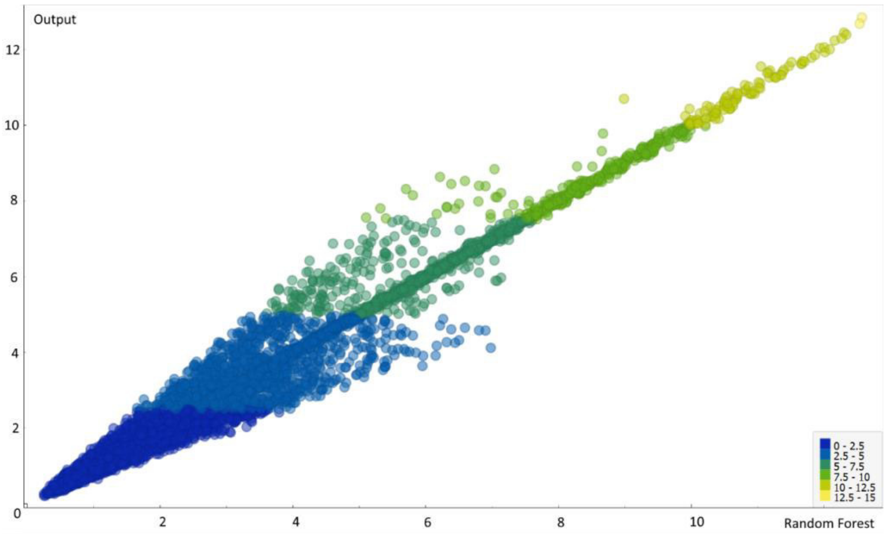

Fig. 6 Correlation of the set of correctly calculated values of the observed strength in relation to the values obtained by the proposed solution for all five elements of the input vector

Fig. 7 shows two violin diagrams based on all five observed parameters of the input vector. Fig. 7.a shows the presented set based on calculated values, which we consider correct, while Fig. 7.b shows the output values from the proposed model. A high degree of similarity can be observed in all parameters, except in the slope of the middle part of the figure on the side edges, which indicates a very soft volume of the total amount of arms for all trees in the forest of trees.

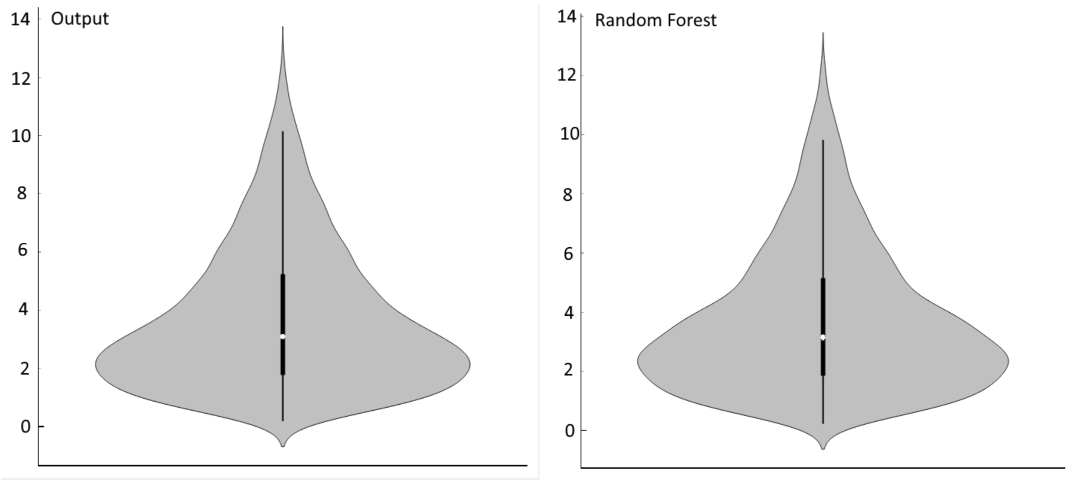

Fig. 7 Comparative analysis of the violin plot diagram for the set of correctly calculated values of the observed strength and the values obtained by the proposed solution for all five elements of the input vector

One of the indicators of the obtained classification of the proposed algorithm can be visually displayed using the diagram in Fig. 8. This diagram shows the obtained set of classified output results in different shades of color in relation to the normalized compressive strength of the masonry element. The normalized strength used is obtained when, as a product of the shape, which depends on the height and the minimum dimension of the masonry element. What can be seen in Fig. 8 is that colors of similar intensity are grouped very close to each other, which indicates a good segmentation according to the criterion, which as a result corresponds well to its surroundings, while at the ends of the diagram there are colors with exceptional differences, which clearly separate the fenced classified groups that have no similarities among themselves.

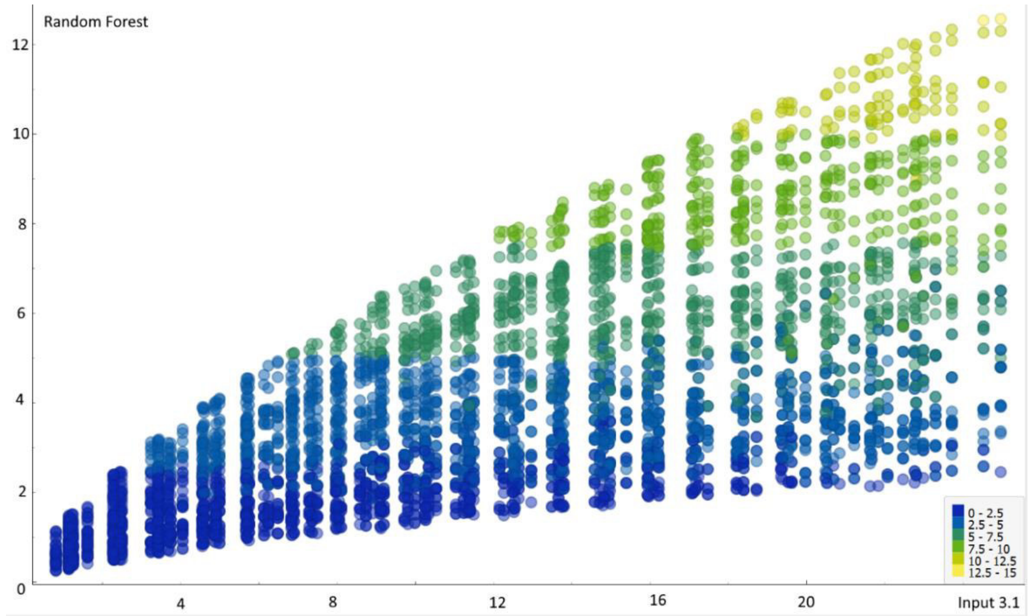

Fig. 8. Classification obtained when using the Random Forest algorithm in relation to the normalized compressive strength of the masonry element

As shown in Fig. 8, the classification of the proposed algorithm in relation to the compressive strength of mortar is presented in a similar way in Fig. 9.

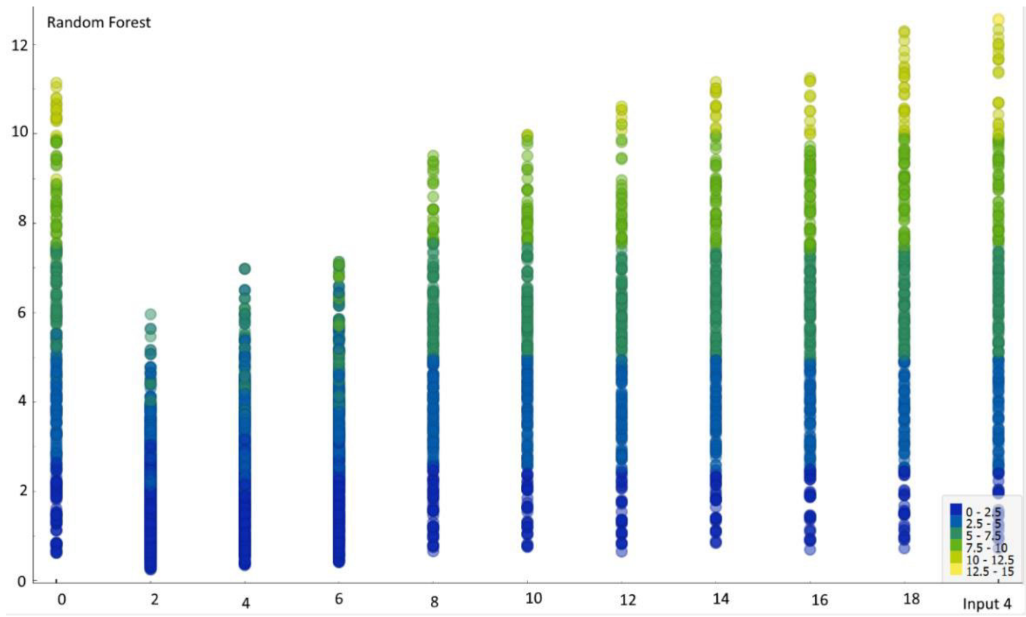

Fig. 9. Classification obtained when using the Random Forest algorithm in relation to the compressive strength of the mortar

In Fig. 9, this type of classification is even better observed because the dependence is quite linear, so the grouping of the obtained clusters perceives more clearly. Four rough groups marked in blue, dark green, light green and yellow are clearly visible. Overlaps of diametrically opposite classes, in the form of color, almost do not exist, except in the part when, at the lowest values along the y axis, some dark blue elements overlap with light blue. This indicates that the clarity of the clustering at those levels behaves somewhat worse than in the central and higher values, so it makes sense to think about changing the application of the algorithm in those extremely initial areas.

5. CONCLUSION

Within this paper, the possibility of implementing artificial intelligence for solving practical problems in construction engineering is shown. By applying one of the Machine Learning artificial intelligence algorithms that provides good data segmentation and prediction results, the problem of defining the compressive strength of the wall was solved based on the data obtained by applying empirical expressions defined in Eurocode 6. After training the algorithm with previously known data, the possibility of segmentation was tested and predictions of a training set of input data with unknown compressive strength of the wall. By analyzing the results obtained based on the tested samples, it is concluded that the results obtained based on the proposed algorithm are in very satisfactory values and that there is a small error on the entire set of input data. It is concluded that the proposed algorithm can be applied to determine the compressive strength of the wall based on arbitrary input parameters, whereby the obtained values are approximately equal to the values obtained based on the empirical expressions given in Eurocode 6.

REFERENCES

[1] Evrokodovi za konstrukcije Evrokod 6: EN 1996-1-1:2005, Proračun zidanih konstrukcija. Deo 1-1:Opšta pravila za armirane i nearmirane zidane konstrukcije, Građevinski fakultet Univerziteta u Beogradu, Beograd,

[2] Milošević, B. "AmQuake: Statička i dinamička analiza zidanih konstrukcija", Akademija tehničko umetničkih strukovnih studija u Beogradu, Fakultet za mašinstvo i građevinarstvo u Kraljevu, Univezitet u Kragujevcu (Srbija), (2022)

[3] Breiman, L. (2001). Random forests. Machine learning, 45, 5-32.

[4] Dick, S. (2019). Artificial intelligence. Harvard Data Science Review, 1(1), 1-8.

[5] Zhou, Z. H. (2021). Machine learning. Springer Nature.

[6] Liu, Y., Wang, Y., & Zhang, J. (2012). New machine learning algorithm: Random forest. In Information Computing and Applications: Third International Conference, ICICA 2012, Chengde, China, September 14-16, 2012. Proceedings 3 (pp. 246-252). Springer Berlin Heidelberg.

[7] Schonlau, M., & Zou, R. Y. (2020). The random forest algorithm for statistical learning. The Stata Journal, 20(1), 3-29.

[8] Shannon, C. E. (2001). A mathematical theory of communication. ACM SIGMOBILE mobile computing and communications review, 5(1), 3-55.

[9] Pal, M. (2005). Random forest classifier for remote sensing classification. International journal of remote sensing, 26(1), 217-222.

[10] Du, S., Zhang, F., & Zhang, X. (2015). Semantic classification of urban buildings combining VHR image and GIS data: An improved random forest approach. ISPRS journal of photogrammetry and remote sensing, 105, 107-119.

[11] Sun, Y., Li, G., Zhang, J., & Qian, D. (2019). Prediction of the strength of rubberized concrete by an evolved random forest model. Advances in Civil Engineering, 2019, 1-7.

[12] Lang, L., Tiancai, L., Shan, A., & Xiangyan, T. (2021). An improved random forest algorithm and its application to wind pressure prediction. International Journal of Intelligent Systems, 36(8), 4016-4032.

[13] Fang, Y., Lu, X., & Li, H. (2021). A random forest-based model for the prediction of construction-stage carbon emissions at the early design stage. Journal of Cleaner Production, 328, 129657.

[14] Zhang, R., Guo, J., Yang, D., Shirakawa, H., Shi, F., & Tanikawa, H. (2022). What matters most to the material intensity coefficient of buildings? Random forest-based evidence from China. Journal of Industrial Ecology, 26(5), 1809-1823.

[15] Kim, J., Hatzis, J. J., Klockow, K., & Campbell, P. A. (2022). Building Classification Using Random Forest to Develop a Geodatabase for Probabilistic Hazard Information. Natural Hazards Review, 23(3), 04022014.

[16] Hoła, A., & Czarnecki, S. (2023). Random forest algorithm and support vector machine for nondestructive assessment of mass moisture content of brick walls in historic buildings. Automation in Construction, 149, 104793.

INTERNATIONAL SCIENTIFIC CONFERENCE
INTEGRATION, NOVELTY, DESIGN,
INTERDISCIPLINARITY, SUSTAINABILITY

iNDiS2023

SEISMIC DEMANDS FOR RIGID ANCILLARY ELEMENTS IN THE SECOND GENERATION OF EUROCODE 8

Vladimir Vukobratović[1]

Summary:

Ancillary elements basically refer to non-structural components and secondary systems (e.g., architectural, mechanical, electrical, and plumbing), and to building contents, not contributing to the bearing structure resistance. Part 1-2 draft of the second generation of Eurocode 8 contains significantly improved provisions related to seismic demands for ancillary elements compared to its predecessor. The determination of demands for rigid elements according to the draft new Eurocode 8 is presented in the paper, and its application is illustrated on a four-storey confined masonry building. It is shown that the numerical procedure is fairly simple, and that the seismic demands can be easily and quickly obtained, which is beneficial for everyday practice.

Key words: seismic demands, rigid ancillary elements, Eurocode 8, masonry building

[1] Assoc. Prof., Faculty of Technical Sciences, University of Novi Sad, Serbia, vladavuk@uns.ac.rs

1. INTRODUCTION

Ancillary elements basically refer to non-structural components and secondary systems (e.g., architectural, mechanical, electrical, and plumbing), and to building contents, not contributing to the structural resistance. The draft of the second generation of Eurocode 8 (Part 1-2) [1] contains significantly improved provisions related to seismic demands for ancillary elements compared to its predecessor. As a basic rule, ancillary elements whose failure poses a risk to human life or affects a main structure or services of facilities, shall, along with their supports, be verified to resist design seismic actions in two main orthogonal horizontal directions.

Seismic analysis should be based on a realistic model of a relevant structure, and on an appropriate floor response spectrum (FRS) derived by considering the response of the supporting structural members. Dynamic interaction between an ancillary element and a structure can be neglected when the element mass is smaller than the floor mass at least one hundred times, which is actually fulfilled in the majority of practical situations. In the opposite case, such an analysis (uncoupled) would lead to conservative results.

The goal of the paper is to show a simplified analysis procedure for the determination of seismic demands for rigid ancillary elements provided in [1]: cantilevering parapets or ornamentations, signs and billboards, chimneys and masts not taller than 4 m, elements with natural period not exceeding lower corner vibration period of the constant spectral acceleration range. Such elements are common in practice, and their seismic demands are primarily dependent on peak floor accelerations (PFAs).

2. SEISMIC DEMANDS FOR RIGID ANCILLARY ELEMENTS

According to [1], ancillary elements and their connections to the main structure should be verified for the seismic design situation in two main orthogonal horizontal directions. The effects of seismic action on ancillary elements in a considered horizontal direction may be determined by applying a force

$$F_{\mathrm{ap}} = \gamma_{\mathrm{ap}} m_{\mathrm{ap}} S_{\mathrm{ap}} / q'_{\mathrm{ap}} \tag{1}$$

where F_{ap} is the horizontal seismic force, acting at the ancillary element mass centre, in the most unfavourable direction; γ_{ap} is the performance factor of the element; m_{ap} is the element mass; S_{ap} is the FRS value; and q'_{ap} is the period-dependent behaviour factor of the element, defined as

$$q'_{\mathrm{ap}} = q_{\mathrm{ap,S}} q'_{\mathrm{ap,D}} \tag{2}$$

Ancillary element overstrength is considered through the behaviour factor component $q_{\mathrm{ap,S}}$, which can be taken as 1.3 unless another value is specified or documented, while deformation and energy dissipation capacities of the ancillary element are taken into account through the frequency-dependent behaviour factor component $q'_{\mathrm{ap,D}}$. The latter should be determined as

$$q'_{\mathrm{ap,D}} = \begin{cases} 1, & T_{\mathrm{ap}} \le T_{\mathrm{B}} \\ \text{linear between 1 and } q_{\mathrm{ap,D}}, & T_{\mathrm{B}} \le T_{\mathrm{ap}} \le 0.8T_{\mathrm{p1}} \\ q_{\mathrm{ap,D}}, & T_{\mathrm{ap}} \ge 0.8T_{\mathrm{p1}} \end{cases} \tag{3}$$

where T_{ap} is the natural period of the ancillary element; T_{B} is the lower corner vibration period of the constant spectral acceleration range; T_{p1} is the fundamental period of the building in the considered direction; and, unless properly documented or provided in the relevant parts of EN 1998, $q_{\mathrm{ap,D}}$ values should not exceed those given in Tab. 1.

As an alternative, in the case of a rigid-plastic ancillary element, having an acceptable displacement denoted as d_{ap}, q'_{ap} may be calculated as

$$q'_{\mathrm{ap}} = 1 + 5\left(\frac{d_{\mathrm{ap}}}{T_{\mathrm{p1}}^{2} a_{\mathrm{ap,R}}}\right)^{0.59} < 1.8 \tag{4}$$

where $a_{ap,R}$ denotes the acceleration capacity of the ancillary element, given by its force capacity $F_{ap,R}$, divided by its total mass m_{ap}.

Tab. 1 Maximum values of $q_{ap,D}$

<table>
<tr><th>Elements not able or not allowed to dissipate energy by inelastic deformation</th><td rowspan="4">1</td></tr>
<tr><td>Cantilevering parapets or ornamentations</td></tr>
<tr><td>Signs and billboards</td></tr>
<tr><td>Chimneys, masts, and tanks on legs, acting as unbraced cantilevers along more than one half of their total height</td></tr>
<tr><th>Elements dissipating energy by inelastic deformation</th><td rowspan="6">2</td></tr>
<tr><td>Exterior and interior walls</td></tr>
<tr><td>Partitions and façades, claddings, veneers</td></tr>
<tr><td>Chimneys, masts, and tanks on legs, acting as unbraced cantilevers along less than one half of their total height, or braced or guyed to the structure at or above their centre of mass</td></tr>
<tr><td>Anchorage elements for permanent cabinets and book stacks supported by the floor</td></tr>
<tr><td>Anchorage elements for false (suspended) ceilings and light fixtures</td></tr>
</table>

For out-of-plane assessment of ancillary masonry walls, in the cases of unreinforced and confined ones $q_{\mathrm{ap,D}} = 1.25$, whereas in the case of reinforced ones $q_{\mathrm{ap,D}} = 1.5$.
It can be seen that in the draft new Eurocode 8 the nonlinearity of ancillary elements is taken into account explicitly, through the factor q'_{ap}, which is applied at the very end of the F_{ap} determination. It should be noted though that, at least in the draft cited here [1], the definition of q'_{ap} is such that the force reduction is mainly related to the fundamental mode. Such an approach is acceptable in the case of rigid ancillary elements considered herein, but leads to conservative results for non-rigid elements, for which higher modes of structural vibrations influence the response and demands.
The floor acceleration spectral (FRS) values S_{ap} should be determined for each of the two considered horizontal directions. When FRS are determined in the whole range of periods, the S_{ap} value at the floor j, denoted as $S_{ap,j}$, in the considered direction, should correspond to T_{ap} and the ancillary element damping of 2%, which is the default value in [1] (values ≠ 2% are also permitted). In some other standards, e.g., in ASCE 7-22 [2], the default damping value for non-structural elements is set to 5%, although 2% has been considered as an option [3].
For rigid ancillary elements, in the considered direction, at the floor j, the $S_{ap,j}$ value can be determined as

$$S_{\mathrm{ap,j}} = \Gamma_1 \frac{z_{\mathrm{j}}}{H} \frac{\eta S_{\alpha}}{q'_{\mathrm{D}}} \geq \frac{S_{\alpha}}{F_{\mathrm{A}}} \tag{5}$$

which is a special case that corresponds to $T_{ap} = 0$, i.e., to an infinitely rigid ancillary element (the PFA governs the seismic demand). S_α is the value at the plateau of the elastic response spectrum; η is the coefficient accounting for building damping ($\eta = 1.0$ for 5% damping); and z_j/H defines the vertical position of the floor j. The participation factor of the fundamental mode Γ_1 may be determined by the simplified formula $\Gamma_1 = 3N_s/(2N_s + 1)$, where N_s is the number of storeys. F_A is the ratio between S_α and peak ground acceleration PGA, so the PGA represents the lower bound for floor accelerations [4]. q'_D is the period-dependent behaviour factor for the building structure, commonly denoted as R_μ in the literature, which can be determined as

$$q'_D = \begin{cases} 1, & T_{p1} \leq T_A \\ \text{linear between 1 and } q_D, & T_A \leq T_{p1} \leq T_C \\ q_D, & T_{p1} \geq T_C \end{cases} \quad (6)$$

where q_D is the component of the building behaviour factor accounting for deformation and energy dissipation capacities, and is provided in the draft new Eurocode 8 for different structural systems and different materials; and T_A and T_C are corner periods in the response spectrum, i.e., T_A is the period where the spectrum starts to increase from the PGA value, whereas T_C is the period at the end of the plateau. Behaviour factor q'_D should be determined only for the fundamental vibration mode, while for higher modes (which are irrelevant for rigid ancillary elements) $q'_D = 1$.
In the end, the value of the performance factor γ_{ap} of ancillary elements should not be smaller than 1. Except for elements participating to safety systems (anchorage elements of machinery or equipment), for which, in general, $\gamma_{ap} = 1.5$ can be used, the value of γ_{ap} should be set to 1.

3. FRS FOR NON-RIGID ANCILLARY ELEMENTS

If an ancillary element does not meet the criteria to be classified as a rigid one, FRS should be determined in the whole period range, according to the normative Annex C of [1]. The procedure for the FRS determination is mainly based on the direct FRS method developed by Vukobratović and Fajfar (VF) [5]. The details of the Eurocode 8 approach and the VF method are not provided herein, but their main differences are:

- in the VF direct method, the nonlinear behaviour of ancillary elements is taken into account through an increased damping (10% and 20% for element ductilities of 1.5 and 2, respectively), and, as said above, in the draft new Eurocode 8 it is taken into account explicitly, through the factor q'_{ap}; and
- the reduction of seismic demands due to an ancillary element nonlinear behaviour is taken into account in the whole period range in the VF direct method, whereas it is limited mainly to the fundamental mode in the draft new Eurocode 8, which leads to conservative results in the cases of non-rigid ancillary elements whose response and demands also depend on higher structural modes.

In the procedure for the FRS determination provided in Annex C of [1], the S_{ap} values at floors of interest should be determined for all considered modes, and should then be combined in order to obtain the resulting FRS. Out of resonance regions, the procedure is based on the theory of structural dynamics, whereas in resonance regions empirical values and well-established approaches are used for considering nonlinear effects.

4. NUMERICAL EXAMPLE

In order to illustrate the determination of seismic demands for rigid ancillary elements according to the draft new Eurocode 8, a confined masonry building typical for Serbian practice is considered, along with an appropriate seismic input.

4.1. STRUCTURE AND SEISMIC INPUT

A four-storey confined masonry building was designed for vertical loads according to the provisions of Eurocode 6 (Part 1-1 [6]). Besides the building self-weight, additional

dead load applied at every floor amounted to 1.5 kN/m^2, variable load applied at every floor (except roof) was equal to 2.5 kN/m^2, and the snow load considered on the roof was taken as 1.0 kN/m^2. Three-dimensional model of the building, and the layout of the characteristic storey (the dimensions are in cm), is shown in Fig. 1 (adapted from [7]).
Storey heights are 320 cm, and all masonry walls are 25 cm thick, with the clear height of 300 cm. They are designed in hollow clay blocks belonging to Group 2 (f_b = 11.5 MPa), with the general purpose mortar M5 (f_m = 5 MPa). The characteristic compressive strength (f_k) of the wall amounts to 4.0 MPa, modulus of elasticity (E) is equal to 4,000 MPa, and shear modulus (G) equals 1,600 MPa. In the case of the confining elements, concrete C25/30 (f_{ck} = 25 MPa) was used, with the steel S500 (f_y = 500 MPa). Vertical confining elements have a square cross-section 25/25 cm, and they are reinforced with four 14 mm diameter longitudinal bars, and 6 mm diameter stirrups spaced at 15 cm. Horizontal confining elements have a rectangular cross-section 25/20 cm, and they are reinforced in the same way as the vertical ones. Solid concrete slabs (C25/30) of 20 cm depth were designed in all storeys, including the roof. It is adopted that $q'_{\mathrm{D}} = 2$.

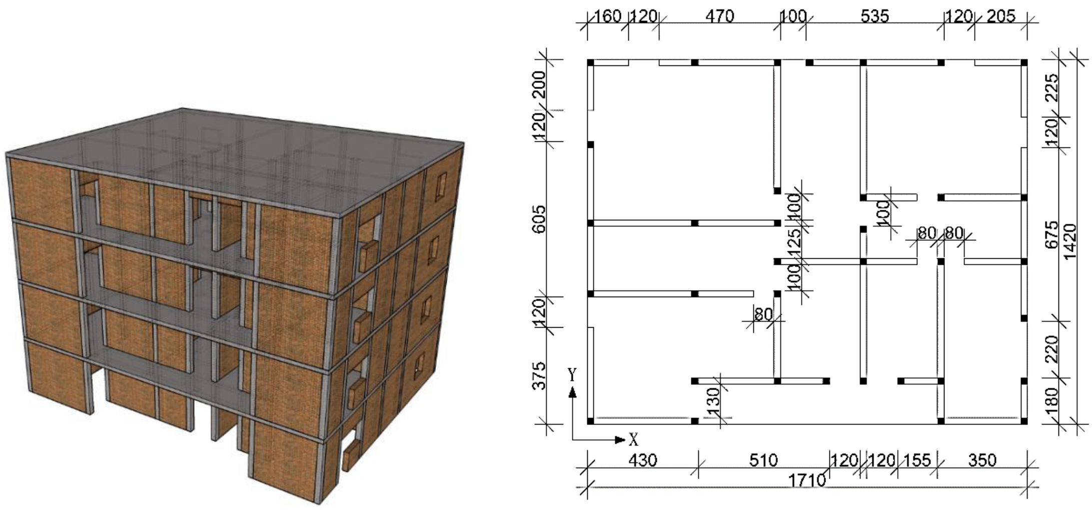

Fig. 1 Three-dimensional model of the building (left) and the characteristic storey layout (right)

Seismic hazard in the draft of the second generation of Eurocode 8 (Part 1-1) [8] is represented with the reference maximum spectral acceleration $S_{\alpha,\mathrm{ref}}$, which corresponds to the constant acceleration range of the horizontal 5%-damped elastic response spectrum, and on the reference spectral acceleration $S_{\beta,\mathrm{ref}}$ at the vibration period T_β = 1 s of the horizontal 5%-damped elastic response spectrum, both on site category A and for the return period T_{ref}. By considering that T_{ref} = 475 years, and maps provided in Annex A of [8], it is adopted that $S_{\alpha,475}$ = 0.25 g and $S_{\beta,\mathrm{ref}}$ = 0.05 g. By considering site category C (site factor 1.5), along with regular topography, it is obtained that S_α = 0.38 g. Finally, according to [8], the value of F_A (the ratio of S_α with respect to the zero-period spectral acceleration), needed for the calculation of the S_{ap} lower limit, amounts to 2.5.

4.2. RESULTS

For the sake of simplicity, the following is assumed: m_{ap} = 1 t, γ_{ap} = 1, $q'_{\mathrm{ap,D}} = q_{\mathrm{ap,D}} =$ 1 (elastic ancillary elements), and $q_{\mathrm{ap,S}} = 1.3$, resulting in $q'_{\mathrm{ap}} = 1.3$. Furthermore, it is assumed that structural damping amounts to 5% (η = 1.0), and considering the number of storeys, it yields that Γ_1 = 1.33.
The obtained results are presented in Tab. 2. It can be seen that seismic demands at the lowest three levels are governed by the lower limit defined by the PGA (S_α/F_A).

Tab. 2 Seismic demands for the assumed properties of ancillary elements

<table>
<tr><th>Floor</th><th>z_j/H</th><th>$\eta S_\alpha/q'_D$ [g]</th><th>S_α/F_A [g]</th><th>S_{ap} [g]</th><th>F_{ap} [kN]</th></tr>
<tr><td>4 (roof)</td><td>1</td><td rowspan="5">0.19</td><td rowspan="5">0.15</td><td>0.25</td><td>18.8</td></tr>
<tr><td>3</td><td>0.75</td><td>0.19</td><td>14.3</td></tr>
<tr><td>2</td><td>0.50</td><td rowspan="3">0.15</td><td rowspan="3">11.3</td></tr>
<tr><td>1</td><td>0.25</td></tr>
<tr><td>0 (ground)</td><td>0</td></tr>
</table>

5. CONCLUSIONS

The determination of seismic demands for rigid ancillary elements according to the draft new Eurocode 8 is presented, and its application is illustrated on a four-storey confined masonry building and seismic input typical for Serbian practice. It is shown that the procedure is fairly simple, and that the demands can be easily and quickly obtained, which is beneficial for everyday practice.

ACKNOWLEDGEMENT

This research has been supported by the Ministry of Science, Technological Development and Innovation through project no. 451-03-47/2023-01/200156 "Innovative scientific and artistic research from the FTS domain".

REFERENCES

[1] CEN (2022). prEN 1998-1-2 Eurocode 8 — Design of structures for earthquake resistance — Part 1-2: Buildings (working draft). European Committee for Standardization, Brussels.

[2] ASCE (2021). Minimum Design Loads and Associated Criteria for Buildings and Other Structures. Structural Engineering Institute of American Society of Civil Engineers, Reston, VA.

[3] ATC (2018). NIST GCR 18-917-43: Recommendations for improved seismic performance of nonstructural components, National Institute of Standards and Technology, Gaithersburg, MD.

[4] Fajfar P., Vukobratović V. (2022). Floor Acceleration Spectra: From Research to Seismic Code Provisions. *Fifth International Workshop on the Seismic Performance of Non-Structural Elements*, Stanford University, Palo Alto, CA, 5-7 December, pp. 2-14–2-26.

[5] Vukobratović V., Fajfar P. (2017). Code-oriented floor acceleration spectra for building structures. *Bulletin of Earthquake Engineering*, Volume 15, Issue 7, pp. 3013–3026. https://doi.org/10.1007/s10518-016-0076-4.

[6] CEN (2005). EN 1996-1-1 Eurocode 6: Design of masonry structures — Part 1-1: General rules for reinforced and unreinforced masonry structures. European Committee for Standardization, Brussels.

[7] Manojlović D., Jovanović Đ., Vukobratović V. (2018). Pushover analysis of a four-storey masonry building designed according to Eurocode. *14th International Scientific Conference iNDiS – Planning, Design, Construction and Building Renewal*, Faculty of Technical Sciences, Novi Sad, Serbia, 21-23 November, pp. 547–554.

[8] CEN (2021). prEN 1998-1-1 Eurocode 8 — Design of structures for earthquake resistance — Part 1-1: General rules and seismic action (working draft). European Committee for Standardization, Brussels.

CONSTRUCTION COST ANALYSIS OF RURAL TOURISM FACILITIES

Dragana Stanojević[1], Vladimir Mučenski[1], Mirjana Terzić[1], Milena Senjak Pejić[1], Igor Peško[1], Milan Trivunić[1]

Summary:

The construction of rural tourism facilities is a specific type of construction project process that requires careful planning and efficient resource management. One of the key processes preceding the construction of such facilities is the cost prediction of construction projects, The objective of this analysis is to provide insights into the costs of constructing of rural tourism facilities according to groups and types of works based on the established database. Aim is to identify the factors that have the greatest impact on overall costs and provide guidelines for efficient cost management. Within the analysis, key types of works have been identified, encompassing the construction of rural tourism facilities, such as rough construction works, finishing works, installations, and landscaping works. Based on the results of this research, conclusions have been drawn regarding the percentage contribution of individual work groups, as well as the most significant factors influencing the costs of rural tourism facility construction.

Key words: Construction, Costs, Rural Tourism, Facilities.

[1] University of Novi Sad, Faculty of Technical Sciences, Department of Civil Engineering and Geodesy, Novi Sad, Serbia

1. INTRODUCTION

The construction industry, as a large consumer of resources, belongs to a complex sector of the economy that includes a wide range of stakeholders, as it creates demand for the production of goods and services associated with other related industries. According to a literature review, construction activities affect almost every aspect of the economy [1]. The biggest problem in the construction industry is cost or budget overruns. According to McKinsey [2], 98% of large construction projects exceed costs by more than 30%. Overruns are often caused by poor cost estimation during the planning phase. In order to solve the mentioned problems, construction economics deals with methods that enable economic decisions to be made in order to reduce costs, optimize available resources and maximize organization. Due to the complexity and volume of modern construction projects, there is a need for tools that would optimize construction processes in order to save time and money [2], [3].

Project size, technology requirements, project location, choice of materials, type of construction, terrain configuration, site equipment, and access to the site are just some of the factors that affect construction project costs [5]. Cost analysis is very important for the construction sector for the above reasons. It provides designers and investors with a better insight into the flow of funds spent and how to manage them more efficiently during the construction of buildings. In order to conduct a cost analysis of a construction project, it is necessary to break down the costs according to groups and types of work and then assess which of them has the greatest impact on the total price.

This research aims to analyze the costs of different types of work during the construction of rural tourism facilities and discuss the key factors that shape costs in residential and tourist facilities. Costs are analyzed according to groups of works such as rough, finishing and installation works. At the same time, the percentage participation of certain groups in relation to others is given, looking at the total construction costs.

2. METHODOLOGY

The cost analysis presented in the paper refers to selected construction cases of facilities to provide tourist services. The database necessary for the analysis was created for ten buildings based on technical documentation, more specifically, a design for a building permit with a detailed estimate and estimate of works.

Based on the created database, the relevant data on the objects related to dimensions and construction are presented in a table, which can be seen in Table 1. Within this research, various parameters were analyzed to specify the characteristics of the objects under study more clearly. Among the key parameters that were the subject of the analysis is the GROSS area that ranges from 70.13 m2 to 480.85 m2, width-a, length of buildings-l, total height-h, and number of floors. The construction of buildings, structural systems, type of foundation, wall and ceiling materialization were further analyzed.

The cost analysis was performed according to groups of works such as rough construction, finishing, and installations (water supply and sewerage, thermo-technical and electrical installations). The structure of construction costs of rural tourism facilities is shown in Table 2.

Tab. 1 Description of facilities

No.	Bruto P [m2]	Object dimensions				Type and description of construction	
		a [m]	l [m]	h [m]	storey	type	foundations; wall; floor construction
1	70.13	5,48 +2,30	9.12	4.65	P	massive	strip; block; ribbed slab + wooden
2	89.61	5.76	1.88+ 2.1	7.77	P+Pk	skeletal (timber construction)	strip; wooden planks; wooden
3	92.49	8.9	9.10	6.21	P+Pk	skeletal	strip; block; ribbed slab
4	115.92	8.00	6.30	6.54	P+Pk	massive	strip; block; ribbed slab
5	116.48	8.08	10.71	6.92	P+Pk	massive (cabin)	strip; log + paneling + gypsum board; wooden
6	136.08	7.70	7.70	6.67	P+Pk	massive	strip; block; ribbed slab
7	155.95	9.85	8.70	8.29	Su+P+ Ga	skeletal	strip; block + RC (basement); ribbed slab+flat plate+ wooden
8	167.00	9.85	17.06	2.92	P	massive	strip; block; ribbed slab
9	168.17	7.00	11.00	8.63	Po+P+ Pk	massive (timber girders)	strip; facade panels + gypsum board; wooden
10	347.00	10.90	14.25	5.72	P	massive	strip; block; ribbed slab

Tab. 2 Costs by type of work expressed in dinars

No.	Construction works		Installations		
	Rough	Finishing and Craftsmanship	Plumbing and sewerage	Mechanical	Electrical
1	2,945,960.00	2,267,580.00	303,500.00	91,400.00	286,700.00
2	7,314,200.40	5,349,792.00	1,351,500.00	493,570.00	719,881.00
3	2,919,301.45	4,444,060.70	218,124.35	687,224.20	549,452.72
4	4,660,400.00	3,604,800.00	530,000.00	115,800.00	582,200.00
5	4,241,994.00	2,361,335.00	262,693.00	201,000.00	386,970.00
6	6,518,549.90	4,717,044.10	361,000.00	288,550.00	759,140.00
7	3,929,093.80	4,128,564.80	588,162.00	1,714,913.00	1,363,672.00
8	9,247,042.50	3,634,996.00	970,480.00	282,988.00	930,280.00
9	4,604,340.00	6,192,843.00	403,608.00	504,510.00	1,862,949.00
10	10,773,256.30	4,682,174.00	1,967,390.00	2,191,828.00	798,570.00

3. RESULTS AND DISCUSSION

Cost analysis showed that a significant part of the total investment costs belongs to the construction part, which participates with 69-89%, while the MEP part (water supply and sewerage installations, electrical installations and thermo-technical installations) makes up 11-31%, depending on the specific project. The percentage representation of costs according to groups of works may vary depending on different parameters of the facilities, as seen in Table 3.

Tab. 3 Percentage representation of expenses by groups %

No.	Construction works		Installations		
	Rough	Finishing and Craftsmanship	Plumbing and sewerage	Mechanical	Electrical
1	50%	38%	5%	2%	5%
2	48%	35%	9%	3%	5%
3	33%	50%	2%	8%	6%
4	49%	38%	6%	1%	6%
5	57%	32%	4%	3%	5%
6	52%	37%	3%	2%	6%
7	34%	35%	5%	15%	12%
8	61%	24%	6%	2%	6%
9	34%	46%	3%	4%	14%
10	53%	23%	10%	11%	4%

The percentage representation of costs was determined in more detail by analysing the data according to the types of work. Based on the obtained results, the mean value of the percentage representation of costs according to the types of works was determined for all ten facilities, as seen in Table 4. The average percentage representation of the costs of rough construction works is 46.97%, of which concrete and reinforce concrete (RC) works stand out, making up 15.17% of the total costs, followed by carpentry and masonry, which make up 11.72% and 11.06%, respectively. As for final crafts, the average percentage representation is 35.21%. The costs for installing construction carpentry and locksmithing with 10.19% and facade work with 5.18% are separately allocated within this group of works. Works on water supply and sewage installations occupy 5.25% of total costs, among which works on the installation of sanitary devices stand out the most with 3.36% representation. The average percentage representation of thermo-technical installations is 4.93%, and heating installations contribute the most with 4.32%. Regarding electrical installations, their costs comprise 7.88% of total costs, among which power supply has the greatest impact.

Tab. 4 The mean value of the percentage representation of costs by type of work per m2 of area for ten buildings, expressed in %

No.	Types of works	The mean value of the percentage representation of costs for all 10 facilities
Construction works	Rough	46.97%
	Preparatory and final works	1.31%
	Dismantling and demolition	0.09%
	Ground works	3.25%
	Concrete and RC works	15.18%
	Masonry	11.06%
	Insulation works	4.36%
	Carpenter	11.72%
	Finishing and Craftsmanship	35.21%
	Construction carpentry and locksmithing	10.19%
	Roofing works	3.67%
	Sheet metal works	1.19%
	Ceramic works	4.65%
	Floor laying works	2.42%
	Dry construction works	1.32%
	Facade works	5.81%
	Painting works	2.21%
	Stone cutting works	0.33%
	Various works	2.89%
	Glass cutting works	0.34%
	Assembly works	0.19%
Installations	Plumbing and sewerage	5.25%
	Preparation works	0.03%
	Water supply installations	0.98%
	Sewage installations	0.71%
	Sanitary devices	3.36%
	Other works	0.18%
	Mechanical	4.93%
	Heating	4.32%
	Ventilation	0.34%
	Air condition	0.28%
	Electrical	7.88%
	Power supply	7.62%
	Structural system	0.25%

By evaluating the costs of construction works in the studied facilities, it can be noted that the construction of the facility's structure, followed by the finishing and finishing of the facility, significantly impacts the total cost of the works. As far as installation works are concerned, electrical installations have the predominant influence on the investment, followed by water and sewage installations, all depending on the needs of the building. In the following text, the costs will be analyzed in more detail according to the groups of works and by m2 of the object's surface, which can be seen in Table 5.

Tab. 5 The cost of a group of works per m2 of area in din/m2

No.	Construction works		Installations		
	Rough	Finishing and Craftsmanship	Plumbing and sewerage	Mechanical	Electrical
1	42,007.13	32,333.95	4,327.68	1,303.29	4,088.12
2	81,622.59	59,700.84	15,082.02	5,507.98	8,033.49
3	31,563.43	48,049.09	2,358.36	7,430.25	5,940.67
4	40,203.59	31,097.31	4,572.12	998.96	5,022.43
5	36,418.22	20,272.45	2,255.26	1,725.62	3,322.20
6	47,902.34	34,663.76	2,652.85	2,120.44	5,578.63
7	25,194.57	26,473.64	3,771.48	10,996.56	8,744.29
8	55,371.51	21,766.44	5,811.26	1,694.54	5,570.54
9	27,379.08	36,824.90	2,400.00	3,000.00	11,077.77
10	31,046.85	13,493.30	5,669.71	6,316.51	2,301.35

3.1. ROUGH WORKS

Within the framework of investments in rural tourism, rough works represent a key aspect that predominantly has the greatest impact on total costs, which was confirmed by comparing the costs of groups of works per m2 of building area. These works cover various activities and represent the basic structure on which all other works are based. Different works have been identified within the rough work group, including preparatory, preliminary, earth, concrete, reinforcement, masonry, carpentry, and insulation. The shares of the mentioned types of works in the total investment may vary in completion due to certain factors and characteristics of the facilities.

From the data shown in Table 5, it can be concluded that the largest share in the costs of rough construction works per m2 of the building surface belongs to building number 2, with a price of 81,622.59 din/m2. The observed building is of the bungalow type, and its primary structural elements are made of wood, which indicates an increased volume and cost of carpentry work. The cost of the carpentry works of the observed building was most influenced by the construction of the hand-built construction of the walls, as well as the construction of the porch.

On the other hand, buildings numbered 8 and 3 require significant financial expenditures for concrete and reinforcement works due to the large investment in the construction of the foundation structure. Larger foundation depths in a certain part of the building, due to the configuration of the terrain, are one of the key reasons that affect the scope and cost of reinforced concrete works in the mentioned projects.

The investment amount can depend a lot on the masonry work, which is especially pronounced in the case of masonry buildings. The construction of load-bearing and partition walls and the plastering process are key items that significantly affect the total costs of the building, as is the case with building number 6.

3.2. FINAL CRAFT WORKS

As part of the analysis of finishing crafts, it is important to point out that different aesthetic and qualitative design requirements vary according to the object's specific function and architectural form, which significantly affects the volume and unit price of these works. It is especially important to note that, in the context of facilities intended for the tourism and hospitality industry, factors such as comfort and aesthetics play a key role in increasing the cost of finishing works. Different types of work have been identified within the finishing crafts group, including facade, masonry painting, ceramics, glass cutting, carpentry, locksmith, tinsmith, sub-laying, roofing, dry assembly, and other works.

From the data shown in Table 5, can be seen that building numbered two stands out for the highest costs of finishing work, with a price of 59,700.84 din/m2 of the building area. As already mentioned, the observed object is of the bungalow type. In the case of this building, facade works makeup about 50% of the total costs of the finishing works, which is a consequence of covering a large area of the facade with wooden planks.

A similar case occurs with the object numbered 3, with a price of 48,049.09 din/m2 of the object's surface. In this case, apart from the cost of covering the facade with wooden planks, the work of laying stone cladding also greatly impacts the price. The next type of work issued at this facility is the installation of construction carpentry and locksmithing. This type of work appears in many projects as a significant factor that affects the price, as seen in Table 4. Building carpentry and locksmithing contribute to the cost of making external carpentry of terraces and various window constructions such as glazed window displays, fixed partitions, panel doors or installation of sliding windows.

Some of the projects contain specific elements which increase the cost of finishing works, such as a fireplace or a prefabricated, retrofitted staircase, which is the case in building number 9, with a price of 36,824.90 din/m2. The staircase price increases further when covering the tread with different materials or installing a stainless steel, glass or wood fence.

3.3. INSTALLATION OF WATER PLUMBING AND SEWERAGE

Water supply and sewage installations are vital parts of every building. They enable the supply of clean drinking water and the efficient removal of wastewater, making facilities functional and hygienically safe. When considering the costs, the level of detail includes installations related to the building only, without considering the installation of ground floor arrangements, such as installing facilities such as septic tanks, inspection shafts or wells. Within the group of water supply and sewerage installations, works on the construction of the water supply and sewerage network and works on the installation of sanitary devices and equipment were identified. Comparing the costs by type of work, is evident that work on installing sanitary devices is the most demanding budgetary resource. If one were to compare the costs of building a water supply and sewerage network, one could notice that higher investments are needed in constructing a water supply network than sewage.

Table 5 shows a significant cost jump for object number 2, with a price of 15082.02 din/m2. The bungalow-type building is separate from the city's water and sewer network, which results in increased construction costs for this type of installation. The costs were additionally increased due to the performance of preparatory and final works on the sewerage and water supply network and sanitary devices. Geodetic surveying of works on constructing the water supply and sewerage network was also carried out. All these positions together contribute significantly to the costs of this group of works.

According to Table 5, it can be noted that the building numbered 8, with a price of 5,811.26 din/m2, also deviates from the average. This particular building contains as

many as three bathrooms. Therefore, the number and price of sanitary devices are significantly higher than other buildings, making the investment more expensive.
Immediately below object number 8, object number 10 stands out, with a price of 5,669.71 din/m2 of surface area. The costs of this facility are increased due to having a jacuzzi. The price of the jacuzzi is 3,779.82 din/m2. These data indicate that the jacuzzi accounts for 66% of the total costs of this group of installations in the observed facility.

3.4. HVAC INSTALLATIONS

In the context of rural tourism, thermo-technical installations play a key role in providing comfort and convenience. This group of works includes heating, air conditioning, ventilation, and solar installations. By analyzing different buildings, it was observed that those with a larger area require more complex systems for temperature regulation, including the installation of heat pumps, underfloor heating, boiler rooms or fan-coil devices. Although the initial costs of these investments can be significant, the payback is reflected in the long-term savings in energy consumption compared to conventional air conditioners and heaters.
A big jump in the price of thermo-technical installations was observed at the object numbered 7, with a price of 10,996.56 din/m2. In this facility, the investment is significantly influenced by the price of the boiler room, which accounts for about 65% of the total costs of thermo-technical installations.
A similar case occurs in the facility number 3, where boiler installations also cause large expenditures.
Based on Table 5, it can be seen that the high cost of the installation is also noticeable in the building numbered 10, with a price of 6,316.51 din/m2. The price was significantly influenced by the installation of the elements of the substation with accessories, which also includes the costs of installing the heat pump. This type of installation accounts for half of the investment of thermo-technical installations. Also, it should be noted that a significant factor in this building is the installation of the FAN-COIL system, which additionally increases the total costs by 1,506.15 din/m2 of the building's surface.

3.5. ELECTRICAL INSTALLATIONS

Electrical installations in buildings are crucial for providing electricity and the functionality of the building. This group of works includes the installation of electrical networks, more precisely, the installation of sockets, switches, power cables, junction boxes, switchboards, and cabinets. Also, electrical installations include lighting, telecommunications, signalling, and lightning protection installations. When looking at the costs of electrical installations, the work on the installation of the entire electrical network and the installation often make up the largest part of the total electrical work, especially in the case of the required lighting needs.
According to Table 4, it can be observed that the building under serial number 9 significantly jumps compared to the average, with a price of 11,077.77 din/m2. The costs of this facility are significant due to the installation of certain devices, such as a photovoltaic power plant, which significantly increases the cost of electrical installations. The price of this type of device accounts for two-thirds of the total cost of electrical installations and amounts to 7,377.77 din/m2 of the object's surface.
Regarding buildings numbered 2 and 7, the investment price is high due to the significant investment in lighting.

4. CONCLUSION

The goal of the research is to analyze the costs of building rural tourism facilities, focusing on identifying key factors that significantly influence the total cost of facilities. The analysis was carried out based on the created database of objects. The database was designed with the help of relevant technical documentation and detailed estimates and estimate of works. The created database includes detailed descriptions of objects and information on the costs of groups of works.

Analyzing the objects of rural tourism, we conclude that the price of the objects from the database varies from 58,827.72 din/m2 to 95,341.80 din/m2, whereby rough works are singled out from the group of construction works whose price varies from 25,194.57 din/m2 to 55,371.51 din/m2, which accounts for 34% to 61% of total costs. Looking at the costs from the group of installation works, the works on electrical installations stand out as the most influential, the price of which varies from 2,301.35 din/m2 to 11,077.77 din/m2, which accounts for 4% to 14% of the total costs.

The cost varies depending on various parameters, including engineering features such as the construction of the facility, topography of the terrain, aspects of aesthetics, and level of service.

Understanding these parameters is essential not only for effective project management but also for contributing to sustainable development.

ACKNOWLEDGEMENT

This research (paper) has been supported by the Ministry of Science, Technological Development and Innovation through project no. 451-03-47/2023-01/200156 “Innovative scientific and artistic research from the FTS (activity) domain”.

REFERENCES

[1] Renata S.-B., Marek P. (2015). Construction Costs Analysis and its Importance to the Economy. *Procedia Economics and Finance*, Volume 34, pp. 35–42, https://doi.org/10.1016/S2212-5671(15)01598-1.

[2] https://www.mckinsey.com/~/media/McKinsey/Industries/Capital%20Projects%20and%20Infrastructure/Our%20Insights/The%20construction%20productivity%20imperative/The%20construction%20productivity%20imperative.pdf Website sccessed:08.10.2023.

[3] Dian L., Heng L., Hongwei W., Chao Q., Timothy R. (2020). Discrete symbiotic organisms search method for solving large-scale time-cost trade-off problem in construction scheduling. *Expert Systems with Applications*, Volume 148, p. 113230, https://doi.org/10.1016/j.eswa.2020.113230.

[4] Santosh M., Lyes B., Young-J. S., M.K.T. (2013). A fuzzy clustering-based genetic algorithm approach for time–cost–quality trade-off problems: A case study of highway construction project. *Engineering Applications of Artificial Intelligence*, Volume 26, Issue 8, pp. 1953–1966, https://doi.org/10.1016/j.engappai.2013.05.006.

[5] https://www.tebodin.bilfinger.com/fileadmin/tebodin/Facelift_News/2020/BILFINGER_TEBODIN_Cost_analysis_CEE_2019.pdf Website accessed: 08.10.2023.

FINITE ELEMENT ANALYSIS OF CFRP CONFINED CONCRETE CYLINDERS

Goran Chapragoski[1], Golubka Nechevska-Cvetanovska[2]

Summary:

The utilization of carbon fibre-reinforced polymer (CFRP) jackets as external confinement is gaining popularity, especially in seismic areas, owing to their ability to enhance the strength and ductility of reinforced concrete. This study introduces enhanced models specifically designed for cylindrical concrete members wrapped with CFRP. In this case, CFRP sheets with fibres perpendicular to the element axis were installed on the concrete cylinders. Based on the previous experimental work of CFRP-wrapped concrete cylinders, the proposed model was verified using finite element analysis (FEA), performed in the computer program ABAQUS. The comparison between the finite element analysis and experimental results revealed a notable agreement. The average percentage deviations between the experimental and FEA outcomes were attributed to variations in testing conditions, assumptions made during the analysis, and the precision of the testing instruments.

Key words: CFRP material, finite element analysis, confining, modelling

[1] Ass., M.Sc., Ss. Cyril and Methodius University in Skopje, IZIIS, R. N. Macedonia, e-mail: goran@iziis.ukim.edu.mk
[2] Professor, Ss. Cyril and Methodius University in Skopje, IZIIS, R. N. Macedonia, e-mail: golubka@iziis.ukim.edu.mk

1. INTRODUCTION

The structural system of a number of new and existing RC structures built in seismically prone regions needs to be strengthened and/or repaired. The majority of the reasons are due to poor material quality and failing to meet modern seismic design standards. Recently, in earthquake regions, advanced FRPs are being used for the urgent retrofitting, rehabilitation and strengthening of damaged structures. It is due to the advantages of increasing the ductility and strength of reinforced concrete (RC) columns wrapped with externally FRPs confinements. The increase in axial strength and strain of RC columns is the main reason for the attraction of the use of FRP confinements (Hollaway et al. 2004). According to Seffo et al. 2012, the confinement of FRP is affected by the elastic modulus of FRP (Ef), the thickness of FRPs, the orientation angle of FRP wraps, and the unconfined strength of concrete material (f'co). In fact, the increase in strength and ductility of concrete members after FRPs wrapping is due to the confinement and prevention of the lateral expansion of concrete material. When the FRP wrapping resists lateral expansion, the concrete would be subjected to multiaxial loads, so this confinement effect is more pronounced in a triaxial state (Ann et al. 2013).

Analytical studies using finite elements are becoming more common due to the complexity of the strengthened cross-section created by using FRP material, laboratorial boundary conditions, and required time (Abed et al. 2020; Kadhim and co. 2020). In this study, analytical models for the axial strain of confined concrete compression members (cylinders) were proposed based on the experimental laboratory investigations. These models played a significant role in predicting the approximate analysis results.

2. LABARATORY TESTS OF CFRP CONFINED CONCRETE CYLINDERS

In order to see the CFRP confining effect of concrete cylinder subjected to axial load, experimental tests on six cylinders were performed. Three of them were referent concrete cylinders, while the other three were concrete cylinders wrapped with CFRP material. The CFRP materials were installed with the fibres set in perpendicular direction along the element axis. The cylinders were with dimension of 150mm diameter and 300mm height. All of them were exposed to monotonously increasing compressive force up to failure (Figure 1) (Roshi, A. 2020). The characteristics of the CFRP material are given in the table 1.

Tab. 1 Characteristics of the CFRP material

CFRP sheets with fibres in one direction	Parameters
Module of elasticity (KN/mm^2)	240
Fibres tensile strength (N/mm^2)	3800
Fibre weight (g/m^2)	300
Density (g/cm2)	1.7
Thickness (mm)	0.176
Maximal dilatation of fibre rupture (ε_{max} -%)	1.55

The Laboratory for Mechanical Testing within the Institute for Testing Materials and Development of New Technologies "Skopje", ZIM "Skopje" AD Skopje was responsible for the execution of the experimental tests. On the figure 1 the experimental investigations from preparation of the models up to axial compression are presented.

Fig. 1 Unconfined and confined concrete cylinder subjected to axial compression

Based on the results obtained, it was concluded that the force inducing failure of concrete cylinders without CFRP amounts to 296kN, while for the cylinder with one CFRP layer, it amounts to 670kN. In other hand, the compressive strength amounts to 17Mpa for the concrete cylinder and 38Mpa for the CFRP confined cylinder (Table 2).

Tab. 2 Compressive strength and modulus of elasticity of concrete cylinders obtained experimentally

Series	Dimensions [cm]	Weight [g]	Force [t]	Compressive strength [MPa]	Modulus of elasticity [MPa]
Referent concrete cylinder	15/30	12200	29.6	17	28200
Concrete cylinder with one layer of CFPR	15/30	12700	67	38	33000

The most relevant for estimation of the static modulus of elasticity is the mean value of the recorded entries of strain gages, after dissolution in the last cycle. For these estimations, the following formulas were used:

$$[\Delta\sigma = \sigma_A - \sigma_B] \; ; \; \left[\Delta\varepsilon = \frac{\Delta l}{l}\right] ; \quad \left[E = \frac{\Delta\sigma}{\Delta\varepsilon}[MPa]\right] \; ; \; E_b = 9.25x\sqrt[3]{f_{bk}+10} \qquad (1)$$

All the results obtained for all three series of concrete cylinders are presented in the table 3.

Tab. 3 Compressive strength and modulus of elasticity of concrete cylinders obtained empirically

Series	Dimensions [cm]	Weight [g]	Force [t]	Compressive strength [MPa]	Modulus of elasticity [MPa]
Referent concrete cylinder	15/30	12200	29.6	16.759	27667
Concrete cylinder with one layer of CFPR	15/30	12700	67	37.933	33601

3. FINITE ELEMENT ANALYSIS (FEA) OF THE CONCRETE CYLINDERS

Numerical models and their results are validated based on the experimental investigations. The finite element modelling of cylinders was done using the commercial software ABAQUS, based on the parameters obtained during the experimental examined models. A control cylinder was used to propose a numerical model after the calibration of different parameters such as dilation angle, viscosity parameter of concrete, mesh size and element types of the concrete. The behaviour of concrete was simulated by using concrete damaged plasticity (CDP) model (Table 4).

Tab. 4 CDP concrete parameters, based on ABAQUS recommendations

Parameter	Value	Descriptions
Ψ	30	Dilatation angle
Ɛ	0.1	Eccentricity
f bo/f co	1.16	The ratio of initial equibiaxial compressive yield stress to initial uniaxial compressive yield stress
K	0.667	Kc, the ratio of the second stress invariant on the tensile meridian
M	0.0001	Viscosity Parameter

In this case, CFRP wraps were simulated using Hashin's damage model (Hashin, Z. 1980). The definition of the bonding behaviour between the CFRP sheets and concrete is very important for the precise predictions. The bottom end of cylinders was fixed for displacements and rotations in all directions. In addition, displacement control technique was used for the application of load on the top surface.

The numerical model of the control cylinder presented here is highly depending upon the mesh size because of the strain localization phenomena. To achieve better results of control specimen, it is important to use smaller mesh size but not enough smaller to enhance the analysis time and burden of computer additionally to solve the equations formed by the FEA (Figure 2).

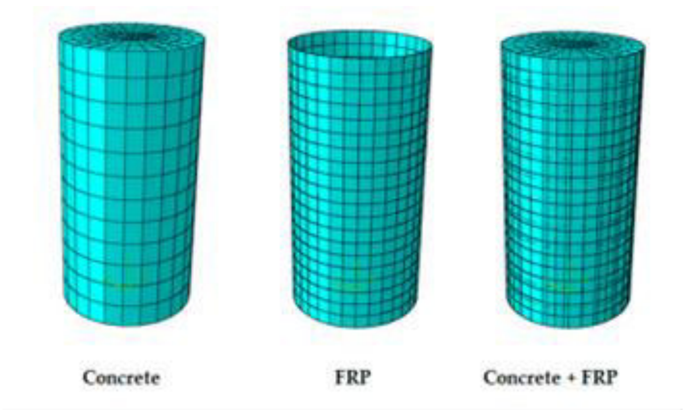

Fig. 2 Finite element mesh of the cylinders

The concrete part was composed of meshed elements with 20mm size and modelled by eight - nodes brick element (C3D8R). In other hand, the CFRP sheets were modelled by four-node shell elements (S4R), while the connection between the CFRP material and concrete was simulated by eight-node three-dimensional cohesive elements (COH3D8). According to given recommendations by the FEA method, some idealizations for the embedded materials were done.

3.1. FINITE ELEMENT RESULTS

Based on the performed finite element analysis, using the commercial software program ABAQUS SIMULIA, the following results for both cylinders (referent concrete cylinder and CFRP wrapped cylinder) were obtained.

3.1.1. Finite element results of the concrete cylinders

The finite element crack patterns were represented through maximum principal plastic strains. It is because the concrete damaged plasticity model (CDPM) assumes that the cracks in the concrete start when there is a positive value of maximum principal plastic strain. The FEA cracks in concrete can also be represented by tensile principal stresses. Figure 3 represents the cracking patterns of a concrete cylinder followed with its maximum stress and strains. It can be visualized that the FEA crack patterns are in a close agreement with the experimental cracks, proving that the FEA software ABAQUS accurately predicted the behaviour of the concrete. The average percentage discrepancies between the experimental and FEA results of CFRP confined concrete cylinder were 15% for axial compressive strength.

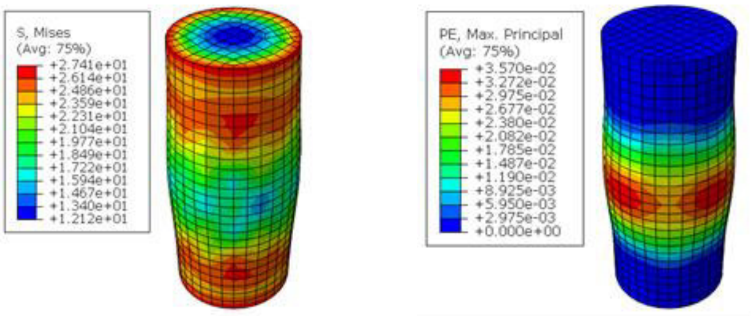

(a) (b)

Fig. 3 (a) Stress and (b) Strains in the concrete cylinder

3.1.2. Finite element results of the CFRP confined concrete cylinders

The experimental results of the concrete cylinders confirmed the increase in strength and ductility with adding of CFRP confinement. It shows that the CFRP confinement is effective in low strength concrete for both strength and ductility of concrete.

The average percentage discrepancies between the experimental and FEA results of CFRP confined concrete cylinder were 7.3% for axial strength. These discrepancies may be due to the minor inaccuracies due to the difference between actual and testing and boundary conditions, assumptions made during FEA and the accuracy of the testing instruments.

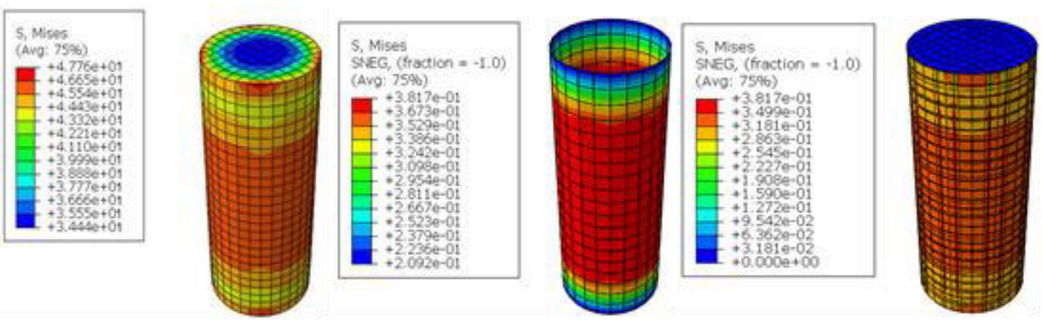

(a) (b) (c)

Fig. 4 Stress in the (a) concrete, (b) CFRP and (c) CFRP wrapped cylinder

Same as the referent concrete cylinder, the finite element crack patterns for the CFRP confined concrete cylinder were represented through maximum principal plastic strains (Figure 4). Regarding the obtained results, it can be noticed that the FEA crack patterns are in a close agreement with the experimental cracks. This shows that the FEA done in the computer program ABAQUS SIMULIA accurately predicted the behaviour of CFRP-wrapped concrete. In table 3, compressive strength comparison of the experimental tests and FEA is presented.

Tab. 3 Comparison between compressive strength of the concrete cylinders obtained experimentally and by FEA

Series	Experimental tests [MPa]	Finite element analysis [MPa]
Referent concrete cylinder	17	20
Concrete cylinder with one layer of CFPR	38	41

4. CONCLUSIONS

The present study aims to evaluate the effectiveness of CFRP wrapping on plain concrete. According to the results obtained, the main conclusions derived from the present study work are as given:

- The experimental tests and performed finite element analysis in this study, illustrated that externally bonded CFRP confinement is a simple and good solution towards enhancing the strength and ductility of concrete cylinders subjected to axial load.
- The rupture of carbon fibres marks failure of all confined cylinders. It occurs prematurely, for stress level appreciably lower than the ultimate strength of the CFRP composite.
- The discrepancies between the experimental and FEA results were 3MPa for axial compressive strength for CFRP confined concrete cylinders and for unconfined concrete cylinders. These discrepancies may be due to the minor inaccuracies due to the difference between actual testing and boundary conditions, assumptions made during FEA and the accuracy of the testing instruments.
- From this study, it can be concluded that the proposed FEA models can predict the axial stress and strain of CFRP-confined concrete with certain accuracy.

REFERENCES

[1] Hollaway, L.C.; Chryssanthopoulos, M.; Moy, S.S. (2004). Advanced Polymer Composites for Structural Applications in Construction: ACIC 2004; Woodhead Publishing: Sawston, UK; Volume 1, pp. 771–772.

[2] Seffo, M.; Hamcho, M. (2012). Strength of concrete cylinder confined by composite materials. Elsevier, 19: 276-285.

[3] Ann, K.; Cho, C.-G. (2013). Constitutive behaviour and finite element analysis of FRP composite and concrete members. Materials 2013, 6, 3978–3988.

[4] Abed, F., Oucif, C., Awera, Y., Mhanna, H., Alkhraisha, H. (2020). FE modeling of concrete beams and columns reinforced with FRP composites. Defence Technology, Production by Elsevier.

[5] Kadhim. M.M.A., Jawdahari, A.R., Altaee, M.J, Adheem, A.H. (2020). Finite Element Modelling and Parametric Analysis of FRP Strengthened RC Beams under Impact Load. Journal of Building Engineering 101526.

[6] Roshi, A., Nechevska-Cvetanovska, G. (2020). Application of innovative buildings materials for repair and strengthening of RC columns in seismically active regions. Doctoral dissertation, Skopje, March 2020.

[7] Hashin, Z. (1980). Failure criteria for unidirectional fibre composite. Journal of Applied Mechanics, 47(2): p. 329-334.

[8] SIMULIA (2016): Analysis user's manual. Providence, Rhode Island, USA., SIMULIA, Dassault Systèmes.

INFLUENCE OF RECYCLED RUBBER ON PROPERTIES OF CONCRETE

Marko Stojanović[1], Ksenija Janković[2], Dragan Bojović[3], Anja Terzić[4], Lana Antić Aranđelović[5]

Summary:

Global warming and the emission of CO_2 into the atmosphere is becoming a bigger problem in the world every year. The desire for a global increase in production and the ever-increasing development of industry are the cause of the increased amount of waste in landfills and environmental pollution. Concrete is the most used construction material in the world, and the production of its main ingredient, cement, is responsible for about 7% of CO_2 emissions in the world. Application of waste materials and by-products that end up as waste during some industrial process in production can find further application in concrete. Such materials can be used as mineral additives or as aggregate fillers, for partial or complete replacement of natural stone aggregate and/or cement. In this work, volume replacement of the fine fraction with 2.5 and 7.5 % crushed rubber was performed. Based on the test results of fresh concrete, in concrete with rubber addition, the slump consistency and bulk density decrease, and the air content increases. A drop in compressive strength of concrete was observed with an increase in the rubber content of 7.5%.

Key words: Recycled rubber, consistency, air content, compressive strength

[1] PhD Candidate, IMS Institute, Belgrade, Serbia, marko.stojanovic@institutims.rs
[2] Principal Research Fellow, IMS Institute, Belgrade, Serbia, ksenija.jankovic@institutims.rs
[3] Research Associate, IMS Institute, Belgrade, Serbia, dragan.bojovic@institutims.rs
[4] Principal Research Fellow, IMS Institute, Belgrade, Serbia, anja.terzic@institutims.rs
[5] Professional adviser, IMS Institute, Belgrade, Serbia, lana.antic@institutims.rs

1. INTRODUCTION

Recycled and waste materials are increasingly used in concrete to overcome environmental problems and save energy. Improvements in concrete properties as well as environmental benefits due to the use of waste materials encourage further research into the production of green concrete. Finely crushed rubber (CR), which is obtained by crushing used pneumatic tires, is one of the waste materials that can be used in concrete, as a partial or complete replacement of coarse or fine aggregate or both [1].
According to the European Tire and Rubber Manufacturers Association (ETRMA), world tire production was 5.1 million tons in 2018 [2]. From an ecological perspective, the use of (CR) in concrete is beneficial, as it leads to the conservation of mineral resources, i.e. aggregates and thus minimizes the need for new landfills needed to dispose of waste tires, thus solving related environmental problems [3].
Concrete is a brittle material that, when it reaches its maximum load capacity, the structure breaks. Therefore, the ductility of CR particles can be used to reduce the brittleness of concrete [4]. Also, several advantages of recycled rubber concrete (CRC) have been reported in research papers, such as improving its deformation capacity, energy absorption, wetting capacity and resistance to cyclic freezing and thawing, reducing water permeability, chloride penetration and thermal expansion [5],[6]. However, the reduction in compressive strength of CRC compared to ordinary concrete is the biggest drawback found in this material. This deficiency, however, can be overcome by increasing the amount of cement, reducing the water-cement ratio and using appropriate chemical and mineral additives [6].
The paper presents the possibility of using crushed rubber in concrete as a volumetric replacement of fine aggregate with 2.5 and 7.5% of crushed rubber. The design of three concrete mixtures was carried out, with each of them tests of fresh concrete were carried out: Slump consistency, bulk density and air content. The change in the properties of fresh concrete was monitored over time, after 10, 30 and 60 minutes from the moment of adding water to the concrete mix. Tests of hardened concrete, bulk density and compressive strength at the ages of 3, 7, 28 and 56 days were performed.
A comparison was made of the obtained results of concrete with 2.5 and 7.5% volumetric replacement of the fine fraction with crushed rubber in relation to the reference concrete, which was made with a water-cement ratio of w/c=0.5.

2. EXPERIMENTAL WORK

2.1. THE COMPOSITION OF CONCRETE

During the design of the concrete mix, volume replacement of fine aggregate in the amount of 2.5 and 7.5% with crushed rubber, water-cement ratio w/c=0.5 and cement amount of 360 kg/m^3 was performed.
Three types of concrete mixtures were designed:
- Mixture 1 – Ordinary concrete,
- Mixture 2 – Concrete with replacement of 2.5% fine aggregate with crushed rubber,
- Mixture 3 – Concrete with replacement of 7.5% fine aggregate with crushed rubber,

The component materials for making CRC are cement, fine and coarse aggregate in fractions 0/4, 4/8 and 8/16 mm, crumb rubber, superplasticizer and water.
Ordinary Portland cement clinker, strength class 42.5 R, produced by "Lafarge BFC" was used. The specific mass of cement is 3110 kg/m^3, the specific surface is 4320 cm^2/g. The chemical composition of cement is shown in Table 1.
Natural, fractionated stone aggregate, of limestone origin, fractions 0/4, 4/8, 8/16 mm, specific mass 2650 kg/m^3, and fineness modulus of 3.06 was used. The granulometric composition of the aggregates is shown in Figure 2.

Finely crumbled rubber (CR - Figure 1), which is obtained by crushing used pneumatic tires, was obtained from the producer of recycled rubber waste "ECO-RECYCLING" doo, the specific mass of the rubber is 1170 kg/m^3, the granulometric and chemical composition are shown in Figure 2 and Table 1.

Superplasticizer based on polycarboxylate "Sika Viscocrete 4077x", manufactured by "Sika Serbia", specific mass 1050 kg/m^3 and tap water were used in this research.

Tab. 1. Chemical composition of cement and crumb rubber

	SiO_2	Al_2O_3	Fe_2O_3	CaO	MgO	Na_2O	K_2O	SO_3	Cu mg/kg	Pb mg/kg	Co mg/kg
Cement	19.83	4.26	2.51	63.41	1.67	0.25	0.78	2.80			
Crumb rubber	0.78	0.18	0.12	0.24	0.08	<0.01	0.07	3.05	147	26	276

Fig. 1. Crumb rubbers CR, fraction 0/1 mm, manufacturer "Eco Recycling"

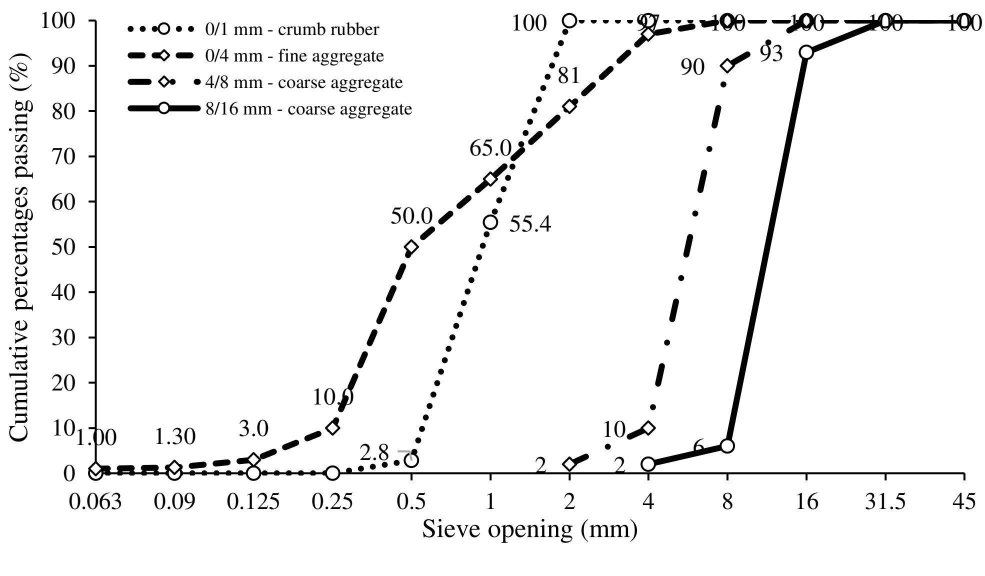

Fig. 2. Particle size composition of crumb rubbers (CR) and natural aggregate

In the mix-design of concrete with crumb rubber, natural, separated river aggregate with 0/4, 4/8, and 8/16 mm fractions, crumb rubber, and combination (Mix-2 - crumb rubber: river sand = 2.5:97.5 by volume and Mix-3 - crumb rubber: river sand = 7.5:92.5 by volume) were employed. The percentage share of aggregate per fraction was 45 % for 0/4 mm, 15% for 4/8 mm, and 40% for 8/16 mm. Fig. 3. depicts a grain-size study of aggregate mixtures.

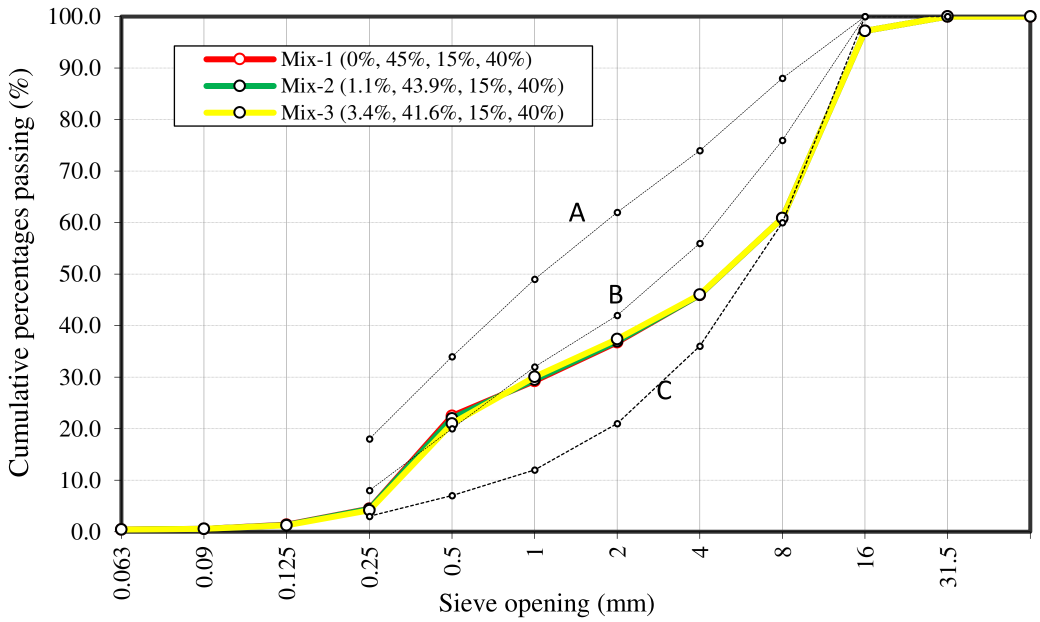

Fig. 3. Grading curves of aggregate mixtures for concrete (red mixture – natural river sand aggregate; green mixture – 2.5% of crumb rubber and 97,5% of natural river sand aggregate; and yellow mixture – 7.5% of crumb rubber and 92,5% of natural river sand aggregate)

2.2. CONCRETE MIXTURE

Concrete mixing was performed in a laboratory planetary mixer with a volume of 0.150 m^3. Order of adding components into mixer:

- Mixtures 1 - aggregate, cement, water, superplasticizer,
- Mixtures 2 - aggregate, crumb rubbers – 2.5%, cement, water, superplasticizer,
- Mixtures 3 - aggregate, crumb rubbers – 7.5%, cement, water, superplasticizer.

Mixing time for all concrete Mixtures was 90 seconds.
The quantities of component materials of concrete mixes are shown in Fig. 4.

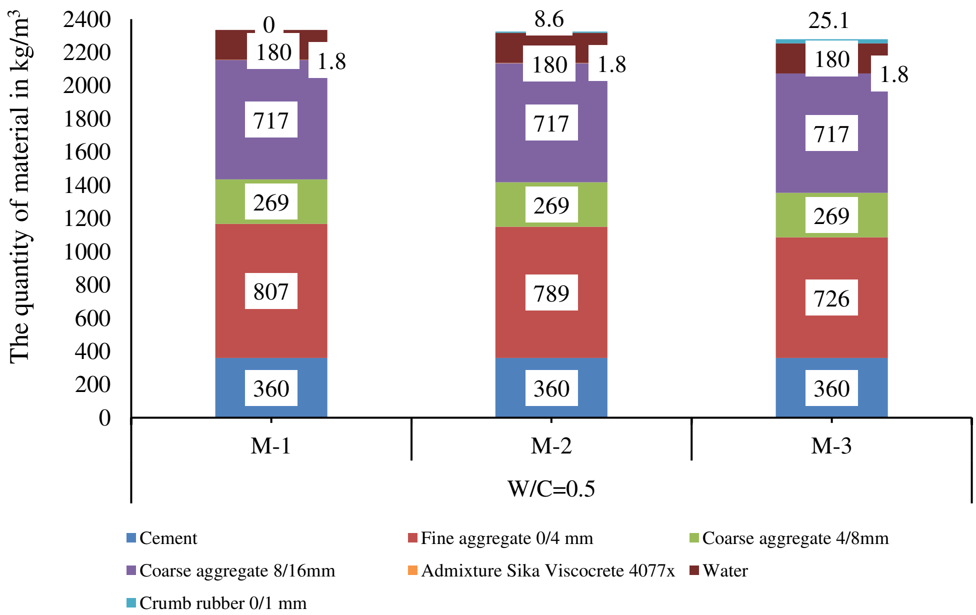

Fig. 4. Compositions of concretes (values are given in kg/m^3)

2.3. PROPERTIES OF FRESH CONCRETE AND DISCUSSION OF THE OBTAINED RESULTS

The testing of concrete properties in fresh state was performed: consistency by the slump method, air content and bulk density (10, 30 and 60 minutes after the addition of water).
The consistency test of fresh concrete was conducted according to the SRPS EN 12350-2 method. Test results of consistency by the slump test method are shown in Fig. 5.

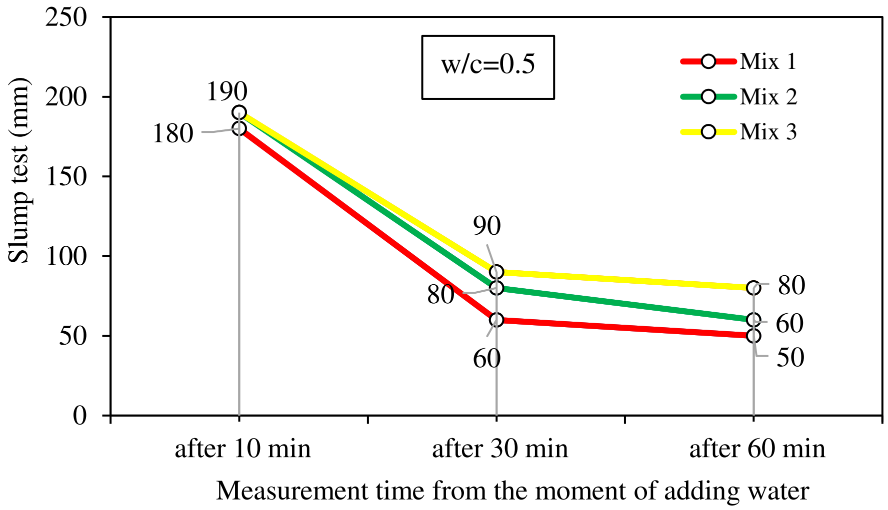

Fig. 5. Properties of fresh concrete after 10, 30 and 60 min: Slump test method

Based on the results obtained by testing all concrete, after 10 minutes the results of 180 to 190 mm were obtained, which belong to the consistency class S4 (160-210 mm). It was observed that after 30 minutes the consistency slump tests decreases, it is from 60 mm for Mix-1 to 90 mm for Mix-3. After 60 minutes, the slump test consistency also decreases and it is from 50 mm for Mix-1 to 80 mm for Mix-3.
The air content test was carried out according to SRPS EN 12350-7, using the pressure method. The values obtained by testing are shown in Fig. 6.

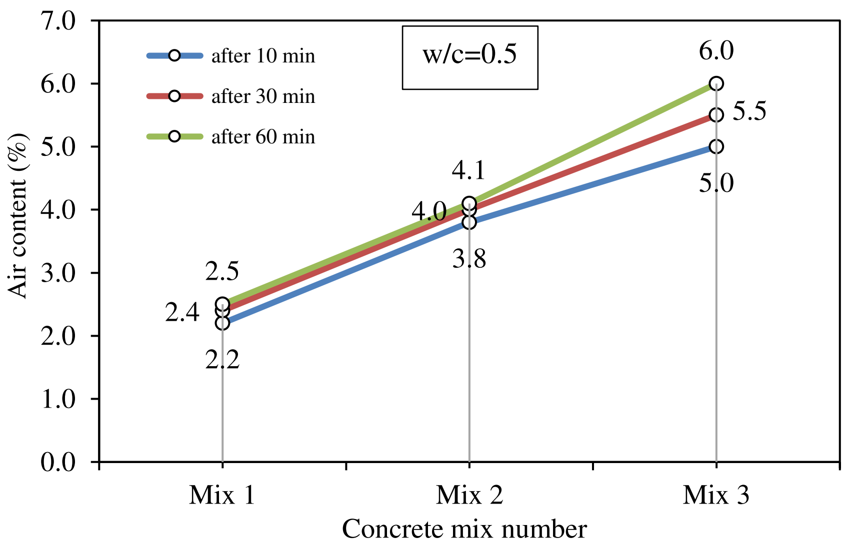

Fig. 6. Propert of fresh concrete after 10, 30 and 60 min: Air content

The obtained values of air content in concrete with the addition of rubber Mix-2 and Mix-3 are higher by 42%, 45%, 46% and 56%, 60% and 63% compared to the values obtained in concrete Mix-1 measured after 10, 30 and 60 minutes (from the moment of adding water). The highest value of air content was obtained for Mix-3.

Bulk density was carried out according to the SRPS EN 12350-6 method. A vessel with a volume of $0.008m^3$ was used, and the method of placing the concrete was carried out according to the obtained consistency using the fresh concrete settling method. The values obtained by testing are shown in Fig. 7.

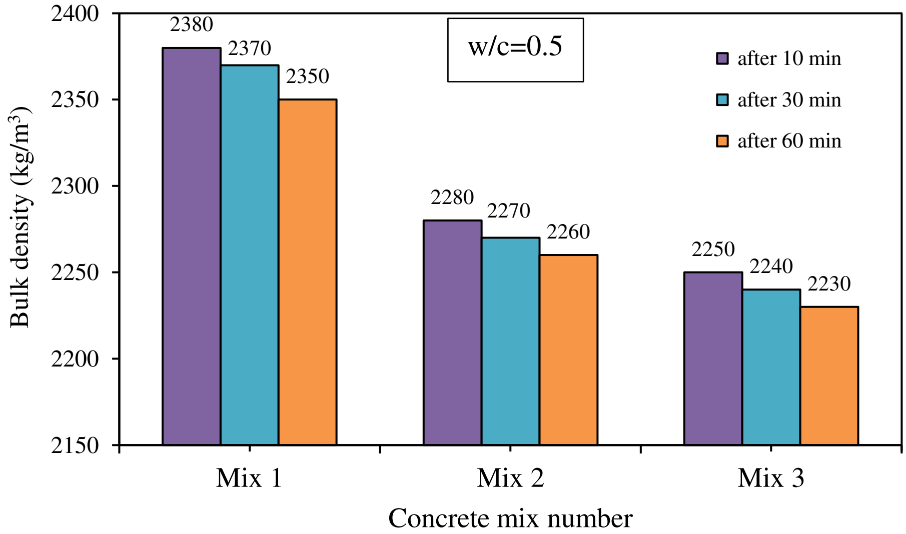

Fig. 7. Property of fresh concrete after 10, 30 and 60 min: Bulk density

The bulk density of fresh concrete ranged from 2240 to 2380 kg/m^3. Concrete mixes Mix-2 and Mix-3 with the addition of rubber of 2.5 and 7.5% have higher air content values compared to Mix-1. As a result, smaller volumetric masses were obtained in the fresh concrete in the Mix-2 and Mix-3 mixtures compared to the Mix-1 mixture.

2.4. PROPERTIES OF HARDENED CONCRETE AND DISCUSSION OF THE OBTAINED RESULTS

2.4.1. Compressive strength

Samples for testing compressive strength of concrete were made. Concrete was compacted on the vibrating table in cube shaped molds, edge d=150 mm, which were cured in water at a temperature of + 20 ° C until the moment of testing according to SRPS EN 12390-2 standard. Testing of compressive strength of concrete at the age of 3, 7, 28 and 56 days was carried out according to SRPS EN 12390-3 standard. The hardened concrete's bulk density was determined using the SRPS EN 12390-7 standard. The bulk densities obtained ranged from 2250 to 2370 kg/m^3. The test results are shown in Fig. 8.

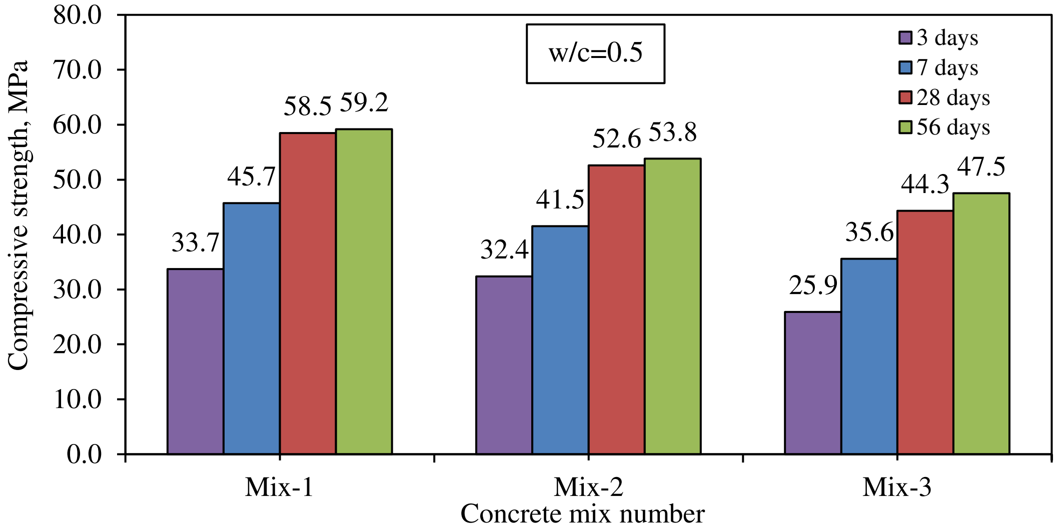

Fig. 8. Compressive strength of concrete at the age of 3, 7, 28 and 56 days

The highest obtained values of compressive strength at the age of 3, 7, 28 and 56 days had concrete Mix-1. Compared to Mix-1, the decrease in compressive strength for Mix-2 was 3.9%, 9.2%, 10.1% and 9.1%, after testing of 3, 7, 28 and 56 days. Compared to Mix-1, the decrease in compressive strength for Mix-3 was 23.1%, 22.1%, 24.3% and 19.8%, after testing of 3, 7, 28 and 56 days.

3. CONCLUSION

Based on the results obtained by researching concrete with volume replacement of fine aggregate with rubber in values of 2.5% and 7.5%, we can conclude the following:

- The consistency of fresh concrete decreases over time,
- The consistency of fresh concrete with the addition of rubber has a greater settlement than concrete without rubber because the rubber crumbs bring with them additional air content in the fresh concrete that contributes to making the mixture more mobile.
- The values of the volumetric mass of fresh concrete in the mixes Mix-2 and Mix-3 with the addition of rubber crumbs are lower than the control mix Mix-1,
- The values of air content in fresh concrete are higher in Mix-2 and Mix-3 containing crumb rubber compared to Mix-1,
- The values of volume masses of hardened concrete in Mix-2 and Mix-3 are lower compared to Mix-1,
- The compressive strength values of Mix-2 and Mix-3 at all ages are lower than Mix-1.

Based on the obtained compressive strength values of concrete with volumetric replacement of fine aggregate with crumb rubber in the amount of 2.5% and 7%, we can conclude that it is possible to use such concrete in load-bearing structures. The obtained test results give us an incentive for further research of this type of concrete, which will be exposed to the effect of frost without or with the presence of a salt solution for defrosting.

ACKNOWLEDGMENTS

This investigation is financially supported by the Ministry of Science, Technological Development and Innovation of the Republic of Serbia (Contract No.: 451-03-47/2023-01/ 200012) and 2021-2023 bilateral cooperation project between Turkey and Serbia: "Tailor made self-compacting heavyweight concrete with waste materials".

REFERENCES

[1] Y.C. Guo, J.H. Zhang, G.M. Chen, Z.H. Xie, Compressive behaviour of concrete structures incorporating recycled concrete aggregates, rubber crumb and reinforced with steel fibre, subjected to elevated temperatures, J Clean Prod, 72 (2014), pp. 193-203,

[2] Etrma (2018), pp. 1-52, http://www.etrma.org,

[3] A.A. Gheni, M.A. ElGawady, J.J. Myers, Mechanical characterization of concrete masonry units manufactured with crumb rubber aggregate, ACI Mater J, 114 (2017), pp. 65-76,

[4] M.K. Ismail, A.A.A. Hassan, Use of steel fibers to optimize self-consolidating concrete mixtures containing crumb rubber, ACI Mater J, 114 (2017), pp. 581-594,

[5] K. Strukar, T. Kalman Šipoš, I. Miličević, R. Bušić, Potential use of rubber as aggregate in structural reinforced concrete element – a review, Eng Struct, 188 (2019), pp. 452-468,

[6] H. Zhu, Crumb Rubber Concrete Bridge Deck, 39 (2017),

[7] SRPS EN 12350-2:2019: Testing fresh concrete - Part 2: Slump test,

[8] SRPS EN 12350-6:2019: Testing fresh concrete - Part 6: Density,

[9] SRPS EN 12350-7:2019: Testing fresh concrete - Part 7: Air content - Pressure methods,

[10] SRPS EN 12390-2:2019: Testing hardened concrete - Part 2: Making and curing specimens for strength tests,

[11] SRPS EN 12390-3:2019: Testing hardened concrete - Part 3: Compressive strength of test specimens,

[12] SRPS EN 12390-7:2019: Testing hardened concrete - Part 7: Density of hardened concrete,

RECONSTRUCTION OF A TYPICAL RESIDENTIAL BUILDING AFTER THE EARTHQUAKE IN PETRINJA

Šime Serdarević[1], Dalibor Gelo[2], Ivan Volarić[3], Dean Čizmar[4].

Summary:

In 2020, Sisak-Moslavina county was hit by two earthquakes of magnitude 5.0 and 6.2 on the Richter scale. A large number of buildings were destroyed or damaged. The aim of this paper is to present an example of the Elaborate of the existing state of the building structure and the Project of retrofitting of the building structure of a typical residential building. This paper will deal with a residential building at the location Ulica Artura Turkulina 43A, Petrinja. The building was built in 1965, with approximate floor plan dimensions of 18.9×9.8 m, storeys B+GF+3F. The main load-bearing system of the building consists of masonry walls. The condition of the building structure before the reconstruction process will be presented, strengthening measures of load-bearing and load non-bearing structural elements will be proposed for the defined level of reconstruction, and the earthquake resistance of the building will be proved by calculation after the strengthening measures have been implemented.

Key words: earthquake, epicenter, design, magnitude, intensity

[1] Lecturer, Tehničko veleučilište u Zagrebu, Zagreb, Hrvatska, sime.serdarevic@tvz.hr
[2] Lecturer, Tehničko veleučilište u Zagrebu, Zagreb, Hrvatska, dalibor.gelo@tvz.hr
[3] Lecturer, Tehničko veleučilište u Zagrebu, Zagreb, Hrvatska, ivan.volaric@tvz.hr
[4] Associate professor, Tehničko veleučilište u Zagrebu, Zagreb, Hrvatska, dean.cizmar@tvz.hr

1. INTRODUCTION

In 2020, Sisak-Moslavina county was hit by two earthquakes of magnitude 5.0 and 6.2 on the Richter scale. The highest intensity was estimated to be VIII-IX (eight to nine) degrees of the EMS scale. Earthquakes damaged a large amount of buildings in terms of damage to their load bearing and load non-bearing elements. A large number of buildings have been completely collapsed. Buildings that did not collapse, suffered damage to load non-bearing and load bearing elements. Damage to load non-bearing elements (damages that do not impact the global mechanical resistance and stability of the structure) include mostly damage or collapse of parts of chimneys and gable walls, collapse of cornices, cracks and collapse of load non-bearing walls, falling plaster, gutters and roof tiles. The most common damages of the load bearing elements (damages that impair the global mechanical resistance and stability of the structure) are larger or smaller cracks in load bearing walls and the separation of load bearing walls from slab structures (due to an improperly connection between wall - slab structure or horizontally non rigid (wooden) slab elements). The causes of damage to load non-bearing elements are usually incorrectly load non-bearing elements (chimney construction without support or with insufficiently rigid support (defective or poor quality wooden roof elements), poor-quality materials (bricks and mortar), incorrect connection with the slab elements. Causes of damages to load bearing elements are also low-quality and construction, incorrect structural details, irregular layout, uncontrolled local weakening of load-bearing elements, non rigid horizontal wooden slab elements without sufficient rigidity to support high slender masonry walls.

2. QUICK REVIEW AND ASSESSMENT OF BUILDING USEABILITY

Construction engineers - volunteers soon after the earthquake, began to quickly inspect the damaged buildings - assess the usability of the buildings. After the inspection, the buildings were assigned the following marks: green (usable building - which is undamaged or has minor damage that is not a threat to the building's usability), yellow (temporarily unusable building - which can become usable with emergency intervention measures or needs to be inspected in detail. Recommendations are given to remove the danger). Red mark (unusable building - the danger may be from massive parts collapsing onto a buildings in close area or the building is dangerous due to a large scale of damage in the load-bearing system). (1)

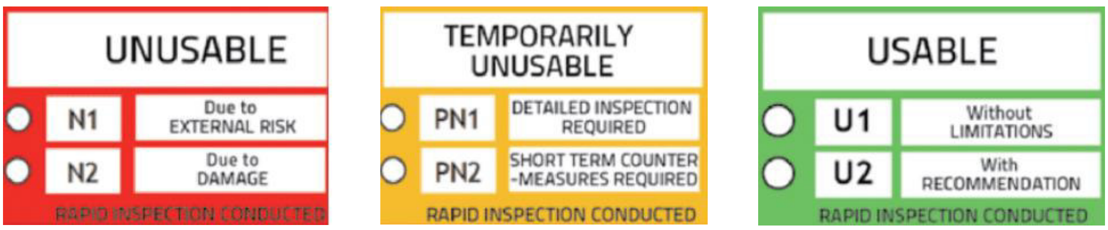

Fig. 1 Usability marks (1)

2.1. LEVELS OF RECONSTRUCTION (1)

The levels of reconstruction are defined by expert guidelines for the reconstruction of earthquake-damaged buildings created by a group of experts. Professional guidelines define four levels of reconstruction for damaged buildings.

2.1.1. Level 1

Level 1 reconstruction assumes that the load bearing structure of the building after the earthquake is undamaged or with very minor damages that do not significantly affect its bearing capacity. It includes repairing of covers, gables, parapets, partition walls, chimneys, local reconstruction of the roof structure and elevators.

2.1.2. Level 2

Level 2 reconstruction involves the repair or replacement of structural (load bearing) elements that were damaged in the earthquake, and certain improvements are made to the structure of the building as a whole, related to earthquake resistance. At this level, reconstruction should be carried out by performing acceptable operations in order to achieve at least the original resistance.

2.1.3. Level 3

Level 3 reconstruction would increase the resistance of the building structure. Resistance level would not be as required by the existing Technical Regulation for building structures and standards for the design of structures – HRN EN. This particularly applies to:
a) Buildings with the status of architectural heritage where it is not acceptable to carry out radical interventions that do not comply with conservation conditions.
b) Buildings with the status of architectural heritage that have a structure and overall architectural features that cannot be brought to a level of resistance by acceptable renovation procedures according to the regulation and the standards for designing structures (HRN EN and TPGK) without significantly disrupting their basic and original architectural identity (for example Zagreb Cathedral, some Church buildings, part of historical buildings and others).
c) Buildings with insufficient original earthquake resistance, where reconstruction to the full level of earthquake resistance is not justified (remaining building life, value of the building, costs reconstructing building up to a full level higher than the building replacement building, etc.).
In the case of the buildings mentioned in a), b) and c), the reconstruction should be carried out as a significant strengthening of the structure to an acceptable level of resistance, whereby the highest possible level of earthquake resistance should be achieved. Reinforcement of the structure is carried out according to the project of the building structure with proof of the mechanical resistance and stability of the structure. Project will define the level of resistance in relation to the required seismic resistance according to standards for designing structures.

2.1.4. Level 4

Level 4 reconstruction implies increasing the resistance to the effects of earthquakes, which is prescribed by the current regulation and standards for designing structures (HRN EN and TPGK). This level includes other basic building requirements, such as fire safety, hygiene, health and environment, and others if necessary.

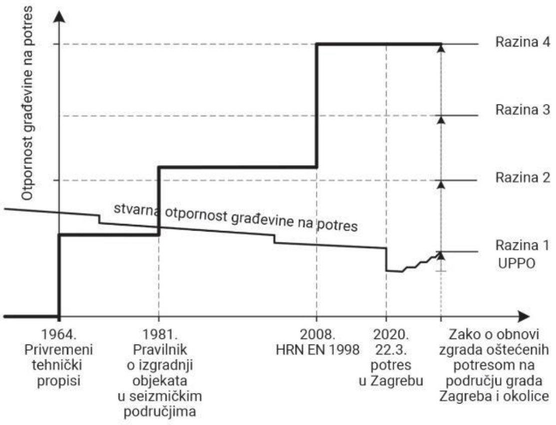

Fig. 2 Required resistance of buildings according to regulations (1)

3. RESIDENTIAL BUILDING (LOCATION: ARTURA TURKULINA 43A, PETRINJA)

3.1. BUILDING LOCATION AND CONSTRUCTIVE SYSTEM

Building location is: ulica Artura Turkulina 43A, 44250 Petrinja (k.č.br. 433/1 k.o. Petrinja).

Fig. 3 Location - cadastral plan

Building is approximately rectangular in shape, maximum floor plan dimensions are 18.9×9.8 m, approximately 830 m^2. It has basement, ground floor and three floors (B+GF+3F). The foundations are made of reinforced concrete, unknown dimensions. The walls are made of solid bricks, 38 cm thick. The slab structure consists of reinforced concrete panels with ribs. Multi-roofed roof structure is made of solid wood.

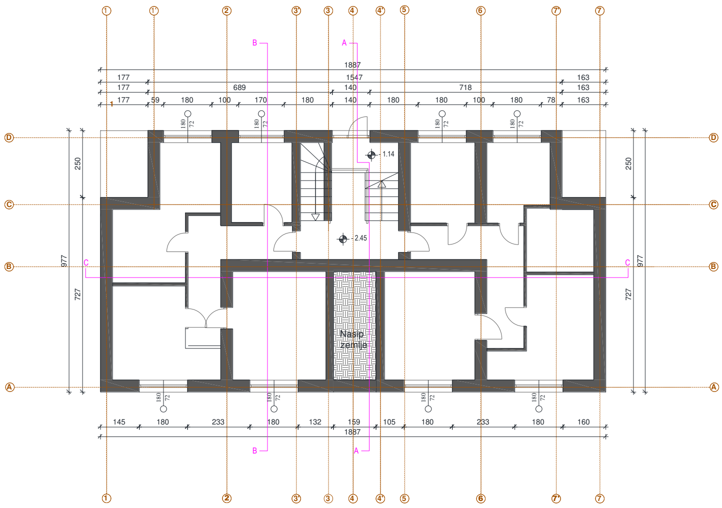

Fig. 4 Basement floor plan

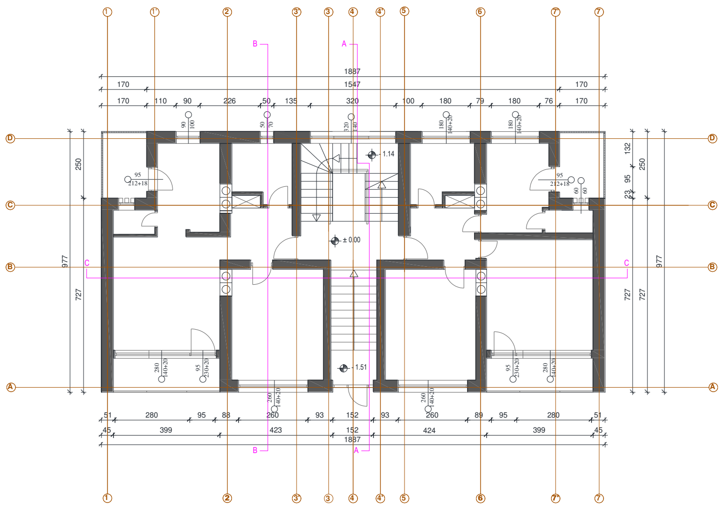

Fig. 5 Ground floor plan

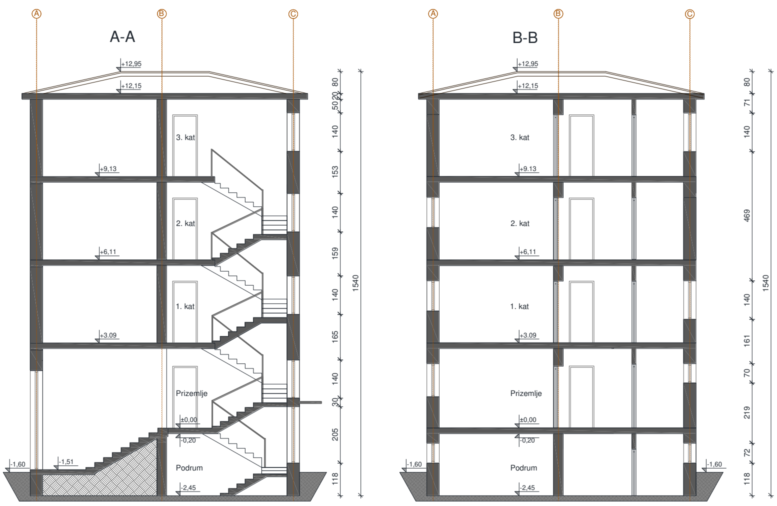

Fig. 6 Sections A-A and B-B

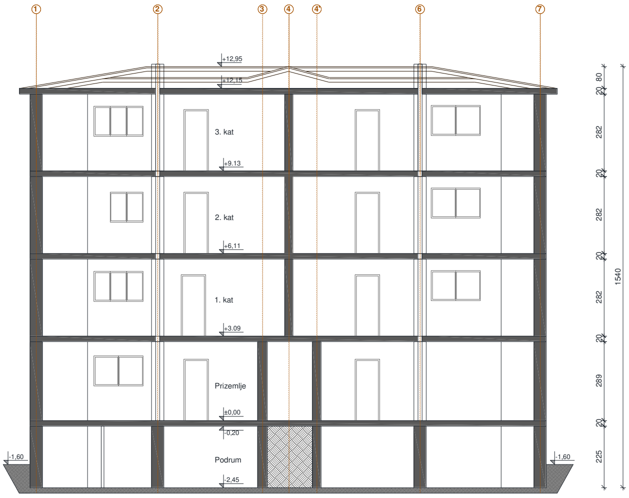

Fig. 7 Section C-C

Fig. 8 South-east and north-east facades

Fig. 9 North-west and south-west facades

3.2. DESCRIPTION OF BUILDING DAMAGE DUE TO EARTHQUAKE EFFECTS

The building structure suffered moderate damages of load bearing and significant damages of load non-bearing elements. Horizontal, diagonal and vertical cracks different thickness appeared on almost all load bearing and load non-bearing brick walls through all floors. Regarding the assessment of the building's usability, the building is marked with a yellow mark.

Fig. 10 Damages of the building

3.3. MECHANICAL RESISTANCE AND STABILITY VERIFICATION

The verification and analysis of the fulfillment of the basic requirement of mechanical resistance and stability and the analysis of the seismic resistance of the existing structure by linear multimodal analysis was performed using the SCIA Engineer 22.0 software package.

3.3.1. Loads

Load combinations are defined in accordance with the HRN EN 1990:2011 standard and the national annex HRN EN 1990:2011/NA:2011.

Permanent load

Selfweight of individual structure elements is generated by a computer program based on the dimensions and material of the element.

The slab structure as a rigid diaphragm connects the walls and enables the correct distribution of the load on the walls, which is especially important in case of an earthquake. In the structure model, ribbed slab, which represents a rigid diaphragm, is modeled with "master-slave" connections defined by the "line rigid link" option. This option connects the point in the slab (master-node) to all the walls (slave-line).

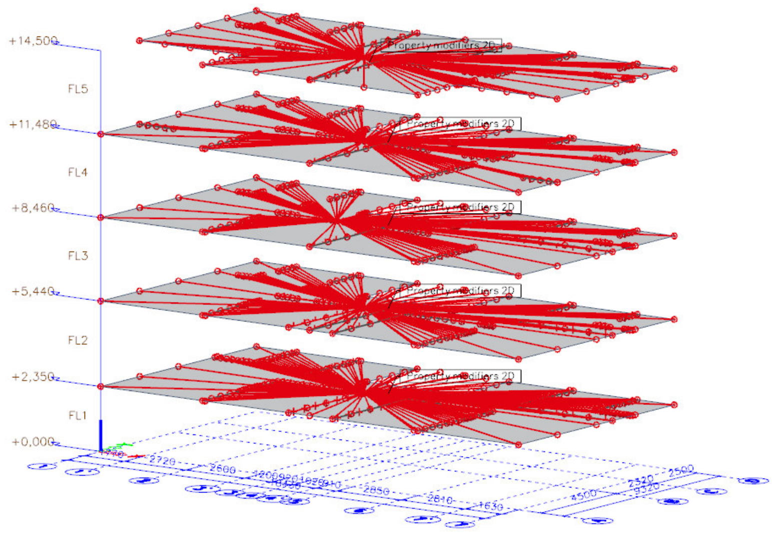

Fig. 11 Master-slave connection with the "line rigid link" option

All loads from the slab are transferred directly to the load-bearing walls as a line load. Slabs selfweight in the model is excluded. These loads are applied as a line load on the walls under the load case "LC3 - Additional permanent".
Building was modeled without wooden roof structure, but the estimated weight of the entire wooden roof with the covering was applied to the model of the masonry structure in the amount of 1.1 kN/m^2. This load was applied under the load case "LC2 - Selfweight of the roof".

Additional permanent load

The weight of the layers in the calculation is taken in accordance with the standard HRN EN 1991-1-1:2012: Eurocode 1: Actions on structures - Part 1-1: General actions - Densities, self-weight, imposed loads for buildings.

Tab. 1 The weight of the characteristic slab structure

	m×kN/m^3 = kN/m^2
Flooring:	= 0.024×6.00 =0.14
Non bearing concrete:	= 0.050×25.00 =1.20
Ribbed slab	= 0.091×25.00 =2.30
Reed and plaster:	= 0.020×20.00 =0.40
TOTAL:	**= 4.00 kN/m2**

Live load

Live load is taken in accordance with the standard HRN EN 1991-1-1:2012: Eurocode 1: Actions on structures - Part 1-1: General actions - Densities, self-weight, imposed loads for buildings. Live load for residential buildings is 2kN/m^2, 3kN/m^2 for staircases and corridors, 4kN/m^2 for terraces. Live load for attic spaces is 1.5 kN/m^2.

Snow load

Snow load is applied according to the standard HRN EN 1991-1-3:2012: Actions on structures - Part 1-3: General actions - Snow loads. The characteristic snow load on the ground was obtained by linear interpolation for an altitude of 106m, and for the 3rd area

- continental Croatia (1.02 kN/m^2). The calculated value of the snow load is 0.82 kN/m^2 (a value of 1 kN/m^2 was taken for the calculation).

Seismic load

Seismic calculation was carried out according to standard HRN EN 1998-1:2011: Design of structures for earthquake resistance - Part 1 : General rules, seismic actions and rules for buildings.

According to the seismic map of the Republic of Croatia, Petrinja is located in the zone of seismic intensity with peak ground acceleration as shown in the table:

Tab. 2 Peak ground acceleration for building location

Return period	agR/g =
475 years (TNCR = 475 g.)	0.15
225 years (TNCR = 225 g.)	0.11
95 years (TNCR = 95 g.)	0.07

The importance factor of the building was adopted with the value II – ordinary building. Ground type was classified as category C. The value of the behavior factor was adopted with a value of 1.50. For the calculation, peak ground acceleration for 95 years was adopted (0.07).

3.3.2. Modeling of brick walls

Masonry is modeled with the "Masonry Wall - 2D member" option. This option is characterized by the "Masonry Orthotropy" possibility, with which is possible to define the coefficient (multiplier) of the shear stiffness of the masonry (matrix member d_{33}). Masonry walls that participate in seismic load transfer are modeled as masonry walls with 95% shear stiffness (d_{33}=0.95). Masonry walls that do not participate in seismic load transfer (walls for vertical load transfer only) are modeled with 1% shear stiffness (d_{33}=0.01).

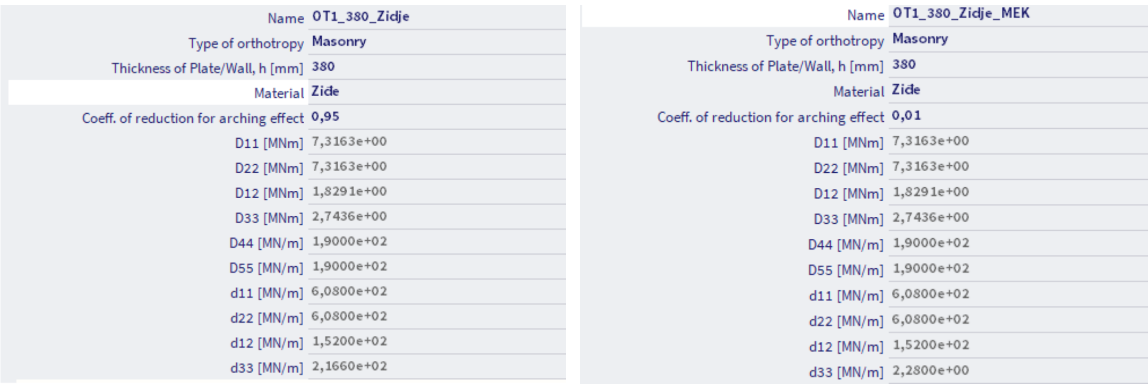

Name	OT1_380_Zidje
Type of orthotropy	Masonry
Thickness of Plate/Wall, h [mm]	380
Material	Zide
Coeff. of reduction for arching effect	0,95
D11 [MNm]	7,3163e+00
D22 [MNm]	7,3163e+00
D12 [MNm]	1,8291e+00
D33 [MNm]	2,7436e+00
D44 [MN/m]	1,9000e+02
D55 [MN/m]	1,9000e+02
d11 [MN/m]	6,0800e+02
d22 [MN/m]	6,0800e+02
d12 [MN/m]	1,5200e+02
d33 [MN/m]	2,1660e+02

Name	OT1_380_Zidje_MEK
Type of orthotropy	Masonry
Thickness of Plate/Wall, h [mm]	380
Material	Zide
Coeff. of reduction for arching effect	0,01
D11 [MNm]	7,3163e+00
D22 [MNm]	7,3163e+00
D12 [MNm]	1,8291e+00
D33 [MNm]	2,7436e+00
D44 [MN/m]	1,9000e+02
D55 [MN/m]	1,9000e+02
d11 [MN/m]	6,0800e+02
d22 [MN/m]	6,0800e+02
d12 [MN/m]	1,5200e+02
d33 [MN/m]	2,2800e+00

Fig. 12 Parameters for modeling brick walls

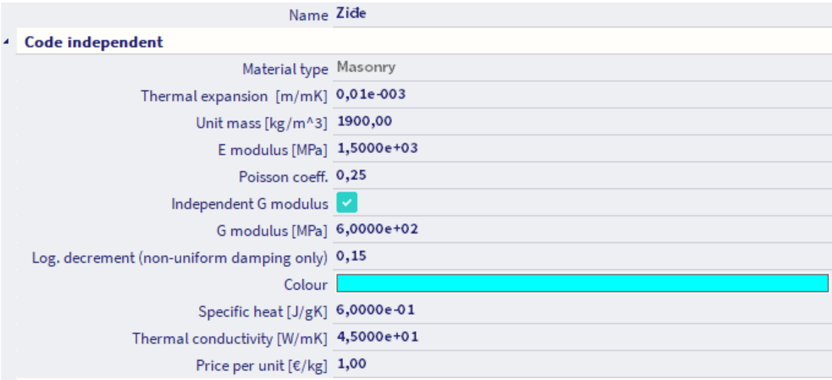

Fig. 13 Characteristic values for modeling brick walls

3.3.3. Modeling of mixed brick-reinforced concrete walls

The existing vertical load-bearing structure consists of solid brick masonry walls without vertical concrete elements, therefore, the vertical load-bearing structure can be defined as an unbounded masonry structure. In addition to the existing load-bearing walls around the staircase (axis 3' and 5) with a thickness of d=38 cm, new reinforced concrete walls with a thickness of d=15 cm and a length of 3.3 m are being added on all floors of the building. In addition to the existing load-bearing walls (axis B) with a thickness of d=38 cm, new reinforced concrete walls with a thickness of d=15 cm and a length of 3.3 m are being added on all floors of the building. All added RC walls have new foundations connected with existing foundations of brick walls.
On this positions new wall consists of existing brick wall and new reinforcement concrete wall. Replacement thickness and weight is determined according to the table below.
E_{AB}= 31000000 kN/m^2 – modulus of elasticity of reinforced concrete wall;
E_o= 1500000 kN/m^2 – modulus of elasticity of brick wall;
E_o/E_{AB}= 0.05 – modulus of elasticity ratio;
γ_{AB}= 25 kN/m^3 – specific weight of reinforced concrete;
γ_o= 19 kN/m^3 – specific weight of brick wall.

Tab. 3 Mixed wall parameters

Thickness of the existing brick wall [cm]	Thickness of the new reinforced concrete wall [cm]	Thickness of the replacement wall [cm]	Design weight of the wall [kN/m^3]	Replacement wall weight multiplier
38	15	17	65	2.60

Fig. 14 Calculation values of the weight and mass multiplier of the replacement wall in the computer program with the "2D property modifier" option

3.3.4. Modeling of structure and calculation results

First mode is displacement in direction X, 63% of mass is activated. Second mode is displacement in direction Y, 70% of mass is activated. In total 10 modes, approximately 90% of mass is activated in direction X and Y. In Tab. 4 and Fig. 17 results of the calculation is presented.

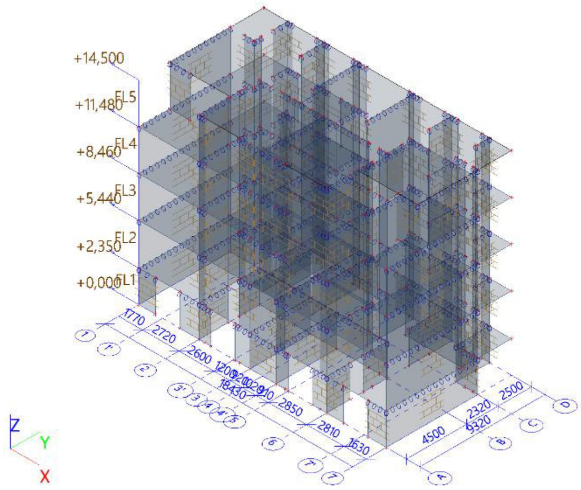

Fig. 15 3D model of the building in the computer program SCIA Engineer 22.0 (axis dimensions in mm)

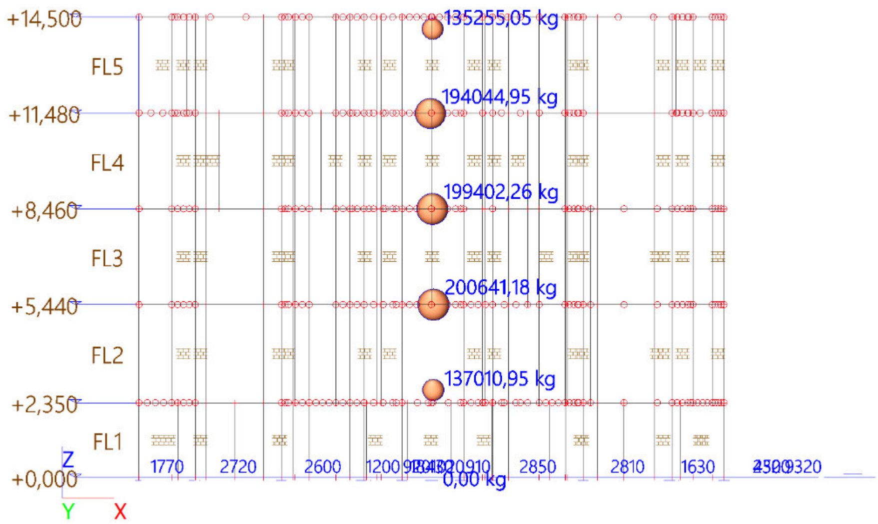

Fig. 16 Mass distribution of the building

Tab. 4 Period with frequencies and activated masses

Mode	Frequency f [Hz]	Period T [s]	W_{xi}/W_{xtot}	W_{yi}/W_{ytot}	W_{zi_R}/W_{ztot_R}
1	5.49	0.18	0.6328	0.0586	0.1440
2	5.52	0.18	0.0758	0.6973	0.0000
3	5.88	0.17	0.1264	0.0114	0.7080
4	13.22	0.08	0.0546	0.0000	0.0001
5	14.48	0.07	0.0024	0.0000	0.0004
6	14.59	0.07	0.0202	0.0000	0.0037
7	15.05	0.07	0.0003	0.0001	0.0743
8	15.80	0.06	0.0000	0.0836	0.0004
9	16.94	0.06	0.0000	0.0287	0.0006
10	17.74	0.06	0.0000	0.0107	0.0018
			0.9127	0.8905	0.9332

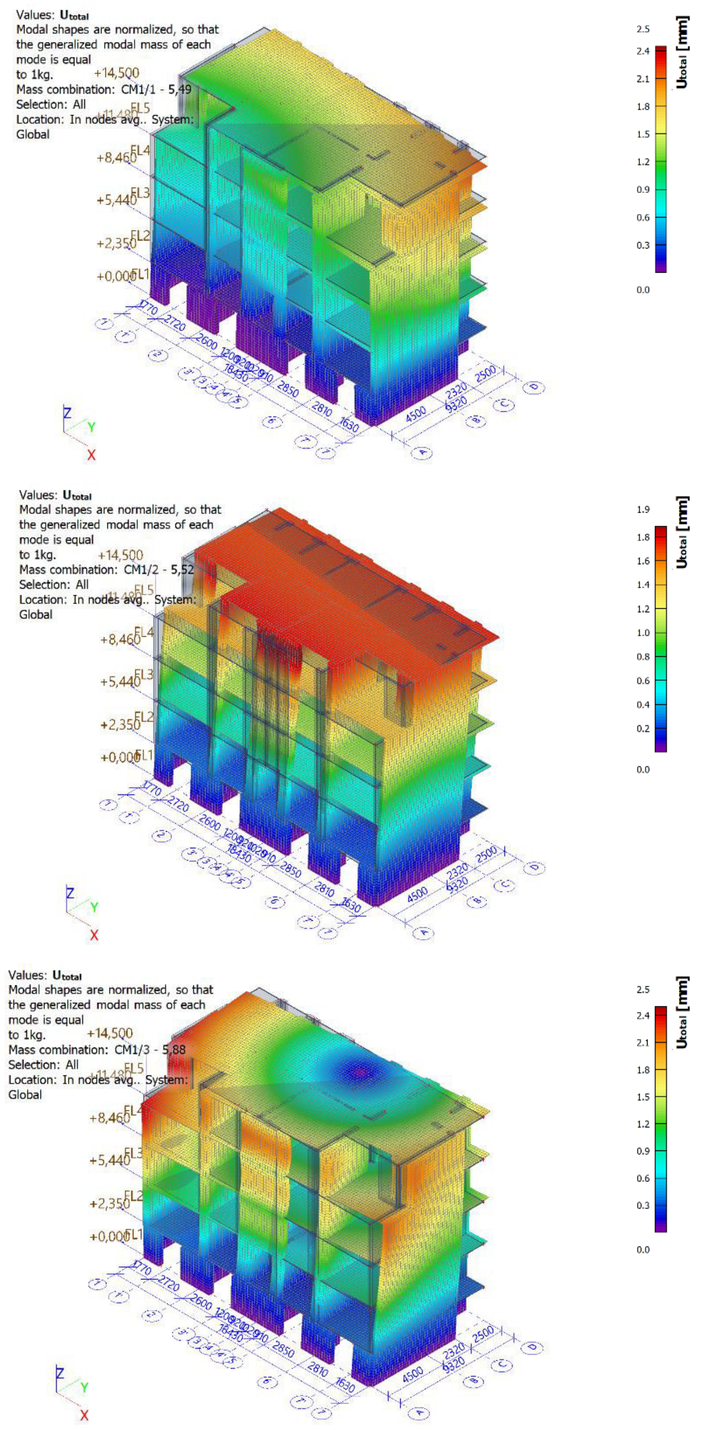

Fig. 17 First three modes

3.3.5. Check of the bearing capacity of masonry walls for horizontal loads

According to the internal forces obtained by computer program (results of seismic combination and input data), verification of all brick walls is presented in Fig. 18 and Fig. 19.

Tab. 5 Input data

Design load capacity for transverse force:	$V_{Rd} = f_{vk} \times t \times L_c/\gamma_M \times FP$
	$L_c = (L/2) \times [1 + (L \times N_{Ed}/6 \times M_{Ed})] \leq L$
Initial shear capacity of walls:	$f_{vk,0} = 0.15\ N/mm^2$
	$f_{vk} = f_{vk,0} + 0.4 \times \sigma_d\ N/mm^2$
Compressive strength:	$f = 10\ N/mm^2$
Normalized compressive strength:	$f_b = 9.72\ N/mm^2$
Characteristic compressive strength:	$f_k = 2.70\ N/mm^2$
Form factor:	$\delta = 0.81$
Confidence factor:	$FP = 1.35$

SMJER X																			
ZID	Duljina zida $L\,[m]$	$t\,[m]$	γ_m	$N_{Ed}\,[kN]$	$M_{Ed}[kNm]$	$V_{Ed}[kN]$	$L_C[m]$	$\sigma_d = \frac{N_{Ed}}{L_c \cdot t}\,[N/mm^2]$	$f_{vk0}[N/mm^2]$	$f_{vk}[N/mm^2]$	$f_{vk} \leq 0{,}065 \cdot f_b$	$V_{Rd}[kN]$	$V_{Ed}/V_{Rd}\,[\%]$	$V_{Rd} > V_{Ed}$	$V_{Ed,ETAŽE}[kN]$	$V_{Rd,ETAŽE}[kN]$	$V_{Ed,ETAŽE}/V_{Rd,ETAŽE}[\%]$	$V_{Rd,ETAŽE} > V_{Ed,ETAŽE}$	ETAŽE
PO_XA_1	1,23	0,38	1,50	82,46	2,01	6,90	1,23	0,176	0,15	0,221	0,221	50,91	14%	Zadovoljava	250,48	1425,74	18%	Zadovoljava	PODRUM
PO_XA_1	1,23	0,38	1,50	82,46	2,68	5,70	1,23	0,176	0,15	0,221	0,221	50,91	11%	Zadovoljava					
PO_XA_2	2,33	0,38	1,50	158,33	8,97	10,65	2,33	0,179	0,15	0,222	0,222	96,86	11%	Zadovoljava					
PO_XA_2	2,33	0,38	1,50	158,33	8,86	10,91	2,33	0,179	0,15	0,222	0,222	96,86	11%	Zadovoljava					
PO_XA_3	3,96	0,38	1,50	277,32	23,89	22,82	3,96	0,184	0,15	0,224	0,224	166,25	14%	Zadovoljava					
PO_XA_3	3,96	0,38	1,50	277,32	23,66	22,51	3,96	0,184	0,15	0,224	0,224	166,25	14%	Zadovoljava					
PO_XA_4	2,34	0,38	1,50	163,31	9,07	11,15	2,34	0,184	0,15	0,223	0,223	98,13	11%	Zadovoljava					
PO_XA_4	2,34	0,38	1,50	163,31	9,17	10,59	2,34	0,184	0,15	0,223	0,223	98,13	11%	Zadovoljava					
PO_XA_5	1,37	0,38	1,50	96,32	3,52	7,48	1,37	0,185	0,15	0,224	0,224	57,59	13%	Zadovoljava					
PO_XA_5	1,37	0,38	1,50	96,32	2,64	8,62	1,37	0,185	0,15	0,224	0,224	57,59	15%	Zadovoljava					
PO_XB_1				**1696,99**	**152,10**	**371,74**	**NOVI AB ZID DEBLJINE 15 CM**												
PO_XB_1				**1696,99**	**204,11**	**254,13**													
PO_XB_2				**886,22**	**12,17**	**171,97**													
PO_XB_2				**886,22**	**14,19**	**171,49**													
PO_XB_3				**1717,05**	**182,57**	**250,44**													
PO_XB_3				**1717,05**	**165,63**	**371,67**													
PO_XC_1	1,77	0,38	1,50	72,51	3,95	21,24	1,77	0,108	0,15	0,193	0,193	64,15	33%	Zadovoljava					
PO_XC_1	1,77	0,38	1,50	72,51	4,12	21,76	1,77	0,108	0,15	0,193	0,193	64,15	34%	Zadovoljava					
PO_XC_2	1,63	0,38	1,50	71,67	3,54	20,77	1,63	0,116	0,15	0,196	0,196	60,04	35%	Zadovoljava					
PO_XC_2	1,63	0,38	1,50	71,67	3,81	21,11	1,63	0,116	0,15	0,196	0,196	60,04	35%	Zadovoljava					
PO_XD_3	1,80	0,38	1,50	47,82	12,42	14,19	1,80	0,070	0,15	0,178	0,178	60,11	24%	Zadovoljava					
PO_XD_3	1,80	0,38	1,50	47,82	14,82	7,89	1,77	0,071	0,15	0,178	0,178	59,28	13%	Zadovoljava					
PO_XD_4	1,80	0,38	1,50	46,76	14,74	9,13	1,75	0,070	0,15	0,178	0,178	58,62	16%	Zadovoljava					
PO_XD_4	1,80	0,38	1,50	46,76	9,68	17,06	1,80	0,068	0,15	0,177	0,177	59,90	28%	Zadovoljava					
PR_XB_1				**433,63**	**41,15**	**44,01**	**NOVI AB ZID DEBLJINE 15 CM**												PRIZEMLJE
PR_XB_1				**433,63**	**42,22**	**44,71**													
PR_XB_2				**1045,88**	**318,26**	**347,30**													
PR_XB_2				**1045,88**	**316,57**	**347,12**													
PR_XB_3				**1182,65**	**409,02**	**439,00**													
PR_XB_3				**1182,65**	**402,83**	**438,24**													
PR_XB_4				**279,18**	**13,32**	**14,35**													
PR_XB_4				**279,18**	**12,83**	**14,05**													
1K_XB_1				**284,45**	**15,92**	**18,27**													1. KAT
1K_XB_1				**284,45**	**17,81**	**20,25**													
1K_XB_2				**694,65**	**70,56**	**258,26**													
1K_XB_2				**694,65**	**66,69**	**170,62**													
1K_XB_3				**627,26**	**20,10**	**250,85**													
1K_XB_3				**627,26**	**9,01**	**248,24**													
1K_XB_4				**700,39**	**131,47**	**168,57**													
1K_XB_4				**700,39**	**102,67**	**262,01**													
2K_XB_1				**425,78**	**47,47**	**128,50**													2. KAT
2K_XB_1				**425,78**	**47,01**	**181,45**													
2K_XB_2				**174,40**	**7,29**	**188,16**													
2K_XB_2				**174,40**	**13,65**	**188,98**													
2K_XB_3				**388,96**	**17,80**	**91,42**													
2K_XB_3				**388,96**	**48,23**	**146,16**													
3K_XB_1				**81,03**	**3,98**	**5,64**													3. KAT
3K_XB_1				**81,03**	**4,04**	**5,66**													
3K_XB_2				84,12	1,58	21,19													
3K_XB_2				84,12	2,08	11,67													
3K_XB_3				**114,82**	**1,39**	**44,67**													
3K_XB_3				**114,82**	**1,65**	**33,55**													
3K_XB_4				**187,67**	**0,90**	**69,02**													
3K_XB_4				**187,67**	**1,31**	**67,75**													
3K_XB_5				**229,53**	**20,74**	**54,53**													
3K_XB_5				**229,53**	**19,37**	**76,66**													
3K_XB_6				**54,66**	**1,36**	**3,26**													
3K_XB_6				**54,66**	**1,35**	**3,41**													

Fig. 18 Verification of the bearing capacity of the walls in the X direction for horizontal load

SMJER Y																			
ZID	Duljina zida $L[m]$	$t\,[m]$	γ_m	$N_{Ed}\,[kN]$	$M_{Ed}[kNm]$	$V_{Ed}[kN]$	$L_c[m]$	$\sigma_d = \frac{N_{Ed}}{L_c \cdot t}\,[N/mm^2]$	$f_{vk0}[N/mm^2]$	$f_{vk}[N/mm^2]$	$f_{vk} \leq 0{,}065 \cdot f_b$	$V_{Rd}[kN]$	$V_{Ed}/V_{Rd}\,[\%]$	$V_{Rd} > V_{Ed}$	$V_{Ed,ETAŽE}[kN]$	$V_{Rd,ETAŽE}[kN]$	$V_{Ed,ETAŽE}/V_{Rd,ETAŽE}[\%]$	$V_{Rd,ETAŽE} > V_{Ed,ETAŽE}$	ETAŽE
PO_Y1'_1	2,50	0,38	1,50	91,68	23,16	26,76	2,50	0,097	0,15	0,189	0,189	88,48	30%	Zadovoljava	878,80	2998,30	29%	Zadovoljava	PODRUM
PO_Y1'_1	2,50	0,38	1,50	91,68	14,40	26,28	2,50	0,097	0,15	0,189	0,189	88,48	30%	Zadovoljava					
PO_Y1_1	6,82	0,38	1,50	379,94	111,06	93,85	6,82	0,147	0,15	0,209	0,209	267,02	35%	Zadovoljava					
PO_Y1_1	6,82	0,38	1,50	379,94	321,71	94,27	6,82	0,147	0,15	0,209	0,209	267,02	35%	Zadovoljava					
PO_Y2_1	2,18	0,38	1,50	140,03	9,19	19,32	2,18	0,169	0,15	0,218	0,218	89,02	22%	Zadovoljava					
PO_Y2_1	2,18	0,38	1,50	140,03	17,46	18,89	2,18	0,169	0,15	0,218	0,218	89,02	21%	Zadovoljava					
PO_Y2_2	2,02	0,38	1,50	79,28	3,17	14,74	2,02	0,103	0,15	0,191	0,191	72,52	20%	Zadovoljava					
PO_Y2_2	2,02	0,38	1,50	79,28	5,74	14,33	2,02	0,103	0,15	0,191	0,191	72,52	20%	Zadovoljava					
PO_Y2_3	3,30	0,38	1,50	128,50	50,05	30,26	3,30	0,102	0,15	0,191	0,191	118,27	26%	Zadovoljava					
PO_Y2_3	3,30	0,38	1,50	128,50	31,22	28,63	3,30	0,102	0,15	0,191	0,191	118,27	24%	Zadovoljava					
PO_Y3'_1				**1140,65**	**544,04**	**293,12**	**NOVI AB ZID DEBLJINE 15 CM**												
PO_Y3'_1				**1140,65**	**296,37**	**294,27**													
PO_Y3_1	4,50	0,25	1,50	181,62	17,49	30,55	4,50	0,161	0,15	0,215	0,215	119,21	26%	Zadovoljava					
PO_Y3_1	4,50	0,25	1,50	181,62	60,62	31,02	4,50	0,161	0,15	0,215	0,215	119,21	26%	Zadovoljava					
PO_Y4'_1	4,50	0,25	1,50	182,73	17,30	31,83	4,50	0,162	0,15	0,215	0,215	119,43	27%	Zadovoljava					
PO_Y4'_1	4,50	0,25	1,50	182,73	60,63	32,41	4,50	0,162	0,15	0,215	0,215	119,43	27%	Zadovoljava					
PO_Y5_1				**1162,55**	**306,97**	**314,41**	**NOVI AB ZID DEBLJINE 15 CM**												
PO_Y5_1				**1162,55**	**559,99**	**311,27**													
PO_Y6_1	1,75	0,38	1,50	116,47	11,18	15,21	1,75	0,175	0,15	0,220	0,220	72,27	21%	Zadovoljava					
PO_Y6_1	1,75	0,38	1,50	116,47	6,53	15,64	1,75	0,175	0,15	0,220	0,220	72,27	22%	Zadovoljava					
PO_Y6_2	2,02	0,38	1,50	95,69	5,87	17,34	2,02	0,125	0,15	0,200	0,200	75,76	23%	Zadovoljava					
PO_Y6_2	2,02	0,38	1,50	95,69	9,70	16,47	2,02	0,125	0,15	0,200	0,200	75,76	22%	Zadovoljava					
PO_Y6_3	3,20	0,38	1,50	129,74	33,14	29,55	3,20	0,107	0,15	0,193	0,193	115,70	26%	Zadovoljava					
PO_Y6_3	3,20	0,38	1,50	129,74	49,10	31,73	3,20	0,107	0,15	0,193	0,193	115,70	27%	Zadovoljava					
PO_Y7'_1	2,50	0,38	1,50	98,45	17,02	28,10	2,50	0,104	0,15	0,191	0,191	89,82	31%	Zadovoljava					
PO_Y7'_1	2,50	0,38	1,50	98,45	25,93	28,18	2,50	0,104	0,15	0,191	0,191	89,82	31%	Zadovoljava					
PO_Y7_1	6,82	0,38	1,50	403,39	326,98	102,31	6,82	0,156	0,15	0,212	0,212	271,65	38%	Zadovoljava					
PO_Y7_1	6,82	0,38	1,50	403,39	116,34	101,13	6,82	0,156	0,15	0,212	0,212	271,65	37%	Zadovoljava					
PR_Y1'_2	1,08	0,38	1,50	30,71	5,16	5,69	1,08	0,075	0,15	0,180	0,180	36,47	16%	Zadovoljava	779,15	2402,85	32%	Zadovoljava	PRIZEMLJE
PR_Y1'_2	1,08	0,38	1,50	30,71	3,78	5,83	1,08	0,075	0,15	0,180	0,180	36,47	16%	Zadovoljava					
PR_Y1_1	6,82	0,38	1,50	471,46	455,48	111,38	6,82	0,182	0,15	0,223	0,223	285,10	39%	Zadovoljava					
PR_Y1_1	6,82	0,38	1,50	471,46	70,49	111,49	6,82	0,182	0,15	0,223	0,223	285,10	39%	Zadovoljava					
PR_Y2_1	2,18	0,38	1,50	183,73	25,89	20,70	2,18	0,222	0,15	0,239	0,239	97,66	21%	Zadovoljava					
PR_Y2_1	2,18	0,38	1,50	183,73	13,12	20,12	2,18	0,222	0,15	0,239	0,239	97,66	21%	Zadovoljava					
PR_Y2_5	1,70	0,38	1,50	51,85	14,23	12,96	1,70	0,080	0,15	0,182	0,182	58,09	22%	Zadovoljava					
PR_Y2_5	1,70	0,38	1,50	51,85	8,72	13,09	1,70	0,080	0,15	0,182	0,182	58,09	23%	Zadovoljava					
PR_Y3'_1				**1020,44**	**277,09**	**319,33**	**NOVI AB ZID DEBLJINE 15 CM**												
PR_Y3'_1				**1020,44**	**749,94**	**320,96**													
PR_Y3_1	4,95	0,25	1,50	224,25	20,83	35,77	4,95	0,181	0,15	0,222	0,222	135,96	26%	Zadovoljava					
PR_Y3_1	4,95	0,25	1,50	224,25	100,62	34,51	4,95	0,181	0,15	0,222	0,222	135,96	25%	Zadovoljava					
PR_Y4'_1	4,95	0,25	1,50	223,67	7,84	40,67	4,95	0,181	0,15	0,222	0,222	135,85	30%	Zadovoljava					
PR_Y4'_1	4,95	0,25	1,50	223,67	87,56	39,58	4,95	0,181	0,15	0,222	0,222	135,85	29%	Zadovoljava					
PR_Y5_1				**1006,53**	**304,17**	**344,59**	**NOVI AB ZID DEBLJINE 15 CM**												
PR_Y5_1				**1006,53**	**777,67**	**346,15**													

Fig. 19 Verification of the bearing capacity of the walls in the Y direction for horizontal load – part 1/2

PR_Y6_1	1,75	0,38	1,50	148,27	9,97	16,05	1,75	0,223	0,15	0,239	0,239	78,55	20%	Zadovoljava				
PR_Y6_1	1,75	0,38	1,50	148,27	16,67	16,69	1,75	0,223	0,15	0,239	0,239	78,55	21%	Zadovoljava				
PR_Y6_4	1,70	0,38	1,50	50,17	9,98	14,57	1,70	0,078	0,15	0,181	0,181	57,76	25%	Zadovoljava				
PR_Y6_4	1,70	0,38	1,50	50,17	15,50	14,47	1,62	0,081	0,15	0,183	0,183	55,60	26%	Zadovoljava				
PR_Y7'_1	1,05	0,38	1,50	28,11	4,03	6,21	1,05	0,070	0,15	0,178	0,178	35,11	18%	Zadovoljava				
PR_Y7'_1	1,05	0,38	1,50	28,11	5,30	6,13	1,01	0,073	0,15	0,179	0,179	33,96	18%	Zadovoljava				
PR_Y7_1	6,82	0,38	1,50	458,50	473,43	126,57	6,82	0,177	0,15	0,221	0,221	282,54	45%	Zadovoljava				
PR_Y7_1	6,82	0,38	1,50	458,50	90,50	126,67	6,82	0,177	0,15	0,221	0,221	282,54	45%	Zadovoljava				
1K_Y1'_2	1,08	0,38	1,50	23,64	4,17	5,17	1,08	0,058	0,15	0,173	0,173	35,07	15%	Zadovoljava	566,76	1677,00	34%	Zadovoljava	1. KAT
1K_Y1'_2	1,08	0,38	1,50	23,64	3,40	5,33	1,08	0,058	0,15	0,173	0,173	35,07	15%	Zadovoljava				
1K_Y1_1	6,82	0,38	1,50	318,36	59,44	99,61	6,82	0,123	0,15	0,199	0,199	254,86	39%	Zadovoljava				
1K_Y1_1	6,82	0,38	1,50	318,36	292,55	99,03	6,82	0,123	0,15	0,199	0,199	254,86	39%	Zadovoljava				
1K_Y2_1	2,18	0,38	1,50	121,36	11,83	18,86	2,18	0,146	0,15	0,209	0,209	85,34	22%	Zadovoljava				
1K_Y2_1	2,18	0,38	1,50	121,36	19,54	19,08	2,18	0,146	0,15	0,209	0,209	85,34	22%	Zadovoljava				
1K_Y2_4	1,70	0,38	1,50	39,22	7,88	12,23	1,70	0,061	0,15	0,174	0,174	55,60	22%	Zadovoljava				
1K_Y2_4	1,70	0,38	1,50	39,22	11,06	12,04	1,70	0,061	0,15	0,174	0,174	55,60	22%	Zadovoljava				
1K_Y3'_1				**700,28**	**245,21**	**298,21**	NOVI AB ZID DEBLJINE 15 CM											
1K_Y3'_1				**700,28**	**528,79**	**298,62**												
1K_Y5_1				**687,83**	**549,76**	**320,09**												
1K_Y5_1				**687,83**	**265,42**	**319,71**												
1K_Y6_1	1,75	0,38	1,50	97,38	13,00	15,26	1,75	0,146	0,15	0,209	0,209	68,49	22%	Zadovoljava				
1K_Y6_1	1,75	0,38	1,50	97,38	8,95	15,02	1,75	0,146	0,15	0,209	0,209	68,49	22%	Zadovoljava				
1K_Y6_4	1,70	0,38	1,50	37,73	8,81	14,01	1,70	0,058	0,15	0,173	0,173	55,30	25%	Zadovoljava				
1K_Y6_4	1,70	0,38	1,50	37,73	12,01	13,98	1,60	0,062	0,15	0,175	0,175	52,35	27%	Zadovoljava				
1K_Y7'_1	1,05	0,38	1,50	21,46	3,57	5,74	1,05	0,054	0,15	0,172	0,172	33,79	17%	Zadovoljava				
1K_Y7'_1	1,05	0,38	1,50	21,46	4,28	5,63	0,98	0,058	0,15	0,173	0,173	31,73	18%	Zadovoljava				
1K_Y7_1	6,82	0,38	1,50	306,71	71,40	113,12	6,82	0,118	0,15	0,197	0,197	252,56	45%	Zadovoljava				
1K_Y7_1	6,82	0,38	1,50	306,71	303,31	112,65	6,82	0,118	0,15	0,197	0,197	252,56	45%	Zadovoljava				
2K_Y1'_2	1,08	0,38	1,50	17,11	2,77	4,60	1,08	0,042	0,15	0,167	0,167	33,78	14%	Zadovoljava	414,61	1479,81	28%	Zadovoljava	2. KAT
2K_Y1'_2	1,08	0,38	1,50	17,11	2,36	4,71	1,08	0,042	0,15	0,167	0,167	33,78	14%	Zadovoljava				
2K_Y1_1	6,82	0,38	1,50	207,90	163,59	72,34	6,82	0,080	0,15	0,182	0,182	233,04	31%	Zadovoljava				
2K_Y1_1	6,82	0,38	1,50	207,90	25,90	72,83	6,82	0,080	0,15	0,182	0,182	233,04	31%	Zadovoljava				
2K_Y2_1	2,18	0,38	1,50	78,25	12,50	15,20	2,18	0,094	0,15	0,188	0,188	76,82	20%	Zadovoljava				
2K_Y2_1	2,18	0,38	1,50	78,25	7,94	15,07	2,18	0,094	0,15	0,188	0,188	76,82	20%	Zadovoljava				
2K_Y2_5	1,70	0,38	1,50	28,20	5,41	9,85	1,70	0,044	0,15	0,167	0,167	53,42	18%	Zadovoljava				
2K_Y2_5	1,70	0,38	1,50	28,20	7,20	9,66	1,70	0,044	0,15	0,167	0,167	53,42	18%	Zadovoljava				
2K_Y3'_1				**440,63**	**321,51**	**218,00**	NOVI AB ZID DEBLJINE 15 CM											
2K_Y3'_1				**440,63**	**155,82**	**217,40**												
2K_Y5_1				**435,37**	**171,39**	**232,79**												
2K_Y5_1				**435,37**	**337,66**	**233,28**												
2K_Y6_2	1,75	0,38	1,50	63,06	8,59	12,63	1,75	0,095	0,15	0,188	0,188	61,72	20%	Zadovoljava				
2K_Y6_2	1,75	0,38	1,50	63,06	6,18	12,47	1,75	0,095	0,15	0,188	0,188	61,72	20%	Zadovoljava				
2K_Y6_5	1,70	0,38	1,50											Zadovoljava				
2K_Y6_5	1,70	0,38	1,50	27,59	7,94	10,80	1,24	0,058	0,15	0,173	0,173	40,47	27%	Zadovoljava				
2K_Y7'_1	1,05	0,38	1,50	15,99	2,52	4,82	1,05	0,040	0,15	0,166	0,166	32,71	15%	Zadovoljava				
2K_Y7'_1	1,05	0,38	1,50	15,99	2,91	4,72	0,77	0,055	0,15	0,172	0,172	24,89	19%	Zadovoljava				
2K_Y7_1	6,82	0,38	1,50	203,14	35,90	82,65	6,82	0,078	0,15	0,181	0,181	232,10	36%	Zadovoljava				
2K_Y7_1	6,82	0,38	1,50	203,14	172,75	82,26	6,82	0,078	0,15	0,181	0,181	232,10	35%	Zadovoljava				
3K_Y1'_2	1,08	0,38	1,50	10,34	1,42	3,06	1,08	0,025	0,15	0,160	0,160	32,44	9%	Zadovoljava	654,98	1115,16	59%	Zadovoljava	3. KAT
3K_Y1'_2	1,08	0,38	1,50	10,34	1,25	3,17	1,08	0,025	0,15	0,160	0,160	32,44	10%	Zadovoljava				
3K_Y1_1	4,50	0,38	1,50	68,76	30,56	26,73	4,50	0,040	0,15	0,166	0,166	140,25	19%	Zadovoljava				
3K_Y1_1	4,50	0,38	1,50	68,76	10,11	26,86	4,50	0,040	0,15	0,166	0,166	140,25	19%	Zadovoljava				
3K_Y2_1	2,18	0,38	1,50	43,60	6,04	10,08	2,18	0,053	0,15	0,171	0,171	69,98	14%	Zadovoljava				
3K_Y2_1	2,18	0,38	1,50	43,60	3,69	9,99	2,18	0,053	0,15	0,171	0,171	69,98	14%	Zadovoljava				
3K_Y2_4	1,70	0,25	1,50	17,13	2,67	6,62	1,70	0,040	0,15	0,166	0,166	34,87	19%	Zadovoljava				
3K_Y2_4	1,70	0,25	1,50	17,13	3,50	6,47	1,70	0,040	0,15	0,166	0,166	34,87	19%	Zadovoljava				
3K_Y3'_1				**195,84**	**59,73**	**107,86**	NOVI AB ZID DEBLJINE 15 CM											
3K_Y3'_1				**195,84**	**143,79**	**108,10**												
3K_Y5_1				**199,53**	**70,43**	**119,68**												
3K_Y5_1				**199,53**	**154,75**	**119,93**												
3K_Y6_1	1,75	0,38	1,50	35,93	3,19	9,24	1,75	0,054	0,15	0,172	0,172	56,36	16%	Zadovoljava				
3K_Y6_1	1,75	0,38	1,50	35,93	4,45	9,33	1,75	0,054	0,15	0,172	0,172	56,36	17%	Zadovoljava				
3K_Y6_5	1,70	0,38	1,50	17,59	4,05	7,52	1,70	0,027	0,15	0,161	0,161	51,33	15%	Zadovoljava				
3K_Y6_5	1,70	0,38	1,50	17,59	3,23	7,66	1,70	0,027	0,15	0,161	0,161	51,33	15%	Zadovoljava				
3K_Y7'_1	1,05	0,38	1,50	10,48	1,43	3,75	1,05	0,026	0,15	0,161	0,161	31,63	12%	Zadovoljava				
3K_Y7'_1	1,05	0,38	1,50	10,48	1,58	3,66	1,05	0,026	0,15	0,161	0,161	31,63	12%	Zadovoljava				
3K_Y7_1	4,50	0,38	1,50	71,25	33,37	32,54	4,50	0,042	0,15	0,167	0,167	140,74	23%	Zadovoljava				
3K_Y7_1	4,50	0,38	1,50	71,25	13,34	32,73	4,50	0,042	0,15	0,167	0,167	140,74	23%	Zadovoljava				

Fig. 20 Verification of the bearing capacity of the walls in the Y direction for horizontal load – part 2/2

4. CONCLUSION

Building in location ulica Artura Turkulina 43A, 44250 Petrinja (k.č.br. 433/1 k.o. Petrinja) was modelled in computer program SCIA Engineer v22.0. Building is approximately rectangular in shape, maximum floor plan dimensions are 18.9×9.8 m, approximately 830 m^2. It has basement, ground floor and three floors (B+GF+3F). The foundations are made of reinforced concrete, unknown dimensions. The walls are made of solid bricks, 38 cm thick. The slab structure consists of reinforced concrete panels with ribs. Multi-roofed roof structure is made of solid wood. The existing vertical load-bearing structure consists of solid brick masonry walls without vertical concrete elements, therefore, the vertical load-bearing structure can be defined as an unbounded masonry structure. In the series of earthquakes in 2020., building structure suffered moderate damages of load bearing and significant damages of load non-bearing elements. According to the standards and technical regulations, all loads and combination were applied in model of the building. New RC walls with new foundations were added. For calculation, return period of 95 years was adopted. Calculation proved maximum utilization of brick wall of 45%. This means that building has 222% resistance for return period of 95 years (peak ground acceleration of 0.07g). With this calculation, after adding new series of RC walls, resistance of the building is proven for peak ground accelereation of 0.15g (peak ground acceleration for 475 years return period).

REFERENCES

[1] UPPO – Urgentni program potresne obnove, Građevinski fakultet Sveučilišta u Zagrebu, Hrvatska komora inženjera građevinarstva, Zagreb, svibanj 2020.

[2] Eurokod 8: Projektiranje potresne otpornosti konstrukcija – 1. dio: Opća pravila, potresna djelovanja i pravila za zgrade (HRN EN 1998-1:2011)

[3] Eurokod 8: Projektiranje potresne otpornosti konstrukcija – 3. dio: Ocjenjivanje i obnova zgrada (HRN EN 1998-3:2011)

[4] Eurokod 6: Projektiranje zidanih konstrukcija – Dio 1-1: Opća pravila za armirane i nearmirane zidane konstrukcije (HRN EN 1996-1-1:2012)

MATHEMATICAL MODELLING OF GROUNDWATER FLOW IN POROUS MEDIUM

Marijana Milić[1], Goran Jeftenić[2], Ljubomir Budinski[3], Danilo Stipić[4], Slobodan Kolaković[5]

Summary:

The subject of this paper's research is based on mathematical modelling of groundwater flow in porous medium, observing the flow as a two-dimensional, in-plane behaviour. With the Laplace's equation (in the form of Poisson's partial differential equation), groundwater flow is considered numerically, by the method of finite differences, using software, not explicitly designed for that purpose. Considering that numerical methods are based on approximation and give approximately accurate results, it is shown to what extent the accuracy of the solution is affected by the idealization of the physical model, the change of boundary conditions, the dimensions of the computational grid and the change of the environment in which the analysis is performed. The obtained solution in the selected software package (Microsoft Excel) was compared with the one obtained using software that enables more accurate modelling (GMS). Despite the deviations that occurred, the model results match well as far as the groundwater level is concerned, which justifies the use of the selected software for the purpose of mastering physical laws.

Key words: groundwater, diaphragm, Microsoft Excel, GMS

[1] Teaching Assistant, MSc, University of Novi Sad, Faculty of Technical Sciences, Novi Sad, Serbia, marijana.milic@uns.ac.rs
[2] Assistant Professor, PhD, University of Novi Sad, Faculty of Technical Sciences, Novi Sad, Serbia, goran.jeftenic@uns.ac.rs
[3] Full Professor, PhD, University of Novi Sad, Faculty of Technical Sciences, Novi Sad, Serbia, ljubab@uns.ac.rs
[4] Teaching Assistant, PhD, University of Novi Sad, Faculty of Technical Sciences, Novi Sad, Serbia, danilostipic@uns.ac.rs
[5] Associate Professor, PhD, University of Novi Sad, Faculty of Technical Sciences, Novi Sad, Serbia, kolakovic.s@uns.ac.rs

1. INTRODUCTION

Groundwater and snow/glaciers comprise more than 97% of all fresh water on Earth [1]. Moreover, they are one of the most important sources of drinking water, used for various purposes such as agriculture, industry, water supply to the population, etc. Groundwater research has been gaining importance in recent years due to the growing awareness of the need for groundwater and the increasing deterioration of its quality and quantity. Although, due to its good characteristics, it represents a widespread type of water supply, groundwater can still cause certain problems.

One of the many problems that arise during groundwater research is the lowering of the groundwater level for building construction. In order to start the construction of a certain object (e.g., underground garages), it is necessary first to lower the groundwater level in the construction pit to ensure construction in dry conditions. The data most often requested for these purposes are the groundwater flow or the groundwater level itself. However, getting to them and solving a specific problem like the one mentioned above is often a challenge because a porous medium does not work in the same way as open channels and pressurized systems. The problem with underground flow is reflected in the involvement of the soil in the entire analysis, and the flow through that soil is based on some other laws (the most important of all, Darcy's[1] law).

The solution for these and similar processes has been searched for centuries by modelling and describing the groundwater flow process in different conditions and environments. Numerical modelling has proven to be a powerful tool for better understanding groundwater flow and obtaining information on relevant groundwater parameters. The most important aspect of using such models is obtaining data on the real conditions within the observed environment, meaning that such models provide us with enough information to manage groundwater resources efficiently [2]. The first step in the modelling process is creating a conceptual model. In the next step, this conceptual model is converted into appropriate mathematical expressions combined with boundary conditions to form a mathematical model. Although these models are quite complex and characterized by a large amount of input data, their application is extensive.

In this paper, by applying mathematics, software and the available literature, the given topic is considered and discussed through the prism of the engineering profession. The aim was to consider the required number of wells in order to lower the level of groundwater (which flows through a porous medium with a free surface, previously determined by exploratory wells at the subject location) to the level required by the project, which is necessary to ensure construction in dry conditions. Numerical analysis was carried out in the Microsoft Excel program package (2D simulation) and compared with the model created in the GMS software, which enables more accurate modelling due to the possibility of 3D simulations. Two possible cases were considered: state without diaphragms and state with diaphragms carried out to an impermeable floor. For both cases, analyses were made with different grid and cell dimensions. The wells were defined by flow using the discretized Laplace's equation according to the finite difference method. The flow was set iteratively to meet the filtration stability criteria at the entrance to the filter structure, which was controlled by the velocities at the entrance to the well.

2. MATHEMATICAL MODEL

Many physical processes, solved as a plane problem, are expressed mathematically with Laplace's equation (ϕ is called potential, and the change of that parameter enables the process to take place) [3]:

[1] Henry Philibert Gaspard Darcy (1803-1858), French engineer

$$\frac{\partial^2 \Phi}{\partial x^2} + \frac{\partial^2 \Phi}{\partial y^2} = 0 \tag{1}$$

When groundwater flows in a phreatic aquifer, the potential Φ should be taken as $h^2/2$ (the case considered here, where the parameter h represents the depth), while in the case of an artesian aquifer, the potential difference, which enables the flow, represents the piezometric elevation, i.e. Φ = Π. Laplace's equation, which has been proven to be able to describe the simulation of well pumping, has the form of a partial differential Poisson's equation:

$$K\frac{\partial^2 \left(\frac{h^2}{2}\right)}{\partial x^2} + K\frac{\partial^2 \left(\frac{h^2}{2}\right)}{\partial y^2} + W = 0 \tag{2}$$

The parameter W describes the function of the source, that is, the sink in this particular case. Regarding groundwater flow, some sources and sinks include recharge from leakage, infiltration, underflow, evapotranspiration, springs, seeps, drains, etc. In other words, this parameter allows a certain amount of water to be introduced into the system or removed from it. If something like that exists in the system, it must be considered in the continuity equation, i.e. the law of mass invariance must be applied. In this expression, the sink W will keep a constant value because the flow that does not change over time is discussed. It is presented in the form of:

$$W = \frac{Q}{A} \tag{3}$$

In equation (3), the parameter Q represents the flow that will be set iteratively in the simulations, and the parameter A is the cross-sectional area perpendicular to the water pumping direction. The representation of the indexes used in the discretization of the equation (2) is shown in Figure 1.

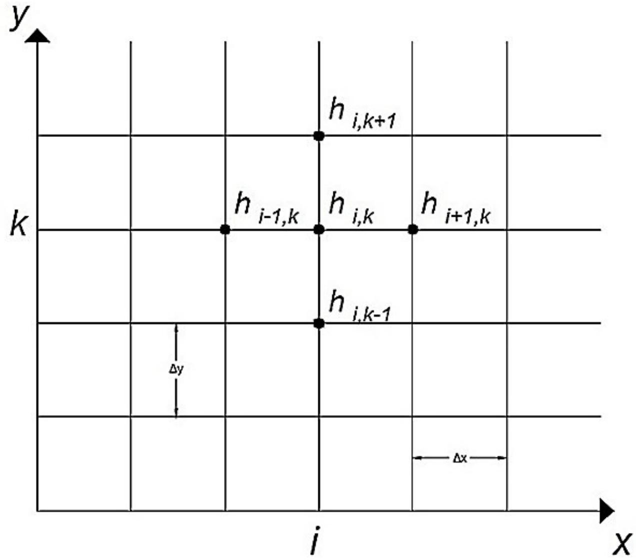

Fig. 1 Plane discretization

For this analysis, it was adopted that the dimension of the well corresponds to the dimensions of one cell to simplify the scheme. As the finite difference method dictates, the discretisation process begins by replacing differentially small increments with finite increments. Instead of the symbol for the partial derivative ∂, the symbol for the total derivative Δ is used. After the discretization of equation (2) in the x and y directions, in order to obtain the final expression used for analysis purposes, certain simplifications

were introduced, such as adopting the same filtration coefficient in both directions and using a square computational grid ($\Delta x = \Delta y$).
The final equation used in the numerical calculation (4) is, in fact, a function (for a steady state) dependent on the surrounding depths (groundwater levels), the flow rate, Q (which is set iteratively) and the filtration coefficient, K:

$$h_{i,k} = \sqrt{\frac{\left(h_{i+1,k}^2 + h_{i-1,k}^2 + h_{i,k+1}^2 + h_{i,k-1}^2\right)}{4} - \frac{Q}{2K}} \tag{4}$$

As the formula used in the finite difference method has been derived, it is necessary to set the boundary conditions as the method requires. They will be mentioned in the following chapters within the specific case to be considered.

3. METHODOLOGY

Analytical solutions have been found in the literature [3] for cases with simple boundary conditions, for example, when a perfect, isolated well (pressed down to an impermeable floor with no influence of other circumstances on its operation) is considered. It is clear that if the physical model were complicated, solving the equations in this way would become much more complicated. At some point, reaching an exact solution would no longer be possible. The solution would be approximate, while other methods start precisely to obtain a sufficiently accurate solution.
Numerical methods used for analysis represent an iterative process suitable for computer work. The accuracy of the results depends on the formation of the model itself, although it is known in advance that the results will be approximate. The finite difference method chosen for this analysis is based on the discretization of the considered area where differentially small quantities are replaced by finite increments. The first step in discretization is the division of the modelled area (flow area) by a regular grid (square or rectangular, orthogonal) into a series of sub-areas (spatial, planar or linear control elements). In order to achieve the simplest and most universal numerical algorithm, a grid of dimensions *nxn* is formed and placed to cover the entire area under consideration and a part of the area where there is no groundwater flow. Once universality is achieved, applying one algorithm with a change in input data to a range of real conditions will be possible. In the parts of the model where there is no flow, the condition of the so-called solid boundary is set. It is crucially important when modelling groundwater to choose the boundary values correctly because in the case of different boundary conditions, significantly different results can be obtained.
Creating a mathematical model involves setting up the flow equation with initial and boundary conditions. When talking about modelling the groundwater flow, the initial conditions would represent the potential level, that is, the groundwater level, while the boundary conditions are those under the influence of which water movement occurs.
The computational grid is created using the "Microsoft Excel" program, an integral part of the "Microsoft Office" software package. The well is simulated with one cell (due to technical conditions). However, an error in the result is expected because the well is 0.2m in diameter in the specifically considered case, while the adopted calculation cells will be of significantly larger dimensions.
The first thing that is set in the software is the grid density. When applying the finite difference method, the derivative approximation error is proportional to the discretization step, which means that with a smaller spatial step, a smaller error is obtained. After that, the boundary conditions are set. In this case, they represent the potential level without the influence of the well at the assumed distance so that they are outside the radius of action of the well (the zone where the influence of the depression cone is not felt). When an equalized level of potential is obtained on the entire grid,

wells are iteratively assigned to fulfil the required task, i.e. lower the groundwater level to the required elevation.
Assumptions used for the modelling process are:

- The flow is observed as in-plane behaviour;
- A grid with square cells was adopted where different dimensions of both cells and grids will be considered;
- Wells defined by flow are considered;
- Wells are located in one cell;
- Fixed elevations give the boundary conditions that describe the system's boundary.

4. RESULTS AND DISCUSSION

This paper's main goal is to compare the results obtained by mathematical modelling in "Microsoft Excel" with those obtained in the paper [4], where the lowering of the groundwater level to construct the "Underground Garage" facility in Novi Sad, was considered using GMS software. Execution of works on the subject location required lowering the groundwater level from the adopted level of 76.00 m above sea level to 63.00 m above sea level in the phreatic aquifer. In order to complete the mathematical model, the filtration coefficient was adopted at a value of $K = 3.0x10^{-4}$ (m/s) based on a geotechnical study. In the constructive solution of the facility, it was predicted that diaphragms would be constructed to secure the foundation pit, given that the object was being built in a densely built-up area of the city, and ground subsidence may cause disturbance of the stability of buildings nearby.
There were three possible cases. The first presented a solution without diaphragms (wells placed exclusively around the pit). The second one was the case of a partially constructed diaphragm, where the diaphragm was performed in the aquifer without interfering with the impermeable floor. It was planned to lower the levels in the construction pit by combining wells around and inside the pit. The third case presented the condition where the diaphragm was carried out to the depth of the impermeable floor. It thus formed a closed contour (reservoir), where it was planned to lower the level by constructing wells exclusively inside the construction pit.
This analysis did not consider the second case since 3D simulations cannot be done in "Microsoft Excel" (a plane state is observed).

4.1. LOWERING GROUNDWATER LEVELS TO A STATE WITHOUT DIAPHRAGMS

To consider the obtained results, it was necessary first to know the process that led to them. Namely, creating a model for simulating the real situation was done iteratively.
The starting assumption was the size of the grid to be displayed. In order to know the groundwater level at each point, the modelled grid must cover an area that will be larger than the zone where the influence of the depression cone is felt. If this were to be ignored and if a grid was created to the borders of which the effect of the well reaches, in addition to not knowing the groundwater level in points that are further from the considered area, one would not even have a realistic picture of the observed environment because it was influenced by the proximity of the border given as a fixed elevation.
The first iteration was a grid with a radius of 300 m on each side of the facility. Since the object has 100 m × 30 m dimensions, the grid was estimated to be 700 m × 630 m. However, after setting up the wells, it turned out that the effect of the wells reached the assumed limits of the system, and for the reasons mentioned above, the grid was increased. The next one was a grid with 1100 m × 1030 m dimensions, meaning the object was located in the middle of the observed area with a distance of 500 m on each

side. For this one, as for the previous grid, the boundary condition was the elevation of the groundwater level around the system's perimeter. A value of 76.0 m was used for the initial condition, while a groundwater level of 76.6 m was adopted for the boundary condition. Laplace's equation converted to fit the finite difference method was first assigned to the entire grid. The iterative calculation in "Microsoft Excel" is conditioned either by the number of iterations or by the fact that it will stop if the difference between two iterations is less than the given one. Changing the number of iterations brought the calculation to an end. However, it physically did not make sense (because it is known that without setting up the wells, the groundwater level must be the same everywhere). So, the program was set to stop when the change between two iterations differed to the tenth decimal place. With the parameters set in this way, the grid was brought to the real state found on the site (identical water level in all the points of the considered area). After that, the wells were simulated by the flow drawn from them.
The requirements that the grid should fulfil were:

- Lower the groundwater level in the area of the facility below 63 m above sea level;
- The boundaries of the system must capture larger dimensions than the radius of action of the well;
- Limit velocities so that suffusion does not occur.

For the first iteration, 14 wells with a flow rate of 20 l/s were adopted, which was insufficient. The problem was that the level was descending too slowly, which initiated an increase in precision (i.e., decreasing the differences between the two iterations) so that Excel would continue to iterate. Increasing accuracy requires a larger grid because it increases the radius of action of the well. Considering these facts, the number of wells and the flow rate per well increased iteratively. Thus, a solution with 36 wells with a flow rate of 40 l/s was obtained. The discretized Laplace's equation used for the numerical calculation as an initial condition in the cells representing the wells, specifically for the square grid used in the analysis, is given as equation (4). The same one, in the case of an artesian aquifer, can be found in [5]. The flow was iteratively set in addition to the steady part of Laplace's equation. These 36 wells were simulated by inserting so-called flow function (4) into the cells representing wells.
The representation of the groundwater level in the adopted case is given in Figure 2. The wells were placed around the construction pit as symmetrically as possible, and only the object zone and 10 m around the object zone are shown in order to have a closer view of the area of interest.

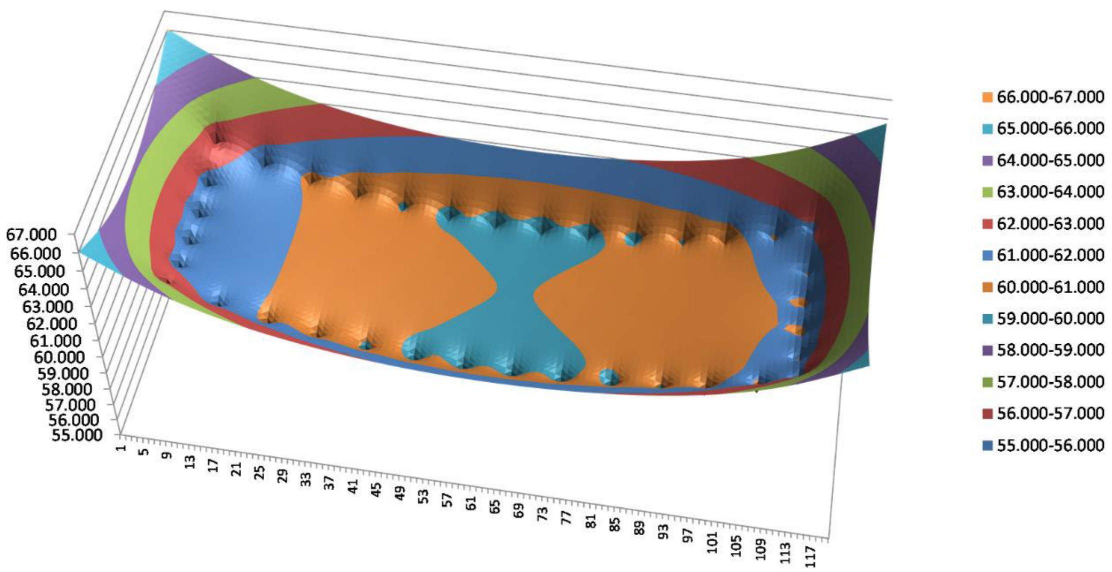

Fig. 2 Display of the groundwater level in the area of the facility and 10 m around the facility with 36 wells (cell 1 m x 1 m)

In addition to lowering the groundwater level to the required elevation (below 63 m above sea level), it was necessary to check the filtration stability. Filtration stability was evaluated by velocities at the entrance of the filter of the well, which were compared with the limit value (critical speed) adopted according to Abramov and Sichardt. It should be emphasized that these are velocity estimates at a distance of about 0.5 m from the well structure itself due to the adopted grid with cell dimensions of 1 m x 1 m. In comparison, the wells are 0.2 m in diameter (considering the very small diameter of the well located in a much larger cell, the well is considered a point). Since there was no possibility to obtain the exact velocity at the entrance to the well without thickening the grid, these estimated velocities were considered. Criteria for limiting velocities to suffosion, according to Abramov and Sichardt, depends on the filtration coefficient, which was estimated at 0.0003 m/s. Considering that, the critical speed, according to Abramov is 0.0022314 m/s, and according to Sichardt 0.0011547 m/s. By applying Darcy's formula, velocities were expressed around the perimeter of the cell of the considered grid in which the well was located. The labelling of the velocities at the entrance of the well cell is shown in Figure 3, and following that labelling, the velocities in m/s for each of the 36 wells are shown in Figure 4.

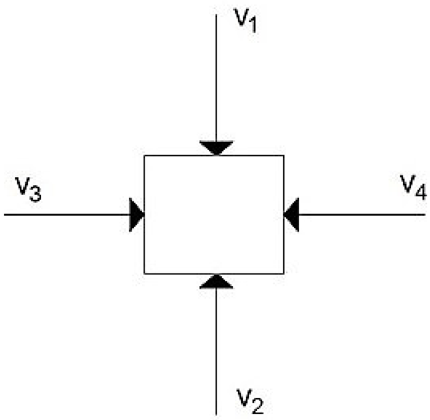

Fig. 3 Labeling the velocities at the entrance of the well cell

W1	v_1 = 0.000426	**W10**	v_1 = 0.000286	**W19**	v_1 = 0.000405	**W28**	v_1 = 0.000263
	v_2 = 0.000213		v_2 = 0.000427		v_2 = 0.000278		v_2 = 0.000412
	v_3 = 0.000436		v_3 = 0.000388		v_3 = 0.000329		v_3 = 0.000283
	v_4 = 0.000209		v_4 = 0.000307		v_4 = 0.000334		v_4 = 0.000370
W2	v_1 = 0.000364	**W11**	v_1 = 0.000403	**W20**	v_1 = 0.000278	**W29**	v_1 = 0.000425
	v_2 = 0.000275		v_2 = 0.000272		v_2 = 0.000405		v_2 = 0.000241
	v_3 = 0.000439		v_3 = 0.000357		v_3 = 0.000329		v_3 = 0.000275
	v_4 = 0.000224		v_4 = 0.000298		v_4 = 0.000334		v_4 = 0.000373
W3	v_1 = 0.000332	**W12**	v_1 = 0.000272	**W21**	v_1 = 0.000406	**W30**	v_1 = 0.000242
	v_2 = 0.000307		v_2 = 0.000403		v_2 = 0.000278		v_2 = 0.000422
	v_3 = 0.000428		v_3 = 0.000358		v_3 = 0.000322		v_3 = 0.000271
	v_4 = 0.000233		v_4 = 0.000298		v_4 = 0.000341		v_4 = 0.000376
W4	v_1 = 0.000305	**W13**	v_1 = 0.000403	**W22**	v_1 = 0.000277	**W31**	v_1 = 0.000433
	v_2 = 0.000333		v_2 = 0.000276		v_2 = 0.000406		v_2 = 0.000215
	v_3 = 0.000434		v_3 = 0.000351		v_3 = 0.000322		v_3 = 0.000196
	v_4 = 0.000234		v_4 = 0.000308		v_4 = 0.000341		v_4 = 0.000452
W5	v_1 = 0.000272	**W14**	v_1 = 0.000275	**W23**	v_1 = 0.000406	**W32**	v_1 = 0.000361
	v_2 = 0.000368		v_2 = 0.000403		v_2 = 0.000275		v_2 = 0.000281
	v_3 = 0.000437		v_3 = 0.000351		v_3 = 0.000314		v_3 = 0.000221
	v_4 = 0.000225		v_4 = 0.000308		v_4 = 0.000347		v_4 = 0.000447
W6	v_1 = 0.000221	**W15**	v_1 = 0.000404	**W24**	v_1 = 0.000275	**W33**	v_1 = 0.000332
	v_2 = 0.000419		v_2 = 0.000278		v_2 = 0.000406		v_2 = 0.000311
	v_3 = 0.000434		v_3 = 0.000344		v_3 = 0.000313		v_3 = 0.000234
	v_4 = 0.000208		v_4 = 0.000318		v_4 = 0.000348		v_4 = 0.000440
W7	v_1 = 0.000414	**W16**	v_1 = 0.000278	**W25**	v_1 = 0.000408	**W34**	v_1 = 0.000309
	v_2 = 0.000248		v_2 = 0.000404		v_2 = 0.000271		v_2 = 0.000334
	v_3 = 0.000377		v_3 = 0.000344		v_3 = 0.000307		v_3 = 0.000235
	v_4 = 0.000269		v_4 = 0.000317		v_4 = 0.000350		v_4 = 0.000439
W8	v_1 = 0.000248	**W17**	v_1 = 0.000404	**W26**	v_1 = 0.000270	**W35**	v_1 = 0.000278
	v_2 = 0.000412		v_2 = 0.000278		v_2 = 0.000408		v_2 = 0.000366
	v_3 = 0.000380		v_3 = 0.000337		v_3 = 0.000306		v_3 = 0.000223
	v_4 = 0.000265		v_4 = 0.000326		v_4 = 0.000350		v_4 = 0.000444
W9	v_1 = 0.000404	**W18**	v_1 = 0.000278	**W27**	v_1 = 0.000412	**W36**	v_1 = 0.000223
	v_2 = 0.000265		v_2 = 0.000405		v_2 = 0.000263		v_2 = 0.000426
	v_3 = 0.000364		v_3 = 0.000337		v_3 = 0.000285		v_3 = 0.000195
	v_4 = 0.000287		v_4 = 0.000326		v_4 = 0.000368		v_4 = 0.000451

Fig. 4 Estimated velocities (m/s) around the perimeter of the well cell (1m × 1m) with a flow rate of 40l/s (state without diaphragm)

Each of the velocities is significantly lower than the critical ones, and it can be concluded that suffusion would not occur in this simulation.
The difference in the number of wells and the elevation at which the whole process is stabilized in this analysis and the one done using GMS [4] is presented in Table 1.

Tab. 1 Comparison of 2D (cell 1m x 1m) and 3D models (state without diaphragm)

Number of wells in the study [4] (3D model, GMS)	36
Estimated flow rate (in l/s) per well in [4] (3D model, GMS)	12
Number of wells in the numerical scheme (2D, MS Excel)	36
Estimated flow rate (in l/s) per well in MS Excel	40
Elevation at which the process was stabilized in [4] (m)	62.5
Elevation at which the process was stabilized in the numerical scheme (m)	59.5 - 62.3

4.2. LOWERING GROUNDWATER LEVELS TO A STATE WITH DIAPHRAGMS

Within this part of the research, lowering the groundwater level of the construction pit was analyzed in the case of a fully constructed diaphragm. The diaphragm represents an impermeable barrier, and as it is placed on all four sides of the construction pit and pressed to the impermeable floor, it forms a reservoir from which water needs to be drained. The zone of interest, in this case, was only the zone of the object, i.e. a grid measuring 100 x 30 m. The very concept of setting up the numerical scheme came down to the fact that initially, the level in the zone of interest was at the maximum expected groundwater level (76.6 m above sea level). Then wells were defined by flow, and as a boundary condition that would simulate the existence of a diaphragm (an impermeable vertical barrier through which no flow occurs) a solid boundary was created. Thus, it was considered as if the water was in contact with a solid boundary on both sides of the diaphragm (where there was no contact between the outer and inner water), so the model could be reduced to not considering the zone outside the pit. Only a pit surrounded by an impermeable barrier (similar to a tank) was observed. When a solid boundary is considered a boundary condition, an appropriate condition describing such a flow (in this case, a flow break) is imposed on those boundary cells. Three grids with cells of dimensions 1 x 1 m, 0.5 x 0.5 m and 0.25 x 0.25 m were considered because the area of interest is significantly smaller than in the previous case. A grid with a cell size of 0.25 x 0.25 m was adopted, which was as close as possible to the dimensions of the well, bearing in mind the technical limitations of the program in which the analysis was carried out.

To lower the groundwater level, in a grid with cells measuring 0.25 m x 0.25 m, 7 wells with a flow rate of 3.5 l/s were required. The depressions in the wells were estimated at around 60.9 m above sea level, while the groundwater levels at the most critical point were at around 61.1 m above sea level. The representation of the groundwater level for this particular state is given in Figure 5.

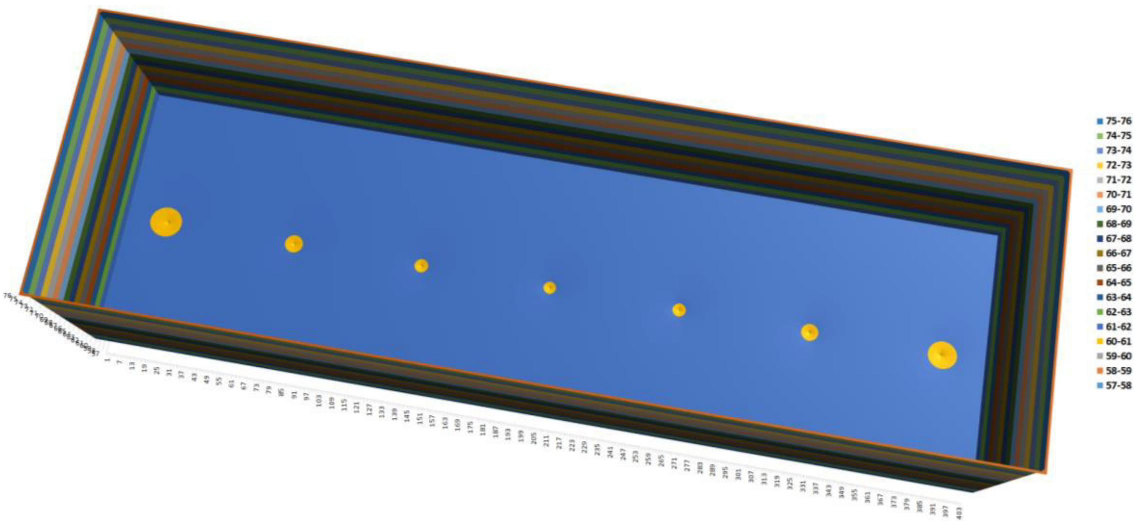

Fig. 5 Display of the groundwater level inside the pit - case with a fully pressed diaphragm (cell size 0.25 m x 0.25 m)

The velocities at the entrance of the well were again compared to the critical velocity, according to Sichardt and Abramov. The velocities in m/s for each of the 7 wells are shown in Figure 6, again following the labels in Figure 3.

W1	v_1 = 0.0001128	W5	v_1 = 0.0001152
	v_2 = 0.0001128		v_2 = 0.0001152
	v_3 = 0.0001128		v_3 = 0.0001152
	v_4 = 0.0001152		v_4 = 0.0001152
W2	v_1 = 0.0001152	W6	v_1 = 0.0001152
	v_2 = 0.0001152		v_2 = 0.0001152
	v_3 = 0.0001128		v_3 = 0.0001152
	v_4 = 0.0001152		v_4 = 0.0001152
W3	v_1 = 0.0001152	W7	v_1 = 0.0001128
	v_2 = 0.0001152		v_2 = 0.0001128
	v_3 = 0.0001152		v_3 = 0.0001152
	v_4 = 0.0001152		v_4 = 0.0001128
W4	v_1 = 0.0001152		
	v_2 = 0.0001152		
	v_3 = 0.0001152		
	v_4 = 0.0001152		

Fig. 6 Estimated velocities (m/s) around the perimeter of the well cell (0.25 m x 0.25 m) (state with diaphragm)

It can be concluded that suffusion would not occur because these velocities (although estimated very close to the well) are less than the critical ones. They are low because of the small value of the pumped flow, causing the small depression cones and small velocity gradients. For this case, there was also a difference depending on the modelling environment, as shown in Table 2.

Tab. 2 Comparison of 2D (cell 0.25 m x 0.25 m) and 3D models (state with diaphragm)

Number of wells in the study [4] (3D model, GMS)	5
Estimated flow rate (in l/s) per well in [4] (3D model, GMS)	3.5
Number of wells in the numerical scheme (2D, MS Excel)	7
Estimated flow rate (in l/s) per well in MS Excel	3.5
Elevation at which the process was stabilized in [4] (m)	60
Elevation at which the process was stabilized in the numerical scheme (m)	60.9 – 61.1

5. CONCLUSION

This paper discussed the process of lowering the groundwater in the program package, which was not specifically designed for that purpose. The results were compared with those of the 3D model made using the GMS software in the paper [4]. The execution of the works at the subject location required lowering the groundwater level to an elevation of 63.00 meters above sea level from the adopted groundwater level of 76.00 meters above sea level. An analysis was performed for two cases of lowering the levels.

The first case involved lowering the groundwater levels without constructing diaphragms, so the wells were placed exclusively around the foundation pit. With a cell size grid of 1m x 1m and wells defined by flow, in the 2D model, the required number of wells was equal to the required number of wells from the study with the 3D model (36 wells in both cases). However, the capacity per well was 3.3 times higher (according to the 2D model, the capacity was 40 l/s per well, and according to the 3D model, 12 l/s). Given that the modelled area, filtration coefficient and other characteristics matched those from the study [4], it was concluded that such a difference in the mentioned flow occurred precisely because of the grid cell size. Therefore, the mentioned difference came from the fact that in the software used in the analysis (MS Excel), there was no possibility of local densification of the grid and setting the well as a point source, in contrast to the 3D model where the approach of different grid resolutions was chosen for the formation of the computational grid. This primarily implies the formation of a grid of higher resolution in hydraulically less demanding zones (smaller level gradients) and using a denser grid in the locality where more intense changes in hydraulic parameters are expected, i.e., the area around the object itself. As there was no possibility to perform such a thing in MS Excel, it could be noticed that the velocities that were calculated to check the suffusion were not near the critical ones because they were not at the border of the well construction (where the velocity should be checked) but in its surroundings, (the cell has significantly larger dimensions than the diameter of the well). If the grid were more dense (which was technically not feasible), observing the current field closer to the well, where the velocity gradients are significantly higher, would be possible.

In the second case, the option of a fully constructed diaphragm to the depth of an impermeable floor was analyzed, i.e., lowering the levels by placing wells exclusively inside the construction pit. Since the location of the building is in the very center of the city, where there is a great risk of subsidence of the surrounding buildings, this solution was adopted. In [4], the hydraulic calculation for this case required 5 wells evenly distributed inside the construction pit, with a capacity of 3.5 l/s. Since a smaller area of interest was considered, three grids were tested, but with significantly smaller dimensions of computational cells, which confirmed the conclusions from the first part. The grid with the smallest cells (0.25 m x 0.25 m) was adopted for the analysis since it was the closest to the dimensions of the well. As a result of the 2D simulation in MS Excel, a solution of 7 required wells with a capacity of 3.5 l/s was obtained.

The difference in the results of both simulations comes from several reasons. One of them implies that in the study [4] a 3D simulation was made, which cannot be done in MS Excel, but a 2D model was made. Based on the soil type data through which water flows and the groundwater levels determined based on geotechnical wells, the exact soil profile at the subject location was reconstructed and imported into the model [4]. In the 2D simulation, there is no way to consider that water enters the well only through the filter structure, i.e. one perforated part. However, the model is made as if water is collected along the entire height of the well, along the entire aquifer to the impermeable floor. Secondly, to obtain a computational grid that most credibly describes the process of water drawing on the field, in [4] an unsteady mathematical model was used. Unlike the steady state (made in MS Excel), this model, for its mathematical basis, uses 3D Poisson's partial differential equations. Those equations can be used to describe much more accurately the time distribution of the lowering process and the relevant values (flow per well) needed to define the configuration of the well. Bearing that in mind, based on 3D simulation, an insight into the time required for the entire process to stabilize is obtained. That was omitted in the 2D simulation because a steady flow was considered. Thirdly, the size of computational cells is crucial to obtaining a usable solution in terms of flow, which entails the interpretation of velocities. For accurate results, it is necessary to have a denser grid in areas where high velocity gradients are expected, i.e. where significant changes are expected, while moving away from the points where the central events take place, it can be sparsed.

However, in addition to the deviations in the results that have occurred, the model fit is quite good as far as the groundwater level is concerned. In this specific analysis, a steady state was used. When compared to the unsteady one done in [4], after two days of pumping when the process was stabilised, it can be seen that the groundwater level oscillates slightly around the required elevation to which it was necessary to lower the level.

The obtained results directly depend on the adopted assumptions and network modelling methods. Namely, the theory of flow through a porous medium has been proven, as well as the applied mathematics, which means that the accuracy and precision of the results depend on the human factor. When talking about the accuracy of the results, the rules of the engineering profession should be taken into account. The simulation model cannot be expected to exactly match the actual physical model, implying that absolutely accurate results will never be obtained. The question is whether these models were justifiably applied. They are, because the engineering profession dictates what error size can be tolerated without jeopardizing safety.
By modelling different cases, the goal of this paper was fulfilled, i.e. it was shown how the obtained solutions could differ due to the change of the boundary conditions, dimensions of the grid and, in general, by changing the environment in which the analysis is carried out. It has been proven that in addition to the mathematical apparatus that functions and the theory of groundwater flow that is justified, the results can only oscillate depending on the combination of the application of these two domains.

ACKNOWLEDGEMENT

This study has been supported by the Republic of Serbia, Ministry of Education, Science and Technological Development through project number 451-03-47/2023-01/200108. The research has been conducted within the project "Scientific theoretical and experimental research and improvement of educational process in the field of civil engineering", developed at the Department of Civil Engineering and Geodesy, Faculty of Technical Sciences, University of Novi Sad, Serbia.

REFERENCES

[1] Jisun K., Sung-Wook J., Hyoun Soo L., Jeonghoon L., Ok-Sun K., Hyoungseok L., Soon Gyu H. (2020). Hydrogeological characteristics of groundwater and surface water associated with two small lake systems on King George Island, Antarctica. *Journal of Hydrology*, Volume 590 https://doi.org/10.1016/j.jhydrol.2020.125537

[2] Yidana S.M., Essel S.K., Addai M.O., Fynn O.F. (2015). A preliminary analysis of the hydrogeological conditions and groundwater flow in some parts of a crystalline aquifer system: Afigya Sekyere South District, Ghana. *Journal of African Earth Sciences*, Volume 104, pp. 132-139. https://doi.org/10.1016/j.jafrearsci.2014.12.011

[3] Hajdin G. (2009). *Mehanika fluida, knjiga treća, dodatna poglavlja*. Beograd, Građevinski fakultet Univerziteta u Beogradu, Republika Srbija.

[4] Jeftenić G., Budinski Lj., Kolaković S., Stipić D., Milić M. (2022). Matematičko modeliranje snižavanja nivoa podzemne vode primenom GMS. *Međunarodna konferencija GNP*, Kolašin, Crna Gora, 08-12 Mart.

[5] Đula F., Budinski Lj. (2021). *Potpovršinske vode*. Fakultet tehničkih nauka, Univerzitet u Novom Sadu, Republika Srbija.

INTRODUCTION OF POPLAR WOOD IN BUILDING CONSTRUCTION SECTOR: REASONS AND POSSIBILITIES

Tatjana Kočetov Mišulić[1], Branislav Kovačević[2], Aleksandra Radujković[3], Ivan Lukić[4], Slobodan Šupić[5]

Summary:

With a set of European standards for the design of timber structures, poplar wood is classified into strength classes together with soft coniferous wood. Intensive cultivation of fast-growing poplar species, especially in areas with suitable conditions, gives an opportunity to obtain convenient building material in conditions of coniferous wood deficit. The introduction of poplar wood as a building material follows modern trends in green building and tends to reduce the unfavourable impact of construction sector on the environment. Before the harmonization of design regulations with European norms, the poplar was not allowed to be used for structural purposes in Serbia and therefore there are no essential data on the poplar' properties at the national level. The aim of the paper is to review the palette of poplar industrial applications, as well as the reasons and advantages of its application in structural design and products, followed by research achievements.

Key words: poplar, clones, density, strength properties, durability, EN standards

[1]Assist. Prof., Faculty of Technical Sciences, University of Novi Sad, Serbia, tanya@uns.ac.rs
[2]Sci. Advisor, Institute of Lowland forestry and Environment, University of Novi Sad, branek@uns.ac.rs
[3]Assist. Prof., Faculty of Technical Sciences, University of Novi Sad, Serbia, leksa@uns.ac.rs
[4]Assoc. Prof., Faculty of Technical Sciences, University of Novi Sad, Serbia, lookic@uns.ac.rs
[5]Assist. Prof., Faculty of Technical Sciences, University of Novi Sad, Serbia, ssupic@uns.ac.rs

1. INTRODUCTION

The built environment generates about 47% of annual global CO_2 emissions. Of those total emissions, building operations are responsible for 27% annually, while building materials and construction (typically referred to as embodied carbon) are responsible for an additional 20% [1]. It is expected that the global building floor area will double by 2060, necessitating the strong answer worldwide. In last few decades Europe proclaimed the multiple actions about zero carbon built environment, which are oriented to bio-economy and sustainability. Dominantly, the actions were based on building with timber, what was/is supported by development and implementation of new timber engineering products (wood fibre insulation boards, glulam, cross-laminated timber and laminated veneer, timber-green concrete composite structures). The wood became the trending material of the 21th century, but the concerns about forest eco-systems stability and sustainability arose. Although the timber is material from renewable recourses, the rotation length for coniferous trees (dominant in building industry) could ranging from approximately 50 to sometimes 200 years [2], especially in northern countries which are one of the biggest suppliers with industrial timber. For this reason, the EU community decided to include fast-growing species in construction sector, with poplar wood being included in the first place.

The relatively fast growth of poplars and the possibility of their plantation cultivation with planned forestation and relatively short rounds of rotation, classify poplar wood as a locally available material, whose suitability for construction purposes has not been sufficiently explored in our region. With the introduction of poplar wood as a building material within the EU (2016), the aspects of the use of wood in construction sector were expanded, which follows the contemporary trends of green building and tends to reduce the unfavourable impact of construction sector on the environment. With a set of European standards for the design of timber structures (EN 1995 and accompanying standards), poplar wood is classified into same strength classes as soft coniferous timber, giving it a new purpose and design importance.

The alluvial areas of Vojvodina provide very good conditions for the development of poplars in our country, which made it possible to consider poplars as the leading species in the forestry of Vojvodina, both in terms of area and total annual wood production. Before the legislative harmonization of Serbian design standards with European norms, which took place in 2022, the use of poplar for structural purposes was not allowed, and therefore there are no basic data on the poplar properties essential for use in constructions i.e. for the strength class classification: density, modulus of elasticity and bending strength.

The aim of the paper is to review the palette of poplar industrial application, as well as the reasons and advantages of its application in structural design and products, followed by research achievements. The second goal of the paper is to promote the short-term scientific project about the characterization of the elasto-mechanical properties of the most widespread poplar clones in AP Vojvodina and to introduce the poplar timber into domestic construction engineering practice.

2. POPLARS

Poplars, as the members of the *Salicaceae* family, are trees with many valuable characteristics which have led to multiple beneficial uses for society and the environment since the ancient times. Poplars are deciduous trees, characteristic for the temperate climate zone of the northern hemisphere. They are spread from subtropical regions to the boreal forests in Europe, East and Central Asia, Middle East, North America, Mexico and in North Africa, dominantly in big rivers valleys.

Culture of poplars has a long history. In fact, the Latin *Populus* was derived from the Roman appellation *arbor populi* or 'tree of the people', because poplars were so widely planted. Historically, poplars often were part of an agro-forestry system and were managed to supply timber, fuel-wood, forage and windbreaks [3].
The poplars are taxonomically divided into six sections, while taxa in section *Aigeiros* (usually referred as "black poplars") – both pure species and interspecies hybrids – have been the most important and spread members of the *genus Populus* worldwide. Desirable accessions of their spontaneous offsprings have been cloned and brought into commercial culture for hundreds of years. Additionally, for many decades, geneticists have purposely bred hybrids that have been deployed in poplar-culture throughout the world. The characteristic of the black poplars is fast growth, ease of vegetative reproduction, predisposition to hybridization and numerous use values of their wood.
Some of the most important clones of this taxa belong to interspecies hybrid species derived from hybridization *Populus deltoides* × *Populus nigra*, known collectively as *P.×euramericana*, i.e. the Euramerican or Canadian poplars. *Populus deltoides* (Eastern cottonwood) is one of the most silviculturally important poplars naturally distributed over USA and Canada. *Populus nigra* (European black poplar) is a pioneer species, growing mainly along rivers in Europe and the western and central Asia and northern Africa (Fig. 1a). The wood of black poplar is highly regarded, so its culture in plantations is long standing. Because this species is as genetically diverse and pliant as any member of the *genus Populus*, it has been frequently used in breeding programs to increase poplar wood production. The clones of Euramerican hybrids have been immensely significant in poplar-culture because of their rapid growth rate, straight stem form and tolerance to fungal, bacterial and viral diseases [3].

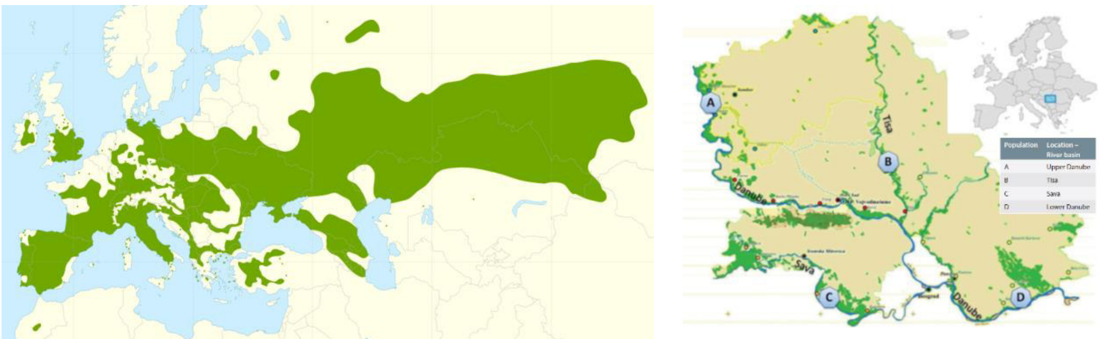

Fig. 1 Distribution map of Populus Nigra: a) EuroAsia [4], b)Vojvodina, Serbia [5]

2.1. POPLARS IN EU AND SERBIA

Currently, in the EU there are approximately 450000 hectares of production-oriented poplar forests and plantations, mainly concentrated in France, Spain, Italy and Hungary.
Among all artificially established broadleaved stands in Serbia, poplar plantations are the most widespread, where poplar forest area covers 48000 ha, 32000 ha of which in form of plantations. During 2022 [6], 1422ha of new poplar plantations were established in Serbia, out of which 1104 ha in Autonomous Province of Vojvodina (Fig. 1b).
The autochthonous stands of European black poplar (*P.nigra* L.) and White poplar (*P.alba* L.) were dominant in lowlands of Serbia, but became rare and endangered due to substitution with plantations of more productive poplar species (Euramerican poplar). Due to introduction of new poplar cultivars and technologies, in the period of forty years (from the 50's to 80's of 20th century), felling cut was increased by around 10 times, and the value of wood volume was increased by around eighteen times. From 1990's until nowadays, this rise stagnated, but many developments have contributed that poplar forest plantations come into the spotlight again [7].

Due to climate change, the need for preservation of natural habitat and biodiversity, flooding control and water quality control, as well as the needs for integrated approach in bio-economy considering fast growing hardwood as building material, the poplars became recognised as the trees of the 21th century.

Many international organizations are established in order to support management of fast-growing tree species, like IPC (FAO) - International Commission on Poplars and other Fast-Growing Trees sustaining People and the Environment, ProPopulus - European poplar association [8], IUFRO - International Union of Forest Research Organizations, etc. Also, the breeding and clone development programmes with cooperation and close integration of basic investigations between countries are networked, while the commercialization of newly developed cultivars are regulated to varying extents throughout the world. The EU has the most sophisticated system – the Organization for Economic Cooperation and Development (OECD) – which stipulates the conditions under which both individual cultivars and mixtures can be marketed and traded among its member states.

Hybrid poplar genetics and breeding are the topic issues in poplar cultivation, so the production-oriented poplar countries produce numerous successful clones based on their own or foreign origin (Fig. 2). Poplar breeding began in Italy 1922. Their most famous clone is *P. ×euramericana cl.* I-214 clone, developed by Giovanni Jacometti in 1929, that is perhaps the most widely planted Populus clone worldwide. In Serbia, there are numerous registered poplar clones (around 26). The leading institution that is involved in the improvement of poplar wood production in former Yugoslavia and now in Serbia, from 1950-ties until nowadays, is Institute of lowland forestry and environment in Novi Sad. The most currently used poplar cultivars in afforestation and reforestation in Serbia are *P. x euramericana cl.* I-214 and *cl.* "Pannonia", as well as new Eastern cottonwood selections of the Institute, such as *Populus deltoides cl.* Bora and *cl.* B-81.

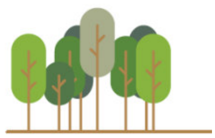

(Source: FAO, EPF, Tragsatec)

Country	Production-oriented poplar plantations (ha)
France	212.000
Spain	123.000
Hungary	109.300
Italy	59.859
Belgium	35.000
Serbia	32.000
Germany	12.500
Romania	8.000
Greece	7.500
Poland	7.500
Sweden	4.000
Czech Republic	2.500
UK	1.300

Fig.2. a) Main Salicaceae family genotypes planted in Europe; b)Production-oriented poplar plantations in Europe [9]

In neighbouring and cooperating countries generally some of the same/similar clones are present: Croatia has 16 registered cultivars that include selections of *P. ×euramericana cl.* I-214, *cl.* Pannonia etc; and *P. Deltoides cl.* S1-8 well known in ex-YU. In Hungary the number of hybrid poplar clones exceeds 20, with most belonging to *P. ×euramericana* cultivars among which the most frequently used are *cl.* I-214, *cl.* Pannonia, *cl.* Kopecky, *cl.* Agathe F, *cl.* Koltay and *cv.* Robusta.

The quality of poplar wood for industrial purposes depends on many factors: characteristics of clones, planting density, growing conditions, habitat, applied technology (plant protection, plantation establishment, rotation period etc.). Generally, the expected rotation length for sawlogs and veneers production is the longest, while for pulpwood and bio-energy is the shortest.

2.2. POPLAR BASED PRODUCTS

Besides the known benefits of poplars for ecosystem and environmental issues (global warming mitigation, control of flooding and irrigation rates, wind shelters and buffer zones, land restoration...), the primary focus of short-rotation poplar planting in industrialized world is always in the source for new products: a source of renewable energy feedstock with advantages of high biomass yields and a source of fast growing wood material for engineered wood products (EWP) for use in construction and industry.
The large-scale uses and benefits provided by the whole tree of poplars are illustrated in Fig 3, summarized by van Acker [10].

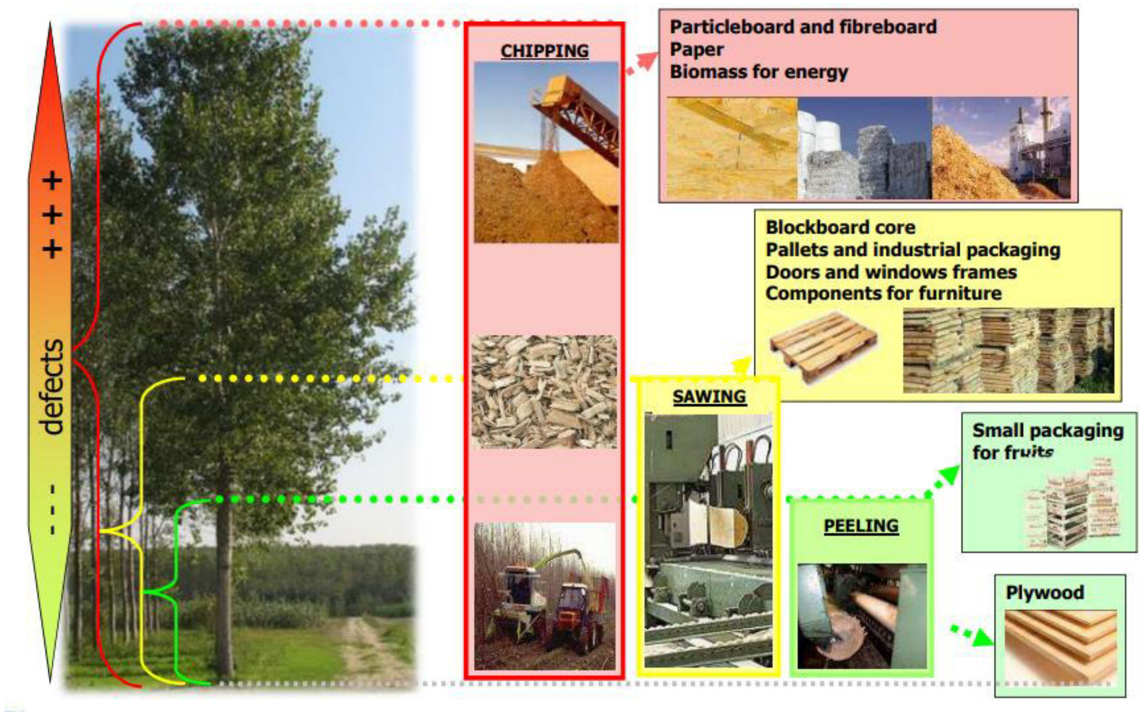

Fig. 3 Treeconomics of poplar wood [10]

At the end of the 20th and in 21st century, besides the energy obtained from biomass, the primary focus of poplar plantings was production of raw material for wood and fibre products: lumber, veneers or strands/particles which bounded together with ecologically improved structural resins are used in order to form palette of poplar EWPs (Fig 4.).
The innovative EWPs made of coniferous wood (OSB boards, plywood, laminated veneer lumber LVL, glue laminated timber GLT, cross laminated timber CLT, I joists) were developed through decades. The replacement of coniferous wood by poplars in EWPs introduced new challenges in research and production technology development. From structural point of view, density and the modulus of elasticity and bending strength of different poplar clones are of the essential importance for construction purposes.

Fig. 4 a) Plywood and OSB boards, b) GLT, c)LVL and LSL, d) CLT

3. SHORT LITERATURE REVIEW OVER THE ESSENTIAL STRUCTURAL PROPERTIES OF POPLARS

The use of poplars for structural purposes was not allowed in Serbia before the harmonization of design standards with Eurocodes in 2022, so the basic data on the properties essential for use in constructions are missing in Serbian literature. In order to obtain the referent frame for comparison, the literature review is oriented to testing results of different clones widely spread in Europe and China regarding three key parameters - density, modulus of elasticity (MOE) and bending strength (MOR) parallel to the grains. Where it was possible, the referent frame was made to the most produced clones in Vojvodina, generally to the Italian clone "I-214" as a good example of an exceptional clone adapted to a large variety of growing conditions.

Generally, poplars are classified as low-density tree species, and it could be stated that the poplar wood is similar to softwoods, as far as density is concerned. This comparison is mainly based on their potential for structural applications. Density of poplar wood has a wide range between taxonomic sections and between clones.

The Italian clone "I-214" shows low density values (around 300 kg/m^3), while some other "Euramerican" clones such as "Robusta" show high average density values of over 550 kg/m^3 [3].

In the report [11] about species grown in natural forests in North America, as well as of hybrid poplars, it is stated that average relative density is in the range of 310 to 370 kg/m^3, MOR in the range of 27 to 37 MPa and MOE in range 5.2 to 7.0 GPa. Visually stress-graded poplar dimension lumber is acceptable for light-framing applications and has lower allowable design stresses than the predominant S-P-F (Spruce-Pine-Fir) species group. The properties of analyzed samples greatly depend on hybrid clone types and habitat locations.

In Spain, Gallego et al. [12] have investigated the influence of the age and stand density of "I-214" on MOE. The *P.× euramericana* hybrid "I-214" clone is one of the most used in poplar plantations in Spain. MOE (mean value) was ranged from 8.8 GPa (for 13 years old trees) to 7.1 and 7.0 GPa (for 9 years old trees), while basic density in timber samples varied in range of 330 to 353 kg/m^3 - with the largest value in lower stand density. It was concluded that the elastic modulus of the "I-214" poplar timber is more associated with the age of the plantation than with its stand density.

Due to the possibility of using poplar wood in building structures in Spain, Casado et al. [13] conducted the experimental investigations to evaluate the structural properties of poplar wood (*P.×euramericana cl.* I-214) in order to grade it by the strength class system according to EN 338. It was concluded that poplar timber from clone "I-214" has acceptable flexural strength, but a comparatively low elastic modulus. The low values in elasticity considerably limit the possible structural application of the species, so the average strength classification would be C14, according to the EN 338 (2009) standard.

Research efforts from China are interesting because of nearly 8 millions of hectares under poplar plantations (European vision is to cultivate about 1 million of hectares) and use of numerous *P.×euramericana* clones (own and of European origin).
Density and bending MOE of *P×euramericana cl.* 74/76 planted near Beijing were investigated in study presented by [14]. The average density of the wood samples (four and five year old poplar trees) at 12% moisture is from 400 to 403 kg/m^3. In this study, the wood density of the poplar clone is mainly higher than that reported previously in various investigations. These differences may be caused by the methods used to determine wood density, clone variation within hybrids, different environmental conditions, and variation in anatomical features. The average MOE of tested clone "74/76" was 9.3 GPa at breast height, which is similar to other poplars with normal growth.
The paper [15] analyzed the physical and mechanical properties of three clones belonging to different species of sections *Aigeiros* (*P. x deltoides cl.* 55/65 introduced from Yugoslavia, *P.×euramericana cl.* Guariento from Italy and *P.nigra cl.* N179 from Germany), that were introduced from Europe in 20th century and were cultivated with the same forest management at the same site in China. For three poplar clones (nine years old) the average density ranged from 408 to 458 kg/m^3, the average MOR from 65.8 to 68.0 MPa, and the MOE values within the range of 9.18–9.97 GPa. The obtained results indicated that the density property can be used to estimate and indirectly select the mechanical properties of MOR and MOE in these three poplar clones and for two of the three considered clones, a radial variation of the properties was noticeable.
For strength class classification of poplars, the investigations conducted in neighbouring countries and in Serbia are of significant importance.
The physical properties of poplar clones "I-214" and "S1-8" from one locality in Croatia were determined in [16]. Average wood density in absolutely dry condition of clone "I-214" was 388 kg/m^3, while for clone "S1-8" was 372 kg/m^3. The remarks about optimal rotations in poplar breeding according to application purpose and the effect of age on wood properties are also highlighted in the paper (up to 15 years for best utilization of wood for non-structural products and higher age for structural purposes due to large portion of juvenile core wood of poplar clones). The juvenile zone is characterized by fast growth rate, lower density and strength, while wood properties generally change from pit outward, meaning that in mature wood zone nearly all properties are relatively constant.
In Hungary, a lot of research dealing with breeding new varieties and enhancing the technical performances of existing poplar wood material recently are presented. In order to find the good alternative to the widely used coniferous species in construction sector, Hungarian scientists made contribution investigating the clone "Pannonia" from different locations and comparing the properties between examined locations according to static and dynamic MOE tests [17]. The comparative analysis shown that investigated clone shows rather good results according to both methods (around 11GPa), what ranks the examined clones to high position considering MOE (usually referred as the lowest property in poplar clones).
The investigations about poplar clones in Serbia are dominantly devoted to genetic, chemistry and plantation aspects and only few results are dealing with density.
In [18] is presented that the nominal density of poplar clones (taken from stems of age from 12 to 24 years) in Vojvodina: for *P.x euramericana*, *cl.* I-214 it is 284 kg/m^3 and for cultivar "Robusta" 350 kg/m^3, while for *P.deltoides,* clone "457" is 390 kg/m^3 and clone "618" is 352 kg/m^3.
The other similar research [19], performed on 10 years old stems, indicated the similar basic density of 285 kg/m^3 for clone "I-214", while for clones of *P. deltoides* ("S1-8", "S6-36", "S6-20", "S1-3") a significantly higher basic density is reported - up to 40%. For poplar wood as a diffuse-porous species with a low wood density, a significant

increase in volumetric mass is observed only after the fifteenth year of growth i.e. the specific weight of wood increases with age. In the case of *P.deltoides* clones there were no major changes in specific gravity with age and the increase was only 10% in adult wood compared to juvenile wood.
Research from Serbia show that optimal rotation period of industrial poplar plantations is longer and to produce the quality structural logs it requires from 22 to 32 years [7].

4. SHORT-TERM PROJECT ABOUT STRENGTH CLASSIFICATION OF POPLAR TIMBER IN VOJVODINA

As the leading tree species and locally available in the forestry of Vojvodina, poplars provide wood material whose suitability for construction purposes has not been sufficiently explored in our region. Investigation and observation of the basic structural properties is a prerequisite for the development of the potential further poplars' use in structures. Also, that is a starting point to evaluate poplar raw material that, combined with adequate types of coniferous wood, leads to the application of EWPs in construction engineering.
The proposed research project refers to the experimental evaluation of elasto-mechanical properties (flexural strength and modulus of elasticity in bending parallel to the grains), based on standardized procedures according to EN 408 (four-point bending test), and on sets of samples separated from the most widespread poplar clones (*Populus x euramericana cl.* I-214 and *cl.* Pannonia) in Vojvodina. Research within this project is considered as a preliminary, with at least one representative sample from each clone (n $\geq$ 40 test specimens). Also, the density will be examined as one of the basic relevant properties for the quantification of the strength class, which can be used as a control data in relation to the existing tests of the same clones conducted for other purposes. Three basic properties enable the evaluation of other elasto-mechanical properties of poplar parallel and perpendicular to the grains, which are necessary in the calculation and design of timber structures according to limit states with the required safety coefficients for the material (EN 1995). The quantification and verification of test results, as well as the assessment of strength classes, will be carried out by statistical methods prescribed by the relevant EN standards (EN 384, EN 14358). Experimental tests will be preceded by a visual classification of wood according to EN 14081-1, as a traditional way of classifying wood into quality classes, and as a prerequisite for classification into strength classes according to EN 338.
A preliminary classification of dominant black poplar clones in Vojvodina according to strength classes (EN 338 and EN 1912) will indicate the possibilities and scope of poplar wood applications in construction sector and will be the potential basis for the National Document for the application of EN 1995 in the field of timber structures.

5. CONCLUSION

Poplar clones, traditionally used for a number of purposes (in production of fibers for pulp and paper, solid timber and engineered wood production), nowadays are also used as in production of biomass for energy, for carbon sequestration and phytoremediation of environmental problems. By increased international demand for wood and so called "Green deal" with the planet Earth, poplar cultivation experienced a shift in a trend, making it competitive and attractive to a number of consumers and researchers, dominantly from the field of genetics, but also in the field of innovative structural design. Serbia and Vojvodina must follow this trend, because of own natural resources and possibilities.
As a very versatile tree, with low wood density similar to some softwood tree species, poplar clones could be with relatively high strength values compared to limited density,

and therefore could find the application in demanding tasks of structural engineering. The advantages, such as the size, straightness and the uniformity and homogeneity of logs, as well as high tolerance to prevalent diseases and pests, easy draying with minimal movement in performance and splitting, with pretty easy cuts, give the additional values to poplar use in industry and structures.
All mentioned above imposed the necessity of research and structural quantification of poplars from domestic resources, which would create a prerequisite for introducing of additional value in potentials of widespread poplar clones in the area of AP Vojvodina.

ACKNOWLEDGEMENT

This paper has been supported by the Provincial Secretariat for Higher Education and Scientific Research of APV through sort-term researh project no. 142-451-3132/2023-01/01 “Forming of prerequisites for the use of poplar wood in building construction - assessment of the mechanical properties of the most wide spread clones in poplar cultivation of Vojvodina".

REFERENCES

[1] Agopian, N. (2022). Countering climate change: Building decarbonization + Building resiliency = Improved human condition. *RenewAire* white paper. 6p.

[2] Felton A, Sonesson J, Nilsson U, Lämås T, Lundmark T, Nordin A, Ranius T, Roberge JM. (2017). Varying rotation lengths in northern production forests: Implications for habitats provided by retention and production trees. *Ambio,* Volume 46(3), pp. 324-334. http://doi.org/10.1007/s13280-017-0909-7

[3] Isebrands JG., Richardons J. (2014). *Poplars and Willows: Trees for Society and the Environment.* FAO & CABI Publishing International, USA & UK

[4] https://en.wikipedia.org/wiki/Populus_nigra (accessed 10.10.2023)

[5] Čortan D., Schroeder H., Šijačić-Nikolić M., Wehenkel C., Fladung M. (2016). Genetic structure of remnant black poplar (Populus nigra L.) populations along biggest rivers in Serbia assessed by SSR markers. *Silvae Genetica*.65(1) http://doi.org/10.1515/sg-2016-0002

[6] Šumarstvo u Republici Srbiji, 2022. Bilten. Republički zavod za statistiku. ISSN 0354-3641

[7] Pilipović A., Orlović S., Dabić S., Maksimović Z. (2016). *Activities related to poplar and willow cultivation and utilization. Country National Reports: Serbia*. International Poplar Commission. Insitute of Lowland Forestry and Environment, Novi Sad, Serbia

[8] https://propopulus.eu/en/ (accessed 10.10.2023)

[9] Oliveira N., Perez-Cruzado C., Canellas I., Rodriguez-Soalleiro R., Sixto H. (2020). Poplar Short Rotation Coppice Plantations under Mediterranean Conditions: The Case of Spain. *MDPI Forests. Special issue Growth and Development of Short Rotation Woody Crops for Rural and Urban Applications.* Volume 11(12). http://doi.org/10.3390/f11121352

[10] Van Acker J. (2022). Poplar, the Tree of the 21st Century. *Treeconomics: Wood in sustainable economy.* ProPopulus. Madrid, Spain, June 22, 2022. 19p.

[11] Balatinecz J.J., Kretschmann D.E., Leclerq A. (2001). Achievements in the utilization of poplar wood – Guideposts for the future. *The Forestry Chronicle.* Volume 77 (2). pp. 265-269. http://doi.org/10.5558/tfc77265-2.

[12] Gallego A., Ripoll M.A., Timbolmas C., Rescalvo F., Suarez E., Valverde I., Rodriques M., Navarro F.B., Merlo E. (2021). Modulus of elasticity of I-214 young poplar wood from standing trees to sawn timber: influence of the age and stand density. *Eur. J. Wood Prod.*79, pp. 1225–1239. https://doi.org/10.1007/s00107-021-01675-5

[13] Casado M., Acuña L., Basterra L., Ramón-Cueto G.,Vecilla D. (2012). Grading of structural timber of *Populus×euramericana* clone I-214. *Holzforschung*, *66*(5), pp. 633-638. https://doi.org/10.1515/hf-2011-0153

[14] Rongjun Z., Chunli Y., Xianbao C., Jianxiong L., Benhua F., Yurong, W. (2014). Anatomical, Chemical and Mechanical Properties of Fast-Growing *Populus×Euramericana* cv. ‘74/76’. *IAWA Journal.* 35(2), pp. 158-169. https://doi.org/10.1163/22941932-00000057

[15] Jia R., Wang Y., Wang R., Chen X. (2021). Physical and Mechanical Properties of Poplar Clones and Rapid Prediction of the Properties by Near Infrared Spectroscopy. *Forests*. 12(2):206. pp14. https://doi.org/10.3390/f12020206

[16] Ištok I., Sedlar T., Šefc B., Sinković T., Perković T. (2016). Physical Properties of Wood in Poplar Clones "I-214" and "S1-8’. *Drvna industrija,* 67(2), pp. 163–170. https://doi.org/10.5552/drind.2016.1604

[17] Kannar A., Csiha C. (2021). Comparative Analysis of Static and Dynamic MOE of Pannonia Poplar Timber from Different Plantations. *Wood Research*, 66(2), pp. 195-202. https://doi.org/10.37763/wr.1336-4561/66.2.195202

[18] Klašnja B., Orlović S., Drekić M., Radosavljević N., Marković M. (2007). Mogućnosti korišćenja drveta topola u hemjskoj i mehaničkoj preradi. *Topola*, *179/180*, pp. 4-14.

[19] Klašnja B., Orlović S., Galić Z., Kebert M., Stevanov M. (2009). Hemijski sastav drveta odabranih klonova topola. *Topola*, *183/184*, pp. 29-37.

AN OVERVIEW OF BUILDING INFORMATION MODELLING AND ARTIFICIAL INTELLIGENCE INTEGRATIONS IN THE CONSTRUCTION INDUSTRY

Mirjana Terzić [1], Jasmina Dražić[2], Milena Senjak Pejić[3], Dragana Stanojević[4]

Summary:

Researchers in the AEC/FM industry have been working intensively for several years on applying information technology, robotics and other modern technologies in design and construction. Artificial intelligence stands for the science of creating intelligent applications that indicate thinking, learning, knowledge, communication, perception, planning, and the ability to move and control objects. Industry 4.0 has given a challenge by providing insight into the potential of digitalization of construction facilities, with the availability of digital data and online digital access that automatically collects and processes data. Building Information Modelling (BIM) is the centre of digitalization of construction. This paper presents an overview of integrating BIM and AI technologies in the construction industry in all life phases of the facility. Existing research has been analysed, basic terms have been defined, and examples of these integration applications in recent research are given.

Key words: Building Information Modelling, Artificial Intelligence, Construction industry

[1] Teaching Ass., Faculty of Technical Sciences, University of Novi Sad, Serbia, terzic.mirjana@uns.ac.rs
[2] Full Prof., Faculty of Technical Sciences, University of Novi Sad, Serbia, dramina@uns.ac.rs
[3] Teaching Ass., Faculty of Technical Sciences, University of Novi Sad, Serbia, senjakm@uns.ac.rs
[4] Teaching Ass., Faculty of Technical Sciences, University of Novi Sad, Serbia, dragana.stanojevic@uns.ac.rs

1. INTRODUCTION

The growth of the construction industry is limited by the many complex challenges it faces, such as cost and time overruns, construction site safety, productivity gaps and labour shortages. Also, the construction industry is one of the least digitised industries in the world, making it difficult to solve the problems it is currently facing. Advanced digital technology and artificial intelligence (AI) are revolutionising many industries, such as manufacturing. Fields of artificial intelligence, such as machine learning, knowledge-based systems, computer vision, and robotics, have been successfully applied in other industries to achieve greater profitability, efficiency, safety, and security [1]. Researchers in the AEC/FM (Architecture, Engineering and Construction / Facility Management) industry have worked intensively on applying information, robotics and other modern technologies in design and construction for several years. Their theories of what could be done far outweighed the practical, technical, commercial, cultural and organisational constraints that had to be overcome [2].

According to the National Building Information Modeling Standard (NBIMS) definition, Building Information Modeling (BIM) is a digital representation of an object's physical and functional characteristics. As such, it serves as a common source of knowledge for information about the object, which forms a reliable basis for all decisions during its life cycle, from planning to demolition of the building. The basic idea of BIM is the cooperation of different stakeholders in different phases of the object's life cycle in order to define, extract, update or modify the information in the BIM model [3].

Artificial intelligence plays a key role in the Fourth Industrial Revolution (Industry 4.0), i.e. the era of digitisation, in which intelligent systems and technologies are used to create a connection between the physical and virtual worlds. Artificial intelligence is the science of creating intelligent machines that exhibit thinking, learning, knowledge, communication, perception, planning, and the ability to move and control objects [4]. Industry 4.0 has given a challenge to the construction industry by providing insight into the potential of digitisation of construction facilities, with the availability of digital data and online digital access that automatically collects and processes electronic data. Information modelling of buildings represents the centre of digitisation of construction within the domain of planning, and together with Industry 4.0, in the domain of production, it tries to close the digital gap that still exists and maintain an influence on future construction processes.

This paper summarises the overview of the integration of BIM and AI technologies in the construction industry in all phases of the facility, explains key concepts, mentions advanced techniques and technologies, and summarises examples of BIM-AI integrated applications, summarised through two perspectives: the main AI techniques integrated with BIM and the main integrated applications applied in the AEC/FM industry.

2. RECENT STUDIES

This chapter gives the existing data on the number of research and published works. Further, in the paper, examples of the application of this integration in recent research are given.

F. Zhang et al. [5] conducted a review study analyzing BIM-AI integration in the AEC/FM industry. A systematic bibliometric analysis was conducted in which 183 relevant references from the literature participated. The study defined the protocols of a systematic review of the literature for the identification of relevant articles. Then, a bibliometric analysis of 81 references was performed. The results were further analyzed and summarized BIM-AI integrations from different aspects, including the main AI techniques integrated with BIM, their integration in the whole life cycle of AEC/FM projects and the main fields of their application. Finally, current challenges and future development directions of BIM-AI integrations are proposed. This review contributes to the systematic research of the application of BIM-AI integrations in the AEC/FM industry and provides valuable future research directions.

A. Zabin et al. [6] also conducted a systematic literature review identifying and summarizing common areas of application and use of machine learning in the context of BIM-generated data. While research into the use of BIM data through machine learning has grown over the past decade, it is still in its infancy, which is why this paper aims to assess where the industry is today. The observed limitations suggest prominent future research directions focusing on information and data architecture, application scalability, and human-to-human information interactions. This paper aims to provide insight into machine learning research applied to BIM-generated data, considering the different stages of the BIM-based project life cycle.

Over 60% of the research on the application of artificial intelligence in construction has been carried out in the last decade and has caused or enhanced the emergence of advanced technologies. In the early 2010s, BIM-related research was quite immature, and only a few studies investigated the possibilities of BIM-AI integration from 2010 to 2013. After 2014, the number of articles began to grow. A significant increase in BIM-AI publications occurred from 2017 to 2020, suggesting that BIM-AI applications have entered the AEC/FM industry. This increase can be attributed to the fact that over the past three years, many countries have encouraged the implementation of BIM and developed national artificial intelligence strategies, significantly promoting BIM-AI applications in the AEC/FM industry [5–7].

3. ARTIFICIAL INTELLIGENCE TECHNIQUES IN INTEGRATION WITH BIM

Artificial intelligence is proving to be an effective alternative advanced approach to classical modelling techniques. AI refers to the branch of computer science that develops machines and software with human-like intelligence. Compared to traditional methods, AI offers advantages in solving problems associated with uncertain results and is an effective aid for solving complex problems. There has been a growing interest in all engineering branches in recent years. Artificial intelligence methods that have attracted considerable attention during the last decade are machine learning, pattern recognition and deep learning, focusing on their application in the AEC/FM industry [8].

Based on the analysis of review papers, four main categories of AI techniques integrated with BIM were determined: knowledge-based reasoning, metaheuristics, machine learning and hybrid artificial intelligence. A detailed classification of these methods is shown in Fig. 1.

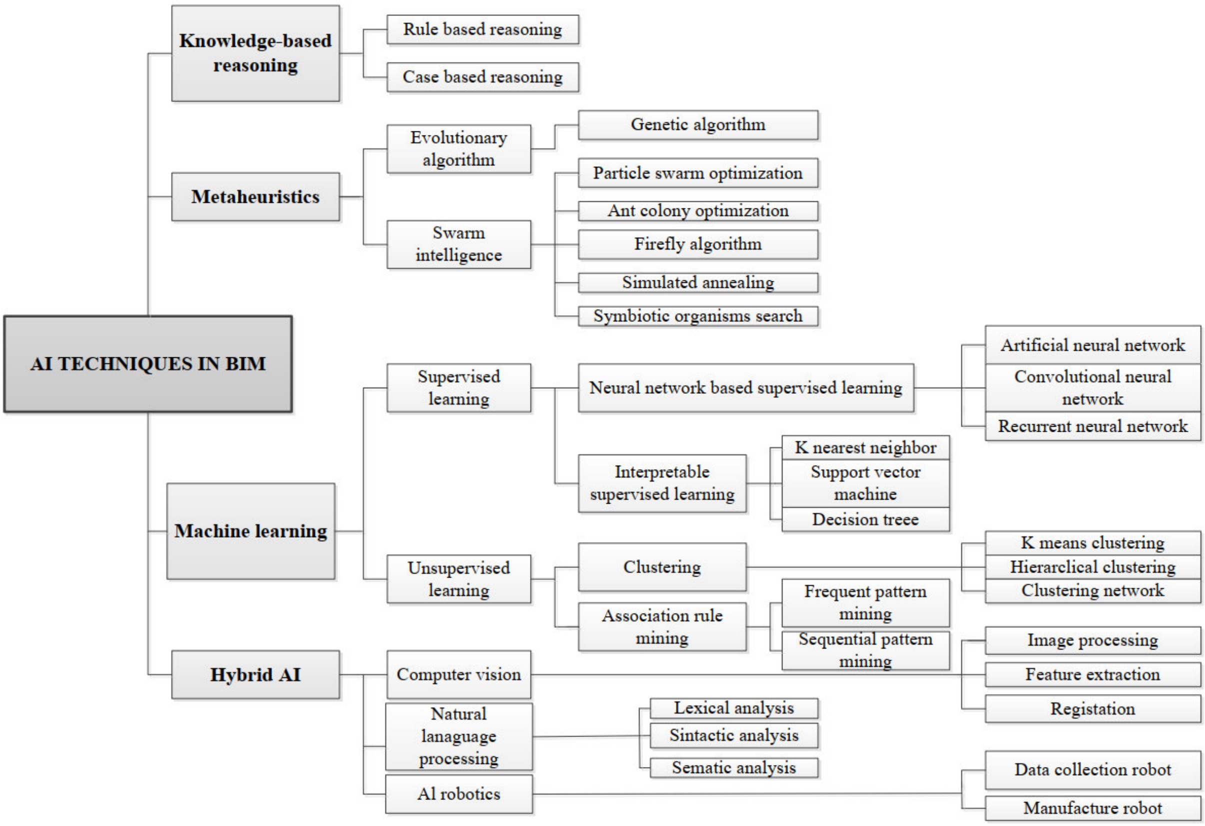

Fig. 1 - Classification of the most commonly used AI techniques in integration with BIM - according to [5]

3.1. KNOWLEDGE-BASED REASONING

Knowledge-based reasoning (KBR) is an early form of artificial intelligence that uses a symbolic representation of domain knowledge (e.g., expert experience and previous projects) to build knowledge-based systems rather than using complex algorithms. KBR can be divided into Rule-based reasoning (RBR) and Case-based reasoning (CBR).

Instead of relying only on general knowledge of the problem domain or making connections between problems and conclusions, CBR can use knowledge from problems from previous cases to identify solutions to new problems. CBR is also an approach to sustainable learning since new experience is retained each time a problem is solved, making it immediately available for future problems. A typical CBR system works according to the following steps: identify the current problem, search past cases similar to the new one, find the most similar case to solve the current problem, evaluate the proposed solution, and update the system by learning from this experience [9]. In the integration with BIM, relevant information is gathered from the BIM model, and the case-based reasoning module gathers knowledge based on it.

Rule-based reasoning (RBR) is one of the popular methods of identification or diagnosis on certain domain systems. They have been proven effective in pattern recognition, decision-making, control, planning, and similar due to the transparency of knowledge reasoning and the consistency of reasoning results. However, despite their advantages, rule-based systems require considerable time to acquire the knowledge required [10].

3.2. METAHEURISTICS

The metaheuristic approach is a generic structure of algorithms for almost all optimization problems. Among the different types of metaheuristic algorithms, the Evolutionary algorithm (EA) and Swarm Intelligence (SI) received the most attention.

In addition to the many model revisions designers deal with, the key factor often affecting project delivery time is the number of design iterations. For example, designers must attend coordination meetings to detect element collisions and revise the design accordingly. Over the past few decades, heuristic optimization approaches and their advancements have been widely adopted to simulate iterated processes to avoid the problems of finding the optimal solution in construction projects effectively [11].

3.3. MACHINE LEARNING

Unlike knowledge-based reasoning and metaheuristic algorithms, machine learning is a technique in which a model learns all the steps between the initial input stage and the final output result. It is a deep learning process where all the different parts are trained simultaneously instead of sequentially. This process requires a large data set but less expert analysis and fine-tuning. Supervised and unsupervised learning are two typical branches of machine learning in BIM.

Recent studies have proposed several machine learning applications to improve AEC practice at various project stages and the built facility's life cycle [12]. For example, in the design and planning stages, the proposed application of machine learning includes predicting the effectiveness of design alternatives based on previous designs, increasing the building performance based on previous simulations, and information mining [2,12]. Researchers have proposed machine learning prototypes for pre-construction phases that predict project costs, dynamics and profits, and the potential for successful tendering [13,14]. For the construction phase, existing prototypes have largely focused on object recognition and tracking (workers, building components, facilities and equipment) based on imagery, GPS, or laser scanning data to predict, monitor and control project progress and estimate safety and conditions in the construction phase [15,16]. For post-construction phases, machine learning applications have advanced analysis methods of built structures, maintenance and condition assessment [17,18].

3.4. HYBRID AI

Nowadays, BIM research involves the use of digital transformation. Many modern technologies have been adopted in BIM by integrating different artificial intelligence algorithms, called Hybrid artificial intelligence. Three key hybrid techniques of artificial intelligence are most often used: Computer vision (CV), Natural language processing (NLP) and Robotics.

F. Pour Rahimian et al. [19] conducted one of the studies and provided an overview of existing technologies for automated construction monitoring, focusing on image processing and visualization methods. Then, they developed a proposed framework for the integration of BIM, artificial intelligence and virtual reality, followed by prototype design details, applied techniques and algorithms, and development strategies, facilitating the coordination of the flow of information between the construction site and the BIM model. The study proposed computer vision and machine learning techniques to assist in the preparation and assembly of site photos with projected BIM models. The proposed hybrid photo processing and BIM model application facilitates model updates while monitoring construction progress. The integration performed in the VR environment allows users to participate actively in evaluating progress and detect inconsistencies in time.

4. MAIN FIELDS OF BIM-AI INTEGRATION IN AEC/FM INDUSTRY

Building Information Model/Modelling/Management represents a new approach to design, static analysis, time and cost calculation, and building management throughout its entire life cycle. BIM is an approach that can be seen as a technology and as a methodology. As a "technology", it defines a digital representation of the physical and functional characteristics of the object. As a "methodology", it enables the cooperation of different participants in different phases of the object's life cycle. BIM enables data reuse for multiple purposes, including building management and maintenance.

The development of BIM software has helped BIM application and research, providing automated platforms for the efficient project management and processing of "big multidimensional data" throughout the life cycle of an object, and AI techniques are at the core of these platforms. Fig. 2 shows a map of the most commonly used BIM software sorted by the project phase.

Fig. 2 The most commonly used BIM software sorted according to the project phase [20]

The BIM approach integrated with AI techniques is applied in all life stages of the project - planning, design, construction, management of facilities and their maintenance, demolition, cost estimation, life cycle dynamics, work automation, and sustainable development. The scheme of the main application of BIM-AI integration is given in Fig. 3.

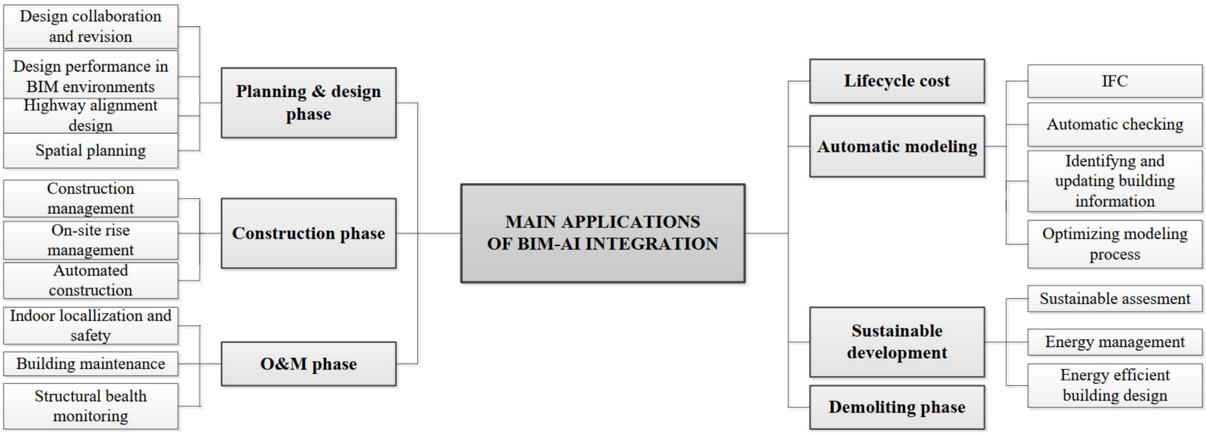

Fig. 3 The scheme of the main application of BIM-AI integration - according to [5]

BIM primarily provides a 3D model that evolves into 4D by adding a time dimension and then into 5D by adding a cost dimension. Multidimensional models have improved planning productivity and facility design [5]. Integrated AI techniques in BIM can improve design efficiency by making recommendations that the program has learned from previous projects [2,18], supporting design decisions by retrieving knowledge and experience, and optimizing building components to balance multiple goals [21]. In their work, Abdirad and Mathur [12] presented a study that developed an artificially intelligent system that minimizes inefficient work associated with manual search and content retrieval when working with BIM tools. The increased need to deliver digital information in projects has imposed new demands on engineers to create, standardize, maintain and reuse thousands of object templates in their digital BIM libraries. Data from a real company was used for this study, with the research extracting content from over 30,000 technical BIM plans (e.g., sections, views, details) from previous projects. Simulation on more than 6,000 real BIM views and experimental implementation of the BCRS system achieved 80% more efficiency in predicting the required content and a significant saving of 15% of the time spent on conventional BIM work habits.

Construction is a complex and dynamic process that involves many elements, such as building materials, machines, workers, managers and time. BIM captures, analyzes and manages the vast dynamic information generated during the construction phase. Integrating AI techniques in the construction phase can improve construction management, risk management and automation. BIM-AI integration can automate the display of construction progress, determine the optimal balance between construction duration and costs, and minimize overlapping construction activities with high risks [21,22]. For the construction phase, existing prototypes mentioned earlier have largely focused on object tracking in situ, based on imagery, GPS, or laser scanning data to control and manage project progress and conditions in the construction phase [15,16].

The exploitation and maintenance phase is the longest period in the life cycle of buildings. BIM can capture, process and analyze the large amount of digital information generated during the maintenance phase. That information is recorded in the BIM model and provides the basis for subsequent processes, but manual records often have incorrect entries. Artificial intelligence techniques are integrated with BIM to solve this problem. One proposed system uses information modelling and knowledge system functions to facilitate maintenance work. The proposed system consists of two modules: A BIM module for gathering relevant information and a case-based reasoning module for knowledge gathering. The system can help maintenance teams learn from past experience and track the full history of a building element and all elements affected by previous maintenance operations [9].

In the final period of a building's life cycle, owners must determine whether the building should be renovated to start a new life cycle or demolished to build a new one. Several artificial intelligence techniques are adopted at this stage. In one of the studies, construction and demolition waste was predicted by S-curve fitting, using machine learning to train the relationship between building characteristics and S-curve parameters [24]. Examining the model with S-curve, the study raises construction waste management to a level equivalent to project cost management.

5. CONCLUSION

Although BIM-AI integration is still in development, it seems that artificial intelligence could be a key factor in the advancement of BIM modelling technology, where data that is explicitly or implicitly present in the model – including that coming from sensors, IoT devices and simulation – can produce new data linked to other data sets within the BIM model. Digitization is conditioned by generating a huge amount of data that can be used in the future through artificial intelligence. Artificial intelligence enables the analysis of such data, leading to improvements in construction techniques and the early detection and prevention of problems.

The BIM approach integrated with artificial intelligence techniques is applied in all life stages of the project - planning, design, construction, management of facilities and their maintenance, demolition, and also in the field of lifetime cost estimation, work automation and sustainable development. This integration enables increased efficiency and productivity of the project, simplification and optimization of processes, better cooperation between teams and better flow of information, reduction of resource losses and risks caused by human error, learning from experience and existing projects, and reduction of costs and time.

The construction of our environment today is often managed without an immediate and accurate understanding of the condition of the facility built on site, leading to increased project costs and poor schedules. Existing BIM solutions provide users with information on the latest project status; however, a secure and accurate record of changes, updates and decisions is essential. All this requires a detailed process of planning and standardization in order to use new technologies and artificial intelligence in the right way. Although introducing this integration of advanced technologies requires financial costs (purchase of software and training equipment), these costs will be compensated in the future by reducing the costs of designing, organizing the construction and maintaining the facility.

ACKNOWLEDGEMENT

This research (paper) has been supported by the Ministry of Science, Technological Development and Innovation through project no. 451-03-47/2023-01/200156 “Innovative scientific and artistic research from the FTS (activity) domain”.

REFERENCES

[1] S. O. Abioye *et al.*, “Artificial intelligence in the construction industry: A review of present status, opportunities and future challenges,” *Journal of Building Engineering*, vol. 44. Elsevier Ltd, Dec. 01, 2021. doi: 10.1016/j.jobe.2021.103299.

[2] R. Sacks, M. Girolami, and I. Brilakis, “Building Information Modelling, Artificial Intelligence and Construction Tech,” *Developments in the Built Environment*, vol. 4, Nov. 2020, doi: 10.1016/j.dibe.2020.100011.

[3] National Institute of Building Sciences, “National Building Information Modeling Standard Version 1 - Part 1: Overview, Principles, and Methodologies,” 2007.

[4] A. Darko, A. P. C. Chan, M. A. Adabre, D. J. Edwards, M. R. Hosseini, and E. E. Ameyaw, “Artificial intelligence in the AEC industry: Scientometric analysis and visualization of research

activities," *Automation in Construction*, vol. 112. Elsevier B.V., Apr. 01, 2020. doi: 10.1016/j.autcon.2020.103081.

[5] F. Zhang, A. P. C. Chan, A. Darko, Z. Chen, and D. Li, "Integrated applications of building information modeling and artificial intelligence techniques in the AEC/FM industry," *Automation in Construction*, vol. 139. Elsevier B.V., Jul. 01, 2022. doi: 10.1016/j.autcon.2022.104289.

[6] A. Zabin, V. A. González, Y. Zou, and R. Amor, "Applications of machine learning to BIM: A systematic literature review," *Advanced Engineering Informatics*, vol. 51, Jan. 2022, doi: 10.1016/j.aei.2021.101474.

[7] DEVB, "Adoption of Building Information Modelling for Capital Works Projects in Hong Kong," 2021.

[8] H. Salehi and R. Burgueño, "Emerging artificial intelligence methods in structural engineering," *Engineering Structures*, vol. 171. Elsevier Ltd, pp. 170–189, Sep. 15, 2018. doi: 10.1016/j.engstruct.2018.05.084.

[9] I. Motawa and A. Almarshad, "A knowledge-based BIM system for building maintenance," *Autom Constr*, vol. 29, pp. 173–182, Jan. 2013, doi: 10.1016/j.autcon.2012.09.008.

[10] W. Y. Lin and Y. H. Huang, "Filtering of irrelevant clashes detected by BIM software using a hybrid method of rule-based reasoning and supervised machine learning," *Applied Sciences (Switzerland)*, vol. 9, no. 24, Dec. 2019, doi: 10.3390/app9245324.

[11] H. C. Hsu, S. Chang, C. C. Chen, and I. C. Wu, "Knowledge-based system for resolving design clashes in building information models," *Autom Constr*, vol. 110, Feb. 2020, doi: 10.1016/j.autcon.2019.103001.

[12] H. Abdirad and P. Mathur, "Artificial intelligence for BIM content management and delivery: Case study of association rule mining for construction detailing," *Advanced Engineering Informatics*, vol. 50, p. 101414, Oct. 2021, doi: 10.1016/j.aei.2021.101414.

[13] Y. Xu, Y. Zhou, P. Sekula, and L. Ding, "Machine learning in construction: From shallow to deep learning," *Developments in the Built Environment*, vol. 6, May 2021, doi: 10.1016/j.dibe.2021.100045.

[14] M. Bilal and L. O. Oyedele, "Guidelines for applied machine learning in construction industry—A case of profit margins estimation," *Advanced Engineering Informatics*, vol. 43, Jan. 2020, doi: 10.1016/j.aei.2019.101013.

[15] A. Braun and A. Borrmann, "Combining inverse photogrammetry and BIM for automated labeling of construction site images for machine learning," *Autom Constr*, vol. 106, Oct. 2019, doi: 10.1016/j.autcon.2019.102879.

[16] R. Akhavian and A. H. Behzadan, "Construction equipment activity recognition for simulation input modeling using mobile sensors and machine learning classifiers," *Advanced Engineering Informatics*, vol. 29, no. 4, pp. 867–877, Oct. 2015, doi: 10.1016/j.aei.2015.03.001.

[17] M. Q. Huang, J. Ninić, and Q. B. Zhang, "BIM, machine learning and computer vision techniques in underground construction: Current status and future perspectives," *Tunnelling and Underground Space Technology*, vol. 108, Feb. 2021, doi: 10.1016/j.tust.2020.103677.

[18] J. C. P. Cheng, W. Chen, K. Chen, and Q. Wang, "Data-driven predictive maintenance planning framework for MEP components based on BIM and IoT using machine learning algorithms," *Autom Constr*, vol. 112, Apr. 2020, doi: 10.1016/j.autcon.2020.103087.

[19] F. Pour Rahimian, S. Seyedzadeh, S. Oliver, S. Rodriguez, and N. Dawood, "On-demand monitoring of construction projects through a game-like hybrid application of BIM and machine learning," *Autom Constr*, vol. 110, Feb. 2020, doi: 10.1016/j.autcon.2019.103012.

[20] "Integrated BIM." Accessed: Oct. 13, 2023. [Online]. Available: https://integratedbim.com/

[21] F. Amer and M. Golparvar-Fard, "Modeling dynamic construction work template from existing scheduling records via sequential machine learning," *Advanced Engineering Informatics*, vol. 47, Jan. 2021, doi: 10.1016/j.aei.2020.101198.

[22] W. He, Y. Shi, and D. Kong, “Construction of a 5D duration and cost optimisation model based on genetic algorithm and BIM,” *Journal of Engineering, Design and Technology*, vol. 17, no. 5, pp. 929–942, Sep. 2019, doi: 10.1108/JEDT-12-2018-0214.

[23] V. Faghihi, K. F. Reinschmidt, and J. H. Kang, “Construction scheduling using Genetic Algorithm based on Building Information Model,” *Expert Syst Appl*, vol. 41, no. 16, pp. 7565–7578, Nov. 2014, doi: 10.1016/j.eswa.2014.05.047.

[24] W. Lu, Y. Peng, X. Chen, M. Skitmore, and X. Zhang, “The S-curve for forecasting waste generation in construction projects,” *Waste Management*, vol. 56, pp. 23–34, Oct. 2016, doi: 10.1016/j.wasman.2016.07.039.

CRITICAL AMOUNTS OF PRECIPITATION FOR ACTIVATING LANDSLIDES IN THE DONJI MILANOVAC – TEKIJA REGION

Nikolina Ćirić[1]

Summary:

In practice, those caused by heavy rainfall stand out as a special type of landslide, which is the case on the ground in the section Donji Milanovac-Tekija. The work aims to determine the dependence of the landslide activation on the critical amount of precipitation based on the available data on daily precipitation amounts in the researched area in a certain period in which a particular landslide was activated. To obtain a complete picture of recent processes, the geological characteristics of the area, which were placed in the context of this work, were also considered. The results of the research showed the existence of a functional relationship between the activation of landslides and the amount of precipitation. The influence on the activation of landslides has a smaller amount of precipitation in a longer duration, depending on the local conditions. In addition, extreme precipitation is also particularly important for activating landslides. This research highlights the need to systematically monitor landslide activations in similar terrains to manage these natural disasters.

Key words: landslide, rainfall, Donji Milanovac, Tekija

[1] Teaching associate, Department of Civil Engineering, Faculty of Technical Sciences, Dositej Obradović square 6, Novi Sad, email nikolina.ciric@uns.ac.rs

1. INTRODUCTION

Donji Milanovac and Tekija are settlements in the eastern part of Serbia near the Danube. Favourable geographical, climatic, and geological conditions, such as landslides and floods, characterize natural disasters of various origins.

This paper emphasizes the study of landslides due to heavy and prolonged rainfall as one of the most common factors for triggering landslides. The rapid movement of soil, rocks, mud or other materials down the slope characterizes this dynamic phenomenon. The causes of landslides are numerous, but intense multi-day rains play a key role when we talk about large amounts of precipitation. When rainfall soaks the soil, the soil becomes heavier and loses its strength. This loss of stability can lead to catastrophic landslides that can cause extensive damage to infrastructure, housing and agricultural land. Apart from material losses, landslides seriously threaten human life and safety [1]. This picture was most clearly confirmed in practice during September 2014, when the settlements of Tekija, Donji Milanovac and Kladovo were threatened due to the activation of massive landslides along the Danube (Đerdap) highway [2].

This work aims to use publicly available data on the time of landslide activation, as well as published meteorological data on the amount of precipitation in that time, to define, using statistical methods, the functional dependence of landslide activation in the investigated area of Tekija-Donji Milanovac on the critical sum of precipitation in a certain period, which led to the sliding of a certain mass.

2. CHARACTERISTICS OF THE AREA

The researched area of Tekija-Donji Milanovac has the name Danube Key in a broader sense (Figure 1). From a hydrographic point of view, the watercourses belong to the Danube River basin. The most important watercourses include Podvrška river, Valja Mare and Kamenička river. A continental climate with hot summers and little precipitation and cold winters with abundant precipitation characterises the area. Winds are frequent and strong in this area, accompanied by heavy rainfall.

Figure 1: Terrain map of the investigation area, according to [3]

Terrain morphology is closely related to the geological structure. Areas with Quaternary and Neogene sediments are flat, while parts of the terrain with older geological formations are hilly. The research area is characterized by a Paleozoic basement, a dominant Mesozoic sedimentary succession with accompanying volcanism, and a Tertiary sedimentary cover (Figure 2).

a) Paleozoic/Proterozoic

Crystalline rocks with a high degree of metamorphism correspond to the Proterozoic. Plagioclase gneisses (Gp) and microcline-plagioclase gneisses (Gmi) dominate. Mica schists (Sbm) and typical Permian sandstones are also widely distributed [4].

b) Mesozoic

Units of Mesozoic age occupy the largest part of the research area.

Among the units of Jurassic age, sandstones, claystones, ferruginous limestones, and subordinate limestones with cherts stand out.

Sinai flysch-like strata, sandstones, marls, clays and limestones of Cretaceous age also dominate the study area. In the Upper Cretaceous, the so-called Bananita formation stands out, a characteristic volcanic rock in the area [4].

c) Tertiary

When we talk about the youngest sediments, conglomerates and sandstones stand out, especially in the vicinity of Donji Milanovac, as well as Quaternary alluviums, sepals, and river terraces, just near Tekija [4].

Of the geological factors, the existence of landslides is primarily indicated by the lithological type of the rock mass and its state of freshness, i.e. decades. Landslides are often formed in rock masses that easily and quickly change their physical and mechanical properties under atmospheric conditions. These include weakly bound rocks (clays, marls, diluvial and semi-vial sediments) and semi-rocks (clays, marls, sandstones with a clay binder and all types of schists of lower crystallinity). Landslides also occur in other rocks where the decay crust is of considerable thickness [5].

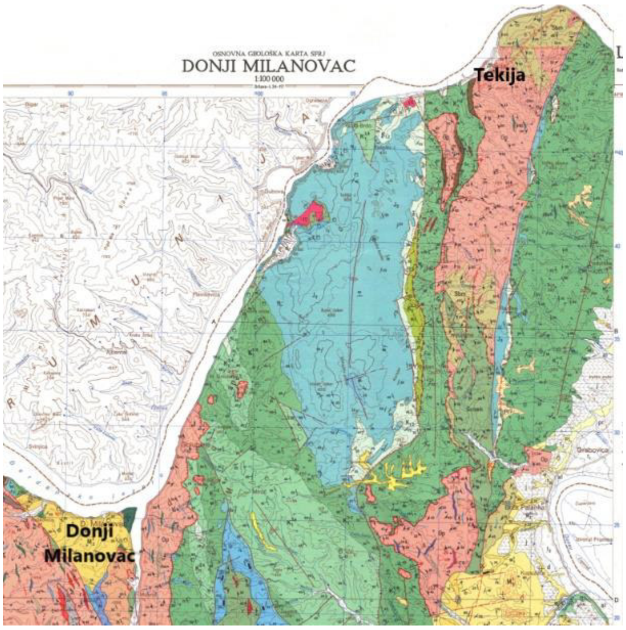

Figure 2: Geological structure of the Eastern part of Serbia, according to [4]

Figure 3 shows a hazard map segment from the occurrence of landslides in the broader investigation area. Just by looking at the map, we can see that in the places where mapped landslides are marked in the research area, the hazard for landslides is higher.

According to available literature sources [2], most landslides (11) in the area of Tekija and Donji Milanovac were formed in flysch sediments of Cretaceous age, which are lithologically represented by sandstones, clays and marls. 37% of landslides were formed in the contact zone of the two lithological environments, and only 7% of landslides were formed along faults. Interestingly, 10% of landslides are formed in igneous rocks. These landslides were formed in the surface zone of decomposition and the zone of contact with other lithological environments [1].

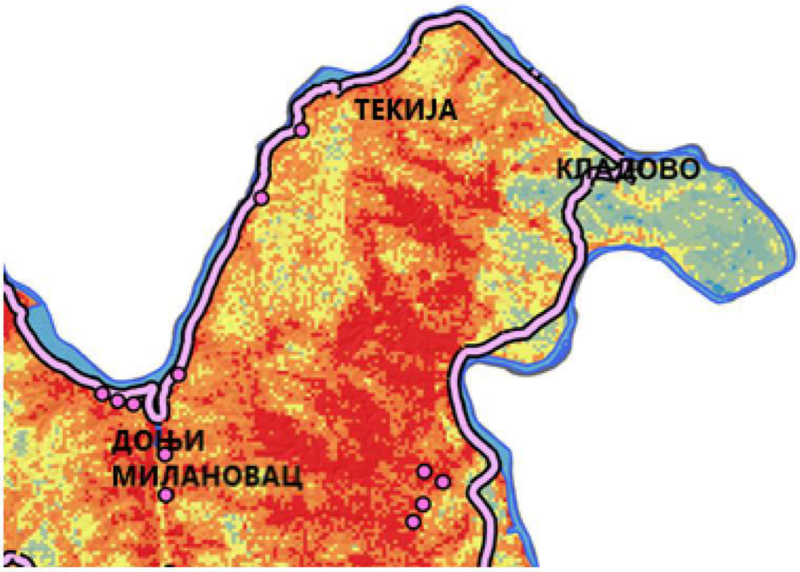

Figure 3: Segment of the landslide hazard map of the wider Donji Milanovac-Tekija research area, according to the Landslide Hazard Map of the Republic of Serbia [6] (purple dots – recorded landslides)

3. METHODOLOGY

This work collected the data, approximate locations and times of activating six landslides in the investigated area of Tekija-Donji Milanovac, which were activated in a previous period. The dating of the landslide was carried out based on available newspaper articles, internet portals of daily newspapers, local governments, reports of road companies, etc., which are placed in the context of this work.

For the wider research area, official data on daily precipitation amounts in 20 years were also collected from the nearest main meteorological station of the Republic Hydrometeorological Institute (RHMZ) in Negotin. The Negotin synoptic station is located at 42 meters above sea level and is one of the main stations in eastern Serbia where measurements have been made since 1947 (https://www.hidmet.gov.rs/ciril/meteorologija/stanica_moss.php?moss_id= 13295). Data on daily precipitation amounts were taken from the Meteorological Yearbook of the RHMZ from 2006-2022. For June 2023 (when the last considered landslide in the area was activated), data on daily precipitation amounts from the RHMZ Monthly Bulletin were used. For this paper, the daily amounts of precipitation corresponding to the temporal activation of the landslide (before and during activation) were considered.

After collecting the available data on the time and location of landslide activation in the researched area and the precipitation regime during and before the landslides' activation, the modelling of critical precipitation sums was started. The statistical model presented in [7] and [8] was used in this paper. First, the located and dated landslide in the researched area is joined with appropriate precipitation values (at the moment of activation and in a certain interval before activation - a few days, a week) based on the published data of RHMZ. Modelling involved the formation of a diagram of the amount of precipitation E (mm) and the duration of precipitation D (h) so that each isolated landslide in the area represents one-point data on the diagram. Then, the statistical analysis of the obtained data was started, which establishes the function of the dependence of the amount of precipitation on the duration of precipitation (1), which in the models used is based on the power rule [7,8].

$$E = a \cdot \mathrm{Db} \qquad (1)$$

Based on the obtained data, a model of the critical sums and duration of precipitation required for activating the considered landslides was defined in the investigated area of Tekija-Donji Milanovac [8].

This methodological approach allows us to study earlier occurrences in the researched area and form a certain dependence on the critical amount of precipitation and the activation of landslides in the future [8]. It is important to point out that with an increase in the number of observed landslides in an area and synoptic parameters before and during their activation (amount of precipitation, duration of precipitation), the accuracy of the used models of critical sums of precipitation significantly increases, taking into account their statistical nature. The resulting models can be used in practice so that in the case of expecting a larger amount of precipitation in a certain period, the competent services can react appropriately. It should be noted that there are numerous more complex global and regional models in engineering practice and more complex multifactor models of landslide activation that consider many different climatic, geological and geomorphological parameters [9]. In our immediate environment, the models were mostly made in the territories of Serbia, Croatia, and Slovenia [8] [10].

4. RESULTS AND DISCUSSION

Data was collected on the approximate location and time of activating six landslides on the Donji Milanovac-Tekija section based on publicly available sources. For the established dates of activation of individual landslides, official data of the RHMZ on the amount and duration of precipitation in the wider research area were collected, based on which the modelling of critical sums of precipitation in the research area was performed according to the above-described methodology.

Table 1 shows the landslides considered in this paper, their designations, determined dates of activation, and synoptic precipitation parameters (E and D), which were used to form the model. and their labels, established dates of activation, as well as synoptic parameters of precipitation (E and D), which were used to form the model.

Tab. 1 Considered landslides in the Donji Milanovac-Tekija area with the determined activation time on the corresponding data on the rainfall regime

Label	Landslide	Activation date	E, mm	D, h
T1	Tekija 1	17.9.2014	192.4	168
T2	Tekija 2	8.9.2014	108.9	168
T3	Tekija 3	9.3.2008	15.5	72
DM1	Donji Milanovac 1	15.3.2006	54.6	144
DM2	Donji Milanovac 2	29.3.2006	5.9	60
DM3	Donji Milanovac 3	17.6.2023	110.1	288

From the table, we can see that the activation of 3 landslides in the wider Tekija region and three landslides in the area of Donji Milanovac has been determined. The times of activation of the mentioned landslides date from 2006 to 2023. It is necessary to highlight the landslides Tekija 1 and Tekija 2, activated during extreme weather events in September 2014 and caused the most negative consequences for the population, infrastructure, and environment. The conditions and mechanisms of the occurrence of these landslides are explained in more detail in the relevant literature [2].

Based on the presented data, a model of critical rainfall sums for activating the considered landslides in Donji Milanovac-Tekija was formed. In Figure 4, we can see a graphical representation of the formed model as a dependence of the total amount of precipitation (E, mm) on the duration of precipitation (D, h). The degree of dependence function was used to approximate the model, the parameters of which are shown in the same picture.

The results of modelling the critical sums of precipitation indicate the existence of a functional dependence of landslide activation in the investigated area of Donji Milanovac-Tekija on the critical sum of precipitation. If we look at the model itself, the amounts of precipitation marked as extreme (over 100 mm) for a longer duration (several days), which correspond to the largest number of activated landslides (especially when it comes to massive landslides such as the Tekija 1 and Tekija 2 landslides). For other landslides, it is noticeable that even smaller amounts of precipitation over a longer period can be considered critical.

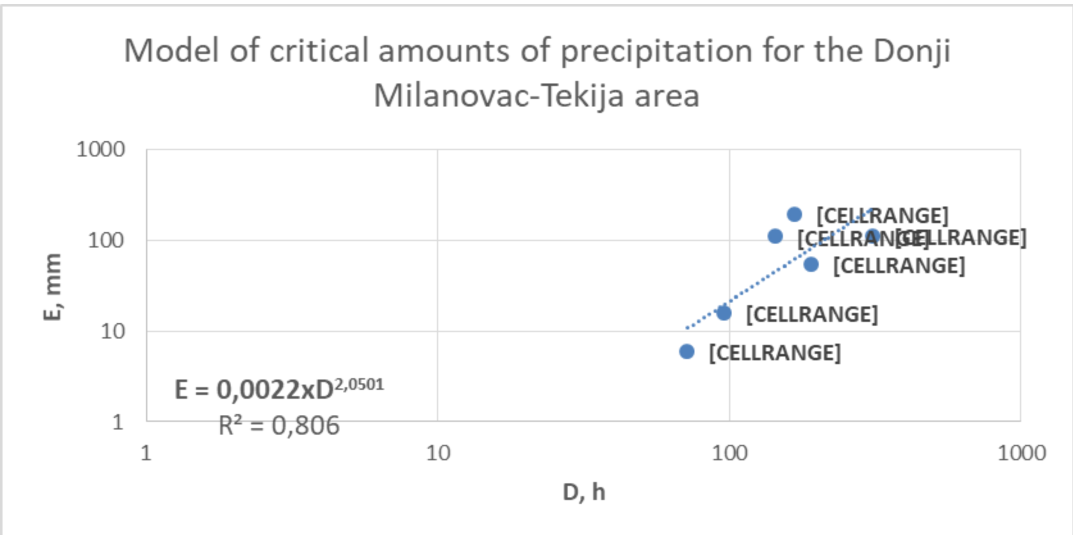

Fig. 4: Model of critical precipitation sums for the Donji Milanovac-Tekija area (blue dots - observed landslides, names - landslide marks from Table 1, logarithmic scale)

Concerning the geological causes of the formation of landslides in the researched area, the disintegration of the surface part of the rock mass, the marked morphometry of the slopes (primarily the slope of the terrain towards the Danube) and the erosion of the foot of the slopes should be highlighted. The soil-debris crust of the decomposition of gneisses in the researched area mostly contributed to the formation of landslides. As a result of several days of intense rainfall, in most cases, the soil-debris crust of the disintegration of the gneiss was saturated with water and its movement down the steep slope. The sliding of the rock masses also contributed to the subduction of the foot of the slope due to the formation of torrential flow, which is an example of the landslide in the area of Tekija from 2014. Based on the available sources, it can be determined that the engineering-geological mapping on the ground established that the ravine was cut by about 0.5-1.0 m. At the time of mapping, water seepage was found in the body of the landslide and the gully, which is another confirmation of this mode of landslide activation [2].

5. CONCLUSION

By applying the model of critical precipitation sums, the climatological conditions that led to the activation of 6 studied landslides on the stretch of Donji Milanovac-Tekija in eastern Serbia from 2006 to 2023 are described. The functional dependence between the determined amounts of precipitation and the duration of precipitation in the context of activating the considered landslides is defined. It is assumed that the greatest hazard from landslides comes from extreme amounts of precipitation (over 100 mm) lasting several days (for example, the Tekija landslide from 2014). Also, lower amounts of precipitation over a longer duration impact the activation of landslides, depending on local conditions. In terms of the geological, morphological and pedological conditions of occurrence of the landslides in the researched area, it was determined that the disintegration of the rock mass, pronounced slopes of the slopes and erosion of the slopes themselves by torrential flows play an important role.

Of course, making such an analysis often requires a certain number of data on landslides that are not easily available, and this paper emphasizes the importance of forming a proper cadastre of landslides, where, in addition to numerous data on the phenomena themselves, one will also find that on the times of activation and reactivation. The need to collect more data on landslides in the researched area of eastern Serbia from other sources is certainly emphasized to form a more precise model of critical rainfall sums for their activation. Also, in future considerations, it is advisable to model the causes of landslide activation in the researched area based on other methods used in practice.

LITERATURA

[1] National Research Council of the United States (1964) Landslides: Investigation and Mitigation, Special report 247.

[2] Đokanović S., (2016). Intense perticipation as a reason for the occurrence of landslides during September 2014 in the municipality of Kladovo. TECHNOLOGY - MINING, GEOLOGY AND METALLURGY 67 (2016) 6, doi:10.5937/tehnika1606823D

[3] Google Earth Pro

[4] Bogdanović P., Marković M., Dragić D., Dolić D., et al. (1980). Basic geological map 1:100 000. Interpreter for sheets Donji Milanovac. Oršova, Baja de Arama i Turnu Severin. Federal Geological Institute, Belgrade

[5] Jevremović D., Kostić S., (2017). Engineering geology. University of Nis, Faculty of Civil Engineering and Architecture, Nis.

[6] Marijanović M., Jevremović D., Lazić M., Damnjanović D., et al. (2017). Landslide hazard map of the Republic of Serbia 1:300,000, Ministry of the Interior of the Republic of Serbia

[7] Guzzetti F., Peruccacci S., Rossi M., Stark C.P. (2008). The rainfall intensity duration control of shallow landslides and debris flows: an update. Landslides 5/1, pp. 3-17.

[8] Marjanović M., Krautblatter M., Abolmasov B., Đurić U., Sandić C, Nikolić V. (2018). The rainfall-induced landsliding in Western Serbia: A temporal prediction approach using Decision Tree technique, Engineering Geology 232, pp. 147–159.

[9] Rossi M., Luciani S., Valigi D., Kirschbaumc D., Brunetti M.T., Peruccacci S., Guzzetti F. (2017). Statistical approaches for the definition of landslide rainfall thresholds and their uncertainty using rain gauge and satellite data. Geomorphology 285, pp. 16 27.

[10] Marijanović M., Abolmasov B., Đurić U., Krušić J., (2020). Practicum in engineering geology (Electronic source), University of Belgrade, Faculty of Mining and Geology, Belgrade

SKID RESISTANCE AND NOISE EMISSION OF DIFFERENT TYPES OF ASPHALT PAVEMENTS

Panta Krstić[1], Milan Marinković[2], Dragana Stanojević[3]

Summary:

Pavements with asphalt surface layers represent the world's most frequently built type of pavement. Besides monitoring pavement unevenness, cracks and possible deformations on the roadway, roadway maintenance nowadays also includes timely monitoring and measurement of pavement friction, ensuring traffic safety. As a consequence of the irregular texture of the pavement, traffic noise may appear due to contact between the tires and the pavement. A comparison of dense-graded, stone-mastic, and porous asphalt mixtures was made in the context of skid resistance, pavement texture, and noise emission. The analysis led to the conclusion that porous and stone-mastic asphalts have better skid resistance properties, especially in terms of macrotexture. Thanks to the air voids in its structure, the use of coarser fractions of aggregates, and the negative texture, porous asphalt concrete emits a significantly lower noise level than dense-grade and stone-mastic mixtures.

Key words: tire-pavement friction, pavement texture, asphalt mixtures, traffic safety, pavement noise

[1] Teaching Assistant, Faculty of Technical Sciences, University of Novi Sad, Serbia, panta.krstic@uns.ac.rs
[2] Assistant Professor, Faculty of Technical Sciences, University of Novi Sad, Serbia, milan.marinkovic@uns.ac.rs
[3] Teaching Assistant, Faculty of Technical Sciences, University of Novi Sad, Serbia, dragana.stanojevic@uns.ac.rs

1. INTRODUCTION

The friction between the vehicle's tires and the pavement plays a major role in keeping the vehicle on the road and improves the ability to control and manoeuvre the vehicle in both the tangential and radial directions. The basic condition for vehicle movement on the road is the existence of friction force. If the friction between the pavement and the wheel did not exist, the wheel, which would receive angular acceleration would rotate in place, slipping concerning the road surface. In order to bring the tire to its natural state of rolling on the surface, a necessary condition is the existence of a force of friction, i.e. adhesion. As a result of the contact between the tires and the surface, traffic noise is created that can be a significant problem in urban areas.

When designing the road, special attention must be paid to critical locations for traffic safety (sharper curves, sections with higher climbs, and approaches to intersections). The need for an adequate coefficient of friction is greatest in these places since this is where friction is most easily reduced and lost. The aggregate's type, origin and characteristics, and therefore the type of asphalt mixture, can have the greatest influence on the formation of micro and macrotexture of pavement and, therefore, the overall coefficient of friction. Also, locations near hospitals, schools and other public institutions must be protected in a certain way from the harmful effects of noise. This paper analysed the available friction and noise emission in the case of different types of dense, stone-mastic (SMA) and porous asphalt mixtures.

2. FRICTION IN TYRE AND PAVEMENT CONTACT

The friction force in the tire and road surface case is due to the adhesion component of the friction force and hysteresis. Adhesion is a component of friction that enables the formation of strong intermolecular forces at the actual contact points between the tire and the road. The strength of molecular forces is directly dependent on the size of the contact surface, i.e. the strength of intermolecular adhesion increases directly with the increase of the contact surface. Increasing the surface contact for the same vertical load decreases the contact pressure, which implies an increase in intermolecular adhesion. When sliding occurs, the adhesion is impaired, which contributes to the reduction of the coefficient of friction during sliding compared to static vehicles. Intermolecular adhesion is the dominant reason for resisting tire slippage on dry surfaces [1].

Hysteresis occurs due to energy loss during tire deformation. The vertical pressure of the tire on the surface causes its deformation and wedging of the tire into the microstructure of the road surface. Hysteresis can be defined differently as the sum of the resistance on all unevenness of the contact between the tyre and the surface. Unlike adhesion, the increase in hysteresis does not occur due to increased surface contact but due to increased contact pressure. In the case of wet pavement, hysteresis plays a dominant role in preventing slippage [1].

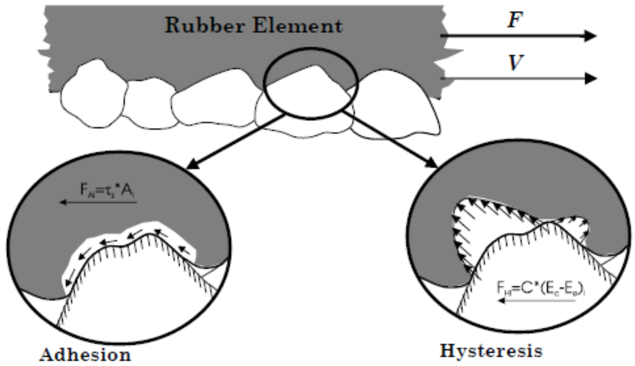

Fig. 1 Mechanisms of pavement and tire friction – adhesion and hysteresis [2]

Although there are other components of the friction force, they are insignificant compared to adhesion and hysteresis. Therefore, the friction force in the case of tires and pavement can be defined as the sum of hysteresis and adhesion components. Both components depend dominantly on the pavement texture and tire characteristics [2].
The micro and macrotexture of the roadway, the pavement type and the method of construction, climatic influences such as the presence of water, snow or ice on the roadway and the possible presence of oil, dust or other pollutants could affect available friction the most [2].

2.1. ROAD TEXTURE AND FRICTION COEFFICIENT

Pavement texture can be explained as the deviation of the pavement from an ideally flat surface that can occur due to various factors (type and size of aggregate used for pavement construction, granulometric composition, type of pavement construction, properties of the applied binder, void content, etc.). Deviations from the ideal texture have a key impact on traffic safety. Pavement texture imperfections are observed at different levels depending on the wavelength λ and amplitude A. The three basic levels in which pavement texture is considered, according to foreign and domestic standardization, are [2]:
1. Microtexture (λ<0.5mm; A=1-500 μm) – The roughness of the road surface visible under a microscope. It depends primarily on the mineralogical properties and origin of the aggregates used to prepare the asphalt mixture [3];
2. Macrotexture (0.5mm-λ-50mm; A=0.1-20 mm) – Roughness that is defined by the type, size or granulometric composition of aggregates used for asphalt mixture production and the construction method of the surface layer;
3. Megatexture (50mm-λ-500mm; A=0.1-50 mm) – Defects and distresses on the road surface, cracks, potholes and other damages resulting in noise and rolling resistance;
4. Pavement unevenness (λ>500mm) – all wavelengths over 500 mm are considered as significant roughness of the pavement surface in the longitudinal direction.

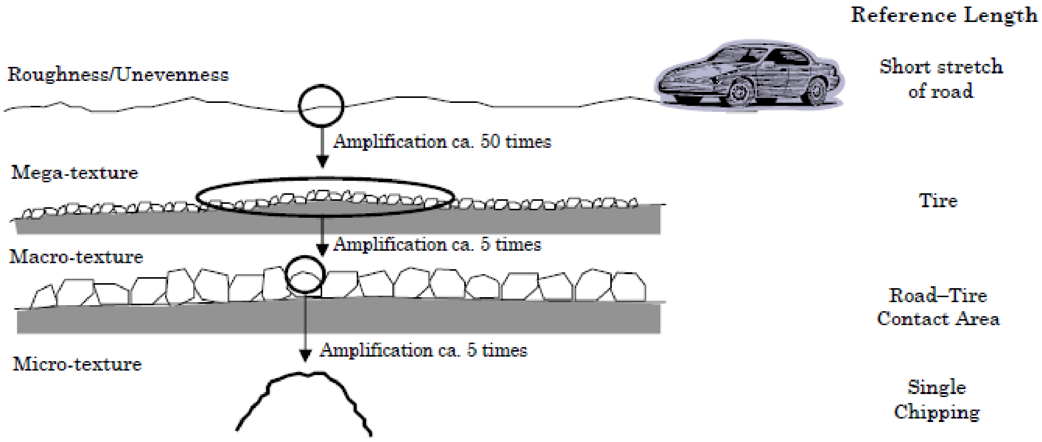

Fig. 2 Texture ranges of a pavement surface [2]

Microtexture, as an adhesive component, is responsible for achieving optimal friction at lower speeds (up to 50 km/h) in ambient conditions that do not include water on the road. At higher speeds, a properly established macrotexture allows the removal of water under the tire and re-establishing the adhesion component of friction. Hysteresis is dominant in friction at higher speeds (95% of total friction comes from hysteresis for speeds higher than 105 km/h) and prevents aquaplaning [2]. The adhesion component that depends on the microtexture is the most important for establishing friction on dry and polished surfaces. In contrast, hysteresis as a friction component is crucial in the case of wet and rougher pavement surfaces [3]. In cases of inadequate friction, it is necessary to increase the roughness of the pavement surface by various technologies of milling, grooving or pavement recycling.

The British pendulum tester (BPT) is one of the most commonly used devices for indexing friction in laboratory conditions or on the field. Friction, defined by the pendulum, refers primarily to the conditions of vehicle movement at lower speeds. The device defines the numerical value of friction (British pendulum number - BPN) based on recording the loss of kinetic energy when sliding a pendulum with a rubber slider that simulates the friction between the tire and the road. The device is used primarily to indicate the pavement microtexture, while the volumetric Sand Patch Test (SPT) is used to evaluate the macrotexture. The measured BPN value roughly corresponds to the theoretical coefficient of friction multiplied 100 times; the equation $BPN=330\mu/(3+\mu)$ [4] applies.

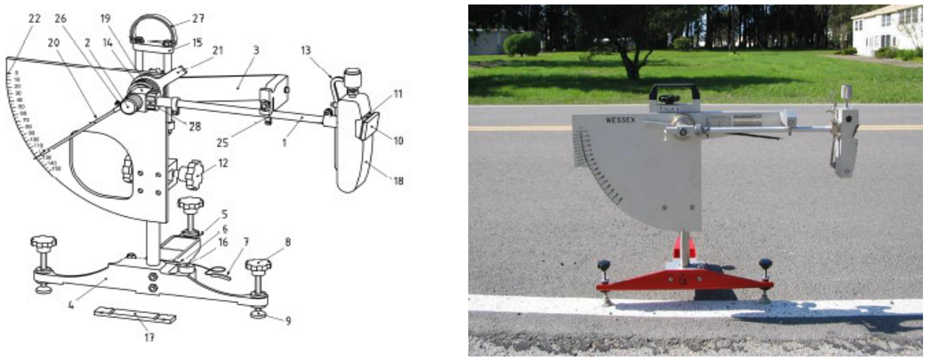

Fig. 3 British Pendulym Tester

The basic prerequisite for a good microtexture is properly selected aggregate fractions for making the asphalt mixture. The aggregate makes up 92-96% of the volume of all asphalt mixtures and, therefore, is in contact with the vehicle's tires to the greatest extent. Different fractions of aggregates and their content in the mixture can act differently on establishing micro or macrotexture. Fine aggregates with more irregular grain shapes and sharper edges generally contribute to a better microtexture. In contrast, rounded and elongated grains contribute to reducing the microtexture [2].
In addition to grain size, hardness, mineralogy, shape, texture and edge sharpness, aggregate polishing resistance can also significantly impact pavement performance in terms of achieved coefficient of friction. Aggregates resistant to polishing retain their microtexture due to a large number of intervals of traffic loads. The polishing resistance of the surface of the aggregate grain is measured by the stone polishing coefficient (PSV - Polished stone value) in laboratory conditions. Aggregate grains are subjected to polishing, and their resistance to polishing is measured using a device with a pendulum. Higher values of this coefficient imply higher resistance to polishing (higher aggregate roughness) [5].

2.2. SKID RESISTANCE OF DIFFERENT TYPES OF ASPHALT MIXTURES

Dense-graded asphalt mixtures are produced as hot mix asphalts, have a small percentage of voids and are relatively waterproof. They can be classified as fine-grained and coarse-grained, depending on the aggregate size in the asphalt mixture. They are suitable for use in all pavement base and surface layers, under all traffic conditions [6]. Depending on specific site and traffic conditions, they are made from fine and coarse aggregate fractions and 5-6% bituminous binder. When it comes to the micro and macrotexture of the surface course, in general, they have a lower macrotexture depth (0.4-0.6mm for fine-grained and 0.6-1.2mm for coarse-grained mixtures) compared to SMA and porous asphalt mixtures. SMA mixtures are applied as a wearing surface of roads with heavier traffic loads. Within this mixture, there is a higher content of the coarse aggregate fraction, which enables the formation of a skeletal structure, i.e. the entrapment between the aggregate grains. They have a higher content of bituminous binder (6-9%) and a lower content of air voids in the mixture [6] [7]. Unlike SMA and dense-graded, porous asphalt mixtures are designed to be water-permeable, using aggregates in the form of crushed stone and modified bituminous binder. Porous asphalt is designed as an open mixture with 18-25% air voids, with a typical layer thickness of 4-5cm. Its permeability enables a full pavement-tire friction coefficient since retaining a film of water on the road surface is extremely rare [8]. Due to the use of larger aggregates in their mixture, SMA and porous asphalts have a more pronounced macrotexture than dense mixtures (over 1mm texture depth for SMA and 1.5-3mm for porous asphalts) [7].

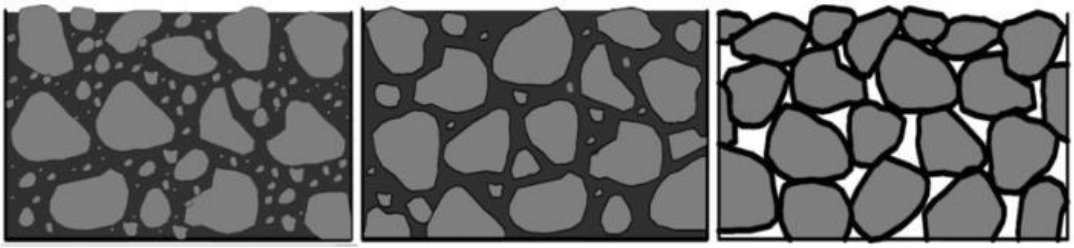

Fig. 4 Structure of dense-graded, SMA and porous asphalt mixtures (from left to right) [9]

The study from 2014 [10] investigated the performance of SMA, asphalt concrete (AC) and porous asphalt concrete (PAC) sections of highway in China in terms of skid resistance, rutting, roughness and noise level. The skid resistance properties of three surface layers (SMA-13, AC-13 and PAC-13) were evaluated through standard BPT protocol and sensor-measured texture depth, observing a period of four years. The authors concluded that BPN values decreased over time, with the PAC section remaining with the highest friction coefficient. Regarding macrotexture, the results indicated that the PAC had the highest texture depth, followed by SMA and dense-graded asphalt.

The influence of temperature and moisture on the friction properties of different types of asphalt mixtures was discussed in [8]. Compared to classic AC-13 and SMA-13 asphalt mixtures, PAC-13 had the highest skid resistance values in microtexture evaluated with BPT. The BPN values gradually decreased with increasing temperature in every mixture type. The skid resistance of porous asphalt decreased, on average, 37.4% for every 20 °C increase in temperature.

A skid resistance comparison of different asphalt mixtures made from local limestone aggregate and slag addition, with different bitumen contents, was made in [11]. The samples analyzed were prepared according to Marshall's method, with samples containing optimal bitumen content, 0.5 and 1% increased bitumen content and compared with mixtures designed according to Superpave methodology and SMA. It was concluded that increased bitumen content beyond the optimum decreased the skid resistance of asphalt mixtures. Mixtures designed according to the Superpave methodology were shown to be better in skid resistance compared to SMA and asphalt mixtures designed according to Marshall. Although with a higher bitumen content, SMA asphalt mixtures, recorded slightly higher BPN values than classic AC.

Observing the skid resistance of porous and dense asphalt mixtures and comparing the obtained BPN values established that porous asphalts have higher friction coefficients than classic AC [12]. According to this study, PAC had a friction coefficient higher by an average of 10 BPN measured units. This fact was confirmed in a similar study made in Iran by Ahadi et al. [13]. When comparing the texture properties of dense-graded and open-graded asphalt mixtures (grade four and five) at the optimal binder content, it was concluded that PAC has significantly better friction properties than classic AC, especially in macrotexture. This can be based on the higher level of void space and coarser aggregate used in the mixture, affecting the road macrotexture.

Table 1 summarizes the typical skid resistance (BPN values) of the different asphalt mixtures analyzed in the abovementioned studies.

Tab. 1 Skid resistance of considered dense, SMA and porous asphalt mixtures

Reference	Asphalt mixture (N_{max})	Standard	Friction coefficient (BPN)	Remark
[10]	AC (13mm)	JTJ059-95	75	*Results obtained for the truck lane and first year measurement
	SMA (13mm)		76.3	
	PAC (13mm)		80.3	
[8]	AC (13mm)	-	42.5	*Results obtained for testing temperature of 20°C ** Laboratory testing
	SMA (13mm)		42.3	
	PAC (13mm)		44.3	
[11]	AC (-)	ASTM E303-93	87.2	* Laboratory testing
	SMA (-)		92.4	
[12]	AC (-)	ASTM E303-74	40 – 76	*Testing of different existing road sections
	PAC (-)		61 - 69	
[13]	AC (-)	ASTM E303-93	69.4; 97.65	*Optimal bitumen content and two mixture grades **Laboratory testing
	PAC (-)		95.9; 93.4	

3. NOISE EMISSION

The noise generated by the movement of vehicles on the road can be a serious environmental problem. In extreme situations, it can negatively affect flora and fauna, as well as people who live near the road with a significant level of noise. Traffic noise can be due to car operation, aerodynamic origin, or the interaction between vehicle tires and the road surface [14]. Standard outdoor methods for measuring tyre-pavement noise are pass-by, close-proximity and on-board sound intensity methods [15].

When it comes to pavement texture, an increase in noise is inevitable in the case of rougher roads with more pronounced macrotexture, which can be undesirable in the case of roads that pass through populated areas or near buildings of public importance. The noise generation depends on the distribution of wavelengths on the pavement surface (positive or negative texture), shown in *Figure 5* [16]. Pavements with a positive texture have a significant number of aggregate grains above the plane of the pavement surface. The negative texture, represented mainly in SMA and PAC [17], contributes to reducing noise between the tire and the pavement due to a flatter contact surface. Among the other factors that can influence noise generation are the temperature and age of the pavement, the size of the maximum aggregate grain in the mixture and the granulometric composition, the percentage of voids in the mixture and the type of asphalt mixture [14]. When it comes to the connection between friction and noise, there is a negative correlation, generally speaking - increased safety is related to a more distinct texture of the pavement and, therefore, to greater noise [14].

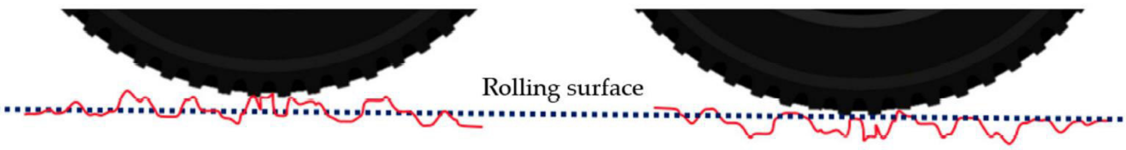

Fig. 5 Positive (left) and negative (right) pavement texture [16]

The typical values of noise levels, in terms of absolute sound pressure level, can exceed 84 dB for dense-graded mixes [14]. Different authors analysed the noise reduction effect by applying SMA or PAC surface layers instead of AC.

Yang et al. analyzed the performance of porous and SMA mixtures (PAC-13 and SMA-13) in the context of noise generation [18]. In addition to reducing the stopping distance during braking, using PAC reduced noise emission by 2-6 dB compared to SMA mixtures, at test vehicle speeds of 80 and 100 km/h. Also, with an increase in the speed of the test vehicle, the general increase in noise level is lower for porous compared to SMA mixtures. The authors explained this phenomenon by the joining air voids in the structure of porous asphalt mixtures and the effect of "air pumping" by the absorption of noise using the bound voids of PAC.

In addition to measuring skid resistance, Khaki et al. compared tire-pavement contact noise for dense and porous asphalt mixtures [12]. The testing was carried out on existing roads at speeds of the test vehicle of 50 km/h, whereby the recorded noise levels were significantly lower in the case of PAC. It is emphasized that using classic and multi-layered PAC or SMA can reduce the noise level due to the passing of a vehicle tire by up to 8 dB. In their study, Yu et al. [10] compared the noisse emission in the case of three different asphalt mixtures. The noise levels were considered when the test vehicle passed at speeds of 50, 80 and 100 km/h over different types of pavements. It was determined that there was a noise reduction in porous mixtures of 1.5 to 4 dB compared to the other two types of pavement surfaces.

4. CONCLUSION

The available friction between the tire and the road surface is crucial for ensuring traffic safety, especially in conditions of increased pavement moisture. Although they have increased resistance to deformations and higher bearing capacity in surface layers, SMA mixtures have similar and sometimes lower skid resistance in terms of microtexture than dense asphalts, mainly due to the higher binder content. Compared to dense-graded, the good macrotexture properties in SMA mixtures can be explained with the coarser aggregate used in the mix. The mixtures that stood out as the most favourable regarding skid resistance are PAC due to the coarser aggregates used for their preparation and primarily the greater void content. Porous asphalt mixtures emit a lower level of noise when in contact with the tire, which is a consequence of their negative texture and the effect of air pumping and noise absorption. Considering the above, applying PAC is advantageous in unsafe and dangerous locations where it is necessary to ensure a high coefficient of friction and good drainage. Porous asphalt mixtures can represent a good design solution for ensuring traffic safety. However, their lower load capacity in cases of heavy traffic loads and the increased maintenance costs should be considered.

ACKNOWLEDGEMENT

The research has been conducted within the project "Scientific theoretical and experimental research and improvement of educational process in the field of civil engineering", developed at the Department of Civil Engineering and Geodesy, Faculty of Technical Sciences, University of Novi Sad, Serbia.

REFERENCES

[1] Stojić B. (2012). *Teorija kretanja drumskih vozila – skripta.*, Faculty of Technical Sciences, Novi Sad, Serbia

[2] Hall J. W., Smith K. L., Titus-Glover L., Wambold J.C., Yager T.J., Rado Z. (2009). *Web-Only Document 108: Guide for Pavement Friction*, National Cooperative Highway Research Program, Transportation Research Board.

[3] Kouchaki S., Roshani H., Prozzi J. A., Garcia N. Z., Hernandez J. B. (2018). Field Investigation of Relationship between Pavement Surface Texture and Friction. *Transp Res Rec*, Volume 2672, pp. 395–407. https://doi.org/10.1177/0361198118777384.

[4] Chu L., Guo W., Fwa T. F. (2022). Theoretical and practical engineering significance of British pendulum test. *International Journal of Pavement Engineering*, Volume 23, pp. 1–8. https://doi.org/10.1080/10298436.2020.1726351.

[5] SRPS EN 1097-8:2010 (2010). Određivanje koeficijenta poliranja kamena, Institute for standardization of Serbia.

[6] Uzelac Đ. (2015), *Kolovozne konstrukcije*, Faculty of Technical Sciencess, Novi Sad, Serbia

[7] Kogbara R.B., Masad E. A., Kassem E., Scarpas A., Anupam K. (2016). A state-of-the-art review of parameters influencing measurement and modeling of skid resistance of asphalt pavements. *Construction and Building Materials*, Volume 114, pp. 602–617. https://doi.org/10.1016/j.conbuildmat.2016.04.002.

[8] Zhao S., Zhang H., Feng Y., Guo Z., Yang H., Li Y. (2023) Effect of temperature and water conditioning on noise and skid resistance of dense-graded, open-graded and gap-graded asphalt mixes. *Ain Shams Engineering Journal*, https://doi.org/ 10.1016/j.asej.2023.102281.

[9] Babalghaith A. M., Koting S., Ramli Sulong H. R., Hossain Khan M. Z., Milad A., Md. Yusoff N. I., Ibrahim M.R., Nagor Mohamed A. H. (2022). A systematic review of the utilization of waste materials as aggregate replacement in stone matrix asphalt mixes, *Environmental Science and Pollution Research*, Volume 29, pp. 35557–35582, https://doi.org/10.1007/s11356-022-19447-w.

[10] Yu B., Jiao L., Ni F., Yang J. (2015). Long-term field performance of porous asphalt pavement in China, Road Materials and Pavement Design, Volume 16, pp. 214–226. https://doi.org/10.1080/14680629.2014.944205.

[11] Asi I. M. (2007) Evaluating skid resistance of different asphalt concrete mixes, *Building and Environment*, Volume 42, pp.325–329. https://doi.org/10.1016/j.buildenv.2005.08.020.

[12] Khaki A. M., Forouhid A. E., Zare M. (2015). Comparison of the noise level and the skid resistance of asphalt pavement mixtures on road surface, *Journal of Measurements in Engineering*, Volume 3, pp. 71-76.

[13] Ahadi M. R., Nasirahmadi K. (2013). The Effect of Asphalt Concrete Micro & Macro Texture on Skid Resistance, *Journal of Rehabilitation in Civil Engineering* , Volume 1-1, pp. 15-28

[14] Sirin O. (2016). State-of-the-Art Review on Sustainable Design and Construction of Quieter Pavements-Part 2: Factors Affecting Tire-Pavement Noise and Prediction Models, *Sustainability (Switzerland)*, Volume 8. https://doi.org/10.3390/su8070692.

[15] Ling S., Yu F., Sun D., Sun G., Xu L. (2020). A comprehensive review of tire-pavement noise: Generation mechanism, measurement methods, and quiet asphalt pavement, *Journal of Cleaner Production*, Volume 287. https://doi.org/10.1016/j.jclepro.2020.125056

[16] Callai S. C., Sangiorgi C. (2021). A review on acoustic and skid resistance solutions for road pavements, *Infrastructures*, Volume 6. https://doi.org/10.3390/infrastructures6030041

[17] Liu M., Huang X., Xue G. (2016). Effects of double layer porous asphalt pavement of urban streets on noise reduction, *International Journal of Sustainable Built Environment*, Volume 5, pp. 183–196. https://doi.org/10.1016/j.ijsbe.2016.02.001.

[18] Yang Z., Xu B., Cao D. (2019). Comparative Analysis of Performance of Porous Asphalt Pavement and SMA Pavement Based on Deck Pavement Structure, *IOP Conference Series: Earth and Environmental Science*, Institute of Physics Publishing, https://doi.org/10.1088/1755-1315/283/1/012053.

UNCONFINED COMPRESSIVE STRENGTH OF DIFFERENT SOIL TYPES STABILIZED WITH CEMENT AND CLINOPTILOLITE MIXTURE: A REVIEW

Panta Krstić[1], Tijana Majkić[2], Tiana Milović[3], Milan Marinković[4]

Summary:

To improve the mechanical characteristics of the soil, stabilization is carried out with standard binders such as lime and cement. Considering the negative impacts of cement production on the environment, replacing cement with different types of sustainable materials is necessary. A review of the available literature analyzed the possibility of using clinoptilolite as a partial substitute for cement in stabilizing different types of soil. By observing the unconfined compressive strength as the main property that defines the bearing capacity of the soil, it was concluded that the maximum strength values were achieved for a curing period longer than 28 days. With the use of clinoptilolite up to 30% measured by the weight of the binder, there was an increase in the unconfined compressive strength compared to samples stabilized only with cement.

Key words: chemical soil stabilization, natural zeolite, clay, sand, loess

[1]Teaching Assistant, Faculty of Technical Sciences, University of Novi Sad, Serbia, panta.krstic@uns.ac.rs
[2]Teaching Assistant, Faculty of Technical Sciences, University of Novi Sad, Serbia, majkictijana@uns.ac.rs
[3]Research Associate, Faculty of Technical Sciences, University of Novi Sad, Serbia, tiana.milovic@uns.ac.rs
[4]Assistant Professor, Faculty of Technical Sciences, University of Novi Sad, Serbia, milan.marinkovic@uns.ac.rs

1. INTRODUCTION

Low bearing capacity of soil is a severe problem in the construction sector because it can decrease construction stability, causing cracks in buildings and even the collapse of structures. It is mainly enunciated in soft soils or soils prone to wetting and reduced bearing capacity. In order to maintain the safety and reliability of infrastructure projects, it is necessary to take appropriate measures to improve the bearing capacity of the soil.
Cement stabilization of the soil, as one of the most used chemical stabilization methods [1], involves mixing the soil with proper percentages of cement in order to enhance its strength and stability. The natural minerals in the soil react with the cement, creating new mineral bonds that increase the bearing capacity of the soil. This method also reduces the soil's sensitivity to moisture, preventing it from swelling, and increasing strength.
Although soil stabilization with cement is an effective solution, the cement industry has a significant negative impact on the environment, as it is an intensive source of fuel consumption and greenhouse gases (GHGs) emissions. This industry is responsible for 5% of GHGs emissions and is among the top industrial sources of carbon dioxide (CO_2) emissions [2]. Demand for cement will continue with the ongoing trend of urbanization, as it is an active component in concrete, and concrete is the most widely used material by humans, after water [3].
The use of clinoptilolite, one of the most abundant natural zeolites, as a partial substitute for cement in soil stabilization is a sustainable alternative that provides numerous benefits in environmental protection. Clinoptilolite is a natural microporous mineral composed of an open network of silicon-oxygen and aluminium-oxygen tetrahedra which is easily found in nature, meaning its exploitation has a minimal impact on the environment compared to the harmful effects of cement production. In [4], it was shown that natural zeolite contributes to the compressive strength development over time in blended cement mortars as a substitution for ordinary Portland cement.
This paper gives an overview of the available literature on the influence of clinoptilolite as a partial replacement of cement on soil strength. The strength of the stabilized soil was determined on the mixed samples through the Unconfined Compression Strength (UCS) test. The effect of this stabilization on different types of soil, such as sand, clay, loess and road layers, is shown.

2. UNCONFINED COMPRESSION STRENGTH

The UCS test is used in most geotechnical engineering designs, such as design and stability analysis of foundations, retaining walls, slopes, and embankments, as it provides the necessary information on the mechanical behaviour of soil under axial load. It is often applied to saturated, cohesive soils collected from samples obtained from thin-walled sampling tubes. In the reviewed papers, the UCS tests were conducted to determine the efficient and optimum percentages of the zeolite needed to improve the soil strength properties based on *Standard Test Method for UCS of Cohesive Soil* [5].
UCS was evaluated in kilograms per square centimeter or megapascal (MPa) in order to measure the strength of different soil–stabilizer mixtures. All the tests of different soil types, such as sand, clay and loess, mixed with different percentages of cement–zeolite stabilizer were conducted with a standard uniaxial compression testing protocol. The steps of sample preparation for the UCS test are shown in Fig. 1, while the alteration of failure modes of the UCS test specimens with 12% cement and different percentages zeolite after 28 days of curing is shown in Fig. 2. Generally, the zeolite–cement stabilized specimens experienced a significant strength improvement compared to ordinary soil-cement mixture. Most of authors reported that the optimal percentage of cement replacement with zeolite was around 30%. The further increase of zeolite

content in the zeolite-cement stabilizing mixture led to a decrease in UCS, primarily due to the restriction of pozzolanic reaction [6].

Fig. 1 Steps of sample preparation for the UCS test [7]

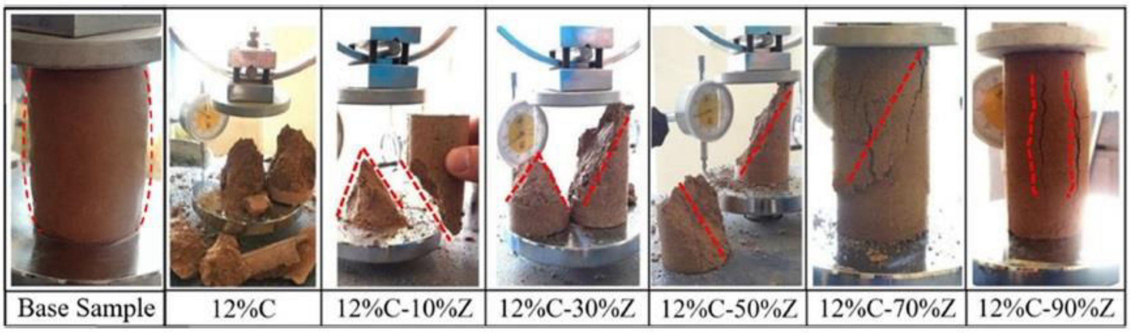

Fig. 2 Alteration of failure modes of the UCS test specimens with 12% cement and different % zeolite after 28 days of curing, for Rc of 98% [7]

2.1. SANDY SOILS

Various studies have been done in order to evaluate the strength parameters of sands stabilized with cement and clinoptilolite, and some of them are summarized in Tab. 1. Problematic soils, such as loose sands, tend to decrease their shear strength when exposed to static or cyclic load, so the primary goal of sand stabilization is to increase the strength parameters of the soil, with the additional benefits of increasing the sulfate resistance and reducing the soil stiffness [6]. Various authors investigated the optimum proportion of clinoptilolite as a cement replacement and the strength increase of sandy soil by conducting a series of UCS tests. Kushawa and Yadav [8] reported a significant increase in UCS values of sandy soil (poorly graded sand – SP by USCS) when stabilized with cement and clinoptilolite mixture. The increase was recorded for all binder contents, from 4 to 10%, for the optimum cement replacement with zeolite (30% by cement mass). The UCS improvements varied from 16 to 33% compared to cement-only stabilized samples. The brittle behaviour of cemented sand was also reduced by adding natural clinoptilolite. The optimum zeolite proportion of 30% for the cement replacement in the cement-zeolite stabilization was also obtained in a 2016 research [9] when stabilizing poorly graded sand (SP) with different binder contents. The strength improvement with clinoptilolite was 20-78% for 28 days of sample curing time. By observing the strength parameters for a 7 day curing period, a decrease in the UCS was recorded, so the authors emphasized the curing time of 28 days and more as appropriate for the development of the pozzolanic reaction and subsoil improvement. When comparing soil samples with different relative densities, it was noticeable that the zeolite impact and effectiveness were higher for less compacted samples and samples with greater cement content. The UCS values expectedly dropped when increasing the compacted samples porosity, with the UCS loss rate higher for cemented soils. A group of researchers confirmed strength improvements by adding clinoptilolite [10], in a cement and sand mixture with a slightly higher optimum percentage of natural zeolite. In this research, the sand samples experienced the greatest UCS improvements when replacing cement with zeolite in an optimum proportion of 40%, so the recorded UCS increase was from 128 to 209% when considering the 14 and 28 days sample curing times. The increase of the clinoptilolite rate was once again proven to reduce the brittle behaviour of the cemented soil samples.

Tab. 1 UCS of sandy soils stabilized with cement and clinoptilolite mixture

Reference& Standard	Cement content (%)	Cement type	Zeolite content (%)	Referent cement UCS (MPa)	Zeolite-cement UCS (MPa)
Kushawa U., Yadav R.K. 2018 [8] IS 2720: Part10 1991	4	CEM I	10, 20, 30	0.44	0.45-0.51 (7d)
	6			1.09	1.14-1.36 (7d)
	8			1.83	1.87-2.34 (7d)
	10			2.27	2.38-3.01 (7d)
Mola–Abasi H. et al. 2016 [9] (Results obtained with the 50% relative density) ASTM D2166 2000	2	CEM II	10, 30	cca 0.06	cca 0.05-0.04 (7d)
				cca 0.15	cca 0.18-0.24(28d)
	4			cca 0.16	cca 0.13-0.09 (7d)
				cca 0.38	cca 0.48-0.68(28d)
	6			cca 0.35	cca 0.31-0.23 (7d)
				cca 0.85	cca 1.08-1.50(28d)
	8			cca 0.66	cca 0.60-0.42(7d)
				cca 1.30	cca 1.66-2.28(28d)
Mola–Abasi H. et al. 2016 [9] (Results obtained with the 85% relative density) ASTM D2166 2000	2	CEM II	10, 30	cca 0.1	cca 0.09-0.07 (7d)
				cca 0.20	cca 0.22-0.24 (28d)
	4			cca 0.25	cca 0.23-0.18 (7d)
				cca 0.52	cca 0.58-0.68 (28d)
	6			cca 0.59	cca 0.51-0.38 (7d)
				cca 1.17	cca 1.26-1.60 (28d)
	8			cca 1.0	cca 0.90-0.69 (7d)
				cca 1.69	cca 1.83-2.39 (28d)
Salamatpoor S. et al. 2018 [10] ASTM D2166 2006	3	CEM II	20, 40	cca 0.15	cca 0.13-0.09 (7d)
				cca 0.52	cca 0.57-0.67(28d)
	7			cca 0.60	cca 0.52-0.38 (7d)
				cca 1.10	cca 1.48-2.29 (28d)

2.2. CLAYEY SOILS

Expansive clayey soils are one of the most problematic for facility construction due to their small particle size and high specific surface area, leading to a high potential for soil volume change and low bearing capacity [11]. The swelling of expansive soil, due to the water saturation and volume expansion of the soil, can severely damage the structures built on it unless soil stabilizes first. The effect of cement and clinoptilolite mixture for stabilizing expansive soils was investigated by Chenarboni et al. [7] for clays with high expansion potential. Samples of expansive clay (CH by USCS) were mixed with different proportions of cement and clinoptilolite additives to determine the optimum percentage of clinoptilolite for improving the soil UCS. The maximum in UCS was evaluated for samples with 12% of cement replaced with 30% of natural clinoptilolite, while the further increment of clinoptilolite led to the UCS decrease. By observing the relative compaction of the samples, it was concluded that the reduction in relative compaction from 98 to 95% leads to a decrease in strength. Zeolite addition reduced the brittleness of the clayey soil, as with sand samples mentioned before. Alhaji et al. [12] compared the UCS values of cemented clay and clay stabilized with the mixture of cement and zeolite in different proportions. A significant increase in strength was recorded, especially when comparing unstabilized with stabilized specimens. The maximum UCS values were obtained when adding 6% of clinoptilolite and 6% of cement to the soil dry unit weight for the curing time of 60 days, increasing the original clay strength by 3.68 times. Basic data and obtained results are presented in Tab. 2.

Tab. 2 UCS of clayey soils stabilized with cement and clinoptilolite mixture

Reference& Standard	Cement content (%)	Cement type	Zeolite content (%)	Referent cement UCS (MPa)	Zeolite-cement UCS (MPa)
Alhaji M. M. et al. 2021 [12] BS 1924 1992	2	Portland cement	3 and 6% out of dry unit weight	cca 0.21	cca 0.37-0.40 (7d)
				cca 0.24	cca 0.40-0.43 (28d)
	4			cca 0.51	cca 0.64-0.70 (7d)
				cca 0.61	cca 0.77-0.97 (28d)
	6			cca 1.04	cca 1.10-1.29 (7d)
				cca 1.30	cca 1.34-1.39 (28d)
Chenarboni H.A. et al. 2021 [7] (For relative compaction of 95%) ASTM D2166 2016	6	CEM II	10, 30	cca 1.93	cca 2.18-2.44 (28d)
	8			cca 2.29	cca 2.64-2.86 (28d)
	10			cca 2.81	cca 3.07-3.37 (28d)
	12			cca 3.40	cca 3.61-3.93 (28d)
Chenarboni H.A. et al. 2021 [7] (For relative compaction of 98%) ASTM D2166 2016	6	CEM II	10, 30	cca 2.26	cca 2.54-2.78(28d)
	8			cca 2.61	cca 3.00-3.14 (28d)
	10			cca 3.27	cca 3.39-3.75 (28d)
	12			cca 3.69	cca 4.06-4.38 (28d)

2.3. LOESS SOIL

Loess is a specific type of sedimentary soil with an eolian origin, made of silt-sized particles containing clay and sand. Loess soil can be hazardous when saturated due to its high porosity, weak structure and sensitivity to moisture content [13]. Stabilizing loess soil is one of the solutions to improve its stability and strength. Adding cement, clinoptilolite, and recycled polyester fiber (PET) to loess soil samples significantly improved UCS values [14]. By evaluating the UCS of loess soil samples (CL by USCS) mixed with different percentages of cement (4 and 8% of dry unit weight) and different zeolite percentages as partial cement replacement, it was concluded that the optimum zeolite contents were 10 and 30% for 4 and 8% of total binder weight, respectively. Further increment of zeolite content led to a downward trend. The addition of PET to the zeolite-cement-loess mixture increased the UCS and caused an increase in failure strain which can effectively overcome the brittle nature of cemented loess. The effect of curing time on the UCS was significant at optimal clinoptilolite content. With the increment of the optimum water content up to 1.2 times, the increase of the strength of loess soil samples was recorded, while any further water addition resulted in the UCS decrease.

2.4. ROAD LAYERS

Stabilizing road pavements represents improving the strength parameters of pavement layer materials, which can deteriorate due to heavy traffic load or lack of quality. Various pavement layer stabilization methods imply using different natural or artificial materials with pozzolanic properties to stabilize road base, subbase, or subgrade layers [15]. A study conducted by Sheikh et al. [16] investigated the possibility of applying the natural clinoptilolite instead of cement in different proportions for stabilization of the road base layers, soil classified as gradation D by AASHTO M147 standard. Materials used in the mentioned study are shown in Fig. 3. The most significant improvement of the UCS was achieved for an optimum zeolite content of 30%, with the samples containing clinoptilolite having lower UCS than the ones containing only cement after 7 days of curing time. It was concluded that zeolite as a material was not expected to improve the UCS of the base layer in a short period. In most cases, the samples containing both clinoptilolite and cement had higher strength than soils stabilized only with cement for 28 days of curing time.

Fig. 3 Consumable materials for road base layer stabilization – aggregate (left), clionoptilolite (center) and cement (right) [16]

3. CONCLUSION

By observing different types of soils, different percentages of clinoptilolite as a cement substitute, the UCS development and curing time of soil specimens, the following conclusions can be summarized:

- Using optimum clinoptilolite percentage as a replacement of cement improves bearing capacity for all types of considered soils.
- The optimum cement with clinoptilolite replacement percentage is around 30%.

- Further increase of clinoptilolite above optimum percentage leads to a decrease of the UCS values.
- The optimum curing time for the development of the UCS increase by adding clinoptilolite is 28 days or more.
- Partial substitution of cement with clinoptilolite reduces the brittle behaviour of the stabilized sandy and clayey soils.
- Regarding sandy soils, clinoptilolite impact and effectiveness are higher for less compacted samples.
- When stabilizing loess soils with a mixture of cement and clinoptilolite, increasing the optimum water content up to 1.2 times results in a UCS enhancement.

Considering the above facts and environmental sustainability, cost-effectiveness and reduced energy consumption, clinoptilolite is a good alternative to ordinary binder such as cement for soil stabilization as its partial replacement.

ACKNOWLEDGEMENT

This paper has been supported by the Ministry of Science, Technological Development and Innovation through project no. 451-03-47/2023-01/200156 "Innovative scientific and artistic research from the FTS domain".

REFERENCES

[1] IRC:SP:89 (2010). Guidelines for Soil and Granular Material Stabilization Using Cement, Lime and Fly Ash, Indian Road Congress, New Delhi.

[2] Benhelal E., Shamsaei E., Rashid M.I. (2021). Challenges against CO_2 abatement strategies in cement industry: A review. *Journal of Environmental Sciences*, Volume 104, pp. 84-101. https://doi.org/10.1016/j.jes.2020.11.020.

[3] https://carbonre.com/three-technologies-to-reduce-climate-change/ Website accessed: 16.07.2023.

[4] Milović, T., Šupić, S., Malešev, M., Radonjanin, V. (2022). The Effects of Natural Zeolite as Fly Ash Alternative on Frost Resistance and Shrinkage of Blended Cement Mortars, Sustainability, Vol. 14, 2736.

[5] ASTM D2166 (2016). Standard Test Method for Unconfined Compressive Strength of Cohesive Soil, ASTM Int..

[6] Salamatpoor, S., Jafarian, Y., Hajiannia, A. (2018). Physical and mechanical properties of sand stabilized by cement and natural zeolite, The European Physical Journal Plus, Vol. 133.

[7] Chanarboni, H.A., Lajevardi, S.H., MolaAbasi, H., Zeighami, E. (2022). The effect of zeolite and cement stabilization on the mechanical behavior of expansive soils, Construction and Building Materials.

[8] Kushawa, U., Yadav, R.K. (2018). Effect of Zeolite and Cement Addition on Properties of Granular Soil, International Journal for Research in Applied Science & Engineering Technology, Vol. 6, No. 6, pp. 783-788.

[9] Mola-Abasi, H., Kordtabar, B., Kordnaeij, A. (2016). Effect of Natural Zeolite and Cement Additive on the Strength of Sand, Geotechnical and Geological Engineering, Vol. 34, No. pp. 1539-1551.

[10] Salamatpoor, S., Jafarian, Y., Hajiannia, A.: Physical and mechanical properties of sand stabilized by cement and natural zeolite, The European Physical Journal Plus, Vol. 133, 2018.

[11] Vorwerk, S., Cameron, D., Keppel, G. (2015). Clay soil in suburban environments: Movement and stabilization through vegetation. In Indraratna B., Chu J., Rujikiatkamjorn C.(Eds.), *Ground improvement case histories*, Butterworth-Heinemann, pp. 655–682, https://doi.org/10.1016/B978-0-08-100191-2.00022-8

[12] Alhaji, M. M., Alhassan, M., Adejumo, T. W., Luka, M. H., Abdulkadir, H. (2021). Microstructural and Strength Characteristics of Cement Treated Clay Stabilized with Zeolite for Road Base Application, IOP Conf. Series: Earth and Environmental Science, Iraq, 856.

[13] Delage, P., Cui, Y., & Antoine, P. (2006). Geotechnical problems related with loess deposits in Northern France. *Proceedings of International Conference on Problematic Soils*

[14] Mariri, M., Moayed, R.Z., Kordnaeij, A. (2019). Stress–Strain Behavior of Loess Soil Stabilized with Cement, Zeolite, and Recycled Polyester Fiber, Journal of Materials in Civil Engineering.

[15] Kamal, I., & Bas, Y. (2021). Materials and technologies in road pavements - an overview. *Materials Today: Proceedings*, *42*, 2660-2667. https://doi.org/10.1016/j.matpr.2020.12.643

[16] Sheikh, A., Akbari M., Shafabakhsh, G. (2022). Laboratory Study of the Effect of Zeolite and Cement Compound on the Unconfined Compressive Strength of a Stabilized Base Layer of Road Pavement, Materials, Vol. 15, No. 7981.

WATER VAPOR PERMEABILITY OF MASONRY MORTAR BLENDED WITH A HIGH SHARE OF WASTE MATERIALS

Vladan Pantić[1], Slobodan Šupić[2], Ivan Lukić[3]

Summary:

The use of waste materials as a cement substitute in the production of masonry mortar is becoming an increasingly common practice, aiming to achieve economic and environmental benefits. Diffusion of water vapor through the elements of the thermal envelope of buildings is a significant phenomenon in construction, which can have serious consequences on the quality of buildings. Therefore, choosing the right materials from the perspective of water vapor permeability is crucial for maintaining the caliber of building structures. The goal of this study is to examine the evolution of the water vapor diffusion resistance factor in masonry mortars that contain a significant amount of locally accessible waste materials, specifically fly ash (FA), corn cob ash (CCA) and ceramic waste powder (CWP), with a 50% volume replacement ratio of cement (OPC). The findings demonstrate that the blended masonry mortars have comparable values of the water vapor diffusion resistance factor with the reference cement-lime masonry mortar.

Key words: water vapor permeability, masonry mortar, biomass ash, fly ash, waste

[1] Teach. assist., Faculty of Technical Sciences, University of Novi Sad, Serbia, pantic_vladan @uns.ac.rs
[2] Assis. prof., Faculty of Technical Sciences, University of Novi Sad, Serbia, ssupic@uns.ac.rs
[3] Assoc. prof., Faculty of Technical Sciences, University of Novi Sad, Serbia, lookic@uns.ac.rs

1. INTRODUCTION

Industrial and agricultural waste materials, such as harvest residues ashes and ceramic waste, could be viable supplementary cementitious materials (SCMs), particularly in terms of sustainable development [1][2]. However, the effects of using various SCMs as a binder replacement in masonry mortars have not been thoroughly examined yet. The ceramic waste powder as a pozzolanic material has only been briefly studied, while there is no published research on the cement-lime ma-sonry mortar incorporating corn cob ash as a SCM. Such research is especially impactful for geographical regions around the world that are subjected to anthropogenic pollution. In this study, the authors evaluated the influence of locally sourced agricultural and industrial wastes: corn cob ash (CCA), fly ash (FA) and ceramic waste powder (CWP) on water vapor permeability of masonry mortar. Furthermore, characterization of selected SCMs was performed, which comprised all essential chemical, physical, mechanical, and pozzolanic tests.

2. MATERIALS AND METHODS

2.1. MATERIALS

The material used was Ordinary Portland Cement (OPC), produced by the Lafarge cement plant in Vojvodina. The cement is characterized by a density of 3.1 g/cm^3 and the Blaine fineness of 4.000 cm^2/g.
Fly ash, corn cob ash, and ceramic waste powder were used as cement replacement materials in the cement-lime masonry mortars.
Fly ash was provided by the thermal power plant Nikola Tesla B in Obrenovac, Serbia.
Corn cob ash was collected from ALMEX-IPOK in Zrenjanin, Serbia. To obtain a material with a satisfactory level of fineness, the collected ash sample was ground in a laboratory ball mill.
The ceramic waste powder was produced from ceramic manufacturing waste, consisting of damaged clay hollow blocks discarded in the production facility NEXE - Stražilovo in Petrovaradin, Serbia. These elements were firstly roughly crashed and, then, finely ground in a lab ball mill up to the appropriate level of fineness.
The appearance of the collected samples of SCMs is shown in Fig. 1.

(a) (b) *(c)*

Fig. 1 (a) Corn cob ash, (b) Fly ash, (c) Ceramic waste powder

The river sand was used as fine aggregate for mortar production. Its specific gravity and fineness modulus were determined to be 2.3 g/cm^3 and 0.97, respectively.
Tap water was used for producing masonry mortar. The water-to-binder ratio (w/b) was adjusted in order to achieve the required workability of masonry mortar (175±10 mm), as advised by SRPS EN 1015-2:2008.

2.2. METHODS

The chemical composition of raw materials was assessed according to SRPS EN 196-2:2015 and ISO 29581-2:2010.

The water vapor permeability of hardened masonry mortars was determined using SRPS EN 1015-19 [3]. Mortar was cast in cylindrical moulds, with a diameter of 175mm and thickness of 30mm, placed on an autoclaved aerated concrete base covered with two layers of cotton gaze. Specimens were cured in the storage chamber at a relative humidity of 95% ± 5% and a temperature of 20°C ± 2°C. After 5 days, mortar specimens were detached from the substrate and stored at a temperature of 20°C ± 2°C and a relative humidity of 50% ± 5% for the remaining 28 days of total curing. Prepared specimens were measured and placed in test cups with a saturated solution of potassium nitrate (KNO_3) to generate a high indoor humidity (>90%) – wet cup method. The volume of the solution was determined so that the specimens were separated from it by approx. 1cm. Specimens edges were sealed to cups with appropriate sealant and stored at a temperature of 20°C ± 2°C and a relative humidity of 50% ± 5%. The weight of the cups was measured on a daily basis, and a graph of the mass of the cups against time was drawn until the flow stabilized (i.e., three consecutive measurements on a straight line). The following equation was used to compute water vapor permeability (Wvp) and a diffusion resistance factor (μ):

$$\mathrm{W}_{vp} = \frac{\mathrm{d}}{A \cdot \Delta_p/(\Delta G/\Delta t) - R_A} \; (kg/m \cdot s \cdot Pa) \tag{1}$$

$$\mu = \frac{\mathrm{W}_{vp,air}}{\mathrm{W}_{vp}} \tag{2}$$

where d, A and ΔG are sample thickness, area and mass change; Δt is the time interval; Δp is the water vapor pressure difference between a saturated solution and samples storing chamber and R_A is the resistance to water vapor diffusion in the air between the sample and the KNO_3 saturated solution ($0.048 \cdot 10^9$ Pa·m^2·s/kg, for 10 mm of interspace); $W_{vp,air}$ is air permeability ($1.94 \cdot 10^{-10}$ kg/(Pa·m·s)) in test conditions (20 °C and 50% relative humidity).

2.3. MIXING AND PROPORTIONING OF MORTARS

Four different mortar mixtures were cast in the experimental study. The volume mixing ratio of components of reference cement-lime mortar was 1:1:5 (cement/lime/sand). In the remaining three mixtures, 50% of cement was replaced by FA, CCA, or CWP, by volume. Based on the designed workability, the appropriate amount of water was determined. Tab. 1. shows the labels and quantities of component materials for each masonry mortar.

Tab. 1 Labels and component material quantities for designed masonry mortars

Mortar	m_c (g)	m_l (g)	m_s (g)	m_{scm} (g)	w/b	m_w (g)
C	161.4	74	1350	/	1.15	270.7
FA-50	80.7	74	1350	49.6	1.35	275.9
CCA-50	80.7	74	1350	57.3	1.30	275.6
CWP-50	80.7	74	1350	61.8	1.30	281.5

m_c—mass of cement; m_l—mass of lime; m_s—mass of sand; m_{scm}—mass of SCM; w/b–water to binder; ratio; m_w—mass of water.

3. TEST RESULTS AND DISCUSSION

3.1. MATERIAL CHARACTERIZATION

3.1.1. Chemical Analyses of Cementitious Materials

The main oxides of FA and CWP are SiO_2 and Al_2O_3, which together account for more than 75% weight of all oxides. The Tab. 2. also demonstrates how abundant Fe_2O_3 is in these materials, accounting for up to 80% weight of the oxides in their chemical compositions. CCA primarily consists of 45.76% of silica and then of CaO and K_2O. The estimated total alkali content of CCA (Na_2O + 0.658 K_2O) is 8.62%, which is higher than the permitted value of 5% outlined in SRPS EN 450-1:2014. Hence, the detrimental effects of potential alkali-silica reaction (ASR) should be taken into consideration while analyzing the durability aspects of mortars blended with this material. [4]. The results of testing the chemical composition of SCMs are summarized in Tab. 2.

Tab. 2 Chemical compositions of SCMs

	FA	CCA	CWP
Loss of ignition at 950 °C	1.50	2.40	3.3
SiO_2, %	53.64	45.76	60.86
Al_2O_3, %	25.74	5.91	16.38
Fe_2O_3, %	7.36	3.37	6.81
Na_2O, %	0.30	0.00	0.77
K_2O, %	1.48	13.10	2.39
MgO, %	3.09	8.30	3.89
CaO, %	7.15	14.08	9.38
SO_3, %	2.75	1.26	0.80
P_2O_5, %	0.06	2.81	0.14
Content Cl-, %	<0.01	0.50	0.002
Reactive SiO_2, %	48.16	38.21	50.26

3.1.2. Physical Properties of Cementitious Materials

In comparison to cement, SCMs have a slightly higher specific surface area, which may be advantageous in terms of their reactivity and packing capacity. All investigated materials showed positive pozzolanicity due to enough amorphous silica concentration and a good level of fineness, although FA and CWP had Class 10 pozzolanic activity while CCA had Class 5 pozzolanic activity.

The FA and CWP samples complied with the activity index requirements, while CCA not only satisfied the standards but also obtained compressive strength greater than that of the reference cement sample. This is likely caused by the mortar mix's improved compactness, which was combined with finer biomass ash particles.

All tested materials met the other physical properties-requirements from the applicable standards, as indicated in Tab. 3.

Tab. 3. Physical properties of SCMs.

	Criteria	**Standard**	FA	CCA	CWP
Specific gravity (g/cm^3)	/	SRPS EN 196-6:2019	2.046	2.494	2.633
Specific surface area (cm^2/g)	/	SRPS EN 196-6:2019	6159	6834	4809
Fineness (%)	≤12 % (S) ≤40 % (N)	SRPS EN 933-10:2009 SRPS EN 450-1:2014	0.80 Category S	1.6 Category S	3.30 Category S
Pozzolanic activity	Class 5 $f_{cs} \geq 5$ MPa $f_{fl} \geq 2$ MPa Class 10 $f_{cs} \geq 10$ MPa $f_{fl} \geq 3$ MPa	SRPS B.C1.018:2015	Class 10	Class 5	Class 10
Activity index	$AI_{28} \geq 75$ % $AI_{90} \geq 85$ %	SRPS EN 450-1:2014	$AI_{28} = 96$ % $AI_{90} = 99$ %	$AI_{28} = 101$ % $AI_{90} = 103$ %	$AI_{28} = 93$ % $AI_{90} = 99$ %
Initial setting time (min)	≥60	SRPS EN 196-3:2017 SRPS EN 197-1:2013 SRPS EN 450-1:2014	245	270	155
Final setting time (min)	≤2 times the setting of the test cement alone	SRPS EN 196-3:2017 SRPS EN 197-1:2013 SRPS EN 450-1:2014	330≤ 2 x 210	395≤ 2 x 210	235≤ 2 x 210
Soundness (mm)	≤10	SRPS EN 196-3:2017 SRPS EN 450-1:2014	0.2	0.4	0.2

3.2. WATER VAPOR PERMEABILITY

In order to control moisture and avoid problems like condensation, mold growth, and damage to building materials, mortars' property to diffuse water vapor is crucial in the construction industry. Water vapor permeability factor was determined as an average value of three measurements, using the wet cup method, as illustrated in Fig. 2.

Fig. 2. Appearance of the tested samples

The results for water vapor permeability and water vapor resistance factor are shown in Tab. 4.

Tab. 4. Water vapor permeability (Wvp) and water vapor resistance factor (μ).

Mortar	Water vapor permeability		Water vapor resistance factor	
	Wvp (kg/m·s·Pa)	ΔWvp (%)	μ	Δμ (%)
C	5.37·10-11 ± 3.48·10-12	0.00	3.63 ± 0.236	0
FA-50	4.05·10-11 ± 3.29·10-12	-24.53	4.82 ± 0.370	32.77
CCA-50	4.88·10-11 ± 3.55·10-12	-9.22	4.00 ± 0.291	10.28
CWP-50	4.36·10-11 ± 2.40·10-12	-18.85	4.46 ± 0.236	23.07

All mortar has a water vapor resistance value that falls between 3.4 and 5.2. For general-purpose masonry mortars, SRPS EN 998-1:2017 does not specify limit values, whereas EN 12524:2000 recommends a value of 6 for water vapor resistance for masonry mortars evaluated using the wet cup method.
The results of monitoring the change in cup weight on a daily basis are displayed in the following graphs (Fig. 3). As previously noted, the measurements were taken until the flow stabilized (i.e., three consecutive measurements on a straight line), as indicated in the right section of each graph.

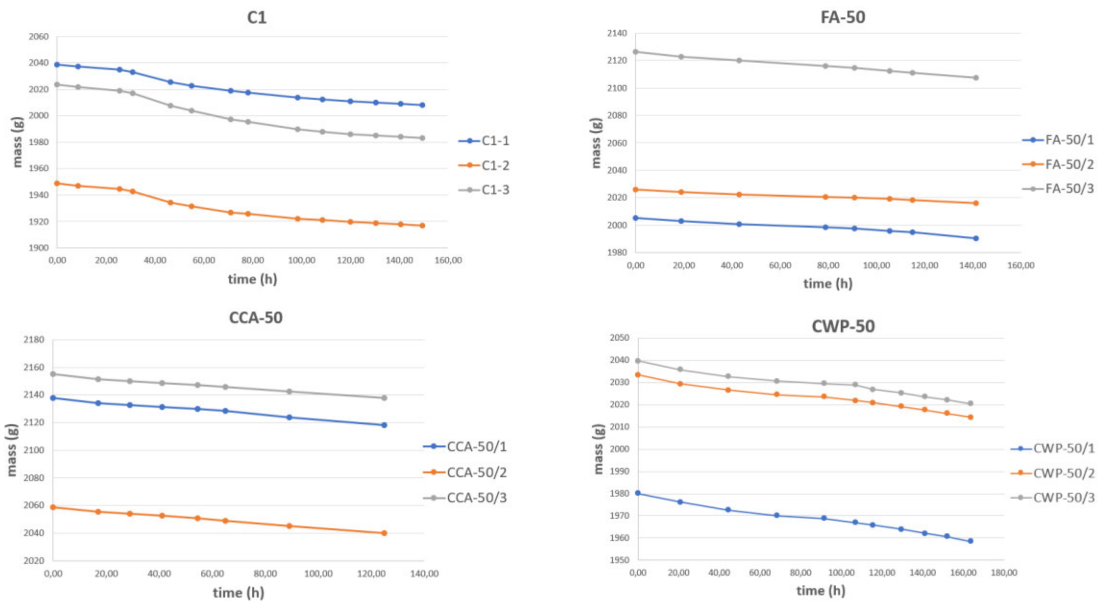

Fig. 3. Changes in cups weight with time

4. CONCLUSIONS

The study's main conclusions are as follows:

- As a result of an effective grinding procedure, the specific surface area of all tested SCMs is slightly higher than that of cement, which could be beneficial from the aspect of their reactivity and packing capacity, i.e., filler effect.
- Fly ash and ceramic waste powder met the criteria for pozzolanic class 10, while corn cob ash reached the class 5 of pozzolanicity.
- The fly ash and ceramic waste powder samples met the activity index requirements, whereas the corn cob ash sample not only met requirements but also had compressive strength greater than the reference cement sample.
- The results reveal that blended masonry mortars produced have water vapor diffusion resistance factor values comparable to the reference cement-lime specimen, regardless of the SCM type. Hence, it can be stated that the substitution

of cement with the specified waste materials, does not jeopardize this property of the mortar.

ACKNOWLEDGEMENT

The research has been conducted within the project "Scientific theoretical and experimental research and improvement of educational process in the field of civil engineering", developed at the Department of Civil Engineering and Geodesy, Faculty of Technical Sciences, University of Novi Sad, Serbia.

REFERENCES

[1] Pantić V., Šupić S., Vučinić-Vasić M., Nemeš T., Malešev M., Lukić I., Radonjanin V. (2023). Effects of Grinding Methods and Water-to-Binder Ratio on the Properties of Cement Mortars Blended with Biomass Ash and Ceramic Powder. Materials , Volume 16.

[2] Nayak D.K.N., Abhilash P.P., Singh R., Kumar R., Kumar V. (2022). Fly ash for sustainable construction: A review of fly ash concrete and its beneficial use case studies. Cleaner materials, Volume 6.

[3] SRPS EN 1015-19. *Methods of test for mortar for masonry*; Part 19. Determination of water vapor permeability of hardened rendering and plastering mortars. Institute for Standardization of Serbia; 2008.

[4] Šupić S., Malešev M., Radonjanin V., Pantić V., Lukić I., Bulatović V. (2022). Characterization of harvest residues ashes and ceramic waste powders originating from Vojvodina as potential supplementary cementitious materials. Building Materials and Structures, Volume 65(4), pp. 155-166.

CONTEMPORARY TREND IN HIGH EDUCATION: HOW, WHY AND HOW MUCH?

Dušan Kovačević[1], Leposava Grubić Nešić[2]

Summary:

It is analyzed one not so new tendency in studying, which unfortunately becomes a "bad trend" and "anti-development concept" in all educational areas and especially on engineering faculties. This is not something dictated "from above" or "from out", but personal and/or collective choice which is consequence of "not very common sense decision" to go on "the path of low resistance". While new times need different view on intellectual, ethical, emotional and social aspects of studying, some "old fashion" and commonly accepted "educationally aided" good traditions are still preferable. This will be illustrated by description and analysis of studying and teaching experience from the any level of studies on two departments of Faculty of Technical Sciences, University of Novi Sad, with principal goal to increasing of interest for technical studies, because technical development is base of general development.

Key words: high education, new "strategy", traditional studying

[1] Prof. Ph.D., Department for Civil Engineering and Geodesy, Faculty of Technical Sciences, University of Novi Sad, Serbia, dusan@uns.ac.rs
[2] Prof. Ph.D., Department of Industrial Engineering and Engineering Management, Faculty of Technical Sciences, University of Novi Sad, Serbia, nesle@uns.ac.rs

1. INTRODUCTION

Global changes in the concept of education contributed to the idea for the creation of this paper. Usual attitudes about "needed knowledge" and therefore "good education" were changed in the direction of a rational and pragmatic approach, but with a strong effort to emphasize the essence of the studied phenomena. A significant result of these changes are the great possibilities of increasing the efficiency of acquiring real knowledge, during the "full life self-studying", which was contributed, above all, by the development in the sphere of information technologies. The availability of these possibilities has enabled the acquisition of knowledge to be focused on primary and essential aspects for analysis and solving of engineering problems.

Previous are the positive circumstances, but what are "relicts"? The current education in the engineering field is slightly overloaded by contents and forms that are unnecessary and sometimes hide the essence of engineering application. Explanation is the fact that those who impose only a theoretical approach are not engineers, but only trainers, educators and/or professors. This circumstance is particularly pronounced in well-established university environments. The principal idea of our intentions is increasing of attractiveness of engineering studies in universities on small countries, through innovative, entrepreneurial and soft-skill oriented educational concept, according to principles of European Higher Education Area (EHEA).

Goal of the proposed ideas are reasonable changes in the education concept, which will be the base of a new professional profile of a graduated engineer: with enthusiasm and advanced competencies. In that sense we plan to formulate a design of "New kind of engineer" - oriented towards resolving a wide area of technical and non-technical problems that feature today's social environment. As a positive consequence we will achieve a "New status of engineer's profession" - status of a dedicated with increased motivation and effectiveness for impact on a wide range of matters, [5].

In the sense of previous, we need some kind of innovative concept of teaching and, especially, examination of the students' knowledge for their real understanding of the principles of functioning of engineering systems. "Old fashion" learning, oriented to the "encyclopedia knowledge", by adoption of "each problem by a different method" strategy, possibly provide wider "quiz-like information" and contributes to some of "technical culture", but it ruins enthusiasm of students in reaching of so-called "functional knowledge". "Functional knowledge" is not only ability of practical use of studying results, but capacity to establishing of new knowledge by self-studying. In that sense, one of possible definition of intelligence is "the wish and possibility of obtaining of new knowledge by studying". Here is important to make difference between "high school learning" and "college studying" and avoid continuation of "high school in faculty building".

According to these facts, teaching and studying focused to a few dominant principles and methods give the results that establish the most competent kind of the engineering education. In this way, we make not only "scholarly graduated student", but also real and functional graduated engineer.

Consequently, the implementation of education's quality decides how much the advantages of this concept will be recognized as successful and used.

In connection to this, arises the problem of phases or parts of educational process concept. In addition to highly solid knowledge in the primary profession, also is needed:

- basic knowledge in boundary technical fields (other technical sciences, dedicated and general purpose software technology and quality evaluation),
- certain knowledge in engineering knowledge distribution (sense for human resources management, marketing and public relations) and

- high level of knowledge in personal engineering orientation (obtained during technical, scientific, educational, management and other references and experience).

2. CURRENT CIRCUMSTANCES OF STUDYING OF ENGINEERING

State of high education depends primarily on studying possibilities, students, education curriculums and finally - on teaching staff.

We all agree that current studying possibilities for obtaining of functional knowledge, professional competence and expert level of proficiency are undoubted and almost without limits in comparison with "good old times". Opposite to mentioned times, when students have to been in more or less equipped and dedicated libraries during 24/7 period, today all of us enjoy plenty of data, information, papers, books, learning aids in electronic form in the global environment. Plenty of information is an advantage if person will and maybe disadvantage if person must. In that sense, here we have old proverb: "the one who wants is much better than any three which must".

Students are very significant factor in the success of high education system because of their intellectual, ethical and emotional performances and because reason given in above proverb. Their possible solid intellectual potential maybe cannot be expressed and used if their willpower and motivation features are modest. Questions are: why this is often situation and what are the reasons for it?

Curriculums and teaching programs are made by teaching staff what is better situation than case typical for high school education, when state (by elected experts or "not quite experts") offers and order unique teaching programs for all schools on that level of education. Unfortunately, this better situation of freedom is not enough used for preparation of corresponding curriculums, way of performing the lectures and kind of examination with the goal of check the level of knowledge of students.

It is well known that principal factor for selection of future teaching staff are someone's success of studying, his wish to make academic career as well as human qualities of the person, [2]. Not quite big number of candidates fulfil these conditions and therefore possibilities of wide and good choice are limited. Additional problem is narrative that "only persons with limited professional skills go into universities" but it is only psychological compensation mechanism well known as "sour grapes", because it is well known work in academic environment is intellectual and social privilege, what sometimes isn't case for academic community.

3. ABOUT STUDENTS

One anecdotal example for better understanding essence of our problems… One of author of this paper always ask his students, immediately after start of first lecture, following question - who will achieve higher academic success:

- our domestic students which are relocated on high ranked world universities where professors are well reputable and maybe Nobel prize winners or
- foreign students, from "well developed countries", which are relocated to some our technical faculty by our professors with "only" PhD academic titles?

About 90% answers are - our domestic students will be more successful and explanation is following: our student are much more resourceful, because of harder life conditions in comparison with foreign students, which are "spoiled because they have all in life". Only one or two students in past twenty years point to foreign students as potentially successful, but without wider explanation.

Such attitudes of majority of domestic students point to our state of "measures of virtues". Unfortunately, instead of studying, achievement of functional knowledge, cognition of real knowledge as an intellectual wealth, our girls and (much more) boys favor resourcefulness, as primary virtue. Thereby they overlook that mentioned "well developed countries" were become such, because of only one important thing: their communities highly appreciate "cult of work" and good results of hard work. Let us remember one well-known statement from that world: "… We will do this not because it is easy, but because it is hard…".

There are many reasons for mentioned model of opinion of majority of our students, and only typical will be discussed here. Let us start from social reasons.

One scientific research dedicated to social status of student of technical faculties given results, which point to the following fact: the most successful high school scholars do not select technical faculties and these professions as a life choice. These young, which are, by the way, from the families of higher middle or high class, select other - mainly medicine, stomatology, law, economy or something from field of so-called social or humanities sciences. As an exception, their reason for choice of some technical studies is consequence of engineering professions of some family members. Young from the families of low or lower middle class go mainly into technical or related faculties, with only two exceptions: architecture and IT. Things are changing, but insufficiently to become new trend. For better progress in this direction, it is necessary to convince students that faculty studying is not only duty, but also social privilege, what is unreachable for many others.

Despite the risk that authors could be misunderstood, it must be emphasized that low level of real success in high schools and allied low level of the so-called "common knowledge and education" are in the relatively modest average life conditions which are characteristic of so-called "transitional communities". Young from "low- and middle class" families, faced with these conditions, take care on existential abilities before personal improvements in educational and cultural manner. Fortunately, some of them realize some technical skills (civil and mechanical engineering, architecture, IT) in addition with school education, what could be useful advantage on technical studies. Additional problem is different level of real and functional knowledge reached in general oriented high schools (gymnasiums) vs. vocational high schools, as well as high schools in urban or not so urban environments, primarily because of different quantity/quality of presented knowledge and different criterion on estimation of educational success.

The first thing our students face is a more liberal viewpoint towards attending lectures, after relatively strict regime in high schools. It is actual for both students and teaching staff, what is almost unthinkable in case of expensive studying fees in some countries. It must to emphasize that active attendance on lectures are needed condition for successful studying. Even the physical presence, only because of check and some undersign by professor, on the end of semester, is more useful than total or partial absence. Student's active attendance on lectures comprehends two phases what make possible much more efficiency in a preparation for examination:

- overview of the teaching material before corresponding lectures and
- interactive and cooperative participation in lectures through free dialog with lecturer by asking for possible unclear details or imprecisely explained or described items of a some topic.

Previously mentioned things are sometimes disgraceful ridiculed by bad average students as "nerd or chair warmer activities" which prefer well-known "preparation five minutes to twelve". This wrong approach is fully compatible with attendance on lectures in following manner (see Fig 1):

- the student is only physically present or even completely absent from lecture in combination with mentioned "campaign preparation" of the examination or
- the student is mentally present on lecture with a solid "following" of the content, but with significant neglect of previously acquired knowledge, which gives results only in subjects that do not request of so-called "synthesis knowledge".

Fig. 1 Active, semi-active and sleeping attendance on lectures

Students incorrectly prefer teaching exercises (performed by assistants) in comparison with lectures (by professors) because exercises are "more useful" for basic preparation of practical part of examination, while main lectures are only presentation of "some boring theoretical aspects and philosophy of profession".

Next important factor is a question of use of literature and other sources for acquisition of real and functional knowledge. It is zone where we are challenged by basic misunderstanding of studying vs. ordinary school learning. Namely, majority of students treat studying as following of high school in another building. In that sense, students unfortunately and pragmatically wish books with clearly defined examination questions together with answers, [1]. Unfortunately, exceptionally respected books by students are wrote in this manner, although those are almost useless for serious studying.

As an illustration of wrong approach of students, an algorithm for pass of the examination will be presented:

- Most often, the examination, colloquium and/or test is prepared "partially", by learning a smaller part of the material, trusting on some probability of a "lucky" outcome.
- In the case of fail, attempts in the following examination periods are based on "calculation": it is better to invest a little additional effort by learning another small part of the material in each following examination period, at the cost of multiple failures, than a reasonably greater effort, with great efficiency of passing in only one examination period.
- In the case of a large number of failures, often go to pressure methods (special requests to dean or vice deans, petitions, student's survey abuse, contact to media and similar) or to the use of illegal means (false representation of knowledge, misleading of teaching staff, use of forbidden things, etc.),
- Most rare case is to go for the proven "learn well - surely pass" approach, where the basic "disadvantage" is the slightly greater required intellectual effort and perseverance.

4. ABOUT TEACHING STAFF AND TEACHING PROGRAMES

Key thing and keyword here is **demystification**. Totally unacceptable and ridiculous is to glorify teaching staff as "They which arrived from Olympus", but as people which are experts in their professions and goodwill colleagues with excellent, and the best in branch, theoretical knowledge what will be transfer to all students. The best results in teaching and making of future engineers will be achieved by teaching staff, which made engineers from himself. In that sense, geeks produce only geeks. Even the excellent geeks are only geeks. In other professions it is maybe acceptable, but not in engineering. Geeks are excellent only for routine purposes, but for development, real engineer is necessary.

First toward importance is professor's approach in lectures and examination concept.

Lectures must be informative, without insignificant details, educative even in language sense (because our students have evident problems with speak communication) and enough interesting, stimulating to discussion, inspiring for personal efforts and even passionate, all according to real situation on possibilities for occupying the attention of young generations of students. In that sense, it could be appropriately to introduce some tricks which "shortening" the time of school class. Sens for humor is important for this purpose and "deadly serious class" are not preferable, unless boredom is some exalted sign of the great level. This kind of "false serious approach" as well as rigidity are the usual sign of lack of professional, scientific and/or educational abilities of professors. Undesirable concepts in lectures have as consequence the low level of success on examinations because of low level of reached knowledge. One old joke shows many concepts for organization of lectures, Fig. 2

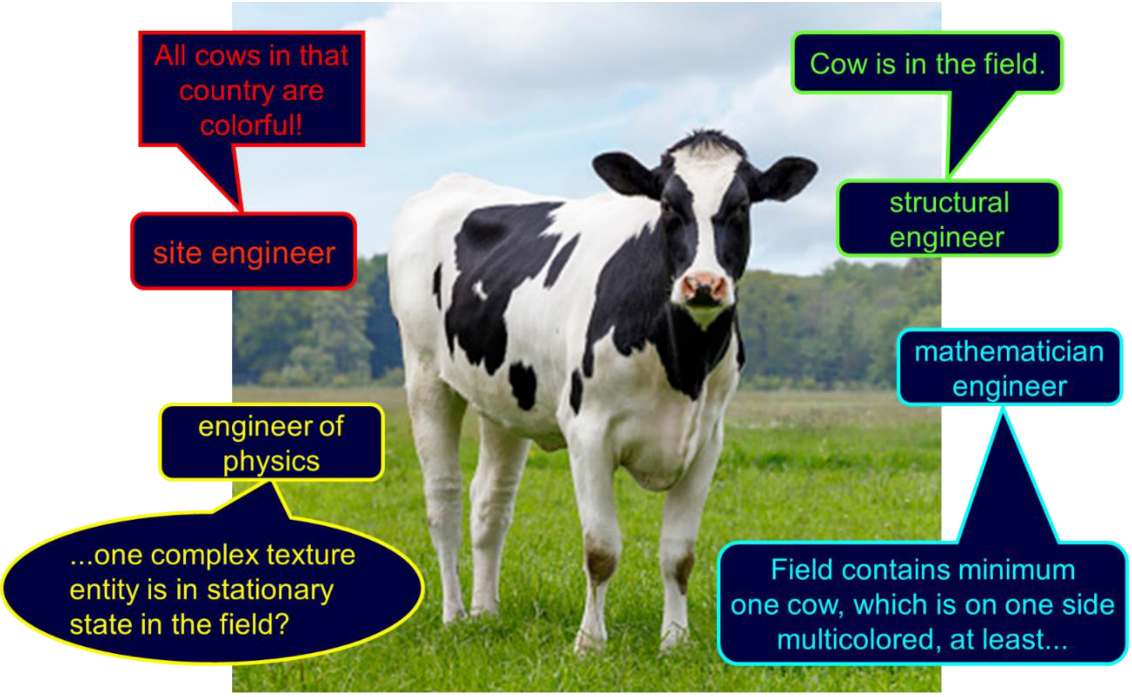

Fig. 2 Old joke about "same thing looks like so different" related to lectures

Examinations must be oriented to check the real and functional knowledge state of students with following grades:

- 6 - **descriptive** knowing of a part of a material,
- 7 - **descriptive** knowing of the whole material and understanding/knowledge of the part of material,
- 8 - **understanding and knowledge** of the whole material,
- 9 - **understanding, knowledge and application** of the whole material and
- 10 - **understanding, knowledge and creative application** of the whole material.

The strategy of grading may vary according to type of subject and these are so-called discrete right of professor staff, which can adjust these during time. Correction of grades must be possible on oral part of examination, but only for students that showed satisfactory level of knowledge (grades 8 or 9) during lectures and practical or written part of examination. If student requests correction of grade 6 or 7, it must be realized by new attempt in following examination period, regards to official regulations of faculty. Teaching staff must to explain reasons of given grade if student insists and explanation must be given with correct answer on examination questions that student did not know.

Next important thing are class books, books or monography publications that are duty of professor on some subject or field. Here there are various examples and typical are illustratively presented of Fig. 3.

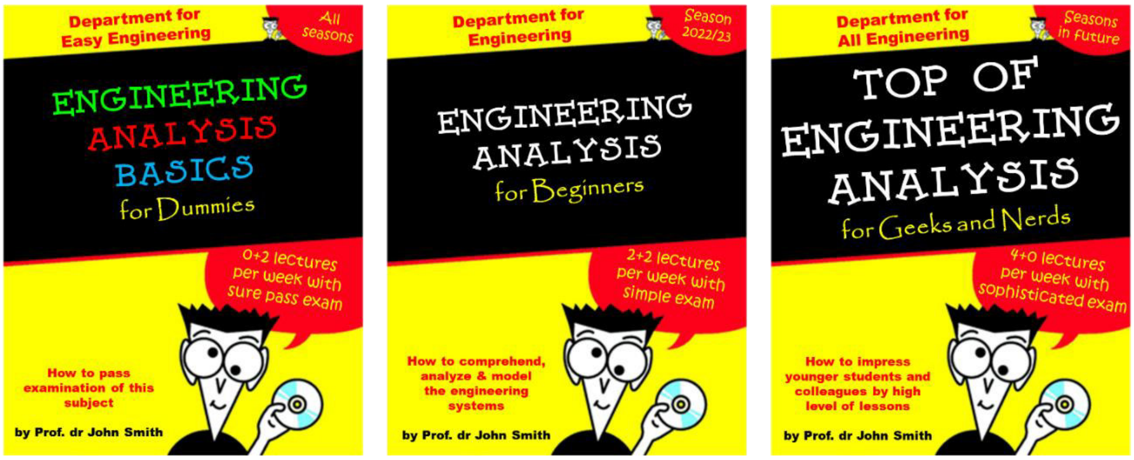

Fig. 3 Various approaches in publishing of book as duty of professor

Three specific approaches in writing class book are:

- so-called **"guidebooks"** which are strictly oriented as collection of lectures after that follows examination tasks, questions and answers, very useful only for pass of examination, but not for real studying,
- **"engineering educative books"** which presents essence of some subject or part of engineering field, very suitable for reaching of real functional knowledge and inspirational for full life personal studying and
- so-called **"Holly Books"** which are some kind of "monument of professor", with primary role to impress naïve observer or superficial reader, but not intellectually curious or well categorized student or professional.

Mentioned publications differ not only in the intentions and content, but also in the language that is used. Guidebooks, as only practical manual for pass the examination, use simple language and short sentences because their users and readers will not to go in deeper levels of mater. Engineering educative books are written in reasonable simple but technically oriented language that is easy for reading and for understanding of the material that is complex and difficult for understanding on first view. Finally, "holly books" are example of use of nontechnical and occasionally completely unsuitable, even "lyric" language, that looks like on language for the basic school home works about some gentle theme, [4].

On the end of these considerations, it must to emphasize, as a special problem, need of publication of papers in well reputable journals, as a main condition in personal progress in academic hierarchy, i.e. for appointment in next academic title, since title of assistant professor to full professor. Authors have attitude that some set of merits must to exist and publishing of important and valuable papers is main factor in that sense, but number of inadequate evaluation of papers, dishonest behavior of reviewers, influence peddling and corruption, request some kind of revision of criterion for development and personal progress. In that sense, dilemma appears which are dignity and respect of professor for their students and colleagues if authorship of these papers is ethically problematic.

5. HOW TO START AND BUILD NEW EDUCATIONAL CONCEPT

Obligation for building the new educational concept is on the side of students, professors and finally on the community. That order is not coincidental but results of our analysis of state and personal experience of almost forty years in this profession.

It is the duty of students to attend lectures regularly and meaningfully, to study by researching material from sources of knowledge, to effectively complete their studies and start a professional career. It is much important if they avoid inertia what is "holy property of mass". It could be much easier to study at a college if there is a passion towards a certain profession or if it is required of oneself, so the passion can come later, [3]. As the help for students, we suggest following measures:

1) Improvement of study conditions with an exclusively morning class schedule and technical improvement of teaching, so that the student's daily engagement is:
   - 08h - 14h ... classes at the college,
   - 14h - 16h ... break for lunch and rest,
   - 16h - 19h ... studying and preparing for the next day and
   - 19h - 22h ... free time.
2) Rationalization of teaching curriculums by giving "optional status" to subjects whose goal is mainly the employment of "surplus teaching staff" and the correction of the schedule of subjects by semesters.
3) Rationalization of teaching programs, i.e. elimination of unnecessary content and tiresome "extracurricular duties", with the transfer and verification of knowledge adapted to the engineering profession while avoiding situation "the status of the subject is above the its goal".
4) Teaching programs of so-called "basic preparation subjects" (mathematics, physics…) should be oriented to understanding of essence of application aspects and solving of engineering problems, opposite to "art for art sake" style, what is such loved by specialists from these sciences.
5) Related to the concept of all lessons… better is "from particular to general", i.e. induction is better than deduction, although opposite principle look likes something sophisticated.
6) More than a quarter of a century ago, technology-intensive industries began to seek workers who could combine professional knowledge and skills with broad, interdisciplinary, collaborative skills.

6. CONCLUSIONS

The development of artificial intelligence simultaneously facilitates and complicates the process of developing teaching at the university. The necessity of combining new knowledge and experiences with the demands of reality must be carried out according to new agile teaching methods. The increased amount of knowledge implies much more activity on the part of university professors, more adaptation to changes in the mental determinations of new generations. The changes that have already taken place in reality in the ways of experiencing and perceiving oneself, and what is happening in the business world, also require a new teacher. Also, engineers of all provenances must know social laws and the ways of their influence on the individual. Without the combined knowledge of technology and man, the development of the educational process is not possible.

ACKNOWLEDGEMENTS

This paper is not scientific or "state of the art" type, but some kind "case of study", without results of our personal formal investigation. Facts given here are the result of our practical monitoring, analysis and assessment of state of educational system of our technical faculty. We are really and curiously interested what other experience about these issues are and all considerations, remarks and suggestions are welcome.
Instead of an apologize to students or professors, because of our sometimes tough statements and comments, we ask they to organize discussion and some kind of "round table" dedicated to this important theme.

REFERENCES

[1] Brunhaver, SR, Korte, RF, Barley, SR, Sheppard, SD. (2017). Bridging the gaps between engineering education and practice. In: US Engineering in the Global Economy, eds Freeman R, Salzman H. Cambridge, MA: National Bureau of Economics Research.

[2] Canary, HE, Taylor, JL, Herkert, JR, Ellison, K, Wetmore, JM, Tarin, CA. (2014). Engaging students in integrated ethics education: A communication in the disciplines study of pedagogy and students' roles in society. Communication Education 63(2):83–104.

[3] Craps, S., Pinxten, M., Knipprath,H. and Langie, G. (2021). Exploring Professional Roles for Early Career Engineers: ASystematic Literature Review. European Journal of Engineering Education 46 (2): 266–286.

[4] Litchfield K, Javernick-Will A, Maul A. (2016). Technical and professional skills of engineers involved and not involved in engineering service. Journal of Engineering Education 105(1):70–92.

[5] Lowe, D., Goldfinch, T., Kadi,A., Willey,K. & Wilkinson,T. (2022). Engineering graduates professional formation: the connection between activity types and professional competencies, European Journal of Engineering Education 47(1): 8-29.

THE DESIGN OF THE WATER PUMP STATION

Dalibor Gelo[1], Šime Serdarević[2], Dean Čizmar[3], Ivan Volarić[4]

Summary:

The plan is to construct a water pump station for the drinking water treatment facility. The location of the water pump station is near river Drava in Croatia. The goal of the paper is to present the design process of the water pump station. The well-lowering approach is applied. The pump station is reinforced concrete construction. Excavation of the soil from inside the walls will reduce the bearing strength of the soil and allow the walls to penetrate the soil under self-weight. The casting of the walls is in phases. The paper will present the process of wall penetration in soil, the stability of the well, and the main reinforcement design.

Keywords: water pump station, design, well-lowering approach

[1] Lecturer, Zagreb University of Applied Sciences, Zagreb, Croatia, dalibor.gelo@tvz.hr
[2] Lecturer, Zagreb University of Applied Sciences, Zagreb, Croatia, sime.serdarevic@tvz.hr
[3] Associate professor, Zagreb University of Applied Sciences, Zagreb, Croatia, dean.cizmar@tvz.hr
[4] Lecturer, Zagreb University of Applied Sciences, Zagreb, Croatia, ivan.volaric@tvz.hr

1. INTRODUCTION

The process of designing and constructing the pumping station near the river Drava in Croatia is explained, with the use of a well-lowering technique.

1.1. WELL GEOMETRY AND MATERIAL

The shape of the well is rectangular, 5.2 m times 6.2 m and the total height of the well is 13 m. The thickness of the walls is 60 cm, only around the knife thickness is 70 cm, and the knife height is 2.0 m.

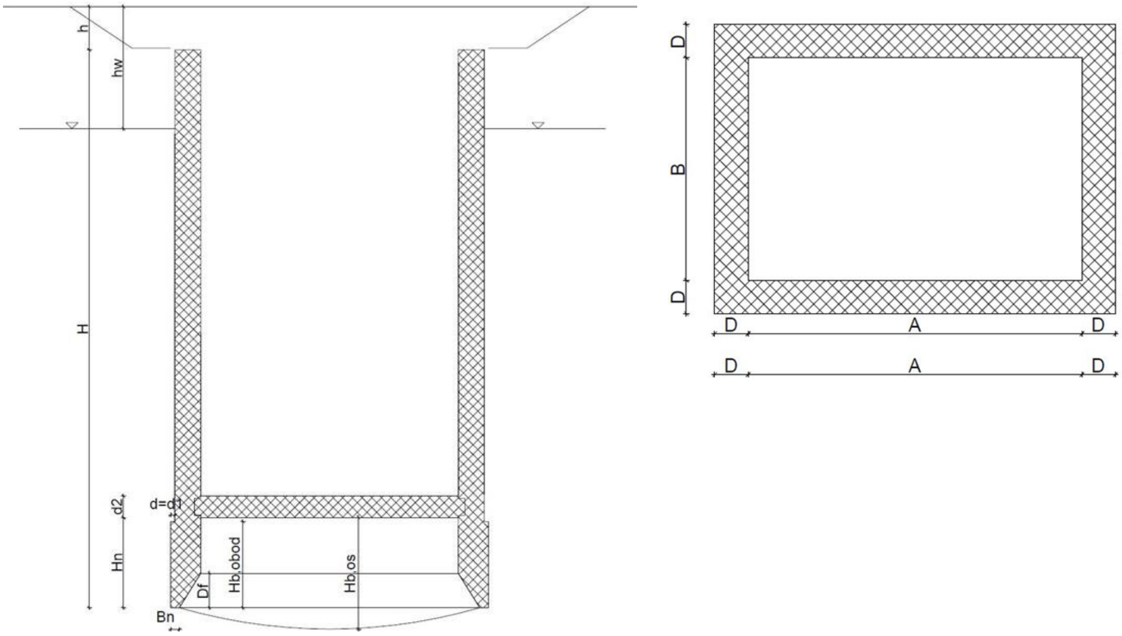

Fig. 1 Drawing of the well.

To prevent the penetration of groundwater, it is necessary to cast concrete cap. The predicted thickness of the concrete lid is 2.0 m at the edge and 2.5 m at the middle of the well. The bottom slab is 40 cm thick. All concretes are class C30/37.

Tab. 1 Well dimensions values

Dimension	H [m]	A [m]	B [m]	D [m]	H_n[m]	B_n [m]	H_{b_obod} [m]	H_{b_os} [m]	d_2 [m]	d_1 [m]	D_f [m]	B_n [m]
Value	13.0	5.0	4.0	0.6	2.0	0.2	2	2.5	0.4	0.1	0.8	0,2

1.2. GEOTECHNICAL DATA

Geotechnical research has been performed, and one drill has been conducted in the middle of the well. The drilling depth is 15 m from the ground surface. Four layers of soil were identified based on the collected data [4]. The first 7.6 meters of the ground consists of mainly clay and dust, while the sand layer starts below it until the end of drilling.

2. WELL DESIGN

It is essential to monitor the stability of the well during the lowering phase and overall stability. Necessary reinforcement and concrete thickness need to be determined. A concrete design is performed for case when the well is completely lowered [3].

2.1. LOWERING PHASE

The structure of the reinforced concrete well is built in several steps. On the working surface at the ground level, concrete casting is performed. Sliding sheeting is used for shaping concrete. When concrete achieves the required strength, digging can start. Removing the soil from the inside of the well reduces the bearing capacity of the soil, and the well begins sinking under its weight. A stability check must be performed for each step. The predicted size of the steps is two meters.

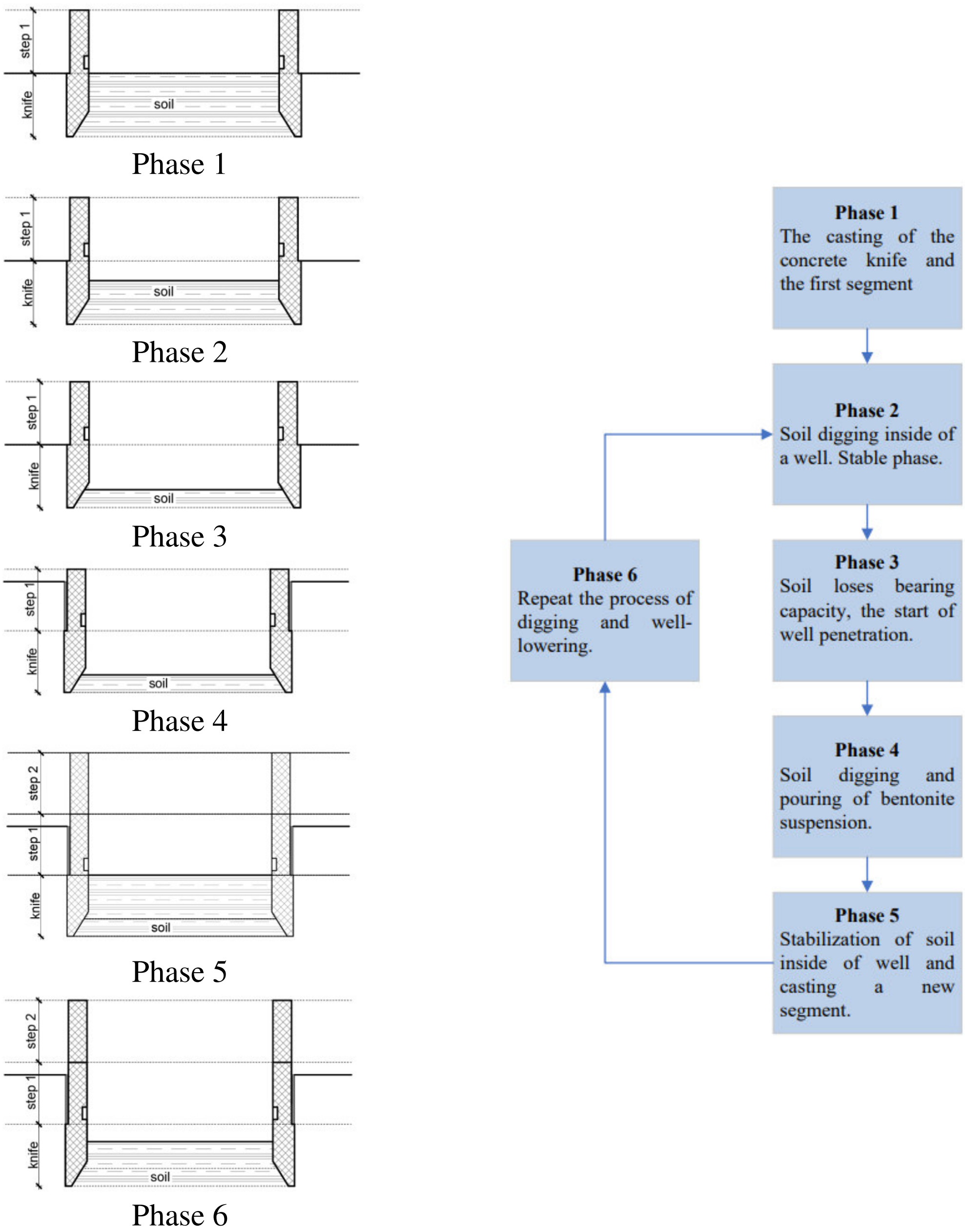

Fig. 2 Phase of well lowering.

Fig. 2 illustrates the six-phase process of lowering a well. Lowering begins in phase three when the soil can no longer bear the concrete weight. The check of this phase is proven by using the equilibrium equations. The following equation determines the effective weight of concrete

$$G' = \big((2\cdot(A+2\cdot D)\cdot D\ +2\cdot\ B\cdot D)\cdot(h_w-h)\big)\cdot\gamma_b+ \\ \big((2\cdot(A+2\cdot D)\cdot D+2\cdot B\cdot D)\cdot(H+h-h_w)\big)(\gamma_b-\gamma_w). \qquad (1)$$

The γ_b and γ_w represent the specific weight of concrete and water, and the h_w determines predicted groundwater levels from the ground surface level. The knife's ability to penetrate the soil is limited by the friction on its surface and the capacity of the soil to bear weight. The friction force is calculated in the middle of the knife height, considering only the outside suffice of the knife.

$$\sigma_v = h_w \cdot \gamma_{soil} + \left(H + h - h_w - \frac{H_n}{2}\right) \cdot (\gamma_{soil} - \gamma_w) \tag{2}$$

$$k_0 = 1 - sin(\varphi) \tag{3}$$

$$\sigma_{h0} = k_0 \cdot \sigma_v \tag{4}$$

$$t_n = tan(\varphi) \cdot \sigma_{h0} \tag{5}$$

Combining equations 2, 3, 4, and 5, it is possible to calculate horizontal specific friction.

Equations 2 and 4 represent vertical and horizontal soil stress at the middle of knife height, while the φ describes the soil friction angle. The total friction force is calculated with equation 6. When concrete walls start to sink, pouring bentonite suspension between walls and surrounding soil is necessary to eliminate friction.

$$T_n = 2 \cdot t_n \cdot H_n \cdot \left((A + 2 \cdot D + 2 \cdot d_1) + (B + 2 \cdot D + 2 \cdot d_1)\right) \tag{6}$$

The bearing capacity of soil is calculated using equation 7, while equation 8 represents the total soil reaction.

$$q_u = c' \cdot N_c + q \cdot N_q + 0.5 \cdot \gamma \cdot B_n \cdot N_\gamma \tag{7}$$

$$Q = q_u \cdot B_n \cdot 2 \cdot (A + 2 \cdot D + B) \tag{8}$$

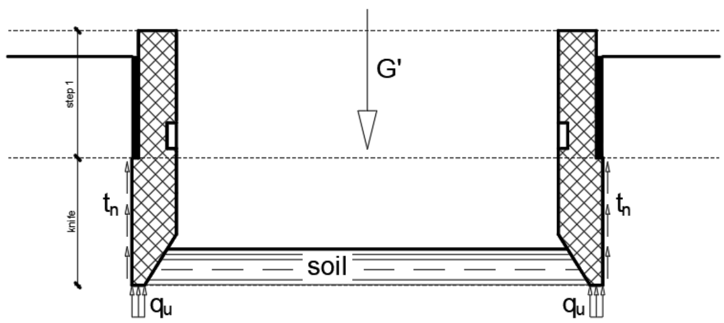

Fig. 3 Force diagram.

Tab. 2 Stability check of well in the phase of lowering, dry state.

Step	H [m]	G' [kN]	T [kN]	Q [kN]	D_f [m]	UC
1	4	1224	278	3297	0.8	2,92
1	4	1224	278	373	0	0,53
2	6	1836	278	3297	0.8	1,95
2	6	1836	278	373	0	0,35
3	8	2448	278	3297	0.8	1,46
3	8	2448	278	373	0	0,27

Tab. 3 Stability check of well in the phase of lowering, wet state.

Step	H [m]	G' [kN]	T [kN]	Q [kN]	D_f [m]	UC
1	4	979	140	1657	0.8	1,84
1	4	979	140	187	0	0,33
2	6	1591	140	1657	0.8	1,13
2	6	1591	140	187	0	0,21
3	8	2203	278	1657	1,2	1,15
3	8	2203	278	187	0,8	0,15

Tables two and three show wet and dry soil forces and UC factors. The UC factor describes the stability of the well. If UC exceeds one, then the well is stable. In the project, only the first 7 to 8 meters of the well will be lowered, as described in this chapter. A large excavation will be carried out for the upper part of the well.

2.2. OVERALL STABILITY

After lowering the well, it is necessary to seal the bottom of the well. The sealing is predicted in two phases. As it's impossible to pump water inside the pumping station due to soil hydraulic issues, a non-reinforced concrete plug made of C30/37 concrete with a minimum height of 2 meters is used to seal the bottom of the pumping station after excavation. Once the concrete has solidified, the water inside the pumping station is pumped out.

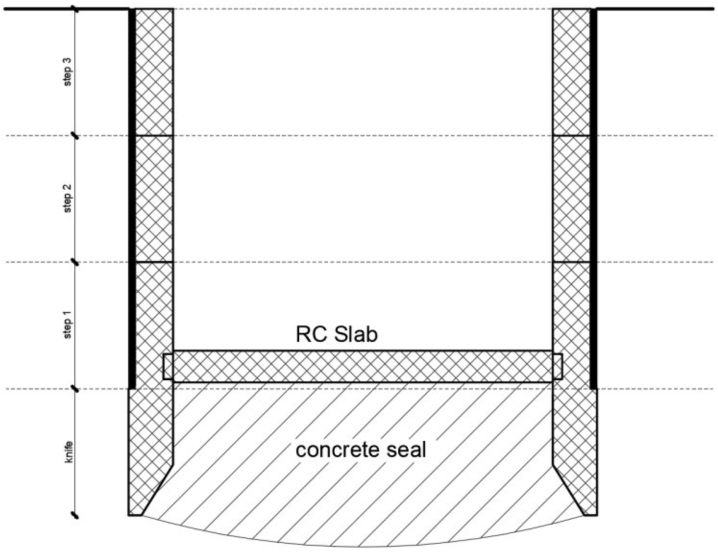

Fig. 4 Non-reinforced concrete seal and RC slab.

Once the sealing process is complete and all water has been pumped out, it is crucial to cast a 40 cm thick reinforced concrete slab over the concrete seal. The well construction is necessary to contract during the dry season when the groundwater level is lower.

$$G_1 = 2 \cdot (A + 2 \cdot D) \cdot D \cdot H \cdot \gamma_b + 2 \cdot B \cdot D \cdot H \cdot \gamma_b \tag{9}$$

$$G_2 = A \cdot B \cdot \left(\frac{\text{Hb\_obod} - \text{Hb\_os}}{2}\right) \cdot \gamma_{b\_seal} \tag{10}$$

$$G_3 = 2 \cdot \big((A + 2 \cdot D + 2 \cdot d_1) + (B + 2 \cdot D)\big) \cdot d_1 \cdot (H - H_n) \cdot \gamma_b \tag{11}$$

$$U = (A + 2 \cdot D + 2 \cdot d_1) \cdot (B + 2 \cdot D + 2 \cdot d_1)(H + h - h_w) \cdot \gamma_w \tag{12}$$

Equations 9, 10, and 11 represent the weight of walls, concrete seal, and RC slab, and equation 12 describes water uplift. The total weight of concrete is 5294 kN, and the force from water uplift is 4493 kN. The safety factor is 1.178.

3. CONCLUSION

The process of constructing a pumping station with a well-lowering technique is explained in the paperwork. The paperwork also confirms that the suggested design process is feasible and the dimensions of the well meet the requirements for the lowering and use phase. When writing this paperwork, the construction has begun, and comparing predictions and actual progress will be interesting. [1, 2, 4]

REFERENCES

[1] HRN EN 1990, Eurocode: Basis of structural design
[2] HRN EN 1991, Eurocode 1: Actions on structures
[3] HRN EN 1992, Eurocode 2: Design of Concrete Structures
[4] HRN EN 1997, Eurocode 7: Geotechnical Design

FROST RESISTANCE OF HEAVYWEIGHT SELF-COMPACTING CONCRETE

Ksenija Janković[1], Dragan Bojović[2], Marko Stojanović[3], Anja Terzić[4], Srboljub Stanković[5]

Summary:

Self-compacting concrete (SCC), a non-shaped composite building material, has improved microstructure packing, strength, and durability thanks to the use of fly ash, a highly effective mineral additive. Performances of SCC with fly ash and conventional SCC with limestone filler were compared. Additional experimental self-compacting concretes were made and adjusted with various types of fine aggregates, fillers, and unique additives to increase freeze-thaw resistance. The relationship between the proportion of barite sand and additives and the properties of SCC was investigated and discussed. Tests of freeze-thaw resistance with and without de-icing salts are the main focus of these articles.

Key words: Fly ash, Recycling, Limestone filler, Barite, Durability

[1] Principal Research Fellow, IMS Institute, Belgrade, Serbia, ksenija.jankovic@institutims.rs
[2] Research Associate, IMS Institute, Belgrade, Serbia, dragan.bojovic@institutims.rs
[3] PhD Candidate, IMS Institute, Belgrade, Serbia, marko.stojanovic@institutims.rs
[4] Principal Research Fellow, IMS Institute, Belgrade, Serbia, anja.terzic@institutims.rs
[5] Senior Research Associate, Vinča Institute of Nuclear Sciences, University of Belgrade, National Institute of the Republic of Serbia, Belgrade, Serbia, srbas@vinca.rs

1. INTRODUCTION

The use of secondary raw waste-based materials such as recycled aggregate (i.e., crushed concrete), fly ash, various forms of slag, foundry sand, and so on is an appropriate modern solution for environmental difficulties as well as resource depletion challenges. Large quantities of waste and recycled materials available at reasonable prices all around the world provide an excellent answer for decreasing the carbon footprint of concrete. These compounds also serve as a binder for the stabilization of contaminated waste materials [1, 2].

Traditionally, the problem of industrial waste disposal has been tackled by the construction of planned landfills. However, landfills take up enormous expanses of land, and trash removal is usually complicated and costly. The use of industrial byproducts and waste materials such as fly ash in the construction of concrete overcomes the problem of their disposal, thus instead of generating new landfills, new ecological materials are developed [3, 4].

Cement is very expensive and energy-intensive component of concrete. Cement production accounts for 2.5 % of global CO_2 emissions from industrial capacities. One solution to this problem is the use of alternative secondary raw materials, such as fly ash, which is a byproduct of numerous manufacturing processes. Coal combustion residues (fly ash and bottom ash) are generated when coal is ignited in power plants. Fly ash is a lightweight powdery raw material that is collected directly from a filter. Fly ash is composed primarily of spherical hollow particles. Coal ash comes in a variety of hues and features, depending on the type of coal, the geolocation of the deposit, the furnace structure, and the combustion procedure utilized in the thermal power plant [5].

When compared to ordinary vibrated concrete, self-compacting concrete (SCC) has a higher flow rate. High flowability is achieved by using a high proportion of extra fine mineral fillers in the mix design [6]. Given its availability and affordable cost, fly ash is one of the most frequently used mineral fillers in SCC. The components and their ratios, as well as the type and particle size of the filler, as well as the method of casting, production, and curing conditions of SCC, all have a considerable impact on the qualities of fresh and hardened concrete. The effect of fly ash on the properties of cementitious materials is defined as a combination of plasticizing (because to its spherical shape in tiny part sizes), micro-aggregate (related to its ability to infill), and active (thanks to its pozzolanic ability). This alters the properties of hardened SCC (strength, Young's modulus, water absorption, permeability, and so on) [7-9].

Heavyweight concrete used for radiation shielding in hospitals and/or nuclear facilities is usually made with barite aggregate. Concrete with barite powder as a sand substitute in the range of 0 % to 25 % lowered compressive strength at 28 days by only 10 %, elastic modulus at one year by 20 %, and tensile strength by up to 50 % [10]. The mixing method affects the grading curve of barite more than other aggregates. This changed the characteristics of concrete, increasing workability while decreasing compressive strength and modulus of elasticity [11]. Concrete with magnetite fine aggregate showed improved physico-mechanical characteristics than concrete based on barite and goethite. The compressive strength of high-performance heavy-density concrete including magnetite as fine aggregate was 23 % greater than that of sand-containing concrete [12-13]. The basic properties of regular concrete and heavy-weight concrete with barite were investigated in the context of their usage for gamma radiation shielding [14-16].

As the temperature of saturated concrete in service is lowered, the water held in the capillary pores in the hardened cement paste freezes and expansion of the concrete takes place. If subsequent thawing is followed by re-freezing, repeated cycles have a cumulative effect. Each cycle of freezing causes a migration of water to locations where it can freeze. The location includes fine cracks which become enlarged by the pressure of the ice and remain enlarged during thawing.

Freezing is a gradual process, partly because of the rate of heat transfer through concrete, partly because of progressive increase in the concentration of dissolved salts in the still unfrozen pore water and partly because the freezing point varies with size of the pore. The larger voids in concrete, arising from incomplete compaction, are usually air-filled, not appreciably subject to the action of frost.

There are two possible sources of dilating pressure. First, freeying of water results in an increase in volume of approximately 9 %, so that the excess water in the cavity is expelled [17]. The second dilating force is caused by diffusion of water leading go a growth of a relatively small number of bodies of ice. This diffusion is caused by osmotic pressure brought about by local increases in solute concentracion due to the separation of frozen water from the pore water.

The purpose of this research is to assess the effect of filler (fly ash or limestone), fine aggregate type (quartz, barite, or a combination of the two) and additives on the freeze-thaw resistance with and without de-icing salts of SCC.

2. EXPERIMENTAL WORK

2.1. THE COMPOSITION OF CONCRETE

Portland cement CEM I 42.5R (specific density: 3100 kg/m^3) was utilized to produce self-compacting concrete. A considerable number of small particles are required to produce a self-compacting concrete mixture. Thereby, as fillers, two mineral additives were employed in this case. In particular, in the mix design of the referent concrete, limestone was used, but fly ash was used in the experimental SCC samples. Fig. 1 shows the chemical analyses of aggregates and mineral fillers. Specific densities for river aggregate and barite sand were 2610 kg/m^3 and 3770 kg/m^3, respectively. Fig. 2 illustrates the grain-size analysis of the fly ash and limestone. Properties of the milled fly ash sample are as follows: bulk density - 2310 kg/m^3, specific surface area – 7990 cm^2/g, pozzolanic activity/ flexural strength - 4.9 MPa, and pozzolanic activity/ compressive strength -14.1 MPa.

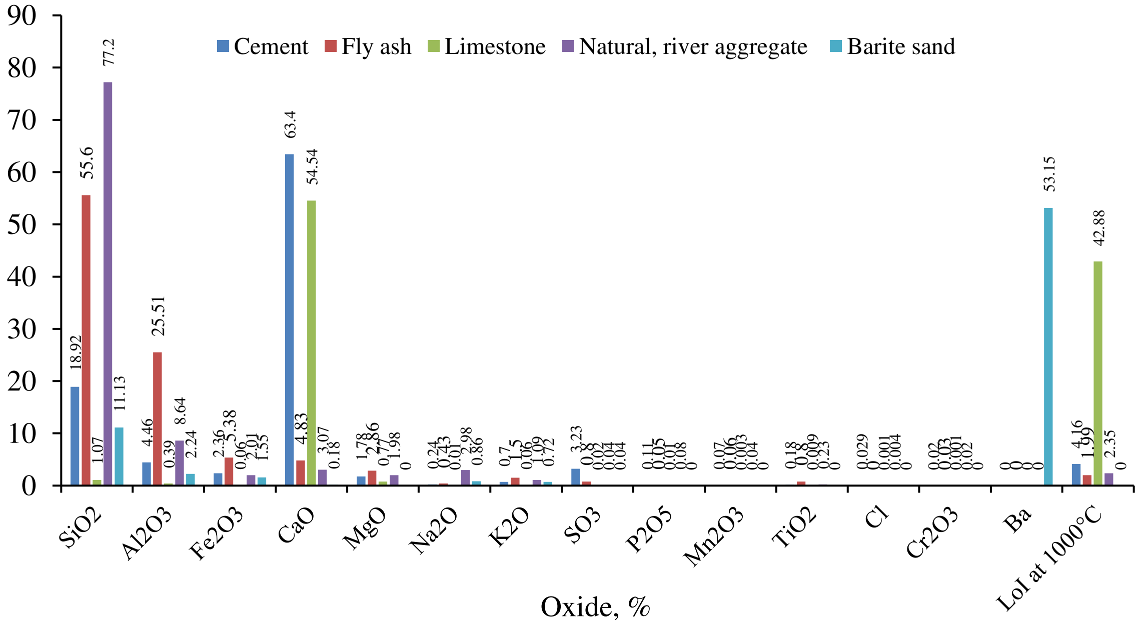

Fig. 1. Chemical compositions of SCC resource materials

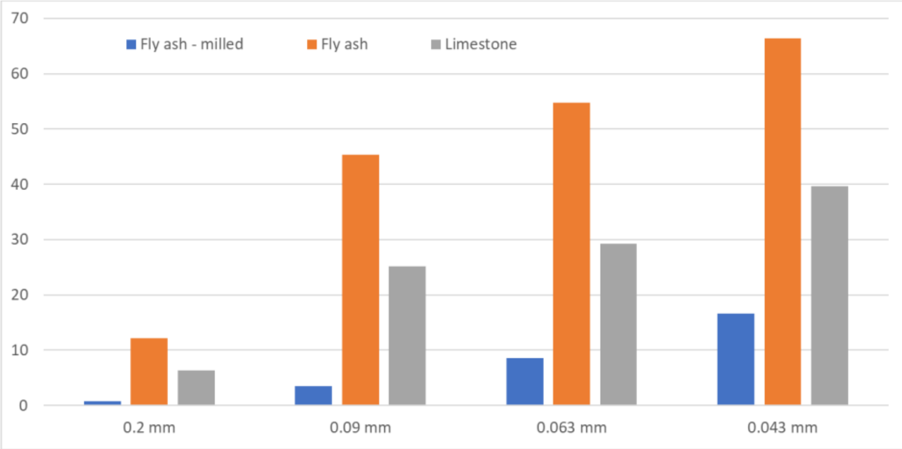

Fig. 2. Grain-size analysis of the fly ash and limestone

In the mix-design of SCC-s, natural, separated river aggregate with 0/4, 4/8, and 8/16 mm fractions, barite sand, and combination (barite: river sand = 75:25 by volume) were employed. The percentage share of aggregate per fraction was 45 % for 0/4 mm, 20 % for 4/8 mm, and 35 % for 8/16 mm. Fig. 3. depicts a grain-size study of aggregate mixtures.

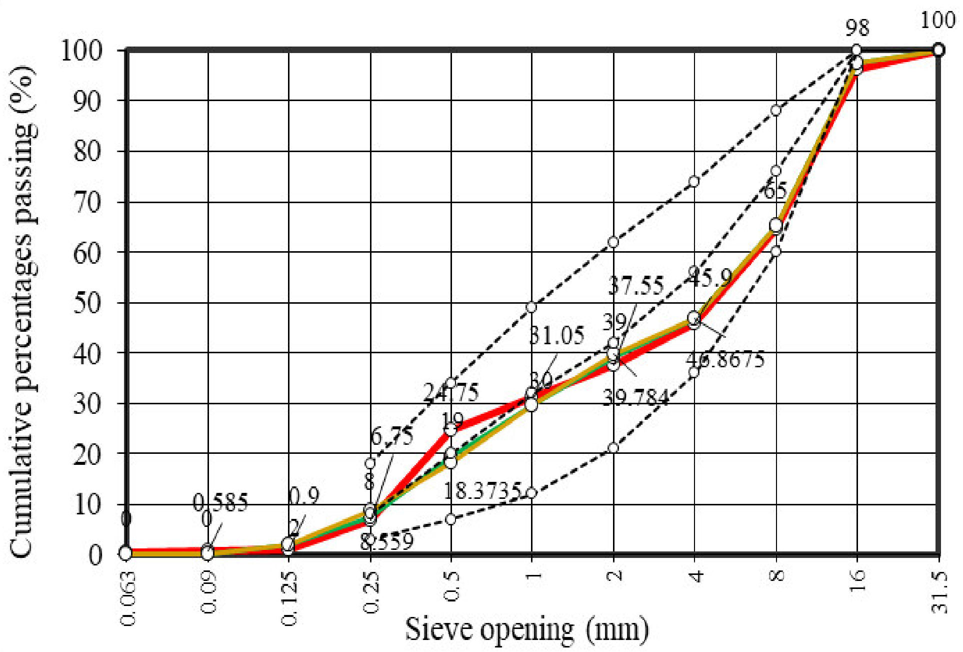

Fig. 3. Grading curves of aggregate mixtures for SCC samples (red mixture – natural aggregate; green mixture – 75% of barite and 25% of natural aggregate; and yellow mixture – barite)

2.2. CONCRETE MIXTURE

Five three-fraction self-compacting concrete mixtures were prepared for this experiment (Figure 4). Bulk densities of P301, P35, P37, P39, and P41 were 2383, 2739, 2743, 2606, and 2611 kg/m^3 respectively.

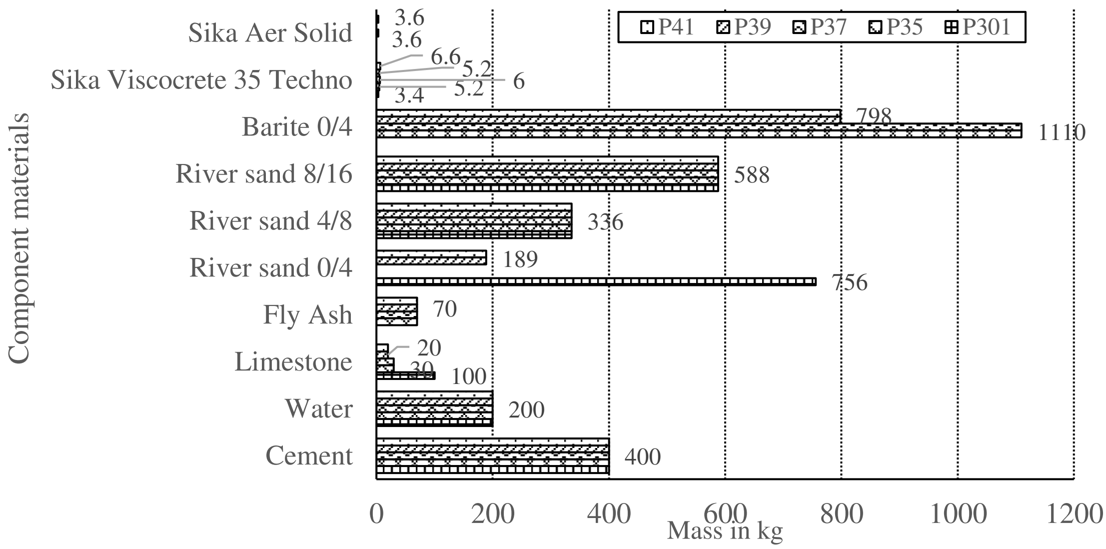

Fig. 4 Compositions of self-compacting concretes (values are given in kg/m^3)

Apart from the previously mentioned cement (CEM I 42.5R), mineral additives - limestone and fly ash, natural river separated aggregate (0/4, 4/8, and 8/16mm fractions), barite sand, and combination of barite and river sand, superplasticizer (Sika Viscocrete 35 Techno) and tap water were used as admixtures. In both combinations, a particular component (Sika Aer Solid) is used to boost freeze-thaw resistance. According to EN 206 requirements, fresh concrete was developed to meet the minimum needed qualities of self-compacting concrete. P301 reference concrete was made with limestone as a filler and natural river aggregate.

The combinations are intended to meet the following requirements: slump-flow 600 ±50 mm, t500> 2s, V-funnel 9 - 25 s, L-box with 3 bars H2/H>1 0.80. All concrete kinds were created with w/c = 0.50. A sufficient amount of superplasticizer was applied to achieve the desired SCC characteristics in the fresh state.

3. RESULTS

3.1. FRESH CONCRETE PROPERTIES

Density, fluidity - slump flow test according to EN 12350-8, viscosity - t500 test according to EN 12350-8, V funnel test according to EN 12350-9, and the ability of the passage between the reinforcement - L box test according to EN 12350-10 were conveyed for the fresh concrete tests. The test results for concrete in the fresh state are shown in Fig. 5 and 6.

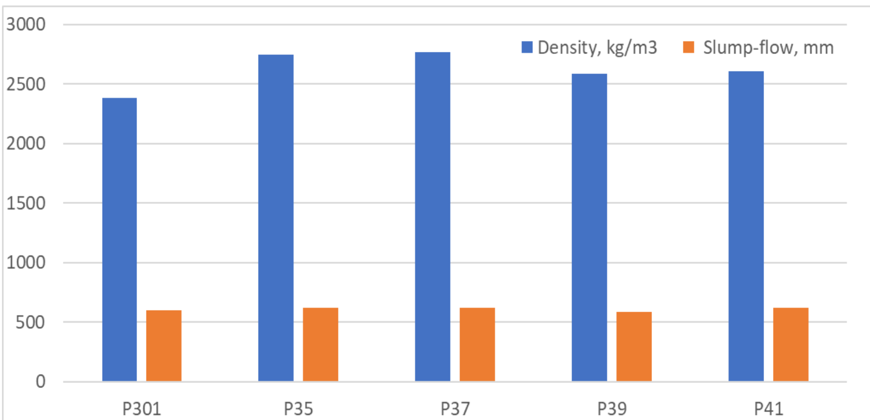

Fig. 5 Density and slump flow of fresh SCC samples

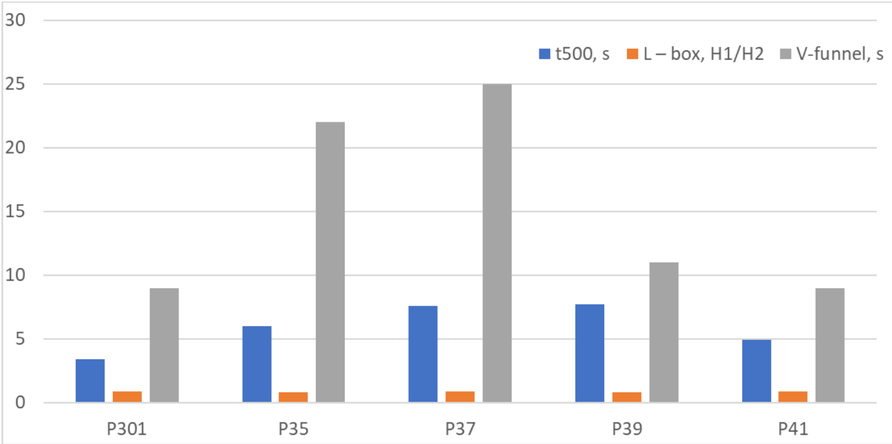

Fig. 6 Properties (T500, L-box, V-funnel) of SCC samples

3.2. COMPRESSIVE STRENGTH

Concrete was compacted without vibration in metal cube-shaped molds with an edge length of d = 150 mm. Following that, the samples were cured in water at a temperature of 20 °C before being tested in line with the SRPS EN 12390-2 standard.

The compressive strength of concrete was tested at the ages of 2, 7, 28, and 56 days using the SRPS EN 12390-3 standard. The hardened concrete's bulk density was determined using the SRPS EN 12390-7 standard. The bulk densities obtained ranged from 2320 to 2720 kg/m^3. The results are shown in Fig. 7.

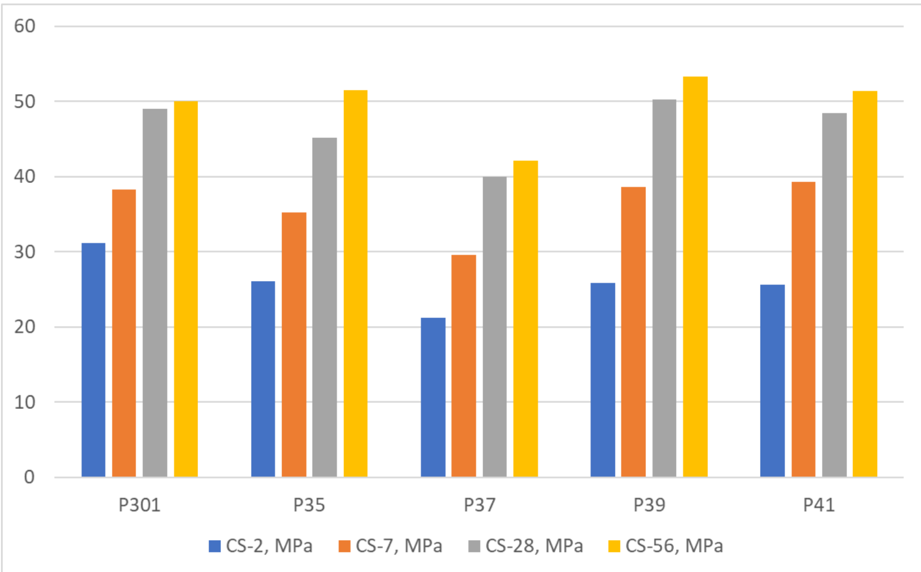

Fig. 7 Test results for concrete compressive strengths (CS) measured on cubic samples (d=150 mm)

3.3. FREEZE-THAW RESISTANCE WITH AND WITHOUT DE-ICING SALTS

The samples were made from each batch to test the freeze/thaw resistance (15x15x15 cm) and resistance freeze/thaw with de-icing agents (15x15x7.5 cm). The samples were made in laboratory conditions. As for the samples tested for the resistance to the effects of de-icing agents, the specimens are preconditioned. Three days before preparing for testing the specimens were covered by water in the room at temperature of 20 ± 2 °C. Plastic frame was set up and sealed, surface was covered with a 3% NaCl solution and after that, they were subjected to freeze/thaw cycles according to the SRPS U.M1.206:2013 – Annex O. The material that has scaled off is collected and weighed and the result is expressed in kg/m2. The test results after 28 cycles are given in Table 1.

Tab. 1 Mass loss after freeze/thaw test

Mass loss after freeze/thaw test (kg/m^2)	Concrete				
	P301	P35	P37	P39	P41
Maximum	0.07	0.23	0.20	0.12	0.06
Average	0.02	0.15	0.11	0.08	0.02

All concrete types satisfied criterion according to SRPS U.M1.206:2023 for class MS-2 (average mass loss value less than 0.20 mg/mm^2 and maximum value less than 0.25 mg/mm^2). Freezing/thawing resistance was testing according to SRPS U.M1.206:2013 – Annex R. One freeze-thaw cycle means that specimens are cured 4h in the water at temperature 20°C and 4h in the freezing chamber at -20°C. The specimens were exposed to 250 cycles. The criterion for estimate the frost resistance according to the SRPS U.M1.206:2023 was that the compressive strength of samples exposed to freezing and thawing cycles must be at least 75% of the reference strength (the samples of equivalent age cured in air at 20°C). All mixtures satisfied that criterion after 250 freeze-thaw cycles.

4. CONCLUSION

Fly ash was employed successfully in the production of self-compacting concretes. All mixtures displayed SF1 flowability. All concrete samples belong to the VF2 viscosity class. All concrete mixtures are classified as VS2 based on t500 values. All concrete types are classified as PL2, because all mixtures satisfied the criteria for the height ratio of the mixture at the ends of the L-box. SCC with barite sand exhibits less strength than river aggregate concrete (reference concrete). All concrete types satisfied resistance class MS-2 according to SRPS U.M1.206:2023 and can use for construction elements were XF4 exposure class is required. All concrete types satisfied resistance class M-2 according to SRPS U.M1.206:2023 and can use for construction elements were XF3 exposure class is required.

ACKNOWLEDGMENTS

This investigation is financially supported by the Ministry of Science, Technological Development and Innovation of the Republic of Serbia (Contract No.: 451-03-47/2023-01/ 200012) and 2021-2023 bilateral cooperation project between Turkey and Serbia: "Tailor made self-compacting heavyweight concrete with waste materials".

REFERENCES

[1] Y.S. Feng, S.J. Zhou, A. Zhou, W. Xia, J. Li, S. Wang, Y. Du, Reuse of a contaminated soil stabilized by a low-carbon binder as roadway subgrade material and mechanical performance evaluation, Engineering Geology 303 (2022).

[2] R. Chen, G. Cai, X. Dong, S. Pu, X. Dai, W. Duan, Green utilization of modified biomass by-product rice husk ash: A novel eco-friendly binder for stabilizing waste clay as road material, Journal of Cleaner Production 376 (2022) 134303.

[3] C. Zhou, Z. Gong, J. Hu, A. Cao, H. Liang, A cost-benefit analysis of landfill mining and material recycling in China, Waste Management 35 (2015) 191-198.

[4] Y. Zhao, L. Song, R. Huang, X. Li, Recycling of Aged Refuse from a Closed Landfill, Waste Management & Research 25(2) (2007) 130-8.

[5] S. Alterary, N. H. Marei, Fly ash properties, characterization, and applications: A review, Journal of King Saud University - Science 33:6 (2021) 101536.

[6] C. Shi et al., A review on mixture design methods for self-compacting concrete, Constr. Build. Mater. 84 (2015) 387–398.

[7] P.L. Domone, A review of the hardened mechanical properties of self-compacting concrete, Cem. Concr. Compos. 29 (2007) 1–12.

[8] Z. Zhang, S. Qian, H. Ma, Investigating mechanical properties and self-healing behavior of micro-cracked ECC with different volume of fly ash, Construction and Building Materials 52 (2014) 17-23.

[9] EFNARC, ERMCO, EFCA, CEMBUREAU, bibm: The European Guidelines for SCC:Specification, Production and Use; May 2005.

[10] K. Saidani, L. Ajam, M. Ouezdou, Barite powder as sand substitution in concrete: Effect on some mechanical properties, Constr Build Mater 95 (2015) 287–295.

[11] M.A. Gonzalez-Ortega, S. Cavalaro, A. Aguado, Influence of barite aggregate friability on mixing process and mechanical properties of concrete. Constr Build Mater 74 (2015) 169–175

[12] A.S. Ouda, Development of high – performance heavy density concrete using different aggregates for gamma - ray shielding. HBRC Journal (2014) http://dx.doi.org/10.1016/j.hbrcj.2014.06.010

[13] A. S. Ouda, Development of high-performance heavy density concrete using different aggregates for gamma-ray shielding, Progress in Nuclear Energy 79 (2015) 48-55.

[14] I. Ahmad, K. Shahzada, M. Imran et al., Densification of Concrete using Barite as Fine Aggregate and its Effect on Concrete Mechanical and Radiation Shielding Properties, Journal of Engineering Research 7(4) (2019) 81-95.

[15] I. Akkurt, C. Basyigit, S. Kilincarslan, B. Mavi, A. Akkurt, Radiation shielding of concretes containing different aggregates. Cem Concr Comp 28 (2006) 153–157.

[16] I. Akkurt, C. Basyigit, S. Kilincarslan, B. Mavi, A. Akkurt, The shielding of gamma – rays by concretes produced with barite, Prog Nucl Energy 46 (1) (2005) 1-11.

[17] A.M. Neville, Properties of concrete. Pearson education limited. England 2000.

IMPLEMENTATION OF CIRCULAR ECONOMY IN THE BUILT ENVIRONMENT

Meri Cvetkovska[1], Camila Cervantes[2], Adriana Salles [3], Rand Askar [4], Ana Trombeva Gavriloska[5], Luís Bragança [6]

Summary:

Facing the increasing concerns about the negative environmental impacts of buildings, governments and general society worldwide have been seeking more efficient and sustainable constructions. Hence, the Circular Economy (CE) emerged as a new paradigm of innovative practice with potential application to the construction industry besides other economic sectors. Following the European Circular Economy Action Plan (ECEAP), multiple efforts have been made to apply circular thinking to construction practices and include resource circularity into sustainability frameworks. The European Cooperation in Science and Technology (COST) recognized the importance of this topic and supported the Action CircularB (Implementation of Circular Economy in the Built Environment-CA21103). CircularB covers an integrated, interdisciplinary and transdisciplinary approach of CE implementation and assessment in the construction and real estate sector, namely buildings, building components, technical systems and construction products.

Key words: circular economy, built environment, circular value chain, sustainable development goals

[1] Prof., Ss. Cyril and Methodius University, Skopje, North Macedonia, cvetkovska@gf.ukim.edu.mk
[2] PhD candidate, University of Minho, ISISE, ARISE, Guimarães, Portugal, pg50902@alunos.uminho.pt
[3] PhD candidate., University of Minho, Guimarães, Portugal, adfsalles@gmail.com
[4] PhD candidate., University of Minho, Guimarães, Portugal, rand.askar@hotmail.com
[5] Prof., Ss. Cyril and Methodius University, Skopje, North Macedonia, agavriloska@arh.ukim.edu.mk
[6] Prof., University of Minho, Guimarães, Portugal, braganca@civil.uminho.pt

1. INTRODUCTION

World's population is constantly growing, facing new needs for new constructions. That is putting enormous stress on our environment and resources. The construction industry is responsible for circa 33% of greenhouse gas emissions, 40% of waste generation, and 40% of materials consumption [1,2]. In response to these figures, the European Commission launched the first Circular Economy Action Plan (ECEAP) in 2015, which holds particular promise for achieving multiple Sustainable Development Goals (SDGs), including SDGs 6 on energy, 8 on economic growth, 11 on sustainable cities, 12 on sustainable consumption and production, and 13 on climate change. A new European Circular Economy Action Plan (ECEAP) [3] was adopted in 2020 with more concrete measures to reduce the pressure on natural resources and create sustainable development. The goal of the ECEAP is to enable an easier transition from the Traditional Linear Economy "take, make, dispose", to a Circular Economy that implies "take the raw materials only once, produce, use and recycle without producing waste", Figure 1.

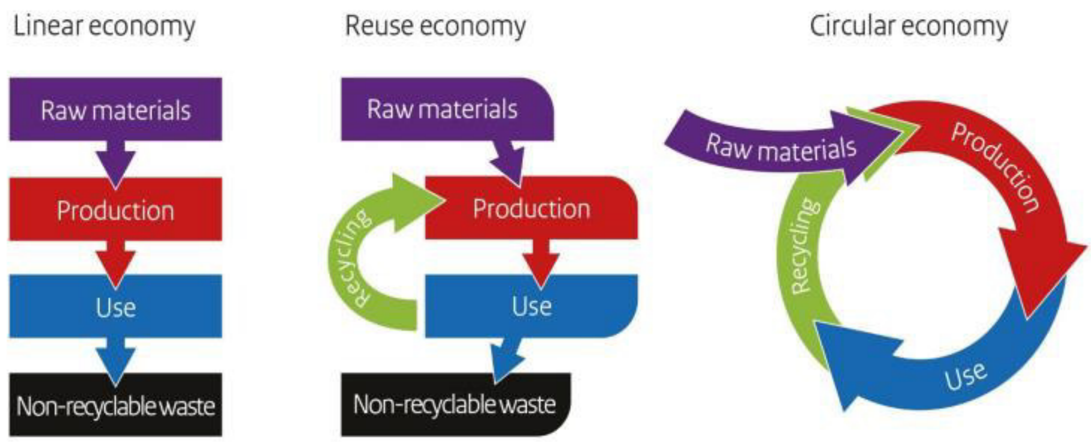

Fig. 1 Transition from Linear to Circular Economy

With very few examples of implementing CE into practice, the practical transformation of a linear business model into a circular one is still the main research gap in terms of consolidated circular practices steering companies towards improving the circularity of their products or services and incentivizing policies to subsidise those.

The application of CE principles in real estate, building design and use (adaptability, durability, waste reduction and high-quality management according to the European Commission [3]) is mainly focused on new buildings where circularity can be embedded and facilitated since the early design stage and consequently throughout the whole life cycle of a building and its components and materials. Conversely, circularity in the context of existing buildings is not so far defined [4].

The multitude of definitions of CE, and more specifically circularity in the built environment, does not contribute to a coherent, systematic approach. CE needs to be viewed as a business strategy, not only waste management or a design strategy. Optimising buildings' use should also be spotlighted instead of only viewing those as potential material banks where components and materials can be recovered, reused or recycled for new constructions [4,5]. Still, recovered materials from existing buildings face a critical barrier in their technical compatibility and quality appraisal, which put their direct reuse in question, leading to down-cycling processes and engaging extra resources and energy flows.

On the other hand, less has been said about the design aspect of circularity integration in buildings (e.g. design for disassembly (DfD), design for adaptability (DfA), design for change (DfC) etc.) and the role of building professionals and supply chain elements in embodying the CE principles into the building sector [6]. In other words, existing practices and concerns focus on the CE principle of "closing the loop" which assumes intensified reuse and upcycling of materials and components.

Most existing knowledge in Circular Economy is based on theoretical or/and analytical studies that often do not involve companies or common stakeholders but rather deliver theoretical concepts merely serving as suggestions to companies and policymakers. Besides, best practices are oriented toward large investments and therefore too complex to be adopted by Small and Medium Enterprises (SMEs). From that aspect, the main aim of the COST Action CircularB is: to define the methodology, to develop a common circularity framework for inclusive application and assessment in new and existing buildings, to support decision-making for all value chain stakeholders, to develop Key Performance Indicators (KPIs) based on current best practices of CE construction and appraise the implementation level of the ECEAP.

The CircularB Action aims to develop a common international framework of a circularity rating tool with Key Performance Indicators (KPIs) based on current best practices of CE construction, state-of-the-art and ECEAP. The tool's framework will allow local application and adaptation by different COST countries and regions. By developing a benchmark database – based on each country/region conditions, culture and traditions – the direct use of the tool is enabled, supporting both designers in developing more sustainable buildings and national/local governments in assessing and promoting their CE targets. Furthermore, construction, assembly, adaptability, deconstruction and business model guidelines will be identified for new and existing buildings to enhance CE in buildings and promote stakeholder knowledge. The rating tool will also be integrated into the Open BIM workflow for better-informed design decisions, automated assessment, efficient value chain management, and circular feedback using central BIM models.

2. CIRCULAR ECONOMY PRINCIPALS AND TOOLS

The CE principle of "slowing the loop" that suggests increasing the life span of buildings and products by preserving their value, quality, and efficiency to the highest possible extent has received less attention so far. This can be justified by the influence of the prevailing construction and design culture during the last decades of viewing buildings as temporal products of limited life service and predefined destiny – demolition. Another key principle of CE that is rarely addressed by existing frameworks is "narrowing the loop" which relies on using fewer resources per product. This principle is inspired from nature's processes that mainly use a limited chemical palette often consisting of six elements: carbon, hydrogen, oxygen, nitrogen, phosphorus and sulphur, while industrial manufacturers follow a different approach, seeking out rare and toxic elements to reach the desired functional properties. Narrowing the loop delivers conditions for recycling by allowing efficient and facilitated material separation and recovery.

Considering the CE principals, several tools have been developed to support the decision-making of designing or/and assessing buildings for circularity. However, many of these tools serve the same purpose with slight differences in goal and scope. The majority were developed to focus on specific aspects of circularity without considering other aspects, such as supporting products and materials choice by only substantiating material-related indicators based on their environmental impacts (e.g. aspects of health, non-toxic composition) and reuse and recycling potentials, such as Materials Passports (MP), Circular Materials Platforms, Material Circularity Index and material flow analysis (MFA) tools. However, these tools fail to address a comprehensive circularity conception and lead to a loss of criticality when used individually since they do not appraise all the other important design aspects, e.g. building composition and connectivity between elements, durability and service life of building components. This is because circularity values come up when specified intrinsic properties (material and product characteristics) cross with relational properties (building design and use characteristics). A building, e.g., can be made of 100% circular materials and products, but when those are unreachable for replacement or maintenance, the building system becomes non-circular.

Multiple sustainability rating tools were used to assess circularity, considering the added value to sustainability. LCA-based tools such as SimaPro, ReCiPe and Open LCA are widely used for the sustainability assessment of buildings. Using LCA tools in the context of circularity assessment considering end-of-life options results in more comprehensive assessments. Yet, these tools only addressed the environmental consequences without other aspects. Similarly, LCC-based tools are used to address the economic aspect of circularity in buildings, investigate the feasibility of circular solutions and conduct financial impact analysis of circular business models. Still, LCA and LCC methods are considered time-consuming and complex to base design choices on [7]. They also rely in parts on inaccessible data for S-LCA or Social Life Cycle Assessment.

Assessment is a relatively recent type of LCA, which has been investigated to complement the triple bottom line of sustainability towards a common sustainability framework. However, S-LCA has rarely been investigated to calculate the social and socio-economic impacts of product circularity.

The multiple aspects addressed by the different types of tools and the similarities among the majority of objectives point out the need to create complementarity rather than establish new ones from scratch. Still, the majority of existing tools so far are developed to support design decisions and perform comparative analyses but not to create solutions and strategies to implement circularity in buildings bearing in mind that the role of design is not merely at the initial planning process but rather persisting along the life cycle of products and services and remains relevant at any point. To fully benefit from circular strategies implementation, supply chain management and monitoring should be key.

The emergence of Building Information Modelling (BIM) has created new opportunities to improve process efficiency and productivity. Among the several applications of BIM for the construction industry, authors have recognised its influence on building sustainability, mainly on decision support, material information storage, managing the building end-of-life scenarios and waste minimisation [8,9]. Despite the great opportunity to link BIM with CE principles, it is still a growing topic with few related investigations. BIM has been widely integrated into some circularityrelated fields, as automated LCA, LCC or sustainability assessment [10]. The role of BIM for circular thinking concerns the capability to accumulate multidisciplinary lifecycle information about a building, together with the possibility of process automation [8].

3. MAIN GOALS OF COST ACTION CIRCULARB

Existing frameworks to implement and assess circularity suffer from a mismatch between supply and need. There is an oversupply of theoretical guidelines and tools that illustrate the basic principles of the CE in buildings. Yet, most of the tools serve the same purpose while there is a need for practical evidence about the utility of these tools and their impact on the design process to highlight best practices.

Considering all previously announced, the CircularB COST Action proposes a holistic framework to create, assess and benchmark circularity in buildings taking into consideration all the lifecycle stages from planning to end-of-life options with all the associated input-output flows of materials, as well as the engagement of a diverse group of stakeholders with interlocking specialities.

Within this context, this COST Action CircularB will attempt to answer the following Research Questions:

- How can circularity be defined as a complex character in buildings?
- How can the principles of circularity be integrated into all stages of a building lifecycle, from its conception to the end of its life considering all of its components, products and systems already during the design of new buildings and larger renovation projects?
- What are the drivers and the barriers of integration of circularity strategies in buildings for COST countries and beyond at the different levels? Are there any best practices established?
- Since existing circularity indicators and assessment frameworks are not satisfactory for delivering a holistic approach to circularity implementation in buildings, what are the other complementary aspects still missing considering all technical, technological, economic, environmental, legal and social factors? How can they be brought together into one inclusive model? Is there a chance to express the circularity as a complex character in one indicator or index or is there a need for a set of indicators?
- Is it possible to quantify the circularity potential of a building, taking into account among others the emerging potentials for disassembly, adaptability, deconstruction, reuse and durability? Is this an application case for module D1 in LCA?
- Does circularity contribute to increased sustainability? What is the relation between sustainability as an overall target and circularity as a partial strategy to support a more sustainable development?
- How to assess the advantages and sustainability of circularity measures? Are there any trade-offs?
- How can the stakeholders within the quadruple helix contribute to achieving building circularity?
- What is their respective role in achieving a circular value chain? And what incentives are needed to make their roles more efficient?
- What strategies and tools should be developed to enable the transformation along the full value chain?
- Are there additional requirements in the design and development for new (next generation) products?
- How will circularity contribute to the availability of secondary materials?
- What kind of new business models are there – from leasing systems to taking back options?

3.1. ORGANIZATIONAL SETTING OF CIRCULARB

The CircularB COST Action aims at delivering a holistic approach to circular buildings including all technical, technological, social, legal, economic and environmental aspects. In order to cover all of the proposed aspects, the research is divided into 4 Working Groups (WGs). The first three interconnected WGs (WG1, WG2, WG3) are focused on the scientific development of the Action, while the fourth (WG4) carries out the monitorisation and coordination of all Action activities and tasks, ensuring active participation of all involved partners, besides communication and dissemination of Action's outcomes.

3.1.1. WG1 - Circularity strategies and best practices

This WG works on developing innovative methods to apply circularity strategies in design and construction activities and identify best practices. Furthermore, this WG aims to create integrated design and engineering solutions for dynamic and circular buildings which by design provide an answer to circularity challenges of resource efficiency and waste prevention through embedding concepts of DfA, DfD, DfC and reversibility among others for new and existing buildings.

3.1.2. WG2 - Circular value chain and stakeholder engagement

This WG works on analysing the full value chain of circular buildings and circular materials and components. The main aim of this WG is to establish a stakeholder platform where an interdisciplinary dialogue can be held among key players including academia, industry, suppliers, governmental bodies and local authorities, construction professionals and the general public. Participatory dialogue among stakeholders is a key to ensuring a closed-loop value chain management and creating new collaboration patterns and business model ideas addressing individual requirements and shared interests.

3.1.3. WG3 - Circular KPIs framework

The WG3 aims to identify and develop relevant, reliable and replicable circular KPIs that can measure the circularity index of new and existing residential buildings. The KPIs will be cross-country (COST countries) applied and based on current and best CE practices, CE Action Plans, governmental reports and national/international practices. Additionally, the KPIs will be grouped under Governmental/Institutional, Environmental, Social, Economic, and Technical dimensions to propose developing an international rating framework. Such a framework will act as a complementary and detailed circular assessment of recognised sustainability schemes to support decision-making.

3.1.4. WG4 - Dissemination and results communication

This WG will ensure the maximisation of the Action's impact via various dissemination, communication, and outreach activities as well as identify opportunities to enlarge the Action's network and communicate with other networks and stakeholders.
The WGs links and interactions are presented on Figure 2.

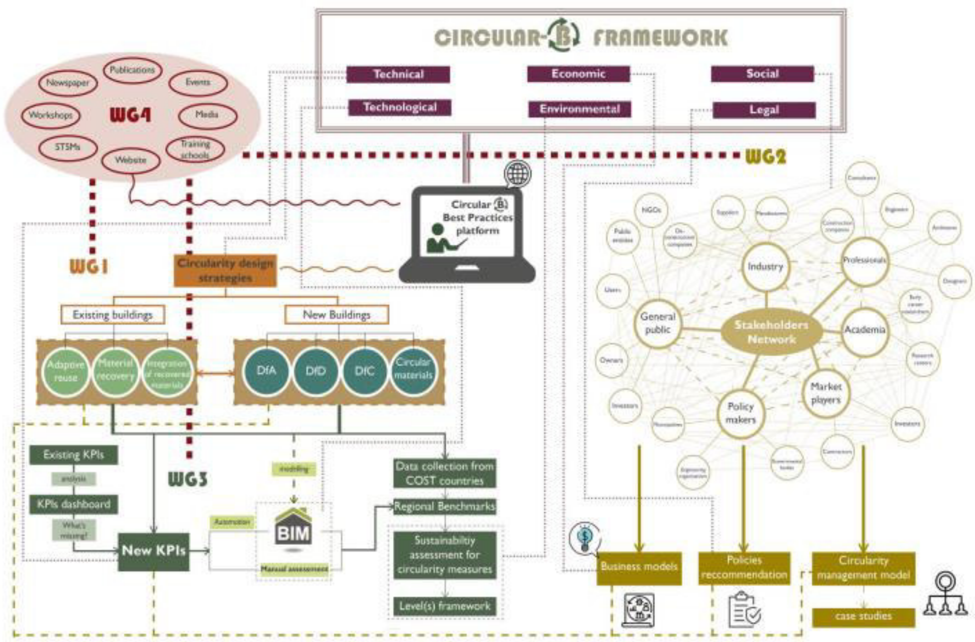

Fig. 2 WGs links and interactions

4. CONCLUSIONS

The CircularB Action is a COST (European Cooperation in Science and Technology) Action dedicated to developing an international circularity framework for the inclusive operation and assessment of new and existing buildings. It supports decision-making for all stakeholders in the value chain and evaluates the implementation level of the European Circular Economy Action Plan (ECEAP). This international framework includes a circularity rating tool with Key Performance Indicators (KPIs) that can be applied and adapted by various countries and regions. The tool can be directly applied to each country/region's specific conditions, culture, and traditions by using a benchmark database that is tailored to its unique conditions, culture, and traditions. In addition to assisting designers in creating sustainable buildings, it assists national/local governments in the evaluation and promotion of Circular Economy targets.
The topics covered Circular Economy (CE) best practices, design strategies and tools, circular materials and building products, adaptive reuse of existing buildings, recovery and reuse of salvaged building materials and products from existing structures, case studies, barriers against CE implementation, efficient waste and circular resource management, circular buildings lifecycle management and decision making, stakeholders relationships and new potential actors in circular management models, CE supporting policies and legal barriers, circular business models, criteria and KPIs for circular building and materials, CE criteria in sustainability frameworks for buildings, digitalization and BIM, and standardization of CE definitions in buildings. In sum, these topics provide a comprehensive overview of the implementation of CE in the built environment.

ACKNOWLEDGEMENT

The authors of this paper would like to thank the European Union for funding and COST (European Cooperation in Science and Technology) for supporting the COST Action CircularB CA21103 www.circularb.eu

REFERENCES

[1] Hossain M. U., Thomas S. N. (2018). Critical Consideration of Buildings' Environmental Impact Assessment towards Adoption of Circular Economy: An Analytical Review. Journal of Cleaner Production 205: 763–80. https://doi.org/10.1016/j.jclepro.2018.09.120

[2] Ness D. A., Xing K. (2017). *Toward a Resource-Efficient Built Environment: A Literature Review and Conceptual Model*. Journal of Industrial Ecology 21 (3): 572–92. https://doi.org/10.1111/jiec.12586

[3] EC. (2020). *Circular Economy - Principles for Buildings Design.* European Commission. https://ec.europa.eu/docsroom/documents/39984.

[4] Kyrö R K. (2020). *Share, Preserve, Adapt, Rethink – a Focused Framework for Circular Economy*. IOP Conf. Ser. Earth Environ. Sci. 588: 1–8. https://doi.org/10.1088/1755-1315/588/4/042034.

[5] Adams K., Osmani T. M., Thorpe T., and Thornback J. (2017). *Circular Economy in Construction: Current Awareness, Challenges and Enablers.* Waste and Resource Management 170: 10.

[6] Kanters J. (2020). *Circular Building Design: An Analysis of Barriers and Drivers for a Circular Building Sector.* Buildings 10 (4): 77. https://doi.org/10.3390/buildings10040077.

[7] Cambier C., Galle W. and De Temmerman N. (2020). *Research and Development Directions for Design Support Tools for Circular Building.* Buildings 10 (8): 142. https://doi.org/10.3390/buildings10080142 .

[8] Akanbi L. A., Oyedele O.L., Akinade O. O., Ajayi O. A., Delgado M. D., Bilal M., Bello A. S. (2018). *Salvaging Building Materials in a Circular Economy: A BIM-Based Whole-Life*

Performance Estimator. Resources, Conservation and Recycling 129 (February): 175–86. https://doi.org/10.1016/j.resconrec.2017.10.026.

[9] Charef R., Emmitt S. (2021). *Uses of Building Information Modelling for Overcoming Barriers to a Circular Economy.* Journal of Cleaner Production 285 (February): 124854. https://doi.org/10.1016/j.jclepro.2020.124854.

[10] Carvalho J. P., Alecrim I., Bragança L. Mateus R. (2020). *Integrating BIM*Based LCA *and Building Sustainability Assessment.* Sustainability 12(18):7468. https://doi.org/10.3390/su12187468.

VALORISATION OF SUNFLOWER HUSK ASH: THE INFLUENCE ON MICROSTRUCTURE AND COMPRESSIVE STRENGTH OF ALKALI-ACTIVATED SLAG MORTARS

Olivera Bukvić[1], Mirjana Malešev[2], Suzana Draganić[3], Marijana Serdar[4], Vlastimir Radonjanin[5]

Summary:

This paper presents a valorisation assessment of the sunflower husk ash (SHA), a locally available waste material, as an alkaline activator for alkali-activated slag. Three alkali-activated mortar mixes were produced with the constant ground granulated blast furnace slag (GGBFS) content and varied SHA content (25, 30 and 35 wt% GGBFS). The experimental programme included thermogravimetric analysis and compressive strength tests after 7 days of sample curing to evaluate the influence of SHA content on the activation of GGBFS. The main hydration products are C,(K)-S-H and C,(K)-A-S-H gels, and hydrotalcite. The highest compressive strength (29 MPa) was observed for the mix with 25% of SHA.

Key words: *alkali-activated materials, sunflower-husk ash, alternative alkali source, biomass ash, circular economy, sustainability*

[1] PhD student, Faculty of Technical Sciences, University of Novi Sad, Serbia, olivera.bukvic@uns.ac.rs
[2] Full prof., Faculty of Technical Sciences, University of Novi Sad, Serbia, miram@uns.ac.rs
[3] Assist. prof., Faculty of Technical Sciences, University of Novi Sad, Serbia, suzanav@uns.ac.rs
[4] Assoc. prof., Faculty of Civil Engineering, University of Zagreb, Croatia, marijana.serdar@grad.unizg.hr
[5] Faculty of Technical Sciences, University of Novi Sad, Serbia, radonv@uns.ac.rs

1. INTRODUCTION

The negative environmental impact of fossil fuels combustion associated with greenhouse gas emissions and depletion of fossil fuels resources has resulted in a tendency to use renewable energy sources. The utilization of biomass, defined as organic matter derived from agricultural, industrial and urban waste, is considered to be a sustainable alternative, as a renewable source with great energy potential [1].

Agricultural activities account for 140Gt of agricultural residues globally [2]. These residues hold immense potential as a valuable source of energy. However, the waste derived from the combustion process – agricultural biomass ash – is usually disposed of in landfills. The successful strategy to tackle the environmental problems associated with waste is its valorisation. This approach aligns with leading European Union strategies and initiatives for reaching sustainable development goals, such as the European Green Deal [3], the Circular Economy Action Plan [4] and the Bioeconomy Strategy [5].

One of the possibilities to valorize agricultural biomass ash is to use it in the construction sector. The application of agricultural wastes as concrete supplementary cementitious materials (SCMs) has already been investigated [6] and can contribute to sustainability goals by resolving waste management problems and decreasing the cement content in concrete composites which can lead to a reduction of CO_2 emissions associated with cement production [2,7].

The potential use of agricultural biomass ashes as an alkali source for alkali-activated materials (AAMs) has been the subject of extensive research in recent years [8]. AAMs are binders based on alumno-silicate-rich precursors (waste materials and industrial by-products, e.g., slag, coal fly ash) and alkaline activators [9]. These cement-free binders have gained increased attention within the research over the past few decades due to their reduced CO_2 footprint, compared to Portland cement-based concrete. The alkaline activators usually employed in AAM technology are alkali hydroxides and silicates. Finding a replacement for these chemical activators has become a topic of interest, due to the high energy requirements of the production process, high costs and potential health and safety issues that can arise from working with highly caustic alkaline solutions [7,10]. Agricultural biomass ashes, in general, can have different chemical compositions, depending on the derivation source. They can be suitable for alkali-activation due to the high amount of potassium and silicon [11].

In the Autonomous Province of Vojvodina, Republic of Serbia, the sunflower husks, generated from the sunflower seed processing, are used as an energy source for the city's heating supply by some oil producers and by Heat and electrical plant in Sremska Mitrovica. The combustion process residue is potassium-rich waste material, sunflower husk ash (SHA). Oil production company Victoria Oil from Šid and Heat and electrical plant in Sremska Mitrovica together generate around 960 tons per year of SHA, according to their data, that is disposed of in landfills.

To date, there is a lack of information regarding the application of SHA as an alternative activator in AAM technology. Therefore, the idea of this research is to investigate the possibility of valorizing locally available SHA as an alkaline activator for alkali-activated slag. The aim of the presented experimental research is to evaluate the microstructural changes and compressive strength of AA mortars with three different SHA contents. The evaluation was performed through the identification of formed hydration products by thermogravimetric analysis (TGA) and compressive strength tests after 7 days of curing.

2. MATERIALS AND METHODS

2.1. RAW MATERIALS

AA mortars were produced from sunflower husk ash (SHA) (Fig. 1), ground granulated blast furnace slag (GGBFS) (Fig. 2), standardized quartz sand (Fig. 3) and water. The GGBFS was provided by Lafarge, Serbia, while the SHA was provided by company Victoria Oil, Sid, Serbia. The chemical composition of the GGBFS and SHA was determined by X-ray fluoresence (Tab. 1).

Fig. 1 Sunflower husk ash

Fig. 2 Ground granulated blast furnace slag

Tab. 1 Chemical composition of GGBFS and SHA (X-ray fluorescence)

Oxide [%]	SiO_2	Al_2O_3	Fe_2O_3	CaO	MgO	SO_3	K_2O	Na_2O	MnO	TiO_2	Cl^-
GGBFS	38.19	10.28	0.31	37.04	9.69	0.75	0.87	0.39	0.52	0.37	-
SHA	5.34	1.19	1.03	12.96	9.94	9.71	44.76	0.68	0.06	-	1.74

Fig. 3 Standardized sand used in experiment: a) 0.08-0.16 mm, b) 0.16-0.5 mm, c) 0.5-1.0 mm, d)1.0-2.0 mm

2.2. MIX DESIGN, MIXING AND SAMPLE CASTING

The water-to-binder ratio (w/b) and GGBFS content were constant in all three AA mortar mixes. The binder content was calculated as the sum of GGBFS and SHA content soluble in water. The SHA content was varied by mass of GGBFS (25%, 30% and 35%). The aggregate-to-binder ratio was 1:3. The mix design of AA mortar mixes is presented in Tab. 2.

Tab. 2 Mix design of three AA mortar mixes

Mix	w/b	GGBFS [kg]	SHA [kg]	Water [kg]	Stand. sand I* [kg]	Stand. sand II* [kg]	Stand. sand III* [kg]	Stand. sand IV* [kg]
M1	0.45	375.0	94.00	187.82	266.80	133.42	400.25	400.25
M2	0.45	375.0	112.50	195.45	270.20	135.10	405.30	405.30
M3	0.45	375.0	131.25	191.63	273.60	136.80	410.35	410.35

*I-0.008-0.16mm; II-0.16-0.5mm; III – 0.5-1.0mm; IV – 1.0-2.0mm

Solid components of the mix were pre-mixed dry and then mixed with water, manually for 1 minute. The mortar was then homogenized in mixer for 5 minutes.
Prism samples (4x4x16 cm) were cast in metal molds and sealed in polymeric films. After 24 hours, the samples were cured for 5 days at 65ºC. For the last 24 hours prior to testing, the samples were cured at ambient temperature.

2.3. METHODS

The compressive strength tests were performed after 7 days of curing on the set of three prism samples for each mix, as prescribed in SRPS EN 1015-11:1999 [12].
TGA was performed using the Labsys evo DTA/DSC1150 (Setaram), by heating approximately 30 mg of samples from 30ºC to 1000ºC, with a constant heating rate of 10ºC/min, in argon atmosphere. The samples for TGA were extracted from the mortar prisms after compressive strength tests. The hydration of the samples was stopped with isopropanol, and threrefore, the TGA results coresspond to the samples at the 7-days of age.

3. RESULTS AND DISCUSSION

The structure and composition of hydration products in AAMs depend on the chemistry and dosage of precursors and activators. The main hydration products of alkali-activated slag systems (i.e., high Ca content systems) are calcium silicate hydrate (C-S-H) and aluminum-substituted C-A-S-H gel. The secondary hydration products are AFm type phases and layered double hydroxide – hydrotalcite in the Mg-rich slags [13,14]. Depending on the alkali source, the C-A-S-H gel can incorporate alkali metal M^+ cations (C,M-A-S-H) [13]. The increase in alkali content from the activator induces the alkali reaction and formation of hydration products, thus leading to an increase in compressive strength [13].
The differential thermogravimetric (DTG) curves of the three mixes are shown in Fig. 4. Three characteristic peaks can be observed. The first peak in three mixes between 30ºC and 157ºC is attributed to the evaporation of structurally unbound water and dehydration of C-S-H [14,15] and C,K-S-H gels [15,16]. The shoulder around 200ºC presents two overlapped peaks: one indicating the formation of C-A-S-H and C,K-A-S-H gels and the other representing the formation of hydrotalcite [14–16]. Due to its layered structure, the hydrotalcite is also associated with peaks around 360ºC [14,15,17]. The same hydration products were identified by TGA in alkali-activated slag

pastes and mortars activated with other biomass ashes: olive stone ashes, almond shell ashes, hazelnut shell, nutshell and mango seed-bark ashes [15,16,18].

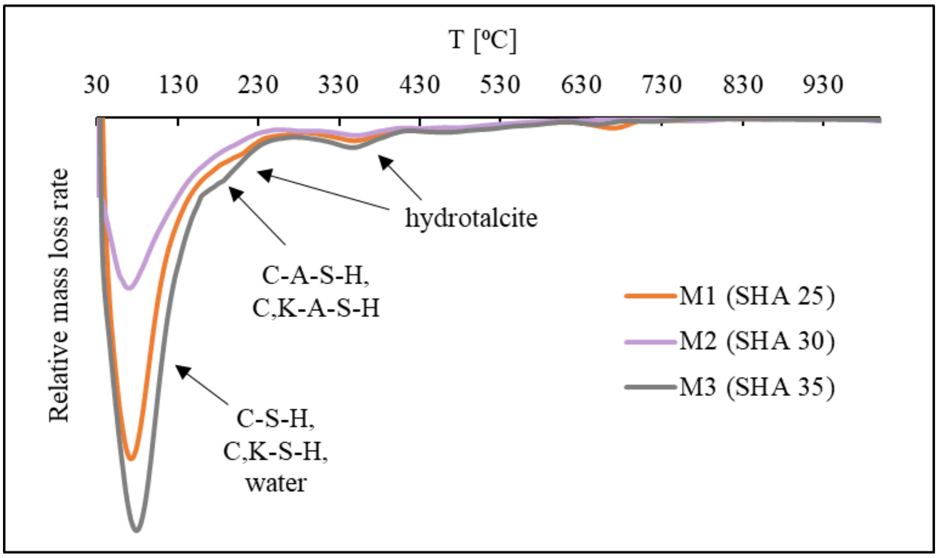

Fig. 4 DTG curves of three AA mortar mixes after 7 days of curing

The highest peaks of all hydration products were observed for the mix M3, then M1 and M2. The higher intensity of the DTG peak should indicate the formation of more hydration products, leading to a higher compressive strength. However, the TGA results did not entirely correspond to the compressive strength tests (Fig. 5). It is not clear why, but similar conflicting results were found in the literature [16].

The compressive strength results for different biomass ash content are reported mostly for 7-day compressive strength (cca 8-40 MPa) [15,19–21] and rarely for 3 (7.8 MPa) [20] and 28-day (25.05-33MPa) [18,22] compressive strength, for mortar samples. Most of the papers found a 7-day curing regime at 65ºC suitable for the slag-based biomass ash activated systems.

The 7-day compressive strength results of SHA activated slag mortars indicated that the highest compressive strength was attained with 25 wt% GGBFS of activator (Fig. 5), reaching 29 MPa. The increase in SHA content for 5% and 10% in the mixes M2 and M3 has led to a slight decrease in compressive strength.

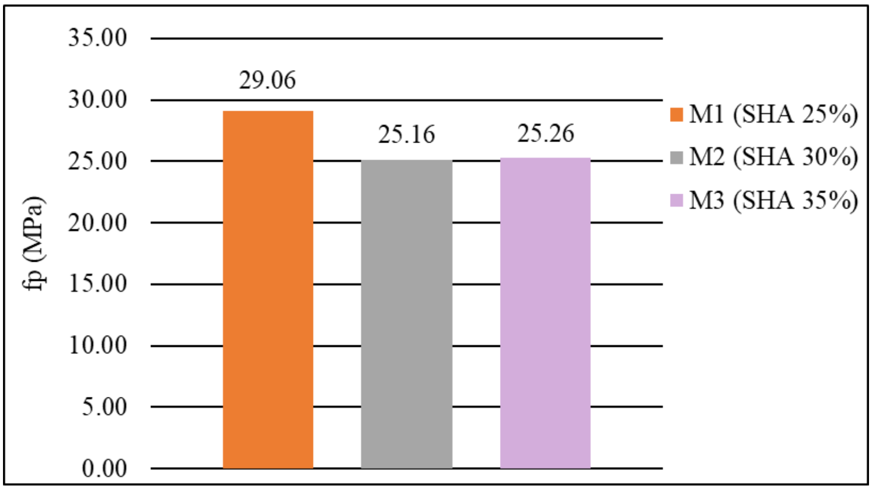

Fig. 5 Compressive strength of three AA mortar mixes after 7 days of curing

Furthermore, there was no difference between the compressive strength of the mixes with increased SHA content (25.16 MPa and 25.26 MPa). This could be explained by the ratio of precursor and alkali in the mix. The highest compressive strength of the given AAM system is achieved when all of the precursor reacts, which is possible if there is enough activator. If there is no unreacted precursor left, the excessive amount of alkalis will not result in strength gain. It is possible that the optimal alkali content for the activation of the whole GGBFS in the system was achieved for the mix M1, with 25% of SHA.

4. CONCLUSIONS

The paper presents the results of TGA and compressive strength analysis of three 100% waste-based AA slag mortars, activated with 25, 30 and 35% of SHA (by mass of slag). The TGA analysis showed that the main hydration products in all mixes are C,(K)-S-H and C,(K)-A-S-H gels, and hydrotalcite. The highest compressive strength (29 MPa) was obtained by mix with 25% of SHA. The formation of the same characteristic hydration products and comparable compressive strengths as reported in the literature are promising in terms of SHA utilization in AAM technology.
Valorizing locally available waste from biomass energy production - SHA - as an alternative activator for cement-free AAMs, would contribute to multiple benefits - not only to the reduction of CO_2 emissions and material costs but also to reinforcing the circular economy concepts in the construction sector.

ACKNOWLEDGEMENT

This research has been conducted within the project “Scientific theoretical and experimental research and improvement of educational process in the field of civil engineering”, developed at the Department of Civil Engineering and Geodesy, Faculty of Technical Sciences, University of Novi Sad, Serbia. Research is also supported by the project “Alternative Binders for Concrete: understanding microstructure to predict durability, ABC”, funded by the Croatian Science Foundation under number UIP-05-2017-4767.

REFERENCES

[1] Agrela F., Cabrera M., Morales M.M., Zamorano M., Alshaaer M. (2019). Biomass fly ash and biomass bottom ash. *New Trends in Eco-efficient and Recycled Concrete*, p. 23–58. https://doi.org/10.1016/B978-0-08-102480-5.00002-6.

[2] Hills C.D., Tripathi N., Singh R.S., Carey P.J., Lowry F. (2020). Valorisation of agricultural biomass-ash with CO_2. *Scientific Reports*, Volume 10:13801. https://doi.org/10.1038/s41598-020-70504-1.

[3] Communication From The Commission To The European Parliament, The Council, The European Economic And Social Committee And The Committee Of The Regions - The European Green Deal 2020.

[4] A new Circular Economy Action Plan For a Cleaner and More Competitive Europe 2020.

[5] A sustainable bioeconomy for Europe: strengthening the connection between economy, society and the environment 2018.

[6] He .J, Kawasaki S., Achal V. (2020). The Utilization of Agricultural Waste as Agro-Cement in Concrete: A Review. *Sustainability*, Volume 12:6971. https://doi.org/10.3390/su12176971.

[7] Ramagiri K.K., Kar A. (2021). Environmental impact assessment of alkali-activated mortar with waste precursors and activators. *Journal of Building Engineering*, Volume 44:103391. https://doi.org/10.1016/j.jobe.2021.103391.

[8] Alnahhal M.F., Kim T., Hajimohammadi A. (2021). Waste-derived activators for alkali-activated materials: A review. *Cement and Concrete Composites*, Volume 118:103980. https://doi.org/10.1016/j.cemconcomp.2021.103980.

[9] Provis J.L. (2014). Geopolymers and other alkali activated materials: why, how, and what? *Materials and Structures,* Volume 47:11–25. https://doi.org/10.1617/s11527-013-0211-5.

[10] Segura I.P., Luukkonen T., Yliniemi J., Sreenivasan H., Damø A.J., Jensen L.S., et al. (2022). Comparison of One-Part and Two-Part Alkali-Activated Metakaolin and Blast Furnace Slag. *Journal of Sustainable Metallurgy*, Volume 8:1816–30. https://doi.org/10.1007/s40831-022-00606-9.

[11] Wang K., Tester J.W. (2023). Sustainable management of unavoidable biomass wastes. *Green Energy and Resources,* Volume 1:100005. https://doi.org/10.1016/j.gerr.2023.100005.

[12] SRPS EN 1015-11-1999 - Methods of test for mortar for masonry. Determination of flexural and compressive strength of hardened mortar 1999.

[13] Provis J.L., van Deventer J.S.J., editors. (2014). Alkali Activated Materials - State of the Art Report TC 224-AAM. vol. 13. Dordrecht: Springer Netherlands; https://doi.org/10.1007/978-94-007-7672-2.

[14] Ben Haha M., Le Saout G., Winnefeld F., Lothenbach B. (2011). Influence of activator type on hydration kinetics, hydrate assemblage and microstructural development of alkali activated blast-furnace slags. *Cement and Concrete Research*, Volume 41:301–10. https://doi.org/10.1016/j.cemconres.2010.11.016.

[15] de Moraes Pinheiro SM, Font A, Soriano L, Tashima MM, Monzó J, Borrachero MV, et al. (2018). Olive-stone biomass ash (OBA): An alternative alkaline source for the blast furnace slag activation. *Construction and Building Materials,* Volume 178, p. 327–38. https://doi.org/10.1016/j.conbuildmat.2018.05.157.

[16] Soriano L., Font A., Tashima M.M., Monzó J., Borrachero M.V., Payá J. (2020). One-part blast furnace slag mortars activated with almond-shell biomass ash: A new 100% waste-based material. *Materials Letters*, Volume 272:127882. https://doi.org/10.1016/j.matlet.2020.127882.

[17] Gruskovnjak A., Lothenbach B., Holzer L., Figi R., Winnefeld F. (2006). Hydration of alkali-activated slag: comparison with ordinary Portland cement. *Advances in Cement Research*, Volume 18, p. 119–128. https://doi.org/10.1680/adcr.2006.18.3.119.

[18] Soriano L., Font A., Borrachero M.V., Monzó J.M., Payá J., Tashima M.M. (2022). Biomass ashes to produce an alternative alkaline activator for alkali-activated cements. *Materials Letters*, Volume 308:131198. https://doi.org/10.1016/j.matlet.2021.131198.

[19] Font A., Soriano L., de Moraes Pinheiro S.M., Tashima M.M., Monzó J., Borrachero M.V., et al. (2020). Design and properties of 100% waste-based ternary alkali-activated mortars: Blast furnace slag, olive-stone biomass ash and rice husk ash. *Journal of Cleaner Production*, Volume 243:118568. https://doi.org/10.1016/j.jclepro.2019.118568.

[20] Font A., Soriano L., Moraes J.C.B., Tashima M.M., Monzó J., Borrachero M.V., et al. (2017). A 100% waste-based alkali-activated material by using olive-stone biomass ash (OBA) and blast furnace slag (BFS). *Materials Letters*, Volume 203:46–9. https://doi.org/10.1016/j.matlet.2017.05.129.

[21] Soriano L., Font A., Tashima M.M.., Monzó J, Borrachero M.V., Bonifácio T., et al. (2021) Almond-shell biomass ash (ABA): A greener alternative to the use of commercial alkaline reagents in alkali-activated cement. *Construction and Building Materials*, Volume 290:123251. https://doi.org/10.1016/j.conbuildmat.2021.123251.

[22] Alonso M.M., Gascó C., Morales M.M., Suárez-Navarro J.A., Zamorano M., Puertas F. (2019). Olive biomass ash as an alternative activator in geopolymer formation: A study of strength, radiology and leaching behaviour. *Cement and Concrete* Composites, Volume 104:103384. https://doi.org/10.1016/j.cemconcomp.2019.103384.

VALORIZATION OF CORN COB ASH AS AN ENVIRONMENTALLY FRIENDLY SCM IN MASONRY MORTAR

Slobodan Šupić[1], Vladan Pantić[2], Gordana Broćeta[3], Ivan Lukić[4], Anđelko Cumbo[5]

Summary:

In response to the urgent demand for more environmentally acceptable building materials made from locally accessible wastes, masonry mortars including the agricultural by-product Corn Cob Ash (CCA) as supplementary cementitious material (SCM) were explored. In the experimental study, four mortar mixtures (volume ratio: 1:1:4) were designed with cement replacement ratios ranging from 0% to 80%, by mass. The basic masonry mortar properties were investigated, including workability, compressive strength, flexural strength, capillary water absorption and adhesive strength. Owing to the higher water demand and, consequently, increased water to binder ratio, the mechanical properties of the blended mortars were reduced, while the porosity and the capillary water absorption rose as the quantity of CCA increased. Nonetheless, some mixtures met the strength criteria for structural masonry mortar, making them both applicable and sustainable.

Key words: masonry mortar, corn cob ash, cement replacement, sustainable

[1] Assist. prof., Faculty of Technical Sciences, University of Novi Sad, Serbia, ssupic@uns.ac.rs
[2] Teach. assist., Faculty of Technical Sciences, University of Novi Sad, Serbia, pantic_vladan @uns.ac.rs
[3] Assoc. prof., Faculty of architecture, civil engineering and geodesy, University of Banja Luka, Bosnia and Herzegovina, gordana.broceta@aggf.unibl.org
[4] Assoc. prof., Faculty of Technical Sciences, University of Novi Sad, Serbia, lookic@uns.ac.rs
[5] Assist. prof., Faculty of architecture, civil engineering and geodesy, University of Banja Luka, Bosnia and Herzegovina, andjelko.cumbo@aggf.unibl.org

1. INTRODUCTION

In recent decades, as urbanization has spread rapidly throughout the world, the volume of industrial and agricultural solid waste has increased as well. One of the biggest obstacles to sustainable urban development is the proper use of these wastes as opposed to landfilling. In Serbia, it is believed that 300 million tons of fly ash (FA) have already been deposited on an area larger than 1500 ha [1]. The utilization rate of FA, which is currently 53.5% worldwide and varies greatly from nearly 100% in Japan to barely a few percentages, such up to 3% in Serbia, is regrettably not as efficient as its production. FA is hence typically disposed of in landfills, posing a variety of disposal and health risks. On a similar line, agricultural waste, which accumulates in increasing volumes every year and constitutes a serious threat to the environment when dumped in landfills, is another solid waste that needs to be taken into account for environmental preservation. With 1.67 tons of oil equivalent, agricultural biomass, or harvest wastes, is Vojvodina's primary renewable energy source (RES). Although only around 2% of this resource is actually used, a large amount of biomass ash (BA), roughly 5000 tons annually, gets produced as a waste product during the combustion of harvest residues.
Other than FA and BA, ceramic waste is an important resource and waste in Vojvodina. Ceramic waste is mostly generated after the demolishing of masonry structures (demolition waste), during the construction of new structures (construction waste), or as a result of manufacturing mistakes (industrial waste). The overall waste generated by ceramic manufacturing facilities accounts for 3-7% of their annual final output. Approximately 6,000 tons of ceramic waste are thought to be produced annually by the Vojvodina ceramic industry [2]. The use of fly ash, corn cob ash (CCA), and ceramic waste powder (CWP) as cement replacement materials in cement-based composites has been the subject of extensive investigation in recent years [3]. Numerous studies have shown that employing these byproducts can improve the durability and microstructure of cement-based mortar and concrete. On another note, there has been scarce research on using industrial and agricultural waste in masonry aplications. The authors of this study assessed the effects of locally sourced agricultural and industrial wastes, including CWP, FA, and CCA, on following masonry mortar properties: workability, compressive strength, flexural strength, capillary water absorption and adhesive bond strength. The results of this study could pave the way for the clever use of FA, CCA, and CWP as more environmentally friendly binder materials in modern construction, which would reduce carbon emissions, increase cost effectiveness, and lessen the damaging environmental effects of waste landfilling.

2. MATERIALS AND METHODS

2.1. MATERIALS

2.1.1. Cement

Ordinary Portland Cement (OPC), produced by the Lafarge cement plant in Vojvodina, was used. The cement has a Blaine fineness of 4.000 cm^2/g and a density of 3.1 g/cm^3.

2.1.2. Corn cob ash

Corn cob ash (CCA) was gathered from the "ALMEX-IPOK" starch factory, which produces large volumes of CCA as a byproduct from using biomass waste (corn cob) as an energy source. The ash sample was processed in a laboratory ball mill to produce a material with acceptable fineness (6800 cm^2/g). The chemical composition of cement and CCA is displayed in the forecoming Table. CCA is characterized with the pozzolanicity class 5, while it met the requirements regarding the activity index (the values of index at the age of 28 and 90 days are 101% and 103%, respectively), in accordance with EN 450-1 [7].

Tab. 1 Chemical compositions of cement and CCA

	LOI	SiO_2	Al_2O_3	Fe_2O_3	Na_2O	K_2O	MgO	CaO	SO_3	P_2O_5	Cl^-	Reactive SiO_2
C	/	17,34	4,53	20,64	0,20	0,59	1,93	50,26	3,06	0,00	0,00	/
CCA	2,4	45,76	5,91	3,37	0	13,1	8,3	14,08	1,26	2,81	0,5	38,21

2.1.3. Fine aggregate

The river sand was used as a fine aggregate in the manufacture of mortar. Sand has a specific gravity of 2.3 g/cm^3 and a fineness modulus of 0.97.

2.1.4. Water

Tap water was used for producing masonry mortar. The water-to-binder ratio (w/b) was adjusted in order to achieve the required workability of masonry mortar (175±10 mm), as advised by SRPS EN 1015-2 [8].

2.2. METHODS

The chemical composition of raw materials was evaluated according to EN 196-2 [9] and ISO 29581-2 [10]. The pozzolanic activity was assessed on specimens prepared in accordance with the instructions provided in SRPS B.C1.018 [11]. Mechanical properties (compressive and flexural strength) were tested in accordance with EN 998-2 [12] and EN 1015-11 [13] guidelines. The workability of fresh mortar (flow value) was detemined in accordance with EN 1015-3 [14]. The water absorption coefficient caused by the capillary action of hardened mortar was estimated using the parameters listed in EN 1015-18 [15]. The EN 1015-12 [16] methodology was followed to measure the adhesive strength of hardened mortars on substrates. The number and the dimensions of the specimens were determined based on the above-listed requirements.

2.3. MIXING AND PROPORTIONING OF MORTARS

Four different mortar mixtures were cast in the experimental investigation. The mixing ratio of components of reference cement-lime mortar (C) was 1:1:4 (cement/lime/sand), by volume. In the remaining three mixtures, 50%, 60% or 80% of cement was substituted with CCA, by volume (cement and CCA have apparent bulk densities of 1000kg/m^3 and 700kg/m^3, respectively). Based on the required workability, the appropriate amount of water was determined. Table 2 shows the labels and quantities of component materials for each masonry mortar.

Tab. 2 Labels and component material quantities for designed masonry mortars

Mortar	m_c (g)	m_l (g)	m_s (g)	m_{scm} (g)	w/b	m_w (g)
C	201.8	92.5	1350	/	0.90	264.9
CCA-50	100.9	92.5	1350	71.6	1.00	265.0
CCA-60	80.7	92.5	1350	85.9	1.03	266.9
CCA-80	40.4	92.5	1350	114.5	1.08	267.2

m_c-mass of cement; m_l-mass of lime; m_s-mass of sand; m_{scm}-mass of SCM; m_w-mass of water; w/b-water to binder ratio.

3. TEST RESULTS AND DISCUSSION

3.1. WORKABILITY OF FRESH MORTAR

The influence of water to binder ratio (w/b) on the necessary workability (175±10 mm) was determined on the flow table. The flow values are given in Figure 1.

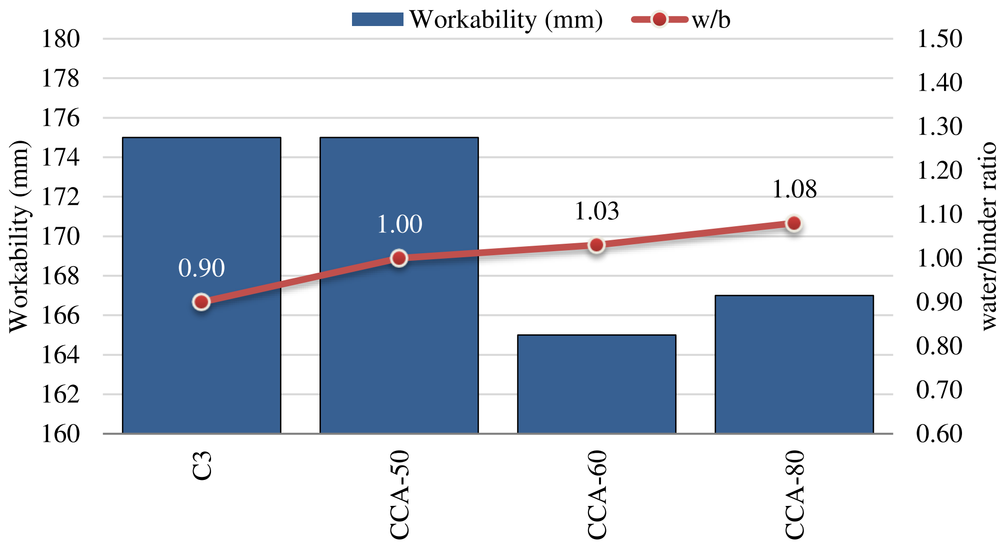

Fig. 1 Flow values of fresh mortar

It is clear that all blended mortar combinations needed more water to reach their targeted flow value. As the workability of cement composites depends mainly on the shape of its particles, this effect can be ascribed to the angularity and sharp edges of ash particles. Resultantly, w/b rises with the increase of CCA content. Furthermore, the higher level of fineness plays its dominating role when CCA content rises, which in turn increases the water demand.

3.2. FLEXURAL STRENGTH OF HARDENED MORTAR

Flexural strength results of the hardened masonry mortar are shown in Figure 2.

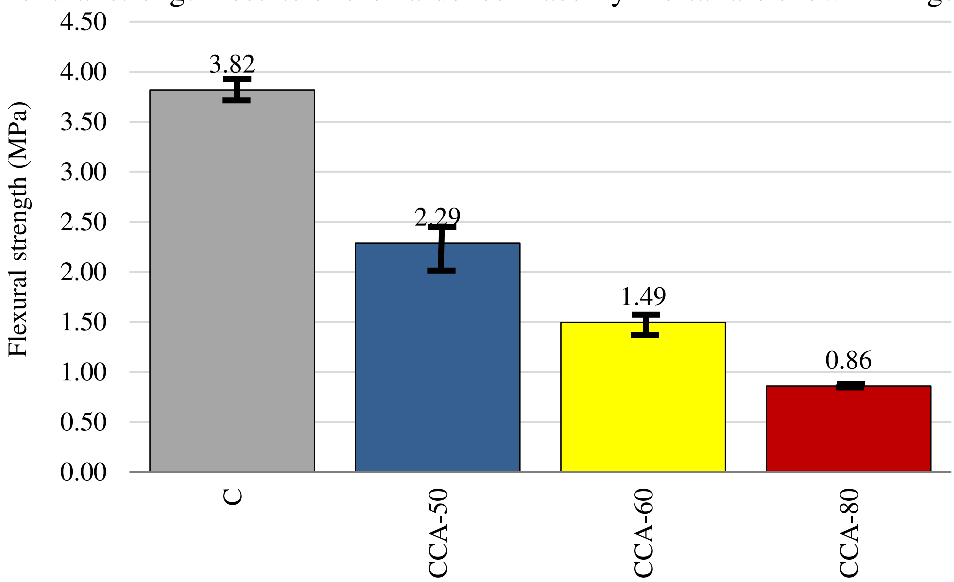

Fig. 2 The flexural strength of mortars

The use of CCA, as cement replacing material, caused a sharp flexural strength decrease. At the 28-day age, blended mixtures (CCA-50, CCA-60 and CCA-80) attained about 60%, 39% and 23% of the control flexural strength, respectively. This remarkable strength reduction can be attributed to 1) the excess water provided for workability adjustment, i.e., increased w/b, and 2) the dilution effect (the reduction in the cement content, i.e., decreased number of hydration products). However, it should be emphasized that, unlike workability, adhesive strength, and compressive strength, flexural strength is not of prime importance for masonry applications.

3.3. COMPRESSIVE STRENGTH OF HARDENED MORTAR

The compressive strength results follow a similar pattern to the flexural strength tests. In general, the trend of the compressive strength reveals that the addition of CCA reduces the strength to a significant extent (Fig. 3).

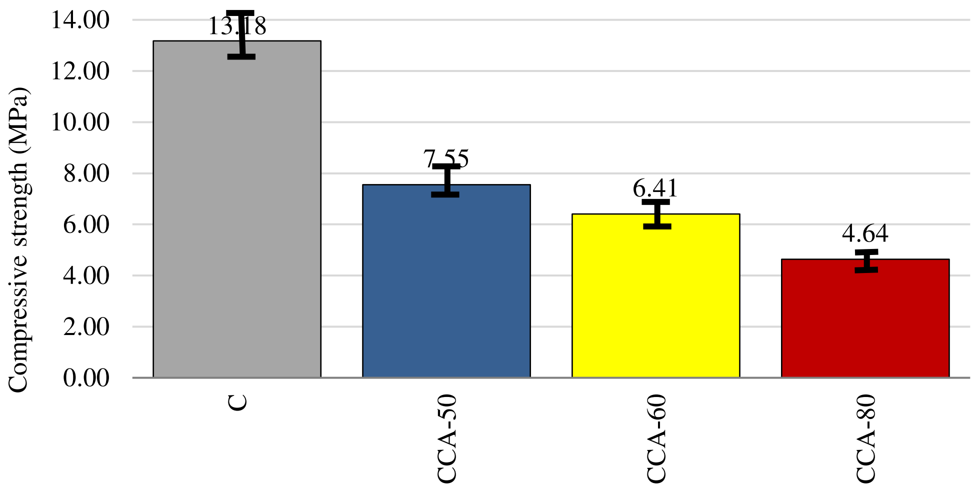

Fig. 3 The compressive strength of mortars

As shown in Figure above, the inclusion of 50%, 60% and 80% of CCA reduced the compressive strength by about 43%, 51%, and 65%, respectively, compared to the control mix. The lower hydration activity of CCA, i.e., the dilution effect could be the reason for the decrease in compressive strength. On a more important note, w/b is also an essential factor influencing the mechanical properties of cement-based composites. Higher w/b caused the mortar blends to have greater total and capillary porosity, which reduced the amount of hydration products and decreased compressive strength.
Masonry mortars are classified into classes depending on their mean compressive strength, as defined by EN 998-2. Eurocode 6 and Eurocode 8 specify a minimum compressive strength of 5MPa for masonry mortars for load-bearing structures, i.e., Class 5. Table 3 shows the average compressive strength and attained class of each mortar.

Tab. 3 Class of masonry mortars based on the achieved compressive strength

Mortar	C	CCA-50	CCA-60	CCA-80
Compressive strength (MPa)	13,18	7,55	6,41	4,64
Class	**10**	**5**	**5**	**2,5**

As displayed in the Table, reference mortar and blends with up to 60% cement replacement meet the criteria for masonry mortar for structural applications, while the mortar CCA-80 achieved the class of 2.5 and can thus be utilized successfully for masonry applications for non-load-bearing elements (such as infill and partition walls).

3.4. CAPILLARY WATER ABSORPTION OF HARDENED MORTAR

Capillary water absorption coefficients of all tested mortar mixtures, as well as the limit for the achieved absorption class, are displayed in Fig. 4.

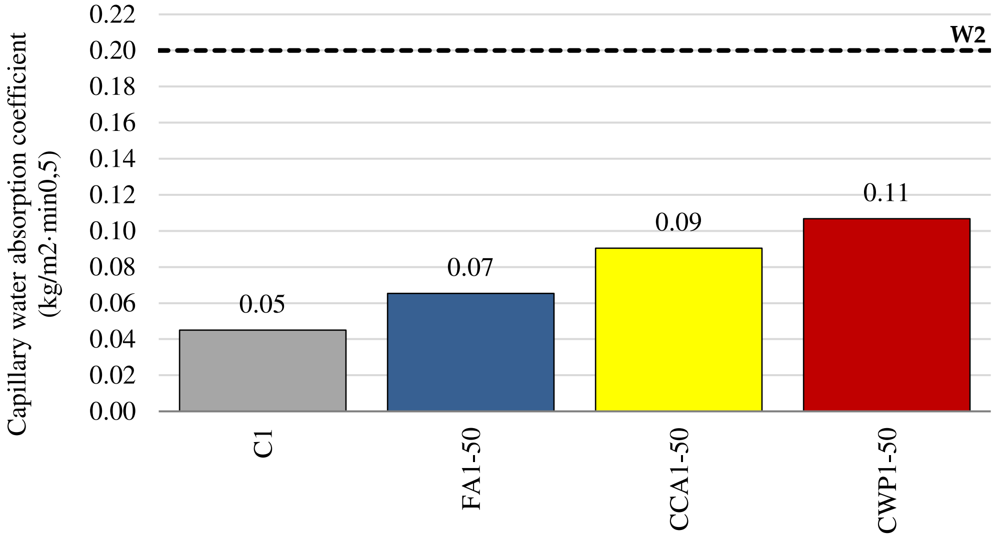

Fig. 4 Capillary water absorption coefficients of mortars

The water-to-binder ratio is one of the crucial factors in cement-based materials that affects the pore structure and capillary water absorption capacities. As aforementioned, all CCA-modified mortars were produced with an additional amount of water aiming to satisfy the required workability. Accordingly, employing a greater w/b ratio, the mortar mixtures' capillary porosity increased as the CCA content grew, leading to a higher absorption coefficient. When compared with the reference mortar, CCA-50, CCA-60 and CCA-80 exhibited higher capillary water absorption coefficients by 44%, 100%, and 138%, respectively.

Based on the computed water absorption coefficient at the age of 28 days, masonry mortars can be categorized, as recommended by EN 998-2. As all mortars satisfy the criterion for the optimal W2 category (<0.2 kg/m^{2}min$^{0.5}$), it can be stated that the substitution of cement with CCA does not jeopardy this property of mortar to a greater extent, regardless of the substitution level.

3.5. ADHESIVE STRENGTH OF HARDENED MORTAR

The adhesive bond strength results are shown in Fig. 5.

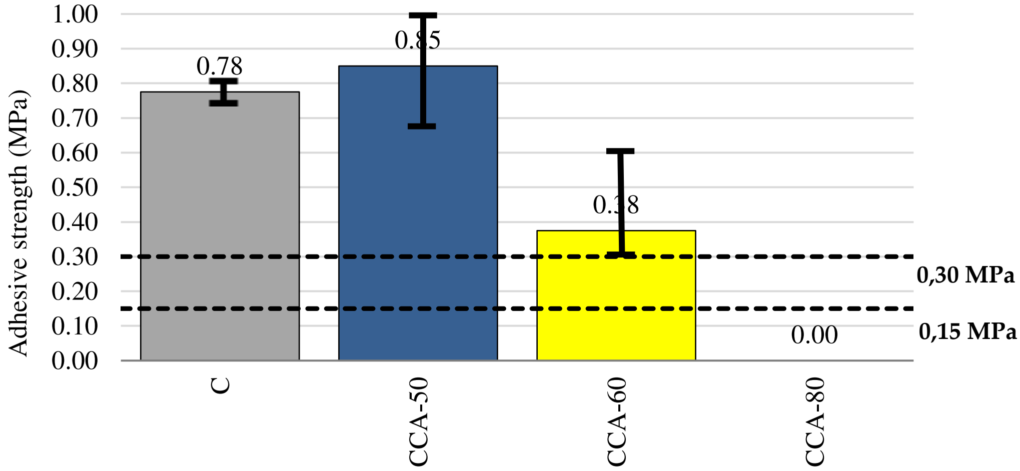

Fig. 5 Adhesive strength of mortars

The results indicate that 50% cement replacement resulted in an increase of the adhesive bond strenght, as CCA-50 exceeded the strength of the reference mortar by 9%. It may be assumed that finer particles of CCA-blended mix might have improved the adhesion of the mortar owing to a smaller number of voids present in between grains. Beyond this replacement level, a sharp strength decrease was observed, i.e., 51% for CCA-60. The adhesive strength of the mix with the largest CCA share was insufficient for the pull off tester to measure it.

A minimum value of 0.3 MPa is required by the EN 998-1 mortar regulation for use in rendering or plastering, while a minimum value of 0.15 MPa is required by the EN 998-2 masonry mortar regulation. All mortar combinations, apart from CCA-80, met the criteria for both plastering and masonry applications.

The EN 1015-12 specification classifies the possible fracture patterns into three categories: a) adhesion fracture: a fracture at the mortar-substrate interface, test value is equivalent to the adhesive strength; b) cohesion fracture: a fracture in the mortar itself, the adhesive bond is stronger than the test value; c) cohesion fracture: a fracture in the substrate material, the adhesive bond is stronger than the test value. Recorded fracture patterns of masonry mortars are listed in fore-coming Table.

Tab. 4 Fracture patterns of mortars

Mortar	C	CCA-50	CCA-60	CCA-80
Pattern	a	b	b	a

4. CONCLUSIONS

The principal findings of the study are as follows:

- Chemical composition of finely ground CCA indicates a relatively high content of amorphous silica, which positively influences the pozzolanic activity and manifests in high activity index,
- CCA, as a conventional pozzolanic material, require more water to ensure that the necessary workability can be attained when used as partial cement replacement material in masonry mortar,
- Taking into account the achieved compressive strength, blended mortars with up to 60% cement substitution met the requirement for structural application, while the blended mortar CCA-80 satisfied the requirement for non-load-bearing masonry elements,
- The capillary water absorption of blended mortar significantly increased as a result of the increased w/b. Despite this pattern, all mixtures exhibited capillary water absorption coefficient values that fell within the W2 category's acceptable range,
- Mortars with up to 60% cement substitution exceeded the required adhesive strength limit of 0.15 MPa, complying with the requirement,
- In light of all the findings, blended mortars CCA-50 and CCA-60 can be rated appropriate in terms of their mechanical and physical performances.

ACKNOWLEDGEMENT

This research was funded by the Provincial Secretariat for Higher Education and Scientific Research of the Autonomous Province of Vojvodina and conducted within the bilateral project between Faculty of technical sciences, University of Novi Sad and Faculty of Architecture, Civil Engineering and Geodesy, University of Banja Luka: “New technologies in the production of environmentally friendly mortar and concrete”, reference number: 142-451-374/2023-01/1.

REFERENCES

[1] Marinković S., Carević V., Dragaš, J. (2021). The role of service life in Life Cycle Assessment of concrete structures. Journal of Cleaner Production, Volume 290, 125610. https://doi.org/10.1016/j.jclepro.2020.125610.

[2] Šupić S., Malešev M., Radonjanin V., Pantić V., Lukić I., Bulatović V. (2021). Characterization of harvest residues ashes and ceramic waste powders originating from Vojvodina as potential supplementary cementitious materials. Building Materials and Structures, Volume 64, pp. 155-166, https://doi.org/10.5937/GRMK2204155S.

[3] Pantić V., Šupić S., Vučinić-Vasić M., Nemeš T., Malešev M., Lukić I., Radonjanin V. (2023). Effects of Grinding Methods and Water-to-Binder Ratio on the Properties of Cement Mortars Blended with Biomass Ash and Ceramic Powder. Materials, Volume 16, 2443. https://doi.org/10.3390/ma16062443.

[4] Malešev M., Radonjanin V., Draganić S., Šupić S., Laban M. (2017). Influence of fly ash and decreasing water-powder ratio on performance of recycled aggregate concrete. Građevinar -Journal of the Croatian Association of Civil Engineers. Volume 69, pp. 811–820. https://doi.org/10.14256/JCE.1379.2015.

[5] Şerbănoiu A.A., Grădinaru C.M., Muntean R., Cimpoeşu N., Şerbănoiu, B.V. (2022). Corn Cob Ash versus Sunflower Stalk Ash, Two Sustainable Raw Materials in an Analysis of Their Effects on the Concrete Properties. Materials, Volume 15, 868. https://doi.org/10.3390/ma15030868.

[6] Olatoyan J.O., Kareem M.A., Adebanjo A.U., Olawale S.O.A., Alao. K.T. (2023). Potential use of biomass ash as a sustainable alternative for fly ash in concrete production: A review. Hybrid Advances, Volume 4, https://doi.org/10.1016/j.hybadv.2023.100076.

[7] EN 450-1. *Fly Ash for Concrete*; Part 1. Definition, specifications and conformity criteria. Institute for Standardization of Serbia; 2014.

[8] EN 1015-2. *Methods of Test for Mortar for Masonry*; Part 2: Bulk sampling of mortars and preparation of test mortars. Institute for Standardization of Serbia; 2008.

[9] EN 196-2. *Method of Testing Cement*; Part 2. Chemical analysis of cement. Institute for Standardization of Serbia; 2015.

[10] ISO 29581-2. *Cement-Test Methods*; Part 2. Chemical analysis by X-ray fluorescence. Institute for Standardization of Serbia; 2010.

[11] SRPS B.C1.018. Non-Metallic Mineral Raws, Pozzolanic Materials, Constituents for Cement Production Classification, Technical Conditions and Test Methods. Institute for Standardization of Serbia; 2015.

[12] EN 998-2. Specification for mortar for masonry; Part 2: Masonry mortar. Institute for Standardization of Serbia; 2017.

[13] EN 1015-11. Methods of test for mortar for masonry; Part 11: Determination of flexural and compressive strength of hardened mortar. Institute for Standardization of Serbia; 2019.

[14] EN 1015-3. Methods of test for mortar for masonry; Part 3: Determination of consistence of fresh mortar (by flow table). Institute for Standardization of Serbia; 2008.

[15] EN 1015-18. Methods of test for mortar for masonry; Part 18: Determination of water absorption coefficient due to capillary action of hardened mortar. Institute for Standardization of Serbia; 2008.

[16] EN 1015-12. Methods of test for mortar for masonry; Part 12: Determination of adhesive strength of hardened rendering and plastering mortars on substrates. Institute for Standardization of Serbia; 2016.

REACTIVITY OF NATURAL POZZOLANS IN LIME MORTARS

Martin Vyšvařil[1], Tomáš Žižlavský[2], Martin Krebs[3], Karel Dvořák[4]

Summary:

Today, lime-pozzolan mortars are being used in the repair of historic buildings, replacing the lime-cement mortars that were previously used in this practice, but were incompatible with historic mortars. In this paper, the pozzolanic reactivity of seven different natural finely ground thermally untreated pozzolans (trass, pozzolanic earth, chalcedonite, pumice, zeolite, spongilite and lava) in lime mortars is investigated. All lime-pozzolan mortars achieved higher strengths than the reference lime mortar, especially after 90 and 180 days. Surprisingly, no clear correlation was observed between the pozzolanic activity of the natural pozzolans, determined by the Chapelle test, and the strength of the mortars. In order to successfully assess the reactivity of a pozzolan, it is not sufficient to determine just the pozzolanic activity, but it is also necessary to know its mineralogical composition and the chemical composition of the amorphous phases in detail and simulate the practical use of the lime-pozzolan mortar.

Key words: amorphous phase, lime mortar, mineralogical composition, natural pozzolan, pozzolanic activity, strength

[1] Assist. prof., Faculty of Civil Engineering, Brno University of Technology, Brno, Czechia, vysvaril.m@fce.vutbr.cz
[2] PhD student, Faculty of Civil Engineering, Brno University of Technology, Brno, Czechia, zizlavsky.t@fce.vutbr.cz
[3] Student, Faculty of Civil Engineering, Brno University of Technology, Brno, Czechia, 214339@vutbr.cz
[4] Assoc. prof., Faculty of Civil Engineering, Brno University of Technology, Brno, Czechia, dvorak.k@fce.vutbr.cz

1. INTRODUCTION

Air lime-pozzolan mortars have a long tradition in application in the construction industry in many places in the world, especially in volcanic areas. Pozzolanic materials are nowadays often ground and sieved into fine particles with a high specific surface area and impart hydraulic properties to air lime mortars. At the same time, air lime-pozzolan mortars retain most of the good characteristics of pure air lime mortars, such as low modulus of elasticity and fast drying. The addition of pozzolans therefore extends the potential range of applications for air lime mortars. The most commonly used natural pozzolans are tuffs, tuffites, diatomaceous earth, zeolites, trass or pumice. The term pozzolanic activity is often used to describe the reactivity of the pozzolan, which includes all the reactions that occur between the active components of the pozzolan, calcium hydroxide and water. Pozzolanic activity essentially defines two values, the maximum amount of lime that the pozzolan can react with (bind) and the rate at which it does so. Both aspects depend on the type of pozzolan used and, above all, on the quality and quantity of the active ingredients it contains. Other influencing parameters are lime/pozzolan ratio in the mix, treatment time, specific surface area, water content in the mix, chemical composition, and temperature [1].

The products of the reaction of pozzolan with calcium hydroxide in water are similar to those formed during the hydration of Portland cement, i.e. hydrated calcium silicates (CSH) and hexagonal calcium aluminates (C_4AH_{13}). By prolonging the reaction time between pozzolan and $Ca(OH)_2$, it is possible to recognize other compounds such as gehlenite (C_2ASH_8) and also monocarboaluminate ($C_3ACaCO_3H_{12}$), hydrogarnet (C_3AH_6), and hibschite ($C_3AS_2H_2$); if gypsum is present in the lime-pozzolan mixture, ettringite is also formed [1]. Pozzolanic activity can be determined by several direct or indirect methods, where direct methods monitor the presence of $Ca(OH)_2$ and subsequent reduction of its amount during the pozzolanic reaction using analytical methods, e.g. Frattini test according to EN 196-5 or Chapelle test [2]. On the other hand, indirect methods are based on measuring mainly the physical properties of the tested samples or the composition of the pozzolan, which is an indicator of the degree of pozzolanic activity. These methods include chemical and mineralogical analysis of pozzolan, determination of reactive SiO_2 in pozzolan according to EN 196-2, electrical conductivity test [3], calorimetric measurements [4], strength characteristics (ASTM C 593-19), or determination of Strength Activity Index (SAI) described in ASTM C311. The mentioned methods for determining pozzolanic activity differ from each other in terms of complexity, method of evaluation, time-consuming and price of their execution. Some methods determine whether and to what extent a given raw material is pozzolanic active, others only characterize a certain property that affects the level of pozzolanic activity. The results of pozzolanic activity obtained by several methods are not always similar or comparable. Donatello et al. [5] compared different test methods for determining pozzolanic activity, namely the SAI, the Frattini test and a similar Frattini test, where the cement in the reaction mixture was replaced by lime water. A certain functional dependence was found only when comparing the Frattini test and the SAI. The results from the test with a saturated solution of $Ca(OH)_2$ did not correspond at all. Liu et al. compared the differences of six pozzolanic evaluation methods on five pozzolanic materials [6] and concluded that SAI is more objective in evaluating the activity based on strength, but there is also the aggregate effect on strength. The electrical conductivity test method is more suitable for evaluating the early pozzolanic reactivity. The evaluation results of the pozzolanicity test are limited by the slow dissolution rate of the active phase, and the dissolution characteristics of $Ca(OH)_2$. The high temperature in the modified Chapelle test makes the method more suitable for evaluating low-reactivity materials. The evaluation system of the thermogravimetric method is reasonable and most similar to the evaluation results of SAI. A modified R3

method is proposed to realize a more accurate simulation of the interstitial solution and a more accurate evaluation of pozzolanic reactivity [6].
Due to ambiguous results when comparing pozzolanic activity by different methods, the content of this paper focuses on the correlation between the chemical and mineralogical composition of seven different natural pozzolans with their pozzolanic activity determined by the Chapelle test and the strength characteristics of lime-pozzolan mortars.

2. MATERIALS AND METHODS

Hydrated lime CL90-S (Carmeuse Czech Republic s.r.o.) was used as a main binder in prepared mortar mixes. Washed quartz sand meeting EN 13139 (fraction 0/2 mm supplied by Filtrační Písky s.r.o.) was used as an aggregate. Seven different natural pozzolans was used as a lime substitute, namely, the trass (0–125 µm, Tubag), the pozzolanic earth (0–125 um, Kremer Pigmente GmbH & Co), the zeolite (0–125 µm, Zeocem, a.s.), the fine chalcedonite powder with the maximum particle size of 40 µm (CRUSIL Spółka z o.o.), the pumice (0–125 µm, Vulkalit WR, Vulcatec Riebensahm GmbH), the spongilite powder (0–125 µm, Kalcit s.r.o.), the ground lava sand (0-125 µm, Der Naturstein Garten). The particle size distribution of the natural pozzolans determined by laser particle analyzer in isopropyl alcohol solution is compared in Figure 1. It is evident that the chalcedonite powder consisted mainly of particles between 1 and 20 µm, i.e. smaller than the other pozzolans, which is reflected in its largest specific surface area (Table 1). The other pozzolans contained mainly particles with sizes between 5 and 70 µm.

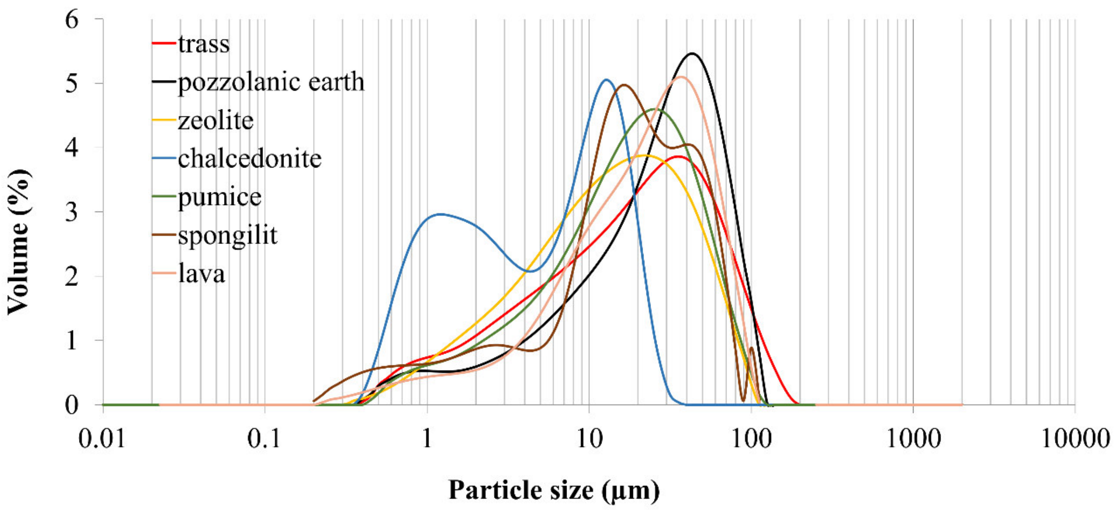

Fig. 1 Particle size distribution of natural pozzolans

Fundamental physical parameters of natural pozzolans such as particle density, specific surface area (S_g) and loose bulk density as defined by EN 196-6 are summarized in Table 1. The low loose bulk density values of zeolite and chalcedonite are caused by the porous structure of their particles and, in the case of zeolite, also by the low particle density. The specific surface of pozzolans varied depending on particle size distribution and particle morphology. The amount of amorphous phase in the pozzolan also plays a part - as its content increases, the specific surface area also increases. The chemical composition (X-ray fluorescence analysis) of all initial materials is given in Table 2 and the phase compositions obtained by the X-ray diffraction analysis (XRD) are presented in Table 3.

Tab. 1 Fundamental physical parameters of natural pozzolans

	Trass	Pozzolanic earth	Zeolite	Chalcedonite	Pumice	Spongilite	Lava
Loose bulk density [kg m^{-3}]	900	1050	570	590	640	770	1000
Particle density [kg m^{-3}]	2460	2660	2110	2540	2290	2370	2560
$S_{g\ Blaine}$ [m^2 kg^{-1}]	4420	3360	6550	9420	8250	6200	4210

Tab. 2 Chemical composition of initial materials (wt. %)

	SiO_2	Al_2O_3	Fe_2O_3	CaO	MgO	K_2O	Na_2O	P_2O_5	TiO_2	SO_3	LOI
Lime	0.92	0.71	0.39	68.09	1.33	0.48	0.11	0.05	0.10	0.19	27.94
Sand	98.50	0.38	0.15	0.01	0.03	0.09	0.01	0.04	0.09	0.02	0.12
Trass	50.08	17.61	5.46	4.16	1.70	4.67	3.61	0.34	0.81	0.05	10.05
Pozzolanic earth	47.98	17.64	9.09	7.67	3.51	3.35	2.59	0.53	1.02	0.07	5.41
Zeolite	67.46	11.73	1.37	2.84	0.73	3.02	0.50	0.03	0.17	0.01	11.57
Chalcedonite	98.92	0.94	0.04	0.05	0.03	0.04	0.05	0.03	0.02	0.01	0.07
Pumice	54.27	20.50	2.07	0.65	0.11	5.62	9.20	0.07	0.21	0.07	6.38
Spongilite	60.37	3.11	1.41	16.12	0.51	1.13	1.09	0.34	0.19	0.06	15.41
Lava	43.20	13.54	10.73	11.93	8.82	2.81	3.76	0.47	2.63	0.05	0.40

The hydrated lime had typical chemical and mineralogical compositions meeting the EN 459-1 standard. The used quartz sand had a high degree of purity, thus the mortar properties could not be affected by impurities in the sand. The chemical composition of pozzolans showed a high content of hydraulic oxides (SiO_2, Al_2O_3, Fe_2O_3) which provided very good conditions for its high pozzolanicity as according to the ASTM C618, the total pozzolanic content (i.e., the sum of SiO_2, Al_2O_3, and Fe_2O_3) must be a minimum of 70% for class N pozzolans. All pozzolans except spongilite and lava fulfilled this condition.

The reactivity of pozzolans is significantly influenced by its mineralogical composition. The quantitative mineralogical composition of natural pozzolans was determined using XRD and Rietveld refinement and quantification of the amorphous phase in pozzolans was performed using the internal standard method (20% CaF_2). It is clear from the results that, with the exception of chalcedonite and spongilite, the pozzolans contained an amorphous phase, mostly pumice, which was almost completely amorphous. However, the spongilite contained pozzolanically reactive opal and chalcedonite consisted of porous quartz grains with cryptocrystalline SiO_2 (with crystals only distinguishable under the electron microscope), with very small crystal grains of μm size filling the void space of the quartz grains (Figure 2). The content of these small grains was reflected in the distinct specific surface area of the chalcedonite particles. It is these small SiO_2 grains that play a crucial role in the pozzolanic activity of chalcedonite, even though it is not truly amorphous SiO_2. XRD cannot distinguish classic crystalline quartz from cryptocrystalline quartz (chalcedonite). From the mineralogy of the pozzolans, it was expected that spongilite and lava would have the least pozzolanic activity. However, spongilite had a relatively high specific surface area, which can enhance pozzolanic reactivity.

Tab. 3 Mineralogical composition of initial materials (wt. %)

	Lime	Sand	Trass	Pozz. earth	Zeolite	Chalcedon.	Pumice	Spongilite	Lava
Albite	–	–	–	–	2.6	–	–	–	–
Analcime	–	–	16.6	15.1	–	–	–	–	–
Anortite	–	–	–	33.5	–	–	–	–	–
Augite	–	–	–	23.9	–	–	–	–	17.0
Biotit	–	–	–	–	1.9	–	–	–	0.8
Brucite	0.5	–	–	–	–	–	–	–	–
Calcite	1.8	–	–	–	–	–	–	37.5	–
Corundum	–	–	–	–	–	0.9	–	–	–
Cristobalite	–	–	–	–	9.3	–	–	15.5	–
Diopside	–	–	–	–	–	–	–	–	24.8
Glauconite	–	–	–	–	–	–	–	3.1	–
Hematite	–	–	–	1.0	–	–	–	–	5.7
Chabazite	–	–	15.0	–	–	–	–	–	5.7
Illite	–	–	–	–	2.0	–	–	–	–
Kaersutite	–	–	–	–	–	–	–	–	1.5
Kaolinite	–	–	1.9	–	–	–	–	–	–
Klinoptilolite	–	–	–	–	50.5	–	–	–	–
Leucite	–	–	–	–	–	–	–	–	9.9
Muscovite	–	–	16.1	2.5	–	–	1.5	–	–
Nepheline	–	–	–	–	–	–	–	–	9.7
Opal	–	–	–	–	–	–	–	14.6	–
Orthoclase	–	–	16.6	–	–	–	–	4.8	11.2
Portlandite	97.1	–	–	–	–	–	–	–	–
Quartz	–	98.3	12.0	–	3.4	98.9	1.0	24.3	1.9
Staurolite	–	1.5	–	–	–	–	–	–	–
Amorphous phase	**–**	**–**	**21.8**	**23.6**	**30.2**	**–**	**97.5**	**–**	**17.1**

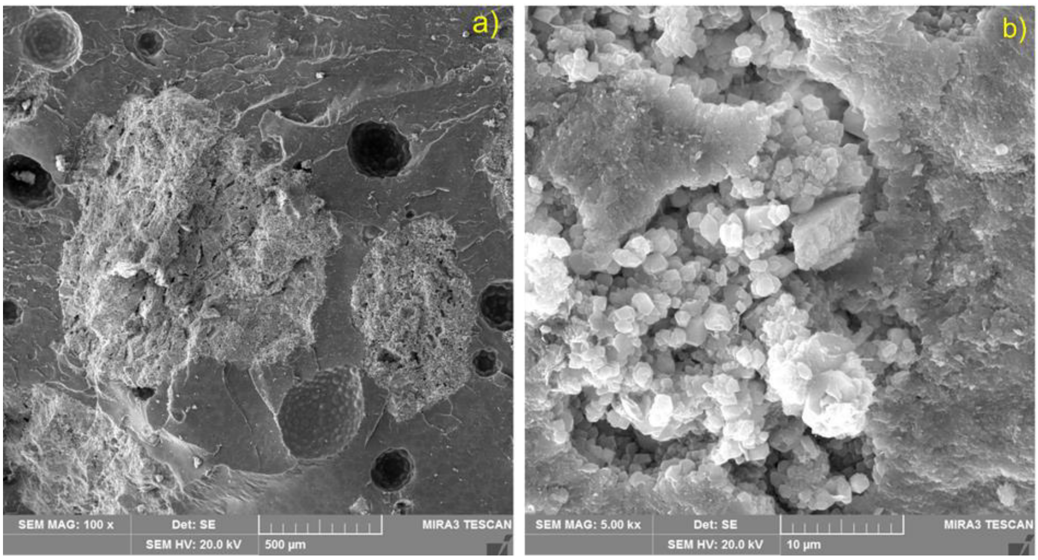

Fig. 2 SEM images of chalcedonite particles: a) magnification 100×, b) magnification 5000×

The content of amorphous hydraulic oxides in pozzolans (Table 4) was calculated from the total content of the respective hydraulic oxides, the known representation of individual minerals containing hydraulic oxides and the total content of the amorphous phase in particular pozzolans. It should be noted that in the case of chalcedonite, it was not possible to calculate the content of amorphous hydraulic oxides due to the indistinguishability of cryptocrystalline SiO_2 (chalcedony) and quartz by XRD. And also, there was 14.6 wt. % of opal in spongilite; opal is pozzolanically active, but is not a typical amorphous phase (it is detectable by XRD). As can be seen from Table 4, pumice had the highest content of hydraulic oxides, which together with its large specific surface area determined its high pozzolanic activity.

Tab. 4 Content of amorphous hydraulic oxides in pozzolans (wt. %)

	Trass	Pozzolanic earth	Zeolite	Chalcedonite	Pumice	Spongilite	Lava
SiO_2	4.1	7.8	14.3	0.0	52.6	0.0	0.0
Al_2O_3	1.0	0.0	2.6	0.0	19.9	0.0	3.9
Fe_2O_3	5.5	8.1	0.1	0.0	2.1	0.0	4.7
Σ	10.1	15.1	17.0	0.0	74.6	0.0	8.6

The pozzolanic activity of pozzolans was determined by the Chapelle test method according to NF P 18-513 [2] after 1 day and also after 2, 3, 4, and 5 days of reaction with $Ca(OH)_2$ in an autoclave at 90 °C (Table 5). Very high values of pozzolanic activity were achieved by zeolite and chalcedonite, partly due to their porous nature and thus large specific surface area, and also due to the content of reactive SiO_2. This confirmed that cryptocrystalline SiO_2 (chalcedony) is pozzolanically active. Pumice, which had a significantly higher content of amorphous hydraulic oxides than zeolite, had lower pozzolanic activity values after two or more days. It is possible that after the rapid initial pozzolanic reaction, it was further slowed down by the rapid increase of reaction products on the pumice grains and the slowing down of the diffusion of the $Ca(OH)_2$ solution to the surface of the pumice grains. The moderate pozzolanic activity of the spongilite confirmed the reactivity of the opal. Pozzolanic earth did not reach very high values of pozzolanic activity despite the considerable content of the amorphous phase, due to the fact that more than half of the content of amorphous oxides was Fe_2O_3, which is the least and slowest reactive of them. The higher content of amorphous Fe_2O_3 at the expense of SiO_2 or Al_2O_3, together with the overall low content of amorphous hydraulic oxides, resulted in relatively low values of the pozzolanic activities of the trass and especially of the lava. If the pozzolans were evaluated according to Raverdy's criterion [7], where the material is considered as pozzolanically active if its Chapelle reactivity is 650 mg $Ca(OH)_2$ per 1 g of test material and more, it is clear that zeolite, chalcedonite, pumice and spongilite were pozzolanically active already after 1 day of treatment with $Ca(OH)_2$. Pozzolanic earth met this condition after 2 days, trass after 4 days, and lava is not pozzolanically active according to this criterion.

Tab. 5 Pozzolanic activity of pozzolans (mg $Ca(OH)_2$/1 g)

	Trass	Pozzolanic earth	Zeolite	Chalcedonite	Pumice	Spongilite	Lava
1 day	516	513	729	755	887	694	359
2 days	618	685	1220	1259	910	803	370
3 days	641	795	1263	1341	958	849	382
4 days	735	870	1390	1349	1002	887	447
5 days	762	871	1395	1369	1022	910	515

Mortar mixtures were prepared with a constant volume ratio of binder to aggregate of 1:1. This ratio was used based on a practical point of view, historical traditions, and results obtained by Lanas et al. [8]. Fine natural pozzolans were used as a partial replacement of lime in 40% of the lime weight. The composition of mortar mixes expressed in weight proportions is given in Table 6. The amount of water required to achieve the same workability of 160±5 mm, determined in accordance with EN 1015-3, was added. The freshly casted samples (40 × 40 × 160 mm) were freely covered by polyethylene foil to avoid their cracking caused by rapid drying. Hardened mortar specimens were demolded after 48 h and then cured in a wet chamber at temperature T = (22 ± 3)°C and a relative humidity RH = (95 ± 5)% for 26 days. The samples were then stored under laboratory conditions at T = (22 ± 3)°C, RH = (50 ± 5)%. During the entire ageing period, the samples were placed on plastic grids to make their surface as accessible as possible for carbonation. High relative humidity promoted the pozzolanic reaction, whereas ambient curing allowed carbonation of hydrated lime mortars.
The basic physico-mechanical properties of mortars were determined after 28, 90, and 180 days of curing. The flexural strength and compressive strength of the samples were determined according to EN 1015-11. For the particular mortar mixture, a set of three prisms was evaluated.

Tab. 6 Composition of mortar mixtures (T – trass, PE – pozzolanic earth, Z – zeolite, CH – chalcedonite, P – pumice, S – spongilite, L – lava)

Mixture	Lime [g]	Natural pozzolan [g]	Quartz sand [g]	Water [ml]
L-ref	100	0	358	100
LT-40	60	40	259	77
LPE-40	60	40	238	75
LZ-40	60	40	327	90
LCH-40	60	40	321	78
LP-40	60	40	309	80
LS-40	60	40	283	88
LL-40	60	40	246	69

3. RESULTS AND DISCUSSION

Time evolution of mortar strengths is presented in Figures 3 and 4. All lime-pozzolan mortars achieved higher strengths than the reference lime mortar, especially after 90 and 180 days. It should be noted that the increase in strength was to a certain extent also due to the lower amount of mixing water used in the preparation of lime-pozzolan mortars for the same workability as the reference mortar. The strengths of the mortars at the age of 28 days were affected by the increased humidity in the mortars, as the samples were tested immediately after removal from a humid environment. For comparison, it is therefore better to use the strength values of mortars at the age of 90 and 180 days. Relatively high strengths were achieved by mortars with trass, pozzolanic earth and pumice, on the other hand, low strength values were documented for mortars with lava and chalcedonite. Unexpectedly low strength values of mortars with chalcedonite and high strength values of mortars with trass and pozzolanic earth did not completely correspond to the pozzolanic activity of these pozzolans. A very good correlation of achieved mortar strengths and pozzolanic activity is evident only for lava (Figure 5). Due to the high values of pozzolanic activity of chalcedonite and zeolite, significantly higher strengths were expected for these lime-pozzolan mortars.

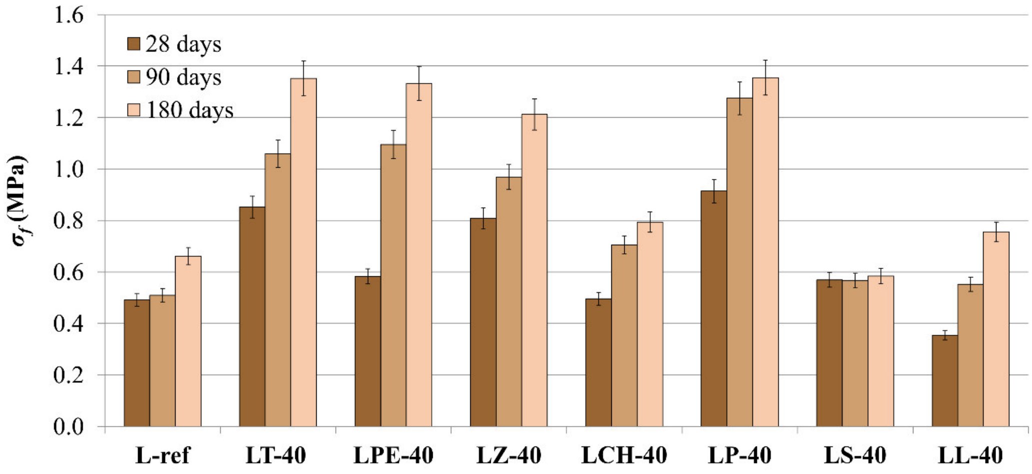

Fig. 3 Flexural strength of lime-pozzolan mortars

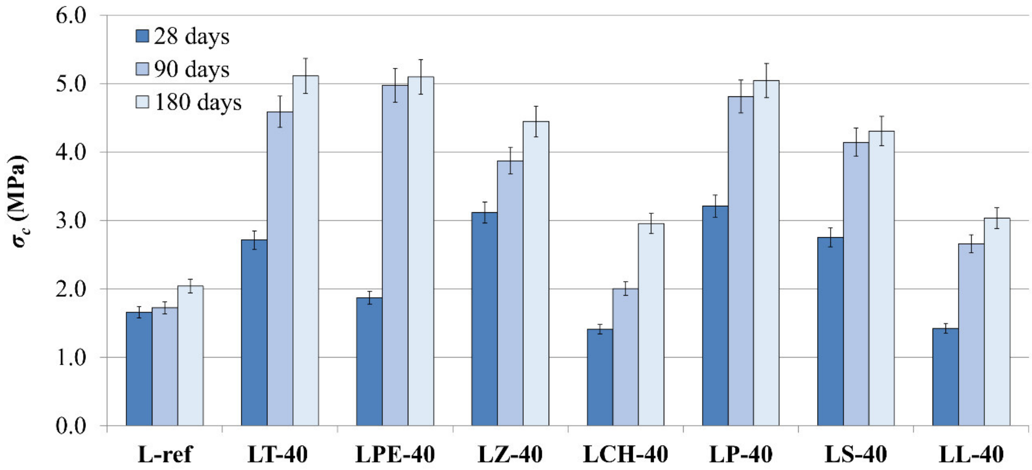

Fig. 4 Compressive strength of lime-pozzolan mortars

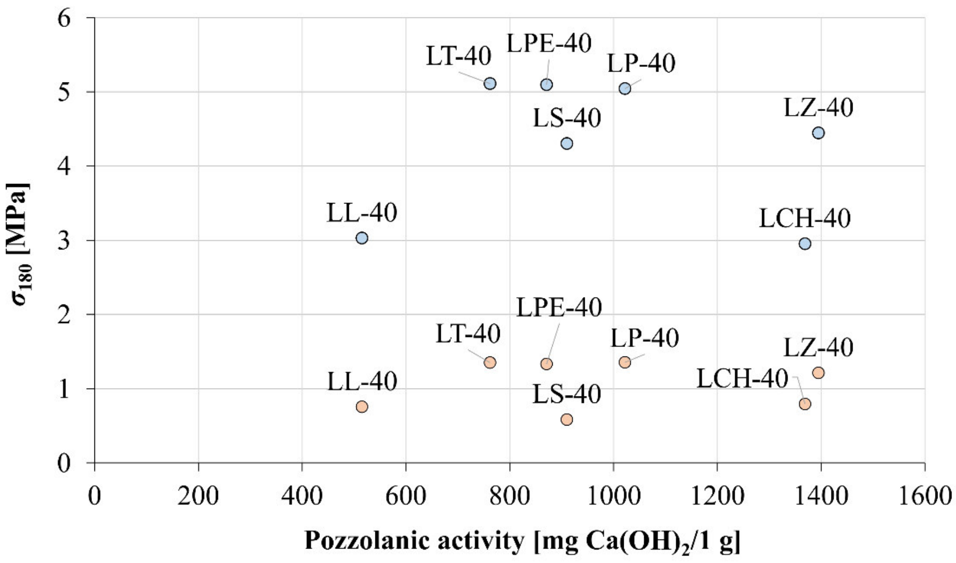

Fig. 5 Correlation of strengths of lime-pozzolan mortars after 180 days and pozzolanic activity of pozzolan.

The long-term strengths also did not correspond very well with the content of amorphous hydraulic oxides. According to Table 4, pumice mortar had the best preconditions for high strengths, which were also achieved. However, the similarly high strengths of mortars with trass and pozzolanic earth did not correspond to the significantly lower content of amorphous hydraulic oxides in these pozzolans.

4. CONCLUSIONS

The pozzolanic reactivity of seven different natural finely ground thermally untreated pozzolans in lime mortars has been investigated. Pozzolans were characterized by their basic physical properties, chemical and mineralogical composition, their pozzolanic activity was determined using the Chapelle test, and they were used as a 40% replacement for lime in lime mortars. The use of all pozzolans led to an increase in the strength of the mortars, especially in the long term. The pozzolanic activity of the pozzolans correlated relatively well with the content of amorphous hydraulic oxides and the specific surface area, but the correlation of the strength of the produced lime-pozzolan mortars with the pozzolanic activity of the pozzolans was insufficient.
As can be seen from the results obtained, when selecting a suitable pozzolan for lime mortars, it is not enough to determine the physical properties of pozzolans, or only to carry out chemical and mineralogical analyses, or to determine the pozzolanic activity. In some cases, during the production of lime-pozzolan mortars suitable for practical use (i.e. with sufficient workability), it may happen that the strengths obtained are higher or lower than expected. It is therefore necessary to analyse the given pozzolan as thoroughly as possible and also to simulate the practical use of the lime-pozzolan mortar. Procedures and reaction conditions given in some guidelines for the determination of pozzolanic activity may lead to an overestimation of the reactivity of the pozzolanic material, which may not manifest itself in its practical use.

ACKNOWLEDGEMENT

The financial support received from the Czech Science Foundation under project No 21-06582S is greatly acknowledged.

REFERENCES

[1] Hewlett P.C. (2004). *Lea's chemistry of cement and concrete*. 4th ed., Elsevier, Oxford, Great Britain.

[2] NF P 18-513 (2009). *Pozzolanic Addition for Concrete-Metakaolin: Definitions, Specifications and Conformity Criteria, Annex A*; Association Francaise de Normalisation, Paris, France.

[3] Luxán M.P., Madruga F., Saavedra J. (1989). Rapid evaluation of pozzolanic activity of natural products by conductivity measurement. *Cement and Concrete Research*, Volume 19, No. 1, pp. 63-68, 1989.

[4] Avet F., Snellings R., Diaz A.A., Haha M.B., Scrivener K. (2016). Development of a new rapid, relevant and reliable (R3) test method to evaluate the pozzolanic reactivity of calcined kaolinitic clays. *Cement and Concrete Research*, Volume 85, pp. 1-11, https://doi.org/10.1016/j.cemconres.2016.02.015.

[5] Donatello S., Tyrer M., Cheeseman C.R. (2009). Comparison of test methods to assess pozzolanic activity. *Cement and Concrete Composites*, Volume 32, Issue 2, pp. 121-127, https://doi.org/10.1016/j.cemconcomp.2009.10.008.

[6] Liu Y., Yuan Q., Tan Y., Garba M.J. (2023). Comparative analysis and modification of evaluation methods for the pozzolanic reactivity of natural volcanic powders, *Journal of Building Engineering*, Volume 78, 107590, https://doi.org/10.1016/j.jobe.2023.107590.

[7] Raverdy M., Brivot F., Paillére A.M., Dron R. (1980) Appréciation de I'Activité Pouzzolanique des Constituents Secondaires. In *Proceedings of the 7th International Congress on the Chemistry of Cement*, Éditions Septima, Paris, France, 30th June–4th July, Volume 3, pp. 36–41.

[8] Lanas J., Alvarez-Galindo J.I. (2003), Masonry repair lime-based mortars: Factors affecting the mechanical behavior, *Cement and Concrete Research*, Volume 33, pp. 1867-1876, https://doi.org/10.1016/S0008-8846(03)00210-2.

VERIFICATION OF BUCKLING ANALYSIS OF BEAM FINITE ELEMENT MODEL INCLUDING WARPING IN MATRIX 3D

Tanja Nožica[1], Đorđe Jovanović[2], Drago Žarković[3], Andrija Rašeta[4]

Summary:

This paper presents a beam model for linear and stability analysis, which includes warping. Commercial software have a built-in buckling calculation, however, few consider the seventh degree of freedom. The influence of the seventh degree of freedom can be considered by using shell elements to model the structure. Such an analysis is time-consuming, which initiates the need for less time-consuming analyses. In the software Matrix 3D, a method is developed that considers the seventh degree of freedom for beam elements, where torsion warping transmission at frame joints is also considered. For validation, several examples of planar and spatial frames were presented, the results of which were compared with the same frames obtained using shell elements in the software Abaqus.

Key words: warping, warping transmission, buckling, seventh degree of freedom.

---

[1]Teaching Assistant, Faculty of Technical Sciences, University of Novi Sad, Serbia, nozica.tanja@uns.ac.rs
[2] Asst. prof., Faculty of Technical Sciences, University of Novi Sad, Serbia, djordje.jovanovic@uns.ac.rs
[3] Asst. prof., Faculty of Technical Sciences, University of Novi Sad, Serbia, dragozarkovic@uns.ac.rs
[4] Assoc. prof., Faculty of Technical Sciences, University of Novi Sad, Serbia, araseta@uns.ac.rs

1. INTRODUCTION

The application of steel constructions is very wide, especially moment steel frames. Steel structures are predominantly composed of thin-walled open sections that generally have low torsional stiffness; as such, they have a problem with torsion, therefore warping displacements. Steel structures are usually slender structures compared to other materials. Due to possible stability problems, it is necessary to check the structure's or its part's global stability. The warping deformation plays an important role in the local buckling behaviour for thin-walled or open sections. If torsional deformation is neglected, the calculated critical buckling load can be much higher than the actual value, resulting in an unsafe system. Therefore, it is important to consider warping deformation when performing buckling analysis for thin or open-walled sections. Commercial software have a built-in buckling calculation, however, few consider the seventh degree of freedom. Beam elements in commercial software packages usually consider six degrees of freedom (DOFs) at each node, based on Euler-Bernoulli or Timoshenko beam theories and uniform (St. Venant) torsion theory.

Implementing Vlasov's theory implies adding one degree of freedom, warping, and an additional force, bimoment, at each element's end. The implementation of warping implies that the engineer is familiar with the warping phenomenon to be able to define the support conditions at the ends of the elements, that is, whether warping is free, fixed or continuous. In the case of choosing free warping for all structural elements, the analysis does not differ in any way from the standard Saint Venant analysis. When choosing fixed or continuous warping, the construction is stiffer. One option for correct modelling of warping and its joint transmission in software is using shell elements, which creates a problem because this type of analysis is time-consuming for more complex constructions.

Over the years, several researchers have significantly contributed to the theoretical and numerical modelling of thin-walled sections. Baigent and Hancock [1] formulated the matrix displacement method incorporating the warping torsion for the linear elastic analysis of general thin-walled sections. They also introduced warping as the 7th degree of freedom at the beam ends and successfully implemented it for the analysis of single channel-section portal frames. Yang et al. [2] derived a new stiffness matrix for the analysis of thin-walled beams where nonuniform torsion is included by adopting the principle of sectorial areas for cross-sectional displacements. McGuire et al. [3] developed MASTAN2, a structural analysis program capable of considering warping torsion and second-order effects. MASTAN2 predicts the elastic critical global buckling force, the warping torsion, and the second-order forces. Lebastard et al. [4] proposed analytical formulations for evaluating the critical bending moment for lateral-torsional buckling of a beam, considering warping restraints at supports. Fatmi [5] presented a beam theory (BT) with a non-uniform warping, including the effects of torsion and shear forces and valid for any homogeneous cross-section made of isotropic elastic material. Murin [6], [7] proposed a new 3D beam finite element including non-uniform torsion where the secondary torsion moment deformation effects are included in the stiffness matrix. Evangelos et al. [8] presented an advanced 32×32 stiffness matrix and the corresponding nodal load vector of a 3-D beam element of arbitrary cross-section, taking into account shear deformation, generalised warping (shear leg effects) and distortional effects due to both flexure and torsion. Basaglia et al. [9], [10] reported research work concerning the use of Generalised Beam Theory (GBT) to analyse the local, distortional and global buckling behaviour of thin-walled steel frames. Zhang et al. [11] incorporated the warping degree of freedom in OpenSees and used the method for the nonlinear analysis of doubly symmetric sections.

One of the major difficulties associated with the analysis of the global behaviour of plane and space thin-walled frames stems from the need to handle the torsion-warping

transmission at the joints connecting two or more non-aligned members. Basaglia et al. [12] developed a simple kinematic model to simulate the warping transmission or restraint at the joints of thin-walled frames in beam finite element analysis. The model relies on the facility of most structural analysis software (e.g. ABAQUS and ANSYS) to impose "linear constraint equations", which establish constraint conditions between the torsion warping degrees of freedom of the member end nodes. Shayan and Rasmussen [13] developed a method for warping transmission where the joint is modelled as an assemblage of shell elements and analysed a priori as a substructure. Using static condensation, the substructuring technique produces a small stiffness matrix that can be converted to a warping stiffness matrix. The warping stiffness matrix components are then applied as springs associated with linear constraint equations. The advantage of this method is that it applies to arbitrary 2D and 3D joint types.
To improve buckling calculation in the academic software Matrix 3D, linear and geometric stiffness matrices 14x14, that include non-uniform torsion, are implemented. Based on this, it is possible to consider the warping deformation influence during the eigen buckling analysis, including warping transmission at joints for different joint configurations. Still, it is also possible to calculate bimoments and warping deformations.

2. FORMULATION

The stiffness method approach for calculating elastic critical loads, including warping, is presented here. The stiffness matrix for an element in pure torsion developed by the virtual displacement approach is adequate for the analysis of many systems with small torsional effects. Still, it is limited because it neglects resistance to cross-sectional out-of-plane warping. Warping resistance can be significant in the response of many frames consisting of members of open cross-sections. Certainly, it can be the dominant factor in their resistance to torsion and combined torsional-flexural effects if the warping deformation is restrained in any way.
The principle of virtual displacements is used to develop an element stiffness matrix that accounts for the warping restraint [3]. The numerical solution of the equation is approximate, but it is found to be in good agreement with analytical solutions of representative problems.

$$[k]=\left[GJ\begin{bmatrix}\frac{6}{5L} & -\frac{6}{5L} & \frac{1}{10} & \frac{1}{10}\\ & \frac{6}{5L} & -\frac{1}{10} & -\frac{1}{10}\\ sym. & & \frac{2L}{15} & -\frac{L}{30}\\ & & & \frac{2L}{15}\end{bmatrix}+\frac{EI_w}{L}\begin{bmatrix}\frac{12}{L^2} & -\frac{12}{L^2} & \frac{6}{L} & \frac{6}{L}\\ & \frac{12}{L^2} & -\frac{6}{L} & -\frac{6}{L}\\ sym. & & 4 & 2\\ & & & 4\end{bmatrix}\right]$$

In the given expression L is the beam length, J is the torsional constant, and I_w is the warping constant. The 12-degree of freedom stiffness matrix can be modified and augmented by the elements of [k] to form a 14-degree-of-freedom stiffness matrix for the linear elastic analysis of members subject to combined axial force, bending, and nonuniform torsion.
For the analysis of the bifurcation stability of line systems, which are composed of a series of elements interconnected in joints, the most suitable is the matrix formulation which is implemented in the Matrix 3D software. From the conditions of existence of a non-trivial solution, the following condition is obtained.

$$det(K_e+K_G)=0$$

In the given expression K_E is a conventional stiffness matrix of a system, while K_G is a geometric stiffness matrix, both extended by an additional degree of freedom (warping) so that the dimensions of the matrices are 14x14.

$$[k_E]=\begin{bmatrix}
\frac{EA}{L} & 0 & 0 & 0 & 0 & 0 & -\frac{EA}{L} & 0 & 0 & 0 & 0 & 0 & 0 & 0\\
 & \frac{12EI_Z}{L^3} & 0 & 0 & 0 & \frac{6EI_Z}{L^2} & 0 & -\frac{12EI_Z}{L^3} & 0 & 0 & 0 & \frac{6EI_Z}{L^2} & 0 & 0\\
 & & \frac{12EI_Y}{L^3} & 0 & -\frac{6EI_Y}{L^2} & 0 & 0 & 0 & -\frac{12EI_Y}{L^3} & 0 & -\frac{6EI_Y}{L^2} & 0 & 0 & 0\\
 & & & \left(\frac{6GJ}{5L}+\frac{12EI_W}{L^3}\right) & 0 & 0 & 0 & 0 & 0 & -\left(\frac{6GJ}{5L}+\frac{12EI_W}{L^3}\right) & 0 & 0 & \left(\frac{GJ}{10}+\frac{6EI_W}{L^2}\right) & \left(\frac{GJ}{10}+\frac{6EI_W}{L^2}\right)\\
 & & & & \frac{4EI_Y}{L} & 0 & 0 & 0 & \frac{6EI_Y}{L^2} & 0 & \frac{2EI_Y}{L} & 0 & 0 & 0\\
 & & & & & \frac{4EI_Z}{L} & 0 & -\frac{6EI_Z}{L^2} & 0 & 0 & 0 & \frac{2EI_Z}{L} & 0 & 0\\
 & & & & & & \frac{EA}{L} & 0 & 0 & 0 & 0 & 0 & 0 & 0\\
 & & & & & & & \frac{12EI_Z}{L^3} & 0 & 0 & 0 & -\frac{6EI_Z}{L^2} & 0 & 0\\
 & & & & & & & & \frac{12EI_Y}{L^3} & 0 & \frac{6EI_Y}{L^2} & 0 & 0 & 0\\
 & & & & & & & & & \left(\frac{6GJ}{5L}+\frac{12EI_W}{L^3}\right) & 0 & 0 & -\left(\frac{GJ}{10}+\frac{6EI_W}{L^2}\right) & -\left(\frac{GJ}{10}+\frac{6EI_W}{L^2}\right)\\
 & & & sym. & & & & & & & \frac{4EI_Y}{L} & 0 & 0 & 0\\
 & & & & & & & & & & & \frac{4EI_Z}{L} & 0 & 0\\
 & & & & & & & & & & & & \left(\frac{2GJL}{15}+\frac{4EI_W}{L}\right) & -\left(\frac{GJL}{30}-\frac{2EI_W}{L}\right)\\
 & & & & & & & & & & & & & \left(\frac{2GJL}{15}+\frac{4EI_W}{L}\right)
\end{bmatrix}$$

$$[k_G]=\begin{bmatrix}
\frac{F}{L} & 0 & 0 & 0 & 0 & 0 & -\frac{F}{L} & 0 & 0 & 0 & 0 & 0 & 0 & 0\\
 & \frac{6F}{5L} & 0 & \frac{11M_{Y1}-M_{Y2}}{10L} & \frac{M_X}{L} & \frac{F}{10} & 0 & -\frac{6F}{5L} & 0 & -\frac{M_{Y1}-11M_{Y2}}{10L} & -\frac{M_X}{L} & \frac{F}{10} & \frac{M_{Y1}}{10} & -\frac{M_{Y2}}{10}\\
 & & \frac{6F}{5L} & \frac{11M_{Z1}-M_{Z2}}{10} & -\frac{F}{10} & \frac{M_X}{L} & 0 & 0 & -\frac{6F}{5L} & -\frac{M_{Z1}-11M_{Z2}}{10L} & -\frac{F}{10} & -\frac{M_X}{L} & \frac{M_{Z1}}{10} & -\frac{M_{Z2}}{10}\\
 & & & \frac{6FI_P}{5AL} & -\frac{2M_{Z1}-M_{Z2}}{5} & \frac{2M_{Y1}-M_{Y2}}{5} & 0 & -\frac{11M_{Y1}-M_{Y2}}{10L} & -\frac{11M_{Z1}-M_{Z2}}{10L} & -\frac{6FI_P}{5A} & -\frac{2M_{Z1}+M_{Z2}}{10} & \frac{2M_{Y1}+M_{Y2}}{10} & \frac{FI_P}{10A} & \frac{FI_P}{10A}\\
 & & & & \frac{2FL}{15} & 0 & 0 & -\frac{M_X}{L} & \frac{F}{10} & -\frac{M_{Z1}+2M_{Z2}}{10} & -\frac{FL}{30} & \frac{M_X}{2} & -\frac{(3M_{Z1}-M_{Z2})L}{30} & \frac{M_{Z1}L}{30}\\
 & & & & & \frac{2FL}{15} & 0 & -\frac{F}{10} & -\frac{M_X}{L} & \frac{M_{Y1}+2M_{Y2}}{10} & -\frac{M_X}{2} & \frac{FL}{30} & \frac{(3M_{Y1}-M_{Y2})L}{30} & -\frac{M_{Y1}}{30}\\
 & & & & & & \frac{F}{L} & 0 & 0 & 0 & 0 & 0 & 0 & 0\\
 & & & & & & & \frac{6F}{5L} & 0 & \frac{M_{Y1}-11M_{Y2}}{10L} & \frac{M_X}{L} & -\frac{F}{10} & -\frac{M_{Y1}}{10} & \frac{M_{Y2}}{10}\\
 & & & & & & & & \frac{6F}{5L} & \frac{M_{Z1}-11M_{Z2}}{10L} & \frac{F}{10} & \frac{M_X}{L} & -\frac{M_{Z1}}{10} & \frac{M_{Z2}}{10}\\
 & & & & & & & & & \frac{6FI_P}{5AL} & \frac{M_{Z1}-2M_{Z2}}{5} & -\frac{M_{Y1}-2M_{Y2}}{5} & -\frac{FI_P}{10A} & -\frac{FI_P}{10A}\\
 & & & sym. & & & & & & & \frac{2FL}{15} & 0 & -\frac{M_{Z2}L}{30} & -\frac{(M_{Z1}-3M_{Z2})L}{30}\\
 & & & & & & & & & & & \frac{2FL}{15} & \frac{M_{y2}L}{30} & \frac{(M_{y1}-3M_{y2})L}{30}\\
 & & & & & & & & & & & & \frac{2FI_P}{15A} & -\frac{FI_P}{30A}\\
 & & & & & & & & & & & & & 2FI_P
\end{bmatrix}$$

The axial forces in the element necessary for forming the K_G matrix can be determined by the first-order theory for an arbitrarily chosen value of a given load. Suppose the intensity of the load changes linearly, in proportion to the parameter λ. In that case, the intensity of the axial forces in the elements of the system also changes in proportion to the parameter λ. Thus, at load $\lambda \times Q$, the matrix of initial stresses is $\lambda \times K_G$. Therefore, the next expression is obtained:

$$det(K_E+\lambda K_G)=0$$

where λ is a parameter of the linear change in the load intensity. This expression defines the state of bifurcation equilibrium of a system which is in the developed form a polynomial of n^{th} degree by the parameter λ, whose roots λ_1, $\lambda_2 \ldots \lambda_n$, represent characteristic values corresponding to the axial forces S_1, S_2, ... Sn in the elements of the system at which neutral equilibrium states are formed.

One of the key challenges in analysing the overall performance of plane and spatial slender frames lies in addressing the transmission of torsion warping at the connections where two or more members aren't aligned.
Matrix 3D uses a numerical model that considers the transmission of warping torsion and local displacement compatibility at frame joints of various configurations [12].
For each beam, two additional global degrees of freedom (warping) are added, which are used for the formation of the system matrix. After adding the warping degrees of freedom, the total number of degrees of freedom is increased by 2 × number of beams. After the formation of the system matrix, link elements that describe warping transmission in the joint are formed.

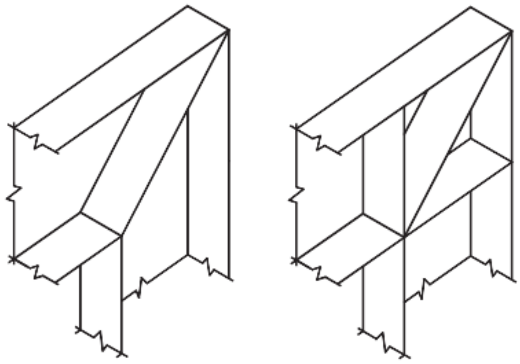

Fig. 1-Diagonal-stiffened and diagonal/box-stiffened joints

Link characteristics are defined by a coefficient describing the transmission of warping between the nodes. A diagonal joint (Fig. 1 left) provides complete and direct warping transmission, and a diagonal/box joint (Fig. 1 right) does not provide transmission, which is why their coefficients are 1 and 0, respectively. The link element matrices for the two joint configurations (Fig. 1) are shown below:

$$k_{link1} = \begin{bmatrix} 1E+10 & -1E+10 \\ -1E+10 & 1E+10 \end{bmatrix}$$

$$k_{link2} = \begin{bmatrix} 1E+10 & 0 \\ 0 & 1E+10 \end{bmatrix}$$

where the first matrix k_{link1} is used for the diagonal-stiffened joints and the second k_{link2} for the diagonal/box-stiffened joints.

3. VALIDATION

To validate the implementation of the seventh degree of freedom in Matrix 3D software and its transfer in nodes for a certain joint configuration, three models, a console, a planar frame, and a spatial frame [12], are presented in this part. In the case of a planar and spatial frame, two variants of the node configuration (diagonal and diagonal-box) are shown. The steel used is S235 with a modulus of elasticity E=205-210 GPa and Poisson's coefficient μ=0.3 Results from the beam finite element in Matrix 3D are compared with "exact" values yielded by shell finite element in the software Abaqus, except for the console whose results are compared with line element in the Abaqus. Current programs that use beam-column elements with warping degrees of freedom are Abaqus and ANSYS, among others. The Abaqus element is called B32OS, and the ANSYS element is named BEAM189. Some results are also compared with the results shown in the literature.

3.1. CONSOLE

The first example of validating the seventh degree of freedom in the buckling calculation in the software Matrix 3D is a cantilever, laterally supported at the ends and loaded with a concentrated force of the intensity of 40 kN at the free end. The cross-section of the console is IPE 400, and the span is 6 m. In this example, the check was performed using the LTBeam and Abaqus software, where the element B320S (line element open beam section in space with the option of 7 degrees of freedom per node) was chosen. The length of each element in the beam analyses is taken as 0.5 m. The modulus of elasticity is taken as E = 210 GPa

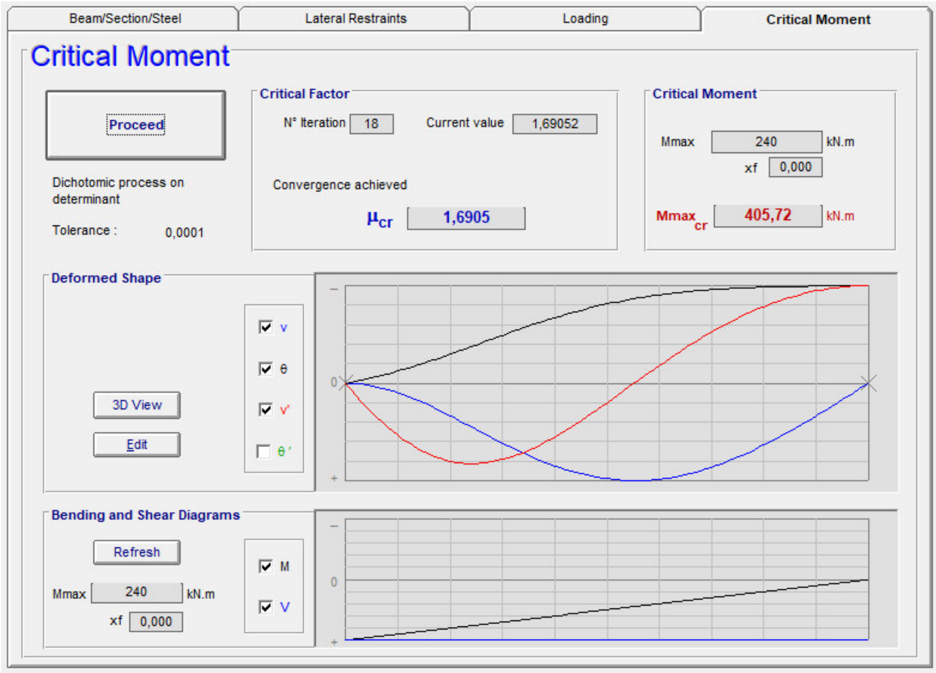

Fig. 2-Critical buckling load in LTBeam

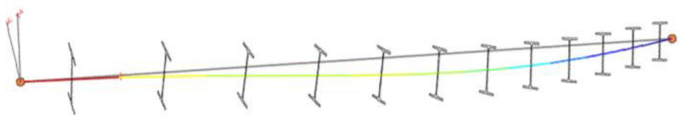

Fig. 3- First mode in Matrix 3D -λ1=1.69

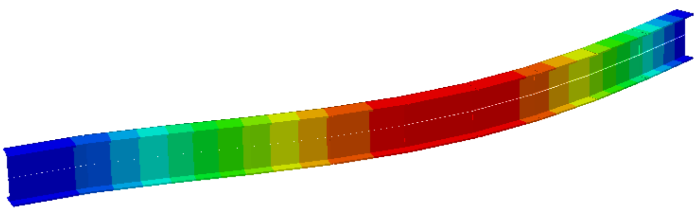

Fig. 4- First mode in Abaqus -λ1=1.64

The result of the critical buckling load in the software Matrix 3D and LTBeam match. Both software give the same result of parameter λ=1.69. While in the Abaqus software, a small deviation is observed where the parameter is λ=1.64.

3.2. PLANAR FRAME

This part presents the buckling analysis of an L-shape plane frame [13]–[15]. The frame is formed by one fixed ended 4 m long column member and an orthogonal 8 m long rafter members with the cantilevered end. A vertical concentrated unit load has been applied at the end of the cantilever. The beam and column are made from 150UB14 sections. The modulus of elasticity has been taken as E = 210 GPa. The shell finite element analyses are based on the discretisation of the flanges and webs into two and three elements, respectively, while the length of each element in the beam analyses is taken as 0.50 m. Two L-shape frame node configuration variants were made: diagonal and diagonal-box (Fig. 1). Tab. 1 presents the beam finite element and shell finite element frame critical buckling loads for the two column-to-beam joint configurations considered. Where it can be seen that the differences are negligible.

Tab. 1 Plane frame critical buckling loads parameter

Joint configuration	Beam element (Matrix 3D)	Shell element (Abaqus)	(%)
Diagonal-stiffened	0.778	0.794	-2.0
Diagonal/Box-stiffened	0.849	0.836	1.5

Fig. 5-8 show the buckling shapes of the L-shape frame first tone for diagonal-stiffened, and diagonal/box stiffened joint configuration. It can be observed that beam finite element analysis in Matrix 3D gives a similar buckling shape to shell finite element analysis in Abaqus.

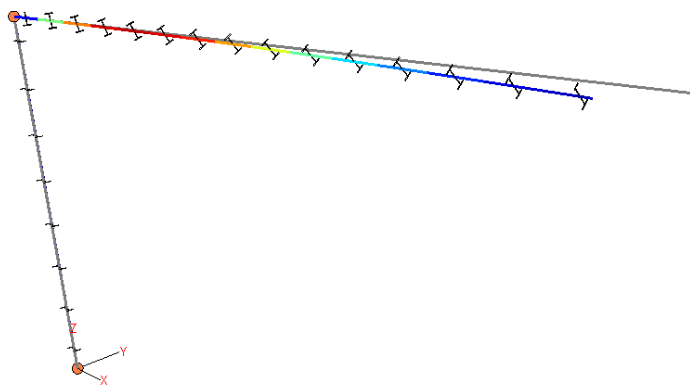

Fig. 5-Diagonal-stiffened joint, first mode in Matrix3D-λ1=0.778

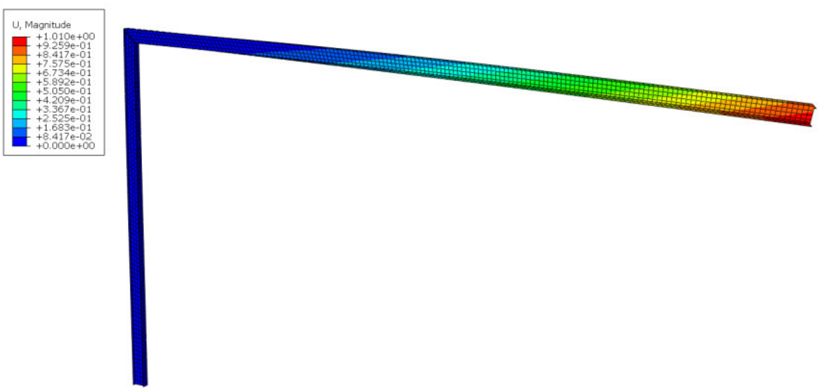

Fig. 6- Diagonal-stiffened joint, first mode in Abaqus-λ1=0.794

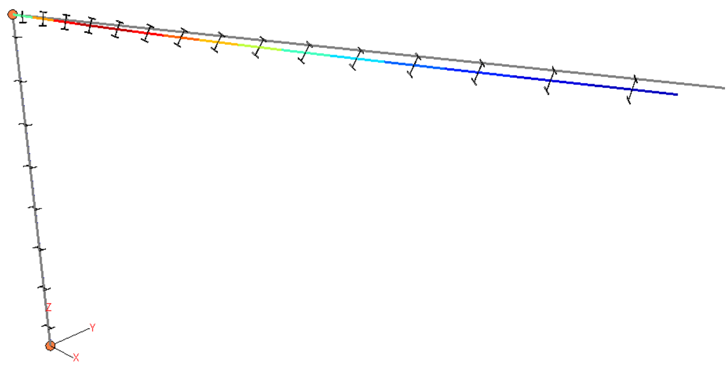

Fig. 7-Diagonal/box-stiffened joint, first mode in Matrix3D-λ1=0.849

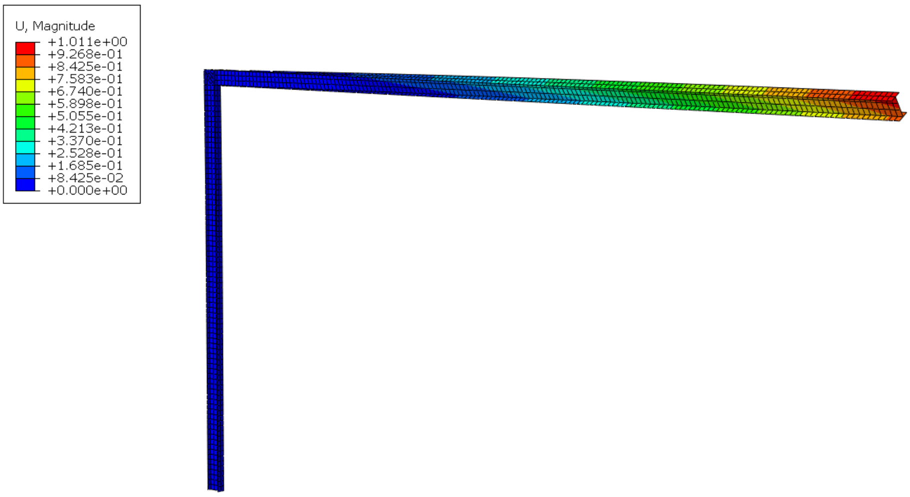

Fig. 8- Diagonal/box-stiffened joint, first mode in Abaqus-λ1=0.836

3.3. SPACE FRAME

This part presents the buckling analysis of a symmetrical spatial frame. The frame consists of two planar frames connected by a transverse beam. The frame is loaded with a point load of the intensity of 1 kN at the tops of the columns and in the middle of the transverse beam. The frame members are built from steel profiles with E=205 GPa (Young's modulus). All elements have the same cross-section I300x8. While the column-to-beam joints exhibit web continuity, there is flange continuity in the beam-to-beam ones. The column bases are fixed, the column-to-beam joints cannot move along Z and X, and the displacement along X of the transverse beam midspan cross-section is also prevented. All these displacement restraints are located at the corresponding cross-section mid-web points (Fig. 9). The shell finite element analyses are based on discretisation of the flanges and webs into four and six elements, respectively, while the beam finite element analysis is based on frame discretisation into 72 finite elements.

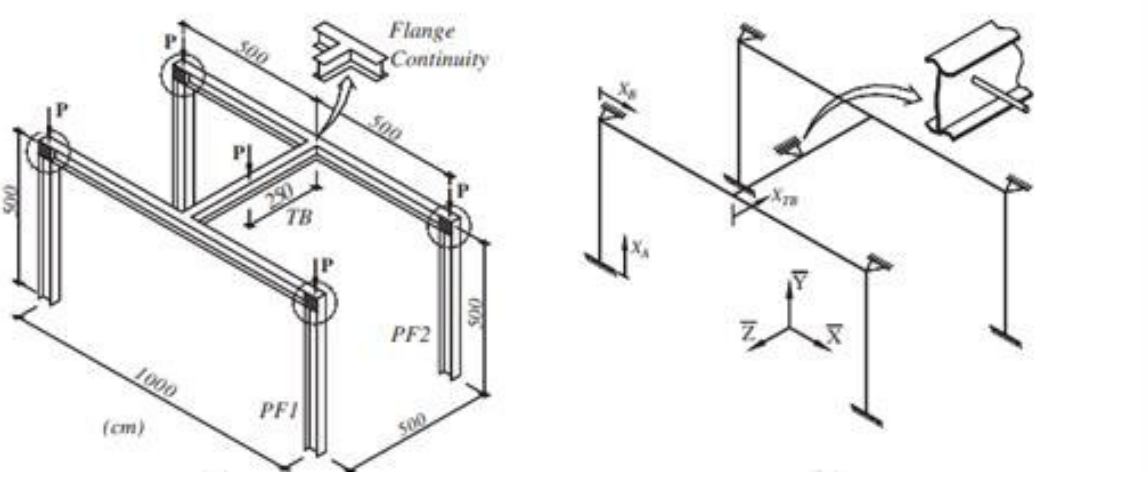

Fig. 9- Space frame geometry, loading and support conditions.

Two spatial frame node configuration variants were made: diagonal and diagonal-box (Fig. 1). Tab. 2 presents the beam finite element and shell finite element frame critical buckling loads for the two column-to-beam joint configurations considered. It can be seen that the deviations of beam analysis from shell analysis are negligible.

Tab. 2 Space frame critical buckling loads parameter

Joint configuration	Beam element (Matrix 3D)	Shell element (Abaqus)	(%)
Diagonal-stiffened	324.32	329.72	-1.6
Diagonal/Box-stiffened	342.57	341.25	0.4

Fig. 10 and Fig. 11 show the buckling shapes of the first tone. Matrix 3D, which uses less time-consuming analysis (beam finite element analysis) for the buckling calculation (including warping), gives a comparable buckling shape to Abaqus, which uses shell finite element analysis.

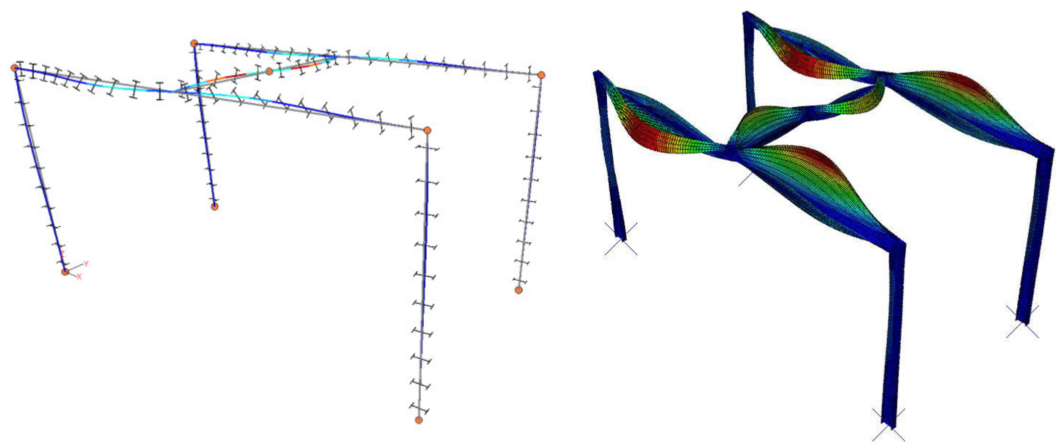

Fig. 10- Diagonal-stiffened joint, first mode in Matrix 3D (λ1=324.32) and Abaqus (λ1=329.72)

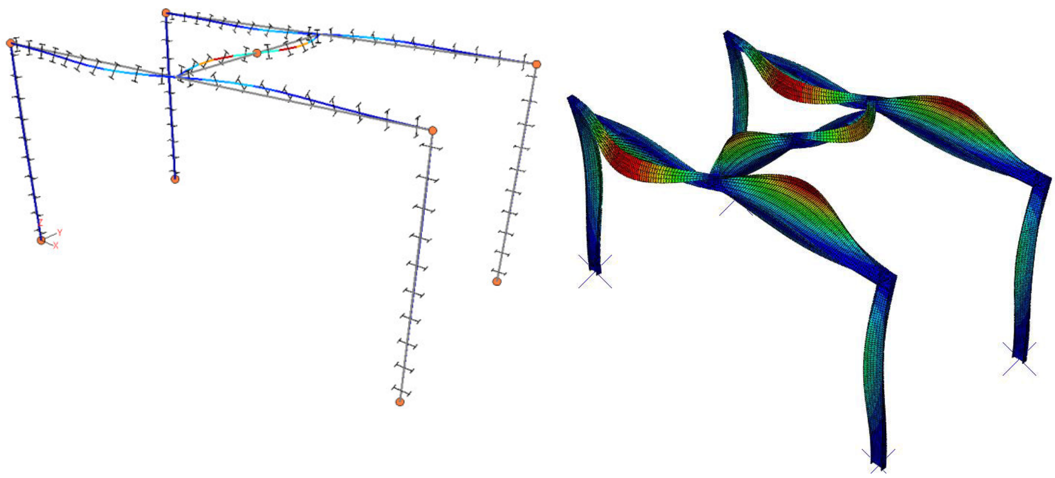

Fig. 11- Diagonal/box-stiffened-joint, first mode in Matrix 3D (λ1=342.57) and Abaqus (λ1=341.25)

Further, the results of torsion and warping of the beam and transverse beam for two joint configurations are shown (Fig. 12). The results are in agreement with [12].

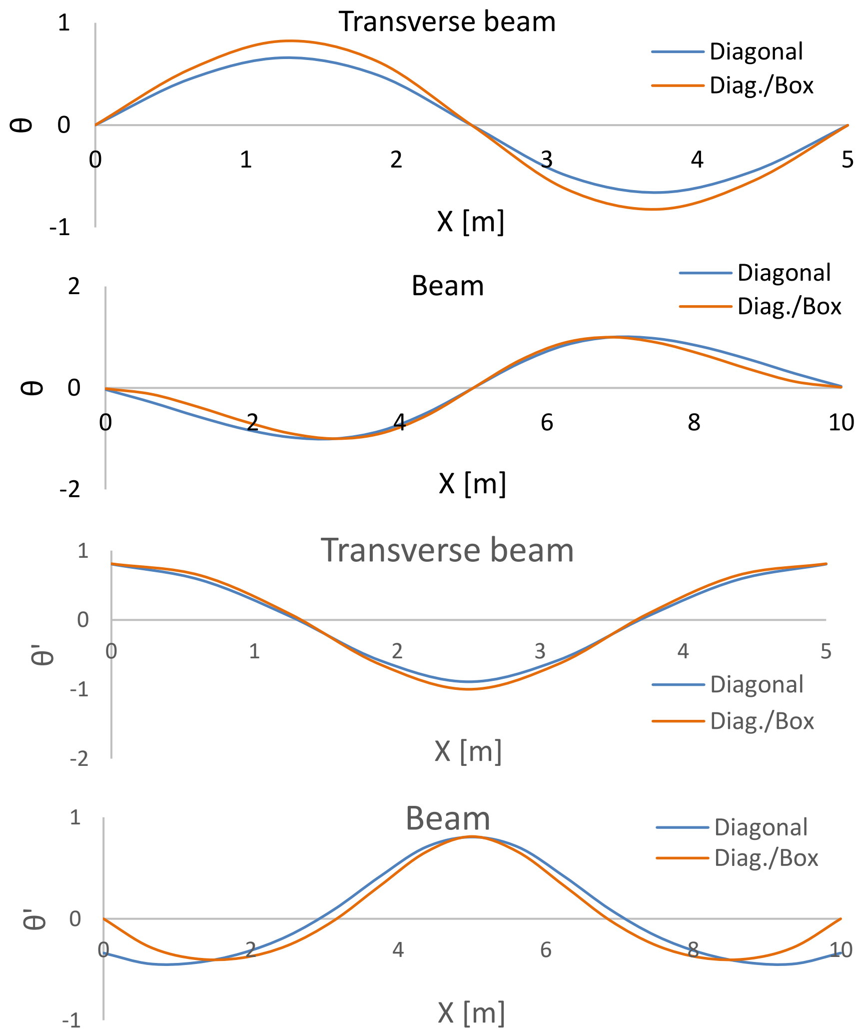

Fig. 12-Torsional rotation functions and derivates

4. CONCLUSION

This paper is dealing with the beam finite element analysis for calculating the critical buckling load, considering warping transfer in nodes for different node configurations (diagonal-stiffened and diagonal/box-stiffened joints). The matrices (linear and geometric) needed to account for the seventh degree of freedom are shown, as well as the link elements needed to consider a warping transmission in the nodes. The performed verification shows that the presented method can accurately predict the values of the critical buckling forces and the buckling shapes compared to the precise results obtained with shell finite elements but with the use of considerably less computation time. This modelling can be built into general finite elements software working with 7DOF beam elements.

ACKNOWLEDGEMENT

This research has been supported by the Ministry of Education, Science and Technological Development through project no. 451-03-68/2022-14/ 200156 “Innovative scientific and artistic research from the FTS (activity) domain”.

REFERENCES

[1] Baigent, A.H., Hancock, G.J. (1982). Structural analysis of assemblages of thin-walled members. Engineering Structures,Volume 4, Issue 3, 207-216. https://doi.org/10.1016/0141-0296(82)90010-4.

[2] Yang Y.B., Asce A.M., Mcguire W., Asce F. (1986). Stiffness matrix for geometric nonlinear analysis. J StructEng, 112(4), 853-877.

[3] McGuire W., Gallagher R.H., Ziemian R.D. (2000). Matrix structural analysis. John Wiley

[4] Lebastard, M., Couchaux, M., Santana, M. V. B., Bureau, A., & Hjiaj, M. (2022). Elastic lateral-torsional buckling of beams with warping restraints at supports. Journal of Constructional Steel Research, 197. https://doi.org/10.1016/j.jcsr.2022.107410

[5] El Fatmi, R. (2007). Non-uniform warping including the effects of torsion and shear forces. Part II: Analytical and numerical applications. International Journal of Solids and Structures, 44(18–19), 5930–5952. https://doi.org/10.1016/j.ijsolstr.2007.02.005

[6] Murín, J., Kutiš, V., Královič, V., & Sedlár, T. (2012). 3D beam finite element including nonuniform torsion. Procedia Engineering, 48, 436–444. https://doi.org/10.1016/j.proeng.2012.09.537

[7] Murín, J., & Kutiš, V. (2008). An effective finite element for torsion of constant cross-sections including warping with secondary torsion moment deformation effect. Engineering Structures, 30(10), 2716–2723. https://doi.org/10.1016/j.engstruct.2008.03.004

[8] Sapountzakis, E. J., & Dikaros, I. C. (2019). Advanced 3-D beam element including warping and distortional effects for the analysis of spatial framed structures. Engineering Structures, 188, 147–164. https://doi.org/10.1016/j.engstruct.2019.03.006

[9] Basaglia, C., Camotim, D., & Silvestre, N. (2009). GBT-based local, distortional, and global buckling analysis of thin-walled steel frames. Thin-Walled Structures, 47(11), 1246–1264. https://doi.org/10.1016/j.tws.2009.04.003

[10] Basaglia, C., Camotim, D., & Silvestre, N. (2008). Global buckling analysis of plane and space thin-walled frames in the context of GBT. Thin-Walled Structures, 46(1), 79–101. https://doi.org/10.1016/j.tws.2007.07.007

[11] Zhang, X., & Rasmussen Hao Zhang, K. (2011). Formulation and implementation of three dimensional doubly symmetric Beam-column analyses with warping effects in Opensees. http://sydney.edu.au/civil

[12] Basaglia, C., Camotim, D., & Silvestre, N. (2012). Torsion warping transmission at thin-walled frame joints: Kinematics, modelling and structural response. Journal of Constructional Steel Research, 69(1), 39–53. https://doi.org/10.1016/j.jcsr.2011.07.016

[13] Shayan, S., & Rasmussen, K. J. R. (2014). A model for warping transmission through joints of steel frames. Thin-Walled Structures, 82, 1–12. https://doi.org/10.1016/j.tws.2014.03.017

[14] Vaszilievits-Somjen, B., & Szalai, J. (2020). Simple superelement model of warping transfer in moment connections between I sections. Proceedings of the 9th International Conference on Advances in Steel Structures, ICASS 2018. https://doi.org/10.18057/ICASS2018.P.036

[15] Vaszilievits-Sömjén, B., Szalai, J., & Rad, M. M. (2019). Validation of simple superelement model of warping transfer in moment connections of portal frames. Ce/Papers, 3(3–4), 373–378. https://doi.org/10.1002/cepa.1069

ARCHITECTURE AND URBAN PLANNING

RETHINKING THE TERM GENERAL CITY CENTRE IN CONTEMPORARY URBAN PRACTICE AND ARCHITECTURAL EDUCATION

Dragana Konstantinović[1], Maja Momirov[2], Nina Čegar[3]

Summary:

In the current urban practice, the concept of a *general city centre* is present in a series of planning documents of different levels, used as an adaptive determinant of the purpose of specific plots, enabling the construction of primarily residential buildings and complexes without considering the real needs of the gravitational area and the impact on the existing infrastructure. During the academic year 2022/2023, Master Studio *Architectural Design-Complex Programs* was dedicated to rethinking this concept. The studio was focused on examining all physical, programmatic, spatial, and other basics that can determine the specificity of the realisation of this type and its spatial and programmatic outcomes. The paper aims to show that the general city centre cannot be considered a generic type but rather a representation of the city`s spatial potential for realising public space, facilities with contextually determined programmes and functioning comprehensive infrastructure.

Keywords: urban planning, architectural design, general city centre, Novi Sad, type, public space

[1] Associate Professor, Department for Architecture and Urbanism, Faculty of Technical Sciences, Novi Sad, Serbia, e-mail: konstan_d@uns.ac.rs
[2] Teaching Assistant, Department for Architecture and Urbanism, Faculty of Technical Sciences, Novi Sad, Serbia, e-mail: maja.momirov@uns.ac.rs
[3] Teaching Associate, Department for Architecture and Urbanism, Faculty of Technical Sciences, Novi Sad, Serbia, e-mail: nina.cegar22@gmail.com

1. INTRODUCTION

The concept of a *general city centre* is present in a series of planning documents of different levels. However, using this flexible determinant is focused primarily on the city's strategic development. In the current urban practice, the term is often used as an adaptive determinant of the purpose of specific plots, enabling the construction of primarily residential buildings and complexes without considering the real needs of the gravitational area and not considering the impact on the existing infrastructure, primarily traffic. Additionally, the urban parameters of the realisation of these complexes are very stretchy and undefined, therefore opening the possibility for the interpretation of regulatory parameters in often speculative ways.

In 2022, the new General Urban Plan for the city of Novi Sad came into force, defining the direction of city development until 2030. The turbulent period of public discussions about the plan, which preceded its adoption, brought into focus numerous issues, including implementing the type of *general city centre* (GCC further in the text) and its broad definition regarding programmatic and urban parameters. This strategy was recognised as a point of possible speculation and interpretation of the general city centre type, mainly when it programmatically includes housing in an undefined spatial ratio to public functions.

During the academic year 2022/2023, *Studio 01A Architectural Design-Complex Programs*, within the master programme of Architecture, was dedicated precisely to the topic formed around the term GCC. The assumption is that at this level of study, students can rely on the acquired knowledge in the field of architectural analysis, design processes, urban design, contemporary architectural and urban planning theory and that they can critically reflect on current architectural and urban practice through their creative contributions. The studio was conceptualised around the broader understanding of *complexity,* not exclusively as the diversity of utilitarian functions in a building, but as the complexity of relations, influences and interactions between architecture and environment. [1] Thus, the studio focused on examining all physical, programmatic, spatial, and other basics that can determine the specificity of the realisation of the general city centre and its spatial and programme outcomes.

2. GENERAL CITY CENTRE

The centre of the city, or any settlement, represents a zone that regarding its position inside the city, dominant traffic directions, the significance of certain buildings, the concentration of public programmes, appearance of built structures, communicational capacity of place and other criteria, residents identify as a city centre. [2] The role of residents as the identifying party suggests the importance of the centre to meet its users' wide range of needs, from functional to aesthetic. Different subcategories of centres are planned and developed especially for the purpose of decentralisation, activating central functions in other city areas.

General city centres represent spaces where programmes can be organised into polyfunctional spatial units according to the type and importance of facilities and areas whose population meets. As such, forming primarily public facilities outside the historical centre enables a polycentric way of city development. This concentration of social, cultural, and commercial activities and services defines central urban spaces as specific urban forms of these functions. [3] The flexibility of the determinant of the GCC requires thoughtful and place-sensitive translation into more detailed parameters and conditions related to each location. The fulfilment of infrastructural, primarily traffic, prerequisites is necessary to overcome the possible adverse outcomes of decentralisation, such as the formation of under-capacity centres or isolation by duplicating functions, which occurs primarily due to imprecise programming and the development of general city centres based on the detection of gaps in the urban fabric. [4] The structure of the GCC programme should be formed concerning the role in the entire system of general and line centres, predominantly developed along significant traffic directions and the specific position within the city area.

3. RECONSIDERING THE TERM GCC – ALTERNATIVE APPROACHES

Although research and design are often regarded as separate fields that naturally follow the general process of separating theory and practice, the studio emphasised the necessity of integrating research and design into a unique architectural field. Multifaceted influences regarded through a complex investigation of the architectural programme move, in a way, the domain of research from the investigation of form to the examination of architectural functions [5], stressing the importance of the pre-design research process for the creation of the original design platform. Thus, the research started with analysing the General urban plan for the city of Novi Sad and considering different locations designated as GCC. A dozen locations were whittled down as a shortlist according to criteria related to the specificity of the position concerning dominant natural and relevant urban elements: Danube River or DTD canal waterfront; traffic directions or hubs; entrance directions to the city; typology and programme of surrounding buildings, etc.

The studio highlighted the ambiguity and potential inherent in the concept of a GCC, exploring how these areas can be leveraged to enhance the city's functionality. Reducing these zones to mere housing blocks and office units is a by-product of market-driven construction activities. Alternative approaches, as the studio sought, were aimed at fostering a more liveable, contextually grounded, and human-centred city.

3.1. LOCAL AND DISPERSED: CANAL DTD MICRO-DOSING REGIONALISM (PROJECT 1)

The approach to Project 1[1] involved first determining what the GCC should not be, especially within the specific context of the Canal DTD area. Key points that the authors' manifesto declares are that a GCC does not manifest as a single building, it is not gentrifying the neighbourhood, it does not create a gated community, and it is not investor-driven urbanism. This evaluation was the precursor to defining an alternative solution.

Next, the project proceeds to question the density and character of the GCC, which results in the micro-dosing of programs to preserve the character of a dominantly single-family housing zone while simultaneously introducing a new program to create communal public spaces that are missing in this suburban setting.

Three types were created – worker's hub, community centre, and market, each manifested in a macrostructure that can host large groups of people and microstructures that correspond to their macro equivalent but on a smaller scale and are designed for small groups of people. In this way, a variety of spaces are created, which in their exploitation can be more easily adapted to cater to the needs of its users.

[1] Authors: Luka Radosavljević, Katarina Dojčev, Nina Čegar

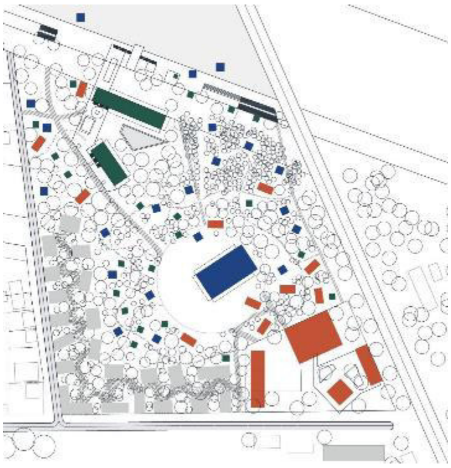

Figure 1 – Plan of Project 1

Figure 2 – Fragment of Project 1: Axonometric view

3.2. THE NETWORK: PROGRAMMATICALLY FLEXIBLE TRANSPORTATION SYSTEM IN JUGOVIĆEVO (PROJECT 2)

Project 2[2] examines the concept of the general city centre from the perspective of traffic infrastructure, with a particular focus on public transport stations as hubs for the movement of people. As a response, the authors have proposed the development of a highly efficient public transportation network that connects various zones within a city, between cities, and internationally, where the spatial capacity of the GCC envisioned in the plan is used within this framework.
The context and the number of users directly condition the programme, type, capacity, and other parameters, so the project presents three primary types of public transport stations, distinguished by their capacity and volume. Further development of each station type is tailored to its specific location. Beyond their central function, serving as public transport hubs, these structures capitalise on the continuous flow of people by incorporating additional features such as commercial spaces, offices, cultural venues, and leisure facilities. In this way, they generate and define a GCC as a spatial network.

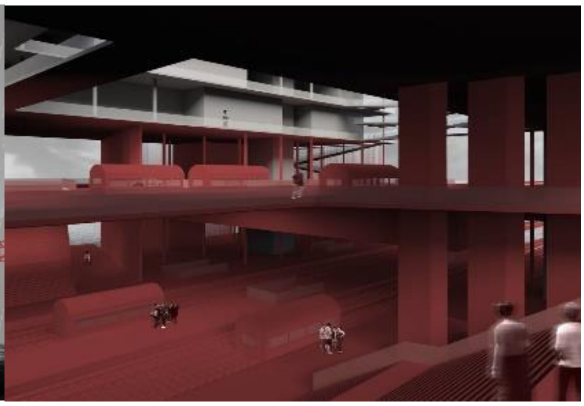

Figure 4 – Medium station in Project 2

Figure 5 – Large station in Project 2

[2] Authors: Tabita Šakanović, Božidar Inđić

3.3. RESPONSIBLE ICON: AGRICULTURE HUB IN FUTOŠKA STREET (PROJECT 3)

Project 3[3] presents a proposal for an Agricultural Hub at a specific location in Futoška Street. The site's characteristics, notably its strategic position at the city's entrance, which serves as a prominent focal point for those approaching the city, have significantly influenced the design decisions and played a pivotal role in shaping the spatial response.

As a result, the mixed-used building, with its programmatic layout and distinct masses, defined the residual space, both outdoors and within the building, simultaneously functioning as a testing ground for various plant cultures and a public area. In this manner, the project explores how a single building can manifest as a GCC, owing to its programmatic and spatial scheme. Furthermore, even the private components, such as agricultural laboratories and institutes, cater to the public interest and are not solely investor-oriented.

Figure 6 – Section of Project 3

3.4. PUBLIC-PRIVATE DIALOGUE: NEW URBAN ORGANISM IN TRANDŽAMENT (PROJECT 4)

Project 4[4] understands the GCC outside the confines of a single multifunctional building, instead regarding it as a composition of urban units. The program and the specific site conditions define the units' form, while a predefined grid system dictates their position.

Although the conventional interpretation of the GCC, encompassing housing and office spaces, serves as the initial reference point, the project expands the programmatic framework and re-evaluates its physical manifestation. This approach offers a unique and distinct spatial response to the urban context.

The project materialises as a mega-block structure at the intersection of architecture and urbanism. It facilitates various types of connections based on desired levels of privacy. Regarding elevation, the ground level is entirely interconnected; the first level functions as a network of public transport and pedestrian routes, and the third level is wholly private and detached.

[3] Author: Đorđe Todorović

[4] Authors: Dajana Stegić, Teodora Jokšić, Yasmina Moumen

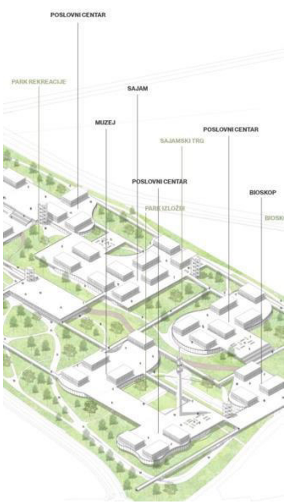

Figure 8 – Axonometric view of Project 4

Figure 9 – Ambiental view of Project 4

4. CONCLUSION

Multiple and heterogeneous forms of problems of contemporary cities, with all the complexities and contradictions that determine them, require polyvalent approaches to activities related to educational and management processes directed towards this issue. [6] Master studies in architecture are precisely the academic level for multi-layered and argumentative analyses of current practices and the creation of innovative strategic frameworks that question the standard planning process and its outcomes. In this respect, understanding the definition, application, and kind of abuse of the GCC type has resulted in a spectrum of new, alternative concepts restoring the urban centre's fundamental qualities.

Analysing the presented projects, clear tendencies can be observed in the answers to the problematic task of reconsidering the term GCC.

Firstly, the topic, which is on some level present in all projects, is the matter of traffic infrastructure as a fundamental precondition for the development of functional systems of city centres. This topic is most dominantly presented in Project 2, which uses one GCC as an example of implementing a much broader coherent system. Project 4 implements a network of public transport and pedestrian routes in the proposal of the GCC as a structure between building and urban development. Even though the other two projects do not directly implement traffic as an element of their design, their concept and programming are directly influenced by the position in immediate contact with significant traffic routes at the entering points of the city.

Secondly, proposals show a significant level of sensitivity to specifics of the exact location. The predominant housing typology of the surrounding area and a deep understanding of the environment's social, cultural, and urban dimensions were crucial for Projects 1 and 4. The dominant city entrance vista and prominent location were taken as an advantage in Project 3, but with the idea that the dialogue between the building and the environment should also be provided on the scale of the community. Thus, the resulting urban design demonstrates innovative formal relations and possibilities for new architecture to emerge.

Thirdly, all the proposals rest on programming, which reflects the public interest within the private or public-private investment framework. The programmatic balance is crucial for providing urban quality and desirable improvement of the neighbourhood on two levels: by understanding and transposing the actual needs of the inhabitants of the

gravitational area, on the one hand, and considering the position and functions of the GCC within the city's centres network, on the other hand.
The presented research and its outcomes undoubtedly show that GCC cannot be considered a generic type. Although the studio was not designed with ambition or the scale to resolve the evident problems of city planning, it indicates, through argumentative and creative proposals, the spectre of the indispensable influences that shape cities and their public and private spaces.

ACKNOWLEDGEMENT

This research has been supported by the Ministry of Education, Science and Technological Development through project no. 451-03-47/2023-02/200012.

REFERENCES

[1] Konstantinović D., Momirov M., Jović S. (2021). Lessons from Mišeluk: Innovative methodology for urban architecture design process. *15th International Scientific Conference iNDiS – Planning, Design, Construction and Building Renewal*, Faculty of Technical Sciences, Novi Sad, Serbia, 24-26 November, pp. 211–220.

[2] Pravilnik o sadržini i izradi urbanističkog plana. Službeni glasnik RS. br. 33; 16. jul 1999.

[3] Badovinac, P. (1997) *Centralne urbane funkcije – centri.* Arhitektonski fakultet Univerziteta u Beogradu, Beograd.

[4] Kara-Pešić Ž. (1971). Komparativna analiza Sistema centara u Novom Sadu. *Arhitektura urbanizam*, Volume 63, pp. 43–44.

[5] Konstantinović D., Zeković M. (2015). Research and Pre-Design. *International Conference on Architecture Research ICAR 2015 - Re[Search] Through Architecture,* Ion Mincu Publishing House, Bucarest, 26-29 March, not paginated.

[6] Zeković M., Konstantinović D. (2022). Interdisciplinarno obrazovanje za savremeni grad. XXVIII Skup TRENDOVI RAZVOJA: “UNIVERZITETSKO OBRAZOVANJE ZA PRIVREDU”, Kopaonik, 14-17 February, pp. 32-35.

THE VALUATION'S ELEMENTS FOR UNEQUAL APARTMENTS STRUCTURE IN THE SAME LOCATION

Željko Jakšić[1], Milan Trivunić[2]

Summary:

A good offer of apartments on the real estate market should represent (imply) their production, as good as the housing stock that satisfies a determined level of well-defined qualities, considering the financial user-ability. That engages some questions that include apartment end-users, directly or indirectly: 1) What does the quality of an apartment mean exactly, and how to define it? 2) How a future end user can estimate an apartment's value, whether it is newly built or already in use? 3) What the dwelling spatial levels are, that the end-user influences, and in what scope? The crucial element of quality is the value of the dwelling's area - apartment and an immediate dwelling's environment, which can be analysed upon a few aspects: constructing value, market value, use value, and value during the exploitation.

Keywords: the quality of the apartments, the structure of the flats, the end-user, the estimation of the apartment value

[1] Docent, Fakultet tehničkih nauka, Univerzitet u Novom Sadu, Srbija, alt96@uns.ac.rs
[2] Profesor, Fakultet tehničkih nauka, Univerzitet u Novom Sadu, Srbija, trule@uns.ac.rs

1. INTRODUCTION

The cost price of an apartment is crucial for the user, defining his status as both - a buyer (private sources, loans, subsidies, etc.) and a user (owner, tenant). Providing a satisfactory quality against the invested money, following its requirements, is an ultimate interest for the end-user.

The mechanism of formation of affordable prices by the state has proven to be unsustainable and counterproductive throughout the history of the functioning of the Western real estate market, i.e. if unilaterally the worth of the real estate market, then by the actual laws of the market, or you get an offer of apartments of an inadequate level of quality for the modern conditions of life in the city, or there are simply no goods on offer. The contemporary market regulation mechanisms introduce a designed system of real estate price control, which includes:

- defined level of housing quality introduced into the legal regulation and standards,
- subsidizing housing policy that includes construction apartments, housing assistance, renting apartments, legal security, etc....,
- Shifting from "providing" strategies to "enabling" processes includes other housing providers, such as local communities and organizations, non-governmental organizations and the private sector.

Learned from earlier experiences, developed societies do not want to make a mistake in terms of security and the corresponding minimum housing quality. The evaluation system must have essential importance, not only to determine an existing housing quality but also to influence the raising of that level in a feedback loop, whether through legislation, technical infrastructure or something else.

On a basic level, there are two participants - an end-user and an architect. There are several levels of relationship between these two main participants (illustrated in Fig.1).

Informative level

- information points divided by sectors of basic needs users of the city, which concerns the area of residence - *the built environment* - spatial planning of housing - I phase of information,
- information point in the field of housing - the built environment - offer on the market of (finished) apartments - II phases of information,
- information point in the field of housing - the built environment - offer on the market of designers (natural and - or legal entities) or advisors (tutors) - III phase of information.

Organization level

- presentation (display) of the project process from origin to source - I phase of education,
- defining the level of decision-making availability of immediate users - II phase of education,
- a checklist used to establish direct contact with the user//designer - III phase of dialogue (an interview),
- performance requirements derived from user requirements - IV phase dialogue (performance specification).

Executive level

- getting to know about the supplier of materials, components and elements - I, II, III phase of information,
- acquaintance with companies for the execution of (all types of) works - I, II, III phase of education,
- acquaintance with companies specialising in maintenance objects - I, II, III phase of dialogue.

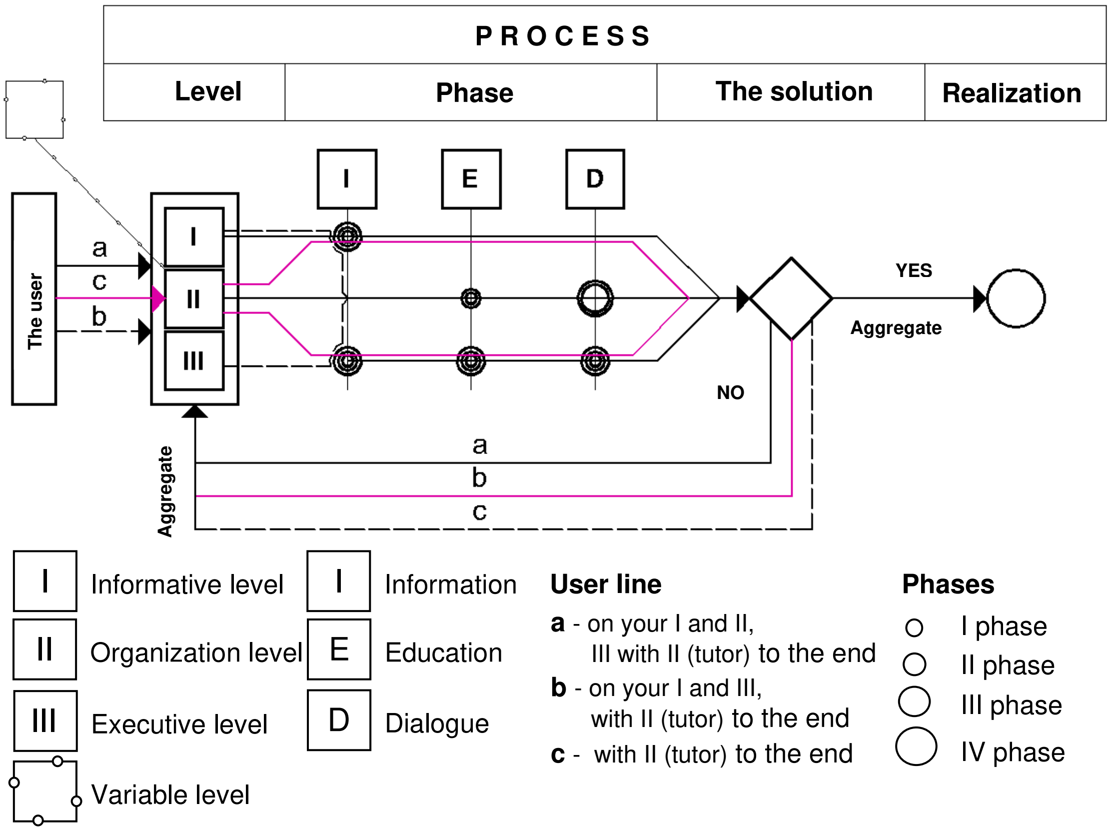

Fig. 1 Proposal of lines of user participation (route) or "logical (rational) path" method [1]

It should be emphasized that the mentioned levels do not condition each other, so the system does not have to be arranged and rounded, but such a state is recommended. More precisely, in the initial phases, when this area is regulated, particular action of regulated parts is also possible; however, the regulated nature of performance-based principles will gradually (automatically) lead to the self-regulation of the entire area (chain reaction). In the feedback loop, the coordinator of these levels can be the chosen designer in several iterations. If the solution selection is unsatisfactory, the option can be the designer excluded from the entire process and replaced by a new one.

2. CITY HOUSING AND MULTI-FAMILY HOUSING

Unacceptable spatial dispersion of cities is not only the consequence of the increased population but also their uneven spatial redistribution (various causes) and non-maintenance of the existing housing stock. To respond to the significant deterioration in the quality of the engaged housing stock, regulations and incentives need to be developed for a mixed approach that will combine repair and renovation schemes with the construction of new buildings only where necessary. The city should not expand.

The issue of relations between users of apartments in multi-family housing facilities is civilizational and more cultural. It manifests itself through several characteristic aspects:

- a population with different habits and customs,
- the uneven economic status of tenants of the same building,
- the level of education is a cause of mutual misunderstanding, and so the appearance of various forms of antagonism,
- different ages.

Most of the past experiences related to the apartment user direct participation mainly dealt with the level of action post-festum, that is, in an already spatially and functionally defined housing structure. That is equally valid when it comes to the design phase and the construction phase. In such a situation, the immediate user acts in a limited space with many restrictions.

Developed countries consider the traditional approach, which does not include the immediate user. The main benefit of this approach is its flexibility (openness) in specific cases, respecting cultural (ordinary) and spatial characteristics of the area (genius loci) to which the solution relates. Contemporary trends allow the end-user greater degrees of freedom, which are included in activities through city forums and making judgments about the meaning of some spatial solutions (they may also concern the policy of spatial development of the city, but also issues directly related to them) and up to deciding on the immediate space of the apartment. There are many limitations to this process. One of the significant limitations is the end-user by himself, which realises his interests in community with the other people, but beyond too. The other side, the opposite, of the human personality is a product of genetic and cultural heritage, education, and habits acquired in the family and the environment in which it developed. All this together limits the degree of freedom of participation in the circulation of multiple users.

3. DETERMINATION OF VALUE PARAMETERS AND COEFFICIENTS FOR EVALUATION OF THE UTILITY VALUE OF THE APARTMENT

An "apartment of quality", according to the interpretation adopted so far, represents a set of standard elements of the organization of the apartment space in interrelationships. That is most often related to the number of rooms combined with the achieved interconnections - communications, the equipment of auxiliary rooms and the apartment area. This "hard" structure has a more/less closed concept that was partly developed, to the maximum, to the extent that it implied the "movement" of the apartment space.

3.1. POTENTIAL FOR DEVELOPMENT AND CAPACITY FOR VARIABILITY

There are certain limitations when talking about the potential for spatial variability of the immediate residential area by zone:

- The strict city centre downtown is, to a greater or lesser extent, a space of historical, ambient, cultural and architectural value, which tends to be preserved mostly as authentic.
- The wider downtown area is characterized by the emphasized need for transformation, especially when being infrastructural equipped, and represents the city's administrative and business area.
- Areas in the suburbs are historically specific for most settlements, specifically when the cities become larger: they were affected by the Industrial Revolution of the 19th century and then the wave of urbanization in the 20th century as satellite settlements.

The capacity of variability represents the ultimate possibilities of development or adaptability at a spatial level, and it is conditioned by the provisions of the regulation in the part when its solutions are specified. *"Knowing this indicator makes it possible to specify the performance of the building in terms of its adaptability to the diverse requirements of the users. Aspects that indicate the 'capacity for variability' are classified into aspects of the decision-making level, the construction of the object and the parts for installation."* [2] That one should represent the presence of inventive design, that is, the act of established (continuous) planning and build-up of the residential environment.

3.2. TECHNICAL POSSIBILITIES OF DEVELOPMENT AND VARIABILITY

The existence of "hard" project solutions for housing structures on elementary spatial levels produces "locked" solutions of flexibility and adaptability, too. Modern man demands changes. Modern man requires changes, but often not the place of residence (apartment, building or neighbourhood). From that point of view, it takes the "openness" of the structural system and the technical solutions as additional non-standard quality.

3.2.1. Development potential

Development potential represents the area of intervention in the residential environment within the limits defined by the legislation for the domain, municipality or city. Limitations specified through design conditions are often related to site characteristics. Additional limitation elements are the character of the applied technical system (hard and soft) and the spatial levels (three spatial levels - apartment, building, and neighbourhood) directly related to the decision-making of an end-user.

Development potential (as well) represents a real possibility of the housing area quality changing according to existing environmental conditions (social, technical, and normative). Its factors are - a) accessibility of the road and its fit-out, b) a reserved area for potential expending, c) the structure with reserve loadbearing, d) adaptable structure, e) partitions, (de)mountable - all or some of them, f) installations - allows apartment adaptability.

3.2.2. Changeability capacity

In the technical area, changeability capacity reflects through all possible solutions of the requested satisfactory performance to allow end-users to make choices. Due to that, we can get an answer to the question: " What the specific space can offer us?" The predictable solutions process and the space transformation limits are some of the main characteristics of that process.

There is a significant connection between the processes of designing and production of the components and elements for quality implementation of the changeability capacity. For example, the choice of quality solutions requires the ability to choose from a "product catalogue", but a wide selection from the catalogue is the rolled practice result that is the product of stimulated inventive design (by the city government and upwards). Therefore, the evaluation of this indicator represents a path from desires to possibilities.

3.2.3. Determining aspects of the utility value of the apartment - performance levels

An essential parameter of the useful is the analysis of needs that regulates the basic assumptions for creating all working places (sleeping, eating, rest, learning, etc.). In the circumstances of a 'motile' apartment area (dwelling area at all), it takes both: a) essential and b) adaptiable needs.

Basic housing needs are relatively "firmly" defined because they are applied for a long time without supplementing the content; they represent a model of everyday life. The teacher designer needs to familiarize the user with these needs, which implies his high information of these.

Adapted (adaptable) housing needs represent non-standard variable values: they are subjective, with an individual character, even among members of the same family. The nature of these needs ranges from technical (material - exact) to aesthetic (intangible - abstract). At these needs, the tutor designer can also point out which he reached based on the created user profile (social, economic, professional, biological-anatomical, etc.).

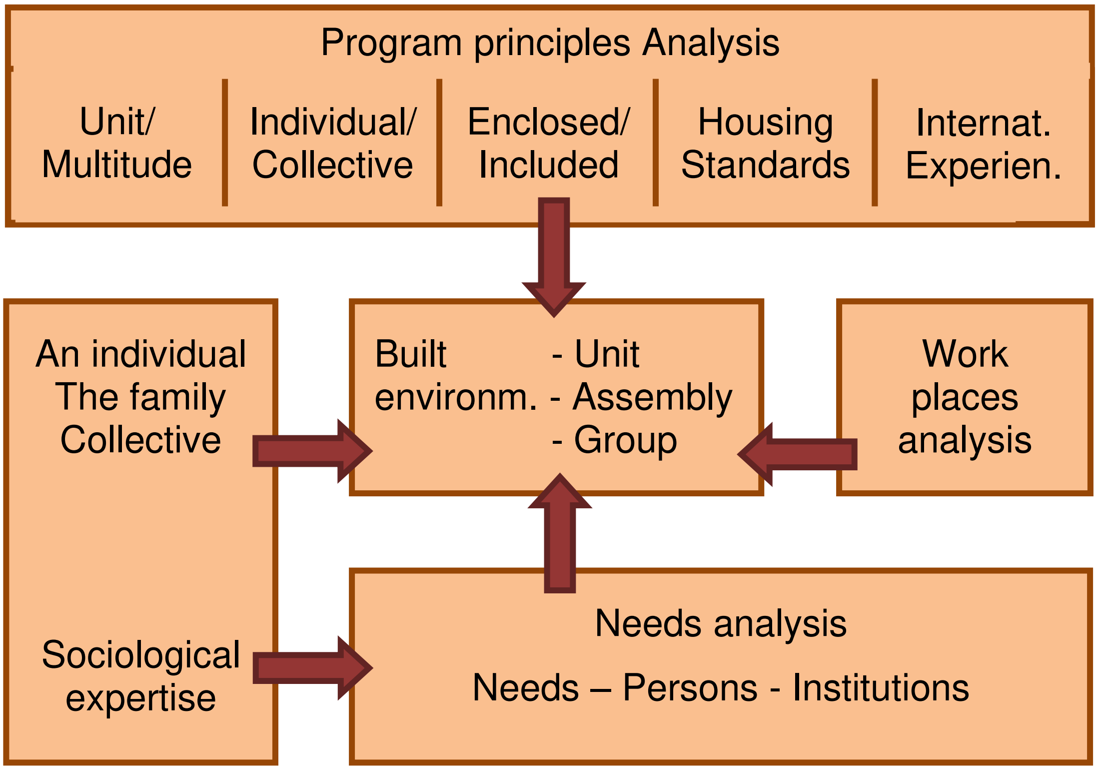

Fig. 3 General scheme of program action [3]

The tutor designer can also point out the needs that he reached by creating a user profile (social, economic, professional, biological-anatomical, etc.). Several aspects are in use to observe the apartment growth, divided as follows::

- quantitative, by physically increasing the spatial contents within the limits of the existing boundaries: a) dimensions of the building (or outside it - in horizontal or vertical projection); b) apartment or by floor (on the same floor joining two apartments or parts of the space of two apartments, or as duplex between two floors);
- qualitative: a) by equipping with devices to support physical and technical functions of housing (Fig. 2); b) by introducing the logical relationship between the head and auxiliary rooms; c) establishing quality communication flows.

The growth phenomenon is a necessary quality observed from the valuation point, specifically related to the life cycle. However, the growth aspect is not necessarily a priority during the valuation; the and-user can recommend that the apartment consists of fully defined qualitative characteristics (hard designing).

4. ASSESSMENT OF APARTMENT USEFUL VALUE

After end-user request analyses, the designer-tutor assesses the elements and the apartment's utility aspects (or housing).

For a simplified process of review, the spreadsheets are in use.

As human needs determine elements of building properties, it is necessary to define them duly within the developing performance criteria process. This process should include research on people's behaviour towards the built environment, which covers the fields of physiology, psychology, sociology, anthropology, and ergonomics, as well as for special populations (such as the older and people with disabilities). Quantifying these criteria requires the application of uncertainty modelling and probabilistic methods. That is necessary if multi-level performance levels have meant developing.

'If a building is viewed as a matrix of parts and attributes, the main difference between the traditional prescriptive approach and the performance approach can be illustrated as shown in Figure 2. In the prescriptive approach, the building parts are described, specified, and procured, resulting in a building with an implicit set of attributes (Fig. 2a). In the performance approach, the building attributes are described and specified, and many different building parts combinations could be procured for which can be demonstrated that the specified attributes will be provided (Fig. 2b).' [4]

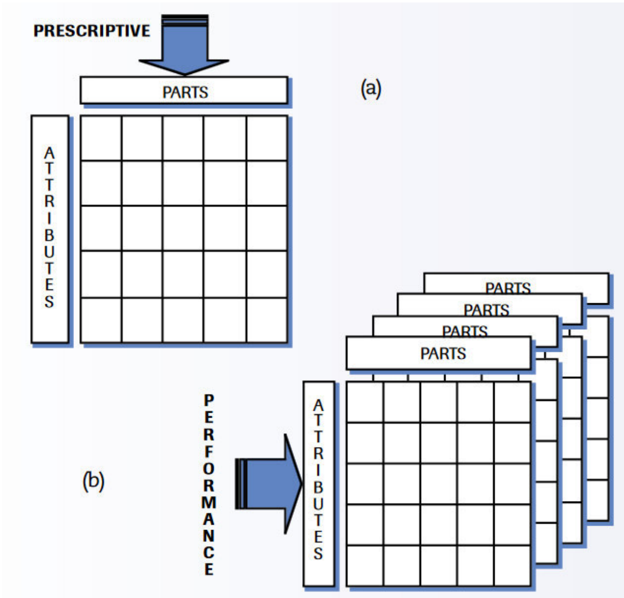

Fig. 2 A matrix of parts and attributes: (a) The prescriptive and (b) the Performance approach [4]

The valuation of the residential environment starts with the monetary value that the future user is ready to invest. For determining the final worth, the market value of the m2 of the apartment is crucial. However, it is inadmissible for the final price to be formed only based on one or two key parameters (e.g. the location's attractiveness). Due to that, the overall worth valuation is conditioned by the performance concept.

In that process, the client (user) decides in what percentage the market (production price) will participate and in what percentage the influence of performance. The highest ratio is 1:1 or 50%:50% when the highest worth of the residential environment is formed based on high quality. The lowest proportion of these two parameters is 99%:1% in favour of the apartment production price. That proportion shows expressed user disinterest in the quality of the environment in which he lives.

The following equation explains the total value (in monetary terms) of the residential environment:

$$C=PT_c \tag{1}$$

Where is:
C – the total value of the residential environment in currency,
P – estimated performance value,
T_c – production price for a specific area (location) in currency.
The estimated performance value represents a specific part of the equation of the several parameters. Defining the relationship between the impact of production price and performance is a procedure left to the future user to determine as "impact bidding". The following equation shows the determination of the estimated performance value:

$$P = Lk_u/3 \tag{1.1}$$

Where is:
L – bidding coefficient,
k_u – value parameter of all three spatial levels (apartment, building or neighbourhood),
3 – number of evaluated spatial levels

Based on the bidding, the *bidding coefficient* (L) is:

$$L = (1/l_{tc})100 \qquad (1.1.1)$$

Where is:
l_{tc} – share of the market price (%).
For all three spatial levels (apartment, building or neighbourhood) were Value parameters (kn), and for each was assigned the maximum value of 1 (one). The parameter value is obtained from the selected attributes ratio and attributes total number. These value parameters are determined tabularly.

$$k_u = k_1 + k_2 + k_3 \qquad (1.1.2)$$

Where is:
k_1 – total value parameter for the levels from region to settlement,
k_2 – total value parameter for the level of immediate housing environment,
k_3 – total value parameter for the housing unit level of multi-family housing with a typical floor and for the residential level units – apartment.
The final value can be lower ($1<k<3$), and if the sum of all three coefficients about the ku value is below the percentage share of the production price, the production price then reduces. When all three levels are fully satisfied (according to the established criteria), they carry 3 (three) quality points. The residential environment price (the price expressed through the apartment price) in the newly built facilities must not contain the coefficient $P<1$ caused by a lack of reference elements quality (location, residential building, residential unit - apartment).

5. CONCLUSION

Housing is not only the apartment where an end-user spends most of his life (no less important factor) but also the apartment's immediate environment - the building and micro-location. Satisfying the direct user's requests forms a matrix for finding more complex solutions for a suitable residential environment. The "ideal concept" (the basic creative principle of the 20th century) is no longer sustainable because no phenomenon or process is complete. It lasts (grows and develops), especially for human needs. Here are the needs of people in the time-space of one hundred to two hundred years, but also about the needs of one user's generation. Valuation of the two higher spatial levels (building or neighbourhood - apartment is the first and founded) in that process for the end-user has a crucial place.

The implementation of the *location's characteristics* valuation from the level of the region to the city level for the user as informative data is significant, but above all, as a condition that can be significant for him if, during the valuation, he gives equal importance to several life functions (e.g. housing and work - life in an industrial or business area).

Valuation *The immediate residential environment* is significant for the housing quality because this level interacts with the housing level - the apartment. Almost all the quality features of a residential unit become worthless if the environment (a similar) quality to the apartment does not follow. At this level, the priority is to form residential structures that affect the definition of the public/private relationship without or with elements of physical separation assigning desired characteristics.

However, for this or a similar valuation methodology to come to life and apply in practice, its implementation is necessary for a valuation system within the appropriate legislation and not just a measure of personal choice of the housing users.

ACKNOWLEDGEMENT

The research has been conducted within the project "Scientific theoretical and experimental research and improvement of educational process in the field of civil engineering", developed at the Department of Civil Engineering and Geodesy, Faculty of Technical Sciences, University of Novi Sad, Serbia.

REFERENCES

[1] Jakšić Ž. (2007). Performance concept and utility value of apartments in multi-family housing facilities. Doctoral thesis (in Serbian), University of Novi Sad, Serbia.

[2] Krstić A. (1997). The variability of housing structures as a condition for fulfilling user requirements. Architecture and Urbanism 4, Belgrade, Serbia. YU ISSN 0354-6055 (in Serbian)

[3] Milenković B. Elements for defining the project task. University in Belgrade, Architecture faculty, postgraduate study, a course - housing, notebook 8. (in Serbian)

[4] Hattis D. (1996). Role and significance of human requirements and architecture in the application of the performance concept in building. In: Proc. 3rd CIB-ASTM-ISO-RILEM Inter. Symp. R. Becker. and M. Paciuk, eds. Vol. 1. National Building Research Institute, Haifa, Israel.

THE INFLUENCE OF THE NEIGHBORHOOD BUILT ENVIRONMENT OF COLLECTIVE HOUSING ON QUALITY OF LIFE: AN EXAMPLE FROM NOVI SAD, SERBIA

Violeta Stefanović[1]

Summary:

The dominant way of city living is in the form of collective housing blocks, which represent a crucial spatial frame. The structure, morphology, programming and microclimate conditions of these residential areas highly impact the resulting quality of life, creating preconditions for the type of experiences residents can have in their primary surroundings. Relying on cross-disciplinary studies, theories and research referring to the relation between the neighborhood built environment and the physical, social and mental well-being of residents, this paper aims to analyze a selected residential block from Novi Sad (Serbia) in order to evaluate the quality of life its physical characteristics can generate. The criteria for analysis are based on key components of residential blocks such as open public spaces, green areas, morphology and programming, which are in a direct relation to the well-being of its users.

Key words: neighborhood, built environment, collective housing, quality of life, well-being of users, Novi Sad

[1] M.Sc. Arch. and PhD candidate, Senior Scientific Researcher, University of Novi Sad, Faculty of Technical Sciences, Department of Architecture and Urbanism, Novi Sad, Serbia, violeta.stefanovic@live.com / violeta.stefanovic@uns.ac.rs

1. INTRODUCTION

The link between housing and the everyday lives of its users and residents is undeniable and the extent to which various elements of the physical environment affect people has been researched in a multitude of aspects. When it comes to todays' dominant way of city living in the form of collective housing blocks, there is a great complexity of influences generated by physical surroundings created in the urban context.

If we were to define two segments of space within the residential area of a collective housing block in a city, where the first one refers to the individual residential dwelling occupied by a resident – the "inner" segment, while the other one, the "outer" segment refers to the immediate surroundings of the residential building, we can begin to understand the importance of the entire neighborhood as a vital physical frame. The importance and deeper meaning of housing as one of the primary elements of human existence is a never-ending complex matter. While we generally consider the aforementioned "inner" segment of residential space as a private, safe and familiar area, the "outer" segment of a residential area is shared with other residents and users and therefore is not at the same "level of control" as a private dwelling is. However, the physical characteristics of the neighborhood in the sense of urban design and urbanism greatly affect the ambiance, safety, possible uses of the space, as well as its microclimate, directly affecting the type of activities that can be carried out within it, influencing the relationship users can have with the space, as well as with one another. Therefore, the built characteristics of a neighborhood are extremely important for the overall experience and well-being of residents on a daily basis.

As we have already mentioned, housing and its characteristics is of great importance to the general well-being of its residents. The World Health Organization (abbreviated: WHO), in its publication concerning guidelines for housing and health states that healthy housing is shelter that supports a state of complete physical, mental and social well-being. Apart from individual dwellings, or the "inner" segment of residential space, this also depends on factors outside its walls. It depends on the local community, which enables social interactions that support health and well-being. Healthy housing also relies on the immediate housing environment, and the extent to which this provides access to services, green space, and active and public transport options, as well as protection from waste, pollution and the effects of disaster, whether natural or man-made [1].

Therefore, when it comes to the neighborhood built environment of collective residential housing complexes, it needs to provide specific "infrastructure" in terms of programming, green areas, safety, as well as access to public transport and services in order for the residents of that residential area to have a good quality of life.

Focusing on the elements described in this chapter, this paper aims to analyze an example of a collective housing block in Novi Sad, Serbia in terms of the overall neighborhood built environment with regard to influencing quality of life of the residents. Relying on crucial aspects of built environments that can influence life quality pointed out by various researchers, as well as relevant social-humanistic theories, focusing on spatial infrastructure that promotes the physical, mental and social well-being of its residents, we will be able to evaluate the quality of life that can be established in a specific housing block which is a prime example of collective housing in Novi Sad, Serbia.

2. ANALYSIS OF A COLLECTIVE HOUSING BLOCK IN NOVI SAD, SERBIA IN TERMS OF ITS INFLUENCE ON THE QUALITY OF LIFE OF ITS RESIDENTS

When it comes to selecting a relevant example of a collective residential housing block in Novi Sad, it is important to mention the genesis of this form of cohabitation in this city. The city of Novi Sad went through numerous changes in the past, but its modernization is what characterizes it in a significant way even today. The biggest changes to the city's urban fabric were made after the Second World War, during the socialist period when the building activity was extremely high. The city went through several radical changes carried out by means of official urban planning documents. As for housing, this period introduced large collective housing complexes guided by the ideas of the modernism, as well as socialist paradigms of equality. Before this, traditionally built, privately owned houses were predominant. These collective complexes are characterized by their large scale - the land was then owned by the state (or public), making it possible to execute large projects on generally previously unbuilt land. These blocks usually feature vast green areas, as well as other urban elements intended for public use (i.e., urban furniture, plateaus, sport courts). These housing concepts were continually developed throughout the duration of the socialist period [2]. The period of political and economic crisis in the 1980s, which culminated with the 90s' armed conflicts, eventually led to the official disintegration of the Socialist Federal Republic of Yugoslavia. This brought with it new economic, cultural, social and political circumstances that also resulted in a new approach to housing. In post-socialism, private investors predominately shape the housing fund, usually erecting buildings on small lots previously occupied by single-family houses, with little or no provided public space for the residents.

Therefore, generally speaking, there are two types of collective housing forms present in the urban fabric of Novi Sad today. However, for the purposes of this paper, a block from the socialist period was chosen as an example for analysis. This was done in accordance to the fact that multiple official and unofficial public surveys were conducted over the years concerning the public's opinion about the "best" area in Novi Sad to live in, and the results always indicate that the general public prefers the areas built during the socialist period. For example, a poll created by a local news outlet in 2021 reported that 23.95% of poll participants (1671 out of 6978 participants) would choose to live in the Liman area of Novi Sad (built between the 1960s and 1980s) [3]. Thus, it will be interesting to see whether the physical characteristics of the residential area which is the choice of the general public concerning perceived quality of life correspond to the aspects of the neighborhood built environment stated by research to be relevant for establishing good life quality.

2.1. A COLLECTIVE HOUSING BLOCK THE LIMAN AREA

The Liman area is a part of the city of Novi Sad that is actually comprised of four segments, with the names of these segments corresponding to the order in which they were realized. Therefore, the blocks in the Liman I area were the first to be built, during the 1960s, while the blocks in the Liman IV area were part of the last instalment, built during the 1970s (Figure 1). This timeline is especially relevant considering the fact that these housing concepts were continually developed.

Fig. 1: Segments of the Liman area; source of the original image: Geosrbija (https://a3.geosrbija.rs/)

For the purposes of this paper, a block from the Liman IV area will be analyzed, considering that it is a prime example of that which was envisioned and established by the architects working on housing concepts during the socialist period. During the seventies, having realized the minimum standards for the state's functioning, socialist Yugoslavia reached a state of utter well-being. This period was characterized by strong enthusiasm and zest, which made way for more innovation regarding architecture and its programs. In terms of residential architecture, the impact this development had on housing can be seen through the further development of housing concepts and the wider programming of the blocks. Numerous realizations and the forming of entirely new city areas were also accompanied by theoretical and other research in the fields of habitology [4].

The block in question will be thoroughly presented, portrayed and analyzed throughout this chapter, along with the relevant aspects of the built environment that influence physical, mental and social well-being that were previously described. With the aim of providing a clear overview of the analysis, the next part of this paper will be divided into four segments, each one of which referring to specific aspects of the neighborhood built environment regarding the framework set up in the beginning of this paper. These segments will be: safety, vegetation, community and other important aspects for everyday life.

2.1.1. Safety

When it comes to safety in terms of collective housing blocks, it is worth considering the fact that there are two types of safety to be evaluated: physical safety (the dominant way in which we perceive safety), as well as psychological safety, which is more personal, referring to the feeling of security people experience. Both are important, but the presence of one does not always guarantee the other [5].

In their work, which researches the correlation between the happiness of residents and the built environment of a neighborhood, authors Pfeiffer and Cloutier, relying on the existing research of numerous authors, mention the feeling of security of residents as well: A neighborhood's physical characteristics also affect its "eyes on the street" which monitor activities and can discourage disorder and decay, as well as criminal opportunities of crime. For instance, residents living in neighborhoods with buildings that have more street frontage and windows facing the street may be more aware of

what is happening in the neighborhood and able to contest threats to personal security. In turn, neighborhoods with fewer problems, such as vacant or deteriorating buildings and unlit spaces hidden from public view, may have fewer places where people can engage in elicit behaviors, deterring criminal activity [6].
When it comes to the collective housing block selected for analysis, its morphology indicates that it can be considered as an "open" block, meaning that the buildings are positioned in a way that enables passage from the streets and throughout the entire block (Figure 2). The parking spaces are located in the corners of the block, making the inner part of the outer area to be more accessible and safer for pedestrians. Residents and other users are able to spend time in the shared courtyard without having to look out for ongoing traffic, which in turn increases the possibilities for children to participate in activities, considering the fact that there is no threat of encounters with vehicles. There are a few paths intended for access to parking garages which are in the basements of the buildings, but they are divided from the public spaces via height difference and street barriers. Regarding the feeling of security, we can establish that a lot of the dwellings look out onto the inner courtyard, making the "eyes on the street" phenomenon extremely present. That, along with the fact that the area is well lit by street lamps makes this area safe at night as well.

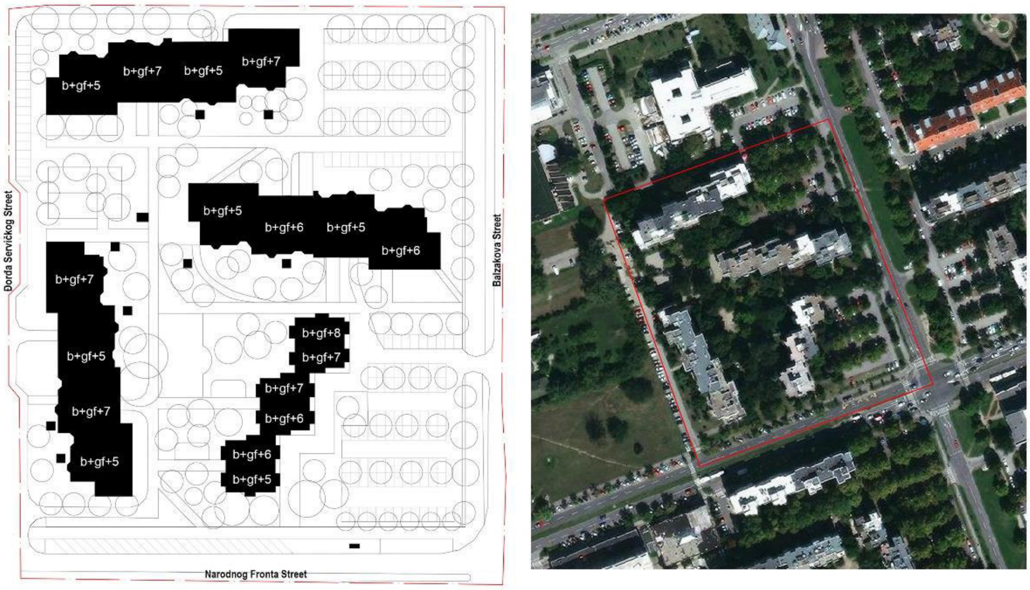

Fig. 2: A block in the Liman IV area: morphology (left); source: author; ortophoto (right), source of the original image: Geosrbija (https://a3.geosrbija.rs/)

2.1.2. Vegetation

The health benefits of urban green space are well recognized for children, whose physical and mental development is enhanced by living, playing and learning in green environments. The elderly also benefit significantly from visiting green and blue spaces, through improved physical health and social well-being. The World Health Organization recommends that all people reside within 300m of green space [7]. The importance and lack of green public spaces in city residential areas has been highlighted in recent years, especially during and after the Covid-19 pandemic lockdowns. Having access to these kinds of areas not only benefits the living conditions in terms of microclimate, but it also benefits the overall health and mental health of residents.

Fig. 3: A block in the Liman IV area: vegetation; source: author, July 2022

From the satellite image (Figure 2) of the block in the Liman IV area, it is clear that a major part of the shared outer space of the block is enriched by vegetation. Apart from green areas, the high number of trees provide a favorable microclimate (Figure 3). The trees also create suitable shade during the hot summer months, meaning that residents are more likely to be able to spend time outdoors than they would be if there were no trees or green areas, seeing that concrete absorbs the heat which raises the overall temperature of the space.

2.1.3. Community

If communities are defined as aggregates of people who share common activities and/or beliefs and who are bound together principally by relations of affect, loyalty, common values, and/or personal concern (i.e., interest in the personalities and life events of one another) [8] and a city community rests and survives on territorialized social relations which are mediated by urban interventions in space [9], the link between the shared residential area and the resulting community is undeniable. Also, the physical characteristics of a neighborhood, including its housing design and density, street connectivity, land use mix, and the availability of public spaces, may lead to more or less opportunities for social engagement among neighbors [10]. Therefore, the built environment of a neighborhood can provide necessary infrastructure in terms of urban elements and designated spaces intended for public use. The opportunity to spend time in shared public spaces, taking part in shared activities and socializing creates a base for interpersonal relationships between residents, which in turn form a community. Therefore, the more opportunities there are for encounters and socialization, the stronger the community can become. Communities enrich the overall quality of life by aiding the mental and social aspects of a person's well-being, which is extremely important.

Fig. 4: A block in the Liman IV area: public spaces; source: author, July 2022

The block being analyzed contains numerous pathways, plateaus and two sport courts (for basketball and futsal), along with urban furniture intended for sitting. This ensures that residents of all ages are able to spend their free time in these spaces, participating in collective activities both spontaneous and planned (Figure 4). Of course, they can spend their time alone as an individual as well, seeing that the vegetation and safety mentioned before allows for carefree leisure. The possibilities for social encounters are plentiful, meaning that there are preconditions for the establishing of a strong community which not only satisfies the social needs of its members, but also creates the feeling of security which is highly important for mental well-being as well.

2.1.4. Other important aspects for everyday life

Apart from the most important aspects for physical, mental and social well-being, there are other aspects that are relevant when it comes to the quality of everyday life in cities. It is worth noting that the analyzed block has two bus stations in its immediate surroundings, with a total of 5 city bus lines passing through them. Surrounding the block, there are numerous shops and cafes, as well as other services (along the Narodnog Fronta and Bulevar cara Lazara streets). There is also a kindergarten adjacent to the block, and primary schools nearby. All of these added aspects make everyday life more convenient and easier for the residents and should be considered in terms of evaluating life quality.

3. DISCUSSION

The analyzed block located in the Liman IV area is one that provides a lot of different elements that residents can benefit from. The morphology of the block and the parking solution ensures physical safety, whilst the number of courtyard-facing dwellings and numerous street lamps ensure for the feeling of security as well. The rich vegetation present in the entire block area creates a favorable microclimate and ambiance, whilst creating the possibilities for residents to spend time in the shared open space even in hot extremely hot weather. Also, seeing as the courtyard has been widely programmed, containing different public spaces and urban furniture intended for different purposes, it is clear that there are a lot of possibilities for social gatherings and encounters. This ensures that relationships can be built between the residents, which is the foundation of establishing a community. The more the residents become interconnected, the stronger and more complete a community becomes. These are all elements of the neighborhood built environment which enable the satisfaction of people's complex needs. These characteristics of the physical surroundings of a collective residential block beneficially influence the quality of life, in terms of physical, social and mental aspects of a person's well-being.

4. CONCLUSION

Through the analysis conducted in this paper, concerning the evaluation of quality of life that can be established in a block in the Liman IV area in regards to research-based aspects pertaining to a person's well being has shown that the built area of this neighborhood beneficially influences the everyday life of the residents. The fact that the results of the previously cited poll indicate that the majority of the respondents would prefer to live in the Liman area in Novi Sad, whilst the results of this paper indicate life quality to be of a high standard in this area shows that the general public is good at recognizing built characteristics of neighborhoods that are favorable for everyday living. That being said, it is important to realize just how much of an impact the built environment of a neighborhood has on the lives of its users. Many residential areas in the city do not possess enough green areas, urban elements, public spaces or safely divided pedestrian areas. These are ongoing issues many cities are facing and only the future will tell whether the needs of citizens in terms of good life quality pertaining to the mental, physical and social aspects of well-being will be met more often through the planning of collective residential areas. By conducting a wider programming of the shared residential areas of collective housing blocks, establishing public spaces created with intention, while not neglecting the need for green spaces and general safety, it is possible to create residential areas which encourage life in a community where people feel comfortable spending time in collective spaces. This leads to a more fulfilling life for residents, enhancing their well-being in a multitude of aspects.

ACKNOWLEDGEMENT

This research (paper) has been supported by the Ministry of Science, Technological Development and Innovation through project no. 451-03-47/2023-01/200156 "Innovative scientific and artistic research from the FTS (activity) domain".

REFERENCES

[1] World Health Organization. (2018). WHO Housing and health guidelines. World Health Organization, Geneva.

[2] Stefanović, V. (2023). Razvoj urbanih zajednica u Novom Sadu. U D. Konstantinović, i M. Zeković (Urednici), Novi Sad - Moderni grad (str. 130-157). Novi Sad: Fakultet tehničkih nauka, Univerzitet u Novom Sadu i BAZA-platforma za prostorne prakse.

[3] 021.rs. (15.07.2021.). Anketa: Koji je najbolji novosadski kvart? Preuzeto 07.09. 2023 sa internet stranice medijskog portala „021": https://www.021.rs/story/Novosadske-price/279380/ANKETA-Koji-je-najbolji-novosadski-kvart.html

[4] Alfirević, Đ., Simonović Alfirević, S. (2018). "Socijalistički stan" u Jugoslaviji: obrazac ili tendencija? *Spatium,* Volume 40, pp. 8-17.

[5] Stefanović, V. (2022). Promena u stepenu urbane bezbednosti i formiranju zajednica - od socijalističkog do post-socijalističkog višeporodičnog stanovanja u Novom Sadu. *Druga naučna konferencija; Urbana bezbednost i urbani razvoj,* Univerzitet u Beogradu, Fakultet bezbednosti, Beograd, Srbija, 1. Jul, pp. 73-83.

[6] Deirdre, P., Cloutier, S. (2016). Planning for Happy Neighborhoods. *Journal of the American Planning Association*, Volume 82(3), pp. 1-13.

[7] The European Environment Agency. (2022). Who benefits from nature in cities? Social inequalities in access to urban green and blue spaces across Europe. The European Environment Agency. doi:10.2800/041176

[8] Brint, S. (2001). Gemeinschaft Revisited: A Critique and Reconstruction of the Community Concept. *Sociological Theory*, Volume 19, pp. 1-23.

[9] Pajvančić-Cizelj, A., Knežević, J. (2017). Socio-prostorna transformacija i susedski odnosi u Novom Sadu. *Annual Review of the Faculty of Philosophy*, Volume XLII-2, pp. 441-455.

[10] Deirdre, P., Cloutier, S. (2016). Planning for Happy Neighborhoods. *Journal of the American Planning Association*, Volume 82(3), pp. 1-13.

LOGIC OF FORM VS. FORMALISM: TEACHING DESIGN IN ARCHITECTURE

Višnja Žugić [1], Maja Momirov [2]

Summary:

This paper focuses on the topic of Design in Architecture, and the problem of teaching the basic principles that regulate architectural form on the level of perception and visual poetics, to first-year architecture students. To overcome the challenge of focusing on the logic of form without promoting formalism as such, the course is designed around the idea of engaging students to think and realise their ideas creatively, on an abstract level. Students are taught basic principles of spatial articulation and ways of applying these principles as the visual qualities of spatial compositions along with managing them as specific tools in a creative process. Through analysing a number of students` works, the paper aims to show that the architectural form is not the goal of architectural design but its result, which is primarily informed by our intentions, shifting the focus away from formalism, towards a deeper understanding of the logic of form.

Key words: design principles, architecture, architectural form, spatial articulation, education

[1]Assoc. Prof., Faculty of Technical Sciences, University of Novi Sad, Serbia, zugic.visnja@uns.ac.rs
[2]Teaching Assistant, Faculty of Technical Sciences, University of Novi Sad, Serbia, maja.momirov@uns.ac.rs

1. INTRODUCTION: UNDERSTANDING THE LOGIC OF FORM

This paper focuses on the topic of Design in Architecture, and the problem of teaching first-year architecture students the basic principles that regulate architectural form, on the level of perception and visual poetics. The course Design in Architecture – Introduction[1] presents the basic principles related to the Theory of Form, and their appropriation in the context of architecture. Given the fact that the course is taught at the very beginning of students' engagement with architecture studies, its thematic framework, and especially practical outcomes are relieved from all those influential forces and complex parameters which inform the process of architectural design - the limitations of the location; climate; context (physical, morphological, temporal, social, political or cultural); users and their needs; specificities of a programme, etc. Such a thematic framework that essentially focuses on architectural form without prior knowledge and awareness of all the complex inputs that influence the design process, can be easily interpreted as a framework that promotes a rather formalistic approach to architecture. To overcome the challenge of focusing on the logic of form without promoting formalism as such, the course is designed around the idea of engaging students to think and realise their ideas creatively, on an abstract level. Rather than focusing on buildings, the course is dedicated to the analysis, understanding and articulation of space. Exploring spatial relations, as a problem of three-dimensional morphology and composition, brings a certain level of abstraction that is needed in the process of studying and understanding the poetics of architectural and spatial form.

2. BASIC PRINCIPLES OF DESIGN IN ARCHITECTURE

The logic of architectural form and the articulation of space is taught through two groups of exercises, each focusing on model-making as both the final product and the tool of the research process. This practice-based methodology that results in a number of individually made, abstract spatial compositions, encourages the students to explore space through physical, thematic and technical constraints, engaging directly with the spatiality of the construction process. Furthermore, this process of model-making is understood as the process of exploring, sometimes with unintended outcomes, rather than a representational tool for the previously (and rationally) shaped ideas. Limiting the number of materials intended for the creation of the final models focuses the students' attention on spatial relations, rather than the colours and textures of the materials, since their apparent tangibility can divert students from engaging in a deeper understanding of the principles of spatial articulation. Models are made on a flat base with predefined dimensions. This establishes the spatial framework for the realisation of the model, but it also represents an equally important element of the composition itself, to which the students relate their compositions through proportions, positioning and relationships between built and unbuilt space.

The first part of the course is dedicated to introducing the basic principles of design in architecture: *Rhythm*, *Volume & In-Between Spaces*, and *Variation*. The second part of the course slightly shifts the focus, introducing the immaterial aspects of spatial design, such as textuality of form, ambience and atmosphere. With a different methodological approach, the second group of exercises demonstrates the creative implementation of the previously exercised principles.

---

[1] The course Design in Architecture – Introduction is taught within the first semester of the Undergraduate Academic Studies of Architecture at the Faculty of Technical Sciences at the University of Novi Sad, Serbia

2.1. RHYTHM

In the context of architecture, rhythm is defined as the repetition of a motif or formal element in a specific pattern, at regular or irregular intervals, in the same or modified form. It can be expressed as a repetition of linear architectural elements, shapes, spatial segments, materials and colours, textures or other formal characteristics of the built structures. The principle of repetition or a sequence of architectural elements can be used to direct perspectives or movements in space and time. As a design principle, rhythm in architecture is understood through the organisation of repetitive forms, elements and physical units in space, according to a clearly established pattern. Depending on the system that regulates an architectural form, rhythm appears in architecture as a regular, alternating, irregular, fluid or progressive rhythm of elements.

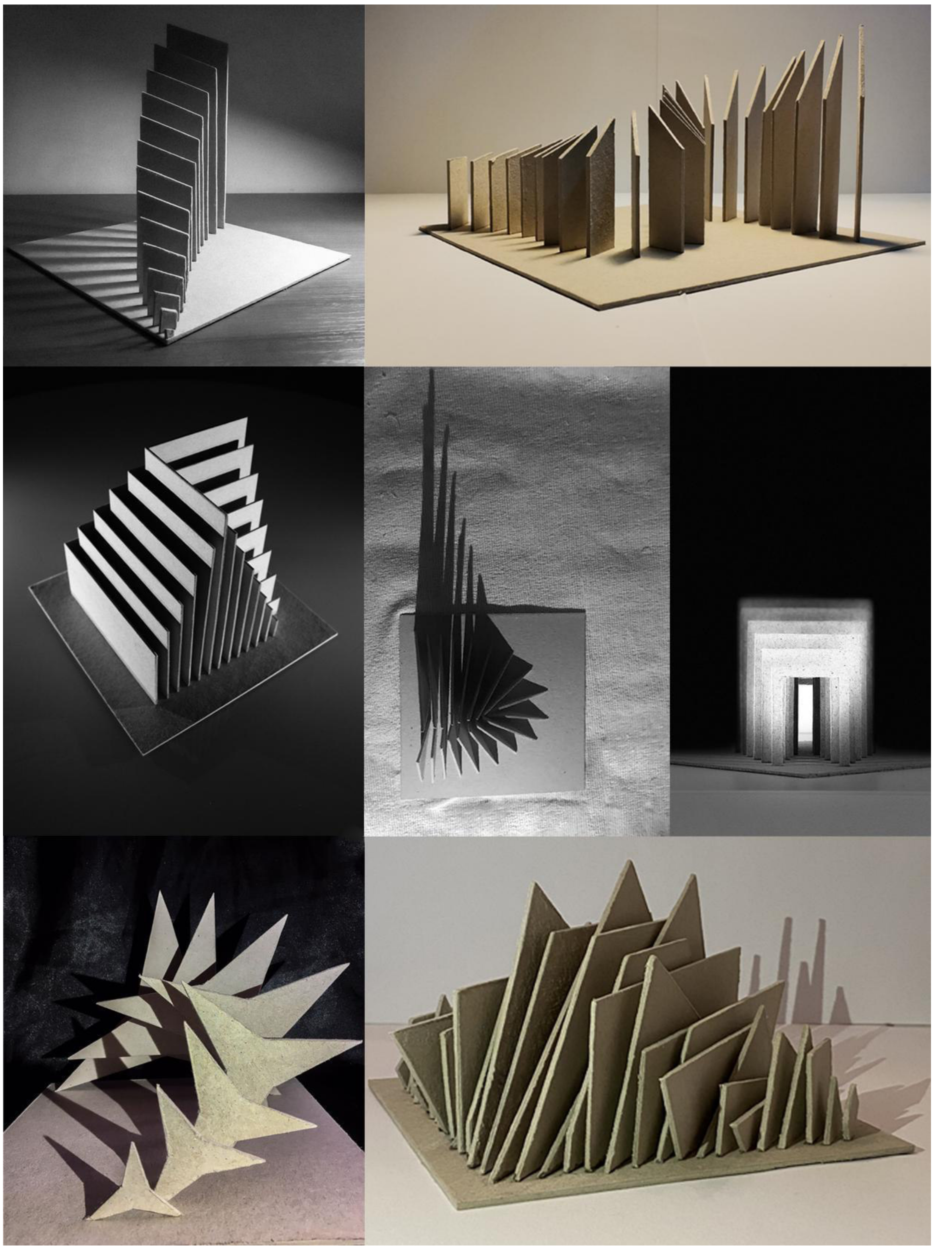

Fig. 1 The collage of students' works that resulted from exploring the principle of Rhythm[2]

In the students' works related to the topic of rhythm, spatial compositions are based on different types of rhythmic gestures. Combined with the restriction of using only vertical elements, the creative research on rhythm in space results in a certain order in

[2] Authors (from left to right). first row: Aleksandra Čubrak, Aleksandar Skendžić; second row: Nikolina Bulajić, Sandra Čanji, Sofija Pavličić; third row: Lea Lanc, Snežana Gajić

students' designs. Focusing on rhythm as a guiding design principle brings regularity, simplicity and visual balance into the students' works, which results in achieving a certain consistency in the realisation of an idea. Therefore, the prevailing conclusion is that the repetition of specific motifs with clearly defined rules for their movements and/or transformations always generates a visual order in a spatial composition (Figure 1). One of the main topics that emerge through the research on rhythm and rhythmic spatial structures, is related to proximity and distance of the elements within the composition. This aspect influences how clearly the notion of rhythm is reflected through the overall design, but it also opens the awareness towards the importance of the in-between space or voids in architecture.

2.2. VOLUME AND IN-BETWEEN SPACE

In its basic meaning, the notion of volume signifies a certain mass, the amount of space that a substance or object occupies, enveloped by a specific, clearly defined membrane. In the most pronounced way, the principle of volume reflects the spatiality of architecture as a discipline and foregrounds the architectural assemblies as three-dimensional units - as opposed to a two-dimensional approach to architecture as an *image*. Singular planes, which in some cases can generate the overall concept of an architectural design, in this context, become secondary, while the focus remains precisely on spatiality, three-dimensionality and morphology of architectural structures. The most straightforward application of the principle of volume in the articulation of space can be found in architectural concepts that rely on a single, free-standing mass - the *mono-volume*. For students and their process of exploring volume as the design principle, most often, the starting points were precisely the regular, basic geometric shapes and bodies.

Doubling and further multiplication of geometric bodies within the composition opens the space, both literally and metaphorically, to the second relevant element of a spatial composition based on volume: *the empty space* in between. The accumulation of volumes thus introduces the subject of the "negative", in-between, unbuilt spaces, or spatial voids into architectural design. This process leads towards establishing the concept known as *the group form* in architecture. One of the main goals of researching the principle of volumes and in-between spaces within the course is to make the students aware of the equal importance of unbuilt and built spaces when considering architectural structures, their composition, poetics and design. Manipulation, or the conscious management of the in-between spaces becomes a tool for establishing the relationships between the volumes, thus working with voids is emphasised as a process inseparable from developing the volumes themselves. Even though these two spatial aspects must be considered and developed simultaneously, and with equal attention, working with the immaterial aspects of spatial design remains the biggest challenge for students. In such a context, insisting on spatial relationships, once again draws the students' attention away from the formalistic approach to designing surfaces, towards the spatiality and the logic of the group form in conceiving the design idea.

The introduction of voids as integral elements of a spatial composition leads the students towards exploring different spatial qualities that mark their works. Besides the overall quality of mass and three-dimensionality, the compositions explore symmetry, tension, accents, modularity, spatial "negative" as an articulated void, accumulation, dynamics, harmony, deconstruction of the basic geometric bodies in defining volumes, etc. All these approaches demand an articulated attitude towards the relations between the elements, as well as the relations of the individual parts towards the composition as a whole (Figure 2).

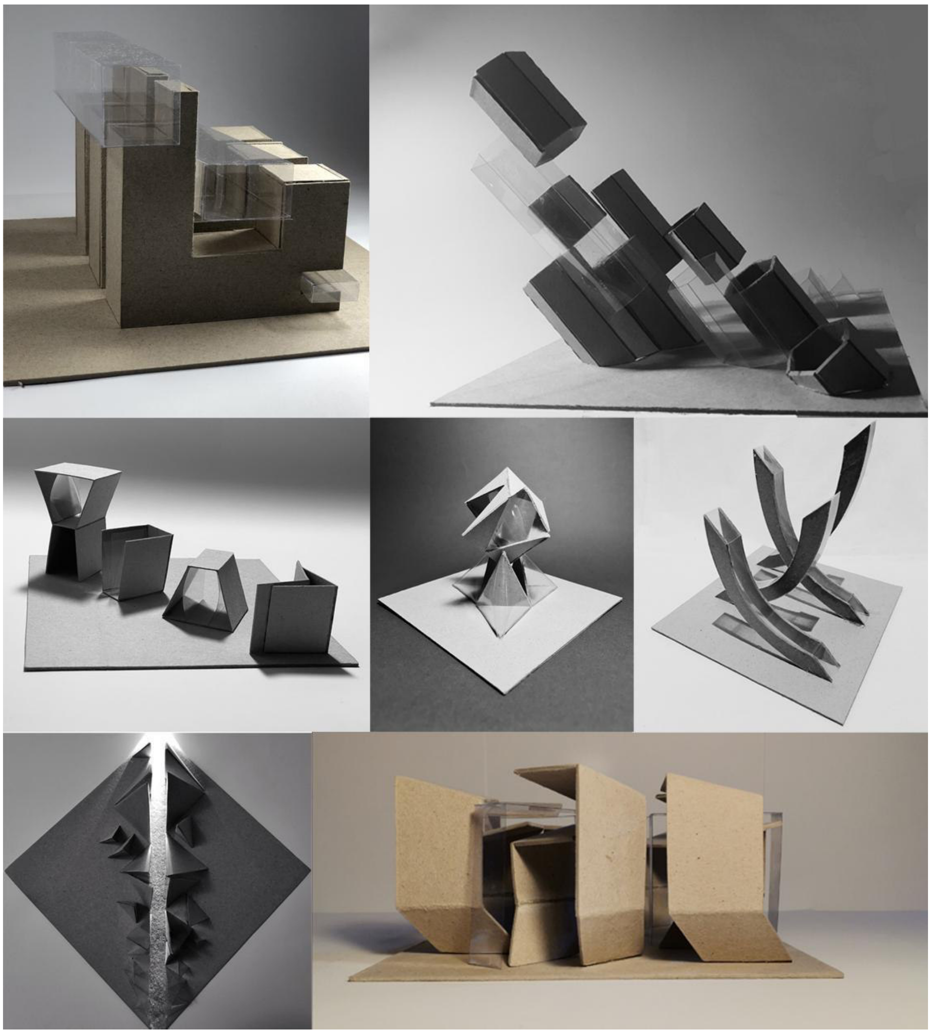

Fig. 2 The collage of students' works that resulted from exploring the principle of Volume / In-between Spaces[3]

2.3. VARIATION

As a general design principle, variation refers to the repetition of motifs, followed by changes in one or more characteristics that occur within a certain (given) limit or framework. In another interpretation, variation can be understood as a principle that produces another or different form or version of something. As a more complex principle, variation incorporates rhythm (through repetition), but the key feature of this principle comes from changes that take place with each recurrence of a visual motif, or, in the context of architecture, a spatial element or structure.

Through the carefully set limitations that essentially define the frame within which the transformations occur, the principle of variation results in an important visual quality: *unity in diversity.* Rather than achieving a disordered and chaotic collection of different spatial structures or elements, variation introduces a *readable theme* among the multitude of different visual motifs that form the composition as a whole. In order to achieve this, the differences have to vary within certain constraints. Therefore, the elements that form a composition based on variation are, on some level, all equal, but at the same time all different as well.

In the exercise that is dedicated to variation, students are given three architectural elements as a starting point for exploring the spatial composition (e.g. a staircase, a wall with an opening, a slab). Through different relations, these elements form a sub-structure that multiplies and transforms through the variation of its proportions, shapes,

[3] Authors (from left to right). first row: Tamara Mitrović, Nikola Radanović; second row: Branka Stanojević, Tea Gnip, Aleksa Todorić; third row: Anica Šijaković, Aleksandar Skendžić

type of elements, etc. The overall composition is then created as a collection of these varied sub-structures, where the focus remains mainly on the logic of variation between the parts, rather than on the composition as a whole. The second dominant approach to variation combines the given elements in a singular structure, within which the individual elements multiply and vary on a certain level. This approach results in a more integral approach to articulating a spatial composition, without losing the focus on the theme of variation (Figure 3).

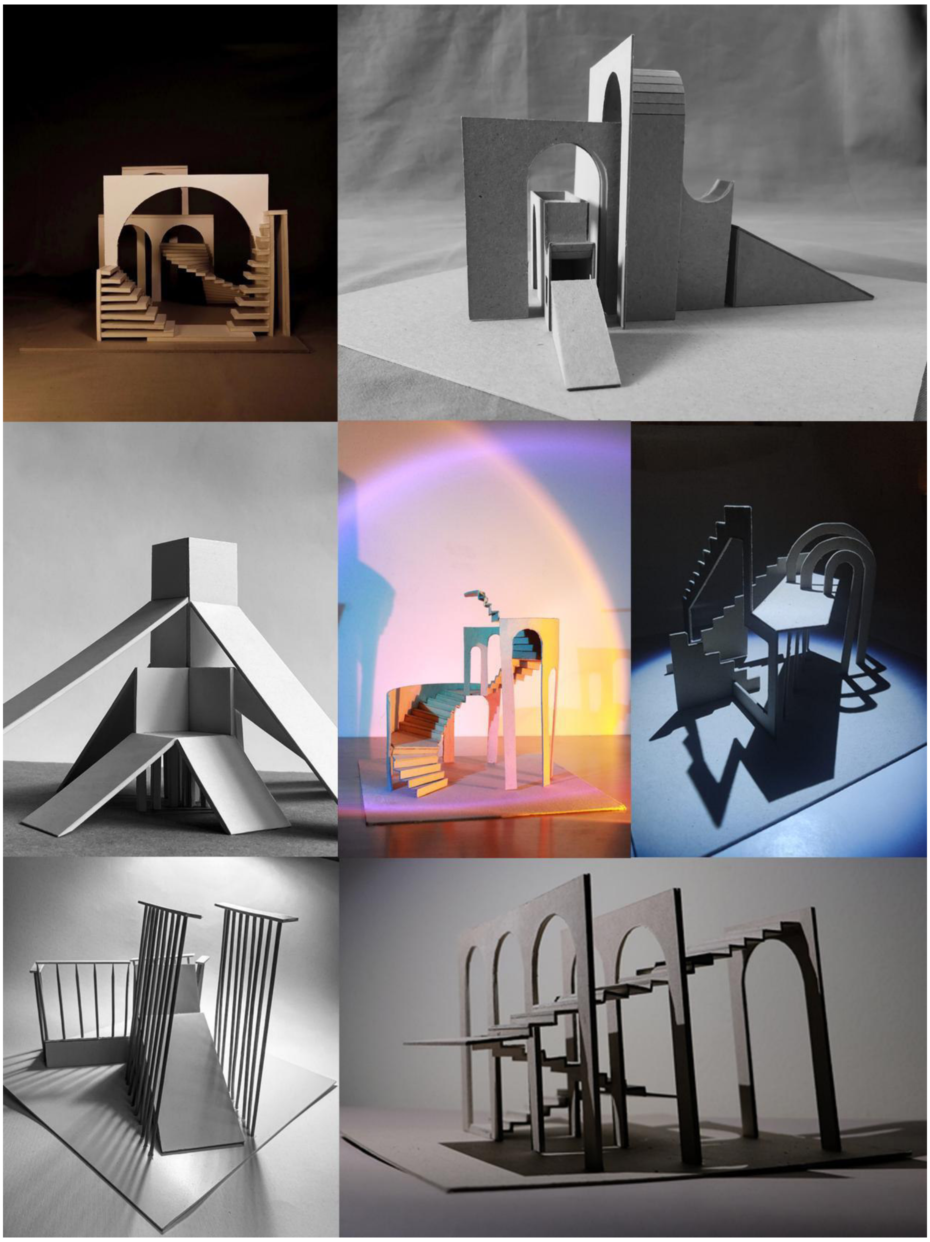

Fig. 3 The collage of students' works that resulted from exploring the principle of Variation[4]

The most important outcome of this exercise refers to understanding the value of manipulating the principle spatial attributes (dimensions, proportions, etc.) in order to achieve diverse results in spatial design. At the same time, through the analysis of different outcomes, their formal relations, visual qualities and dynamics, students shape their skills in achieving balance, harmony, and readable correlations between the elements.

[4] Authors (from left to right): first row: Elena Ogrizović, Marija Simović; second row: Mia Janjić, Milica Aleksić, Teodora Fojkar; third row: Ana Cvejić, Laura Oberhauzer

3. IMPLEMENTATION

Further implementation of the basic principles of spatial articulation are exercised through a more complex set of tasks, in which students respond to specific creative methodologies in architectural design. The first one, the Narrative Embodiment [1] refers to a method of translating the main idea, effects and experiences, from a visual medium - a photography, to a physical medium - a spatial composition. The narrative in this case refers to a textual articulation of the experience of watching the image, which then becomes a starting point for its spatial embodiment.

The final exercise refers to the creation of a Spatial Construct through the medium of collage. In this task, the students are asked to reinterpret an existing model (one that they already produced through previous exercises in the semester), creating a new, fictional space out of photographs of the existing model. The main goal is to explore the potentials of an existing model, its spatial segments and parts, in creating a completely new, imaginary space, unburdened by real technical constraints. Additionally, the new space created as a construct has to attain qualities that the starting spatial composition didn't have. Through this kind of reinterpretation of the given spatial elements, this exercise employs the creation of a new spatial narrative, as the final outcome of this process. Since methodologically both exercises focus on different kinds of spatial textuality, and not necessarily on one specific principle that regulates the architectural form, all of the principles from the previous exercises become tools in articulating the spatial idea.

3.1. NARRATIVE EMBODIMENT

In the process of the narrative embodiment, the starting point for students' works are images by famous photographers that embody some spatial aspects and qualities but don't explicitly depict buildings and architecture. The main aim of the exercise is not to literally translate the physical aspects of the image through a symbolic representation of its elements in space but to capture the essence of the effect the image has on its observer, and translate this same effect into a spatial system.

Besides the more confident use of rhythm, volume, variation and spatial voids in this exercise, the students' works show an important stride towards several tools, in order to reflect specific feelings, themes and effects: the treatment of space, its qualities, atmosphere, the direction of views and the photographic representations of the final works. The analysis of the students' works shows diverse approaches to the task, often combining several principles in the realisation of the idea.

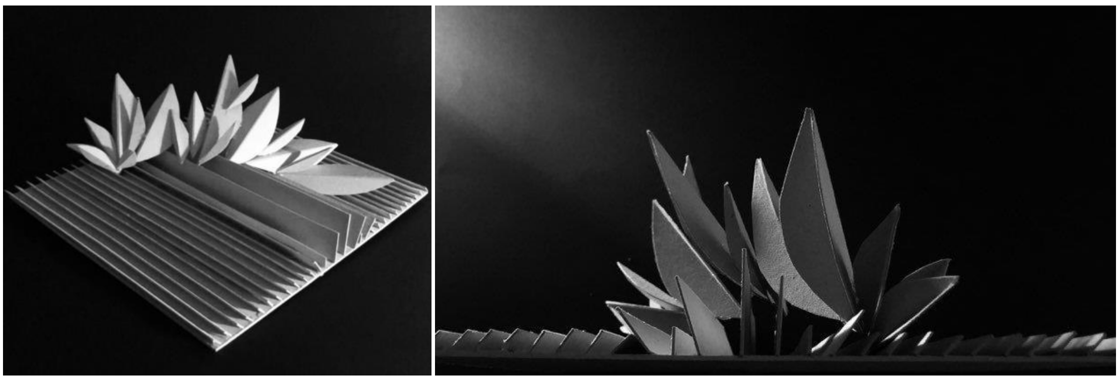

Fig. 4 Photos of the model representing the Narrative Embodiment method: Spatial structure that reflects the atmosphere of fluidity and movement, with a specific treatment of the flat surface of the base, which becomes an integral part of the composition. Author: Maša Lukić

In a work that responds to the keywords of dynamics, fluidity and freedom (Figure 4) the biggest shift in conceptualising the model happens in the way the flat base is used.

In an almost two-dimensional treatment of the entire surface, which would essentially be a principle to avoid when dealing with the spatiality of an abstract composition, the very base, with its texture and tectonics, becomes an integral part of the composition as a whole. Its repetitive qualities emphasise the overall rhythmicity of the composition, while its regularity and symmetry balanced out the rather irregular and fluid movement of the rest of the composition. Through this relationship, this work showcases the important principle of simplicity which is often needed, but at the same time “not enough” [2], balancing between regular and irregular, symmetrical and asymmetrical aspects of a design. This balance contributes to the overall harmony and dynamics of spatial structures.
The second example relies on a predefined perspective when developing the concept for the model. Introducing a strictly articulated surface with an opening, which marks the point where the spatial experience begins, this work achieves a specific scenic and theatrical quality, utilising the spatial concept that resembles the conventional fourth-wall theatre setting. Even though the overall composition is partially hidden by the elements positioned on the perimeter, which should be considered a principle to be avoided in developing spatial compositions, these decisions were made consciously in order to represent and translate the character and atmosphere of the initial work of art into the spatial system. The scenic character of the composition was additionally highlighted through the use of directional lighting and shadows, emphasising the depth of space and the layering of spatial planes (Figure 5).

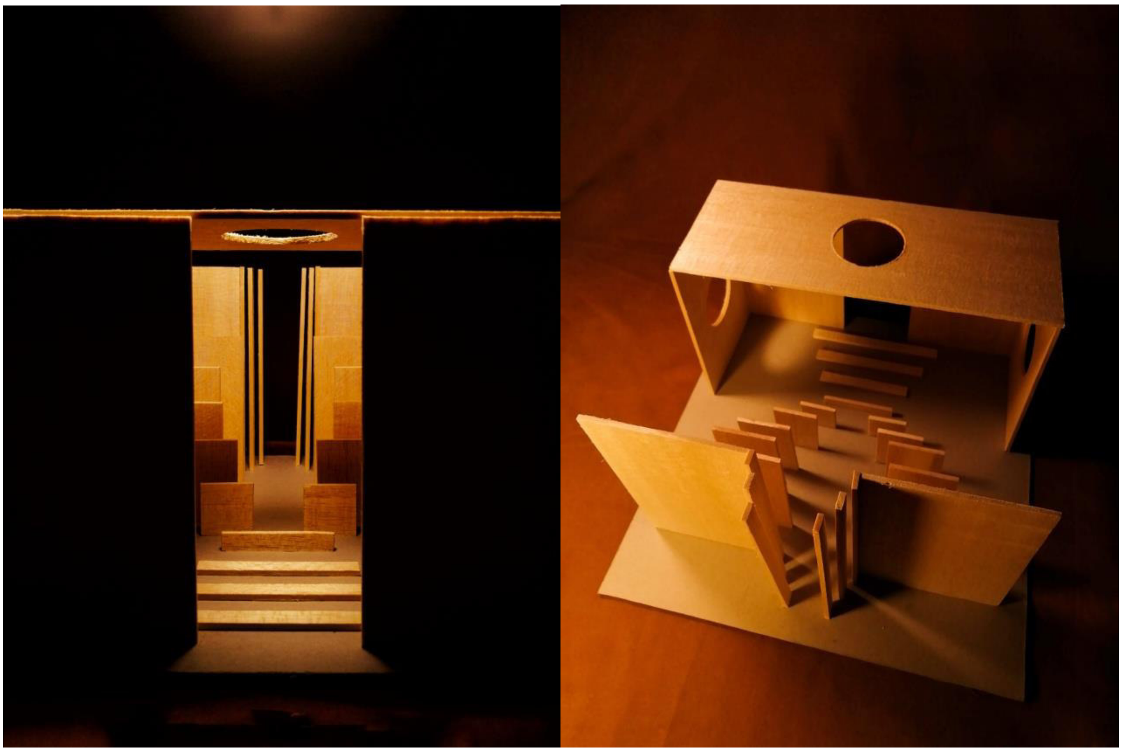

Fig. 5 Photos of the model representing the Narrative Embodiment method: The scenic qualities of the composition, highlighting the depth of space. Author: Elena Ogrizović

The third model represents a more common approach to Narrative Embodiment among the students’ works, where one precise theme or keyword guides the development of the concept. In this case, students often use the combination of previously exercised principles, in order to communicate the defined narrative. A significant group of works rely on different approaches to articulating a *threshold* in space, embracing the qualities of duality, liminality and contrast. The third example of the Narrative Embodiment method shows a model that embodies duality as the basic quality (Figure 6). It is achieved by using the principles of balance and contrast, which are in this case realised through confronting vertical and horizontal; the straight gesture and the movement; the full and the porous surface; order and disorder; regular and irregular rhythm; static and dynamic features. Besides rhythm, as the main tool in the articulation of this spatial entity, the visual connection between the opposite parts of the composition is achieved through utilising variation as the guiding principle regulating the overall form.

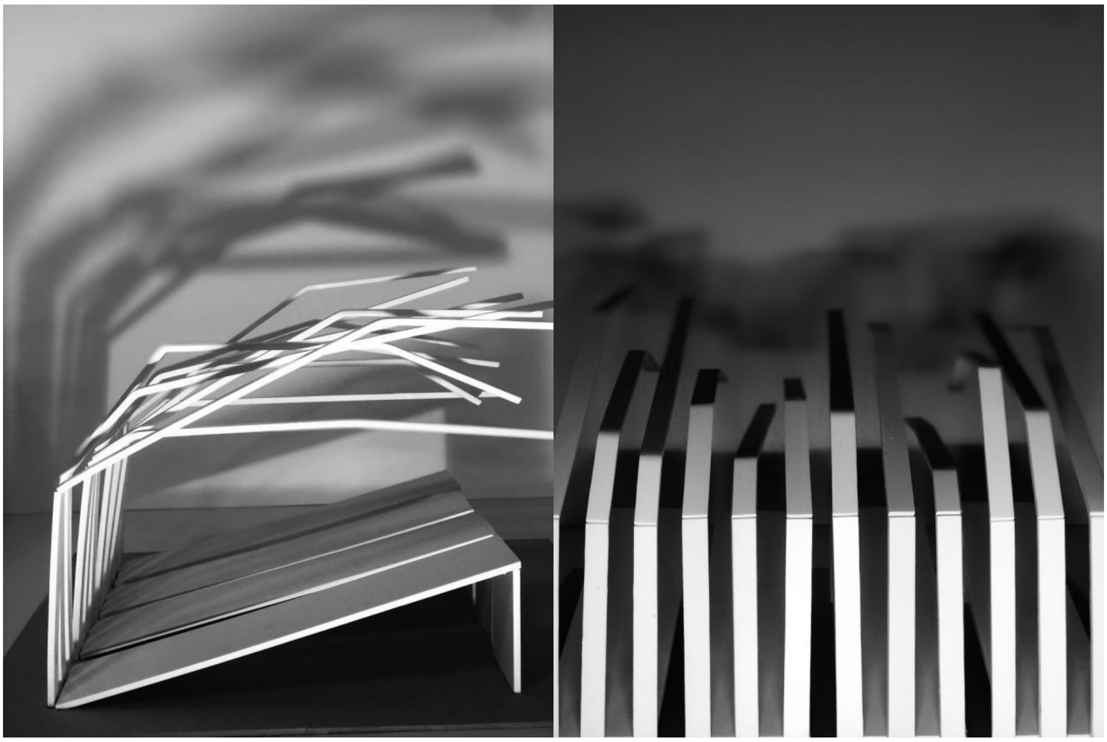

Fig. 6 Photo of the model representing the principle of the Narrative Embodiment: Principle of Rhythm as a tool in achieving duality, balance and contrast. Author: Tamara Mitrović

3.2. SPATIAL CONSTRUCT

Within the realisation of the spatial construct, students are asked to create a space represented in a collage technique, using segments of photographed models that explore the previously researched topics. Through the analysis of the students` works, several principles in the construction of space can be observed: *the abstract spatial system*, *the tower* and *the group form*.

The principle of the abstract spatial system refers to the formation of a three-dimensional stretched-out space that is equally developed both horizontally and vertically through a series of planes and connecting elements. Through the change of position, scale and relations of the chosen elements, rhythmic development and perspective view are created. Simultaneously, utilising the change of the scale introduces new spatial layers, as shown in the example where the staircase element is used in its original role, but also as a form of perforated partition. (Figure 7) This layer deepens the perception of space through the development of relationships *here and there* in which *here* is known and there is *unknown* [3], contributing to the excitement and dynamics of the created space.

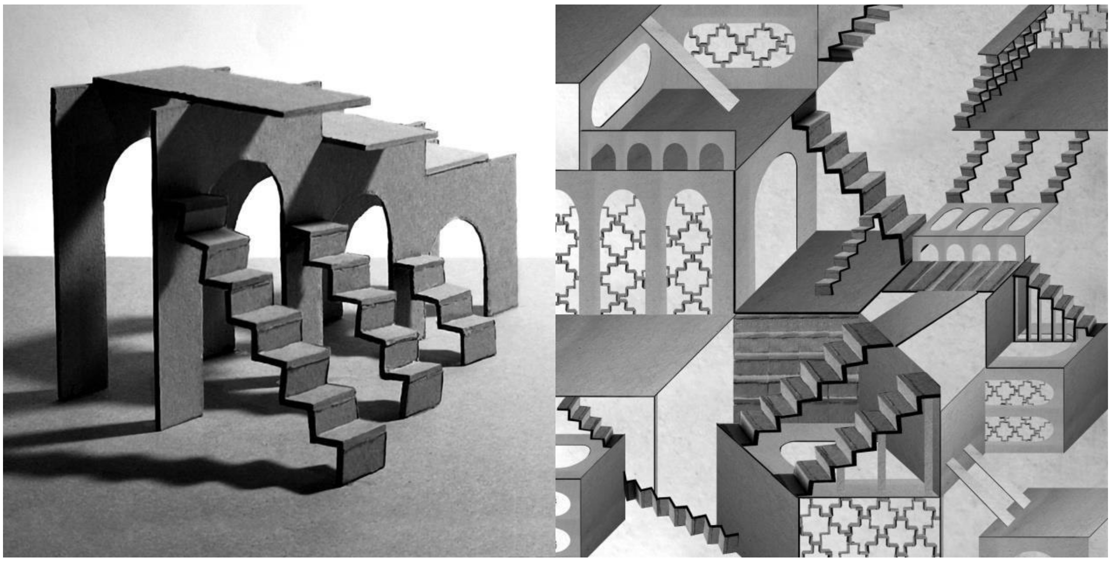

Fig. 7 Photo of the model representing the principle of Variation (left); Collage representing Spatial Construct developed from the photos of the model (right). Author: Vasilije Adamović

The tower, as the second principle, displays the vertical development of the composition. In this case, the space is primarily created by multiplying the segments, with or without variations, through the vertical spatial plane. Depending on the used elements, connections between levels are realised in different manners: using the suggestion of stairs or ramps as architectural elements intended for vertical communication, or in more abstract representations, by interweaving elements between levels. Some examples show a dominant vertical element that permeates the entire composition. This approach to creating a spatial construct introduces, in addition to the principle of the rhythm through which the towers are developed, the idea of relationship with the surrounding space, often represented as flattened and seemingly empty, contrasting the verticality of the composition. (Figure 8)

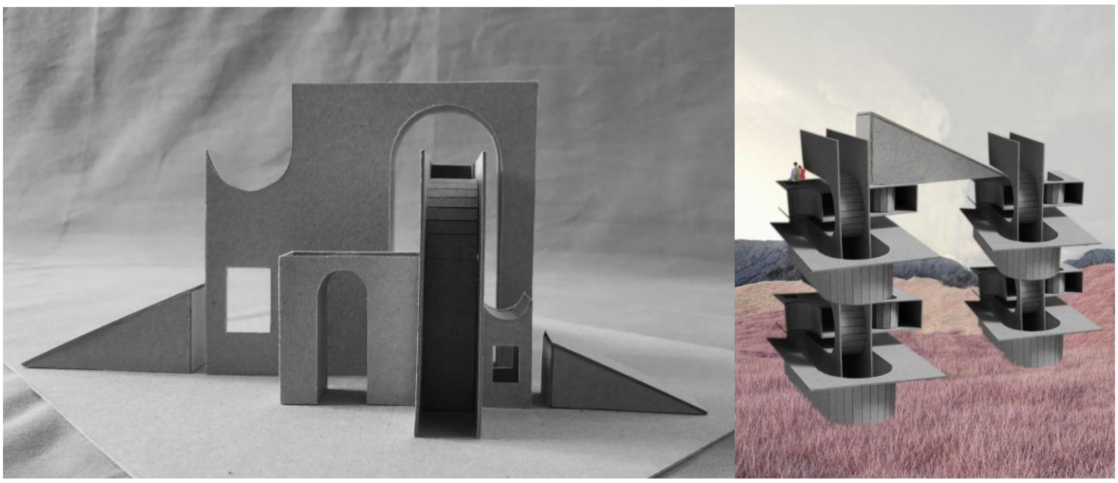

Fig. 8 Photo of the model representing the principle of Variation (left); Collage representing Spatial Construct developed from the photos of the model (right). Author: Marija Simović

The third principle that we can single out in the students` works refers to the use of group form in the realisation of a spatial construct. The group form represents the type of form that is developed from the system of generative elements in space.[4] In these examples, space is articulated primarily by introducing volume into the spatial scope. Volumes are further multiplied, often with variations in dimensions or position, building an integral spatial framework. It is noticeable that in the works that were conducted with this approach, the built-up spatial coverage is at a significantly higher level than with the first two approaches. The elements form a compact space, which achieves dynamics through the subtle variations of gaps in its rhythmicity. (Figure 9)

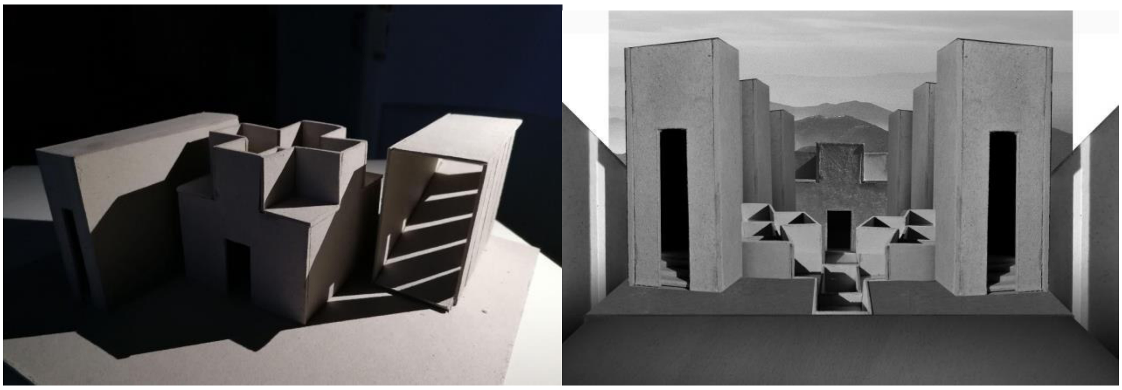

Fig. 9 Photo of the model representing the principle of Volume and In-between Space (left); Collage representing Spatial Construct developed from the photos of the model (right). Author: Aleksandar Tomić

3.3. ANALYSIS OF THE ACHIEVED SPATIAL QUALITIES

Tab. 1 Parallel presentation of the analysed student' works that resulted from the exploration of Narrative Embodiment and Spatial Construct, and their specific qualities in relation to the basic principles of spatial articulation and design

Student's works	Figure 4 / NE	Figure 5 / NE	Figure 6 / NE	Figure 7 / SC	Figure 8 / SC	Figure 9 / SC
Principles employed	Rhythm (regular and irregular / fluid)	Volume, Rhythm	Rhythm, Variation	Repetition (rhythm); Variation; Abstraction	Volume, Rhythm	Volume and In-Between Spaces; Rhythm
Additional qualities achieved	Texture, Depth, Balance, Movement	Scenic character; Spatial depth; Control of perspective	Contrast, Balance, Porosity, Movement	Creative use of Perspective and Scale, Infinity	Verticality, Dynamics, Modularity	Symmetry, Density, Order, Monumental Space

4. CONCLUSION: LOGIC OF FORM VS. FORMALISM

Each principle of spatial articulation that the course Architectural Design - Introduction addresses, draws the focus towards analysing, understanding and applying a readable system which regulates an architectural or spatial form. In the first phase that focuses on Rhythm, Volume, In-Between Spaces and Variation the educational process centres on the methods and mechanisms of applying these principles as the visual qualities of spatial compositions. The second phase of the course is dedicated to learning ways to manage those principles as specific tools in a creative process. This way, the basic principles of architectural and spatial design, at first, become the goal of exploration through the abstract scale models, while in the second phase, they become the means of expression for the more complex ideas.
The analysed examples of the students' works showed that the focus on the articulation of thoughts, which are translated into spatial systems through diverse creative methods, inevitably leads to achieving additional spatial qualities along the way, besides the basic principles that are mastered throughout the semester. Through this process, students are gradually taught that the architectural form is not the goal of architectural design but its

result. Primarily informed by our intentions, this process shifts the focus away from formalism, towards a deeper understanding of the logic of form.

ACKNOWLEDGEMENT

This research was done as a part of the project: *Innovative approaches and advancement of processes and methods in higher education in Architecture, Urbanism and Scene Design*, led by the Department of Architecture and Urbanism, Faculty of Technical Sciences, University of Novi Sad, Serbia.

REFERENCES

[1] Zeković, M., Konstantinović, D., Žugić, V. Conquering Space: Experiments in Architectural Education. *International Conference on Architectural Research ICAR' Proceedings*, 'Ion Mincu' Publishing House, Bucharest, Romania, 2015, ISSN 2393-4425, pp.151

[2] Arnhajm, R. (1998). *Umetnost i vizuelno opažanje.*, Univerzitet umetnosti u Beogradu i Studentski kulturni centar, Beograd.

[3] Cullen G. (1990). *Gradski pejzaž.*, Građevinska knjiga, Beograd.

[4] Maki F., Otaka M. (1660). Neka razmišljanja o kolektivnoj formi. *Teorija arhitekture XX veka - antologija*, ed. Perović M. R. Građevinska knjiga, Beograd, Serbia, pp. 356–372.

TRANSFORMATION OF ARCHITECTURE AND URBANISM DUE TO CHANGE OF GENDER ROLES IN SOCIETY

Enis Hasanbegović[1],Melisa Alcan[2], Lejla Zećirović[3], Julija Aleksić[4], Danilo Dragović[5]

Summary:

Giving certain spaces, architectural features and layouts the quality of "femininity" or "masculinity" had a strong impact on cultural and sociological shifts. In this paper, we will examine the historical nature of these shifts and how the architecture can direct the position of all genders towards equality.The subject of the paper is the transformative value of architecture and urbanism induced by gender changes in society, as well as overcoming gender with the aim of segregation decrease.The purpose of the paper is a chronological examination of architecture and urbanism through both feminist and gender theory. The goal is also to debunk the linguistic and cognitive premise that compares specific architectural spaces with the female body (and dedicate it to it) and some others we liken with the male`s build. The paper will demonstrate the architectural transformation through the women's movement, as well as the transformation through the reduction of the sociological difference between private and public spheres.

Key words: *gender equality, feminism, machism, transformation, architecture, public, private*

[1] PhD student, M.Arch, Assistant, State University of Novi Pazar, Novi Pazar, Serbia, ehasanbegovic@np.ac.rs
[2] PhD student, M.Arch, Assistant, State University of Novi Pazar, Novi Pazar, Serbia, malcan@np.ac.rs
[3] PhD student, M.Arch, Assistant., State University of Novi Pazar, N. Pazar, Serbia, lzecirovic@np.ac.rs
[4] Associate professor, Faculty of Technical Sciences in Kosovska Mitrovica, University of Priština, Serbia, julija.aleksic@pr.ac.rs
[5] PhD student, M.Arch, Assistant, State University of Novi Pazar, N. Pazar, Serbia, ddragovic@np.ac.rs

1. INTRODUCTION

Gender has tremendously influenced both how we perceive space and time, and how we allocate and value them. The division into public and private spheres had a lot to do with gender and gender roles, stereotyping, and generalization, as well as the identification of gender and sex [1]. Architecture was not an exception in male dominance; on the contrary, it often supported it, pushing women into limited private spaces such as kitchens and bedrooms, "intimate spaces" where "women rule," thereby limiting their movement and safety in so-called "male" spaces. The epithet of femininity was attributed to decorative architecture, and it was followed by tender, impractical, and even dysfunctional notions. The epithet of masculinity, on the other hand, was attributed to stable, potent, pompous, and authoritative buildings, and "masculine" spaces allowed men greater mobility simply because they belonged to the public sphere. Therefore, so-called masculine architecture is seen as superior to so-called feminine architecture because it has a purpose [2]. Until relatively recently, architecture and urban planning, unfortunately, were often dominated by a single gender. However, as (post-post) modernism demands increased awareness and the intertwining of sociological, political, artistic, and personal aspects, architecture is also undergoing significant political transformations.

2. HISTORICAL CONTEXT

If we begin to read architecture through gender, we will notice even in antiquity "masculinity" or "femininity" was evaluated through two extremes: massiveness and decoration. So we have a Doric column that is characterized as "male" and an Ionic column as "female". The famous Vitruvius describes the Doric column as a male body and says that it depicts "the proportion and strength of the male body". Ionic, of course, with a female body, and female slenderness, and recommends that Ionic columns be used in temples of "calm, not too strong" deities, i.e. deities of water and earth (as opposed to powerful fire and air ones). The Corinthian column, as the most slender, was attributed to the characteristics of a virgin girl. And since the Corinthian column occupies the least space and is the most decorated, its appearance and comparison with the virgin girl can easily be read as fashion anorexia in a feminist key today.

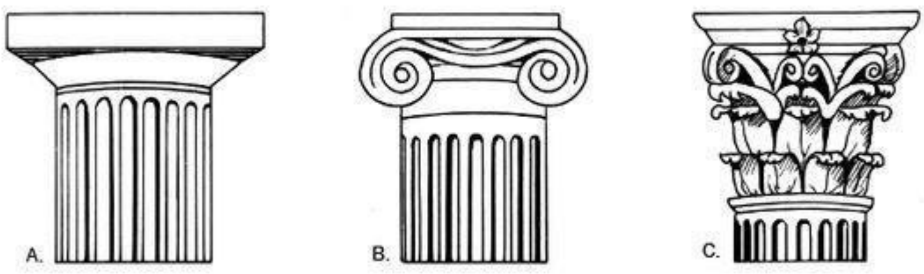

Fig. 1 Doric, Ionic and Corinthian styles

Rococo is later considered feminized, and the "female building" continues to retain the character of naivety and tenderness, in contrast to the "masculine" one, which is even more deeply constituted as functional, serious representative, stable, and significant.

The attitude towards decoration and ornamentation in the modern age is best represented by Adolf Loos, who considers any kind of decoration a crime: "The evolution of culture is simultaneous with the removal of ornamentation from useful objects. [3] " Loos describes the decoration as infantile, disdainfully stating that people with body tattoos are either criminals or freaks and as the decoration was strictly related to "female architecture", the concept of femininity once again acquired a childish, immature character in architecture. Several times Loos cites utilitarianism as the opposite of ornamentation, which places decoration in the category of uselessness or leisure. Architects will also use the gendering of architecture capitalistically, like Sullivan, who "feminized" the appearance of the shopping center in order not to attract the female part of the population, to whom shopping is still stereotypically associated to this day.

Fig. 2 Sullivan, ground floor of the mall

Masculine architecture reached its bottom in the period preceding the Second World War, in the fascist regime that preferred extreme masculinity. It is precisely the end of the world war that will return women to the privacy of the home, and architecture and urbanism, like women, will have a hard time recovering from the baby boom generation and the concept of the suburbs, which deepens the issue of women's gender and private space.

3. PUBLIC AND PRIVATE

As John Ruskin poetically explains in his text "Sesame and Lilies", "within his home, where she rules" there is "the true nature of home" [4]. Later, in his essay on women and war [5], he underlines again: "Once again: women must use their practical influence within the home, for the sake of peace in it." This is a picture of the 19th century and one of the most influential English thinkers, which inevitably reflected on architecture, that is, the feminization of the interior of the house. No matter how poetically Ruskin presented it, these moves to place women in the private sphere were also moving women away from the centers of power.

The urban peak of the "privatization of women" took place in the era of the suburbs, i.e. the ideality of the house in the suburbs, which places women much more seriously on the outskirts, making their mobility even more difficult. In that period, strictly male spaces became business, office, and economic centers. Dolores Hayden calls this moment of the suburbs "a scene of gender inequality [6]" - where a clear demarcation is made between what is male work (public, paid) and what is female (private, unpaid) and how architecture supports the sustainability of such a system. Public spaces are being kept "masculine" even more segregated and becoming more and more exclusive, while private spaces are kept "feminine" at the level of apparent authority inside houses that women did not legally own.

The gender division into interior-feminine and exterior-masculine, as stated by Anna-Maria Adams and Peta Tancred, conditioned the later feminization of interior design, as well as the duration of the premise of "women's innate understanding of household things" [7]. Such a strict division also meant a clear delineation of the influence of one sphere on another, so Susana Torres [8] divides the influence of feminism on the transformation in architecture into six categories:

- 1. Home space design;
- 2. Changing the structure of the suburbs - initiatives to integrate the suburbs still exist today, given that urban zoning additionally kept women in areas with more crime and a worse education system (of course, these initiatives are met with strong conservative resistance);
- 3. Development of new types of buildings; redefinition of old and design of new constructive forms:

  The integration of the "women's building" first all happened in 1893 quite literally, forced by the rich feminist Breta Palmer, the Woman's Building was created, designed, and built for the World's Columbian Exposition (later in 1973, this building functioned as an important cultural center and art school). When it comes to redefining constructive forms, one thinks primarily of what distinguishes "women's clubs" from "men's clubs", for example, the mandatory existence of space for self-education, and this was insisted on by both white women and African-American women at the beginning of the 20th century.

Fig. 3 Gender roles

In the 1970s, the first Childbirth Center was created in America (after the removal of restrictions on abortion) - and this greatly changed not only the sociological view of childbirth as such (tabooed and isolated), but also the architectural approach in which birthing rooms can accommodate more people who then participate in the birthing process, and today already include a jacuzzi and a more comfortable atmosphere at home.

Fire station number 5[1], in Indiana, can serve as a good example of the realized direct influence of feminism on architecture. Namely, the mayor at the time wanted to include more women in the fire service - she hired Susana Torres to design the new fire station - and that meant redesigning the doors, toilets, buses, and everything else that until then was intended only for a highly capable male body. Tore also designed the parks around the station to accommodate people with special needs and parents with baby carriages.

[1] https://www.susanatorre.net/architecture-and-design/making-room-for-women/fire-station-five/

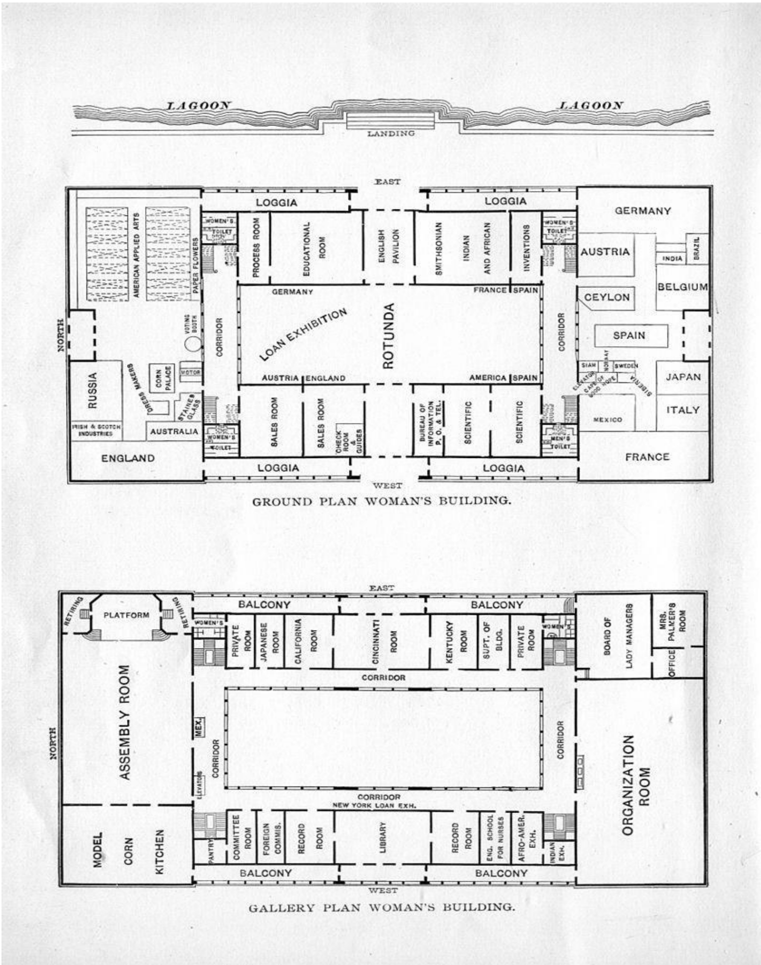

Fig. 4 Woman's Building, 1893.

- 4. Changes in the way we experience the engraving of collective memory;
- 5. A radical revision of the attitude towards nature conservation and the introduction of sustainable design as an ecological practice;
- 6. Feminist identity as a legitimate paradigm in design:
  Tore is not talking here about the question of whether men and women design differently, but about ways of implementing women's concerns and needs in design and urbanism. Feminist identity also means consideration of femininity and the nature of femininity, and in addition to Zaha Hadid's famous buildings, we can also find a visual representation of feminist identity in architecture in, say, the Spanish "Basket" pavilion in Shanghai.

4. KITCHEN AND BATHROOMS AS SPACES OF SEGREGATION

After the disappearance of the concept of domestic service, the domestic space is even more deeply divided by gender, as a consequence, the most gendered room of all appears: the kitchen.

Building and maintaining family peace and comfort inside the house, as well as the emphasis on motherhood and housekeeping, made the kitchen the most "female" space. The kitchen, because of all the above, experienced perhaps the strongest transformations: from the Frankfurt school and the kitchen of Margareta Šita-Lihocki, a kitchen that saves space, all the way to the open plan of the kitchen and rituals as the central event in the central room.

The Frankfurt kitchen, although initially characterized as a feminist project because it made a kitchen for a modern woman who also worked outside the home and thus saved time with this efficient kitchen, in the long term stationed women in the small, sterile space of the dining car. Shyta-Lihocki's serious intention to professionalize housework later suffered heavy criticism in feminist theories, because not only was that work unpaid, but with that procedure, household work was guaranteed to be assigned to women.

That's why it was a rather disturbing exhibition at the MoMA museum in 2011, in which the work of Shita-Lihocki was presented as a huge success and modernization in kitchen design, despite the then steady pile of feminist analyses on the subject of pushing women into small isolated spaces. Modernization in kitchen design, according to Susana Torres, does not mean modern kitchen design as such, but also the emancipation of women and their exit from rigid assigned household roles:

"I don't believe that any architect today would design a kitchen for one woman. The challenge is to design for the integration of all household members in the care and maintenance process. [8]"

Fig 5. Frankfurt Kitchen (1926)

Fig 6. Open plan kitchen

Placing a woman in the role of a housewife made this kitchen space lonely at first, so the Frankfurt kitchen began to be used "incorrectly", that is, by introducing other family members into it, which did not make the kitchen a less "feminine" space, but it did make it less private. With that, over time, the kitchen was adapted into a more open space where you spend time and not just work. Today's kitchens are significantly less gendered, connected to the living room, without walls, thus confronting all family members, members of both sexes, with kitchen elements and kitchen work, which is thereby demystified.

Social feminism, however, believes that the kitchen as a repressive room can be transformed only by taking it out of the home and placing it in the public sphere: wage-earning and professionalizing the kitchen would, according to that theory, make the kitchen finally genderless. In the works of Dolores Hayden, we find feminist plans (the 1880s and later) that transcend the boundaries of the home and expand into neighborhood design - even then she suggests ideas of shared highly-equipped almost industrialized kitchens and laundries.

However, just as cooking itself is slowly losing its gendered character, kitchens are becoming, albeit within the home, gathering spaces of all genders and all ages. The task of the architect is to, knowing all this, try to deconstruct the collective memory that is inscribed in the space of the kitchen.

Bathrooms, unlike kitchens, encroached a large part of the public sphere, so segregation was even more obvious, but due to the intimacy of the bathroom - and more accepted.

Although the idea of separate, private bathrooms and toilets seems very modern, the history of the Roman Empire teaches us otherwise. Unfortunately, as with the kitchen, the toilets were also chronologically not an easy obstacle for women. Until the Victorian era, all public bathrooms and toilets were for men only, which again meant that women could not (physically) be in public spaces for long, that is, it sent a clear message: women stayed in their homes. It's important to put things in perspective: the first gender-separated toilet (that we know of) was in Paris in 1739 [9], however, in India, for example, women today try not to eat or drink too much while out and about - due to the lack of women's toilets. So from this point of view, gender segregation of toilets can be seen as an important development for women.

Architecture tried to prevent or at least mitigate all possible negative products of the existence of "completely private rooms" in the public sphere. Therefore, public toilets, toilets in the workplace, in clubs, restaurants, were in a kind of open plan with a lot of visual obstacles: this was an attempt to guarantee the safety of the users, but also to reduce the abuse of that space: sex and drugs were things that tried to avoid by design.

However, the psychological phenomenon of gender segregation did not only harm women here. From Lacan's "urinary segregation" to the vulnerability of male sexuality in public men's toilets, the influence of gender has changed the perception and use (or non-use) of urinals in the last few decades. Discretion was characterized as a feminized trait - so women's toilets tended to be closed and cramped, with much more space for privacy than in men's.

The design differences between men's and women's toilets didn't hit a major stumbling block until recent years when ignoring the difference between sex and gender became unsustainable. Transgender people have posed a real challenge to architects and sociologists together. And, although gender-neutral "for all genders" toilets are increasingly being seen and the walls between women's and men's toilets in clubs have been demolished, the safety of women in these not-always-so-neutral spaces is once again slightly violated or at least questioned. Therefore, at least as far as public toilets are concerned, we are in an interesting moment in time where the task of architects is to listen carefully to the needs of all genders and not rush to unified solutions.

When it comes to bathrooms, the inevitable phenomenon of the Turkish hammam teaches us how the purpose of already existing rooms can be redefined, and how this intimate, almost sacred space changed under the influence of gender. Hammams are generally designed as double (couple-hammams), rigidly divided into two parts - male and female, which are almost symmetrically placed around the massive wall that separates them.

Fig. 7 Jean Auguste Dominique Ingres - Turkish bath, 1863.

At first glance, the female and male parts of the hammam look identical, however, it is interesting that the hood of the female part of the hammam is wider and, therefore more spacious than the male part. It is also logical because women used this room more often to rest after bathing. In addition, in the women's Kapalua, according to custom, there was especially a shelter (pillow) for girls, who came just before the wedding, and

mattresses for women, who visited the hammam for the first time after giving birth, after 40 days, with a certain ceremony.
Apart from the mentioned changes, the changes in the status of women significantly influenced the abandonment of these facilities, which lost their main clientele due to the departure of women from them. During the Ottoman era, women used hammams as a kind of "café" where the most important news, gossip, and even scandals were invented. Women were, therefore, much more attached to the hammam space than men because it was a place where they could socialize without the presence of a man (because in the tradition of Islam, it is required that a woman does not go anywhere alone without a man accompanying her). After the rapid emancipation of women in the second half of the twentieth century, an increasing number of them work and pursue careers - hammams lost their target group, which now uses other spaces for socialization.

Fig. 8 - Turkish bath/Hamam

Nevertheless, hammams regain their charm and influence on public and social life, precisely by gender neutralization. In the Western world (especially Germany, Holland, and Hungary), gender-neutral hammams - i.e. inclusive hammams - are becoming a hit, a combination of care and enjoyment in public bathing with modern materials and rooms designed to offer full comfort and safety for every person. They again become a space for socialization: couples go for romantic treatments for couples (only in this century is it possible for a man and a woman to go to the hammam together and plan), groups hold specific celebrations or gatherings, and it is no longer rare to schedule a meeting in the hammam, which it allows with its new structure.

5. CONCLUSION

Architecture and urbanism at the same time both inform and are informed about how the human body is perceived, and how body and gender were almost philosophically inseparable - architecture had to be extremely gendered throughout history. However, this is no longer the case and does not have to be. The work on gender neutralization of architecture is already well underway.
The gender criterion is more and more consciously applied to projecting and designing space, as well as to urban planning. It is a criterion that must be used carefully and responsibly, taking into account the different needs of people when it comes to gender. Inevitably, cities, neighborhoods, and private spaces will transform more and more into oases of safety and equal opportunities, without gender-based privileging.
The paper emphasizes the need for an inclusive architecture that does not favor any gender. Architects and urban planners should carefully consider gender and equality in their projects to create a space that reflects inclusivity and comfort for all, regardless of gender.
Binary gender roles are associated with specific colors, materials, objects, symbols, spaces, and many more. In a world of segregation, architecture can play a key role in

bringing people together, accommodating everyone, holding space for differences and promoting inclusivity.

In essence, the work explores how changes in society and understanding of gender roles have shaped architecture and urbanism and calls for further reflection and action in creating spaces that promote equality and unity.

REFERENCES

[1] Butler, Judith (1990): " Gender Trouble: Feminism and the Subversion of Identity", Routledge, United States.

[2] Forty, Adrian (1986): "Objects of Desire", Pantheon Books, University of Michigan, United States.

[3] Loos, Adolf (1913): " Ornament and Crime ", Penguin, 2019, London, UK.

[4] Ruskin, John (1865), "Sesame and Liliesi", Yale University Press; New edition (September 1, 2002), New Haven and London, UK.

[5] Ruskin, John (1875), Littell's Living Age/Volume 127/Issue 1645/ On Women and War, Littell & Gay, Boston, United States

[6] Hayden, Dolores (2003): " Building Suburbia: Green Fields and Urban Growth, 1820-2000", Pantheon Books, 2003, the University of Michigan, United States.

[7] Ceawford, Lucas (2015) : "Transgender Architectonics: The Shape and Change in Modernist Space", Ashgate Publishing, Farnham, UK.

[8] Torre, Susana (1977) "Women in American Architecture: A Historic and Contemporary Perspective", Whitney Library of Design, Susana Torre, "Women in American Architecture: A Historic and Contemporary Perspective", New York, United State.

[9] Cavanagh, Sheila (2010) : "Queering Bathrooms: Gender, Sexuality, and the Hygienic Imagination", University of Toronto Press, Torronto, Canada.

[10] Bonnevier, Katarina: (2007) "Behind Straight Curtains: Towards a Queer Feminist Theory of Architecture", Axl Books, Stockholm, Norway.

[11] De Beauvoir, Simone. (1949) The Second Sex. Trans. H.M. Parshley. Middlesex, Penguin, London, UK.

HARMONIZATION AND IMPLEMENTATION OF SEISMIC VULNERABILITY ASSESSMENT OF THE URBAN HISTORIC CENTER OF SKOPJE

Aleksandar Zlateski[1], Veronika Shendova[2], Elena Delova[3]

Summary:

The vulnerability assessment of historic masonry buildings in a given urban area, is a key prerequisite for evaluating global risk. The considered vulnerability index method, obtained by the calculation of a score for a building as weighted sum of characteristic parameters related to the building's seismic response and distributed into vulnerability classes, represents an innovative hybrid methodology for bridging the gap between empirical and analytical methods providing initial seismic vulnerability assessment by using simplified scoring method. The paper will present selecting the specific independent parameters, characteristic for the urban historic center in the old part of the city of Skopje and establishing the relation between the chosen specific parameters and the vulnerability class levels for each of them, as well as calibration of the weight parameter by ranging the importance of each of the parameters. The method will be implemented for a representative part of Skopje Old Bazaar.

Key words: Architectural Heritage, Risk Management, Masonry Structures

[1] Research Assistant, M.Sc., "Ss. Cyril and Methodius" University in Skopje, Institute of Earthquake Engineering and Engineering Seismology (IZIIS), Skopje, North Macedonia, azlate@iziis.ukim.edu.mk
[2] Prof. PhD, "Ss. Cyril and Methodius" University in Skopje, Institute of Earthquake Engineering and Engineering Seismology (IZIIS), Skopje, North Macedonia, veronika@iziis.ukim.edu.mk
[3] Research Assistant, M.Sc., "Ss. Cyril and Methodius" University in Skopje, Institute of Earthquake Engineering and Engineering Seismology (IZIIS), Skopje, North Macedonia, delova@iziis.ukim.edu.mk

1. INTRODUCTION

Urban historic centers are important part of the cultural heritage. Beside their cultural-historic value, they usually represent important economic and touristic centers. Within the broad range of construction techniques and building materials that might be included in the urban historical centers, seismically very vulnerable unreinforced stone and brick masonry structures, constructed before the introduction of a more demanding seismic design code, are one of the most common not only in Europe, but worldwide.
On the territory of the historic city of Skopje, various cultures and spheres of influence intertwined, whose material remains have always attracted the interest of scholarly circles. Each of these cultures left its own mark both in the material and spiritual culture of the people. However, it seems that the Ottoman presence of five hundred years (XIV to early XX century) left a special mark and permanent traces in the physiognomy of the city which in this period achieved their cultural and economic rise.
In addition, for urban historic center located in one of the seismically most active regions in Europe, the vulnerability assessment of historic masonry buildings in this urban area, is a key prerequisite for evaluating global risk. Within the framework of this work, the available literature on seismic vulnerability assessment of historical centers, that has been accumulated over the past decades and calibrated based on broad damage data obtained from post-earthquake damage surveys, has been chosen. The gained knowledge has been used to set-up of vulnerability index method, harmonized with the specific characteristics of urban historic center in Skopje, the capitol of N. Macedonia.

2. HISTORIC CENTER OF SKOPJE (OLD BAZAAR) AND ITS RECENT SEISMIC HISTORY

The capital city of Skopje is situated in the Skopje valley on the banks of the biggest Macedonian river Vardar. Next to the river is located heart of the city, the old part of Skopje, known as Skopje Old Bazaar, (Figure 1). It is one of the oldest and largest marketplaces in the Balkans and its trade and commerce center since at least XII century. Besides, it is known for its cultural and historical values. Although Ottoman architecture is predominant, remains of Byzantine architecture are evident as well, while recent reconstructions have led to the application of elements specific to modern architecture.

Fig. 1 Historic center of Skopje - Skopje Old Bazaar

The Ottoman influence left a special mark and permanent traces in the physiognomy of the historic city of Skopje. The building of Ottoman structures reached its peak in the XV and XVI century, when a large number of mosques, baths, covered bazaars, inns and other facilities, mostly visible in the old part of today’s Skopje, were built as a reflection of the economical and politic circumstances, and represent an expression of the cultural and artistic tendencies and potentials of respective periods. Among them, Mustafa Pasha, Sultan Murat and Ishak Bay Mosques are among the oldest and best-preserved mosques in the Balkan region, while Kurshumli Inn, Suli Inn and Kapan Inn, all of them from XV century, together with Chifte Hammam and Daut Pasha Hammam represent the commercial and public bath areas. In addition, the presence of individual commercial buildings should be emphasized. They form almost 70% of the structure of the entire historic center.

The urban configuration of the historic center of Skopje is characterized with huge authenticity. The buildings are placed in the irregular urban mesh, with a couple of main quite wide streets and the narrowness of the other streets and passes between them. A great percentage of the built urban stock is constituted without any earthquake resistant criteria. The masonry walls constitute the main structural elements with the timber floor slabs resulting in a very simple box-type structure. Brick and stone masonry are the most common building materials but adobe masonry with timber bracing can be found too. Regarding the geometry in height, the buildings usually are constituted by ground floor, one or two elevated floors.

During XX century, the region of Skopje was affected by series of damaging earthquakes, which lasted from August to September 1921 with a magnitude of 4.6 to 5.1. Besides the local earthquakes, region of Skopje has suffered several times from earthquakes occurring at a distance.

In the early hours of July 26, 1963, Skopje was struck by an earthquake with magnitude 6.1, one of the most severe catastrophes in its history. The entire territory of SR Macedonia was shaken with intensities varying between V and IX, MCS. Major earthquake effects were manifested by loss of 1070 human lives and 3300 injuries, destruction and severe damage to a large number of buildings and other public and social facilities, damage to the infrastructure, lifelines, urban furniture, etc. Damage to existing buildings was tremendous. Out of the total building area 80.7% was destroyed or heavily damaged and about 75.5% of the inhabitants were left homeless. Only 19.7% remained non - or slightly damaged, which, in accordance with the damage and usability criteria were usable immediately after the earthquake, (Petrovski 2013) (Velkov 2013).

In addition to the damage to residential and public buildings the catastrophic 1963 Skopje earthquake inflicted inestimable damage to cultural monuments and historic buildings. The entire monument fund of historical center of Skopje was damaged, while part of it was destroyed. Damages were manifested by failure of individual parts of the structures, large cracks, inclination and deformations of the walls, the vaults, the columns and other structural elements.

Through the years following the catastrophic earthquake, there were works on protection of cultural historic structures considering their value and importance. Structural consolidation has been performed in the first phase, while during the renovation of the buildings, particularly those adapted to modern needs whose structural systems did not provide the necessary seismic safety, the principle of repair and seismic strengthening has been applied, involving reinforced concrete bearing structure, columns and belt courses interconnected and incorporated into the existing masonry. Cement as a material was also applied in repair of the medieval churches and monasteries through injection of the occurred cracks or rebuilding of the ruined parts and seismic strengthening

On September 11, 2016, the city of Skopje and its surroundings was hit by a series of earthquakes with main shock of moderate size moment magnitude of 5.1. The main shock was felt in the urban city area with intensity of about VI to VII degrees according to EMS. Immediately after the occurring of the main shock, an activity of rapid visual screening was performed by IZIIS, within a framework of which 15 cultural heritage buildings and monuments were inspected, located in the old historic part of the city, (Shendova et al. 2018)

After the fast visual screening vast majority of inspected monumental buildings were assessed as safe and usable, since their damage varies from slight non-structural one, (failing of pieces of mortar or bricks from the cornices or facade walls, hair cracks in mortar joints on facade walls and ceiling, breaking of glass from large windows), to very localized or negligible structural damage, (initial cracks to the walls and ceiling elements, falling of large patches of mortar from wall and ceiling surface, considerable cracks or partial failure of chimneys). However, there are isolated cases of considerable structural damage manifested as widening and elongating of older cracks or occurring of newly developed cracks, usually in the walls or along with the connection between the walls and vaults or domes.

3. HARMONIZED VULNERABILITY INDEX FOR URBAN HISTORIC CENTER OF SKOPJE

The vulnerability assessment of historic masonry buildings in a given urban area is a key prerequisite for evaluating global risk. This is not only important because of the obvious physical consequences in the possible occurrence of an event but also because of its relationship with human presence and evacuation support systems, which are essential aspects in the definition of effective risk reduction strategies. The combination between vulnerability assessment of existing buildings and the implementation of appropriate seismic retrofitting and emergency planning solutions can help to reduce physical damages, human losses and critical emergency conditions for the population, as well as the economic impact of future events.

The available literature on seismic vulnerability assessment of historical centers, related to the collected data that has been accumulated over the past decades about post-earthquake damage surveys and interventions in the historical center of Skopje, opens a unique opportunity to set-up of vulnerability index method, harmonized with the specific characteristics of the specified urban historic center. This was the starting point of the internal IZIIS' project as a contribution to the governmental long-term project on Skopje Old Bazaar revitalization.

The considered vulnerability index method represents an innovative hybrid methodology for bridging the gap between empirical and analytical methods and provides seismic vulnerability assessment by using simplified scoring method. This method has been originally developed by (Benedetti et al. 1984), adapted and applied to several historic centres in Portugal (Vicente et al. 2011), (Ferreira et al. 2013), (Maio et al. 2015), and calibrated using post-earthquake damage data, (Ferreira et al. 2017). This methodology also has been successfully calibrated and implemented for vulnerability assessment in order to evaluate, manage and mitigate the earthquake risk in the historical center of Coimbra, Portugal, with the urban configuration very similar to Skopje old Bazar, (Zlateski et al. 2020).

The vulnerability index is obtained by the calculation of a score as the weighted sum of 14 parameters,

$$I_{vf} = \sum_{i=1}^{14} c_{vi}\, p_{vi} \tag{1}$$

Each parameter shown in Table 1 covers one aspect related to the building's seismic response and is distributed into four vulnerability classes (cvi) of growing vulnerability: A, B, C and D, while two sets of weights show those originally proposed and recently calibrated by post - eq data, (Ferreira et al. 2017).

Beside the weight parameter, essentially the most important issue in this method is to prescribe the vulnerability class for each of the parameter, which should be in relation with the specificity of historic buildings in the urban historic center in consideration. The most important part of this harmonization is setting up the specific independent parameters, characteristic for the urban historic centre in the old part of the city of Skopje, capital of N. Macedonia, and establishing the relation between the chosen specific structural parameters and the vulnerability class levels A, B, C, D for each of them.

Tab. 1 Vulnerability index associated parameters classes and weights

Parameters	Class, C_{vi} A	B	C	D	Weight, p_i Original	Calibrated
1. Structural building system						
P1. Type of resisting system	0	5	20	50	0.75	2.50
P2. Quality of resisting system	0	5	20	50	1.00	2.50
P3. Conventional strength	0	5	20	50	1.50	1.00
P4. Maximum distance between walls	0	5	20	50	0.50	0.50
P5. Number of floors	0	5	20	50	1.50	0.50
P6. Location and soil condition	0	5	20	50	0.75	0.50
2. Irregularities and interactions						
P7. Aggregate position and interaction	0	5	20	50	1.50	1.50
P8. Irregularity in plan	0	5	20	50	0.75	0.50
P9. Irregularity in height	0	5	20	50	0.75	0.50
3. Floor slabs and roofs						
P10. Alignment of openings	0	5	20	50	0.50	0.50
P11. Horizontal diaphragms	0	5	20	50	1.00	0.75
P12. Roof systems	0	5	20	50	1.00	0.50
4. Conservation status and other elements						
P13. Fragilities and conservation status	0	5	20	50	1.00	1.00
P14. Non-structural elements	0	5	20	50	0.50	0.75

Based on the acquired knowledge for Old Bazaar' structures, what follows are established relation between the chosen specific independent structural parameters, (P1, P2, P4, P5, P6, P7, P8, P9, P10 and P11) and the vulnerability class levels, (Table 2, 3, 4, 5). The content of the Tables 3, 4, 5 and 6, along with the corresponding schemes and necessary explanations, like those presented on Figures 2, 3 and Figure 4, represent the part of harmonized vulnerability index regarding the independent parameters and associated vulnerability class levels, specific for the historic buildings in Skopje Old Bazaar.

Tab. 2 Harmonized independent parameters associated to vulnerability class, Type of resisting system P1, Quality of resisting system P2 (P3, P13)

Class C_{vi}	P1 Resisting system	P2, Quality of resisting system Mortar	w kN/m^3	f_c kPa	f_t kPa	E MPa	G MPa	P3, P13 Cracked stiffness
A	Confined masonry	Cement	22	800	40	4200	1400	1.00
B	Brick/stone masonry	Lime/cement	20	600	30	3300	1100	0.83
C	Brick/stone masonry	Lime	19	400	20	2100	700	0.67
D	Adobe masonry	Adobe mud	18	100	5	450	150	0.50

Tab. 3 Harmonized independent parameters associated to vulnerability class, Distance between walls P4, Number of floors, P5, Location and soil type P6

Class C_{vi}	**P4 Maximum distance between walls (l/d, h_0/d) wall thickness:**	**P5 Number of floors**	**P6 Location and soil condition (according EN 1998-1)**
A	0.60 m	1	A
B	0.50 m	2	B
C	0.40 m	3	C
D	0.30 m	enlarging/ upgrading	D, E

Tab. 4 Harmonized independent parameters associated to vulnerability class, Position - interaction P7, Irregularity in plan P8, Irregularity in height P9

Class C_{vi}	**P7**	**P8**	**P9 change in vertical elements' geometry**
A	Figure 2, a	Figure 3, a	0%
B	Figure 2, b	Figure 3, b	up to 10%
C	Figure 2, c, d	Figure 3, c	(10 -20) %
D	Figure 2, e, f	Figure 3, d	(20 – 30) %

Tab. 5 Harmonized independent parameters associated to vulnerability class, Alignment of openings P10, Horizontal diaphragms P11, (Roof structure P12)

Class C_{vi}	**P10 Alignment of openings**	**P11, P12 Horizontal diaphragms (Roof structures)**
A	Figure 4, a, regular and aligned	Rigid and well connected
B	Figure 4, b, horizontal misalignment	Flexible and well connected
C	Figure 4, c, horizontal and vertical misalignment	Rigid and poorly connected
D	Figure 4, d, large openings in ground floor	Flexible and poorly connected

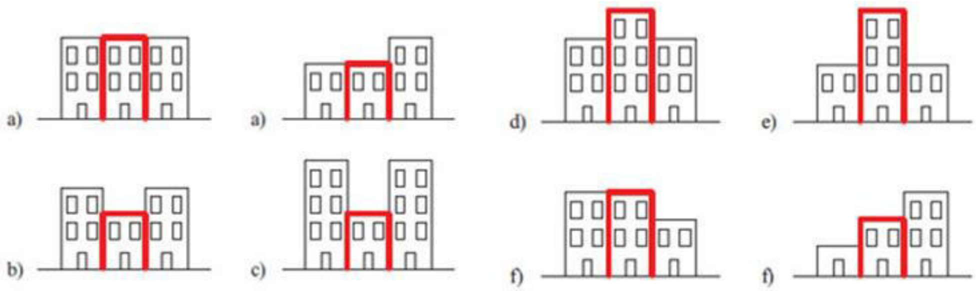

Fig. 2 Building position

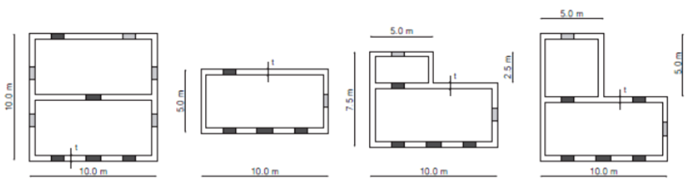

a) b) c) d)

Fig. 3 Plan regularity

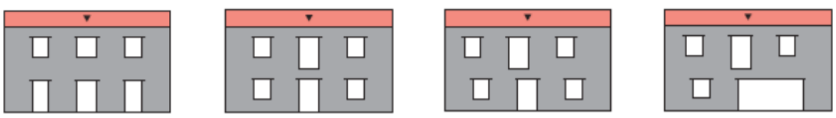

a) b) c) d)

Fig. 4 Alignments in openings

With this part is prepared an understandable guideline for pre-earthquake vulnerability assessment of specific historic urban centre, which can be easily applied by the key target groups such as architects and civil engineers involved in the earthquake protection of structures pertaining to cultural heritage. The final aim is to be reached the vulnerability index method related to the specific independent parameters and associated vulnerability class levels, specific for the historic buildings in Skopje Old Bazaar.

4. APPLICATION OF THE HARMONIZIED METHOD TO THE HISTORICAL CITY CENTRE OF SKOPJE

The seismic vulnerability assessment of one representative street of the historical city center of Skopje was carried out by applying the harmonized vulnerability index methodology, shortly presented in section 3. Because the methodology requires accurate knowledge of the building characteristics, which can only be obtained via thorough and detailed inspection, the 33 buildings were analyzed, in function of the detail of the information available and used on its seismic vulnerability assessment.
It is important to note that during the field assessment and analysis of the buildings, 6 buildings were observed that were reconstructed using reinforced concrete. These buildings were not exempted from the seismic assessment.
The methodology applied herein and results obtained are presented resourcing to a Google Earth application. Figure 5 shows the assessed urban area with marked buildings.
As already referred, the seismic vulnerability index Ivf was calculated resorting to Equation (1). The values of the Iv are presented in Table 4.

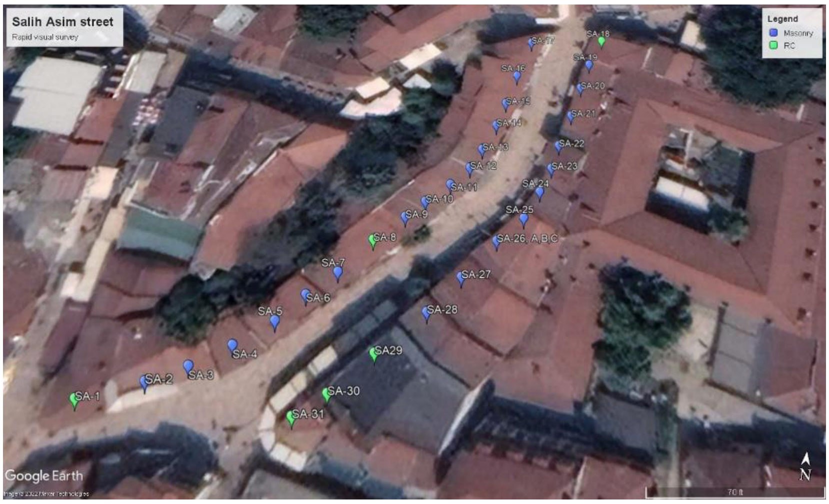

Fig. 5 The assessed urban area with marked buildings – Salih Asim street (Skopje old Bazaar)

Tab. 6 vulnerability index values for the whole study area

No.	Ivf	No.	Ivf
SA-1	0	SA-17	320
SA-2	295	SA-18	0
SA-3	325	SA-19	245
SA-4	290	SA-20	275
SA-5	255	SA-21	275
SA-6	255	SA-22	285
SA-7	255	SA-23	275
SA-8	0	SA-24	245
SA-9	275	SA-25	275
SA-10	270	SA-26-A	247.5
SA-11	245	SA-26-B-C	197.5
SA-12	217.5	SA-27	227.5
SA-13	107.5	SA-28	345
SA-14	195	SA-29	0
SA-15	245	SA-30	0
SA-16	275	SA-31	0

As already mentioned, seismic vulnerability results were mapped using the Google Earth tool, developed to provide a global overview of the vulnerability assessment results and the consequent risk scenarios.

Based on the previous seismic vulnerability values of the buildings within the study area, descriptive damage grades were estimated for seismic scenarios with macroseismic intensity IX.

The proposed damage for this work, according to the vulnerability, is presented to table 7. Figure 6 presents the spatial distribution of the vulnerability index values for the whole study area and, also presents the damage scenario for seismic intensity IMS-98= IX.

From the results, it is observed that for earthquake intensities IX, 10% of the buildings would collapse, 64% of them would have severe damage, 10% would have minor damage, and 16% would remain undamaged. In this 16 percent, reinforced concrete constructions are placed (Figure 7).

Tab. 7 Damage grade, according to vulnerability

	Damage - Intensity IX - MSC
(green)	Ivf=0-100 - No damage
(yellow)	Ivf =101-200 - Slight / moderate damage
(orange)	Ivf =201-300 - Severe damage
(red)	Ivf >300 - Very severe damage / destruction

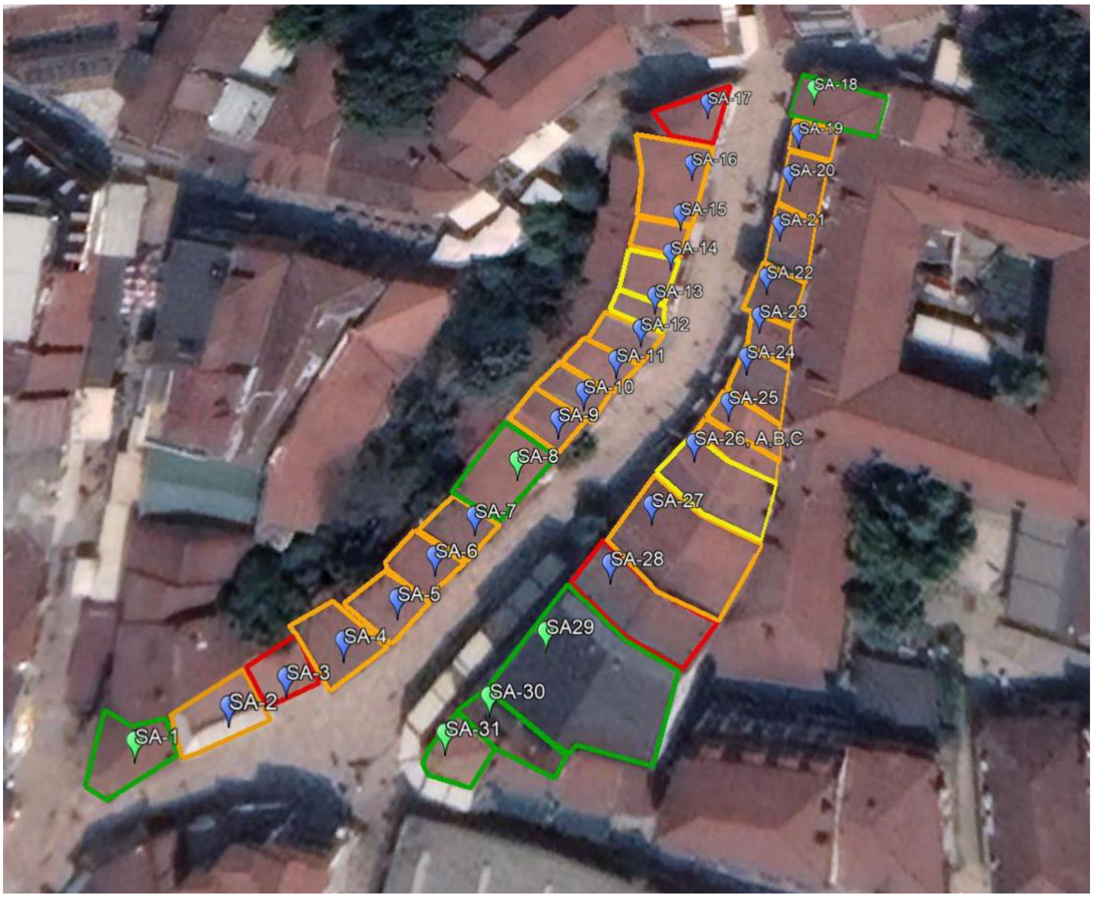

Fig. 6 The assessed urban area with marked buildings – Salih Asim street (Skopje old Bazaar)

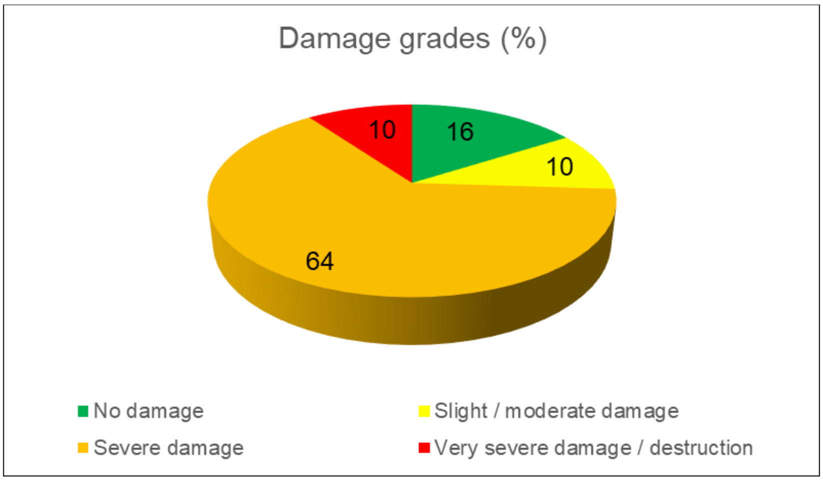

Fig. 7 Percentage representation of different damage grades

5. CONCLUSIONS

The vulnerability assessment of masonry buildings in a given historical urban area is a key prerequisite for evaluating global risk which is defined as the probability of the occurrence of a seismic event of a certain intensity, at a specific site, during a determined period of time. The vulnerability analysis is not only important because of the obvious physical consequences in the possible occurrence of an event but also because of its relationship with human presence and evacuation support systems, which are essential aspects in the definition of effective risk reduction strategies.

In fact, the combination between vulnerability assessment of existing buildings and the implementation of appropriate seismic retrofitting and emergency planning solutions can help to reduce physical damages, human losses and critical emergency conditions for the population, as well as the economic impact of future events. Particularly regarding the seismic vulnerability assessment of masonry buildings in historical centers, the amount of knowledge that has been accumulated over the past decades, together with the broad damage data obtained from post-earthquake damage surveys, opens a singular opportunity to harmonized and calibrate effective seismic vulnerability assessment approaches.

Given that the achievements were obtained as a result of recent knowledge in the field, calibrated methods using databases from previous earthquakes, as well as specific knowledge on the characteristics of the Old Bazaar' historic buildings over time, the result are undoubtedly sustainable and could be successfully applied and easily modified in the case of a new event in the future.

The proposed harmonized vulnerability index method, obtained by the calculation of a score for a building as a weighted sum of characteristic parameters related to the building's seismic response and distributed into vulnerability classes, represents an innovative and effective tool for bridging the gap between empirical and analytical methods providing initial seismic vulnerability assessment.

REFERENCES

[1] Benedetti D., Petrini V. (1984): Sulla vulnerabilità sismica di edifici in muratura: Un metodo di valutazione, L'industria delle costruzioni, 149, 66–74, 1984.

[2] Ferreira T.M., Maio R., Vicente R. (2013): Seismic vulnerability assessment of historical urban centres: case study of the old city centre in seixal, Portugal, Bulletin of Earthquake Engineering, 15 (5), 1753–1773.

[3] Ferreira T.M., Maio R., Vicente R. (2017): Seismic vulnerability assessment of the old city centre of Horta, Azores: Calibration and application of a seismic vulnerability index method, Bulletin of Earthquake Engineering, 15(7): 2879–2899.

[4] Maio R., Vicente R., Formisano A., Varum H. (2015): Seismic vulnerability of building aggregates through hybrid and indirect assessment techniques, Bulletin of Earthquake Engineering, 13 (10), 2995–3014.

[5] National Conservation Center (1983): Monography marking 20 years of renovation of the Skopje monuments and historic buildings, (in Macedonian).

[6] Petrovski J. (2013): Damaging Effects of July 26, 1963 Skopje Earthquake, Proceeding of the International conference Skopje Earthquake – 40 years of European Earthquake engineering, Skopje.

[7] Shendova V., Zlateski A., Delova E. (2018): Skopje 11th September 2016 earthquake: post-earthquake visual screening on cultural heritage buildings, Proc. of the 16ECEE, Thessaloniki.

[8] Velkov D. (2013): Skopje 1963 Earthquake, Damages and Reconstruction, Proceeding of the International conference Skopje Earthquake – 40 years of European Earthquake engineering, Skopje

[9] Vicente R., S. Parodi, Lagomarsino S., Varum H., Mendes da Silva J.A.R. (2011): Seismic vulnerability and risk assessment: Case study of the historic city centre of Coimbra, Portugal, Bulletin of Earthquake Engineering, 9(4):1067–1096

[10] Zlateski A., Lucesoli M., Bernardini G., Ferreira T. M. (2020): Integrating human behaviour and building vulnerability for the assessment and mitigation of seismic risk in historic centres: Proposal of a holistic human-centred simulation-based approach, International Journal of Disaster Risk Reduction, 43, doi: https://doi.org/10.1016/j.ijdrr.2019.101392

VALUE CRITERIA OF CITIZENS IN PERCEIVING THE FUNCTION OF PUBLIC SPACES

Sofija Priljeva[1]

Summary:

This research focuses on examining the value criteria of citizens from Novi Sad in relation to the variability of the basic functions of public spaces. The analysis aims to explore the interdependence between the passage of time and the spatial (physical, aesthetic) and functional changes, in order to determine to what extent, the declining societal value system allows for changes in the physical structure of the city. Additionally, it seeks to answer the question of whether the community itself is contributing to the deterioration of the quality of the living space. For the purpose of this analysis, two well-known public spaces in Novi Sad were selected, both of which possess a rich tradition and are recognized as cultural, tourist, and reference points within the city center. The analysis focuses on occasional spatial changes that arise from cultural demands and the corresponding content that meets those demands. Two examples of such changes include the winter amusement park with an ice rink called "The Ice Forest" ("Ledena Šuma") in the Danube Park (Dunavski park), as well as the New Year's concerts held at the public square The Liberation Square (Trg slobode). The survey conducted among the citizens of Novi Sad led to the conclusion that it is important that events and activities take place in the city, even if these events pose a potential aesthetic and/or functional threat to the existing urban landscape.

Key words: community, public space, public interest, citizen participation

[1] Assistant - Master. Faculty of Technical Sciences, University of Novi Sad, Serbia, sofija.priljeva@uns.ac.rs

1. INTRODUCTION

Collective, as the most common form of association among people, represents a community with pronounced shared values of its members. Values are therefore a very important factor in the formation and functioning of the community, with clear criteria and rules by which members of the collective are guided. Values are relatively stable and hierarchically organized characteristics of individuals and groups, formed through the interaction of historical, social, cultural, and individual factors, directing the behavior of their bearers towards specific goals [11]. Adler however defined four basic types by which the concept of values can be simplified. The first type represents the existence of absolute, eternal values that are common to the vast majority and are often not even questioned (for example, the existence of God). The second type of values is essentially material or immaterial and is usually assigned through factual consideration. The third type represents values that are seen as part of the individual, and they arise from a more subjective assessment, where values are experienced as something personal, characteristic of the individual. Finally, the fourth type of values are those that are identified with actions and are defined by behavior [1]. However, these types often overlap, giving rise to their modifications. This means that every community is determined by a combination of universal values and values nurtured by its members, who influence the overall image of the community through their behavior. In addition to values, elements that are important to mention in the context of a community include a sense of belonging, human interaction, and a common space, more precisely, the physical framework in which a community exists. Space, whether virtual or real, is crucial for the existence of a community because it serves as the platform for all common activities. If there are no activities or the space, the community cannot be sustained. Therefore, the spatial framework and values represent inseparable elements in the life of a social community. The connection between these two elements will be the subject of research in this paper, with a special focus on analyzing the factors that influence the change in value criteria in the perception of the function of public spaces. The research is based on examining the causes and consequences of changes in the consciousness of citizens regarding the basic function of certain public spaces, such as the square and park in the center of Novi Sad, Serbia. The examination of the interdependence of the passage of time on the one hand and spatial (physical, aesthetic) and functional changes on the other should provide an overview of how the declining value system of society in practice allows for the change in the physical structure of the city and answer the question of whether the community itself undermines the quality of the space in which it lives. The issue of different collective behaviors that affect the (non)fulfillment of public interest will be presented as one of the problems, through the analysis of specific examples of changes in the function of the square and park and by surveying the citizens of Novi Sad. The results of the research will also show whether and to what extent important decisions, which have a direct impact on the arrangement of public urban space, are made in accordance with its preservation or to meet the expectations of different interest groups, including the citizens themselves – the space users.

2. CULTURAL NEEDS AND CULTURAL CONSUMPTION

Every expression of human spiritual life can be understood as a kind of language, and this understanding, as the truthful method does, opens up new questions everywhere [2]. Thus, cultural values, which are part of spiritual life, represent the language through which a community expresses its cultural needs. These needs are reflected in various cultural contents that are "consumed" and used as a kind of resource, and the criteria for selecting content depend on the aforementioned values of the community that prevail at that moment. Marx's theory of the base and superstructure could be used to confirm the relationship between the socio-political circumstances in Serbia and cultural consumption. The fact that less than one percent of the state budget for the year 2023 is allocated for culture[1] (and this amount has been exponentially decreasing from year to year) could indicate an unfavorable financial situation or a lack of interest from government leaders in promoting cultural values in society. In this case, both are contributing factors, but it is most concerning that almost one-third of the citizens have expressed the opinion that the state should not finance any form of cultural activities. This already speaks to unmet expectations regarding the basic needs of a society, where the "base and superstructure" thesis can be drawn as a parallel to the satisfaction of essential needs, such as material security in life, and "higher" cultural needs. In the cultural market, as in any other, the alignment of supply and demand is not merely a simple effect of production imposed on consumption, nor is it a conscious effort to cater to consumers. Instead, it is the result of an objective coordination of two independent logics. Tastes depend on the goods that are offered, so any change in taste, resulting from a transformation of the conditions of existence, tends to, directly or indirectly, transform the field of production itself [3]. The most common factors influencing the choice of cultural content are the political system and socio-economic conditions. The first factor is institutional and relates to the lack of public policy, while the second factor arises as a direct consequence of the first and encompasses unequal social conditions, uneven and rapid accumulation of material wealth by individuals, thereby deepening the financial and intellectual gap among different segments of the population. All of this has also been significantly influenced by the transition, which "bridged" certain stages in the maturation of society through the process of modernization. Interest in culture and cultural content became diluted, and the identity formed and maintained through them became inert. This has led to today's mass media audience, which is larger, and the entire program is designed around it. In maintaining such programs, there is a change in the function of public space, which is often disrupted, and since space is a complex phenomenon of social production, it is impossible to observe it outside of the social framework [8]. Lefebvre, also known as a pioneer in the critique of everyday life, believed that the city (space) is shaped by social activities during specific historical periods, raising a question that is still relevant today – Is the city the result of or a product of social interactions [8]. Does the society that creates it contribute to its value as a work[2] through its values, or does it merely shape it for the sake of the formal existence of urban space? According to Debord, the fundamental intention of capitalism is to restructure society without community, translating spectacle into a new pseudo-culture. The function of the spectacle is to bury history in culture, exerting pressure on the novelties of its modernity and putting them in the service of a strategy that will further define it [4]. Considering that moral norms and value structures in Serbia are very unstable and inconsistent, the question arises to what extent cultural consumption dictates current physical changes in the city, leaving lasting consequences on it. Hillier believes that we can understand a society's culture simply by examining the way they order their built environment. And, likewise, understanding a society's culture helps clarify its architecture and urbanity [6]. This primarily applies to spaces that have developed over a long period, in accordance with social customs, tradition, and beliefs. However, certain short-term spatial interventions also arise as a result of the influence of prevailing cultural values during that period.

[1] According to Parliamentary Committee for Culture and Information
[2] Referring to an artistic work

3. ANALYSIS OF SPECIFIC CHANGES IN PUBLIC SPACES – THE LIBERATION SQUARE AND THE DANUBE PARK IN NOVI SAD

In this chapter will be analyzed spaces that periodically change their purpose, simultaneously altering their fundamental, primarily aesthetic and functional characteristics. For analysis – case study, two well-known public spaces in Novi Sad with a long tradition and the reputation of being cultural, tourist, and focal points of the city center have been selected. The analysis includes occasional spatial changes that result from cultural demand and content that satisfies that demand, such as hosting New Year's concerts on The Liberation Square (Trg slobode) and the winter amusement park “The Ice Forest“ (Ledena šuma) in the Danube Park (Dunavski park).

3.1. THE LIBERATION SQUARE AS A CENTRAL URBAN LOCATION

Squares have always been significant points of activity in cities, dating back to ancient times. People gathered in squares for trade and the exchange of goods, but also for the exchange of ideas, participating in public debates and political events. The most famous square in Novi Sad, the Liberation Square (Trg slobode), was known as the Main Square (Glavni trg) for almost two centuries. Around 1900 it changed its name, and later, after World War II, it received its current name. This fact speaks to how public spaces, in this case squares, reflect what is happening within the collective – after being renamed following World War I, it was called Freedom Square (Trg Oslobođenja), and after World War II, Liberation Square (Trg slobode).

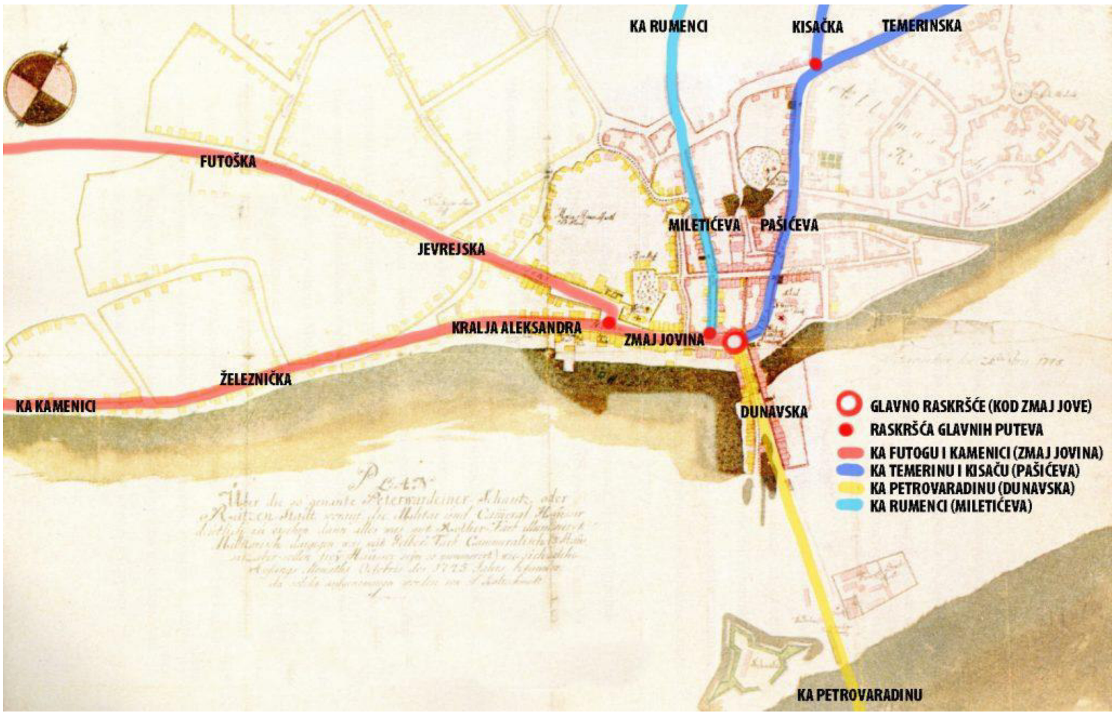

Fig. 1 The oldest map of Novi Sad (1745)

According to the 1745 map of Novi Sad, the Liberation Square had been a crossroads of main roads since the founding of the city – one leading to Kamenica and the other to Futog. It was also referred to as the Great Market (Velika pijaca) for a long time because market days were held there, during which it was bustling with people and carts.

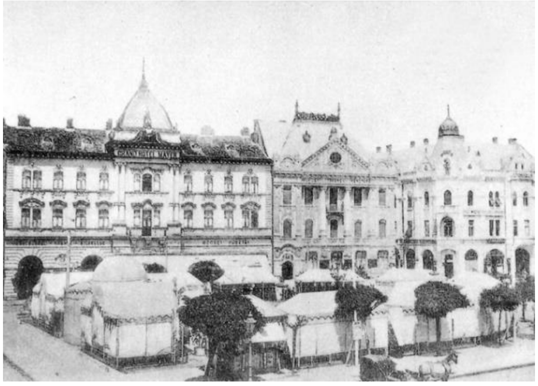

Fig. 2 and 3 The Liberation Square during a market, at the end of the nineteenth century

From 1911 to 1958, trams also operated in the Liberation Square, which further confirms its significance and the fact that it has always been a center for various activities, including transportation.

Fig. 4 and 5 The Liberation Square in the early and mid-twentieth century

3.2. LIBERATION SQUARE − CENTER OF NEW YEAR'S EVENTS

The celebration of New Year's Eve, as well as the organization Christmas events in main city squares, is a tradition in cities across Europe. The same holds true in Novi Sad, where multiple public spaces are used for these festivities, with the Liberation Square being undoubtedly the most attractive location.

For many years now, both New Year's Eve celebrations (on December 31st) and Orthodox New Year celebrations (on January 13th) have featured concerts by various performers. Since 2016, as part of the competition for the European Capital of Culture 2021, the "Doček"[3] (New Year's Eve celebration) has been introduced.

[3] The sequence of events in December and January, which includes concerts at Trg slobode, where a large number of local and foreign performers from various music genres have participated so far.

Figure. 6 The New Year's Eve celebration of 2018 attended by 50,000 people

In addition, from December 1st to December 28th each year, the "Zimzolend" winter festival takes place in the Liberation Square. This winter festival is inspired by Christmas markets in Europe and features around thirty stalls where visitors can sample various food and drinks and purchase artisanal products.

Figure. 7 Stalls at "Zimzolend"

3.3. DANUBE PARK – NOVI SAD ICE RINK

This oldest park in Novi Sad was established at the end of the 19th century on the site of a muddy depression, which was a former branch of the Danube River called Liman. Even back then, at the end of what is now the park and what was then known as the Promenade (corso), there was a lake, part of the Small Liman, which served as an ice skating rink in winter, while during the summer, visitors could rent boats and paddle on it [9].

Fig. 8 and 9 The lake in the Danube Park (part of Mali Liman) at the beginning of the nineteenth century

In the mid-1930s, this area was filled with soil, and pathways were added, giving it the name it bears today – the Danube Park. In the 1960s, the park acquired its current appearance while retaining existing trees. Floral elements were added, a central lake with a weeping willow in the middle was formed, and to this day, it has preserved as many as six hundred plant species.

The park covers an area of nearly 40,000 square meters and houses several sculptures by prominent Yugoslav artists. It also features a gazebo, which holds a special place and serves as an oasis of peace and a pleasant natural setting.

In 1998, by a decree of the Government of the Republic of Serbia, the Danube Park was designated as a nature monument of the second category. This is an important aspect to emphasize within the scope of this analysis, as it impacts the change in purpose and physical characteristics of the space.

As previously mentioned, a sort of improvised ice skating rink existed in the Danube Park as far back as the late 19th century. However, during the interwar period, on the outskirts of the park, a tennis court across from the Sokolski dom began to be used as a skating rink. Just before the war, this location even hosted the Novi Sad high school championship in speed skating.

Figure. 10 Ice skating on the Promenade at the end of the nineteenth century

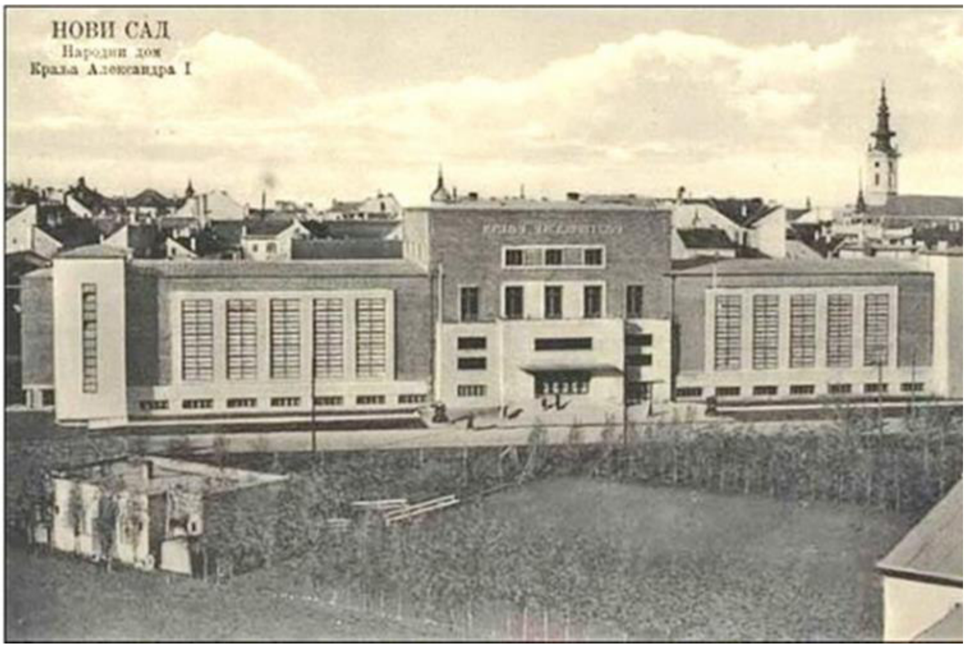

Figure. 11 The tennis court in the Danube Park from the 1930s, which was used as an ice skating rink

3.4. “THE ICE FOREST“ – TRADITION OR POPULISM?

The event "Ice Forest" („Ledena šuma“), which offers a central ice skating rink, music performances, shows, and a certain gastronomic selection, has been held every winter in the Danube Park since 2016. At the outset, this event faced sharp criticism from the public, sparking many discussions.

The first issue raised concerned the budgeting of the event, specifically questioning whether the citizens of Novi Sad, as taxpayers, were financing the construction and maintenance of "The Ice Forest" and its ice rink, which charges an entrance fee. The second issue was related to environmental protection and its impact on the natural beauty of the park, which has been declared a natural monument and should consider numerous legal provisions before any adaptation or addition of content.

Environmental activists emphasize each year that the construction seriously damages this green oasis, leaving grassy areas damaged, while decorative lighting and fireworks have consequences for the environment. They point out that the Regulation on the Protection of Natural Monuments explicitly prohibits the installation of electrical installations, and this decision was issued to the organizers in 2016. The same applies to the use of chemical substances used to create ice and fireworks. However, the Institute for Nature Conservation states that, *"...the structure of the ice rink was set up during the vegetation dormant period, above the lawn, and additionally, with the aim of improving the condition of the protected natural area, an obligation was placed to repair the lawn after the completion of work and activities by the beginning of spring"*[4]. The authorities confirm that this is being followed, but it will be revealed over time whether this indeed is the case.



Figures. 12, 13 and 14 The Danube Park after the removal of “The Ice Forest“

[4] Udruženja pitaju ko je i kako dozvolio „Ledenu šumu" u Dunavskom parku, organizatori i nadležni odgovaraju. https://www.021.rs/story/Novi-Sad/Vesti/229343/Udruzenja-pitaju-ko-je-i-kako-dozvolio-Ledenu-sumu-u-Dunavskom-parku-organizatori-i-nadlezni-odgovaraju.html (june 2023)

Undoubtedly, it is a fact that citizens love to visit “The Ice Forest“. When the it was first held in 2016, approximately two hundred thousand people passed through the Danube Park during this event. The New Year's euphoria is likely the primary reason for the popularity of this happening, which is not a bad thing. However, for it to truly be meaningful and thematically, visually, and conceptually closer to similar events in European cities during the New Year and Christmas "markets", all limiting factors and potentials of the given space should be taken into account without altering it beyond necessary measures.
Is "The Ice Forest" a kind of "memory" of the former corso and ice rink, or is the change in purpose and the addition of similar content in a different way merely a coincidence? What sets apart these two forms of entertainment from different times is the position of the ice rink itself, the users' (visitors) relationship with the space, and their awareness of collective well-being, as the values cultivated in the past were not reflected in periodic events that left lasting consequences on the surroundings.

4. SURVEY

The survey conducted among the citizens of Novi Sad from June 15th to June 22nd 2023, aimed to collect information about the value criteria related to the changing function of public spaces. A total of 115 people participated in the survey, providing different responses and thereby expressing the opinions of a part of the population regarding the identity, usage, aesthetic value, and accessibility of two public spaces: The Liberation Square and the Danube Park.

4.1. QUESTIONS AND RESULTS

1.

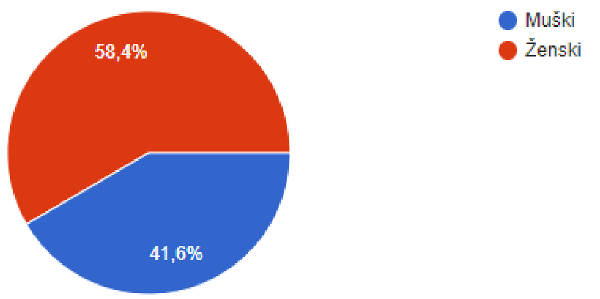

Chart. 1

The first question in the survey related to the gender structure of the respondents, which was roughly equal (the percentage of women was about one-seventh higher than that of men).

2.

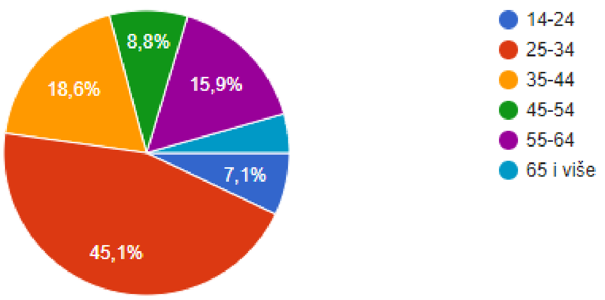

Chart. 2

The second question pertained to the age structure, with the majority of respondents falling in the category of 25 to 34 years old. Other categories were less represented.

3.

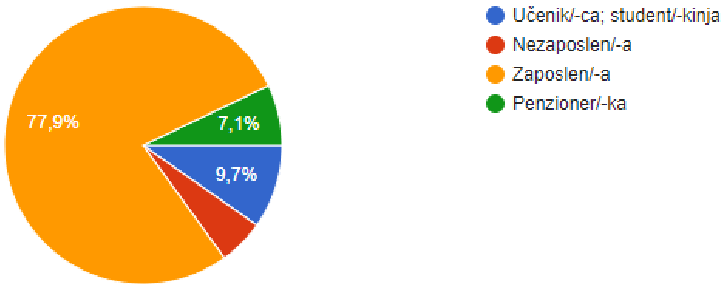

Chart. 3

The third question was related to occupation, and it was determined that the largest number of respondents belonged to the category of employed individuals.

4.

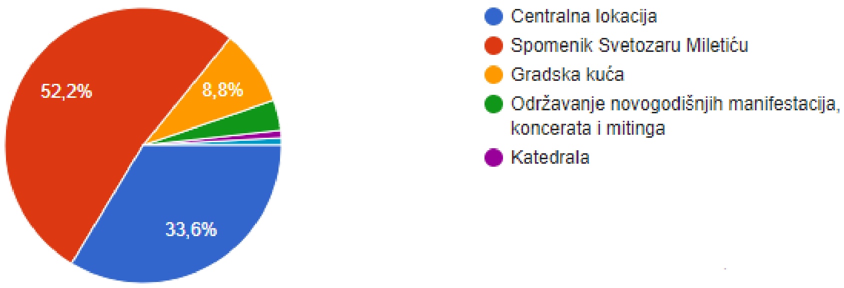

Chart. 4

As the strongest association with the Liberation Square, the monument to Svetozar Miletić proved to be the most prominent. The second in line was the central location of the square, while only 3,5% of the respondents (4 out of 115) chose it as a location for New Year's events. An additional response that was not offered was “The Cathedral“, referring to the Church of the Name of Mary (Crkva imena Marijinog).

5.

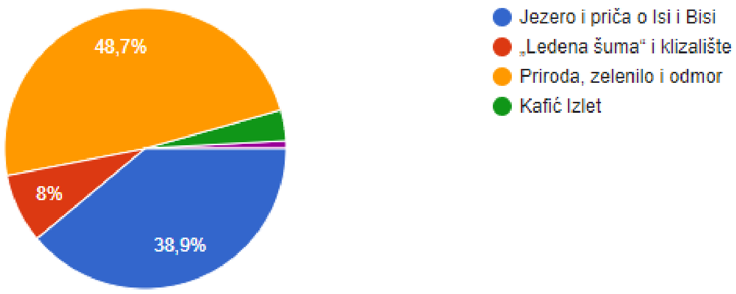

Chart. 5

The strongest association with the Danube Park among the people of Novi Sad is undoubtedly relaxation in nature, while the next one is the story of a pair of swans, Isa and Bisa.

6.

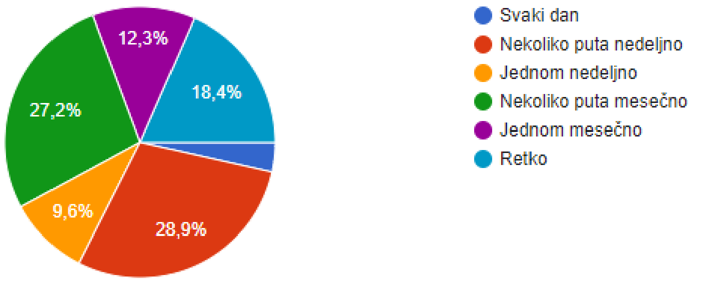

Chart. 6

Regarding the frequency of visits to the Liberation Square, the majority of respondents (28,9%) answered that they visit it several times a week...

7.

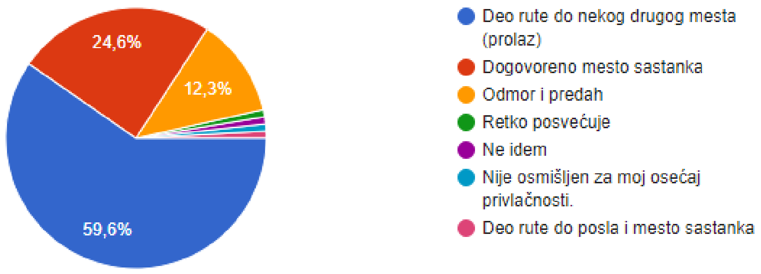

Chart. 7

...mostly in passing through. Almost a quarter of the respondents answered that the reason for visiting the square is a pre-arranged meeting place, indicating its significance as one of the focal points of Novi Sad. One respondent stated that the square was not designed to be attractive, which could refer to its appearance or the activities that take place there.

8.

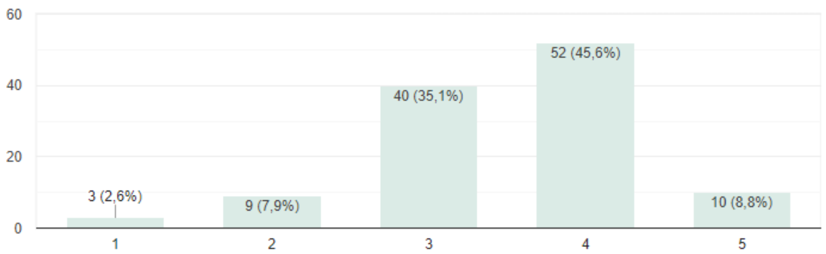

Chart. 8

The majority of respondents rated the aesthetics of the square with a rate of 4, indicating that citizens are generally satisfied with the appearance of the Liberation Square.

9.

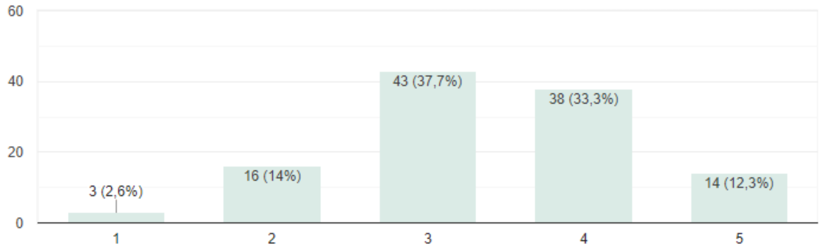

Chart. 9

When it comes to the square's amenities such as urban furniture and similar elements (benches, lighting, trash bins, pavement quality), the majority of respondents gave a moderate rating, with rates of 3 or 4.

10.

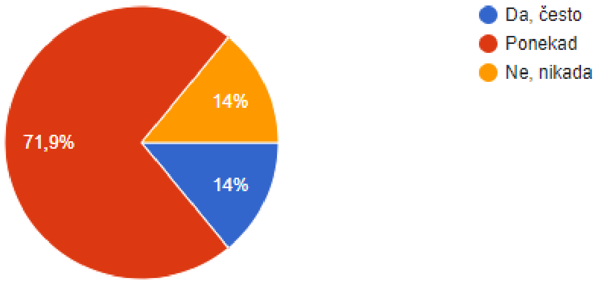

Chart. 10

Regarding the attendance of the square during New Year's events, the majority of respondents (71,9%) answered that they visit the square occasionally, while an equal number of people come frequently or never visit it during these events.

11.

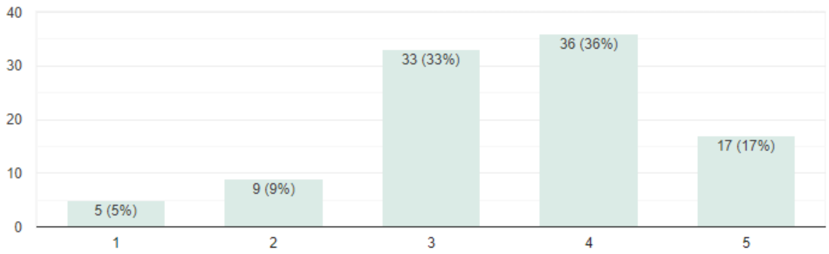

Chart. 11

When asked to rate the aesthetics of the Liberation Square during New Year's events and concerts, only those who attend them answered, and the results are similar to when these events are not taking place – most respondents gave it a middle rating (3 and 4).

12.

Chart. 12

The last question related to the Liberation Square was about the impact of stalls, stages, and accompanying equipment at events and concerts on the aesthetic value of the Square and its use. Almost half of the respondents answered that it reduces the aesthetic value, but at least something is happening and the city needs it.

13.

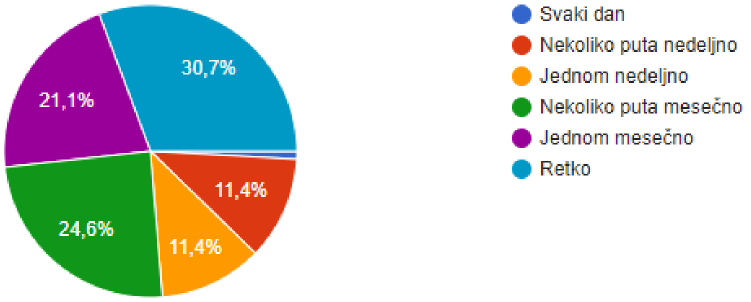

Chart. 13

To the question about the frequency of visits to the Danube Park, the majority of respondents (30,7%) answered that they rarely visit it, followed by those who visit it several times a month (24,6%) or once a month (21,1%).

14.

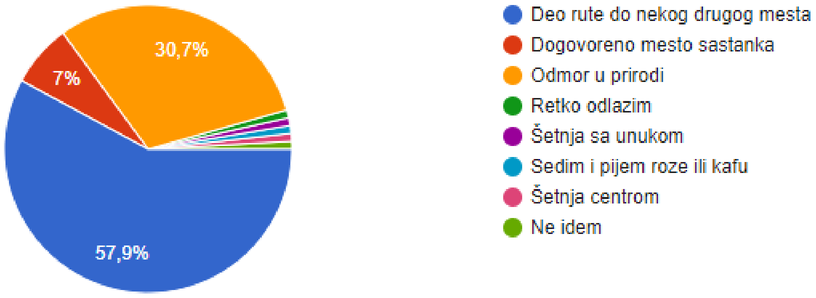

Chart. 14

As the most common reason for their visits, respondents mentioned that the park is just an "in passing" stop for them, while its primary function, relaxation in nature, was mentioned as the second most common reason.

15.

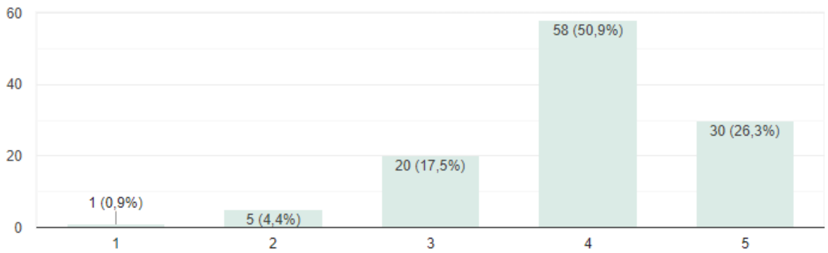

Chart. 15

The aesthetics of the park were mostly rated with very good and excellent ratings (4 and 5), indicating that even though they don't spend a lot of time in it, the respondents still find the park "beautiful."

16.

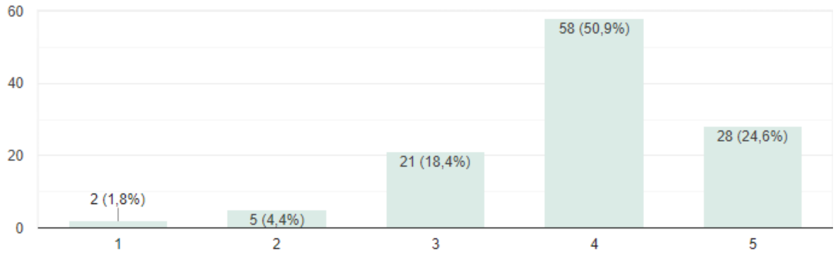

Chart. 16

The quality and quantity of greenery, as well as the equipment of the Danube Park with urban furniture and similar elements (benches, lighting, trash cans, quality of paving), were also mostly rated with very good and excellent ratings (4 and 5), while a small percentage believe that there is not enough greenery and that the park is not adequately equipped.

17.

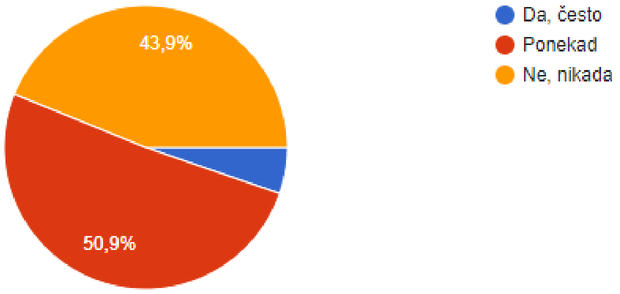

Chart. 17

When it comes to visiting the park during “The Ice Forest“ ice rink, a little over half of the respondents (50,9%) answered that they sometimes visit it, while a significant number of them never come to the park during the winter period when the event is held.

18.

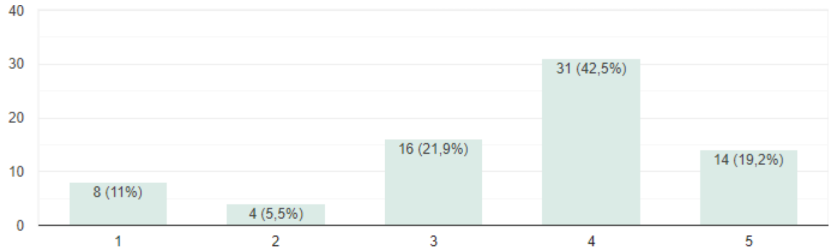

Chart. 18

As for the aesthetics of the park during the “The Ice Forest“, which was assessed only by those who visit the park during that time, it received diverse ratings, but mostly with a rating of 4. Therefore, it can be said that respondents are generally satisfied with how the park looks during “The Ice Forest“.

19.

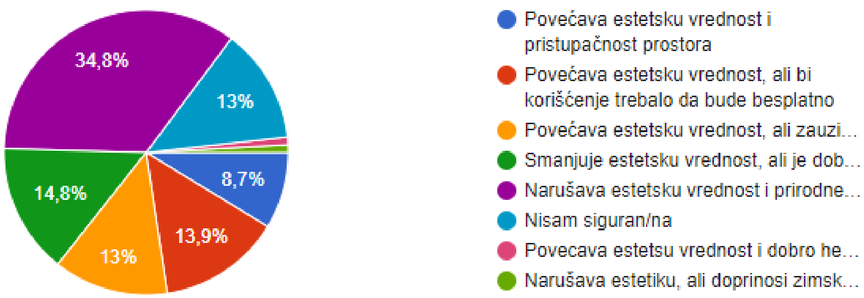

Chart. 19

The majority of respondents (34,8%) answered that following elements (ice rink, stalls, and accompanying equipment) negatively affect the aesthetic value and natural elements of the park, making it difficult to move around. A slightly smaller number believe that the aesthetic value decreases but that the park is a good location for the ice rink. The number of those who believe that the aesthetic value increases but the ice rink takes up a large area, as well as those who believe that usage should be free, is equal to the number of those who did not provide an opinion on this matter.

4.2. ANALYSIS OF RESULTS

Based on the obtained responses, it can be concluded that a part of Novi Sad's residents (115 surveyed individuals) consider the change in the function of the analyzed public spaces as a positive intervention due to the introduction of new content and activities in the city. However, the way in which these changes are implemented has not generally received a positive response. It appears that people place a higher importance on their involvement in decision-making and the presence of diverse activities rather than the physical appearance and practical use of these spaces.

Regarding the Liberation Square, the most common association was with the monument to Svetozar Miletić, a well-known landmark and a place where many people arrange to meet. During regular use, the square is primarily seen as a part of the route through the city center. However, during the winter months (New Year's festivities), a significant number of residents choose the square as their destination in the city center, where it becomes a stopping point for spending a certain amount of time.

On the other hand, whether due to its location or underdeveloped habits related to spending time in nature, the Danube Park remains less visited compared to the square, despite its primary function as a place for nature, greenery, and relaxation. Regarding the winter amusement park "The Ice Forest", reactions were mostly negative, although less than expected. Opinions are divided – some believe that the ice rink must not take place in the park as it occupies a large area, makes movement through the park difficult, and disrupts the natural ambiance. However, many do not have aesthetic issues with "The Ice Forest" and see it as an appealing attraction for both adults and children, contributing to the New Year's atmosphere. The only criticism observed relates to the admission fee, as many feel that usage should be free since it is a public space, accessible for everyone.

The research thus demonstrates that people value having events and activities in the city, regardless of the potential aesthetic or functional impact on the existing urban landscape. This means that citizens themselves, as users of the space, sometimes inadvertently act counter to their own interests and the broader goal of preserving and enhancing the urban environment.

5. CONCLUSION

When considering the situation regarding the possibility of organizing various events in cities, it becomes evident that at the present moment, there is less emphasis on promoting values in the interest of all stakeholders (both city officials and citizens). Due to the lack of cultural activities, stemming from neglected cultural values, urban environments change, and public spaces are modified, often using superficial criteria that disregard those that were valid in the past.

Entertainment and recreation have always been essential aspects of city life. From ancient times to the present day, outdoor activities have been designed for people to spend their leisure time. However, the approach to adapting urban environments to different functions has changed over time.

"We are bored in the city, there is no more Temple of the Sun", stated Gilles Ivain, using this sentence as a starting point for his Situationist ideas and views in the preface to the New Urbanism. What is boredom, and is it possible, considering the emergence and development of cities, that it exists as a part of urban life? The first association with the word *city* is certainly not stagnation and monotony but rather speed, congestion, sounds, and life. The Situationists believed that boredom was the price we paid for living in a world where *"darkness and obscurity have been driven away by artificial*

lighting, and the seasons are air-conditioned“[5]. However, today it seems that boredom is driving greater demand for “instant“ culture, with its consumers becoming more numerous and louder, seeking easily accessible entertainment.
According to modern urban theory and practice, the understanding and planning of a city are defined as the result and synthesis of all human activities in space and the life processes of the community in constant change [5]. Using a more open interpretation, this means that there is a constant cause-and-effect relationship between the city (space) and the community developing in that space.
According to the conducted survey, entertainment happenings such as New Year's concerts and “The Ice Forest“ are needed in the city, and the citizens (the audience) positively assess the organization of such events. However, from the responses can be concluded that the choice of the event location is worthy of broader discussion involving a larger number of citizens. This could consider other locations where the “The Ice Forest“ atmosphere could be recreated, utilizing the potential of craftsmen and artists, while preserving the ambiance of the Danube Park, a natural monument and a true oasis. Even New Year's concerts could be moved from the city center to some underutilized venues.
Architecture should put itself in the middle of the public debate of space. Space accommodates current and future political, economic, and societal demands. Architecture can facilitate the convergence of this debate and bring it to reality. Architects can actively visualize this process and comment it [10].
Critical theory has to be communicated in its own language – the language of contradiction, dialectical in form as well as i n content: the language of the critique of the totality, of the critique of history. Not a negation of style, but the style of negation [4].

REFERENCES

[1] Adler, F. (1956). The value concept in sociology. *American Journal of Sociology*, Volume 62(3), pp. 272-279. https://www.jstor.org/stable/2772921

[2] Benjamin, W. (1974). *Eseji*. Nolit, Beograd.

[3] Bourdieu, P. (1984). Dinsticion: A Social Critique of the Judgement of Taste. Harvard Press, Cambridge.

[4] Debord, G. (1995). *Society of the Spectacle*. Zone Books, New York.

[5] Grozdanić, M. (2006). Savremeni koncept urbanog razvoja i kontekst u R. Bogdanović, *Urbani dizajn*. Društvo urbanista Beograda, Beograd.

[6] Hillier, B. (1984). The Social Logic of Space u J. Sauser, *Measuring the Social Experience of Urban Spaces*. Cambridge University Press, Cambridge.

[7] Joachim Åström (2020). Participatory Urban Planning: What Would Make Planners Trust the Citizens? *Urban Planning*, Volume 5(2), pp. 84–93.
https://doi.org/10.17645/up.v5i2.3021

[8] Lefebvre, H. (1991). *The Production of Space*. Blackwell Publishing, Ltd., Oxford.

[9] Mirosavljević, J. (1995). *Novi Sad - Atlas ulica*. Prometej, Novi Sad.

[10] MVRDV. (2005). *KM3: Excurions on Capacity*. ActarD, Inc., New York.

[11] Pantić, D. (2005). *Da li su vrednosti bivših komunističkih zemalja slične?*. Zbornik Matice srpske za društvene nauke, Novi Sad.

[5] Ivan Chtcheglov, most known as Gilles Ivain

NOVI PAZAR CITY CENTER`S DETAILED URBAN PLAN FROM 1968. SEEN AS A STAGE

Enis Hasanbegović[1],Melisa Alcan[2], Lejla Zećirović[3], Branko Slavković[4], Džemila Beganović[5]

Summary:

Through this paper, we`ll try to expound the detailed urban plan of the Novi Pazar city center, which dates back in 1968, as an attractor of events that creates an illuminated open stage that awaits the unfolding of a drama, in which the observer becomes a participant who engages all his senses. Further, we`ll explain the inseparble connection of the scenic potential with the city space. In certain segments of the paper, the relationship between the spectacle and the city will be examined, like the issues of the city's spatial framework intended for that very spectacle as well. The goal of this paper is to find a new approach in the observation process of urban plans, as well as a peculiar call to respect the already existing architectural scenario. Looking at the urban plan as a scenic area - myriad of possibilities open up, both functional and aesthetic, both for the architect (director), and for the residents (spectators), who are also the protagonists at the same time.

Key words: stage, urban plan, scene, Novi Pazar, spectacle, city

[1] PhD student, M.Arch, Assistant, State University of Novi Pazar, Novi Pazar, Serbia, ehasanbegovic@np.ac.rs
[2] PhD student, M.Arch, Assistant, State University of Novi Pazar, Novi Pazar, Serbia, malcan@np.ac.rs
[3] PhD student, M.Arch, Assistant, State University of Novi Pazar, Novi Pazar, Serbia, lzecirovic@np.ac.rs
[4] PhD Assistant professor, State University of Novi Pazar, Novi Pazar, Serbia, bslavkovic@np.ac.rs
[5] PhD Assistant professor, State University of Novi Pazar, Novi Pazar, Serbia, dzbeganovic@np.ac.rs

1. INTRODUCTION

Interpreting the meaning and significance of urban theatricalization, D. Konstantinovic and M. Zekovic (2011) provide a crucial definition: "The emergence of theater onto the streets, into the city, sought new stimuli that new environments brought. This process is not an isolated phenomenon of modern cities but a result of the desire to explore new spaces and investigate their scenic potential, as well as the aspiration for unhindered communication and the intention to engage ordinary citizens as the audience. The demystification of theatrical play by placing it within familiar urban contexts is just one form of new theatrical action. Simultaneously, there is a general theatricalization of various aspects of urban life, serving various socio-economic needs of the moment. Regardless of the reasons for these changes, this process has irreversibly altered the function of the theater building, permanently shifting the play beyond the boundaries of its constructed structure."This implies that the space for play, as a space of presentation, can be any environment within the city, whether planned for it or exploited for the purpose of artistic presentation [1][1].

Experiencing urban space also demands the ability for scenographic perception of the city[2]. As explained by Tajtana Dadic Dinulovic in her work, paraphrasing Roland Barthes, the city can only be semantically approached by viewing it as a structure and an abundance of offered signs, without attempting to fill the structure with definitive meanings, or, more precisely: "With every cultural or psychological complex, we find ourselves facing endless metaphorical chains, whose meanings are always different. [3]"

Thus, this work not only explores the relationship between urban planning and theatricality in general but also specifically analyzes the urban project of Novi Pazar from 1968, shedding light on it in terms of theatricalization. This project will be regarded as a stage for the performance, consciously or unconsciously designed by architects, for the display of events.

William Shakespeare writes: "All the world's a stage, and all the men and women merely players: They have their exits and their entrances, And one man in his time plays many parts... [4]“

Therefore, through this work, I will attempt to read the urban plan of the center of Novi Pazar, a city in southern Serbia with a population of over one hundred and twenty thousand, as an attractor of events that creates an illuminated and open stage awaiting the unfolding of a drama, where the observer becomes a participant engaging all the senses. Additionally, this work will explain the inseparable connection between scenic potential and urban space. In various segments of the text, we will consider the relationship between spectacle and the city, as well as questions related to urban spatial frameworks intended for spectacle.

The aim of this work is to find a new approach to the observation of urban plans and to call for the appreciation of the existing architectural scenario. By viewing the urban plan as a scenic space, numerous possibilities, both functional and aesthetic, open up for the architect, i.e., director, as well as for the viewers, i.e., residents.

2. THE STAGE OF NOVI PAZAR (DETAILED URBAN PLAN OF THE CITY CENTER OF NOVI PAZAR)

In an attempt to redefine architecture, B. Zevi distances himself from art and the images of bygone eras, focusing on architecture as a stage: "Above all, it is a framework, a stage on which our life unfolds.[5]“

---

[1] Paraphrased, Danilo Dragović in his text "City, Spectacle, Identity: The Stage and Semantic Variability of the City,"

This stage can be defined as the one that broadcasts intriguing scenes from the „grand performance.[5]“ It is the stage through which we experience the spectacle. After World War II, architects, including protagonists, directors, stage designers, inspectors, and virtuosos of this project, Amir Corovic and Toma Milovanovic, endeavored to create the grand stage. These two architects founded the Institute of Urban Planning in 1963, along with the later-established design bureau "Sandzakprojekt," which became the leading institution for the architectural and urban development of Novi Pazar and its surroundings. This project departed from the previous linear structure and made a sharp break from traditional construction. Work on the project for the city center began in 1965 and lasted until 1968 (see Figure 1).

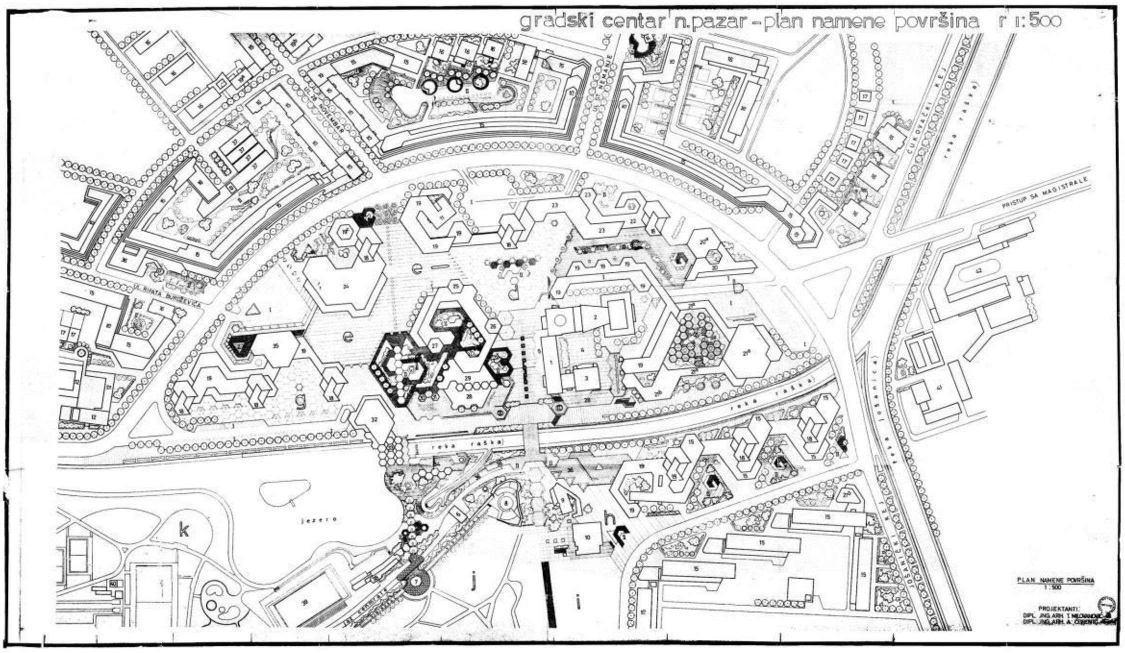

Fig. 1 Area plan of the city center of Novi Pazar, 1968.

Observing this plan, we notice that the design began with the historical core of Novi Pazar's fortress, known as the "old watchtower," specifically one of its three bastions—the northern bastion. This particular bastion served as a kind of center where a six-pointed star was fixed, and a circle was then described, outlining the framework of the newly designed central core of the city, which now serves as our main stage (see Figure 1 and 4).

AVNOJ Street tangentially surrounds the entire pedestrian zone, transforming it into a stage on one side, while on the other side, there are arc-shaped residential blocks, now serving as auditoriums, through their form, facades, and position in relation to the stage. AVNOJ Street itself will be the fourth wall of the theater, separating the audience from the actors. Behind the arc-shaped buildings, multi-family and single-family housing is planned, while in front, the center with all its public institutions is situated, with the arc-shaped buildings enclosing it, preventing its expansion to the north. This street collects and terminates all the radial street directions of the city, those leading toward the main stage (Figures 2 and 4).

"The life of the city has two aspects—one is public and social, where everything unfolds in the open and intertwines. This is the life of streets and squares, large parks and public spaces, and the lively activities and bustle of commercial districts... There is also another aspect of life in the city—private and withdrawn from the world, personal, secluded, life centered on the individual, seeking peace, shelter, and seclusion. [6]“

Expanding upon the earlier quote, when discussing this project, it is impossible to overlook its main criticism, specifically that the arc-shaped buildings undeniably segregate the city into public and private, lifeless and vibrant segments. Designed with terraces, numerous loggias, and balconies facing the city center, these arc-shaped buildings in shape and form resemble the tiers of an arena, with the front rows predictably reserved for wealthier citizens. In both their form, materialization, and function, these arc-shaped residential buildings imitate the Novi Pazar fortress, more precisely, the bastion. (Figure 2 and 3).

Fig. 2 Arc-shaped residential buildings

Fig. 3 The bastion of Novi Pazar fortress

Consequently, if we regard this highly theatrical project as an expansive stage, we can observe that all the "spotlights" are directed toward the historical core, (Figure 3) , which we now perceive as the principal actor on the stage, capable of delivering its monologue while the rest of the city slumbers. Conversely, the arc-shaped buildings rise (Figure 2), as the fourth imposing wall of the stage, with their residents forming the audience who react to events in the squares and scenes by venturing out onto their loggias and balconies.

Deeper scrutiny and analysis of the project as a theatrical scene, quite literally, enable us to perceive the space enclosed by the arc-shaped buildings to the River Raska as a space replete with squares that function as scenes. During major events, spectacles, and happenings, these squares collectively serve as a magnificent and diverse stage for performances.

3. SCENES IN THE PEDESTRIAN ZONE

It is not only in the theater that the audience feels that the actors are larger than life. This is also a characteristic illusion created by the city, as the urban center is, in fact, a theater [7].

The conditions of urban space are diverse, ranging from ambient values to physical characteristics, and extending to social and cultural usage patterns of the city and urban environments. In terms of the physical characteristics of the city, places where artistic expression is most frequently manifested are squares, streets, and parks, where different forms of expression occur depending on the character and ambiance. Today, the design of urban space is approached from an interdisciplinary perspective, aiming to connect various scales of physical structure and disciplines, all with the goal of improving urban life.[2]

A prominently observable characteristic of the focal "stage" is the interconnectedness of its scenes or squares; differentiation is achieved through various pavements and levels. The transformation of the city into a stage begins at the bus station (Square B), where the visitor automatically becomes a participant in the scene upon arrival and the first step. The bus station itself is a reservoir of highly emotive scenes, making it quite spectacular because it is precisely on such squares that we can witness various life performances, including numerous farewells, as well as reunions and reconciliations (Figure 4).

[2] Danilović-Hrastić N., Vukotić-Lazar, M., AU34/2012, contemporary art in the public-political space.

This square borders the circular traffic road to the east and connects to the market square (Square A) to the west, where equally emotional and bustling scenes of bargaining, selecting, and touching the textures and colors of fruits and vegetables take place. You can hear the loud vendors, a constant presence in this scene. This vibrant scene is, in fact, an open market resolved in the form of a large atrium among the market buildings. It has an irregular hexagonal shape in a modular network, open to numerous passages through the market buildings or under wider pergolas. Stalls, each with its miniature scenography, are shaped and arranged in a modular network on the market square.

From the market square, there is a sudden transition to the somewhat cooler postal square (Square C), where the main post office, the district court, and various business premises are located. It is connected to the municipal or administrative square (Square D), whose central position designates it as the main gathering place. The actors on this square are young lovers who nervously meet there, clerks running late for work with a pastry in hand, revelers who do not notice the transition from night to morning, musicians, animators, performance artists, and more.

From the market square, there is a sudden transition to the somewhat cooler postal square (Square C), where the main post office, the district court, and various business premises are located. It is connected to the municipal or administrative square (Square D), whose central position designates it as the main gathering place. The actors on this square are young lovers who nervously meet there, clerks running late for work with a pastry in hand, revelers who do not notice the transition from night to morning, musicians, animators, performance artists, and more.

Apart from the pavement, the postal and municipal squares are also separated vertically by a one-meter difference in height. This difference is overcome by a staircase interspersed with six seating platforms, each of them with a regular hexagonal shape and an area of 1.5 modules (which will be discussed later), functioning as mini chamber scenes for 8-10 participants, mostly high school students, who gather there at precisely the same time every school day to share their impressions (Figure 8).

Continuing our journey, we arrive at the cultural square, which consists of the Culture

Continuing our journey, we arrive at the cultural square, which comprises the Culture Centre, an open-air stage, and the Workers' University (the current municipality building). Across from the Culture Centre, there is Bezistan (Square F), where Amir-agin han has been preserved, a legendary scene that has continued to exist since the founding of Novi Pazar. On this square, several buildings have been designed: the museum, library, reading room, exhibition gallery, and clubs for various social organizations, including engineers, technicians, medical professionals, educators, and more.

Bezistan intentionally has the lowest plateau compared to other squares. Through its materialization, position, and content, it was intended to represent the most interesting and aesthetically arranged corner of the overall scene. This plateau has been vividly designed in a modular network. The objects on it offer extremely scenic views through the courtyards' passages of the museum building, towards all parts of the square, facilitated by its central position. Additionally, numerous terraces on the buildings located in Bezistan face south and overlook the river, the watchtower, and the old bazaar with the fortress.

To the west of Bezistan, we encounter the strictly commercial square (Square E), where the Beogradjanka department store (now Maxi) and numerous small retail shops have emerged. Here, we witness almost a television production of organized shopping scenes and casual snacks, with costumes featuring branded suits, dresses, and high heels.

On this somewhat futuristic set, along the left bank of the River Raska, stretches Freedom Square, which widens toward the lake and Vrbak island, Tvrđava city park, and the recreation center – the main green areas in the city center.

The park's greenery in the very center of the city is complemented by the vertical blooming of space; specifically, every window and balcony on the arc-shaped building has planters with soil that bring vitality to the monumentality and uniformity of the building.

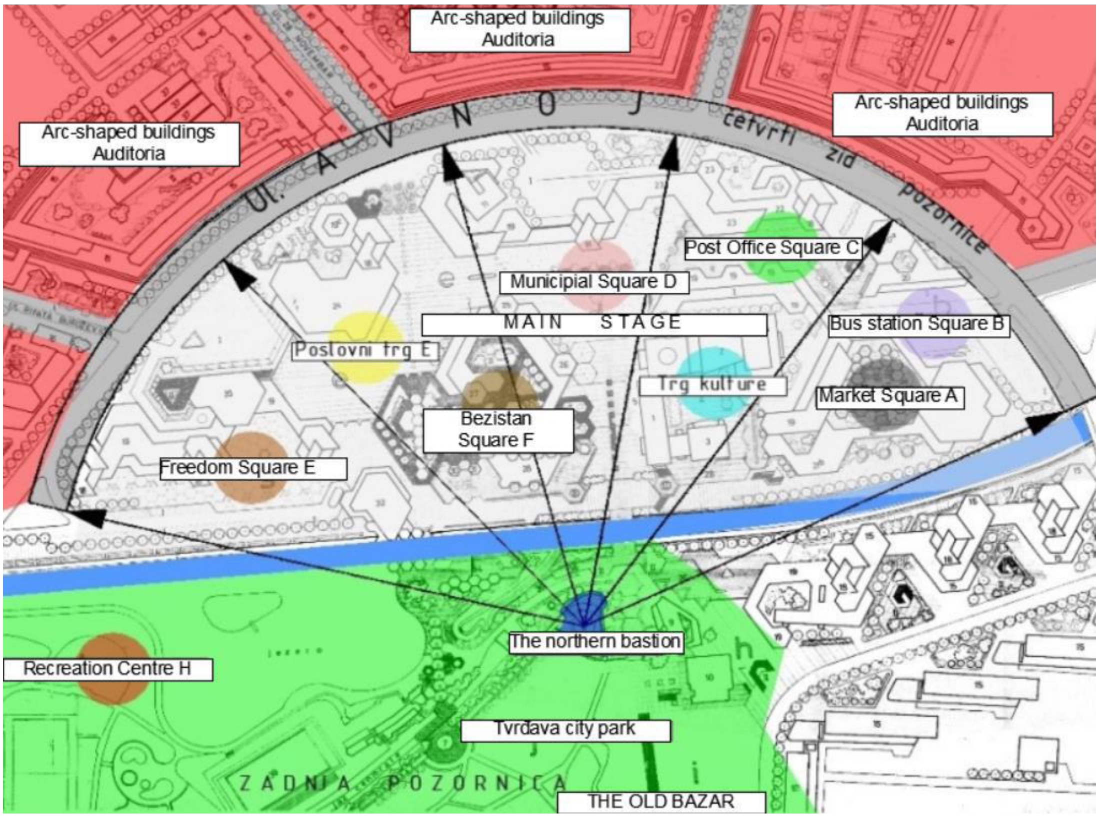

Fig. 4 Schematic Representation of the City/Stage

The most tragic character in this historical drama was the weeping willow tree near the hotel, after which the Hotel Vrbak was named. We can easily regard it as the narrator of all city stories because, by staying in the same place for many years, it accumulated the energy, tradition, and narratives that unfolded in this area. Despite all these and clearly decorative reasons, it was planned to keep the tree - although relocated to the Flower Square (Bezistan). Unfortunately, the new scenographers of this space decided that future performances on the city stage would take place without a narrator, and therefore, without memories.

In addition to all the mentioned scenes that rapidly change, there are many smaller ones that have not been mentioned but can be viewed as intimate stages and mini-stages, such as numerous rest areas in the form of semicircular plazas, fountains, Vrbak hotel bridge, Vrbak hotel terrace, and more.

Going south from River Raska, like a backdrop, lies the old bazaar with a hammam and Novi Pazar fortress, which towers over the newly designed pedestrian realm and, together with the viewpoint, the watchtower, Altun Alem Mosque, and Arap Mosque, create an ambient theater that "utilizes the city as a stage, as a scene that no one will need to construct and reconstruct because it already exists much more adequately than any subsequently designed simulation of reality. [8]“

4. MISE EN SCÈNE AND VISIBILITY OF THE STAGE

The shaping of the identity of the contemporary city is largely determined by the observer's position and how people experience the city. Thus, every city is characterized by multiple identities that define and shape the city's character, culture, and „personality.“ These identities vary depending on whether we perceive the city as a street, neighborhood, center, or part of a region, or as a collection of positive and negative experiences held by an individual or a community.[2].

For a city to be truly experienced, it is necessary, above all, for the observer to actively participate in urban life. Indeed, movement through urban space determines how we perceive it and the extent to which we evaluate its quality. One of the fundamental elements of urban life is the activity of its residents or the specific "choreography of the city." However, the influence of urban space on its "readers" cannot be easily determined or generalized because it is not about a homogeneous mass but a group of individuals who use urban space, experience it, and then interpret it. These individuals are, like the audience in a theater, simultaneously both individual and a collective entity; "the audience, for whom the actor performs in the theater, although an individual, is by definition a collective phenomenon. [2]“

The architects of this project, while constructing the "stage" and scenography, also directed the mise-en-scène, which they referred to as pedestrian promenades (1, 2, 3, 4, 5, and 6). The pedestrian promenades (see Image 6) ensured visibility of the stage from any seat in the theater so that everyone in the audience could see all the events and scenography on this vast stage.

Each promenade had a different pavement compared to the rest of the squares they passed through, and this distinctive pavement guided pedestrians to follow a specific path, making it easier for them to traverse the entire stage. In this movement, pedestrians had the opportunity to experience views of all parts of the stage and beyond it.

The pedestrian, in this context, is a participant on the stage. The journey begins at the bus station (pedestrian promenade 1) located to the east, where they leave their belongings at the station square, and then proceed parallel to the River Raska towards the west, ultimately reaching the commercial square (E), which serves as the endpoint of this promenade, along with the National Bank (Figure 5 and 6).

The Commercial Square with Fortress Park connects to Promenade 2 (Figure 5 and 6) in a straight line to the Watch Tower (where the crosswalk Vidikovac is located, connecting two bastions in the park), passing over the bridge of the Hotel Vrbak, which, with its form and position, represents a unique scene.

On the path of Promenade 1, squares are lined up on both the left and right sides. After the station square on the left side, there is the marketplace square, and on the right, the postal square with the main post office building. Halfway through its route, Promenade 1 intersects with Promenade 3, which goes over the Culture Square and the bridge over River Raska, then continues along 1. May Street towards the old bazaar. It is precisely at the junction of these two promenades that the wide municipal square is situated. Other squares near the municipal square are closely connected to it, so they can serve as its expansion in case of event-related needs.

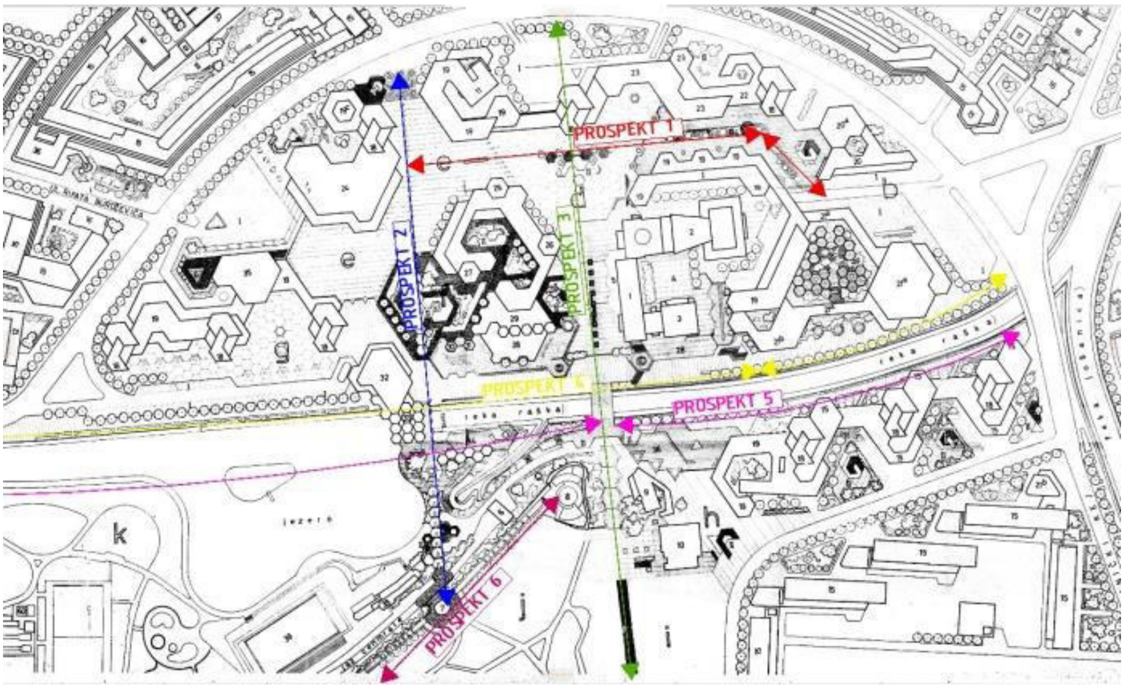

Fig. 5 – Pedestrian Promenades

The last two promenades serve as the primary pedestrian links between the two halves of the city center on both banks of the River Raska. They intersect both banks of the River Raska at the river's height, which is also parallel to the first station promenade (Figure 5 and 6).

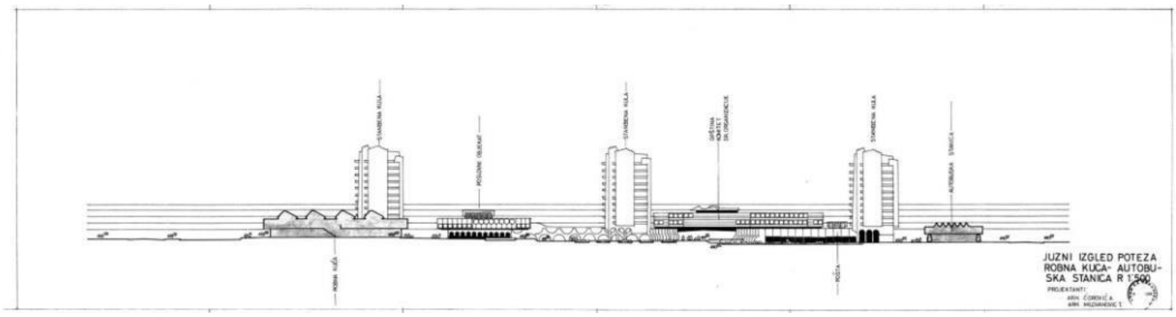

Fig. 6 – Pedestrian Promenade 1 - Section

The left bank of the River Raska connects the station and marketplace squares, the Culture Square, Bezistan, and the Hotel Square on its southern side, extending further to the Parice Quay at the western end of the center.

On the right bank of the River Raska, to the east, it starts from the Josanica River, runs along the residential and commercial block "Pothamam," proceeds along the bastion and the power plant, and enters the recreational center, where it branches out in four directions.

The sixth promenade is the Vidikovac promenade, corresponding to the rear stage or hinterba. This "stage" is the highest point in the center and serves, among other things, as a viewpoint for city observation, presenting another ambivalent space within the city.

The entire southern part of the city center, located south of the river (with higher elevation than the northern part), forms the "overstage" of this stage.

It is noticeable that this orthogonal scheme is oriented toward the most important actors of this scene, including the River Raska, the Bastion, Hotel Vrbak, the Watch Tower, as well as 1. May Street, i.e., the old bazaar.

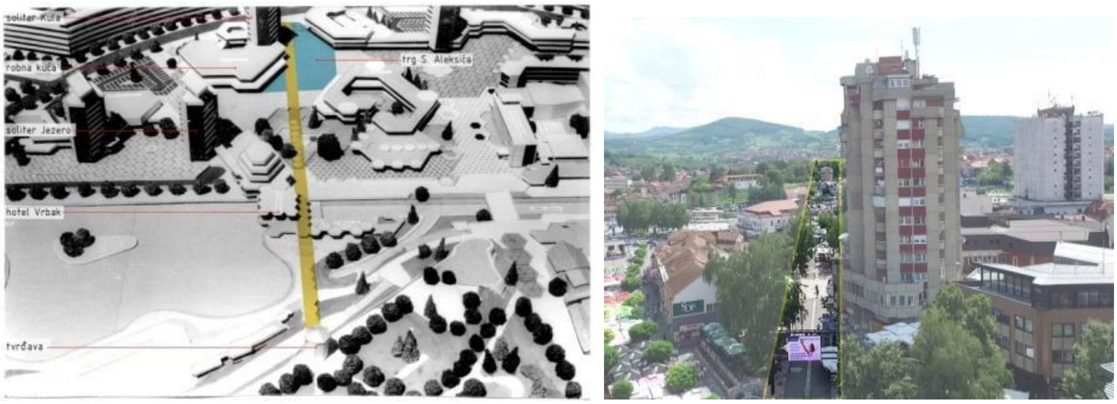

Fig. 7 – Pedestrian Promenade 2

In addition to the imposed movement and cleverly designed vistas, which establish the functional framework of the center, numerous secondary pedestrian pathways aim to immerse participants (i.e., residents) in a labyrinthine layout, guiding them through various passages. This approach places participants in a specific interactive state, where they constantly explore what lies around the next corner.

The plan included rows of red chestnut trees along the streets and squares. Even in the selection of these trees, the importance of vistas for the concept of this urban plan is evident. The crown of the red chestnut tree is of medium size, allowing for unobstructed views within the central complex and beyond. Additionally, rows of deciduous maples, catalpas, silver linden trees, large-leaved linden trees, silver spruces, shaped yews, and junipers were planned [9]. All the greenery had both ecological and decorative functions, outlining and emphasizing the highlighted vistas.

Fig. 8 – Urban furniture as mini chamber scenes on stage

5. POLYGONAL

In the development of the detailed urban plan for Novi Pazar, one of the essential elements of sound urban design is the establishment of clearly defined vistas, as discussed in the previous chapter.

For this reason, a polygonal geometric modular scheme for the city center was created. The primary modular scheme, which provides the dimensions of the center's buildings and plazas, is based on a network with the basic element being an equilateral triangle with a height of 6 meters. The base of the triangle runs from east to west, parallel to River Raska.

You might wonder why this particular module was adopted. The base of the triangle, functioning in the east-west direction, and the height, functioning in the north-south direction, align well with the orthogonal scheme of the main pedestrian promenades in the city center. These promenades include the station - department store, department store - tower in the park, station - Melaj Mosque, municipality - Altun Alem Mosque, as

well as vistas along River Raska promenade and through 1 May Street. The other two sides of this triangle roughly follow several main radial streets and directions in the city: Stevana Nemanje Street, 28. Novembar Street, Josanica Quay, and Cukovac Quay (see Image 1). This choice of module ensures and diversifies vistas [9].
Additionally, this module provides a hexagonal grid with a spacing of 6 meters, which offers rational structural spans for various types of buildings. In this grid, a regular hexagon, whose side is equal to the side of the equilateral triangle (6.928 meters), with an area of 20.78 square meters [9] , appears as a secondary module. This creates a hexagonal grid for the center, expanding the possibilities for shaping the dimensions of buildings and plazas.
The dimensions obtained in this way harmoniously interact with the dimensions of the city walls and the Watch Tower, creating a delicate continuity between the old and the new. All volumes of buildings and plazas are given in a combination of triangular and hexagonal schemes, resulting in lively, scenic, interesting, and sculptural forms of dimensions. This module was also applied to the facades of some buildings (e.g., the business premises of Novi Pazar Branch of Belgrade United Bank, 1970) designed by this duo (Figure 9).

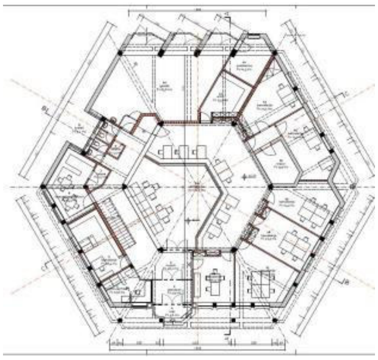


Fig. 9 The business premises of Novi Pazar Branch of Belgrade United Bank, 1970

Not only was it later used on facades, but this entertaining module was also employed to define the vertical playfulness of plazas and the buildings on them.
Besides the leveling differences as a secondary plastic element, these famous plazas also differ in terms of third-order spatial plasticity, or surface treatments.
For example, market and pedestrian areas were adorned with noble materials according to the importance of the square [9].
In addition to very scenic paving, all squares were designed with urban appliances such as fountains, channels, flowerbeds, pots, and vases, as well as staircases and benches, transforming public space into an open sculpture gallery (Figure 8).

6. PERMANENT PERFORMERS AND MAIN STARS ON THE STAGE

6.1. HOTEL VRBAK

While we perform live on this stage, it is impossible not to notice the main actors, leading roles, and stars of this scene. Besides the mentioned City Wall (Bedem), the unquestionable star is the Hotel Vrbak (Figure 10). With its unusual spatial and architectural structure [10], captivating presence, artistic and sculptural qualities, and attractive location on the main city square, this building has earned its position as the most essential element in constructing the visual and symbolic identity of the contemporary urban core of Novi Pazar.
Milan Popadic, in his text „How to Read a City" [10] , analyzes the architecture of Vrbak and paraphrases Charles Jencks, who posits that in contrast to multivalent architecture, which emphasizes the existence of many levels of meaning and complex

values, there is univalent architecture characterized by a simple accumulation of elements or parts. Popadic suggests that the architecture of Vrbak could be analyzed from both of these perspectives: „Its meanings are so numerous that they are simply very difficult to read or overloaded to illegibility. In a simplified interpretation, Vrbak's visual identity could be structured on several levels: synthetic tradition, which could parallel '1001 Nights' in literature, uncritical hybridity, and camp aesthetics, as an urban pastoral, as Susan Sontag would put it. In this triangle, or triad, of pseudo-tradition, hybridity, and camp, Hotel Vrbak is both a manifestation and materialization of the desire and will for 'otherness.' Certainly, unless it's something else. [10]"

Viewed as camp architecture, Hotel Vrbak suddenly becomes much clearer, more intelligible, and communicative, especially when we consider that camp is a form of historicism seen theatrically. The oscillation between the magnificent and the comical, broad gestures, a challenge to conventionality, arrogance, and other camp tendencies are aspects of camp architecture recognizable in Vrbak. Additionally, it is now possible to find explanations for the most problematic elements, such as the monumental dome of the accommodation part of the building. The camp stance on Vrbak's colonnade is straightforward, while we can speculate that the semantic interpretation might suggest that the hyperboloid shape of the columns (Figure 10) represents ecstatic dervishes, gnawed apples, or spinal columns, among other possibilities [11].

6.2. KULA MOTRILJA: WATCH TOWER

The most scenic sight is the staircase leading to Watch Tower itself, (Figure 10) which gathers all views from the main stage. This staircase starts from Vrbak, at an elevation of 493 meters over an earthen dam, and ascends to the tower at an elevation of 503 meters. A height difference of 10 meters is overcome with about ten step-like platforms of a hexagonal shape. Along this axis, there is a tiered water surface planned, where water flows from the gap into the fountain on Vrbak Island. From there, this water is channeled through ditches or underground pipes to the river on the left bank, starting from Bezistan, and from there, it flows to the other squares towards the municipal square. The tower in the park and the promenade connect two ramparts (which also have a semicircular shape and are often used as summer stages and viewpoints) serving as the highest points, and the canopies have an ambivalent role as an audience and a stage. The pedestrian paths branch off to the left and right from this staircase, with the right side leading to the recreational center and the left side passing by the electric plant to the craft bazaar. From this staircase, the waterfalls of the electric plant can be clearly seen, further enhancing the attractiveness/scenic quality of this pedestrian avenue. Each stepped platform, like other platforms on the squares that overcome level differences, is enriched with flower pots, flowers, and benches for sitting and viewing [11].

Fig. 10 Hotel Vrbak and colonnade of hyperboloid columns

Fig. 11 - Watch Tower

7. SCENE DESTROYERS AND THE ABSURDIST DRAMA

After the construction of the first phase of the Novi Pazar center, this urban plan, in its initial phase, was taken over by other architects whose aspirations leaned towards the theater of the absurd. The new protagonists of this scene, along with the claque[3] and less-educated prompters, continue to act and encore uninvited.

Unfortunately, to this day, only two-thirds of the mentioned project has been built, and instead of completing the story, entirely new objects (mostly residential) have been introduced that do not communicate in any way with the rest of the plan; on the contrary, they are completely disconnected from it. Without a sense of scenography and the dynamics of the city, these new architects, mostly politically biased, have blocked almost all the views that were carefully planned before. Thus, most of the scenes in the city are now fenced off, and life „performances" take place under the same veil of secrecy under which such projects are approved and sponsored.

Fig.12 Illustration of N. Pazar, F. Hajdinović

Fig.13 Blemish on the urban fabric

Failing to grasp the depth of Tomo and Amir's idea to create a unique urban plan with a strong sense of the city's heritage using a triangular and hexagonal modular network, the architectural political milieu that followed rejected all aesthetic norms (but not in a good way) and focused purely on the capitalist value of the objects. This means that objects are built using the offset technique in relation to the plot, without considering either the previous modular network or the future one.

In an effort to profit as much as possible from each square meter, various protuberances and gaffes appear on the objects. For the latest example, one only needs to look at the newly emerged blemish on the urban fabric of Novi Pazar (Figure 13) , right in front of the Vrbak Hotel. Even to complete amateurs, it is clear how this object is in complete contrast (again, not in a good way) in terms of form, style, and function compared to the object that was once a symbol of the city, but also compared to the entire surrounding area. This cube in front of the hotel partially blocks the passage from the square to the Parice Quay and is built illegally on the plot of the city square. The Vrbak colonnade (Figure 14) has been demolished, and instead of the recessed part of the ground floor of the accommodation part of Vrbak, there are business premises that will never be read as an integral part of Vrbak, on the contrary.

Right across from Vrbak is the largest architectural transformer in the city. The building of the Islamic religious community, formerly Grmija department store and now the Islamic Faculty building, has expanded and continues to expand to the detriment of the main square. Namely, the part of the building that serves as a restaurant extends onto Isa Beg Ishakovic Square with its terrace.

[3] Klaka (from French "claque" - slap): Paid support through applause (and sometimes shouts like "bravo" or "encore") in the theater. A paid group of the audience that, on command, supports specific performers or plays in the theater. Claqueurs can also be helpful - they train inexperienced audience members when to applaud without disrupting the performance.

Fig.14 Business premises replaced the Vrbak colonnade, 1999 - 2020

This, by itself, would not be so problematic if, every year, the terrace were not covered, becoming a closed part of the building, while at the same time, a new terrace is formed, occupying a new part of the square. With this move, unimpeded by anything, the Islamic Faculty building is moving deeper into the square, consuming the most public space in the city.

However, when viewed from the perspective of the 1968 urban plan, the most detrimental aspect of this intervention is that the illegally constructed object intersects with Prospect 2 and obstructs the view of the Watch Tower. Moreover, just beneath the tower, residential houses have been erected, further obscuring the tower's visibility. The tower now timidly peeks out behind houses whose yards are often occupied by livestock, resulting in a transformation of the city center into a village (Figure 15).

Fig.15 A view of the Watch Tower today; The Islamic Faculty building

Lejlek and Melaj's Mosque are now entirely concealed behind oversized residential buildings that exceed the legally permitted height. All the meticulously selected pavement has been replaced, and the squares have been surfaced with new concrete pavers, chosen with an emphasis on maximizing material utilization and minimizing waste. On the "subscene," residential buildings with ground-floor commercial spaces now stand, completely obstructing the former stage.

These are just a few examples drawn from the portfolio of the new builders, and there will undoubtedly be many more. Much like an absurd drama, these new builders adhere to principles such as the instability of value, a lack of communication, irrationality, illogicality, and alienation – embodying the absurdity of existence.

Despite persistent efforts to dismantle the stage, numerous scenes continue to unfold in Novi Pazar, and the spectacle persists, unfolding and being experienced. A theatrical performance endures even in the absence of the demolished stage, echoing the sentiments of Tatjana Dadic Dinulovic in the conclusion of her work, "The Contemporary City as a Space of Spectacle: Stage or Scene." She writes, "The city today becomes a performance that cannot be said to ever end. Thus, this permanent theater, open to the 'audience' as well as to the participants, continuously unfolds throughout the entire day, featuring its own program that is not entirely anarchic, improvised, or entirely devoid of form." (...)[2].

If we follow the idea that „the theater represents every kind of visibility that, performed on stage, is applied and experienced by the viewer, or the audience“ [1], in Novi Pazar, now on narrow squares and streets lined with illegal construction that blocks all views, we can still experience and see scenes of children playing, street fights, young people walking, and old people chatting, who become extras or main actors in an endlessly long performance. Not only that, there are also various performances, festivals, and fairs, but also numerous protests against the authorities and the illegality of certain (not only) urban procedures; we can also experience other spectacles - familiar to this city.

In the example described by Tatjana Dadić Dinulović: if we give each visitor a small bell, with a small effort, we create the sound of seventy thousand bells, creating an incredible spectacle of sound. I recognize the spectacle that occurs in Gazi Isa-beg Ishaković Square[4], where every year, on the night of Laylat-Ul-Qadr5, thousands of people perform the night prayer[6].

As passive observers (if we can even be such in the face of such a spectacle), without religious involvement, we notice that with each synchronized ritual movement, „thousands of small bells“ can be „heard“, enriching the city and reminding its residents of the theatrical potential of this wounded space (Figure 16).


Fig. 16: Nighttime prayers at Isa Beg Ishakovic Square as a spectacle.

8. CONCLUSION

As mentioned in the introduction, the scenic potential of the city and the desire for unrestricted communication are closely intertwined. The need for communication is not one-sided; it does not solely originate from an architect desiring to connect with the audience but also from the viewers or residents seeking to engage in a dialogue with architectural elements individually and with entire urban plans. The project conceived and partially realized by Amir Corovic and Toma Milovanovic aimed at fostering open dialogue and transparency between the stage and the audience. Respecting key elements of the city, such as the ramparts, Watch Tower, and Vrbak Hotel, was just one of the initial ways in which the architects conveyed to the residents that their voices were heard. Open and expansive vistas, along with diverse pavements in the squares, encouraged viewers to engage in discussions about past and future aesthetics while simultaneously inviting them to participate in new dramaturgy.

---

[4] It is usually prayed in squares and streets because all the mosques are too small to accommodate such a large number of worshippers on this special night.

[5] Laylat-Ul-Qadr, The night of Power, the holy night, more valuable than a thousand months; Muslims believe that this night should be spent in various forms of worship, such as reading and reciting the Quran, performing the night prayer, seeking forgiveness, and repentance.

[6] Namaz (Fiker – e- akhirat) is the Islamic ritual prayer that involves various bodily movements and recitations, including Quranic recitation. Namaz is prayed five times a day at specific times, while the mentioned nightly voluntary prayer, the „nafile“ namaz (*nafl, nafil, nawafil*), is performed on the eve of the twenty-seventh night of the month of Ramadan, in the third third of the night.

A simple change of architects reveals that the architectural scene is continually interlinked with society: the curtains have been lowered on many stages within the grand stage. This transformation can be observed on both sociological and behavioral levels in the city: segregation is on the rise, and opacity is cultivated as a virtue.

Nonetheless, this socio-economic shift does not extinguish the architectural theater with its off-set moments and the utilization of space. The stage still endures, albeit in a state of disrepair; it functions as long as people interact within it. The scenery and costumes of the city evolve, and with them, the roles played on the stage.

Just as in any congestion or blockage, in architecture, the closing of vistas, unlawful segregation, and the privatization of public spaces lead to the emergence of new assertive roles, including protests and engaged performances.

The lingering question is whether this severely wounded space can ever rejuvenate and once again provide participants with a comprehensive sensory experience.

REFERENCES

[1] Danilo Dragović (Autor poglavlja), Radivoje Dinulović, Velimir Savić (Urednici), Prostor u scenskoj umetnosti; Grad, spektakl, identitet: scenska i značenjska promenljivost grada, 2016, SCEN – Centar za scenski dizajn, arhitekturu i tehnologiju, OISTAT Centar Srbija, Departaman za arhitekturu i urbanizam, Fakultet tehničkih nauka Novi Sad, 90, ISBN 978-86-7892-879-6

[2] Tatjana Dadić Dinulović, (2010) "The Contemporary City as a Space of Spectacle: Stage or Scene," Singidunum University, Academy of Fine Arts, Beograd, Serbia no. 126-1, p. 84-93

[3] Bart R. (1973) according to Eco U., "Culture, Information, Communication," Nolit, Belgrade.0

[4] William Shakespeare, "As You Like It," Jacques (II, VII), 1938, Belgrade.

[5] B. Zevi, "Architecture and Space," edited by C. Norberg-Schulz in "Existence Space and Architecture," 1971, page 12.

[6] Laurens Halprin (1974) : "Cities," Construction Book, Belgrade.

[7] L.Mumford (1988), The City in History, Publisher: Naprijed, Zagreb, Croatia, p.70

[8] Milena Dragičević - Šešić, "The City as a Space of Spectacle."
http://www.scen.uns.ac.rs/wp-content/uploads/2017/11/Dragicevic-Sesic-M-grad-kao-prostor-spektakla.pdf

[9] T. Milovanović, A. Ćorović, Detailed Urban Plan of the City Center in Novi Pazar – Program Document, Institute for Urban Planning - Novi Pazar 1968.

[10] Milan Popadić, "How to Read the City," 2014, Belgrade.
https://bif.rs/2014/08/milan-popadic-kako-citati-grad/

[11] Milan Popadić (2007), "On the Architecture of the Hotel 'Vrbak' in Novi Pazar," Novopazarski zbornik no.30, Publisher: Muesum Ras, Novi Pazar, Serbia ISBN 0351-3017, UDK 930.(08).

INTERNATIONAL SCIENTIFIC CONFERENCE
INTEGRATION, NOVELTY, DESIGN,
INTERDISCIPLINARITY, SUSTAINABILITY

iNDiS2023

NISH STEEL BRIDGES ON NISHAVA

Hartmut Pasternak[1], Nataša Živaljević Luxor[2], Thomas Krausche[3]

Summary:

The Nišava River is one of several rivers in Nish however it is considered the most important one because it determines the primar axis of the city. It is fast river with strong and abundunt torrential waters. Therefore, possibilities for construction of bridges are limited. However, many bridges were built since the second half of the 20th century, as necessesary for the growth of the city, following arrangement of the river bed through the city and the construction of the dam upstream. Only four of bridges are made of steel: the fortress main gate bridge, two railway bridges and pedestrian bridge in Brzi Brod. They were all built in the 20th c and are continiously used. We briefly examined the design and the current state of the structure. These aspects are disscussed in the context of sustainability of steel bridges, maintainance and the higher education in this discipline.

Key words: Steel, bridges, sustainability, maintenance, higher education

[1] Full Professor, Brandenburg University of Technology, Cottbus, Germany, hartmut.pasternak@b-tu.de
[2] PhD, PE Institute for Urban Planning Nish, Serbia, natasa.zivaljevic@zurbnis.rs
[3] PhD, Engineering.Office IPP, Braunschweig and Cottbus, Germany, i-p-p@gmx.de

1. INTRODUCTION

The Nishava runs from East to the West and flows into South Morava, which runs almost precisely from South to the North, and their confluence is locted in the territory of the City of Niš, at its western border. The Nišava River is one of several rivers in Nish however it is considered the most important one because it determines the primar axis of the city, which spreds linerly along it. It is a fast river with strong and abundunt torrential waters. Therefore, possibilities for construction of bridges are limited. Inspite that, many bridges were built since the second half of the 20th century, as necessesary for the growth of the city. That was made possible by three earlier projects. On two occasions the river bed was arranged for prevention of the repeating flooding of the left bank as well as for other reasons, including gentrification. The upstream dam, near Pirot, further contributed to the better control of the river.

Among existing bridges, the most numerous are composite and concrete ones, and only four bridges out of 16 are made of steel (Nish has over 30 bridges on all its rivers). However, since early 20th c the most prestigious bridge – the one in front of the main gate of the fortress of Nish in the city center – is repeatedly made of steel. Two railway bridges and one pedestrian bridge are also made of steel and they are curretly in use (Figure 1). We briefly exemined the design and present state of these bridges.

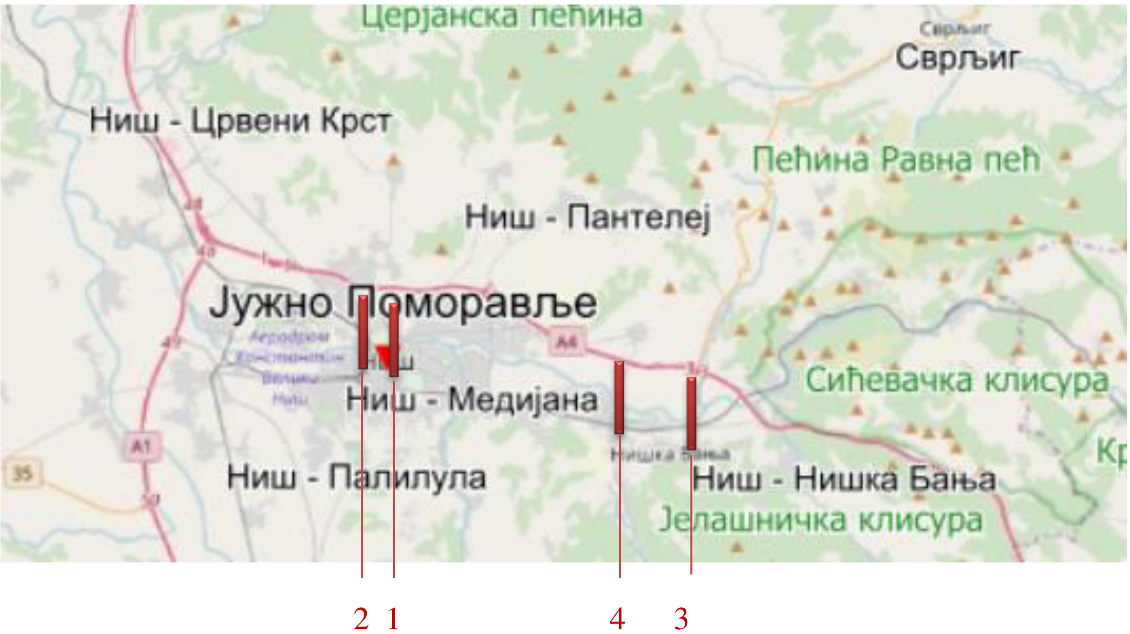

Fig. 1 The locations of Nish steel bridges on Nishava 1-The main-gate fortress bridge 2-The centre railway bridge 3 – The edge railway bridge 4- The pedestrian bridge in Brzi Brod

2. THE MAIN-GATE FORTRESS BRIDGE

This bridge is situated on the most prestigious location in the city center of one of Serbia's oldest and most historically rich cities. This bridge serves nowadays as pedestrian only, but it is historically the most important one and for many centuries the only one in the area. Under the bridge there are presented in situ remains of Ancient Roman bridge (Figure 2).

Fig. 2 Bridge ahead of the main gate of the fortress (called Stambol-kapija), known as the Blade-bridge due to the slim structure.

Built as a single-span over the Nisava (span is 66.7m) and was originally staged in 1961 (replacing old iron bridge from 1900). The last reconstruction was completed in August 2021.

Designed as an haunched bridge with two box girders and orthotropic deck slab. The haunched design provides added structural strength and stiffness to the bridge, making it more capable of handling heavy loads and distributing them effectively. The two separate box girders running parallel to each other along the length of the bridge. The use of two girders adds redundancy to the structure, enhancing safety and load-carrying capacity. Box girders are closed rectangular or trapezoidal structures that provide excellent torsional stiffness and resist bending forces. An orthotropic deck slab is a specialized type of deck that is lightweight and designed to efficiently distribute loads, that include a stiff, thin plate with transverse ribs, longitudinal stiffeners, and edge beams. This design reduces the dead load on the bridge while maintaining structural integrity and is known for its durability and fatigue resistance.

It is particulary interesting that the box girders are welded as the assembly joints riveted. This might result of the different building stage times and also availability do the joining methods.

When inspecting the bridge, the bridge is in good shape. Structural elements are sound, with only minor signs of wear or damage. Routine maintenance is required.

3. THE TRUSS BRIDGE FOR THE RAILWAY IN THE CENTER OF NISH

As a representative example of a railway bridge the bridge consists of two separate two-span bridges crossing the Nišava River aproximtely 700m from the previously mentioned bridge. The lenght of the bridge is 66.5m.
The trough bridge with parallel chords design is characterized by its structural elements, primarily the shape of the bridge and the arrangement of the chords (horizontal members). The bridge has a trough-like or U-shaped cross-sectional profile, resembling an open-topped rectangular box or a trough. This shape provides natural support for the bridge deck, allowing it to distribute loads efficiently over the length of the bridge.

Fig. 3 The truss bridge for the railway in the centre of Nish

This bridge is probably best known to the public due to the black-and-white photography of partly sank structure under the bombs, taken in 1915 (Fig 3.e).
The bridge is in poor condition and requires immediate repair. Visible deformations have resulted from impacts. Corrosion between the plates on the lower chord and crack

(c) is advanced and ongoing, posing a significant threat to the bridge's future usability. Addressing this corrosion is essential. Additionally, a diagonal crack has formed on the lower chord due to the impact (d), further jeopardizing the bridge's integrity and safety.
The importance of this bridge is expected to diminish after relocation of the main railway station which was announced in September 2023 by the city authorities, in which case it will not be part of the railway Belgrade-Nish.

4. THE TRUSS BRIDGE FOR THE RAILWAY AT THE EDGE OF THE CITY

This is one of the railway bridges whose apperance is identified accross Serbia as typical domestic railway bridge. Being many times tested, the shape of the bridge is considered to be good. It has span of 57.3m, The structural components are generally in good condition, showing only minor indications of wear or damage.

Fig. 4 The truss bridge for the railway at the edge of Nish

Fig. 5 The truss bridge for the railway at the edge of Nish - details

5. THE PEDESTRIAN BRIDGE

Fig. 6 The Pedestrian bridge

This pedestrian bridge provides a safe and convenient means for people to cross over barriers between Brzi Brod and Donja Vrezina. It has span of 70.3m and was built as a riveted suspension bridge with orthotropic roadway (a, b).

To ensure horizontal stiffness, prestressed cables were necessary (c, d), but one is not prestressed (e). That means the horizontal stiffness is absent and the bridge is exposed to horizontal loads such as pedestrian loads (that issue also accrued at the Millennium Bridge in London after the first construction phase) and wind or seismic loads. The cables are also exposed to the air and need protection from the environmental influences.

6. DISCUSSION AND CONCLUSION

Steel bridges are not common in the area of Nish. Furthermore steel bridges on territory of Serbia are not even often discussed in scientific literature. Regarding public opinion, it is common belief that composite bridges have the best performances in Serbian climate conditions, that it is easier to find reliable craftsmen for composite structures than for pure steel, that they require regular maintenance which cannot be guaranteed in Serbia and that even in aesthetic terms massive composite bridges fit better bit local mentality, apart from railway bridges which are typically made of steel. In favour of the last, let's point out that the main gate fortress bridge is known as a "blade bridge" due to its slim structure not in favourable manner, and that there were many concerns regarding the oscillations of bridge during regular use, prior to the recent reconstruction. The second reflects certain mistrust in public pole regarding steel bridges. Needless to argue indications of prejudices regarding steel bridges in this case or a lack of understanding, we would like to stress out that civil engineering in Serbia has a long tradition, and that all of them are well ranked in the world university rankings, not to mention that that all civil engineering faculties in Serbia have well established steel departments. However, what Serbia doesn't have is the following:

- built ways for dissemination of knowledge of steel bridges in advantages in terms of sustainability and circular economy
- public competitions for practicing of designing and building well designed steel bridges, so that young generation do not lose this skill, and which would further inspire excellence in higher education
- instruments for the efficient enforcement of regular maintenance.
- local supply chain which would act in favour of steel bridges.

Diversification of structural design of bridges in Serbia is welcome, in particularly if it contributes sustainability and overall progress. In simple words, it would be good to have more steel bridges in Nish in the future. In meantime, the focus should be on regular maintenance of the existing ones.

REFERENCES

[1] Xie J., Fu Q., Yan J. (2019). Compressive behaviour of stub concrete column strengthened with ultra-high performance concrete jacket. *Construction and Building Materials*, Volume 204, pp. 643–658. https://doi.org/10.1016/j.conbuildmat.2019.01.220.

[2] Crank J. (1975). *The Mathematics of Diffusion*. 2nd ed., Clarendon Press, Oxford, Great Britain.

[3] Kusunoki K., Yeow T., Kajiwara K. (2021). Tackling earthquake disaster by using E-defense shaking table facility. *15th International Scientific Conference iNDiS – Planning, Design, Construction and Building Renewal*, Faculty of Technical Sciences, Novi Sad, Serbia, 24-26 November, pp. 32–43.

[4] Hozjan T. (2009). Nelinearna analiza vpliva požara na sovprežne linijske konstrukcije. Doctoral thesis (in Slovenian), University of Ljubljana, Slovenia.

19TH CENTURY FRONT TERRACED RURAL HOUSES AT THE VRMAC PENINSULA-THE BAY OF KOTOR (MONTENEGRO)

Dušan Tomanović[1], Marta Grbić[2],Tijana Tomanović[3]

ABSTRACT

Traditional settlements and their constituent traditional houses are culturally relevant artefacts; in that, they are products of building traditions handed down from one generation to another. They are the most important places that represent the lifestyle of the past. They consistenly adopt to the change of time and suitably transform according to the changing circumstances. There is a rich diversity of building types in the Vrmac Peninsula. With its simple organization, these houses are often arranged in rows. Courtyards are small and rarely enclosed [1]. In its main features, it corresponds to some basic principles that are perceived in every rural architecture [2]. The aim of this research is to investigate front terraced traditional houses at the Vrmac Peninsula and describes the basic principles of these houses. The existing houses shown in this paper are those that survived the devastating earthquaqe of 1979. as well as modern age destruction.

Key words: Rural settlements, Terraced houses, Vrmac peninsula

[1]PhD Prof. Faculty of Technical Sciences, Department of Architecture, University of Priština, K.Mitrovica

[2] ass, Faculty of Technical Sciences, Department of Architecture, University of Priština, K.Mitrovica

[3] English language teacher, Radivoj Popović elementary school, Belgrade - Zemun

1. INTRODUCTION

The motiv of the frontal terrace is present in various forms in the residential architecture of the Bay of Kotor during the whole Baroque period. These terraces are enriched with frontal yards in different combinations. During this period, it was the nobility, sailors, warriors and artists who raised the towns and villages of the region to a higher degree of economic and cultural bloom [3].

Baroque architecture (religious art) began in Italy in the late 16th century. It took the Roman vocabulary of Renaissance architecture. The central concept of the Italian Renaissance - the concept of perfect proportion - disappeared in Baroque, while the interest was not related to existence, but to reality [4].

A Baroque building always stimulates to movement and the true values of its details are viewed only through the change of perspective. The foundations and facades became motional, abundant in convex and concave surfaces, and the structure of the building was often hidden. The novelty brought by the Baroque was the concept of absolute unity. Beautiful individual parts no longer assembled in harmony but subordinated to one dominant overall motive, and only the synergy with the whole gave them the meaning and the beauty [5].

Until mid of the 17th Century, the Baroque style had found its secular expression in the form of grand palaces.

Venetian influence on the Baroque architecture of the Bay of Kotor is recognizable in the second half of the 17th century. Their influence is expressed primarily in the volume design of the raised central part (belvedere–scenic viewpoint) [6]. The volume composition with the dominating belvedere is even more efficient owing to the front terrace. During the 18th century, this element settled in the Bay of Kotor as a sign of recognition of residential architecture, especially those located in the surrounding area.

The frontal terraces in the Bay of Kotor were first to be seen in two baroque noble palaces in Perast, immediately after the great Battle of Perast in 1654 when the Turkish attack was repelled and Herceg Novi was liberated in 1687, thus eliminating the Turkish presence from the Bay of Kotor [7].

Fig. 1 The palace of Bujović family– Perast

Fig. 2 The palace of Smekja family– Perast

The Bay of Kotor architecture found its inspiration in its adjacent and distant neighbourhood, where some builders and masons came from. In the first place in the Dubrovnik architecture; however, the South-Italian influences should not be forgotten as the frontal terraces or terraces along the frontal walls of large households are characteristic of Apulia, for example, Palmieri family (the 17th c.), Calderoni (the 19th c.), Viglione (the 17th c.), Lamberti (the 18th c.), Caracciolo (18th c.) [8].

Figure 3. Masserie- didattiche – Puglia

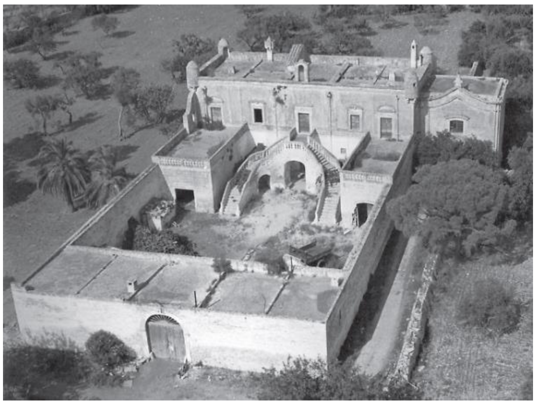

Figure 4. Masseria Lamberti – Bari

The intertwined cultural influences are normal having in mind the strong commercial and maritime connections of Dubrovnik and the Italian cities with the cities of the Bay of Kotor [9].

The most effective design elements of the frontal terrace are stone balusters (balustrade).[1]

Fig. 5 Balusters in front of the Church of Our Lady in Prčanj

Fig. 6 Balusters on the balconies were replaced by iron fences in the 19th century

Another feature of these houses is the base with central bearing wall that divides the space into two parts. It was primarily formed within the fortifications of Dubrovnik during the Baroque reconstruction, after the earthquake in 1667, as the result of merging older particles inside the double row houses [10].

[1] During the present renovation, the balusters were modeled on the example of stone balusters that were preserved.

2. CASE STUDY

2.1. TERRAIN CONFIGURATION

The massif of the Vrmac Peninsula consists of a high main ridge (seven hundred meters above the sea level) spread in the south–north direction with a slightly lower and less emphasized southern ridge, a central delve and slopes descending towards the sea - steep and rugged northeast slopes and somewhat milder southwest slopes.
The geologic foundation consists of sporadic waterproof layers, so that seasonal surface currents and springs of drinking water can be found in this field. Fertile soil is mainly located on the mild slopes and depressions.
Along the seaside, the terrain is pebbly and very porous and loose with clayey soil appearing in some places. The most cultivated fertile land on the Vrmac Peninsula is mainly located on the southern and south-western slopes.
The northeast side facing Kotor is sharply separated by steep slopes. The layers on this side of Vrmac consist of clayey limestone and flysch with occasional karst. This side is incomparably more difficult in every aspect than that of Tivat, and we can notice that the places in this part, both the coast and the hills, are disappearing.

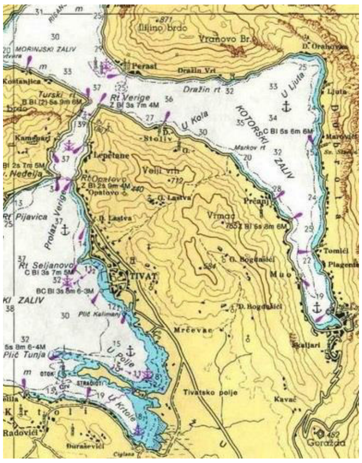

Fig. 7 Topographic map of Vrmac peninsula

Fig. 8 Vrmac peninsula

2.1.1. Settlement

Settlements, house assemblies and groups with their mutual relations as well as their attitude towards the landscape reflect the traditional way of life and the principle of socio-economic organization. Traditional settlements and a landscape created by man were not a product of a particular activity separated from life. They are the result of a way of life and a strategy of community survival in a specific climate [11]. Urbanization of the Vrmac village occurred probably under the strong influence of the towns (Kotor, Perast), adopting city forms and striving for the monumental. The village area in the Bay of Kotor has irregular borders as the result of its spontaneous formation and terrain configuration. Apart to terrain, climate and hydrographical factors are also important for the position of the settlements [12].

There are four important periods in the history of the Bay of Kotor and the organization of settlements in these periods and the attitude of a man towards his environment can be, more or less, reconstructed in the following manner:

a) Appearance of rural settlements in the hills, far away from the sea and the main communications (the Middle Ages);

b) Consolidation of settlements on inaccessible terrains with more intensive use of the territory, deforestation and transformation of the landscape (the Venetian period);

c) Settling of the lower terrains and development of new activities (the Austrian period);

d) Abandonment of upper villages, growth of urban centres and degradation of the landscape (the post-war period).

At the beginning of the 19th century, the coastal bay area became attractive for settling and the sea became the most important traffic road. The existence of the population in this period still depended on the traditional economy. Care for the land continued to be the condition of survival. Strengthening of industry at the end of the 19th century within the seemingly traditional relations, the conditions for change of the settlement structure were created. The breakthrough of the coastal road by the Austro-Hungarian authorities at the beginning of the 20th century and the breakthrough of the main road in the course of the 1960's significantly determined the way in which the settlements were organized. They enabled a rapid development of the coastal area, thus neglecting other areas.

In the period between the two World Wars, with the emergence of industry, the need for food production was decreased and agricultural parcels were transformed into building lots. The change of the Vrmac landscape continued with increased intensity. Intensive construction did not pay the least consideration for the traditional architecture.

After the Second World War (caused by a new way of life), migration of the population is even more noticeable than in the previous period. The Tivat Bay area experienced rapid growth owing to its favourable position. However, this movement was reduced only to the change of location and descending of upper settlements towards the sea, especially in the period after the catastrophic earthquake in 1979. In the Bay of Kotor, this process started somewhat later, but it had similar migration course as in the Tivat Bay. The consequences were the formation of new settlements (already densely populated at the time) along the sea coast and abandonment of the upper villages. The main motive is the rapid development of industry (navy arsenal in Tivat, industry in Kotor, shipbuilding in Bijela), various schools, developed administration and, later, tourism. Today, the largest number of the peninsula inhabitants lives in a narrow coastal area. The existing and disappeared settlements, about which there are reliable historic data, can be divided into two groups: the lower and the upper settlements. The lower settlements are located in the coastal area, from Muo and Prčanj, Stoliv, Lepetani, Donja Lastva to Tivat. Almost all of these settlements are located along the coast line and the road and availed of no predispositions to be the centre as they form the groups of the same or similar rank along the coast. The upper settlements located between two mountain ranges in the longitudinal valley at the altitude of 250 - 450 meters and far from the sea include the following places: Bogdašići, Gornji Stoliv, Veće Brdo, Gornja Lastva, whereas in the Middle Ages there were also the villages of Pasiglav, Rozgovac and probably Gradac, which no longer exist. In the upper villages of the Vrmac massif, the buildings are arranged in a row according to the neighbourhood principle with maximum use of the terrain slope. The rock itself represents one of the walls wherever possible. These buildings were mostly single-cell residential buildings (barns).

Fig. 9 The lower settlement- Muo; the residential settlement in which the road passes directly in front of the house's facades, i.e. through the yard

Fig. 10 The upper settlement - Gornja Lastva; each individual house adapts to naturaltopography so well that no house hinders the view of the house located behind

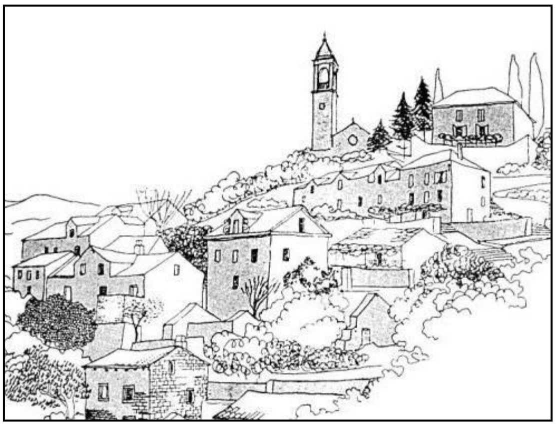

Fig. 11 The upper settlement- Gornji Stoliv; houses are grouped around the church in the center of the settlement.

Fig 12 The lower settlement- Lepetani; houses are grouped along the main street by the sea

At the seaside, the terrain configuration is much gentler allowing construction of the multi-floor houses. The houses started to stand out and inflict themselves along the seaside. On the steep terrains around the houses, drainage channels had to be excavated to drain huge amount of water. Terrain delevelling was mastered by the construction of supporting stone walls. Terrain configuration also affected the functional organization of the house. It conditioned the function not only horizontally, but also vertically. There has always been a tendency, and it is present even today, that a house has as many views towards the sea and the surrounding as possible.

2.2. HOUSES WITH FRONT TERRACES – EXAMPLES

Terrain configuration at the Vrmac Peninsula (a falling terrain) prompted the formation of stepped terraces in front of the house. Terraces were most often raised to the height of the first floor of the house. The ground floors of these terraces are occupied by warehouses, cisterns and taverns. Depending on the situation, the terrace was located in the front, on the side or the back of the yard.
Each individual house adapts to natural topography so well that no house hinders the view of the house located behind. In this way, the desirable effects of nature, like prevailing wind for ventilation and solar orientation, are also admitted to indoors.
Some of these houses will be described in the following examples from Donji Stoliv, Lepetani and Gornji Stoliv.

2.2.1. Example A

The building shown here is located on the slopes of Vrmac, in the village of Gornji Stoliv. It is located on the northern slope of the Vrmac Peninsula, parallel to the very steep terrain contours. The house has a trapezoid-shaped base and consists of the ground floor, the first floor and the attic. The thick stone wall divides the middle of the ground floor into two asymmetrical sections. The two parts have their own entrances from the outside and are not interconnected. The interior stairs, however, are connected with the floor. These rooms were used for storage and processing of food products. The main entrance to the house is on the first floor through the front terrace and a single-staircase set next to the outer wall on the north facade. The terraces are surrounded with stone benches for sitting.
The thick stone wall on this floor divides the building into two parts, but here they are interconnected. Both parts were probably a single room at the time of construction, but over time, one part was divided into rooms. On the right side of the entrance, there is a staircase on the first floor leading to the attic. The attic is located below the scenic viewpoint in the form of a shutter, with its two windows on the north facade. The kitchen is in the attic. Food is prepared there, and the central motif is the fireplace (chimney). Tanks were almost the only way for water supply during the summer months. In this case, it is located below one of the two front terraces, which is also the main entrance to the house. The whole mechanism (horizontal and vertical gutters) that drained the water from the roof into the tank itself is made of stone. All windows and doors are framed by the thresholds of Korčula stone. The two-gabled roof is covered with roof tiles ("ćeramida").

2.2.2. Example B

An interesting example of this type is the house at Lepetani, built in the second half of the 19th century. It is located on the western slope of the amphitheatre. By placing the longer side of the house parallel to the terrain contours, the main facade got the western horizon. On the other three cardinal directions, the foundation walls are buried into the ground. A harmonious simplicity marks the facade of the house. A narrow, curved path

that passes under the arched front terrace gives the access to the pedestrian path on the north side.
The house consists of the ground floor, the first floor and the attic. The ground floor space is divided into two parts with a solid stone wall. The cattle were kept in one part and household food supplies in another. The space in front of the building is also divided, one for people and another for the animals. In order to get to the main entrance on the first floor, the outer staircase led through the front terrace on two levels. The terrace is on two levels, surrounded by a stone bench ("pižuo"). The floor arrangement is dominated by three rooms, one of which was transient and probably used as a dining room. The other two served for rest and representation. On the eastern facade there was a kitchen (a small built-up building) that descended from the attic in the second half of the 19th century. The cistern is built next to it. The wooden staircase connects the floor with the attic. The space below the staircase was used to store firewood supplies.
The single room in the attic is now dedicated for rest and sleep. On this floor, on the facade, there is a sightseeing platform, a wall in the form of a tympanum with a two-gabled roof. This scenic viewpoint has a window on each east and west sides, giving the attic a good lighting. Dimensions of all house windows are the same: 121.69 / 86.9; the side ratio is 5:7. All windows and doors are framed with the thresholds of Korčula stone whose size is 1/2 of the Venetian foot, which equals 17 cm.

2.2.3. Example C

Another example of this type is in Donja Lastva. It is located on the south-western slope of the amphitheatre with western orientation. Due to its good position, openness of the space in front and behind the house, it has two main facades oriented to the east and west. The first facade is accentuated by its openness and a large number of windows and doors, while the other is emphasized by the entrance staircase, the spacious front terrace and the entrance door. The terrace is bordered with a stone bench. The base is trapezoidal-shaped. Its longer side is parallel to the terrain contours, and the main entrance to the house is from the east. It consists of the ground floor, the first floor and the attic. The ground floor area (tavern) is divided into three asymmetrical parts, two of which are interconnected. The third space was transient and connected with the first floor by the inner staircase. The purpose of this space was of economic character. In order to get to the main entrance on the first floor, the outer staircase led through the front terrace on two levels. The outer staircase on the facade leads to the main entrance of the house on the first floor. In front of the main entrance, there is a frontal terrace which covers the area on the ground floor (most likely a cattle storage area, because it has a separate entrance from the north side). The terrace is surrounded on all sides with stone benches for seating ("pižuo") and paved with stone slabs from local stone pits. There is a small hallway on the first floor, from which the narrow angular stairs lead into the attic area. Most of this space was used for living. Both the floor and the attic were divided by thin partition walls to a large number of rooms, the bigger ones in the centre whereas the lateral ones were smaller, all of which were used for dwelling and rest.
It is assumed that the kitchen was in the attic, and of all the traces leading to such a presumption there is only a stone sink left. In the later period (at the beginning of the 20th century), the kitchen with the dining room descended into a separate building annexed to the building on the southern facade. The equipment of the house was very modest. A few beds in the sleeping rooms, two or three chests, a "kasuna"(a crate in which clothes, goods and laundry were kept) and several chairs made all of the furniture. All walls have a kind of closet on all floors (''panjega"is a kind of safe), where lamps and keys were kept. There were enough window and door openings on the house. The window dimensions were: small 104.31 / 69.54 - ratio 3:2, and large 121.69 / 86.9 ratio 7:5. The doors on the ground floor as well as those at the entrance to the

house are folding doors, which offer a good protection, with a door lock and latch system. All plastic elements on this house are made of stone from the island of Korčula.

3. GENERAL ADVICE FOR ALTERATIONS

Since I've been involved in numerous reconstruction and revitalization projects in this area, I suggest the following guidelines. A lot of the materials and craft techniques used in the construction of these terrace houses are still available today. It is rarely advisable to depart from traditional practice when carrying out alterations or repairs. As a general rule, alterations should preserve the structure, character and appearance of the buildings. In a conservation area it is vital to consider the way the house fits into the wider context of the street and any alterations should preserve or enhance the character of appearance of the area. The front elevation and other parts visible from the street are particularly sensitive. Alterations should not impair or destroy the overall shape and proportion of a house, or detract from its historic character, in particular its roof profile or the shape, design, and appearance of window and door openings.

Many old buildings appear to suffer from the arising structural weaknesses. These weaknesses manifested during a catastrophic earthquake that struck the Montenegrin coast in 1979. when most of the houses were more or less damaged. Inadequate structural intervention can easily turn limited weaknesses into serious defects, resulting in a rapid escalation of work, loss of original interior or, possibly, a collapse. An adequate structural intervention involves the participation of experts.

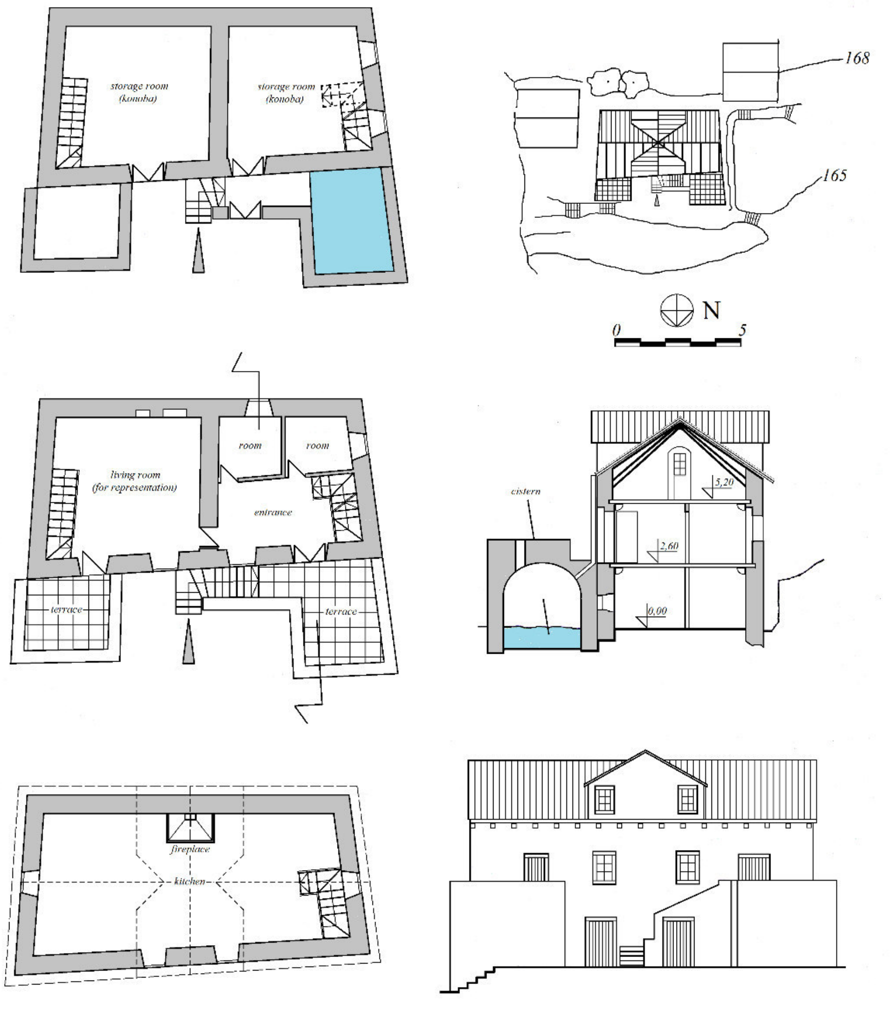

Fig. 13 This type of house is characteristic for the settlements: Gornji Stoliv and Gornja Lastva

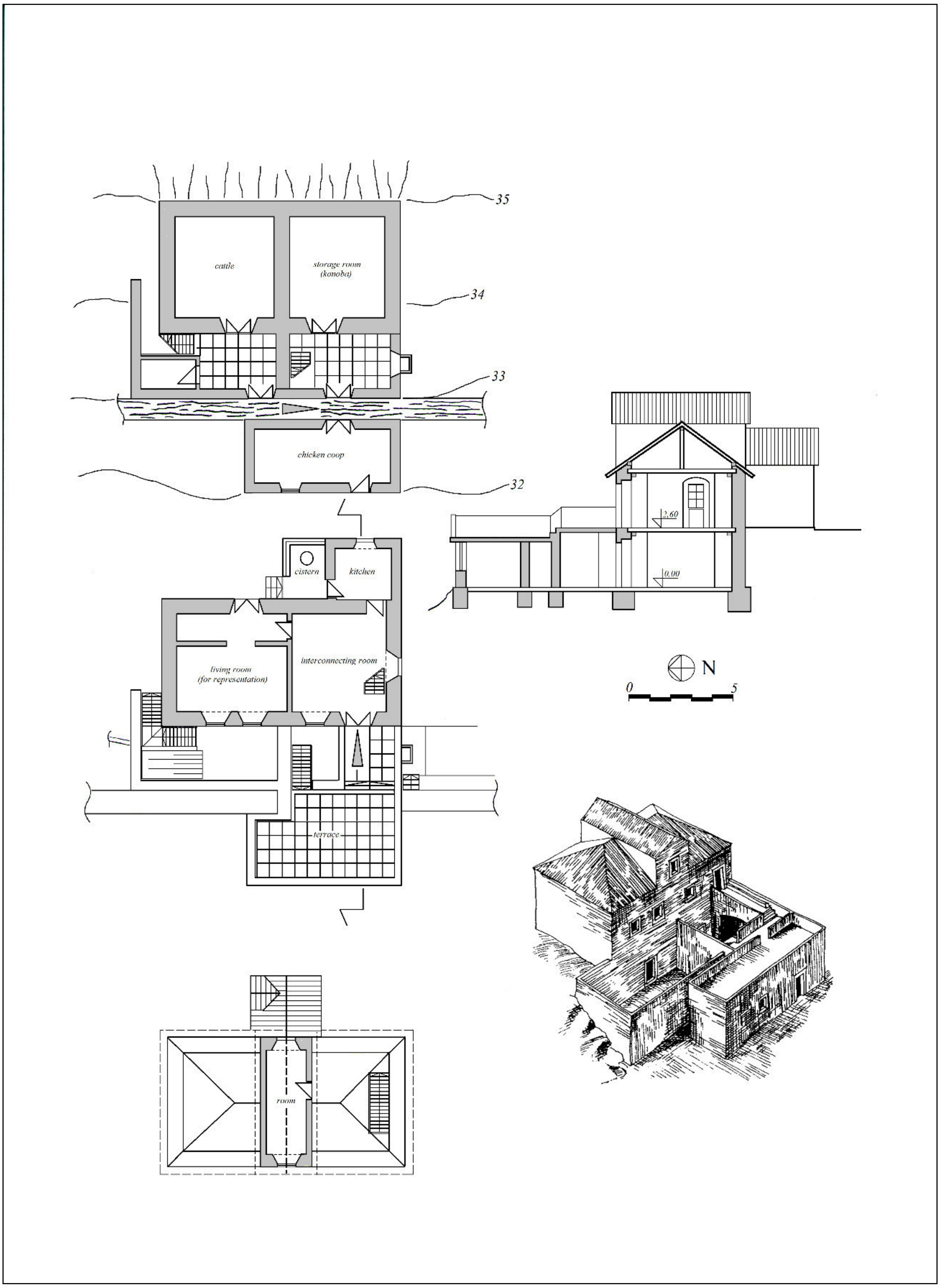

Fig. 14 This type of house is characteristic for the settlements : Lepetani, Donji Stoliv, Prčanj, Muo, Donja Lastva

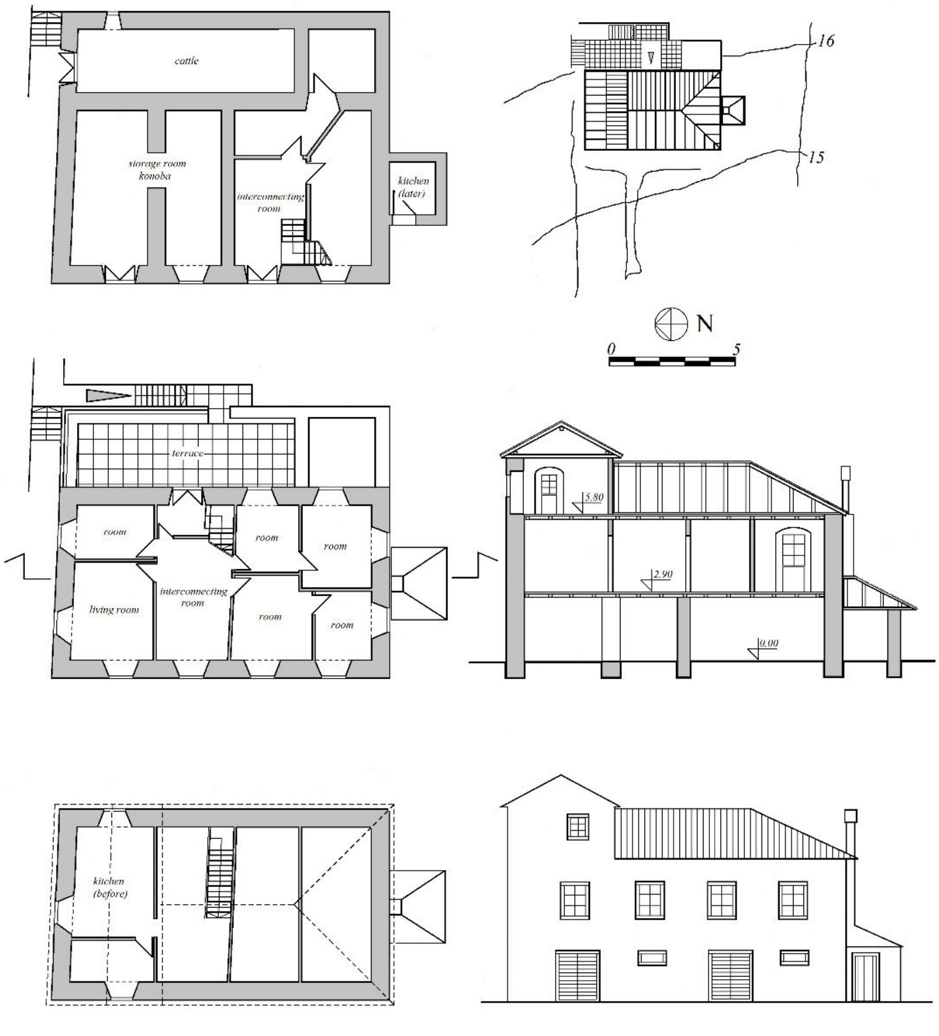

Fig. 15 This type of house is characteristic for the settlements: Lepetani, Donji Stoliv, Prčanj, Muo, Donja Lastva

4. CONCLUSION

The terrace houses are of outstanding importance for the historical development of the houses at the Vrmac Peninsula and the whole of The Bay of Kotor. For over 300 years they have provided accommodation for domestic and commercial purposes. Today, vernacular built forms and traditional construction techniques with use of local materials are disappearing. The planning principles adopted in the 19th century lost its importance in the society and are being forgotten for the time being.

Important advancement in protecting the architectural heritage began to take place at the turn of the last century. Then, it has become clear that rural heritage is a potential tourist attraction that can help develop specific forms of the tourism offerings. The recognition and categorization of various types of architecture can lead to better understanding of the environment, its conservation and the establishment of new design methods. Absence of recognition and appreciation for these buildings by the authorities and public audience will gradually lead to their destruction and replacement by contemporary buildings.
The future architects should study these types of houses.
Conservation of these houses should be the goal. This requires organization and funding. Preserving the features of these houses helps in maintaining the architectural heritage and culture of the region.

PHOTOS AND DRAWING SOURCES

Figure 1,2,6,9,10,12 - Made by author of the article

Figure 3 - Masseria di Puglia, courtesy of *www.storienogastronomiche.it*

Figure 4 - Masseria Lamberti - Bari, courtesy of *www.hevelius.it*

Figure 5 - Our Lady Church in Prčanj, courtesy of w*ww.upoznajcrnugoru.com*

Figure 7 -Topographic map of Vrmac peninsula, courtesy of *www.bestofboka.com*

Figure 11 - Drawing made by prof. Zoran Petrović

Figure 13-15 - Drawings made by author of the article

LITERATURE

[1] Božović, G., Naselja i kuće Tivatskog zaliva, Centar za planiranje urbanog razvoja, Beograd, 1981., 12

[2] Kojić, B., Spomenik CIII S.A.N.,Beograd, 1953., 174

[3] Milošević, M., I caratteri stilistici del Barocco nelle Bocche di Cattaro, Vittore Branca, Sante Graciotti, Firenca, 1983., 141-146

[4] Velfin, H., Osnovni pojmovi istorije umetnosti, Veselin Masleša, Sarajevo, 1965., 20-21

[5] Velfin, H., Osnovni pojmovi istorije umetnosti, Veselin Masleša, Sarajevo, 1965., 190

[6] Maretto, P., La casa veneziana nella storia della cita dalle orgini all Ottocento, Venezia, 1986.

[7] Butorac, P., Boka kotorska u 17. i 18. stoljeću – politički pregled, Perast, 2000., 56-64

[8] Vujičić, R., O nekim karakteristikama baroka u likovnim umjetnostima Boke Kotorske, Godišnjak Pomorskog muzeja u Kotoru XXXIX –XL, 1991-1992., 19-25

[9] Burdelez, I., Prinos kulturnoj povijesti Cavtata,u: Konavle u prošlosti i sadašnjosti i budućnosti (bilj.11), 144-145

[10] Levaj, K., Barokne kuće s terasama u Cavtatu – prilog istraživanju umjetničkih veza Dubrovnika i Boke Kotorske, Institut za povijest umjetnosti, Zagreb, 2005., 232

[11] Božović G., Projekat oživljavanja seoskih naselja Tivatskog zaliva, Centar za planiranje urbanog razvoja CEP, Beograd, 1986., 7

[12] Petrović Z., Selo i seoska kuća u Boki Kotorskoj, Zbornik arhitektonskog fakulteta- treća knjiga, Beograd, 1956-57., 5

ADAPTIVE REUSE OF NEGLECTED AREAS IN SKOPJE BY IMPLEMENTING OF THE CIRCULAR ECONOMY

Ana Trombeva - Gavriloska[1], Teodora Mihajlovska[2], Liljana Dimeska Sofronieska[3], Meri Cvetkovska[4]

Summary

The urban landscape holds significant potential in steering the shift towards a circular economy, particularly given the substantial resource consumption and waste output associated with building construction. This paper delves into the prospect of repurposing abandoned industrial structures, examining the sustainability implications within the framework of a circular economy in Skopje, North Macedonia. Repurposing vacant industrial buildings has the capacity to yield environmental, social, and economic advantages by adopting urban strategies rooted in circular economy principles and innovative methodologies. In the context of Skopje's urban development and the metamorphosis of its industrial zones for reuse, this research identifies potential abandoned industrial sites within the city. The research examines these abandoned industrial sites by assessing their functional transformation and adaptive reuse.

Key words: circular economy, neglected areas, adaptive reuse

[1] Prof., Faculty of Architecture, Ss. Cyril and Methodious University in Skopje, North Macedonia, agavriloska@arh.ukim.edu.mk
[2] Asist., Faculty of Architecture, Ss. Cyril and Methodious University in Skopje, North Macedonia, mihajlovska.teodora@arh.ukim.edu.mk
[3] Asist., Faculty of Architecture, Ss. Cyril and Methodious University in Skopje, North Macedonia, dimevska.liljana@arh.ukim.edu.mk
[4] Prof., Faculty of Civil Engineering, Ss. Cyril and Methodious University in Skopje, North Macedonia, cvetkovska@gf.ukim.edu.mk

1. INTRODUCTION

The urban landscape holds a pivotal role in steering the transition to a circular economy (CE), particularly in light of the substantial resource consumption and waste generation inherent in building construction. The CE model of production and consumption emphasizes activities such as sharing, leasing, reusing, repairing, refurbishing, and recycling existing materials and products for as long as possible [1]. This stands in stark contrast to the linear economy approach, characterized by the transformation of natural resources into products destined to become waste, encapsulated in the "take, make, waste" paradigm [2].
While the prevailing mindset often views buildings as having a limited useful life and thus destined for eventual discard, CE seeks to challenge this paradigm. Recognizing that a significant portion of the existing building stock will remain in use for the next century [3], there is an imperative to not only devise strategies for designing durable and adaptable new construction projects but also to formulate sustainable CE approaches for existing buildings.
Adaptive reuse (AR) emerges as a strategic avenue for enhancing the environmental, social, and financial aspects of a building, site, or area by repurposing them from disused structures into ones with a renewed function [3, 4, 5]. In the context of the transition towards a circular economy, adaptive reuse assumes a pivotal role in rendering buildings as regenerative and reusable resources. While adaptability stands as a fundamental principle in the design of circular buildings, facilitating their longevity and averting premature demolition, AR approaches can also be applied retrospectively to existing structures not originally conceived with CE principles.
This paper is dedicated to investigating the potential of implementing AR on underutilized or abandoned industrial sites in Skopje, North Macedonia, contributing valuable insights to innovative approaches within the framework of CE initiatives. Through a comprehensive analysis of historical and contemporary urban plans, the evolution of industrial sites in Skopje is delineated. The study includes an examination of identified abandoned industrial sites, evaluating their functional transformation potential and assessing their susceptibility to prevailing demolition practices.

2. SPATIAL DEVELOPMENT OF SKOPJE

2.1. HISTORY

Industrial buildings in Skopje have played a pivotal role in the city's economic development and historical landscape. The establishment of the first industrial enterprises in Skopje occurred towards the end of the 19th century, marking the commencement of machine production. Following the Second World War, during North Macedonia's tenure as part of the Socialist Federal Republic of Yugoslavia, the region experienced a significant surge in economic and industrial activities.
However, this trajectory faced a major setback in 1963 when a devastating earthquake obliterated 80% of the city's buildings. In response, a new General Urban Plan was devised in 1965, aiming at the reconstruction and development of the city. Despite the seismic interruption, the commitment to industrialization persisted, leading to an expansion of the city's borders and an increase in the city's territory to 11,156 hectares. Approximately 10.9% of this area, equivalent to 1,215 hectares, was earmarked for industrial purposes. The city's industry was strategically organized into planned industrial zones, including the Zhelezara industrial zone, Eastern industrial zone, Southern industrial zone, and a new Western industrial zone, Figure 1.

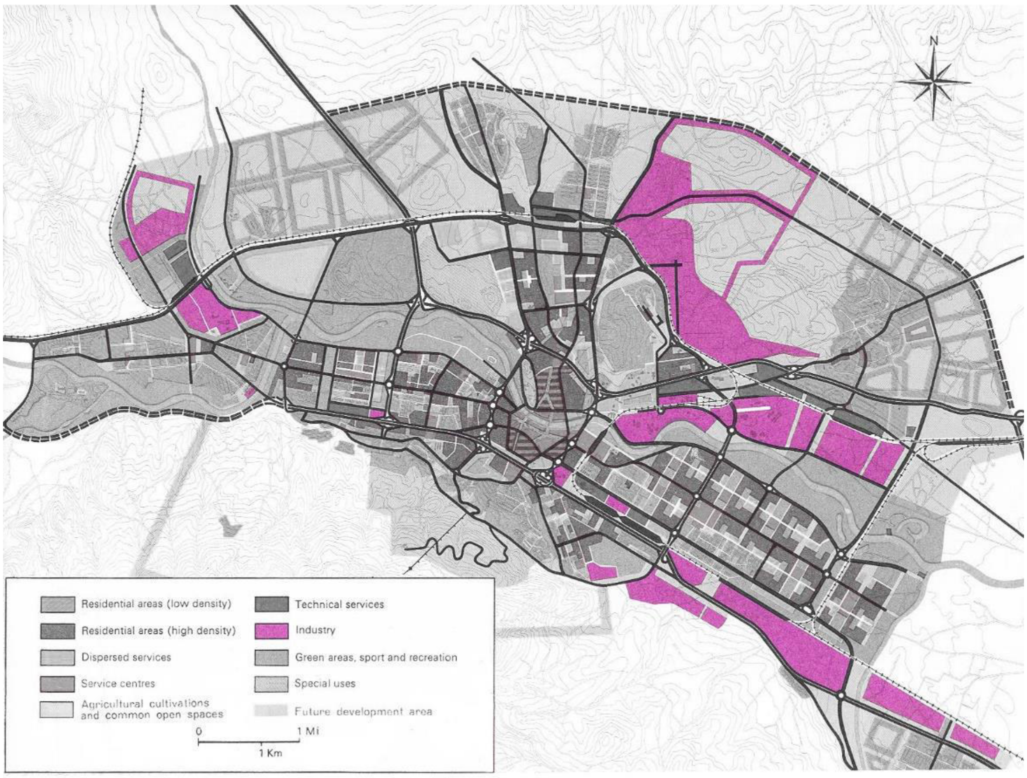

Fig. 1 Industrial zones – General Urban Plan 1965

In 1985, a new General Urban Plan was adopted due to significant changes in planning parameters, including disproportionate population growth and unmet planning goals. However, this plan merely affirmed the existing industrial zones established by the 1965 plan. A crucial shift occurred in 2001, Figure 2, with the introduction of a new General Urban Plan, emphasizing the imperative of rational and efficient use of space and land. Aligned with the vision of a 'sustainable city' integrated into the natural environment, this plan marked a departure from extensive industrialization.

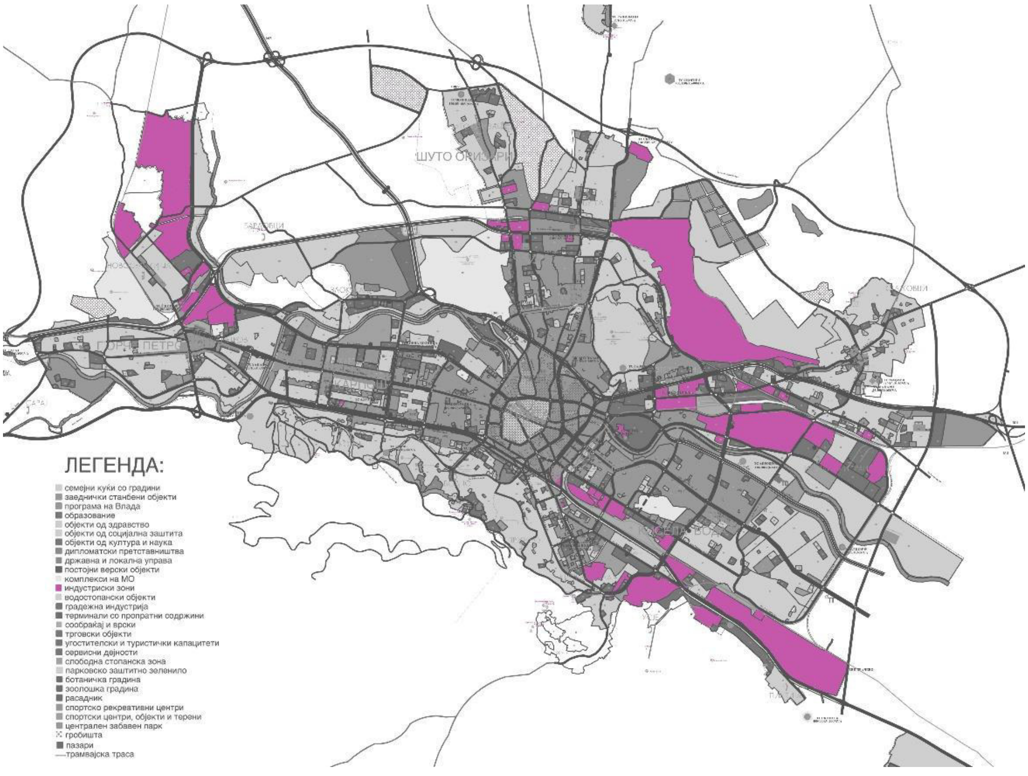

Fig. 2 Industrial zones – General Urban Plan 2001

Illustrating this shift, the planned reduction of industrial area in the city decreased from 1,269.6 hectares envisioned by the 1985 Plan to 1,050.29 hectares outlined in the 2002 Plan—a reduction of 219.31 hectares. This trend of decreasing industrial areas in the urban landscape continued with the General Urban Plan of 2012, Figure 3, further reducing the area to 782.19 hectares compared to the 2002 Plan, signaling a decrease of 268.1 hectares.

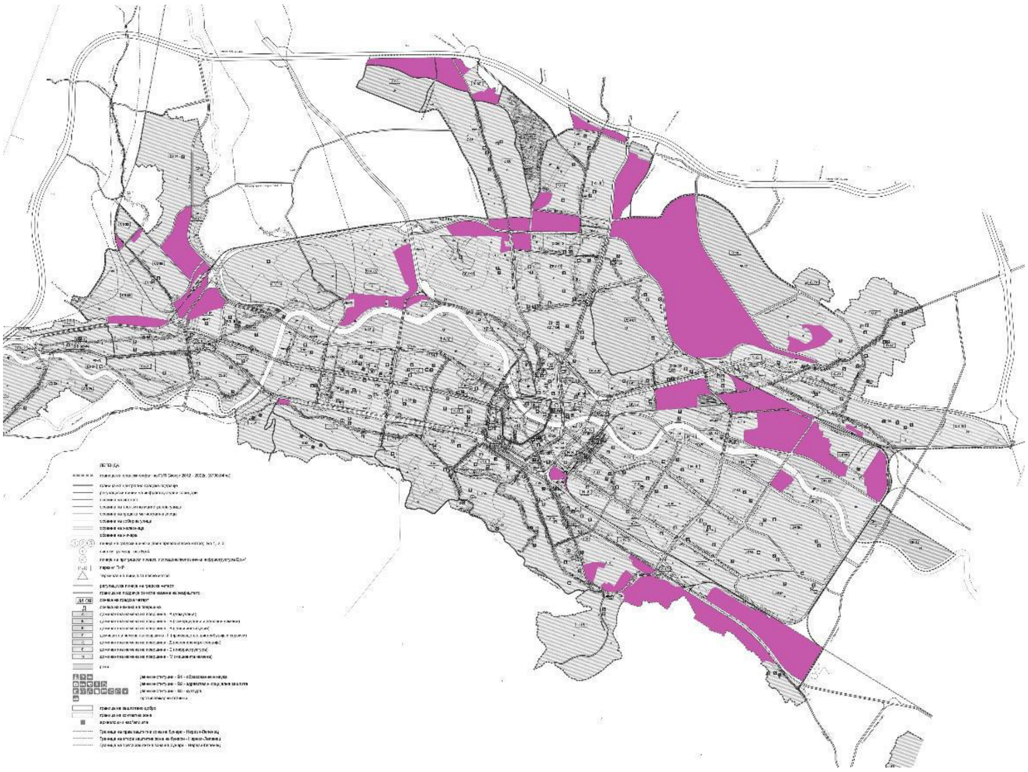

Fig. 3 Industrial zones – General Urban Plan 2012

2.2. CURRENT STATE OF INDUSTRIAL SITES IN SKOPJE

The shift in industrial enterprises during the post-socialist period, driven by the transition to a new socio-economic and political system, resulted in the abandonment or transformation of many of these sites. For the purpose of this research, a total of 163 individual industrial sites in Skopje, covering an area of 849.79 hectares, were considered.

Data for these sites were gathered by scrutinizing studies conducted for the new General Urban Plan for Skopje (2022-2032), currently in development, as well as any relevant preceding urban plans. The research focused on former industrial sites, revealing that the industrial zones in the city are undergoing fragmentation and adaptation to new functions. The once-exclusive industrial areas are undergoing changes influenced by processes such as deindustrialization, functional transformation, and industrial reconstruction. These sites were categorized into three groups: (1) Abandoned – sites that are completely inactive or severely underused; (2) Restored – sites that are actively used for industrial purposes; and (3) Transformed – sites that underwent complete changes and are now utilized for non-industrial purposes [6]. This classification provides insight into the dynamic evolution of industrial spaces in Skopje, reflecting the city's response to changing socio-economic and industrial dynamics.

The data presented in Table 1 indicates that the total number of abandoned industrial sites, comprising 42 sites, accounts for 25.76% of the overall analyzed 163 industrial sites in the city, while 51.53% of sites, 84 sites, have been successfully restored and remains functional as an industrial complex. Notably, 22.70% of the industrial sites, 37 sites, have undergone successful transformation and repurposing. In the scope of this paper, the focus will be on examining the abandoned sites due to their significant potential and the apparent need for the application of AR. Additionally, attention will be given to the transformed sites to understand the nature and extent of functional transformations achieved thus far.

Tab. 1 Overview of transformation of researched industrial sites in Skopje, 2022 [7]

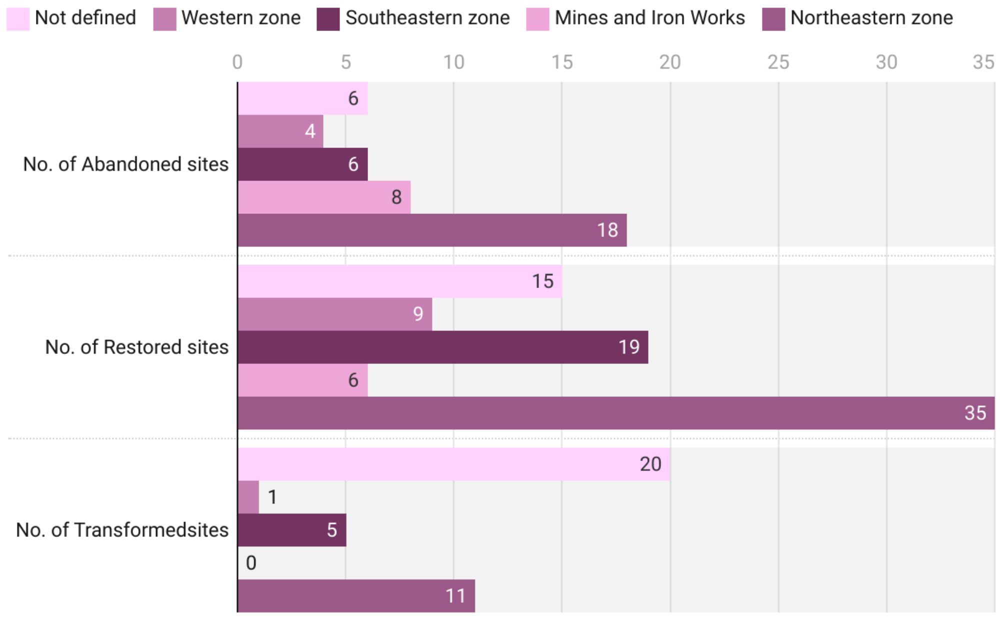

The determination of the status of these abandoned sites, presented in Table 2, takes into account the degree of use, classified as follows: (1) Inactive Sites: These are completely deserted sites with no ongoing activity; (2) Underused Sites: Referring to sites where the degree of use falls short of matching the size and potential of the site: (3) Occasionally Used Sites: These sites experience intermittent use, suggesting a sporadic utilization pattern. This classification based on the degree of use provides a nuanced understanding of the status of abandoned industrial sites, allowing for a comprehensive analysis of the varied conditions and potentials associated with each site.

Tab. 2 Overview of abandoned industrial sites in Skopje, 2022 [7]

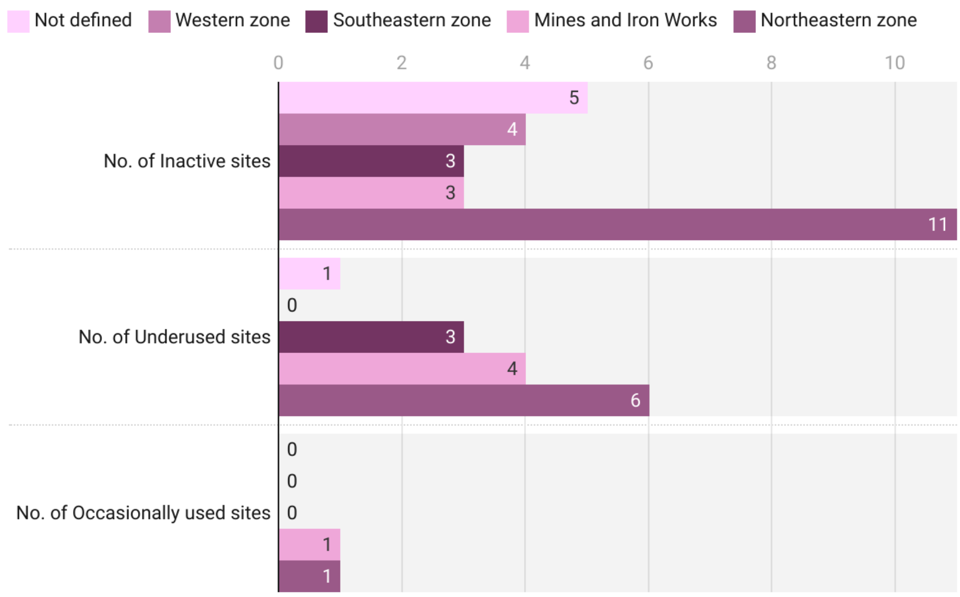

Based on the data outlined in Table 3, it is evident that a modest proportion of the abandoned industrial sites has undergone functional transformations. The predominant functions to which these sites have been transformed are as follows: (1) Commercial Transformation: Approximately 46.38% of the sites have been converted for

commercial purposes, indicating a notable trend toward repurposing industrial areas for business and commercial activities; (2) Housing Transformation: Following closely, about 32.43% of the sites have been transformed into housing which highlights a significant shift in land use, converting former industrial spaces into residential areas; (3) Green Spaces and Parks: A smaller yet noteworthy percentage of sites, amounting to 8.11%, has been cleared and repurposed into green surfaces and parks. This reflects an effort to introduce more environmentally friendly and recreational spaces.
These findings underscore the diverse range of transformations undertaken, showcasing the adaptability of abandoned industrial sites to new functions that contribute to commercial, residential, and green spaces within the urban landscape.

Tab. 3 Overview of transformed sites in Skopje according to new purposes in 2022 [7]

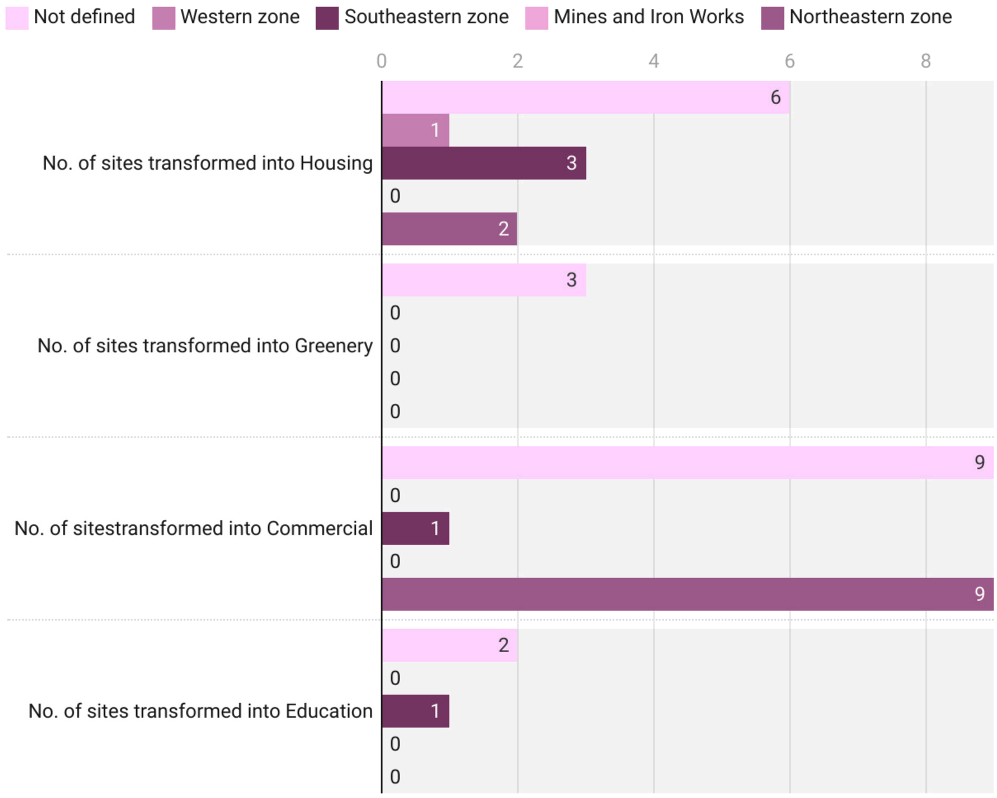

The shift in function observed in these abandoned industrial sites is a consequence of evolving economic structures. The prevailing trend favors the most economically lucrative transformations within the city, notably the construction of residential and commercial buildings. This inclination toward profitable transformations is influenced by the changing economic landscape, and the locations of these sites within the urban fabric further support this trend.
As the city expanded and industrial zones underwent fragmentation, some sites found themselves surrounded by incompatible residential and commercial functions. Consequently, those proximate to the city center tend to be repurposed for commercial use, while sites within residential areas are predominantly developed for new residential buildings. Examining the spatial distribution of abandoned industrial sites reveals that they are dispersed across the entire territory of the city. These abandoned sites are not confined solely to the three designated industrial zones but also extend to isolated locations outside these zones, Figure 4.

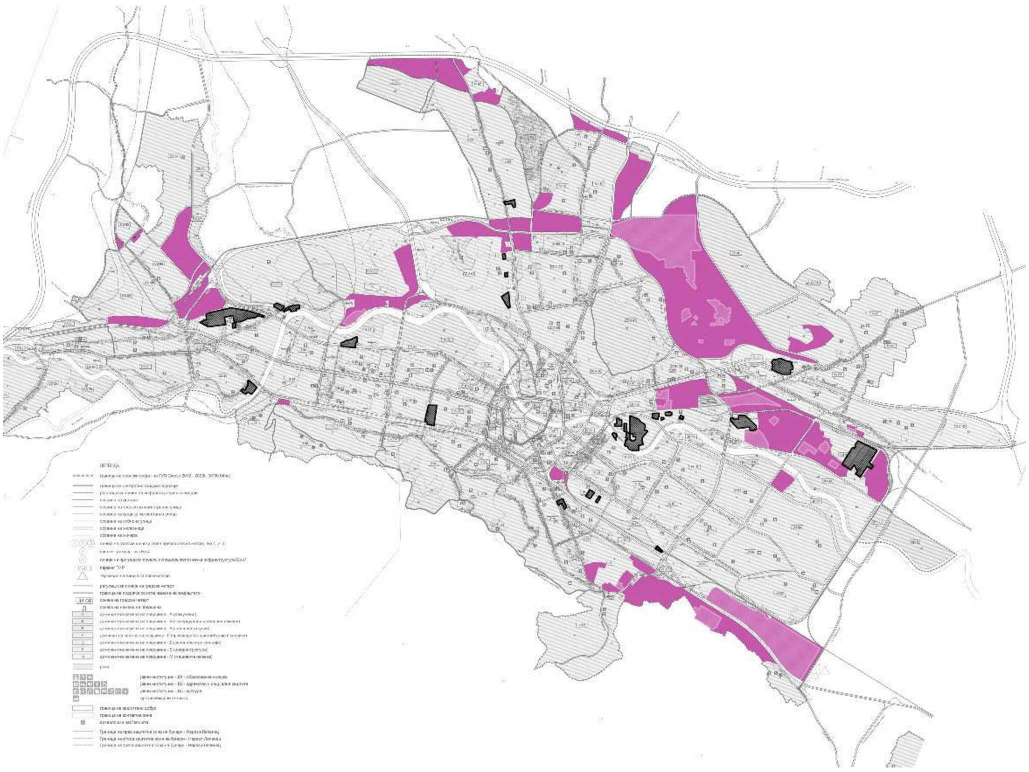

Fig. 4 Sites located outside of current industrial zones

While the transformation of these sites is deemed necessary, the current approach predominantly involves demolishing existing industrial structures and erecting new ones. This approach not only generates waste but also contributes to additional resource consumption. Adopting an AR approach for the remaining locations would not only mitigate these challenges but also bring about environmental, social, and economic benefits. AR represents a sustainable alternative, allowing for the preservation of existing structures, reduction of waste, and the integration of innovative solutions to breathe new life into these industrial sites. This approach aligns with principles of CE, fostering a more resilient and sustainable urban development model.

3. EXAMINING THE POTENTIAL FOR AR

Not all abandoned industrial sites necessarily require functional transformation through adaptive reuse. Some sites, still located within current industrial zones, can retain their original purpose. The vulnerability arises for sites that, according to the General Urban Plan of the city, are no longer situated within industrial zones. Buildings on these sites cannot serve their original function and, as observed in the analysis of transformed sites, are at risk of demolition.

To identify these vulnerable sites, the map of abandoned industrial sites is overlapped with the industrial zones planned in the most recent General Urban Plan for Skopje. Abandoned industrial sites near the central city area and in areas where the dominant function (mostly housing) clashes with industry are earmarked for a change in function. To explore the potential of these sites, an analysis was conducted in the context of other urban studies made for the master plan, particularly focusing on economic perspectives and environmental protection.

The study for environmental protection highlighted two critical aspects: the presence of brownfield sites and pollution [8]. Soil measurements revealed significant contamination with heavy metals around the "Ohis" organic-chemical industry, the "Makstil" iron and steel production and processing industry, and the "Godel" tannery. These sites are identified as industrially contaminated "hotspots," ranking among the 14 largest in the Republic. The risk posed by these localities due to high soil contamination emphasizes the need for soil remediation before any AR activities can proceed. Of particular concern is the Ohis site, storing hazardous chlorinated organic substances for more than two decades.

The second significant issue impacting AR feasibility is air pollution. Air quality measurements, particularly for suspended particulate matter pollution like PM10 particles, reveal a citywide problem. The highest concentrations are recorded at the Lisiche station and in the city center. This data becomes crucial in determining suitable future functions for these sites, emphasizing the importance of considering environmental factors in the planning and implementation of adaptive reuse initiatives.

The study on the economic perspectives of the city identified issues in the urbanization policy, emphasizing the lack of a comprehensive strategy for even development across the entire city area [9]. The absence of a polycentric dispersion of business buildings and commercial facilities, along with a dispersed distribution of economic and social contents in the broader area, were highlighted. Commercial buildings, primarily concentrated in the city center and surrounding neighborhoods, showcased a spatial concentration.

The study proposed potential solutions, suggesting the development of industrial zones through the establishment of business incubators and technology parks to support entrepreneurship. It also recommended expanding and diversifying contents in peripheral zones, particularly through the creation of commercial centers. This strategy could have a dual impact by fostering business development in these zones and alleviating the burden on the city center. This decentralization could enhance accessibility, mobility, reduce pollution in the city center, and achieve a more even distribution of commercial and business facilities.

However, the study falls short by not considering the AR potential of certain buildings, overlooking the opportunity for a sustainable CE approach. Instead, it leans toward a conventional linear approach where introducing new functions involves the construction of entirely new buildings. The analyzed abandoned industrial sites present an alternative solution to this problem, given that historically, most of these sites were located on the outskirts of the city. Although these areas are now integrated into the city, they still represent its most peripheral zones. Recognizing the AR potential of these sites can contribute to a more sustainable, resource-efficient, and circular development approach, aligning with the principles of the circular economy. This approach could also complement the proposed strategy for the polycentric development of the city, fostering a more balanced and resilient urban landscape.

4. CONTINUING THE ASSESSMENT OF AR POTENTIAL

The evaluation of the potential of adaptive reuse is extremely complex and dynamic because the process involves different stakeholders [10] and a number of aspects need to be taken into consideration for each individual building. So far, this research has been focused on the city level, and exploring the potential benefits for an AR approach at this scale. However, in order to evaluate whether or not the specific buildings have the physical capacity to adapt to new functional needs, a number of aspects at the building scale need to be examined. Their compliance with health and safety requirements needs to be checked; their energy performance needs to be assessed in comparison to current standards; their infrastructures such as electricity, drainage, mechanical systems evaluated; the presence of hazardous materials assessed etc. [11].

Ball [12][13] investigated the industrial property stock in Stoke-on-Trent in the UK and identified the characteristics of buildings that were reused or reoccupied in comparison to the vacant ones. He argued that the characteristics suggested the potential of a building's adaptive reuse. This approach could be implemented in Skopje, since a number of the mentioned sites have been transformed, an analysis of the type of function and location in the city of these sites could help identify which ones could be next. The redevelopment of brownfield and reuse of industrial buildings has attracted considerable research interest but only a handful of researchers attempted to find solutions for the evaluation of adaptive reuse potential [14].

5. CONCLUSION

This paper analyzed the abandoned industrial sites in Skopje, North Macedonia in order to explore the potential for AR of underused or abandoned buildings in order to help improve current practices that are not aligned with CE. From the analyzed data it can be concluded that the city of Skopje is undergoing a transformation of its industrial zones. Currently a large number of former industrial sites are underused or completely abandoned, with a number of sites located in areas where according to the current urban plans no industrial functions are planned. These sites will inevitably undergo a functional transformation in the future. The small percentage of sites that adapted to a new function, have been transformed by means of demolition and new construction, which results in waste creation and depletion of resources. This research identifies the sites where by developing a proper AR strategy the buildings can be repurposed, rather than demolished. The AR of vacant industrial buildings can bring environmental, social, and economic and help change the perspective of buildings as products with a limited useful life. The development and implementation of such strategies is crucial in the transition towards CE in the built environment. Further research should look into the specific conditions of the sites identified by this paper and focus on developing a clear plan for AR of the buildings. This type of applicative use of adaptability on existing industrial buildings can be helpful in developing a more general strategy for AR on buildings with different functions. Finally, an in-depth analysis of the application of more sustainable approach from the perspective of CE and AR would provide a set of useful guidelines for practitioners.

ACKNOWLEDGEMENT

The authors of this paper would like to thank the European Union for funding and COST (European Cooperation in Science and Technology) for supporting the COST Action CircularB CA21103 www.circularb.eu

REFERENCES

[1] European Commission. Directorate General for Communication., *Circular economy action plan: for a cleaner and more competitive Europe.* LU: Publications Office, 2020. Accessed: Feb. 13, 2023. [Online]. Available: https://data.europa.eu/doi/10.2779/05068

[2] Ellen MacArthur Foundation, "A new textiles economy: Redesigning fashion's future", 2017. [Online]. Available: http://www.ellenmacarthurfoundation.org/publications

[3] P. Bullen and P. Love, "Factors influencing the adaptive re-use of buildings", *Journal of Engineering, Design and Technology*, vol. 9, no. 1, pp. 32–46, Mar. 2011, doi: 10.1108/17260531111121459.

[4] F. Abastante, S. Corrente, S. Greco, I. M. Lami, and B. Mecca, "The introduction of the SRF-II method to compare hypothesis of adaptive reuse for an iconic historical building", *Oper Res Int J*, vol. 22, no. 3, pp. 2397–2436, 2022, doi: 10.1007/s12351-020-00611-4.

[5] I. M. Lami, "Shapes, Rules and Value", in *Abandoned Buildings in Contemporary Cities: Smart Conditions for Actions*, vol. 168, I. M. Lami, Ed. Cham: Springer International Publishing, 2020, pp. 149–162. doi: 10.1007/978-3-030-35550-0_9.

[6] G. Mickovski, "Transformation of industrial space in the context of post-socialist transition of the city of Skopje", University of Belgrade, Belgrade, 2015.

[7] Faculty of Architecture - UKIM, “Study of the Development of the industry of the City of Skopje for General Urban Plan 2022-2032”, 2022.

[8] Faculty of Architecture - UKIM, “Study for the Environmental protection of the City of Skopje for General Urban Plan 2022-2032”, 2022.

[9] Faculty of Architecture - UKIM, “Study for the Economic development of the City of Skopje for General Urban Plan 2022-2032”, 2022.

[10] E. Kurul, “A qualitative approach to exploring adaptive re-use processes”, *Facilities*, vol. 25, no. 13, pp. 554-70, 2007.

[11] P. Bullen and P. Love, “A new future for the past: a model for adaptive reuse decision-making”, *Built Environment Project and Asset Management*, vol. 1, no. 1, pp. 32-44, 2011.

[12] R. M. Ball, “Vacant industrial premises and local development: a survey, analysis and policy assessment of the problem in Stoke-on-Trent”, *Land Development Studies*, vol. 6, pp. 105–28, 1989.

[13] R. M. Ball, “Re-use potential and vacant industrial premises : revisiting the regeneration issue in Stoke-on-Trent”, *Journal of Property Research*, vol. 19, no. 2, pp. 93-110, 2002.

[14] Urban Task Force, Towards a Strong Urban Renaissance, London: Urban Task Force, 1999.

THE MULTI-CRITERIA DECISION MAKING MODELS IN ARCHITECTURE: APPROACH DEVELOPMENT THROUGHOUT THE HISTORY

Damjana Nedeljković[1], Tatjana Jurenić[2], Aleksandra Čabarkapa[3]

Summary:

Multi-criteria models for decision-making are an instrument used in various fields within processes that require a choice between several alternatives, and are based on the comparison of various aspects of potential solutions, among which it is possible to establish a hierarchy. A certain number of such models are also applied in the field of architecture, and they are intended, among other things, to evaluate the potential of buildings for various types of adaptations or to select an adequate intervention in relation to the current state and characteristics of the observed object and its location. The paper represents the historical development of models for decision-making and the influence on the creating of contemporary multi-criteria models, the application of experiences from other fields, grouping according to certain criteria and the shaping of elements of multi-criteria models throughout history.

Key words: multi-criteria decision making models, historical aspect, development, types of models, elements

[1] Teaching Assistant, University of Belgrade – Faculty of Architecture, Belgrade, Serbia, damjana@arh.bg.ac.rs
[2] Assistant Professor, University of Belgrade – Faculty of Architecture, Belgrade, Serbia, tanja@arh.bg.ac.rs
[3] Assistant Professor, University of Belgrade – Faculty of Architecture, Belgrade, Serbia, aleks@arh.bg.ac.rs

1. INTRODUCTION

Depending on the problem to be solved, the number and characteristics of the solutions offered and the differences in the interests of the participants, the decision-making process can be very complex. In those cases, participants use techniques, which can be formal (cost-benefit analysis, multiple criteria decision analysis, decision trees, etc.) and informal (which are not the subject of research in this paper) to help making decisions. All formal decision support techniques are similar in that they contain a set of clearly defined rules on the basis of which the necessary data are selected and evaluated. Multi-criteria models for decision-making represent one of the formal techniques for decision-making support. These models represent mathematical instruments that are used to more successfully solve problem tasks in various fields.[1] The research is primarily directed towards multi-criteria decision-making models applicable in architecture, but many findings are general and applicable to all models of this type.
In the paper there are two parts.
The first part of the paper, the development of the approach itself, which preceded the emergence of multi-criteria models for decision-making, is presented, various approaches to aid in decision-making are explained and the structure with basic elements is shown, which applies to all multi-criteria models, regardless of their purpose, while the second part of the paper presents nine multi-criteria models that have different uses in architecture.
The main goal of the research is to improve understanding of how to use multi-criteria models for decision-making and their more frequent application in decision-making processes in all suitable fields.

2. DEVELOPMENT OF THE MULTI-CRITERIA DECISION-MAKING MODELS

2.1. APPROACH DEVELOPMENT

The beginnings of the formal research of the decision-making process are not known, but within the process itself, two lines of research are recognized: the first relates to analyzing the origin of decisions and the second relates to utility theory and multiple objective mathematical programming.
Within the first line, Edgeworth's (Francis Ysidro Edgerworth) early work on the indifference contours from the 1880s, Ramsey's (Frank Ramsey) and Finetti's (Bruno de Finetti) subjective expected utility model from the 1930s and von Neumann's (John von Neumann) and Morgenstern's (Oscar Morgenstern) utility theorem from the 1940s.
Multiple objective mathematical programming was mostly developed during the 1970s. The basic characteristic of this approach is a certain reconsideration of explicit estimates of values or utility functions and the focus is on finding ways to choose the most suitable solution.
The author of one of the first known models that have the form of the multi-criteria decision making model that we know today is the American statesman Benjamin Franklin. His way of making decisions, which he called "Moral Algebra", was based on the formation of a list with arguments in favor of the issue and against it. Then, on both sides of the list, arguments that had approximately equal importance were removed, until all arguments were removed on one side. The result is a position with which a number of unremoved arguments remain.[2]

2.2. DECISION AIDING APPROACHES

In the decision-making process, there are different approaches to problem solving, which depend on the profile of the participants in solving the problem. In this paper it

will be presented four basic approaches: normative approaches, descriptive approaches, prescriptive approaches and constructive approaches.
Normative derive models of rationality from a priori established norms. Such norms are an integral part of rational behavior and can refer to ethical, religious norms and laws. Deviation from these norms would result in errors in the decision-making process from a rational aspect. Models with a normative approach are universal and can be applied to help solve problems in any field.
Descriptive approaches derive models of rationality from the perspective of the decision makers themselves. These models are general and applicable to different types of decision makers who are making a decision on a similar type of problem.
Prescriptive approaches find models of rationality for a particular client by interpreting his answers to questions related to preferences. The model is based on the discovery of the decision maker's value system. Therefore, these models are not general, but closely adapted to a particular decision maker and the specifics of his problem.
Constructive approaches, similar to the previously described approach, derive models of rationality from the answers the decision maker gives to questions about preferences. Nevertheless, the "discussion" between the decision-maker and the analyst he addressed is not neutral, but is part of the decision-making process, forming a presentation of the problem with indications of a potential solution. In this approach, structuring and formulating the problem is as important as arriving at a solution.
Previously listed approaches can be divided into two groups. The first group consists of normative and descriptive approaches that are universal, use general models of rationality that are formed independently of the decision maker, while the second group consists of prescriptive and constructive approaches that adapt the model of rationality to the specific decision maker and the specific problem.
Normative and descriptive approaches differ in the process of model formation. Normative models are based on abstract economic facts, and descriptive models are based on empirical observation. The difference between prescriptive and constructive models is also, to a large extent, in the process of forming the model. Prescriptive approaches seek to reveal the value system that exists in the decision-maker himself, before considering the decision-making process. On the contrary, within the framework of constructive models, the existing value systems are not considered, but the decision-maker forms the value system during the formation of the model, noting that these two processes are mutually conditioned. [1]

2.3. BASIC ELEMENTS OF THE MULTI-CRITERIA DECISION MAKING MODELS

Although multi-criteria decision-making models differ from each other depending on what they are intended for, the same basic elements are recognized in the structure of each of them. The creation of each multi-criteria model begins with the definition of the problem, then the system of preferences is determined, a set of criteria is formed, and one or more outranking methods with a weighting system are determined. Each of these elements will be explained in Table 1.

Tab. 1 Preview of the basic elements of the multi-criteria decision-making models

<table>
<tr><td rowspan="13">Basic elements of the multi-criteria decision making models</td><td colspan="2">Defining a problem</td></tr>
<tr><td>Formulating a problem</td><td>Problem structuring</td></tr>
<tr><td>- to translate the decision maker's problem in decision support language into a "formal" problem so that decision support techniques and methods can be used in solving;
- the formulation of the problem directs the further steps of decision-making.[1]</td><td>- to find a suitable decision and/or evaluation model, based on the previously formulated problem;
- some of the well-known methodologies for structuring problems are: cognitive mapping, strategic choice, soft systems methodology, valued focused thinking, integrating approaches. [1]</td></tr>
<tr><td colspan="2">Preference detection system</td></tr>
<tr><td colspan="2">- recognition of the decision-maker’s preferences over the set of alternatives;
- detection of preference relation among alternatives previously evaluated according to certain dimensions;
- some of the preference detection systems with many variations:
pointwise evaluations on an ordinal scale, pointwise evaluations on an interval scale, pointwise evaluations on a ratio scale, interval evaluations on an ordinal scale, etc.[1]</td></tr>
<tr><td colspan="2">Criteria</td></tr>
<tr><td colspan="2">- different types of criteria and indicators according to which alternatives are evaluated;[1]
- three groups of criteria are recognised in multi-criteria decision-making models used in a field of architecture: general criteria and indicators, specific criteria and indicators determined by the type of adaptation and specific criteria and indicators determined by the specific context.[3]</td></tr>
<tr><td colspan="2">Outranking methods</td></tr>
<tr><td colspan="2">- aggregation methods used for creating a global preference relation which is based on pairwise comparisons of the alternatives;
- some of the outranking methods used in multi-criteria decision-making models are: ELECTRE, PROMETHEE, MAUT, TACTIC,etc.[1]</td></tr>
<tr><td colspan="2">Weighting system</td></tr>
<tr><td colspan="2">- determination of the relative importance of the different criteria using weights – non-negative numbers, which values are independent from measurements units of the criteria.[3]</td></tr>
</table>

3. THE MULTI-CRITERIA DECISION MAKING MODELS IN ARCHITECTURE

After basic steps in decision making process and structural elements of every multi-criteria decision making model, in this part of paper a brief review of nine multi-criteria decision making models used in architecture is presented.

3.1. THE CONVERSION METER MODEL

The *Conversion meter* model is intended to assess the potential for conversion of commercial buildings into permanent and temporary housing. The first version of the model was created at the end of the twentieth century in the Netherlands, when a large number of business buildings were out of use. The evaluation of the potential is done in several steps, through several lists of criteria, and each positive answer is worth one point. Value ranges are determined on a numerical scale that are linked to a certain level of potential of a business object for conversion. The specificity of this model is the use of "veto" criteria, which, if not met, stop further evaluation.[4]

3.2. THE TOBUS MODEL

The *TOBUS (Tool for selecting office building upgrading solutions)* model is the result of joint research by experts from several European countries (Denmark, France, Greece, Switzerland and the Netherlands) and was developed within the European research program JOULE III. It is intended to assess the current state of the business facility, on the basis of which a set of interventions for improvement is proposed. Essentially, the model has the ability to propose a large number of different scenarios and an analysis of the financial and energy aspects of the realization of a potential adaptation. In order to make it easier to use, the software of the same name was developed, which, initially, uses data related to the territory of Switzerland, but the structure of the software is designed so that it is possible to enter data relevant to other countries.[5]

3.3. THE XENIOS MODEL

The *XENIOS* model or methodology is a multi-criteria model intended to help in the decision-making process related to different scale of adaptations of hotels. The model offers a technical and economic assessment of potential interventions, taking into account the specifics of this group of buildings, while relying on experiences in the field of different types of adaptations of residential and commercial buildings. For potential users of the model, the software which is programmed to estimate the total costs of various scenarios - potential types of adaptation and to recommend related to improving the energy properties of buildings, installation of renewable energy sources can be obtained, was designed. Through special modules for assessing the sustainability of buildings and their impact on the environment, techniques are proposed for the rational use of energy.[6]

3.4. THE MEDIC MODEL

The *MEDIC* model is designed so that it can be used with the *EPIQR* model, which will be explained below. The model divides each object into fifty elements, and, through the use of four codes (which are also used in the *EPIQR* model) an assessment and description of the state of all elements of the object is performed. Based on the experience gathered by analyzing a large number of other objects and data related to a specific object, using the *MEDIC* model , the remaining "expected life" of the object can be calculated. The expected remaining duration of building elements is not only one of the criteria when choosing the type of adaptation, but also when evaluating the energy and environmental characteristics of the building. The above estimates are important when planning investments, since they allow the owner and/or investor to decide what is the most reasonable moment to start the adaptation of the building.[7]

3.5. THE EPIQR MODEL

The *EPIQR (Energy performance indoor environmental quality retrofit)* model is based on a detailed description of the object for which some type of adaptation is being considered. As described in the part with the *MEDIC* model, in the model, the building is divided into fifty elements such as facades, installation systems, etc. Each of the elements is described by one of the four degrees of degradation (represented through the codes discussed in the part about the *MEDIC* model). More than eight hundred potential descriptors are used to define the state of the object. The assessment of the potential for some kind of adaptation is considered through criteria that are grouped into four aspects: the quality of the interior space, the required amount of energy, potential costs and measures of subsequent equipment. The analysis of these aspects can help when choosing the optimal way to adapt the building.[8]

3.6. THE ARP MODEL

The assessment of the potential for the conversion of commercial to residential buildings using the *ARP (Adaptive reuse potential)* model is based on the consideration of the (temporal) moment in which the building is located in relation to its estimated useful life. In the model, first of all, the physical life of the object is evaluated, that is, the possibility of the object's duration as a physical structure, based on a list of criteria. The useful life, that is, the period in which the object is expected to be used for the purpose for which it was built, represents the physical life reduced by various factors. In this model, result is displayed graphically, through a diagram, and through a numerical scale within which the ranges of values associated with the specific potential of the business object for repurposing are determined.[9]

3.7. THE ADAPTSTAR

The *AdaptSTAR* model is a tool designed to assess the future adaptive potential of buildings under construction. The future possibility of the building adaptive reuse is considered as one of the key criteria during the process of building design. In order to check the adaptive reuse potential of the building, the *ARP* model will be used. The *AdaptSTAR* model is designed as a weighted checklist for different design strategies aimed at high-potential of buildings for future conversion. The list of criteria for the building design was compiled based on the assessment of professionals from the architectural profession. The model is based on the analysis of case studies, interviews with experts and surveys conducted among participants in the processes of adaptive reuse in practice.[10]

3.8. THE ICONCUR MODEL

The *iconCUR* model considers the potential of a business object for various types of adaptations, based on a set of criteria. The evaluation takes place through a diagram, which is designed as a spatial grid, the sides of which are different types of adaptations, and the object is positioned according to certain coordinates. The distance of the object from the sides of the spatial grid is measured. By using this model, it is possible to see the potential of several objects simultaneously or of one object over time. The specificity of this model is the establishment of a hierarchy among the criteria, which has an impact on the final result.[11]

3.9. THE PAAM MODEL

The *PAAM (Preliminary assessment adaptation model)* model is intended to assess the potential of business facilities for upgrading. This paper discusses the large number of criteria that are important for all types of adaptations and the way of establishing a hierarchy among the criteria. The selection of the criteria of this model, as well as the method of valorization, is based on statistical data collected by analyzing a large number of objects on which this type of adaptation was carried out, where the influence (in percentage) of each criterion on the final outcome is estimated, and the percentage share is determined by the mathematical method *PCA (Principle Component Analysis)*. Criteria that affect the object's potential for this type of adaptation to the same extent are ignored in all analyzed cases.[12]

4. DISCUSSION AND CONCLUSION

Multi-criteria models represent one of the formal forms of assistance in the process of solving problems in various fields. Through the analysis of the development of ideas on which multi-criteria decision making models are based, it can be concluded that the need for rationalization and formatting of thought processes and opposing views in the decision-making process existed long before the emergence of today's forms of models in this area.

The first part of the paper is generally aplicable for multi-criteria decision models intended for use in any field and presents the basic ways of thinking on which the logic of multi-criteria decision making models is based and the basic elements recognized in the structure of each of those models. Each of the elements has a number of variations, the combination of which provides the possibility of forming a multi-criteria decision making model that corresponds to the specifics of individual cases.

In the second part of the paper, an overview of multi-criteria decision making models used in different parts of the architectural field is presented. Some of these models are intended for choosing the best solution among the offered alternatives, others are focused on assessing the degree of suitability of one solution in a specific case. It was noticed that some of the analysed models were created together, within the same larger project and that they complement each other. This fact indicates the development of the idea of applying multi-criteria decision making models in architecture, and it is expected that the application of these models in the early stages of decision-making during the design process will greatly contribute to the quality of the final product - built environment.

ACKNOWLEDGEMENT

This research was done at the University of Belgrade – Faculty of Architecture, within the Research Laboratory: *Optimal lighting design in architecture*.

REFERENCES

[1] Bouyssou, D., Marchant, T., Pirlot, M., Tsoukias, A. & Vincke, P. (2006). Evaluation and decision models with multiple criteria. New York, Springer Science+Business Media, Inc.

[2] Koksalan, M., Wallenius, J. & Zionts, S. (2005). An Early History of Multiple Criteria Decision Making. In: Greco, S. (Ed.). *Multiple Criteria Decision Analysis: State of the Art Surveys.* Springer: London: New York. 3- 17.

[3] Nedeljkovic, D., Jurenic, T. & Djokic, L. (2023). Comparative analysis of multi-criteria models for decision-making in the process of building adaptation. *Heliyon* 9 (6), doi: 10.1016/j.heliyon.2023.e16620.

[4] Geraedts, R. P., Van der Voordt, T. & Remoy, H. (2018). Conversion Potential Assessment Tool. In book. S. Wilkinson & H. Remoy (Eds.), *Building Resilience in Urban Settlements through sustainable change in use* (121-151). Willey Blackwell.

[5] Flourentzou, F, Genre, J. & Roulet, C-A. (2002). TOBUS software – an interactive decision aid tool for building retrofit studies. Energy and Building 34: 193-202.

[6] Dascalaki, E. & Balaras, C. (2004). XENIOS – A methodology for assessing refurbishment scenarios and the potential of application of RES and RUE in hotels. *Energy and Buildings* 36 (11), 1091 – 1105.

[7] Flourentzou, F., Brandt, E. & Wetzel, C. (2000). MEDIC – A method for predicting residual service life and refurbishment investment budgets. *Energy and Buildings* 31 (2), 167 – 170.

[8] Jaggs, M. & Palmer, J. (2000). Energy performance indoor environmental quality retrofit – a European diagnosis and decision making method for building refurbishment. *Energy and Buildings* 31 (2), 97 – 101.

[9] Langston, C. (2014). Identifying Adaptive Reuse Potential. In. S.J. Wilkinson, H. Remoy and C. Langston. *Sustainable Building Adaptation: Inovation in Decision-Making*. Wiley Blackwell.

[10] Conejos, Sh., Langston, C. & Smith, J. (2012). AdaptSTAR model: A climate-friendly strategy to promote built environment sustainability. Habitat International 37, 95 – 103.

[11] Langston, C. (2014). Modelling Building Performance Using iconCUR. In. S.J. Wilkinson, H. Remoy and C. Langston. Sustainable Building Adaptation: Inovation in Decision-Making. Wiley Blackwell.

[12] Wilkinson, S.J. (2014). The preliminary assessment of adaptation potential in existing office buildings. *International Journal of Strategic Proprety Management* 18 (1), 77-87.

THE BUILDING HERITAGE OF DEPOPULATED RURAL SETTLEMENTS IN THE MUNICIPALITY OF CRNA TRAVA AS A PARAMETER OF THE REVITALIZATION MODEL

Olivera Nikolić[1], Ana Momčilović Petronijević[2], Mirko Stanimirović[2], Marko Joksimović[3], Vladan Nikolić[2]

Summary:

Crna Trava is a municipality in southern Serbia characterized by pronounced depopulation, as well as an unfavorable age structure of the population. The previous research determined the natural resources, economic and tourist potential, as well as the state of the infrastructure in the Municipality, on the basis of which four models of the revitalization of rural settlements in the Municipality were created. The villages of Zlatanci and Mlačište were highlighted as villages with the greatest potential for regeneration and economic development. In this paper, the building fund of Crna Trava Municipality, especially villages with revitalizing potential, was researched. After the analysis of residential architecture throughout history, a basic typology of residential buildings was made, and an assessment of the condition of the existing building stock was made through field research. The aim of the work is to determine the level of preservation of abandoned buildings and the possibility of their revitalization, as a basic parameter in the process of population return.

Key words: built heritage, depopulated settlements, revitalization, development

[1] PhD Student, Junior Teaching Assistant, Faculty of Civil Engineering and Architecture, University of Niš, Serbia, olivera.nikolic@gaf.ni.as.rs

[2] Assoc. prof., Faculty of Civil Engineering and Architecture, University of Niš, Serbia, ana.momcilovic.petronijevic@ gaf.ni.as.rs, mirko.stanimirovic@gaf.ni.ac.rs, vladan.nikolic@gaf.ni.ac.rs

[3] Assoc. prof., Faculty of Geography, University of Belgrade, Serbia, dellmare@gmail.com

1. INTRODUCTION

After the last population census conducted in 2022, the fact that there is a trend of continuous decrease in the number of inhabitants in Serbia is even more pronounced, primarily in rural areas. This phenomenon is most drastic in the mountainous rural areas of southern and southeastern Serbia. The poor demographic picture of the settlements causes the natural and economic potential of the municipalities to be underutilized, which stops the economic development of the region.

A team of scientists from Serbia composed of architects, civil engineers, geographers, mathematicians, economists and programmers gathered around the idea of using scientific methods to determine the revitalization potential of depopulated settlements, which would serve as a basis for incentive programs for resettlement.

In this work, which builds on previous research, and the results of which are applied to the case study of the Municipality of Crna Trava, the existing building stock of abandoned settlements with a pronounced revitalization potential will be investigated, with the aim of determining the number and condition of buildings and the level of interventions for returning them to their intended purpose and preservation of architectural heritage. The method of field recording, observation, historical and statistical methods, as well as the method of analysis and synthesis were applied in the work.

2. BACKGROUND

As one of the most sparsely populated municipalities, with many years of constant population decline, Crna Trava was chosen as a typical representative of municipalities with a large percentage of depopulated settlements. In the Municipality of Crna Trava, only 2 out of 26 settlements have more than 100 inhabitants, where one settlement is a town itself, and ten settlements have less than 10 inhabitants. The previous research on the topic of revitalization of depopulated settlements resulted in the establishment of a methodology for determining natural and economic potential, as well as a methodology for creating economic models of revitalization. The methodology was applied on the example of the Municipality of Crna Trava, and it, like the principle of creating the model, could also be applied to other depopulated rural settlements in the territory of the Republic of Serbia, with adaptation to specific cases [1][2].

In the Municipality of Crna Trava, it is possible to develop four economic models for the revitalization of populated areas - MODEL 1 based on animal husbandry and milk and meat processing, MODEL 2 based on forestry and processing of wood raw materials, MODEL 3 based on forestry and processing of non-wood forest products and MODEL 4 based on tourism (Fig. 1). In the town of Crna Trava, and the settlements of Darkovce and Gradska, models 2 and 3 are applicable, while economic revitalization in the settlements of Jovanovce and Bajinci can be realized according to model 1 and model 3.

The village of **Zlatance** in the southeast of the municipality and **Mlačište** in the southwest of the municipality stood out as places with a particularly strong economic potential because three models of revitalization can be developed in them, model 1, model 3 and model 4.

A previous survey determined that there are 2,959 households with at least one residential building and one or two auxiliary buildings in the area of Crna Trava Municipality [sa barem jednom stambenom zgradom i jednom ili dva pomoćna objekta [3]. Among them, 2,043 residential buildings are used occasionally, while 312 of them are uninhabited or abandoned. Of the total number of residential buildings, very few are in permanent use. The largest percentage is made up of those that are used occasionally, mostly during the summer months, as holiday homes.

In addition to unused natural resources and economic potential, in a village that loses its inhabitants, buildings that have been created by generations remain. Abandoned households, first of all residential buildings, but also objects intended for the economy such as stables, mills, barns, granaries become an unused building fund that collapses together with the infrastructure and the economy. This trend follows a decrease in the number of inhabitants and results in a decline in economic activity in the area [4].

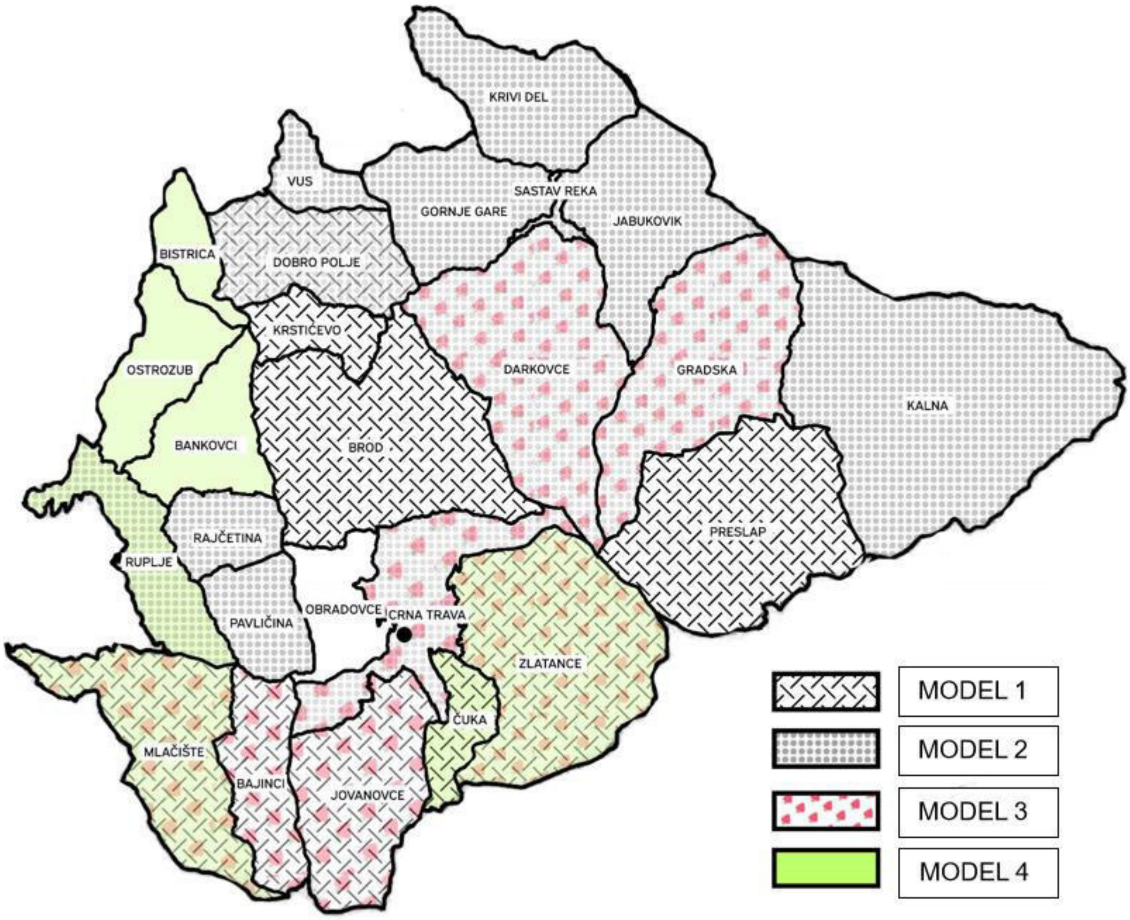

Fig. 1 Rural settlements of Crna Trava Municipality with applicable models of revitalization [2]

In this paper, which continues directly on the aforementioned previous research [1][2], an analysis of the condition of buildings in the villages of Zlatance and Mlačište, as villages with the most potential for revitalization, is carried out, in order to determine the type and level of intervention needed to the buildings themselves are revitalizing and returning them to the function of housing.

3. RESEARCHED AREA

Crna Trava is a small municipality in southern Serbia. Administratively, it borders with several municipalities - Babušnica, Vlasotince, Leskovac, Vladičin Han and Surdulica, as well as the neighboring country of Bulgaria. The mountainous environment has contributed to the fact that the Municipality of Crna Trava, apart from extending along the border and having a peripheral position, is naturally isolated from the rest of Serbia [5].

It belongs to the Jablanica district, from the center of which, Leskovac, is 66 km away. The only important traffic connection is the road to Leskovac via Vlasotince and Surdulica, which connects it to the Niš-Skopje motorway. Except for this road, it is traffic-isolated in relation to other road corridors.

It covers an area of about 300 km2. It is located in the upper and middle course of the Vlasina River, surrounded by the Grdelica Gorge and the South Morava Valley from the west, the branches of the Suva Planina from the north, the Serbian-Bulgarian border from the east, and Mount Vardenika and Vlasina Lake from the south.
The reason for the research in the area of this municipality is a very bad demographic picture. According to the data of the Statistical Office [6][7], the number of inhabitants of this municipality, during the second half of the 20th century, is decreasing alarmingly fast, and the municipality is on the verge of disappearing in a demographic sense (Fig 2). A little more than 10% of the population that lived there 50 years ago lives in the municipality now.

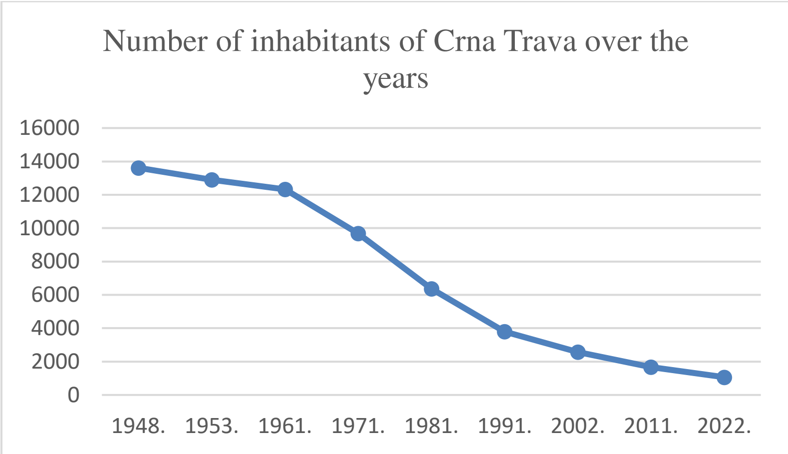

Fig. 2 Graphic representation of population decline over the years

4. DEVELOPMENT OF HOUSES IN THE RESEARCHED AREA

On the territory of Serbia, there are rural areas that have not been sufficiently explored in the context of architecture and rural development. Although it is known what type of settlements, housing and houses exist, the specifics in the establishment and development of these rural areas and agglomerations have been poorly researched. Those specificities have influenced their current character and important differences compared to similar areas, which makes them special and sets them apart from existing divisions and classifications [8]. One of these under-researched areas is the area of Crna Trava Municipality.
The type of a house that is built is determined by the way of life, the degree of development of technique and technology, the available building materials, and many factors that directly or indirectly influence the development of the construction[9]. The most common division that can be found among the few authors who have been engaged in researching the architecture of this area is into buildings that were built:
• up to 1830 (period I),
• in the period from 1830 to 1878 (period II),
• in the period from 1878 to 1914 (period III),
• in the period between the two world wars (period IV) [10]
• in the period after the Second World War (period V).
The houses of **the first period** were one-room huts, with mud-plastered wicker walls, a hearth in the middle of the house, and a thatched roof. In some households, such huts also had the function of a barn. There are no such buildings preserved in the territory of Crna Trava Municipality.
The second period is characterized by the appearance of post and petrail system of building, which appears here with a delay compared to Pomoravlje [11]. The buildings are still one-room, with the hearth retaining its central position. More complex objects, with a "house" and a room, appear less frequently. Straw as a roof covering was the

most common in this period. The construction of this type of a house remains until the liberation from the Turks. Buildings constructed in this period are no longer present either.

The period from 1878 to 1914, i.e. from the liberation of southern Serbia from the Turks to the beginning of the First World War, is the most significant in terms of the architectural heritage that was created in it, and the new tendencies that were developed in it, in the chronology of the development of houses in this part of Serbia [8].

The most dominant type of a house was the post and petrail type with a wooden skeleton and some kind of infilling. The most common type is the one where hewn crossbars were nailed over the wooden frame. The space between was filled with mud mixed with chopped straw. The walls were also covered with mud on both sides. If they were built on the sloping ground, the lower part was built with stone and used as a basement. Instead of straw, the roof covering becomes tiles. Four-gable roofs predominate, which later received the four-gable incised or three-gable variant. In contrast to the Moravian type of the house, whose basic design element was the porch, the porch is rare in the researched area. Apart from post and petrail houses, brick houses were also built to a much lesser extent.

In a functional sense, in this period, in lower and more developed areas, the creation of houses with additional rooms next to the main house began noticeably. This type of architectural concept arrived in these parts through seasonal migrations, which influenced the development of local houses in a similar order as in already developed areas. [9].

The appearance of the so-called "dunđer" houses, known as “the house in the shape of letter L” brought a certain interruption and stagnation in the development and design of traditional houses in the countryside of this area. This style of construction deviated from the traditional forms and patterns that previously existed in rural areas. This phenomenon, which appeared at the beginning of the 20th century, had a greater impact on the development path of the local house than some generally recognized social processes, such as the First World War.[8]

The oldest buildings that can still be found in the villages come from this period.

The period between the two world wars is characterized by significantly more frequent construction of brick houses. Houses with more rooms are being built. Seasonal working as a characteristic of this region, caused a more intense movement of people to various parts of the country, who, returning home, applied the old type of house construction with innovations in construction, number of rooms, appearance, use of new details. In a word, the culture of housing and the way of life in the countryside strive to reach the urban way of life. Unfortunately, the brick country houses of that period began to fall under the influence of construction in cities, which brought qualitative changes to their appearance. Houses began to lose their local authenticity, being built with less and less pronounced characteristics that were inherent to the area, houses with a weaker overtone of the local features [9].

The period after the Second World War is characterized by the construction of buildings that have largely lost the traditional elements characteristic of country houses. The country house now to a certain extent imitates the city house, often the one from remote areas [12] More often houses were built in the shape of the Cyrillic letter G, letter P or even letter T. Builders who, building in larger towns or the outskirts of larger towns, accept architectural elements of that space and transpose them into their village [13]. The positive aspect of the influence of modern architecture is reflected in the functionality and furnishing of buildings, primarily in the inclusion of sanitary facilities in buildings. On the other hand, the style characteristic of the country house is slowly being lost.

A comparative analysis of the development of a country house in Crna Trava Municipality with the development of a house in Pomoravlje leads to the knowledge that the functional development of a country house in these areas is delayed, in the first stages of research, by more than fifty years compared to Pomoravlje. Over time, the houses in Crna Trava slowly catch up with the houses in the Pomoravlje area, and in the later researched periods this delay is drastically less.[9]

Today, the picture of the building fund is mostly a picture of the later stages of development, with a lot of elements of city architecture.

5. THE BUILDING FUND OF ZLATACE AND MLAČIŠTE VILLAGES

The research on the ground of the building fund of the targeted settlements Zlatance and Mlačište was carried out at the beginning of September 2023. On that occasion, residential and auxiliary buildings within one household were recorded, while for residential buildings, the period of construction was determined, that is, the age of the building was assessed, structural and facade elements, primary and secondary elements of the building were inspected, the damage was determined, the possibility of returning the building to its intended purpose was assessed or the possibility of conversion. Adaptations and reconstructions were also recorded. All auxiliary objects in the household were also recorded, in order to be taken into consideration for possible conversion. The access to the interior of the buildings was not possible in most households because the owners were not found, therefore this research did not record the layout of the functional units. The questionnaire for assessing the condition and quality is shown in Table 1.

Tab. 1 The questionnaire used in the field research

settlement															
Hamlet/mahalla															
The owner of the household															
		storey	**Condition of the primary elements**			**Condition of the seconda.elements**		**Facility maintenance**		**Living conditions**			**Housing**		
			walls	roof	staircase	windows	doors	original state	adapted	good condition	necessary adaptation	collapsed	permanent	temporarily	abandoned
number of residential buildings															
number of economic buildings															

The village of Zlatance is located in the south of Crna Trava municipality and borders the town on the west side. The average altitude of the village is 1480m. It is of a scattered type and made up of hamlets or mahallas, whereby the field surveys of the building fund included the mahallas in bold letters: **Vujinci, Čurčisci, Čukurusci, Barkinci, Blatarci**, Ćosinci, Gornji Slavkovci, Gornji Strumićevi, Donji Strumićevi, **Dubisci, Makinci, Vesinci, Golusci**, Popadisci, **Lulinci**, Čauševi, Leponjci, Vidićevi, **Samokov**. The town of Crna Trava is only connected to the nearest hamlets by an asphalt road, while the more distant hamlets can be reached by an unpaved, dirt road, which has been damaged by torrential waters in several places. Certain villages can only be reached by off-road vehicles or on foot. The nearest store is in Crna Trava. The school building is not in the function of education.

The demographic decline in the village, as well as in the Municipality, was continuous, and today only 49 inhabitants live in the village. According to the latest census, the village has 220 residential units with a total area of 10,771 m2, of which 30 are inhabited, two are abandoned and 188 are occasionally inhabited. [3]

Tab. 2 Data from the field survey of the rural settlement Zlatance

settlement	**Hamlet/mahalla**	**Number of households**	**Number of residential buildings**	**Number of economicbuildings**	**Condition of buildings**		**The quality of the residential building**			**Housing**		
					original condition	adapted	good condition	necessary adaptation	collapsed	Permanently inhabited	temporarily in use	abandoned
Zlatanci – in tottal	19	207	220	128								
Number of recorded objects	10		121	50	72	49	71	37	11	11	85	25
	Vujinci	**15**	**15**	**19**	**10**	**5**	**8**	**3**	**4**	**4**	**7**	**4**
	Čurčisci	**19**	**20**	**7**	**15**	**5**	**10**	**7**	**3**	**1**	**15**	**4**
	Čukurusci	**11**	**11**	**5**	**9**	**2**	**4**	**7**	**0**	**0**	**11**	**0**
	Barkinci	**5**	**6**	**1**	**5**	**1**	**2**	**2**	**2**	**0**	**3**	**3**
	Blatarci	**5**	**5**	**2**	**2**	**3**	**4**	**1**	**0**	**1**	**4**	**0**
	Ćosinci	6	6	5								
	Gornji Slavkovci	8	8	0								
	Gornji Strumićevi	10	11	5								
	Donji Strumićevi	10	10	6								
	Dubisci	**12**	**12**	**1**	**8**	**4**	**8**	**4**	**0**	**3**	**9**	**0**
	Makinci	**9**	**11**	**3**	**4**	**7**	**7**	**3**	**1**	**0**	**8**	**3**
	Vesinci	**8**	**8**	**3**	**4**	**4**	**7**	**1**	**0**	**0**	**7**	**1**
	Golusci	**11**	**12**	**2**	**7**	**5**	**9**	**3**	**0**	**0**	**6**	**6**
	Popadisci	39	43	42								
	Lulinci	**15**	**16**	**2**	**6**	**10**	**10**	**5**	**1**	**1**	**11**	**4**
	Čauševi	12	13	14								
	Leponjci	6	7	4								
	Vidićevi	1	1	2								
	Samokov	**5**	**5**	**5**	**2**	**3**	**4**	**1**	**0**	**1**	**4**	**0**

In the field, 121 residential buildings and 50 economic buildings were recorded, in 10 hamlets out of a total of 19. According to information collected in the field, from residents in 11 permanently inhabited buildings, the number of abandoned buildings is higher than that shown in the census books. Of the 121 recorded, 25 are abandoned, while 85 are used occasionally. 71 buildings are suitable for living, and adaptation is recommended for 37 of them. 11 buildings have completely collapsed (Table 2). The percentage values are shown in Chart 1.

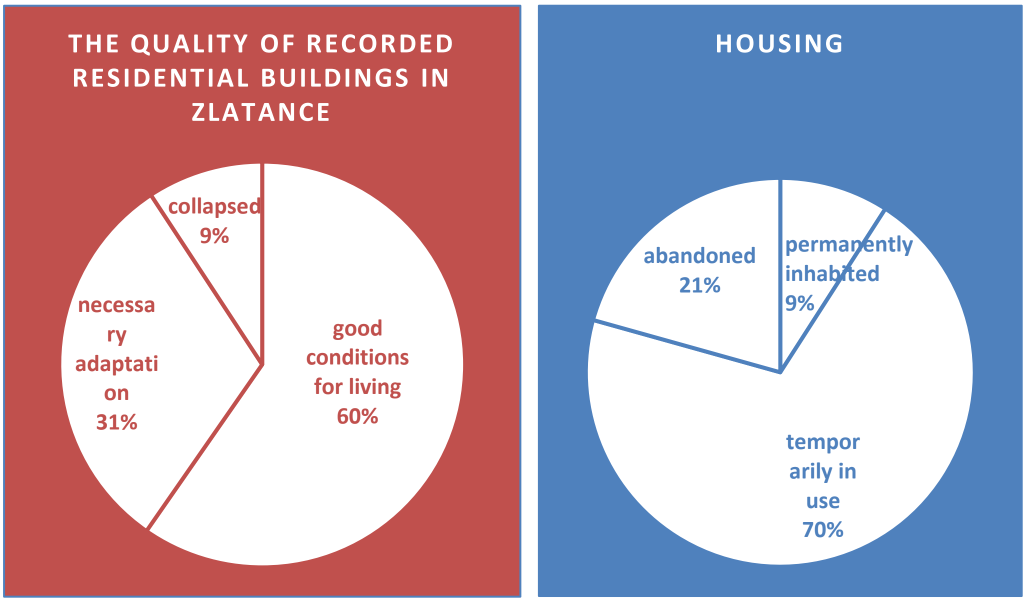

Chart 1 Percentage data from the field research Zlatanci

It has been noted that the damage to the buildings starts from the roof structure, and then it is transferred to the walls, until it completely collapses, as in the example of the "L" shaped warehouse in the hamlet of Čurčišci (Fig. 3) or the abandoned, brick building at the end of the street in the same hamlet (Fig. 3).

Fig. 3 The damage to buildings in the mahalla of Čukurusci

Due to the non-maintenance of abandoned residential and economic buildings, the replacement of elements of the roof structure and roof covering is required. In most buildings, even those built after 1980, it is necessary to replace secondary elements such as windows and doors, as well as the arrangement of facade coverings (Fig. 4).

Fig. 4 Examples of buildings where replacement of secondary elements is necessary in the mahallas of Vujinci, Golusci, Makinci, Barkinci

The hamlet of Čukurusci stands out as an architectural unit with preserved post and petrail houses on a stone wall and as such could be used for the purpose of promoting ethnic tourism. The advantage of this hamlet is the asphalt road that connects it to Crna Trava, it is located on the southern slope, a mountain stream with drinking water flows through the gardens (Fig. 5).

Fig. 5 Architectural ensemble of buildings in the hamlet of Čukurusci

Another prominent architectural unit can be found in the hamlet of Lulinci. It is characterized by residential buildings with elements of urban architecture built between the two wars. There is a public fountain in the central part of the village. Objects of larger dimensions dominate compared to objects found in other mahallas. They were built on the extremely steep terrain. The lower level, the basement, was built with hewn stone that is flat pointed on the outside. The residential, higher floor, is accessed from a higher ground level. This part is built of solid brick, with prominent pilasters at the corners. The final treatment of the pilasters is either facade brick, while the space between the pilasters is plastered, or horizontal flutings that imitate masonry with hewn stones. Around the windows, architectural stucco is present on some buildings. In one building, an unusual window treatment in the form of double arches was observed at the level of the attic space. The roof cornice is not decorated (Fig. 6).

Fig. 6 Examples of buildings in the hamlet of Lulinci

The village of Mlačište is located southwest of the municipality, on the gentle slopes of Čemernik, facing the Grdelica gorge, at an altitude of 1100-1300m. It is 16 km away from Crna Trava, which is the nearest place for supplies. Only 3 km of the state road 232 Crna Trava - Predejane are asphalted, the rest is crossed on an unpaved road, through the forest. The village consists of 8 hamlets connected by a damaged and unpaved road. Houses in hamlets are built at a short distance, and the gardens are small.
In the village of Mlačište, according to the data of the Statistical Office, there is a total of 93 residential units, with a total area of 7361 m2, 6 of which are inhabited, two are temporarily uninhabited, 3 are abandoned and 82 residential units are used occasionally, during vacations. Two occupied business premises were also recorded.[3]
During the recording in the field, it was observed that there are 93 households and 102 residential buildings, while the number of economic buildings is significantly smaller, only 32 (Table 3). The reason is reflected in the fact that there are 38 abandoned buildings in the village, 62 are used occasionally, and only 2 are permanently inhabited, one of which is a school building, adapted for housing needs of one family and one single person. The percentage values are shown in Chart 2.
The village of Mlačiška mehana stands out as a whole with the potential for the expansion of the village. This hamlet is located on a wide plain and is surrounded by pastures. Several types of houses can be found in the architecture of residential buildings, from 19th-century post and petrail houses to modern residential houses. The yards are spacious. There is also a school building in the hamlet, which is currently used for residential purposes. Mountaineers and nature lovers have at their disposal a wagon shelter with water and a solar source of electricity on the plot (Fig 7).

Tab. 3 Data from the field survey of the rural settlement Mlačište

settlement	**Hamlet/mahalla**	**Number of households**	**Number of residential buildings**	**Number of economic buildings**	**Condition of buildings**		**The quality of the residential building**			**Housing**		
					original condition	adapted	good condition	necessary adaptation	collapsed	Permanently inhabited	temporarily in use	abandoned
Mlačište – in tottal	8	93	102	32								
Number of recorded objects	8	93	102	32	51	51	57	34	11	2	62	38
	Mlačiške meane	**18**	**19 +school +wagon**	**6**	**16**	**5**	**9**	**8**	**4**	**1**	**13**	**7**
	Vitel	**1**	**1**	**0**	**0**	**1**	**1**	**0**	**0**	**0**	**1**	**0**
	Miljkovci	**20**	**20**	**8**	**12**	**8**	**9**	**9**	**2**	**0**	**8**	**12**
	Najdina bara	**1**	**1**	**1**	**1**	**0**	**0**	**1**	**0**	**0**	**1**	**0**
	Paunovci	**15**	**16**	**9**	**7**	**9**	**10**	**5**	**1**	**0**	**9**	**7**
	Radivljovci	**16**	**17**	**4**	**7**	**10**	**10**	**6**	**1**	**0**	**10**	**7**
	Kukulinci	**16**	**18**	**2**	**6**	**12**	**12**	**3**	**3**	**1**	**13**	**4**
	Kamenjari	**6**	**8**	**2**	**2**	**6**	**6**	**2**	**0**	**0**	**7**	**1**

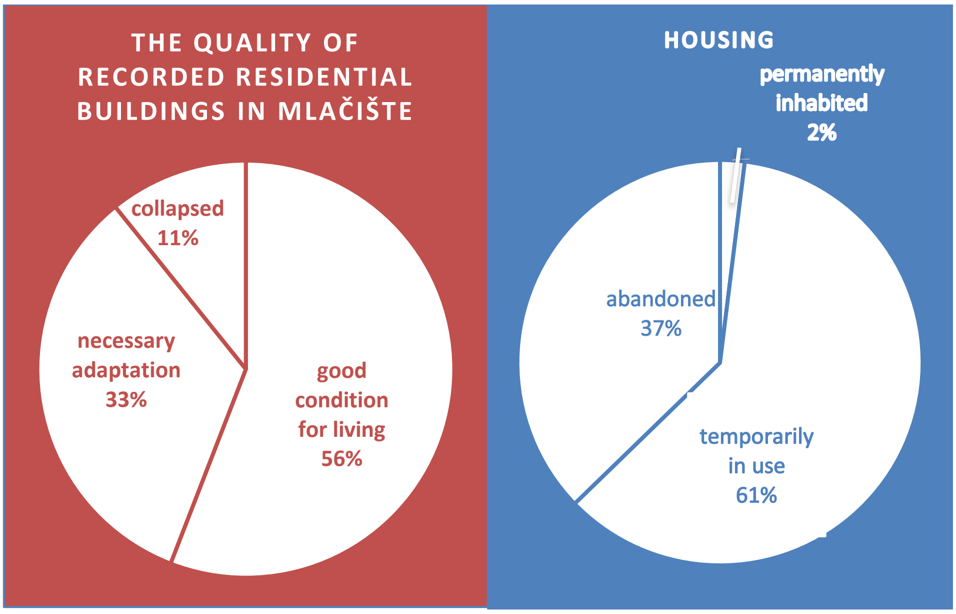

Chart 2 Percentage data from the field research Mlačište

Fig. 7 Examples of buildings in the hamlet Mlačiške meane

6. DISCUSSION

Both investigated villages have a significant building fund that is not in constant use. According to the typology, residential buildings could be classified into two types: post and petrail houses and brick buildings.

The villages of Zlatance and Mlačište differ in their location and position in relation to the administrative center of the Municipality. Zlatance is a scattered village with distant hamlets surrounded by a forest, on very steep slopes, but close to the town. Mlačište is further away from the center of the Municipality, there are fewer hamlets that are close and interconnected. The natural environment is more gentle, even the hamlet of Mlačiška mehana is on a wide plain. In terms of the quality of the recorded residential buildings, these villages are almost indistinguishable. On average, 58% of existing residential buildings are conditionally livable, in 32% it is necessary to carry out a certain intervention regarding the roof and roof structure, very rarely on the load-bearing walls, in order for the buildings to be functional again. On average, 10% of residential buildings are completely or partially collapsed and economically unprofitable for any adaptation (Chart 3).

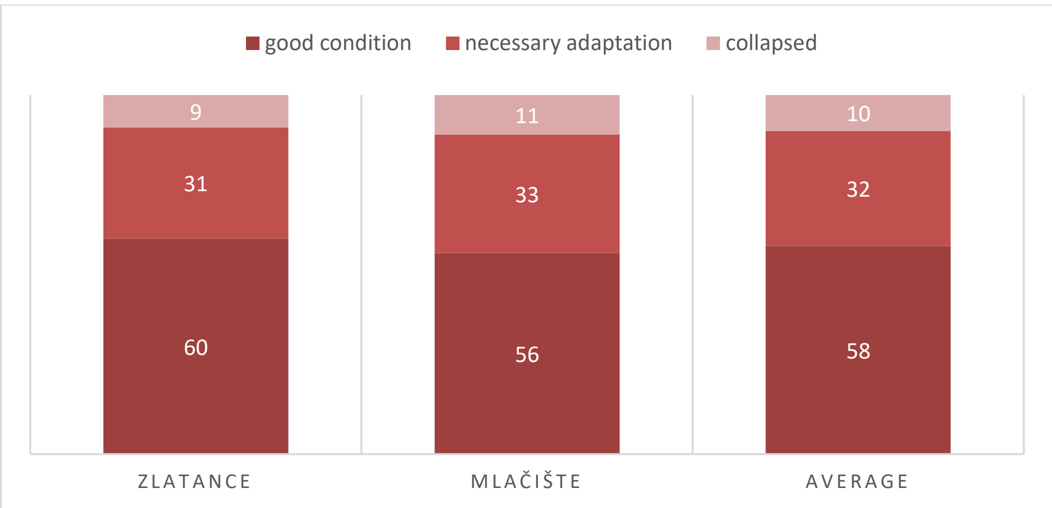

Chart 3 The quality of recorded residential buildings

A significant difference is observed in terms of the percentage of facilities used. As the village of Mlačište is on the verge of extinction, far from the source of supply of basic foodstuffs, with poor road infrastructure, the difference in the percentage of permanently inhabited, occasionally inhabited and abandoned buildings is not surprising (Chart 4).

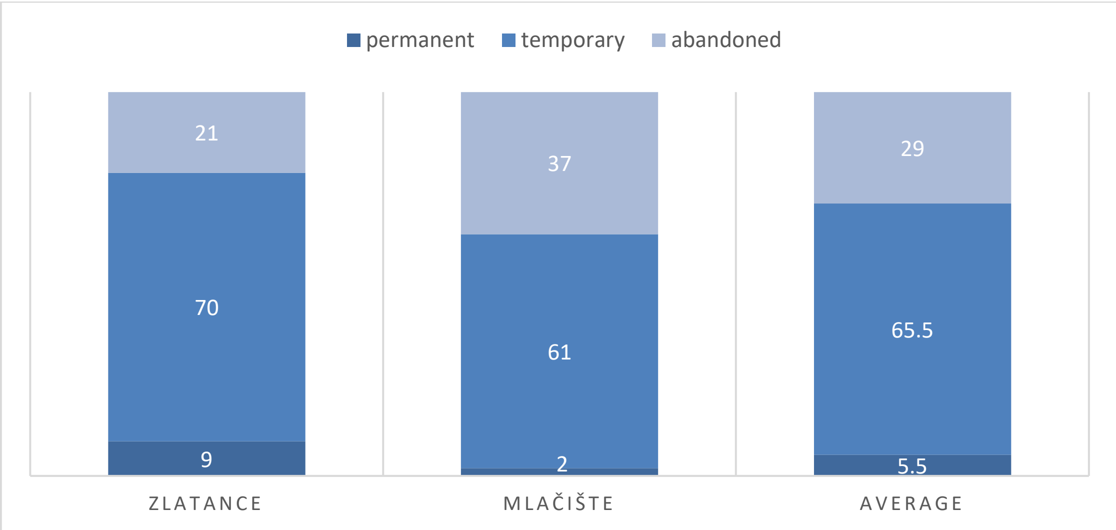

Chart 4 Housing in recorded buildings

The oldest types of buildings that can be observed in the researched area, and at the same time the buildings with the most pronounced stylistic characteristics of traditional architecture, are buildings created before the First World War. Most of the buildings were built between the two wars, but there are also more recent buildings. In Zlatanci, out of 121 recorded buildings, only 9 are post and petrail houses, the other 112 are brick-built. In Mlačište, out of 102 residential buildings, 13 are post and petrail houses, and 89 are brick. Whether it's wooden structures or masonry structures, they are found to be deteriorating due to lack of maintenance. Partial or complete falling off of the mud plaster from individual walls is characteristic of post and petrail houses. Due to the effect of moisture, the wood swells and dilatations occur that the mud plaster cannot accept, and it cracks, crumbles and falls off. In this way, the structural wooden elements remain exposed, even more exposed to the weather, and eventually rot, causing significant structural damage. Minor damage to the facade plaster was noted on the brick buildings, mostly on the corners of the buildings, most often caused by the effect of water falling from the eaves. It is interesting that no damage was found in the foundation walls, which were built of stone, on the steep terrain. The skill of the builder is also reflected in the foundation buttresses that were placed on some leveled locations, perhaps as a precaution. (Fig 8).

Fig. 8 Strengthening of buildings, Paunovci and Lulinci hamlets

In the buildings that collapsed, the damage started from the roof structure, and due to lack of maintenance, it spread to the walls.
Houses that are inhabited permanently or occasionally have most often undergone certain adaptations and reconstructions, whether it is structural repairs and reinforcements, or there was a need to expand the living space, which is the more frequent case. The problems that arise in this case are of an aesthetic nature.
Aesthetic problems, which could not be subsumed under devastation, and greatly impair the visual identity, often arise from the inadequate implementation of inappropriate small and large plastic elements, subsequently installed and not in harmony with the original architecture. Inadequate "collage" of elements belonging to various time and architectural instances are common and create the impression of visual and architectural chaos (Fig 9).

Fig. 9 Subsequent additions to the buildings

As expected, the buildings built after the Second World War are in the best condition, they require the least investment in renovation, but at the same time have the least features of traditional architecture characteristic of these areas.

Fig. 10 Multi-owner buildings

The appearance of different treatment of multi-ownership buildings was observed. In Mahalla Lulinci in the village of Zlatanci, half of the building has been adapted, it even contains added elements (the originally missing toilet), while the other half is in its original state. It is similar with the house in the hamlet of Miljkovci, in Mlačište. The village of Vijunci in Zlatanci is perhaps even more illustrative of this phenomenon. Half of the building is permanently inhabited, while the other part is completely demolished. (Fig 10).

Only every third household has an economic facility in its yard. Those that have survived are generally in good condition and show us information about the different construction techniques and materials used for their construction (Fig 11).

Fig. 11 Economic facilities in the hamlets Miljkovci, Radivoljovci and Vesinci

7. CONCLUSION

Both villages, which were the subject of the research, in addition to the natural and economic potential, which were a prerequisite for the conducted field research, have a housing fund as a parameter for the successful implementation of settlement revitalization procedures. Newly inhabited population in 58% of the existing housing stock would have basic conditions for housing, and 32% of the existing housing facilities could be used for housing again with minimal construction interventions. The damage that was observed on the buildings is mainly on the plaster coating, roof covering, secondary elements of the building, less often constructive, and their rehabilitation would not represent a significant problem. The lack is road infrastructure, the outdated electricity grid in the village of Mlačište and the distance from facilities for supplying basic foodstuff.

In addition to assessing the condition and quality of residential buildings, the research also included economic buildings. They are two thirds less than residential ones. The existing abandoned barns, granaries and storerooms are generally in good condition and with minimal interventions could once again become facilities for accommodation and care of animals, or could have another purpose under certain conditions.

In terms of architectural values, it would be good to preserve: 6 post and petrail houses in the hamlet of Čukurisci in the village of Zlatanci, which form one ambient unit, buildings with elements of urban architecture built between the two wars in the hamlets of Golusci and Lulinci in the same village. In Mlačiške mehane, it is necessary to preserve the construction technique, the shape and the number of floors of the buildings. An example of good practice is revealed in the hamlet of Paunovci, where the facilities have been adapted in such a way that the layout and purpose of the room adapt to the needs of modern comfort, without damaging the appearance of the facade plastic and without changing the authentic appearance of the facade planes.

REFERENCES

[1] Momčilović Petronijević A., Nikolić O., Stanimirović M., Joksimović M., Nikolić V. (2023). Development of the revitalization model of depopulated villages on the example of the Municipality of Crna Trava – part I. *International Conference Synergy of Architecture & Civil Engineering SINARG 2023,* Science and Technology Park, Niš, Serbia, 14-15 September, pp. 22-22.

[2] Momčilović Petronijević A., Nikolić O., Stanimirović M., Joksimović M., Nikolić V. (2023). Development of the revitalization model of depopulated villages on the example of the Municipality of Crna Trava – part II. *International Conference Synergy of Architecture & Civil Engineering SINARG 2023,* Science and Technology Park, Niš, Serbia, 14-15 September, pp. 22-22.

[3] Republički zavod za statistiku, Podaci popisa 2022 - Broj i površina stambenih jedinica https://publikacije.stat.gov.rs/G2023/Pdf/G20234002.pdf (30.08.2023.)

[4] Mitrović, M. (2015): Sela u Srbiji, promene strukture i problemi održivog razvoja (Popis stanovništva, domaćinstava i stanova 2011. Popis poljoprivrede 2012.) Republički zavod za statistiku, Beograd.

[5] Strategija održivog razvoja 2013-2018 Opštine Crna Trava https://www.opstinacrnatrava.org.rs/assets/strategija-razvoja-op%c5%a1tine-crna-trava.pdf (30.08.2023.)

[6] Uporedni pregled broja stanovnika 1948,1953,1961, 1971, 1981, 1991, 2002. I 2011. https://pod2.stat.gov.rs/ObjavljenePublikacije/Popis2011/Knjiga20.pdf (09.06.2023.)

[7] Republički zavod za statistiku, Podaci popisa 2022 – Nacionalna pripadnost https://publikacije.stat.gov.rs/G2023/Pdf/G20234001.pdf (09.06.2023.)

[8] Videnović A. (1996). *Crna Trava, život, kriza i nada*. Zaduzbina Andrejević, Beograd.

[9] Momčilović Petronijević A. (2010). Razvoj seoske kuće u jugoistočnoj Srbiji na primeru triju opština. *International Conference PhIDAC2010,* Novi Sad, Serbia, pp. 181-188.

[10] Bogojević V., Milošević Č., Tomić B. (1987). *Kalna crnotravska*. IRO Gradina, Niš..

[11] Simonović S. (1983). *Pečalbarstvo i neimarstvo crnotravskog kraja*. SIZ kulture Crna Trava, Crna Trava.

[12] Ćirić J. (1979). *Osnove sociologije naselja i sociologija sela*. Gradina, Niš.

[13] Momčilović Petronijević A., Vasić Č., Bjelić I.: Traditional Architecture in the Context of Preserving the Traditional Values, *International Scientific Conference Tradition, Modernization, Identities 2: The Traditional and the Modern in the Culture of Serbian and the Balkan Nations*, Niš, pp. 611-618.

PLANNING OF WORKPLACE LIGHTING

Dragan Hristovski[1]

Summary

The quality of lighting in the workplace can have a significant impact on productivity. With adequate lighting, workers can produce more products with fewer errors, which can lead to a 10-50% increase in productivity. All sources of light have a particular colour. Some of these, such as sodium, can make coloured text and diagrams difficult to read. Sudden contrasts in light levels eg coming out of a well-lit area into a dark area or vice versa can be a problem because it takes the eye several seconds to adapt to new lighting conditions. In general, workrooms should have enough free space to allow people to move about with ease. Whether in industrial or office settings, proper lighting makes all work tasks easier. People receive about 85 percent of their information through their sense of sight. Appropriate lighting, without glare or shadows, can reduce eye fatigue and headaches; it can prevent workplace incidents by increasing the visibility of moving machinery and other safety hazards.

Key words: Planning, Lighting, Productivity, Quality, Safety and Health, Continuous Improvement

[1] MSc. Industrial Engineering, Expert consultant, Occupational Safety Association 28 April, Skopje, N.Macedonia, vestak.hristovski@gmail.com

1. INTRODUCTION

Good lighting can reduce errors by 30-60%, as well as reduce eye strain and the headaches, nausea, and neck pain that often accompany eye strain. Adequate planning lighting allows workers to better concentrate on their work, which increases productivity.
Good lighting in the workplace means:

- reduced risk of accidents at work and health problems;
- better concentration and accuracy in work;
- a brighter, cleaner workplace that results in a more active, cheerful environment;
- improved work performance;
- better visibility, improved accuracy and increased work speed, which increases production.

Here are some low-cost measures that promote a safe work environment, reduce workload and increase productivity. These measures are easily implemented in small and medium-sized enterprises.

1.1. MAKE THE MOST OF DAYLIGHT

Natural lighting is most effective in improving lighting. Using daylight improves morale and is free. Examine the workplace layout, material flow and worker needs, then try these tips on how to make the most of daylight:

- provide skylights, for example by replacing roof panels with transparent ones;
- equip the workplace with additional windows;
- place machines near windows;
- move works that require more light near windows.

1.2. CONSIDER THE FOLLOWING BEFORE PLANNING AND INSTALLING WINDOWS AND SKYLIGHTS:

- Consider the height, width and position required for windows or skylights. More light is available when the window is placed high on the wall;
- Install blinds, screens, louvres, canopies or curtains on windows and skylights to protect the workplace from outside heat and cold while taking advantage of natural light
- orient skylights and windows away from direct sunlight to obtain constant, but less intense light;
- point the skylights and windows towards the sun if the variations in the brightness levels during the day do not disturb the workers;
- avoid storing or placing flammable liquids in direct sunlight as the increase in solar heat can cause the liquid to evaporate and increase the risk of fire.

Illumination level and illumination uniformity refer to maintaining the minimum average illuminance required to perform a specific task in a work area [1].
The nature of the light source, the position and height of installation, the type of lamp and the distribution of light determine the quantity, quality and uniformity of lighting in the workplace. Research shows that the right lighting level and uniformity improve visual perception and reduce signs of fatigue, including eye pain and headaches [2].
Light has a dual nature. It appears as both a wave and a particle, and the wavelength of light determines the colour that the eye registers. In the visible region ranging from ≈380 nm to 780 nm, short wavelengths between 380 nm and 500 nm are considered violet and blue light [2]. Photons in this region have high energy, and it is known as high-energy visible light.
Epidemiological evidence shows that people who work night shifts have a higher incidence of cancer and a higher rate of breast cancer among the female population, especially in industrialized countries [3]. Metabolic syndrome, osteoporosis, bone

fractures, reduced sleep quality, increased body weight, and higher prevalence of cardiovascular disease [5] are also among the health effects caused by inadequate light exposure. The effect of these symptoms in the critical phase increases the susceptibility of individuals to diseases [6], mental and psychological discomfort and job dissatisfaction and thus reduces productivity and work efficiency [4].

2. WHAT ARE THE BASIC TYPES OF ARTIFICIAL LIGHTING?

There are three basic types of lighting:

2.1. GENERAL LIGHTING

General lighting provides fairly even lighting. An example would be ceiling fixtures that illuminate large areas.

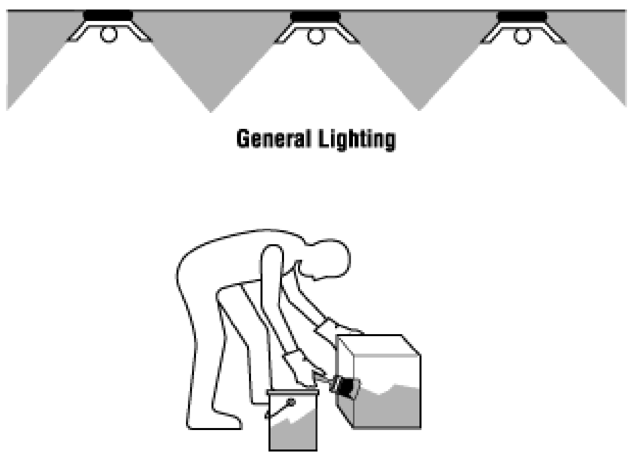

Fig. 1 General lighting [7]

2.2. LOCALIZED LIGHTING

Localized general lighting uses overhead fixtures in addition to ceiling fixtures to increase lighting levels for specific tasks.

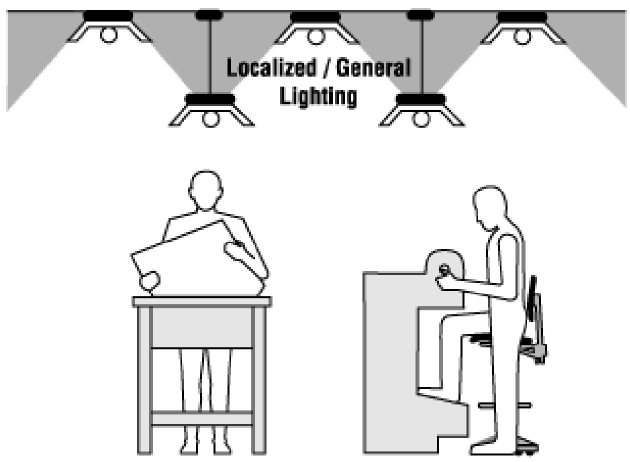

Fig. 2 Localized lighting [7]

2.3. LOCAL LIGHTING

Local (or default) lighting increases light levels in the workplace and immediate surroundings. Local lighting often allows the user to customize and control the lighting and provides flexibility for each user.

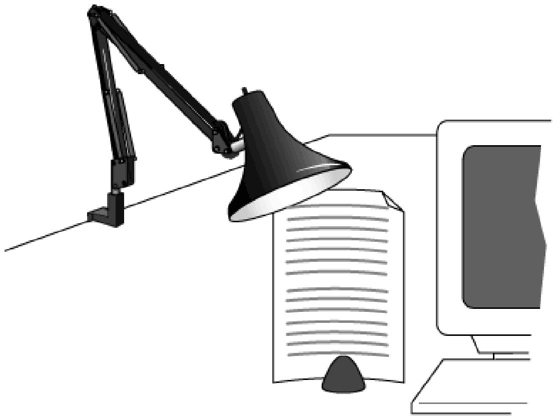

Fig. 3 Local lighting [7]

2.4. DIFFERENT TYPES OF LAMPS

Different types of lamps are designed to distribute light in different ways. These devices are known as:

- Direct.
- Direct-indirect.
- Indirect.
- Protected (different types).

No one type of lamp is suitable for every situation. The amount and quality of lighting required for a particular workstation or task will determine which lighting unit is most suitable.

2.5. DIRECT LAMPS

project 90 to 100 percent of their light down toward the work area. Direct lighting tends to create shadows.

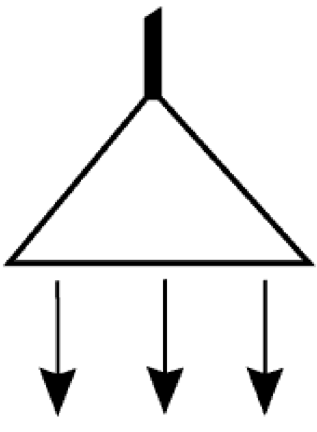

Fig. 4 Direct lighting [7]

2.6. DIRECT-INDIRECT LAMPS

distribute light equally upwards and downwards. They reflect light from the ceiling and other surfaces of the room. Little light is emitted horizontally, which means direct glare is often reduced. They are usually used in "clean" production areas.

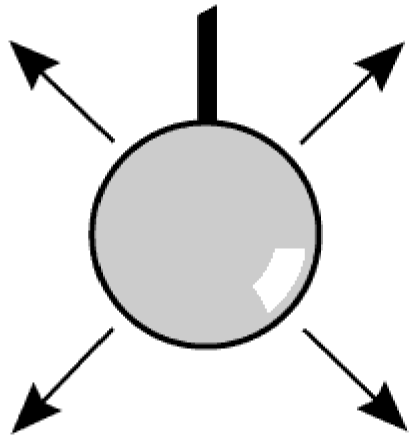

Fig. 5 Direct-reflective lighting [7]

2.7. INDIRECT LIGHT FIXTURES

distribute 90 to 100 percent of light upward. The ceiling and upper walls must be clean and highly reflective in order for light to reach the workspace. They provide the most uniform illumination of all types of lamps and the least direct glare. Indirect lights are usually used in offices.

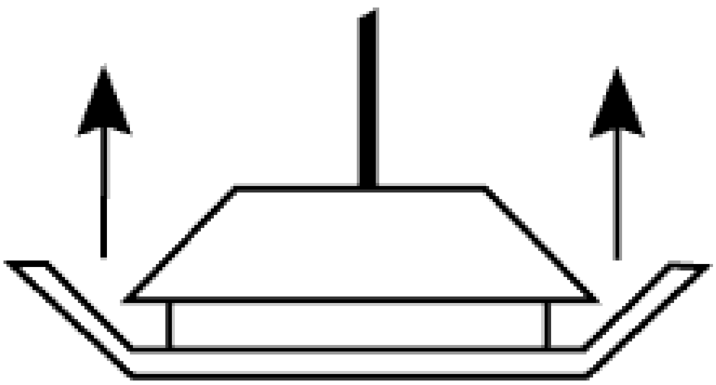

Fig. 6 Indirect lighting [7]

2.8. SHIELDED LIGHTS

Use diffusers, lenses and openings to cover the bulbs from direct view; therefore, it helps prevent glare and distribute light.

- Diffusers are transparent or semi-transparent (see-through) covers usually made of glass or plastic. They are used on the bottom or side of the lights to control brightness.
- Lenses are clear or transparent glass or plastic covers. The lens design includes prisms and grooves to distribute light in specific ways.

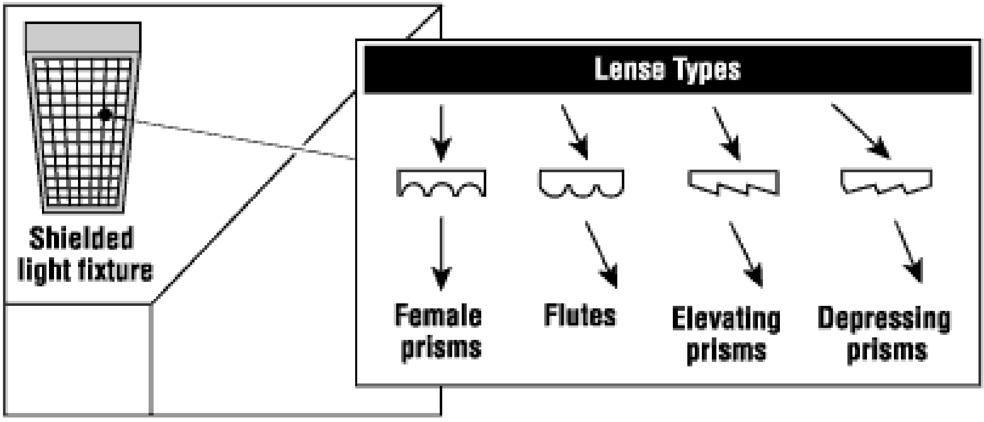

Fig. 7 Types of lenses [7]

Slats are partitions that protect the bulb from view and reflect light. Baffles can be shaped to control light and reduce brightness. Parabolic gratings are specially shaped gratings that concentrate and distribute light.

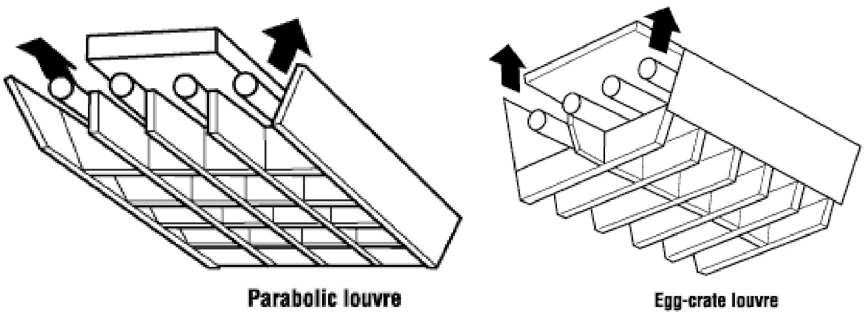

Fig. 8 Parabolic gratings [7]

3. CONCLUSIONS

Buildings are established to be functional and satisfy the needs of their occupants. Hence, the goal of a building cannot be accomplished if its occupants are discontented by its performance. Daylight utilization significantly contributes to energy savings in office buildings. However, daylight integration requires careful design to include variations in daylight availability and maintain a balance between factors such as lighting quality and heat gain or loss. Designers with proper planning can not only improve the visual environment and create higher-quality spaces but simultaneously minimize energy costs for buildings. We conclude that it is more rewarding for the companies that increase and decrease the light levels all over the day and should promote healthier human beings, who in turn will become more motivated, and happier and will contribute to the good results of the company profits. Simultaneously, improved visual comfort and a more appealing spatial impression are created.

4. REFERENCES

[1] J.-H. Lee, J. Moon, and S. Kim, “Analysis of occupants' visual perception to refine indoor lighting environment for office tasks,” Energies, 2014;

[2] N. Wessolowski, H. Koenig, M. Schulte-Markwort, and C. Barkmann, "(The effect of variable light on the fidgetyness and social behavior of pupils in school," Journal of Environmental Psychology, 2014;

[3] SM Pauley, "Lighting for the human circadian clock: recent research indicates that lighting has become a public health issue," Medical Hypotheses, 2004;

[4] H. Jusl´en and A. Tenner, "Mechanisms involved in enhancing human performance by changing the lighting in the industrial workplace," International Journal of Industrial Ergonomics, 2005;

[5] EA Lucassen, CP Coomans, M. van Putten et al., "Environmental 24-hr cycles are essential for health," Current Biology, 2016;

[6] Working Woman Education Fund, Health Hazards for Office Workers, an Overview of Problems and Solutions in Occupational Health in the Office, Working Woman Education Fund, Cleveland, OH, USA, 1981.

[7] http://www.ccohs.ca/oshanswers/ergonomics/lighting_general.html

GEODESY AND GEOINFORMATICS

TRANSFORMATION PARAMETERS OF LOCAL FITTING OF DIGITAL ELEVATION MODELS IN THE AREA OF KOVILJSKO-PETROVARADINKI RIT

Nikola Santrač[1], Pavel Benka [2], Mehmed Batilović[3]

Summary:

The digital elevation model is one of the most essential spatial data used for various purposes. The global digital elevation model may deviate significantly from the actual situation in a local area. In this paper, the accuracy analysis of three digital elevation models (TanDEM-X, SRTM, and ASTER GDEM) was performed to improve the accuracy and determine the transformation model that best reflects the actual terrain for the SRP "Koviljsko-Petrovaradin rit". Using control points measured in the field and applying the least squares method, three transformation models were defined for each digital elevation model. The results of the experiment indicate that the accuracy of the existing digital elevation models is improved with the applied methods. After determining the transformation parameters, it was concluded that the TanDEM-X model best reflects the actual terrain. Still, errors were also observed in certain parts of the model, such as errors on the surface of the Danube, etc.

Keywords: Digital elevation model, Least squares method, Koviljsko-petrovaradinski rit, TanDEm-X, SRTM, ASTER GDEM

[1] Teaching associate, MSc, Faculty of Agriculture, University of Novi Sad, Novi Sad, Serbia, e-mail: nikola.santrac@polj.edu.rs
[2] Full professor, PhD, Faculty of Agriculture, University of Novi Sad, Novi Sad, Serbia, e-mail: pavel.benka@polj.edu.rs
[3] Assistant professor, PhD, Faculty of Technical Sciences, University of Novi Sad, Novi Sad, Serbia, e-mail: mehmed@uns.ac.rs

1. INTRODUCTION

The Digital Elevation Model (DEM) is regularly defined as being the key to representing the terrain of the Earth to provide fundamental data for a raised-relief map [1]. DEM is an essential parameter to assess in any procedure using topography analysis, including its derived features (slope, curvature, roughness, drainage area and network, etc.). It has been used in scientific applications, such as hydrological, geological, geomorphologic, development, urban planning, and surveying [2, 3, 4, 5]. The accuracy of the DEMs application has affected the results of the scientific applications as mentioned in the previous studies. DEM is established using various techniques, for example, stereoscopic photogrammetric using airborne or satellite borne, interferometer of RADAR or SAR, laser scanning using airborne, and conventional surveys. Each technique has a limitation depending on price, accuracy, sampling density, and preprocessing requirements. The DEM-generated procedure is normally about four steps, such as data acquisition, grid spacing resampling, height interpolation, repeating, and accuracy assessment [6]. DEM's error is related to the resampling methods to grid spacing and interpolating techniques [7]. Errors on a spatial DEM have been classified as gross errors based on data collection, systematic errors based on the stereo image with setting elevation height values, and random errors from unknown errors. Their errors vary on terrain are depend on topography conditions [8]. DEM's quality is affected by many factors, such as sensor types, algorithm, terrain type, grid spacing, and characteristics, which is widely investigated based on the causes and consequences of errors. The free provided DEM, including ASTER GDEM from METI of Japan and NASA of USA (30 m), SRTM provided by NIMA and NASA of USA, and TanDEM-X implemented by German Aerospace center and EADS Astrium. For application modeling on a global and local scale, the vertical accuracy of DEM on a specific location is a requirement. The approach of DEM accuracy investigation on a specific location is assessed using the reference point to examine the vertical accuracy that the field measurements use high-precision equipment, such as the Global Navigation Satellite System (GNSS) [9, 10, 11]. This is also an investigation of DEM accuracy in Serbia especially in "Koviljsko-Petrovaradinski Rit"(KPR).

The main objective of this study is to improve the accuracy and determination of transformation models that best reflects the actual terrain using ground control points (GCPs).

2. MATERIALS AND METHODS

2.1. STUDY AREA

The selected study case is located in the southern part of Vojvodina Province (Serbia) (Figure 1), declared a special nature reserve KPR. KPR is situated on the left and right bank of the Danube River, near the City of Novi Sad, the capital of Vojvodina Province. It covers a surface of 5886 ha, and its total length is 22 km.

KPR presents a very important floodplain in the Danube catchment. The floodplain complex is a combination of forest, meadow, swamp, pond, and wetland ecosystems recognized on an international level. A fertile plain surrounds the reserve on one side, while the foothills of the National Park Fruška Gora are on the other.

The process of creating the transformation model and the analysis itself is shown in Figure 2. First, to assess the vertical accuracy of ASTER GDEM, SRTM, and TanDEM-X, GCPs are used. Second, three transformation models are defined for the three mentioned digital elevation models using residuals obtained in the previous step by comparing GCP elevations to elevations on the DEMs. And third, the accuracy of the created models is analyzed based on check points (ChPs).

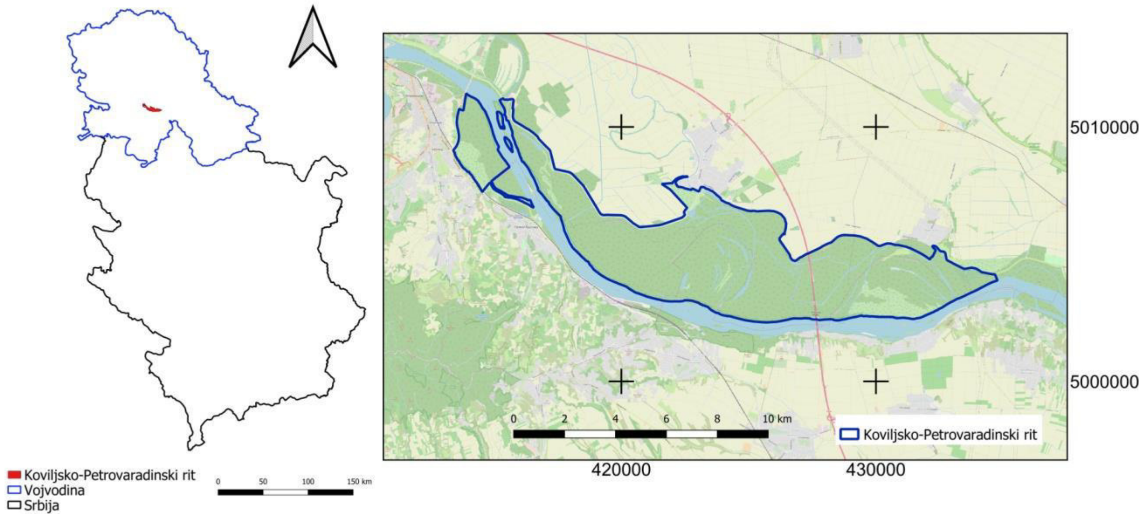

Figure. 1 Study area

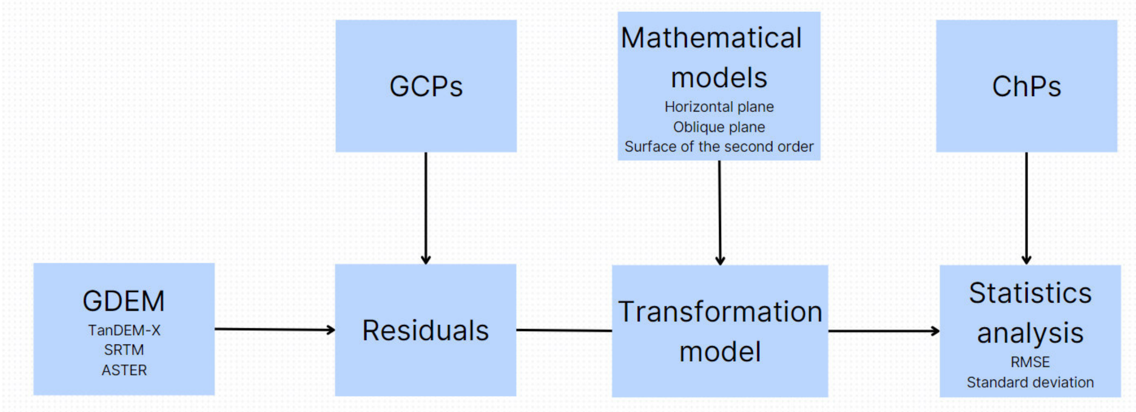

Figure. 2 Workflow

2.2. DATASET DESCRIPTIONS

There are several DEMs are commonly used in many applications such as ASTER GDEM, SRTM, and TanDEM-X. All these DEMs have different usage and implications according to their characteristic and specification.

The ASTER GDEM sensor [12] was launched in December 1999 onboard the Terra satellite, with the capability of generating along-track stereoscopic images on the Near Infra-Red wavelength (0.78–0.86 μm) with telescopes aligned to nadir (3N band) and backward (3B band), with 15 m spatial resolution. In 2009 ASTER GDEM version 1 was released, covering all land areas between 83°N and 83°S [13]. ASTER GDEM V.1 was produced by automatically processing the entire ASTER GDEM archive (about 1,500,000 scenes acquired from 2000 to 2008) [14, 15]. ASTER GDEM V.2 was released in 2011 [15] and improves on the first version on the processing algorithms, inclusion of scenes acquired between 2008 and 2011 (about 250,000 scenes), better georeferencing of data and increase of effective spatial resolution from 120 m to 70 m. At 95% confidence, ASTER GDEM has an estimated accuracy of 30 m horizontal and 20 m vertical [16].

SRTM is the most commonly used in various scientific studies, especially in regional geoid modeling. This DEM was an international project spearheaded by the National Geospatial-Intelligence Agency and NASA generated from SRTM. The DEM derived from the SRTM mission that using a C-band (5.6 cm wavelength) Interferometric Synthetic Aperture Radar (InSAR), covers the earth between latitude of 60 °N to 56°S,

or more than 80% of Earth's land surface [17]. In the beginning, SRTM provided the most complete and highest DEM resolution in the world with global vertical errors ± 16 m and ± 6 m for absolute and relative accuracy, respectively [17, 18].
TanDEM-X is an Earth observation radar mission that consists of a SAR interferometer produced by almost twin satellites flying in close orbit. As mentioned by [19], both satellites have been flying at 500km altitude since October 2010. The establishment of TanDEM-X mission is to provide unprecedented accuracy and precision for 3D land surface maps. According to [19] and [7], the use of SAR data for the DEM production was acquired in Strip Map mode with horizontal transmit and receive polarization between December 2010 and January 2015. To facilitate unwrapping the dual-baseline phase, All land masses are covered at least twice. The TanDEM-X mission offers a new era in space borne synthetic aperture radar (SAR) due to its latest and the most current global consistent and accurate data [20]. The TanDEM-X is widely used in earth sciences, environmental science, and defenses such as geology, oceanography, land monitoring usage, urban planning, and navigation. One of the elements that make TanDEM-X differ from other DEMs is it uses reference datum WGS84 ellipsoid. Thus, it produces ellipsoidal height.

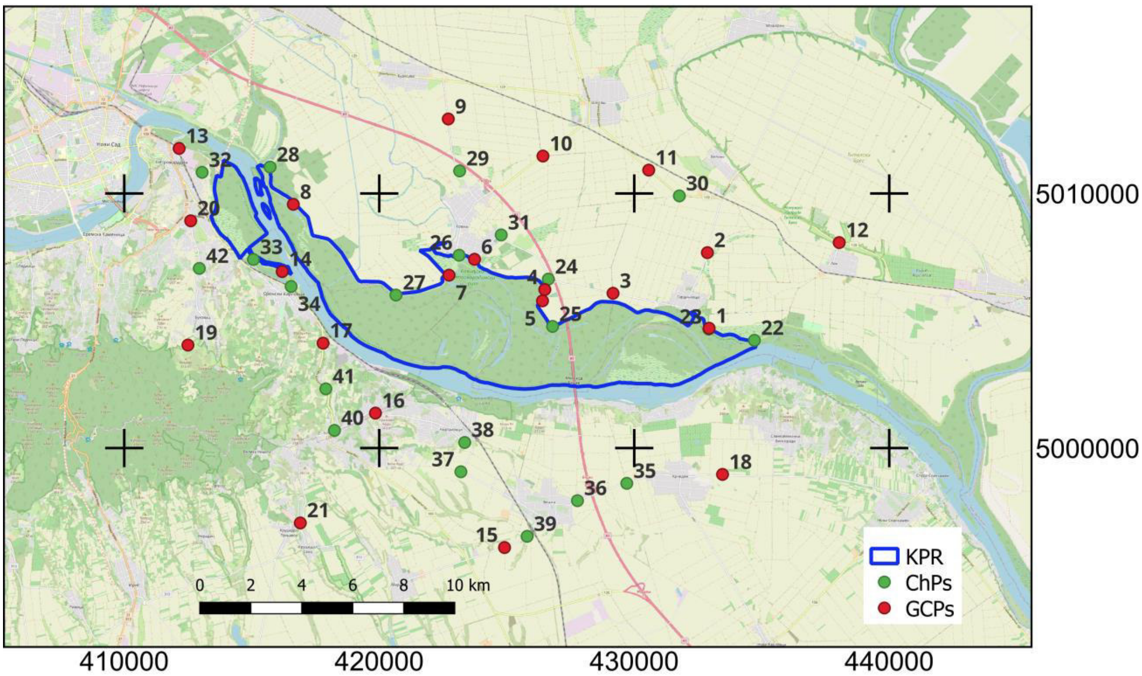

Figure. 3 Distribution of GCPs and ChPs

The DEMs assess accuracy to contain numerous GCPs to achieve reliable measures of high accuracy. The accuracy of the GCPs and ChPs might be at least three times greater than the DEM elevations [21]. The American Society of Photogrammetry and Remote Sensing (ASPRS) has mentioned a minimum of ChPs about 20 observed in each major land cover type. The GCPs and ChPs in this study were observed from the GNSS survey method. The GNSS has an accuracy of less than 2 cm on observation. Figure 3 presents the observed GCPs and ChPs. GCPs and ChPs are typically positioned outside the KPR itself to obtain a more detailed representation and to avoid errors at the boundaries of the area.
In this study, 42 points were stabilized and divided into two equal sets, meaning there are 21 GCPs and 21 ChPs. GCPs are used for model creation, while ChPs are solely used for the final accuracy control. Data for the E, N, and H coordinates of these points are provided in Table 1. The E and N coordinates were defined in the official coordinate system of the Republic of Serbia ETRS89/UTM34 (EPSG: 25834). The H coordinate is

defined in the state vertical system using the Grider application, which transforms it into orthometric heights.

Tab. 1 Coordinate of GCPs and ChPs

GCPs				ChPs			
No.	E [m]	N [m]	H [m]	No.	E [m]	N [m]	H [m]
1	5004705.44	432936.63	75.96	22	5007676	432868.5	75.33
2	5007675.93	432868.47	76.06	23	5008071	438038.3	79.64
3	5006079.18	429168.27	80.78	24	5004705	432936.6	80.7
4	5006225.3	426494.01	80.46	25	5006079	429168.3	80.36
5	5005781.85	426402.76	80.11	26	5005782	426402.8	80.11
6	5007415.2	423735.29	78.41	27	5007415	423735.3	80.3
7	5006789.32	422737.4	80.12	28	5006789	422737.4	80.62
8	5009572.37	416630.86	79.85	29	5009572	416630.9	81.91
9	5012925.31	422707.78	81.78	30	5010917	430568.2	80.98
10	5011468.4	426419.92	81.19	31	5006225	426494	80.66
11	5010917.02	430568.16	80.16	32	5004045	412497.3	77.41
12	5008070.76	438038.26	77.48	33	5004119	417796.6	80.68
13	5011768.29	412152.09	77.65	34	4997058	416904.6	80.32
14	5006932.82	416194.19	80.54	35	4998965	433462.5	120.49
15	4996091.13	424913.71	144.89	36	5001373	419850.5	112.1
16	5001373.25	419850.53	248.34	37	5008925	412606.4	177.56
17	5004119.23	417796.6	117.92	38	5012925	422707.8	131.3
18	4998965.06	433462.48	109.25	39	5006933	416194.2	117.94
19	5004045.48	412497.26	259.59	40	5011468	426419.9	263.39
20	5008925.1	412606.38	97.63	41	4996091	424913.7	211.88
21	4997057.58	416904.58	172.33	42	5011768	412152.1	118.12

2.3. MATHEMATICAL MODELS OF TRANSFORMATIONS

To determine the transformation model that best represents the actual surface conditions for the KPR, the least squares method was applied. Three transformation models were defined: horizontal plane, oblique plane, and surface of second-order. Equations 1-3 represent these mentioned models, respectively.

Horizontal plane:

$$H_i = \mathrm{F}, \quad (1)$$

where H_i represents the measured values, while F is an unknown value.

Oblique plane:

$$H_i = \mathrm{F} - DN_i - EE_i, \quad (2)$$

where:

H_i- measured values,

N_i and E_i - GCPs coordinates,

D and E - unknown parameters, which represent the slopes of the plane along the N and E axes, F – intersection of the plane with the H-axis.

The surface of second-order:

$$H_i = AN_i^2 + BE_i^2 + CN_iE_i + DN_i + EE_i + F, \tag{3}$$

where:
H_i- measured values,
N_i and E_i- GCPs coordinates,
A, B, C, D, E i F - unknown parameters.
For a better representation of the obtained results, the accuracy of specific transformation models was assessed using RMSE, as shown in Equation 4.

$$RMSE = \sqrt{\frac{\sum(H_{transf} - H_{ChPs})^2}{n}} \tag{4}$$

3. RESULTS AND DISCUSSIONS

After the residuals were calculated for each of the three DEMs, the determination of the transformation model that best reflects the actual state of the surface was determined using the method of least squares. Where the residuals represented the measured values. A total of 3 transformation models were defined (horizontal plane, an oblique plane, and a surface of second-order are defined). Table 2 shows the values of unknown parameters that were calculated based on equations 1, 2, and 3.
The first step of the analysis represents the extraction of heights from 3 DEMs and comparison with orthometric heights from 21 GNSS GCPs. To determine all the vertical errors from DEMs, residuals were calculated for each point. Based on that, residuals were obtained, three residuals were obtained for each GCP, and one for each DEM. Which is shown in Table 3.
After defining the transformation model, the height values of those transformation models were calculated in the places where the ChPs are located, where then those values were compared with the actual height values measured by the GNSS method. The results of the comparison are shown in Tables 4, 5 and 6.

Tab. 2 Values of unknown parameters

Transformation models	DEM	Unknown parameters					
		A	B	C	D	E	F
Horizontal plane	Tan DEM-X	x	x	x	x	x	43.39
	SRTM	x	x	x	x	x	-3.31
	ASTER GDEM	x	x	x	x	x	-1.31
Oblique plane	TanDEM-X	x	x	x	4.55E-05	2.64E-05	282.58
	SRTM	x	x	x	1.45E-04	-5.07E-05	700.14
	ASTER GDEM	x	x	x	1.27E-04	3.42E-04	780.15
The surface of second-order	TanDEM-X	1.22E-11	-1.95E-09	4.04E-09	-1.78E-03	-1.86E-02	-8217.36
	SRTM	-2.50E-08	-6.46E-09	1.77E-09	2.50E-01	-3.44E-03	624812.19
	ASTER GDEM	5.22E-08	1.11E-08	3.83E-08	-5.39E-01	-2.01E-01	-1390476.93

Tab. 3 GCPs residuals

No.	H [m]	TanDEM-X [m]	SRTM [m]	ASTER GDEM [m]	H - DEM(residual)		
					TanDEM-X [m]	SRTM [m]	ASTER GDEM [m]
1	75.96	119.09	75	74	-43.13	0.96	1.96
2	76.06	119.21	74	73	-43.15	2.06	3.06
3	80.78	123.97	78	78	-43.2	2.78	2.78
4	80.46	124.07	77	76	-43.61	3.46	4.46
5	80.11	123.75	76	80	-43.63	4.11	0.11
6	78.41	120.94	75	80	-42.53	3.41	-1.59
7	80.12	122.69	73	78	-42.57	7.12	2.12
8	79.85	123.08	73	86	-43.22	6.85	-6.15
9	81.78	125.02	77	82	-43.24	4.78	-0.22
10	81.19	124.24	78	69	-43.05	3.19	12.19
11	80.16	123.12	76	76	-42.96	4.16	4.16
12	77.48	120.3	75	68	-42.82	2.48	9.48
13	77.65	121.69	76	76	-44.05	1.65	1.65
14	80.54	123.17	75	82	-42.63	5.54	-1.46
15	144.89	188.2	144	139	-43.31	0.89	5.89
16	248.34	292.85	246	252	-44.51	2.34	-3.66
17	117.92	161.87	117	121	-43.95	0.92	-3.08
18	109.25	153.43	106	109	-44.17	3.25	0.25
19	259.59	303.67	251	256	-44.08	8.59	3.59
20	97.63	141.39	97	104	-43.76	0.63	-6.37
21	172.33	215.92	172	174	-43.59	0.33	-1.67

Tab. 4 ChPs residuals on horizontal plane

No.	H	Mathematic transformation			H – Transformation(residual)		
		TanDEM-X [m]	SRTM [m]	ASTER GDEM [m]	TanDEM-X [m]	SRTM [m]	ASTER GDEM [m]
22	75.33	75.43	75.31	73.31	-0.09	0.02	2.02
23	79.64	78.85	77.31	75.31	0.79	2.33	4.33
24	80.7	81.22	81.31	85.31	-0.51	-0.61	-4.61
25	80.36	80.82	81.31	86.31	-0.45	-0.95	-5.95
26	80.11	78.79	77.31	74.31	1.32	2.8	5.8
27	80.3	79.21	75.31	80.31	1.09	4.99	-0.01
28	80.62	79.87	79.31	88.31	0.75	1.31	-7.69
29	81.91	80.79	80.31	96.31	1.11	1.6	-14.4
30	80.98	80.77	83.31	72.31	0.22	-2.33	8.67
31	80.66	79.76	77.31	84.31	0.89	3.35	-3.65
32	77.41	78.09	77.31	80.31	-0.68	0.1	-2.9
33	80.68	80.25	81.31	83.31	0.43	-0.63	-2.63
34	80.32	81.35	80.31	87.31	-1.02	0.02	-6.98
35	120.49	119.77	120.31	129.31	0.72	0.18	-8.82
36	112.1	112.07	114.31	101.31	0.03	-2.21	10.79
37	177.56	177.81	176.31	180.31	-0.24	1.25	-2.75
38	131.3	132.53	133.31	131.31	-1.23	-2.01	-0.01
39	117.94	117.94	119.31	116.31	0	-1.37	1.63
40	263.39	263.86	261.31	260.31	-0.47	2.08	3.08
41	211.88	212.29	210.31	221.31	-0.41	1.57	-9.43
42	118.12	118.24	118.31	117.31	-0.12	-0.19	0.81

Tab. 5 ChPs residuals on an oblique plane

No.	H	Mathematic transformation			H – Transformation(residual)		
		TanDEM-X [m]	SRTM [m]	ASTER GDEM [m]	TanDEM-X [m]	SRTM [m]	ASTER GDEM [m]
22	75.33	75.75	75.07	76.7	-0.41	0.26	-1.36
23	79.64	79.32	76.87	80.51	0.32	2.77	-0.87
24	80.7	81.4	80.64	88.34	-0.7	0.06	-7.64
25	80.36	80.97	81.03	88.23	-0.6	-0.67	-7.86
26	80.11	78.85	77.13	75.24	1.26	2.98	4.87
27	80.3	79.28	75.5	80.54	1.02	4.8	-0.24
28	80.62	79.88	79.46	88.12	0.74	1.16	-7.5
29	81.91	80.77	81.17	94.38	1.14	0.73	-12.48
30	80.98	81.17	83.66	75.32	-0.19	-2.68	5.66
31	80.66	79.85	77.19	85.33	0.81	3.47	-4.67
32	77.41	77.71	77.58	76.27	-0.3	-0.17	1.15
33	80.68	80.01	81.32	81.09	0.67	-0.64	-0.41
34	80.32	80.76	79.35	83.89	-0.44	0.98	-3.56
35	120.49	119.71	118.78	131.79	0.78	1.71	-11.3
36	112.1	111.76	113.82	99.44	0.34	-1.72	12.66
37	177.56	177.65	177.28	176.92	-0.08	0.28	0.64
38	131.3	132.82	134.35	131.89	-1.52	-3.05	-0.59
39	117.94	117.79	119.81	113.9	0.15	-1.87	4.04
40	263.39	264.18	261.95	261.97	-0.79	1.44	1.42
41	211.88	211.87	208.8	220.5	0.01	3.08	-8.62
42	118.12	118.2	119.72	114.13	-0.08	-1.59	3.99

Tab. 6 ChPs residuals on the surface of second-order

No.	H	Mathematic transformation			H – Transformation(residual)		
		TanDEM-X [m]	SRTM [m]	ASTER GDEM [m]	TanDEM-X [m]	SRTM [m]	ASTER GDEM [m]
22	75.33	75.76	75.19	76.96	-0.42	0.14	-1.63
23	79.64	79.15	76.13	82.78	0.49	3.52	-3.14
24	80.7	81.28	80.92	87	-0.58	-0.22	-6.29
25	80.36	81.02	81.67	86.92	-0.65	-1.3	-6.55
26	80.11	78.94	77.94	73.61	1.17	2.17	6.5
27	80.3	79.4	76.22	79.26	0.9	4.07	1.04
28	80.62	80	80.26	86.64	0.63	0.36	-6.02
29	81.91	80.71	81.17	93.68	1.2	0.74	-11.77
30	80.98	81.35	83.31	77.57	-0.37	-2.33	3.41
31	80.66	79.95	77.97	83.83	0.71	2.69	-3.17
32	77.41	77.67	77.78	76.81	-0.26	-0.37	0.6
33	80.68	80.09	82.06	80.17	0.59	-1.38	0.51
34	80.32	80.98	78.65	87.77	-0.66	1.68	-7.44
35	120.49	119.3	118.07	129.88	1.19	2.42	-9.39
36	112.1	111.89	114.42	99	0.21	-2.32	13.1
37	177.56	177.42	176.96	176.45	0.14	0.6	1.11
38	131.3	132.95	133.55	133.72	-1.65	-2.26	-2.42
39	117.94	117.78	120.27	112.89	0.17	-2.33	5.06
40	263.39	264.37	261.67	263.48	-0.98	1.72	-0.09
41	211.88	211.87	207.82	221.83	0.01	4.07	-9.94
42	118.12	117.84	118.47	114.26	0.29	-0.35	3.87

To more simply and easily define the accuracy of determining the transformation, Table 7 shows measures of central tendency and RMSE calculated according to formula 4.

Tab. 7 Measures of central tendency and RMSE

No.	Horizontal plane			Oblique plane			Surface of second-order		
	Tan DEM-X [m]	SRTM [m]	ASTER GDEM [m]	Tan DEM-X [m]	SRTM [m]	ASTER GDEM [m]	Tan DEM-X [m]	SRTM [m]	ASTER GDEM [m]
average	0.10	0.54	-1.56	-0.10	-0.54	1.56	-0.10	-0.54	1.56
min	-1.23	-2.33	-14.40	-1.26	-4.80	-12.66	-1.20	-4.07	-13.10
max	1.32	4.99	10.79	1.52	3.05	12.48	1.65	2.33	11.77
RMSE	0.72	1.95	6.31	0.71	2.13	6.26	0.75	2.13	6.16

Upon analyzing the obtained values in Tables 3, 4, and 5, we observe significant differences in elevation values between different data sources TanDEM-X, SRTM, and

ASTER GDEM. These differences reflect the variation in accuracy of each data source and how each source interprets the terrain. This is crucial for understanding regional disparities and specificities in the results. Furthermore, mathematical transformations have a significant impact on elevation values, as evidenced by residual values that vary between positive and negative values. This indicates that transformations can significantly affect the final elevations, underscoring the importance of understanding how these transformations are applied and interpreted. It is important to note that some points stand out as exceptions, where deviations from reference values were notably large after the application of transformations. These exceptions point to special terrain characteristics or areas that may require further investigation to understand the causes of these discrepancies.

The results highlight that the TanDEM-X model provided significantly better accuracy in determining elevation values after the application of transformations compared to the SRTM and ASTER GDEM models. This difference in accuracy is particularly emphasized by the fact that only TanDEM-X can precisely determine elevations in centimeters. This is crucial for applications requiring high precision in elevation measurements, such as engineering projects, geodetic mapping, or terrain analyses where centimeter-level accuracy plays a pivotal role in decision-making and planning.

4. CONCLUSION

In this study, the accuracy of three different DEMs (TanDEM-X, ASTER GDEM, and SRTM) was tested using a specific transformation model determination for an area of KPR. Using the GNSS method, GCP and ChPs were measured on site, and based on them, the transformation models and height accuracy control of the model were determined. By comparing 3 different models, we concluded that the models created based on TanDEM-X best correspond to the actual situation on the ground. The remaining two models gave far worse results. It was also concluded that changing the transformation model does not improve model accuracy much. From this study, it can be concluded that by transforming TanDEM-X DEM, the best mapping of the model for the KPR area can be obtained. However, although a transformation was created based on TanDEM-X, which in this case best corresponds to ChPs, errors were observed in certain parts of the model, such as errors on the surface of the Danube where the height values are equal to zero.

LITERATURE

[1] Guth, P. L. (2006). Geomorphometry from SRTM: Comparison to NED: Photogrammetric. *Engineering and Remote Sensing, v. 72, no. 3*, 269.

[2] Pakoksung, K., & Takagi, M. (2015). Remote sensing data application for flood modeling. *JAST*, *26*, 115-122.

[3] Lee, S. J., Komatitsch, D., Huang, B. S., & Tromp, J. (2009). Effects of topography on seismic-wave propagation: An example from northern Taiwan. *Bulletin of the Seismological Society of America*, *99*(1), 314-325.

[4] Weibel, R., & Heller, M. (1990, July). A framework for digital terrain modeling. In *Fourth International Symposium on Spatial Data Handling, Zurich, Switzerland* (pp. 219-229).

[5] Fraser, C. S., Baltsavias, E., & Gruen, A. (2002). Processing of Ikonos imagery for submetre 3D positioning and building extraction. *ISPRS Journal of Photogrammetry and Remote Sensing*, *56*(3), 177-194.

[6] Li, J., Chapman, M. A., & Sun, X. (2006). Validation of satellite-derived digital elevation models from in-track IKONOS stereo imagery. *Ontario Ministry of Transport, Toronto*.

[7] Fisher, P. F., & Tate, N. J. (2006). Causes and consequences of error in digital elevation models. *Progress in physical Geography*, *30*(4), 467-489.

[8] Hebeler, F., & Purves, R. S. (2009). The influence of elevation uncertainty on derivation of topographic indices. *Geomorphology*, *111*(1-2), 4-16.

[9] Gonga-Saholiariliva, N., Gunnell, Y., Petit, C., & Mering, C. (2011). Techniques for quantifying the accuracy of gridded elevation models and for mapping uncertainty in digital terrain analysis. *Progress in Physical Geography*, *35*(6), 739-764.

[10] Kolecka, N., & Kozak, J. (2014). Assessment of the accuracy of SRTM C-and X-Band high mountain elevation data: A case study of the Polish Tatra Mountains. *Pure and Applied Geophysics*, *171*, 897-912.

[11] Forkuor, G., & Maathuis, B. (2012). Comparison of SRTM and ASTER derived digital elevation models over two regions in Ghana-Implications for hydrological and environmental modeling (pp. 219-240). London: INTECH Open Access Publisher.

[12] Yamaguchi, Y., Kahle, A. B., Tsu, H., Kawakami, T., & Pniel, M. (1998). Overview of advanced spaceborne thermal emission and reflection radiometer (ASTER). *IEEE Transactions on geoscience and remote sensing*, *36*(4), 1062-1071.

[13] ASTER, G. (2009). Earth Remote Sensing Data Analysis Center (ERSDAC).

[14] Abrams, M., Bailey, B., Tsu, H., & Hato, M. (2010). The aster global dem. *Photogrammetric Engineering and Remote Sensing*, *76*(4), 344-348.

[15] Tachikawa, T., Hato, M., Kaku, M., & Iwasaki, A. (2011, July). Characteristics of ASTER GDEM version 2. In *2011 IEEE international geoscience and remote sensing symposium* (pp. 3657-3660). IEEE.

[16] Tachikawa, T., Kaku, M., Iwasaki, A., Gesch, D. B., Oimoen, M. J., Zhang, Z., ... & Carabajal, C. (2011). *ASTER global digital elevation model version 2-summary of validation results*. NASA.

[17] Rabus, B., Eineder, M., Roth, A., & Bamler, R. (2003). The shuttle radar topography mission—a new class of digital elevation models acquired by spaceborne radar. *ISPRS journal of photogrammetry and remote sensing*, *57*(4), 241-262.

[18] Smith, B., & Sandwell, D. (2003). Accuracy and resolution of shuttle radar topography mission data. *Geophysical Research Letters*, *30*(9).

[19] Lachaise, M., Fritz, T., & Bamler, R. (2017). The dual-baseline phase unwrapping correction framework for the TanDEM-X mission part 1: Theoretical description and algorithms. *IEEE Transactions on Geoscience and Remote Sensing*, *56*(2), 780-798.

[20] Wessel, B., Breunig, M., Bachmann, M., Huber, M., Martone, M., Lachaise, M., ... & Zink, M. (2016, June). Concept and first example of TanDEM-X high-resolution DEM. In *Proceedings of EUSAR 2016: 11th European Conference on Synthetic Aperture Radar* (pp. 1-4). VDE.

[21] Athmania, D., & Achour, H. (2014). External validation of the ASTER GDEM2, GMTED2010 and CGIAR-CSI-SRTM v4. 1 free access digital elevation models (DEMs) in Tunisia and Algeria. *Remote Sensing*, *6*(5), 4600-4620.

INTEGRATED SYSTEMS FOR GEODETIC MEASUREMENTS IN ENGINEERING

Bogdan Bojović[1], Žarko Nestorović[2], Milan Trifković[3], Miroslav Kuburić[4], Jelena Tatalović[5]

Summary:

The development of geodetic technologies conditioned their specialization, that is, in a certain way, maximized their performance in certain geodetic measurements, while on the other hand it limited their other possibilities. In order to achieve an optimal response to increasingly demanding conditions from other engineering fields, it is necessary to properly combine geodetic technologies and integrate them depending on the project's requirements. In this paper the equality of surveying results accuracy obtained by aero photogrammetry and GNSS were analysed.

Key words: geodetic technologies, accuracy, statistical hypothesis

[1] MsC, Faculty of civili engineering Subotica, University of Novi Sad, Serbia, bojovic@gf.uns.ac.rs
[2] mr, Public Company of Electricity Production – EPS, Branch “DJerdap”, Kladovo, zarko.nestorovic@djerdap.rs
[3] Professor, Faculty of civili engineering Subotica, University of Novi Sad, Serbia, mtrifkovic@gf.uns.ac.rs
[4] Professor, Faculty of civili engineering Subotica, University of Novi Sad, Serbia, mtrifkovic@gf.uns.ac.rs
[5] PhD, Faculty of civili engineering Subotica, University of Novi Sad, Serbia, jelena.tatalovic@gf.uns.ac.rs

1. INTRODUCTION

In this research the theoretical and practical aspects of integrated geodetic measurement systems are considered. Concept of integrated surveying systems is created as a result of geodetic technologies specialization and their recent rapid development. Actually, from the beginning of total station development, GNSS equipment, digital photogrammetry and laser scanners development their advantages and disadvantages were noticed. For example: total stations could provide great accuracy but are quite inefficient because they need geodetic networks developed and auxiliary workers. The development of GNSS technologies reduced the inefficiency but also reduced the accuracy of points' position in case of RTK methods or increased the time needed for high accuracy achievement in case of static measurements. Digital photogrammetry increased the number of points obtained as a result of surveying but the points' position accuracy is dependent on the geodetic frame in which the position of camera is determined. Terrestrial laser scanners could collect the huge number of points' position in a short time at relatively high accuracy but they also need positioning in space.

According to Haddad [1]: "Modern technology has changed matters in documentation radically and promises to continue to bring rapid changes. Photographic and non-photographic (graphic) documentation tools are merging in one process, in which the digital photographic technology is the main base." This statement, even though appeared almost a decade earlier, has been continually proven in geodetic field. Continual improvement of geodetic technologies permanently increase the efficiency of geodetic data processing and shorten the period from starting measurement to final report. But the question of accuracy still remains important in providing survey by utilizing combined technologies.

Bearing in mind advantages and disadvantages of different geodetic technologies it is possible to combine their advantages and obtain the better results than using only one technology in practical surveying. For example it is possible to combine the digital photogrammetry for obtaining the position of points in a short time with their global positioning by utilizing the GNSS system based on the AGROS system of points. In this research the differences of points' coordinates obtained by GNSS and aerophotogrammetry technology were investigated in order to check the hypotheses about normality of differences' distribution and gross errors existence. The statistical tests were formulated in standard form [2, 3]. For normality of data distribution was used Shapiro-Wilk statistics [4, 5] and calculator available on internet [6]. The issue of coordinates' correlation is researched by utilizing the Pearson correlation coefficient [7].

2. MATERIALS AND METHODS

In this research the differences of 3D coordinates of 31 point obtained by GNSS and digital aerophotogrammetry method were analysed. The area for surveying was the industrial zone in Požega (approximate WGS coordinate: φ= 43°50'41.67"N and λ= 20° 3'14.59"E). The surveying area is illustrated on figure 1, while the position of control points are given on figure 2.

Fig. 1 Approximate area of surveying

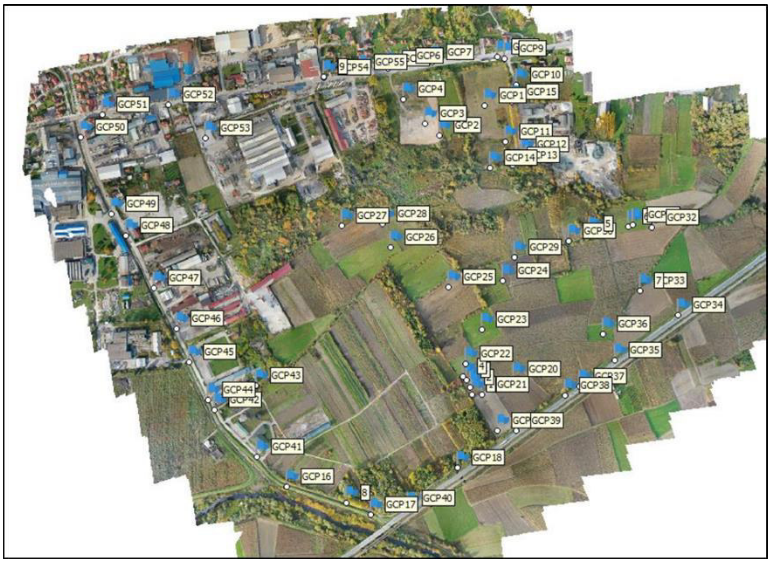

Fig. 2 Position of control points

The statistical analysis encompassed further hypothesis:

- Hypotheses about normality of coordinates' differences
- Hypotheses about gross errors of coordinates' differences and
- Hypotheses about correlation between coordinates' differences.

Hypotheses about normality of coordinates' differences distribution are formulated as follows:

H_0: Coordinates differences' are normaly distributed,

H_a: otherwise.

These hypotheses are checked by utilizing the Shapiro-Wilk test.

Hypotheses about gross errors existence in set of coordinates' differences distribution are formulated as follows:

H_0: Coordinate differences' contains gross errors,

H_a: otherwise.

These hypotheses are checked by utilizing the student's statistics as follows

$$t = \frac{a}{m_a} \sim t_{f,1-\alpha} \quad (1)$$

where:

t – statistics

a – estimation of regression coefficient

m_a – mean root square error of regression coefficient a.

f – degrees of freedom and

α – level of significance ($\alpha = 0.05$).

Hypotheses about correlation existence in set of coordinates' differences distribution are formulated as follows:

H_0: Coordinate differences' are correlated,
H_a: otherwise.
These hypotheses are checked by using following statistics:

$$r_{x,y} = \frac{K_{x,y}}{\sigma_x \sigma_y} \tag{2}$$

where:
r – correlation coefficient (Pearson)
$K_{x,y}$ – covariation
$\sigma_x, \ \sigma_y$ – coresponding standard deviation of coordinates.
Criteria for accepting null hypothesis reads:

$$r \geq 3 * \frac{1 - r^2}{\sqrt{n}} \tag{3}$$

3. RESULTS AND DISCUSSION

The data processing encompassed the systematization of coordinates' differences, calculation of average values and standard deviations. These data are the initial for further analysis. The data of coordinate differences are given in table 1.

Tab. 1 The coordinate differences

item number	Point name	ΔX [cm]	ΔY [cm]	ΔZ [cm]	Total (cm)
1	GCP5	0.16	-1.00	-0.11	1.02
2	GCP7	0.63	-0.01	0.41	0.75
3	GCP9	0.48	0.70	0.02	0.85
4	GCP10	-0.35	-0.02	0.16	0.38
5	GCP11	-0.24	-1.41	0.50	1.51
6	GCP12	-0.51	0.76	0.38	0.99
7	GCP14	-0.14	-0.06	-0.67	0.69
8	GCP17	-0.56	1.49	-0.62	1.71
9	GCP19	-0.88	0.90	0.80	1.49
10	GCP20	-0.21	-0.64	-0.36	0.77
11	GCP22	0.05	0.88	-0.24	0.91
12	GCP25	-0.12	0.30	-0.28	0.43
13	GCP26	0.27	0.46	-0.09	0.54
14	GCP27	-2.09	-4.76	2.82	5.91
15	GCP28	0.92	-1.00	-0.79	1.57
16	GCP29	0.30	1.17	0.16	1.22
17	GCP31	1.06	-0.95	-0.30	1.46
18	GCP34	0.39	0.45	0.26	0.65
19	GCP36	-1.87	0.82	0.21	2.06
20	GCP37	0.61	-0.16	0.14	0.64
21	GCP39	1.14	-1.08	-0.07	1.57
22	GCP40	0.72	-0.88	-0.11	1.14
23	GCP41	-1.44	0.56	0.34	1.58
24	GCP42	-1.33	1.18	1.08	2.09
25	GCP43	2.61	-1.60	-2.28	3.82
26	GCP46	-1.20	-0.16	0.42	1.28
27	GCP48	-1.00	-0.17	1.04	1.46
28	GCP50	-0.24	-0.18	0.59	0.66
29	GCP52	1.17	-1.34	-1.08	2.09
30	GCP54	-0.45	0.76	-0.67	1.11
	$\overline{X}$	-0.07	-0.17	0.06	1.41
	σ_X	1.00	1.22	0.85	1.09

After the data tabulation the Shapiro-Wilk test was utilized for normality of distribution testing and obtained results are given in table 2.

Tab. 2 The results of Shapiro-Wilk test

item number	Coordinate	W	Hypothesis not rejected	Note
1	X	0.982	H_o	Without maximal difference elimination
2	Y	0.856	H_o	After elimination Y value for GCP27
3	Z	0.930	H_o	After elimination Z value for GCP27
4	T	0.945	H_o	After elimination Z value for GCP27 and GCP43

The results of Shapiro-Wilk test suggests that only points GCP27 and GCP43 deviate from the normal distribution.
The statistical test about gross errors in set of coordinates' differences which overcome critical values are given in table 3 with accepted hypothesis in brackets.

Tab. 3 The student's test

item number	Point name	t(X)	t(Y)	t(Z)	t(T)
1	GCP27	2.08 (H_a)	3.90 (H_a)	3.33 (H_a)	5.42 (H_a)
2	GCP43	2.60 (H_a)	1.31 (H_o)	2.69 (H_a)	3.49 (H_a)

The test of gross errors suggests that coordinates of points GCP27 and GCP43 significantly deviate from others differences in researched set.
The obtained correlation coefficients are given in table 4 with accepted hypotheses in brackets.

Tab. 4 The correlation coefficients

item number		ΔX	ΔY	ΔZ	ΔT
1	ΔX	-	-0.13 (H_o)	-0.73 (H_a)	-0.17 (H_o)
2	ΔY		-	-0.21 (H_o)	-0.67 (H_a)
3	ΔZ			-	0.27 (H_o)
4	ΔT				-

The obtained results about correlation analysis suggest that only coefficient of correlation $r_{x,z}$ and $r_{y,T}$ are significant. Bearing in mind relatively small sample the research of correlation should be provided on the bigger sample (at least with 50 points [3]).
The results of statistical analysis suggest that, in researched set of data, there are negligible deviations of coordinates' differences. Also, in practical sense, the deviations of coordinate's differences for points GCP27 and GCP43 are not significant because their differences still do not exceed required accuracy of surveying.

4. CONCLUSION

The results of statistical analysis of coordinates' differences obtained by two different methods (aerophotogrammetry and GNSS) imply the high level of concordance. This means that the obtained accuracy of different methods of surveying allows their integration in engineering task solving. The small numbers of differences which exceed the 95% criteria of significance support the statement of high concordance of coordinates' obtained by two different technologies. The correlation coefficient is significant only between x and z coordinates and between y coordinates and total differences T. Bearing in mind relatively small number of points the correlation coefficient deserves further analysis in cases with bigger sample.

REFERENCES

[1] Haddad, Naif Adel. "From ground surveying to 3D laser scanner: A review of techniques used for spatial documentation of historic sites." Journal of King Saud University-Engineering Sciences 23.2 (2011): 109-118.

[2] Perović, G. "Račun Izravnanja I – Teorija grešaka merenja", Naučna knjiga, Beograd, 1989.

[3] Perovic, Gligorije. "Least Squares." Monograph, University of Belgrade, Faculty of Civil Engineering, Belgrade (2005).

[4] Kim, Namhyun. "The limit distribution of a modified Shapiro-Wilk statistic for normality to Type II censored data." Journal of the Korean Statistical society 40.3 (2011): 257-266.

[5] Jurečková, Jana, and Jan Picek. "Shapiro–Wilk-type test of normality under nuisance regression and scale." Computational Statistics & Data Analysis 51.10 (2007): 5184-5191.

[6] https://www.statskingdom.com/shapiro-wilk-test-calculator.html

[7] Szöcs, H. L., and C. S. Hujber. "Some problems of the correlation analysis especially in geodesy." Journal of geodynamics 18.1-4 (1993): 23-31.

THE POSSIBILITY OF USING INTEGRATED GIS SYSTEMS AND PUBLICLY AVAILABLE REMOTE SENSING DATA FOR THE PURPOSES OF LAND VALUATION IN LAND CONSOLIDATION

Dragana Skorup[1], Goran Marinković[2], Marko Božić[3], Miroslav Vujasinović[4]

Summary:

The improvement of conditions in rural areas is influenced by the implementation of sustainable programs and projects that aim to achieve agricultural, economic, and ecological prosperity. One such project is land consolidation. A crucial aspect of its implementation is the project of land valuation, which ensures fairness in land re-allotment and compensation, if necessary. This paper will demonstrate the utilization of remote sensing data, primarily the CORINE database containing land cover information, DSMW soil map, as well as DEM, to determine some of the criteria used for defining land valuation classes in land consolidation. The integration of CORINE, DSMW, and DEM will be presented using QGIS. The objective of this study is to showcase the potential reduction in the workload of land valuation through the application of publicly available data and visual representation using one of the GIS software packages.

Key words: land valuation, land consolidation, remote sensing, GIS.

[1] Assistant, Faculty for Architecture, Civil Engineering and Geodesy, University of Banja Luka, Banja Luka, BiH, dragana.skorup@aggf.unibl.org
[2] Assoc. prof., Faculty of Technical Sciences, University of Novi Sad, Serbia, goranmarinkovic@uns.ac.rs
[3] Engineer, Meixner d.o.o., Zagreb, Croatia, marko.bozic@meixner.hr
[4] Assistant, Faculty for Architecture, Civil Engineering and Geodesy, University of Banja Luka, Banja Luka, BiH, miroslav.vujasinovic@aggf.unibl.org

1. INTRODUCTION

Land consolidation is represented by a land reform that is carried out in areas characterized by pronounced fragmentation, with the aim of reorganizing parcels and their associated rights for the purpose of more efficient utilization of agricultural land [1]. There is no universal definition for land consolidation, and various models are employed in its implementation by different countries. Serbia has a long-standing tradition of land consolidation dating back to the time of the Austro-Hungarian Empire. Today, land consolidation in the Republic of Serbia is closely tied to the development of agriculture and the execution of large-scale infrastructure projects [2]. According to the Law on Agricultural Land in the Republic of Serbia, land consolidation is conducted when rational use of agricultural land is rendered impossible due to extensive fragmentation and irregular shapes of cadastral parcels. This is done in cases involving the construction of infrastructure facilities such as drainage and irrigation systems, rural road networks, public roads, railways, reservoirs, riverbed regulation, urban expansion, as well as erosion control works [3].

The implementation of land consolidation is carried out through several interconnected phases. The first phase constitutes the preparatory stage in which a legal framework is established for the execution of land consolidation. Subsequently, geodetic-technical works are conducted, distinguishing between the phases of planning and implementation, along with investment activities that accompany this process. Given that the land consolidation process consists of a series of interrelated projects, the realization of each individual project plays a crucial role in the overall success of the completed one. One of the fundamental projects without which it would be impossible to redistribute parcels and group them is the process of land valuation in land consolidation [2].

In accordance with the Regulations on Geodetic-Technical Standards, Methods, and Procedures in the Field of Land Arrangement through Land Consolidation (in further text: Regulations), land valuation represents the process of determining the value of land within the consolidation area. The land valuation consists of two parts. The first part pertains to the approximate land valuation, requiring a reconnaissance of the terrain to select locations for pedological profiles. The second part concerns the classification of land into appraisal categories based on various characteristics. These characteristics encompass land suitability, climatic factors, and economic factors [4].

To achieve appropriate cost-effectiveness in land valuation in land consolidation, it is necessary to consider the potential use of new technologies that could be employed to optimize this procedure. In works [5]–[9], researchers attempt to identify new standardized models for land valuation that could be applicable in various complex land administrations. To facilitate the preliminary land consolidation process in determining the locations where pedological profiles need to be dug, the paper describes the utilization of the Coordination of Information on the Environment (CORINE) database. CORINE Land Cover (CLC) is the oldest and most sought-after database within the Copernicus Land Monitoring Service (CLMS) system. This service provides information on land, its changes, land use patterns, vegetation conditions, water status, and energy variables across the Earth's surface for a wide range of applications worldwide. The first CLC database was created in 1990 based on Landsat-5 MSS/TM single data. The first update was conducted in 2000, with the latest update occurring in 2018. CLC2018 utilizes data obtained from ESA Sentinel-2 and Landsat 8 [10]. The multifaceted applications of the CLC database in various contexts are described in works [11]–[14]. This paper will demonstrate the method of using the CORINE database to determine land types within the area of interest. Based on the updated CORINE database, the commission responsible for a land valuation could provide a solid foundation for a detailed assessment, as data derived from land records are often outdated and may not correspond to the actual conditions.

The FAO Digital Soil Map of the World (DSMW) is one of the series of free tools that, through integration with other acquired data, could represent a smoother and more expeditious path towards the optimization of land valuation. The DSMW is a digital version of the FAO-UNESCO soil map produced in a paper version at scale 1:5 million. Based on this map, soil types are categorized into 106 groups, with an additional four groups that do not qualify as soils [15]. This paper will demonstrate the method of integrating DSMW into the QGIS software to streamline the approximate assessment [15]–[17].

The Digital Elevation Model (DEM) represents a three-dimensional portrayal of the Earth's surface and finds utility across a broad spectrum of disciplines, including geomorphology, precision agriculture, defense, sports, tourism, telecommunications, urban planning, hydrology, and land arrangement [18]. The application of DEM for determining various soil characteristics has been showcased in works [19]–[21]. This paper will illustrate the use of DEM models for the purpose of ascertaining specific soil suitability characteristics such as terrain relief, slope, erosion, and exposure in the detailed soil assessment process.

2. MATERIALS AND METHODS

In this section of the paper, an overview will be provided of the area of interest, the method by which separate data sets are acquired, and their integration into QGIS.

2.1. STUDY AREA

The cadastral municipality chosen as an example for the integration of remote sensing and GIS data from the perspective of applying new technologies to optimize land valuation in land consolidation is Izbište. Izbište is a cadastral municipality that belongs to the city of Vršac and is situated between the South Banat loess plateau, which represents a continuation of the Deliblatska peščara, and the East Banat depression. The topographical structure of the project area is generally flat and close to flat. It spans between 21°6' - 21°14' E and 44°56' - 45°3' N, Figure 1. The land consolidation area of the Izbište cadastral municipality falls within the Bela Crkva administrative district and covers an area of 4501 hectares, of which 303 hectares are designated as the construction zone. The cadastral boundaries of this area were established 135 years ago, and no changes had occurred until the land consolidation process began. The land survey was conducted using the fathom measurement system and stereographic projection, while the cadastral plans were prepared at a scale of 1:2880. The maps used were very outdated, and any modifications made to them were difficult and unreliable for registration. The total number of property sheets amounted to 1914. All of these factors indicated the outdated nature of cadastral data, which presented an unrealistic depiction of property and legal relationships in this area.

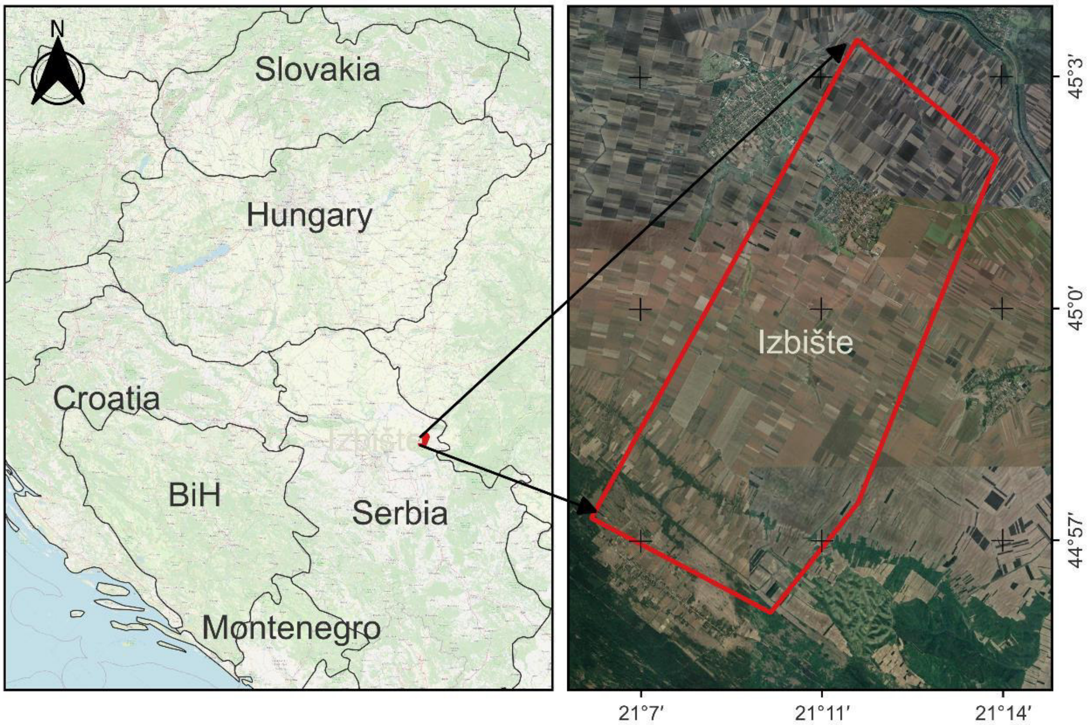

Fig. 1 Study area

2.2. DATA ACQUISITION

For the purpose of developing the land valuation model, data has been acquired from multiple sources. To determine land cover in the Izbište cadastral municipality, data from the CLC database has been obtained. The land consolidation process in the Izbište cadastral municipality was conducted in 2018; therefore, the CLC database for the year 2018 will be presented. Since the exact date of the land valuation is unknown to the author, it is possible that an earlier update from 2012 had to be used during that period. Given that this is a purely research-oriented project without applicability to a specific case in the Izbište cadastral municipality, precise data is not necessary for the integration process with other datasets.

CLC2018 represents an updated version of the previous CLC2012. The project is coordinated by the European Environment Agency (EEA), and its key characteristics include [22]:

- The use of Sentinel-2 satellite imagery as the primary dataset for land cover representation;
- Filling data gaps based on Landsat-8 data;
- Reduced production time compared to earlier models (one and a half years);
- Geometric accuracy of CLC data is better than 100 m;
- Thematic accuracy exceeding 85%.

The Corine Land Cover GeoPackage database for the year 2018 was obtained from the Copernicus website [23].

DSMW represents a digital version of the FAO-UNESCO soil map at a 1:5 million scale. It displays 4931 mapping units consisting of various soil types categorized into 106 soil groups based on the FAO-UNESCO legend. The classification of soil is done based on the estimated proportions of component soil units, the presence of relevant constraint factors or phases, and the estimated proportions of all soil units within one of 9 texture-slope classes. Physical and chemical characteristics in the topsoil and subsoil are assessed for soil units. The DSMW shapefile format digital map was obtained from the FAO Map Catalog [24].

The Shuttle Radar Topography Mission (SRTM) represents the first single-pass Synthetic Aperture Radar (SAR) interferometer in space, developed as a joint project between the National Aeronautics and Space Administration (NASA), the National Imagery and Mapping Agency (NIMA, now known as the National Geospatial-Intelligence Agency - NGA), and Deutsches Zentrum für Luft - und Raumfahrt (DLR) [25]. SRTM introduced the first freely available, nearly global, high-resolution digital elevation model of consistent quality [26]. Data for this mission were collected in February 2000 over an eleven-day period, and height files with a resolution of 1 arc-second (SRTM1) were initially produced for the United States [27], [28]. Currently, 30 m (1 arc-second) resolution SRTM data is publicly accessible on the USGS Earth Explorer for a significant portion of the world. USGS Earth Explorer was used to obtain the SRTM DEM model for the Izbište cadastral municipality area [29].

2.3. METHODOLOGY

Following the acquisition of the aforementioned data, their integration was carried out within the QGIS software package. The acquired databases and rasters were clipped to the area for which the land valuation is required, specifically, the Izbište cadastral municipality. Based on the CLC database, the vegetation cover in the Izbište cadastral municipality area was visualized. The DSMW has been integrated with the Soil and Water Assessment Tool (SWAT) model to display soil types in QGIS.
From the SRTM .tiff model, contour lines, slope, aspect, and ultimately a 3D terrain model were generated to obtain a comprehensive depiction of the terrain in this area. The flowchart of steps and methods for this study is depicted in Figure 2.

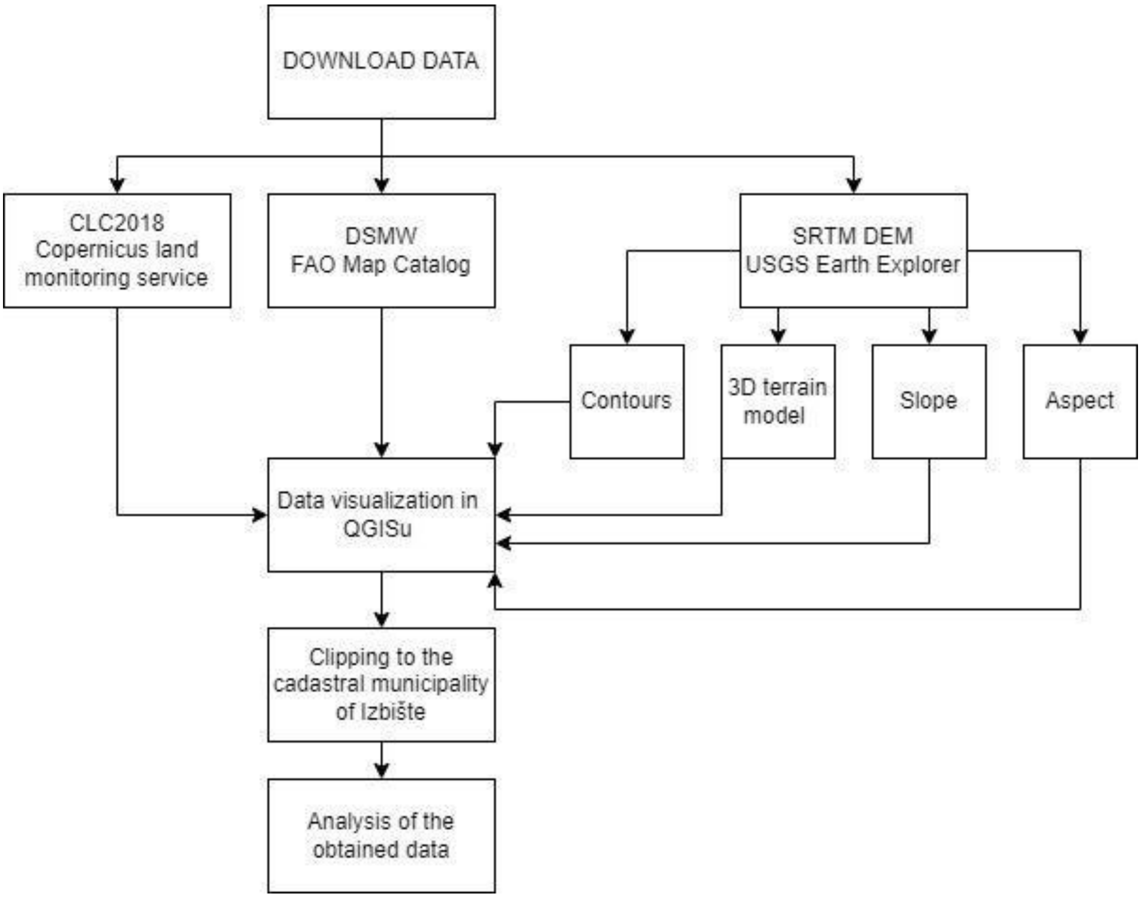

Fig. 2 Flowchart of steps and methods for this study.

3. RESULTS

After loading the acquired data into QGIS, they underwent analysis. The analysis of the CORINE database was conducted with the perspective of displaying land cover types in the Izbište cadastral municipality, as shown in Figure 3. Additionally, raster data was acquired for the purpose of analysis. Using the "Raster layer unique values report" and "Zonal histogram" tools, diagrams were created (Figure 3) to illustrate the relationship between different vegetation types in the Izbište cadastral municipality. Furthermore, by grouping specific subcategories into broader classes as follows:

- Greater than or equal to 100 and less than 200 in Class 1 - Built-up area;
- Greater than or equal to 200 and less than 300 in Class 2 - Agricultural area;
- Greater than or equal to 300 and less than 400 in Class 3 - Forested area;
- Greater than or equal to 400 and less than 500 in Class 4 - Wetland area;
- Greater than 500 in Class 5 - Water area.

Polygons were formed to calculate the area and percentage occupied by each vegetation type in the Izbište cadastral municipality (Table 1).

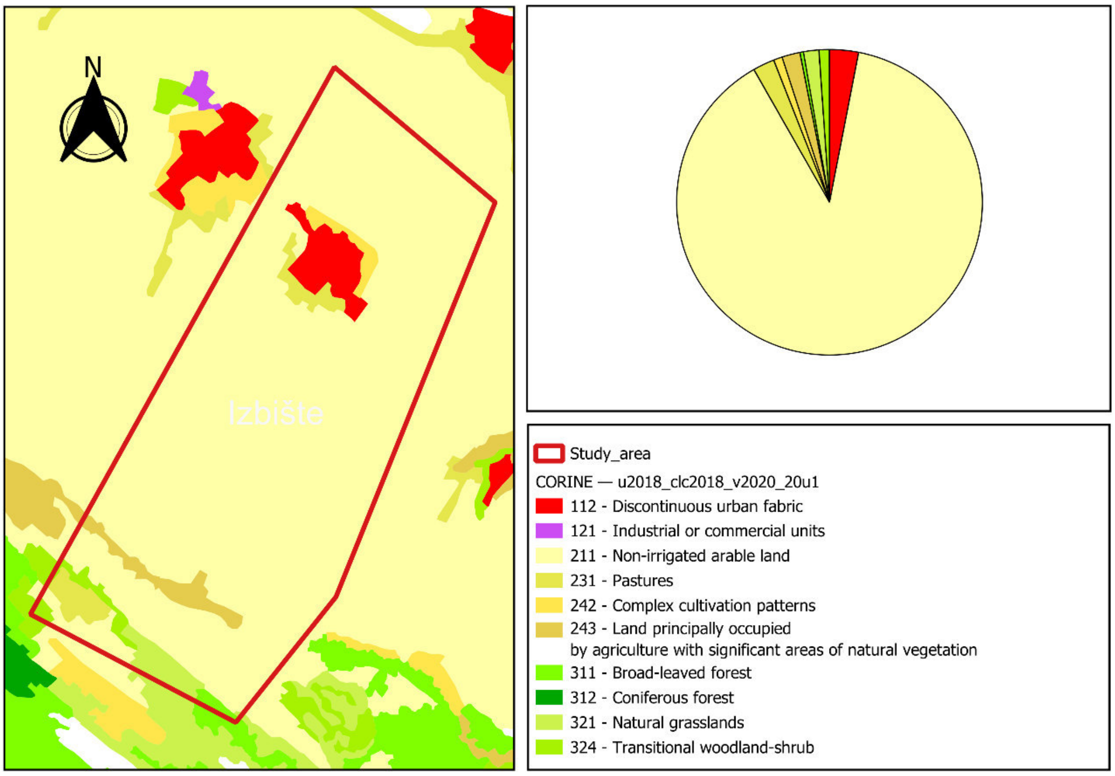

Fig. 3 The representation of vegetation cover based on the CORINE database, along with the diagram.

Tab. 1 Display of the surface areas of individual vegetation classes.

Code	Level	CatchArea [m^2]	ClassArea [m^2]	Percentage [%]
211	2	62200765	58407427	93.9
311	3	62200765	1890194	3
112	1	62200765	1904099	3.1

Based on the CORINE database, non-irrigated arable land is the most prevalent form of vegetation in the Izbište cadastral municipality.

The DSMW represents the second acquired database related to land types within the territory of the Izbište cadastral municipality. SWAT model was acquired along with DSMW, which was used for land classification, resulting in the creation of Table 2 summarizing the fundamental soil characteristics.

Tab. 2 Display of the surface areas of individual vegetation classes.

Code	Texture	Clay	Silt	Sand	Rock
6516	Clay Loam	37	39	24	0
3033	Loam	24	44	32	0

This database could facilitate the land valuation commission, primarily agricultural engineers, in the part of the assessment that pertains to selecting locations for pedological profiles. Of course, further analysis would be complemented by the CORINE database and relief maps, which, in turn, influence the choice of locations for opening pedological profiles.
Based on the acquired database, a map displaying land types within the territory of the Izbište cadastral municipality was created, as shown in Figure 4.

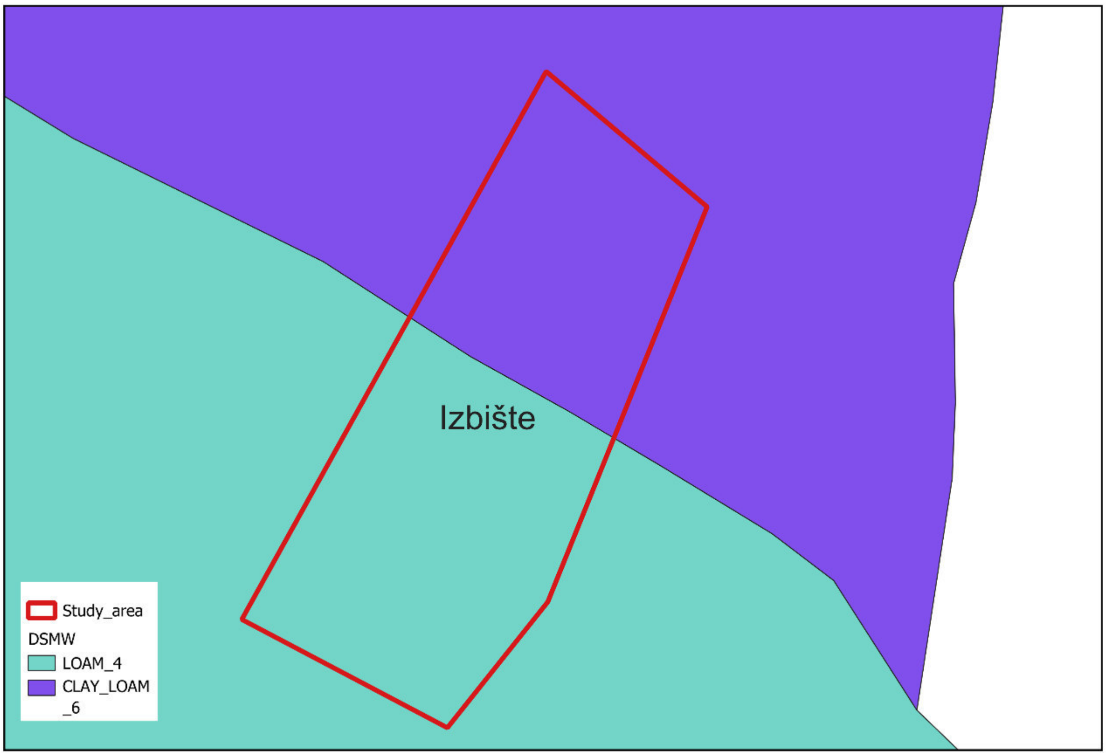

Fig. 4 Soil types in the Izbište cadastral municipality based on the DSMW.

Given that it is a digitized map at a 1:5 million scale, it is evident that the level of detail required for optimizing the approximate land valuation process cannot be expected. However, by combining it with other available data, it is possible to optimize the number of pedological profiles and, consequently, make the entire process more cost-effective. For the purpose of supplementing the DSMW model, the SRTM DEM was acquired.
Based on the DEM, contour lines, slope, and aspect were visualized within the QGIS software package. The presentation of these three maps is depicted in Figure 5.

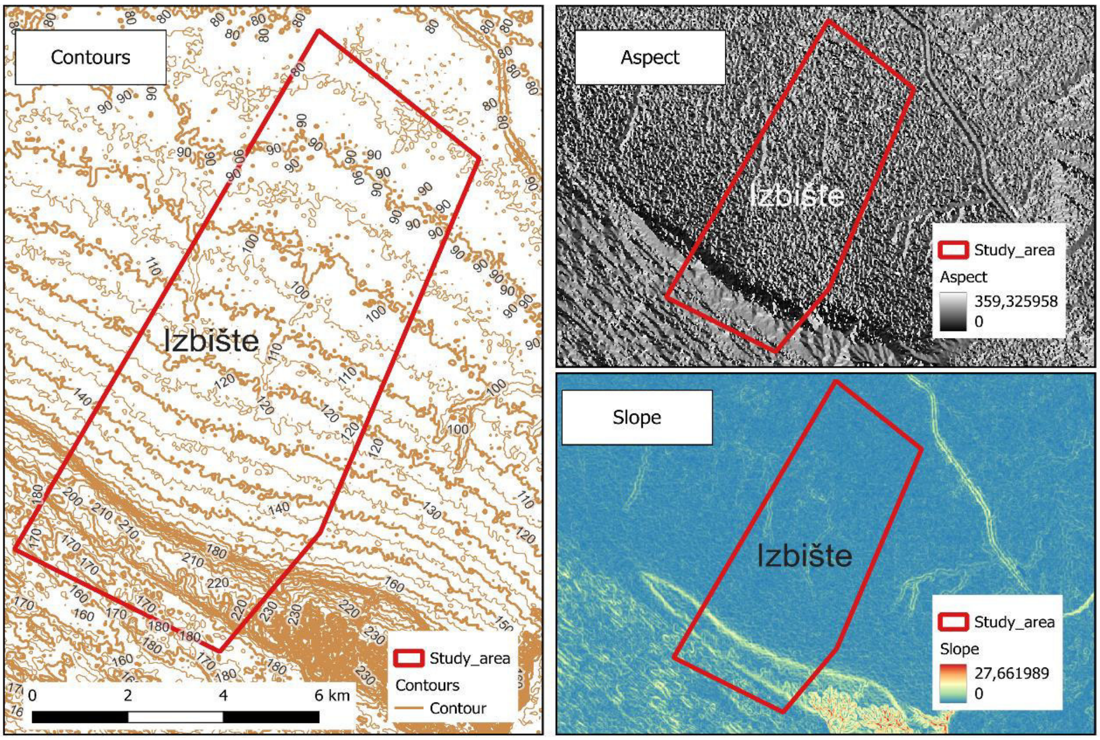

Fig. 5 The representation of contour lines, slope, and aspect in the Izbište cadastral municipality.

Based on the 3D Map Views, the creation of a 3D terrain model was also carried out, as shown in Figure 6.

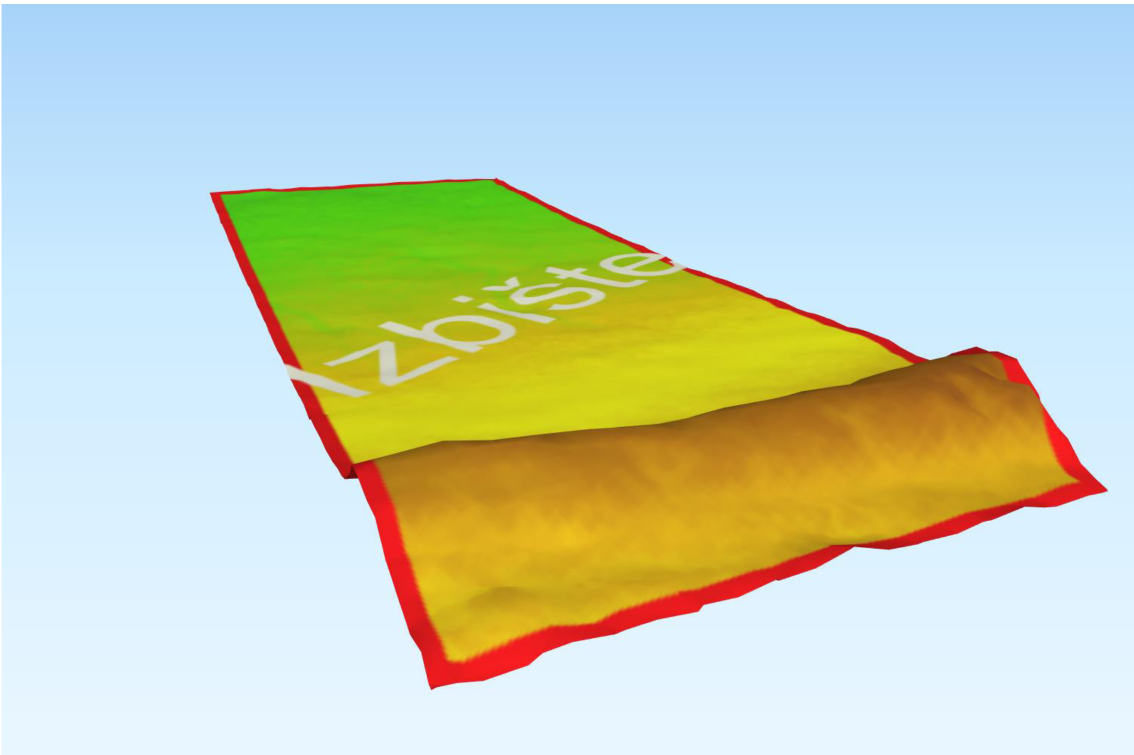

Fig. 6 3D Terrain Model of the Izbište cadastral municipality.

All the aforementioned models have been created with the aim of facilitating a faster and more cost-effective means of reviewing the cadastral municipality for the purposes of the land valuation report. The terrain relief, slope, and aspect are used for detailed land valuation, categorizing parcels into specific valuation classes. The use of freely available tools does have its limitations, primarily in terms of accuracy and detail, for this type of project. However, in areas lacking adequate non-commercial tools, such as pedological maps, higher spatial resolution DEMs, or recent surveys dating back several hundred years, these methods will undoubtedly assist in decision-making and preparing the necessary data for the land valuation process. This aspect of the project is, of course, highly significant, and reliance solely on this data is insufficient for its execution.

4. DISCUSSION

The land valuation process represents a crucial part of the land consolidation project, upon which the success of its implementation and the satisfaction of all parties involved largely depend. To ensure fair compensation for the land consolidation, it is important for the valuation commission to clearly define the conditions under which specific land is classified into various valuation categories in accordance with the Regulations. Efficient implementation requires a large dataset whose integration can yield valid results.

This paper demonstrates the use of publicly available data to obtain the necessary data for both approximate and detailed land valuation. Based on these data, conclusions can be drawn regarding the necessary further steps in the valuation process. Using the CORINE database, it is possible to determine the vegetation cover in the desired area and identify changes that occur over time by comparing two desired sets of data. Vegetation cover information can provide insights into the use of individual parcels, which may differ from what is recorded in cadastral records, as they rely on measurements from several decades ago.

Another used database related to soil types is suitable for approximate land valuation purposes with the goal of optimizing the location for soil profile excavation. It should be noted that the database used is not detailed, as it pertains to a world map, but in conjunction with terrain data, it can be utilized to streamline the approximate land valuation planning process.

The use of DEMs is important for determining detailed land valuation criteria related to terrain, slope, and aspect. Many countries have developed their own DEMs with better spatial resolutions than those obtained from SRTM, resulting in more detailed and accurate results for valuation purposes. In the absence of such models, the use of freely available DEMs is significant for defining the aforementioned criteria.

Ultimately, the integration of all these data sources is feasible through GIS software systems, enabling various spatial data analyses, their overlap, and the creation of databases suitable for manipulation.

In the course of this work, only a brief overview of some of the possibilities of using publicly available datasets has been provided, which, of course, needs to be supplemented with data collected from official records and data generated during the determination of the factual state.

Future research will focus on the potential combination of different land consolidation factors obtained from all the aforementioned sources to create a mathematical model for the land valuation boundary. This model could facilitate the fieldwork of the land valuation commission, thereby reducing the likelihood of making significant errors due to subjective boundary determination.

REFERENCES

[1] W. T. de Vries, “Social Aspects in Land Consolidation Processes,” Land, vol. 11, no. 3, p. 452, 2022, Doi: https://doi.org/10.3390/land11030452.

[2] T. Veršinskas, M. Vidar, M. Hartvigsen, K. Mitic Arsova, F. Van Holst, and M. Gorgan, “Legal guide on land consolidation,” 2020.

[3] Official Gazette of the Republic of Serbia no. 62/06, Law on agricultural land. 2006.

[4] Republic Geodetic Authority, Regulation on geodetic-technical standards, methods and procedures in the field of land consolidation (in Serbian). Serbia, 2020.

[5] S. Branković, L. Parezanović, and D. Simović, “Land consolidation appraisal of agricultural land in the GIS environment.,” Geod. Vestn., vol. 59, no. 2, 2015, Doi:10.15292/geodetski-vestnik.2015.02.320-334.

[6] D. Demetriou, “The assessment of land valuation in land consolidation schemes: The need for a new land valuation framework,” Land use policy, vol. 54, pp. 487–498, 2016, Doi: https://doi.org/10.1016/j.landusepol.2016.03.008.

[7] D. Demetriou, “Automating the land valuation process carried out in land consolidation schemes,” Land use policy, vol. 75, pp. 21–32, 2018, Doi: https://doi.org/10.1016/j.landusepol.2018.02.049.

[8] A. Tezcan, K. Büyüktas, and S. T. A. Aslan, “A multi-criteria model for land valuation in the land consolidation,” Land use policy, vol. 95, p. 104572, 2020, Doi: https://doi.org/10.1016/j.landusepol.2020.104572.

[9] Z. Muchová, L. Konc, and F. Petrovič, “Land plots valuation in land consolidation in Slovakia: a need for a new approach,” Int. J. Strateg. Prop. Manag., vol. 22, no. 5, pp. 372–380, 2018, Doi: https://doi.org/10.3846/ijspm.2018.5221.

[10] G. Büttner et al., “Copernicus Land Monitoring Service-CORINE Land Cover. User Manual,” 2021.

[11] I. Cieślak, A. Biłozor, and K. Szuniewicz, “The use of the CORINE land cover (CLC) database for analyzing urban sprawl,” Remote Sens., vol. 12, no. 2, p. 282, 2020, Doi: https://doi.org/10.3390/rs12020282

[12] U. Myga-Piatek, A. Żemla-Siesicka, K. Pukowiec-Kurda, and J. Sobala Michaland Nita, “Is there urban landscape in metropolitan areas? An unobvious answer based on corine land cover analyses,” Land, vol. 10, no. 1, p. 51, 2021, Doi: https://doi.org/10.3390/land10010051

[13] D. Tešić, “Corine land cover change detection in Serbia and Bosnia and Herzegovina,” Zb. Rad. Departmana za Geogr. Turiz. i Hotel., no. 51–2, pp. 98–110, 2022, Doi: 10.5937/ZbDght2202098T.

[14] B. Drašković, M. Gutalj, S. Stjepanović, and B. Miletić, “Estimating recent forest losses in Bosnia and Herzegovina by using the Copernicus and Corine land cover databases,” Šumarski List, vol. 145, no. 11–12, pp. 581–589, 2021, Doi: https://doi.org/10.31298/sl.145.11-12.7.

[15] X. M. Baxromjon o‘g‘li and others, “History of the development of soil mapping,” PEDAGOG, vol. 6, no. 5, pp. 750–754, 2023.

[16] “FAO/UNESCO Soil Map of the World.” https://www.fao.org/soils-portal/data-hub/soil-maps-and-databases/faounesco-soil-map-of-the-world/en/, accessed: 9. 6. 2023.

[17] K. C. Abbaspour, S. A. Vaghefi, H. Yang, and R. Srinivasan, “Global soil, landuse, evapotranspiration, historical and future weather databases for SWAT Applications,” Sci. data, vol. 6, no. 1, p. 263, 2019.

[18] P. L. Guth et al., “Digital elevation models: terminology and definitions,” Remote Sens., vol. 13, no. 18, p. 3581, 2021, Doi: https://doi.org/10.3390/rs13183581.

[19] I. Milevski, S. Dragićević, and S. Kostadinov, “Digital elevation model and satellite images an assessment of soil erosion potential in the Pcinja catchment,” Glas. Srp. Geogr. društva, vol. 87, no. 2, pp. 11–20, 2007.

[20] M. H. Greve, R. B. Kheir, M. B. Greve, and P. K. Bøcher, “Using digital elevation models as an environmental predictor for soil clay contents,” Soil Sci. Soc. Am. J., vol. 76, no. 6, pp. 2116–2127, 2012, Doi: https://doi.org/10.2136/sssaj2010.0354.

[21] P. D. Sreedevi, P. D. Sreekanth, H. H. Khan, and S. Ahmed, “Drainage morphometry and its influence on hydrology in an semi arid region: using SRTM data and GIS,” Environ. earth Sci., vol. 70, pp. 839–848, 2013.

[22] G. Büttner, B. Kosztra, T. Soukup, A. Sousa, and T. Langanke, “CLC2018 technical guidelines,” Eur. Environ. Agency Copenhagen, Denmark, vol. 25, 2017.

[23] "Copernicus Land Monitoring Service." https://land.copernicus.eu/pan-european/corine-land-cover/clc2018, accessed: 1. 6. 2023.

[24] "FAO Map Catalog." https://data.apps.fao.org/map/catalog/srv/eng/catalog.search#/metadata/446ed430-8383-11db-b9b2-000d939bc5d8, accessed: 10. 6. 2023.

[25] M. Werner, "Shuttle radar topography mission (SRTM) mission overview," Frequenz, vol. 55, no. 3–4, pp. 75–79, 2001, Doi: https://doi.org/10.1515/FREQ.2001.55.3-4.75.

[26] L. Yang, X. Meng, and X. Zhang, "SRTM DEM and its application advances," Int. J. Remote Sens., vol. 32, no. 14, pp. 3875–3896, 2011, Doi: https://doi.org/10.1080/01431161003786016

[27] T. Bašić and G. Buble, "Usporedba globalnog modela visina SRTM3 s postojećim digitalnim modelima reljefa na području Hrvatske," Geod. List, vol. 61, no. 2, pp. 93–111, 2007.

[28] G. Marinković, M. Ilić, M. J. Lazić, and I. Grgić, "Komparacija digitalnih modela terena: Studija slučaja opština Bela Crkva i Brus", 11th International Scientific Conference "Science and Higher Education in Function of Sustainable Development", Mećavnik – Drvengrad, Užice, Serbia, 2019.

[29] "USGS Earth Explorer." https://www.usgs.gov/educational-resources/earth-explorer, accessed: 14. 6. 2023.

REGISTRATION OF PROPERTY RIGHTS ON THE CONSTRUCTION LAND

Gordana Nataroš[1], Marina Davidović Manojlović[2]

Summary:

By different Laws in Serbia from 1958, 2003, 2009, respectively, private construction land was nationalized, then partially returned, and finally, privatized again. According to the Law on Planning and Construction, the basis for obtaining a construction permit in the regular and in the legalization procedure, is the registered private property of the investor, i.e., natural person on the subject parcel. Previously valid Laws did not allow alienation or conversion of nationalized property, which turned away potential foreign investors.

This paper deals with a comparative analysis of previously valid Laws related to the registration of property rights on construction land in the Cadastre, with the currently valid Laws, and provides an overview of the draft of the new Law. A case study of registration, i.e., change of property rights in the Cadastre on land that was public property, while the objects on it were private property, will be presented.

Key words: cadastre, construction land, property right

[1] Mast inž geod., Savetnik za nekretnine, Novi Sad, Srbija, jeja023@gmail.com
[2] Mast inž geod., Istraživač saradnik, Fakultet tehničkih nauka, Univerzitet u Novom Sadu, Srbija, marina.davidovic@uns.ac.rs

1. INTRODUCTION

Urban construction land in Serbia has gone through many changes in the last 70 years. It was nationalized, partially restored and, finally, privatized again.
After the Second World War, large areas of arable land, forests, construction land, buildings, factories, etc. were confiscated by the authorities. The socialist state took complete control over the majority of private property, using one of the first and most radical economic-political measures, i.e. nationalization. This happened in several stages, and the most significant nationalization was in 1958, when all urban construction land was nationalized. That land was first converted into public, and then transferred into social ownership. The owners of the land became only its usufructuary, and that usufructuary right could be inherited, but not sold. This situation stopped the development of the real estate market. It happened that some people sold their right of use on construction land, but there was no possibility of legal transfer [1].
Three important laws on nationalization should be noted:

1. Law on Nationalization of Rental Buildings and Construction Land (Official Gazette of FNRY, no. 52/58 24/61);
2. Law on determining construction land in cities and settlements of urban character (Official Gazette of the SFRY No. 5/68);
3. Law on determining construction land in cities and settlements of urban character (Official Gazette of SRS No. 32/68...39/73).

In the period from 1958. that is, from 1968 onwards, the previous owner could not transfer to any legal or physical person the right of use either by sale, exchange, gift or any other way. This was valid for all except the municipality, which was authorized to exempt construction land, allocate and manage construction land.
In 2003, the Law on Planning and Construction was passed, which under certain conditions enabled the sale and transfer the right of use for nationalized undeveloped construction land (Article 84) [2]. It was a formal and legal acceptance of established practice. The law also enabled the formation of construction plots.
However, this Law did not change the status of land. The purchase still meant only the purchase of the right of use. Many potential foreign investors could not accept or understand that their million dollar investments can be located on land that they can lease for 99 years, but it cannot be their property. They wanted full ownership like anywhere in the West. This Law was the first step forward in the domestic real estate market, but insufficient for successful and rapid development [1]
The new Constitution of Serbia, adopted in October 2006, opened the door to the privatization of construction land. A new Law that would finally return the land to its owners should be passed. This happened with the new Law on Planning and Construction in Serbia (Official Gazette of RS, no. 72/2009), which entered into force on September 11, 2009 [3]. This new Law regulates the conversion of the right of use of nationalized developed land into the right of ownership, while the problem of what to do with unbuilt nationalized land remains.
All these changes had to be implemented in public books, ie. Cadastre.
The Constitution of the Republic of Serbia (Official Gazette of RS, No. 98/06) recognizes three forms of property: private, public and cooperative.
Construction land can be: built and unbuilt. The term built-up construction land means a plot of land on which a legal object of permanent character is located. Unbuilt construction land is a plot on which there are no objects, that is, a plot on which there are illegal objects.
The basis for obtaining a construction permit in the regular procedure and in the legalization procedure is the registered ownership right on the land.
It should be mentioned that the transfer of the plot can be performed and certified by a notary only if the ownership of the land, and not the right of use, is registered.

2. CASE STUDY (CM ZRENJANIN I)

For the case study of registration, i.e. change of rights on land that was public property, while the objects on it were private property, the example of the cadastral municipality (hereinafter, CM) Zrenjanin I, cadastral plot number 6714 was taken.

This plot, with an area of 1,662 m², is registered as public property of the City of Zrenjanin, while the objects (six them in total), are registered as a legal entity of LTD Eurobiro with private ownership. LTD Eurobiro is a company that was founded from its own capital, which means that it was not bought in bankruptcy. This further provides the possibility of registering property rights on the land, by applying the Law on Planning and Construction (hereinafter , LPC) [3].

In this case, it is not about conversion, because that procedure has already been carried out, as the City of Zrenjanin converted the right of land use into public property.

Before submitting a request to the competent authority for state survey and cadastre affairs, i.e. to the Republic Geodetic Institute (hereinafter, RGI) for the registration of property rights on land (LPC - Article 102, paragraph 3 and Article 105, paragraph 1), it is necessary to obtain a Decision determining the land for regular object use and the formation of a construction plot (LPC , Article 70, paragraph 1).

The request for the determination of land for the regular object use and the formation of a construction plot is submitted to the body of the local self-government unit responsible for property-legal affairs (LPC, Article 70, paragraph 10), which was done in this case as well.

When passing the Decision, the competent authority was obliged to obtain:

1. From RGI
   - Immovable property list,
   - A copy of the cadastral plan (Figure 1 - the red marked is the plot of interest),
   - Land registry file (Figure 2),
   - Statement of identification (Figure 3),
   - Notification when the plot is formed.
2. From the Restitution Agency
   - Notification of whether there is a request for the return of confiscated property.
3. From the Department of Urban Planning
   - Report whether the cadastral plot meets the conditions to be designated as land for regular object use

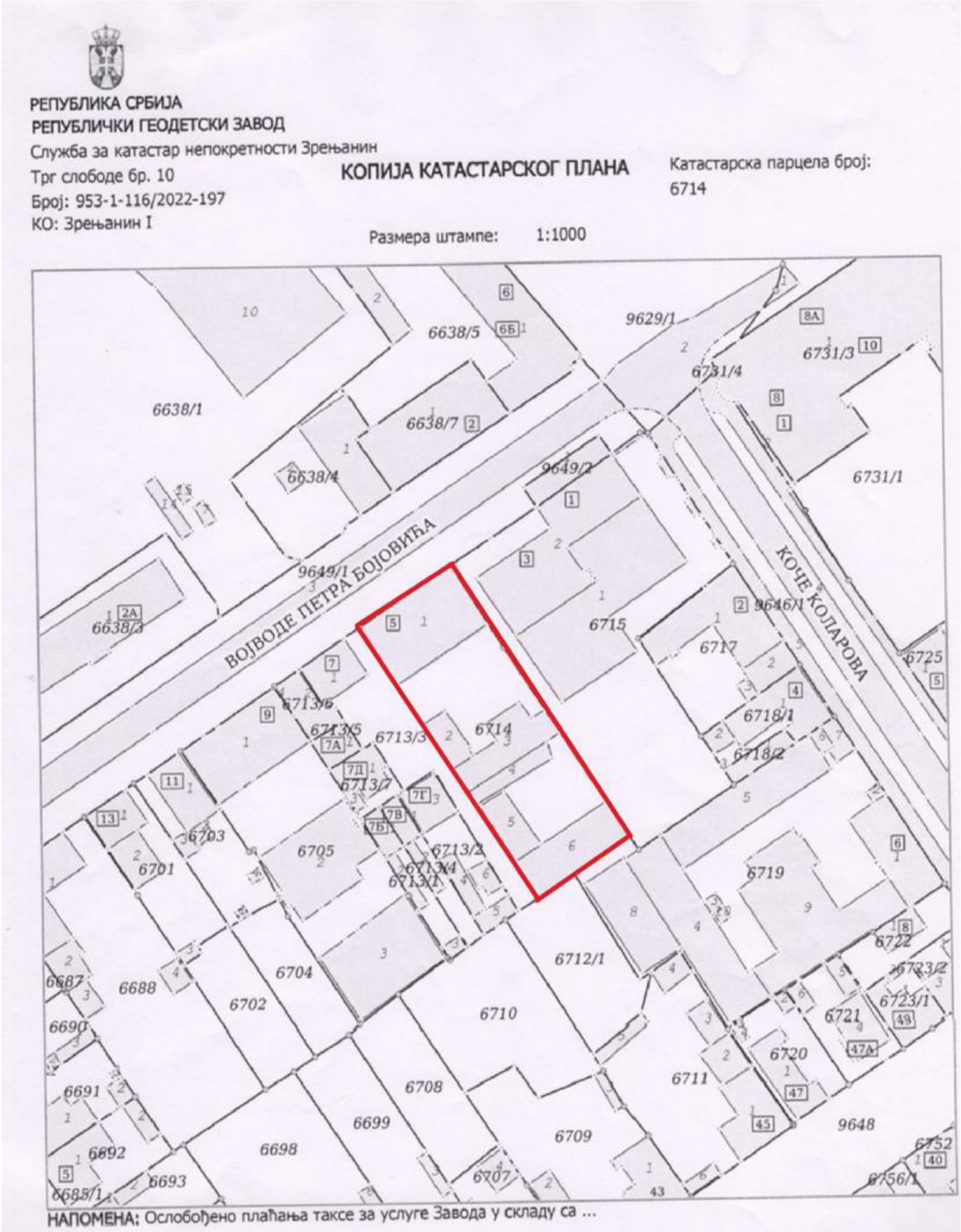

Figure 1. Copy of the cadastral plan

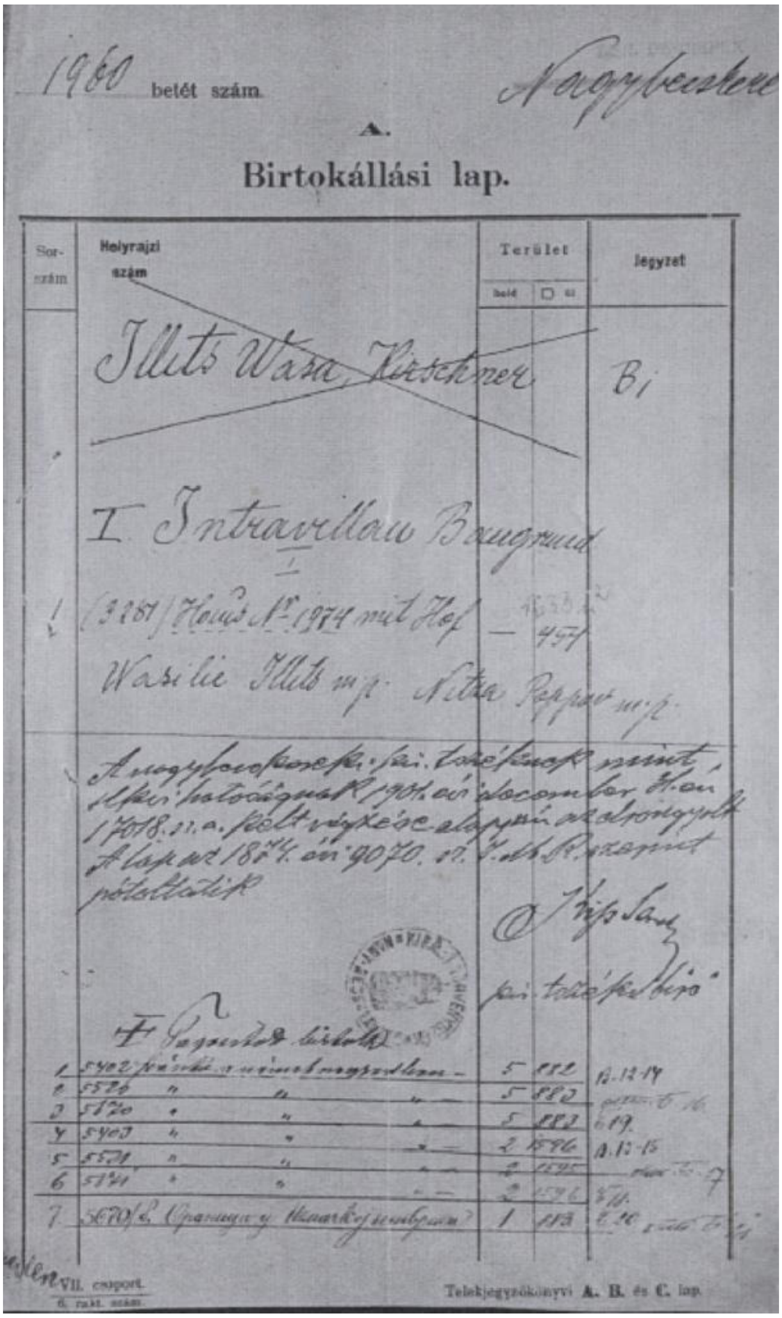
1980 betét szám. Nagybecskerek

A.

Birtokállási lap.

Sor-szám	Helyrajzi szám	Terület hold	Terület □ öl	Jegyzet
	~~Illits Wasa, Kirschner~~			B/
	I. Intravillan Baugrund			
1	(3281) Haus № 1974 mit Hof	—	457	
	Wasilie Illits m/p. Nitza Poppov m/p.			
1	5402	5	882	A.12-14
2	5526	5	882	
3	5170	5	883	6.19.
4	5403	2	1596	A.12-15
5	5531	2	1595	
6	5141	2	1596	
7	5670/2.	1	883	

VII. csoport.

Telekjegyzőkönyvi A. B. és C. lap.

Figure 2. Land registry insert

страна бр. 1

РЕПУБЛИКА СРБИЈА
РЕПУБЛИЧКИ ГЕОДЕТСКИ ЗАВОД
Служба за катастар непокретности Зрењанин
Број: 952-116-33107/2022
Дана 20.04.2022
ЗРЕЊАНИН

Ваш број: 463-24/2022

РГЗ Служба за катастар непокретности Зрењанин по захтеву:

Градска управа, Одељење за имовинско-правне послове и управљање имовином, Зрењанин

ИЗДАЈЕ
УВЕРЕЊЕ О ИДЕНТИФИКАЦИЈИ

К.О. Зрењанин I

СТАЊЕ ПО КАТАСТРУ ЗЕМЉИШТА						СТАЊЕ ПО ЗЕМЉИШНОЈ КЊИЗИ					СТАЊЕ ПО КАТАСТРУ НЕПОКРЕТНОСТИ					
број П.Л.	број парцеле	ку. кл.	површина ха	а	м2	зкњ.ул. број	број парцеле	површина ха	а	м2	број ЛН.	број парцеле	ку. кл.	површина ха	а	м2
						1960	3281		16	33	4287	6714	об. 1		03	52
													об. 2			67
													об. 3		01	80
													об. 4			69
													об. 5			92
													об. 6		02	17
													уз об.		06	85
															16	62

НАПОМЕНА:Подаци из катастра земљишта заснивају се на службеној евиденцији коју води Републички геодетски завод Служба за катастар непокретности Зрењанин.
Идентификација парцела катастра земљишта и катастра непокретности са подацима земљишне књиге заснива се на неслужбеној евиденцији.

Идентификовао: Гордана Јанков

Оверава

Figure 3. Statement of identification

With complete documentation, the Department for Property-Legal Affairs and Property Management, Section for Property-Legal Affairs, issues a decision determining the land for regular object use and the formation of a construction plot.
When the Decision has become legally binding, it is officially forwarded to RGI and with the request of the party, RGI issues a Decision allowing changes to be made in the database of the real estate cadastre, where LTD Eurobiro with a 1/1 share in the land is entered.
Since LTD Eurobiro was registered on this plot on all six objects (having area 977 m², with a plot occupancy rate of 58.78%) as private property, and the city of Zrenjanin did not have a separate object part, Eurobiro became the owner of the plot 1/ 1 free of charge.

3. CONCLUSION

This was the procedure of registering property rights on the land, which takes time, due to the collection of all documents. A lot of people are not familiar with the procedure and waste even more time and money on consulting services, lawyers etc. All these flaws indicated the need to change the legal regulations. Finally, the new Law is passed in July this year , i.e. 2023: Law on Planning and Construction (Official Gazette of RS, no. 72/2009, 81/2009 - corrected, 64/2010 - US decision, 24/2011, 121/2012, 42/2013 - US decision, 50/2013 - decision US, 98/2013 - decision US, 132/2014, 145/2014, 83/2018, 31/2019, 37/2019 - other laws, 9/2020, 52/2021 and 62/2023) [4].
Analyzing the aforementioned Law that is presented in this paper, a following conclusion is reached: since 2009, the same Law has undergone numerous additions and changes of certain articles, all for the purpose of faster and simpler solutions to the problem of land ownership registration. The same Law shows that there were various decisions, then decrees and other laws. Certain articles of the Law are put out of force

from the moment of adoption of new amendments and additions to the articles of the Law. By amending the Law on Planning and Construction, the previous procedure and heavy paperwork is not needed, but the procedure is shortened, where a party or a legal entity directly submits a request and immediately registers the property on the land based on Article 102 [4]:

"The right of use on construction land is converted into the right of ownership, free of charge.

The ownership right from paragraph 1 of this article is acquired on the day this law enters into force, and the registration of the ownership right is carried out by the authority responsible for state survey and cadaster, ex officio.

The ownership right on the cadastral plot is registered in favor of the person who is registered as the owner of the object, that is, the objects located on that plot, or the person who is registered as the holder of the right of use on the cadastral plot on unbuilt construction land."

When it comes to conversion, which for years has hindered a large number of investments, according to the amended law, the right of use on construction land is converted into the right of ownership without compensation.

REFERENCES

[1] Nataroš G. (2010). Cadaster changes on nacionalized land in Municipality Zrenjanin. *Geodetski žurnal,* Vol. 38, pp. 11–16.

[2] Law on Planning and Construction, Official Gazette of RS, no. 47/2003 (Zakon o planiranju i izgradnji, Službeni glasnik RS, br. 47/2003)

[3] Law on Planning and Construction, Official Gazette of RS, no. 72/2009 (Zakon o planiranju i izgradnji, Službeni glasnik RS, br. 47/2003)

[4] Law on Planning and Construction, Official Gazette of RS, no. 62/2023 (Zakon o planiranju i izgradnji, Službeni glasnik RS, br. 47/2003)

PARALLELISM OF STRAIGHT LINES DETERMINED BY GEODETIC METHODS TESTING

Goran Marinković[1], Žarko Nestorović[2], Zoran Ilić[3], Marko Božić[4]

Summary:

Determination geometry of linear objects by utilizing geodetic methods is based on their discretization i.e. determination of points' coordinates by which they are defined. For linear objects such as railway lines or crane tracks it is necessary after their realization and during exploitation, along with designed range, to check their parallelism. Discretization of two lines whose parallelism is to be verified, in general case is not possible in two opposite points. That is the reason to express the set of points with formula and compare it with the formula which defines another line. The inevitable measurement errors and their influence on points' coordinate determination cause process of decision making about parallelism of two lines during statistical hypothesis testing quite complex. This research considers parallelism of two lines from theoretical and practical aspect in the horizontal plane.

Key words: discretization, statistical test, accuracy, statistical hypothesis formulation

[1] Assoc. prof., Faculty of Technical Sciences, University of Novi Sad, Serbia, goranmarinkovic@uns.ac.rs
[2] mr, Public Company of Electricity Production – EPS, Branch "DJerdap", Kladovo,, nzarko07@gmail.com
[3] Engineer, Academy of Technical and Educational Vocational Studies, Aleksandra Medvedeva 20, 18000 Nis, Serbia zoran.ilic.ni@akademijanis.edu.rs
[4] Engineer, Meixner d.o.o., Hermanova 16/G, 10000 Zagreb, Croatia, marko.bozic@meixner.hr

1. INTRODUCTION

In this research the theoretical and practical aspects of two line parallelism determination is considered. Linear objects especially objects with higher accuracy requirements like crane tracks and/or railway tracks.
In the general case determination of two lines parallelism is derived to the discrete case: the track shall be surveyed and coordinates of points which represent the tracks are determined. The parallelism of tracks could be determined by comparing the distance between opposite points. This could simple idea could not fulfil the aim because line determined by two opposite points could not be perpendicular on tracks' axis. On the other side the attempt of staking out the opposite points on their right position consume a lot of time and it is burdened by additional errors. In this research the linear regression was utilized and results were discussed. The mathematical model of regression is well known and described in literature (for example [1]).
From literature are known different methods for straightness of each track but they do not often provide the information about relative distance between pair of rails [2]. Even though the geodetic method usually does not provide ultra-high accuracy in tracks parallelism determination the mathematical model shall be provided in order to obtain correct conclusion about parallelism and straightness of tracks. The geodetic methods could provide the accuracy of measurements in the millimetre or submillimetre range and could determine deviation from straightness and parallelism of lines dependently on the measurement accuracy and the deviation's size.

2. MATERIALS AND METHODS

In this research straightens and parallelism of cranes tracks surveyed by geodetic methods were modelled and statistically tested. The cranes tracks were about 200 m long and discretized by 39 points each. The accuracy of each point's position was $\sigma_x =$ 1 mm. The statistical hypotheses formulation is also given in further text.
The model of linear regression is described as follows:

$$Y_i = aL_i + b + \varepsilon_i \tag{1}$$

where:
Y_i – deviation from the straight line
L_i – distance from the beginning of the line
a – coefficient of inclination
b – constant coefficient and
ε_i – random error.
It is assumed that random errors have following properties:

$$E(\varepsilon_i) = 0 \tag{2}$$

$$E\left(\varepsilon_i \varepsilon_j\right) = 0 \tag{3}$$

$$E(\varepsilon_i \varepsilon_i) = \sigma^2 \tag{4}$$

where E denotes mathematical expectation. The coefficients of linear model (1) were estimated by utilizing the least squares method [1] assuming that all weights are equal.
It is also assumed that coefficients of regression follow the student's distribution:

$$t = \frac{a}{m_a} \sim t_{f,1-\alpha} \tag{5}$$

where:

- t – statistics

- a – estimation of regression coefficient
- m_a – mean root square error of regression coefficient a.
- f – degrees of freedom and
- α – level of significance ($\alpha = 0.05$).

The root mean square errors are assumed to follow F-distribution:

$$F = \frac{m_i^2}{m_j^2} \sim F_{f_i, f_j, 1-\alpha} \tag{6}$$

where:

- F – F distribution
- f_i – degrees of freedom of numerator
- f_j – degrees of freedom of denominator and
- level of significance ($\alpha = 0.05$).

The statistical hypotheses are utilized for determining if deviation from straightness of tracks exists, if the tracks are parallel and if the tracks are inclined. Formulation of statistical hypotheses is based on the null (H_o) and alternative (H_a) hypothesis formulation and decision based on the value of statistics.

The statistical hypotheses about equality of two models read as follows:

- H_o: two models are equal and
- H_a: otherwise.

The equality of two models is tested as follows:

$$F = \begin{cases} \dfrac{m_i^2}{m_j^2} < F_{f_i, f_j, 1-\alpha} \text{ then } & H_o \text{ is not rejected} \\ \dfrac{m_i^2}{m_j^2} \geq F_{f_i, f_j, 1-\alpha} \text{ then } & H_a \text{ is not rejected} \end{cases} \tag{7}$$

The statistical hypotheses about parallelism of two lines read as follows:

- H_o: two lines are parallel and
- H_a: otherwise.

The parallelism of lines is tested as follows:

$$t = \begin{cases} \dfrac{a_{M_i} - a_{M_j}}{\sqrt{\dfrac{m_{a_{M_i}}^2}{n_{M_i}} + \dfrac{m_{a_{M_j}}^2}{n_{M_j}}}} < t_{f,1-\alpha} \text{ then } & H_o \; is \text{ not rejected} \\ \dfrac{a_{M_i} - a_{M_j}}{\sqrt{\dfrac{m_{a_{M_i}}^2}{n_{M_i}} + \dfrac{m_{a_{M_j}}^2}{n_{M_j}}}} \geq t_{f,1-\alpha} \text{ then } & H_a \; is \text{ not rejected} \end{cases} \tag{8}$$

The statistical hypotheses about deviations from straightness of measured points read as follows:

- H_o: two lines are parallel and
- H_a: otherwise.

The deviation from straightness is tested in two ways:

$$F = \begin{cases} \dfrac{m_i^2}{\sigma_x^2} < F_{f_i, \infty, 1-\alpha} \text{ then } & H_o \text{ is not rejected} \\ \dfrac{m_i^2}{\sigma_x^2} \geq F_{f_i, \infty, 1-\alpha} \text{ then } & H_a \text{ is not rejected} \end{cases} \tag{9}$$

$$t = \begin{cases} \dfrac{Y_i - Y_{M_i}}{\sqrt{\sigma_x^2 + \dfrac{m_{M_i}^2}{n_{M_i}}}} < t_{f,1-\alpha} \text{ then } \; H_o \text{ is not rejected} \\ \dfrac{Y_i - Y_{M_i}}{\sqrt{\sigma_x^2 + \dfrac{m_{M_i}^2}{n_{M_i}}}} \geq t_{f,1-\alpha} \text{ then } \; H_a \text{ is not rejected} \end{cases} \tag{10}$$

Formulae (7), (8) and (9) imply that there is a global deviation in the model while formula (10) identifies the local deviation for certain point from straightness.
The degree of freedom in formulae (8) and (10) is calculated according Perović [3]:

$$\frac{1}{f} = \frac{c^2}{f_1} + \frac{(1-c)^2}{f_2} \tag{11}$$

$$c = \frac{\dfrac{m_1^2}{n_1}}{\dfrac{m_1^2}{n_1} + \dfrac{m_2^2}{n_2}} \tag{12}$$

Testing significance of coefficients of linear regression are also hypotheses of importance for detailed parallelism analysis. The hypothesis in this case reads:

- H_o: the coefficient of linear regression is zero ($a = 0$) and
- H_a: otherwise.

The significance of linear regression coefficient statistics reads as follows:

$$t = \begin{cases} \dfrac{a}{m_a} < t_{f,1-\alpha} \text{then } \; H_o \text{ is not rejected} \\ \dfrac{a}{m_a} \geq t_{f,1-\alpha} \text{then } \; H_a \text{ is not rejected} \end{cases} \tag{5}$$

3. RESULTS AND DISCUSSION

After data processing by the model (1) of linear regression, calculating test statistics and hypothesis testing the obtained results about global statistical tests are presented in table 1. The deviations are given in millimetres [mm].

Tab. 1 The global statistical tests

item number	Test	Model	Hypothesis not rejected
1	The equality of two models	$\frac{10.7^2}{6.1^2} = 3.0769 > F_{37,37,0.95}$=1.7304	H_a
2	The parallelism of lines	$\frac{-8.0650 * 10^{-5} - (-1.1165 * 10^{-4})}{\sqrt{\frac{(1.7439 * 10^{-5})^2}{39} + \frac{(3.0491 * 10^{-5})^2}{39}}} = 6.3756 > t_{62,0.95} = 1.9990$	H_a
3	The deviation from straightness for first line	$\frac{10.7^2}{1^2} = 114.4900 > F_{37,\infty,0.95} = 1.4113$	H_a
4	The deviation from straightness for second line	$\frac{6.1^2}{1^2} = 37.2100 > F_{37,\infty,0.95} = 1.4113$	H_a
5	Significance of linear regression coefficient for first line	$\frac{\lvert -1.165110^{-4} \rvert}{3.0491 * 10^{-5}} = 3.8212 > t_{37,0.95} = 2.0262$	H_a
6	Significance of linear regression coefficient for second line	$\frac{\lvert -8.0650 * 10^{-5} \rvert}{1.7439 * 10^{-5}} = 4.6246 > t_{37,0.95} = 2.0262$	H_a

The result of global tests about parallelism of analysed two straight lines shoved as follows:

- The deviations between models were significant (lines deviate from each other straightness significantly)
- The lines are not parallel
- The deviation from straightness for both lines are significant
- Linear regression coefficients are significant for both lines.

These conclusions are significant but, in practical sense, they are not acceptable base for crane tracks correction. The examination of each point deviation from straightness is required in order to correct the crane tracks. The statistics and hypothesis are given in tables 2 and 3.

Tab. 2 The local statistical tests for Line 1

item number	L1:$Y_i - Y_{M_i}$	L1:$\sigma_x^2 + \frac{m_{M_i}^2}{n_{M_i}}$	L1: t	L1: Hypothesis
1	-2.8	1.1	2.4632	*Ha*
2	-6.4	1.1	5.6292	*Ha*
3	-9.5	1.1	8.3958	*Ha*
4	-10.4	1.1	9.1013	*Ha*
5	-12.2	1.1	10.6856	*Ha*
6	-24.6	1.1	21.5018	*Ha*
7	-16.7	1.1	14.5924	*Ha*
8	2.2	1.1	1.8951	*Ho*
9	-3.0	1.2	2.5868	*Ha*
10	3.4	1.2	2.9229	*Ha*
11	1.3	1.2	1.0843	*Ho*
12	7.3	1.2	6.2822	*Ha*
13	5.9	1.2	5.0140	*Ha*
14	9.0	1.2	7.6287	*Ha*
15	10.5	1.2	8.8555	*Ha*
16	15.3	1.2	12.8155	*Ha*
17	10.7	1.2	8.9245	*Ha*
18	13.4	1.2	11.0914	*Ha*
19	16.0	1.2	13.1486	*Ha*
20	8.7	1.2	7.0593	*Ha*
21	9.6	1.2	7.7253	*Ha*
22	3.9	1.2	3.0966	*Ha*
23	-1.7	1.3	1.3746	*Ho*
24	-0.7	1.3	0.5540	*Ho*
25	1.2	1.3	0.9481	*Ho*
26	4.7	1.3	3.6766	*Ha*
27	3.0	1.3	2.3022	*Ha*
28	2.7	1.3	2.0323	*Ha*
29	6.1	1.3	4.5971	*Ha*
30	8.7	1.3	6.5088	*Ha*
31	14.8	1.4	10.9592	*Ha*
32	8.4	1.4	6.1804	*Ha*
33	-1.9	1.4	1.3996	*Ho*
34	-7.0	1.4	4.9948	*Ha*
35	-9.0	1.4	6.3695	*Ha*
36	-8.9	1.4	6.2980	*Ha*
37	-8.7	1.4	6.0925	*Ha*
38	-18.3	1.5	12.5959	*Ha*

Tab. 3 The local statistical tests for Line 2

item number	L2:$Y_i - Y_{M_i}$	L2:$\sigma_x^2 + \frac{m_{M_i}^2}{n_{M_i}}$	L2: t	L2: Hypothesis
1	16.1	1.9	1.0464	Ha
2	7.9	1.9	1.0465	*Ha*
3	6.8	1.9	1.0468	*Ha*
4	6.3	1.9	1.0472	*Ha*
5	3.2	2.0	1.0479	*Ha*
6	-3.8	2.0	1.0487	*Ha*
7	-3.8	2.0	1.0498	*Ha*
8	2.5	2.0	1.0510	*Ha*
9	2.6	2.0	1.0523	*Ha*
10	-7.1	2.1	1.0539	*Ha*
11	-9.7	2.1	1.0557	*Ha*
12	-4.7	2.1	1.0576	*Ha*
13	-12.8	2.2	1.0597	*Ha*
14	-7.4	2.2	1.0620	*Ha*
15	-12.1	2.3	1.0645	*Ha*
16	-8.0	2.3	1.0672	*Ha*
17	-6.5	2.4	1.0700	*Ha*
18	1.6	2.4	1.0730	*Ho*
19	-1.1	2.5	1.0762	*Ho*
20	-1.9	2.5	1.0795	*Ho*
21	5.3	2.6	1.0830	*Ha*
22	4.6	2.7	1.0867	*Ha*
23	4.6	2.7	1.0905	*Ha*
24	1.5	2.8	1.0945	*Ho*
25	2.4	2.8	1.0987	*Ha*
26	2.2	2.9	1.1031	*Ho*
27	-2.6	3.0	1.1075	*Ha*
28	0.4	3.0	1.1122	*Ho*
29	-0.6	3.1	1.1170	*Ho*
30	1.7	3.2	1.1219	*Ho*
31	-0.8	3.2	1.1270	*Ho*
32	0.8	3.3	1.1323	*Ho*
33	2.0	3.4	1.1377	*Ho*
34	-0.3	3.5	1.1432	*Ho*
35	9.7	3.5	1.1489	*Ha*
36	6.3	3.6	1.1547	*Ha*
37	-1.7	3.7	1.1607	*Ho*
38	-6.3	3.8	1.1668	*Ha*

According to obtained results it is possible to conclude that 33 positions of crane tracks shall be corrected for line 1 (crane track 1) and 26 position for line 2 (crane track 2) in order to achieve their straightness and parallelism in concordance with achieved accuracy. Global test only proved that crane tracks significantly deviate from straightness and parallelism but only the local deviations could be identified only by local statistical test. Statistical hypothesis selection and formulation are of the crucial importance in the process of identifying the straightness and parallelism of two lines on the certain level of accuracy. It is necessary to bear in mind that improvement of accuracy and density of points will increase the reliability of conclusions.

4. CONCLUSION

In this paper the method based on linear regression model and statistical analysis was utilized for determination straightness and parallelism of two lines (case study was utilized on the crane tracks of approximately 200 meters length and approximated by 39 points for each track). The conclusions were made on the global and local level of statistical hypothesis testing. In practice the global tests are of less importance because they give only the information about straightness and parallelism but not about the location were the correction shall be provided. Only local tests could identify the positions were correction shall be provided and the scale of correction. That is reason why proper selection and formulation of statistical hypotheses shall be made at the beginning of analysis. Global statistical test also should not be the only base for conclusion about parallelism and straightness of lines because the level of accuracy also defines the straightness and parallelism of two lines.

ACKNOWLEDGEMENT

The research has been conducted within the project "Scientific theoretical and experimental research and improvement of educational process in the field of civil engineering", developed at the Department of Civil Engineering and Geodesy, Faculty of Technical Sciences, University of Novi Sad, Serbia.

REFERENCES (STYLE: LITERATURA)

[1] Perovic, Gligorije. "Least Squares." Monograph, University of Belgrade, Faculty of Civil Engineering, Belgrade (2005).

[2] Hwang, Jooho, et al. "A three-probe system for measuring the parallelism and straightness of a pair of rails for ultra-precision guideways." International Journal of Machine Tools and Manufacture 47.7-8 (2007): 1053-1058.

[3] Perović, G.. “Račun Izravnanja I – Teorija grešaka merenja”, Naučna knjiga, Beograd, 1989.

FOREST CHANGE DETECTION BASED ON SENTINEL 2 IMAGES

Isidora Knežević[1], Gordana Jakovljević[2], Miro Govedarica[3]

Summary:

The increased availability and volume of remote sensing data, such as Sentinel or Landsat missions, have allowed analysis of land use/land cover and change detection. However, the accuracy of created maps and detected changes is highly influenced by image classification accuracy. Due to that, the performance of two popular machine learning algorithms for forest mapping and change detection is tested. The results show that although both provide high accuracy (overall accuracy and kappa coefficient higher than 0.96 and 0.87 respectively), Random Forest outperforms the Supported Vector Machine. The results of accuracy assessment and visual inspection indicated that RF and Sentinel 2 images were efficient in forest mapping, change detection, and forest type mapping providing insight into the forest dynamics that occurred in the period from 2016-2020.

Key words: forest mapping, change detection, machine learning, Sentinel 2

[1] BS.c, Faculty of Architecture, Civil Engineering and Geodesy, University of Banja Luka, Republic of Srpska, isidora.knezevic@student.aggf.unibl.org
[2] Assistant professor, Faculty of Architecture, Civil Engineering and Geodesy, University of Banja Luka, Republic of Srpska, gordana.jakovljevic@aggf.unibl.org
[3] Full professor, Faculty of Technical Science, University of Novi Sad, Serbia, miro@uns.ac.rs

1. INTRODUCTION

Forests cover more than a third of the Earth's land area. They contribute to the balance of oxygen and carbon dioxide in the air, protect river areas and water sources, and are the most biologically diverse ecosystems on the Earth. Due to the growth of population, inadequate management, fires, changes in water regimes, insects, rodents, bacteria, fungi, air pollution, soil, and water pollution, etc. forest cover throughout the world is subjected to deforestation and degradation. According to the United Nations data, 13 million hectares of forest disappear annually worldwide, leading to a 12 to 20% increase in greenhouse gas emissions, accelerating climate change [1].
Understanding and monitoring the dynamics of forest cover changes, their intensity, drivers, and impacts represents an important goal in forest management providing useful information for sustainable development [2]
Large-scale changes in land cover and repeated monitoring of forests have populated remote sensing as a credible tool for understanding spatiotemporal and spectral characteristics of land use changes that have been used by decision-makers and planners to design forest-related policies, provide sustainable development, and mitigate negative impacts.
The increasing availability of open high spatiotemporal resolution remote sensing data, such as Landsat and Sentinel satellite images, and improvements in tools and classification algorithms have allowed the generation of land use/land cover (LULC) maps [3], [4]. LULC monitoring is one of the most important applications of Earth observation since it provides a comprehensive overview, accurate classification of different land cover types, change detection, and cost-effective monitoring of large geographical areas.
Many studies investigating methods to monitor LULC changes from satellite images have focused on the biophysical properties through the use of spectral data or derived indices such as the Normalized Difference Vegetation Index (NDVI). The changes are generally detected by comparing the difference between the images in two different time phases. Therefore, change detection involves multi-temporal data sets to quantify the changes.
The methods for change detection include image differencing, principle component analysis, post-classification comparison, change vector analysis, etc [5], [6]. The accuracy of those approaches is limited by classification accuracy, availability of images in the same season, etc. To improve classification accuracy and decrease processing time, machine-learning algorithms have been used for LULC mapping such as k-Nearest Neighbors (kNN), Supported Vector Machine (SVM), Random Forest (RF), Artificial Neural Network (ANN), Decision Tree (DT), etc. [7] was compared RF and SVM for LULC classification in a heterogeneous coastal landscape using RapidEye imagery. Both algorithms performed comparatively similarly with kappa coefficient 0.92. [8] tested the performance of four ML algorithms DT, k-NN, SVM, and RF for LULC mapping based on EuroSAR dataset. Validation results of classification algorithms show that RF provides the highest accuracy with an Overall Accuracy (OA) of 57.6 % followed by SVM with OA:50.85 %. [9] used ANN for monitoring LC changes based on Landsat images from 1990 to 2002 resulting in OA of 89.7% and kappa 0.61. [10] compared performance of SVM and RF form LULC mapping in complex urban areas using Sentinel 2 images. An overall classification accuracy of 90,82% with a kappa value of 0,87 and 88,29 with a kappa value of 0,84 was achieved using SVM and RF. [11] was used the SVM for forest cover classification based on Sentinel 2 images with high OA (96.7-99.6%) and a kappa coefficient (93.3-99.2). Similarly, [12] compared RF, SVM, and classification and regression tree (CART) for extraction of Mediterranean forest habitats from Sentinel 2 time series. The best results were achieved using RF (OA:83%).

In this paper, the goal is to apply ML approaches using two classification algorithms (RF, SVM) to map and quantify changes in forest cover in the period from 2016-2020, and to provide a comparison of those algorithms in a continental forest setting. In addition to comparison, the goal of this study is to produce accurate forest cover maps, detect changes, and better understand the impact of socioeconomic and demographic changes on LULC. In addition, the maps of forest type i.e. deciduous and coniferous forests will be made.

2. STUDY AREA

This study focuses on the municipality of Mrkonjić Grad (Figure 1.). It is located in the southwest part of the Republic of Srpska, Bosnia and Herzegovina. The municipality covers the area between 16° 47' and 17° 15' east longitude and 44° 12' and 44° 35' north latitude. Mrkonjić Grad is situated at an elevation of 591 meters above sea level, and the municipality covers an area of 677.43 km².

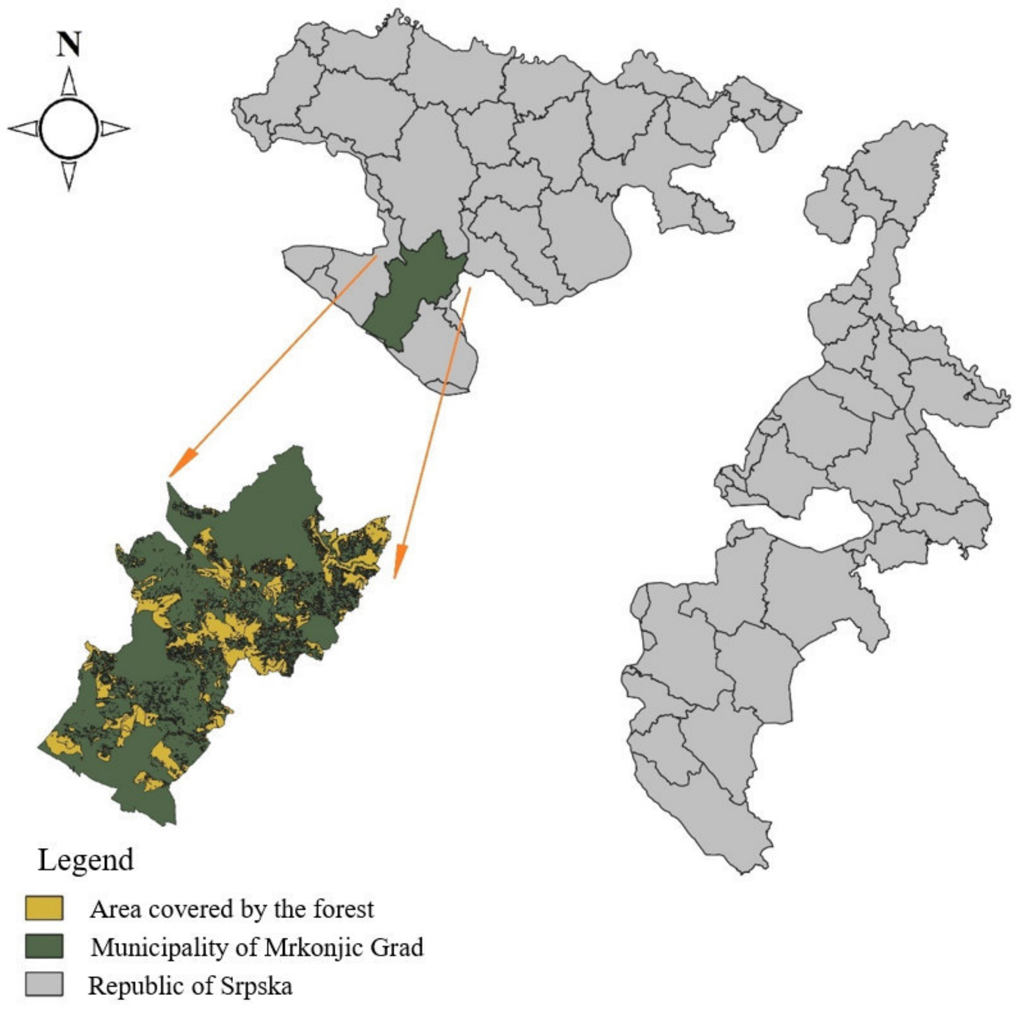

Fig. 1 Study area

Agricultural land occupies 54.0% of the total land surface. Forested areas represent a very significant natural resource, constituting 44.0% of the total municipality area. Although a substantial portion of the land is covered by forests, their structure is unfavorable. The total forested area is 32,710 hectares of which approximately 79.0% (25,957 hectares) is owned by the state, and are mainly concentrated in the Ovčara, Dubička Gora (part of the Manjača mountain), Lisine, and Dimitar mountain areas.

Private forests cover around 21%, or 6,753 hectares of the area, and are distributed throughout the municipality territory [13].

3. MATERIALS

Platform for data processing: The acces to and processing of EO data is preformad at Google Earth Engine (GEE) by using JavaScript language. GEE is a geospatial processing service powered by the Google Cloud Platform. The GEE represents public data catalog, compute infrastructure, and geospatial API providing planetary-scale analysis capabilities [14]. Its data catalog contains a wide range of datasets, including Landsat and Sentinel images, numerous MODIS collections, and many vector datasets. Therefore GEE allows the researcher to combine their processing algorithms with a forty-years-long earth image time series to detect changes, map trends, quantify differences, visualization, and data sharing.
Satellite data: In this paper, forest cover mapping and change detection is based on a time series of Sentinel 2 satellite images. Sentinel-2 is an Earth observation mission developed by the European Space Agency (ESA) as part of the Copernicus program. The mission consists of the twin satellites flying in the same orbit but phased at 180°, and is designed to give a high revisit frequency of 5 days at the Equator. Sentinel-2 provides high-resolution multispectral images of the Earth's surface. Sentinel-2 images consist of 13 spectral bands: four bands at 10 m (B2, B3, B4 visible and B8 Near infrared specter)), six bands at 20 m (B5, B6, B7, B8a Near Infrared, and B11, B12 Shortwave Infrared) and three bands at 60 m spatial resolution [15]. The Sentinel 2 Level 1A product from 2016, 2018, and 2020 was used. In addition to spectral bands, NDVI index was used.
In-situ data: In order to perform supervised classification in-situ data. In this study, there are two classes of interest: forest and non-forest. For these purposes, 100 samples in the form of polygons were collected, 50 for each class, which are approximately evenly distributed within the areas of interest. The training polygons are created by using official cadastral data and visual inspection of high-resolution images. The samples were randomly selected and split to 80% for model training and 20% for accuracy assessment of performed classification.

4. METHODOLOGY

The methodology used in this paper for forest mapping and change detection is presented in Figure 2. It includes three phases: preprocessing, classification, and change detection.

4.1. PREPROCESSING

Reflectance of the object detected by the sensor is affected by a heterogeneous and dense atmosphere composed of water vapor, aerosols, and gases resulting in atmospheric absorption and scattering that causes the difference in the reflectance value od satellite images and actual object [16]. Removing the atmospheric effects on optical remote sensing data is critical for the application of EO in environment monitoring. Atmospheric correction includes simulation of the radiation transmission process between atmosphere-surface sensors [17]. After determining the atmospheric parameters it is possible to separate the contribution of gases at the ground from radiation information obtained by the sensor and then calculate the bottom-of-atmosphere reflectance [18]. In this paper, Sensor Invariant Atmospheric Correction (SIAC) is used [19]. The obtained BOA values are used to calculate NDVI index.

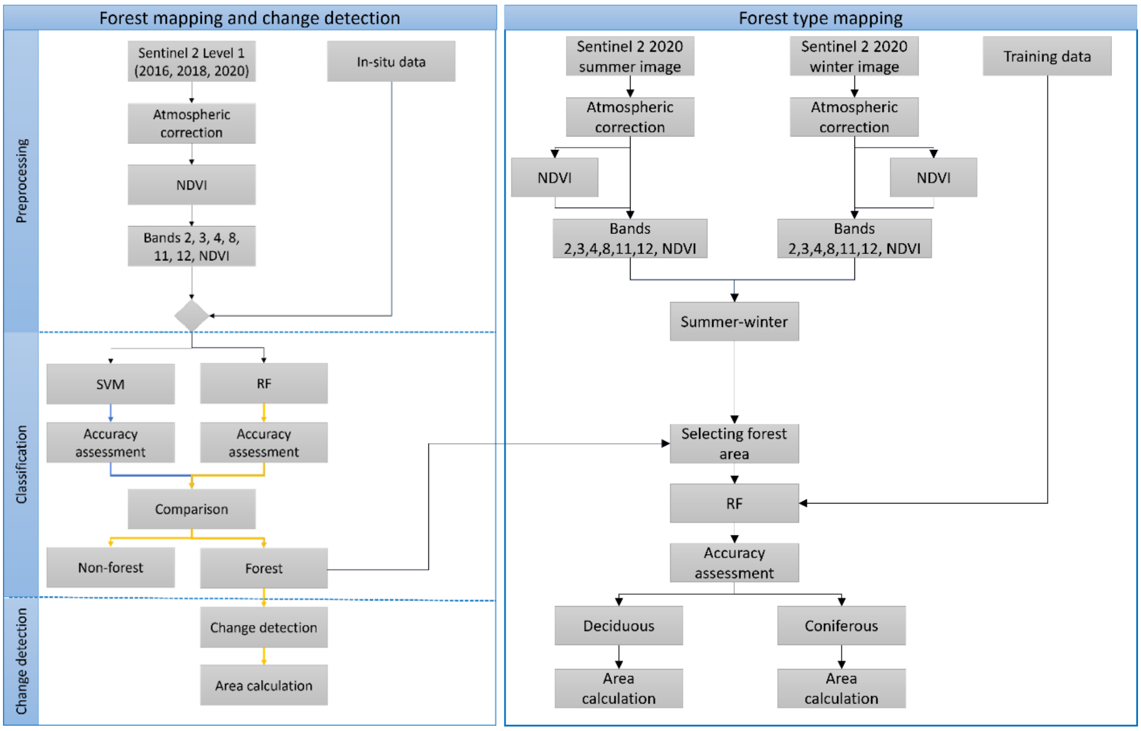

Fig. 2 Workflow

4.2. CLASSIFICATION

The preformance of two ML algorithmes, SVM and RF, for mapping of forest and change detection is tested in this paper.

Random forest: In recent years, RF have become popular in classification of remote sensing data due to high accurate prediction, simplicity and flexibility. It is supervised algorithm that containes a multipe decision trees and each tree is trained on a random subset of the data and uses a random subset of features for making decisions at each node. To increase the diversity of trees, an RF uses bagging or bootstrap aggregation to make the trees grow from different training subsets [20]. Therefore, each tree "votes" for a specific class, and the final prediction is determined by taking a majority of votes. The generalization error of RF depends on the strength of the individual trees in the forest and the correlation between them [21].

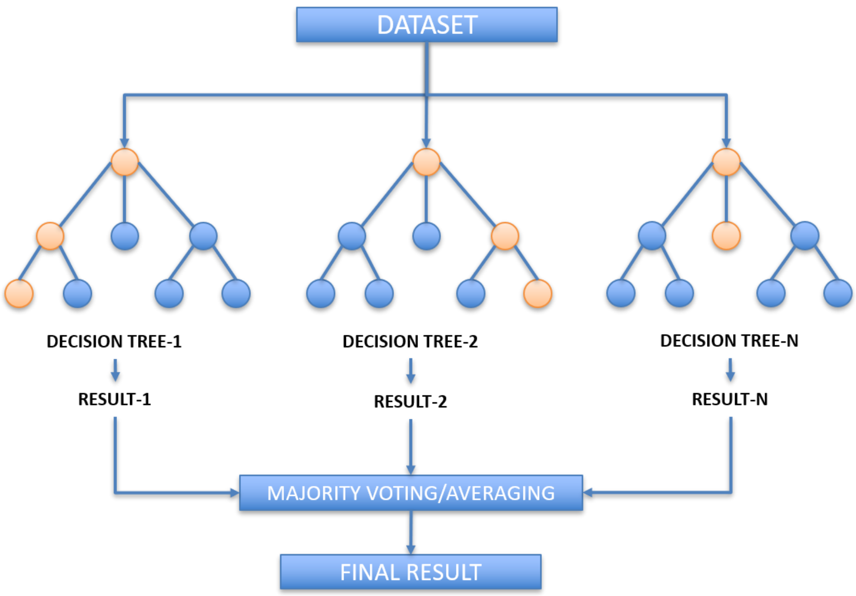

Fig. 3 RF classifier

SVM: SVM is a supervised ML algorithm that can be used for classification or regression tasks. SVM is based on statistical learning theory whic aims to determine the optimal hyperplain in an N-dimensional space to achieve optimal seperation between classes in feature space. If classes are lineary separable it is possible to define multiple hyperplain but there is only one n dimensional optimal hyperplain which is founded by maximizing the margin between closest points of different classes. The dimension of hyperplain is a function of the number of features. The data points that are closest to the hyperplane are called „support vectors“. while the margin represents the distance between the hyperplane and support vectors (Figure 4.).

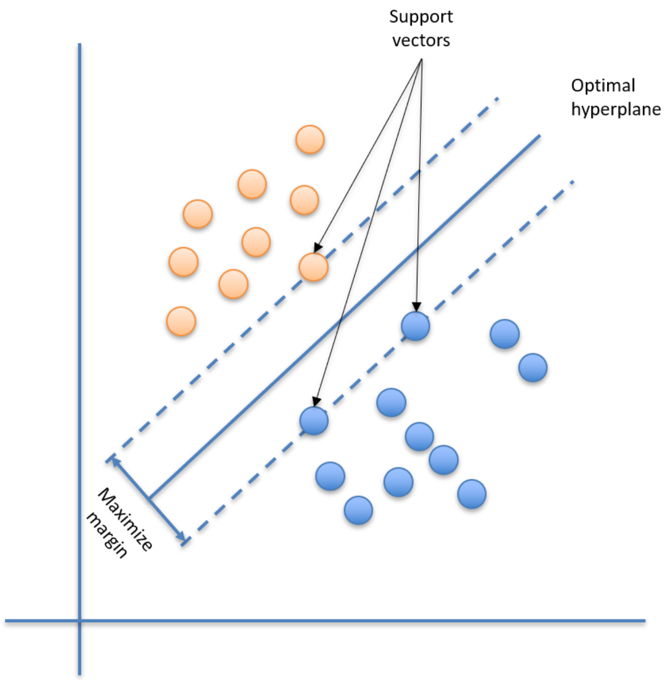

Fig. 4 SVM classifier

In addition, the SVM can be used for non-linear classification by mapping original input data points into high dimensional feature spaces in order to easily determine hyperplane even if the data points are not linearly separable in the original input space by employing kernel. In this paper, the Radial Basis Function (RBF) is used as the kernel.

Accuracy assessment: After classification, it is necessary to perform an accuracy assessment. Confusion matrix is commonly used for standard pixel-based accuracy assessment. A confusion matrix is a simple cross-tabulation of the prediction class label against the reference data for the sample at a specific location. The overall classification accuracy is defined as the ratio of the total number of correctly classified for all classes to the total number of pixels. In addition to overall accuracy, the confusion matrix can be used to calculate omission and commission error which represents the errors related to individual classes. Comision error represents pixels that belong to another class but are labeled as belonging to the target class while omission error represents the pixels that belong to a class but fail to be classified into that class.

Additionally, kappa statistics defined by Cohen [22] is used as a measure of classification accuracy reduced for accidentally correct class agreement. The value of the kappa coefficient can be between 0 and 1 where 0 implies that the used model didn't provide better results that can be expected from random chance while 1 represents a model that made all predicts perfectly.

Change detection: The post-classification comparison represents the most popular approach in change detection analysis. This method is based on the classification of images from different time periods independently. Afterward, a comparison of multi-temporal images is preferred to detect change matrices and create change maps. The final accuracy of detected changes depends on the classification accuracy for each image. In order to detect changes, the pixel values of the two images are subtracted from each other on a per-pixel basis. The resulting image represents the difference image that shows the change magnitude between to acquisition data. Pixels that have experienced changes will have non-zero values in different images, while unchanged areas will be equal to 0.

Forest type classification: In addition to forest mapping and change detection, forest-type detection (deciduous and coniferous forests) is performed. Only images from 2020 were used for the classification of forest type. Since the largest difference between deciduous and coniferous forests can be obtained during winter the difference between summer and winter images was used in order to emphasize the contrast between classes. Only area covered by forest was used as input. Training data were created by visual interpretation of high-resolution images. Totally 100 polygons were used, 50 per class. Training data were split to 80% for training and 20 % for validation. RF classifier was used for the detection of forest type.

5. RESULTS AND DISCUSSION

In this paper, the comparison of RF and SVM for forest mapping and change detection is tested. The same satellite images and training data are used for both algorithms. The forest maps detected by using RF and SVM algorithms are presented in Figure 5.

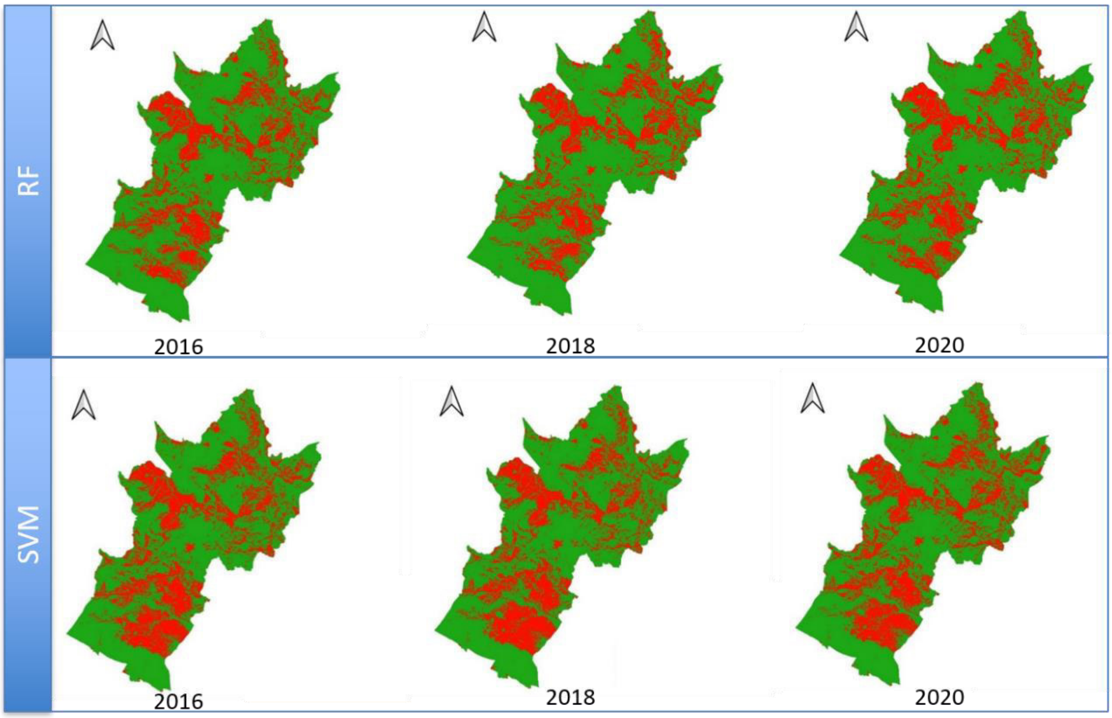

Fig. 5 The results of Sentinel 2 classification based on RF and SVM for 2016, 2018, and 2020 (red color represnets forest and green represents non-forest class)

The results of image classification was validated by pixel-by-pixel accuracy assessment. Same validation data set is used for RF and SVM. Table 1 and Table 2 provide overall and per class classification accuracy.

Tab. 2 Accuracy assessment for forest detection by RF and SVM

Classifier	Year	Overall accuracy	Kappa
RF	2016	0.992	0.968
	2018	0.993	0.973
	2020	0.986	0.946
SVM	2016	0.976	0.912
	2018	0.970	0.893
	2020	0.964	0.871

Tab. 2 Accuracy assessment for forest detection by RF and SVM

Classifier	Year	Class	Omission error [%]	Commission error [%]
RF	2016	Forest	0.50	0.50
		Non-forest	2.90	2.60
	2018	Forest	0.30	0.30
		Non-forest	2.90	2.90
	2020	Forest	0.90	0.9
		Non-forest	4.40	4.40
SVM	2016	Forest	2.40	0.40
		Non-forest	2.30	12.00
	2018	Forest	2.90	0.60
		Non-forest	3.30	14.00
	2020	Forest	3.40	0.90
		Non-forest	4.80	16.00

According to visual inspection and results presented in Tables 1 and 2, both classifiers produce high overall accuracy and can be used for the creation of forest maps and change detection. The classification achieved an overall accuracy higher than 98.6 % for RF and 96.4 % for SVM. Similarly, both methods result in a high kappa coefficient (RF: 0.946-0.973; SVM: 0.871-0.912). The obtained results are in line with previous studies where the Kappa coefficient ranged from 0.933-0.992 [11], 0.95-0.97 [10] and 0.92 [7]. However, the RF provides slightly better performance compared with SVM. These results are in line with results in [8], and [12]. This is mainly due to higher commission error for the non-forest class for all years meaning that SVM tends to misclassify the non-forest pixels as forest. In other words, while 96% of the non-forest class is correctly identified, only 85% of the area identified as non-forest in the classification actually represents other land types. Similar results were obtained in [10], where the SVM method also resulted in higher errors for the forest class. Based on the analysis conducted, it is evident that the RF method achieves better results for forest classification and it is used for change detection.

The changes are detected for the period 2016-2020. The results of change detection are presented in Figure 6 where red color represents deforestation while blue color marks new areas covered by forest.

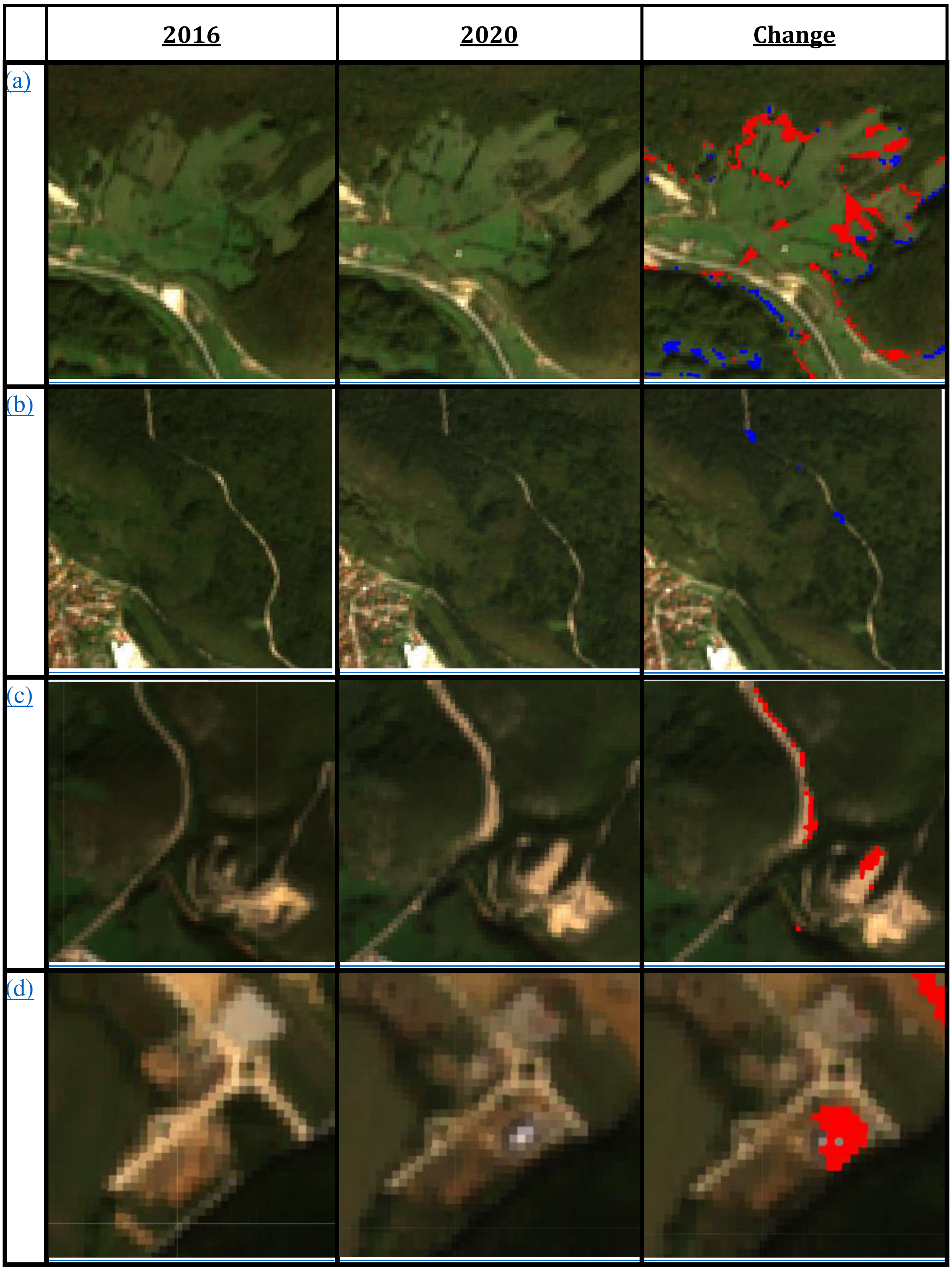

Fig. 6 The detected chages in forest cover for 2016-2020 period

By comparing the classification results of images from 2016 and 2020, numerous changes in forest vegetation during that time period were identified. Visual analysis of forest vegetation changes revealed that the most significant changes occurred in the peripheral areas of large forested regions (Table 7 (a)) and due to the construction of commercial and infrastructure objects (Table 7 (c) and (d)). However, visual analisi of results (Table 7), shows that some of the detected changes are actually errors. In Table 7 (b), it is noticeable that a portion of the road was detected as a newly formed forest, which is not the case in reality. The reason for this is that the spatial resolution of used satellite images (10 m) is insufficient for monitoring changes for narrow objects, and due to the occurrence of mixed pixels (one pixel representing two classes, in this case, forests and roads). If vegetation dominates such a pixel, the entire area it covers will be classified as vegetation, as happened in this example.

The results of accuracy assessment for forest type detection is presented at Table 3 and Table 4.

Tab. 3 Accuracy assessment of forest type mapping

Year	Training		Kappa	
	Overall accuracy	Kappa	Overall accuracy	Kappa
2020	0.996	0.992	0.982	0.963

Tab. 4 Accuracy assessment of forest type mapping per class

Year	2020	
	Omission error [%]	Comission error [%]
Deciduous	17	17
Coniferous	21	20

The results of forest type mapping are presented in Figure 7 where yellow color represents deciduous while blue color marks coniferous forest.

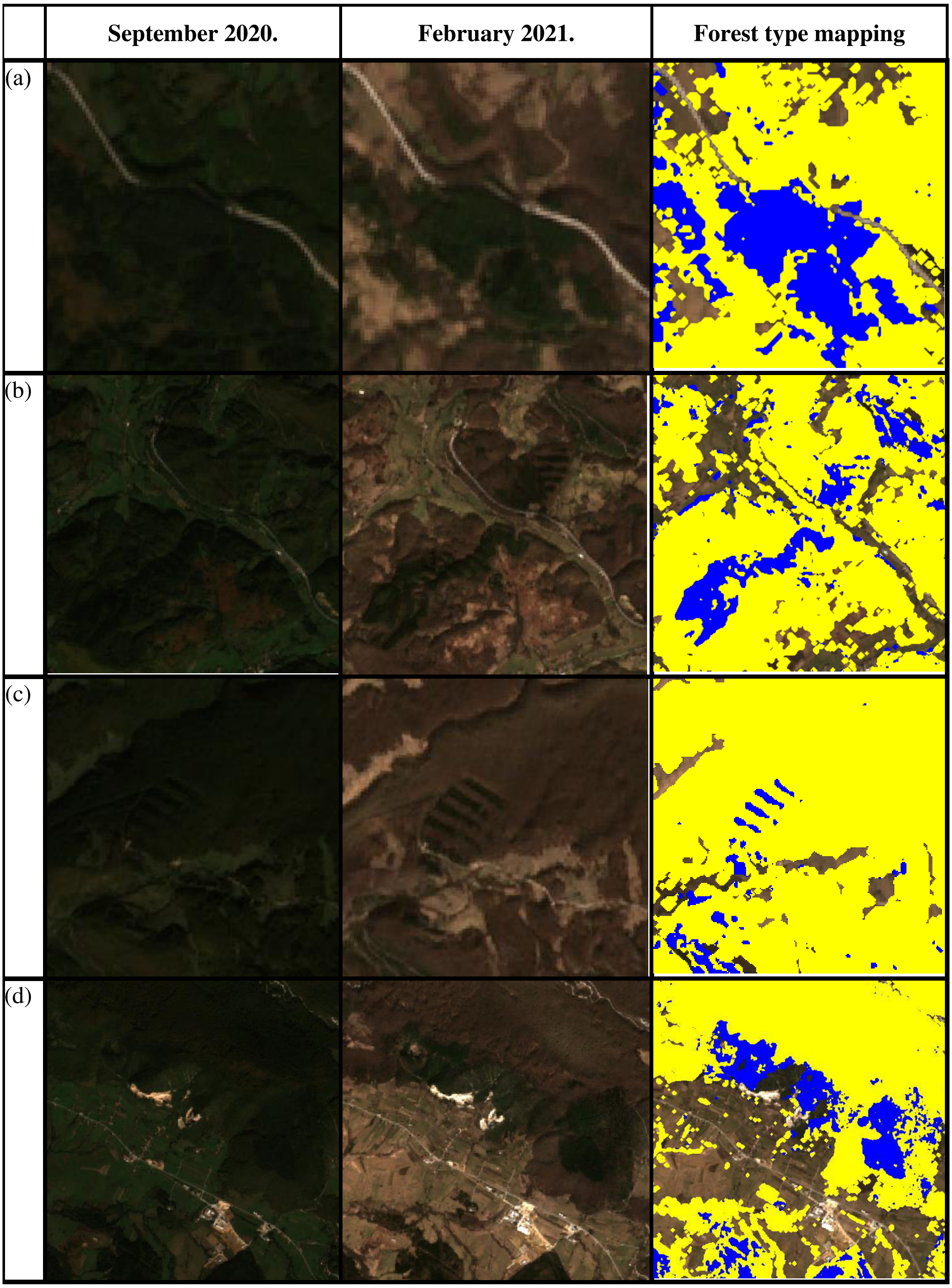

Fig.7 Visual interpretation of forest type mapping

Result of accuracy assessment shows that RF provide high overall accuracy (98.2%), while kappa coefficient was 0.963. Visual inspection of results are in line with accuracy assessment. Algorithm was able to detect large (Figure 7 (a) and (d)) but also small (Figure 7 (b) and (c)) areas covered by different forest types. It is estimated that 439.161 km^2 i.e. 65.71 % of municipality area is covered by deciduous while 111.736 km^2 (16.72 %) represents coniferous forest.

6. CONCLUSION

In this study, two machine learning algorithms were employed for forest mapping and change detection based on multispectral satellite images and cloud computing service.
Accuracy assessment of results shows that Random Forest algorithm provide higher accuracy compared with Supported Vector Machine (kappa coefficient 0.973 vs 0.912). This is mostly due to SVM tendency to misclassify the non-forest pixels as forest. The obtained results indicate that 82 % of study area is coverd by forest. Comparasion between classified images from 2016 and 2020 shows that there were numerous changes in forest vegetation in this time period. The largest differences are visible in the peripheral parts of large forest areas.
The results shows that Earth Observation data and machine learning algorithms are extremely valuable data source for the analysis and development of strategies for sustainable forest management. Usage of these technologies can provide continuous monitoring of forest status on a global level.

REFERENCES

[1] D. Brack, „Forests and Climate Change," UN Forums on Forests, 2019.

[2] D. Lu, P. Mausel, E. Brondizion i E. Moran, „Change detection techniques," t. 25, 2003.

[3] M. Schmidt, R. Lucas, P. Bunting, J. Verbesselt i J. Armston, „Multi-resolution time series imagery for forest disturbance and regrowth monitoring in Queensland, Australia.," t. 158, 2015.

[4] M. Mohajane, A. Essahlaoui, F. Oudija, M. El Hafyani, A. El Hmaidi, A. El Ouali, G. Randazzo i A. C. Teodoro, „Land Use/Land Cover (LULC) Using Landsat Data Series (MSS, TM, ETM+ and OLI) in Azrou Forest, in the Central Middle Atlas of Morocco," t. 5, br. 12, 2018.

[5] J. Chen, X. Chen, X. Cui i J. Chen, „Change vector analysis in posterior probability space A new method for land cover change detection," t. 8, 2011.

[6] D. Lu, P. Mausel, E. Brondizio i E. Moran, „Change detection techniques," t. 25, br. 12, 2004.

[7] E. Adam, O. Mutanga, J. Odindi i E. M. Abdel-Rahman, „Land-use/cover classification in a heterogeneous coastal landscape using RapidEye imagery: evaluating the performance of random forest and support vector machines classifiers," t. 35, br. 10, 2014.

[8] R. Thakur i P. Panse, „Classification Performance of Land Use from Multispectral Remote Sensing Images using Decision Tree, K-Nearest Neighbor, Random Forest and Support Vector Machine Using EuroSAT Data," t. 10, br. 1, 2022.

[9] L. Silva, A. P. C. Xavier, R. M. de Silva i C. Santos, „Modeling land cover change based on an artificial neural network for a semiarid river basin in northeastern Brazil," t. 21, 2020.

[10] G. Jakovljevic, D. Sekulovic i M. Govedarica , „LULC mapping from Sentinel 2 using machine learning algorithms," u PROCEEDINGS of International conference on Contemporary Theory and Practice in Construction XIII, Banja Luka, 2018.

[11] A. Mironczuk i A. Hoscilo, „Mapping tree cover with Sentienl 2 data using the Supported Vector Machine," t. 9, br. 1, 2017.

[12] S. Pratico, F. Solano, S. Di Fazio i G. Modica, „Machine Learning Classification of Mediterranean Forest Habitats in Google Earth Engine Based on Seasonal Sentinel-2 Time-Series and Input Image Composition Optimisation," t. 13, 2021.

[13] O. M. Grad, „Mrkonjic Grad," [Na mreži]. Available: https://www.mrkonjic-grad.rs/ . [Poslednji pristup 2022 06 01].

[14] Google, „Google Earth Engine," [Na mreži]. Available: https://earthengine.google.com/. [Poslednji pristup 29 8 2023].

[15] Copernicus, „Sentinel," [Na mreži]. Available: https://sentinels.copernicus.eu/web/sentinel/user-guides/sentinel-2-msi/resolutions/spatial. [Poslednji pristup 30 8 2023].

[16] L. Fibriawati, Koreksi Atmosfer Citra SPOT-6 Menggunakan Metode MODTRAN4 = Atmospheric Correction of SPOT-6 Image With MODTRAN4 Method, LAPAN, 2016.

[17] S. Liang i J. Wnag, Advanced Remote Sensing (Second Edition), Academic Press, 2020.

[18] M. Bilal, A. Mhawish, M. Ali, Z. Qiu, de Leeuw i M. Kumar, „etrieval of aerosol optical depth from satellite observations: Accuracy assessment, limitations, and usage recommendations over South Asia," u Atmospheric Remote Sensing, Elsevier, 2023.

[19] F. Yin, P. E. Lewis i J. L. Gomez-Dans, „Bayesian atmospheric correction over land: Sentinel-2/MSI and Landsat 8/OLI," t. 15, 2022.

[20] V. F. Rodriguez-Galiano, M. Chica-Olmo, F. Abarca-Hernandez, P. M. Atkinson i C. Jeganathan, „Random Forest classification of Mediterranean land cover using multi-seasonal imagery and multi-seasonal texture," t. 121, 2012.

[21] L. Breiman, „Random Forests," t. 45, 2001.

[22] J. Cohen, „ Coefficient of Agreement for Nominal Scales," t. 20, 1960.

PERFORMANCE AND ACCURACY ANALYSIS OF LEICA P20 SCANNER AND IPHONE LIDAR SENSOR IN SCANING OF CULTURAL HERITAGE OBJECTS

Igor Ruskovski[1], Milan Gavrilović[2], Miro Govedarica[3]

Summary:

According to the definition of UNESCO, cultural heritage includes artifacts, monuments, groups of objects and museums that have different symbolic, historical, artistic, aesthetic or anthropological value. Objects of cultural heritage must be properly documented, preserved and protected from destruction. One of the methods of preserving cultural heritage is digitization through various methods and storage of digital material in an appropriate manner. Laser scanning is a method of collecting spatial data on the basis of which it is possible to create detailed 3D models of objects. This paper analyzes the possibilities of creating a point cloud in two ways: with an industrial terrestrial laser scanner and a sensor more accessible to a wider range of users, which is installed in mobile phones. An analysis of the performance and accuracy of both methods was performed and a conclusion was given on the degree of their usability. The results of the work show the possibility of using both methods in the preservation of cultural heritage.

Key words: cultural heritage, lidar, iPhone, laser scanning

[1] Teaching assistant, Faculty of Technical Sciences, University of Novi Sad, Serbia, rus_igor@uns.ac.rs
[2] Teaching assistant, Faculty of Technical Sciences, University of Novi Sad, Serbia, milangavrilovic@uns.ac.rs
[3] Full Professor, Faculty of Technical Sciences, University of Novi Sad, Serbia, miro@uns.ac.rs

1. INTRODUCTION

Cultural heritage can be described as a spectrum of various artifacts, traditions and practices that have shaped the identity of societies across many generations. It can include tangible and intangible elements. Historical buildings, archeological sites, monuments can be examples of cultural heritage that stand as a testament to the richness of human history and creativity. Fig. 1 shows detailed UNESCO's classification of cultural heritage [1].

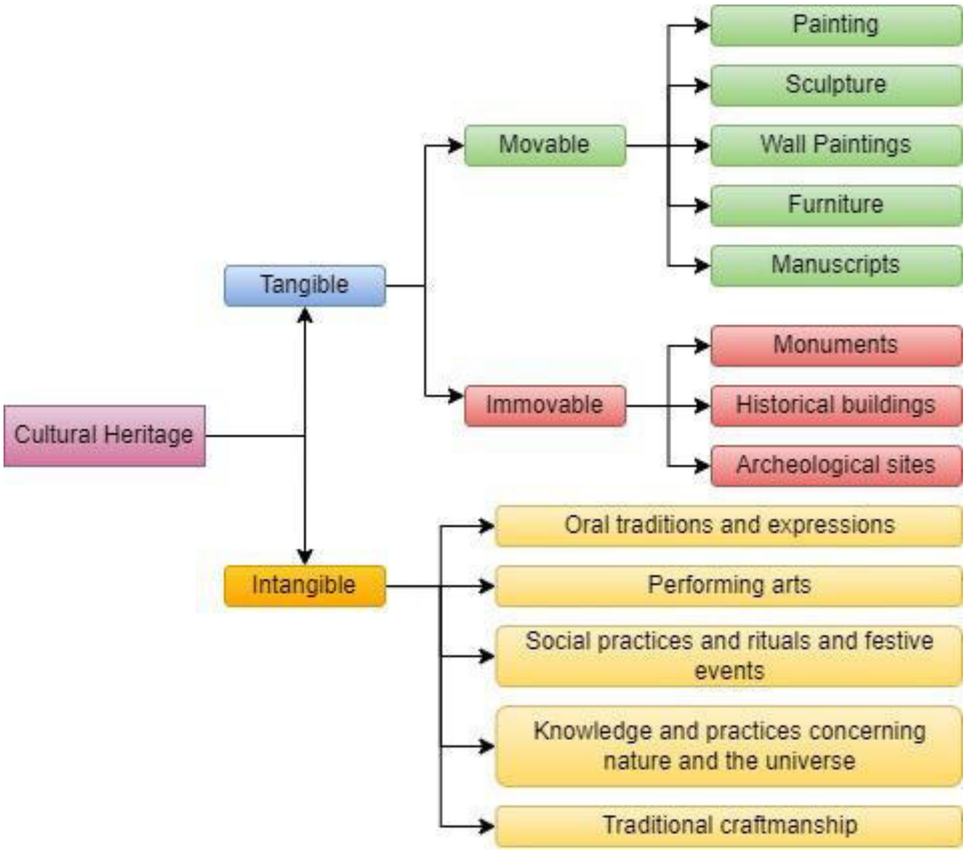

Fig. 1 UNESCO classification of cultural heritage

In the world of rapid expansion and urban development, these elements can be subject to deterioration and damaging. Causes can be environmental, anthropogenic, biocontamination, natural disasters and climate changes [2], [3]. This is one of the main reasons why the conservation of cultural heritage must be a priority. Conservation of cultural heritage means to maintain the physical and cultural characteristics of the object to ensure that its value is not diminished and that it will outlive our limited time span [1]. Written description, photos, high quality 3D models [4] and other digital material can be a mean to conserve and protect cultural heritage.

Among the modern technologies available today, several of them stand out from others by providing large amount of data rich in details that can serve as a starting point in developing credible 3D models of objects of tangible cultural heritage [5]. Laser scanning is one of them, and up untill a few years ago, the only way to collect laser scanning data was to use a professional laser scanner. Today, there is another option that seems to be faster, simpler and generally more accesible to the wider public and it does not require specific training or knowledge on the usage in comparison to aforementioned professional laser scanner. This option is an integrated LiDAR sensor in iPhone smartphones that has the potential to achieve the needed quality of the data.

The authors performed scanning with a professional terrestrial laser scanner and a smartphone sensor and compared the gained results from the point of view of details, precision and accuracy. The object of interest in this paper is a monument to Milutin Milankovic, Serbian mathematician, located in front of Faculty of Sciences in Novi Sad (Fig. 2).

Fig. 2 The object of interest in this paper, a monument to Milutin Milanković

Several measurements on the monument were taken as true values that will later be used to compare the accuracy of both technologies. The goal of this paper is to determine whether the iPhone LiDAR sensor can be used to collect the data for conservation of cultural heritage.

2. RELATED WORK

Apple has been using LiDAR tech in cell phones since 2020 with the launch of the iPhone 12 Pro. Ever since then, many authors have questioned and researched the abilities of this sensor compared to professional LiDAR in various fields. Authors in [6] explored the possibilities of integration of LiDAR equpped iPhones in geoscience fieldwork. By utilizing LiDAR capabilities, the paper demonstrates the potential for improved accuracy in capturing topographic and structural information, leading to more efficient and detailed geological assessments. Another paper [7] focuses on using the iPhone LiDAR sensor in the area of forensics and capturing the data in the context of crime and vehicular crash scenes. The authors conclude that this technology holds promise for enhancing forensic analysis. Applicability of this sensor for the purpose of 3D indoor mapping is a topic of [8] where authors conclude that this approach is a more accessible and cost effective solution for certain mapping applications. As for the point of view of data processing, paper [9] explores the possibilities of point cloud segmentation with the question of iPhone LiDAR sensor accuracy and noise in mind. Authors in [10] researched a line structure extraction method and conducted their experiments on a point cloud acquired by the iPhone 12 Pro MAX and their results performed well in comparison with other related results. Papers [11] and [12] suggest using targets on objects and point cloud sections as a mean of comparing different point clouds and testing the true measured distances against distances taken from point clouds, both professional and phone generated. The former paper also suggests using iterative closest point (ICP) algorithm for point cloud registration in order to properly compare point clouds from different sources. Results of [13] confirm that the Polycam app used on iPhone 13 Pro can capture data with sufficient accuracy.

3. MATERIALS AND METHODS

The data used for this paper consists of two separate point clouds. The first point cloud was acquired using Leica P20 terrestrial laser scanner. Important hardware specifications are shown in Tab. 1.

Tab. 1 Leica ScanStation P20 relevant specifications [14]

Accuracy of single measurement	3mm at 50m, 6mm at 100m
Angular accuracy	8’’ horizontal, 8’’ vertical
Range	0.4 – 120m
Resolution	0.8-50mm @ 10m

For this study, a resolution of 3.1mm @10m was chosen, which is the 3nd best that the scanner can scan with and it provides sufficient point density and object coverage. The object was scanned from 3 stations (Fig. 3) and registration was done using targets with a minimal registration error of 0.001m and maximal error of 0.004m. Initial point cloud consists of approximately 32M points and it was reduced to approximately 4M after extracting the object of interest.

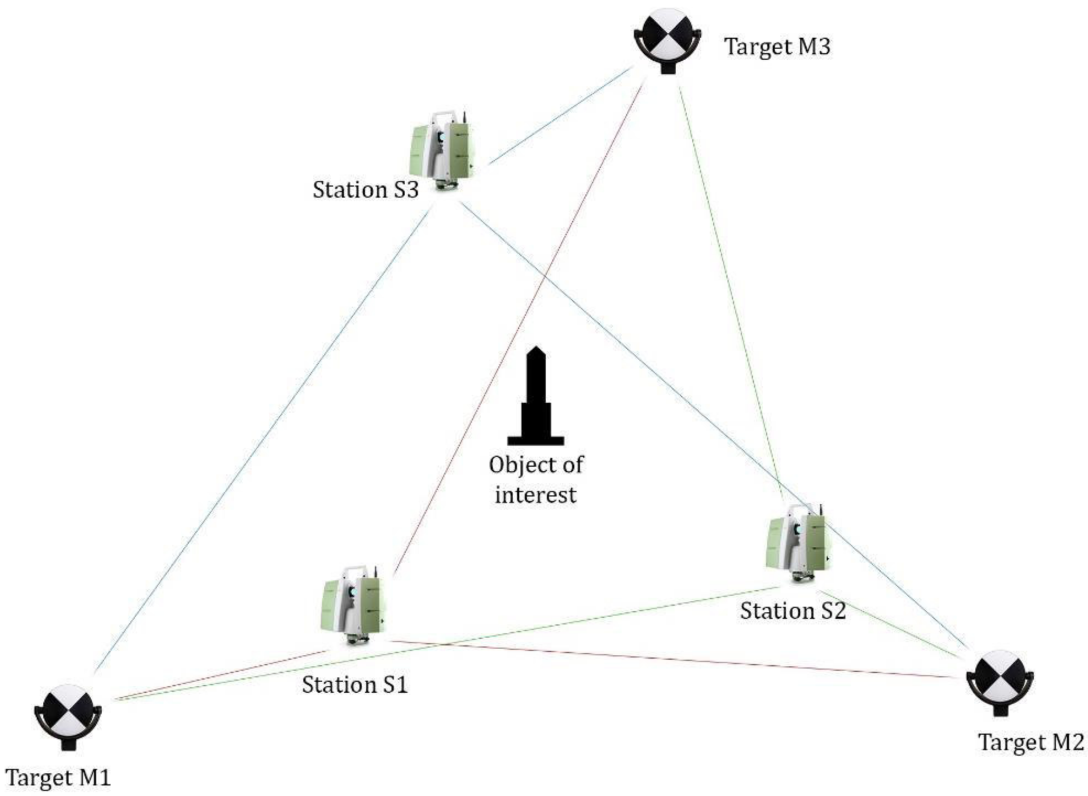

Fig. 3 Position of TLS and targets during scanning

As for the phone sensor, iPhone 13 Pro with Polycam app was used to collect the data. Tab. 2 explains important parameters in the app and their values for the scan.

Tab. 2 Polycam app parameters

Parameter	Explanation	Value
Depth range	Depth range used for processing each frame of the capture sequence. Useful to exclude background material from an object capture	5m
Voxel size	Voxel size used when processing the capture	6mm
Simplification	Amount of simplification to apply to the mesh before texturing	45%

The data was then exported to *.las format and used in future process. This point cloud consists of just below 2M points. Additionally, 6 black and white targets were placed across the object and some of them were used for measuring the distances, both with tape on site and from each of the point clouds later. Fig. 4 shows both point clouds. Open source software solution *Cloud Compare* was used for point cloud processing and analysis.

Fig. 4 Raw data from TLS (left) and iPhone (right)

Fig. 5 displays the general workflow of the process. After the two approaches of data acquisiton and exporting, the first step is to register the resulting point clouds. Following is cloud-to-cloud distance calculation and analysis on one side, and measurement and comparison with the true values on the other side. From these, a conclusion can be drawn.

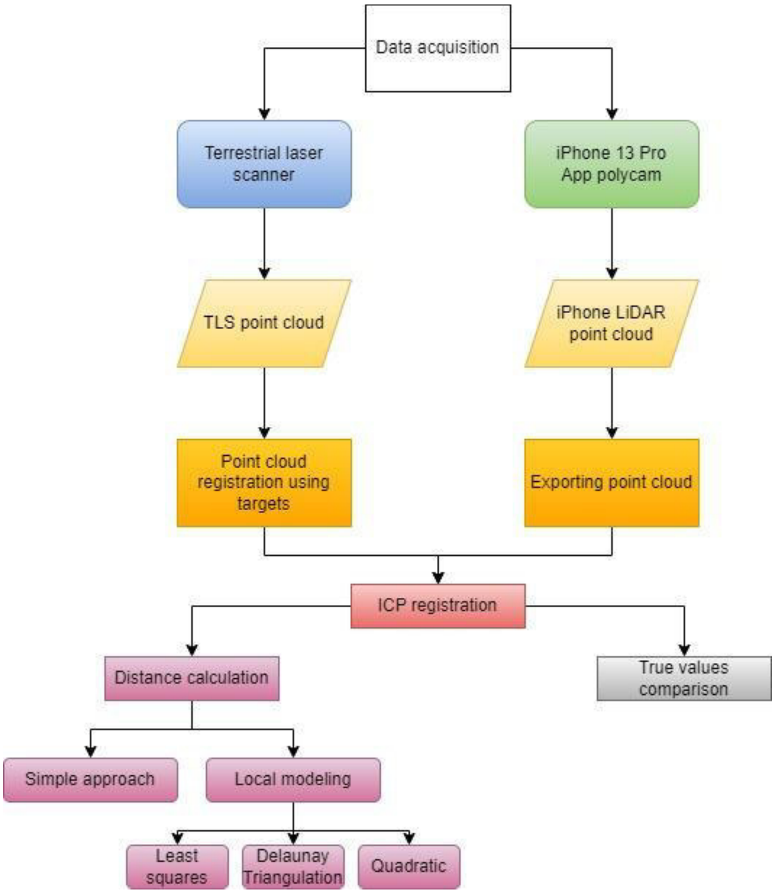

Fig. 5 Workflow

3.1. ITERATIVE CLOSEST POINT – ICP

In order to be able to compare the point clouds, they must be previously registered. One of the approaches to achieve this is through the ICP algorithm. First, both point clouds must be roughly registered and this can be done using other alignment methods, and second, both clouds must represent the same object and/or have overlapping parts. Both conditions were matched before the start of the registration process.

Important parameters for the ICP algorithm are number of iterations and random sampling limit. ICP is an iterative proces which means that during the process, the registration error decreases. By setting the number of iterations or a RMS (root mean square) error treshold, it's possible to stop the process. To increase computation speed on big clouds, optimization scheme is used and it consists in randomly sub-sampling the data cloud at each iteration. Random sampling limit parameter is used to set the maximmum number of sub-sampled points.

3.2. DISTANCE ANALYSIS

The easiest method to compare two point clouds is to calculate cloud-to-cloud distances. This simple approach uses nearest neighbor distance to compute distances between two points. For each point in compared cloud, the nearest point in the reference cloud is searched and their Euclidean distance is computed [15]. It's important to mention that the reference cloud should be the cloud with higher point density and wider extents [16]. Another approach is cloud-to-surface where the distances aren't compared between two points but between point in one cloud and a surface generated based on the points from the other cloud. Several methods to create a surface model are available: least square plane, Delaunay triangulation and Quadric model. Documentation recommendation is to use Quadric model in this approach. The difference in these two approaches is shown on Fig. 6.

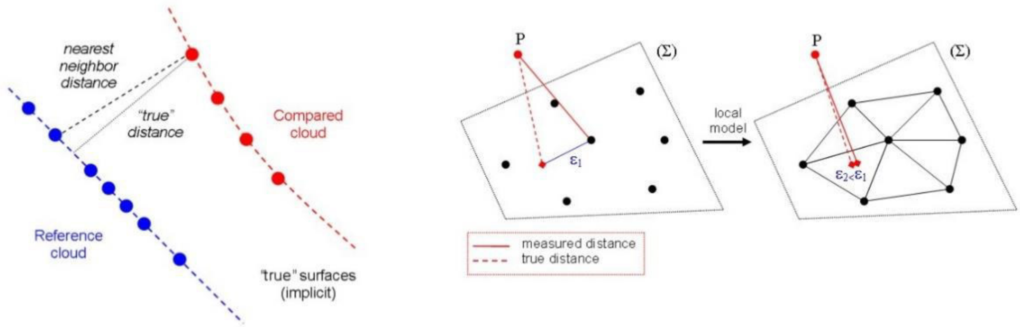

Fig. 6 Distance computation: simple approach (left) and local modeling (right)[17]

3.3. TRUE VALUES COMPARISON

The last part of the point cloud comparison consists of taking several measurements on the object of interest using tape measure and then measuring the same values in both point clouds. By calculating the differences between those values, it can be determined if the accuracy of the point clouds is sufficient for given application. In this case, a total of 4 measurements were taken, three of which were directly on the object and one was between previously set black and white targets.

4. RESULTS

The first step after exporting both datasets was to register them using proposed ICP. Considering the important parameters, several values were tried and the best results were accepted as final for future analysis. Tab. 3 contains results for different values for parameters of ICP and RMSE values. With the increase of number of iterations and number of points, the RMSE value decreases. The final RMSE value was 0.0077 and those clouds were further used.

Tab. 3 ICP results for several different values of parameters

Number of iterations	20	400	800
Number of points	50 000	200 000	500 000
RMSE	0.0096	0.0081	0.0077

As for the distance calculation, all four methods were used (simple approach and 3 variations of local modeling). Local modeling was performed in two ways: creating a surface using a fixed number of points (kNN) and using a sphere of fixed radius where all the points inside the sphere were used to model a surface. Tab. 4 and Tab. 5 present the mean distances and standard deviations for every method for both ways.

Tab. 4 Results of distance calculation based on simple approach and local modeling with kNN as a method of determining nearest neighbour

Method	**Mean distance [m]**	**Standard deviation [m]**
Simple approach	0.0029	0.0066
Least square plane (kNN)	0.0020	0.0047
Delaunay triangulation (kNN)	0.0028	0.0066
Quadric model (kNN)	0.0021	0.0051

Tab. 5 Results of distance calculation based on local modeling using sphere as a method of determining nearest neighbour

Method	**Mean distance [m]**	**Standard deviation [m]**
Least square plane (Sphere)	0.0022	0.0021
Delaunay triangulation (Sphere)	0.0027	0.0066
Quadric model (Sphere)	0.0022	0.0021

These results are also graphically presented in Fig. 7, while Fig. 8 is a visual representation of distances between an iPhone cloud (compared) and TLS cloud (referenced) for the simple approach. The scale on the right side shows that most of the values are not bigger than 0.03m. The biggest differences are located on the top of the statue and the reason behind that is that there is a hole in th TLS cloud on that spot. Similar results were achieved for other methods.

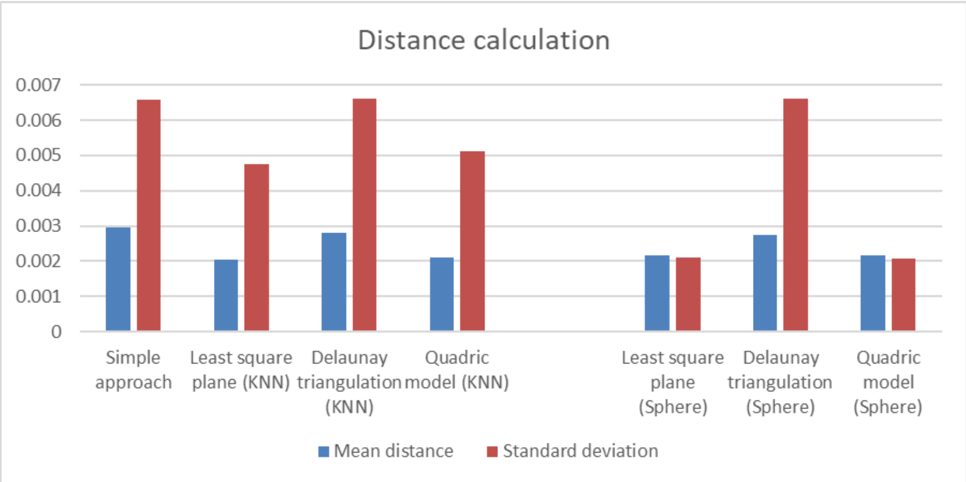

Fig. 7 Results of distance calculation using previously described methods

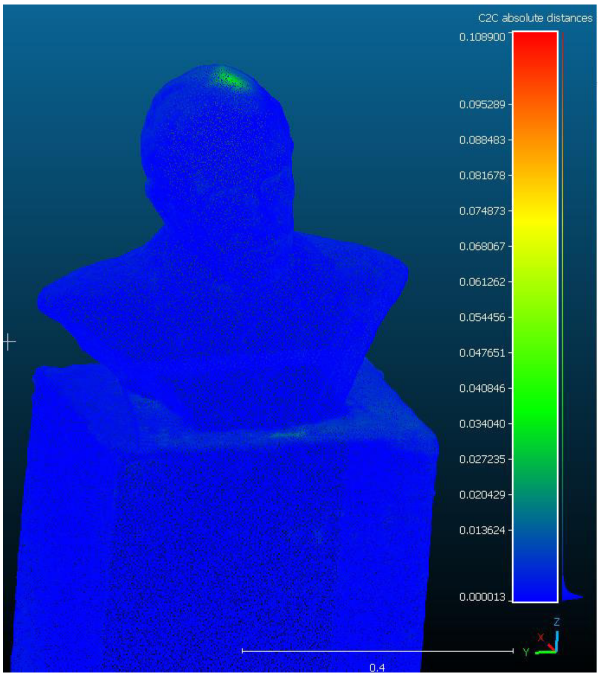

Fig. 8 Absolute distances between two clouds calculated using simple approach

The last part is comparing the true measured values with the ones measured from both point clouds. Tab. 6 contains measured values shown in Fig. 9.

Tab. 6 Measured values and differences between them

Measurement	True value [m]	TLS [m]	iPhone [m]	|True – TLS| [m]	|True – iPhone| [m]
#1	0.499	0.502	0.496	0.003	0.003
#2	0.451	0.453	0.452	0.002	0.001
#3	0.355	0.352	0.351	0.003	0.004
#4	0.298	0.296	0.297	0.002	0.001

From this table it can be concluded that the differences between measured values are noticeable at the 3rd decimal and thus can be considered acceptable.

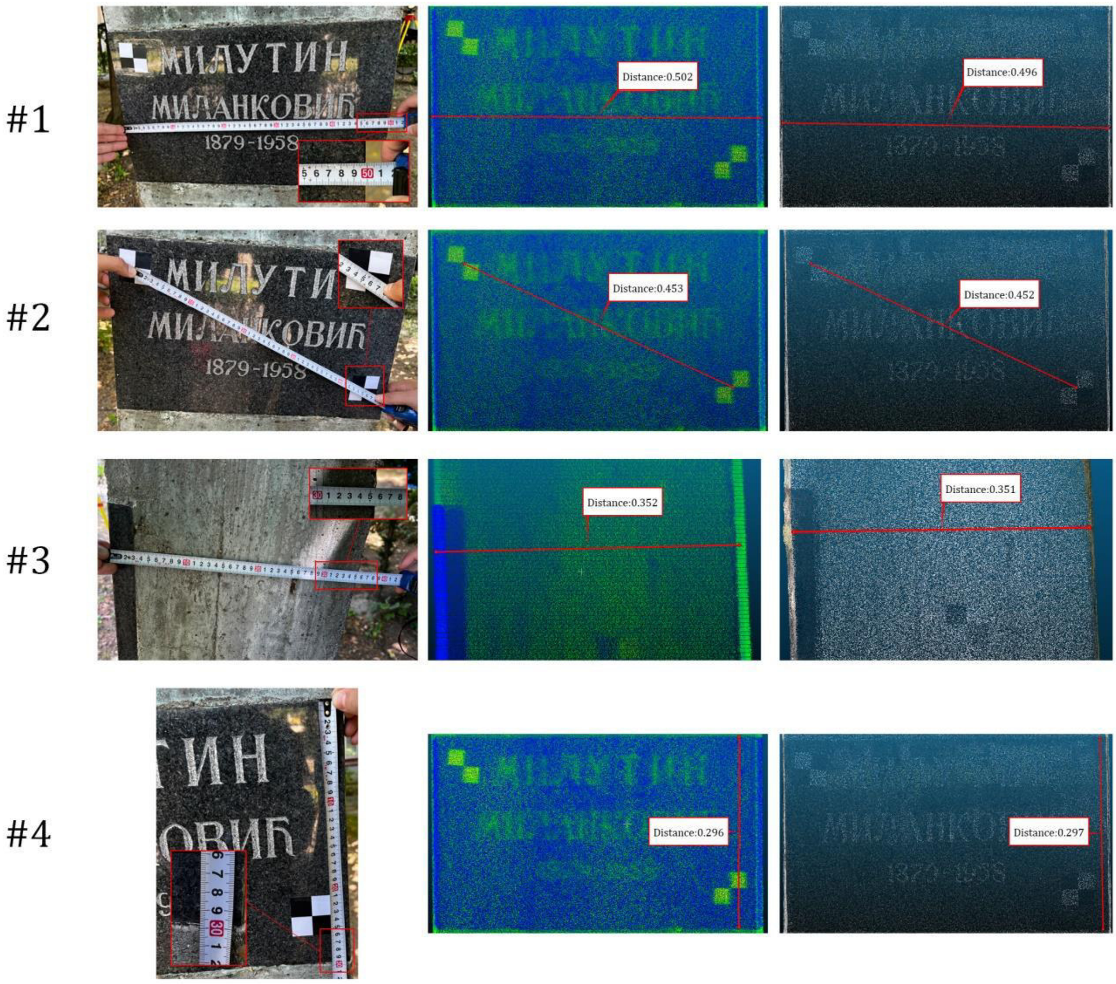

Fig. 9 Measured distances on site (left), from TLS point cloud (middle) and from iPhone point cloud (right)

5. CONCLUSION

After a thorough analysis of two point cloud acquired using two separate methods, a professional laser scanner and a smartphone sensor, it can be concluded that the differences on the example of scanning of cultural heritage object are within the tolerable values. Among four approaches of distance calculation, mean distance was never above 2 milimeters with the least square plane method having the smallest value,

followed by the quadric model. Comparison between true values of distances measured on site and same distances taken from the point clouds also confirmed this hypothesis having differences no larger than 4 milimeters (most values being 2 milimeters on average) and even that can be explained with the nature of point cloud data.
Problems that did occur during the scanning and in the post processing are related to the scanning process. The phone sensor is limited by the distance to the object and its height since the results depend on the possibility of the sensor to get close to the object and capture it from all sides. For taller objects, some sort of tools (e.g. gimbal) would have to be used. As for the TLS, its limitation is similar to the phone but not from the point of view of range, but its position, what can be noticed on the example in this paper where the biggest distance differences occured on the top of the statue and on top of the pedestal where TLS could not reach.
However, the general conclusion is that LiDAR sensor integrated in the smartphone device can create high quality 3D datasets that can be used in the cultural heritage conservation just as much as professional laser scanners, as far as smaller and easier-to-reach objects are concerned.

ACKNOWLEDGEMENT

This research (this paper) is supported by the Ministry of Science, Technological Development and Innovation through project number 451-03-47/2023-01/200156 "Innovative scientific and artistic research in the field of activities of FTN". The authors wish to express their deepest gratitude and warmest recognition to the Geoinformatics Laboratory of the Faculty of Technical Sciences in Novi Sad.

REFERENCES

[1] *THE 2009 UNESCO FRAMEWORK FOR CULTURAL STATISTICS (FCS)*. UNESCO Institute for Statistics.

[2] Baglioni, M., Poggi, G., Chelazzi, D., & Baglioni, P. (2021). Advanced Materials in Cultural Heritage Conservation. *Molecules*, *26*(13), 3967. https://doi.org/10.3390/molecules26133967.

[3] Sesana, E., Gagnon, A. S., Ciantelli, C., Cassar, J., & Hughes, J. J. (2021). Climate change impacts on cultural heritage: A literature review. *WIREs Climate Change*, *12*(4), e710. https://doi.org/10.1002/wcc.710.

[4] Tucci, G., Bonora, V., Conti, A., & Fiorini, L. (2017). HIGH-QUALITY 3D MODELS AND THEIR USEIN A CULTURAL HERITAGE CONSERVATION PROJECT. *The International Archives of the Photogrammetry, Remote Sensing and Spatial Information Sciences, XLII-2/W5*, 687–693. https://doi.org/10.5194/isprs-archives-XLII-2-W5-687-2017.

[5] European Commission. Directorate General for Communications Networks, Content and Technology. (2022). *Study on quality in 3D digitisation of tangible cultural heritage: Mapping parameters, formats, standards, benchmarks, methodologies, and guidelines : final study report.* Publications Office. https://data.europa.eu/doi/10.2759/471776.

[6] Tavani, S., Billi, A., Corradetti, A., Mercuri, M., Bosman, A., Cuffaro, M., Seers, T., & Carminati, E. (2022). Smartphone assisted fieldwork: Towards the digital transition of geoscience fieldwork using LiDAR-equipped iPhones. *Earth-Science Reviews*, *227*, 103969. https://doi.org/10.1016/j.earscirev.2022.103969.

[7] Kottner, S., Thali, M. J., & Gascho, D. (2023). Using the iPhone's LiDAR technology to capture 3D forensic data at crime and crash scenes. *Forensic Imaging*, *32*, 200535. https://doi.org/10.1016/j.fri.2023.200535.

[8] Jakovljević, G., Govedarica, M., & Alvarez Taboada, F. IPHONE 13 PRO VS PROFESSIONAL TLS FOR 3D INDOOR MAPPING. *PROCEEDINGS OF INTERNATIONAL CONFERENCE ON CONTEMPORARY THEORY AND PRACTICE IN*

CONSTRUCTION XV. STEPGRAD2022, University of Banja Luka. https://doi.org/DOI 10.7251/STP2215274J.

[9] Wang, X., Lyu, H., Mao, T., He, W., & Chen, Q. (2022). Point Cloud Segmentation from iPhone-Based LiDAR Sensors Using the Tensor Feature. *Applied Sciences*, *12*(4), 1817. https://doi.org/10.3390/app12041817.

[10] Wang, X., Lyu, H., He, W., & Chen, Q. (2022). Line Structure Extraction from LiDAR Point Cloud Based on the Persistence of Tensor Feature. *Applied Sciences*, *12*(18), 9190. https://doi.org/10.3390/app12189190.

[11] Teppati Losè, L., Spreafico, A., Chiabrando, F., & Giulio Tonolo, F. (2022). Apple LiDAR Sensor for 3D Surveying: Tests and Results in the Cultural Heritage Domain. *Remote Sensing*, *14*(17), 4157. https://doi.org/10.3390/rs14174157.

[12] Costantino, D., Vozza, G., Pepe, M., & Alfio, V. S. (2022). Smartphone LiDAR Technologies for Surveying and Reality Modelling in Urban Scenarios: Evaluation Methods, Performance and Challenges. *Applied System Innovation*, *5*(4), 63. https://doi.org/10.3390/asi5040063.

[13] Mikita, T., Krausková, D., Hrůza, P., Cibulka, M., & Patočka, Z. (2022). Forest Road Wearing Course Damage Assessment Possibilities with Different Types of Laser Scanning Methods including New iPhone LiDAR Scanning Apps. *Forests*, *13*(11), 1763. https://doi.org/10.3390/f13111763.

[14] *Leica ScanStation P20 Product Specifications.* Retrieved August 29, 2023, from http://www.studiotecnicocalvario.it/examples/pdf/P20.pdf.

[15] Antova, G. (2019). Application of Areal Change Detection Methods Using Point Clouds Data. *IOP Conference Series: Earth and Environmental Science*, *221*, 012082. https://doi.org/10.1088/1755-1315/221/1/012082.

[16] *Cloud Compare documentation: Cloud to cloud distance.* Retrieved August 29, 2023, from https://www.cloudcompare.org/doc/wiki/index.php/Cloud-to-Cloud_Distance.

[17] *Cloud Compare documentation: Distance computation*. Retrieved August 28, 2023, from https://www.cloudcompare.org/doc/wiki/index.php/Distances_Computation.

GEODESY AND GEOINFORMATION IN THE SERVICE OF REMEDIATION OF DAMAGES FROM NATURAL DISASTERS, EXAMPLES OF ZAGREB AND PETRINJA EARTHQUAKES IN 2020

Almin Đapo[1], Damir Medak[2], Marko Pavasović[3], Mario Miler[4]

Summary:

Natural disasters such as the recent earthquakes in Zagreb and Petrinja in 2020 have highlighted the need for a practical approach to mitigating the consequences of such events. This paper explores the central role of geodesy and geoinformatics in facilitating damage recovery through several application examples conducted by the Faculty of Geodesy at the University of Zagreb. First, we investigate the implementation of an interactive GIS portal that connects citizens in the affected area and facilitates the coordination and provision of information. We are also investigating the role of an interactive GIS application in the coordination of government services operating in the disaster area, emphasizing the importance of rapid response and effective planning. In addition, we are investigating the application of 3D documentation technologies to accurately assess the damage caused by the earthquake to immovable cultural assets. We are analysing the benefits of such techniques in documenting the actual condition of the objects and their importance for planning future restoration measures. We are also looking at the use of GNSS and InSAR technologies to analyse ground displacements to detect and prove the effect of progressive damages due to the occurrence of two strong earthquakes in nearby areas in the same year. We are investigating their application in monitoring changes and understanding the behaviour of the ground in the context of natural disasters such as earthquakes. This paper uses key examples to show how the Faculty of Geodesy at the University of Zagreb has played an important role in facilitating damage recovery after natural disasters such as earthquakes and provides concrete examples of their application in the Zagreb and Petrinja areas in 2020.

Keywords: Geodesy and Geoinformation, Earthquake, Zagreb, Petrinja, GIS, InSAR, GNSS

[1] Prof., University of Zagreb, Faculty of Geodesy, Zagreb, Croatia, almin.dapo@geof.unizg.hr
[2] Prof., University of Zagreb, Faculty of Geodesy, Zagreb, Croatia, damir.medak@geof.unizg.hr
[3] Assoc.prof., University of Zagreb, Faculty of Geodesy, Zagreb, Croatia, marko.pavasovic@geof.unizg.hr
[4] Assoc.prof., University of Zagreb, Faculty of Geodesy, Zagreb, Croatia, mario.miler@geof.unizg.hr

DISASTER RISK MANAGEMENT AND FIRE SAFETY

DATA COLLECTION ORGANIZATION FOR THE ASSESMENT OF HIGH-RISE BUILDINGS' CONDITION

Milan Trivunić[1], Željko Jakšić[2], Dušanka Plazina-Pevač[3], Igor Peško[4], Vladimir Mučenski[5],

Summary:

High-rise buildings are exposed to risks of injury due to the effects of earthquakes, fires, floods, etc. In populated areas, high-rise buildings have different characteristics (age, applied materials, applied design and construction methods). In order to perform a global assessment of individual injury risks, a range of facility data is required. By analyzing the data availability in populated areas, there are no databases on constructed facilities. The aim of this paper is to systematize data and present one of the ways of collecting data on high-rise buildings, which as such can be further used for the necessary analyses.

Key words: high-rise buildings, characteristics, vulnerability, data collection, organization

[1]Prof., University of Novi Sad/Faculty of Technical Sciences/Department of Civil Engineering and Geodesy, trule@uns.ac.rs
[2] Ass. Prof., UNS /Faculty of Technical Sciences/Department of Civil Engineering and Geodesy, alt96@uns.ac.rs
[3]Head of Engineering Department, IEE Consult s.e. d.o.o., Mičurinova street no.8, Novi Sad, Republic of Serbia,dusanka.plazina@iee.rs
[4] Prof., UNS /Faculty of Technical Sciences/Department of Civil Engineering and Geodesy, igorbp@uns.ac.rs
[5] Prof., UNS /Faculty of Technical Sciences/Department of Civil Engineering and Geodesy, mucenskiv@uns.ac.rs

1. INTRODUCTION

High-rise buildings represent a significant resource in the functioning of the social community, particularly in the economic, physical, aesthetic – functional sense, and the like. As such, its importance is primarily durability, safety, and security, above all for its users and the environment as such.
High-rise buildings are exposed to risks of injury due to natural and artificial sources, like earthquakes, fire, flood, wind, landslides, explosion, etc.
In populated areas, high-rise buildings are of a different characteristic (age, materials used for construction, methods of design and construction, interventions on the building in the previous period as well as maintenance).
With the goal of carrying out a global assessment of the damage risk to objects because of the above-mentioned hazards, a series of data about buildings, as objects, is needed. (According to [1],[2],[3],[4],[5],[6])
By analyzing the availability of data on high-rise buildings in populated areas (in Serbia and beyond), the conclusion is as such that there are no databases on built facilities that could be fully used in assessing the risk of injury due to accident situations.
Since the number and surface area of high-rise buildings is extremely large, it is necessary to collect the necessary data and present them through appropriate databases in an organized manner. An illustrative example of the data collection need is the area of residential buildings, primarily, (collective and individual) in the area of the city of Novi Sad of about 11,500,000 m^2, which is used by approximately 450,000 inhabitants [source: JKP "Informatika" Novi Sad], and when to this amount is added a number of buildings and areas, such as social, hospital, business and other high-rise buildings, the number of buildings and their surface area are increasing significantly, only for the area of one city.
It is necessary to define a systematic and organized data collection method that would enable accurate, fast, and cost-effective data collection on certain facilities.
The aim of this paper is the initial presentation of the data collection organization on existing high-rise buildings to further represent the basis for condition assessment, vulnerability assessment, measures to improve facilities and response in case of various acceding situations.

2. RISK ASSESSMENT OF BUILDING DAMAGE

Risk is the potential for an unwanted outcome resulting from an incident, event, or occurrence, as determined by its likelihood and the associated consequences. Risk is influenced by the nature and magnitude of a threat, the vulnerabilities to the threat, and the consequences that could result [2]. According to the same source, risk quantification can be defined as:

Risk rating = Consequences x Threat (or Hazard) x Vulnerability

Consequences – Degree of impact that would result from the incapacity or destruction of the building's assets (occupants, critical functions, and infrastructure) as a result of a catastrophic event causing fatalities, social and economic losses, and/or business disruption.
Threat – Relative likelihood that a threat or hazard will affect the building.
Vulnerability – Relative weaknesses of functions, systems, and sites in regard to a particular threat/hazard; the likelihood that damage, casualties, and business disruption will occur.

The built environment in which people live consists of facilities with different purposes and distinctive characteristics. Each of the facilities (and groups in a certain area) has technical characteristics that are a possible source of vulnerability in case of hazard.

Especially important element of hazard risk assessment is the characteristics of buildings. Based on the analysis of the observed area and beyond, for many buildings, there are no databases that would be the basis for assessing vulnerability, regardless of the observed hazard (earthquake, fire, flood, wind, landslides, explosion, etc.).
After various events in the previous period, the United States government, Department of Homeland Security, FEMA, are approaching an organized process of risk assessment from various events. Based on this, Integrated Rapid Visual Screening of Buildings (IRVS) [2][3][4] was created.
The IRVS Database is a standalone application that supports the collection and analysis of data to identify risk and resilience, accept or reject risk, and implement effective mitigation measures.
Within[3] it is possible to download the IRVS Software Database Package: MS Access. The IRVS Database supports the IRVS series (buildings, mass transit stations, and tunnels). The IRVS Database is a standalone application that is both a data collection tool and a data management tool.
The Integrated Rapid Visual Screening Series (IRVS) for Buildings enables interactive data collection. Several basic data about the buildings are given in the following Table 1.

Tab. 1 Data - Occupancy Type and Building Systems

Purpose of building, i.e., function of building[2]:	Building Systems/Characteristics - The vulnerability of the following building systems/categories is assessed [2]:
Agriculture and Food, Banking and Finance, Chemical, Commercial Facilities, Communications, Critical Manufacturing, Dams, Defence Industrial Base, Emergency Services, Energy, Government Facilities, Healthcare and Public Health, Information Technology, National Monuments and Icons, Nuclear Reactors, Materials, and Waste, Postal and Shipping, *Residential buildings (not listed in[2]),* Transportation Systems, Water.	Site Architecture Building enclosure Structure Mechanical/electrical/plumbing (MEP) systems Fire protection systems Security systems Cyber/communication infrastructure Continuity of operations

The specifics of the architectural construction engineering design of buildings in a certain area must be considered when collecting data and analysing vulnerability. Based on that in Table 2 is presented a comparative view of Structure Type - building types as a group of data that is selected within the data collection system, and according to [2] also for the analysed area.

Tab. 2 Structure Type - building types

According to [2]	For the observed area
Wood frame	Masonry bearing walls
Steel moment frame	Masonry bearing walls with concrete elements
Steel braced frame	Concrete frame
Steel light frame	Concrete frame with unreinforced masonry infill walls
Steel frame with cast-in-place concrete shear walls	Concrete frame with prestressed elements
Steel frame with unreinforced masonry infill walls	Concrete walls and ceilings
Concrete moment frame	Precast concrete frames
Concrete shear walls	Precast concrete frames with prestressed elements
Concrete frame with unreinforced masonry infill walls	Precast concrete walls and ceilings
Precast concrete tilt-up walls	Steel frame
Precast concrete frames with concrete shear walls	Concrete and steel elements
Reinforced masonry bearing walls with wood or metal deck diaphragms	Wood frame
Reinforced masonry bearing walls with precast concrete diaphragms	Concrete and wood elements
Unreinforced masonry bearing walls	Concrete, steel and wood elements
Manufactured homes	Walls made of unbaked earth and wood elements

Based on the previously mentioned as well as other analyses, there is a need to modify the types of data for analyzing the vulnerability of buildings, risk assessment, respecting the specifics of the architectural construction engineering design of buildings in a certain area, availability of data, etc. This states that either existing systems (such as IRVS) must be modified, or new ones must be created for the collection of data on facilities and risk assessment respecting the specificities of certain areas.

3. ORGANIZATION OF DATA COLLECTION ON FACILITIES

Modification of existing or creation of new systems for collecting data on facilities, exposed to potential risks and assessment of risk intensity, must take into account the following: the specifics of engineering design of facilities or parts of facilities (mechanical, electrical and other installations) of a certain area, location characteristics, availability of data on objects and their shape, etc.

The format of data on facilities is defined by the process of assessing the risk of injury, and in addition to the basic technical data by individual groups (Tab.1 - second part), and is of the utmost importance to include the following data:

- building construction period (implication - applied regulations),
- repairs, upgrades, reconstructions, modernization (improvement of performance compared to the basic condition of the facility),

– current/present condition of the facility (maintenance quality).

In addition to previously presented data groups (Tab.1 - second part), data groups can be organizationally grouped according to the needs of risk assessment of various negative impacts (earthquake, fire, flood, wind, landslides, explosion, etc.), which is given in Fig. 1. Data grouped in this way will enable the attention of those collecting data to be directed towards the aspect of different risks.

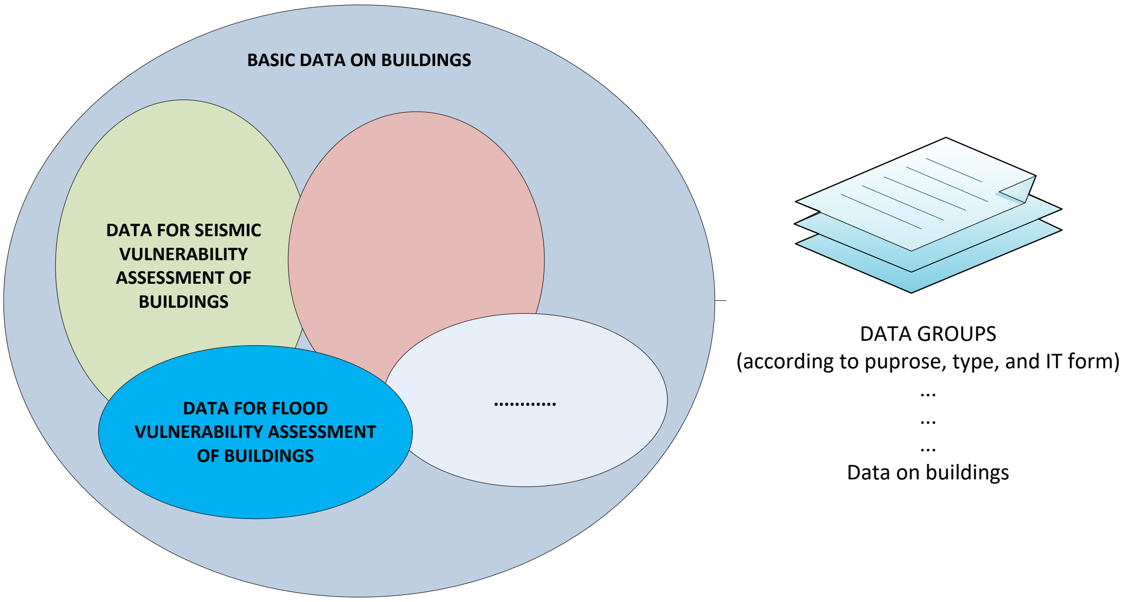

Fig. 1 Facility data groups in relation to risks

By forming a model for collecting and presenting data on the performance of the facility, at any location, it will provide significant support to all specialists, interested in the occurrence of several types of risks. Without such facility database, the risk assessment will not be satisfactory.

The data collected in this way would also have value for all other analyses within the built environment.

Data collection would be organized by using a suitable application (modified IRVS or a new form) that would be used on one of the platforms (laptop, tablet, smartphone). The application is formed in the form of an expert system (ES) that enables an easy selection of the offered solutions - attributes about facilities during a visual inspection of the one. In this way, Visual Screening of facilities (of which there are many) does not have to be done by top experts but can be done by all those who have basic knowledge about high-rise buildings. However, Screeners may use subjective judgment when selecting attribute options for certain characteristics. The information in the catalog (ES) is intended in part to minimize the number of times the screener must use subjective judgment. When subjective judgment is used, the screener should document why the attribute was selected [2].

In Fig. 2 is given a graphic representation of the process of data collection on high-rise buildings.

Based on the collected data on the facilities and the determination of the intensity of the risk of injury due to the effect of some hazard, it is possible to approach their improvement even for facilities that are extremely endangered.

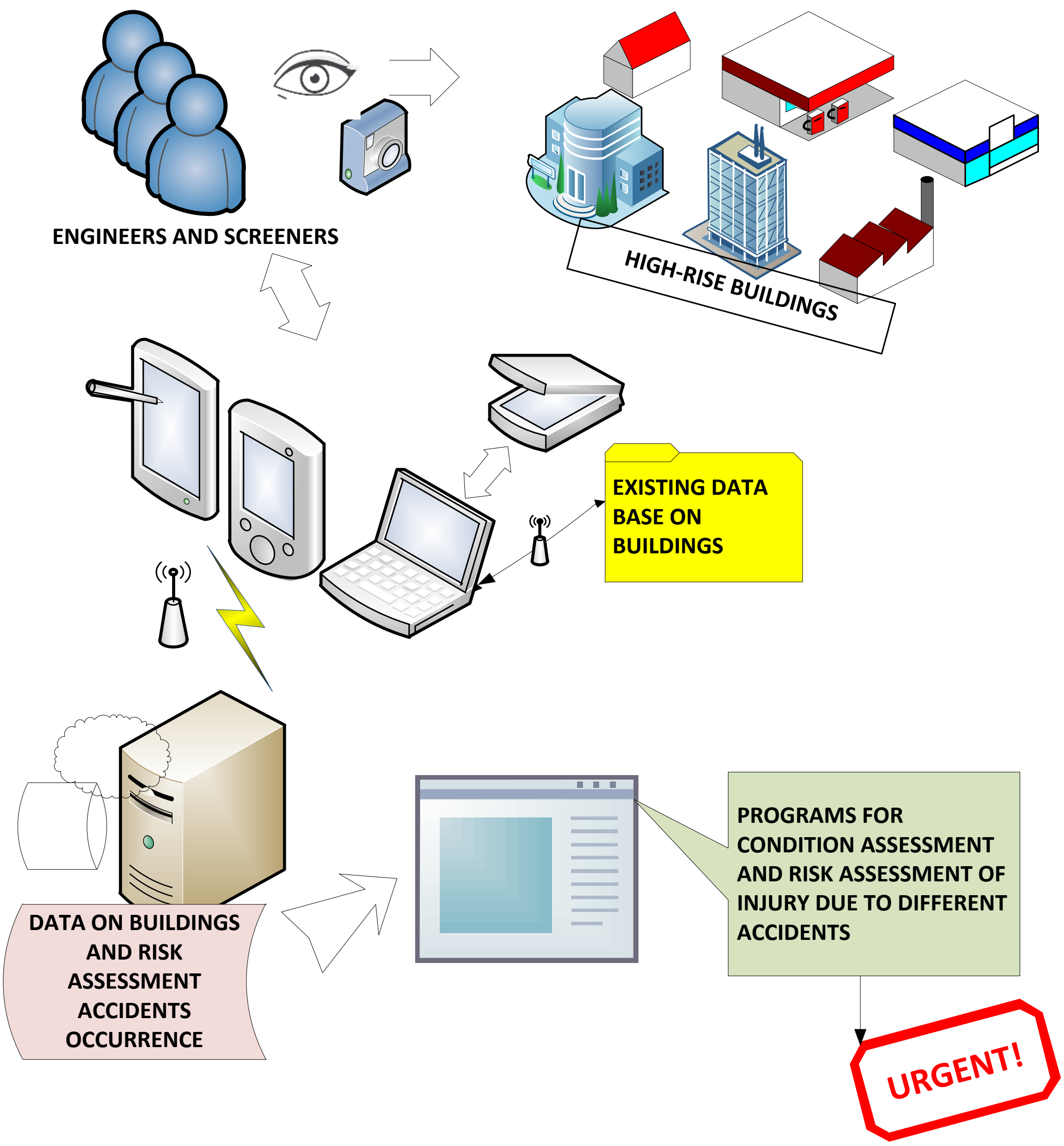

Fig. 2 The process of data collection on high-rise buildings

4. CONCLUSIONS

High-rise buildings represent a significant resource in the functioning of the social community - economic, physical, aesthetic-functional sense. As such, it is important that it be durable, safe, and secure, above all for its users and the environment, so it is very important how they respond to the effects of natural and artificial sources: earthquakes, fires, floods, wind, landslides, explosions, etc.

In the absence of a single database on high-rise buildings with data needed to assess the condition and vulnerability of buildings, it is necessary to collect data on their characteristics.

The collection of data on objects of the built environment can be done by modifying the existing system IRVS (Integrated Rapid Visual Screening Series) or by creating a special program based on the Expert System that considers all the specifics of the engineering design of objects or parts of objects in a certain area, location characteristics, the availability of data on objects and their shape.

ACKNOWLEDGEMENT

The research has been conducted within the project "Scientific theoretical and experimental research and improvement of educational process in the field of civil engineering", developed at the Department of Civil Engineering and Geodesy, Faculty of Technical Sciences, University of Novi Sad, Serbia.

REFERENCES

[1] *Law on Disaster Risk Reduction and Emergency Management*, "Official Gazzette of RS", no. 87/2018

[2] *Integrated Rapid Visual Screening of Buildings*, Homeland Security Science and Technology, BIPS 04/September 2011

[3] https://www.dhs.gov/bips-04-integrated-rapid-visual-screening-series-irvs-buildings

[4] *Integrated Rapid Visual Screening of Schools, A How-to Guide to Mitigate Multi-hazard Effects Against School Facilities* (2014)National Institute of Building Sciences, *US.*

[5] *The Seismic Assessment of Existing buildings, Technical Guidelines for Engineering Assessment, Initial Seismic Assessment, Part B* (2017), New Zealand, ISBN:978-0-478-43366-1.

[6] Bektas, N., Kegyes - Brassai, O. (2023), Development in Fuzzy Logic-Based Rapid Visual Screening Method for Seismic Vulnerability Assessment of Buildings, *Geosciences 2023*, 13,6.https://doi.org/10.3390/geosciences13010006,

[7] https://www.mdpi.com/journal/geosciences., pp. 1/25-25/25.

FIRE RISK ASSESSMENT OF THE ELEMENTARY SCHOOL "VUK KARADŽIĆ" IN BIJELJINA

Mirjana Kačarević[1], Slobodan Šupić[2], Mirjana Laban[3]

Summary:

Schools are facilities accommodating many young people, i.e., vulnerable population, where panic can affect rational behavior in the event of a fire. Therefore, it is of utmost importance that evacuation and rescue procedures are effectively planned and practiced in advance. In this study, in accordance with the Low on risk reduction, the fire assessment of the elementary school "Vuk Karadžić" in Bijeljina was carried out. The risk level was determined by analyzing two scenarios: 1) the most likely adverse event, and 2) the event with the most severe possible consequences. Based on the obtained results, a proposal to enhance conditions in terms of fire protection for school users was given.

Key words: risk assessment, fire, legislation, educational institutions, safety measures

[1] MSc, Faculty of Technical Sciences, University of Novi Sad, Serbia, kacarevic.mirjana00@gmail.com
[2] Assis. prof., Faculty of Technical Sciences, University of Novi Sad, Serbia, ssupic@uns.ac.rs
[3] Full prof., Faculty of Technical Sciences, University of Novi Sad, Serbia, mlaban@uns.ac.rs

1. INTRODUCTION

Residential, commercial, and public buildings, which house a significant number of people, are vulnerable to catastrophic dangers, particularly fire. Fire safety is a complex area in Republic of Srpska, and represents an area of special interest. Fire prevention begins with documentation, which should be present in every public, commercial, and residential building. An essential document among these requirements is an assessment of the risk of fire and explosion, which assesses all the dangers of the present condition in the structure. Furthermore, buildings should have a Fire protection plan that describes the essential actions to prevent and spread fire, as well as a Fire protection design, a Fire protection report, and so on.

The laws and regulations governing fire safety in educational facilities in Republic of Srpska are as follows:

- Law of fire protection [1];
- Rulebook of technical norms of fire protection in objects where a large number of people gather, live or work [2];
- Rulebook of technical norms for the hydrant network for fire extinguishing [3];
- Rulebook of technical norms for accessible roads, turnway and arrangement plateau for fire fighting vehicles near objects with an increased fire risk [4].

The laws and regulations governing fire safety in educational facilities in in Republic of Serbia:

- Law of fire protection [5];
- Fire protection strategy for the period from 2012-2017 years [6];
- Decree of the classification of buildings, activities and land into fire hazard categories [7];
- Rulebook on technical norms for fire protection of residential and commercial buildings and public buildings [8];
- Rulebook on technical standards for firefighting hydrant network installations [9];
- Rulebook on technical norms for access roads, turnstiles and arranged plateaus for fire engines in the vicinity of objects with an increased risk of fire [10];
- Rulebook on technical fire safety requirements for external walls of buildings [11].

As can be seen from the above-listed current legislation, the rules for fire protection in schools are comparable. As a result, the fire safety requirements and analysis could be carried out in accordance with both countries' rules.

This study presents the fire risk assessment of the primary school "Vuk Karadžić" in Bijeljina in accordance with the Law of Risk Reduction.

2. FIRE RISK ASSESSMENT OF "VUK KARADŽIĆ" PRIMARY SCHOOL, BIJELJINA

2.1. BASIC DATA ON THE BUILDING

The elementary school is divided into two floors: the ground floor and the first floor [12]. Elementary school is located at Josif Marinković Street 36. The structure is equipped with paved roads, electricity, water supply, sewerage, and a telecommunications network. The Bijeljina Health Center, which is 2.5 kilometers from the school, provides health treatment. The Territorial Fire Department is 1.5 kilometers away from the elementary school.

The structural system of the building is a frame-structure, consisting of reinforced concrete (RC) elements, with RC columns and RC beams and rigid RC mezzanine

floor-structures constructed of solid slabs. In order to ensure the seismic resistance of the structure, aseismic RC panels were designed and executed. Brick-masonry walls were executed as a infill of the frame structure. The facade elements were made of autoclaved aerated concrete and have a fire resistance rating of 2 hours.
The elementary school "Vuk Karadžić" generates income by delivering educational services. This school's earnings for the year 2021 were 90 million RSD, and this value will be used to determine the level of risk.

Fig. 1 Elementary school „Vuk Karadžić“

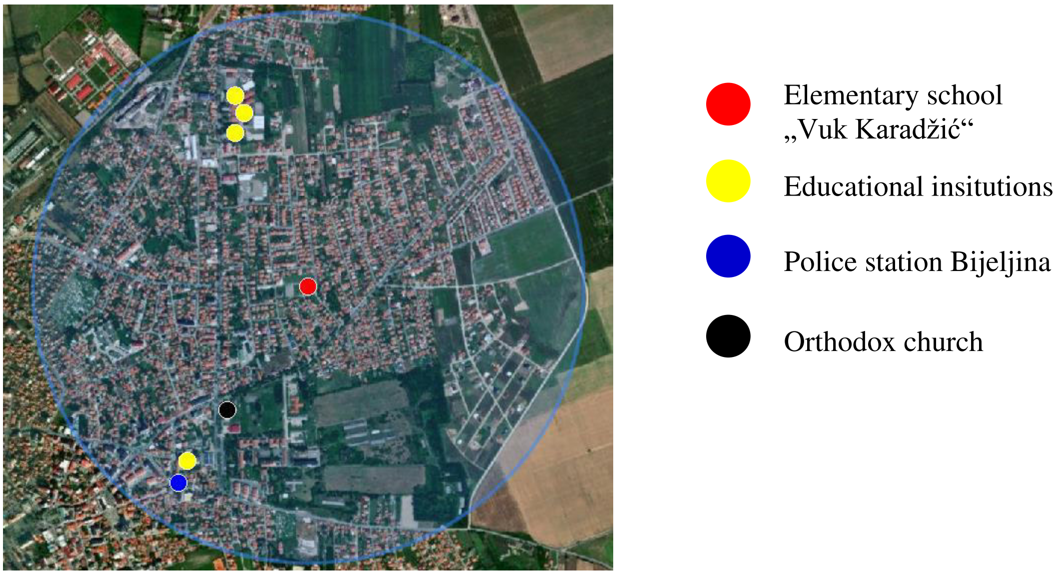

Fig. 2 Vulnerable facilities near the primary school

2.2. FIRE-SAFETY MEASURES

The "Vuk Karadžić" primary school facility comes under the III fire hazard category, according to the Regulation on the categorization of buildings, activities, and land in the fire hazard categories. Entities of this category are obliged to adopt Fire Protection Rules. This criterion is met by the facility.
In terms of passive fire safety measures, the load-bearing structure (reinforced concrete and clay-based masonry parts) is constructed of noncombustible materials, and the cladding and coatings are also fire-proof, as well. The structure is divided in three fire-compartments: 1) the school, 2) children's daycare center, and 3) boiler room with associated rooms.
Within the active fire safety actions, we highlight the hydrant network, electrical installations, fire protection installation, and mobile fire protection equipment as established protection systems.

There are two types of installed detection systems: automated and manual fire alarms, as well as alarm sirens for external and internal mounting [13].
The number of devices for initial fire extinguishment is determined according to the total area of the building, its purpose and fire protection load [13], and it includes:
• S9 apparatus - 18 pieces,
• CO_2 apparatus – 9 pieces.
In accordance with the Law of Risk Reduction [14], a fire risk assesment was carried out for the elementary school „Vuk Karadžić“ in Bijeljina. Two scenarios were analyzed:

1. The most likely adverse event – an event that occurs frequently, and it is reasonable to assume that it could endanger the life and health of individuals in a certain region and cause material damage.
2. The event with the most severe possible consequences – an event that rarely occurs in a certain area, and in the event of its occurrence, has such an intensity that the consequences are serious or catastrophic for certain protected values.

2.3. SCENARIO 1

The scenario 1 (the most likely adverse event) is presented in forecoming Table.

Tab. 1 The scenario 1 (the most likely adverse event), a brief description

Parameter	Basic data	
Danger	Fire and explosions - open fires	
Appearance	A fire broke out on the first floor in the midday hours when the building was not fully loaded, i.e. when 175 people were staying in it.	
Spatial dimension	The fire broke out on the first level of the "Vuk Karadžić" elementary school building owing to a short circuit in the installations.	
Intensity	Occurrence of fire and smoke	
Time	19.9.2023. year at 12 o'clock, the first shift, Malfunction of electrical installations	
Event description	A spark caused the roller shutters in the conference room on the first level to catch fire due to a failure in the electrical installations. As lectures were in session at the time, the fire was not discovered in time, and it spread to office supplies. As the automatic system did not respond, the employee triggered the manual alarm after seeing the fire. All employees and students evacuated and the janitor contacted the Fire Department, which located the fire in 20 minutes. Two persons sought medical attention for smoke inhalation. Electrical equipment, office furniture, and partition walls suffered damaged.	
Duration	The fire took 20 minutes to extinguish, and the evacuation of personnel, pupils, and preschool-aged children was conducted in 10 minutes.	
An early announcement	The whole facility is protected by a fire alarm system, nevertheless it failed owing to inconsistent testing.	
Preparedness	Employees are only partially prepared to respond to a fire. In the event of a fire, the territorial fire service is ready to respond.	
Influence	Protected values	Presentation of the impact of a scenario
	Life and people's health	The total number of people affected: • dead – none • injured and cared for (smoke inhalation) – 2 • evacuated – 173 **total: 175**
	Economy/ecology	Total material damage to the economy and ecology: • health care and treatment: 1500KM – (90000RSD) • all immediate emergency measures (replacement of burnt work equipment, installation, renovation of carpentry and claddings): 45 000KM – (2 700 000RSD) The costs were estimated in consultation with an expert in fire protection and occupational safety.
	Critical infrastructure	Energy (installation damage): Minimal damage
Other dangers	No other hazards generated	
Ref. incidents	No reference incidents	
Public informing	Information is provided directly by the school administration	

As the facility has been in operation for less than ten years, the frequency criterion cannot be applied; thus, the assessment of the probability of fire occurrence will be based on the probability of fire occurrence, as given in Table 2.

Table 2. The probability of the event

Category	**Probability or frequency**			
	(a) Expert assessment	**(b) Probability**	**(c) Frequency**	**Selected**
1	Negligible	< 1%	1 event in 100 years and less often	
2	Small	1 – 5%	1 event in 20 to 100 years	
3	Medium	6 – 50%	1 event in 2 to 20 years	√
4	Large	51 – 98%	1 event in 1 to 2 years	
5	Extremely large	> 99%	1 event per year or more often	

The assessment of the consequences - for people's lives and health is shown in Table 3.

Table 3. Consequences for people's life and health

Category	**The magnitude of the consequences**	**Criterion**	**Selected**
1	Minimal	< 50	
2	Small	50 – 200	√
3	Moderate	201 – 500	
4	Serious	501 – 1500	
5	Catastrophic	> 1500	

The probability level is **medium (3)**, the consequences are **small (2)**, so the risk level is **moderate.**

Consequences for the economy/ecology - are obtained by comparing the damage with the sum of the value of fixed assets and working capital in accordance with the specified criteria shown in the Table 4.

Table 4. The consequences for economy/ecology

Category	**The magnitude of the consequences**	**Criterion**	**Selected**
1	Minimal	the amount exceeds 1% of the budget	
2	Small	the amount exceeds 3% of the budget	√
3	Moderate	the amount exceeds 5% of the budget	
4	Serious	the amount exceeds 10% of the budget	
5	Catastrophic	the amount exceeds 15% of the budget	

The probability level is **medium (3)**, the consequences are **small (2)**, so the risk level is **moderate.**

The consequences for critical infrastructure are presented in Table 5.

Table 5. Consequences for critical infrastructure

Category	**The magnitude of the consequences**	**Criterion**	**Selected**
1	Minimal	< 1% budget	√
2	Small	1 – 3% budget	
3	Moderate	3 – 5% budget	
4	Serious	5 – 10% budget	
5	Catastrophic	> 10% budget	

The probability level is **medium (3)**, the consequences are **small (2)**, so the risk level is **moderate.**

The risk level was computed and displayed in the matrix below based on the assigned degrees of probability and consequences.

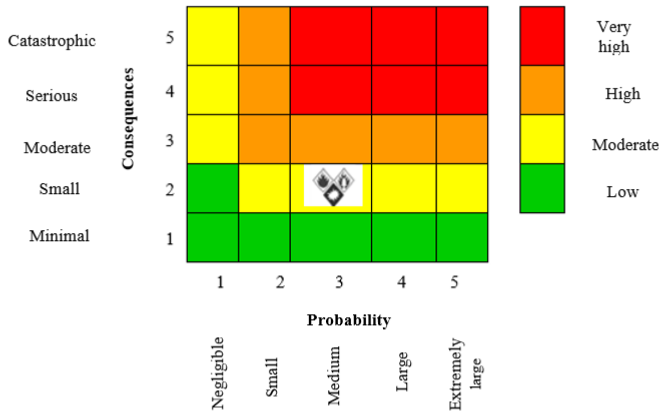

The total risk was determined as the mean value of all risk values in relation to consequences for human life and health (2), economy/ecology (2), and damage to critical infrastructure (1).

$$\frac{2+2+1}{3} = 1{,}67$$

We go with the first greater value: 2.

2.3.1. Risk treatment

Based on the findings, it was determined that safety precautions were required. It is necessary to lower the level of risk to the lowest possible level using the following measures:

- Creation of a protection and rescue plan in emergency situations;
- Appointment of commissioner and deputy commissioner of civil protection;
- Maintaining evacuation routes passable;
- Maintaining evacuation signs visible;
- Check and service of the hydrant network every 6 months;
- Regularly servicing fire extinguishers;
- Conducting an evacuation exercise every 6 months;
- Regular update of the fire protection plan.

2.4. SCENARIO 2

The scenario 2 (the event with the most severe possible consequences) is presented in forecoming Table 6.

Table 6. The scenario 2 (the event with the most severe possible consequences), a brief description

Parameter	Basic data	
Danger	Fire and explosions - open fires	
Appearance	A fire broke out on the first floor in the afternoon, when the building was fully loaded, i.e. when 350 people were staying there.	
Spatial dimension	The fire broke out on the first level of the "Vuk Karadžić" elementary school building owing to a short circuit in the installations.	
Intensity	Occurrence of fire and smoke	
Time	20.03.2024. at 14 o'clock, the second shift, Malfunction of electrical installations	
Event description	A short circuit in the electrical installations caused the fire to start in the library. The books were set ablaze, followed by the bookshelves. The fire swiftly spread throughout the library due to the enormous volume of combustible and easily flammable material. At the moment, no personnel were present in the library. When the janitor came by, the fire had spread to the school's corridor (floor coated with laminates), and he activated the alarm and called the fire department. In 15 minutes, students, parents, and employees were evacuated. The fire service was able to contain the fire in 50 minutes. Smoke inhalation caused 30 persons to be injured.	
Duration	The fire took 50 minutes to extinguish, and the evacuation of personnel, pupils, and preschool-aged children was conducted in 15 minutes.	
An early announcement	The whole facility is protected by a fire alarm system, nevertheless it failed owing to inconsistent testing.	
Preparedness	Employees are only partially prepared to respond to a fire. In the event of a fire, the territorial fire service is ready to respond.	
Influence	Protected values	Presentation of the impact of a scenario
	Life and people's health	The total number of people affected: • dead – none • injured and cared for (smoke inhalation) – 30 • evacuated – 320 **total: 350**
	Economy/ecology	Total material damage to the economy and ecology: • health care and treatment: 25000KM – (1.500.000RSD) • all immediate emergency measures: 100.000KM – (6.000.000RSD) The costs were estimated in consultation with an expert in fire protection and occupational safety.
	Critical infrastructure	Energy (installation damage): Minimal damage
Other dangers	No other hazards generated	
Ref. incidents	No reference incidents	
Public informing	Information is provided directly by the school administration	

The assessment of the probability of fire occurrence was carried out based on the probability of fire occurrence, as given in Table 7.

Table 7. The probability of the event

Category	Probability or frequency			
	(a) Expert assessment	**(b) Probability**	**(c) Frequency**	**Selected**
1	Negligible	< 1%	1 event in 100 years and less often	
2	Small	1 – 5%	1 event in 20 to 100 years	√
3	Medium	6 – 50%	1 event in 2 to 20 years	
4	Large	51 – 98%	1 event in 1 to 2 years	
5	Extremely large	> 99%	1 event per year or more often	

The assessment of the consequences - for people's lives and health is shown in Table 8.

Table 8. The consequences for people's life and health

Category	The magnitude of the consequences	Criterion	Selected
1	Minimal	< 50	
2	Small	50 – 200	
3	Moderate	201 – 500	√
4	Serious	501 – 1500	
5	Catastrophic	> 1500	

The probability level is **small (2)**, the consequences are **moderate (3)**, so the risk level is **large.**

Consequences for the economy/ecology - are obtained by comparing the damage with the sum of the value of fixed assets and working capital in accordance with the specified criteria shown in Table 9.

Table 9. The consequences for economy/ecology

Category	The magnitude of the consequences	Criterion	Selected
1	Minimal	the amount of which exceeds 1% of the budget	
2	Small	the amount of which exceeds 3% of the budget	
3	Moderate	the amount of which exceeds 5% of the budget	√
4	Serious	the amount of which exceeds 10% of the budget	
5	Catastrophic	the amount of which exceeds 15% of the budget	

The probability level is **small (2)**, the consequences are **moderate (3)**, so the risk level is **large.**

The consequences for critical infrastructure are presented in Table 10.

Table 10. Consequences for critical infrastructure

Category	The magnitude of the consequences	Criterion	Selected
1	Minimal	< 1% budget	√
2	Small	1 – 3% budget	
3	Moderate	3 – 5% budget	
4	Serious	5 – 10% budget	
5	Catastrophic	> 10% budget	

The probability level is **small (2)**, the consequences are **minimal (1)**, so the risk level is **moderate.**

The risk level was computed and displayed in the matrix below based on the assigned degrees of probability and consequences.

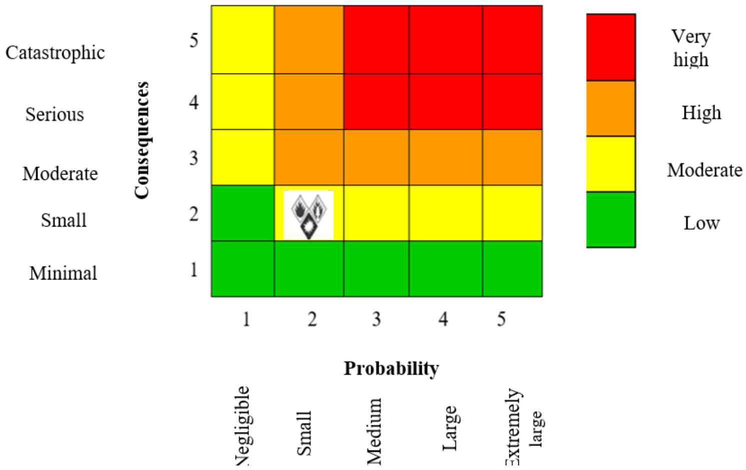

The total risk is determined as the mean value of all risk values in relation to consequences for human life and health (3), economy/ecology (3), and damage to critical infrastructure (1).

$$\frac{3+3+1}{3} = 2{,}33$$

Since the value is less than 2.5 we use the value: **2**

2.4.1. Risk treatment

Based on the findings, it was determined that safety precautions were required. The following measures must be taken to reduce the amount of risk to the lowest possible level:

- Creation of a protection and rescue plan in emergency situations;
- Appointment of commissioner and deputy commissioner of civil protection;
- Maintaining evacuation routes passable;
- Maintaining evacuation signs visible;
- Maintaining passable plateaus for the access of firefighting vehicles;
- Conducting employee education once a year with the aim of faster and more efficient evacuation;
- Check and service of the hydrant network every 6 months;
- Regular service of fire extinguishers;
- Conducting an evacuation exercise every 6 months;
- Smoking not permitted in the office or kitchen;
- Regular update of the fire protection plan.

3. CONCLUSION

This study presented a fire risk assessment for "Vuk Karadžić" Primary School in Bijeljina in compliance with current legislation. Two scenarios were developed to represent probable negative occurrences that could occur in the event of a fire.

By examining the first scenario for the most likely adverse outcome, it was determined that the risk is moderate and tolerable, implying that safety precautions are required. In this sense, it is critical to keep the risk level as low as possible.

The second scenario analysis concluded that the risk is moderate and acceptable. A risk treatment is carried out in the case of this level of risk, which defines methods and solutions to lower the level of risk to the lowest feasible level.

The training of the fire protection personnel, as well as regular training of the employees at this facility, should be prioritized in the implementation of fire-safety procedures. Regular inspections, services, and maintenance of the active fire-safety measures are of utmost importance for timely and safe evacuation in case of an eventual hazard.

Acknowledgement

The research has been conducted within the project "Scientific theoretical and experimental research and improvement of educational process in the field of civil engineering", developed at the Department of Civil Engineering and Geodesy, Faculty of Technical Sciences, University of Novi Sad, Serbia.

REFERENCES

[1] Law of fire protection ("Official Gazette of Republic of Srpska", No. 01-020- 4291/19).

[2] Rulebook of technical norms of fire protection in objects where a large number of people gather, live or work ("Official Gazette of Republic of Srpska", No. 94/19).

[3] Rulebook of technical norms for the hydrant network for fire extinguishing ("Official Gazette of Republic of Srpska", No. 39-2013).

[4] Rulebook of technical norms for accessible roads, turnway and arrangement plateau for fire fighting vehicles near objects with an increased fire risk ("Official Gazette of Republic of Srpska", No. 94/19).

[5] Law of fire protection ("Official Gazette of Republic Serbia", No. 111/2009, 20/2015, 87/2018).

[6] Fire protection strategy for the period from 2012-2017 year ("Official Gazette of RS", No. 21 from 21. march 2012).

[7] Decree of the classification of buildings, activities and land into fire hazard categories ("Official Gazette of RS", No. 76/2010).

[8] Rulebook on technical norms for fire protection of residential and commercial buildings and public buildings ("Official Gazette of RS", No. 22 from 28. march 2019).

[9] Rulebook on technical standards for firefighting hydrant network installations ("Official Gazette of RS", No. 3/2018).

[10] Rulebook on technical norms for access roads, turnstiles and arranged plateaus for fire engines in the vicinity of objects with an increased risk of fire ("Official Gazette of FRY", No. 8/95).

[11] Rulebook on technical fire safety requirements for external walls of buildings ("Official Gazette of RS", No. 59/2016, 36/2017 and 6/2019).

[12] Architectural and construction project of Elementary school "Vuk Karadžić", PC "Directorate for Construction and development of the city Bijeljina".

[13] Fire protection report for the Elementary school "Vuk Karadžić", PC "Directorate for Construction and development of the city Bijeljina".

[14] Law of Risk Reduction and emergency management ("Official Gazette of RS", No. 87/2018);

[15] Methodology for the preparation of vulnerability assessments from natural disasters and other accidents and protection and rescue plans in emergency situations ("Official Gazette of RS", No. 80/2019).

INTERNATIONAL SCIENTIFIC CONFERENCE
INTEGRATION, NOVELTY, DESIGN,
INTERDISCIPLINARITY, SUSTAINABILITY

iNDiS2023

CONTEMPORARY METHODS FOR EVACUATION SAFETY ANALYSIS

Jana Opačić[1], Suzana Draganić[2], Mirjana Laban[3]

Summary:

Amphitheatres, theatres, cinemas and similar spaces, where a large number of people temporarily gather, require a higher level of fire safety. The fire safety performance of the amphitheatre block at the Faculty of Technical Sciences in Novi Sad was checked in the context of evacuation, using the Pathfinder software package and current national technical regulations. Three distinctive simulations of evacuation scenarios were applied: the scenario deemed fastest by the program itself, the scenario based on an existing evacuation plan and the estimated fastest scenario. The simulations derived from the three evacuation scenarios highlight the problems which may occur in real-life situations, as well as the problems which were not solved by meeting the basic technical requirements. It is necessary to recognize the complexity of the problem and find an appropriate solution based on building performances needs.

Key words: amphitheatres, fire safety, evacuation scenario, software simulation

[1] Student, Faculty of Technical Sciences, University of Novi Sad, Serbia, jana.opacic99@gmail.com
[2] Assist. Professor, Faculty of Technical Sciences, University of Novi Sad, Serbia, suzanav@uns.ac.rs
[3] Full Professor, Faculty of Technical Sciences, University of Novi Sad, Serbia, mlaban@uns.ac.rs

1. INTRODUCTION

For the past couple of decades evacuation has become an important research topic with the intention of reducing the number of injured and victims. The main goals of the successful evacuation are speed, efficiency and safety of building users. Helbing et al. [1] have developed a "social force" model which “predicts” the dynamics of evacuation based on quantitative theories. Researching stampedes caused by panic research has shown that during evacuation, the density of users increases at key points (doors, vertical communications and exits from the facilities) compared to the movement of users under normal conditions. Using the "lattice-gas" model, Tajima and Takashi [2] simulated the flow of people from the hall and thus proved the correlation between evacuation efficiency and door size. By simulating an evacuation on a model of a shopping center in China, Fang et al. [3] have discovered a connection between the complexity of the building and unfamiliarity with the area with an increase in the number of injured and victims. The efficiency of evacuation is dominantly affected by: panic, knowledge of space, increase of the flow and density of people throughout exits and passages, increase in capacities of vertical communications, spatial configuration of the building, etc.

This research analyzed the Amphitheater block at the Faculty of Technical Sciences in Novi Sad by applying the Pathfinder software package, where the results of the evacuation simulation serve as a starting point for assessing the safety of users in the event of a fire.

2. FIRES AT EDUCATIONAL INSTITUTIONS

In the period 2014-2018 fire brigades in USA have responded to approximately 3,230 school fires, where the largest number of fires occurred in secondary schools [4]. Data collected in the National Fire Incident Reporting System (NFIRS) shows that 43% of fires that broke out in US schools were caused intentionally (Fig. 1).

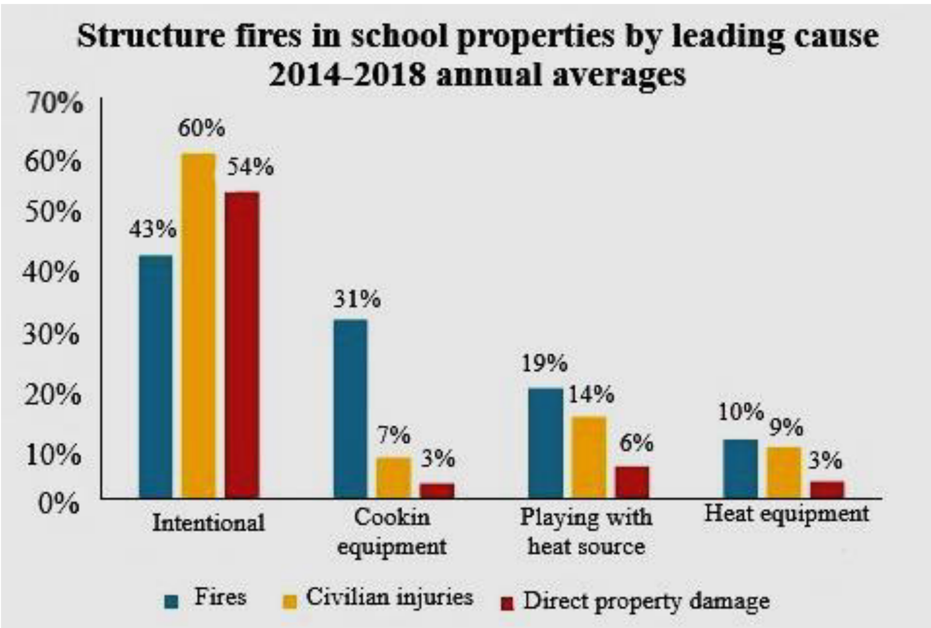

Fig. 1 Leading cause of structure fires in American schools (2014-2018) [4]

In Sweden there is a "vision zero" practice, which aims to reduce the level of mortality and injuries caused by fires or to be more precise "no one in Sweden should die or be seriously injured in fire-related incidents" [5]. Annually 25,000 fires break out in Sweden, of which 10-15% are intentionally caused (Fig. 2) [6]. On average between 60-70% of fires that occur in schools are caused accidentally or intentionally using open flames by young people (Fig. 3) [7]. In order to prevent the occurrence of fires, Sweden introduced, through national regulations, the implementation of preventive programs whose focus is fire protection systems, information campaigns, educational initiatives, national conferences, etc. [8]. Between 1952 and 2013, a total of 6,232 people died in incidents caused by fires in Sweden [9].

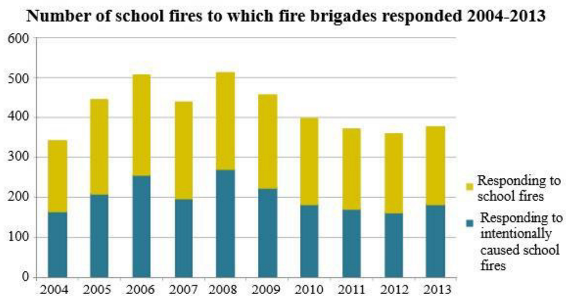

Fig. 2 Sweden: Number of school fires to which fire brigades responded

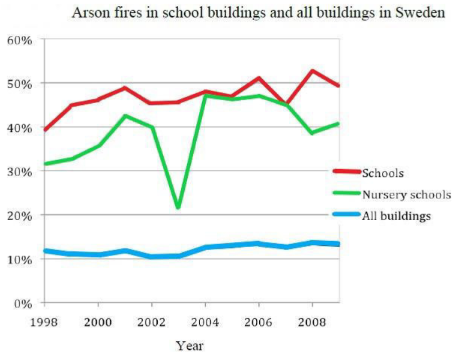

Fig 3. Annual overview of arson fires in school buildings

As schools and universities are specially equipped institutions where a large number of people is present, the implementation of fire prevention measures and systems is of key importance for ensuring safe schooling. Fires in these facilities cause great material losses due to the compactness and nature of the materials needed for education [10]. The fire load represents the amount of fuel that is present in the space and which "feeds" the fire, thus it allows fire to grow and spread [11]. Fuel represents a key factor in controlling and preventing fire outbreaks. On the other hand, factors related directly to the structure of the building that control the size of the fire are air flow and heat loss. Although the air dictates the speed and size of fire development, the fact is that large concentrations of air in the room slow down the fire spread, i.e. put it out. In addition to matter and the presence of oxygen, the third key factor is the size of the room. It is believed that the larger the space, the greater the amount of fuel, as well as that further entering into the room follows the rise of temperature of the fire due to the lack of air cooling [12].

Fast spread of fire reduces the *Available Safe Egress Time* (ASET) in comparison to the *Required Safe Egress Time* (RSET) and thus reduces the success of safe evacuation.

3. CASE STUDY – EVACUATION FROM AMPHITEATERS

3.1. BASIC DATA ON THE BUILDING

The Amphitheater block is one of the buildings that belong to the Faculty of Technical Sciences in Novi Sad, Serbia (Fig. 4). The total area of the building is 3,500 m^2 and the maximum number of people who can be present at the same time in the building is 1,200. According to the regulation [13], the building of the Amphitheater block belongs to the II risk category.

Fig. 4 The Amphitheater block

Except for the four amphitheaters, there are also classrooms (12), porter's office, script room, copy room, warehouse (2), library, study hall, offices (4), post office, sanitary facilities, storeroom, professor's club room and printing office in the building.

The building structure is made of reinforced concrete – RC columns and slabs, the external walls are made of brick and plastered. The partition walls are made of plasterboard or light wood. The roof is flat and impassable. The floor height is 3.45 m, while the maximum height in the amphitheaters is 7.40 m. The building has one main entrance and 5 side entrances. The building is connected by passarellas to three adjacent blocks of the faculty - the Teaching block, the Tower block and the ITC block. All the doors open in the direction of evacuation, except for the internal windbreak door at the main entrance. Vertical communications are achieved through the RC staircases, which are located opposite to the main building entrance.

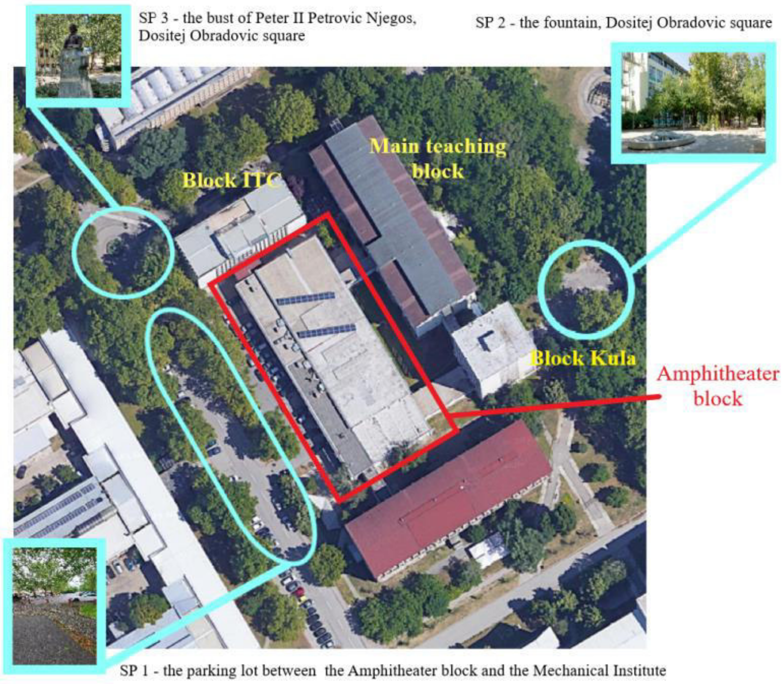

Fig. 5 Safe areas around building

The entire building of the Amphitheater block is one fire sector. There are no evacuation corridors or safety stairs in the building. Evacuation routes are wider than technically required (min. 1.2 m). The corridors are passable in the middle, but there are benches, flower pots with decorative flowers, high tables and sideboards on the sides. The rooms of the amphitheaters have cascades, where the floor height on the lower side is 1.5 m above the ground level, and the floor height on the higher side is at a height of 3.45 m. According to the technical regulations, the rooms of the amphitheater should

have a minimum of 2 first exits in the form of double doors; however, in the case of amphitheaters A3 and A4, this measure was not fulfilled. On the amphitheaters A1 and A2, the two pairs of doors leading to the hall on the ground floor are double doors with a light width of 1.8 m, and the single-leaf wooden doors leading to the hall to the teaching block have a width of 0.9 m. The double doors in the amphitheaters A3 and A4 are 1.8 m wide.
There are 18 fire extinguishers available, which are placed in visible and accessible points; there are no internal hydrants, only two external ones. The fire alarm system is only one call point in the entire building and is located between amphitheater A2 and A3. Panic lights and evacuation signs are installed at prescribed heights and places. The Evacuation Plan for the ground floor is placed on the ground floor wall between the study hall and the professor's club room. Three gathering safe areas were identified in the vicinity of the building (Fig. 5).

3.2. EVACUATION SCENARIOS

3.2.1. The Pathfinder parameters

The Pathfinder software package is an agent-based simulator of people moving and leaving spaces. The program includes an integrated user interface that is primarily used for designing simulation models and their display in 2D and 3D visualizations [14].
In order to successfully perform an evacuation simulation, it is necessary to determine the characteristic behaviors of the actors. Behaviors represent the command of directing the actors towards the given final exits. In the pictures shown in the scenarios, certain rooms are framed with different colors, which are indicators of which final exits the actors were sent to, or more precisely, which characteristic behaviors were assigned to the actors (Tab. 1).

Tab. 1 The legend of exits

Exit	Colour
Post office	Red
Main exit of the block	Blue
GRID’s side exit	Yellow
GRID’s main exit	Purple
Exit by the amphitheater’s toilet	Green
Main teaching block	Pink
Tower block	Orange
Block ITC	Brown

The speed of movement assigned to the actors in the simulation is the speed of undisturbed movement - 1.5 m/s [13]. In the evacuation scenarios, the model settings are the same, however, the differences occur in the number of people directed to certain final exits, which makes the evacuation routes loaded or unloaded. The number of actors managed in the simulation is 1,200.

3.2.2. Scenario 1 – Evacuation according to the evacuation plan

The presented evacuation simulation was performed based on the existing evacuation plan. The scenario shows the evacuation from all floors where the actors are activated simultaneously. The real time of evacuation with the set parameters of the movement speed and the use of certain final exits is 5.13 min. The simulation according to the evacuation plan is a reflection of the actual situation in the building. Certain exits are locked and thus it is impossible to fully use the available capacities (end exits). Fig. 6-8 show the building’s floor plans with characteristic behaviors of the actors.

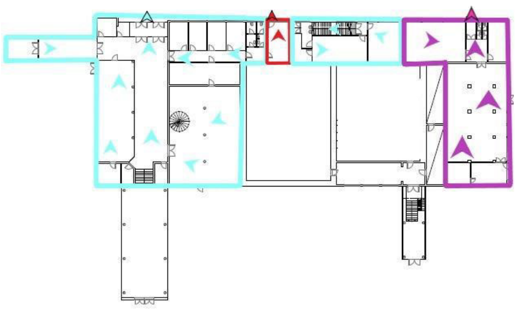

Fig. 6 Simulation 1 – evacuation route from the basement

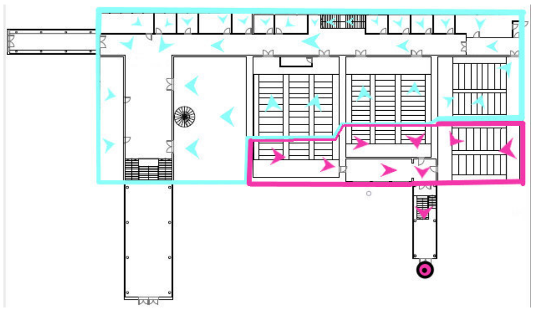

Fig. 7 Simulation 1 – evacuation route from the ground floor

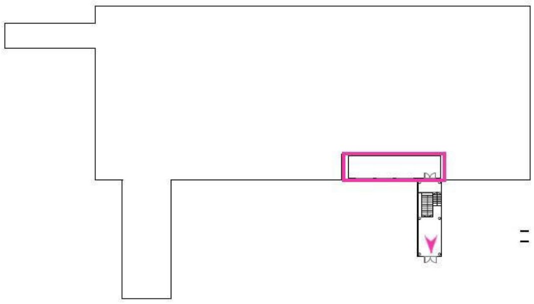

Fig. 8 Simulation 1 – evacuation route from the first floor

At the very beginning of the simulation, the highest density of people is in the amphitheaters (Fig. 9). By starting the simulation, the first actors who successfully evacuated were those who were in the rooms whose first exits coincide with the final exits and in the rooms located immediately next to the final exits, namely the post office and GRID premises. Actors, who are in other rooms of the basement, even though they are near the main exit, are unable to evacuate before the actors from the ground floor descend via the main staircase into the basement. The movement of actors from a higher floor to a lower one leads to the creation of short stops on the first exits in the library.

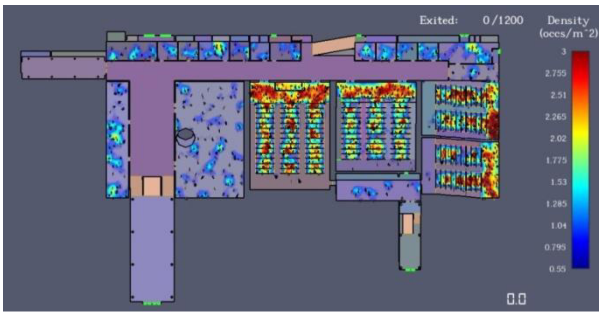

Fig. 9 Initial arrangement of the actors in the simulations scenario

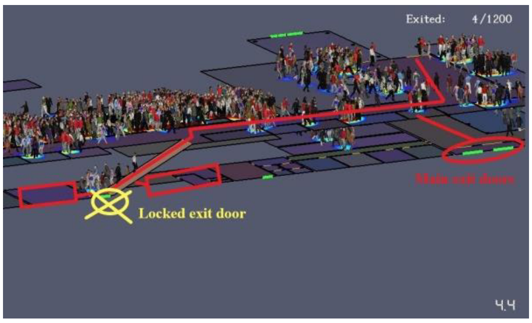

Fig. 10 The actor's movement path from the indicated part of the basement

Actors who are in the basement near the toilet are not able to evacuate through the exit by the amphitheaters toilet because the exit is not functional. Instead they are forced to use the staircase leading to the main hall on the ground floor (Fig. 10). Here the actors join the actors whose starting place was the ground floor and following the evacuation route leading to the main staircase, they evacuate through the main exit of the building.
The small capacities of the doors of the first exits and the large flow of actors in the hallway on the ground floor prevent the actors from leaving the amphitheaters and the study hall. On the main staircase, in the passages between the benches in the amphitheaters and the first exits from the amphitheaters, bottlenecks were created, which caused the actors to stay longer in these places and additionally slowed down the evacuation (Fig. 11).

The last person moving towards the main exit of the building left the room of their starting point in the second minute of the simulation. During that time, the last 48 actors staying in amphitheater A4 and those actors from A1 and A2, whose evacuation route leads to the exit through the teaching block, still did not leave the room before the evacuation began. The problem at this end of the building is the small capacity of the door from the amphitheaters and the narrow staircase which leads to the exit through the main teaching block. It is important to point out that although the actor's movement speed in the simulation is set to 1.5 m/s, the program itself recalculates the movement speed when the actors move up or down the stairs. This feature of the program further reduces the speed of the evacuation. The last actor from the room of the amphitheater A4 successfully carried out the evacuation through the exit of the teaching block in 3.27 minute. The last actor, whose evacuation route led via the main staircase to the main exit in the basement, successfully completed the evacuation at 5.13 minutes.

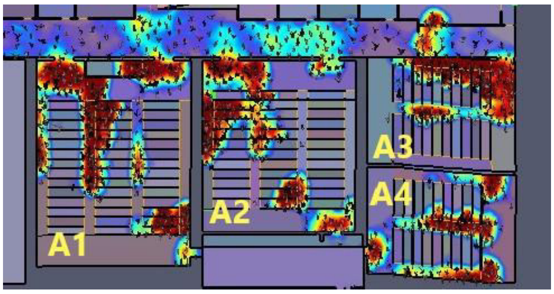

Fig. 11 Delays on evacuation routes

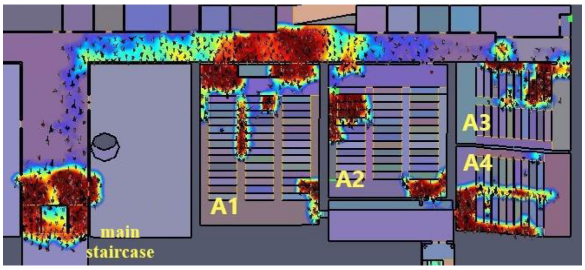

Fig. 12 Critical points in evacuation simulation 1

The critical points in the simulation are located in front of the amphitheater A1 due to the large influx of actors from the direction of the amphitheater A2 and A3 and the classrooms located across from these amphitheaters, the main staircase located opposite the main entrance and the staircase leading to the teaching block (Fig. 12).

3.2.3. Scenario 2 - Evacuation determined by the program as the fastest

In the second scenario, the actor's movement speed is the same as in the first, while the number of open final exits presented in Tab. 1 and the actor's behavior differ. In order to reduce the evacuation time, the exits that were locked in the previous scenario are now open. With the only set parameter of the actor's movement speed (1.5 m/s) the Pathfinder program modeled this evacuation simulation as the fastest. In scenario 2, none of the actors were directed to the exit Tower block (Figs. 13 and 14). Evacuation and characteristic behavior for actors from the first floor is the same as in the previous scenario. The evacuation time with the given parameters is 6.15 minutes.

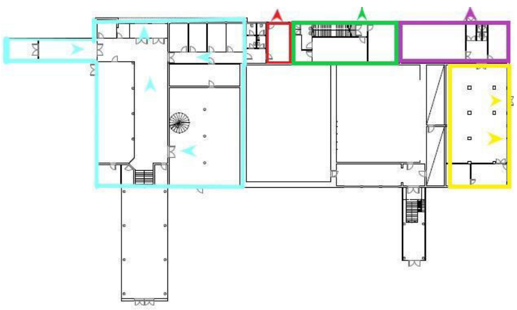

Fig. 13 Simulation 2 – evacuation route from the basement

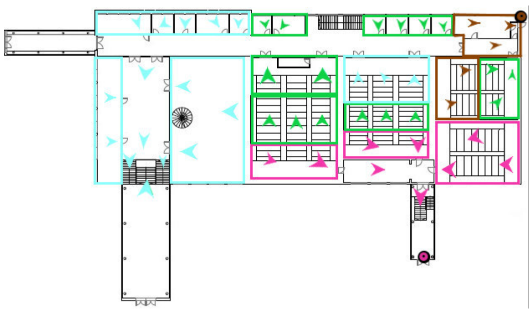

Fig. 14 Simulation 2 – evacuation route from the ground floor

The actors of the simulation are evacuated in the same way as the actors from the first scenario simulation, with the exception of actors located in the premises of the GRID, who are this time evacuated through GRID's main and side exits, and the actors who are in the rooms near the exit by the amphitheaters toilet, which are evacuated through the nearest exit door to the parking lot. The evacuation time for all actors from the basement was 41 seconds (Fig. 15).

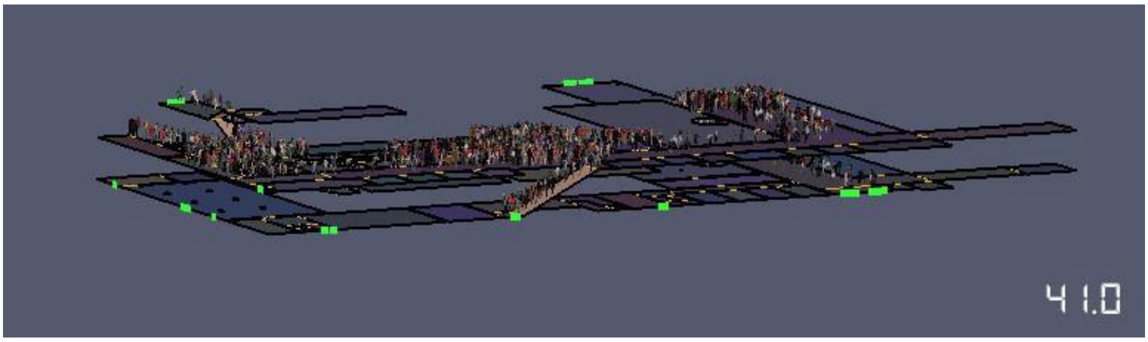

Fig. 15 Overview of the building after the completed evacuation of the basement

As in the first simulation, the first delays occur at the exits from rooms where a large number of people stay (amphitheaters and study hall). The movement of people from the direction of the amphitheaters towards the main staircase creates congestion on the main staircase, first exits from the amphitheater A1 and A2 and the study hall. Due to the heavy traffic in front of the upper first exits from the amphitheaters, a large number of actors from the lower stands were trapped on the stairs in the amphitheaters (Fig. 16). Actors whose starting place was in the amphitheater A2 are directed to the staircase leading to the exit by amphitheaters toilet. Here, due to the large flow of people, congestion occurs. As in the first scenario, the situation on the part of the staircase leading to the main teaching block is progressing slowly and the first exit from the amphitheater A4 is still overloaded. The evacuation of some of the actors from the A3 amphitheater is carried out through the exit Block ITC, and here, with minor delays, the evacuation takes place successfully.

Fig. 16 Congestions at critical locations in scenario 2

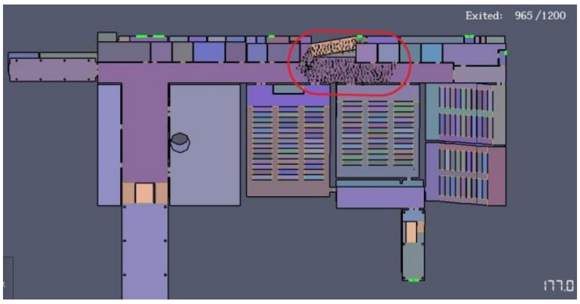

Fig. 17 Overload of the staircase near the exit by the amphitheaters toilet

The last place from which evacuation takes place is on the staircase near the amphitheater's toilet. In 177 seconds, all actors who were directed to other evacuation exits evacuated safely (Fig. 17). The remaining number of actors trapped in the building near the stairwell by the toilet is 235. The starting place of the last actor who evacuated after 6.15 minutes was the upper tribune of the amphitheater A3.

3.2.4. Scenario 3 – The fastest evacuation

The settings in the third scenario are as follows: as in the previous scenarios, the movement speed of the actors is set to 1.5 m/s, the number of actors sent to the final exits is changed and all exits are open for use in order to optimize the speed of the evacuation. The real evacuation time with the given parameters is 3.07 minutes. Figs. 18 and 19 show the building's floor plans with characteristic behaviors. As in the previous scenarios, the evacuation route of the actors on the first floor is led through the exit from the main teaching block.

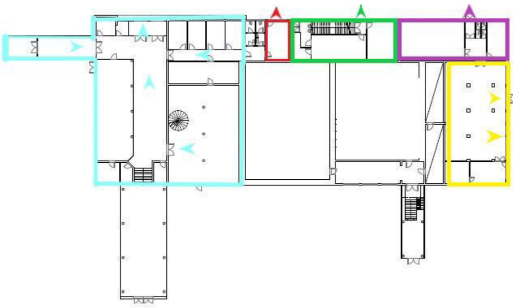

Fig. 18 Simulation 3 – evacuation route from the basement

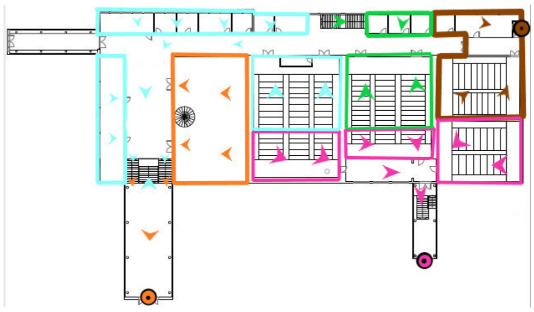

Fig. 19 Simulation 3 – evacuation route from the ground floor

Actors who were in the basement at the initial moment of evacuation, arrived at the safe places 1 and 3, in 30 seconds after the simulation started. The classrooms were the first emptied rooms at the ground floor. With the beginning of the evacuation, traffic jams occur on the first exits from all the amphitheaters and the study hall and at the exit Block ITC. Evacuation through the exit Block ITC is difficult due to the large influx of actors from the surrounding classrooms and amphitheater A3 and the obstacle in the form of a small vestibule (marked with a yellow circle in Fig. 20) where the exit Block ITC is located. Observing the further flow of the simulation, as in the previous scenario simulations, significant delays are observed not only on the first exits from the amphitheaters but also on the main staircase, the staircase leading to the exit by amphitheaters toilet and on the passages between the rows of benches in the amphitheaters. The very beginning of the simulation proceeds with difficulty, with large delays in the places marked in Fig. 21.

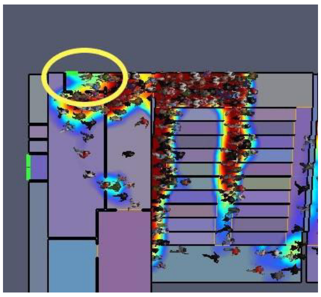

Fig. 20 The situation at the exit Block ITC

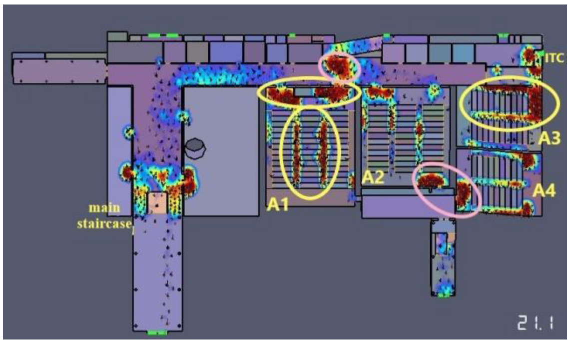

Fig. 21 Places of accumulation of actors and creation of stagnation

The continuation of the simulation continues to produce similar results as the beginning. The bottlenecks on the stairs continue to increase, the exit from the amphitheater A4 is overloaded and the evacuation of actors through the main teaching block is proceeding slowly. The stagnation and accumulation of actors at the exit Block ITC is slowly clearing up. The actors from the first floor and basement classrooms quickly and safely evacuated. Actors from the classroom on the ground floor, study hall and amphitheater A2 successfully completed the first stage of evacuation. At the end of the simulation, the exits through which the evacuation is still taking place are: the exit by amphitheater's toilet and the exit of the main teaching block. The starting point of the last actor who successfully evacuated in 3.07 minutes is amphitheater A4.

3.3. COMPARATIVE ANALYSIS OF RESULTS

In all three simulations, the number of actors, the spatial geometry and the number of exits are the same. The differences in the scenarios that played a crucial role in changing the evacuation time are the behavior of the actors (differences in the number of actors that were sent to the selected exits) and the number of exits which were open to the flow of people. The following table shows the exact number of actors that were sent to certain final exits.

Tab. 2 Number of actors sent to certain exits

Scenario 1		**Scenario 2**		**Scenario 3**	
Main exit of the block	907	Main exit of the block	394	Main exit of the block	353
		Exit by the amphitheater's toilet	441	Exit by the amphitheater's toilet	211
GRID's main exit	29	GRID's main exit	9	GRID's main exit	9
		GRID's side exit	20	GRID's side exit	20
		Block ITC	97	Block ITC	190
Main teaching block	264	Main teaching block	239	Main teaching block	263
				Block Tower	154

As previously mentioned, the limitation of the use of all capacities (exits) led to the extension or reduction of the evacuation time. In the first evacuation scenario according to the evacuation plan, the non-use of exits led to overloading of the main staircase and the main exit, which caused the evacuation to proceed slowly. The second scenario, although considered the fastest by the program, is actually the longest simulation. The main factors that resulted in the extension of the evacuation time are the redirection of a large number of actors to the exit of low flow capacity and the non-use of all available exits (exit Block Tower), which would relieve the load on other stairs.

In the fastest simulation (scenario 3), all final exits were used. Minimizing collisions and cutting the evacuation routes of the actors to a minimum generated the results of a quick and efficient evacuation. Although critical points appear in this simulation (places where a large number of people stay for a long time), their scattering is faster than in the previous two scenarios. Crucial factors in reducing the simulation time are the use of exit Block Tower, sending more actors to staircases with a higher capacity and to exits that have a higher flow rate. The simulation of the fastest evacuation ended 188 seconds before the simulation the program determined as the fastest.

4. CONCLUSION

The Amphitheater block is a spacious building, where a large number of people temporarily gather, making evacuation challenging if the building is not properly constructed.

The building complies with the requirement of using non-combustible materials in evacuation routes. However, there is a significant presence of flammable items throughout the faculty premises. Items found in the amphitheater halls, classrooms, offices, and other areas are primarily constructed from plastic or chipboard, with a limited use of textiles, leading to the generation of substantial smoke in the event of ignition. Furthermore, the final layers of floors and decorative wall coverings in amphitheaters and reading rooms consist of wooden panels coated with flammable finishes, exacerbating the fire risk. Additionally, benches, tables, potted plants, and sideboards are positioned in the corridors on various floors, creating minor obstacles that could marginally impede evacuation. In crowded situations, visibility of the floor is reduced, and low objects may pose risks of individuals becoming trapped or items falling.

The evacuation simulations, conducted by the Pathfinder software package, highlight the problems which may occur in real-life situations in the Amphitheater block, as well as the problems which were not solved by meeting the basic technical requirements. Research results indicate that although the building is designed in compliance with relevant rules and regulations, this alone does not guarantee a safe and swift evacuation. Consequently, it is necessary to recognize the complexity of the problem and find an appropriate solution based on building performances needs.

Case studies of this nature hold significant value, as the prompt utilization of simulations leads to timely adjustments of implemented organizational and technical safety measures, ultimately leading to a higher number of survivors in fire and other emergency situations. In addition to addressing building construction measures, efforts focused on educating and informing the public about fire procedures prove to be beneficial.

LITERATURE

[1] Helbing, D. Farkas, I. Vicsek, T. (2000) Simulating dynamical features of escape panic. *Nature*, vol. 407, str. 487-490

[2] Tajima, Y. Nagatani, T. (2001) Scaling behavior of crowd flow outside a hall. *Physica A: Statistical Mechanics and its Applications*, vol. 292, str. 545-554

[3] Han, F. Liu, L. Zhang, Y. (2020) Pathfinder-based simulation and optimization of personnel evacuation modeling of a shopping mall. *Journal of Physics: Conference Series*, vol. 1757, str. 1-9.

[4] Campbell, R. (2020) *Structure fires in schools*. National Fire Protection Association. Massachusetts, USA.

[5] Swedish Civil Contingencies Agency (MSB) (2014) Räddningstjänst I siffror 2013. MSB. Karlstad, Sweden.

[6] Swedish Civil Contingencies Agency (MSB) (2010) National strategy to enhance fire safety. MSB. Karlstad, Sweden.

[7] Uhnoo, S. Persson, S. Ekbrand, H. Lindgen, SA . (2014) Juvenile school firesetting in Sweden: cause and countermeasures. *Journal of Scandinaviaan Studies in Criminology and Crime Prevention*, vol. 16, br. 1, str. 25-40.

[8] Jonsson, A. Nilson, F. Runefors, M. P. Särdqvist. (2015) Fire related mortality in Sweden, temporal trends 1952 to 2013. Fire technology.

[9] Hassanain, M. Aljuhani, M. Hamida, M, B. Salaheldin, M,H. (2022) A framework for fire safety management in school facilities. *International Journal of Built Environment and Sustainability*, vol. 9, br. 2, str. 901-909

[10] Ehab, Z. (2011) Validation of methodologies to determine fire load for use in structural fire protection, Fire Protection Research Foundation

[11] Hassanain, M. (2006) Towards the design and operation of fire safe school facilities. *Disaster Prevention and Management: An International Journal*, vol. 15, br. 5, str. 838-846

[12] Уредба о разврставању објеката, делатности и земљишта у категорије угрожености од пожара („Службени гласник РС“, бр. 76/2010)

[13] Thunderhead : Pathfinder user manual, last accessed 5.9.2023.:

https://support.thunderheadeng.com/docs/pathfinder/2023-2/

RISK ASSESSMENT FOR POSITION OF THE CHIEF FIRE OFFICER

Dubravka Mandić Ilić[1], Senka Bajić[2]

Summary:

Firefighting is considered as a physically demanding job. The commander of the Fire and Rescue Brigade (FRB) is the person responsible for the work of the FRB completely, where command and control of the unit require many qualities that cannot be guaranteed by the rank alone. The focus of this study is risk assessment from the aspect of safety and health at work. Furthermore, various measures to reduce the adverse impact of the included dangers and harms for the position of the Chief Fire Officer were suggested. The assessment was made on the basis of research, conversations with the Chief Fire Officer, as well as on the basis of documentation provided for inspection by the Fire and Rescue Brigade in Novi Sad (Serbia). For the purpose of risk assessment, the Fine-Kinney method was used. After the risk assessment, different measures to reduce the risk were proposed, apropos, to maintain the risk at an acceptable level.

Key words: Firefighting, The Chief Fire Officer, Risk assessment, Safety and Health at Work, Fire safety, Disaster response, Risk management

[1] PhD student, Faculty of Technical Sciences, University of Novi Sad, Serbia, dudart2022@gmail.com
[2] Asst. Prof., Faculty of Technical Sciences, University of Novi Sad, Serbia, senka.bajic@uns.ac.rs

1. METHODOLOGY OF THE RISK ASSESSMENT

Work position risk assessment is based on determining, recording and evaluating all factors in the work process - possible types of hazards and harm in the work positions and in the working environment, which can cause injury at work, impairment of health or illness of the employee. While, second part of the risk assessment is introduction of the methods and measures for their elimination or risk reduction, to the extent that prevents or reduces the risk of injury at work, impairment of health or illness of employees [1].

This paper focused on the identification of dangers and harmfulness on the basis of a conversation with an employee at the work position of the Chief Fire Officer (CFO), as well as an insight into the technical and other documentation available to the CFO.

1.1. PROCEDURE FOR IMPLEMENTING THE RISK ASSESSMENT PROCEDURE

Method of obtaining information for risk assessment:
- preparing and processing the check list,
- conversation with the employee,
- observation, monitoring and
- other ways of collecting the necessary information.

1.2. THE METHOD USED FOR RISK ASSESSMENT AT WORK AND IN THE WORK ENVIRONMENT - FINE-KINNEY

In this research, the Fine-Kinney method was used to estimate the risk value. The Fine-Kinney method [2,3], which was first introduced as a tool for work position risk assessment from the aspect of safety and health at work in the 1970s, is a systematic methodology that gives us a mathematical formula for calculating the risk that arises from a certain hazard or harm. [4].

According to the original version of the Fine-Kinney method, the risk (R) value is calculated as the result of mathematical multiplication of parameters as seen in Equation (1):

$$R = P \times F \times C \tag{1}$$

Where:

• P is probability of injury/disease (P),
• F is frequency of exposure to hazards/harms (F) i
• C is the consequences, i.e. the severity of a possible injury or illness (C) [5],

2. RISK ASSESSMENT FOR THE POSITION OF THE CHIEF FIRE OFFICER

The commander of the Fire and Rescue Brigade (FRB) is the person responsible for the work of the FRB, where command and control require many qualities that cannot be guaranteed by rank alone.

"The position of commander requires theoretical, practical skills and the ability to know human relations" [6]. The assumption is that the position of the CFO is a position with high risk. This assumption was made in the first place because of the responsibility of the employee in the position of the CFO, which is the main characteristic of this position.

The job description as well as the organization of work at the observed work position were analyzed by reviewing the documentation of the Ministry of Internal Affairs, as well as by talking to an employee at the work position of the CFO in Novi Sad.

Considering the nature of the work, it is necessary to mention that the personal protective equipment of the members of the Fire and Rescue Brigade is significantly different from the personal protective equipment intended for employees in all other services, activities, or industries.

2.1. OVERVIEW OF POSSIBLE HAZARDS AND HARMS AT THE WORK AND IN THE WORKING ENVIRONMENT

Recognition and determination of hazards and harms at the work position and in the working environment was carried out based on data collected from documentation, by observing and monitoring the work process at the work position, obtaining the necessary information from employees and information from other sources and classifying them into defined hazards and harms which the data indicates. When determining data on hazards and harms at the work position and in the working environment, the starting point is the existing state of safety and health at work. Hazards and harms are grouped depending on their type and nature [1].

2.2. RECOGNIZING AND DETERMINING HAZARDS AND HARM IN THE WORK ENVIRONMENT AND AT THE WORK POSITION OF THE CHIEF FIRE OFFICER

Table 1 presents list of recognized hazards and harms at the work position and in the working environment, based on the collected data, analysis of jobs and working conditions at work position and in the working environment, as well as on the basis of the information obtained on the spot and an employee survey (Table 1) [7].

Table 1. Recognized hazards/harms [7]

Work position		Code	Description of hazards/harms for the observed work position
	Hazar	Mechanical hazards	
		02	Free movement of materials - during the intervention there is a possibility of injury due to the movement of parts of the building that burn and fall from the building

THE CHIEF FIRE OFFICER	ds	04	Dangerous means that can cause fire or explosion - during the intervention of technical-technological accidents, chemical spills
		05	Impossibility of removal - due to the changing working environment on interventions, there may be the possibility of sudden danger - dangerous chemicals, sudden explosions and similar to that
		06	Other factors that can appear as a source of danger - participation in traffic towards intervention (stress, accident: lying down, fractures, cuts, fatal outcomes, etc.)
		Hazards related to work position characteristics	
		07	Contact with dangerous surfaces, sharp edges, rough surfaces of furniture and equipment in the work area (possible injuries, cuts, bruises, etc.)
		09	Working in a confined, limited and dangerous space - although the CFO is in the so-called safe zone during the intervention, no zone is completely safe during large-scale interventions
		10	The possibility of slipping or stumbling in the work area; (possible injuries, sprains, fractures, death, etc.)
		12	Consequences due to the mandatory use of personal protection means or equipment - Given the use of suits during interventions with chemicals, carcinogenic substances and mutagens, there is a possibility of danger/harm with prolonged effects due to non-decontamination of the suit after the intervention
		Dangers due to the use of electricity	
		16	Danger of indirect contact with parts of electrical installations or equipment (electric shock)
	Harms	Harms that arise or appear in the work process	
		21	Chemical hazards, dust and fumes (inhalation, suffocation, introduction into the body, penetration into the body through the skin, burns, poisoning, etc.) - during interventions, even if it is in the so-called protected zone
		22	Physical harm (noise and vibration) - during the intervention, when raising the alarm, as well as during practical exercises
		23	Biological damage (infections, exposure to microorganisms, allergens) - There is always a possibility of interventions; Also, if the epidemiological situation is unfavorable, there is an increased possibility of infection

		26	Harmful effects of radiation (IR and UV radiation) - In the burned area, the temperature is over 8000 °C and it is accompanied by strong radiation that causes injuries: heat stroke and heat stress - Increased temperatures are also in the so-called safe zone
		27	Harmful climatic influences (outdoor work) During interventions and exercises
		28	Harms caused by the use of dangerous substances - during interventions with dangerous chemicals
		29	Working with a screen (sight impairment) - The commander spends part of his working day using a computer
		Harms due to mental and psychophysical efforts	
		31	Non-physiological position of the body - sitting (injuries of the bone-muscle system)
		32	Efforts that occur when performing certain tasks that cause psychological burdens (stress)
		33	Responsibility in receiving and transmitting information, using appropriate knowledge and skills, responsibility in rules of conduct, responsibility for rapid changes in work procedures, intensity of work, spatial conditioning of the workplace, conflict situations, responsibility in management - all of the above causes stress
		34	Harms related to the organization of work, such as: work longer than full-time (overtime), night work, preparedness in case of intervention, etc. - consequences stress

In the following, risk assessment according to the specified method, and for recognized hazards and harms with high risk will be presented in Table 2:

Table 2. Risk Assessment [7]

	C consequences	P probability	F frequency	R risk
32 Efforts that occur when performing certain jobs that cause psychological burdens (stress)	6 Very serious	6 Quite possible	10 Continuous	360 High risk
33 Responsibility in receiving and transmitting information, using appropriate knowledge and skills, responsibility in rules of conduct, responsibility for rapid changes in work procedures, intensity of work, spatial conditioning of the workplace, conflict situations, responsibility in management - all the above causes stress	6 Very serious	6 Quite possible	10 Continuous	360 High risk
34 Harms related to the organization of work, such as: work longer than full time (overtime), night work, preparedness in case of intervention, etc. - consequences stress	6 Very serious	6 Quite possible	10 Continuous	360 High risk

Given that the numerical value of the risk, R=360 was obtained, as well as considering the synergistic effect of dangers and harms, i.e., the total effect of dangers and harms that appear simultaneously, it is concluded that the job of the Chief Fire Officer belongs to the group of jobs with high risk [7].

2.3. PROPOSED MEASURES TO ELIMINATE, REDUCE OR PREVENT RISKS FOR HAZARDS WITH R=360

For the recognized harms, under the codes, 32, 33, 34, a numerical risk value of 360 was obtained. The measures proposed to reduce high risk values are: Anti-stress program according to one's own needs and possibilities; Balanced diet; Organizing a meeting after each critical event and, if necessary, individual advisory services; Regular systematic reviews; Regular physical activity/Recreation; Distribution of responsibilities and duties; Holiday; Constant improvement through continuing education, following appropriate literature, visiting counseling and general exchange of information, visiting other FRB and adopting good solutions, engagement of advisory bodies or individuals (mentors, experts from certain fields - chemicals, safety and health, psychology, data processing etc., education of the population in the field of fire protection, analysis of previous events, follow-up in the introduction of novelties in their work and the work of FRB; Creation of a strong, trained team; Non-deviation from standard safety procedures; Defining and determining the real needs for upgrading the general culture in connection with raising the degree safety in regular work, through the establishment of a realistic system of management, leadership, supervision in work and general and personal responsibility for safe and healthy work; Elaboration and application of all standards related to training and further training, as well as certification - specialization for certain work operations in depending on the jobs expected of them in regular work; Adequate training of the entire staff; Adequate equipment and maintenance provided; Adequate communication; Elaboration and application of forms of psychophysical preparation prescribed or recommended by professional organizations for members of the FRB; Collection and specification of own experiences with the aim of including them in the further improvement of safety and health measures at work; Exploitation of all technological innovations, especially in situations where they directly contribute to raising the level of security; Emphasis on psychophysical preparations; Insisting on the tightening of legal regulations, as well as the control of the law and the request for the installation of more systems for detection and automatic extinguishing of fires [7].

3. CONCLUSION

In order to reduce stress and share responsibility, apart from the measures mentioned in the previous chapter, it is very important to have a person (Officer) for safety in each fire brigade (who would be in charge of training, personal protective equipment - procurement and examination, medical examinations, monitoring of safety procedures, analysis of injuries, etc.). Furthermore, psychological support in each Fire and Rescue Brigade should be included, and mandatory periodic talks with each member of the FRB and their families in case of large-scale incidents or injuries during intervention.
A good law, with clear obligations and responsibilities, as well as frequent control of the implemented legal measures, is also a very important link in reducing the risk of both the CFO, and every member of the FRB.
Mandatory medical examinations of each member of the FRB should be scheduled every 6 months, as well as after every major intervention. The introduction of citizen education at the state level through the media and practical exercises for responding to emergency situations would be a good preventive measure for fire protection. Education of children in schools in the field of fire safety is practiced in some countries through mandatory subjects and it has been shown to give good results in raising safety awareness.
The introduction of standard procedures, modelled after the American Fire Service [8], for all individual items and the division of responsibilities for controlling the application of standards by item, would greatly reduce the possibility of error by each member of the Fire and Risk Brigade, and thus the amount of stress. [7]

ACKNOWLEDGEMENT

This research (paper) has been supported by the Ministry of Science, Technological Development and Innovation through project no. 451-03-47/2023-01/200156 “Innovative scientific and artistic research from the FTS (activity) domain”.
We would like to thank the Fire and Rescue Brigade and Stojan Milovac, the Chief Fire Officer of the Fire and Rescue Brigade in Novi Sad during the research, for enabling practical research work. We would also like to thank professor Mirjana Laban, for cooperation in research work.

REFERENCES

[1] Правилник о начину и поступку процене ризика на радном месту и у радној околини, "Сл. гласник РС", br. 72/2006, 84/2006 - испр., 30/2010 i 102/2015

[2] Fine in J Saf Res 3:157–166, 1971; Kinney and Wiruth in Practical risk analysis for safety management. Naval Weapons Center, pp 1–20, 1976

[3] Fine, W. T. (1971). Mathematical evaluations for controlling hazards. Journal of SafetyResearch,3(4),157–166.2. Kinney, G. F., & Wiruth, A. D. (1976). Practical risk analysis for safety management (pp. 1–20). Naval Weapons Center

[4] Gul M., Mete S., Serin F., Celik E. Fine–Kinney-Based Fuzzy Multi-criteria Occupational Risk Assessment: Approaches, Case Studies and Python Applications. Springer, 2021

[5] Kleut, N.: O određivanju rizika, Zaštita u praksi, str. 15-23, Beograd, 2009

[6] Grimwood P. (2008) Euro firefighter: global firefighting strategy and tactics, command and control and firefighter safety, Huddersfield, Jeremy Mills Publishing.

[7] Mandić Ilić D. (2022). Master thesis - Risk assessment for the position of the Chief Fire Officer, Faculty of Technical Sciences, Novi Sad, Serbia.

[8] National Fire Protection Association, Standard On Personal Alert Safety Systems (Pass), dosutpno na: https://www.nfpa.org/codes-and-standards/all-codes-and-standards/list-of-codes-and-standards?mode=code&code=1982, Pristupljeno: 05.08.2022.

JOINED FOR SUSTAINABILITY – BUILDING CLIMATE RESILIENT COMMUNITIES IN WB AND EU

Mirjana Laban[1], Suzana Dragnić[2], Marko Marković[3], Ljiljana Popović[4], Srđan Popov[5], Meri Cvetkovska[6]

Summary:

Economic and social development is widely affected by the impacts of climate change. It is of critical importance that higher education system contributes to building capacities and interdisciplinary knowledge for a sustainable and resilient society, able to build back better our vulnerable economies. Investors, insurers, businesses, cities and citizens across the EU and the Balkans should be able to access data and to develop instruments to integrate climate change into their risk management practices. Erasmus+ project 1FUTURE aim and specific objectives are in line with "Green Deal" EU overarching priority, as a project that supports action within higher education systems for creating climate resilient communities. Based on the performed needs analysis the broader aim of the project is to mainstream a holistic approach towards on climate and sustainability action.

Key words: climate change, resilient society, higher education

[1] Full Prof., University of Novi Sad, Faculty of Technical Sciences, Department of Civil Engineering and Geodesy, mlaban@uns.ac.rs
[2] Assis. Prof. University of Novi Sad, Faculty of Technical Sciences, Department of Civil Engineering and Geodesy, suzanav@uns.ac.rs
[3] Assoc. Prof. University of Novi Sad, Faculty of Technical Sciences, Department of Civil Engineering and Geodesy, marko_m@uns.ac.rs
[4] University of Novi Sad, Faculty of Technical Sciences, Department of Industrial Engineering and Engineering Management, ljiljana.popovic@uns.ac.rs
[5] University of Novi Sad, Faculty of Technical Sciences, Department of Computing and Control Engineering, srdjanpopov@uns.ac.rs
[6] Ss. Cyril and Methodius University in Skopje, Faculty of Civil Engineering, Department of Structural Mechanics and Earthquake Engineering, cvetkovska@gf.ukim.edu.mk

1. INTRODUCTION

Economic and social developments are widely affected by the impacts of climate change. It is of critical importance that higher education system contributes to building capacities and interdisciplinary knowledge for a sustainable and resilient society, able to build back better our vulnerable economies. Investors, insurers, businesses, cities and citizens across the EU and the Balkans should be able to access data and to develop instruments to integrate climate change into their risk management practices.

*Fig. 1 The **1FUTURE** Erasmus+ project team* (https://1future.feut.edu.al/)

Climate action and sustainability are set as priorities of WB governance. Leaders from Western Balkans, gathered in Sofia in 2020, at the WB Summit acknowledged the need to set the basis for a major transformation of WB region that would turn sustainability and resilience challenges into opportunities and transpose elements of the European Green Deal in all interrelated priority sectors. Among other issues, they agreed to develop a plan for economy-specific and regional awareness-raising activities, reflecting the Green Agenda for the Western Balkans in the reforms of the education systems.
Therefore, the HEI curricula across WBC should embrace the issues of green economy, climate change and sustainability in order to implement and develop the institutional reforms and to satisfy the requirements of the labor markets in the future. It is widely recognized that education is key to positively affect behaviors regarding the environment, starting from an early age. By reforming curricula and raising awareness within WBC communities, the youth of the region can contribute decisively to the implementation of the Green Deal Agenda and building a regional higher education area in the field of climate, sustainability and resilience.
Addressing these observations, and based on a sound needs analysis, the 1FUTURE project team (Fig. 1) deems the inclusion of Green Deal Goals into the WBC HEIs agenda as a necessity. The progress will be achieved through the revision and improvement of existing courses programmes, provision of short intensive courses to students and practitioners, development of new lectures materials, training of teaching staff and encouraging the research work in climate and sustainability. Furthermore, positioning university research in strategic areas of development can help inform good policies and find sustainable social, economic, environmental and technical solutions to today's problems. Considering the collaboration with the business sector as the key for achieving long-term sustainable goals, a joint collaboration platform, uniting student, staff and business communities within the Western Balkan countries, is planned to be created within the project under the name **1Future Platform**. The platform will give access to decision makers in government, business, and society, offering this way transversal knowledge and skills required to shape the future through embracing a climate resilience culture.

The wider aim of the project is to improve regional capacities in implementing Green Deal goals within higher education system, initiating an action towards environment, climate change, sustainability and resilience. Achievement of this aim requires the involvement of all stakeholders, gathered under a holistic approach. Regional cooperation provides the opportunity for tackling common problems and for sharing knowledge and transferring good practice. In line with the broader integration goals of WB countries to the EU, the support from EU funding and the cooperation of HEIs from the EU Member states or third countries associated to the programme is essential in capturing the full potential of this project.
The role of University of Novi Sad (UNS) in *jOiNEd For sUsTainability - bUilding climate Resilient* (1FUTURE) Erasmus+ project is an advisory, since Serbia became the program country in 2020.

2. NEEDS ANALYSIS

This project has been conceived after a thorough evaluation of the needs for the outcomes it will produce. Our needs analysis has used a systematic approach (using desk research, surveys and interviews) to studying the state of knowledge, ability, interest, and attitude of stakeholders included in the project. Elements of the needs analysis are outlined also in other parts of this project (impact, project concept and methodology), but the main outcomes of the process are summarized here. We have organized the needs analysis in 4 main parts:

- *impact*, outlining how education system can reach the targeted audience;
- *awareness*, outlining the gaps in the education provision within the existing programs and the needs to raise awareness among stakeholders;
- *demand*, outlining the potential demand of stakeholders for the knowledge and capacities developed under the project;
- *approaches*, outlining the methodologies we are using to reach the stakeholders.

In summary, the Needs Analysis revealed the following challenges across WBC HEIs, and advised on the possible areas of intervention:

- Absence of climate centers/hubs affiliated to the WBC HEIs;
- Limited or missing climate and sustainability courses;
- Limited typologies of teaching and learning methodologies applied in teaching process;
- Lack of professional courses in the field of climate and sustainability;
- Lack of students activities targeting climate and sustainability;
- Very limited collaboration capacities with business sector in the field of climate;
- Lack or very limited efforts to implement climate smart solutions within HEI services.

2.1. 1 FUTURE PROJECT - IMPACT

Climate issues and sustainability targets are at the core of international discourse, and have intensified since the UN Paris Agreement in 2015. It has become obvious that the environmental ambitions of the European Green Deal will not be achieved by acting only within the EU, as climate change and disaster risk do not know borderlines. The future sustainability will not be accomplished if all the households, business entities, private and public institutions do not act on these challenges to contribute to building back better our economies after a shock is experienced.
Education institutions play a crucial role in this process, by contributing in the development of knowledge and attitude toward sustainable behavior and resilience practices of all potential learners. Although the role of education in addressing these challenges is being increasingly recognized, and the development agendas in Western

Balkan Countries call for more action toward climate resilience and sustainability [1-3], the ability of education system of the region to contribute to adaptation and mitigation measures is yet a way to go.
Western Balkan countries share a similar political context, coming from a communist past, which, to various extents, continues to affect their higher education systems. The implementation of Climate Change and Sustainable Development Education in the Western Balkan countries requires profound reforms and initiative. Issues such as green economy and climate change represent new challenges for the region. Knez et. al. in 2022 [4], suggests that EU must use its influence, expertise, and financial resources to mobilize its' neighbors to join them on a sustainable path. The study revealed that in WB Balkan countries the implementation of the necessary regulations and strategies towards climate change mitigation is at a low level. According to the authors, the reason for this most often lies in the insufficient commitment of decision-makers to make significant changes in the field of climate change transition. This low level of commitment may be due to the low level of awareness that several entities have on issues on climate change and sustainability.

2.2. 1 FUTURE PROJECT - AWARENESS

A high gap between climate and sustainability education in EU and the Western Balkans has been observed during the development of this needs analysis. A review of programs of studies conducted within an EU project showed that over 107 education programs in the field of resilience and risk management are offered in EU and UK (K-force, 2017) [5]. In many cases these programs are of interdisciplinary nature, where the technical elements of the field, such as climate science, disaster risk, societal safety, etc. are integrated with economics, finance and insurance issues. Holloway, in 2014 [6], has reviewed the academic offerings in the field of sustainability and found around 100 masters-level programmes offered in 48 countries that involve several topics such as climate change and other disaster risks, sustainability and resilience topics.
A survey of education programs in the Western Balkan area showed that few countries of the region have operationalized the inclusion of topics related to green economy, climate change adaptation, energy markets, sustainability governance, resilience, etc. [5]. The number of graduates is insufficient for regional or national needs. Consequently, there is a need for education of experts who will be able to create a sustainable plan for building economic, social and infrastructure resilience in the region. At this moment, existing higher education programs do not meet the mentioned WB countries' needs for qualified staff. Moreover, climate and sustainability basic terminology in Balkan languages is very scarce. Cultural inflexibility, a traditional education system, and a generally restricted labor market are barriers for implementing such requirements in higher education.
During the post-communist era (1990 to the present), higher education curricula in the Western Balkans have been heavily revised to incorporate the principles of the Bologna Process. The European Union has supported the higher education sector in the region, and most countries have reciprocated by embracing western education practices, such as multidisciplinary or interdisciplinary approaches. While bachelor programs in WB tend to be more traditional in terms of content and focus, postgraduate programs are making a concerted effort to diversify their content. The creation of master programs that straddle across faculties is evidence of that, reflecting the needs of the increasingly challenging future described above.
In 2016, an EU funded project entitled *Knowledge for a resilient Society* (K-FORCE), contributed to building a sustainable educational foundation in the field of Resilience in the Western Balkans. In 2018, six new programs in the field of Disaster Risk Management, including topics related indirectly and directly to resilience, climate and sustainability, such as: disaster risk management, climate change adaptation, financial

resilience toward hazards, disaster risk modeling, disaster risk evaluation, etc. were implemented at Partner Universities in Serbia, Bosnia and Herzegovina and Albania. The programs have pursued after the end of the project, forming professionals in the field since 2020, proving the sustainability of the project outputs. Other EU funded projects that aimed at the enhancement of environmental awareness were implemented through the joint collaboration of HEIs in Iceland, Serbia, Bosnia and Herzegovina, and Romania. Through them, teaching and lectures, and open educational resources in the field of environment sustainability were developed. The success of these projects shows that there is a strong potential in filling the gap between climate and sustainability action undertaken by education institutions in EU and the Balkans.

2.3. 1 FUTURE PROJECT - DEMAND

While identifying the rationality of this project in relation to the education gap between EU and WBC HEIs in sustainability, climate, and resilience fields, the specific demand from different stakeholders, including student communities and business sector, has been appraised.

In framework of K-FORCE project, a *Youth Safety Culture survey* [7] was conducted aiming to gain an understanding of how safe and prepared for disasters management the youth of Western Balkan countries feel and how much they would be willing to engage in education on sustainability, resilience and climate. About 59% responded that they had no chance of learning on resilience practices in their High Schools or Universities. This survey has discovered the willingness among most of the respondents to engage in courses related to resilience, climate and sustainability. A significant number, around one fifth of respondents, expressed interest in doing a master's degree in the field. Such results indicate that there is a potential to create and leverage the human capital and improve the climate culture in the future years in order to provide an adequate answer to the challenges that the region would face in this area.

Another survey conducted by *Finget et al.* in 2021 [8] was addressed to students of WBC communities, to find out the perception about who is responsible to provide environmental education. The result from the survey showed a strong demand of students of the region for climate and sustainability education, concluding that that funding for international collaboration on Environmental Education is of fundamental importance to promote and facilitate the implementation of the concepts of the environmental citizen into the curriculum of universities.

Business entities are also not immune to the climate changes and disaster risks. Businesses entities that do not adapt will be at risk, while those that embrace change will see greater opportunities. Therefore, business entities should embrace sustainability practices in order to contribute to a green economy.

The *OECD's SME Policy Index*, has identified that, SME greening measures and policies are now included in overall SME strategies in almost all of the WB economies, but with limited implementation. The existing SME strategies of WBC, include measures related to providing advice and guidance to SMEs on improving resource efficiency (in particular energy efficiency), promoting Eco-innovation and introducing financial incentives for SME greening [9].

In the framework of the K-FORCE project, another survey aiming to monitor the existing practice and gather information on the preferences of the practitioners and experts for more education, was conducted [10]. The results indicated that currently the vocational education systems in the WB region cannot be considered as structured systems for the purpose of life-long education of professionals and do not offer much in terms of education for climate and resilience. The respondents indicated the needs practical skills, followed by improved theoretical knowledge. Among others, the survey relieved a significant interest to take part in the future professional courses, even if under a voluntary scheme.

The results of another survey conducted by *Shyle* in 2018 [11] in Tirana (Albania) highlight the level of knowledge and awareness that people and business have about sustainable development. The study results show low levels of knowledge by students and businesses to the concepts of sustainable development and the need for further measures to improve this situation in the future.

To further support and validate the planned activities and the broader aim of the project, the project WBC beneficiaries undertook a series of interviews with key institutions representatives in Albania, Bosnia and Herzegovina and Montenegro. The willingness of these stakeholder to take part in disseminating events and other broader activities of the project was also discussed during this process. More specifically, the target groups of interviewees included: in-line ministries and public institutions representatives in charge of environmental management, water resources, civil emergencies, and climate legislation; representatives of key municipalities (*Tirana, Lukavac, Sarajevo and Podgorica*); and UNDP Climate change Program in Albania representative. Participants in these interviews addressed thoroughly the need of consolidation of legislation and institutions in the field of climate change and sustainability as a prerequisite for strengthening the labor market for future professionals in the field.

The representatives underlined the lack of expertise in the current labor market in relation to climate change and sustainability. These stakeholders emphasized as well that for too long the region has been supported by international experts in this field, and it is very important to create local experts who need to acquire in depth knowledge from their studies.

2.4. 1 FUTURE PROJECT - APPROACHES

Based on the identified demand for education and initiatives within HEIs in the WBC to engage in climate action, we planned on the methods to implement these initiatives that would best address this demand.

The design of innovative curricula by introducing innovative elements in the existing curricula, the implementation of innovative learning and teaching methods (i.e. learner-centred and problem-based teaching and learning), the engagement with the business world by organizing joint programmes and activities with and within enterprises and the establishment of efficient networks for scientific and technological innovation within WBC and EU countries are some of the methods planned for addressing the needs of the project. We planned on activities that would best fit the needs, and be as flexible as possible in order to achieve a natural engagement of stakeholders to the project activities, through flexible and friendly tools. The characteristics of the methods we chose based on the needs of different stakeholders.

3. 1FUTURE SPECIFIC OBJECTIVES

The broader aim of the project is to mainstream a holistic approach towards climate and sustainability action. This will be achieved by improving regional capacities in implementing Green Deal goals in higher education system, particularly those related to the need for action to contribute to the green transition and to strengthen the sustainability competences of stakeholders. In line with the broader integration goals of WBC to the EU, the another aim of this project is to create a joint network of interdisciplinary collaboration between Western Balkans Universities and EU Universities, which would contribute to the sustainability of climate action and to promoting sustainability culture within the university governance. The collaboration with the business sector is another aspect considered as crucial for achieving the goals of the project. Therefore, specific outcomes of the project have been designed exactly to ease this collaboration, and to make is feasible and flexible for all participants.

Based on the performed needs analysis the broader aim of the project was defined: *Mainstream and holistic approach towards climate and sustainability action.* In addition, the following specific objectives are developed:

- SO1: Establish Knowledge Hubs for Climate and Sustainability (KHCS) within each WBC HEIs;
- SO2: Mainstream climate and sustainability culture within WBC HEIs;
- SO3: Raise awareness of staff and student community on the needs for climate action within HEIs;
- SO4: Increase Synergies between academia, business sector and government for implementing joint initiatives for climate and sustainability and
- SO5: Reinforcement of networking and collaboration between staff and student communities of WBC and EU about climate and sustainability actions.

1FUTURE project is planned in three phases: Initiation, Development and Implementation. Phases are intertwined, following the natural course of improvement of regional capacities in implementing climate and sustainability goals in higher education system. Each phase is linked to one Working Package (WP) led by two or more Lead Beneficiaries, who will be in charge for reaching its milestones and produce its deliverables. In addition, each WP is composed of specific tasks, leaded by one of or more project partners, depending on the complexity of the task. A total of 6 WP have been conceived, where WP1, WP5 and WP6 are related to project management, dissemination and quality assurance, while WP2, WP3, W4 represent the main WPs that will develop the main outputs of the project. The flow of WPs and tasks follow a linear course: activities of the project start with WP2 and end in WP4.

The roles and responsibilities have been divided between project partners, following a homogeneous division of tasks and duties. Competences, knowledge, experience, expertise and skills of project partners have been taken into account when dividing the roles, in order to create a reliable environment for the achievement of planned project activities as well as responsible, timely, cost effective and efficient task and project completion.

4. CONCLUDING REMARKS

The 1FUTURE Project is conceived following one of the main actions and priorities of EU, the *Green Deal*. This project envisages actions, tasks and deliverables that contribute to the field of climate change and sustainability in accordance with the main actions and priorities of the EU. It combines HEIs of the EU and WBC under a common goal: enhancing climate action within HEIs. While the path of EU HEIs towards this goal is greatly advanced, in the WBC HEIs more initiatives and actions are needed.

An alliance between EU HEIs and WBC HEIs provides a basis for achieving the green deal ambition for Higher Education in WBC. The further involvement of non-HEIs in the partnership fosters the collaboration and the ambitions of the project.

The 1FUTURE project has assessed the European Added Value following 5 specific criteria, as defined in the EU Report: "*European Added Value of EU Science, Technology and Innovation actions and EU-Member State Partnership in international cooperation*".

Networking: The Project's potential for strengthening the networking capacities between EU and WBC HEIs is very important. Activities are aimed at strengthening the joint initiatives between HEIs across Europe. In addition, the project would serve to support and widen the already established networks between partners. In fact, this partnership is built upon previous successful collaborations initiated within other EU programs in the past.

Facilitating excellence and capacity building: As a CBHE action, this project would support the international cooperation, by increasing excellence in teaching and further supporting research capacities in WBC. The joint work of partners and the exchange of experiences and best practices between EU and WBC countries would help to solve complex issues related to the green deal goals. Partners could make use of the best methods, tools and subjects available. European research and innovation experience in climate field can be transferred to WBC countries and make the contribution to their progress towards excellence and capacity building.

Coordination of critical mass: The complexity of this project requires the support and assistance of European counterparts. The initiation of climate action within a single HEI or country is very difficult, and even impossible, as climate impacts are not confined by national borders. Support in terms of expertise, knowledge transfer, financial resources and guidance is crucial for WBC. Initiating climate action within Higher Education systems requires joint efforts. In fact, climate and sustainability action goes beyond one single institution, one single sector, and even one single country. Multidisciplinary collaboration is essential.

Fostering mutual learning and harmonization in the EU and WBC: This joint effort for achieving the goals of the project would lay the ground for more standardization and harmonization of teaching and research practices between EU HEIs and WBC HEIs. The transfer of knowledge from EU counterparts would be reflected in concrete steps taken by WBC HEIs to make the services of education sector more compliant with EU practices.

Rationality and Economic Efficiency: This partnership involves 18 partners who jointly have taken the initiative to engage in climate action or support climate action developed within HEIs of WBC. The project results would provide gains in efficiency gains by pooling the costs of the action with more units and achieving a wide impact. In addition, this cooperation addresses one of the main areas of action of the EU, the EU Green Deal; therefore, it contributes to the achievement of wider EU policy goals, targeting both economic and societal objectives.

ACKNOWLEDGEMENT

The research has been conducted within the Erasmus+ project *jOiNEd For sUsTainability - bUilding climate Resilient communities in WB and EU* (1FUTURE, 101082815) and the project "Scientific research and improvement of educational process in the field of civil engineering", developed at the Department of Civil Engineering and Geodesy, Faculty of Technical Sciences, University of Novi Sad, Serbia.

REFERENCES

[1] The National Strategy for Development and Integration 2015-2020 (NSDI II) Retrieved from https://www.ips.gov.al/en/the-national-strategy-for-development-and-integration-nsdi/

[2] The Foreign Policy Strategy of Bosnia and Herzegovina 2018-2023 Retrieved from http://www.predsjednistvobih.ba/vanj/default.aspx?id=79555&langTag=en-US

[3] The National Strategy for Sustainable Development by 2030 (NSSD) Retrieved from https://www.gov.me/en/article/174209--national-strategy-for-sustainable-development-by-2030-nssd

[4] Knez, S., Štrbac, S. & Podbregar, I. Climate change in the Western Balkans and EU Green Deal: status, mitigation and challenges. Energ Sustain Soc 12, 1 (2022) Available at: https://doi.org/10.1186/s13705-021-00328-y

[5] K-FORCE (2017) Report on existing master programmes in EU. Retrieved from: http://www.kforce.gradjevinans.net/images/Fajlovi/Po_tackama/1.1/Report%201.1_part%20II_Report_on_existing_master_programmes_in_EU.pdf

[6] Holloway, A. (2014). Srategic Mobilisation of Higher Education Institutions in Disaster Risk Reduction Capacity Building: Experience of Peripero U. Research Alliance for Disaster and Risk Reduction (RADAR), Stellenbosch University, South Africa. Retrieved

from https://www.preventionweb.net/english/hyogo/gar/2015/en/bgdocs/Holloway,%202014.pdf

[7] K-Force (2017) Report on the Youth Safety Culture Survey in Western Balkan Countries. Retrieved from: http://www.kforce.gradjevinans.net/images/Fajlovi/Po_tackama/1.2/KFORCE_Report%20on%20Youth%20Safety%20Culture%20in%20WBC.pdf

[8] Finger, D.C.; Draghici, C.; Perniu, D.; Smederevac-Lalic, M.; Halbac-Cotoara-Zamfir, R.; Sehic, A.; Kapović Solomun, M. The Importance of International Collaboration to Enhance Education for Environmental Citizenship. Sustainability 2021, 13, 10326. Available at: https://doi.org/10.3390/su131810326

[9] OECD, SME Policy Index, Western Balkans and Turkey 2019, Chapter 11. SMEs in a green economy (Dimension 9) in the Western Balkans and Turkey, https://www.oecd-ilibrary.org/sites/948f4170-en/index.html?itemId=/content/component/948f4170-en

[10] K-Force (2017) Report on WBC needs for LLL courses. Retrieved from: http://www.kforce.gradjevinans.net/images/Fajlovi/Po_tackama/6.1/KFORCE_Report_on_WBC_needs_for_LLL_courses.pdf

[11] Irma SHYLE, 2018. "Awareness of Individuals and Businesses in Albania for Sustainable Development," European Journal of Multidisciplinary Studies Articles, Revistia Research and Publishing, vol. 3, Issue 1 https://revistia.com/files/articles/ejms_v3_i1_18/Irma.pdf

SPONSORS

УНИВЕРЗИТЕТ У НОВОМ САДУ
UNIVERSITY OF NOVI SAD

ФАКУЛТЕТ ТЕХНИЧКИХ НАУКА
FACULTY OF TECHNICAL SCIENCES

Факултет техничких наука, основан 1960. године, једна је од најсавремније организованих високообразовних институција у региону. Факултет је данас научно-образовна институција састављена од 13 департмана, 10 стручних служби и 38 научно-стручних центара. Лоциран је у неколико зграда и располаже са преко 35.000 m^2. Има око 1.200 запослених и око 17.000 студената. Факултет техничких наука изводи наставу на свим нивоима академских и струковних студија из следећих области високог образовања:

1. Машинско инжењерство
2. Електротехничко и рачунарско инжењерство
3. Грађевинско инжењерство
4. Саобраћајно инжењерство
5. Архитектура
6. Индустријско инжењерство и инжењерски менаџмент
7. Инжењерство заштите животне средине и заштите на раду
8. Геодетско инжењерство

Интердисциплинарне студије:

1. Графичко инжењерство и дизајн
2. Мехатроника
3. Управљање ризиком од катастрофалних догађаја и пожара
4. Примењена математика
5. Рачунарска графика
6. Енергетска ефикасност у зградарству
7. Сценски дизајн
8. Биомедицинско инжењерство
9. Техничка механика
10. Енергетске технологије
11. Урбанизам и регионални развој
12. Третман и заштита вода
13. Инжењерство информационих система
14. Информациони инжењеринг

ВИСОКО МЕСТО У ДРУШТВУ НАЈБОЉИХ

Трг Доситеја Обрадовића 6, 21000 Нови Сад
021/6350-413, 021/485-2055

The Faculty of Technical Sciences, which was established in 1960, is one of the best organized high-educational institutions in the region. Today, Faculty of Technical Sciences is scientific and educational institution of 13 departments, 10 administrative sectors and 38 scientific technical centers. The Faculty is located within the University campus in several separate buildings of 35.000 m^2 in area, with about 1.200 employed personal and about 17.000 students. The Faculty of Technical Sciences offers the following profiles of high education:

1. Mechanical engineering
2. Electrical engineering and computing
3. Civil engineering
4. Traffic engineering
5. Architecture
6. Industrial engineering and engineering management
7. Environmental engineering and occupational safety engineering
8. Geodesy

Interdisciplinary studies:

1. Graphic engineering and design
2. Mechatronics
3. Disaster Risk Management and Fire Safety
4. Applied mathematics
5. Computer graphics
6. Energy Efficiency in Buildings
7. Scene design
8. Biomedical engineering
9. Technical Mechanics
10. Energy technologies
11. Urban planning and regional development
12. Water treatment and protection engineering
13. Information Systems Engineering
14. Information Engineering

HIGH PLACE IN TOP SOCIETY

Trg Dositeja Obradovica 6, 21000 Novi Sad
021/6350-413, 021/485-2055

www.ftn.uns.ac.rs

ИНЖЕЊЕРСКА
КОМОРА
СРБИЈЕ

"AXIS GRAĐEVINSKI BIRO" DOO

AXIS

Sremska Kamenica

VOJVODE PUTNIKA 79,
SREMSKA KAMENICA

OFFICE@AXISBIRO.CO.RS

МОРАВСКИ КОРИДОР | MORAVA CORRIDOR

BECHTEL

ENKA

MORAVA CORRIDOR
MOTORWAY PROJECT


JADRAN
WE BUILD THE FUTURE.
WE PRESERVE TRADITION.
jadran-bg.rs


ČELIK
PROJEKTOVANJE
PROIZVODNJA I
MONTAŽA ČELIČNIH
KONSTRUKCIJA
Novosadska 119
21234 Bački Jarak, Srbija
www.celikdoo.rs
office@celikdoo.rs

Institut za ispitivanje materijala a.d.

Beograd, Bulevar vojvode Mišića 43

tel: +381 11 2650 322
fax: +381 11 3692 772

office@institutims.rs

www.institutims.rs

ŽIVOT JE LEPŠI
KADA BIRATE
KVALITETNO
MAPEI
ŽIVI KVALITETNO
www.mapei.rs

best
izgradnja
NOVI SAD

iNDiS2023

ISBN 978-86-6022-615-2